LIBRARIES SMITHSONIAN INSTITUTION

SMITHSONIAN INSTITUTION LIBRARIES

113

PALAEONTOGRAPHICA AMERICANA

(Founded 1917)

VOL. VII

NO. 42

TORREITES SANCHEZI (DOUVILLÉ) FROM JAMAICA

By

PETER JUNG

1970

Paleontological Research Institution
Ithaca, New York, U.S.A., 14850

SMITHSONIAN
SEP 10 1970
LIBRARIES

PALEONTOLOGICAL RESEARCH INSTITUTION

1969 - 1970

PRESIDENT	WILLIAM B. HEROY
VICE-PRESIDENT	DANIEL B. SASS
SECRETARY	REBECCA S. HARRIS
DIRECTOR, TREASURER	KATHERINE V. W. PALMER
COUNSEL	ARMAND L. ADAMS
REPRESENTATIVE AAAS COUNCIL	DAVID NICOL

Trustees

REBECCA S. HARRIS (Life)
AXEL A. OLSSON (Life)
KATHERINE V. W. PALMER (Life)
W. STORRS COLE (1964-1970)
DANIEL B. SASS (1965-1971)
KENNETH E. CASTER (1966-1972)
DONALD W. FISHER (1967-1973)
WILLIAM B. HEROY (1968-1974)
VIRGIL D. WINKLER (1969-1975)

BULLETINS OF AMERICAN PALEONTOLOGY

and

PALAEONTOGRAPHICA AMERICANA

KATHERINE V. W. PALMER, *Editor*
MRS. FAY BRIGGS, *Secretary*

Advisory Board

KENNETH E. CASTER
A. MYRA KEEN
HANS KUGLER
JAY GLENN MARKS
AXEL A. OLSSON

Complete titles and price list of separate available numbers may be had on application.

For reprint, Vols. 1-23, Bulletins of American Paleontology see
Kraus Reprint Corp., 16 East 46th St., New York, N.Y. 10017 U.S.A.

For reprint, vol. I, Palaeontographica Americana see Johnson Reprint Corporation, 111 Fifth Ave., New York, N. Y. 10003 U.S.A.

Subscription may be entered at any time by volume or year, with average price of $18.00 per volume for Bulletins. Numbers of Palaeontographica Americana invoiced per issue. Purchases in U.S.A. for professional purposes are deductible from income tax.

For sale by

Paleontological Research Institution
1259 Trumansburg Road
Ithaca, New York 14850
U.S.A.

PALAEONTOGRAPHICA AMERICANA

(Founded 1917)

VOL. VII

NO. 42

TORREITES SANCHEZI (DOUVILLÉ) FROM JAMAICA

By

PETER JUNG

July 27, 1970

Paleontological Research Institution
Ithaca, New York, U.S.A., 14850

SMITHSONIAN INSTITUTION AUG 26 1970

Library of Congress Card Number: 72-125866

Printed in the United States of America
Arnold Printing Corporation

CONTENTS

Page

Abstract 5

Systematic description 5

References 7

Plates 9

Index 13

TORREITES SANCHEZI (DOUVILLÉ) FROM JAMAICA

PETER JUNG
Naturhistorisches Museum
Basel, Switzerland

ABSTRACT

Torreites sanchezi (Douvillé), a hippurite rudist, is reported from the Campanian *Barrettia* Limestone of the Green Island Inlier of Hanover Parish, western Jamaica, W.I. It represents the first record of the genus outside Cuba.

Early in 1969 I found two specimens of a rudist belonging to the family Hippuritidae in the Campanian *Barrettia* Limestone of the Green Island Inlier of Hanover Parish, Jamaica, W.I. They are identified as *Torreites sanchezi* (H. Douvillé) and seem to be worth describing as they represent the first record of the genus in Jamaica. *Torreites* was so far known only from the Upper Cretaceous of Cuba.

I wish to thank Dr. L. J. Chubb of Kingston, Jamaica, for reading the manuscript.

SYSTEMATIC DESCRIPTION

Genus **TORREITES** R. H. Palmer

Palmer, R. H. 1933, Revista de Agricultura, Comercio y Trabajo, vol. 14, Nos. 15, 16, p. 99.

Type species (by original designation), *Hippurites (Vaccinites) sanchezi* H. Douvillé. Upper Cretaceous of Cuba.

General form cylindrical to conical, straight or somewhat curved, colonial or solitary. Umbo excentrical, situated anteriorly. Anterior side with a shallow, longitudinal depression. Ligamental ridge long, slightly tapering towards the interior. S and E pillars almost parallel-sided, rounded at their ends. E pillar considerably shorter than S, about half the length of L. Cardinal apparatus arranged on a straight line which forms an angle of 35° to 40° with the ligamental ridge. Left valve with three slots through which L, S, and E reach to the surface. Left valve consists of two layers: an inner layer with pores radiating from the umbo and an outer, imperforate layer.

Up to now only two species of the genus *Torreites* are known, both originally described from Cuba. Chubb (1961) included *T. tschoppi* MacGillavry in the *Durania* fauna of the Loma Yucatán limestones, whereas *T. sanchezi* (H. Douvillé) is part of the *Barrettia* fauna of the lower Habana Formation. According to Chubb (1961, pp. 419, 420), therefore, the range of the genus *Torreites* is Santonian or Coniacian to Campanian.

The origin of *Torreites* is as yet unknown. Douvillé (1927, p. 55) suggested an European ancestor based on analogies with the genus *Pironaea,* but according to Sénesse (1958, p. 647) it was derived from the genus *Pseudovaccinites.*

Torreites sanchezi (H. Douvillé)

Plates 1-3; Text figures 1,2

1927. *Hippurites (Vaccinites) sanchezi* H. Douvillé, Bull. Soc. Géol. France, ser. 4, vol. 27, fasc. 1, 2, p. 54, pl. 4, fig. 1.
1933. *Torreites sanchezi* Douvillé, Palmer, Revista de Agricultura, Comercio y Trabajo, v. 14, Nos. 15-16, p. 100, pl. 7, figs. 1-2, pl. 8, figs. 1-2.
1936. *Torreites sanchezi* (Douvillé), Rutten, Jour. Paleont., vol. 10, No. 2, p. 135, text-fig. 4g.
1937. *Torreites sanchezi* (Douvillé), Vermunt, Jour. Paleont., vol. 11, No. 4, p. 269.
1937. *Torreites sanchezi* (Douvillé), MacGillavry, Geogr. Geol. Meded., Physiogr.-Geol. Reeks, No. 14, p. 128, pl. 5, figs. 4e-h.

Diagnosis. — See description of genus.

Material and occurrence. — Only two specimens are available (Naturhistorisches Museum Basel Nos. G 14065 and G 14066). Both have been found as blocks in sugar cane fields near Green Island, Hanover, 400 m SSW of Church Hill School, in a small valley running from south to north. Trechmann (1922, pp. 506, 507) described the succession of rocks in this area.

Specimen G 14065. — This is an almost complete specimen somewhat eroded on top and near the base. The right valve is conical, its axis curved. Anterior side with a longitudinal, shallow depression. Outer shell layer of right valve with numerous, narrow infolds which are marked by longitudinal ridges on the surface all around the valve. These are connected by transverse riblets at irregular intervals. The left valve has three slots through which L, S, and E reach the surface. Inner layer of left valve with pores radiating from the umbo. The outer layer of the left valve is imperforate, but only parts of it are preserved.

After casting the complete specimen four transverse sections were made to show the ontogenetic development of the internal structure (Text figs. 1, 2; Pl. 2, figs. 1a-1d). L is long and slightly tapering towards the interior; E is shorter than S. All three pillars have about the same width. The myophore for the posterior muscle is horseshoe-shaped and does not pass the tip of S.

Measurements. — Greatest diameter: 125 mm. Height of complete specimen: 135 mm. The measurements of the pillars in the different sections are tabulated below (in mm):

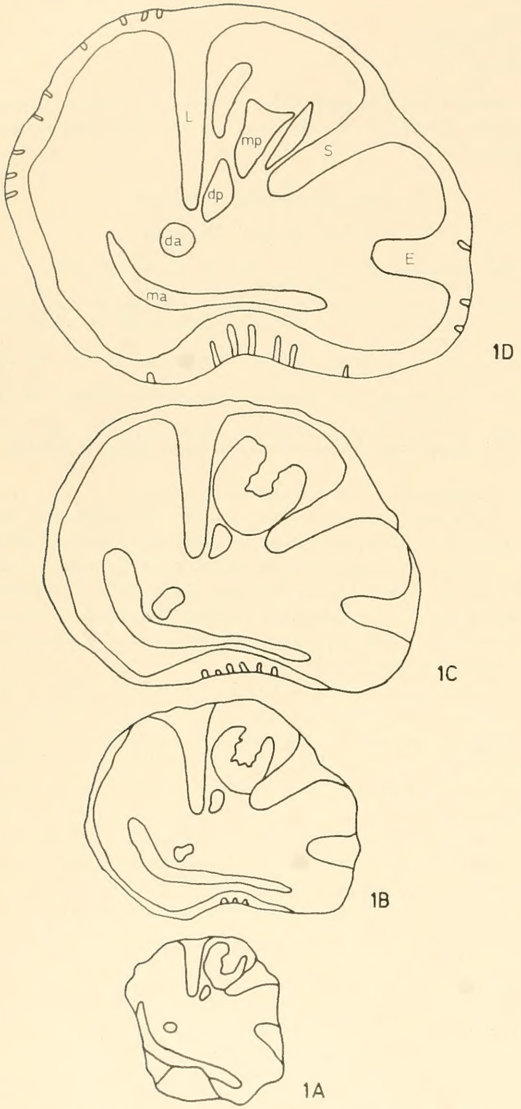

Text-figure 1.—Diagrams of sections A to D of specimen G 14065 (compare Pl. 2, figs. 1a-1d) showing ontogenetic development of internal structures. L: ligamental ridge. S and E: pillars. mp: myophore for posterior muscle. ma: attachment area for anterior muscle. dp: posterior tooth. da: anterior tooth.

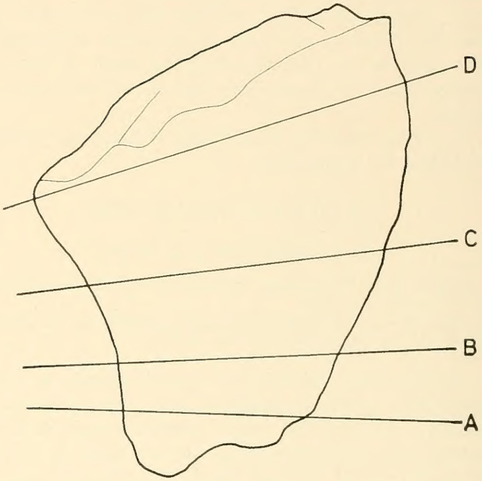

Text-figure 2.—Sketch of specimen G 14065 showing position of transverse sections A to D of Text-figure 1.

	section D		section C		section B		section A	
	length	width	length	width	length	width	length	width
L	48	8	36	7	25	6	15	4
S	35	8	28	8	20	7	13	5
E	21	10	18	8	13	7	10	5

The angles between the pillars and between L and the cardinal apparatus (= ca) are as follows:

angle between	section D	section C	section B	section A
L and ca	40°	38°	36°	39°
L and S	58°	63°	55°	58°
L and E	94°	103°	95°	110°

The measurements for the width of the pillars represent average figures. The lengths of the pillars in sections A and B are approximate only, because the shell wall is not or only partly preserved.

Specimen G 14066. — Only part of the right valve is preserved. This specimen is not conical in shape, but parallel-sided. It is strongly eroded and only small parts of the outer shell layer are preserved. L is proportionately longer than in specimen G 14065, and E is exceptionally narrow (about half the width of S).

Measurements. — Greatest diameter: 118 mm.
L: length 62 mm; width 6 mm
S: length 43 mm; width 7 mm
E: length 24 mm; width 3 mm
angle between L and cardinal apparatus: 34°
angle between L and S: 70°
angle between L and E: 105°

Comparison. — The differences between *T. sanchezi* and *T. tschoppi* MacGillavry have been pointed out by MacGillavry (1937, p. 129). *T. tschoppi* is a much smaller species; it lacks infoldings in the outer layer of the shell, and the angle between L and E is considerably smaller. So far all the specimens of *T. sanchezi* known are solitary, whereas the type of *T. tschoppi* is a colony.

Distribution. — According to Chubb (1961, pp. 419, 420) *T. sanchezi* is restricted in Cuba to the *Barrettia* fauna of the lower Habana Formation the age of which is Campanian. The specimens from Jamaica here described represent the first record of the genus outside Cuba. They derived from the *Barrettia* Limestone of the Green Island Inlier, Hanover. The age of this *Barrettia* Limestone is thought to be Upper Campanian by Chubb (1960, p. 17), but has been considered to be of older age in earlier publications. *T. sanchezi* is here associated with *Antillosarcolites macgillavryi* Chubb (1968, p. 26), a few other molluscan species, and corals.

The locality from where the two specimens of *T. sanchezi* described above were collected is the type locality of *Pseudorbitoides trechmanni* H. Douvillé 1922. This species has been dealt with extensively by Brönnimann (1955), who also noted the presence of "rare *Sulcoperculina* cf. *S. vermunti* (Thiadens), rare small, benthonic foraminifera, and abundant algal and rudist fragments." On the basis of comparison with related species of *Pseudorbitoides* Brönnimann assigned a Campanian or Maestrichtian age to the *Barrettia* Limestone of Green Island.

Chubb (in press) is describing a fragment from the Peters Hill Limestone of the Central Inlier, Jamaica, as *Torreites* cf. *sanchezi* which is associated with *Praebarrettia coatesi* Chubb (1968, p. 30) and the age of which is given as probably Turonian or Coniacian.

REFERENCES

Brönnimann, P.
1955. *Upper Cretaceous orbitoidal Foraminifera from Cuba. Part III. Pseudorbitoides H. Douvillé, 1922.* Contr. Cushman Found. Foram. Research, v. 6, pt. 2, pp. 57-76, pls. 9-12, text-figs. 1-17.

Chubb, L. J.
1960. *The Antillean Cretaceous geosyncline.* Trans. Second Carib. Geol. Conf., Puerto Rico, pp. 17-26, 2 figs.
1961. *Rudist assemblages in Cuba.* Bull. Amer. Paleont., v. 43, No. 198, pp. 411-422.
1968. *New rudist species from the Cretaceous rocks of Jamaica.* Jour. Geol. Soc. Jamaica, v. 9, 1967 (published November 1968), pp. 24-31.
(In press). *Rudists of Jamaica.* Palaeontographica Americana.

Douvillé, H.
1927. *Nouveaux rudistes du Crétacé de Cuba.* Bull. Soc. Géol. France, ser. 4, v. 27, fasc. 1-2, pp. 49-56, 2 figs., pl. 4.

MacGillavry, H. J.
1935. *Remarks on rudists.* Proc. Koninkl. Akad. Wetensch. Amsterdam, v. 38, No. 5, pp. 558-565.
1937. *Geology of the Province of Camaguey, Cuba, with revisional studies in rudist paleontology.* Geogr. Geol. Meded., Physiogr.-Geol. Reeks, No. 14, pp. 1-168, pls. 1-10, 1 map.

Palmer, R. H.
1933. *Nuevos rudistas de Cuba.* Revista de Agricultura, Comercio y Trabajo, v. 14, Nos. 15-16, pp. 95-125, pls. 1-10.

Rutten, M. G.
1936. *Rudistids from the Cretaceous of northern Santa Clara Province, Cuba.* Jour. Paleont., v. 10, No. 2, pp. 134-142, figs. 1-4.

Sénesse, P.
1958. *Considérations sur l'évolution des Hippuritidés d'après des matériaux des Corbières et de l'Ariège.* Bull. Soc. Géol. France, ser. 6, v. 7, fasc. 6, pp. 631-652, text-pls. 1-2.

Trechmann, C. T.
1922. *The Barrettia beds of Jamaica.* Geol. Mag., v. 59, No. 701, pp. 501-514, pls. 18-20.

Vermunt, L. W. J.
1937. *Cretaceous rudistids of Pinar del Rio Province, Cuba.* Jour. Paleont., v. 11, No. 4, pp. 261-275, pls. 36-37, text-figs. 1-3.

PLATES

EXPLANATION OF PLATE 1

All figures natural size

Figure		*Page*
1-3.	*Torreites sanchezi* (H. Douvillé)	5
	Three views of complete specimen (G 14065). Note longitudinal ridges marking position of infolds of outer shell layer of right valve.	

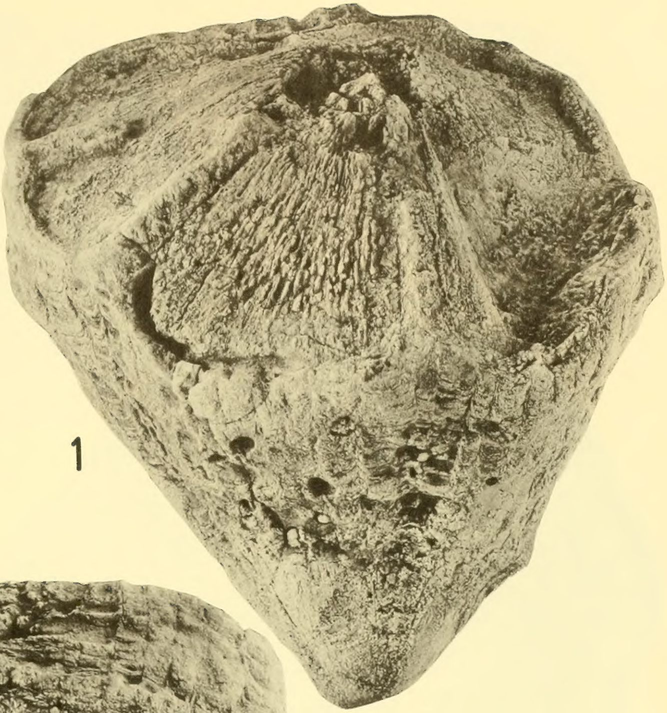

1

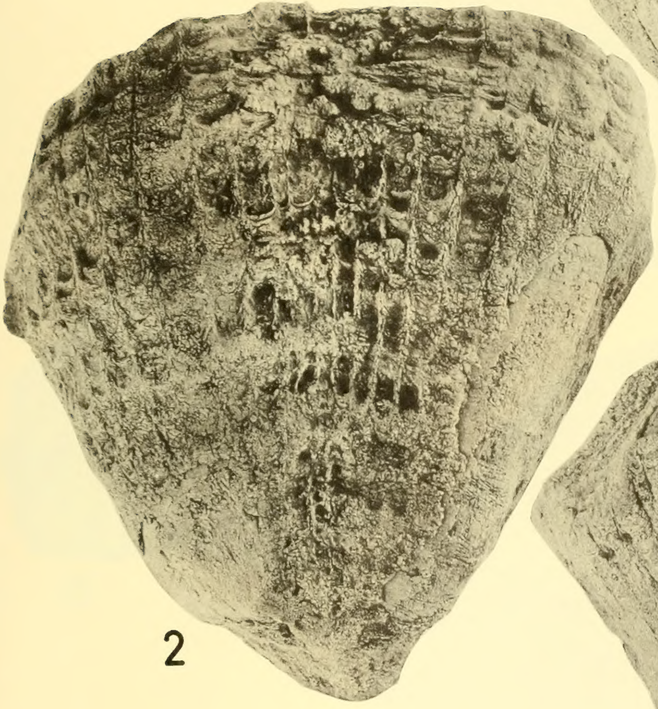

2

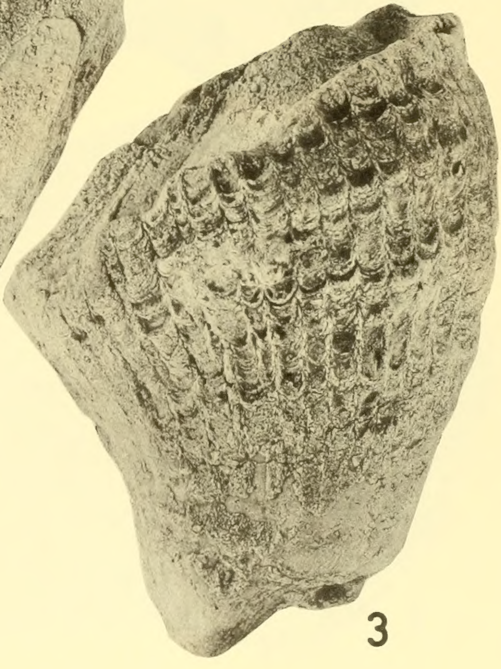

3

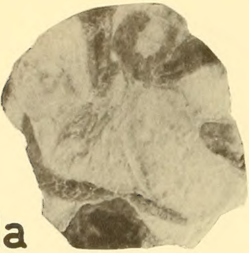
1a

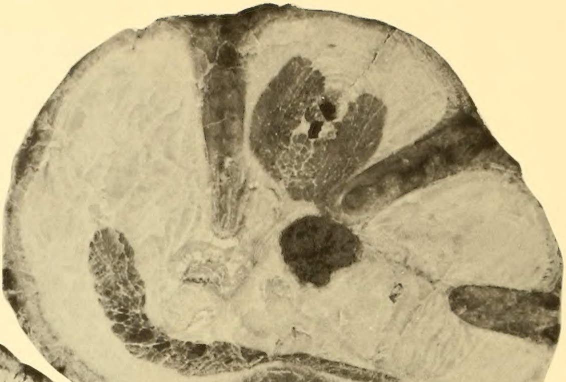
1c

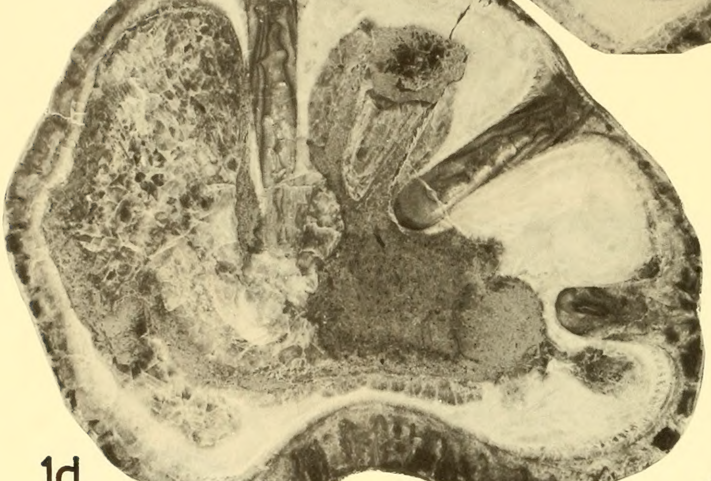
1d

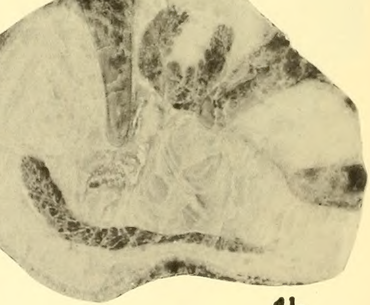
1b

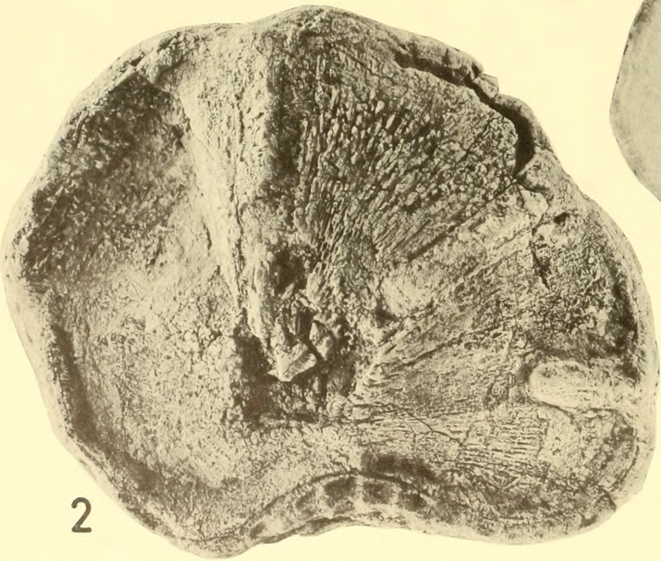
2

EXPLANATION OF PLATE 2

All figures natural size

Figure		*Page*
1,2.	*Torreites sanchezi* (H. Douvillé)	5

1a-1d. Transverse sections of specimen G 14065 corresponding to those of Text-figure 1A-1D. 2. Top view of specimen G 14065. L, S, and E reach above the surface of the left valve. The left valve is seen to consist of two layers: the areas to the left of L and just below the E pillar show remains of the outer, imperforate layer. The inner layer of the left valve with radiating pores is best seen between L and S. In figure 1d part of this inner layer is sectioned to the left of L.

EXPLANATION OF PLATE 3

All figures natural size

Figure		*Page*
1-3.	*Torreites sanchezi* (H. Douvillé)	5

Sections of specimen G 14066. 1. Transverse section. 2. Longitudinal section (same specimen as fig. 3a). 3a-3b. Oblique views of two matching pieces sectioned at about right angles. For explanation of symbols see Text-figure 1.

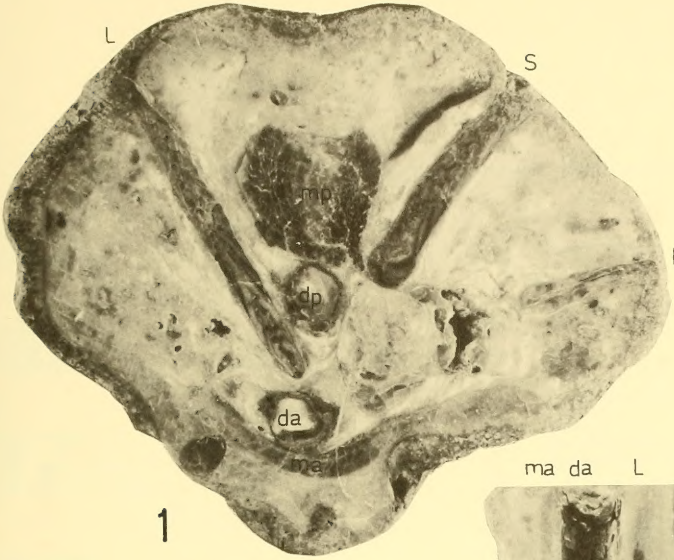

1

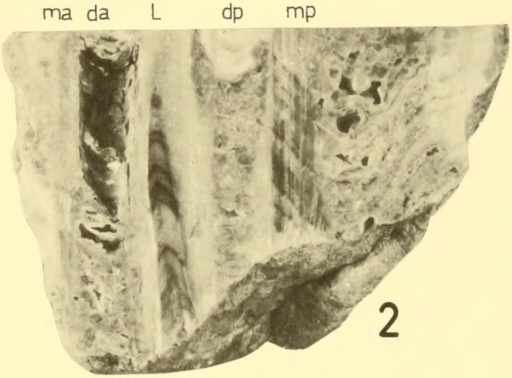

2

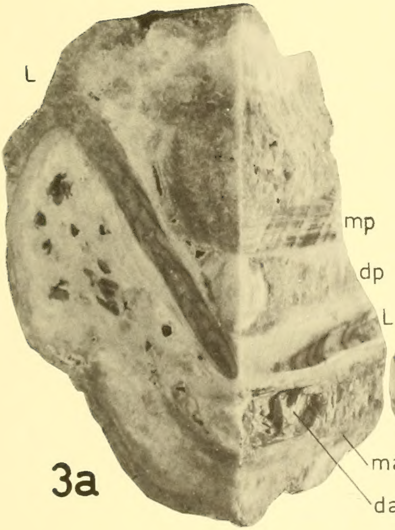

3a

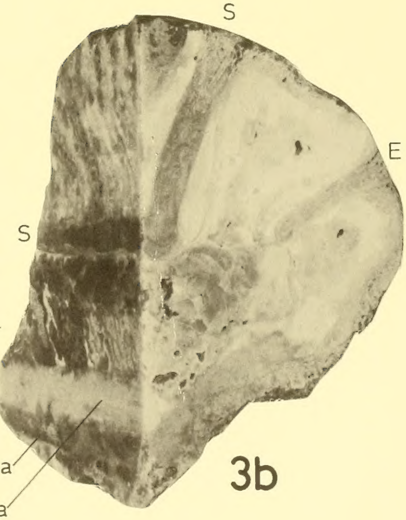

3b

INDEX

Note: Light face type refers to page numbers. Bold face type refers to plate number.

A

Antillosarcolites 7

B

Barrettia fauna 5, 7
Barrettia Limestone 5, 7
Brönnimann, P. 7

C

Central Inlier 7
Chubb, L. J. 5, 7
Church Hill School 5
coatesi, Praebarrettia 7

D

Durania fauna 5
Douvillé, H. 5

G

Green Island, Hanover 5, 7
Green Island Inlier 5, 7

H

Habana Formation 5, 7
Hanover Parish 5
Hippurites 5

L

Loma Yucatán limestones 5

M

macgillavryi, Antillosarcolites 7

P

Palmer, R. H. 5
Peters Hill Limestone 7
Pironaea 5
Praebarrettia 7
Pseudorbitoides 7
Pseudovaccinites 5

S

sanchezi, Torreites **1, 2, 3,** 5, 7, 10 11, 12
sanchezi, Torreites cf. 7
Sénesse, P. 5
Sulcoperculina 7

T

Torreites 5
Trechmann, C. T. 5
trechmanni, Pseudorbitoides 7
tschoppi, Torreites 5, 7

V

Vaccinites 5
vermunti, Sulcoperculina cf. 7

XLI.	(Nos. 185-192). 381 pp., 35 pls. Australian Carpoid Echinoderms, Yap forams, Shell Bluff, Ga. forams. Newcomb mollusks, Wisconsin mollusk faunas, Camerina, Va. forams, Corry Sandstone.	16.00
XLII.	(No. 193). 673 pp., 48 pls. Venezuelan Cenozoic gastropods.	18.00
XLIII.	(Nos. 194-198). 427 pp., 29 pls. Ordovician stromatoporoids, Indo-Pacific camerinids, Mississippian forams, Cuban rudists.	16.00
XLIV.	(Nos. 199-203). 365 pp., 68 pls. Puerto Rican, Antarctic, New Zealand forams, Lepidocyclina, Eumalacostraca.	16.00
XLV.	(No. 204). 564 pp., 63 pls. Venezuela Cenozoic pelecypods	18.00
XLVI.	(Nos. 205-211). 419 pp., 70 pls. Large Foraminifera, Texas Cretaceous crustacean, Antarctic Devonian terebratuloid, Osgood and Paleocene Foraminifera, Recent molluscan types.	16.00
XLVII.	(Nos. 212-217). 584 pp., 83 pls. Eocene and Devonian Foraminifera, Venezuelan fossil scaphopods and polychaetes, Alaskan Jurassic ammonites, Neogene mollusks.	18.00
XLVIII.	(No. 218). 1058 pp., 5 pls. Catalogue of the Paleocene and Eocene Mollusca of the Southern and Eastern United States.	18.00
XLIX.	(Nos. 219-224). 671 pp., 83 pls. Peneroplid and Australian forams, North American carpoids, South Dakota palynology, Venezuelan Miocene mollusks, *Voluta.*	18.00
L.	(Nos. 225-230). 518 pp., 42 pls. Venezuela and Florida cirripeds, Antarctic forams, Linnaean Olives, Camerina, Ordovician conodonts, Niagaran forams.	18.00
LI.	(Nos. 231-232). 420 pp., 10 pls. Antarctic bivalves, Bivalvia catalogue.	18.00
LII.	(Nos. 233, 236). 387 pp., 43 pls. New Zealand forams, Stromatoporoidea, Indo-Pacific, Miocene-Pliocene California forams.	18.00
LIII.	(Nos. 237-238). 488 pp., 45 pls. Venezuela Bryozoa, Kinderhookian Brachiopods.	18.00
LIV.	(Nos. 239-245). 510 pp., 50 pls. Dominican ostracodes, Texan pelecypods, Wisconsin mollusks, Siphocypraea, Lepidocyclina, Devonian gastropods, Miocene Pectens Guadaloupe.	18.00
LV.	(Nos. 246-247). 657 pp., 60 pls. Cenozoic corals, Trinidad Neogene mollusks.	18.00
LVI.	(Nos. 248-254). 572 pp., 49 pls. American Foraminifera, North Carolina fossils, coral types, Belanski types, Venezuelan Cenozoic Echinoids, Cretaceous Radiolaria, Cymatiid gastropods.	18.00
LVII.	(Nos. 255-256). 321 pp., 62 pls. Alaskan Jurassic ammonites, Pt. II, Jurassic Ammonitina New Guinea.	18.00

PALAEONTOGRAPHICA AMERICANA

Volume I.	See Johnson Reprint Corporation, 111 Fifth Ave., New York, N. Y. 10003 Monographs of Arcas, Lutetia, rudistids and venerids.	
II.	(Nos. 6-12). 531 pp., 37 pls. Heliophyllum halli, Tertiary turrids, Neocene Spondyli, Paleozic cephalopods, Tertiary Fasciolarias and Paleozoic and Recent Hexactinellida.	23.00
III.	(Nos. 13-25). 513 pp., 61 pls. Paleozoic cephalopod structure and phylogeny, Paleozoic siphonophores, Busycon, Devonian fish studies, gastropod studies, Carboniferous crinoids, Cretaceous jellyfish, Platystrophia and Venericardia.	28.00
IV.	(Nos. 26-33). 492 pp., 72 pls. Rudist studies Busycon, Dalmanellidae, Byssonychia, Devonian lycopods, Ordovican eurypterids, Pliocene mollusks.	28.00
V.	(Nos. 34-37). 445 pp., 101 pls. Tertiary Arcacea, Mississippian pelecypods, Ambonychiidae, Cretaceous Gulf Coastal forams.	32.00
VI.	(Nos. 38-40). 275 pp., 56 pls. Lycopsids and sphenopsids of Freeport Coal, Venericardia, Carboniferous crinoids.	20.75

BULLETINS OF AMERICAN PALEONTOLOGY

Vols. I-XXIII.	See Kraus Reprint Corp., 16 East 46th St., New York, N. Y. 10017, U.S.A.	
XXIV.	(Nos. 80-87). 334 pp., 27 pls. Mainly Paleozoic faunas and Tertiary Mollusca.	12.00
XXV.	(Nos. 88-94B). 306 pp., 30 pls. Paleozoic fossils of Ontario, Oklahoma and Colombia, Mesozoic ehinoids, California Pleistocene and Maryland Miocene mollusks.	12.00
XXVI.	(Nos. 95-100). 420 pp., 58 pls. Florida Recent marine shells, Texas Cretaceous fossils, Cuban and Peruvian Cretaceous, Peruvian Eogene corals, and geology and paleontology of Ecuador.	14.00
XXVII.	(Nos. 101-108). 376 pp., 36 pls. Tertiary Mollusca, Paleozoic cephalopods, Devonian fish and Paleozoic geology and fossils of Venezuela.	14.00
XXVIII.	(Nos. 109-114). 412 pp., 34 pls. Paleozoic cephalopods, Devonian of Idaho, Cretaceous and Eocene mollusks, Cuban and Venezuelan forams.	14.00
XXIX.	(Nos. 115-116). 738 pp., 52 pls. Bowden forams and Ordovician cephalopods.	18.00
XXX.	(No. 117). 563 pp., 65 pls. Jackson Eocene mollusks.	16.00
XXXI.	(Nos. 118-128). 458 pp., 27 pls. Venezuelan and California mollusks, Chemung and Pennsylvanian crinoids, Cypraeidae, Cretaceous, Miocene and Recent corals, Cuban and Floridian forams, and Cuban fossil localities.	16.00
XXXII.	(Nos. 129-133). 294 pp., 39 pls. Silurian cephalopods, crinoid studies, Tertiary forams, and Mytilarca.	16.00
XXXIII.	(Nos. 134-139). 448 pp., 51 pls. Devonian annelids, Tertiary mollusks, Ecuadoran stratigraphy paleontology.	16.00
XXXIV.	(Nos. 140-145). 400 pp., 19 pls. Trinidad Globigerinidae, Ordovician Enopleura, Tasmanian Ordovician cephalopods and Tennessee Ordovician ostracods and conularid bibliography.	16.00
XXXV.	(Nos. 146-154) 386 pp., 31 pls. G. D. Harris memorial, camerinid and Georgia Paleocene Foraminifera, South America Paleozoics, Australian Ordovician cephalopods, California Pleistocene Eulimidae, Volutidae, and Devonian ostracods from Iowa.	16.00
XXXVI.	(Nos. 155-160). 412 pp., 53 pls. Globotruncana in Colombia, Eocene fish, Canadian Chazyan Antillean Cretaceous rudists, Canal Zone Foraminifera, fossils, foraminiferal studies.	16.00
XXXVII.	(Nos. 161-164). 486 pp., 37 pls. Antillean Cretaceous Rudists, Canal Zone Foraminifera, Stromatoporoidea.	16.00
XXXVIII.	(Nos. 165-176). 447 pp., 53 pls. Venezuela geology, Oligocene Lepidocyclina, Miocene ostracods, and Mississippian of Kentucky, turritellid from Venezuela, larger forams, new mollusks, geology of Carriacou, Pennsylvanian plants.	18.00
XXXIX.	(Nos. 177-183). 448 pp., 36 pls. Panama Caribbean mollusks, Venezuelan Tertiary formations and forams, Trinidad Cretaceous forams, American-European species, Puerto Rico forams.	16.00
XL.	(No. 184). 996 pp., 1 pls. Type and Figured Specimens P.R.I.	18.00

15

PALAEONTOGRAPHICA AMERICANA

(Founded 1917)

VOL. VII

No. 43

THE CANCELLARIID RADULA AND ITS INTERPRETATION

By

AXEL A. OLSSON

1970

Paleontological Research Institution
Ithaca, New York, U.S.A. 14850

SMITHSONIAN
SEP 10 1970
LIBRARIES

PALEONTOLOGICAL RESEARCH INSTITUTION
1969 - 1970

President	William B. Heroy
Vice-President	Daniel B. Sass
Secretary	Rebecca S. Harris
Director, Treasurer	Katherine V. W. Palmer
Counsel	Armand L. Adams
Representative AAAS Council	David Nicol

Trustees

Rebecca S. Harris (Life)
Axel A. Olsson (Life)
Katherine V. W. Palmer (Life)
W. Storrs Cole (1964-1970)
Daniel B. Sass (1965-1971)
Kenneth E. Caster (1966-1972)
Donald W. Fisher (1967-1973)
William B. Heroy (1968-1974)
Virgil D. Winkler (1969-1975)

BULLETINS OF AMERICAN PALEONTOLOGY
and
PALAEONTOGRAPHICA AMERICANA

Katherine V. W. Palmer, *Editor*
Mrs. Fay Briggs, *Secretary*

Advisory Board

Kenneth E. Caster
A. Myra Keen
Hans Kugler
Jay Glenn Marks
Axel A. Olsson

Complete titles and price list of separate available numbers may be had on application.

For reprint, Vols. 1-23, Bulletins of American Paleontology see
Kraus Reprint Corp., 16 East 46th St., New York, N.Y. 10017 U.S.A.

For reprint, vol. I, Palaeontographica Americana see Johnson Reprint Corporation, 111 Fifth Ave., New York, N. Y. 10003 U.S.A.

Subscription may be entered at any time by volume or year, with average price of $18.00 per volume for Bulletins. Numbers of Palaeontographica Americana invoiced per issue. Purchases in U.S.A. for professional purposes are deductible from income tax.

For sale by

Paleontological Research Institution
1259 Trumansburg Road
Ithaca, New York 14850
U.S.A.

PALAEONTOGRAPHICA AMERICANA

(Founded 1917)

VOL. VII

No. 43

THE CANCELLARIID RADULA AND ITS INTERPRETATION

By

Axel A. Olsson

August 17, 1970

Paleontological Research Institution
Ithaca, New York, U.S.A. 14850

Library of Congress Card Number: 75-128176

Printed in the United States of America
Arnold Printing Corporation

CONTENTS

Abstract 19

Introduction 19

Acknowledgment 19

The cancellariid radula 19

- The upper shield or mandible 20
- The inner shield 20
- The radula proper 20

Conclusions 20

Additional notes 21

Bibliography 21

Plates 23

Index 27

THE CANCELLARIID RADULA AND ITS INTERPRETATION

Axel A. Olsson*

ABSTRACT

This paper deals with the cancellariid radula which, up until now, has been so imperfectly known that the classification of this interesting family of marine snails has remained uncertain. The study also presents a new approach to research upon radulae and their proper illustration by photomicrographs of the whole structure rather than by sketches of a few parts. The study also demonstrates that the so-called family Cancellariidae warrants recognition as a separate and distinct ordinal group of the Prosobranchia. The radula in this group is unique and differs so fundamentally from those of other named taxa that a new term based upon radular structure is necessary. For this order, the name Nematoglossa is proposed in allusion to the threadlike shape of its highly modified radular teeth.

The food requirements of the cancellariids are unknown. It is assumed that they feed mainly upon soft-bodied interstitial micro-organisms, which they are able to capture by means of the petaloid structure at the distal end of the anterior set of filiform teeth, and to transmit through the tubular formation of the filaments into the central area of the radula and from there into the alimentary system of the snail. Until the mode of life of the cancellariids becomes known more fully, preferably through direct observation of the living animals, the functional operation of the radula must remain conjectural.

INTRODUCTION

The Cancellariidae comprise a very select family of marine gastropods with a well-documented geologic history extending back into the Cretaceous. Their shells may show a high degree of diversification in shape and coil permitting arrangement in various genera and subgenera, nevertheless they display a unique degree of family likeness and hence are always readily recognizable and seldom if ever confused with other gastropod groups. Until lately, our knowledge of the cancellariid radula has been incomplete, puzzling, and their position in classification uncertain. Troschel (1866) first assigned the family to the Toxoglossa on broad generalities while Thiele (1929), in the *Handbuch der Systematischen Weichtierkunde,* referred them to the Rachiglossa between the Volutes and the Marginellas. Graham (1966) indicated that the foregut of the Cancellarias is essentially stenoglossate provided with an extensible muscular proboscis which would seem to imply a carnivorous diet. The food habits of the family are unknown and until more directly determined, this aspect of their life activities will remain largely speculative.

This paper presents a study of the radula of five cancellariid species, mainly through the medium of direct microphotographs which have not been retouched to any marked degree. It introduces a different approach to radular research by means of photographs rather than the usual visual one of hand or camera lucida sketches of a few teeth or elements. Although the cancellariid radula is of average size, high magnification is necessary to show its complicated structure and especially the shape and nervation of the petaloids at the distal extremities of the filaments. The radula each of the following species is figured herein.

Cancellaria cremata Hinds Gulf of Panama. IMAS
urceolata Hinds Panama. Petit
indentata G. B. Sowerby I Gulf of Panama
ovata G. B. Sowerby I Galapagos. Petit
scalata G. B. Sowerby I (as *lamellosa* Hinds). Petit
Trigonostoma bullatum (G. B. Sowerby I) Gulf of Panama. IMAS

ACKNOWLEDGMENT

This study has been made possible along the present lines through the use of exceptionally well-preserved material from two sources. In the first instance, I am grateful to Professor Ferderick M. Bayer of the Institute of Marine and Atmospheric Sciences of the University of Miami (IMAS) for material from the Gulf of Panama collected by their Research Vessel "Pillsbury" in 1967; secondly to Mr. Richard E. Petit of Ocean Drive Beach, South Carolina, for alcoholic material from Panama, Galapagos, and Europe. Also my thanks are offered to Dr. Katherine V. W. Palmer, Director of the Paleontological Research Institution of Ithaca under whose editorial guidance this paper is published.

Coral Gables, Florida
March 2d, 1970

THE CANCELLARIID RADULA

The radular organ of the Cancellariidae differs fundamentally from that of all other marine gastropods in its multiple construction or in having accessory structures in which the radula proper is contained, as well as by the peculiar features of the radula itself. In most extractions using an alkaline reagent (KOH) for the dissolution of the fleshy tissue, the upper accessory element generally becomes separated from the radular proper, and if noticed at all floating free in the solution, its connection as an intimate part of the whole radula organ would hardly be suspected. Two accessory structures are present which for convenience of description may be termed: the Upper Shield or Mandible and the Inner Shield. Both structures are of chitonous nature since they withstand the action of strong alkalies. The radula itself bears no resemblance to that of other Prosobranchs having sharp cusped teeth in transverse rows attached to a basal ribbon and forming a fixed pattern for each major group and on which our basic classification is so largely founded. In the cancellariids, the radula has a short middle section of no appreciable width and from

---

*Honorary Research Associate Smithsonian Institution; Research Associate Paleontological Research Institution and of the Academy of Natural Sciences of Philadelphia.

which arise coarsely veined strands of flexible filaments in single file and diverge in opposite directions; one set forward or anteriorly, the other backward or posteriorly. Because these filaments are resistant to the action of strong alkalies, they can be interpretated as highly modified radular teeth. The alignment of these filaments is longitudinal or uniserial, and if this feature has any meaning, a possible relations with the uniserial rachiglossate radula of the Volutes is indicated. The function of the radular filaments in the procurement of food is not clear. Barnard (1957) who gave us the first full description and figures of the cancellariid radula suggested that only the anterior set of filaments were functional, the hinder one being replacements but both sets are equally well developed and differs also in other respects so that both sets are functional at the same time but in different ways.

THE UPPER SHIELD OR MANDIBLE

The presence of an chitinous structure above the radular proper was first noticed by Thiele, although it was separated from that organ in the extracting solution. Thiele named this structure a "kiefer" or a modified jaw and its position near or within the mouth of the muscular proboscis warrants this interpretation. When separated and spread open, flat in a slide mount, it bears a striking resemblance to the cast-off carapace of a crustacean. Its shape varies a little between species but in general it is wide and winged in the middle and back and prolonged into a long, narrow, hollow snout in front. In position, it is laterally folded with the radula proper within. Although the mandible is described as an accessory structure, it is merely an adjunct in the proper operation of the radula and hence a different morphological element. This situation is indicated by the ease in which the radula and the mandible become separated during extraction even when special care is taken to keep them together.

THE INNER SHIELD

The presence of an inner shield directly enclosing the radula was first indicated by Barnard. The structure is homologous to the membraneous-winged flaps seen on a rachiglossate radula (*Olivella*) and by means of which the radula is attached to the buccal mass or the buccal wall.

THE RADULA PROPER

The essential features of the radula proper have been mentioned, its filiform teeth and their straight, linear alignment. Figures on the plates show its appearance as seen in different slide mounts or as floating free in the extraction fluid. In its normal, undisturbed position, it lies within the folded flaps of the Upper Shield or Mandible with the anterior set of strands lying within the hollow, tubelike interior of the snout, the posterior set extending out beyond the limits of the shield in the back. When removed entirely from the Upper Shield, it may appear as in figure 1, with both sets of strands separated into numerous, tentacular-like filaments. This figure also shows the membraneous Inner Shield to which the radula is directly attached.

The individual filaments when flattened in a slide mount resemble narrow blades of grass with coarse, parallel venation (like a monocotyledonous leaf) traceable throughout their length. At the terminal ends of each individual strand, they may be divided into a cluster of loose, open tubes as in figure 17. In other species, as in *Cancellaria ovata* (figure 10), they form petaloid expansions composed of a similar aggregation of tubelike structures. It is evident that these terminal modifications are adaptations for the capture and screening of food particles to be pulled into the hollow, rectangular spaces formed by the coarse venations and carried through these canals into the central area of the radula and from there into the ailimentary system itself. The nature of these food particles is unknown but we may assume with some probability that they are soft-bodied microorganisms of various sort.

CONCLUSIONS

The radula of the Cancellariidae with its accessory elements (shields) which surround it and its tentacular or filiform teeth is remarkably different from all other radular patterns shown by the Prosobranchs and warrants separate naming and classification. For this pattern, the term *Nematoglossa* is proposed with reference to the threadlike form of the radula teeth.

In its normal position, the radula lies within the folded flaps of the Upper Shield or Mandible with its anterior set of filaments within the hollow, tubelike interior of the snout, and the great length of these filaments show that they can be protruded a distance beyond the end of the snout.

When completely separated from the Mandible as usually happens in an average extraction, the radula is seen attached to the membraneous flaps of the Inner Shield and the two sets of strands divided into its separate filaments which hang loosely from each end. The Inner Shield is believed to be homologous with the similar structure seen on most rachiglossate ribbons and by means of which the radula is attached to the buccal mass or to the muscles which activates its movement.

The petaloids at the end of the radular strands are aggregates of rectangular tubes which form a canal system which traverse the whole length of radular filaments, the walled partition between them imparts to the lot its coarsely veined appearance. Examined under relatively high power, the tubes at the terminal end of each individual strand are paired at least in some species. In *Trigonostoma,* these tubes are capped by two, small globular objects (see figures 20, 25, 26) whose purpose is not known but may be a device for the sorting and picking of minute food particles or merely act as valves opening and closing the entrance to the tubes as occasion requires.

The tubular snout of the mandible held in the mouth of the muscular proboscis is believed to be a probing instrument capable of poking into holes and crevices, in the search for suitable food particles.

The essential characteristics of the cancellariid radular organ have been established. It can be assumed for the present, that the main subsistence or prey requirements of the cancellariids are furnished by soft-bodied microorganism screened and captured by the petaloids of the anterior set of filiform strands and carried through their canal system to the central zone of the radula and backwards into the oesophagus.

Positive determination of the food requirements of the cancellariids remains and on which a more sound interpretation of the function of the filiform teeth must be based. Perhaps the best approach to this question may be through patient observation of captive snails.

ADDITIONAL NOTES

The anatomy of the cancellariid foregut has recently been described by Graham (1966) and closely compared with that of *Marginella.* Both groups have a muscular, extensible proboscis with the radula attached to a buccal mass in the front section of the proboscis, the general anatomy being that of a typical stenoglossate which in most genera of the Neogastropoda would imply a carnivorous diet. There are marked differences between the two groups, especially in that of the radula. The cancellariid radula was not closely examined by Graham but some pertinent points were mentioned such as its unusual form and arrangement of its teeth (described as forming a brush). Its position in the proboscis is shown by his figure 5 (a longitudinal dissection) as lying on a large, elliptical buccal mass and described as covered by a cuticle (Upper Shield or Mandible) and to which are attached protractor and retractor muscles by means of which the buccal mass and buccal papilla are moved backward and forward as well as by the muscles of the proboscis. In front of the buccal mass, his sketch shows a long, narrow extension which contains the anterior set of radular filaments, its end retracted only a short space from the mouth of the proboscis; this section, therefore, represent the tubelike snout of the mandible. As to the food requirements of the cancellariids, Graham concluded as follows: — because they live mostly on sandy muddy bottoms, then the only food available would be diatoms and other microscopic forms; and that the unusual form and arrangement of the radular teeth, which form a brush can be projected from the mouth, is a device for loosening or picking up such particles, which can then be sucked into the gut. He also mentioned that no trace of food was visible in the specimens dissected or sectioned. Graham did not mention the work of Barnard or list it in his bibliographic references. Also no mention was made of the posterior set of radular filaments.

To anyone not directly versed in molluscan anatomy, Graham's explanation of the growth of the cancellariid radula is not clear. In my extractions of the radula I have not found any of the filaments in a nascent condition. It also appears to me that the small organ indicated in Graham's sketch as the radular sack is something else. The present author ventures to suggest that from the formation of the cancellariid radula itself and the fishbone shape of its stem that the strandlike filaments begin their growth within the radula itself and from this central zone are diverted towards the front or back according to their position. It is also possible that after the radula has been fully formed, the filaments seldom need replacement because they do not perform any abrasive action.

BIBLIOGRAPHY

Adam, William, and Knudsen, Jorge

1955. *Note sur quelques especes du Mollusques marins nouveaux ou peu connus de L'Afrique Occidentale.* Institut royal des Sciences naturelles de Belgique, Bull., tome XXXI, No. 61, pp. 18, 19, text fig. 4. Gives figures of the distal end of a few filiform teeth showing their rectangular tubular form, and the terminal end of the snout of the mandible of *Sveltia lyrata* (Brocchi).

Barnard, K. H.

1957. *The radula of Cancellaria.* Journal of Conchology, vol. 24, No. 7, pp. 243, 244, text figures of the radula of *Cancellaria* cf. *lyrata* Brocchi. Although the paper is short, it presents the fullest account of the cancellariid radula and its acessory structure published up to this date.

Graham, Alastair

1966. *The fore-gut of some marginellid and cancellariid Prosobranchs.* Studies Tropical Oceanography, Miami, 4 (part 1), pp. 134-151 (with especially reference to figure 5).

Thiele, Johannes

1925. *Die beschalten Gastropoden der deutschen Tiefsee-Expedition.* II, 1898-1899, pp. 171-172, Taf. IX (IV), figs. 69, 70.

1929. *Handbuch der Systematischen Weichtierkunde.* Erster Teil, pp. 351-353, fig. 422.

Troschel, F. H.

1866. *Das Gebiss der Schnecken.* Zweiter Bandes, Erste Leiferung, pp. 45, 46, Taf. IV, figs. 10-13.

PLATES

EXPLANATION OF PLATE 4

Radular features of *Cancellaria indentata* Sowerby, *C. urceolata* Hinds, and *C. lamellosa* Hinds (=*scalata* Sowerby).

Figure *Page*

1-3. *Cancellaria indentata* G. B. Sowerby I 19

Full radula within the inner shield, length of shield 1.4 mm. Anterior set of radular filaments on left, posterior set on right. Pillsbury Station 501, Gulf of Panama. IMAS. Full magnification about × 35. 2,3. Distal petaloids of a pair of anterior radular filaments.

4. *Cancellaria scalata* G. B. Sowerby I 19

(In collection of *C. lamellosa* Hinds.) Mandible or Upper Shield, open and flattened in slide.

5. *Cancellaria indentata* G. B. Sowerby I 19

Shell. Length 27.6 mm, diameter 13.7 mm. Pillsbury Station 501, Gulf of Panama. IMAS.

6. *Cancellaria scalata* G. B. Sowerby I 19

Shell. Length 25.2 mm, diameter 14.5 mm. Petit.

7. *Cancellaria urceolata* Hinds 19

Side view of the Upper Shield or Mandible containing the radula, the anterior set within the snout of the mandible. Snout distorted into its curved shape by flowage of the mountant. Panama. Petit.

8. *Cancellaria urceolata* Hinds 19

Shell. Length 31.4 mm, diameter 18.5 mm. Panama. Petit.

9. *Cancellaria indentata* G. B. Sowerby I 19

Basal section of a group of posterior set of filaments showing their linear arrangement along the basal membrane and their coarse, grasslike venation. Highly magnified.

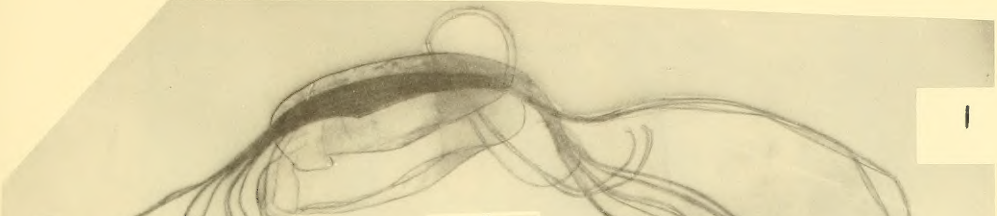

1

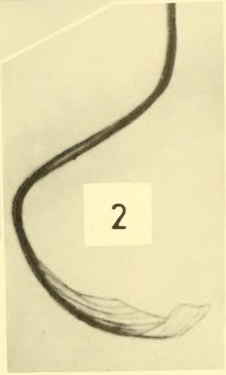

2

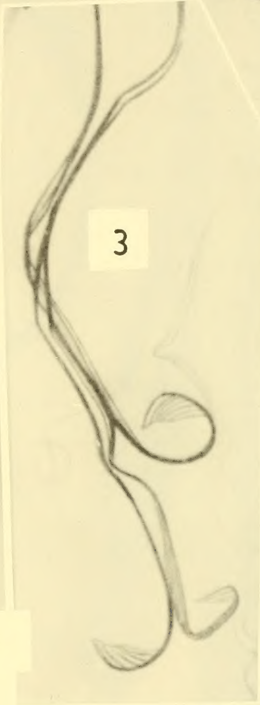

3

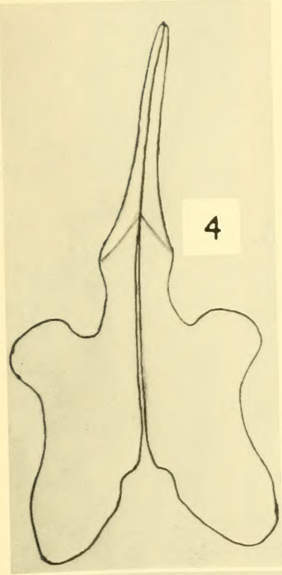

4

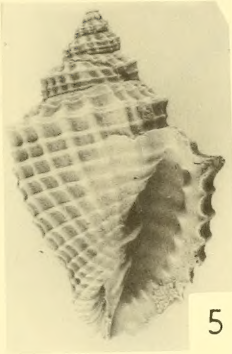

5

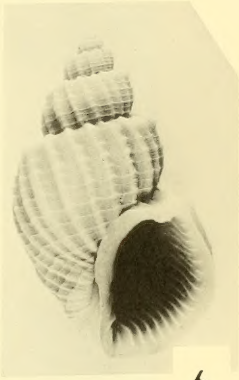

6

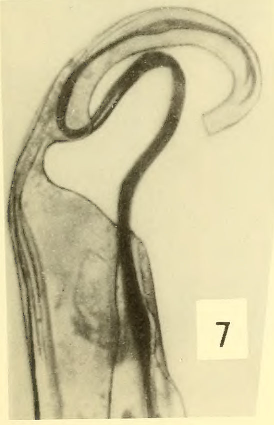

7

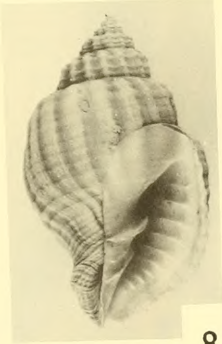

8

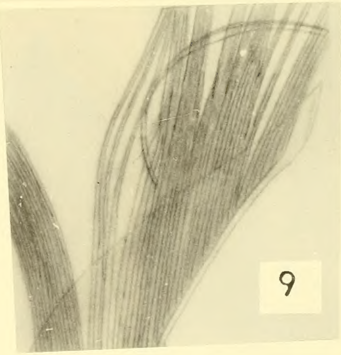

9

Plate 5

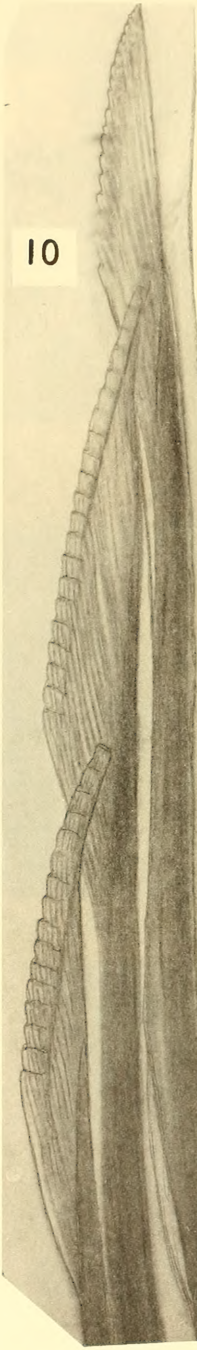

10

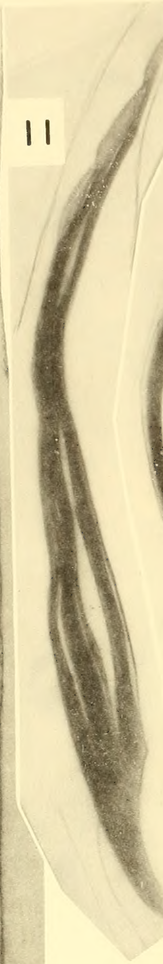

11

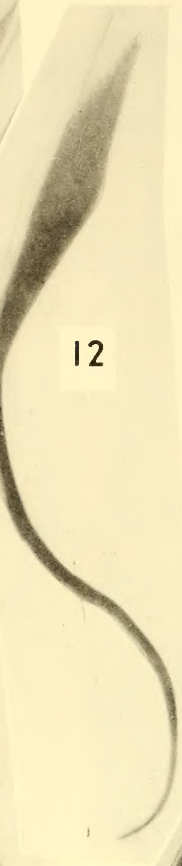

12

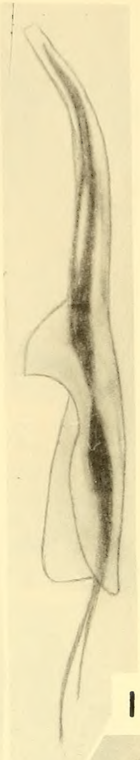

13

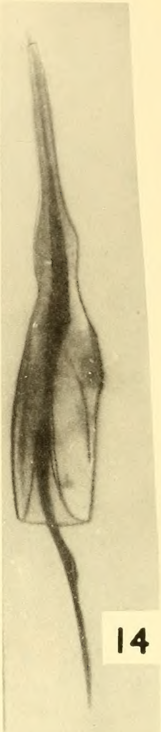

14

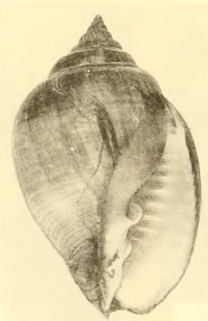

15

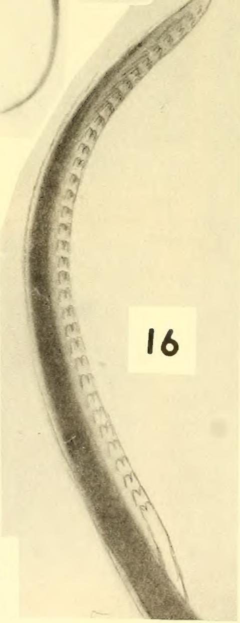

16

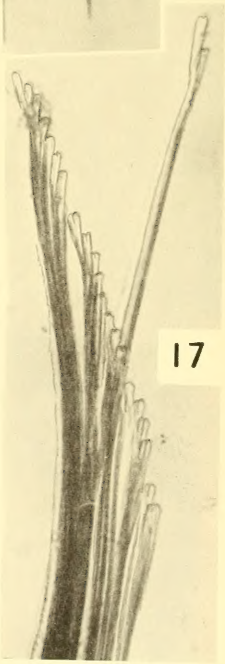

17

EXPLANATION OF PLATE 5

Figure *Page*

10-14. *Cancellaria ovata* G. B. Sowerby I 20

Radular features of *Cancellaria ovata* Sowerby, mainly Santa Cruz, Galapagos Islands. Petit. Petaloids at the distal ends of the three, radular strands of the anterior set. Magnification about 216. 11, 12. Two halves of the whole radula. Anterior set (fig. 11); posterior set (fig. 12). 13, 14. Radula within the Mandible or Upper Shield in lateral and basal views, the anterior set of strands lying extended within the tabular snout. Microphotographs taken before mounting as the organ laid floating free in the cleansing solution shortly after extraction.

15, 16. *Cancellaria ovata* G. B. Sowerby I 20

Shell. Length 41.7 mm, diameter 25.7 mm. 16. Petaloids along the distal end of the posterior strand in uniserial alignment. × 216.

17. *Cancellaria scalata* G. B. Sowerby I 19

Distal extremities of the posterior set of strands. Magnification about 216.

EXPLANATION OF PLATE 6

Figure		*Page*
18-26.	*Trigonostoma bullatum* (G. B. Sowerby I)	21

Details of radula and accessory structure extracted from a single specimen (shell fig. 23). Pillsbury Station 516. Gulf of Panama. IMAS. Slides 875, 876.

18. Full length of radula within the inner shield. Anterior set of strands on the left; posterior on the right. Length of radula 4.1 mm. General magnification × 53.

19. Anterior radular strand showing a continuous row of petaloid paired tubes.

20. A portion of the petaloid shown in figure 19, the paired tubes and the capping device. × 520.

21. Central portion of the radular stem within the inner shield and showing its herring-bone like structure.

22. Distal ends of the three, posterior radular strands and petaloid development.

23. Shell. [*Trigonostoma bullatum* (G. B. Sowerby I)]. Length 43.0 mm, diameter 31.5 mm.

24. Upper Shield or Mandible as spread open and flat in slide.

25, 26. Outline sketches from microphotographs of two posterior petaloids showing their paired tubes and capping devices. × 520. Note their larger size than those of figure 20.

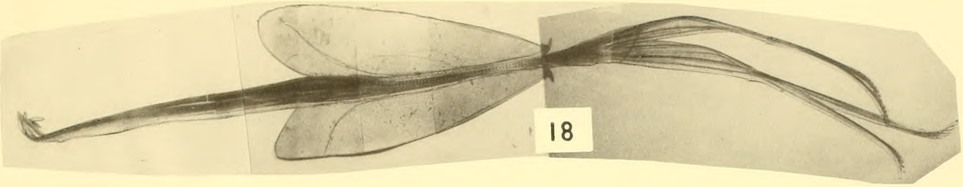
18

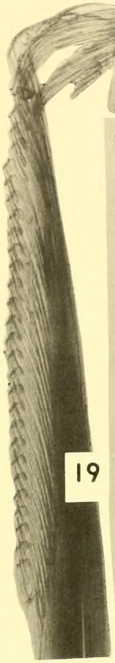
19

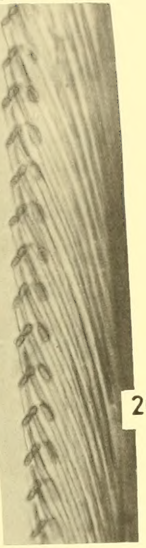
20

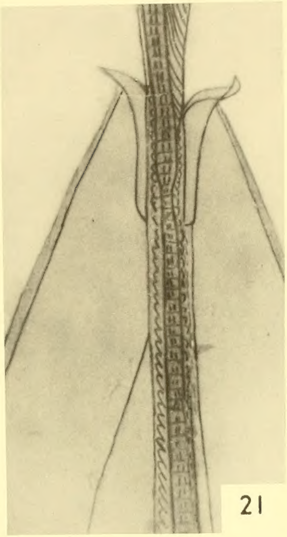
21

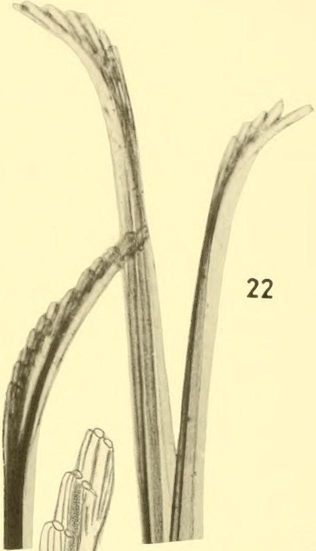
22

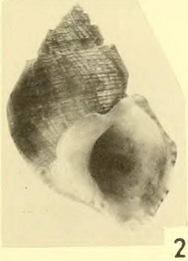
23

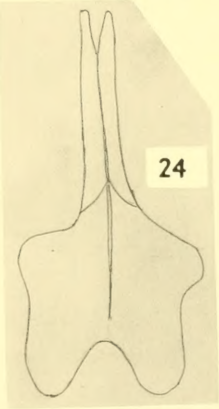
24

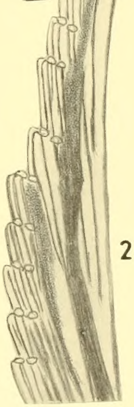
25

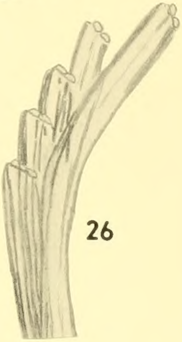
26

INDEX

Light face type refers to page. Bold face type refers to plate number.

B

Barnard, K. H. 20
bullatum, Trigonostoma **6** 19

C

Cancellaria 19, 20
cremata, Cancellaria 19

G

Graham, Alastair 19, 21

I

indentata, Cancellaria **4** 19

L

lamellosa, Cancellaria 19

M

Marginella 21

N

Nematoglossa 20
Neogastropoda 21

O

Olivella 20
ovata, Cancellaria **5** 19, 20

P

Prosobranchia 19

S

scalata, Cancellaria **4, 5** 19

T

Toxoglossa 19
Thiele, Johannes 19, 20
Trigonostoma 19, 21
Troschel, F. H. 19

U

urceolata, Cancellaria **4** 19

XLI.	(Nos. 185-192). 381 pp., 35 pls. Australian Carpoid Echinoderms, Yap forams, Shell Bluff, Ga. forams. Newcomb mollusks, Wisconsin mollusk faunas, Camerina, Va. forams, Corry Sandstone.	16.00
XLII.	(No. 193). 673 pp., 48 pls. Venezuelan Cenozoic gastropods.	18.00
XLIII.	(Nos. 194-198). 427 pp., 29 pls. Ordovician stromatoporoids, Indo-Pacific camerinids, Mississippian forams, Cuban rudists.	16.00
XLIV.	(Nos. 199-203). 365 pp., 68 pls. Puerto Rican, Antarctic, New Zealand forams, Lepidocyclina, Eumalacostraca.	16.00
XLV.	(No. 204). 564 pp., 63 pls. Venezuela Cenozoic pelecypods	18.00
XLVI.	(Nos. 205-211). 419 pp., 70 pls. Large Foraminifera, Texas Cretaceous crustacean, Antarctic Devonian terebratuloid, Osgood and Paleocene Foraminifera, Recent molluscan types.	16.00
XLVII.	(Nos. 212-217). 584 pp., 83 pls. Eocene and Devonian Foraminifera, Venezuelan fossil scaphopods and polychaetes, Alaskan Jurassic ammonites, Neogene mollusks.	18.00
XLVIII.	(No. 218). 1058 pp., 5 pls. Catalogue of the Paleocene and Eocene Mollusca of the Southern and Eastern United States.	18.00
XLIX.	(Nos. 219-224). 671 pp., 83 pls. Peneroplid and Australian forams, North American carpoids, South Dakota palynology, Venezuelan Miocene mollusks, *Voluta.*	18.00
L.	(Nos. 225-230). 518 pp., 42 pls. Venezuela and Florida cirripeds, Antarctic forams, Linnaean Olives, Camerina, Ordovician conodonts, Niagaran forams.	18.00
LI.	(Nos. 231-232). 420 pp., 10 pls. Antarctic bivalves, Bivalvia catalogue.	18.00
LII.	(Nos. 233, 236). 387 pp., 43 pls. New Zealand forams, Stromatoporoidea, Indo-Pacific, Miocene-Pliocene California forams.	18.00
LIII.	(Nos. 237-238). 488 pp., 45 pls. Venezuela Bryozoa, Kinderhookian Brachiopods.	18.00
LIV.	(Nos. 239-245). 510 pp., 50 pls. Dominican ostracodes, Texan pelecypods, Wisconsin mollusks, Siphocypraea, Lepidocyclina, Devonian gastropods, Miocene Pectens Guadaloupe.	18.00
LV.	(Nos. 246-247). 657 pp., 60 pls. Cenozoic corals, Trinidad Neogene mollusks.	18.00
LVI.	(Nos. 248-254). 572 pp., 49 pls. American Foraminifera, North Carolina fossils, coral types, Belanski types, Venezuelan Cenozoic Echinoids, Cretaceous Radiolaria, Cymatiid gastropods.	18.00
LVII.	(Nos. 255-256). 321 pp., 62 pls. Alaskan Jurassic ammonites, Pt. II, Jurassic Ammonitina New Guinea.	18.00

Palaeontographica Americana

Volume I.	See Johnson Reprint Corporation, 111 Fifth Ave., New York, N. Y. 10003 Monographs of Arcas, Lutetia, rudistids and venerids.	
II.	(Nos. 6-12). 531 pp., 37 pls. Heliophyllum halli, Tertiary turrids, Neocene Spondyli, Paleozic cephalopods, Tertiary Fasciolarias and Paleozoic and Recent Hexactinellida.	23.00
III.	(Nos. 13-25). 513 pp., 61 pls. Paleozoic cephalopod structure and phylogeny, Paleozoic siphonophores, Busycon, Devonian fish studies, gastropod studies, Carboniferous crinoids, Cretaceous jellyfish, Platystrophia and Venericardia.	28.00
IV.	(Nos. 26-33). 492 pp., 72 pls. Rudist studies Busycon, Dalmanellidae, Byssonychia, Devonian lycopods, Ordovican eurypterids, Pliocene mollusks.	28.00
V.	(Nos. 34-37). 445 pp., 101 pls. Tertiary Arcacea, Mississippian pelecypods, Ambonychiidae, Cretaceous Gulf Coastal forams.	32.00
VI.	(Nos. 38-41). 444 pp., 83 pls. Lycopsids and sphenopsids of Freeport Coal, Venericardia Carboniferous crinoids, Trace fossils.	35.00

BULLETINS OF AMERICAN PALEONTOLOGY

Vols. I-XXIII.	See Kraus Reprint Corp., 16 East 46th St., New York, N. Y. 10017, U.S.A.	
XXIV.	(Nos. 80-87). 334 pp., 27 pls. Mainly Paleozoic faunas and Tertiary Mollusca.	12.00
XXV.	(Nos. 88-94B). 306 pp., 30 pls. Paleozoic fossils of Ontario, Oklahoma and Colombia, Mesozoic ehinoids, California Pleistocene and Maryland Miocene mollusks.	12.00
XXVI.	(Nos. 95-100). 420 pp., 58 pls. Florida Recent marine shells, Texas Cretaceous fossils, Cuban and Peruvian Cretaceous, Peruvian Eogene corals, and geology and paleontology of Ecuador.	14.00
XXVII.	(Nos. 101-108). 376 pp., 36 pls. Tertiary Mollusca, Paleozoic cephalopods, Devonian fish and Paleozoic geology and fossils of Venezuela.	14.00
XXVIII.	(Nos. 109-114). 412 pp., 34 pls. Paleozoic cephalopods, Devonian of Idaho, Cretaceous and Eocene mollusks, Cuban and Venezuelan forams.	14.00
XXIX.	(Nos. 115-116). 738 pp., 52 pls. Bowden forams and Ordovician cephalopods.	18.00
XXX.	(No. 117). 563 pp., 65 pls. Jackson Eocene mollusks.	16.00
XXXI.	(Nos. 118-128). 458 pp., 27 pls. Venezuelan and California mollusks, Chemung and Pennsylvanian crinoids, Cypraeidae, Cretaceous, Miocene and Recent corals, Cuban and Floridian forams, and Cuban fossil localities.	16.00
XXXII.	(Nos. 129-133). 294 pp., 39 pls. Silurian cephalopods, crinoid studies, Tertiary forams, and Mytilarca.	16.00
XXXIII.	(Nos. 134-139). 448 pp., 51 pls. Devonian annelids, Tertiary mollusks, Ecuadoran stratigraphy paleontology.	16.00
XXXIV.	(Nos. 140-145). 400 pp., 19 pls. Trinidad Globigerinidae, Ordovician Enopleura, Tasmanian Ordovician cephalopods and Tennessee Ordovician ostracods and conularid bibliography.	16.00
XXXV.	(Nos. 146-154) 386 pp., 31 pls. G. D. Harris memorial, camerinid and Georgia Paleocene Foraminifera, South America Paleozoics, Australian Ordovician cephalopods, California Pleistocene Eulimidae, Volutidae, and Devonian ostracods from Iowa.	16.00
XXXVI.	(Nos. 155-160). 412 pp., 53 pls. Globotruncana in Colombia, Eocene fish, Canadian Chazyan Antillean Cretaceous rudists, Canal Zone Foraminifera, fossils, foraminiferal studies.	16.00
XXXVII.	(Nos. 161-164). 486 pp., 37 pls. Antillean Cretaceous Rudists, Canal Zone Foraminifera, Stromatoporoidea.	16.00
XXXVIII.	(Nos. 165-176). 447 pp., 53 pls. Venezuela geology, Oligocene Lepidocyclina, Miocene ostracods, and Mississippian of Kentucky, turritellid from Venezuela, larger forams, new mollusks, geology of Carriacou, Pennsylvanian plants.	18.00
XXXIX.	(Nos. 177-183). 448 pp., 36 pls. Panama Caribbean mollusks, Venezuelan Tertiary formations and forams, Trinidad Cretaceous forams, American-European species, Puerto Rico forams.	16.00
XL.	(No. 184). 996 pp., 1 pls. Type and Figured Specimens P.R.I.	18.00

P15

PALAEONTOGRAPHICA AMERICANA

(Founded 1917)

VOL. VII

NO. 44

ONTOGENY AND SEXUAL DIMORPHISM OF LOWER PALEOZOIC TRILOBITA

By

Chung-Hung Hu

1971

Paleontological Research Institution
Ithaca, New York, U.S.A. 14850

SMITHSONIAN
APR 8 1971
LIBRARIES

PALEONTOLOGICAL RESEARCH INSTITUTION

1970 - 71

PRESIDENT	WILLIAM B. HEROY
VICE-PRESIDENT	DANIEL B. SASS
SECRETARY	REBECCA S. HARRIS
DIRECTOR, TREASURER	KATHERINE V. W. PALMER
COUNSEL	ARMAND L. ADAMS
REPRESENTATIVE AAAS COUNCIL	DAVID NICOL

Trustees

REBECCA S. HARRIS (Life)
AXEL A. OLSSON (Life)
KATHERINE V.W. PALMER (Life)
DANIEL B. SASS (1965-1971)
KENNETH E. CASTER (1966-1972)
DONALD W. FISHER (1967-1973)
MERRILL W. HAAS (1970-1973)
PHILIP C. WAKELEY (1970-1973)
WILLIAM B. HEROY (1968-1974)
VIRGIL D. WINKLER (1969-1975)

BULLETINS OF AMERICAN PALEONTOLOGY

and

PALAEONTOGRAPHICA AMERICANA

KATHERINE V. W. PALMER, *Editor*
MRS. FAY BRIGGS, *Secretary*

Advisory Board

KENNETH E. CASTER
A. MYRA KEEN
HANS KUGLER
JAY GLENN MARKS
AXEL A. OLSSON

Complete titles and price list of separate available numbers may be had on application.

For reprint, Vols. 1-23, Bulletins of American Paleontology see
Kraus Reprint Corp., 16 East 46th St., New York, N.Y. 10017 U.S.A.

For reprint, vol. I, Palaeontographica Americana see Johnson Reprint Corporation, 111 Fifth Ave., New York, N. Y. 10003 U.S.A.

Subscription may be entered at any time by volume or year, with average price of $18.00 per volume for Bulletins. Numbers of Palaeontographica Americana invoiced per issue. Purchases in U.S.A. for professional purposes are deductible from income tax.

For sale by

Paleontological Research Institution
1259 Trumansburg Road
Ithaca, New York 14850
U.S.A.

PALAEONTOGRAPHICA AMERICANA

(Founded 1917)

VOL. VII

NO. 44

ONTOGENY AND SEXUAL DIMORPHISM OF LOWER PALEOZOIC TRILOBITA

By

CHUNG-HUNG HU

April 2, 1971

Paleontological Research Institution
Ithaca, New York, U.S.A. 14850

Library of Congress Card Number: 70-135053

Printed in the United States of America
Arnold Printing Corporation

CONTENTS

Page

- Abstract 31
- Introduction 31
  - Acknowledgments 32
- I. Sexual Dimorphism 33-36
- II. Ontogeny of Polychaetes, Crustaceans, and Merostomes 37
  - 1. Ontogenetic development of polychaetes 37
    - A. Examples of the ontogenic development of polychaetes 38
    - B. The prostomium 41
    - C. Segmentation problem 43
  - 2. Ontogeny of crustaceans 44
  - 3. Ontogeny of Merostomata (*Xiphosura*) 46
- III. Ontogeny of Trilobita 48
  - 1. Protaspid period 48
  - 2. Meraspid period (traditional) 54
    - A. Meraspid period (reconsidered) 54
    - B. Types of meraspides 54
  - 3. Holaspid period 57
  - 4. Rate of growth in trilobites 57
    - A. Variation in larval size 57
    - B. Growth rate correlated with instar periods 58
  - 5. Cephalic segmentation 59
    - A. Primary segments 59
    - B. Post-oral segments 62
  - 6. Formation of the post-cephalic segments 64
    - A. Thoracic segmentation 64
    - B. Pygidial segmentation 65
- IV. Phylogeny of Trilobita 65
  - 1. The problem of primary somites 66
  - 2. The problem of secondary segments 67
  - 3. The problem of cephalic segments 67
  - 4. The problem of appendages 68
  - 5. Polychaete origin of the Trilobita 71
  - 6. On the major classification of trilobites 71
  - 7. Remarks 72
- V. Systematic Paleontology 73
  - Family Spinagnostidae Howell 73
  - Family Pagetiidae Kobayashi 75
  - Family Olenellidae Vogdes 76
  - Family Dolichmetopidae Walcott 81
  - Family Anomocaridae Poulsen 83
  - Family Parabolinoididae Lochman 87
  - Family Raymondinidae Clark 90
  - Family Crepicephalidae Kobayashi 92
  - Family Alokestocaridae Resser 95
  - Family Pterocephaliidae Kobayashi 97
  - Family Ptychaspididae Raymond 100
  - Family Olenidae Burmeister 101
  - Family Leistegiidae Bradley 107
  - Family Missisquoiidae Hupé 109
  - Family Encrinuridae Angelin 111
  - Family Proetidae Salter 113
  - Family Pterygometopidae Reed 115
  - Family Calymenidae Burmeister 117
  - Family Trinucleidae Hawle and Corda 120
  - Family Asaphidae Burmeister 122
  - Dimorphism trilobite Problematica 124
- References 126
- Plates 135

TEXT-FIGURES

1. Sexual dimorphism of the stag-beetle *Lucanus;* 2. *Hepatus ephelitus* (*Linnaeus*) 34
3. Showing pig sexual ratio at different growth stages; 4. Sexual dimorphism of the milkweed bug, *Oncopeltus fasciatus* (Dallus) 35
5. Mating of the horse-shoe crab, *Xiphosura polyphemus* (Linné) 36
6. Showing sexual dimorphism of *Uca pegilator* (Bosc); 7. Sexual ratio of *Uca pegilator* (Bosc); 8. Human sexual ratio 37
9. External and internal views of the trochophore of *Polygordius*........ 38
10. Embryonic development of *Tomopteris helgolandica* Greeff; 11. Planktonic larvae of *Pisione remota* (southern) 39
12. Three larvae of *Pisione remota* (Southern) at different stages of metamorphosism; 13. The early embryonic development of *Scolplos armiger* Müller 40
14. Early metatrochophore of *Arenicola cristata* Stimpson; 15. An ontogenetic sequence of *Arenicola cristata* Stimpson 41
16. Showing the growth stages and ecological phases during the ontogenetic development of *Arenicola cristata* Stimpson 42
17. Two naupliar larvae of crustaceans 44
18. Early embryonic stage of a palaemonid crustacean 45
19. A growth sequence of *Balanus amphitrite* "var." *denticulata* Broch 46
20. Ontogeny of a limulid 47
21. Embryo of *Xiphosura;* 22. Early embryos of *Xiphosura polyphemus* (Linné) 48
23. Showing various author's divisions of the ontogenetic development of trilobites 49
24. Graph; showing the rate of growth of trilobites and their size distribution through the Cambrian and Ordovician 57
25. Showing the cranidial growth rate at different ontogenetic stages of trilobites 58
26. Showing the ontogenetic development of the librigenae and the migration of the eyes of trilobites. Schematic 60
27. Annelid and arthropod brains 67
28. Correlation chart showing the head components of the Polychaeta and non-Hexapoda groups of Arthropoda 68
29. Types of appendages of the crayfish (*Cambarus*); 30. Showing the differentiation of appendages of *Xiphosura polyphemus* (Linné)........ 69
31. A comparison of the appendages in xiphosurans, trilobites, and crustaceans; 32. Showing the correlation of various arthropod pleurae to the notopodium of polychaete 70
33. Showing cephalic structure in relation to the librigeno-rostrum 72
34. A growth sequence of *Kormagnostus simplex* Resser 74
35. *Pagetia clytia* Walcott. 36. *Olenellus truemani* Walcott 75,77
37. *Laudonia canadiensis,* n. sp. 79
38. A growth series of *Ptarmigania aurita* Resser 80
39. *Glyphaspis* cf. *parkensis* Rasetti 82
40. *Iohomia sickia,* n. gen., n. sp. 85
41. A growth series of *Apomodocia conica,* n. gen., n. sp. 86
42. *Cedarina cordillerae* (Howell and Duncan) 88
43. *Crepicephalus deadwoodiensis,* n. sp. 90
44. A growth sequence of *Dunderbergia ? anyta* (Hall and Whitfield) 92
45. *Dytermacephalus granulosus* Palmer 95
46. *Ptychaspis bullasus* Lochmand and Hu 98
47. A growth series of *Olenus gibbosus* (Wahlenberg) 100
48. A growth sequence of *Acerocare ecorne* Anglin 101
49. A growth series of *Highgatella faciala,* n. sp. 103
50. *Kepisis stenotoides* (Matthew), n. gen. 106
51. A growth sequence of *Missisquoia cyclochila,* n. sp. 108
52. *Libertella corona,* n. gen., n. sp. 110
53. *Phaseolops conus,* n. sp.; 54. *Calliops strasburgensis* Ulrich and Delo 112,114
55. A growth sequence of *Flexicalymene granulosa* (Foerste) 116
56. *Cryptolithus bellulus* (Ulrich) 118
57. *Isotelus stegops* Green 120
58. *Flexiclymene meeki* (Foerste); 59. *Acidaspis cincinnatiensis* Meek 123

ONTOGENY AND SEXUAL DIMORPHISM OF LOWER PALEOZOIC TRILOBITA

Chung-Hung Hu*

ABSTRACT

In the present research 26 genera and species of Lower Paleozoic trilobites are described. These include four new genera and seven new species. Among these, 23 species show an excellent sequence of ontogenetic stages, and 12 species show distinct bimodalism of adults which is thought to be attributable to sexual dimorphism. The life cycle of trilobites is divisible into three periods: the protaspid, meraspid, and holaspid periods. The protaspid period is subdivided sequentially into anaprotaspid, metaprotaspid, and paraprotaspid stages, based primarily on the number of axial rings and the presence or absence of the protopygidium. The meraspid period is likewise subdivided into early and late meraspid stages, based mainly on the presence or absence of the anterior cephalic brim, position of the palpebral lobes, and facial sutures. The holaspid period shows ephebic characters which are those customarily employed for specific diagnosis and are essentially unaltered throughout the remainder of the life span. The presumed adult sexual differences comprise variation in body size, nature of the prosopon ("ornament"), and bimodal ratio. The "females" have a statistically larger body, without distinct prosopon, and are less numerous than the "male" forms. The relative abundance of the two forms is the "sexual ratio." The ontogenetic development of the polychaete worms, crustaceans, and xiphosurans is compared with that of trilobites. Both trilobite and crustacean larvae possess two primary somites and five cephalic segments, whereas the xiphosuran larva has four primary somites and six or seven cephalic segments. If these criteria are of phylogenetic significance, it would seem that Trilobita and Crustacea may be more closely related to one another than are trilobites to merostomes. The undifferentiated serial appendages of trilobites are similar to those of polychaetes, whence they may well be derived, and probably can serve as a paradium of the primitive limb structure within the Arthropoda. The variously diversified appendages of crustaceans and xiphosurans are functional, and all are possibly derived from serially uniform appendages such as those of trilobites. Simplification, complication, and differentiation have been evolutionarily operative in the divers arthropod groups. Examination of the larval development of the polychaete, *Pisione remota,* shows many similarities to that of earliest trilobites, especially *Laudonia* and *Olenelloides* of the Lower Cambrian. In both these annelids and the trilobites the cephalization is accomplished by a forward migration of the body segments and elongation of the eye rings. These ontogenetic similarities, together with the generalized nature of trilobite appendages, seem strongly to support the hypothesis of "polychaete origin of the trilobites."

The degree of separation of the librigenae and rostrum of trilobites appears to have great phylogenetic and classificatory significance. Four groups can be differentiated on this basis: Monorostraloid, Trirostraloid, Birostraloid, and Holorostraloid. These relations may eventually serve as major taxobases. The agnostids are viewed as representing an Architrilobitoid group, and as deserving a taxonomic rank equal to Trilobita. Both ontogenetic and morphologic characters of the architrilobites are different from those of the rest of the trilobites. The architrilobite larvae possess the same number of primary somites as typical trilobites, but the adult has four (instead of five) cephalic segments. The similarity of the architrilobite cephalic and pygidial shields in size and shape, and the presence of only two or three thoracic segments further sets them apart.

INTRODUCTION

There has been great progress in the ontogenetic study of trilobites during recent years. This has been especially due to the discovery of silicified materials which have not only the dorsal morphologic characters well preserved, but also the marginal spines and certain ventral structures, including the hypostoma and rostrum. These fine specimens give new insight into the larval mode of life and afford new data of taxonomic importance. The most notable studies of this new material have been done by Whittington and Evitt, (1953), Whittington (1956e, 1959a), working on Middle Ordovician trilobites of Virginia; by Palmer (1957, 1962) and Robison (1964), studying the Lower to Upper Cambrian trilobites of Nevada and Utah; and by Ross (1951a, b) and Hintze (1952), studying the Lower Ordovician trilobites of Nevada and Utah.

Because of the extraordinary perfection of the silicified larval remains and the recentness of their discovery and study, and especially the ease with which this material can be recovered by acid treatment, other types of larval documentation have tended to be neglected or discounted. Non-silicious remains require far more time and pains for extraction and preparation, yet for many places and horizons, these are the only larval evidence available. Moreover, as the photographs here presented show, the calcareous remains may rival the siliceous if properly pursued with microscope and fine dissecting needle.

The materials here studied include both calcareous and silicified specimens representing 23 species, ranging in age from Lower Cambrian through Upper Ordovician and showing continuous ontogenetic sequences. Except for two genera from the Scandinavian Peninsula, the materials were mostly collected from North America: from Mexico to the Canadian Rockies and from New Brunswick to Utah (Index Map).

Statistical studies of adult specimens commonly show that a given species of trilobite possesses bimodally distributed characters, a phenomenon here attributed to sexual dimorphism. It is the assumption here that the most abundantly represented specimens were males, either having relatively small bodies without special prosopon, or large bodies with strongly modifying prosopon. The less numerous female are large-bodied without special prosopon or small-bodied with slightly modifying prosopon. These morphologic and sexual ratio differences seem to correlate with sexual dimorphism in Recent Arthropoda, such as Insecta, Crustacea, and Merostomata. Twelve species are described which show these bimodal traits. By extension, this phenomenon is to be expected as a general trait of trilobites. Its recognition may well materially reduce the number of "species" now current in trilobite literature.

The ontogenetic development of a complete growth sequence is divided into three periods: the protaspid, meraspid, and holaspid. The protaspid period is subdivided into anaprotaspid, metaprotaspid, and paraprotaspid stages; the meraspid period into early and late meraspid stages; and the holaspid period lacks subdivisions.

---

[*] Doctoral dissertation, University of Cincinnati.

In the earliest ontogenetic developmental instars, or anaprotaspid stage of the trilobite larva, the shield contains two primary somites with a procephalon and a generative pygidium. It does not resemble the "trilobite" stage of the ontogenetic development of *Xiphosura ("Limulus")* but rather the nauplius of crustaceans, since the *Xiphosura* larvae have four primary somites whereas both trilobites and crustaceans possess only two. In adults, the cephalon of both crustaceans and trilobites have antennules and four post-oral segments, whereas the xiphosuran lacks antennules and contains more than six post-oral segments. The ontogenetic development and cephalic structure suggest that the phylogenetic relationship between trilobites and crustaceans is closer than that of trilobites to merostomes. The trilobite is a true protarthropod with many morphologic and ontogenetic features similar to those of polychaetes. The morphologic feature of the polychaete, *Pisione,* is similar to that of olenellids and is highly suggestive of the possibility that the Trilobita may be directly evolved from *Pisione*-like polychaetes by secretion of an external skeleton, forward migration of body segments to form a cephalon, and elongation of the eye rings.

The variously differentiated appendages of arthropods, *i.e.,* uniramous, biramous, and triramous appendages, are best interpreted as independent functional adaptation of trilobitiform appendages. Simplification, complication, and differentiation have operated in various derivative evolution. Thus, the uniramous appendages, like those of trilobites or geologically older crustaceans, are original and the biramous (bifurcate) or triramous appendages are derived. If the notopodium of polychaetes is homologous with the pleural spine or tergal spines of trilobites, limuloids, and crustaceans, the neuropodium and parapodial setae should be equivalent to the uniramous or endopodite appendage and gill branch of the epipodite (Text-fig. 32). Therefore, the exopodite of crustaceans would appear to be a subsequent development. The structure and the uniform serial arrangement of trilobite appendages show the same basic plan as those of polychaetes.

The basis for a fundamental classification of Trilobita is by no means yet known. A good case can be made for excluding the agnostids as Architrilobitoids from the Trilobita *ss.* The present study has brought out the potential importance of the Librigeno-rostrum organization as a major taxobasis for the Trilobita *s.s.* Thus, four groups are here distinguished: In the Monorostraloid group the complete rostrum is the perrostrum; this is the condition in olenellids; in the Trirostraloid group the librigeno-rostrum is separated into three parts; this condition is represented by *Redlichia* and most of ptychopariids; in the Birostraloid group the librigeno-rostrum is separated into two parts, as in asaphids, *Bathynotus,* and *Remopleurides;* and the Holorostraloid group lacks separation but differs from the monorostraloids by the dorsal or super-marginal suture; examples are the trinucleids, phacopids, and dalmanitids. The Architrilobitoids are not strictly comparable with typical trilobites, because their cephalon comprises four segments only: a procephalon and three post-oral segments. They may not even represent a trilobite taxon due both to the ontogenetic and morphologic differences. The agnostids, eodiscids represent this group. They may equate in taxonomic rank with Trilobita.

The terminology of the present study for the most part follows the *Treatise on Invertebrate Paleontology, (Part O, Arthropoda 1).* The figured and type specimens are mainly stored in the Geological Museum, University of Cincinnati, Cincinnati, Ohio (U.C.M.), and partly in the United States National Museum (U.S.N.M.).

ACKNOWLEDGMENTS

The writer wishes to express his gratitude to the many people who have contributed to the successful completion of this work. Special thanks go to Kenneth E. Caster under whose direction this work was prepared. He gave generously of his time and was a constant source of inspiration. Thanks are also due R. Endo, Professor of Geology, Saitama University, Japan, and T. Kobayashi, Professor of Geology, University of Tokyo, Japan, for their long-term encouragement.

I am grateful to H. B. Whittington, Harvard University, and B. F. Howell, Princeton University for their criticism and helpful suggestions. A. R. Palmer, United States Geological Survey, permitted me to describe his Wah Wah Range collection including *Dunderbergia ? anyta* and *Dytremacephalus granulosus;* F. Rasetti, formerly of Johns Hopkins University, permitted me to describe his Virginia collection of *Libertella corona* and *Phaseolops conus;* and Christina Lochman Balk, New Mexico Institute of Mining and Technology, permitted me to describe her Mexico and Missouri collections, including *Olenellus truemani* and *Kormagnostus simplex.* J. L. Wilson, Rice University, generously permitted me to describe his British Columbia collection, including *Laudonia canadiensis.* For their valuable discussion of the identifications, I also extend my warm thanks to these specialists. Many thanks go also to my paleontology classmates at the University of Cincinnati for their contributions during a three year (1963-1966) seminar course on the Arthropoda, through which I

have profited by much information related to the present studies.

The writer is deeply indebted to C. G. Bookhout, Director of Duke University Marine Laboratory, Beaufort, North Carolina, for his many suggestions on the ontogenetic development of modern crustaceans and under whose supervision the writer has had the rare opportunity to study the ontogenetic development of polychaetes in comparison with that of trilobites.

Finally, I must express my heartfelt thanks to my very good friend, Michael Stephens, formerly of the Geology Department, University of Cincinnati (now at California Institute of Technology) for assistance with the English text and discussion of certain problems involved in the present study. To Mrs. Wanda Osborne, secretary of the Geology Department, University of Cincinnati, who typed the manuscript, I also wish to express deep thanks. The financial expenses of the present work were mainly supported by the Museum Fellowship and the Nevin M. Fenneman Fund of the University of Cincinnati, and partly by the National Science Foundation during two summers of study (1966-1967) at the Duke University Marine Laboratory at Beaufort, North Carolina.

I. SEXUAL DIMORPHISM

Statistical study of specimens of the same species of trilobite often shows several variable minor features: the shape, length, and width of the glabella, width of the librigenae and hypostoma, length of the occipital spine, the number of axial rings on the pygidium, the shape of the terminal portion, the width of the marginal border, and the convexity of the skeleton. Moreover, these variables are essentially bimodal in corresponding parts. These variable characteristics have been interpreted by many students as being largely the effects of preservation, or in some instances as specific differences. However, these features are constant and bimodal in undeformed specimens representing many genera and species. Dimorphism seems to be a common feature of trilobites, as it is in many arthropods. This trilobite dimorphism is believed to be sexual and the criteria for ascertaining the sexual identity of dimorphic forms now seem to be at hand.

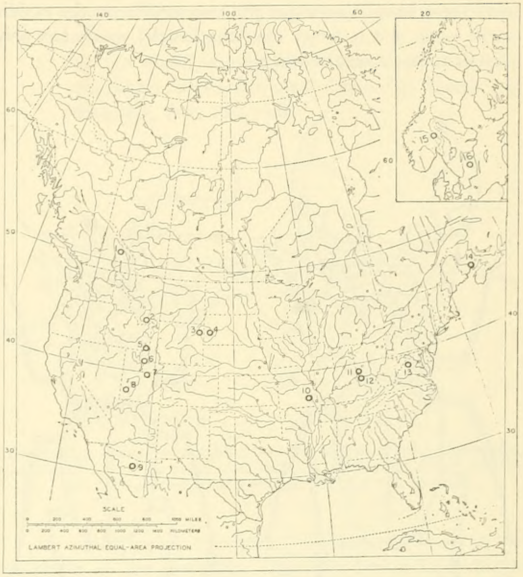

Index map of the geographic distribution of the described materials. Loc. 1. North of Radium, west of the Columbia River, British Columbia, Canada; 2. West side of South Boulder Creek, western Madison County, Montana; 3. Sheep Mtns., Sundance, eastern Wyoming; 4. Lead, Deadwood, South Dakota; 5. North of Mink Creek, Preston Quadrangle, Idaho; 6. Locality ?, Wasatch Mtns., Utah; 7. Santaquin Canyon, northeast side of road, Wasatch Mtns., Utah; 8. Wah Wah Range, Utah; 9. Caborca, northwestern Sonora, Mexico; 10. St. Francois County, South Bonneterre, Missouri; 11. Cincinnati, Ohio; 12. Park Hills, W. Covington, Kentucky; 13. Willow Grove, 3 miles southwest of Woodstock, Virginia; 14. Kennebec River, St. John, New Brunswick, Canada; 15. Ringsaker Station, north of Oslo, Norway; 16. Nye, southeast of Joukoping. Sweden.

1. MORPHOLOGIC CRITERIA

Frequently the male differs from the female in other respects than the nature of the reproductive organs, *i.e.*, in size, prosopon, and the like; when such differences are strongly marked the species is said to be sexual dimorphic. This phenomenon is especially recognized in living organisms. The differentiation of species into two distinct sexual forms is universally found in all higher animals as well as in many plants and lower animals. In modern animals, especially in arthropods, the spinosely armored, large individuals of a species are commonly male, while those without armour or slender and smaller sized are the female. In West Indian Hercules beetle [*Dynastes hercules* (Linnaeus)], the male has a larger body and two large horns on the middle of the head, whereas the female has a small body and a hornless head. In the stag-beetles *(Lucanus)* (Text-fig. 1), the male is larger and has two hypertrophis mandibles, whereas the female has shorter specialized mandibles. In the boreal primitive-weevil [*Eupsalis minuta* (Drury)], the male is larger than the female and has a pair of powerful mandibles, the female has considerably smaller mandibles, which are prolonged into a slender snout. In the rhinoceras-beetle [*Dynastes tityus* (Linnaeus)], the male bears three horns, one larger and two smaller on the middle of the head, and is larger than the female, which has only a small tubercle on the head.

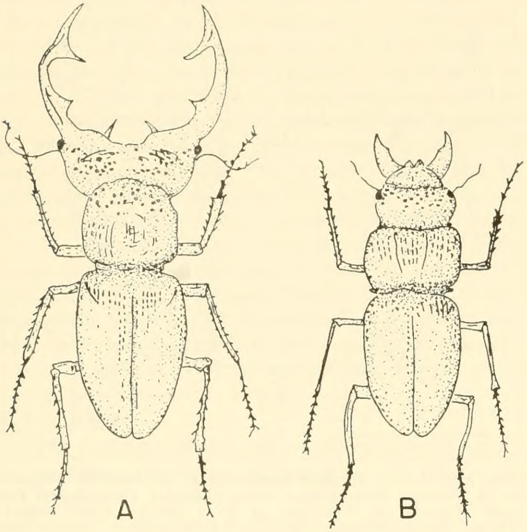

Text-fig. 1—Sexual dimorphism of the stag-beetle *Lucanus.* A. Male form; B. Female form. (Redrawn from Hanson, 1964).

In *Hepatus ephelitus* (Linnaeus) a common decapod crab, (collected in channels a few fathoms in depth at Beaufort, North Carolina) the female is smaller than the male, and possesses a broad abdomen and shorter chelipeds (Text-fig. 2).

In other cases the male may be smaller (dwarf male) than the female. For example, in the oriental cockroach *(Blatta orientalis* Linnaeus) the smaller male has longer antennae and a smaller abdomen. Among certain grasshoppers *(Neoconocephalus)* the smaller males lack caudal spines. The two sexes are alike in carpenter moths *(Prionoxystus robiniae* Peck), except that males are about half the size of females. In the horseshoe crab *Xiphosura ("Limulus")* the female is considerably larger than the male, and the male form possesses larger chelicerae which are modified as sexual claspers. The male of the shrimp *Palaemonetes* differs from the female in being smaller with a more slender rostrum, having the free part of the shorter ramus of the upper antennular flagellum longer in relation to the fused part, with somewhat shorter legs, and the carpus of second leg longer in relation to the chela. Younger female individuals resemble the male. In another shrimp, *Xiphopeneus,* the female's rostrum is somewhat longer than the male's; and in *Hippolyte,* still another, the male's body is more slender than the female's. The extreme examples of dwarf males are represented by many copepods, in which the male forms are sometimes diminuitive parasites upon the female's body.

2. SEXUAL RATIO

The sexual ratio among existing animals affords another clue for the identification of fossil forms. However, the knowledge of this field is poor.

In genetic theory the sexual ratio of animals may be 50:50. The reasoning is that, for example, in the human body the males have XY and the female have XX sexual chromosomes. As a result of maturation, two kinds of sperm are formed in equal numbers with respect to these chromosomes. One kind having X (megasperm) and the other Y (microsperm). Only one kind of egg is formed, containing X. If an egg is fertilized by an X-bearing sperm, a female (XX) results; if by a Y bearing sperm, a male (XY). The proportion of fertilization of potential males and females is 1:1. But the facts do not conform to this hypothesis. The sexual ratio of many animals is more than 100: Human, 103; Cattle, 107.3; Pig, 111.8 (Text-fig. 3); Mouse, 105; Pigeon, 115 (Ishibashi, 1938); *Drosophila melanogastor* Meigen, 300; and Man, 106. (Herskowitz, 1962). Although Ishibashi and Herskowitz give slightly dif-

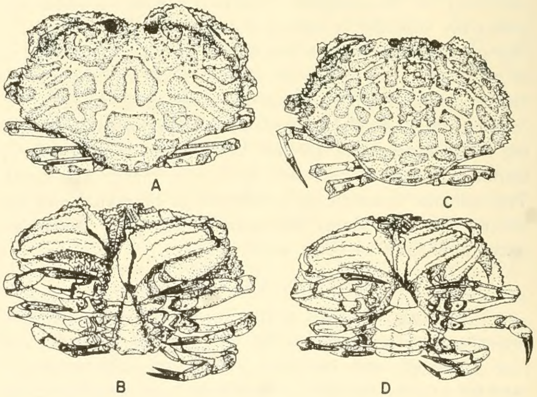

Text-fig. 2—*Hepatus ephelitus* (Linnaeus). A. B. Dorsal and ventral views of male form; C. D. Dorsal and ventral views of female form. Notice the different-sized abdomens.

ferent human sexual ratios, the fact remains that male individuals are more abundant than female.

Weight	Number	Male	Female	Male %
0-100 gr.	281	166	115	59.1 ± 1.98
101-300 gr.	114	65	49	57.0 ± 3.12
300 gr.	188	100	88	53.2 ± 2.45
Total	583	331	252	56.8 ± 1.38

Text-fig. 3.—Showing pig sexual ratio at different growth stages. (After Parker, 1926, from Ishibashi *et al.*, 1938).

These results suggest that the ratio of the fertilization of XY is much higher than XX. The reason for this phenomenon is unknown, but the fact is that male individuals are more numerous than female.

It is not the subject of this paper to discuss the genetic sex determination of animals, but the author would like to point out that the sexual ratio is influenced by environment: such external factors as temperature, light, water salinity, food supply, or internal ones, such as sexual hormones and richness of acidic and alkalic media. These factors could affect the biochemical and biophysical reactions and directly or indirectly act as a partial sexual determinant. The slower motion of megasperm X than that of microsperm Y could be another important factor in sexual determination. Males are not universally more abundant than females, but under natural conditions the sexual ratio of any animal is predictable. In contrast, abnormal or experimental environments can cause the sexual ratio to vary randomly. The secondary reduction of male forms must also be considered. For example, many males die after copulation, are eaten by the female, killed fighting, or are inherently less viable, *e.g.*, human males, and the result is an increase in the relative number of females in the species population.

3. EXAMPLES OF ANIMAL SEXUAL DIMORPHISM

Sex determination in insects usually utilizes characteristics as shape of body, shape of antennae, size of eyes, color patterns and comparative length, or absence of wings. As an illustration, in the large milkweed bug, *Oncopeltus fasciatus* (Dallus), Lever (1966) has given the following criteria for identifying males:

1. They are smaller than the sibling female.
2. They lack the right and left lateral lobes on the dorsal surface of the fifth abdominal segment (fifth tergite). The female's lobes are readily visible when both pairs of wings are raised or removed.
3. The posterior edge of the fourth plate on the ventral surface of the abdomen (fourth sternite) is rounded. The female's is triangular and tapers posteriorly (Text-fig. 4).
4. The last dorsal segment of the male's abdomen (the pygidium) is rounded and shiny. The female's is triangular, dull, and cleft.

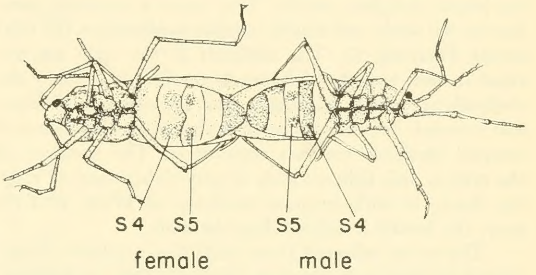

Text-fig. 4.—Sexual dimorphism of the milkweed bug, ***Oncopeltus fasciatus*** (Dallus), shown in copulation. S4, sternite no. 4; S5, sternite no. 5. (Redrawn from a photograph of Lever, 1966.)

In the decapod crustacean, *Callianassa,* there is dimorphism of the chelipeds. The male has a large major cheliped, granular along the proximal lower edge of the carpus, lower edge of the merus and over the entire ischium; the propodus and carpus are about equal in length, twice as broad as the merus and more than three times as broad as the ischium; the merus has a strong tooth on the lower proximal border; whereas the major cheliped of the female is weaker and not granulated; the propodus and carpus are proportionally shorter than those of the male and the merus lacks a tooth on the lower proximal border.

The horseshoe crab, *Xiphosura,* shows sexual dimorphism in the chelae, the males having special graspers. The crabs spawn during the month of May, or in the Spring whenever weather is conducive. The males respond first, awaiting the arrival of the females in the shallow water along the beaches. Generally only one male attaches with his "fist-and-thumb" chela to a female, but a female simultaneously spawning with two or more males is not uncommon. Spawning occurs on the high tides of the new moon and full moon. As each female makes her way to the beach she is accompanied by a male clasping the posterior margin of the female abdomen with specialized claws. At the water's edge she digs a shallow nest in the sand, often practically burying herself, and deposits the clutch of eggs in the shallow depression, where they are fertilized by the spermatozoa washed over the eggs by the waves. The female moves on to make several nests during a single tide. Occasionally a male may remain coupled to the female throughout the year, from one spawning season to the next (Text-fig. 5) (Shuster, 1950).

The sand fiddler crab, *Uca pugilator* (Bosc), is commonly found along the East Coast of North America. The largest male individuals are more than 16 mm in length, and the female is slightly smaller. They occur in countless numbers on the sandy and muddy beaches bordering on the tidal creeks (Text-fig. 6). The chelipeds of the male are unequal in size, and the abdomen is smaller. In females the chelipeds are equal and smaller, and the abdomen is larger and rounded. Intersexual forms having large abdomen and unequal chelipeds are rare occurrences. The carapace of the male is dull, light-purplish or grayish-blue and of varying shape, or with irregular markings of brown or dark grey; the female is lighter than the male.

The writer collected about 3000 *Uca pugilator* (Bosc) individuals during the week of July 6-12, 1966, at Beaufort, North Carolina, near the Duke Marine Laboratory. Among these the smallest specimens are about 5 mm, the largest male form is 17.5 mm, and the female is rarely 16.0 mm long (carapace sag.). The sexual ratio of the smaller sized forms is 120; of the medium-sized, 148.3; and of the large ones, 200.

Although the sexual ratio of this animal would at first seem to be chaotic, the explanation no doubt lies in the fact of near-shore collecting. Under the sampling conditions, probably the population of sexually juvenile forms comes closer to representing the true sexual ratio, whereas the variable sexual ratios of the adult forms are due to the females usually being inactive and commonly hidden, and active males are caught in the sampling.

Von Bälz's (1911) investigation indicated that the human sexual ratio of England is 103.6; Italy 108; Russia 105.4; Germany 105.2; France 104.6; Spain 108.3; and Japan 105. Parker (1915, 1926) reported on the juvenile sexual ratio of the embryonic stage of man is extremely high (120-140). The ratio decreases from infancy to adulthood (Text-fig. 8).

In the United States the sexual ratio averages about 103 from 1850 to 1959 (Year Book, 1961), and the birth and death ratios are 105.4 and 130.4 respectively (World Almanac, 1958). The birth ratio of the male population is much higher and the death rate of male population is also higher than that of the female.

4. SUGGESTIONS FOR IDENTIFICATION OF SEXUAL DIFFERENCES IN TRILOBITES

a. *Sexual ratio.* — As discussed above, statistical studies often show two morphologically differentiated groups in the same species of trilobites. It would seem in conformity with the usual condition in nature, that the larger group of specimens is male and the smaller one female.

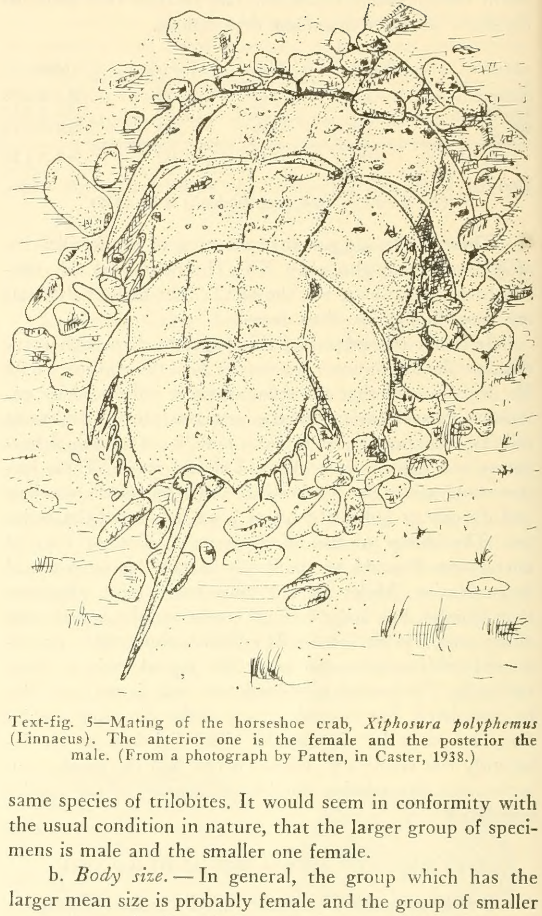

Text-fig. 5—Mating of the horseshoe crab, ***Xiphosura polyphemus*** (Linnaeus). The anterior one is the female and the posterior the male. (From a photograph by Patten, in Caster, 1938.)

b. *Body size.* — In general, the group which has the larger mean size is probably female and the group of smaller mean size male. But if the animal is strongly armored or bears prominent prosopon, the situation appears to be reversed: then, the group of the larger mean size conforms statistically to the male data, and the group of smaller mean size, to the female.

c. *Prosopon.* — Spinous or heavily armored forms are judged to be male, and those without or only slightly armored to be female.

This correlation is derived statistically and represents probability rather than demonstratable truth, because the sexual organs of trilobites are unknown. Biocoenosis, thanatocoenosis, and sedimentologic history need careful exam-

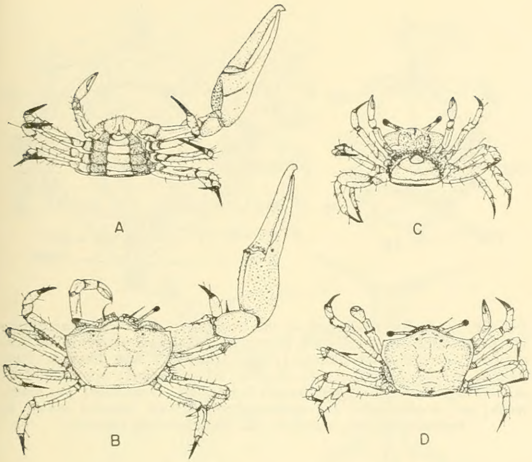

Text-fig. 6—Showing sexual dimorphism of *Uca pugilator* (Bosc). A,B ventral and dorsal views of male form; C,D, ventral and dorsal view of female form. Notice the difference in size of body, chelipeds, and abdomen in the two sexes. (From photographs.)

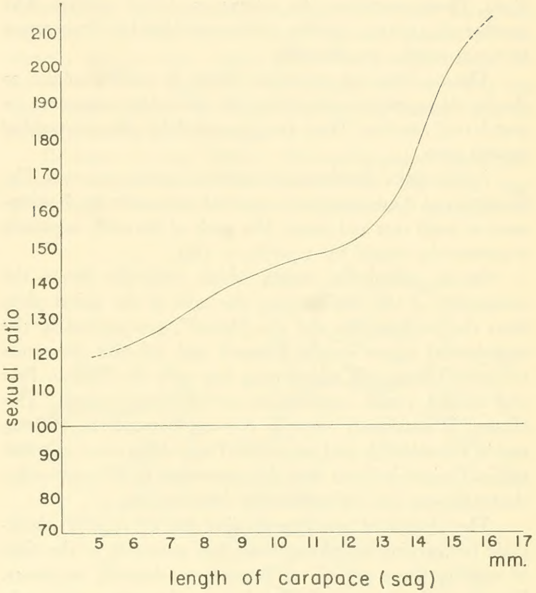

Text-fig. 7—Sexual ratio of *Uca pugilator* (Bosc)

ination for each association, lest these factors distort the true population statistics.

II. ONTOGENY OF POLYCHAETES, CRUSTACEANS, AND MEROSTOMES

1. ONTOGENETIC DEVELOPMENT OF POLYCHAETES

The embryos of polychaetes *(Nereis, Tomopteris, Scoloplos)* develop by means of spiral cleavage and gastrulation to produce the larvae. The embryo at this stage assumes a top-shape and leads a purely pelagic life, moving by bands of cilia that encircle the body. This is the trochophore stage. The fully developed trochophore is divided into two parts by an equatorial ring; an episphere above, and a hyposphere below (Text-fig 9). The hyposphere consists of the metatroch, neurotroch, telotroch, prepygidial growth zone, and the anal region or pygidium. The prepygidial growth zone eventually forms serially all of the trunk segments of the body.

Additional development takes place as the trochophore metamorphoses into adult body form. The most conspicuous feature of metamorphosis is the gradual lengthening of the generative zone due to the formation and development of trunk segments. The segments develop almost simultaneously from anterior to posterior, between metatroch and pygi-

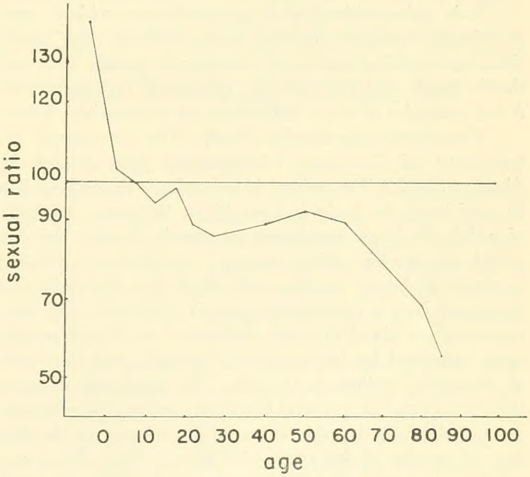

Text-fig. 8—Human sexual ratio. (After Parker, 1915, from Ishibashi, 1938.)

dium. These constitute the primary or larval somites. The number of primary somites varies considerably from taxon to taxon within the Annelida.

The sequence of segments which is serially added to the larval segments comprises the secondary segments or post-larval somites. They are generated by the prepygidial growth zone.

Each somite develops two coelomic compartments. The formation of the segments are marked externally by development of setal sacs and setae. Also each of the early segments is commonly ringed by a girdle of cilia.

In the epispheric region, which originally forms the major part of the trochophore, the cells of the apical plate form the prostomium and the "brain"; concomitantly the mesodermal tissue moves forward and invades the prostomium. The mouth region may fuse with the first or first and second trunk segments from the peristomium. This process is commonly seen in *Nereis, Tomopteris, Pisione,* and in the sabellids and serpulids. These differences in peristomium origin indicate that the peristomia of different polychaete groups are not necessarily homologous.

The elongated metamorphosing larvae remain planktonic for varying lengths of time, but generally at the time of settling there are six or seven setae-bearing segments. However, the larvae of *Ophelia* are free-swimming only until three setae-bearing segments have developed.

A. EXAMPLES OF THE ONTOGENETIC DEVELOPMENT OF POLYCHAETES

It is quite misleading to generalize too widely upon polychaete ontogeny because many variables are operative: *e.g.,* varying segmental processes in pelagic and benthonic larvae and the mode of prostomial metamorphosis. A few examples of these differences are summarized below:

Tomopteris helgolandica Greeff: The ontogenetic development of *Tomopteris helgolandica* was studied by Åkessen (1962). The animal is holopelagic throughout life. In adulthood the body is from 50 to 100 mm. in length, of which the larger specimens are mostly female. The fertilized egg develops spiral cleavage; gastrulation is finished in about 28 hours; at about the third day the embryo is developed into a trochophore; late in the third day, four segments are simultaneously delineated as lateral protrusions separated by intersegmental grooves, and four pairs of parapodial rudiments are seen. The parapodia differentiate into dorsal and ventral branches and bear long bristles. Late in the fifth day the fifth segment appears as the first sign of activity of the prepygidial growth zone. For a surprisingly long time this fifth segment is the only one which buds off from the growth zone. From the fifth day the morphology of the larva changes slowly with respect to the middle and posterior parts of the trunk region and the pygidium. During this period the prototroch and first segment are forced toward the apical pole along with the previously equatorial line (Text-fig. 10).

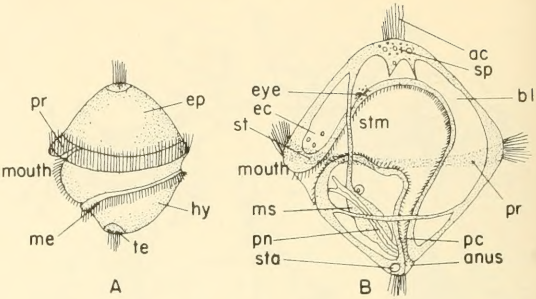

Tex-fig. 9—A. External view of the trochopore of ***Polygordius,*** showing prototroch, metatroch, and telotroch. B. Internal structure of generalized annelid trochophore. (After Dawydoff and Shearer from Barnes, 1963). ac, apical tuft of cilia; bl, blastocoel; ep, episphere; ec, ectomesoderm; ms, mesodermal bands, me, metatroch; pr, prototroch; pc, proctodeum; pn, protonephridium; sp, sensory plate; st, stomodeum; stm, stomach; sta, statocysts; te, telotroch.

The larva differentiate little beyond this stage through the ninth day. By the fifteenth day, the tentacles bud off and the seventh segment appears. At the 9-10 segmental period the tentacles become hollow and connect with the general coelom.

The initial stage of segmentation of the animal first becomes visible in the ectoderm and not in the mesoderm. The first segmental indications are first visible in the lateral ectoderm where the cells arrange themselves in four bulbous structures on each side. The four bands represent synchronously developing primary larval segments. There is, however, a fifth larval segment, the formation of which is delayed at least 24 hours after the fourth primary segment is completed.

Pisione remota (Southern): *Pisione remota* has an interesting larval developmental pattern. It is much like a Lower Cambrian trilobite. The animal is errant in life with planktonic larva early and benthonic later. Åkesson (1961) divided the life period into two stages: planktonic and bottom stages, and eight substages, as listed below.[1]

1. *Planktonic stage* (Text-fig. 11). A) Larva with three pairs of setigerous parapodia; the appendages of the buccal segment not visible; one pair of eyes. B) Larvae with three to four pairs of parapodia; the buccal appendages are visible as rounded protrusions; one pair of eyes. C) Larvae

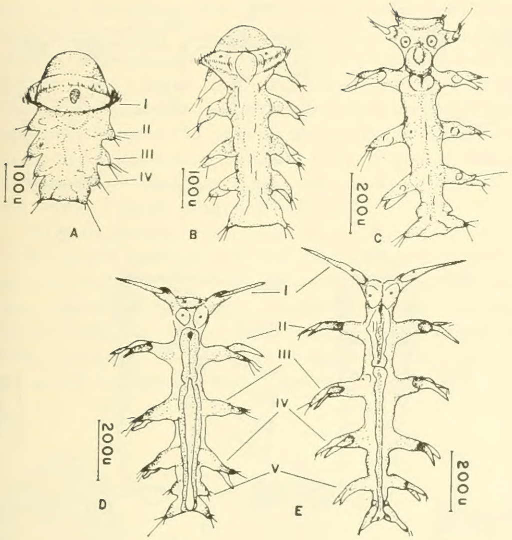

Tex-fig. 10—Embryonic development of *Tomopteris helgolandica* Greeff. A. Four-day embryo; B. Five-day embryo; C. Six-day embryo; D. Seven-day embryo; E. Eleven-day embryo. Note the development of primary somites (I-IV), secondary somite (V), and forward migration of the prototroch and the first pair of setigerous cirri. (Drawn from photographs of Åkesson, 1962.)

with six to seven segments; the dorsal cirri of the buccal segment are longer than the parapodia proper; subulate ventral cirri have developed in the first setigerous segment; two pairs of eyes. D) Larvae with eight segments; the persisting prototroch is somewhat displaced laterally through the forward migration of the buccal parapodia. These larvae are ready for metamorphosis.

2. *Bottom stage* (Text-fig. 12). E) Larvae with eight segments; the prototroch is vestigial or has disappeared. In a dorsal view the brain is circular with four eyes at approximately the same level. F) Larvae with eight segments; two pairs of eyes, one in the posterior of the elongated brain, the other, lateral and elongates (Text-fig. 12B, C). G) Larvae with eight segments; the still more elongated brain extends to the posterior margin of the third setigerous segments. The two pairs of eyes are now located in the anterior and posterior region of the brain respectively. H) Larvae with ten segments; the anterior end now has the adult organization. The anterior, originally lateral, pair of eyes is more or less reduced.

Scoloplos armiger Müller: The embryology of *Scoloplos armiger* was studied by Anderson (1959). The yolky eggs of *Scoloplos armiger* are layed in gelatinous cocoons, and develop by spiral cleavage and gastrulation to produce a yolky trochophore, which then develops 12 primary segments in strict succession. Ciliated bands occur, though development is nonpelagic. Segment-formation ceases after eight days and the embryo hatches and metamorphoses into a free pre-adult, cilia are developed last and yolk resorbed. Additional segments, the secondary ones, are now added (Text-fig. 13).

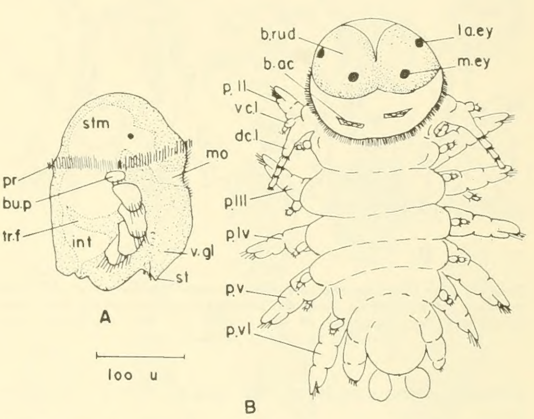

Text-fig. 11—Planktonic larvae of *Pisione remota* (Southern). A. A young metatrochophore; B. Older stage, not yet ready to metamorphose. b.rud, brain rudiment; b.ac, buccal aciculum; dc.I, dorsal cirrus of the buccal segment; dc.II, dorsal cirrus of the second segment; int, intestine; la.ey, lateral eye; m.ey, median eye; p. II-IV, parapodium; ph, pharynx; mo, mouth; pr, prototroch; stm, stomadaeum; tr.f, transversal fold; vc. I-II, ventral cirrus of the first and second segment; v.gl, ventral gland. (After Åkesson, 1961.)

Anterior to the first primary segment lies the prostomium and mouth region derived from the body, or episphere, of the trochophore. Posterior to the primary or secondary segments is a prepygidial growth zone, followed by a terminal pygidium. The primary and the secondary segments have a similar origin and both are formed before ectoderm; each segment contains a pair of hollow meso-

---

As indicated on Text-figures 11 and 12, Åkesson showed this annelid as possessing slender appendages which appear to be both segmented and in part biramous. Further study of this condition is essential, for if this is not pseudo-segmentation of the appendages (*e.g.*, as in the Onychophora), *Pisione* may lie extremely close to the transition from annelids to arthropods in this respect, as it appears to lie in associated cephalic features and other aspects of early larval growth.

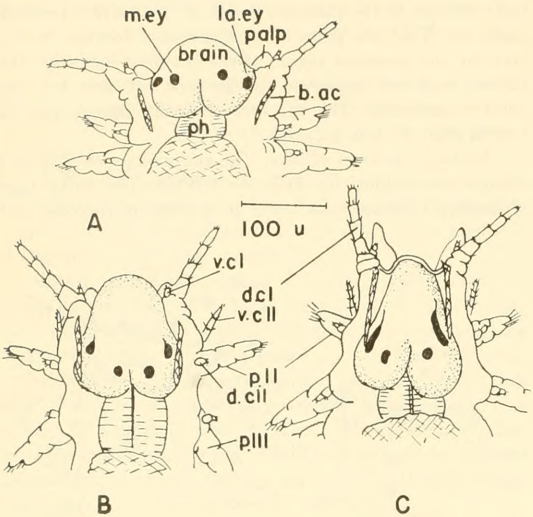

Text-fig. 12—Three larvae of *Pisione remota* (Southern) at different stages of metamorphosis. Note the forward migration of the body segments and the elongation of the lateral eye. For explanation see Text-fig. 11. (After Åkesson, 1961.)

dermal somites, usually of "4d" origin; this is the mesoderm.

Arenicola cristata Stimpson: *Arenicola cristata* inhabits muddy sand at the extreme low water line. The surface of the inhabited area is marked by a large (2″ to 3″ in diameter) low black cone. In life the body is deeply yellowish-green to dark-purple, with 11 pair of branchiae and six pair of rudimentary parapodia in front of a long, non-appended pygidium. It attains a length of eight to ten inches. Eggs are deposited in a large (five inches to two feet in length), spherical, cucumber-shaped gelatinous mass, which is attached to the upper end of the bottom surface by a gelatinous filament. The writer had an opportunity to study the ontogenetic development of the animal during early September to December, 1967, at the Duke Marine Laboratory, Beaufort, North Carolina. The following is a brief discussion of the results of this research.

The gelatinous egg cases of the animal were collected during mid-September to the end of October from Bird Shoals, near Duke University Marine Laboratory and taken to the Laboratory in jars of sea water, where the mass containing developing embryos was separated into finger-bowls containing filtered sea water which was changed daily. Here the embryos hatched from the jelly and entered approximately 20 hours of free-swimming period, after which they built muddy tubes from a small amount of muddy sand added to each bowl. Diatoms liberated from the disintegrating jelly mass served as food for the developing larvae.

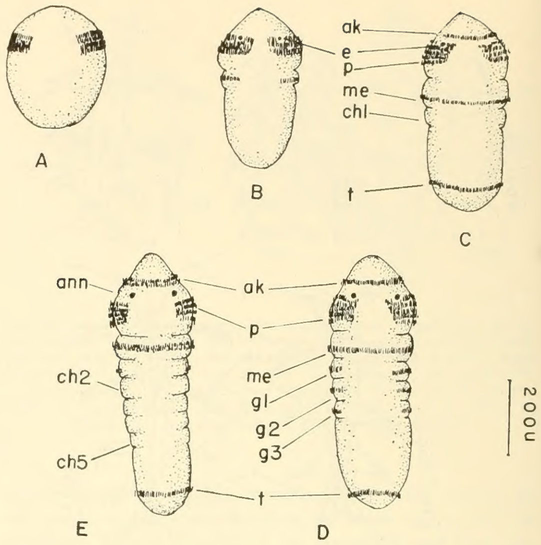

Text-fig. 13—The early embryonic development of *Scoloplos armiger* Müller. A. Unfertilized egg; B. Early 4-day embryo, dorsal view; C. Late 5-day embryo; D. Late 6-day embryo; E. Early 7-day embryo. Note the continuous development of the body segments; ak, acrotroch; ann, post-pro-prostomial antennules; ch. 1, 2, 5, chaetiger 1, 2, 5; e, eye; g, 1, 2, 3, gastrotroch of chaetigers 1, 2, and 3; me, metatroch; p, prototroch; t, telotroch. (After Anderson, 1959.)

The early ontogenetic development of the animal is divisible into four stages and four ecological phases. These stages and phases almost parallel each other, except the Free Swimming Phase is developed within the metatrochophore stage (Text-fig. 16). A brief description of the development of the animal follows:

Embryo-trochophore stage (Text-fig. 14A-C, and Text-fig. 15). The eggs are brownish-yellow, opaque, oval, and about 0.13 to 0.15 mm in diameter. The fertilized eggs develop into embryos about 15 hours after collected in the field. The embryos, rotating within the vitelline membrane, are nearly the same size as the eggs, and are covered with cilia. After approximately 30 hours, the trochophores are hatched out from the vitelline membrane, and are about 0.20-0.22 mm in length, and about 0.10 mm in width, with well-defined proto-, narrow meta-, broad neuro-, and telotrochs. A pair of red eyespots is located laterally at the margin of the prostomium. The larvae, having one or two segments, generally pass through a short free-swimming phase, then attach on a small piece of animal skeleton or alga to enter a six to seven day pseudoplanktonic phase. The pseudoplanktonic life history is demonstrated by both laboratory experiments and planktonic net trawling. The larvae are light-positive, and if a piece of alga is thrown into the finger bowl, the larvae will quickly attach to it and secrete a small gelatinous body cover.

Metatrochophore stage (Text-fig. 15, H-L). The larvae at this period have one oral and one to six setal segments and vary between 0.25-0.75 mm in length. The first segment appears, without setae, shortly after the trochophore hatches from the vitelline membrane; it is well-defined by folded ectoderm. The six pairs of appendages or segments are added sequentially over a period of eight days.

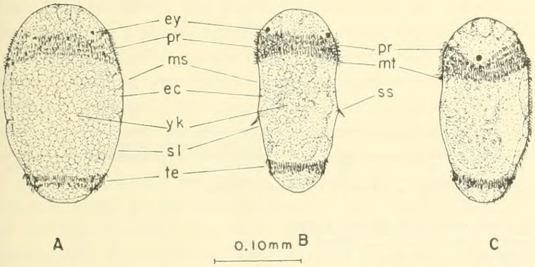

Text-fig. 14—Early metatrochophore of *Arenicola cristata* Stimpson, showing the process of segmentation. A. Note the ectodermal segmentation before formation of mesoderm; B. C. Dorsal and side views of a larva with a single pair of setae; ec, ectoderm; ms, mouth segment; mt, metatroch; pr, prototroch; sl, first segment; ss, first pair state; yk, yolk, te, telotroch. (All drawings were from photographs; the animals were slightly flattened by the cover-glass of the slide mount.)

Early juvenile stage (Text-fig. 15, M-N). The body of the animal contains 7 to 17 setal segments and about 1.00 to 2.30 mm in length. The 7th segment appears three and one-half days after the 6th segment has been completed, and growth continues; the 17th segment being completed approximately 30 days later. The first 17 segments are each with well-developed appendages. The mode of life of the animal from the early stage of this period is burrowing or living in a muddy sand tube.

Late juvenile stage (Text-fig. 15, O). In this period the larvae add the rudimentary segments, *i.e.*, the segments without any appendages behind the 17th segment. The prostomium is proportionally reduced in size and the 7th to 17th appendages are formed into 11 pairs of gills. The length of the animals is more than 3.00 mm.

B. THE PROSTOMIUM

The prostomium is the "head" of the polychaete. It originates from the episphere, or in front of the prototroch of the trochophore, and is composed of mouth, eyes, palps, and nuchal organ. The prostomium is the presegmental region except that mesodermal bands grow forward from the segmental zone into this region on each side to fuse in front of the mouth, and paired sacs may arise within

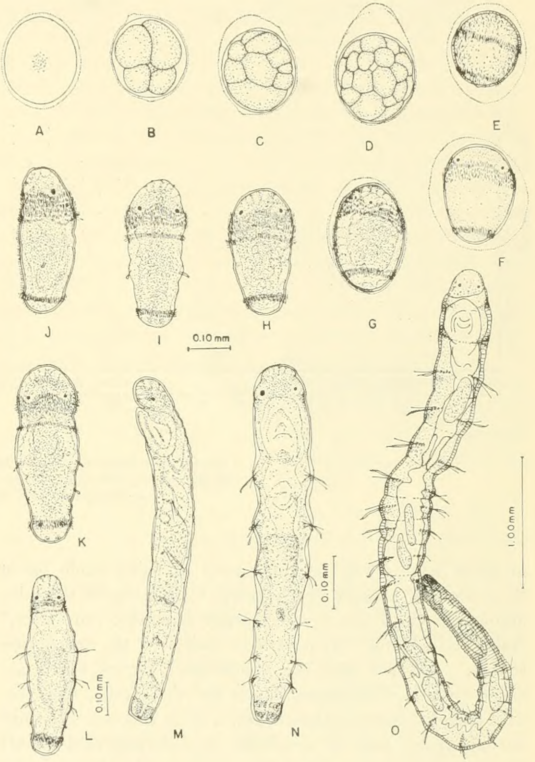

Text-fig. 15—An ontogenetic sequence of *Arenicola cristata* Stimpson. A. Unfertilized egg; B. C. D. Cell cleavage, showing 4, 16, 32 cella stages; E. An early embryo; F. G. Top and side views of trochophore; H-L. A few different sized metatrochophores, note the segmental process; M. N. Side and dorsal views of an early juvenile; O. A late juvenile. (All drawings made from photographs.)

them. Some morphologists have maintained that the occurrence of these sacs lends support to the view that the prostomium is derived from a number of segments which have been reduced by cephalization. The suggestion that the prostomium might contain as many as three segments, however, first came from the studies of the brain, which in many worms has the appearance of being made up of three pairs of ganglia closely fused. Opponents of this idea argue that the brain is functionally separable into "fore," "mid," and "hind" brain regions owing to the correlation centers associated with the paired sense organs which are borne on the prostomium. These are the tactile, and possible chemosensory, antennae, palps, eyes, and chemosensory nuchal organs, none of which has any obvious counterpart on the succeeding segments. In studying the development of *Scoloplos armiger* Müller, Anderson (1959) concluded that there was no evidence for the view that there are vestiges of any segments in front of the first definitive trunk segment; that the brain and the circumoesophageal commissures are presegmental structures; and that the forward growth of the mesoderm and the appearance of the cavities within it are secondary developments. The ganglionic centers occur in the prostomium and they can be presumed to have evolved *in situ* in association with paired prostomial sense organs, and not as the ganglia of cephalized trunk segments; there is no evidence for incorporation of segmental ganglia into the polychaete brain in the manner of arthropods.

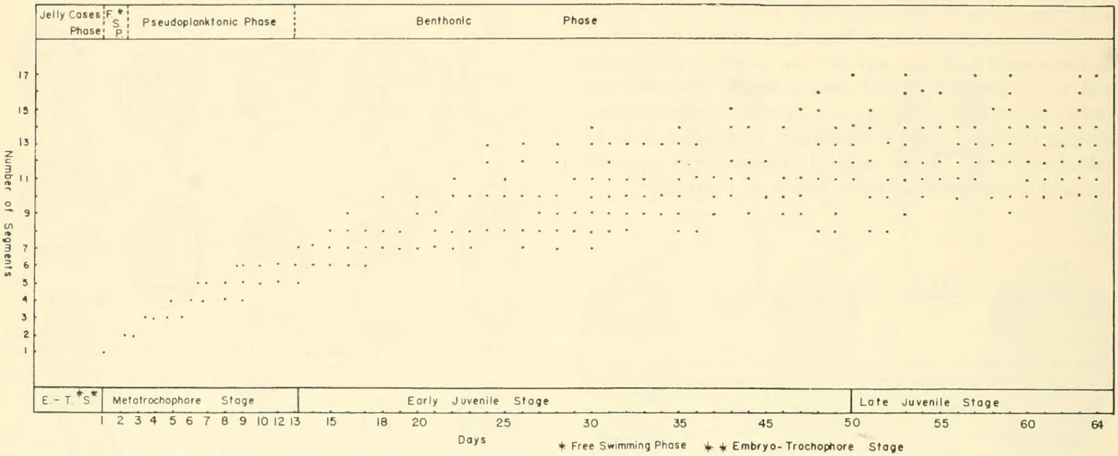

Text-fig. 16—Showing the growth stages and ecological phases during the ontogenetic development of *Arenicola cristata* Stimpson. Note the segmental process ceases from 9th to 13th day.

The peristomium is formed by a fusion of more than one trunk segment immediately behind the prostomium. In *Nereis* and *Tomopteris* the peristomium is formed by two trunk segments, because it bears two pairs of cirri on each side similar to those of the parapodia farther back. *Pisione* has three trunk segments incorporated with the prostomium. The more posterior of the peristomial cirri are innervated by a parapodial ganglion just beneath the bases of the cirri, and are secondarily connected to another ganglion on the circumoesophageal commissure at the same horizontal level; but these parapodial ganglia remain distinctly separated from the brain, even when their individuality is externally masked by a loss of their parapodia in the adult worm. Anderson goes on to say that we can at present only conclude that there is certainly no evidence whatever for the view that any part of the brain, circumoesophageal commissures, or the mouth region, is derived from the most anterior segment by cephalization, and that, on the contrary, the brain and all the structures that it directly innervates, such as the palps and antennae, are presegmental in structure. Structures such as the peristomial cirri, which are manifestly derived from the most anterior segments, are always innervated from ganglia which retain their identity and remain separate from the brain.

C. SEGMENTATION PROBLEM

In a series of papers Iwanoff (1928, 1933, 1944) discussed the primary and secondary segmentation in articulates. The primary segments, or larval segments, which form the main part of the functional embryo, all appear simultaneously and are derived from the ectodermal activity. The secondary segments, or post-larval segments, which give rise to most of the adult body, are budded off in a strict succession from the prepygidial growth zone and primitively contain nephridia and reproductive organs. This heteronomy in segment formation is found not only among the polychaetes but also in other phyla such as arthropods, enteropneusts, and chordates. The number of primary somites varies considerably within the polychaete annelids but seems to be distinct in separate families. Also among the arthropods it has been possible to distinguish primary and secondary somites. Iwanoff demonstrated the presence of four postoral primary somites in the merostomes and has given cogent reasons to believe that the same number of primary somites occurs in Chelicerata and Trilobita, whereas the Crustacea evidently have only two primary somites. For these reasons, Iwanoff came to the conclusion that the varying number of primary somites suggests a polyphyletic origin of the arthropods. This view has been accepted by several writers: Remane (1949), Snodgrass (1938), Størmer (1944), and Beklemischew (1952). It has been rejected by Manton (1949), Tiegs and Manton (1958), Anderson (1959), and Åkesson (1962), who argued that the different numbers of primary somites in polychaete larvae, heteronomous or non-heteronomous, can be interpreted best in terms of functional specialization enhancing the efficiency of the growing organism, whether pelagic or nonpelagic.

Returning to the condition found among the polychaetes, a few examples of the ontogenetic development of polychaetes have been here presented to demonstrate the morphologic variations of the prostomium and heteronomous and non-heteronomous segmental processes of the animals. *Tomopteris helgolandica* Greeff is an heteronomous polychaete, in which three primary segments simultaneously appear between the prototroch and the telotroch by segmentation of the ectoderm, and the second segments are developed from the prepygidial growth zone. The same process is also found in *Eunice kobiensis* (Åkesson, 1967), the Nereidae, Serpulidae. Non-heteronomous or partly heteronomous forms are illustrated by *Scoloplos amiger* Müller (Anderson, 1959), *Halploscoloplos fragilis* (Verrill) (Åkesson, 1961), *Polygordius* which are without any distinction between primary and secondary segmentation; the segment formation in these annelids takes place evenly from anterior backward, with the mesoderm segmenting before the ectoderm. However, these forms do have a shallow segmental break between certain segments, but the segmenting first appears in the mesoderm; it is not like heteronomous segmentation which first appears on the ectoderm.

The observation on the segmental process and the mode of life of *Arenicola cristata* Stimpson and *Axiothella mucosa* (Andrews) has led to the conclusion that Iwanoff's theory is still tenable. These observations do not support Manton, *et al.*, that the heteronomic segmental process is merely a functional response to the needs of the larva during planktonic life. In the larval development of *Arenicola cristata,* the early trochophore has a short free-swimming period (during the 1st and 2nd segmental stage) but lacks heteronomy; *Axiothella mucosa* (Andrews) (Bookhout and Horn, 1949) exhibits heteronomy (three or four primary segments) but no planktonic stage, and in these the ectodermal segmentation precedes mesodermal (Text-fig. 14A). The functional response to the needs of the larvae does not seem to be a convincing argument against Iwanoff's theory. The presence or absence of heteronomy among polychaetes seems to be a fundamental condition and probably indicates separate annelidan origins for derived groups such as the different arthropod classes or mollusks.

Segrove (1951) postulated that the primitive (hypothetical) polychaete produced a large number of small eggs which developed into fully ciliated larvae. These larvae were pelagic and fed on the microplankton for a long time before undergoing metamorphosis. The cilia were mainly for locomotion and perhaps to a much lesser extent for feeding. Another line, characterized by benthonic larvae, developed from this hypothetical type. They produced a small number of large, yolk-laden eggs. The larvae developing from these eggs depend on the yolk and not on an external food supply, hence the feeding and locomotor ciliary apparatus was suppressed. In some of the benthonic types, however, cilia seem to have been retained for a respiratory function. Manton (1949) and Anderson (1959) have also both argued that forms with benthonic mode of life, producing few, large yolk eggs and segmentating in a strictly anterior to posterior manner during development, are primitive, *e.g., Scoloplos, Halploscoloplos* and including the Onychophora. For them the pelagic larvae of *Tomopteris, Nereis* are advanced. It should be noted that the egg of *Arenicola cris-*

tata Stimpson and *Axiothella mucosa* (Andrews) both contain much yolk, but *A. cristata* larvae possess a short free-swimming stage and are non-heteronomic, whereas *A. mucosa* has a heteronomic segmental process but is non-pelagic throughout life. In this light, the Anderson-Manton criteria for determining primitiveness among polychaetes are less than convincing.

2. ONTOGENY OF CRUSTACEANS

Crustaceans eggs are typical centrolecithal and cleavage is superficial; holoblastic cleavage is not uncommon. Often only the initial cleavage divisions are complete, as in some arachnids, but there are a considerable number of species of both Entomostraca and Malacostraca in which a hollow blastula is formed.

Because among the crustaceans the young hatch at different periods of development, the youngest larvae may have diverse forms in the various orders, representing different ontogenetic stages according to the degree of development they undergo within the egg. The earliest and basic type of crustacean larva is the nauplius (Text-fig. 17). It is commonly free-swimming and planktonic, oval or pyriform in shape with the larger end anterior. Three pairs of appendages are present — the antennules, antennae, and mandibles — and a median eye of two or more parts, although there is no visible segmentation of the ectoderm; the presence of appendages and ganglia shows that the nauplius is at least a partly segmented stage of development. The region of the body behind the mandibles is that in which the other segments will be formed later, and their rudiments may be seen beneath the nauplius cuticle. When these segments are formed, however, they are generated by a different method from that which formed the anterior segments. The nauplius is usually followed by a metanauplius stage, during which, in the course of successive molts, trunk segments, and additional appendages are gradually acquired from a subterminal zone of the nauplius; the posterior part of the body is much lengthened; it is now distinctly segmented and bears the rudiments of several pairs of new appendages.

EXAMPLES OF CRUSTACEAN ONTOGENY

a. The ontogenetic development of *Leander squilla* Linnaeus has been studied by Sollaud (1923). The germ bands of *Leander* are at first V-shaped (Text-fig. 18), its two arms diverge forward on the blastoderm from a posterior area of proliferation (GD) in the region of the blastopore, whence also are proliferated forward two corresponding bands of mesoderm. Each mesoderm band soon becomes divided into four consecutive parts, which appear as four lobes on the surface (B). The germ bands themselves gradually become less divergent, and finally their anterior ends curve medially and are united by a bridge between their anterior lobes (C). At the same time the rudiments of three pairs of appendages appear on the second, third, and fourth lobes, which are respectively the antennules (Anu), the antennae (Ant), and the mandibles (Md). The first lobes (Prc) have no appendages, but they give rise to the compound eyes and optic ganglia. These now appear in the ectoderm of the young embryo. Sollaud said that there are transverse grooves which appear before the first segmentation (D). The most anterior groove runs between the antennae and the mandibles, and the third behind the mandibles (D,E). The body of the embryo is thus divided into an anterior prostomial head segment (Prst), bearing the procephalic lobes and the antennules, a second segment (I) bearing the antennae, a third segment (II) bearing the mandibles, and a terminal unsegmented piece (Cdp), which is the caudal papilla. The embryo is now in the nauplius stage. Sollaud claimed that the first segment, bearing the optic lobes and antennules, is the prostomium, the other two segments being the first and second true somites.

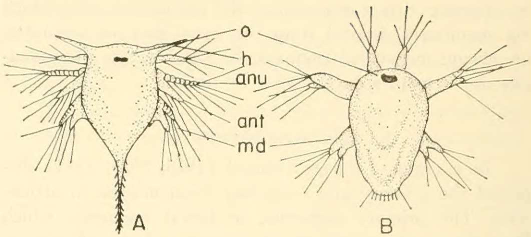

Text-fig. 17—A. A late nauplius of *Balanus* (after Calman from Lankester, 1909); B. First nauplius larva of *Cyclops fuscus* (after Green from Barnes, 1962); anu, antennules; ant, antennae; md, mandibles; h, frontal horn; o, nauplius eye.

The caudal papilla of the malacostracan embryo (Text-fig. 18) projects from the blastoderm. In its distal part, there is a circle of undifferentiated ectodermal (Ect) and mesodermal cella, which are the teloblasts that will generate the postnauplius somites. Beyond the teloblasts is the region of the telson (Tel) containing the anus (An). In its development the caudal papilla bends forward (F) beneath the part of the embryo contained in the blastoderm.

When the malacostracan embryo reaches the metanauplius stage there appear at the base of the caudal papilla the two maxillae and their appendages.

Sollaud (1923), however, asserted that in *Leander* both maxillary somites arise from the base of the caudal papilla before the beginning of activity in the teloblast, and that the first somite of the teloblastic series is that of the first maxillipeds. According to him the four somites of the metanauplius (F), namely, those of the second antennae, the mandibles, the maxillae, and the second maxillae, are primary somites formed directly in the primary embryonic body between the acronal prostomium and the caudal papilla. If so, the primary somites of the crustaceans would agree in number with the Xiphosurida and Trilobita. However, Snodgrass (1938, p. 81) thought this interpretation is erroneous, since the maxillae are derived from the caudal papilla (see below).

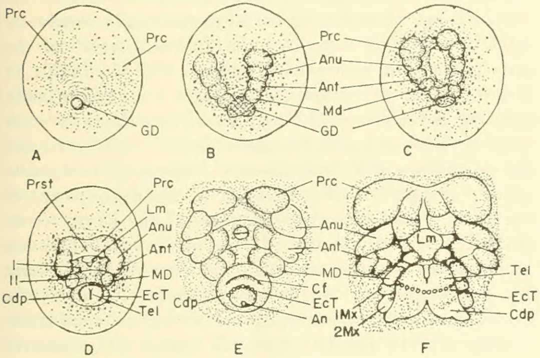

Text-fig. 18—Early embryonic stage of a palaemonid crustacean. Showing the development of the procephalic lobes and the antennules from the unsegmented prostomial region, and cephalic segmentation. A. *Leander squilla* Linnaeus; B-F. *L. serratus* Pennant. Anu, antennules; Ant, antennae; Cdp, caudal papilla; Ect, ectodermal teloblasts; GD, germinal disk; I,II, primary somites; Lm, labrum; MD, mandible; 1Mx,2Mx, first and second maxillae; Prc, procephalic lobe; Prst, prostomium; Tel, telson. (After Sollaud, 1923 from Snodgrass, 1938.)

Manton's (1928, 1934) studies of the embryonic process of secondary segmentation of the crustaceans *Heminysis* and *Nebalia* agreed with the observations of Sollaud for the embryo of *Leander*. In *Heminysis*, she said the nauplius and postnaupliar mesoderms are at first some distance apart, but later the teloblastic ectoderm and mesoderm extend forward to include the first maxillary segment. The teloblasts of *Nebalia* are differentiated at the sides of the posterior blastoporic area, and the ectodermal teloblasts eventually form a complete circle around it; the mesodermal teloblasts are formed from the mesendodermal mass at the blastopore; Fränsemeier (1939) said they are proliferated from the ectodermal teloblasts. The ectodermal teloblasts, according to Manton, join the naupliar ectoderm between the mandibular and first maxillary segments. Thus it seems that all segments between the mandibular segment and the telson are formed by the teloblasts. Therefore, the maxillae represent secondary somites and the primary somites are restricted to the second antennae and mandibles only.

When the last abdominal segment is complete, the teloblasts disappear in both *Heminysis* and *Nebalia.*

b. The ontogenetic development of *Balanus amphitrite* "var." *denticulata* Broch has been studied by Costlow and Bookhout (1958b), who described six naupliar and one cyprid stages. In the naupliar stages one through three the carapace is about 0.15-0.25 mm in length (sag.) and rounded to subrounded with a long terminal process. Two pairs of spines are marked along the margin of the carapace; the anterior lateral pairs are medium-short, and the posterior-lateral ones are rather small. Three pairs of appendages, antennules, antennae, and mandibles, bearing setules are directed laterally and lateral posteriorly; the abdominal process terminates in two short spines. The labrum is located on the anterior mid-central carapace (Text-fig. 19, I-III).

In nauplius stage 4, the carapace is about 0.22 mm in length without a terminal process, but a pair of short spines appear on the posterior edge where the carapace is delimited from the caudal process. Six rows of minute bristles are found on the ventral surface of the abdominal process (Text-fig. 19, IV).

In nauplius stage 5 and 6, the carapace is ovate and about 0.28-0.34 mm in length (sag.) The anterior and posterior pairs of spines of the carapace remain unchanged, except that the posterior ones are slightly more widely spaced than in the previous stage. The abdominal process bears six pair of bristles. A pair of eye spots develops beside the naupliar eye in the later stage (Text-fig. 19, V, VI).

Cyprid stage. The rounded anterior end of the cyprid is the widest portion of the carapace which curves gradually to the posterior end. The degree of pigmentation varies considerably, but some brown pigment is always observed; when the bivalve carapace is closed, both the anterior and posterior ends are smooth.

It should be noted that the early ontogenetic development of *Balanus* is morphologically similar to some protaspides of trilobites, such as *Cryptolithus, Tretaspis* (Whittington, 1959a, pls. 23, 26), and asaphids (Evitt, 1961, pl. 117). Though this similarity may be interpreted as an adaptation to their presumed temporary pelagic life, because the trilobite larvae also represent an early stage of development, it may, on the other hand, be indicative of evolutionary affinities.

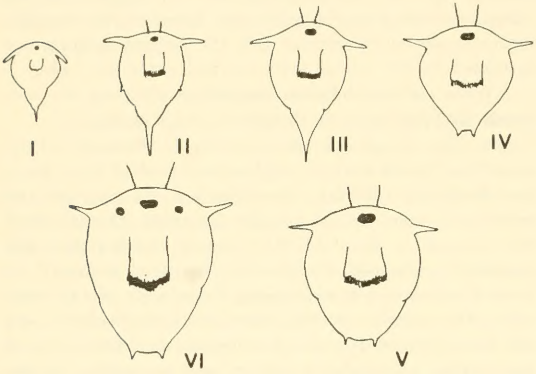

Text-fig. 19—A growth sequence of *Balanus amphitrite* "var." *denticulata* Broch showing the metamorphosis of the carapace. (After Costlow and Bookhout, 1958b.)

3. ONTOGENY OF *MEROSTOMATA (XIPHOSURA)*

According to Shuster (1950, 1960), the eggs of the horseshoe crab are laid between the tide marks on sandy beaches. A month or more later, hatching occurs and the smallest larvae average 4.5 mm in length. These grow by stages, shedding their chitinous skin between each stage. After the first molt the larvae acquire a tail. In the first tailed stage their average length is 6.0 mm and in the next six stages 9.55 mm, 14 mm, 21 mm, 29 mm, 40 mm, and 50 mm, respectively.

During the first few years of life the horseshoe crabs shed their chitinous exoskeletons more than once a year, but when the animal attains a length from 100 to 120 mm there is only one molt a year, and this occurs during midsummer. Some 9 to 12 years elapse before the horseshoe crab is sexually mature. The sexual organs become functional and the accessory reproductive apparatus is developed with the final molt. Throughout the period of growth each horseshoe crab molts 16 to 19 times; when a horseshoe crab reaches the adult, sexually mature, stage, it seems to stop molting. However, occasional exceptionally large adults seem to contradict this.

The opening of the exoskeleton during molt begins just within the ventral margin of the prosoma, the doublure. The first-tailed stage or smaller horseshoe crab emerges within an hour, but an animal 100 mm wide may require over 24 hours.

Measurements of the linear dimensions of the growing animal show that the increments of growth generally decrease during the life cycle after an initial increase. For example, the width of the first-tailed stage is 45% greater than that of the previous stage, 75% greater in the next stage, but then decreases step-wise to a 15% increase in width in the twelfth stage.

Embryologic development of *Xiphosura ("Limulus")*. — The earliest embryologic study of *Xiphosura polyphemus* (Linnaeus) was made by Milne Edwards (1838); the next classical studies of this subject were those of Lockwood (1870) and Packard (1872, 1880a, b); all included detailed studies not only of embryology but also of ecology, anatomy, and histology. Packard strongly argued that the Trilobita and Merostomata are phylogenetically closely related, and he first recognized the "trilobite stage" of the early *Xiphosura* embryos. Kingsley (1892-3, 1897), in a series of papers, recognized 11 stages from egg to early hatching larva. Patten (1896, 1912) divided the early ontogeny of *Xiphosura* into 14 stages. Iwanoff (1933) studied the embryology of *X. maluccanus* (Linnaeus) *("Tachypleus gigas")* and paid special attention to the development of the primary and secondary segments of the larval forms. According to him, the early larvae of *X. maluccanus* has four primary somites, which are the first to appear from the mesoderm, and are secondarily impressed upon the ectoderm. Thus demonstrating his phylogenetic principle. Størmer (1944) followed Iwanoff's theory and separated the ontogenetic development of *Xiphosura* into four stages, namely, the trilobite, synziphosura, prestwichianella, and limulid stages. These growth stages apparently parallel the geological record and phylogenetic development of the animal.

In the earliest *Xiphosura* larva, the trilobite stage (Størmer, 1944) consists of four primary segments in front of the generative pygidium or caudal papilla. The secondary somites, or the new segments, are successively budded off from the prepygidial growth zone and serially added to the primary somites. The formation of the new segments is essentially the same as in annelids and crustaceans, but it seems that after the 6th cephalic, or 3d secondary, somite are formed, the generative pygidium is turned forward, and comes to lie underneath the posterior margin of the cephalon, although Iwanoff failed to show this generative pygidial activity. This is an interesting parallel to the condition shown to occur in the ontogenetic development of the palaemonid crustacean *Leander* (Text-fig. 18). Therefore, as the result of this pygidial inversion, the 7th segment, or 3d secondary somite, divides into two halves (7th and 8th) and a juncture forms between the prosoma with chilaria rudiments and the opisthosoma ridges (Text-fig. 21). The same condition is seen in the occipital ring of olenellids and the cervical groove of crustaceans. Secondary segments are continuously added behind the prosoma to form the opisthosome; these are comparable to and perhaps homologous with the tertiary somites of trilobites. The opisthosomal segments are formed around the margin of the generative pygidium and arranged semi-concentrially at the early stage but later open so as to arch forward and laterally (Text-fig. 21, T). The adult structure of *Xiphosura* contains evidence of the presence of 14 post-oral somites, the last somite being behind the last gill-bearing segment; but Iwanoff said that in the embryo, rudiments of three somites appear in the post-branchial region, thus giving a total of 16 somites anterior to the caudal spine. The caudal spine of the xiphosurids is often called the "telson," but it is situated beyond the segment-forming zone. Therefore, Iwanoff suggested that it might be comparable with the dorsal spine on the posterior segments of certain *Olenellus*, where the spine arises from a segment some distance from the end of the body. Thus the xiphosuran "telson" may not be a true terminal structure, and several small somites beyond it may have been lost. This interpretation may be reasonable, but it should never be taken to mean that this condition has necessarily any phylogenetic significance, because many crustaceans and insects also possess a similar structure, which may be longer or shorter, slenderer or stouter, due to functional differences.

Patten (1912) showed that the early limulid embryo has the lateral eyes situated on the anterior lateral margin of the shield. The eyes migrate to a more dorsal medial position during the later stage (Text-fig. 22). Comparable migration to the eyes is also seen in opisthoparian and proparian trilobites. Moreover, the segmental sense organ (Text-fig. 22, So4), which appears in the early larvae of *Xiphosura* is comparable to and may correlate with the fixigenal node of certain immature trilobites (Text-fig. 38H and 43E).

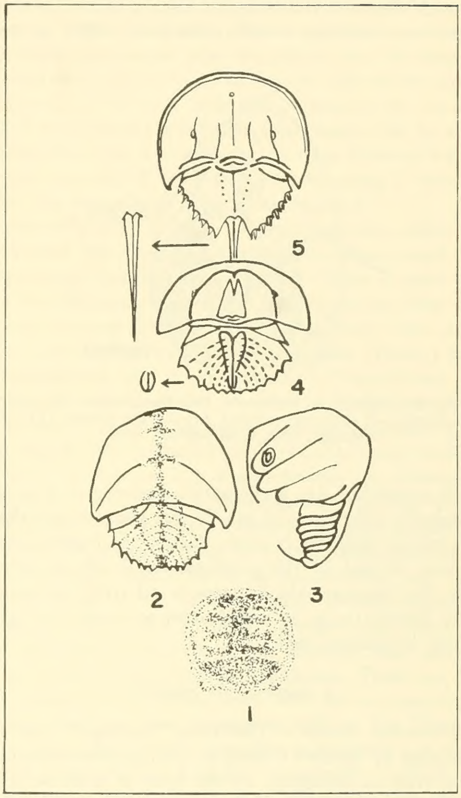

Text-fig. 20—Ontogeny of a limulid. 1-4. *Xiphosura maluccanus* (Linnaeus). 1. Trilobite stage; 2. 3. *Synziphorura* stage; 4. Prestwichianella stage; 5. Limulid stage. (After Størmer, 1944.)

III. ONTOGENY OF TRILOBITA

The ontogeny of trilobites is divided into three periods namely, protaspid, meraspid, and holaspid. Five stages of the periods are recognized: the protaspid period is subdivided into three stages: the anaprotaspid, metaprotaspid, and paraprotaspid; the meraspid period is subdivided into early and late meraspid stages; no stages of the holaspid (adult) period are recognized (Text-fig. 23). Each stage presumably represents several instars (episodes of ecdysial moulting) during the succession of which the changes termed periods and stages of morphologic differentiation were attained. Nothing comparable to hexapod metamorphosis is here involved in the ontogeny. Thus the periods and stages are arbitrarily defined, because the morphologic changes of any trilobite during ontogeny were essentially gradual and continuous. Hypothetically, these morphologic changes have left no gap, no omission, except that conditions of preservation may cause a certain stage to be lacking in growth sequence. Neontologists have sometimes observed the pre-maturation of certain individuals within an ontogenetic assemblage, *i.e.*, an immature specimen may be morphologically older than its age. If this phenomenon should occur among trilobites it would disrupt the regular growth sequence or lead to the misidentification of the growth stages, but because this situation is relatively uncommon in the Recent fauna, it would seem to present no grave problem in ancient ones.

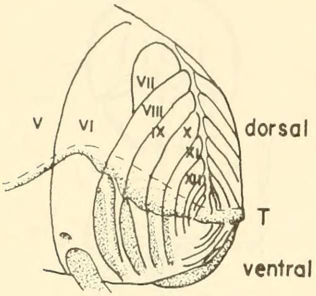

Text-fig. 21—Embryo of *Xiphosura.* Posterior-lateral view, showing the formation of secondary somites around the telson (T). After Iwanoff, 1933, from Størmer, 1952.)

1. PROTASPID PERIOD

Historical review. — The term "protaspis" was first established by Beecher (1895a, p. 169) for the earliest record of trilobite ontogeny, on the basis of features of the dorsal shield. He described it as: "minute, varying in observed species from 0.4 to 1.0 mm in length, circular or ovoid in form, axis distinct, more or less strongly annulated: head portion predominating; glabella with five annulations; abdominal portion usually less than one-third the whole length of the shield, axis with from one to several annulations; pleural portion smooth or grooved; eyes when present anterior, marginal or submarginal; free-cheeks when present very narrow, marginal." This original concept of the protaspis now needs revision because we now know considerably smaller protaspids with only four or five axial annulations and for the most part lacking the abdominal part. Beecher (1859a, p. 169) also suggested that the protaspid period might be subdivided into anaprotaspid, metaprotaspid, and paraprotaspid stages during which the early

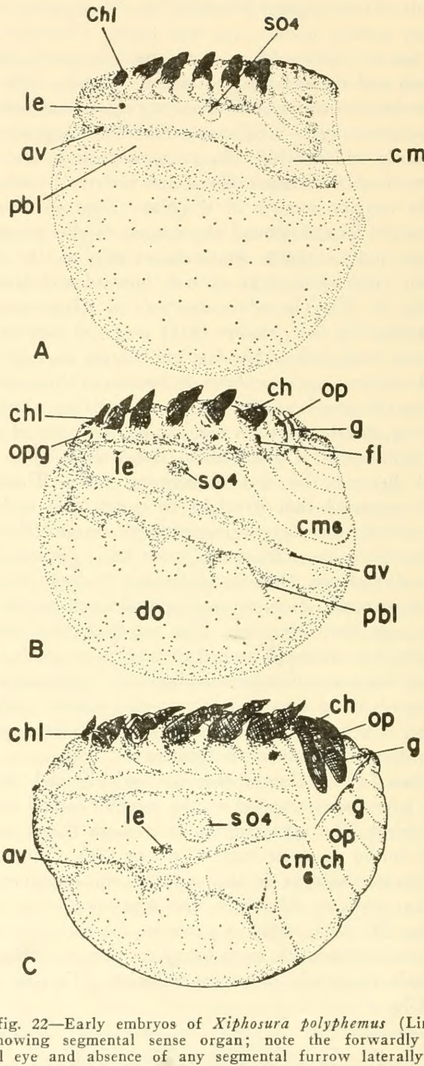

Text-fig. 22—Early embryos of *Xiphosura polyphemus* (Linnaeus). A. Showing segmental sense organ; note the forwardly located lateral eye and absence of any segmental furrow laterally on the prosomal region. B. The lateral eye has moved to the second segmental region C. The abdominal lobe is distinctly marked off; the lateral eye has moved backward and dorsally to 4th cephalic segmental region. av, anterior median ventral margin of the cephalon; ch, cheliceral lobe; cm6, 6th cephalic segment; g, gill; fl, flabellum; le, lateral eyes; op, opercular segments; opg, optic ganglion; pbl, posterior dorsal plate; So4, 4th segmental sense organ. (After Patten, 1912.)

and late molts took place, before the complete separation of pygidium or introduction of thoracic segments. He did not give any distinctive characteristics to define these different stages. Raw's (1925, p. 226) view was that "the protaspid period embraces the various stages that precede the development of a definite transverse suture subdividing the dorsal shield." This definition clearly draws a line between the protaspid and the meraspid periods and is now followed by most authors. Størmer (1942, p. 56) defined the protaspid period as "all the earliest stages from hatching to the appearance of the first transverse dividing of the dorsal shell into two separate shields, and the transitory pygidium." He also further defined the anaprotaspid stage as that in which "the axis has only five segments," and the metaprotaspid stage that which "includes the later stage in which new segments are added beyond those present in the anaprotaspis." Thus he was the first author to give a clear definition of Beecher's stages. However, the paraprotaspid stage was not adopted. In Whittington's (1959b, p. 127) opinion, "the earliest protaspis represents the earliest stage at which, presumably, the exoskeleton is mineralized and therefore may be preserved. A range in length (sag.) from about 0.25-1.0 mm is known, rarely larger. Outline in dorsal aspect is usually subcircular, convexity moderate to strong, and subspherical form may be attained. The axis is at least partially defined in the smallest protaspides . . . and may be completely outlined by furrows. From a length of 0.40 mm upward it is in most specimens divided into rings, the anterior being longer (sag.) than those following it. The 5th . . . ring is the occipital, and behind this is the short axial portion of the protopygidium . . . The pleural regions of the smallest known protaspid . . . are either incompletely divided or not at all. At a length of 0.50 to 0.60 mm the transverse ridge (posterior border of cephalon) and furrow have either appeared or been completed, thus dividing the protaspis into a larger cephalic portion and smaller protopygidium . . . ." I infer from this statement that he subdivided the protaspid period into three stages: the 1st stage being smaller than 0.40 mm, the 2d stage between 0.40 to 0.50 mm, and the 3d larger than 0.60 mm (sag.); however, he did not denominate these three stages.

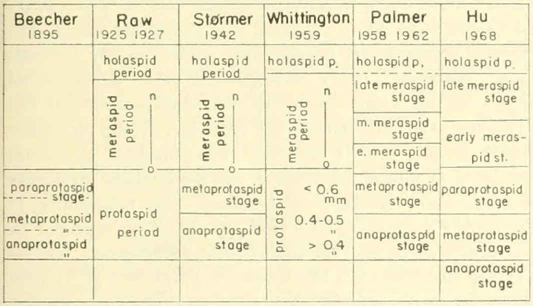

Beecher 1895	Raw 1925 1927	Størmer 1942	Whittington 1959	Palmer 1958 1962	Hu 1968
	holaspid period	holaspid period	holaspid p.	holaspid p.	holaspid p.
	meraspid period n–o	meraspid period n–o	meraspid period n–o	late meraspid stage	late meraspid stage
				m. meraspid stage	early meraspid st.
				e. meraspid stage	
paraprotaspid stage	protaspid period	metaprotaspid stage	protaspid < 0.6 mm	metaprotaspid stage	paraprotaspid stage
metaprotaspid "			0.4-0.5 "		
anaprotaspid "		anaprotaspid stage	> 0.4 "	anaprotaspid stage	metaprotaspid stage
					anaprotaspid stage

Text-fig. 23—Showing various author's divisions of the ontogenetic development of trilobites.

Palmer (1958, p. 165) followed Størmer's definition, and divided the protaspid period into anaprotaspid and metaprotaspid stages, and noted that "there is some evidence that the anaprotaspid axis may have more than five segments anterior to the occipital segment. Also some species, such as *C.* [*"Cassifimbra"*] *walcotti* (Resser) have an unsegmented axis in the protaspis. Nevertheless, the morphologic position of the posterior part of the occipital ring is nearly always apparent. The anaprotaspid stage might thus be less equivocally defined as the stage in which the dorsal exoskeleton is a shield showing no evidence of segmentation of a distinct protopygidium portion to the occipital ring." He recognized Størmer's anaprotaspid and metaprotaspid stages as valid and identifiable subdivisions of the protaspid period for most non-olenellid and non-agnostid trilobites, but used a slightly different notation. The writer agrees with Palmer's statement that there are many trilobite larvae without any distinct axial annulation and distinct protopygidial separation. These are less easily categorized, but those forms with distinct annulation and protopygidium lend themselves well to the Beecher-Størmer protaspid classification. The exceptional, and rarer, forms of protaspids are probably secondarily modified out of the common, and probably more primordial and general, undifferentiated condition. Palmer (1962, p. 92) also further subdivided the metaprotaspid stage into four degrees based on the distinct or indistinct separation and the number of the fixigenal and pygidial spines; these subdivisions generally conform to Ross' (1951b, p. 584) ontogenetic studies of *Pseudocybele nasuta* Ross. Such differences as exist are in minor details.

Thus it can be seen that, there is no complete agreement among trilobite students on the definition of ontogenetic stages; however, there is a consensus as to the reality of protaspid stage and its divisibility despite the hazy and somewhat debatable boundaries of both stages and periods. It is obvious that the different interpretations of trilobite development are due to the study of different materials by the different researchers. The characteristics of all trilobite larvae are not all the same, and hence the different materials present somewhat different information, from which various generalized interpretations have been derived. The situation is well demonstrated by modern crustacean larvae (as well as those of echinoderms, with variously different larval forms). It is now manifest that no single set of criteria can be used as the basis for the determination of ontogenetic stages of all trilobites. In this study an attempt has been made to find a comprehensive interpretation of all known trilobite ontogenies. In the search a certain body of new information has also accrued. Thus, the definition of period and stages used in this work is to some degree different from the definitions of most other workers. However these deviations are held to a minimum to lessen confusion.

A. TERMS USED IN THIS PAPER

The *protaspid period* is the earliest known period in the ontogenetic development of a trilobite: the instars are generally 0.22-0.85 mm in length (sag.) and rounded to subrounded in outline. The shield may be gently to highly convex, with or without distinct axial and pleural lobe differentiations and axial annulation; such differentiation as does occur is fundamental. Surface ornamentation may be present or absent. The smallest instars usually have four axial rings and the largest ones well-developed cephalic and protopygidial shields. The *anaprotaspid stage* is the earliest subdivision of the protaspid period; the shield averages 0.28 mm in length (sag.) and varies from 0.22 to 0.40 mm long (sag.), with or without axial and pleural differentiations. The axial lobe is marked by four distinct or indistinct annulations. A longitudinal fissure may be present along the central axis, and well-preserved material may show one to three pairs of marginal spines, a spinose hypostoma, and the librigeno-rostrum underneath the shield. The *metaprotaspid stage* is the second subdivision of the protaspid period. The shield averages 0.35 mm in length (sag.) and varies from 0.30-0.60 mm (sag.) It may or may not show distinct differentiation of the axial and pleural lobes. Typically, the axial lobe is marked by five annulations; the longitudinal axial fissure of the prior stage may or may not show. Some silificied material shows one or more pairs of marginal spines, a sparsely spinose hypostoma, and undifferentiated librigeno-rostrum. The *paraprotaspid stage* is the third subdivision of the protaspid period. The average total length is about 0.58 mm (sag.) and varies from 0.50-0.80 mm (sag.). The shield is subspherical elongate and well differentiated into cephalic and protopygidial shields by a definite transverse suture. The axial and pleural lobes are well differentiated, with or without axial annulation; the axial fissure may show; facial sutures are dorsal or dorsomarginal; the librigeno-rostrum is separated; the number of hypostomal spines is fewer than in the preceding period. The protopygidium may be divided into a few segments by furrows, with or without marginal spines.

Palmer (1958, p. 165) pointed out that some protaspids have more than four glabellar segments, and Whittington (1959b, p. 134) stated that *Shumardia* larvae have three glabellar rings anterior to the occipital segment. It now appears that four glabellar segments is the general rule in protaspids: when more or less than four are present, it is probably due to secondary segmentation of the frontal lobe or segmental fusion. Such "segments" should not be considered as truly initial segments.

B. REPRESENTATIVE TYPES OF PROTASPIDES

Agnostids. — The ontogeny of agnostids commonly is neglected in discussions of trilobite larval development, and our knowledge of the ontogeny of this group has not advanced much since Barrande's (1852) period. The youngest known form has a cephalon and a pygidial shield. The thoracic segments are subsequently added serially between them. Matthew (1895) distinguished three ontogenetical stages of this group based on the characteristics of the pygidium: the early larval, the later larval, and the adult stages. Šnajdr (1958) described the ontogeny of several species of agnostids but none of the morphologic structures shown pertain to stages earlier than those represented in Barrande's studies: Hunt (1967, pp. 203-208) reported on the development of *Trinodus elspethi* (Raymond) but his silicified material from the Edinburg Formation of Virginia shows no earlier growth stage than was previously known. If there were a protaspis, the stage earlier than the two shields one, it is still unknown.

The present study of *Pagetia clytia* Walcott is the first report on the ontogeny of the eodiscinid group. The earliest instar shows a large cephalic shield and somewhat smaller pygidial shield without any distinct suture between (Pl. 7, fig. 23); well-elevated posterior fixigenal borders are present. The total length of the shield is less than 0.30 mm (sag.). The axial lobe is cylindrically conical, with three indistinct annulations. Judging from the indistinct separation of the cephalic and pygidial shields, and from the size, this specimen belongs to the paraprotaspid stage or between paraprotaspid and early meraspid stages.

Olenellids. — The first ontogenetic work on the olenellids was by Ford (1877) who studied the ontogeny of *Elliptocephala asaphoides* Emmons from the Lower Cambrian of New York. Walcott (1910) studied the same form from the Lower Cambrian of Alberta and *Paedeumias yorkense* Resser and Howell from the Lower Cambrian of Pennsylvania. The ontogeny of *Paedeumias hanseni* Poulsen was described by Poulsen (1932) from the Lower Cambrian of Greenland, and *Holmia kjerulfi* (Linnarson) by Størmer (1942) from the Lower Cambrian of Norway. Most of these ontogenies were reinvestigated by Whittington (1957a, 1957b, 1959b). According to him none of the supposed protaspids of olenellids truly belong to the protaspid period, because the specimens are all too large for the protaspid stage and all have well-developed thoracic segments, a characteristic of later stages.

Palmer (1957) recently described a few silicified specimens from the Lower Cambrian of Nevada. He recognized five different growth stages, designated by Roman numerals I-V, but none of the specimens was judged as protaspis by Palmer or by Whittington (1959b) who reviewed the work.

A few small shields or cephala of *Olenellus truemani* Walcott from the Lower Cambrian of Mexico were examined during the present study. They are about 0.40-0.55 mm in length (sag.), spherical to subspherical in outline and convex, with well-differentiated axial and pleural lobes. The axial lobe is marked by a longitudinal fissure, and the pleural lobes bear well-impressed pleural furrows. Possibly there is a small protopygidium located behind the occipital ring (Pl. 8, figs. 1-5). If a small protopygidium is present behind the occipital ring, it is safe to assign the specimens to the paraprotaspid stage. The Mexican early larvae are different from those of *Olenellus* or related genera which have been published in that the axis is fusiform and marked with a longitudinal fissure; the pleural lobes bear distinct segmental furrows, and the occipital ring is narrow (sag.).

In discussing these specimens with Dr. Whittington at Harvard University in 1966, he suggested that they possibly belong to protaspids. There seems to be no doubt that these specimens are the earliest instars of olenellids yet seen.

Ptychopariids. — The ontogeny of ptychopariids is better known than for any other trilobites. The classical foundations were laid down by Barrande (1852), who figured and described a considerable number of larval stages including those of *Sao hirsuta* Barrande and *Hydrocephalus carens* Barrande, which are well known from illustration in paleontology text-books. Brøgger (1875) described a larval series of *Liostracus linnarssoni* Brøgger from the Middle Cambrian of Norway. Beecher (1895a) reviewed these studies and was the first to make a comprehensive study of the ontogenetic development of trilobites and therefrom attempted a natural classification of the Trilobita. Strand (1927) and Størmer (1942) demonstrated the eye-ridges and cephalic segments of the early larvae of *Olenus gibbosus* (Wahlenberg). Endo (1935) worked on the ontogeny of *Blackwelderia kobayashii* Endo. Kobayashi and Kato (1951) presented detailed illustrations of the growth sequence of *Redlichia chinensis* Walcott. Recently, Palmer (1958, 1962) and Whittington (1941b, 1956e, 1959a), both working on silicified materials of Cambrian and Middle Ordovician ages, contributed much new information on the ontogeny and ventral morphology of early ptychopariid larvae. Whittington (1959b) also reinvestigated many of the old ontogenetic works, restudied original specimens, and has given a complete summary of the ontogenetic development of trilobites.

The material here studied consists both of silicified and calcified forms. The typical protaspis of the ptychopariids is a rounded to subrounded, convex shield; the total length of the instars is about 0.22-0.80 mm (sag.); most of the shields are differentiated into axial and pleural lobes, but undifferentiated forms are common; the axis is either annulated or smooth, often marked with a longitudinal fissure along the axis; a pair of pits occur on the anterior lateral margin of the shield; the under-side of the shield shows a complete librigeno-rostrum of one plate and a spinose hypostoma. The librigenae are well developed in the later stages and occur in front of the first pair of marginal spines. The protopygidium is marked by a few segmental furrows during the later stage.

The *anaprotaspis* varies from 0.22 to 0.28 mm in length (sag.); the axis is composed of four annulations of varying distinctness, which are usually divided by a longitudinal fissure along the central axis and separated by transverse ring-furrows; the librigeno-rostrum is a single plate; the hypostoma is spinose. The typical examples of this stage have been studied for: *Dytrmacephalus granulosus* Palmer (Pl. 15, fig. 1), *Flexicalymene granulosa* (Foerste) (Pl. 25, figs. 1-4), *Welleraspis lata* Howell (Hu, 1964, p. 96, pl. 24, fig. 19), and *Crepicephalus deadwoodiensis*, n. sp. (Pl. 14, figs. 1,2).

In the *metaprotaspid* stage the shield is 0.30-0.45 mm in length; the axis is composed of five annulations of varying distinctness and the axial and pleural lobes are well differentiated. Some forms may present a narrow fringe along the posterior margin of the shield, but not segmented; the librigeno-rostrum is one unit; the hypostoma has a smaller number of marginal spines than the earlier stage. Examples of this stage have been examined in: *Dunderbergia ? anyta* Hall and Whitfield (Pl. 15, fig. 2-6), *Ptychaspis bullasus* Lochman and Hu (Pl. 17, fig. 1), *Olenus* *gibbosus* (Wahlenberg) (Pl. 12, fig. 1-3), *Ptarmigania aurita* Resser (Pl. 10, figs. 6,7), and those of genera described in the anaprotaspid stage.

In the *paraprotaspid stage,* the shield is subrounded and elongate with well-differentiated cephalon and protopygidium; the dorsal furrows are distinct to indistinct; in most of the forms the longitudinal fissure has disappeared; secondary pits appear on the anterior lobe; the facial sutures are dorso-marginal and the palpebral lobes are well defined. The protopygidium is transverse or triangular, with or without marginal spines. The librigenae and rostrum are distinctly separated, and the marginal spines of the hypostoma are reduced. The dorsal furrow and the annulations of most genera show varying shallowness. Examples of this stage have been examined for: *Apomodocia conica,* n. sp. (Pl. 9, figs. 4-8), *Gylyphaspis* cf. *parkensis* Rasetti (Pl. 11, figs. 6,7), *Cedarina cordilleae* (Howell and Duncan) (Pl. 13, figs. 5-8), *Missisquoia cyclochila* n. sp. (Pl. 20, figs. 4-7), *Libertella corona,* n. sp. (Pl. 22, figs. 1-4, 7,8), and for those genera indicated in the previous stages.

Asaphids. — The ontogenetic studies of asaphids have not progressed as far as those of ptychopariids. Ross (1951b, p. 579) studied a complete silicified growth series of *Menoparia genalunata* Ross, from the Lower Ordovician of northeastern Utah. The early instars of this form show the shield strongly enrolled, and the librigenae situated between the anterior and the posterior pair of spines. Whittington (1959a) studied the ontogeny of *Remopleurides* and *Robergilla* and showed that the larval forms are similar to those of *Menoparia genalunata.* All have a pair of posterior fixigenal spines, with the librigenae developed in between them along the lateral margin of the cranidium. Evitt (1961, pp. 986-995) established an excellent growth series of *Isotelus*? which showed again the small instars with a pair of anterior and posterior cranidial spines. Both Whittington's and Evitt's specimens were collected from the Middle Ordovician of Virginia.

Leptoplastus salteri (Callaway) (Raw, 1925, 1927) and *Norwoodella halli* Resser (Hu, 1963) possibly belong to this group because both show a development similar to that of *Isotelus.* The larvae of *Leptoplastus* have the librigenae located between the anterior and posterior fixigenal spines, and those of *Norwoodella* have the protopygidium developed before the cephalic and pygidial shields are differentiated. The early librigenal structures of both genera are unknown.

The *protaspis* of this group is spherical to subspherical in outline, convex, and about 0.25-1.00 mm long (sag.); the surface is roundly smooth with a finely impressed dorsal furrow and anterior pits. The librigeno-rostrum is undivided in the earlier larvae but separated in the larger forms. The large palpebral lobe occurs between the anterior and posterior cranidial horns. The hypostoma is relatively large and spiny. The unity of the shield is characteristic; the protopygidium is well developed before the cephalic and pygidial shields differentiated; it thus seems that the pygidial and cephalic shield developed as a single plate without a distinct suture between them. This marks them as different from the protaspis of ptychopariids where the protopygidium is consistently sutured to the cranidial shield; moreover, the asaphid distinctness is pointed up by the fact that their librigenae occur between the anterior and posterior pairs of cranidial horns, and most of the shields are without distinct axial and pleural lobal differentiation.

In the *anaprotaspid stage* the convex shield is rounded or ovate and ranges from 0.25 to 0.35 mm in length; the axial and pleural lobes are not differentiated except for a longitudinal fissure along the central axis; the anterior pits are distinctly impressed. The silicified specimens show a pair of anterior and posterior shield spines, an undifferentiated librigeno-rostrum, and a spinose hypostoma. During the present study this stage was established for *Isotelus stegops* Green (Pl. 26, fig. 17); possibly Evitt's (1961, p. 988, pl. 117, figs. 1-4, text-fig. 1) asaphid represents this stage, and also Hu's (1963, p. 130, pl. 19, figs. 18-24) study of *Norwoodella halli* Resser.

In the *metaprotaspid stage* the shield is rounded to subrounded, convex, and varies from 0.35-0.45 mm in length (sag.); the axial and pleural lobes are separated by faint dorsal furrows. The longitudinal fissure may be present or absent; the librigeno-rostrum is a single plate and ankylosed with hypostoma. Evitt (1961) stated that the librigeno-rostrum and hypostoma are separated at this stage; this may be questionable since these structures are evidently undifferentiated in ptychopariids of the same stage (Pl. 15, figs. 3, 6), and none of the material examined which seems referable to this stage shows librigeno-rostral-hypostomal sutures. It is unfortunate the shale material which has been studied here of *Isotelus stegops* Green (Pl. 26, fig. 18, 19) fails to preserve these parts. An asaphid illustrated by Evitt (1961, p. 988, pl. 117, figs. 5-9 and text-fig. 2) and *Norwoodella halli* Resser (Hu, 1963, p. 130, pl. 19, figs. 16, 17) are possibly representatives of this stage.

In the *paraprotaspid stage* the shield is elongate and subrounded with the axial and pleural lobes well differentiated. The shield ranges from 0.50-1.00 mm in length (sag.); it lacks a distinct posterior cephalic border and all signs of shield separation; the protopygidium occurs at the posterior margin of the shield; the dorso-lateral facial suture is located between the anterior and posterior cranidial horns. For *Isotelus stegops* Green (Pl. 26, fig. 20,21) and probably for some other asaphis, (*e.g.*, Evitt, 1961, pl. 117, fig. 9-19, text-figs. 3,4) the earlier metaprotaspids are now known. Some of the early instars of *Menoparia genalunata* Ross (Ross, 1951, p. 557, pl. 81, figs. 1-9), *Norwoodella halli* Resser (Hu, 1963, p. 131, pl. 19, figs. 11-15), and Whittington's (1959a, p. 397) described protaspids of *Remopleurides* possibly belong to this stage.

Phacopids and trinucleids. — There are few ontogenetic studies of phacopids and trinucleids, and most have revealed incomplete suites. No early protaspis is known. The classical ontogenetic studies of this group are those of Barrande (1852) on *Dalmanitina socialis* (Barrande) and *Onnia ornata* (Sternberg), both from the Ordovician of Bohemia. Some additional material of *Dalmanitina socialis* was studied by Whittington (1956a). All of the specimens of *D. socialis* and *O. ornata* show well-developed pygidium. Their total length from the anterior border to the posterior pygidial margin is about 1.0 mm (sag.). The ontogeny of *Triarthrus eatoni* Hall from the Utica Shale (Upper Ordovician) of New York State which is possibly a member of this group, was studied by Walcott (1879) and recently re-examined by Whittington (1957a); the smallest known form has both cephalic and protopygidial shield well preserved and may include one or two thoracic segments. Poulsen (1923) published a growth sequence of *Peltura scarabaeoides* (Wahlenberg), and the original specimens were likewise re-examined by Whittington (1958); the smallest form shows five glabellar annulations and a pair of broadly open posterior marginal spines, possibly with a small protopygidium between them. Temple (1952) studied the ontogeny of *Dalmanitina olini* Temple from Scandinavia and North Wales. He did not separate the protaspids into stages, but comparison of the size and morphologic structures of the shield shows that the smallest ones are early paraprotaspids. Whittington (1956a) re-examined Beecher's (1893) supposed odontopleurid protaspis, which belongs actually to a *Phacops;* this specimen also bears a well-developed protopygidium, which indicates that it is a late protaspis. Størmer (1930) described the ontogenetic development of the Norwegian trinucleid, and assigned the smallest forms to "degree O" of the early meraspid period, and none of the specimens could be judged as protaspids.

The growth stages of two genera which belong to this group were reviewed during the present investigation: *Calliops strasburgensis* Ulrich and Delo and *Cryptolithus bellulus* (Ulrich). All bear a well-differentiated protopygidium which indicates that they had developed at least beyond the metaprotaspid stage.

Generally, the smallest instars of this group are similar to those of ptychopariids, except that the librigeno-rostrum remains unseparated throughout life. Three different groups of the larval form are recognizable; all belong to the paraprotaspid stage. 1), In the first group, the shield bears an anteriorly expanded glabella, spinose surface, and small pygidial shield, such as *Dalmanitina socialis* (Barrande) (Barrande, 1852, pl. 26, figs. 1-3; Whittington, 1956a, p. 106, pl. 24, figs. 6,7,10), *Dalmanitina olini* Temple (1952, pl. 9, figs. 1-3, and pl. 10, fig. 6), and undetermined phacopid (Whittington, 1956a, p. 105, pl. 24, figs. 1-5), *Calliops strasburgensis* Ulrich and Delo (Pl. 24, figs. 1,2). 2), In the second group the shield is distinctly separated into cephalic and pygidial shields of almost equal size; the cephalic shield bears punctured fixigenae and a small median eye tubercle. This group includes *Onnia ornata* (Sternberg) (Barrande, 1852, pl. 30, figs. 41,42) and *Cryptolithus bellulus* (Ulrich) (Pl. 26, fig. 1). 3), In the third group, the shield bears a fusiform glabella, with distinct axial ring furrows and finely granulose surface. This group is represented by *Shumartia pusilla* (Sars) (Whittington, 1959b, p. 129, fig. 87A), *Peltura scarabaeoides* (Wahlenberg) (Whittington, 1958, pp. 200-206, pl. 38, fig. 1-7), and *Acerocare ecorne* Angelin (Pl. 19, fig. 1,2).

2. MERASPID PERIOD (TRADITIONAL)

The second division of trilobite growth sequence is the *Meraspid period.* The term was proposed by Raw (1925, 1927), who defined it as follows: "later a suture comes to separate the cephalon from the post-cephalic rudiment, or 'transitory pygidium' of Barrande, and between these the free thoracic segments . . . are later, in effect, interpolated one by one, till the thorax is complete." Following Barrande (1852), he further divided the meraspid period into "degrees", marked by the addition of new segments to the thorax, and numbered them from O to N according to the number of segments in the thorax. These ontogenetic divisions are followed by most authors, but his degrees are difficult to recognize because most of the fossils are compressed, distorted, or disassociated. Hence, the degrees of the meraspid period for such material cannot be ascertained. Furthermore, those having the same number of thoracic segments in different species may not be in the same degree of development, because different trilobite genera or species vary in the same number of thoracic segments. For example, the "degree 8" in *Paedeumia yorkense*

Resser and Howell and the same "degree" of *Isotelus stegops* Green are not at the same age level, the "degree 8" for the *P. yorkense* is juvenile, whereas for *I. stegops* it is an adult. The pygidium of *I. stegops* consists of about 12 segments, whereas that of *P. yorkense* is of one only; therefore, *I. stegops* at "degree 8" has 20 segments (eight thoracic segments and 12 pygidial ones) and is an adult, while *P. yorkense* at the same degree has nine segments only (eight thoracic segments and possibly one pygidial segment) and is juvenile. The "degree" system can be useful only for marking the stages of an individual species. This being true, the term "degree" loses its meaning, since we are looking for terms which uniformly represent the ontogenetic stages common to all trilobites. Raw's definition of the meraspis seems valid. It can be subdivided on the basis of arbitrary criteria into early meraspid and late meraspid stages without any "degrees." This means that whereas Raw's "degree" subdivisions represent the absolute ages of the instars of an individual species, the subdivisions here employed pertain to all trilobites, and are comparable.

Kobayashi and Kato (1951, p. 112) proposed two meraspid terms based on the condition of the facial suture: *anameraspid, i.e.,* without facial suture, and *metameraspid, i.e.,* with facial suture. These terms have not been adopted by any other authors. Palmer (1958, 1961) used early, middle, and late meraspid stages, instead of "degree." This system has much to recommend it. However, here in only early and late meraspid stages designations made because it seems better in keeping with the practice in neontology and makes fossil and Recent ontogenetic data better comparable. Thus, trilobite ontogeny is here considered to be divisible into three periods: protaspid, meraspid, and holaspid. The protaspid period is subdivided into three stages, the meraspid into two, and the holaspid or adult is undivided. In the protaspid period the trilobite larva underwent rapid morphological change, in the meraspid period there was slow change, and in the holaspid little or none (Text-fig. 25).

2A. MERASPID PERIOD (RECONSIDERED)

The meraspid period is the second division in the ontogenetic development of trilobites. The cephalon is about 0.40 to 1.20 mm in length (sag.), rounded to subrounded in outline, and low to high in convexity; the glabella of the early meraspid forms is divided into rings by distinct or indistinct transverse furrows; and become more deeply impressed during the later stages; the anterior brim first appears; palpebral lobes and ridges are well defined; the dorso-facial suture cuts the cranidium into a trapezoidal to subtrapezoidal shape; free thoracic segments and definite pygidium are present. Commonly the instars of this period were disassociated after the molt; the librigenae, thoracic segments and pygidium being scattered. Therefore, if an isolated immature cranidium is found, it is likely to belong to the meraspid period.

In the *early meraspid stage,* the cephalon averages 0.50 mm in length (sag.) and bears transverse glabellar furrows of varying definition. A narrow anterior border appears along the anterior glabellar margin; the palpebral lobe is located in front of the mid-line of the glabella (tr.). The *late meraspid stage,* the cranidium averages about 0.70 mm in length (sag.), and is trapezoidal in outline; the glabellar furrows are completed, and the preglabellar field appears between the anterior border and the anterior glabellar margin. The palpebral lobes are located near to or on the mid-line of the glabella (tr.).

2B. TYPES OF MERASPIDS

Agnostids. — The cephalon of agnostid meraspids varies from 0.25-1.4 mm in length (sag.); the thoracic segments, which are added between the cephalic and pygidial shields, vary from none to two or three. In the *early meraspid stage* of the agnostids the cephalon is about 0.25-0.60 mm in length; the thorax appears with one segment; the pygidial axis is conical or subrounded, *e.g., Kormagnostus simplex* Resser (Pl. 7, figs. 1, 6-8). In the eodiscids, the cephalon averages 0.40 mm in length (sag.) and bears a slenderly conical glabella and narrow anterior border. The glabella bears a frontal lobe, two axial rings and an occipital one. The best examples of this stage are known for *Pagetia clytia* Walcott (Pl. 7, figs. 15-17, 24, 25).

In the *late meraspid stage* the cephalon is about 0.50-1.20 mm in length (sag.) with a broad anterior and broad conical glabella (eodiscid); the pygidial axis is subquadrate or rounded, with more than one thoracic segment (agnostid). This stage is described from instars of *Pagetia clytia* Walcott (Pl. 7, figs. 18,19,26,27) and *Komagnostus simplex* Resser (Pl. 7, figs. 2,4,9,10,12-14).

Barrande (1852) divided the agnostids into five developmental degrees (1-5) from early to adult forms. Whittington (1959b) adopted Raw's "degree" terms but interpreted specimens through the range from no thoracic segments to those with two thoracic segments as pertaining to meraspid degree 0 to 1. This possibly correlates with Barrande's "degrees" 1 to 4. Here the early meraspid stages of *K. simplex* Resser and *P. clytia* Walcott would correspond to Barrande's degrees 1 to 3, and those of the late meraspid stage to degree 4.

Olenellids. — The meraspid period of olenellids is characterized by a rounded shield with broad anterior brim, a cylindrical glabella, narrow crescent palpebral lobes, and a shield length of about 0.60 to 1.90 mm (sag.). This period differs from the previous one in having no longitudinal fissure along the central axis, a narrower glabella and the fixigenal spines appearing laterally.

In the *early meraspid stage* the shield is 0.70 to 1.30 mm in length, roundly convex, without a preglabellar field; the palpebral lobe and the cephalic segmental furrows are distinct. Examples studied are *Olenellus truemani* Walcott (Pl. 8, figs. 6-10,20,23) and *Laudonia canadiensis,* n. sp. (Pl. 9, figs. 20,21).

This stage corresponds to Palmer's (1957) stage I to III of the ontogenetic development of *Olenellus gilberti* Meek and of *Paedeumias clarki* Resser and possibly to Walcott's (1910) early larvae of *Paedeumias yorkense* Resser and Howell (Walcott, 1910, pl. 32, fig. 2; Whittington, 1959b, fig. 96A).

In the *late meraspid stage* the shield varies from 1.42 to 2.0 mm in length (sag.) with a narrow preglabellar field and shorter and broader palpebral lobe; the genal spine appears at the posterior lateral shield margin. The species in which this stage has been studied are: *Olenellus truemani* Walcott (Pl. 8, figs. 11-14,21) and *Laudonia canadiensis,* n. sp. (Pl. 9, figs. 25,28,29). This stage is equivalent to Palmer's (1957) stages IV to V of *Olenellus gilberti* Meek, Størmer's (1942, pl. 2, figs. 6,7, text-fig. 5e) young larva of *Holmia kjerulfi* (Linnarsson), Whittington's (1957a, p. 935, pl. 115, figs. 1-3) *Elliptocephala asaphides* Emmons and to *Paedeumias yorkense* Resser and Howell of Walcott (1910, pl. 1, fig. 3-8), and to *Paedeumias yorkense* Resser and Howell of Whittington (1959b, fig. B and C).

Ptychopariids. — The cephalon of the ptychopariid meraspid period bears well-developed dorsal facial sutures; the cranidium is trapezoidal or subtrapezoidal in outline and varies from 0.60 to 1.60 mm in length (sag.), rarely extending from 0.40 to 1.80 mm; the glabella may or may not bear distinct glabellar furrows; the anterior border appears earlier than the preglabellar field. The pygidial segments are ankylosed and frequently associated with small number of free thoracic segments.

This is the largest group within trilobites, and most of the ontogenetic studies which have been done belong to this group. The immature forms differ from those of olenellids by their smaller palpebral lobe, dorsal facial suture, and shields which lack a horse-shoe-shaped marginal border; but these characteristics are not always distinct and intermediate conditions occur, for example, in *Redlichia, Paradoxides, Hydrocephalus.*

In the *early meraspid stage* the cranidium is trapezoidal or subtrapezoidal in outline, and about 0.60-0.95 mm in length (sag.); the glabellar furrows distinctly or indistinctly cross the axis; the anterior border appears along the anterior glabellar margin; the protopygidial segments are not in a definite form and commonly associated with more than one free thoracic segment. This statement accurately describes certain of the early meraspid larvae but the stage features are more ambiguous. For example, in *Dunderbergia ? anyta* (Hall and Whitfield) (Pl. 15, figs. 13,14,27, 28,33), *Dytremacephalus granulosus* Palmer (Pl. 16, figs. 15,17,24,29,30,32), and *Olenus gibbosus* (Wahlenberg) (Pl. 18, figs. 9-12), the cranidia bear distinct glabellar furrows and hence the age is easily distinguishable, while *Apomodocia conica,* n. gen., n. sp. (Pl. 9, figs. 9-16), *Glyphaspis* cf. *parkensis* Rasetti (Pl. 12, figs. 1,2,10,11) *Crepicephalus deadwoodiensis,* n. sp. (Pl. 24, figs. 11-13,21) and *Cedarina cordillerae* (Howell and Duncan) (Pl. 13, figs. 9,10,26) all lack distinct glabellar furrows. Therefore, it is difficult to know their precise ontogenetic position; but because all of these latter forms, within the appropriate size range, lack a preglabellar field, it appears that they are also early meraspids.

This illustrates the need for less rigidly approaching the stage-dating of trilobite larvae. A broader spectrum of traits than is customarily employed for this purpose has much to recommend it.

In the *late meraspid stage* the cranidium ranges from 0.90-1.60 mm in length (sag.) and is subtrapezoidal to trapezoidal in outline; the glabellar furrows are all complete; the preglabellar field generally appears; the pygidial segments are ankylosed and take on the specific configuration. They are articulated with several thoracic segments. The best examples are presented by several genera as noted in the previous stage. Here again, no limited set of characteristics will serve the whole group for stage recognition. For example, *Ptarmigania aurita* Resser (Pl. 10, figs. 19,20) and *Ptychaspis bullasus* Lochman and Hu (Pl. 17, figs. 8-13,26,27,31) lack of preglabellar field, but comparison of the position of the palpebral lobe, the width of the fixigena, and the differentiation of the glabellar furrows with that of the earlier stage, make stage assignment reasonably secure.

As noted previously, Palmer (1958, 1962) divided the meraspid period into three stages: early, middle, and late meraspid stages. The middle meraspid of Palmer correlates with the early meraspis here; the late meraspis are the same; but his early meraspid stage is equivalent to the paraprotaspid or represents between the paraprotaspid and early meraspid stages here. (Text-fig. 23).

Asaphids. — The cranidium of the meraspid period of asaphids is characterized by well-differentiated axial and fixigenal lobes; the dorsal and glabellar furrows are distinct or indistinct; the palpebral lobes are large and situated at the mid-length of the glabella; the silicified material shows the early forms with a pair of large anterior and posterior cranidial spines, but these spines have disappeared in the larger, later ones; the posterior fixigena is very narrow. The pygidium is rounded to elongate, with or without posterior marginal spines.

In the *early meraspid stage,* the cranidium is quadrate in outline except for a pair of large anterior horns; the anterior border appears; the palpebral lobe is situated between the anterior and posterior fixigenae. The pygidium bears posterior marginal spine. The asaphid species in which this stage has been observed are *Menoparia genulunata* Ross (Ross, 1951b, p. 579, pl. 81, figs. 10-13; 1953, p. 634, pl. 62, figs. 6,7,9,10,13,16), and *Remopleurides,* meraspids degree 0, (Whittington, 1959a, p. 398), and possibly degrees 1-4 or 5 of *Leptoplastus salteri* (Callaway), (Raw, 1925, 1927), and the early meraspid stage of *Norwoodella halli* Resser (Hu, 1963, p. 131, pl. 19, fig. 5-10).

In the *late meraspid stage* the subquadrate cranidium varies from 1.50 to 2.50 mm in length and lacks anterior horns; the anterior border and preglabellar field appear. The palpebral lobe is smaller than in the previous stage. The pygidium lacks marginal spines. Instars belonging to this stage are described for *Isotelus stegops* Green (Pl. 27, figs. 14,15,22-24,27), *Isotelus ?* (Evitt, 1961, p. 99, pl. 117, figs. 20-23), *Menoparia genulunata* Ross and *Scinocephalus solitecti* Ross or *S. solitecti* Ross (1951b, p. 581, pl. 81, figs. 14-19), and larger meraspid cranidia of Whittington (1959a, p. 399). Questionable members of this stage are Raw's (1925) degrees 5 or 6 to 12 of *Leptoplastus salteri* (Callaway) and *Norwoodella halli* Resser (Hu, 1963, p. 131, pl. 19, figs. 3,4).

It should be pointed out that the prostaspids of *Isotelus ?* of Evitt (1961) and the late protaspids of *Remopleurides* of Whittington (1959a) are possibly a continuous growth sequence of the same species and genus; this interpretation is based on both the side of the skeletons and morphologic characters; for example, the largest protaspis of *Isotelus* is about 1.0 mm long with a rudimentary protopygidium and an indistinctly developed posterior fixigenal border; the smallest meraspis of *Remopleurides* is about 1.3 to 1.5 mm in length (sag.) with well-developed protopygidium, posterior fixigenal border, and dorsal furrows; both show continuous morphologic and size variation. Furthermore, both genera came from the same locality and were presumably etched out from the same material, the *Remopleurides* lacking early protaspids and the *Isotelus?* lacking early meraspids. Hence, these larvae could belong to the same growth sequence, or if they really belong to the two genera indicated, then these genera must be phylogenetically closely related. Unfortunately, the ontogenetic evidence of *Isotelus stegops* in the Cincinnati materials is no better than Evitt's, and does not help to resolve the problem.

Phacopids and trinucleids. — The ontogenetic information on phacopids and trinucleids is mostly incomplete, both in the published data and the present material. The only significant morphologic differences from the ptychopariids is the presence of an undivided librigeno-rostrum. Otherwise the description of ptychopariid meraspids serves here, at least until fuller data are discovered. However, there are three distinct types of development: dalmanitid, trinucleid, and triarthrid.

Dalmanitid. — The cranidium is occupied by a forward-expanded glabella and lacks an anterior border; the palpebral lobe varies from small to large and extends from the anterior lateral margin of the cranidium back to the posterior fixigenal border. Examples include *Calliops strasburgensis* Ulrich and Delo (Pl. 24, figs. 3-13), *Dalmanitina socialis* (Barrande) (Barrande, 1852, pl. 26, figs. 4-11), and *Dalmanitina olina* Temple (1952, pl. 9, figs. 4-6; pl. 10, figs. 1-5).

Trinucleid. — The instars all have distinctly separated cephalic and pygidial shields; the cranidium is transverse, semicircular; the fringe increase in width and the eye-ridge decreases in length during growth. Examples include *Cryptolithus bellulus* (Ulrich) (Pl. 26, figs. 2-8,11), *Onnia ornata* (Sternberg) (Barrande, 1852, pl. 30, figs. 43-50 ?), and *Reedolithus carinatus* (Angelin) (Størmer, 1930, p. 34, pl. 4, figs. 2-4; pl. 5, figs. 1-3).

Triarthrid. — The early meraspids all have incomplete glabellar furrows, and a narrow anterior border appears along the preglabella margin. In the late meraspids, the glabellar furrows are well separated, and a narrow preglabellar field appears. Types of this group are *Triarthrus eatoni* (Hall) (Whittington, 1957a, p. 941, pl. 116, figs. 1-9), *Peltura scarabaeoides* (Wahlenberg) (Whittington, 1958, pl. 38, figs. 8-18), and *Acerocare ecorne* Angelin (Pl. 19, figs. 9-12,20,22,26), and possibly *Shumardia pusilla* (Sars) (Whittington, 1959b, p. 129, figs. 87B-G).

3. HOLASPID PERIOD

The holaspid period is the last period of the trilobite life history. The term was introduced by Raw (1925, p.

226): "the Holaspid period covers the development after the completion of the thoracic," and also (1927, p. 16) "the Holaspid period . . . is that of the greatest growth in size, accompanied by a more modern development of form." Stubblefield (1926, p. 351) drew attention to the literal meaning of "Holaspid" — complete shield — and suggested that it should be applied only to trilobites "in which complete post-cephalic segmentation has been attained." Raw's definition is adopted here. During the holaspid period only minor differentiation takes place and the specific characteristics are achieved. Such changes occur as increase in size, the shortening or lengthening of spines, deepening or shallowing of the furrows, widening or narrowing of the border. These changes progress slowly and are complete only after a long period of time, and many molts.

4. RATE OF GROWTH IN TRILOBITES

The skeleton of trilobites covered the dorsal surface of the animal and extended a variable distance under the ventral surface as the doublure. The organic material was strengthened by mineral secretions, probably, mainly of calcium carbonate, but seemingly also of calcium phosphate. Preservation is extremely variable. The exoskeleton may be complete, but far more often it occurs as dissociated parts. The complete skeleton of many species is unknown, and almost no trace of soft parts is preserved. There was undoubtedly also a delicate ventral integument but it too is unknown. From a few localities have come specimens preserving the appendages. These complete or dissociated exoskeletons may be preserved in virtually any kind of marine sediment. In fine-grained sediments the skeletons, though flattened, are sometimes only partly, or not all, disarticulated. In both muddy and relatively pure limestone the exoskeletons are usually not flattened or distorted, though commonly disarticulated. In recent years Whittington, Palmer, Ross, Hintze, and Robison have also recorded beautifully and delicately preserved silicified specimens of both adults and larvae from limestone dissolved in glacial or hydrochloric acid. These materials add greatly to knowledge of trilobite morphology.

A. VARIATION IN LARVAL SIZE

The Early Cambrian olenellid larvae, which have been found by many paleontologists, are all recognized as late protoaspids or early meraspids, and the most immature larvae of the later Cambrian are mostly younger in ontogeny. This phenomenon could be interpreted as being due to the rate of mineralization of the animal skeletons. A statistical study has shown that the rate of the skeletal mineralization has increased during geologic time (Text-fig. 24). Early Cambrian trilobites have mostly large-sized larvae which are preserved only in the later developmental stage, whereas the later Cambrian larvae are smaller and are of early ontogenetic stages. This feature could reflect the relatively unmineralized condition of the exoskeleton of early Cambrian trilobites, such as olenellids. Possibly their early protaspids were not yet mineralized, therefore, no fossils remain; whereas the protaspids of late Cambrian or geologic younger trilobites, such as ptychopariids had mineralized skeletons. This assumption also correlates with the increase in thickness of the trilobite skeleton: geologically earlier forms have thinner skeletons than later forms. Walcott (1918, p. 176) pointed out that "all known trilobites had a more or less chitinous shield or carapace which was thick and strong in the Illaenidae etc., or thin and delicate in the Mesonacidae, *Olenellus* etc.". When olenellid trilobite skeletons have been compacted together or two individuals interplicated, then the features of the lower individuals are always impressed upon the upper one during the compaction following deposition (Resser and Howell, 1938, p. 207, pl. 12, fig. 2). This bespeaks the yielding nature of the integument in the early forms.

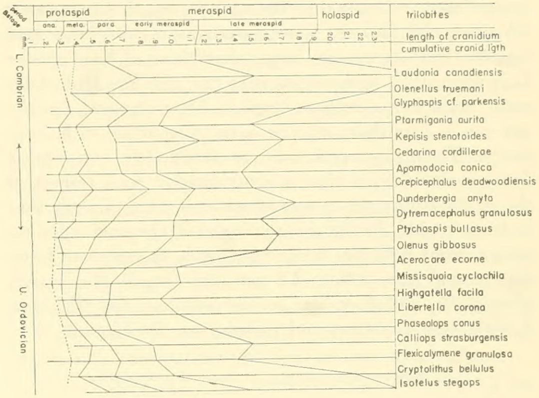

Text-fig. 24. — Graph showing the rate of growth of trilobites and their sizes distribution through the Cambrian and Ordovician.

The size of protaspids is not constant. Størmer (1942, p. 94) noted that "the size of the protaspis seems largely to correspond to the size of the adult." It appears that the protaspid instars average about 0.28 mm in length (sag.). Extremely small instars may be as small as 0.22 mm, such as those of *Ptarmigania, Cedarina,* and *Dunderbergia;* the largest ones are more than 0.80 mm in length (sag.), as in *Olenellus, Glyphaspis, Crepicephalus, Isotelus*. The geologically early larvae are larger than those of later epochs. It is interesting, however, to note that the late Ordovician early larval forms, such as *Calliops, Flexicalymene, Isotelus* are much like those of the early Cambrian with large larvae. Their protaspids average about 0.45 mm (sag.). Thus it would seem that a generalization with respect to the gradual decrease in size of early instars through time is unacceptable. In the meraspid period, the cranidium averages about 0.90 mm in length (sag.), the extreme forms may extend from 0.40 to 2.3 mm long (sag.). *Missisquoia, Highgatella,* and *Acerocare* are the smallest, and *Olenellus, Kepisis, Crypotolithus,* and *Isotelus* are the largest.

B. GROWTH-RATE CORRELATED WITH INSTAR PERIODS

Protaspid period. — During the anaprotaspid and metaprotaspid stages, the shield undergoes distinct changes in its morphologic characters; the most significant is the addition of the new axial segment; whereas the earliest stage has only four, the later instars develop five; the axial rings and the longitudinal fissure may disappear, but little increase in length. During the paraprotaspid stage, the cephalon has five axial rings and a protaspid pygidium is added posterior to the cephalon. In this stage the length may increase more than twice that of the earliest stage (Text-fig. 25).

Meraspid period. — The early meraspid is the great developmental stage of a trilobite as it involves the differentiation and growth of cranidial structures. The glabella grows longer than that of the protaspis; the anterior and posterior cranidial borders are defined. The cranidium shows about a four-fold increase in length from the average-sized protaspis to the end of the early meraspid period. During the late meraspid stage, the cranidium develops a preglabellar field and distinct glabellar furrows, but the rate of the increase of glabellar length is much less than in the early meraspid stage; the cranidium is about five times longer than the average-sized protaspis and about one-fourth longer than that of the early meraspid stage. The growth rate is greatly reduced during this stage, in comparison with the protaspis and early meraspid stages.

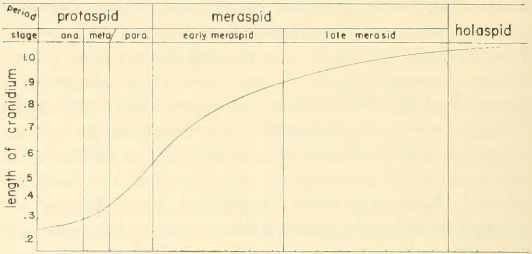

Text-fig. 25 — Showing the cranidial growth-rate at different ontogenetic stages of trilobites. Notice that the length of the cranidium increases rapidly during the paraprotaspid and early meraspid stages. (Data based on Text-fig. 24.)

Raw (1927, p. 15) reported that *Leptoplastus salteri* (Callaway) increased six-fold during the meraspid period (between his degrees 1 and 12) and *Sao hirsuta* Barrande ten times during the meraspid period. Westergård (1936) calculated that *Paradoxides pinus* ? Holm increased 17-fold. Stubblefield (1926) showed that *Shumardia pusilla* (Sars) increased seven times. Whittington (1957b, p. 434) assumed that "during the meraspid period the length of the trilobite increased to some 6 to 14 times that of the largest meraspis . . ." It should be pointed out that the rate of cephalic increases may not correspond to the increases of the thorax. The rate of increase of cephalon and thorax are unequal. The thorax increases in length much faster than the cephalon, because the thoracic segments are added mainly during meraspid period.

The increase in rate of body growth possibly indicated that the animals underwent rapid adaptation. It is reasonable to assume that as the pelagic larvae of trilobites changes their mode of life to the benthonic or borrowing habitat, the rate of growth should increase in order to adapt to the new environment. Hupé (1953b, pp. 3-5, figs. 1,2; 1953, pp. 43,44, fig. 28) pointed out that the more steeply rising growth curves seem to characterize the geologically younger trilobites.

The variation of growth rate corresponding to the age of the individual is also seen in other taxa, the best example that has been given is that of *Xiphosura ("Limulus")* and Green (1961, pp. 66,67, text-fig. 31A) studies on the growth of Crustacea.

5. CEPHALIC SEGMENTATION

Study of the segmentation of trilobites has to depend on external structure only, for nothing of the internal structures are known except for muscular markings on the inside of the skeleton which are occasionally preserved. Commonly, in the modern arthropod the "head" is a complex structure consisting of a large procephalon with a few forwardly migrated body segments joined to it to form a cephalon. This phenomenon has been demonstrated by embryologists and anatomists, but for trilobites this characteristic is inferential and the number of cephalic segments is difficult to determine.

In the late 19th century Bernard (1894), who studied adult trilobites, considered the trilobite cephalon to be composed of five segments, of which four segments were supposed to lie behind the laterally projected and posteriorly curved first segment. Beecher (1895b), from his ontogenetic studies of trilobite carapaces, pointed out that the early larval instars had an axis apparently composed of five segments. Walcott (1910, p. 237) identified seven segments in the trilobite cephalon: 1, an anterior border segment; 2, an ocular segment; 3, a palpebral or first glabellar segment; 4-6, the second to fourth glabellar segments; and 7, the occipital segment. In a later paper, Walcott (1918, p. 126) omitted the anterior border segment, thus postulating a trilobite cephalon composed of six segments. Raw in his several papers believed that the glabella originally included six segments as supposedly shown in several meraspid larvae and certain adult forms. Størmer (1942) studied the ontogenetic development of *Olenus gibbosus* and noted that the earliest known larvae or "anaprotaspis" stage has five primary segments. He tried to correlate these five segments with the primary segments of the *Xiphosura* embryo. Subsequently, Raw (1953), Hupé (1953b), and Palmer (1957), from their morphologic and ontogenetic studies of olenellids, considered the head to be composed of a minimum of eight primary dorsal segments.

The earliest protaspis or anaprotaspis found in the course of this study is about 0.22 mm in length (sag.) with four segments. This has been observed in *Dunderbergia ? anyta* Hall and Whitfield (Pl. 15, fig. 1), *Dytremacephalus granulosus* Palmer (Pl. 16, fig. 1), *Missisquoia cyclochila*, n. sp. (Pl. 20, fig. 1), *Flexicalymene granulosa* (Foerste) (Pl. 25, fig. 1-4), *Welleraspis lata* Howell (Hu, 1964, p. 96, pl. 24, fig. 19). All of the specimens show either a small or a large procephalon (frontal lobe) and three post-oral segments. The pleural segmental furrows, while commonly not distinct, are in some specimens clearly seen.

A. PRIMARY SEGMENTS

The segments of the trilobite body from the anterior margin of the cephalon to the posterior end of the pygidium are differentiated into three regions; the primary, secondary, and tertiary segmental regions. The primary segmental region, or archicephalic region, includes a procephalon and two post-oral segments; the secondary segmental region consists of the third and fourth axial segments, *i.e.*, the preoccipital and occipital segment. The tertiary segmental region consists of the thoracic and pygidial segments.

Procephalon. — The earliest instar of the trilobite consists of four cephalic segments; the procephalon, two postoral, or primary, segments, and a small terminal portion, or the generative disc. The procephalon is the extreme anterior portion of the trilobite head, or archicephalon. It is located anteriorly to the preoral region, and is composed of hypostoma, rostrum, antennules, librigenae, eyes, preglabellar field, and the first glabellar segment. The procephalon is delimited by the posterior branch of the facial suture, palpebral ridges, and dorsally by the first pair of glabellar furrows. This portion is probably homologous with the acron or prostomium of polychaetes, which is not segmented, but superficially divided into a few plates.

The *hypostoma* is the extreme anterior portion of the procephalon. It is separated from the rostrum or librigenorostrum by the rostral suture. This plate, of variable size and shape, lies underneath the anterior-central portion of the cephalon. The early hypostoma is proportionally considerably larger in relation to the body than in late growth stage. The early hypostoma often bears a spinose margin and small, longitudinal median body. This condition is well shown in *Olenellus truemani* Walcott (Pl. 8, fig. 20), *Dunderbergia ? anyta* Hall and Whitfield (Pl. 15, figs. 28,29), and by an asaphid described by Evitt (1961, pl. 9, fig. 5-39). The marginal spines are reduced during the later growth stages while the median body increase in size during ontogeny. The surface of the hypostoma varies from smooth to granulose, ridged, or maculate.

The *maculae,* when present, (and in many trilobites this portion of the hypostoma is preserved), are located on the central lateral sides of the hypostoma or slightly anterior to this. The maculae commonly show a surface pattern of granules, regularly or irregularly disposed, or are roughly reticulated or rather regularly facetted (Pl. 26, fig. 26). Lindström (1901, pp. 35-70) published a comprehensive study of these structures, and concluded that the maculae are true ventral visual organs. This interpretation is favored by Hupé (1953), whereas Raymond (1920b), Størmer (1949), and Whittington and Evitt (1953) regarded them as places of muscle attachment. An alternative suggestion is that these structures reflect the position of the statocyst sacs which are seen in many crustaceans, polychaetes, scyphozoans. In the crustaceans the statocysts are restricted to a few groups of Malacostraca, where only a single pair are present and are diversely located, in the base of the antennules, on the base of the abdomen, uropods, or telson. Each statocyst arises as an ectodermal invagination and is unusually expressed on the exterior. The statolith may be a tissue-secreted structure but commonly is composed of a mass of agglutinated sand grains. The physiology of crustacean statocysts is best known in the decapods (shrimp, crayfish, lobsters, and crabs).

Statocysts of various kinds are also found in certain polychaetes: in several species of *Arenicola,* in several ariciids, in *Loimia* and *Lanica* among terebellids, and in sabellids. All of these are burrowers or tube-dwellers in which orientation may be important. Apart from the ariciids, which may have several pairs of statocysts, a single pair is most commonly found, unusually situated in one of the most anterior segments. There is no doubt that these are all gravity perceptors. Removal or destruction of the statocysts causes the animal to lose its orientation. The nuchal organ of the polychaete, which is located on the frontal lobe of the acron, may also have the same function as statocysts. This nuchal organ is another candidate for possible correlation with the maculae of trilobites.

No detailed examination of this problem has been made, but considering the location of the maculae, their presence or absence on diverse hypostomata, as well as their different morphologic features, this interpretation should be reasonable. If maculae are statocystic, their study may help much in reconstructing the mode of life of trilobites and help to relate them to the habits of modern animals: burrowing, benthonic, or pelagic. The so called "panderian organ" may also have had the same function as statocysts.

Librigeno-rostrum. — This plate, of various sizes and shapes, is located underneath the anterior-ventral margin of the cephalon or rotated onto the dorsal surface to form various types of librigenae. Ontogenetically, the librigena, perrostrum or rostrum are homologous. The librigeno-rostrum may be separated into three parts (a pair of librigenae and a rostrum) or two parts (a pair of librigenae only) or without any separation (Text-fig. 26). In the ptychopariids the librigeno-rostrum is separated into three parts by connective sutures. In the asaphids it is separated into two parts by a median suture, and the olenellids and phacopids are without any separation. Hence the undivided perrostrum may be the original condition and the two or three-part condition derived.

Jaekel (1901), Hupé (1951, p. 473), and Raw (1953, p. 114) named the librigeno-rostrum the "ocular segment." Morphologically, the ocular segment is synonymous with the librigeno-rostrum, but ontogenetically it is doubtful if this part is an independent segment. It seems rather to be a part of the acron or procephalon which became separated by secondary segmentation to facilitate molting. It is not a true segment.

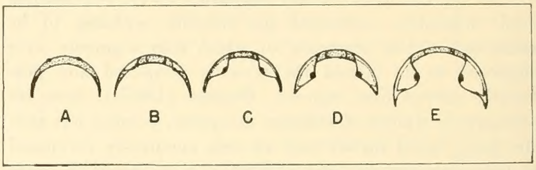

Text-fig. 26 — Showing the ontogenetic development of the librigenae and the migration of the eyes of trilobites. Schematic.

The *eyes* are situated on the librigenae, as most authors believe (Jaekel, 1901; Warburg, 1925; Henrikson, 1926; Størmer, 1942; and Hupé, 1951). Beecher (1897) pointed out that during the earliest larval stage, the lateral eyes migrate from the margin to submargin towards their median position in the adult. This observation is supported by the development of most ptychopariids and a similar migration is also seen in the development of *Xiphosura* (Text-figure 22). However, there are exceptions. In some forms the eyes are initially located dorsally of supermarginally, *e.g.,* in olenellids, trinucleids and harpids (Pl. 8; Pl. 26). Therefore, it seems safer to allocate the eyes simply to the procephalon or acron, and to recognize that several modes of ontogenetic ocular shift occur among trilobites.

The *frontal lobe* is the first glabellar segment and is probably homologous with the posterior portion of the acron of the polychaete. In the early ontogenetic stages this segment is generally larger than in succeeding stages, *e.g., Ptarmigania aurita* Resser (Pl. 10), *Glyphaspis* cf. *parkensis* Rasetti (Pl. 11), and *Calliops strasburgensis* Ulrich and Delo (Pl. 24). However, this condition does not always prevail; *Crepicephalus deadwoodiensis,* n. sp. (Pl. 15), *Ptychaspis bullasus* Lochman and Hu (Pl. 17), *Acerocare ecorne* Angelin (Pl. 19), and *Flexicalymene granulosa* (Foerste) (Pl. 25, fig. 1-4) among others, show a first glabellar segment which is initially relatively smaller than in later instars. The frontal lobe shows varying degrees of separation by glabellar furrows. During later development the frontal lobe may become expanded or reduced in size. Størmer (1942, p. 117) believed that "the strong development of the frontal lobe is apparently dependent on the more powerful development of the alimentary canal, which probably extended forwards from the mouth in a fold below the glabella, just as in *Limulus.*" If the procephalon of trilobites is homologous with the acron of polychaetes, then the frontal lobe, whether small or large, of the early protaspis may be representative of the corresponding brain-case, because it is now known that the longitudinal fissure which characterizes the early protaspid axis disappears during the later growth stages. The disappearance of the longitudinal furrow may reflect expansion of the alimentary canal. This metamorphosis of the axial lobe may indicate that the alimentary canal was not located directly underneath the frontal lobe.

Anterior pits. — A pair of pits of varying definition is located at the sides of the first glabellar segment or frontal lobe. These pits generally appear early on the anterior margin of the protaspid shield and become shallower and indistinct later. In early ontogeny the pits are mostly rounded to oval but become elongate or linear during the later stages. The pits are poorly developed among the olenellids, agnostids during early stages but are well-impressed later (Pl. 8, figs. 16-18; Pl. 7, figs. 4,5). Generally, with these exceptions, the anterior pits are distinctly marked in the early larval stage and become shallow later on. *Ptarmigania aurita* Resser (Pl. 10, figs. 1-23), *Glyphaspis* cf. *parkensis* Rasetti (Pl. 11, figs. 1-15), and *Acerocare ecorne* Angelin (Pl. 19, figs. 1-13) are good examples.

The anterior pits were thought to be attachment for antennules or muscles by Beecher (1895b, p. 179) and Størmer (1942, p. 116). Whittington (1941; 1953, p. 50), who studied both silicified and calcified materials of *Flexicalymene senaria* (Conrad) and *F. meeki* (Foerste), found that the pits correspond to the anterior lateral wing processes of the hypostoma. His view was that "the development of anterior pits and corresponding wing processes on the anterior wings of the hypostoma is interpreted as a mechanism for support (cranidium) but not articulation of the hypostoma." This was a significant discovery.

Palpebral ridges. — The palpebral ridge is a raised strip connecting the proximal side of the eye and the axial furrow behind the anterior lateral corners of the first glabellar segment. In the early ontogenetic stages the ridges are indistinct; they presumably curve forward from the anterolateral margin of the shield to extend behind the anterior pits (Pl. 14, fig. 5,7; Pl. 17, fig. 2), but they are generally not recognizable until the later stages. These ridges sometimes appear in the immature stages but disappear during later immature stages, or perhaps early holaspis, as in *Cryptolithus bellulus* Ulrich (Pl. 26, figs. 1-6). In some forms such as *Isotellus stegops* Green (Pl. 26, figs. 17-30) the ridges are always indistinct and another asaphid described by Evitt (1961, p. 117, figs. 1-23). In the olenellids the ridges are unknown.

The palpebral ridges also appear on the cephalon of agnostids (Pl. 7, fig. 5) where they curve forwardly from the anterior pits to the anterior-lateral margin.

The palpebral ridges may lie along the line of ankylosis of the procephalon and the post-oral segmental tips. An interesting comparison can be made with the formation of the prototroch of the trochophore larva due to forward migration of the peristomium.

Cephalic sutures. — There is on the head of trilobites a single major cephalic suture delimiting the cranidium from the librigeno-rostrum. It presumably reflects a major cleavage during moulting. Various names have been applied to this suture as a whole (*e.g.*, grand suture) or for diverse courses that it pursues: perrostral, opisthoparian, proparian, hypoparian, gonatoparian suture. Some of these courses have been employed in the past as major taxobases.

Beecher (1895b, pp. 177-178) was of the opinion that the librigena had a ventral position in the early stages and migrated toward the margin and backward over the cephalon to the adult position. This interpretation has been validated by subsequent ontogenetic studies of silicified trilobites. Because the librigena originated in a ventral position and migrated onto the dorsal surface during the later growth stages, the grand suture or its derivatives accompanied the migration of the librigeno-rostrum onto the dorsal surface. The submarginal position of the facial suture is primordial in all trilobites; from this location various patterns are derived (Pl. 15, figs. 3,6,11,27; Pl. 16, figs. 3,9,29). From the perrostral or hypoparian sutural types, the opisthoparian, proparian, and grand suture plans are developed.

Hupé (1953) presented supposed evidence of the existence of a dorsal or metaparian suture in the olenellid trilobites, where previously no facial suture had been observed. He suggested that the dorsal suture was present and open in ancestral olenellids but became closed during later evolution. Vestiges of the supposed dorsal sutures are seen on some of his specimens from the Lower Cambrian. His illustration (1952, [1953], pl. 1-5) shows two ridges on the preglabellar field and a pair on the posterior lateral fixigenal areas. However, the ridges (pl. 1, fig. 3,5) on the preglabellar field may not be suture but impressions of the perrostrum. Most of the Lower Cambrian trilobites had thin exoskeletons, as was pointed out earlier. Some of Hupé's illustrations (pl. 1, figs. 1,3,6) shows a well-preserved and undisturbed perrostrum. The coincidence of the limits of the perrostrum and the preglabellar "sutures" make one suspicious of Hupé's conclusion. Moreover, the posterior fixigenal ridges, which show in his photographs, appear not to be a facial suture ankylosis but rather the preoccipital segment ankylosis. The existance of this suture as described by Hupé was denied by Størmer (1942, p. 141) who said "I find no direct evidence of the anterior and posterior eye-line representing trace of a facial suture in the Olenellidae." Moreover, uncompacted calcareous specimens show no preglabellar field ridges or lines such as those seen in Hupé's shaly specimens, and the posterior lateral fixigenal ridges are well marked (pl. 2, figs. 14-19; pl. 3, figs. 28-31). It seems that Hupé's hypothesis is untenable, no facial sutures are recorded on the dorsal surface of the olenellid cephalon.

B. POST-ORAL SEGMENTS

The post-oral segments include the 2d to 4th glabellar and occipital segments, *i.e.,* two primary and two secondary segments. The secondary segments are derived from the generative disc. These segments are possibly homologous with the antennae, mandibles, and maxillae 1 and 2 of crustaceans. The segmental furrow may be distinctly or indistinctly marked; the pleural furrows are shown on *Olenellus truemani* Walcott (Pl. 8, figs. 1-10) and are less impressed on *Olenus gibbosus* (Wahlenberg) (Pl. 18, figs. 4,6), *Dytremacephalus granulosus* Palmer (Pl. 16, figs. 4,5) and others.

The pleural segmental furrows were first demonstrated by Størmer (1942) from his ontogenetic study of *Olenus gibbosus.* Whittington (1957b, p. 467) reinvestigated Størmer's original material and came to the conclusion that the pleural segmental furrow is hypothetical. Whittington's views are in turn subject to review, for, unfortunately, most ptychopariid instars do not show the well-impressed pleural furrows as clearly as olenellids do. In *Olenus gibbosus* and *Dytremacephalus granulosus* the furrows are only vestigial, fine and sometimes they do not oppose each other (due to preservation ?). However, upon closer inspection, especially of well-focused photographs on high-contrast paper and darkly printed pictures, *these furrows* can sometimes be discerned. Hence, Størmer's interpretation seems valid, on the basis of independent demonstration. Whittington is probably correct in concluding that Størmer's material does not reveal the furrow. Hence Størmer's conclusions as to its presence were largely intuitive, albeit vindicated by further study.

The formation of the cephalic segmental furrows is here divided into three steps. In the first of which the furrows are simply parallel on the pleural lobes (Pl. 8, figs. 1-5); in the second the furrows fuse to form introfurrow ridges (Pl. 8, figs. 6-10); in the third the furrow and ridges have all disappeared, and the surface is smooth (Pl. 8, figs. 13-18). Similar morphologic changes are demonstrated by the formation of the pygidial furrows. These steps are illustrated by *Cryptolithus bellulus* Ulrich (Pl. 26, figs. 10-13) where the first two steps are well demonstrated; figs. 10 and 11 correlate with the first step, and figs. 14 and 15 represent the first step, and figure 16 is the second step. The development of the pleural or fixigenal furrows and the pleural furrows of the pygidium follow an analogous course.

The same steps in the formation of the cephalic furrows are also seen in *Crepicephalus deadwoodiensis* n. sp. (Pl. 14, figs. 28,29). Something comparable is also seen in the formation of the axial lobe of the glabella: in most of the earliest trilobite instars the glabellar rings are impressed by a longitudinal fissure separating the glabellar rings into two or three pairs of nodes. The longitudinal fissure at certain growth stages becomes a fine ridge, which subsequently disappears as the glabellar rings are completed (Pl. 8, fig. 7; Pl. 16, figs. 7,8; Pl. 9, figs. 2,3). The process of obsolescence of the longitudinal fissure is exactly similar to the obsolescence of the fixigenal and pleural furrows of the pygidium, which pass through a ridge stage followed by disappearance and a smooth surface in maturity.

The *longitudinal fissure* of the axial glabellar lobe possibly represents a depression along the course of the alimentary canal, and the glabellar nodes the mesodermal compartments or mesoblasts such as are commonly seen in the early embryos of polychaetes and crustaceans (Text-fig. 18).

Some meraspids are distinctly marked with three or four pairs of nodes on the fixigenal regions; these nodes supposedly correlate with the four post-oral segments (Pl. 14, figs. 10-13, and Pl. 10, fig. 14). These nodes disappear in the later ontogenetic stages. They may be representative segmental sense organs, similarly disposed organs occur in the early immatures of *Xiphosura* (Text-fig. 22A,B,C, So4).

Posterior fixigenal ridges. — Moberg (1899) pointed out the presence in *Kjerulfia* of a faintly raised line, which shows its position corresponds to the course of the posterior branch of the facial suture. Kiaer (1916, p. 81) found "a fine raised line, that runs in an arc from the posterior edge of the eye to the posterior margin of the intergenal rim." In both instances the lines were interpreted as vestiges of fused facial sutures. The same structures are also seen in *Elliptocephala, Olenellus, Holmia,* and related genera. The vestigial suture theory was supported by Warburg (1925, p. 37), Raw (1936), and Hupé (1953). Most specialists, however, have either rejected or only conditionally supported this interpretation. Beecher (1897, p. 191), Walcott (1916), and Raymond (1917, p. 206) thought the suture was in a condition of symphysis, the real sutures in a condition of fusion. Størmer (1942, p. 137) and Palmer (1957, p. 126) both out rightly rejected the interpretation.

Størmer (1942, p. 138) believed that the so-called posterior facial suture is due to the procephalic (ocular) segment bending posteriorly to the distal end of the post-oral segmented pleurae (1st and 2d) and ending in front of the pre-occipital segment (3d post-oral segment). Lindström (1901, p. 16) suggested that the ridges or line represent a pre-existing feature prenuncial of the next step in the development of the true facial sutures. Beecher (1897), noting the same phenomenon, thought the ridges represent lines of symphysis — a fused suture. Raw (1936, p. 586) supported Beecher, believing that the posterior fixigenal ridges are the ankylosis of the posterior branch of the facial suture. Whittington (1957b, p. 451) argued that the "fixigenal furrows" are really the intrapleural furrows. The formation of the furrows of both the pygidium and fixigena seems to support Whittington's interpretation.

The ontogenetic development of the posterior fixigenal ridge is clearly indicated by the different growth stages. From the paraprotaspid to the early meraspid stages (Pl. 8, figs. 1-10) the fixigenal furrows are all parallel and curve slightly anterior-laterally from the dorsal furrow to the palpebral lobes, and the 3d post-oral (pre-occipital) segment bears a pair of broad-based spines pointed posteriorly. In the late meraspid stage the fixigenal furrows are all strongly bent posteriorly, and the pre-occipital segment gradually decreases in width and becomes elevated into a pair of ridges; these ridges extend continuously posterior-laterally through the hind border to form a pair of intergenal (or metagenal) spines. This morphologic change is possibly due to posterior bending of the procephalic segment. This seems to support Størmer's interpretation.

Some of the instars often bear a pair of ridges or furrows at the sides of the median tubercle of the occipital segment. This feature is especially clearly indicated by olenellids and related forms, and also in *Acerocare ecorne* (Pl. 8, fig. 16; Pl. 19, figs. 17-19) as presented by Størmer (1942, pl. 2, fig. 4). This is a possible result of the segment-generating disc or caudal papilla warping forward underneath the posterior marginal border as we have seen in crustaceans (Text-fig. 18). Hence, this furrow could be homologous with the cervical groove of Crustacea. If this interpretation is acceptable, then the posterior fixigenal ridges are homologous with the mandibular groove. This explanation would make the "posterior fixigenal ridge" a combination feature of the fused union of bent cephalic segments and a trace of the mandibular and maxillae I segments. The same groove (cervical groove) is possibly indicated by a juncture which lies between the 7th and 8th segments of *Xiphosura,* and which is the result of the warping of the generative disc. Obviously much more detailed study is necessary before this suggestion has substance.

Cephalic spine. — Most silicified trilobite larvae have three pairs of marginal spines along the cephalic shield (Pl. 8, figs. 20-22, 28; Pl. 16, fig. 6; Pl. 15, figs. 3-6); these spines may be preserved, one or two pairs lost during ontogeny. *Acanthoparipha* and *Olenelloides* have three adult pairs; *Holanshina* and *Diceratocephalus* have two pairs, and most ptychopariids lack spines, other than librigenal, in adulthood. The olenellid cephalic spines were termed procranid, genal, and metagenal by Raw (1927, p. 11). Palmer (1962) proposed anterior, mid-, and posterior fixigenal spines for the ptychopariid forms. Hupé (1960) designated them as fixigenal, 1,2,3 from front to rear. These spines are supposedly homologous in olenellid and ptychopariid forms. However, these designations may not apply (or may be only questionably applied) to all forms, because some shields have only two pairs of spines (Evitt, 1961, pl. 117; Ross, 1951b, pl. 81; Whittington, 1959a, pl. 11,16,23,26, etc.) or only one pair (Pl. 23, fig. 1-3). It is difficult, if not impossible, to know whether the spines are fixigenal or pygidial, or if fixigenal, which. Therefore the general terms anterior, lateral, and posterior marginal spines are recommended without any implied homologies. Størmer (1942, p. 12) and Palmer (1957, p. 106) adopt the term "intergenal spine" instead of "metagenal spine" for adult olenellid specimens.

Palmer (1962, p. 88) believed that "the librigenal spine is not acquired by transfer of any one of the fixigenal spines . . . ." As was brought out previously in the present study, the librigeno-rostrum is clearly associated with the procephalon, when it migrates onto the dorsal surface to become the librigenae. The genal spines are essential to posterior tips of the librigeno-rostrum; hence librigenal spines are derived from the procephalon, and the fixigenal ones are thus necessarily derived from the post-oral segments. The two kinds of spines are of different origins and cannot be derived one from the other. Palmer's interpretation of the origin of the genal spine is well supported.

Raw (1937, p. 585) found that the procranidal spines are absent in *Holmia, Elliptocephala,* and *Paedeumias,* but present in the *Olenelloides* cephalon. Therefore, his view was that "the procranidal spines must have reached the genal angle position by evolution, and this would necessarily involve also revolution of the anterior branch of the suture in advance of it." He thought the procranidal spines moved to the genal position during evolution. This explanation has no developmental evidence, for all spines remain in constant position throughout ontogeny (Pl. 9, fig. 20-31), except that the anterior pair gradually disappears, whereas the lateral or posterior pairs gradually increase in length. The larval spines may be an ecological adaptation, comparable with those of planktonic larvae of polychaetes, crustaceans, mollusks. Contrary to the opinion of most students, they seem to be of little or no phylogenetic significance.

It should be pointed out that "genal spine" is a common term for the spines located at the posterior lateral angle of the cephalon. But the genal spines are of two derivations: one is librigenal, and the other fixigenal. The spines originating from the librigenae should be dominated "librigenal spine":, and those from the fixigenae "fixigenal spine." If there is more than one pair of either type of genal spine, they become, from rear to front, 1st, 2d, 3d fixigenal or librigenal spines. See, for example, such forms as *Sphaerocoryphe* cf. *granulatus* (Angelin) (Harrington, 1959, p. 52, fig. 37E), *Acanthoparypha perforata* Whittington and Evitt (Whittington and Evitt, 1953, p. 74, pl. 13, and text-fig. 18), and the odontopleurids.

6. FORMATION OF THE POST-CEPHALIC SEGMENTS

The trilobite body segments, located posterior to the cephalon and constituting the thorax and pygidium, are tertiary in origin. These segments have a slightly different origin from those of polychaetes (see below), but are exactly similar to crustaceans; however, in the Crustacea there is no special term for these segments, all are named secondary somites or segments as they are in the polychaetes.

A. THORACIC SEGMENTATION

In the crustaceans after the maxillar somites are developed, the segmental generative disc or caudal papilla is reflected underneath the posterior margin of the shield and proceeds to form the post-cephalic segment (Text-fig. 18). The more anterior somites, or proximal side of the segmental series, are the earliest formed and early acquire the mature structure. The same phenomenon may occur among the Trilobita, where the generative disc may have undergone the same reflection. In the annelids, on the other hand, the segmental generative disc, or pygidium, does not undergo this deflection process and extends to the extreme posterior end of the body (Text-fig. 10).

Although the segmental generative disc of trilobites has never been observed, it may well be present, but because it would lie underneath the shield, it will never be dorsally observable. In adult specimens of *Paedeumias yorkense* Resser and Howell the skeleton has 14 thoracic segments, a telson, three or four rudimentary segments, and a small pygidium. Within the 14 thoracic segments the 3d one is a macrosomite, and the 15th is the telson. These somites remain in constant position during growth, *i.e.*, the macrosomite is always in the 3d position and the telson formed during the transition to the holaspis. This organization could be well explained by the hypothesis of a reflected generative disc. In Stubblefield's (Whittington, 1957b, p. 442, fig. 11) study of the ontogeneric development of *Shumardia pusilla* (Sars) a fifth segment was shown to be added to the pygidium after the complete number of thoracic segments had been developed. This would mean that after the proximal side of the pygidial segment is added to the thorax, the distal side gained a segment from the generative disc or teloblats which would be necessary in order to maintain a constant segmental number in the pygidium. It, therefore, appears that thoracic segments are developed by transfer from the pygidium during the growth stages; the proximal side of the pygidium gives up segments to the thorax while concomitantly there is distal replacement of pygidial segments from the generative disc. This is known to be the process operative in the ontogeny of the cephalocarid crustacean, *Lightiella incisa* (Sanders and Hessler, 1963, p. 93, figs. 1,2), and all other articulates.

Størmer's (1942, p. 130) views on this matter are that ". . . it is probable that in trilobites the transverse joints between the pleurae of the thoracic segments, or between these and the cephalon or pygidium, are secondary formations crossing the primary segments. Each thoracic pleura probably contains portions of two succeeding segments coalesced along the pleural furrows." Raw (1937, p. 580), and Whittington (1957b, p. 451) interpreted the fixigenal furrows of the early instars of olenellids and the pleural furrows on the thoracic and pygidial segments as being serially homologous; all are intrapleural furrows, and the intersegmental grooves run along the convex line. As was previously pointed out herein Whittington's and Raw's view seems valid. Størmer's observation was strongly influenced by the body structures of *Xiphosura,* and his conviction that trilobites are merostomatous. It is possibly true that the joint of the prosoma and opisthosoma is due to secondary segmentation of a primary segment, but this is not a fundamental pattern. The fundamental process of segmentation has to be primary, the new segments being added to the previous ones along the primary intersegmental boundaries. An alternative interpretation of the secondary segmentation lying between the 7th and 8th segments is that it is a result of under-warping of the segmental disc after the 6th segment was formed in the manner seen in the ontogenetic development of crustaceans. According to this view, the 7th and 8th segment of *Xiphosura* are essentially one segment divided into two halves by the activity of the generative disc (Text-fig. 21).

B. PYGIDIAL SEGMENTATION

In trilobite systematics the relative size of the pygidium compared with the cephalon has been used as taxonomic criterion. A trilobite is said to be "micropygous," "macropygous" or "isopygous" according to whether the pygidium is smaller, larger, or subequal in size to the cephalon. The pygidium is essentially a fusion of a certain number of post-cephalic segments. A large number of pygidial segments generally correlates with a pygidium of large size; a small number with one of smaller size. *Scutellum* and *Dicranopeltis,* are exceptions to this rule. In these genera, the few pygidial segments of the broad marginal fringe create a large pygidium. The smallest pygidium may consist of one or two segments and a terminal portion, such as in olenellids, redlichiids, *Remopleurides.* The largest pygidia contain more than 20 segments, as in phillipsiids, asaphids, and dalmanitids.

The pygidial segmental generative disc would seem to have been located behind the extreme end of the pygidium, or within the terminal zone, since the segments are always concentrically arranged around this portion (Pl. 26, fig. 14; Pl. 25, figs. 23,24; Pl. 15, figs. 32-37). Hence, the segments which lie near the terminal position or distal region are younger than those more proximal. The generative disc supposedly lost its generative power during the end of late meraspid or early holaspid stage after the animal gained the specific condition, just as in the archaic crustaceans *Hemimysis* and *Nebalia.* The generative disc is apparently homologous with the pygidium of polychaetes and the caudal papilla of crustaceans. The growth zone of the Trilobita, or in Crustacea, presumably remained proximal to the caudal furcae which presumably characterized most if not all trilobites despite their rarity in the record. The best record of these caudal appendages is in *Olenoides serratus* (Rõminger) found by Walcott (1912, 1918) from the Middle Cambrian of British Columbia.

IV. PHYLOGENY OF TRILOBITA

Current thought favors a xiphosuran, arachnid affinity for the Trilobita, but the matter is by no means firmly resolved. Trilobites were long considered to be related to the crustaceans, *e.g.*, works of Walcott (1881, 1894), Bernard (1894), Beecher (1895, 1897), Carpenter (1903), Raymond (1920a), and others. They considered that the trilobites were true crustaceans of a primitive type, *i.e.*, an early off-shoot from the line leading from the annellids to the crustaceans. This hypothesis was generally supported by paleontologists and zoologists for a long period, and recently Sanders (1957), from his studies of the Cephalocarda, reasserts their crustacean affinity. Butt (1960), from his comprehensive study of the arthropod head structures, is of the same view and proposed a Trilobita-Crustacea major group of Arthropoda.

The xiphosuran hypothesis was also established early by Dohn (1871), Packard (1880a), and many other students who pointed out the general resemblance between the Trilobita and Merostomata, especially between the larval development of *Xiphosura ("Limulus")* and the larval stages of trilobites. They suggested a genetic relationship between the two groups. Fedotow (1924), Iwanoff (1933), Snodgrass (1938), Sharov (1966), and Størmer (1942, 1944, 1951) forcefully demonstrated important and challenging similarities between the merostomes and trilobites. The subject was especially studied by Størmer (1942, 1944) working mainly with trilobite morphology. He took sharp issue with the crustacean concept. He felt that the trilobite features which decisively separated them from crustaceans are:

a. The tri-lobatation of the dorsal shield and tendency to form a styliform telson.
b. The presence of four posterior larval or primary somites.
c. Highly ramified intestinal diverticulae.
d. Homologus appendages in the Trilobita and Chelicerata and the absence of trilobitan appendages from the Crustacea.

Among these four criteria he strongly emphasized the contrasting ontogenetic development and appendage morphology between xiphosurans-trilobites and crustaceans. He viewed the supposedly different number of primary somites and allegedly different appendage organization of crustaceans and trilobites as fundamental differentia. Tiegs and Manton (1958) and Manton (1960) strongly supported the Chelicerata affinity of Trilobita.

The present study of the ontogenetic development of trilobites does not seem to support the Xiphosuran hypothesis. The development of trilobites does not appear to be similar to that of xiphosurans, but closely resembles that of crustaceans. The early crustacean nauplius and trilobite anaprotaspis both possess two primary somites, whereas chelicerats *(Xiphosura)* larvae have four (Iwanoff, 1933). The result independently supports Butt's (1960) conclusion as to the common Trilobita-Crustacea taxonomic line. The following discussion is mainly a summary of the previously presented data resulting from studies of the ontogenetic development of a variety of invertebrates of possible relevance to the problem of trilobite phylogeny.

1. THE PROBLEM OF PRIMARY SOMITES

It is unfortunate that Iwanoff's (1928, 1933, 1944) hypothesis of primary and secondary segmentation of the articulates has been rejected by several authors since ectodermal segmentation exists in both the heteronomic and nonheteronomic polychaetes, and since both are represented by forms with pelagic and non-pelagic modes of life. Assuredly in the search for reliable indicators of polychaete primitiveness a morphologic-ontogenetic trait such as segmentation is of greater reliability than mode of life. Whatever the primordial ecology of segmented marine worms, they have undergone many environmental adjustments, while they all show initial ectoderm segmentation followed by mesoderm. To abandon the morphologic-ontogenetic approach to systematics and phylogeny is serious retrogression.

In evaluating Iwanoff's hypothesis that the larval ectodermal segmentation in polychaetes is archaic, the ontogenetic history of certain lower, and possibly, antecedent, groups is pertinent. In the kinorhynchs and priapulids the first segment is the head; the second segment, the neck; the trunk in most species contains eleven segments. The cuticle of each segment is subdivided into one dorsal and two ventral plates, and the cuticle between the plates is very thin and flexible, permitting articulation. The body wall of the kinorhynchs is the epidermis thickened to form longitudinal epidermal cords which bulge slightly into the pseudocoel. It is to be noted that these animals develop without coelom or mesoderm. They are a grade below the coelomates, but superficially they are segments, and are similar in appearance to the annelid body structure. This "segmentation" is initiated from the epiderm, and is remarkably like the initial phase of ectodermal segmentation in annelids. It may have genetic-phylogenetic bearing, and, if so, lends support to Iwanoff's idea that this is the primordial annelidan trait.

It is now known that the anaprotaspis of trilobites and the nauplius of crustaceans both consist of two primary segments; a preoral segment and a generative disc or caudal papilla. Contrarily, the early larva or "trilobite" stage (Størmer, 1944) of *Xiphosura ("Limulus")* has more than two primary somites lying between the preoral segment and the generative pygidium.

2. THE PROBLEM OF SECONDARY SEGMENTS

The secondary or body segments in polychaetes are developed from a prepygidial growth zone. Similar development is observed in trilobites and crustaceans. The anterior margin of the generative disc or caudal papilla generates the secondary segments from the teloblasts. In crustaceans, after two secondary segments develop the caudal papilla bends forward beneath the posterior portion of the shield; hence, thereafter the teloblasts of the caudal papilla are essentially located along the posterior margin of the second body segment, and from this new location they continue to generate additional body segments. The same action (generative disc warping) possibly also occurred in trilobites and *Xiphosura ("Limulus")* although it has not been suggested before. The structure and origin of the occipital segment of trilobites and the post-6th (7th-8th) segment of *"Limulus"* makes a plausible comparison. Primary and early secondary segments fuse together to form a cephalon. The additional thoracic and pygidial segments lying between the cephalon, are the true body segments. They are added serially from the teloblasts while the caudal papilla or generative disc moves backward step by step until the animal reaches the adult stage when it is endowed with the specific characters. The composite cephalon of trilobites and Crustacea comprises five segments whereas the merostome (Chelicerata) cephalon has six or six and a half.

3. THE PROBLEM OF CEPHALIC SEGMENTS

Ideally, the segmentation of annelids and arthropods is externally delineated by grooves, and each segment has a pair of appendages externally and a pair of coelomic sacs and ganglia internally. The nature of the segments can sometimes be seen from the early stages of embryonic development and may persist during the later growth stages. The internal criteria for the recognition of segmentation is lacking in fossil arthropods where one must rely on groove evidence preserved in the carapace of early instars. The point is made by Butt (1960) that "it is apparent, therefore, that the ideal type of segment marked off by ring-like grooves, with paired appendages, coelomic sacs, and a ganglion just does not exist." This is part of the perennial problem of reconciliation of neontology with paleontology, and while direct comparisons are commonly impossible when criteria pertain to soft parts, an oblique approach may be rewarding.

In the development of many segmented animals, annelids, arthropods, and vertebrates, the young forms often acquire an active existence during the stage of growth when they possess few segments; these few early segments are often added to the acron in forming an adult cephalon during cephalization. A simplified concept of head segmentation has been presented by Hölmgren (1916) and Hanström (1928) and has been elaborated upon by Snodgrass (1938). According to this thinking, the hypothetical head (Text-fig. 27) consists of an acron which contains a protocerebrum and a deuterocerebrum (together, the archicerebrum) internally. The mouth is located between the acron and the following segment, the second antennal which contains the tritocerebrum. The tritocerebrum sometimes migrates forward to join with the archicerebrum to form the composite brain, but such forms always retain a commissure passing beneath the stomodaeum. The tritocerebrum represents the first post-oral segment, and the protocerebrum and deutocerebrum represent the eye and antennule respectively. Chandonneret (1950), on the basis of studies of thysanuaran *Thermobia domestica* (Packard), concludes that the head comprises seven segments behind the acron; Weber (1952) was of the opinion, that the archetypical head had six head segments behind the acron, and Butt's (1960) modified theory calls for four segments behind the acron. The present study of the cephalic segmentation of the earliest trilobites, *i.e.,* anaprotaspis, and related animals seems to be in keeping with the Hölmgren and Hanström theory.

Archicephalon. — The archicephalon is the embryonic head of the arthropods which according to Crampton *(in* Snodgrass, 1938), consists of an acron with eyes and the labral, antennular antenna and mandibular segments. This structure would correlate with the "ideal head" of Hölmgren and Hanström. In the annelids this would correspond to the prostomium plus two post-oral segments; to the procephalic region (ocular and antennule) and two post-oral segments (2d and 3d glabellar segments) of trilobites; to the procephalic region, antennal, and mandibular segments of crustaceans; and to the procephalic region (ocular only, without antennular), cheliceral, and first leg-bearing segment of xiphosurans, not withstanding the arguments of Butt (1960), Manton (1960), and Tiegs and Manton (1958) as to the cephalic segmentation of arthropods.

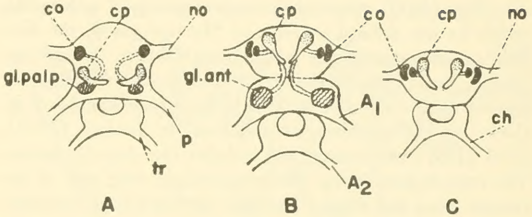

Text-fig. 27 — Annellid and arthropod brains: A. A polychate annelid; B. Mandiblate arthropod; C. A chelicerate arthropod, A1, nerve of antennules; A2, nerve of antennae; ch, nerve of chelicerae; co, optic ganglion; cp, peduncular body; gl-ant, antennal ganglion; gl. palp, palpal ganglion; no, optic nerve; p, nerve to first trunk segment. (From Hanström, 1928 after Vendel, 1949.).

According to Hölmgren and Hanström's theory, the archicephalon would be composed of the archicerebrum and tritocerebrum (Text-fig. 27); however, both the anaprotaspis and nauplius larvae have an acron plus two primary segments, whereas the "trilobite" stage of *"Limulus"* has an acron plus three primary segments. If the "trilobite" stage represents an archicephalon, then obviously the archicephalic structure of *"Limulus"* is not homologous to that of Trilobita and Crustacea. If it is assumed that the chelicerae are homologous with the antennules of crustaceans and trilobites, then the archicephalic structure of the two groups would be similar, for the second and third paired appendages of *"Limulus"* would then correlate with the antennae and mandibles of crustacea, and the chelicerae with the antennules. This facile explanation is not tenable, however, since embryonic studies by Milne-Edwards (1883), Hanström (1928), and Johansson (1938) show that the nerves of the chelicerae belong to the ventral nerve cord which is innervated by the secondary brain. They expressed the opinion that the preoral appendages, *i.e.,* antennules, are absent or reduced in *"Limulus,"* whose ontogeny demonstrates forward migration of the primarily post-oral, or cheliceral segments. In the adult the chelicerae attain a distinctly preoral position, while the ganglia migrate anteriorly and unite with the preoral brain. Therefore, the deuterocerebrum has apparently disappeared during the forward migration of the tritocerebrum, and certainly no antennules are present on the procephalic region of *"Limulus."*

The true cephalon of trilobites consist of a procephalon or acron and four post-oral segments, which correlate with the prostomium and four body segments of annelids; with the procephalic region, antenna, mandibular, and a maxillary segment of crustaceans; and with procephalic region, chelicera, and 1-3 leg segments of xiphosurans. The xiphosuran cephalon consists of six complete and one incomplete (chilarial) segments. Therefore, the 4th and 5th leg segments of xiphosurans correlate with the first two post-cephalic segments of trilobites and crustaceans, and with 6th and 7th segments of annelids (Text-fig. 28).

Butt (1960) proposed three main groups of arthropods, which he has defined as follows: "In one group, the first pair of antennae and a well-formed labrum, second antennae, mandibles, first maxillae and second maxillae are present behind the mouth. This is the group thought to be closest to the trilobites, as indicated by Sanders (1957), Dahl (1956) and others, and includes the class Crustacea. The second great group also preserves the first pair of antennae, has a well formed Labrum, but the second antennae are rudimentary or wanting entirely. The mandibles, the first maxillae and the second maxillae are present behind the mouth. This group includes the Pauropoda, Diplopoda, Chilopoda, and Insecta. In the third great group, the Arachnida, there is no separate head, antennae and antennal lobes of the brain are wanting, the labrum is present and cephalization has taken a rather unusual course, since according to the theory presented here the second postoral pair of appendages have moved forward around the mouth and also have taken a position anterior to the labrum. Thus, the chelicerae would correspond to the mandibles of the insect."

Butt's second group has not come under scrutiny in the present study, but the developmental and anatomical examination of trilobites and limulids supports his views on the major classification of arthropods.

4. THE PROBLEM OF APPENDAGES

The great studies of trilobite appendages were made by Walcott (1881, 1918), Raymond (1920b), and Størmer (1942, 1951). Several genera have revealed well-preserved cephalic and body appendages; among these are: *Olenellus, Olenoides, Kootenia, Ptychoparia, Cryptolithus, Triathrus, Phacops, Asteropyge, Ceraurus, Ogygopsis, Flexicalymene,* and *Isotelus.* These studies were made by direct examination of natural preservation or by grinding serial sections and reconstruction therefrom.

The appendage structures are especially well shown by Størmer (1939; 1942; 1951). All appendages are uniramous; the antennules are simple, whereas the uniramous legs each bear a gill branch (Text-fig. 31E). The legs were thought by Beecher (1895), Walcott (1918), Raymond (1920b), and Calman (1939) to be biramous structures, corresponding to those of Crustacea. According to this older view, the endopodite and exopodite of crustaceans correspond to the segmented leg and gill branch (epipodite) of trilobites, apparently this is misinterpreted. Garstang (1940) and Heegaard (1945) argued that the differences in structure of the appendages of trilobites and crustaceans are due to an increased development of the protopodite and concomitant reduction of the endopodite segments. Størmer in a series of papers demonstrated that the trilobite appendage is more closely similar to the appendage structure of xiphosurans *("Limulus")*: both have multiple joints (nine segments, Text-fig. 31, A and E) and are uniramous; both possess a gill branch (Text-fig. 31, C and E). Størmer concluded largely on the evidence that the Trilobita are phylogenetically more closely related to the *Xiphosura* than to the Crustacea. Sanders (1957, 1959), in connection with his extensive work on the cephalocarid crustaceans, maintained that the triramous (protopodite, endopodite, and exopodite) trunks appendages of cephalocarids are comparable to the trunk appendages of trilobites, and postulated a trilobite origin for crustaceans. Moreover, he believed this triramous structure is the primitive one for all crustacean groups.

Polychaeta		Trilobita		Crustacea		Xiphosura	
prost.	palpus eye	acron	ant. eye hypo. rost. librig. 1rst glabel -sg.	acron	ant. eye labrum epistome	acron	ant-reduced eye labrum ocellus out- opth-area
	mouth		mouth		mouth		mouth
peristomium	seg. 1	leg 1		antennae		chelicerae	
	seg. 2	leg 2		mandible		leg 1	
seg. 3		leg 3		maxillae 1		leg 2	
" 4		leg 4		maxillae 2		leg 3	
" 5		thorax		thorax		leg 4	
" 6		"		"		leg 5	
" 7		"		"		chilaria	
" 8		"		"		thorax	

Text-fig. 28 — Correlation chart showing the head components of the Polychaeta and non-Hexapoda groups of Arthropoda.

So much of trilobite organization and development now seems to be crustacean that Sander's resurrection of the crustacean assignment of trilobites seems highly plausible. There has apparently been far too much reliance of late upon the structure of appendages as fundamental taxobases, especially at a stage when they are still inadequately understood. Moreover, it would be hard to imagine any organs more responsive to ecologic adjustment, more mutable, than equatic arthropod appendages. Homeomorphy may well be rampant in appendages. Moreover within the appendage series of an individual there is enormous differentiation among the post-trilobites. In higher crustaceans, the same animal body commonly possesses both uniramous and biramous (bifurcate: endopodite and exopodite) appendages, and also both of these appendages may be of different shape and structure. The same phenomenon is also found in chelicerates, the prosomal and opisthosomal appendages are not all of the same structure or function. In *Cambarus,* the crayfish (Text-fig. 29, 31), for example, the anterior two pairs of appendages are biramous and have a sensory function; III and IV are uniramous, and serve for chewing and food-handling; V to VIII are biramous and function for touch, taste and food-handling; IX-XIV are uniramous and function for respiration, grasping, walking, and mating; XV to XIX are biramous and function for egg-carrying and swimming. To define the Crustacea as all possessing biramous appendages is manifestly false. Pelagic and benthonic crustaceans have differently constituted appendages. One need only compare isopods, decapods, cirripeds, and phyllopods. The same differentiation occurs in chelicerates. In *Xiphosura ("Limulus")* (Text-fig. 30, 31) the appendages I to V are uniramous, function as grasping, digging, and food-handling, and are similar to appendages III and IV of crustaceans. The structure of VIII to XIII of limulids are similar to IX and XII and XV to XIX of crustaceans, because both function for respiration and swimming (Text-fig. 29, 31, C).

Returning to the trilobites, the appendages are mostly uniform and uniramous (Text-fig. 31, E) except that both anterior and posterior ones are somewhat smaller. Their *shapes* are similar to those of walking-legs of crustaceans (Text-fig. 29, IX to XI) and *Xiphosura* (Text-fig. 31, A, B). This similarity presumably reflects similar function: walking, digging, and food-handling. They also *structurally* resemble the walking legs of crustacea and the abdominal appendages of *Xiphosura* (Text-fig. 31, A, C) in bearing gill branches which in all three served for respiration and swimming.

It is assumed that trilobites were non-predaceous and generally walked, dug, and swam along the bottom or burrowed into the substrate; this relatively simple mode of life permitted the retention of the primordial, uniformly simple, appendages. In their serial uniformity and lack of functional differentiation, trilobite appendages are similar to the parapodia of most polychaetes. The trilobite is the most primitive arthropod radical out of which the highly diversified phylum evolved. There took place both serial "differentiation" of appendages, from uniform to polymorphic for different functions, and "simplification" or reduction of the appendage segmental number, required for increased efficiency in the different ecologies which they eventually assumed. "Complication," also occurred, *i.e.,* development of new types of appendages such as the biramous appendage (endopodite and exopodite; Text-fig. 31, D, F) of many Crustacea which restrict the gill branches to respiratory function, and consequently a new organ (exopodite) was needed for swimming and cleaning. The exopodite seems to be a subsequent development, acquired from a certain endopodite segment — possibly next to the basipod — by lateral branching.

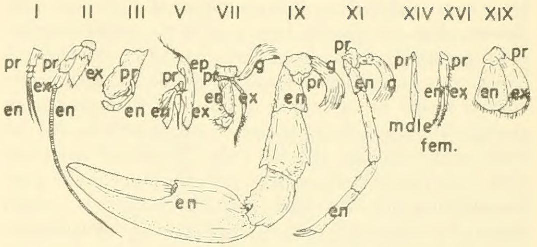

Text-fig. 29. — Types of appendages of the crayfish *(Cambarus)* I-II, sensory; III, chewing; V-VII, food-handling; IX, grasping; XI, walking; XIV, male mating; XVI, female egg carrying; XIX, swimming; pr, protopodite; ex, exopodite; en, endopodite; ep, epipodite; g, gill. (From Storer, 1943.)

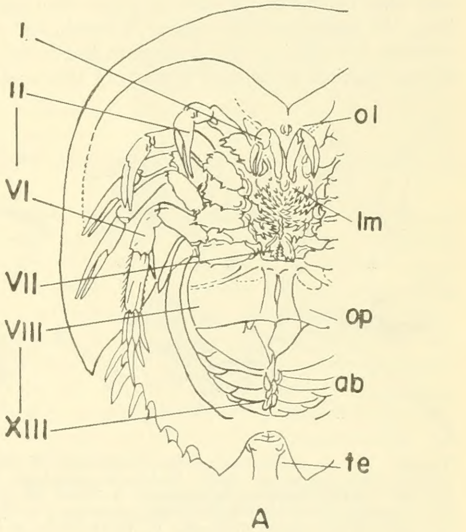

Text-fig. 30 — Showing the differentiation of appendages of *Xiphosura polyphemus* (Linnaeus). I, chelicera; II-VI, chilaria; XIII, opercula; IX-XIII, abdomen; ab, abdominal appendages; lm, labrum; ol, ventral olfactory organ; op, operculaum; te, telson. (After von der Hoeren from L. Fage, 1949.)

Raw (1953) believed that the pleural spines of trilobites were modified appendages inherited from the polychaetes, thus once having been part of the worm's complicated parapodia. If his hypothesis that the notopodium is homologous with pleural spine is acceptable, then the neuropodium should be equivalent to the uniramous appendage (endopodite), and the epipodite or gill branch located between might correlate with the setae. This would mean that there is no branch to homologize with the exopodite of crustaceans; thus this bifurcated appendage (exopodite) would seem to have been subsequently derived from the uniramous appendage of the crustacean nauplius, in many ways recalling the parapodium of the polychaetes, are a larval adaptation. Their evolution may correlate with the development of the chitinous exoskeleton in the nauplius, whereas the polychaete metatrochophore was naked. For a chitin-sheathed, and consequently heavy, planktonic larva strong swimming organs would be necessary to keep it afloat, whereas cilia satisfied in the polychaete. The ecologic correlation of naupliar appendages is demonstrated by the fact that when nauplii live in water of higher than normal salinity, the appendages are reduced in length, and if in abnormally low salinity, they increase in length and number of setae required to maintain bouyancy.[2] This would clearly indicate that the weight of the body influences the structure of appendages in these pelagic organisms. Undoubtedly, natural selection operated along these lines in the process of appendage evolution. It is interesting to note that *Pisione remota* (Southern) also seemingly possesses slender, segmented, and bifurcate appendages. (Text-figs. 11, 12).

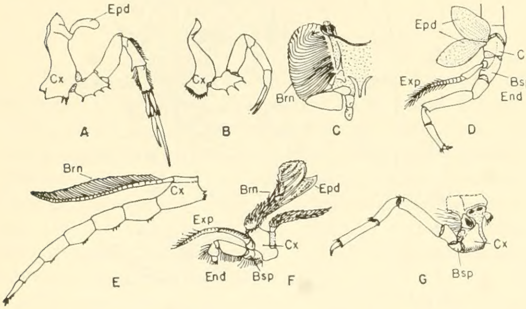

Text-fig. 31 — A comparison of the appendages of xiphosurans, trilobites, and crustaceans. A,B,C. Xiphosura appendages of II, VI, and IX; D,F,G. Crustacena appendages; D. Third left periopod of the crustacean *Anaspides;* E. Trilobite appendage; F. Left second maxilliped of the crayfish *Cambarus;* G. Third left leg of Cambarus. Brn, branchis; Bsp, basipodite; Cx, coxopodite; End, endopodite; Epd, epipodite; Exp, exopodite. (All redrawn from Snodgrass, 1956.)

5. POLYCHAETE ORIGIN OF THE TRILOBITA

It was the view of Raw (1953) that trilobites are the most primitive arthropods, the true protarthropods, and that they occupied an organizational stage between polychaetes and euarthropods. He said: "Their primitive nature is indicated by: I. the uniformity of the segments and appendages throughout the body; II. the retention of pleura throughout the body unreduced; III. the retention of a large hypostoma and, IV. the retention of soft ventrum." These characters of trilobites and of certain other arthropods indicate a derivation of the class from a polychaete, and probably from an archaic polychaete. This theory of trilobite origin is wholly compatible with the observations made in the present investigation. Raw's five hypothetical stages in the transition from annelid to trilobite and arthropod (phyliodocid-life, merocyclism, early protarthropod, late protarthropod, and deutarthropod stages) are, of course, unsubstantiated, but his is an ingenious and stimulating hypothesis.

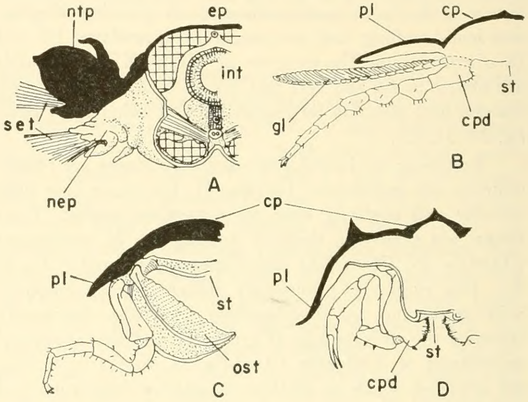

Text-fig. 32 — Showing the correlation of various arthropod pleurae (indicated by solid black) to the notopodium of polychaete. A. The polychaete, *Neries;* B. Section of thoracic segment of a trilobite; C. Section of the second thoracic segment of crustacean, *Ligydia;* D. Section of prosoma behind the third leg of ***Xiphosura.*** cp, carapace; cpd, coxapodite; ep, epidermis; gl, gill; int, intestine; ntp, notopodium; nep, neuropodium; ost, ostegite; pl, pleuron; st, sternum. (Modified from Snodgrass, 1938, 1956.)

---

[2] Personal communication, Dr. William A. Spoor, Professor of Biology, Department of Biology, University of Cincinnati.

The study of the ontogenetic development of polychaetes is of great significance in tracing both the ontogeny and phylogeny of trilobites. Åkesson (1961) found an amazing polychaete in the North Sea, *Pisione,* which looks similar to a Lower Cambrian olenellid trilobite. The mode of ontogenetic development of this animal leads one to speculate that the early larval development of the Lower Cambrian trilobite must be recapitulatory of an adult polychaete of the general *Pisione* organization (Text-fig. 11, 12).

The early pelagic embryos of *Pisione* have a prostomium in front of a few body segments; as metamorphosis continues, the animal assumes a benthonic mode of life; whereupon the first three body segments gradually migrate forward and fuse with the prostomium to form the head. During this process the prostomium is elongated and the mouth is warped beneath the head, and the eyes are stretched and elongated to form a pair of sickle-shaped eye-rings. This head structure is similar to the adult form of *Olenelloides* and to immature stages of olenellids such as *Olenellus, Laudonia canadiensis,* n. sp. (Pl. 9, fig. 20-31), *Paedeumias, Elleptocephala.* If *Pisione* also secreted a calcium-phosphate tergal carapace it would be virtually indistinguishable from olenellids, especially *Olenelloides.* This discovery may render Raw's hypothetical transition stages unnecessary. This interpretation of *Pisione* would seem to be strengthened by the fact that the olenellids and this new annelid seem to share similar modes of life. Both were larvally pelagic and ephebically benthonic. The main difference is that the olenellids developed a thin exoskeleton, whereas *Pisione* does not. However, this difference is probably not of major importance. Paleontologists have not found any early protaspids of olenellids, in contrast with other trilobites; moreover, adult olenellids have thin exoskeletons. Apparently the shell secretion of olenellids was delayed and slow and closely correlated with the ontogenetic change in their mode of life.

6. ON THE MAJOR CLASSIFICATION OF TRILOBITES

It is the concensus here that a sound taxobasis for major subdivision of the Trilobita has yet to be presented. The discovery of the interesting ontogenetic relations of the librigeno-rostrum, whether undivided or diversely separated (Text-fig. 33), offers the basis for a new, and perhaps fundamental, regrouping. Five categories based on these traits are listed below. Further study may elevate them to taxa.

A. *Monorostraloid group.* — In this group the librigeno-rostrum is a narrowly crescentic perrostrum which lies underneath the anterior half of the cephalon. It has submarginal and hypostomal sutures. Examples: *Olenellus, Elliptocephala, Nevadia, Holmia, Olenelloides, Callavia, Kjerulfia, Wanneria.* These are mostly *Olenellidae.* This group of trilobites is absent (or unknown) from the Oriental region. The geologic distribution is limited to the Lower Cambrian.

B. *Trirostraloid group.* — Here the librigeno-rostrum is divided into three parts: the rostrum and paired librigenae; these parts are separated by the hypostomal, connective, and facial sutures. Examples include *Redlichia, Paradoxides,* the ptychopariids, *Conocoryphe, Aphelaspis, Cedaria, Proetus, Oryctocephalus, Dunderbergia, Flexicalymene, Scutellum.* This is the dominant group among the trilobites, having the greatest geographic and geologic distribution. The librigeno-rostral structures of certain Lower and Middle Cambrian forms *(Redlichia,* and certain corynexonechids) are well known, but the most of the forms are unknown.

C. *Birostraloid group.* — The librigeno-rostrum is separated into two parts: paired librigenae only; median, hypostomal, and facial sutures are present. No rostrum is present. In this group belong: *Bathynotus, Pterocephala, Housia, Norwoodella* ?, the asaphids, *Xenostegium, Theodenisia, Remopleurides, Menoparia, Homalopyge.* The earliest known birostral trilobite is *Bathynotus* from the Middle Cambrian of North America, but the dominant forms are the asaphids which were world-wide in distribution during the Ordovician period.

D. *Holorostraloid group.* — The librigeno-rostrum is here a single plate, without any separation; it is limited by the hypostomal and super-marginal or grande sutures. This group contains the illaenurids, *Hungia, Loganopeltis, Lauzenella, Levisella,* the nileids, *Entomaspis,* the trinucleids, phacopids, dalmanitids; and possibly *Triarthrus, Peltura.* The earliest known trilobites of this group are *Levisella, Hungia,* and possibly *Peltura* from the upper-most Cambrian, but the dominant forms are trinucleids, dalmanitids, and phacopids, of world-wide distribution from the Lower Ordovician through the Devonian.

E. *Architrilobitoid group.* — The rostral plate of certain agnostids is similar to that of olenellids or certain holorostraloid forms (the rostrum of the eodiscids remains unknown), but the body structure and the ontogenetic development of this group are entirely different from those of typical trilobites. Resser (1938) placed all agnostids in a separate subclass, equal in rank to the Trilobita; however, he gave no reason for this move. Comparison of the cephalic structure of this group with that of typical trilobites shows that agnostids have four cephalic segments whereas typical trilobites have five. Hence, the agnostids differ from typical trilobites not only in ephebic morphology but in ontogenetic development. There is a growing tendency to separate them into different classes. The relationship of trilobites to agnostids is much like that of polychaetes to archiannelids.[3]

7. REMARKS

In many trilobites the librigenal structures remain unknown, especially for the Middle and Upper Cambrian "ptychopariids." Recently Rasetti (1952) reviewed the literature on this problem and suggested that if the ventral structures were well understood, they might give great insight to both phylogeny and taxonomy of trilobites. Richter (1932) and Stubblefield (1936, p. 411, fig. 2) showed that the rostrum tended to become reduced in size and the librigenae ultimately met so that the connective suture became a median suture. They suggested that this eventually disappeared. There seems to be no ontogenetic evidence to support this hypothesis. Instead, it appears that the tri-, bi-, and holorastraloid types derived from the monorostrum or perrostrum of the olenellid form. Silicified materials of *Dunderbergia ? anyta* (Hall and Whitfield) and *Dytremacephalus granulosus* Palmer show protaspids with a single rostrum and a spiny hypostoma. This early condition of the librigeno-rostrum is exactly like that of the perrostrum of olenellids; during the later growth stages the rostrum divided into three parts: the rostrum and paired librigenae. In asaphids, the development of the rostrum is the same as that of *D. ? anyta,* and *D. granulosus;* the early protaspis has a single rostrum which later separated into two parts. In the development of *Calliops strasburgensis* Ulrich and Delo, the rostrum lacked any separation throughout the trilobite's life. No such recapitulation of the phylogenetic development of the rostrum such as was suggested by Warburg (1925), Richter (1932), and Stubblefield (1936) has been observed.

In any case, the data on the structure of the librigenae are obscure; more study of this structure is badly needed, both for mature and immature forms. Both silicified preservation and shale specimens can be most revealing.

Much of the adult similarity between trilobites is apparently convergence or homeomorphy. It may be that librigeno-rostral features will be exceptionally useful in sorting out true from apparent relationships. Note, for example, the similarities, probably bespeaking similar ecologies and convergent morphologies, between olenellid (monorostraloid) and redlichiids and zacanthoidids (trirostraloid) or the similarity to the remopleurids (birostraloid); nileids (holorostraloid) to illaenids (trirostraloid).

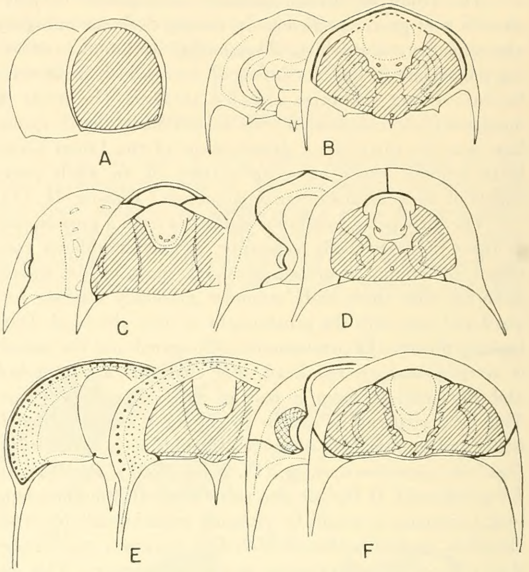

Text-fig. 33 — Showing cephalic structure (solid line) in relation to the librigeno-rostrum. A. Architrilobitoid B. Monorostraloid; C. Trirostraloid; D. Birostraloid; E,F. Holorostraloid. Ruled areas represent the empty cavity of the cephalon as seen from the center. (Redrawn from Harrington, 1959.)

V. SYSTEMATIC PALEONTOLOGY

Family **SPINAGNOSTIDAE** Howell, 1935

Genus **KORMAGNOSTUS** Resser, 1938

Kormagnostus simplex Resser

Pl. 7, figs. 1-14, Text-fig. 34

Kormagnostus simplex Resser, 1938, p. 49, pl. 9, figs. 11-13; Rasetti, 1946, p. 444, pl. 69, figs. 32-34 (see Palmer, 1954, 1965, p. 38, pl. 1, figs. 8, 9); Palmer, 1954, p. 718, pl. 76, figs. 8-12; Lochman and Hu, 1960, p. 822, pl. 99, figs. 5-31.

K. harlanensis Resser, 1938, p. 49, pl. 10, figs. 11, 12.

K. esterius Lochman, 1940, p. 24, pl. 2, figs. 32-35; Lochman and Duncan, 1944, p. 77, pl. 5, figs. 15, 16; p. 141, pl. 12, figs. 13-18; Lochman, 1950, p. 348, pl. 51, figs. 6-9.

K. splendens Lochman, 1940, p. 25, pl. 2, figs. 23-31.

---

[3] It should be pointed out that some of the geologically later trilobites: such as trirostraloid and birostriloid forms have their librigenae or librigeno-rostrum so fused together as to create a *pseudo-holorostraloid* condition in the adult stage. It is seen in *Oryctocephalus,* the proetids, phillipsiids, and some illaenids. Ths feature is indicated by the ankylotc ridges along the position of the suture lines. This is the secondary character and is not included in the present taxonomic category.

Diagnosis. — Cephalon regularly convex. Glabella conical, convex, with rounded posterior margin and a pair of paraglabellar nodes at the base. Occipital ring narrow, curving backward along the posterior margin of the glabella. Dorsal furrow deeply marked. Pleural lobes strongly convex, with a very broad preglabellar field. Marginal border wide and convex, separated by deep and broad marginal furrow. Two thoracic segments, broad axial lobe and shorter pleural bands, pygidium with strongly convex axial lobe and broad concave marginal furrow. Axis expanded slightly posteriorly. Dorsal furrow well defined. Marginal border wide, moderately convex, with a pair of short blunt spines. Surface finely granulose.

Description. — The cephalon is strongly convex, with a conical glabella and broad preglabellar field and marginal brim. The glabella is delimited by a dorsal furrow, and divided into three axial rings by faint glabellar furrows; the frontal lobe or the first glabellar ring, is transverse, subquadrate, and has a pair of anterior pits at the postero-lateral corners; the second axial ring is narrow and bears a median tubercle; the third axial ring is longer and triangular with a rounded posterior margin. The occipital ring is represented by a pair of triangular base lobes or paraglabellar lobes is situated at the posterior lateral corners of the glabella. The preglabellar field is occupied by a low indistinct median boss immediately anterior to the glabellar margin. The cheeks or pleural lobes are rounded, convex, broad anteriorly and narrowing posteriorly; a pair of faint palpebral ridges extend laterally from the anterior pits; the marginal furrow is concave, broadly arching forward and narrowing postero-laterally; a median notch is directed to the anterior margin of the preglabellar field; the marginal border is medium-narrow, convex, and without a marginal spine.

The thoracic segments are narrow, and convex, with a broad axial lobe and short pleural bands; the axis is moderately convex; the pleural bands are distinctly marked by pleural furrows, and the ends of the tips are directed slightly anteriorly.

The pygidium is quadrate in outline and strongly convex. The axial lobe is divided into three rings by a faint furrow; the first ring is narrow and arches slightly anteriorly; the second is of the same nature as the first one, except that it bears a median tubercle; the last ring is broad, semicircular and expanded both slightly laterally and posteriorly. The dorsal furrow is distinct. The pleural lobes are narrow, tapering posteriorly and downsloping laterally to the broad, shallow marginal furrow; the marginal border is of medium width, convex, with a pair of short blunt spines directed posteriorly from the posterior lateral corners.

The surface is covered with minute granules.

Remarks. — This species is represented by more than 30 immature and mature specimens, all recovered from a few pieces of light-grey, medium-crystalline limestone. The smallest instar is about 0.30 mm long (sag.) and the adult forms are more than 3.00 mm. The smallest pygidium is 0.40 mm long, and the larger ones are 2.30 mm in length (sag.); arranged in order of size, they show a continual growth sequence. In the growth stages, the pygidium shows more morphologic change than the cephalon; the pygidial axis, which in the meraspid stage is conical in form and largely separated from the posterior marginal border by the pleural lobes, develops first into a subquadrate form and then into a posteriorly expanded form, separating the pleural lobes and abutting the posterior marginal border. The glabella develops from a conical to a truncate-conical form; and the median furrow disappears in the larger cephala.

As seen in the synonymy, some of Resser's (1938) and Lochman's (1940) "species" are here interpreted as representatives of different growth stages of *K. simplex* Resser. *K. simplex* Resser (U.S.N.M. 94842) and *K. esterius* Lochman, both with largely expanded pygidial lobes, are the adult forms, and the *K. harlanensis* Resser (U.S.N.M. 94863) and *K. splendens* Lochman (U.S.N.M. 98697), developed with smaller narrower pygidial axis, are possibly the respective late and earlier mature forms. Although the conditions of preservation may also have influenced the form in the types of these "species," it seems more likely that they represent different growth stages of a single species.

The agnostid orientation employed here is that urged by Raymond (1917, 1924, 1925) and supported by Kobayashi (1939a). Raymond reversed the generally accepted orientation of these trilobites, urging that: 1) pleural extremities should point posteriorly, and 2) the "ventral plate" appears to be separated from the dorsal shield by a suture. Kobayashi (1939a, p. 74) showed, 1) that in the Condylopygidae which are primitive agnostids, the pleural extremities point posteriorly; the forward bending of later forms was apparently an adaptation which aided in enrolment. Moreover, 2) a "ventral plate" has been found on both shields in one agnostid species by Holm and Westergård (1930) who, however, regarded their "plates" as doublures.

In the course of the present study, it has been observed that the cephalon of *K. simplex* shows a pair of ridges extending laterally from the anterior pits (Pl. 7, fig. 5, Text-fig. 35K). They are presumably palpebral ridges and their presence supports the Kobayashi's interpretation as to agnostid orientation.

Horizon and locality. — Upper Cambrian, Cedaria zone, Bonneterre Dolomite, southern Bonneterre, St. Francois County, Missouri.

Figured specimens. — Complete skeleton, U.C.M. 38722; cephala, U.C.M. 38722a-e; pygidia, U.C.M. 38722f-k.

Kormagnostus Simplex Resser, ontogeny

Early meraspid stage (Pl. 7, fig. 1, 6-8, Text-fig. 34, A,G,H). The cephalon is spherical convex and about 0.30 mm in length (sag.). The glabella is subtriangular, elongate, conical, and restricted to the posterior half of the shield; glabellar furrows are not distinctly marked; the preglabellar field is marked by a longitudinal furrow. The marginal border is narrow and separated by a marginal furrow.

The pygidium is convex, quadrate-spherical in outline, and about 0.40 mm in length. The axial lobe is conical, tapering posteriorly; the axial furrows are not distinctly marked; the median tubercle is borne at the mid-length of the axial lobe. The dorsal furrow is distinct. The pleural lobes are about one-half as wide as the axis, convex, tapering slightly posteriorly. The marginal furrow is distinctly impressed and with the dorsal furrows at the posterior margin of the axial lobe; the marginal border is flat, broad, and tapers anteriorly. Figures 6 and 7 show a pygidium associated with one thoracic segment.

The surface of the skeleton is rough, covered by fine granules.

Later meraspid stage (Pl. 7, figs. 2-4,9,10,12-14, Text-fig. 34 B-F, I). The cephalon is convex and about 0.50-1.20 mm in length (sag.). The glabella is truncate-conical. The preglabellar field is occupied by a small, slightly convex median boss immediately in front of the glabella. The pygidium is subquadrate, convex, with a broad marginal brim. The axial lobe is cylindrical, with a rounded posterior margin; the first axial ring is narrow and transverse; the second is the same as the first one except that it bears a median tubercle; the third ring is rounded and extends to the posterior marginal furrow. The pleural lobes are rather narrow tapering posteriorly, and ending at the sides of the posterior lateral margin of the axial lobe. The marginal furrow is broad and concave; the marginal border is broad, slightly upturned from the marginal furrow and bears a pair of spines at the posterior lateral margin.

The surface is covered by fine granules.

The important features of this stage is the absence in the preglabellar field of a median furrow and the presence of the median boss. The glabellar furrows have first become distinct; the pygidial axis becomes subquadrate to cylindrical and the lateral lobes are narrower than previously.

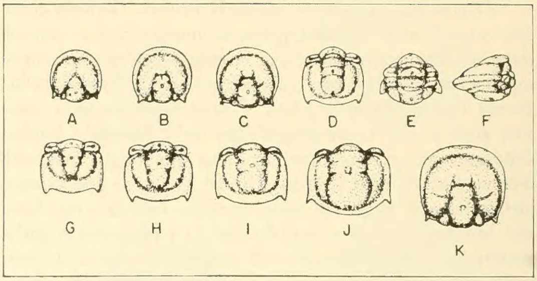

Text-fig. 34 — A growth sequence of *Kormagnostus simplex* Resser. A,G,H. Early meraspids; A. Cephalon, x 53; G,H. Two pygidia each associated with one thoracic segment, x 35, x 34; B-F,I. Late meraspids; B. Cephalon, x 30; C-F. Dorsal, posterior, and side views of a complete specimen, x17; I. Pygidium, x 30; J,K. Top views of a cephalon and a pygidium, x 13 x 8. (Drawings made from photographs.)

Figured specimens. — Early meraspids. U.C.M. 38722a, f-h; late meraspids, U.C.M. 38722, 38722b-d,i,j.

Family **PAGETIDAE** Kobayashi, 1935

Genus **PAGETIA** Walcott, 1916

Pagetia clytia Walcott

Plate 7, figs. 15-32, Text-fig. 35

Pagetia clytia Walcott, 1916, p. 408, pl. 67, figs. 2, 2a-e.
Pagetia (Mesopagetia) clytia Walcott, Kobayashi, 1944, pp. 63-66, pl. 1, fig. 14.

Diagnosis. — Skeleton elongate-ovate, convex. Cranidium having broad, flat marginal fringe and stout occipital spine. Glabella slenderly conical, with two pairs of glabellar furrows. Palpebral lobes small. Proparial facial suture. Pygidium slightly convex, six or seven axial rings, each bearing a tiny median tubercle. Pleural lobes divided into pleural bands. Marginal border narrow, flat, and smooth. Surface finely granulose.

Description. — The cranidium is rounded in outline and moderately convex. The glabella is slenderly conical and divided into three glabellar rings; the first glabellar ring is convex and triangular; the second is narrowly transverse; and the third large, broad, and slightly convex. The occipital furrow is deep along the sides of the glabella and shallow across the axial line; the occipital ring is posteriorly convex and bears a stout posteriorly directed spine. The dorsal furrow is broad and deeply marked. The anterior brim is broad, concave, without clearly separated preglabellar field and anterior furrow; the anterior border is broad, flat, and fringelike, with many elongate radial pits. The flat fixigenae are slightly wider than the glabella and slightly upturned; a pair of tubercles occurs on the posterior-lateral area of the fixigenae near the marginal furrow; the palpebral ridges are faint and curved anteriorly; the palpebral lobe is narrow, medium-sized, and located opposite (tr.) the mid-line of the glabella; the posterior fixigena slope steeply downward and have geniculate posterior-lateral borders. The posterior lateral furrows are deeply marked and broad, running anterior-laterally before reaching the side margins. The anterior branches of the facial suture are strongly divergent and the posterior branches normal to the sagittal line.

The pygidium is triangular in outline and highly convex along the axis; the axial lobe is divided into six or seven rings by distinctly marked ring furrows; a median tubercle occurs on each axial ring; the terminal portion is triangular with a long, posteriorly directed spine. The pleural lobes are convex, sloping down to the narrow, flat marginal border; five or six pleural segments are distinctly separated by fine interpleural grooves; the pleural furrows are wide and deeply impressed. The surface is covered by granules.

Remarks. — This species is represented by more than 80 immature and mature specimens; all were recovered from a few pieces of dark grey, medium crystalline limestone. The smallest instar is approximately 0.30 mm in total length (sag. Text-fig. 23), and the mature forms are about 2.0 mm long (exclusive of the pygidium). This species differs from *P. bootes* Walcott, *P. (Eopagetia) resseri* Kobayashi, and *P. maladensis* Resser in having a narrow, concave preglabellar field without any median furrow; it should be pointed out that the small forms of the present species all show a wide preglabellar field and occupied by a median furrow, whereas the larger one lack both wide field and furrow. The glabella is made of four rings: a frontal lobe, two axial rings and an occipital ring.

Horizon and locality. — Middle Cambrian, *Bathyuriscus-Elrathina* zone. Northeast side of road in Santaquin Canyon, Wasatch Mts., Utah Co., Utah.

Figures specimens. — Cephala, U.C.M. 38732, 38723i-q; Pygidia, U.C.M. 38732a-h.

Pagetia clytia Walcott, ontogeny

Paraprotaspid stage (Pl. 7, fig. 23, Text-fig. 35A). The shield is differentiated into cephalon and pygidium and is about 0.30 mm in total length (sag.). The cephalon is moderately convex, quadrate in outline, with a rounded anterior border. The glabella is slenderly conical with fine but recognizable glabellar furrow. The dorsal furrow is shallow and broad. The anterior brim is deeply concave. The occipital ring is distinctly delimited, possibly bearing a small occipital spine. No thoracic segments are seen. The flat fixigenae are about twice as wide as glabella and are gently upturned from the dorsal furrow, with swollen lateral margins; the palpebral lobes are not known. The posterior lateral border is broad, convex, and separated by shallow, concave marginal furrows. The protopygidium is semicircular, convex, and steeply downward from the posterior margin of the cephalon; the axial and the pleural lobes are without distinct segmentation.

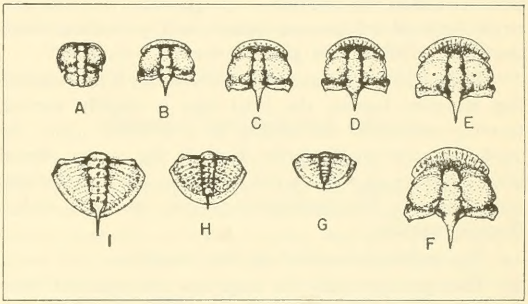

Text-fig. 35 — *Pagetia clytia* Walcott. A. A complete paraprotaspis, x 50; B. An early meraspid cephalon, x 24; C,D,G. Late meraspids; C,D. Two cranidia, x 26, x 28; G. Pygidium, x 25; E,F,I,H. Holaspids; E,F. Two cranidia, x 14, x 13; I,H. Two pygidia, x 13, x 15. (Drawings made from photographs.)

Early meraspid stage (Pl. 7, figs. 15-17, 24,25; Text-fig. 35B). The convex cranidium is quadrate in outline, with palpebral lobes appearing on the dorsal surface. It varies from 0.40-0.50 mm in length. The glabella is slenderly conical with well-developed frontal lobe, two recognizable glabellar rings, and a posteriorly arched occipital ring. The frontal lobe is triangular, convex, and bearing a pair of well-developed anterior pits on the posterior lateral bases. The dorsal furrow is broad, shallow, and deeply impressed. The occipital ring is small and faintly separated by the occipital furrow; the median spine is large, stout, directed posteriorly and has a pair of narrow ridges projecting laterally and anteriorly connected with the fixigenal borders. The preglabellar field is wide and has a longitudinal median furrow. The anterior border is narrow, arching anteriorly and is delimited by the anterior furrow. The convex fixigenae ae slightly wider than the glabella, with palpebral lobes located at the mid-line of the glabella (tr.); the posterior fixigenal borders are narrow and geniculate, about the same width as the glabellar base.

The pygidium is rounded, highly convex, with a narrow, flag marginal border; the axial lobe is slightly conical, tapering posteriorly and ending in a terminal spine; the axial rings are not distinctly divided; the convex pleural lobes are twice as wide as the axial lobe and lack distinct pleural furrows. The pygidium is possibly associated with a thoracic segment.

The surface is covered by fine granules.

The specimens of this stage are distinguished from those of previous ones in having a well-developed anterior border, a distinct frontal lobe and anterior pits; the facial sutures are distinct; the pygidium is articulated with one free thoracic segment.

Late meraspid stage (Pl. 7, figs. 18,19,26,27, Text-figs. 35C,B,G). The cranidium is about 0.50-0.55 mm in length (sag.) and moderately convex. The glabella is cylindrical, slightly tapering forward, with a rounded anterior margin, and divided into three glabellar rings by faintly impressed glabellar furrows. The anterior pits and longitudinal median furrow are shallower and have disappeared in the larger specimens. The fixigenae are of the same width as the glabella or slightly wider. The pygidium has faintly marked axial and pleural furrows and does not incorporate any thoracic segments.

Granules cover the cranidal surface and the pygidal pleural bands.

The present stage differs from the earlier one in having a shorter and wide glabella and fixigena of nearly the same width as the glabella.

Figured specimens. — Paraprotaspis, U.C.M. 38723i; early meraspids, U.C.M. 38723a-c,j,k; late meraspids, U.C.M. 38723d,e,m. 38723.

Family **OLENELLIDAE** Vogdes, 1893

Genus **OLENELLUS** Hall, 1860

Olenellus truemani Walcott

Plate 8, figs. 1-26, Text-fig. 36

Olenellus truemani Walcott, 1913, p. 316, pl. 54, figs. 2-10.
Olenellus (Olenellus) truemani Walcott, Lochman, 1952, p. 89, pl. 18, figs. 6-12.

Diagnosis. — Cephalon semicircular in outline, moderately convex; glabella with large, subrounded frontal lobe, and three unequal glabellar segments; dorsal furrow distinctly defined. Palpebral lobe strongly arcuate, running from side of frontal lobe posterior-laterally to occipital furrow. Metagenal spines smaller than genal spines. Preglabellar field narrow, flat, and distinctly delimited by anterior furrow. A faint posterior fixigenal ridge extends posterior-laterally from the pre-occipital segment to the rear margin to become continuous with a short metagenal spine.

Description. — The cephalon is semicircular in outline, moderately convex at the center and uniformly inclined to the ocular platform and preglabellar field. The glabella is cylindrical with a broad and forwardly expanded frontal lobe which is transversely subcircular, convex above the preglabellar field, and bearing a pair of faint lateral furrows; the second glabellar ring is narrower (sag.) and wider than the following; the third ring is medium-sized; the fourth one is larger than the previous ones and broadly chevron-shaped; the occipital ring is the same size as the fourth one and bears a minute median posterior tubercle. The glabellar furrows are all deeply impressed lateral but shallow across the axis. They are directed posterior-laterally from the dorsal furrow. The occipital furrow curves posteriorly and is deep laterally and shallow axially. The dorsal furrows are distinctly impressed laterally but absent at the lateral marginals of the frontal lobe. The fixigenae are elongate, semiovate, gently convex, and delimited by fine and shallow palpebral furrows. The palpebral lobes are parenthesis-shaped and extend posterior-laterally from the lateral bases of the frontal lobe, to the rear fixigenae, but terminate before reaching the posterior borders. The eye rings are vertically disposed and extend the full length of the lobes. The ocular platform is slightly broader both anteriorly and posteriorly than medially. A narrow marginal furrow runs continuously around the cephalon. It has a median notch towards the preglabellar field; the marginal border is narrow, convex and continuous with a pair of short, slender genal spines. A faint posterior fixigenal ridge extends from the side of pre-occipital ring posterior-laterally to the hind fixigenal border, then curves backwardly, crossing the posterior border to form the metagenal spine.

The hypostoma is roundly triangular in outline, with a strongly convex median body, which is triangular in plan with the anterior region arching forward. The hypostomal maculae are deep and narrow, extending posterior-laterally from the lateral borders; the rear lobe is crescentic, convex, curving posteriorly, with a rather narrow marginal border.

The surface of the skeleton is covered by a fine irregular reticulum of ridges; a row of distinct pits occurs along the cephalic furrow.

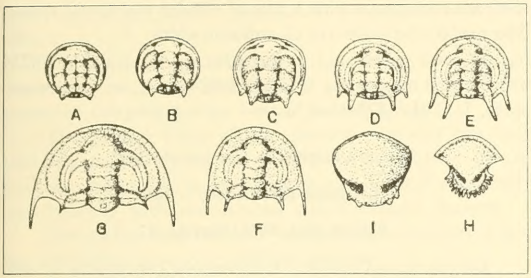

Text-fig. 36 — *Olenellus truemani* Walcott. A. Paraprotaspis, x 40; B,C. Two early meraspids, x 25, x 30; D,E. Two late meraspids, x 17, x 15; F,G. Two holaspids, x 8, x 6; H. An early meraspid hypostoma, x 10; I. A late meraspid hypostoma, x 3; (Drawings made from photographs).

Remarks. — This species is represented by more than 100 immature and mature skeletal fragments; all are prepared from a few small pieces of dark-grey, finely crystalline limestone. The assignment and relationship of this species were thoroughly discussed by Lochman (1952), where she attributed the species to the subgenus *Olenellus (Olenellus)*. It seems that the Mexico specimens here presented have a wider preglabellar field and broader fixigenae in comparison to typical (Canadian specimens) representatives of *O. truemani*. These differences might be due to preservation. The Canadian specimens were deformed, since they are preserved in a shale matrix, whereas the Mexican ones occur in limestone. Discounting discrepancy factors attributable to diagensis and deformation, the Mexican and Canadian material seems to be conspecific. The present form seems to be typically *O. truemani* Walcott and no useful purpose seems to be served in employing the subgeneric designation of Lochman.

The early instars of this species, which I have judged to represent the paraprotaspid stage, are about 0.45 to 0.60 mm in length (sag.). They are spherical in outline and strongly convex. The axial lobe is elongate-fusiform and faintly divided into an obscure median fissure along the axial lobe, axial nodes, and cephalic segmental furrows. Due to these unique characteristics of these instars, this seems to be the earliest growth stage yet known among olenellid trilobites.

The early meraspid are possibly correlated with Palmer's (1957) stages I and II, and the late meraspids correlate with his stages III and IV, judged both from their morphologies and sizes.

Horizon and locality. — Buelina Formation, Lower Cambrian, near Caborca, northwestern Sonora, Mexico.

Figured specimens. — Cephala, U.C.M. 38724, 38724o-q; hypostoma, U.C.M. 38724v; fragments, U.C.M. 38724x-z.

Olenellus truemani Walcott, ontogeny

Paraprotaspid stage (Pl. 8, figs. 1-5, Text-fig. 36A). The shield is about 0.45-0.60 mm in length (sag.). It is characterized by a fusiform axial lobe, longitudinal axial fissure, cephalic segmental furrows, and parenthesis-shaped dorsal furrows. There are three pairs of pits distinctly impressed at the intersection of the dorsal and cephalic segmental furrows. The cephalic segmental furrows are shallow but well defined; they arch slightly forward to the axial lobe and curve backward to the palpebral furrows. The cephalic segmental bands are gently convex, of which the second and third end in the inner palpebral lobes, and the fourth bends laterally and posteriorly to the rear cephalic margin, continuous with a pair of long spines. The last or occipital segment is short and bears a small occipital ring. The first cephalic segment, or the frontal lobe, is gently convex and rounded, with a pair of palpebral lobes extending from the lateral margin, running posterior-laterally and terminating in front of the fourth cephalic segment. The palpebral lobes are elongate and elevated vertically above the marginal border. The palpebral furrows are distinctly marked. The marginal border is narrow and concave, broad anteriorly and narrow posterior-laterally. Neither anterior cephalic or genal spines have been observed. The stout metagenal spines show possible association with a small protopygidium at the hind of the occipital segmental border.

Early meraspid stage (Pl. 8, figs. 6,10,20,23, Text-fig. 36B,C,H). The shield varies from 0.65 to 1.0 mm in length (sag.). It is spherical in outline, with moderately to strong convexity. The axial lobe is divided into a large frontal lobe, three axial rings, and a small terminal ring. The longitudinal furrow is absent. The dorsal furrows are distinctly marked. There are three pairs of pits deeply impressed at the intersections of the cephalic segmental and dorsal furrows. The cephalic segmental furrows are incised laterally but become shallow across the axial lobe. The resulting cephalic segments are gently convex and arch posteriorly to the palpebral lobes; they are elevated above the marginal border and extend from the lateral margin of the frontal lobe, whence they curve posterior-laterally, and end in front of the fourth cephalic segment. No preglabellar field has been observed except for a narrow concave area. The small occipital segment occupies a narrow subtriangular area with a small subrounded occipital ring, which bears a minute, posteriorly directed median node or short spine. Anterior cephalic and genal spines have not been observed. The metagenal spines are long and stout (Text-fig. 23), and extend continuously from the pre-occipital segment.

The convex hypostoma is elongate-subtriangular in outline, with a posterior margin showing 15 dentations. The convex median body is triangular and delimited by deep maculae.

The distinctive feature of this stage is the disappearance of the median longitudinal furrow. The axial lobe is narrower and longer; the marginal border is broader; and the frontal lobe is faint with a pair of furrows.

Late meraspid stage (Pl. 8, figs. 11-14, Text-figs. 36D, E,I). The shield ranges from 1.2 to 1.8 mm in length (sag.), is rounded in outline and moderately convex. The axial lobe is cylindrical and divided into five axial rings by furrows; the frontal lobe or the first glabellar segment is rounded with a pair of finely marked, elongate pits at the sides; the second glabellar segment is smaller and narrower than the first and third ones; the third glabellar segment is broader (sag.) than the second and fourth ones. The fourth glabellar segment is rounded and triangular; the occipital ring is smaller and distinctly separated by an occipital furrow. It becomes a minute median spine. The dorsal furrow is faint. The distinct cephalic segmental furrows arch posterior-laterally to the palpebral furrow; the pre-occipital segment extends laterally and posteriorly to become continuous with a pair of metagenal spines. The palpebral lobes are narrow and crescentic, running from the lateral margin of the frontal lobe to terminate in front of the fourth cephalic segment. The anterior marginal border is narrow and well elevated. The narrow and flat preglabellar field is delimited by a broad, concave anterior furrow. Genal spines are present on the posterior-lateral margin of the shield.

Both the complete hypostoma and the median body are of subtriangular in outline; the median body is more convex than that of the previous stage, but less expanded than that of the holaspis; the posterior marginal dentation has disappeared.

The surface is covered by fine granules.

The important features of this stage are the presence of a pair of genal spines, the cylindrical glabella, and the appearance of the preglabellar field. This stage differs from the holaspid in that the latter has longer genal spines and the cephalic segmental furrows are absent. A pair of strongly elevated ridges extends from the fourth glabellar segment; they are continuous with a pair of slender metagenal spines. The ocular platforms are of uniform width.

Figured specimens. — Paraprotaspids, U.C.M. 38724 a-c,e; early meraspids, U.C.M. 38724f-j, t, w; late meraspids, U.C.M. 38724k-m, u.

Genus **LAUDONIA** Harrington 1956

Laudonia canadiensis, n. sp.

Plate 9, figs. 20-31, Text-fig. 37

Diagnosis. — Cephalon transversely pentagonal in outline, moderately convex, with roundly arching anterior border, and two pairs of spines which project posterior-laterally from the four corners. Glabella cylindrical with rounded and expanded frontal lobe; three distinctly marked glabellar rings, and a broadly convex occipital ring. Palpebral lobe narrow, elevated above the ocular platform. Marginal border narrow, convex, delimited by marginal furrow. Posterior fixigenae marked with a pair of ridges, which extend laterally from the base of the palpebral lobes and continue into the metagenal spines. Hypostoma prominently convex, with large median body and spinose posterior marginal border. Thoracic segments having long pleural spines and serrate lateral margins. Pygidium unknown.

Description. — The cephalon has a transversely pentagonal outline and is moderately convex. The glabella is expanded slightly both anteriorly and posteriorly; the third glabellar segment is triangular and narrower than the fourth one; and the fourth segment is broader (tr.) and larger. The occipital ring is broad and convex, with a median node or short tubercle. The glabellar furrows are separated by the central axis except for the first furrows, which cross the axis behind the frontal lobe. The dorsal furrow is deeply impressed at the sides of the second glabellar ring, but shallower both posteriorly and anteriorly. The narrow palpebral lobes extend in a low arc to the mid-line of the fourth glabellar segment (tr.). The palpebral furrows are deeply impressed. The eyes have vertical sides and extend the full length of the palpebral lobes. The inner fixigena is small and half moon-shaped. The outer fixigenae are of medium width, widening slightly anterior-laterally. The posterior fixigenae are narrow, marked with a pair of well-elevated ridges, which extend from the fourth glabellar segment laterally and posteriorly to the posterior marginal border, and are continuous with a pair of short metagenal spines. The marginal borders are narrow and convex, distinctly marked off by marginal furrows. The genal spines are strong and project outwards from the anterior lateral borders opposite the first glabellar furrows (tr.). The metagenal spines are slender and extend posteriorly and laterally.

The hypostoma is subtriangular in outline, with a large, convex median body; the maculae are deeply marked; the posterior marginal border bears 15 short spines.

The pleural lobes of the thoracic segment are long and flat, and deeply impressed by broad and shallow pleural furrows; the pleural spines are long and directed posteriorly and laterally with saw-toothed anterior-lateral borders.

The surface is covered by fine granules; traceable ridges are developed along the cephalic margins.

Remarks. — The present species was obtained from a single sample of black, medium-crystalline limestone which yielded about 15 immature and mature cephala, three hypostomata, and a few thoracic segments. The material also contains *Olenellus* and *Salterella.* The morphologic features of the present species are close to those of *Laudonia bispinata* Harrington (1956) and *Wanneria ("Laudonia") mexicana prima* Lochman (1952), but it differs from those two forms in that the palpebral lobes are smaller, the marginal furrow is shallower, and the anterior glabella is less expanded. It is interesting to note that the early meraspis most nearly resembles *Olenelloides armatus* Peach (1894) which was found in west of Ross-Shire, Scotland, in the Lower Cambrian, and studied by Peach (1894) and Walcott (1910). Both forms have a pentagonal to hexagonal cephalon, three pairs of cephalic spines, and no facial sutures; however, the immature forms of *L. canadiensis* show the pair of palpebral lobes is larger and the skeletal measurements smaller. Undoubtedly these two genera are closely related.

Horizon and locality. — Lower Cambrian. North of Radium, west side of the Columbia River, British Columbia, Canada.

Figured specimens. — Holotype, Cranidium, U.C.M. 38726; Paratype, Cranidia, U.C.M. 38726a-c, g-i; hypostomata, U.C.M. 38726e, d; thoracic fragment, U.C.M. 38726f.

Laudonia canadiensis, n. sp. ontogeny

Early meraspid stage (Pl. 9, figs. 20,21, Text-fig. 37A). The smallest cephalon varies from 1.2 mm to 1.7 mm in length (sag.); the outline is hexagonal, convex, and bears three pairs of cephalic spines. The cylindrical axial lobe is separated into a rounded, convex frontal lobe and four transverse and undifferentiated axial rings; the last axial ring or occipital ring bears a minute median spine. The palpebral lobes are sickle-shaped and extend from the posterior lateral margins of the frontal lobes to the mid-length of the fourth axial ring (tr.). They are elevated above the fixigenae and delimited by palpebral furrows. The outer fixigenae are broad anterior-laterally, and narrow posterior-laterally; the narrow posterior fixigena is marked by a pair of prominent ridges; the posterior fixigenal ridges extend from the pre-occipital ring to the posterior-lateral corners and are continuous with a pair of spines projecting from the posterior lateral borders. The marginal border is narrow, and convex, and well delimited by a deep marginal furrow. Three pairs of cephalic spines project downward at the cephalic corners.

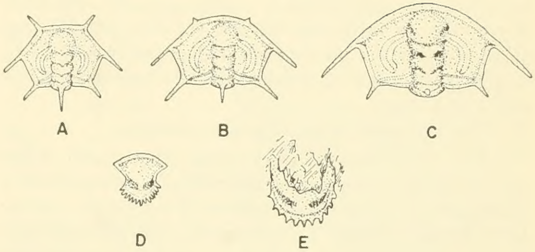

Text-fig. 37 — *Laudonia canadiensis,* n. sp. A. An early meraspis, x 14; B. A late meraspis, x 10; C. Holaspis, x 4.5; D. A late meraspid hypostoma, x 11; E. A broken holaspid hypostoma, x 2.5. (Schematic drawings from photographs.)

The surface of the skeleton is covered by fine granules.

Late meraspid stage (Pl. 9, figs. 25,28,29; Text-fig. 37B). The cephalon is nearly pentagonal in outline, convex, arching forward anteriorly. It ranges from 1.20-2.50 mm in length. The glabella is cylindrical but expands slightly both anteriorly and posteriorly from the third ring; the frontal lobe is spherical and convex above the outer fixigenae; the second glabellar ring is narrow (sag.) and transverse; the third glabellar ring is triangular with the apex pointing backward; the fourth one is of medium width, convex and arches posteriorly; the glabellar furrows are all steep-sided; the first and the second cross the axis, and the third is separated. The convex occipital ring is wider than the other glabellar rings and defined by a steep-sided occipital furrow; it bears a minute median spine. The palpebral lobe is elevated above the fixigenae, sickle-shaped, and divided by palpebral furrow. The outer fixigenae are narrow, gently convex, and slope downward to the deep marginal furrow. The convex marginal border is narrow and bears a pair of cephalic spines anterior-laterally, a pair laterally, and one pair posterior-laterally; the posterior lateral spines are continuous with a pair of posterior fixigenal ridges which extend to the sides of the pre-occipital ring. The hypostoma is subtriangular in outline, elongate and has a convex median body; the maculae are deep laterally and shallow across the central axis; the posterior lobe is U-shaped, gently convex, and bears 15 dentations along the posterior margin.

The surface is covered by fine granules.

The morphologic changes during the growth stages are as follows: the shape of the cephalon changes from a hexagonal to a pentagonal outline; the anterior cephalic spine becomes shorter and disappears; the glabellar rings change in configuration from stage to stage; the posterior fixigenal borders are expanded laterally (tr.); and the size of the median body of the hypostoma increases while the posterior marginal dentations shorten.

Figured specimens. — Early meraspids, U.C.M. 38726a, b; late meraspids, U.C.M. 38726d, g-i.

Family **DOLICHOMETOPIDAE** Walcott, 1916

Genus **PTARMIGANIA** Raymond, 1928

Ptarmigania aurita Resser

Plate 10, figs. 1-23, Text-fig. 38

Ptarmigania aurita Resser, 1939, p. 37, pl. 3, figs. 35,36.
Ptarmigania sp. undetermined, Resser, 1939, p. 42, pl. 3, fig. 34.

Diagnosis. — Dolichometopid trilobites with subquadrate glabella expanding anteriorly; large palpebral lobes located far behind the mid-length of glabella (tr.). Fixigenae about half as wide as glabella (between palpebral furrow and dorsal furrow); narrow in front; narrow behind (subequal to width of occipital ring); dorsal furrow distinct; occipital ring bearing a minute, short, median spine. Anterior border narrow. Librigenae, thoracic segment, and pygidium unknown.

Description. — The cranidium is triangular in outline. The subquadrate glabella, which expands slightly anteriorly, is marked by four pairs of glabellar furrows; the anterior pair is shallow and faint and directed anteriorly from the dorsal furrows; the posterior two pairs are deeper, and directed posterior-laterally from the dorsal furrows. The occipital furrow is deep and narrow; the occipital ring is crescentic, convex, arching posteriorly, and bearing a medium-sized median spine. The fixigenae are gently convex, and flattened near the palpebral furrow area, and about one-half as wide as the glabella between the dorsal furrow and the palpebral lobe. The large and narrow palpebral lobes are delimited by palpebral furrows, extending posteriorly from between the first and second glabellar furrows and ending in front of posterior fixigenal furrows; the palpebral ridges are short and prominent. Both anterior and posterior fixigenae are narrow and convex; the narrow (sag.) posterior lateral borders are about the same width (tr.) as the glabella and are convex above the deep border furrows. The narrow and convex anterior border is adjacent to anterior glabellar margin. The anterior facial suture lines are convergent convex; the posterior ones are almost parallel to the posterior-lateral borders. The surface is finely granulated.

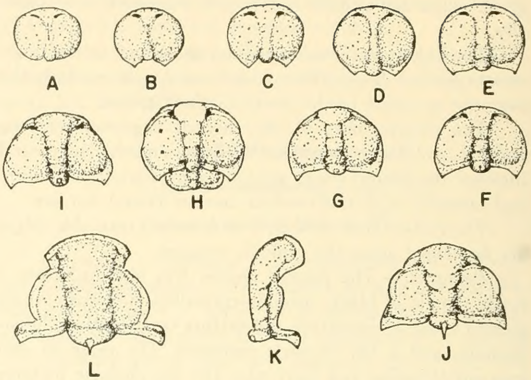

Text-fig. 38 — A growth series of *Ptarmigania aurita* Resser. A-C. Three anaprotaspids, x 40, x 43, x 38; D. A metaprotaspis, x 40; E-G. Three paraprotaspids, x 37, x 35, x 33; H,I. Two early meraspids, x 28, x 30; J. A late meraspis, x 25; K,L. Dorsal and side views of an holaspid cranidium, x 12. (Drawings from photographs.)

The librigenae, hypostoma, thoracic segments, and pygidium are unknown.

Remarks. — This species is represented by more than 55 immature and mature specimens. All were prepared from a few small pieces of dark grey, medium-crystalline limestone. The samples also include both early instars and adults of *Elrathina, Alokistocare,* and *Pagetia.* The immature forms are different from those of ptychopariids in having a narrow axial lobe, and impossible to mistake for those of *Pagetia* since the forms are so characteristic (Pl. 7, fig. 23-26).

The complete skeleton of the type of *Ptarmigania ("Bathyuriscus") rossensis* (Walcott) (type of genus) (1917) shows a cephalon with long genal spines, nine thoracic segments, and a pygidium with a broad marginal border and a pair of anterior-lateral spines. Resser (1939) assigned to this genus a few species based on disassociated body parts. It is, therefore, difficult to evaluate his assignments. It is likely, as pointed out by Rasetti (1951, p. 169), that in most corynexochid trilobites, secure generic and specific determinations can only be based on essentially complete specimens which show the number of thoracic segments and the shape of the pygidium. It is obviously untrustworthy to attribute any single cranidium to species or genus within the group. In the absence of any closely similarly librigena which can be securely correlated with the present cranidium and with no potentially assignable pygidia known, Resser's unsatisfactory assignment is perforce here adopted.

Horizon and locality. — Middle Cambrian, *Elrathina-Bathyuriscus* zone. Santoquin Canyon, northeast side of road, Wasatch Mts., Utah Co., Utah.

Figured specimens. — Cranidium, U.C.M. 38727; cranidia, U.C.M. 38727a-u.

Ptarmigania aurita Resser, ontogeny

Anaprotaspid stage (Pl. 10, figs. 1-5, Text-fig. 38A-C). The shield is spherical to slightly transverse, convex, without distinct dorsal furrows, and ranges from 0.28-0.35 mm in length (sag.). The axial region is slightly elevated with a faint longitudinal fissure along the axis. No axial rings or furrows are present, and the frontal lobe is poorly defined; the anterior pits are transversely elongate and distinctly impressed on the sides of the frontal lobe; a pair of short eyebrow-shaped ridges extend laterally from the anterior lateral margin of the frontal lobe. A terminal tubercle is slightly elevated on the edge of the posterior median margin of the shield. The posterior lateral margin has a pair of short, broad spines directed backward.

The surface is covered by fine granules.

Metaprotaspid stage (Pl. 10, figs. 6,7, Text-fig. 38 D). The shield is rounded, convex, with distinctly divided axial and pleural lobes, it is approximately 0.40 mm long (sag.). Both ends of the axial lobe expand from the second axial ring; both axial rings and furrows are distinctly defined; the frontal lobe is rounded, triangular, with a pair of supercilioid ridges directed laterally and posteriorly from the anterior lateral margin; the anterior pits are elongate and deeply marked; the second axial ring is small, narrow, and elongate; the third and fourth are oval and larger, rounded, and highly convex. The pleural lobe is convex anteriorly and gently sloping downward posterior-laterally towards the margin. A pair of short, broad spines project backward from the posterior-lateral margin. The protopygidium is unknown. The surface is finely granulose.

This stage differs from the previous one in having the shield distinctly divided into axial and pleural lobes, and the axial lobe segmented into five distinct rings.

Paraprotaspid stage (Pl. 10, figs. 8-13, 15, Text-fig. 38 E-G). The cranidium, which is trapezoidal to subtrapezoidal in outline, bears well-developed axial and pleural lobes and ranges from 0.45-0.55 mm in length (sag.). The axial lobe expands both anteriorly and posteriorly from the second axial ring; the frontal lobe is triangular, convex, and arching forward with a pair of eye-ridges; the anterior pits are distinct; the second ring is narrowly elongate, the third and fourth ones are larger, rounded to roundly transverse; the occipital ring is smaller and transverse. The dorsal furrow is deeply impressed. The fixigenae are convex, broad, about three times as wide as the glabella (tr. at mid-length). The supercilioid ridges are prominently elevated, situated behind the frontal pits, and directed posterior-laterally to be connected with the narrow palpebral lobes. The posterior lateral furrows are distinct. The posterior-lateral borders are narrow and have a pair of short spines projecting backward from their mid-line (tr.). The anterior branches of the facial sutures are convergent and the posterior branches are divergent and their course is either sinous or straight. The surface is covered by fine granules.

The characteristics of this stage are the trapezoidal cranidium, the dorsal facial sutures and the appearance of the protopygidium.

Early meraspid stage (Pl. 10, figs. 14, 16-18, Text-fig. 38 H, I). The cranidium is trapezoidal in outline, moderately convex, and varies from 0.55 to 0.65 mm long (sag.). The glabella is strongly expanded forward, with distinct anterior pits on the sides of the first glabellar segment; the glabellar furrows are faint but steep-sided. The dorsal furrow is deep; the convex occipital ring bears a minute median spine. The fixigenae are broadly triangular, convex, less than twice as wide as the glabellar (tr.); the eye ridges are prominently elevated and directed posterior-laterally from the sides of the anterior pits; the palpebral lobe is narrow and long; the posterior lateral border is narrow (sag.) and about twice as wide as the occipital ring (tr.). The surface is finely granulose, and three pairs of prominent nodes occur on the fixigenae.

In comparison to previous stages, the specimens of this stage have a marked forward expansion of the glabella and narrow fixigenae.

Late meraspid stage (Pl. 10, figs. 19, 20, Text-fig. 38 J). The convex cranidium is about 0.80-1.00 mm long (sag.). The important characteristics of this stage are the first appearance of the anterior border; the lengthening of the palpebral lobes, which here extend posteriorly to the posterior-lateral border; and disappearance of the anterior pits. The specimens of the meraspid stage are differentiated from those of the holaspid stage in having wider fixigenae and the palpebral lobes situated at the mid-length of the glabella (tr.).

Figured specimens. — Anaprotaspids, U.C.M. 38727a-e; metaportaspids, U.C.M. 38727 f, g; paraprotaspids, U.C.M. 38727 h-m, o; early meraspids, U.C.M. 38727n, p-r; late meraspids, U.C.M. 38727s, t.

Family **ANOMOCARIDAE** Poulsen, 1927

Genus **GLYPHASPIS** Poulsen, 1927

Glyphaspis cf. **parkensis** Rasetti

Plate 11, figs. 1-30, Text-fig. 39

Glyphaspis parkensis Rasetti, 1951, p. 224, pl. 34, figs. 5-7; Poulsen, 1964, p. 51, pl. 3, figs. 8,9.

Diagnosis. — Skeleton similar to that of *Anomocare*: cranidium quadrate in outline, with wide and concave frontal brim. Fixigenae medium-narrow. Palpebral lobe long, sickle-shaped, and located behind the mid-line of glabella (tr.). Librigenae elongate with a long genal spine. Pygidium larger with broad, usually concave, marginal border. Axial lobe conical and backwardly tapering, divided into seven or eight axial rings and a small posterior terminal portion.

Glyphaspis cf. **parkensis** Rasetti, male?

Plate 11, figs. 15-18, 22, 27, Text-figs. 39 I, L

Description. — The skeleton is large, convex, with semicircular cephalon and pygidium. The cranidium is quadrate in outline. The glabella is conical with a rounded anterior margin and rather shallow, broad glabellar furrows. The dorsal furrow is shallow but well defined. The shallow occipital furrow curves slightly forward at the mid-line (sag.). The frontal brim is indistinctly separated into an anterior border and preglabellar field by a furrow; the anterior border is broad and concave, and marked laterally with delicate furrows; the anterior furrow is faint but well defined; the preglabellar field is narrow, *i.e.*, the anterior border is more than three times as wide as the preglabellar field. The fixigenae are about one-half the width of the glabella; the palpebral lobes are crescentic, more than half as long as the glabella, sickle-shaped and located behind the mid-line of the glabella (tr.); eye ridges are distinctly marked; the posterior fixigenae are narrow and marked by narrow distinct border furrows; the posterior lateral borders are narrow and slender. The anterior facial suture is considerably divergent and cuts the anterior border roundly; the posterior facial suture is almost parallel to the posterior lateral border.

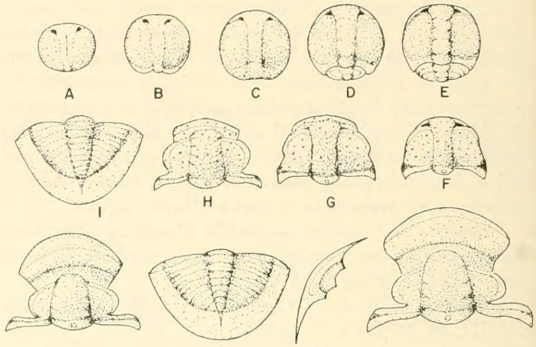

Text-fig. 39 — *Glyphaspis* cf. *parkensis* Rasetti. A,B. Two anaprotaspids, x 53; C. A metaprotaspis, x 45; D,E. Two paraprotaspids, x 40, x 30; F,G. Two early meraspids, x 26, x 24; H. A late meraspis, x 20; I. A "male" pygidium, x 1.7; J. A "female" pygidium, x 1.7; K. Librigena, x 10; L. A "male" cranidium, x 1.6; M. A "female" cranidium, x 7. (Drawings made from photographs.)

The librigenae are elongate and have long genal spines; the librigenal lateral border is broad, and flat or slightly concave, with a faint furrow along the inner marginal border; the lateral furrow is faint but clearly recognizable; the ocular platform is narrow and gently convex; the genal spine is long and arcuate, with a broad base that tapers gradually to the tip.

The pygidium is elongate semiovate in outline, with a convex axial lobe and broad concave border. The axial lobe is slenderly conical, broad anteriorly and tapering posteriorly to the inner marginal furrow; six or seven small axial rings and a small posterior portion are seen; the ring furrows are shallow, and they are slightly curving anteriorly at the central axis. The pleural lobes are convex, gently sloping downward from the dorsal furrow to the inner marginal furrow, and distinctly divided into six or seven pleural furrows.

The surface of the skeleton is covered by fine granules; radial ridges are marked on the preglabellar field and ocular platform of the librigenae, the outer of the cephalic margins are surrounded by fine wrinkles.

Figured specimens. — Cranidia, U.C.M. 38728o-q; librigena, U.C.M. 38728s; pygidium, U.C.M. 38728y; hypostoma, U.C.M. 38728r.

Glyphaspis cf. **parkensis** Rasetti, female?

Plate 11, figs. 19, 20, 26, 28-30, Text-fig. 39 J, M

The characteristics of what are presumed to be females differ from those of the presumed males in that the female body is remarkably larger than the male and has a narrower and less convex anterior border; the glabellar is narrow and longer, and the pygidium has a rounded outline.

Remarks. — This species is represented by 20 mature and 60 immature specimens, all are prepared from a few small pieces of dark-grey oölitic, medium-crystalline limestone. The features of the present species conform to Rasetti's description, but unfortunately the holotype and the paratypes of *G. parkensis* are all slightly deformed; moreover, the holotype was a shale specimen, hence its characteristics are not exactly identical with those of the limestone specimens here studied. The main portion of the preglabellar field of the paratype (U.S.N.M. 116286a) is slightly wider than that of the holotype (U.S.N.M. 116285) and was exfoliated. Therefore, if diagenetic factors are considered, the present material may present the original shape and convexity. The specimens identified as this form which were found in northwestern Greenland by Poulsen (1964) show a narrower frontal brim, and narrower pygidial marginal border than both Rasetti's and present materials. Poulsen's material may represent a "variety" of this species. The sexual ratio of the present species is 125.

Horizon and locality. — Meagher Formation, Middle Cambrian, *Bathyuriscus-Elrathina* Zone. West side of south Boulder Creek, west Madison County, Montana.

Figured specimens. — Cranidium, U.C.M. 38728; pygidia, U.C.M. 38728w, x, z, r.

Glyphaspis cf. **parkensis** Rasetti, ontogeny

Anaprotaspid stage (Pl. 11, figs. 1-3, Text-fig. 39A, B). The convex shield is rounded to subrounded in outline, with a narrow shield margin and varies from 0.25 to 0.30 mm in length (sag.). The axial and pleural lobes are undivided; a narrow but traceable longitudinal axial fissure is well defined on small shield but absent on larger ones. The frontal lobe is delimited by two distinct anterior pits; a pair of short supercilioid ridges extend from the anterior-lateral margin of the frontal lobe. The hind margin of the shield bears a rounded to elongate median tubercle or occipital ring. A pair of short, broad-based marginal spines project from the posterior-lateral margin of the shield. The surface is covered by fine granules. A narrow marginal border surrounds the shield.

Metaprotaspid stage (Pl. 11, figs. 4, 5, Text-fig. 39 C). The shield is subrounded in outline, convex and about 0.40-0.50 mm in length (sag.), with well-defined axial and pleural lobes. No axial ring or glabellar furrows are seen. The anterior pits are deeply impressed; the frontal lobe is broad and convex, with a pair of supercilioid ridges extending posterior-laterally along the front margin. The axial lobe is cylindrical but with a broadly expanded frontal lobe; the posterior axial lobe is distinguished by a prominent tubercle. The lateral lobe is convex and twice as wide as the axial lobe. The posterior margin of the shield arches to the axial lobe, with flat, narrow, and unsegmented marginal fringe. The marginal border is present along most the posterior-lateral shield margin. The surface is covered by fine granules.

The important features of this stage are: the axis and the pleural lobes are well differentiated; the central axial fissure has disappeared; and the posterior shield margin bears a narrow, flat fringe.

Paraprotaspid stage (Pl. 11, figs. 6, 7; Text-fig. 39 D, E). The shield is composed of a cephalon and a protopygidium; it is subspherical in outline and convex, with the length about 0.55-0.75 mm (sag.). The axial and pleural lobes are distinctly separated by dorsal furrows. The glabella is cylindrical with a slightly expanded frontal lobe, four faint glabellar rings and a prominently elevated occipital ring; the glabellar furrows are steeply sided and extend across the axis. The anterior pits are shallower than those of the previous stage, but clearly recognizable. The pleural lobes or fixigenae are convex and about one and one-half the width of the glabella; the posterior-lateral border are backwardly projected. The transversely subtriangular protopygidium is composed of one or two segments. The surface is finely granulose.

This stage differs from the previous one in that the shield is composed of a clearly differentiated protopygidium and cephalon; the pleural lobes are narrower, and the frontal pits are shallower; the palpebral ridges are prominently elevated.

Early meraspid stage (Pl. 11, figs. 8-11, 23, 24, Text-fig. 39 F, G). The convex cranidium is triangular in outline and about 0.60-0.80 mm in length (sag.). The glabella is broadly cylindrical with indistinct glabellar furrows. The dorsal furrows are narrow and deeply impressed. The anterior border is narrow and arches forward. The occipital ring is convex, and bears a small median tubercle. The fixigenae are about the same width as the glabella and are broadly triangular with a distinct posterior lateral border; the eye ridges are prominently elevated; the palpebral lobe is large and situated in front of the mid-line of the glabella (tr.). The pygidium is transversely oval and divided into two or three segments by distinct furrows (figs. 23, 24). The surface is covered with large granules.

This stage is characterized by the appearance of the anterior border; the fixigenae are about the same width as the glabella, which here becomes cylindrical. The pygidium is separated from the cephalon by a few thoracic segments.

Late meraspid stage (Pl. 11, figs. 12-14, 25, Text-fig. 39 H). The cranidium is trapezoidal to quadrangular in outline, moderately convex, and about 1.00 to 1.80 mm in length (sag.). The glabella is truncate-conical with broad, shallowly impressed glabellar furrows. The occipital ring is crescentic, convex, and has a small median tubercle. The preglabellar field first appears in this stage and is separated by the anterior furrow from the border; the anterior brim varies in width, narrower on smaller forms and broader and flat on larger ones. The fixigenae are about one-half the width of the glabella; the palpebral lobe is crescentic, and located at the mid-line of the glabella (tr.). The pygidium is oval or subtriangular with six-seven segments; the marginal border is narrow. The surface is covered by coarse granules in smaller specimens but finer in the larger forms.

The most distinctive characteristics of this stage are: cranidium bears a clearly defined preglabellar field; the glabella becomes truncate-conical, and the palpebral lobes are located at the mid-line of the glabella (tr.). This stage differs from the holaspid stage in that the glabella of the meraspis is less rounded at the frontal margin; the anterior margin has no border furrow; and the palpebral lobe of the holaspis is located slightly behind the mid-length of the glabella.

Figured specimens. — Anaprotaspids, U.C.M. 38728a-c; metaprotaspids, U.C.M. 38728d, e; paraprotaspids, U.C.M. 38728f, g; early meraspids, U.C.M. 38728h-k, t, u; late meraspids, U.C.M. 38728l-n, v.

Genus **IOHOMIA** n. gen.

Diagnosis. — Cranidium subquadrate in outline; glabella conical; glabellar furrows faint; dorsal furrow deep and broad; preglabellar field moderately narrow; anterior furrow broad, well defined, bearing a median pit; anterior border broad and flat. Fixigenae narrow, convex above dorsal furrow; palpebral lobes large and sickle-shaped, situated posterior to the mid-length of the glabella; posterior fixigenae rather narrow; librigenae with broad, flat lateral borders; genal spine unknown. Pygidium rounded to subtriangular in outline, highly convex along the axis; possibly divided into more than ten segments; marginal border rather broad and flat.

Description. — The cranidium is subquadrate, elongate, moderately convex, with a broad flat frontal brim. The glabella is conical, rounded in front, and marked with shallow glabellar furrows. The dorsal furrow is deep and broad, but shallow along the anterior glabellar margin. The occipital ring, which is broad centrally, and narrower laterally, bears a minute median tubercle. The occipital furrow is distinct, shallow across the central axis, and steep-sided. The preglabellar field is narrow and slopes downward to the shallow anterior furrow, which arches forward to a transverse, ovate median pit. The anterior border is broad and flat, subtriangular to crescentic. The fixigenae are narrow, about one-third as wide as the glabella and steeply convex above the dorsal furrow. The larger palpebral lobes are sickle-shaped, and located behind the mid-line of the glabella. The prominent palpebral ridges are obliquely directed anterior-medially from the anterior palpebral lobes to points immediately behind the anterior-lateral corners of the glabella. The narrow posterior fixigenae are deflexed steeply from the posterior palpebral lobes to the deep and broad border furrow, and are larger laterally (tr.) than the occipital ring. The anterior facial sutures are strongly convergently convex, and the posterior ones are divergently sinuous, and nearly transverse.

The librigenae may lack genal spines. The ocular ring is large and located above the ocular platform. The lateral border is broad and flat, or slightly concave, anteriorly, and delimited by a broad shallow lateral furrow.

The pygidium is elongate-subtriangular in outline and convex along the axis. The axial lobe is slenderly conical, tapering posteriorly, and ending before reaching the pygidial margin. It is divided into at least ten narrow axial rings and a small subtriangular terminal portion. The pleural lobes are more than one-half as wide as the axis and marked by shallow pleural furrows which extend into the broad, flat marginal border.

The skeletal surface is covered by fine granules; radial ridges are marked on the preglabellar field, and wrinkles occur along the cephalic margin.

Remarks. — The present genus is similar to *Anomocare* and *Glyphaspis,* but it differs in having a cranidium bearing an anterior median pit, narrower glabella, and subtriangular anterior border. The pygidium is highly convex along axial lobe. The general appearance indicates close relationship to other genera in the family Anomocaridae.

Type species. — *Iohomia sickia,* n. gen. and n. sp.

Iohomia sickia, n. gen. and n. sp., male?

Plate 12, figs. 15, 18, 19, 21, 22, 25, 26, Text-fig. 40 A, D, F

The cranidium is triangular in outline with broadly subtriangular anterior border; glabella conical, broad and short; anterior furrow occupied by a transverse, ovate median pit. Librigenae without genal spines. Pygidium elongate, subtriangular, and highly convex along the axial lobe.

Holotype. — Cranidium, U.C.M. 38737.

Paratypes. — Cranidium, U.C.M. 38737i; pygidia, U.C.M. 38737c, f; librigena, U.C.M. 38737 e; meraspis, U.C.M. 38737a.

Iohomia sickia, n. gen. and n. sp., female?

Plate 12, figs. 17, 20, 23, 24, Text-fig. 40 B, C

The cranidium is subquadrate in outline, with a narrow transverse, crescentic anterior border; the glabella is slightly narrower and longer than that of the male form. The pygidium is semicircular or semioval in outline and uniformly convex.

Remarks. — This species is represented by more than 30 specimens; the smallest form is about 1.5 mm in length (sag.) and represents the meraspid stage; the largest cranidium is about 15.0 mm and the largest pygidium 14.0 mm in length (sag.). All of the specimens were prepared from a few small pieces of dark grey, medium-crystalline limestone.

Horizon and locality. — Meagher Formation, *Bathyuriscus-Elrathina* zone, Middle Cambrian. West side of south Boulder Creek, west Madison County, Montana.

Figured specimens. — Paratypes; cranidia, U.C.M. 38737g, h; pygidia, U.C.M. 38737b, d.

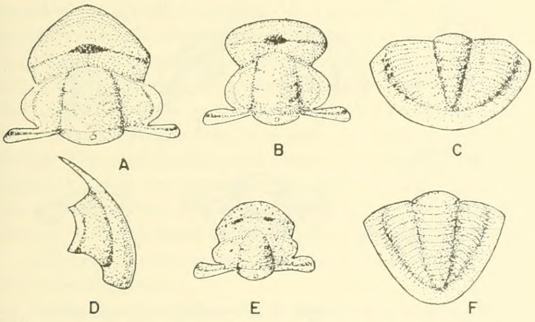

Text-fig. 40 — *Iohomia sickia,* n. gen. and n. sp. A. "Male" cranidium, x 2.5; B. "Female" cranidium, x 4.3; C. A "female" pygidium, x 2.2; D. Librigena, v 5.4; E. A late meraspid cranidium, x 10; F. A "male" pygidium, x 3; (Schematic drawings from photographs.)

Family **PARABOLINOIDIDAE** Lochman, 1956

Genus **APOMODOCIA,** n. gen.

Diagnosis. — Cranidium triangular in outline, elongate, moderately convex. Glabella slenderly conical with three pairs of faint glabellar furrows. Dorsal furrow narrow and shallow. Occipital ring crescentic, convex, bearing a minute median tubercle. Anterior furrow with median notch. Anterior border narrow and convex. Fixigenae narrow about one-third as wide as glabella (tr.). Palpebral lobe small, located in front of the mid-line of glabella (tr.). Fixigenae broad, posteriorly subtriangular, with border the same width as the occipital ring. Librigenae crescentic, elongate with a short genal spine. Hypostoma subquadrate and bearing a broad median body. Convex pygidium, subtriangular in outline, consisting of three or four segments, with a narrow marginal border.

Description. — The cranidium is triangular in outline, elongate, and moderately convex. The glabella is a slender cone, tapering forward with a rounded anterior margin; three pairs of faint glabellar furrows are present; the first pair is short and located in front of the transverse line of the palpebral lobes; the second pair is of medium length and directed posteriorly from behind the transverse line of the palpebral lobes; the third pair of glabellar furrows is longer and deeper than the preceding pairs. The dorsal furrow is narrow and deeply defined. The occipital furrow is deep and steep-sided laterally but shallow across the central axis. The occipital ring is broadly convex, crescentic and bears a minute median tubercle. The anterior brim extends one-third the length of the glabella and is gently convex. The anterior furrow is shallow, broad and distinctly defined with a median notch directed towards the anterior margin of the preglabellar field; the convex anterior border is of medium width. The fixigenae are with slightly expressed palpebral lobes, which are one-third as wide as the glabella (tr.); the narrow palpebral lobes are small and located in front of the mid-line of the glabella; the palpebral furrows are faint. The posterior fixigenae are subtriangular in outline and marked by broad, deeply impressed border furrows. The anterior branches of the facial sutures are straight and diverge anteriorly; the posterior branches are strongly divergent posteriorly and are gently sinuous.

The librigenae are crescentic with short posterior lateral genal spines. The ocular platform is moderately narrow. The lateral border is medium — narrow, slightly convex, and distinctly delimited by a shallow, broad lateral furrow.

The moderately convex pygidium is transversely subtriangular to ovate in outline. The axial lobe is conical, tapering posteriorly and marked by three or four axial rings and a semicircular posterior portion. The dorsal furrow is distinct. The pleural lobes are gently convex, with three pairs of distinct segments; the pleural furrows and the interpleural grooves are distinctly defined. The marginal border is of medium width, narrowing slightly posteriorly, and moderately convex.

The surface is covered by fine granules, and radial ridges are marked on the preglabellar field and the ocular platforms of the librigenae.

Remarks. — This genus differs from *Modocia* Walcott (1924) by its triangular cranidium of low convexity; the glabella of *Apomodocia* is longer and narrower; the dorsal furrow is shallow; the preglabellar field is wider and fixigenae are narrower; the librigenae have shorter genal spines; the pygidium lacks marginal spines. The *Modocia* skeleton is covered by large granules whereas that of *Apomodocia* is smooth or covered with the granules.

The general features of *Apomodocia* are similar to those of *Parabolinoides* Frederickson (1949), and *Maustonia* Raasch (*in* Lochman, 1950), but *Apomodocia* shows a slightly more slender glabella, narrower anterior border, shorter genal spines, and a pygidium lacking marginal spines. On the other hand, the location of the palpebral lobes, the narrow fixigenae, the small ocular ring, the shallow dorsal furrow, and the posteriorly broad fixigenae are similar in all these genera. Like there, *Apomodocia* should be a member of family Parabolinoididae.

Type species. — *Apomodocia conica,* n. gen. and n. sp.

Apomodocia conica, n. gen. and n. sp.

Plate 9, figs. 1-19, Text-fig. 41

Armonia lata (Howell and Duncan), Lochman and Duncan, 1944, p. 122, pl. 15, figs. 30-36 only (*not* figs. 29, 37); Lochman, 1950, p. 346, pl. 51, figs. 11,13-15 only (*not* figs. 10, 12).

Remarks. — This species is represented by more than 50 immature and mature specimens, all prepared from a few pieces of light-brown, medium-coarse crystalline limestone. The material contains also both larval and adult forms of *Cedarina cordillerae* (Howell and Duncan). The larvae of *A. conica* differ from those of *C. cordillerae* by their narrower axial lobes and absence of occipital spines.

The present genus and species present certain taxonomic problems. The holotype (M.S.U.M. T1616) of *Armonia lata* (Howell and Duncan) was originally assigned as *Perioura lata* Howell and Duncan (1939). After a re-examination of the holotype of *A. lata,* Lochman and Duncan (1944) removed the original assignment as a new species of *Armonia lata* and subsequently assigned several specimens to this species. Lochman (1959, Treatise, Part O, p. 306) synonymized *Armonia* Walcott (1924) with *Modocia* Walcott (1924) without giving reasons. The writer had an opportunity to carefully study the original materials of the type species of *Modocia, Armonia,* and *Perioura* with Dr. Lochman at the New Mexico Institute of Mining and Technology a few years ago. It is unfortunate that the holotype of *A. elongata* Walcott (1924) (U.S.N.M. 62811) is an internal mold of an imperfect cranidium and that of *Perioura ("Armonia") lata* (M.S.U.M. T1616) is a cranidium from well-compacted shale. Thus, they could not be exactly compared, but taking into account the preservation, the general shape of the cranidium, the position of the palpebral lobes, it was my conclusion that the types of *Armonia elongata* (Walcott) and *Perioura ("Armonia") lata* Howell and Duncan should belong to the genus *Modocia,* and that the subsequent assignments by Lochman and Duncan (1944) and Lochman (1950) pertain to other genera.

Lochman's *Armonia lata* (1950, pl. 51, figs. 10, 12 only) may belong to the genus *Blountia.* However, this is speculative because of the poor preservation of the material.

Horizon and locality. — Upper Cambrian, *Cedaria* zone. Locality unknown, Wasatch Mts., Utah.

Figured specimens. — Holotype, Cranidium, U.C.M. 38725; paratype, Cranidia, U.C.M. 38725a-p.

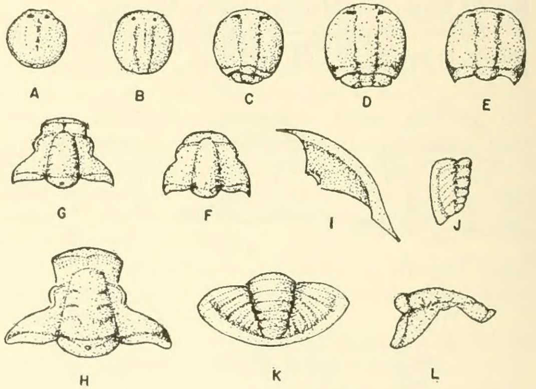

Text-fig. 41 — A growth series of *Apomodocia conica,* n. gen., n. sp. A. Anaprotaspis, x 43; B. Metaprotaspis, x 38; C-E. Paraprotaspids, x 36, x 36, x 36; F. An early meraspis, x 40; G. A late meraspis, x 17; H,L. Dorsal and side views of an holaspid cranidium, x 54; I. A librigena, x 4.3; J,K. Top and side views of a pygidium, x 3.6. (Schematic drawings made from photographs.)

Apomodocia conica, n. gen. and n. sp., ontogeny

Anaprotaspid stage (Pl. 9, fig. 1, Text-fig. 41A). The shield is rounded in outline, moderately convex, and approximately 0.30 mm in length (sag.). The axial and pleural lobes are not well-differentiated except for an elongate median fissure, which extends from the anterior margin to the mid-length of the shield. A pair of anterior pits, which suggest the instars' orientation, are distinctly marked on the anterior lateral margin of the shield. The surface is covered by fine granules.

Metaprostaspid stage (Pl. 9, figs. 2, 3, Text-fig. 41B). The shield is subrounded, moderately convex, and about 0.30-0.40 mm in length (sag.). The axial and pleural lobes are distinctly separated; the dorsal furrows are faint and parallel; no axial ring or ring furrows occur but a small terminal tubercle is situated at the posterior margin of the shield. The anterior pits are rounded and distinctly marked. A pair of supercillioid ridges are directed laterally and posteriorly from the anterior lateral margin of the frontal lobe. The posterior tubercle is rounded, transverse, and faintly separated from the axial lobe by a furrow. The convex pleural lobes are broader than axis; the marginal border is rounded and depressed.

The instars of this stage are characterized by the well-developed axial and pleural lobes; the longitudinal fissure is absent.

Paraprotaspid stage (Pl. 9, figs. 4-8, Text-figs. 41C-E). The shield, which is distinctly divided into cephalon and protopygidium, is subspherical and about 0.45 to 0.50 mm in total length (sag.). The axial lobe is cylindrical and has distinctly defined dorsal furrows. The anterior pits are rounded and distinctly marked; the eyebrow-like ridge taper posterior-laterally from the anterior lateral frontal lobe. The occipital ring is transverse, oval, convex, and defined by the occipital furrow. The convex pleural lobes are about one and a half times as wide as the glabella and have posterior borders terminating in a pair of posteriorly directed spines. The protopygidium is transversely ovate and composed of one or two segments; the ring and pleural furrows are sharply defined. No marginal spines are observed. The surface of the skeleton is covered by fine granules.

This stage is characterized by a well-developed cephalon and protopygidium.

Early meraspid stage (Pl. 9, figs. 9, 10, Text-fig. 41F). The cranidium is convex, trapezoidal in outline, and about 0.45 to 0.70 mm in length (sag.). The glabella is slenderly conical without distinct glabellar furrows; the dorsal furrow is narrow and deeply impressed; the occipital ring is broadly convex and defined by the occipital furrow. A narrow and forward-arching anterior border is present. The convex fixigenae are about the same width as the glabella and have a pair of prominent palpebral ridges, which are directed laterally from the anterior lateral sides of the glabella. The small palpebral lobes are located in the anterior quarter of the cranidium. The posterior fixigenae are broad; the posterior lateral borders are narrow, separated by wide and deeply impressed furrows. The anterior branches of the facial sutures are convergent and the posterior branches are transverse, and divergent immediately from behind the palpebral lobe. The surface is finely granulose.

The skeletons of this stage differ from the skeletons of the previous ones by their triangular to trapezoidal cranidium, slender glabella, absence of anterior pits, and narrower fixigenae.

Late meraspid stage (Pl. 9, fig. 11, Text-fig. 41G). The cranidium is triangular in outline, convex, and about 1.00 mm long (sag.). The glabella is slenderly conical with three pairs of short glabellar furrows; the dorsal furrow is deeply defined; the occipital ring is broadly convex and bears a tiny median tubercle. The preglabellar field is narrow and convex; the anterior furrow is faint but has a median notch directed to the preglabellar field; the anterior border is narrow. The fixigenae are about one-half as wide as the glabella and bear a pair of pronounced palpebral lobes; the posterior fixigenae are broadly triangular, convex, and are deflected laterally. The surface is covered by fine granules.

This stage is characterized by the appearance of the preglabellar field, the anterior furrow with a median notch towards the preglabellar margin, and the narrower fixigenae.

Figured specimens. — Anaprotaspis, U.C.M. 38725a; metaprotaspids, U.C.M. 38725b, c; paraprotaspids, U.C.M. 38725d-h. early meraspids, U.C.M. 38725i, j; late meraspis, U.C.M. 38725k.

Family **RAYMONDINIDAE** Clark, 1924

Genus **CEDARINA** Lochman, 1940

Cedarina cordillerae (Howell and Duncan)

Plate 13, figs. 1-29, Text-fig. 42

Piemontia cordillerae Howell, and Duncan, 1939, p. 9, pl. 1, fig. 4.
Cedarina cordillearae (Howell and Duncan), Lochman, and Duncan, 1944, p. 89, pl. 17, figs. 1-10; Lochman, 1950, p. 347, pl. 50, figs. 20, 21.

Diagnosis. — Conical glabella having three pairs of faint, broad glabellar furrows. Occipital furrow steep-sided and deep. Occipital ring elevated with a large posteriorly directed median spine. Dorsal furrow distinct. Preglabellar field about one-third as long as glabella. Anterior border slightly narrower than preglabellar field. Fixigenae narrow, less than one-half the width (tr.) of the glabella. Palpebral lobes small, located in front of the mid-length of the glabella. Posterior lateral fixigenae broad laterally with border furrows curving forward before reaching lateral margin. Librigenae with long spines and strongly arched genal angles. Hypostoma subquadrate and bearing a strongly convex median body. Pygidium semicircular; four or five fused segments, with a flat, narrow marginal border.

Description. — The elongate triangular cranidium has cedarid form facial sutures. The conical glabella is rounded anteriorly and bear three pairs of faint glabellar furrows. The dorsal furrows are narrow and deeply impressed. The occipital furrow is shallow but steep-sided. The occipital ring is medium width and bears a small median node and a long posteriorly directed occipital spine. The preglabellar field is about one-third as long as the glabella and gently slopes downward to the broad anterior furrow. The anterior furrow arches forward but has a posteriorly directed median notch. The anterior border is broad and slightly convex. The flat to convex fixigenae are narrow and less than one-half as wide as the glabella. The small palpebral lobes lack distinct palpebral furrows and are located anteriorly from the mid-line of the glabella (tr.). The broad palpebral ridges curve posterior-laterally from the anterior-lateral edge of the glabella. The posterior margin of the fixigenae are broad. The wide posterior lateral furrows are shallow, but well-defined. The posterior borders are broad, about the same width as the occipital ring (tr.), and arch forward before reaching the lateral margins. The anterior facial sutures are convergently convex, and the posterior ones are divergently transverse.

The elongate librigenae are narrow with a narrow, slightly convex ocular platform. The marginal furrow is narrow and well defined; the marginal border is of medium width, convex, with a long, large genal spine.

The hypostoma is subquadrate with a rounded posterior margin; its median body is convex. The moderately convex posterior lobe is distinctly separated from the median body by a shallow, broad macular furrow.

The pygidium is narrowly transverse, its axial lobe is conical, tapering slightly posteriorly and divided into three or four axial rings and a terminal portion; the pleural lobes are almost flat, narrower than the axis, with three broad pleural segments. The marginal border is of medium width, flat, and lacking a marginal spine.

The outer surface is covered by fine granules; radial ridges are marked on the preglabellar field and ocular platforms; faint wrinkles are present along the skeletal margins. The inner surface is minutely punctate.

Remarks. — This species is represented by 75 immature and mature specimens. The adult cranidia can be separated into two groups: one with a narrower and longer glabella and the other with a broader and shorter one. These characteristics might indicate sexual dimorphism, but Lochman (1944) stated that there is still another form, *Cedarina prima* Lochman, without an occipital spine. She suggested that *C. prima* may represent a sexual variant. The writer agrees that these forms often do occur together, but in the present material no trilobite resembling *C. prima* has been found. For the time being, it seems best to consider that the broader glabella forms are male and the narrower ones female, because they exhibit bimodal discrepancies such as are commonly correlated with sexual dimorphism. The sexual ratio of the present species is 115.5.

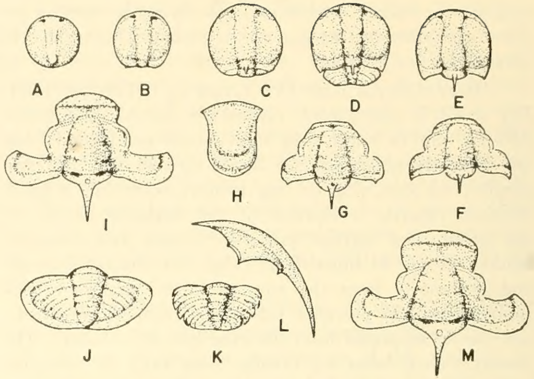

Text-fig. 42. — *Cedarina cordillerae* (Howell and Duncan). A. Anaprotaspis, x 52; B. Metaprotaspis, x 40; C,D,E. Three paraprotaspids, x 42, x 35, x 36; F. An early meraspis, x 26; G. A late meraspis, x 19; H. Hypostoma, x 8; I. A "female" cranidium, x 6; J,K. An adult and a juvenive pygidium, x 6.3, x 26; L. A librigena, x 2.7; M. "Male" cranidium, x 4.2. (Drawing made from photographs.)

The material comes from a fossiliferous, light-brown, medium-crystalline limestone, containing *C. cordilleare* more abundantly than *Apomodocia conica,* n. gen. and n. sp.; the inarticulate brachiopod, *Dicellomus* sp., is also common.

Horizon and locality. — Upper Cambrian, *Cedaria* zone. Locality unknown, Wasatch Mts., Utah.

Figures specimens. — Cranidia ("female"), U.C.M. 38731n, o, q, r. t; cranidia ("male"), U.C.M. 38731, p, s, u. librigena, U.C.M. 38731w; hypostoma, U.C.M. 38731v; pygidia, U.C.M. 38731z, a′, b′.

Cedarina cordillerae (Howell and Duncan), ontogeny

Anaprotaspid stage (Pl. 13, fig. 1, Text-fig. 42A). The shield is spherical in outline and about 0.26 mm in length (sag.). A pair of anterior pits, which suggest the orientation of the specimens, are located on the anterior-lateral margin of the shield. The axial and pleural lobes are not differentiated. The surface is nearly featureless except for the covering of fine granules.

Metaprotaspid stage (Pl. 13, figs. 2-4, Text-fig. 42B). The shield is subspherical, convex and about 0.40-0.50 mm long (sag.). The axial lobe is cylindrical but slightly expanding anteriorly. The anterior pits are rounded, distinct, and seated on the anterior lateral margin of the frontal lobe. The axial rings are not defined, but the terminal tubercle has appeared; it is small, rounded to subrounded, and located at the posterior margin of the shield. A pair of marginal spines project posterior-laterally from the rear margin of the shield. The surface is finely granulose.

This stage is distinguished from the anaprotaspid stage in having the axial and pleural lobes distinctly divided and by the subspherical shield.

Paraprotaspid stage (Pl. 13, figs. 5-8, Text-fig. 42C-E). The subspherical shield consists of a cephalon and protopygidium, and ranges from 0.48 to 0.60 mm in length. The axial lobe is clearly defined by dorsal furrows; no axial ring or ring furrows are seen, except for the occipital ring and the protopygidium. The axial lobe is cylindrical but slightly expanding at the mid-length and narrowing slightly both anteriorly and posteriorly. The pleural lobes are the same width as the glabella or slightly wider. The posterior lateral borders are directly backwardly and terminate in sharply pointed spines. The occipital ring is distinctly marked, transverse, oval, and convex. The protopygidium is transversely subtriangular and curves ventrally behind the posterior margin of the cephalon; the conical and posteriorly tapering axial lobe is divided into one or two axial rings; the pleural lobes are gently convex with two pairs of faint pleural furrows. No marginal spines are preserved. The surface is covered with fine granules.

In this stage the shield is characterized by a distinctly separate cephalon and protopygidium; the posterior lateral fixigenal borders are clearly defined.

Early meraspid stage (Pl. 13, figs. 9, 10, 26, Text-fig. 42F). The cranidium is trapezoidal in outline, moderately convex, and varies from 0.55-0.70 mm in length (sag.). The glabella is slenderly conical, tapering forward, without any distinct glabellar furrows. The occipital ring is definitely separated by an occipital furrow; the occipital spine is directed posteriorly. The anterior border is narrow and is adjacent to the anterior margin of the glabella; no preglabellar field is present. The anterior furrow arches forward and is distinct. The flat to gently convex fixigenae are of the same width as the glabella; their palpebral lobes are medium-sized and occur in front of the mid-line of the glabella (tr.); the posterior lateral fixigenae are transverse and broad; the posterior-lateral borders are narrow; the prominent palpebral ridges arch anteriorly and obliquely to the anterior lateral margin of the glabella. The facial sutures are convergently convex anteriorly and divergently transverse laterally. The pygidium consists of six or seven segments; the posteriorly tapering axial lobe is conical, and six or seven well-divided axial rings and ring-furrows; the pleural lobes are about the same width as the axial lobe; the pleural furrow is wide and deep; the interpleural grooves are narrow and distinct; the pleural bands terminate in a pair of short, broad, and posteriorly directed spines. The pygidium may consist of three segments.

This stage differs from the protaspid stage in that the cranidium is trapezoidal in outline, the glabella is slightly conical, the anterior border appears, and the pygidium develops a few thoracic segments.

Late meraspid stage (Pl. 13, figs. 11-13, 25, Text-fig. 42A). The cranidium is triangular in outline, moderately convex, and ranges from 0.80-1.40 mm long (sag.). The slender, forwardly tapering glabella has three pairs of distinct glabellar furrows; the dorsal furrow is narrow and distinct; the occipital ring is convex with a medium spine directed posteriorly. The anterior brim is divided by a well-defined anterior furrow into a narrow preglabellar field and anterior border. The fixigenae are narrower than the glabella and bear palpebral lobes located in front of the midline of the glabella (tr.). The pygidium is semicircular in outline and consists of three or four segments; there are no marginal spines. The surface is finely granulose.

The definitive features of this stage are as follow: The cranidium appears with a narrow preglabellar field; the fixigenae are narrower than the glabella; the glabella is proportionally shorter and broader; and the pygidium lacks marginal spines. The meraspid stage differs from the holaspid stage in that the meraspid cranidium has a slender glabella; the palpebral lobes are located anteriorly; the fixigenae are wider, and the preglabellar field is narrow. The pygidium of the holaspis is transverse whereas that of the late meraspid stage is semicircular.

Figured specimens. — Anaprotaspis, U.C.M. 38731a; metaprotaspids, U.C.M. 38731b-d; paraprotaspids, U.C.M. 38731e-h; early meraspids, U.C.M. 38731i, j, y; late meraspids, U.C.M. 38731k-m,x.

Family **CREPICEPHALIDAE** Kobayashi, 1935

Genus **CREPICEPHALUS** Owen, 1852

Crepicephalus deadwoodiensis, n. sp.

Plate 14, figs. 1-29, Text-fig. 43

Diagnosis. — Cranidium trapezoidal in outline, gently convex. Glabella regularly conical with three pairs of short shallow glabellar furrows. Eyes medium-sized and located at the mid-line of the glabella (tr.). Fixigenae and preglabellar field medium narrow. Anterior border generally the same width as preglabellar field and convex. Elongate librigenae moderately convex, with large genal spines. Pygidium subquadrate, transverse, gently convex with four or five axial rings. Pleural lobes slightly wider than axis. Indistinct marginal border with a pair of posterior lateral spines.

Description. — The moderately convex cranidium is trapezoidal in outline. The glabella is conical with a rounded frontal margin. The glabellar furrows are wide and shallowly impressed, all project posterior-medially from the dorsal furrows. The occipital ring is a posteriorly curved crescent bearing a minute tubercle; the occipital furrow is well marked, broad at the center and narrowing toward the sides. The dorsal furrow is deep and wide at the sides of the posterior half of the glabella and shallow across the anterior margin. The fixigenae are moderately narrow, about one-third as wide as the glabella and gently convex at the palpebral lobe area; the posterior lateral lobes are narrow with distinct posterior-lateral furrows and moderately narrow marginal borders. The gently convex preglabellar field is about one-third as long as the glabella and slopes downward toward the broad, shallow anterior furrow; the convex and forwardly arching anterior border is the same width as the preglabellar field; the narrow palpebral lobes are located at the mid-line of the glabella (tr.); they are strongly arched laterally and separated by distinct palpebral furrows. The facial sutures are opisthoparian in form; the anterior branches are convergently convex and the posterior ones are divergently sinuous, almost parallel to the posterior borders.

The elongate librigenae bear medium-sized genal spines; the ocular platform is moderately convex and gently downsloping towards the lateral border, which is broad and shallowly concave, extending posteriorly to meet the posterior furrow at the genal angle, then continuing onto the genal spine for a short distance; the convex lateral border is generally narrow, but widens slightly posteriorly.

The pygidium is rectangular, transversely broad, and convex; its axial lobe is slightly narrower than the pleural lobes and consists of four or five axial rings and a smaller terminal portion; the axial furrows are well defined, deeply marked laterally but shallow across the axis. The dorsal furrow is deeply impressed. The pleural lobes slope gently down from the axial lobe, and become flat towards the marginal border; there are three pairs of distinctly impressed pleural furrows, which are shallow and broad; all project posterior-laterally from the dorsal furrows. The marginal border is broad and flat, with an indistinct inner border furrow. A pair of caudal spines with broad bases and slender posterior taper project from the posterior-lateral border. The under side of the pygidium bears a broad and wrinkled doublure.

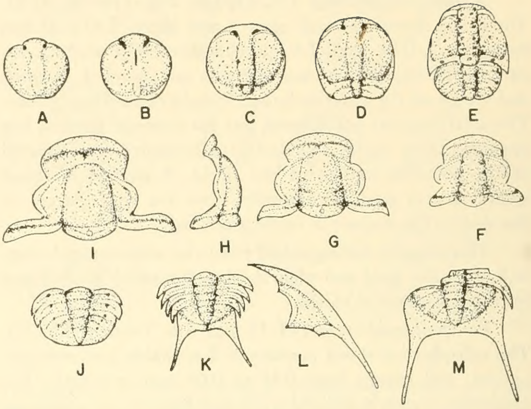

Text-fig. 43 — *Crepicephalus deadwoodiensis*, n. sp. A,B. Two anaprotaspids, x 65, x 68; C. Metaprotaspis, x 63; D. Paraprotaspis, x 40; E. An early meraspis, x 21; F,G. Two late meraspids, x 16, x 12; H,I. Top and side views of an holaspid cranidium, x 5.6; J,K,M. A growth sequence of pygidia, x 27, x 16, x 12; L. Librigena, x 17. (Drawings made from photographs.)

The skeletal surface is covered with fine granules; the preglabellar field is marked with ridges; and the lateral and anterior borders are ridged. The pygidial margin is finely impressed with wrinkles along the flattened border.

Remarks. — This species is represented by 15 adult cranidia and more than 80 immature specimens; all specimens were prepared from a few pieces of light-grey, calcareous interformational conglomerate. The largest cranidium is about 10 mm long and the smallest immature forms are about 0.25 mm long (sag.). The prepared specimens exhibit a continuous growth sequence. Both mature and immature forms are present within the intraformational conglomerate casts and the matrix, indicating that the conglomerate and the matrix formed contemporaneously.

This species is similar to *C. battsi montanensis* Lochman but differs in having a more rounded glabella, posteriorly located palpebral lobes, and shorter genal spines. It differs from the type species *C. iowensis* Owen, by possessing a wider anterior border, narrower posterior-lateral fixigenae, and shorter genal spines.

Horizon and locality. — Upper Cambrian, *Crepicephalus* zone, Deadwood Formation. Lead, northern Black Hills, Lawrence Co., South Dakota.

Figured specimens. — Holotype, cranidium, U.C.M. 38732; Paratype, cranidia, U.C.M. 38732z; librigena, U.C.M. 38732y; pygidia, U.C.M. 38732, u, w, x.

Cripicephalus deadwoodiensis, n. sp., ontogeny

Anaprotaspid stage (Pl. 14, figs. 1, 2, Text-fig. 43A, B). The spherical shield varies from 0.23 to 0.25 mm in length (sag.) and bears a pair of distinct anterior pits and short, broad posterior marginal spines, which suggest the orientation of the shield; the axial and the pleural lobes are not differentiated.

The smallest shield shows no features on the dorsal surface but the larger ones are marked with a longitudinal furrow along the axial region from behind the frontal lobe to the mid-line of the shield (tr.). A tiny elongate node occupies the extreme posterior end of the axial area.

The surface is finely granulose.

Metaprotaspid stage (Pl. 14, figs. 3-7, Text-fig. 43C). The spherical to subspherical shield varies from 0.30-0.40 mm long (sag.). The axial and the pleural lobes are distinctly divided by axial furrows; the axial lobe is fusiform, tapering both forward and backward from the mid-line of the axis (tr.), the axial rings are not well defined; the frontal lobe is delimited by a pair of distinct anterior pits; a pair of short broad supercilioid ridges extend from the posterior lateral margin of the frontal lobe. The occipital ring is delimited by a furrow. The convex pleural lobe is about one and one-half times wider than the axial lobe. A narrow flat fringe surrounds the posterior shield margin. The surface is finely granulose.

Paraprostaspid stage (Pl. 14, figs. 8-10, Text-fig. 43D). The shield is subspherical, about 0.45 to 0.80 mm in length (sag.), with well-differentiated cephalon and protopygidium. The cranidium is subrounded to subtriangular in outline, with distinct axial and pleural lobes; the anterior pits are shallow and disappear in the larger specimens; the frontal lobe tapers from the first segment of the glabella. The occipital ring is convex and transverse. A narrow inward-curving border appears along the anterior margin of the cranidium. The fixigenae are about one and one-half times wider than the glabella and bear a narrow and convex posterior lateral marginal border. The palpebral ridges are prominent; the palpebral lobes are located at one-fourth the length of the glabella (sag.) from the anterior end of the glabella. The facial sutures are present along the anterior-lateral margin and form a convergently convex outline. The protopygidium is transverse; two segments are recognizable. Three pairs of prominent nodes are marked longitudinally on the pleural lobes. The surface of the skeleton is covered with fine granules.

The distinct features of this stage are that the shield is differentiated into cephalon and protopygidium; the facial sutures are present on the dorsal surface; the anterior border is present along the anterior margin, and the fixigenae bear three pairs of large nodes.

Early meraspid stage (Pl. 14, figs. 11-13, 21, Text-fig. 43E). The cranidium is subtrapezoidal in outline and ranges from 1.00 to 1.40 mm in length (sag.). The glabella is cylindrical and gently rounded anteriorly; it lacks distinct glabellar furrows but bears three pairs of large glabellar nodes. The dorsal furrow is distinct. The occipital ring has a tiny median tubercle. The anterior border curves forward. The fixigenae are the same width as the glabella; the posterior-lateral fixigenae are broadly triangular, with borders projecting posterior laterally. The pygidium of three or four segments is semicircular in outline and is associated with three thoracic segments; the axial lobe is divided into three or four distinct rings by distinct ring furrows; the pleural lobes are convex and moderately sloping to the margin; three pairs of faintly marked pleural furrows are seen; the posterior marginal border is slightly recessed and flat.

The important characteristics of this stage are that the anterior border curves forward; the glabella becomes cylindrical; the fixigenae are narrower than those of the previous stage; the facial sutures extend directly to the glabella, and pygidium increases in number of segments.

Late meraspid stage (Pl. 14, figs. 14-17, 22, 23, Text-fig. 43F, G). The cranidium is subtriangular in outline and about 0.90 to 1.50 mm in length (sag.). The glabella is slightly cylindrical or conical, without distinct glabellar furrows. The occipital ring is crescentic, with a median tubercle. The dorsal furrow is distinctly marked. The anterior border is convex and about the same width as the preglabellar field; the anterior furrow is distinct and includes a median notch. The fixigenae are about one-half as wide as the glabella. The surface is finely granulose. The rectangular pygidium is preceded by three or four articulated thoracic segments, and has a pair of short caudal spines projecting posterior-laterally from the rear lateral margin; the axial lobe, which is conical, and tapering posteriorly, is divided into three rings by ring furrows; the pleural bands extend onto the broad and flat marginal border.

This stage differs from the previous one in that the glabella becomes conical; the fixigenae are narrower; the anterior border is wider; and the large pleural nodes have disappeared. The small pygidium is preceded by three to four articulatory thoracic segments and has a pair of short pygidial spines. The meraspis differs from the holaspis in having a slightly cylindrical glabella and wider fixigenae; the pygidium is larger and has a pair of longer pygidial spines.

Figured specimens. — Anaprotaspids, U.C.M. 38732a-b; metaprotaspids, U.C.M. 38732c-g; paraprotospids, U.C.M. 38732h, j; early meraspids, U.C.M. 38732k-m, r; late meraspids, U.C.M. 38732n-q, s, t.

Family **ALOKISTOCARIDAE** Resser, 1939

Genus **DUNDERBERGIA** Walcott, 1924

Dunderbergia ? **anyta** (Hall and Whitfield)

Plate 15, figs. 1-40, Text-fig. 44

Dunderbergia anytus (Hall and Whitfield), Resser, 1937, p. 9.
Dunderbergia ? anyta (Hall and Whitfield), Palmer, 1965, p. 39, pl. 4, figs. 8, 10, 14-16.

Diagnosis. — Cranidium trapezoidal in outline. Glabella truncate-conical with rounded anterior margin. Three pairs of faint glabellar furrows. Preglabellar field of medium width. Anterior border convex, about one-half as wide as preglabellar field. Fixigenae narrow, triangular. Hypostoma subquadrate with a medium-sized median body. Librigenae with wide ocular platform and medium-sized genal spine. Rostral plate transverse, with x-shaped outline. Thoracic segments of two different forms: short and long pleural spines. Convex, semicircular pygidium with axial and pleural lobes of the same width, and consisting of two or three segments.

Surface covered with fine granules; radial ridges marked on preglabellar field and ocular platform.

The taxonomic analysis of this species was given by Palmer (1965, p. 40) in detail and need not be repeated here. The present material can be segregated into two groups based on the convexity of the skeleton, width and length of glabella, and width of the pygidial margin.

Dunderbergia ? **anyta** (Hall and Whitfield), male?

Plate 15, figs. 18, 22, 24, 38, 40, Text-fig. 44K, S

Description. — The convex cranidium is trapezoidal in outline. The glabella is truncate-conical with a slightly rounded anterior margin and three pairs of faint, broad glabellar furrows. The dorsal furrow is deeply marked; a pair of pits is impressed on the anterior lateral convexity of the glabella. The narrow occipital furrow is distinct, composite, and branching laterally; the occipital ring is broadly convex and bears a tiny median node. The preglabellar field is one-third as long as the glabella (sag.). The anterior furrow arches forward; it is distinct and steep-sided laterally but becomes shallow across the axis. The convex anterior border is about one-half as wide as the preglabellar field. The fixigenae are flat to gently convex, and less than one-third as wide as the glabella. The palpebral lobes are sickle-shaped, distinctly divided by palpebral furrows, and located in front of the mid-line of the glabella (tr.). The palpebral ridges are faint, obliquely extended to the dorsal furrow, and terminate immediately behind the anterior lateral corners of the glabella. The posterior fixigenae are broad and triangular, with shallow posterior lateral furrows. The posterior lateral borders are convex, wider than the occipital ring and project slightly posterior-laterally. The anterior facial suture-lines are divergently straight to convergently convex at the anterior-lateral border. The posterior ones are divergently sinuate.

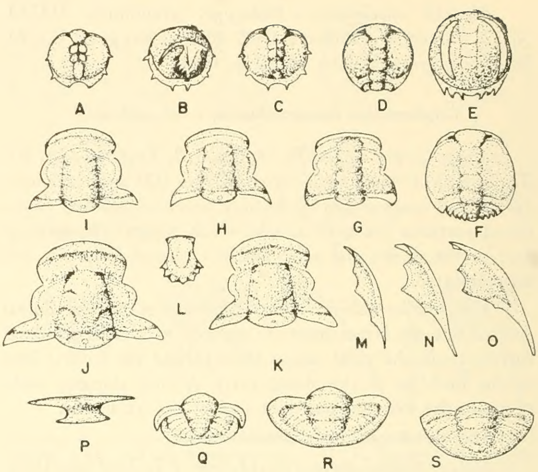

Text-fig. 44 — A growth sequence of ***Dunderbergia* ? *anyta*** (Hall and Whitfield). A. Anaprotaspis, x 58; B,C. Dorsal and ventral views of a metaprotaspis, x 50; D,E,F. Paraprotaspids, x 48, x 42, x 40; G. An early meraspis, x 20; H,I. Two late meraspids, x 14, x 12; J. "Female" cranidium, x 4; K. "Male" cranidium, x 7; L. An immature hypostoma, x 46; M-O. A growth series of librigenae, x 16, x 8, x 3.5; P. Prostrum, x 8; Q. An immature pygidium, x 26; R. "Female" pygidium, x 18; S. "Male" pygidium, x 16. (Drawings made from photographs.)

The librigenae bear long, slender genal spines. The lateral and posterior furrows are not clearly joined at the genal angle. The anterior tip of the doublure is blunt which suggests that the rostral plate has deep, semiparabolic lateral notch (fig. 23). The platform is convex and moderately broad.

The moderately convex pygidium is semicircular in outline. Its axial lobe is broadly conical and tapers slightly backward, divided into two axial rings and a broad terminal portion. The flat to moderately convex pleural lobes are wider than the axis (tr.), and have three pairs of shallow, broad pleural furrows. The marginal furrow is narrow and concave, delimiting a narrow and slightly convex marginal border.

The skeletal surface is covered by fine granules; radial ridges are marked on the preglabellar field and the ocular platform of the librigenae, and fine wrinkles surround the marginal border of the pygidium.

Dunderbergia ? anyta (Hall and Whitfield), female?

Plate 15, figs. 19-21, 25, 36, 39, Text-figs. 44 J, R

Comparison. — In the presumed female form the glabella is narrower and longer than that of the male; the librigenae have narrower platforms and less strongly arched lateral borders; the pygidium is less convex, with a slightly wider marginal border and a median notch on the posterior margin.

Remarks. — This species is represented by a few hundred immature and mature specimens, all of which were etched from a single piece of dark-grey, medium-crystalline limestone. The material also contains *Dytremacephalus granulosus* and a few inarticulate brachiopods. The smallest immature specimen is about 0.25 mm long (sag.) and has four distinct axial rings and a longitudinal fissure marked along the central axis. These are the significant structures which are also seen in some of the other species described in this report. The larger cranidia, librigenae, and pygidia are morphologically divided into two groups, which have been judged sexual dimorphism. The sexual ratio varies 115.

Horizon and locality. — Upper Cambrian, *Dunderbergia* zone, Wah Wah Range, Millard and Beaver Cos., Utah (U.S.G.S. Coll. No. 5503-CO).

Figured specimens. — "Male" form: cranidia, U.C.M. 38733o,t; librigena, U.C.M. 38733v; pygidia, U.C.M. 38733j, l′; rostrum, U.C.M. 38733u; "Female" form: cranidia, U.C.M. 38733p, 38733, 38733r; librigena, U.C.M. 38733w; pygidia, U.C.M. 38733h′,k′; hypostoma, U.C.M. 38733b′.

Dunderbergia ? anyta (Hall and Whitfield), ontogeny

Anaprotaspid stage (Pl. 15, fig. 1, Text-fig. 44A). The shield is spherical, about 0.25 mm in length (sag.), and has three pairs of marginal spines. The axial lobe is fusiform, both ends taper anteriorly and posteriorly from the second pair of axial nodes. The small frontal lobe is delimited by a pair of distinct anterior pits. The second and third axial rings are formed by two pairs of central axial nodes. The fourth axial ring is subtriangular, and its posterior end is located at posterior margin of the shield. A narrow longitudinal fissure is marked along the central axis. The dorsal furrows are faint. The pleural lobes are about as wide as the axial lobe. The first pair of marginal spines are located at one-third of the total length from the anterior margin; they extend horizontally and laterally. The second pair of marginal spines are short and project posteriorly and laterally from a point two-thirds of the cephalic length posteriorly from the anterior margin. The third pair of marginal spines is short and strong, and project posteriorly from the posterior lateral bases of the terminal axial ring. The surface is covered by fine granules.

Metaprostaspid stage (Pl. 15, figs. 2-6, Text-fig. 44B, C). The convex shield is rounded, about 0.27 to 0.35 mm in length (sag.), and bears three pairs of marginal spines. The axial and pleural lobes are sharply divided by dorsal furrows. The axial lobe is slenderly fusiform but with an expanded frontal lobe. The large frontal lobe is delimited by a pair of anterior pits and dorsal furrows. The second, third, and fourth axial rings are formed by three pairs of axial nodes. The terminal ring is smallest. A longitudinal fissure is marked along the axis. The pleural lobes are about twice as wide as the glabella and are convex with a slightly flat marginal border. The first pair of marginal spines is located in front of the mid-line of the shield (tr.); they are short, with broad bases and project laterally or posterior-laterally. The second pair of marginal spines is shorter than the first; they extend posterior-laterally from points two-thirds of the cephalic length posteriorly from the anterior margin. The third pair of spines project posteriorly from the posterior margin of the pleural lobes; they are short with broad bases. The narrow posterior marginal border is medially notched.

The underside of the shield shows a narrow rostral plate with a spiny hypostoma anteriorly and broad doublure posteriorly. The narrow rostral plate is perrostral in form, and its posterior projections in front of the third pair of marginal spines, where the doublure appears. The hypostoma is broadly fusiform with a fused rostral plate anteriorly and spiny margin posteriorly; the triangular median body is narrow with distinct lateral furrows; the first pair of marginal spines is broad, short; they extend laterally from the mid-length of the hypostoma (tr.). The second and third pairs are short, and project posteriorly and laterally along the posterior lateral margin. The terminal spine is longer and extends posteriorly from the axial line. The doublure is broad and rounded along the posterior margin of the shield from the first pair of marginal spines.

The surface of the shield is finely granulose.

The characters of this stage which are different from those of the early ones are the presence of five rings on the axial lobe, and the larger frontal lobe.

Paraprotaspid stage (Pl. 15, figs. 7-12, Text-fig. 44 D -F). The shield is spherical in outline and ranges from 0.40-0.60 mm long (sag.). The cylindrical glabella is composed of four distinctly separated rings; the first ring, or frontal lobe, is large and expanded anteriorly; the second to fourth ones are transverse, oval, and uniform. The occipital ring is convex, oval, and separated by occipital furrows. The elongate anterior pits are shallowly impressed in the dorsal furrows and delimited by a pair of short, laterally projecting eyebrow-shaped ridges from the anterior lateral margin of the frontal lobe. The pleural lobe are approximately one and one-half times as wide as the glabella; the posterior borders are well defined and project posterior-laterally. The protopygidium is subtriangular, with one or two axial rings and sharp, laterally directed pleural spines. The underside of the shield shows a narrow doublure along the protopygidial margin. The hypostoma has reduced marginal spines and a widened median body. The surface is covered by fine granules.

This stage is characterized by the appearance of the protopygidium, the fusion of the axial nodes, and the separation of the rostral plate, librigenae, and hypostoma.

Early meraspid stage (Pl. 15, figs. 13,14,27,28,33, Text-fig. 44G.). The cranidium is trapezoidal in outline and varies from 0.70-1.00 mm in length (sag.). The glabella is cylindrical or slightly constricted at the second glabellar ring. The glabellar rings are all nearly of the same form and separated by shallow glabellar furrows. The glabellar furrows are shallow across the central axis and steep-sided. The dorsal furrows are distinct. The convex occipital ring is crescentic and arches posteriorly. The narrow anterior border appears; it is convex and curves anteriorly. The palpebral lobes are narrow, distinctly divided by palpebral furrows, and located in front of the mid-line of the glabella (tr.). The fixigenae are of about the same width as the glabella. The posterior fixigenae are broad; the posterior borders with their lateral ends directed posterior-laterally. The elongate librigenae each have a narrow ocular platform and a medium-sized genal spine. The hypostoma is about 1.2 mm in length, with an elongate, oval median body; the lateral furrows are deep and narrow. The posterior lobe is U-shaped and broadly convex; the marginal border is narrow and separated by distinct marginal furrows; the first lateral marginal spines are larger and stouter than the following ones, which occur at the lateral margins of the mid-line of the hypostoma (tr.); the posterior marginal spines are small and are located along the posterior marginal border. The pygidium is approximately 1.2 mm in length and bears five or six marginal spines; the axial lobe is divided into five or six axial rings; the pleural lobes are separated into pleural bands by distinct interpleural grooves; the marginal spines extend continuously from the pleural bands; they are turned upward and project posterior-laterally. The pygidium may connect to a few articulated thoracic segments. The surface of the skeleton is covered by moderately large granules.

The definitive characteristics of this stage are: the cranidium has a narrow anterior border; the glabella is cylindrical; the fixigenae are the same width as the glabella; the librigenae are narrower and the pygidial segments are preceded by a few thoracic segments.

Late meraspid stage (Pl. 15, figs. 15-17,26,29,34,35,37, Tex-fig. 44H, I). The cranidium is trapezoidal in outline, about 1.20-1.80 mm in length (sag.). The glabella is conical and marked by three pairs of distinct glabellar furrows. The dorsal furrows are narrow and distinct. The preglabellar field is about the same width as the anterior border. The fixigenae are narrower than the glabella. Each librigenae has a narrow ocular platform. The pygidium bears a conical axial lobe, which is divided by ring furrows; a median notch at the posterior margin. The surface is finely granulose, and radial ridges are marked on the preglabellar field.

The specimens of this stage are distinguished from those of early forms in that the cranidium has a conical glabella, the preglabellar field appears, the fixigenae are narrower than the glabella, and each librigena has a broad ocular platform; the pygidium shows the general outline seen in the holospid pygidium, except that a median notch is marked at the posterior margin, and the pygidium is preceded by one or two thoracic segments.

Figured specimens. — Anaprotaspis, U.C.M. 38733a; metaprotaspids, U.C.M. 38733b-e; paraprotaspids, U.C.M. 38733f-j; early meraspids, U.C.M. 38733k, l, y, z, e′; late meraspids, U.C.M. 38733m, n, o, x, a′, f′, g′, i′.

Family **PTEROCEPHALIIDAE** Kobayashi, 1935

Genus **DYTREMACEPHALUS** Palmer, 1954

Dytremacephalus granulosus Palmer

Plate 16, figs. 1-36, Text-fig. 45

Dytremacephalus granulosus Palmer, 1954, p. 750, pl. 85, figs. 5, 6; 1965, p. 85, pl. 18, figs. 14, 16-19, 21.

Diagnosis. — Cranidium trapezoidal in outline. Glabella broadly conical with three pairs of glabellar furrows. Occipital ring bearing a short median spine. Preglabellar field moderately narrow. Anterior border about the same width as preglabellar field. Fixigenae about one-third as wide as glabella. Palpebral lobe situated in front of the mid-line of glabella (tr.). Anterior facial suture lines convergently convex, and posterior facial suture lines divergently straight. Each librigena with broad ocular platform and short genal spines. Pygidium highly convex, semicircular in outline, having broadly conical axial lobe. Surface covered by moderately large granules.

Dytremacephalus granulosus Palmer, male?

Plate 16, figs. 21,23,25,26,28,35, Text-fig 45L, N

Description. — The cranidium is trapezoidal in outline. The glabella is broadly conical, with three pairs of well-defined glabellar furrows. The occipital furrow curves slightly backward and is deeply impressed laterally. The occipital ring is crescentic and has a short prominent median tubercle. The preglabellar field is steeply declined and strongly depressed laterally. The anterior furrow is shallow and broad. The anterior border is arched forward, convex, and about the same width as the preglabellar field. The flat to slightly convex fixigenae are approximately one-third as wide as the glabella. The palpebral lobes are well defined by palpebral furrows, located in front of the mid-length of the glabella (tr.). The posterior lateral fixigenae are convex and triangular. The posterior borders are more than one-half as wide as the occipital ring (tr.). The anterior branches of the facial sutures are convergently straight, and posterior branches are gently divergent.

Each librigena has a broad ocular platform. The lateral furrow is shallow, wider, and becomes obsolete posteriorly before meeting the rear border furrow. The lateral border is roundly convex and has a long and sharply pointed anterior projection. The doublure is the same width as the lateral border. The posterior border furrow is deep but shallow towards the genal angle. The genal spine is short and sharply pointed posterior-laterally.

The thoracic segments are highly convex; their axial rings are slightly narrower than the pleural lobes and deeply separated by ring furrows. The anterior half-ring is crescentic, convex and arching forward. The posterior ring is delimited by a ring furrow and is about the same width as the half-ring. Each pleural lobe is flat laterally for a short distance and slopes steeply downward to form a long and sharply pointed pleural spine.

The pygidium is semicircular in outline; the dorsal lobe is divided into two axial rings and a large terminal portion. The pleural lobes are narrower than the axis and moderately convex anterior-laterally, and progressively deflect posteriorly. The flat marginal border is of medium width and delimited by a poorly defined inner marginal furrow; the pleural lobes are shallowly impressed by two or three pleural furrows; all curve posteriorly and laterally to reach the inner edge of the border.

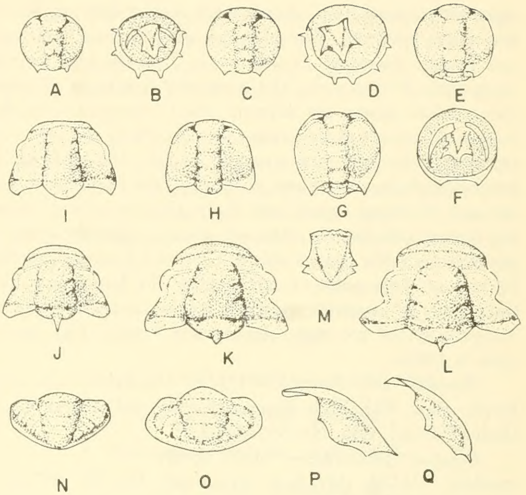

Text-fig. 45 — *Dytremacephalus granulosus* Palmer. A. Anaprotaspis, x 56; B,C. Ventral and dorsal views of two metaprotaspids, x 55; D. Ventral view of a metaprotaspis, x 58; E,F,G. Ventral and dorsal views of two paraprotaspids, x 62, x 50; H. A late paraprotaspis, x 42; I. An early meraspis, x 25; J. A late meraspis, x 15; K. A "female" cranidium, x 9; L. A "male" cranidium, x 10; M. An immature hypostoma, x 15; N. A "male" pygidium, x 13; O. A "female" pygidium, x15; P,Q. Juvenile and adult librigenae, x 9, x 22. (Drawings made from photographs.)

The surface of the skeleton is covered by moderately large granules; ridges occur along the anterior cephalic margin.

Dytremacephalus granulosus Palmer, female?

Plate 16, figs. 20, 22, 27, 36, Text-fig. 45 K, O

Comparison. — The presumed female specimens differ from those of the males in having a narrower conical glabella with a rounded anterior margin; each librigena has a wider ocular platform, and the triangular pygidium has a narrower marginal border.

Remarks. — A few hundred immature and mature specimens were etched from a small piece of dark-grey, medium-crystalline limestone. The material also contains immature and mature forms of *Dunderbergia* ? *anyta* and several inarticulate brachiopods. The immature specimens of these two trilobite genera are different when compared with the same sized instars of the present species: those of *Dytremacephalus granulosus* are strongly convex, the glabella is marked with four complete axial rings, the hypostoma has one pair of lateral spines, and the pygidial marginal spines are shorter and broader; whereas, those of *Dunderbergia* ? *anyta* have a low convex shield; the axial lobe is occupied by two or three pairs of axial nodes; the hypostoma has three pairs of posterior marginal spines; and the pygidial marginal spines are more slender and longer. The sexual ratio is 135.6.

Horizon and locality. — Upper Cambrian, *Dunderbergia* zone, Wah Wah Range, Millard and Beaver Cos., Utah (U.S.G.S. Coll. No. 5503-Co.).

Figured specimens. — "male" form:
cranidia, U.C.M. 38734s,v; pygidium, U.C.M. 38734g′; librigena, U.C.M. 38734z; thoracic segments, U.C.M. 38734 w, x.

"female" form: cranidia, U.C.M. 38734r,t; pygidium, U.C.M. 38734h′; librigena, U.C.M. 38734y.

Dytremacephalus granulosus Palmer, ontogeny

Anaprotaspid stage (Pl. 16, fig. 1, Text-fig. 44A). The highly convex shield is rounded to subrounded in outline, with well-marked dorsal furrows. It is about 0.23 to 0.25 mm long (sag.). The axial lobe is divided into four axial rings by well-defined transverse furrows; the frontal lobe is large, convex, and delimited by a pair of anterior pits; the lateral margin of the frontal lobe is continuous with a pair of supercilioid ridges; the second and third rings are transversely subrounded; the terminal one is rounded; a minute ridge extends along the central axis. The pleural lobes are convex and slightly wider than the glabella (tr.). The presumed marginal spines are not preserved. The surface is covered by fine granules.

Metaprotaspid stage (Pl. 16, figs. 2-6, Text-fig. 44 B, C). The shield is rounded, convex, and approximately 0.26-0.27 mm long (sag.). It bears three pairs of marginal spines and the surface is well divided into axial and pleural lobes by distinct dorsal furrows. The axial lobe consists of five rings; the frontal lobe is triangular with a pair of eyebrow-shaped ridges projecting laterally and posteriorly from the anterior lateral margin; the second, third, and fourth rings are transversely subrounded and of subequal size; the posterior one is the smallest. The anterior pits are well defined and elongated along the sides of the frontal line. The convex pleural lobes slope downward toward the narrow marginal border. The hypostoma is elongately pentagonal in outline, with a straight anterior margin, and a pair of stout lateral spines projecting posterior-laterally; the median body is elongate-triangular, defined by lateral furrows. The underside of the shield is surrounded by a narrow, rounded doublure along the posterior half of the shield margin. The surface is covered by fine granules; the pleural lobes are marked with a few pairs of minute transverse furrows, which possibly are the vestigial cephalic segmental furrows (fig. 5).

Paraprotaspid stage (Pl. 16, figs. 7-14, Text-fig. 45E-G). The shield is spherical ranging from 0.29 to 0.40 mm in length (sag.), and having three pairs of marginal spines at the shield margin (fig. 8). The pleural and axial lobes are divided by dorsal furrows; the cylindrical axial lobe is only slightly expanded forward; the large frontal lobe is convex and expanded forward with a pair of narrow supercilioid ridges projecting laterally from the anterior lateral margin. The second to fourth axial rings are transverse and are all of subequal size; the terminal ring is small. The elongate anterior pits are located along the dorsal furrows at the posterior lateral margin of the frontal lobe. The pleural lobes are convex and about one and one-half times as wide as the glabella. The first pair of marginal spines is located on the anterior-lateral margin of the shield; the second ones are located laterally; the third are situated posteriorly and project from the extreme ends of the posterior lateral border. The protopygidium is transversely subtriangular with one or two segments. The underside of the shield exhibits the perrostral plate and hypostoma anteriorly and the narrow doublure along the posterior margin of the protopygidium. The surface is covered by fine granules.

The specimens of this stage are subspherical with well-defined cephalic and pygidial shield; the larger specimens possess only one pair of spines which are at extreme ends of the posterior lateral border of the cephalon; the transverse pleural furrow and the axial ridge are absent.

Early meraspid stage (Pl. 16, figs. 15-17,24,29-32, Text-fig. 45I). The cranidium is trapezoidal in outline, highly convex, with a well-defined anterior border and facial sutures. It varies from 0.50-0.80 mm in length (sag.). The glabella varies from cylindrical to slightly conical. It is divided into three glabellar segments by complete glabellar furrows; the glabellar furrows are shallow, faint, and directed slightly postero-medially from the dorsal furrows; the occipital ring is broadly convex and crescentic with a tiny median tubercle. The anterior border is narrow, arching forward, and sharply defined by the anterior furrow. The dorsal furrow is distinct. The convex fixigenae are subequal in width to the glabella. The posterior-lateral fixigenae are broad, well defined by border furrows and borders; the width (tr.) of the posterior border corresponds with the width (tr.) of the occipital ring; the narrow, elongated palpebral lobes are located at the first pair of glabellar furrow in the smaller specimens but move posteriorly to the second glabellar in the larger ones. The facial suture lines are convergently straight anteriorly and divergently straight posteriorly from the palpebral lobes. The convex hypostoma is elongate-pentagonal; its anterior margin is straight or slightly arching forward; the lateral spines are located slightly posteriorly from the mid-length of the median body. They extend laterally and slightly posteriorly. The posterior marginal border is convex posteriorly; the median body is narrowly triangular, convex, wedge-shaped, and sharply pointed posteriorly to the posterior margin; the lateral furrows are distinct, deeply marked at the mid-length, and shallow both anteriorly and posteriorly. Each librigena is narrow with an ocular platform of almost uniform width; the genal spine is short and broad, projecting posterior laterally. The pygidium is transversely subspherical with a narrow, convex axial lobe and wider pleural lobes; the axial lobe of six or seven axial rings is conical and tapers sharply posteriorly. The pleural lobes are moderately convex, broad, each having pleural bands running slightly posterior-laterally and ending with a broad terminal spine; the pleural furrow is broad and shallow, and the interpleural grooves are minute. The surface is covered with fine granules. The pygidial axis bears a small tubercle on each ring.

The specimens of this stage are characterized by a forward-tapering glabella, well-separated glabellar segments, distinct anterior border, pygidium preceded by two or three articulated thoracic segments, and librigenae of uniform width posteriorly and anteriorly.

Late meraspid stage (Pl. 16, figs. 18,19,33,34, Text-fig. 45S. The cranidium is trapezoidal in outline and about 1.0 to 1.5 mm in length (sag.). The glabella is conical with a rounded frontal margin; the glabellar furrows are impressed, except for the first pair which are faint. The occipital ring is broad with a tiny median spine extending posteriorly. The fixigenae are about one-half as wide as the glabella but have broad posterior lateral portions. The palpebral lobes are small and located next to the second glabellar furrows (tr.). The palpebral ridges are prominent and project obliquely to the anterior-lateral margin of the glabella. The facial suture lines are convergently straight anteriorly and divergently straight posteriorly. The pygidium is transversely semicircular and has a median notch at the posterior margin. It is associated with one or two thoracic segments. The surface is covered by distinct granules.

This stage differs from the previous one in having a slender, conical glabella, the palpebral lobes located at the level of the second glabellar furrow, a narrow preglabellar field, the pygidium separated from the cephalon by one or two thoracic segments, and a notch at the posterior margin.

Figured specimens. — Anaprotaspis, U.C.M. 38734a; metaprotaspids, U.C.M. 38734b-e; paraprotaspids, U.C.M. 38734f-l; early meraspids, U.C.M. 38734m-o, u, a′-d′; late meraspids, U.C.M. 38734p, q, e′, f′.

Family **PTYCHASPIDIDAE** Raymond, 1924

Genus **PTYCHASPIS** Hall 1863

Ptychaspis bullasus Lochman and Hu

Plate 17, figs. 1-34, Text-fig. 46

Ptychaspis bullasa Lochman, and Hu, 1959, p. 422, pl. 58, figs. 21-42; Bell, and Ellinwood, 1962, p. 405, pl. 58, figs. 14-17.

Diagnosis. — Convex cranidium trapezoidal in outline. Glabella nearly parallel-sided, with rounded frontal margin and two transverse glabellar furrows. Occipital ring crescentic and convex, bearing a median tubercle. Frontal margin narrow and strongly convex. Fixigenae convex, about one-third as wide as glabella. Palpebral lobes located in front of the mid-length of glabella. Posterior fixigenae broadly triangular. Librigenae elongate with a broad-based genal spine. Hypostoma narrow, elongate, with a convex median body and broad triangular wings. Pygidium narrowly transverse, with broad axial lobe and narrow vertically upturned marginal border. Surface densely granulose with large granules, and well-elevated ridges are marked along the skeletal margin.

Description. — The cranidium is trapezoidal in outline with a rounded anterior border. The dorsal furrows are deeply impressed and broad. The glabella is broadly cylindrical, convex, long, nearly parallel-sided with a rounded anterior margin. The first pair of glabellar furrows is faint; the second and third ones are transverse, deeply impressed laterally but shallow across the central axis. The occipital ring is crescentic with a small median node; the occipital furrow is broad and deep. The frontal area is narrow, convex, and steeply declined; the anterior margin is vertical with a blunt median point. The fixigenae are horizontal, slightly convex and more than half as wide as the glabella;

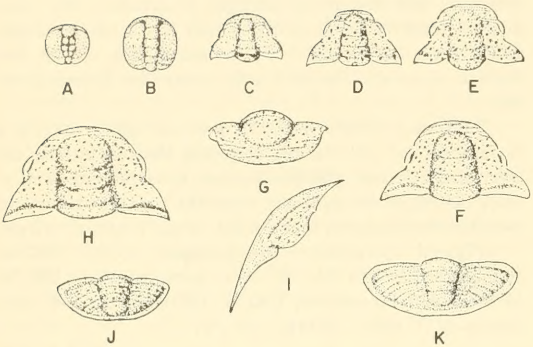

Text-fig. 46 — *Ptychaspis bullasus* Lochman and Hu. A. Metaprotaspis, x 45; B. Paraprotaspis, x 35; C,D. Two early meraspids, x 20, x 13; E. A late meraspis, x 12; F,G,H. Three holaspids, x 8.6, x 3, x 2.7; I. Librigena, x 6.6; J,K. A small and a larger-sized pygidium, x 8, x 3. (Drawings made from photographs.)

the small and narrow palpebral lobes are separated by deeply marked palpebral furrows situated opposite the anterior one-third of the glabella. The posterior fixigenae are broadly triangular, and extend slightly posterior-laterally; the narrow posterior-lateral borders are defined by broad posterior-lateral furrows; the width (tr.) of the rear lateral border is the same as that of the occipital ring (tr.).

Each librigena is elongate with an ocular platform bearing a small ocular ring; the lateral and posterior furrows join at an acute angle, where they are shallow; they are deeper anteriorly and laterally; the convex lateral border is of medium width and gently deflected along the margin; it is continuous posteriorly with a long and broad-based genal spine.

The pygidium is transversely semicircular in outline and moderately convex; the axial lobe is broad, parallel-sided to slightly tapering backward and divided into three well-marked axial furrows and a broad terminal portion, which has a pair of nodes on the posterior lateral margin. The pleural lobes are broad, with three shallow but well-defined pleural furrows and the same number of narrow interpleural grooves. The marginal border is narrow and upturned vertically; the posterior marginal border is slightly indented medially.

The surface is covered by large granules, except in the furrows and well-elevated, irregular ridges are marked along the skeletal margin.

Remarks. — This species is represented by more than 30 adult and 20 immature specimens. The materials are those described in 1959 by Lochman and Hu. The present work attempts a more detailed analysis of the ontogenetic development of the species. The materials also contain some meraspids of *Minkella ("Saratogia") americana* (Lochman and Hu) and *Idahoia wisconinensis* (Owen). The differences between them are obvious. The present species has a more convex shield, a more slenderly conical or nearly fisiform glabella, and broader fixigenae, whereas those of the other two genera have less convex cranidium, cylindrical glabella, and narrower fixigenae.

Horizon and locality. — St. Charles Formation, Upper Cambrian, *Ptychaspis-Prosaukia zone.* North of Mink Creek, Preston Quadrangle, Idaho.

Figured specimens. — Cranidia, U.C.M. 38735, 38735 m-s; Librigenae, U.C.M. 38735t-v; Pygidia, U.C.M. 38735y, z and U.S.N.M. 137100h.

Ptychaspis bullasus Lochman and Hu, ontogeny

Metaprotaspid stage (Pl. 17, fig. 1, Text-fig. 46A). The shield is about 0.24 mm in length with separate axial and pleural lobes. The axial lobe is composed of a big frontal lobe, three pairs of axial nodes, and a small terminal ring; the frontal lobe is rounded and convex, delimited by a pair of deeply marked anterior pits on its anterior-lateral margins; the three pairs of axial nodes are divided by longitudinal fissure along the axis and transverse furrows across the axis; a small terminal tubercle is present near the posterior margin of the shield. The pleural lobes are convex and gently down-sloping toward the marginal border. The surface is covered by fine granules.

Paraprotaspid stage (Pl. 17, figs. 2-4, Text-fig. 46B). The shield is spherical to subspherical in outline and about 0.28 to 0.45 mm in length (sag.). The axial lobe is delimited by dorsal furrows and is cylindrical to slightly fusiform; it is composed of five axial rings and a small protopygidial ring; the glabellar or axial rings are transverse, oval, convex, and connected by a faint median ridge along the central axis; the anterior pits are shallower than in the metaprotaspis but well defined. A narrow border appears along the anterior margin of the shield. The pleural lobes are the same width as the glabella, and marked by a pair of distinct palpebral lobes at the anterior lateral margin. The posterior-lateral borders extend laterally from the sides of the occipital ring with a pair of posteriorly directed spines at the extreme ends. The protopygidium is narrow, transverse, and curves ventrally from the posterior cephalic margin; one or two segments may be present, but the nature of the pleural lobe is obscure.

This stage is distinguished from the previous one in that the three pairs of axial nodes are fused together to form three axial rings; the anterior border and palpebral ridges are recognizable, and the protopygidium appears.

Early meraspid stage (Pl. 17, figs. 5-7,29,30, Text-fig. 46C, D). The cranidium varies from 0.50-1.00 mm in length (sag.), is trapezoidal in outline with a rounded anterior border. The axial lobe tapers slightly forward and is subhemicylindrical in configuration; the first axial ring furrow is faint, but the following furrows are deeper, wider, and strongly impressed laterally. The occipital ring is deeply separated by the occipital furrow and bears a median spine. The pleural lobe is narrow and triangular with palpebral lobes located opposite (tr.) the first glabellar furrows; the posterior lateral borders are delimited by border furrows and have posterior-lateral projections. The pygidium consists of six or seven segments with short blunt marginal spines; it may retain a few articulated thoracic segments. The surface is densely covered with large granules.

The distinguishing characteristics of this stage are: the somewhat conical axial lobe with three long axial rings anteriorly and two short ones posteriorly (sag.).

Late meraspid stage (Pl. 17, figs. 8-13,26,27,31, Text-fig. 46 E). The trapezoidal cranidium is about 1.1-1.80 mm in length (sag.). The glabella is conical with a rounded frontal margin. The first pair of glabellar furrows is faint, shallow, and separated. The second and third ones are deeper and extend slightly backward. The occipital furrow is as deep and as wide as the third glabellar furrow; the occipital ring is convex and bears a median tubercle. The narrow fixigenae are divided by palpebral furrows and located opposite (tr.) the second glabellar furrows. The librigena is broad, crescentic, with lateral and posterior furrows, connected at the genal angle; the genal spine is short with a broad base. The pygidium is subtriangular in outline, and has the axial and pleural lobes divided into three segments by furrows; the pleural lobes are broad and deep; the interpleural grooves are narrow and minute.

The surface is covered by large granules, and irregular ridges are marked along the anterior cephalic margin and ocular platform.

In comparison, the skeleton of this stage differs from those of early ones in that the glabella is wider and shorter; the pygidium is generally of holaspid shape. The meraspid specimens differ from holaspis forms by their conical glabella, palpebral lobes located at the second glabellar furrow (tr.), and librigenae with wider ocular platforms and shorter genal spines. The pygidium lacks a posterior median notch and is semicircular.

Figured specimens. — Metaprotaspis, U.C.M. 38735a; paraprotaspids, U.C.M. 38735b-d; early meraspids, U.C.M. 38735e-f, w, x; U.S.N.M. 137100a; late meraspids, U.C.M. 38735g-l, q.

Family **OLENIDAE** Burmeister, 1843

Genus **OLENUS** Dalman, 1827

Olenus gibbosus (Wahlenberg)

Plate 18, figs. 1-32, Text-fig. 47

Entomostracites gibbosus Wahlenberg, 1821, p. 39, pl. 1, fig. 4 only.
Olenus gibbosus (Wahlenberg), Angelin, 1878, p. 55, pl. 25, fig. 5; Strand, 1927, pp. 320-329, pl. 2, figs. 1-14d; Størmer, 1942, pl. 81, figs. 9a-e, 10a-e; Henningsmoen, 1957, p. 105, pl. 1, fig. 1, pl. 3; pl. 9, fig. 7.

Diagnosis. — Cranidium trapezoidal in outline, moderately convex with a truncate-conical glabella. Dorsal furrow deeply impressed. Fixigenae broad with the palpebral lobe located at the mid-length of cranidium. Librigena of medium width; genal spine continuous with course of lateral margin. Pygidium subtriangular with one or two pairs of marginal spines and five or seven axial rings. Hypostoma subquadrate in outline, with a large convex median body.

Description. — The trapezoidal cranidium is moderately convex; the glabella is truncate-conical, tapering slightly forward, with three pairs of oblique lateral furrows; the preglabellar field is gently convex, more than one-half the length of the glabella (sag.); the anterior border is narrow and separated by a distinct anterior furrow; the fixigenae are broad and more than one-half the width of the glabella (tr.); the palpebral lobes are moderately small and located slightly in front of the mid-line of the glabella (tr.); the palpebral ridges are at a right angle to the anterior-lateral corners of the glabella; the occipital ring bears a small node. The librigena bears a broad ocular platform and a medium-sized genal spine. The convex and elongate hypostoma is subquadrate in outline and has a large median body. The flat pygidium is triangular in outline and has five to seven axial rings and furrows; the pleural lobe is flat, gently upturned from the dorsal furrow, with well-developed pleural furrows; a pair of marginal spines extend from the anterior-lateral corners of the pygidium.

The surface of the skeleton is covered by fine granules, and minute radial ridges occur on the preglabellar field and the platforms of the librigenae.

Remarks. — The ontogeny of this species was first established by Strand (1927) and subsequently re-examined by Størmer (1942). The material here studied was collected by K. E. Caster during a field trip of the International Geologic Congress, 1962. More than 90 immature and mature skeletons have been freed from a small piece of fossiliferous bituminous limestone. The smallest specimen is 0.27 mm long and the largest cranidium about 15.0 mm in length.

Størmer's observation that the earliest instars have the cephalic segmental furrows impressed on the pleural lobes is correct, but they are minute and almost impossible to observe. In addition, a few instars were found in which the axial lobe contains five rings, of which two are formed by four axial nodes, situated in between the frontal lobe and posterior two rings (fig. 1-3). These are similar to features occurring in other young trilobites, which are described in this report.

Horizon and locality. — Upper Cambrian, Zone II, Ringsaker Station, north of Oslo, Norway.

Figured specimens. — Cranidia, U.C.M. 38736 and 38736s,d′,e′; hypostoma, U.C.M. 38736t,u; librigenae, U.C.M. 38736x, y; pygidia, U.C.M. 38736b′, c′.

Olenus gibbosus (Wahlenberg), ontogeny

Metaprotaspid stage (Pl. 18, figs. 1-3, Text-fig. 47A, B). The moderately convex shield is spherical to subspherical in outline and about 0.27 mm in length (sag.). The glabella is composed of a large frontal lobe, two pairs of axial nodes, and two small posterior axial rings. A minute fissure is impressed along the axis of the glabella (sag.). The dorsal furrow is well developed. The pleural regions are gently convex, with three or four poorly defined cephalic segmental furrows. The marginal border is limited by an indistinct marginal furrow. The marginal spines are obscure except for the posterior pair. The surface is covered by fine granules.

Paraprotaspid stage (Pl. 18, figs. 4-8, Text-fig. 47C, D). The shield is circular in outline and about 0.30-0.40 mm in length (sag.). The axis is expanded anteriorly and divided by faint, transverse furrows. The frontal lobe, which consists of a pair of eyebrow-like ridges is larger than most of the axial rings. The anterior pits are shallow and elongate; the pleural lobe is about one and one-half the width of the glabella (tr.), and is surrounded by a narrow marginal border. The prominent palpebral ridge extends from behind the anterior pit and posterior-lateral margin of the frontal lobe and curves laterally and posteriorly to the marginal border. The marginal spines are obscure, except for the posterior pair, which are produced from the posterior-lateral margin.

The protopygidium appears at the posterior margin of the shield, curving ventrally between the posterior spines. It is triangular and consists of two segments. The surface of the shield is covered by fine granules.

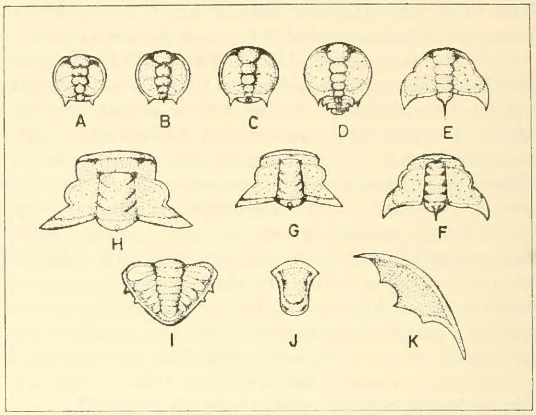

Text-fig. 47 — A growth series of *Olenus gibbosus* (Wahlenberg). A,B. Two metaprotaspids, x 50; C,D. Two paraprotaspids, x 50, x 30; E,F. Two early meraspids, x 20, x 18; G. A late meraspis, x 10; H. Holaspid cranidium, x 7; I. A pygidium, x 7; J. Hypostoma, x 20; K. Librigena, x 4. (Drawings made from photographs.)

The new features in this stage are: the fusion of the two pairs of metaprotaspid glabellar nodes to form two complete glabellar rings; the pleural segmental furrows are not visible; the protopygidium appears; and a pair of short furrows are newly developed on the sides of the frontal lobe.

Early meraspid stage (Pl. 18, figs. 9-12, 29, Text-fig. 47E, F). The trapezoidal shield is about 0.50-0.85 mm in length (sag.). The glabella is hemicylindrical to slightly expanded anteriorly. The frontal lobe is larger than the following axial ring, and bears a pair of short furrows laterally. The prominent palpebral ridges extend from the lateral margin of the frontal lobe and are located slightly posterior to their position in the earlier stage. The anterior pits are absent. The posterior lateral border is expanded laterally with a pair of posterior spines at the extreme ends. The pygidium is elongated, subtriangular, with five distinct axial rings. The pleural lobes are slightly convex above the dorsal furrow; the narrow marginal border bears short marginal spines which are continuous projections of the pleural segments. The surface is covered by medium-sized granules.

The important features of this stage are: the trapezoidal outline of the cranidium, the hemicylindrical form of the glabella, and the first appearance of the anterior border.

Late meraspid stage (Pl. 18, figs. 13-18,25,26,30, Text-fig. 47 G). The trapezoidal cranidium is about 0.90 to 1.50 mm in length (sag.) and moderately convex. The conical glabella is marked by three pairs of glabellar furrows which are deeper laterally and become more shallow toward the axis. The occipital ring is convex and bears a tiny median tubercle. The dorsal furrows are deep and distinct. The anterior border is narrow and separated by a well-developed preglabellar field. The palpebral lobes are prominent ridges. The fixigenae are broadly triangular in outline and about the same width as the glabella (tr.). The posterior lateral border is narrow but prominent. The triangular pygidium, which is not articulated with the cephalon, conical, of four or five segments, all of which are separated by furrows; the conical axial lobe tapers slightly posteriorly; the flat to slightly convex pleural lobes are divided into three or four broad pleural bands; the marginal border is narrow and distinctly delimited by the marginal furrow; no marginal spines are preserved. The librigena is elongate, narrow, and crescentic, with a medium-sized genal spine.

The features which differentiated this stage from the earlier one are: the appearance of the preglabellar field, the axial separation of the glabellar furrows, and the change of the pygidial axis from hemicylindrical to conical.

Figured specimens. — Metaprotaspids, U.C.M. 38736a-c; paraprotaspids, U.C.M. 38736d-h; early meraspids, U.C.M. 38736i-l, z; late meraspids, U.C.M. 38736m-r, v, w, a′.

Genus **ACEROCARE** Angelin, 1854

Acerocare ecorne Angelin

Plate 19, figs. 1-34, Text-fig. 48

Acerocare ecorne Angelin, 1878, p. 46, pl. 25, fig. 10, p. 47; Mober, and Möller, 1898, p. 231, pl. 10, figs. 1-10, p. 231; Henningsmoen, 1957, p 243, pl. 2, fig. 3, pl. 7; pl. 30, figs. 1-8; pl. 31, p. 243.

Diagnosis. — Convex cranidium bearing a broad subquadrate glabella and anteriorly situated palpebral lobes. Preglabellar field narrow, limited by a narrow, subtriangular frontal border. Posterior fixigenae wide bearing a pair of short spines at the posterior lateral border. The semicircular librigena bearing a short, broad, and curved terminal spine. Hypostoma elongate and occupied by an oval and convex median body. Subtriangular pygidium with six or more axial rings and a small terminal portion.

Cephalic surface covered by small granules; fine, radial ridges are present on the preglabellar field and ocular platform. A pair of distinct small nodes is present on the sides of the preglabellar field.

Acerocare ecorne Angelin, male?

Plate 19, figs. 15,17,19,24,32,34, Text-fig. 48H, L

Description. — The cephalon is semicircular in outline and wider (tr.) than long (sag.). The glabella is broadly subquadrate, marked by four pairs of glabellar furrows and a shallow anterior median pit. The dorsal furrow curves around the glabella and has a small median salient into the frontal margin of the glabella; at its mid-line of the glabella (tr.) it is slightly expanded laterally. The crescentic occipital ring is marked laterally by a pair of curving furrows and medially by medium-sized spine or node. A median occipital ridge runs along the occipital ring (tr.). The narrow preglabellar field is limited by a fine but well-defined frontal furrow. The anterior border is narrow, slightly elevated and bluntly pointed anteriorly. The interocular cheek is narrow. The small palpebral lobes are located far forward from the mid-line of the glabella (tr.). The posterior fixigenae are broad and transverse. The prominent and narrow posterior lateral border is delimited by posterior lateral furrows, which curve anterior-laterally. A pair of short fixigenal spine is borne at the lateral margin of the posterior lateral border.

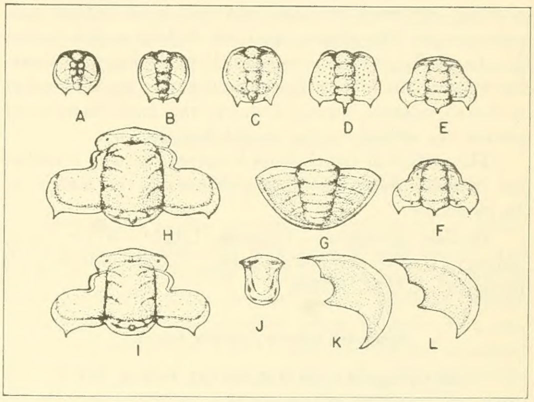

Text-fig. 48 — A growth sequence of *Acerocare ecorne* Angelin. A. Metaprotaspis, x 50; B,C. Two paraprotaspids, x 56, x 47; D. Early meraspis, x 32; E,F. Two late meraspids, x 26, x 22; G. Pygidium, x 6.8; H. "Male" cranidium, x 6.7; I. "Female" cranidium, x 8; J. Hypostoma, x 3.8; K. "Female" librigena, x 7; L. "Male" librigena, x 5. (Drawings from photographs.)

The librigena is semicircular in outline and gently convex. The ocular platform is broad. The convex lateral border is of medium width and defined by a shallow and broad lateral furrow. The anterior and posterior ends of the librigenae are sharply pointed.

The pygidium is subtriangular in outline. The conical axial lobe tapers posteriorly, is divided into four or five axial rings and a small terminal portion. The dorsal furrow is deeply impressed anteriorly and shallow around the posterior margin. The pleural lobes are slightly narrower than the axis (tr.), gently convex, and down-sloping to the narrow margin; the four or five pleural bands are all marked by broad, concave pleural furrows; the faint interpleural grooves are oblique to the pleural furrows.

The surface of the skeleton is covered by fine granules, and irregular ridges are developed around the margin of the pygidium.

Figured specimens. — Cranidia, U.C.M. 38738n, p, r; librigena, U.C.M. 38738w′; pygidia, U.C.M. 38738e′, g′; hypostoma, U.C.M. 38738t.

Acerocare ecorne Angelin, female?

Plate 19, figs. 13,14,16,18,25,30,31,33, Text-fig. 48 I, K

Comparison. — The glabella of the presumed female form is narrower, longer, and more cylindrical than that of the male form; the librigena is longer and narrower; and the pygidium is triangular. The sexual ratio is 115.

Horizon and locality. — Upper Cambrian, *Acerocare* zone ($2d_a$), Nye, Joukoping, Sweden.

Figured specimens. — Cranidia, U.C.M. 38738l, m, o, q; librigena, U.C.M. 38738x; pygidia, U.C.M. 38738c′, d′, f′.

Acerocare ecorne Angelin, ontogeny

Metaprotaspid stage (Pl. 19, figs. 1-2, Text-fig. 48 A). The shield is rounded to subrounded, convex, and about 0.20-0.29 mm in length (sag.). The marginal border of the shield is narrow and has a pair of short and broad spines projecting posteriorly from the posterior-lateral border. The fusiform axis is about the same width as the pleural lobe (tr.) and is delimited by dorsal furrows. It is composed of a frontal lobe, two pairs of axial nodes, and two terminal rings. The paired anterior pits are distinctly marked in the anterior lateral margin of the frontal lobe. The palpebral ridges and the palpebral lobes are indistinct. The surface of the shield is covered by fine granules.

Paraprotaspid stage (Pl. 19, figs. 3-6, Text-figs. 48B, C). The subrounded, convex shield varies from 0.30-0.40 mm in length (sag.), is surrounded by narrow marginal border. The fusiform axis is the same width as the pleural lobe and is divided into five convex, well-defined rings. The rings are connected by a narrow ridge along the median axis (sag.), and the small terminal ring bears a minute median spine. The convex frontal lobe is semicircular in outline and bears a pair of elongate pits on the anterior lateral portion. The distinct palpebral ridges extend laterally from behind the anterior pits to the lateral borders. The extreme ends of the borders are arched posteriorly and laterally and bear a pair of sharp-pointed spines. A small triangular protopygidium, which possibly consists of only one segment, is curved ventrally between the posterior spines from the posterior cephalic margin. The surface is covered by moderately large granules.

This stage differs from the preceding one in that here the axial nodes are fused to form five complete rings and the protopygidium first appears.

Early meraspid stage (Pl. 19, figs. 7-9, 26, Text-fig. 48 D). The cranidium is trapezoidal in outline about 0.40-0.70 mm in length (sag.), and the cranidium is disassociated from the pygidium. The fusiform glabella may be slightly expanded anteriorly and is composed of five distinct axial rings. The terminal or occipital ring is smaller than the preceding rings and bears a medium-sized median spine. The palpebral ridges and the palpebral lobes are situated at the anterior lateral margin of the shield. The posterior fixigenal borders are expanded laterally and bear a pair of spines directed posterior-laterally from the lateral borders. The facial sutures are obscure but may be located at the anterior-lateral corners of the cranidium, as is suggested by the palpebral lobes and the posterior fixigenal borders.

The pygidium is elongate-triangular in outline and slightly convex; its axial lobe is slenderly conical, tapering posteriorly, and divided into four rings, but some of which may be thoracic segments. The pleural lobes are convex above the dorsal furrow, and each segment projects marginally as a pair of short, broad spines. The surface is regularly ornamented with large granules.

In this stage the instars differ from the paraprotaspids in that the shield assumes a trapezoidal outline and the posterior fixigenal border becomes laterally expanded.

Late meraspid stage (Pl. 19, figs. 10-12,20,22,27-29, Text-fig. 48E, F.) The cranidium is trapezoidal in outline and about 0.60-0.80 mm in length (sag.). The subconical glabella is slightly expanded at the mid-line (tr.) and divided by three pairs of complete furrows. The crescentic occipital ring is smaller than the glabellar rings; it arches posteriorly and bears a small median tubercle. The anterior border is narrow, convex, and curves anteriorly. The fixigenae are broad posteriorly and narrow anteriorly; the distinct palpebral lobes and ridges are located at the anterior-lateral corners of the cranidium; the posterior fixigenal borders are delimited by furrow and curve anteriorly and laterally before reaching the margin; a pair of short spines projects from the posterior-lateral margins. The convex hypostoma is subquadrate in outline, with rounded posterior marginal border; its median body is small, subtriangular, and convex; the posterior lobe is wide, convex, and U-shaped. The flat pygidium which is subtriangular in outline, has a slenderly conical axial lobe; the axial lobe is divided into five or six rings; the pleural lobes are about the same width as the axis and marked by three or four distinct pleural bands; the marginal border is narrow and no marginal spines are preserved. The surface is covered by medium-sized granules.

This stage is characterized by a subconical glabella, incomplete glabellar furrows, and a narrow anterior border; the hypostoma has a small median body and a broad posterior lobe; the pygidial axis is slenderly conical; and the librigenae have a narrow platform.

Figured specimens. — Metaprotaspids, U.C.M. 38738a-b; paraprotaspids, U.C.M. 38738d-f; early meraspids, U.C.M. 38738g-i, y; late meraspids, U.C.M. 38738h-k, s, u.

Genus **HIGHGATELLA** Shaw, 1955

Highgatella facilia, n. sp.

Plate 21, figs. 1-26, Text-fig. 49

Diagnosis. — Cranidium trapezoidal to subquadrate in outline, moderately convex. Glabella truncate-conical, marked by three pairs of glabellar furrows. Preglabellar field about one-half the length of glabella. Anterior border narrow. Fixigenae narrow. Eyes medium-sized and located at mid-line of glabella. Posterior lateral fixigena triangular. Dorsal furrow deeply marked. Librigena having medium-wide ocular platform and genal spine. Hypostoma subquadrate, with a large, convex median body. Pygidium oval, convex with two pairs of marginal spines and same number of axial rings; pleural lobe narrower than axis and having distinctly impressed pleural furrow.

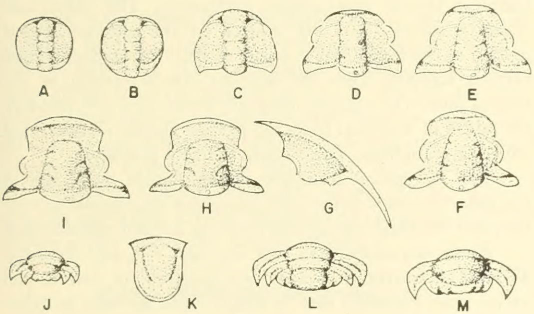

Text-fig. 49 — A growth series of *Highgatella facila,* n. sp. A. A metaprotaspis, x 62; B,C. Two paraprotaspids, x 53; D. Early meraspis, x 40; E. Late meraspis, x 30; F. An early holaspid cranidium, x 14; G. Librigena, x 5; H. "Male" cranidium, x 10; I. "Female" cranidium, x 9; J. Immature pygidium, x 30; K. Hypostoma, x 24; L. "Male" pygidium, x 25; M. "Female" pygidium, x 12. (Drawings made from photographs.)

Highgatella facila, n. sp., male?

Plate 21, figs. 13,14,17,20,21,23,25,26, Text-fig. 49 H, L

Description. — The cranidium is trapezoidal in outline and convex in profile. The glabella is broadly conical with a slightly rounded frontal margin, three pairs of well-defined glabellar furrows; the first pair of glabellar furrows, which are opposite the palpebral ridges, is short and poorly impressed; the second pair of glabellar furrows is deeper and extends a short distance behind the palpebral ridge; the last pair is longer and distinctly marked. The dorsal furrow is narrow and deep. The occipital furrow is shallow but well marked, deep laterally and shallow across the axial line (sag.). The crescentic occipital ring bears a median node. The preglabellar field is one-third as long as the glabella, slightly convex, and curves abruptly into the anterior furrow which is narrow, distinct, and arches anteriorly. The rounded and arched anterior border is narrow, being about one-fourth as wide as the preglabellar field. The fixigenae are narrow and flat, approximately one-fourth as wide as the glabella. The prominent eye-ridges extend from the anterior edges of the palpebral lobes medially to the dorsal furrow just behind the anterior lateral corner of the glabella; the medium-sized palpebral lobes are located on, or slightly forward from the mid-line of the glabella; the posterior fixigenae are triangular, convex, sloping down from the dorsal furrow to the impressed posterior-lateral furrows; the narrow posterior border is about two-thirds the length of the occipital ring. The anterior facial sutures are slightly divergent to parallel; the posterior facial sutures are divergently sinuous and cut the posterior lateral border with a sharp angle.

Librigena is convex, with a medium-wide ocular platform; the lateral furrow is shallow and broad; the lateral border is of medium-width, convex, and slopes gently down to the outer margin; the genal spine is slender and of medium length.

The pygidium is oval, transverse, and convex; the axial lobe is broad and convex above the pleural lobes and divided into two axial rings and a long terminal portion; the pleural lobe is narrower than the axis and marked by two pairs of pleural furrows; the marginal border bears two pairs of short, broad spines, which extend continuously from the pleural segmental tips.

The surface of the skeleton is covered by fine granules; radial ridges are present on the preglabellar field, and a row of distinct pits is present along the cephalic marginal furrow.

Figured specimens. — Paratype, cranidia, U.C.M. 38740n, m, q, r; librigenae, U.C.M. 38740w, x; hypostoma, U.C.M. 38740s; pygidium, U.C.M. 38740u.

Highgatella facila, n. sp., female?

Plate 21, figs. 12,15,16,18,19,22,24, Text-fig. 49I, M

Comparison. — The cranidium of the female differs from that of the male by having a narrower and longer glabella, wider preglabellar field, broader pygidial axis with two axial rings, and narrower pleural lobes.

Remarks. — This species is represented by 20 mature and 50 immature specimens which show a continual growth sequence. The largest female cranidium is about 20 mm long and the male cranidium is about 15 mm (sag.). The matrix material is light-brownish, medium-crystalline limestone. This species is distinguished from the type species *H. gelasinata* (Shaw) (1951, 1955) by its larger and more posteriorly located palpebral lobes.

Recently Winston and Nicholls (1967) assigned *Euloma cordilleri* Lochman (1964) from the Williston Basin to *Highgatella.* The assignment is doubtful. Dr. Lochman's specimens were prepared by the writer while serving as her research assistant; at that time a detailed comparison was made among three closely similar genera, *Euloma, Highgatella,* and *Parabolinella.* The differences are: *Euloma* has a quadrate cranidium, conical glabella, and deeply marked dorsal furrow; whereas *Highgatella* and *Parabolinella* have a trapezoidal to subquadrate cranidium, broadly subquadrate glabella, and shallower dorsal furrow. Moreover the preglabellar field of *Euloma* has a strongly elevated median boss whereas this field in *Highgatella* and *Parabolinella* has none. They are clearly different, but unfortunately, the specimens which were figured by Lochman are not all identical. The specimens which she shows on her plate 63, figures 27-30, 32-34, 36-38 (U.S.N.M. 140714, 140715a, c-f, h-j) are typical *Euloma,* whereas her figure 31 (U.S.N.M. 140715b) is either a member of *Highgatella* or *Parabolinella,* and figure 35 (U.S.N.M. 140715g) is a juvenile pygidium of *Symphysurina* with a peeled surface. These differences are easily discernible. Winston and Nicholl's (1967) specimens on their plate 13, figures 8,11,13 (Ut 12651-12653) are closely similar to Lochman's figure 31 (U.S.N.M. 140715b) and appear to belong to *Highgatella* or *Parabolinella,* whereas Lochman's specimens are referable to *Euloma,* except for her plate 63, figures 31 and 35 (U.S.N.M. 140715b and 140715g). This conclusion was reached after comparison of present material with Dr. Lochman's duplicates and topotypes(?) of *Euloma ornatum* Angelin, from Tremadocian *Ceratopyge* Limestone, Bjerkasholmen, Norway, which were collected by Dr. K. E. Caster during a field trip of the International Geological Congress, 1962.

Horizon and locality. — Deadwood Formation, *Missisquia* zone, Lower Ordovician. Sheep Mt., Sundance, Crook Co., northeastern Wyoming.

Figured specimens. — Holotype, cranidium, U.C.M. 38740; paratype, cranidia, U.C.M. 387401o, p; pygidia, U.C.M. 38740t, v.

Highgatella facila, n. sp. ontogeny

Metaprotaspid stage (Pl. 21, figs. 1-5, Text-fig. 49A). The spherical to subspherical shield is about 0.26-0.30 mm in length (sag.) and distinctly divided into axial and pleural lobes by the dorsal furrow. The axial lobe is fusiform, tapering slightly anteriorly and posteriorly, and lacking distinct rings or ring-furrows. The anterior pits are faint; the frontal lobe tapers continuously from the axial lobes; the last axial, or occipital, ring is oval, transverse, and convex. No protopygidium is seen from the dorsal view. The surface is covered with fine granules.

Paraprotaspid stage (Pl. 21, fig. 6, Text-fig. 49B, C). The cranidium varies from 0.35-0.40 mm in length (sag.), is trapezoidal in outline with a rounded anterior margin. The axial lobe is fusiform to cylindrical and divided into five rings by faint ring furrows; its frontal lobe is large and rounded; the occipital ring is distinctly separated by a deep occipital furrow and arches posteriorly. The faint and elongate anterior pits are located at the anterior lateral margin of the frontal lobe; a pair of short supercilioid ridges extends laterally from the anterior lateral margin of the frontal lobe. The pleural lobes are about one and one-half the width of the axial lobe. No protopygidium is associated with the cranidium. The surface is finely granulose.

The distinction from the metaprotaspid stage lies in the paraprotaspids having the cranidium trapezoidal in outline, and the axial lobe cylindrical with defined ring-furrows.

Early meraspid stage (Pl. 21, figs. 7-9, and Text-fig. 49D). The convex cranidium is trapezoidal in outline and varies from 0.40-0.60 mm in length. The glabella is cylindrical to anteriorly tapered and bears three pairs of glabella furrows. The dorsal furrow is deep and narrow. The occipital ring is crescentic and convex, possibly bearing a median tubercle. The narrow anterior border appears in contact with the frontal margin of the glabella; the anterior furrow is well defined and bends backward at the mid-point of the frontal glabellar margin (sag.). The broadly triangular fixigenae are of the same width as the glabella. The elevated palpebral lobes are located at the anterior one-third of the glabellar length, and are defined by distinct palpebral furrows. The posterior fixigenal border is twice as wide as the glabellar base, and divided by a wide and deep posterior-lateral furrow. The facial sutures converge anterior-medially to form a trapezoidal cranidium. The surface is covered with numerous small granules and occasionally large ones.

The distinctive characteristics of this stage are the conical glabella with three pairs of glabellar furrows and the development of the anterior border.

Late meraspid stage (Pl. 21, figs. 10-11, Text-fig. 49E). The convex cranidium is trapezoidal in outline and varies from 0.65 to 0.90 mm long (sag.). The slenderly conical glabella is marked by three pairs of well-defined glabellar furrows. The dorsal furrow is narrow and deeply marked. The convex occipital ring is distinctly separated by an occipital furrow and bears a small median node. The preglabellar field appears, slightly depressed in front of the preglabellar area. The narrow and convex anterior border is defined by an anterior furrow which curves slightly inward to form a median notch. The fixigenae are about one-third as wide as the glabella (tr.) and bear prominent palpebral ridges; the small crescentic palpebral lobes are deeply separated by palpebral furrows. The posterior fixigenal borders are triangular and of the same width as the glabellar base (tr.). The surface is generally covered by numerous fine granules and scattered large granules are seen on the fixigenae.

This stage differs from the earlier one in that the preglabellar field first appears, the fixigenae become narrow, and the palpebral lobes have moved posteriorly. The meraspis differs from the holaspis in having the glabella slenderly conical and the posterior lateral fixigenae wider. The glabella of the holaspid is truncate-conical; the posterior fixigenae are narrower; and preglabellar field is wider.

Figured specimens. — Metaprotaspids, U.C.M. 38740a-d, e; paraprotaspis, U.C.M. 38740f; early meraspids, U.C.M. 38740g-i; late meraspids, U.C.M. 38740j, k.

Family **LEIOSTEGIIDAE** Bradley, 1925

Genus **KEPISIS**, n. gen.

Diagnosis. — Cranidium trapezoidal in outline, convex; glabella conical with three pairs of distinctly impressed glabellar furrows; dorsal furrow shallowly impressed; preglabellar field of medium width; anterior border convex, same width as preglabellar field, with a stout median spine. Fixigenae about one-half the width of the glabella; palpebral lobe small, situated at the mid-line of the cranidium (tr.). Anterior facial suture lines convergently convex; posterior facial sutures divergent and straight. Librigenae with convex ocular platform and long genal spines. Pygidium transversely subtriangular, convex, divided into five or six segments, pleural lobes about twice as wide as axis; marginal border narrow, flat, and without spines.

Description. — The cranidium is regularly trapezoidal in outline and moderately convex. The glabella is conical, with three pairs of faint, obliquely directed glabellar furrows; the dorsal furrows are shallow and broad, but well defined; the occipital furrow is narrow, steep-sided and shallow across the center; the occipital ring is crescentic, convex, curving backward, and bearing a tiny median tubercle. The preglabellar field is one-fourth as long as the glabella, gently deflected toward the anterior furrow; the anterior furrow, which has a median notch directed toward the preglabellar field, is deep laterally but shallow across the axis; the anterior border is convex, about the same width as the preglabellar field, and bearing a median spine. The fixigenae are flat to gently convex and about one-half as wide as the glabella; the palpebral lobes are small and narrow and indistinctly separated by palpebral furrows; the faint palpebral ridges extend laterally, and gently arch forward; the posterior fixigenae are broad and triangular, with the border wider than the occipital ring.

The librigenae are moderately narrow and elongate with a long genal spine. The convex ocular platform is of medium width. The lateral border is moderately narrow, convex, and well delimited by a lateral furrow. The lateral and posterior furrows are not joined at the genal angle.

The pygidium is subtriangular, transverse, and convex. The axial lobe is cylindrical, slightly tapering posteriorly and ending before reaching the inner marginal furrow. Five axial rings are distinctly recognizable. The pleural lobes are broader than the axis, slightly convex, and well defined by a narrow and flat marginal border. Five pleural bands are divided by pleural furrows, the interpleural grooves being rather faint; the marginal border lacks spines.

Remarks. — There are not many trilobites which have a cranidium with a median spine at the anterior border. *Acrocephalites, Shantongia, Dokimocephalus, Thysanopyge, Zuninaspis, Nascocephalus, Lonchodomas,* and the dalmanitoids have this feature, but their other characteristics are different from those of *Kepisis; e.g.,* the shape, position, and origin of the anterior spines of these forms are dissimilar. For example, in *Shantongia* and some dalmanitoids the spine is developed from the rostral plate; in *Lonchodomas* and some other dalmanitoids the spine is developed from the anterior glabella. In *Nascocephalus, Dokimocephalus,* and *Acrocephalites* it is, however, located at the anterior border, but the shape of the cranidia and spines are completely different in form. The present form has no generic features which could associate it with any of the anteriorly spinose genera so far known.

The present genus is similar to *Chuangia* and *Anomocarella,* except that these two genera have no anterior border spine and possess wider posterior fixigenae and less numerous pygidial segments. On the other hand, *Chuangia, Anomocarella,* and *Kepisis* have some features in common: the shape of the cranidium and the glabella, the convexity, dorsal furrow, and outline of the pygidium are all closely similar in these three genera. Therefore, the present genus *Kepisis* could be a member of either the Asaphiscidae or Leiostegiidae. Age considerations would incline one to prefer the latter family assignment. It should be pointed out that *Kepisis* shows affinities relating it to the Asiatic realm of Cambrian time.

Type species. — *Kepisis stenotoides* (Matthew), n. gen.

Kepisis stenotoides (Matthew)

Plate 12, figs. 1-14, Text-fig. 50

Anomocare stenotoides Matthew, 1898, pp. 139-141, pl. 2, fig. 5a-i.

Remarks. — This species is represented by 15 cranidia, three librigenae, eight pygidia, and a few thoracic segments, prepared from a single piece of dark-grey, finely crystalline limestone. The material was found in the Geology Museum, University of Cincinnati, labeled as "Kennebec River, St. John, N. B.". However, no stratigraphic horizon, detailed locality or identification are given. Dr. F. Rasetti and Dr. B. F. Howell, who are familiar with the geology and paleontology of the New Brunswick area, suggest that the specimens in question may belong to *Anomocare stenotoides,* published by Matthew in 1898. Dr. Rasetti reported that Matthew's types at the Royal Ontario Museum are similar to the present material. Dr. Howell, on the other hand, said that he collected thousands of trilobites from the St. John region but never found any form like the present one. It is his thought that the present forms are a new genus and possibly belong to the Upper Cambrian. Through the courtesy of the Royal Ontario Museum, Matthew's types were loaned for comparison with the present material. The specimens are lithologically and morphologically identical and were probably collected from a same general region and horizon.

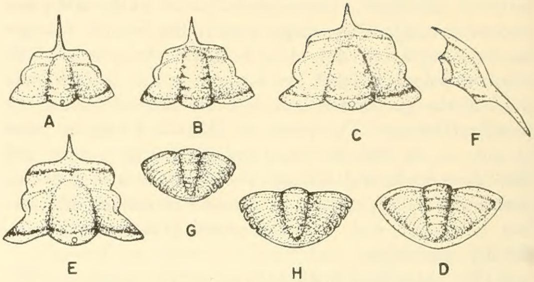

Text-fig. 50 — *Kepisis stenotoides* (Matthew), n. gen. A. An early meraspis, x 17; B. Late meraspis, x 13; C,E. Two holaspid cranidia, x 11, x 5.5; F. A. librigena, x 17; D,G,H. A growth series of pygidia, x 11, x 25, x 16. (Drawings from photographs.)

Horizon and locality. — Probably Bretonian (Upper Cambrian or Lower Ordovician), Kennebec River, St. John, N.B., Canada.

Figured specimens. — Cranidia, U.C.M. 38730f, 38730; librigena, U.C.M. 38730g; pygidia, U.C.M. 38730m; thoracic segment, U.C.M. 38730h.

Kepisis stenotoides (Matthew), ontogeny

Early meraspid stage (Pl. 12, figs. 1,2,10,11, Text-fig. 50A). The cranidium is about 1.0-1.22 mm in length (sag.), trapezoidal in outline, convex, with distinctly impressed dorsal furrows. The slenderly conical glabella tapers forward with a rounded anterior margin and has three pairs of weakly marked glabellar furrows. The crescentic occipital ring curves posteriorly and bears a tiny median node. The narrow anterior border is sharply defined by a wide, concave anterior furrow and bears a long, slender, anterior projecting, median spine. The fixigenae are fairly convex, slightly wider than the glabella, with a pair of elongate sickle-shaped palpebral lobes which approach the glabella at one-third the distance from its front margin. The posterior fixigenal borders are convex, broad, and slightly geniculate. The posterior lateral furrows are broad laterally with a narrow, convex marginal border. The short anterior branches of the facial sutures are convergent; the posterior branches are divergent or slightly transverse.

The convex pygidium is triangular in outline. The axis is slender, tapering posteriorly, convex above the pleural lobes, and divided into at least eight axial rings by transverse furrows. The pleural bands, which slope gently downward to the margins, are well defined by pleural furrows and end with short spines; no marginal borders have been observed.

The surface is covered by fine granules.

Late meraspid stage (Pl. 12, figs. 3-5, 12,13, Text-fig. 50B). The cranidium is convex, trapezoidal in outline, and varies from 1.30 to 1.80 mm in length (sag.). The conical glabella is weakly marked by three pairs of broad, posterior-laterally directed glabellar furrows. The occipital furrow is distinctly marked and delimited by a crescentic, posteriorly arching occipital ring which has a minute median tubercle. The preglabellar field is axially flat but deflected laterally. The narrow anterior border arches forward, with an anteriorly projecting median spine. The anterior furrow is steep-sided but shallow across the axis. The fixigenae are wider than the glabella and bear a pair of small palpebral lobes which are located slightly in front of the mid-line of the cranidium (tr.), and connect with a pair of prominent palpebral ridges. The anterior facial sutures are divergently convex, and the posterior ones are divergently straight. The pygidium is composed of 8 to 14 segments and is subtriangular to semioval in outline; its marginal border is narrow and bears numerous short spines. One specimen (fig. 12) shows a pygidium with at least two articulating thoracic segments.

The surface is finely granulose, and well-defined radial ridges are present on the preglabellar field.

The morphologic changes during ontogeny are as follows: the anterior border spine changes from long to short; a preglabellar field is progressively developed; the initially long slender glabella becomes progressively short and broad; wide fixigenae become narrow; the palpebral lobes migrate from the anterior lateral margin to the mid-length of the cranidium; and the pygidial axis changes from slenderly conical to almost cylindrical, with nearly parallel dorsal furrows; the spiny pygidial margin becomes smooth.

Figured specimens. — Early meraspids, U.C.M. 38730a, b, i, j; late meraspids, U.C.M. 38730c-e, k, l.

Family **MISSISQUOIIDAE** Hüpe, 1953

Genus **MISSISQUOIA** Shaw, 1951

Missisquoia cyclochila, n. sp.

Plate 20, figs. 1-28, Text-fig. 51

Diagnosis. — Cranidium triangular in outline, convex. Glabella parallel-sided to slightly expanding both anteriorly and posteriorly, with two pairs of distinct glabellar furrows. Dorsal furrow deeply impressed. Eye small, located behind mid-line of the glabella (tr.). Fixigena about one-half as wide as glabella. No preglabellar field. Anterior border convex, arching forward. Librigena narrowly elongate, having a short genal spine. Pygidium semicircular, convex, with six or seven axial rings and a small terminal portion.

Description. — The small cranidium is triangular in outline. The convex glabella is parallel-sided or slightly expanded both anteriorly and posteriorly, with a rounded frontal margin and small median notch. Three pairs of glabellar furrows are seen; the first pair is faint, the second and third ones are deeply impressed and extend posterior-laterally from the dorsal furrows. The dorsal furrow is moderately deep at the mid-line of the glabella but becomes shallower both anteriorly and posteriorly. The occipital furrow is distinct, shallow across the central axis and deeper laterally; the crescentic occipital ring is widest at its center and tapers laterally; a minute node is borne on the center of the ring. No preglabellar field is present; the anterior furrow is narrow and deeply marked; the anterior border is narrowly rounded and convex. The fixigena is convex and about one-half the width of the glabella; the small palpebral lobes are located behind the mid-line of the glabella (tr.) and lack furrows; the palpebral ridge is faint, obliquely directed toward the anterior-lateral margin of the glabella. The posterior lateral fixigenae are broad, and convex; the posterior-lateral fixigenal borders are wide, about the same width as the occipital ring. The anterior branches of the facial sutures are straight and converge toward the anterior border; the posterior branches are divergently sinuous.

The hypostoma is subquadrate with a narrow marginal border and a large median body. Its lateral wings are short and broad.

The librigenae are moderately convex, narrow and elongate, with a short genal spine; the ocular platform is narrow and convex; the lateral border is broadly flat, of about the same width as the platform, and separated by a faint lateral furrow. The pygidium is semicircular to triangular in outline and strongly convex; its conical, posteriorly tapering axial lobe consists of six or seven axial rings and a terminal portion. The convex pleural lobes curve ventrally around the margin; the pleural furrows and interpleural grooves are well marked.

The surface of the skeleton is covered by fine to medium-sized granules; elevated and parallel ridges are present along the outside of the cephalic border.

Remarks. — This species is represented by 15 mature and 45 immature specimens which show a continuous growth sequence. The largest cranidium is about 5.0 mm in length (sag.), and the smallest immature specimens 0.22 mm long (sag.). The material is from reddish-brown, medium to coarsely crystalline limestone.

This species differs from *M. typicalis* Shaw, (1951), *M. nasuta* Winston and Nicholls, and *M. inflata* Winston and Nicholls (1967) by its rounded anterior border, palpebral lobes located behind the mid-line of the glabella, librigena with short genal spine, pygidium without any marginal spines, and its pygidial axis not extending to the posterior pygidial margin.

It is interesting to note that the present genus is similar to the genus *Parakoldinoides* Endo (1937), from northern China and southern Manchuria. These two forms are believed to be closely related; the pygidium referred by Endo to *Parakoldinoides* may have been misassociated.

Horizon and locality. — Lower Ordovician, *Missisquoia* zone, Deadwood Formation. South side of Sheep Mt., Sundance, Crook Co., northeastern Wyoming.

Figured specimens. — Holotype, cranidium, U.C.M. 38749; paratype, cranidia, U.C.M. 38749r; librigena, U.C.M. 38749t; hypostoma, U.C.M. 38749s; pygidia, U.C.M. 38749x, y.

Missisquoia cyclochila, n. sp., ontogeny

Anaprostaspid stage (Pl. 20, fig. 1, Text-fig. 51a). The spherical shield has a length of about 0.22 mm (sag.). The fusiform axial lobe is composed of a medium-sized frontal lobe, two pairs of oval notes, and a larger terminal tubercle. The frontal lobe is delimited by a pair of anterior pits; two pairs of central nodes are divided by a longitudinal fissure and transverse grooves; the large terminal tubercle occupies about one-third the length of the axial lobe. The dorsal furrow is faint. The pleural lobe is convex and slightly narrower than the axial lobe. The surface is finely granulose.

Metaprotaspid stage (Pl. 20, figs. 2, 3, Text-fig. 51B). The convex shield is about 0.26-0.30 mm long (sag.) and subspherical in outline. The fusiform to cylindrical axial lobe is distinctly defined by dorsal furrows; the frontal lobe is rounded, convex, with faint anterior pits; the three transverse axial rings are of subequal size, and the terminal tubercle is large, elongate, and convex. The pleural lobes are convex and slightly narrower than the axial lobe. The surface is covered by fine granules.

The important feature of this stage is that the shield is subspherical with five complete axial rings which are apparently formed by the fusion of the axial nodes.

Paraprotaspid stage (Pl. 20, figs. 4-7, Text-fig. 51C). The shield is subspherical, convex, about 0.35-0.55 mm in length (sag.). The axial lobe is cylindrical to slightly fusiform with a larger frontal and three equal-sized axial rings; the frontal lobe is delimited by furrows and anterior pits; a pair of superciliold ridges extend lateral from the anterior-lateral margin of the frontal lobe. The dorsal furrows are distinctly impressed. The pleural lobe is approximately the same width as the axial lobe or slightly wider.

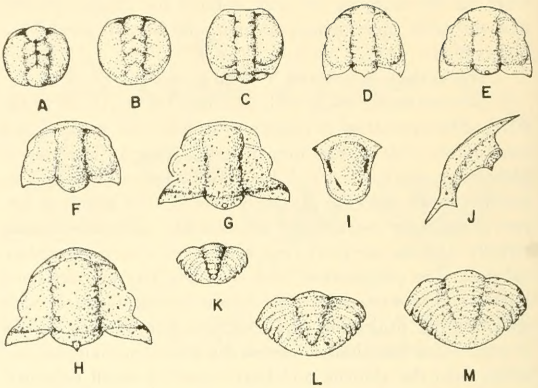

Text-fig. 51 — A growth sequence of *Missisquoia cyclochila*, n. sp. A. Anaprotaspis, x 70; B. Metaprotaspis, x 70; C. Paraprotaspis, x 62; D,E. Two early meraspids, x 43, x 45; F. Late meraspis, x 24; G,H. Two holaspids, x 18, x 12; I. Hypostoma, x 18; J. Librigena, x 20; K,L,M. Growth series of pygidia, x 50, x 28, x 19. (Drawings made from photographs.)

The protopygidium was not observed, but some specimens show a transverse ring behind the fifth axial ring, which suggests the pygidium, although its nature is unknown. The surface is covered by fine granules.

The distinct feature of this stage is the well-developed posterior-lateral border.

Early meraspid stage (Pl. 20, figs. 8-15, 23, Text-fig. 51D, E, K). The subtriangular to trapezoidal cranidium ranges from 0.40 to 0.60 mm long (sag.). The glabella is slenderly fusiform with a slightly expanded frontal lobe. The anterior pits are shallow impressed to almost absent in the larger specimens. The glabellar furrows are deep at the dorsal furrow and shallow across the central axis. The occipital furrow is well defined. The occipital ring is wide at the axial line (tr.), narrowing laterally and bearing a medium tubercle. The convex fixigenae are about one and one-half times as wide as the glabella. The posterior lateral fixigenae are broadly triangular, curve ventrally from the dorsal furrow, and extend posterior-laterally. The rear borders are of medium width, well impressed by a border furrow and terminate with a pair of projections. The facial sutures are only seen on the anterior-lateral corners of the cranidium. The triangular and convex pygidium bears five or six axial rings and a small terminal portion; the pleural lobes are separated into five or six pleural bands; they are convex, and curve ventrally toward the margin; the pleural bands terminate in short, broad marginal spines. The surface is finely granulose; possibly one or two articulating thoracic segments precede the meraspid pygidium.

The distinct features of this stage are the trapezoidal cranidium, broad and shorter glabella, the dorsal facial sutures, and expanded posterior-lateral borders.

Late meraspid stage (Pl. 20, figs. 16,17,24,25, Text-fig. 51F, L). The convex cranidium is trapezoidal in outline and about 0.70-1.00 mm (sag.) long. The glabella is cylindrical to slightly expanded at both the anterior and posterior ends; the glabellar furrows are faint. The dorsal furrows are deeply marked. The occipital furrow is narrow and distinct laterally; the crescentic occipital ring bears a minute tubercle. The anterior border is narrow, roundly arching forward, and delimited by the anterior furrow. No preglabellar field is observed. The fixigenae are of about the same width or slightly narrower than the glabella. The posterior-lateral fixigenae are convex, broad, and triangular. The palpebral lobes lack distinct palpebral furrows and are located at or slightly posterior from the mid-line of the glabella. The facial sutures extend from the posterior-lateral border convergently, forming a trapezoidal cranidium.

The semicircular pygidium has a conical axial lobe which tapers backward to the posterior marginal border and is divided into six or seven axial rings and a small terminal portion. The pleural lobes are composed of five or six pleural bands, all separated by pleural furrows, and bear interpleural grooves. The marginal border is sharply curved in a ventral direction. The surface is covered by medium-fine granules.

This stage is characterized by a subquadrate glabella, the narrow anterior border, and by having the pygidial axis extending to the posterior marginal border.

Figured specimens. — Anaprotaspis, U.C.M. 38749a; metaprotaspids, U.C.M. 38749b, c; paraprotaspids, U.C.M. 38749d-g; early meraspids, U.C.M. 38749h-o, u; late meraspids, U.C.M. 38749p, q, v, x.

Family **ENCRINURIDAE** Angelin, 1854

Genus **LIBERTELLA**, n. gen.

Diagnosis. — Cranidium subtriangular to subtrapezoidal in outline, convex, having a pair of long fixigenal spines. Glabella strongly expanded forward without glabellar furrows. Fixigenae quadrate, broad posteriorly, occupied by a pair of small palpebral lobes. Librigenae narrow with steeply sloping ocular platform. Hypostoma diamond-shaped with a slightly convex median body. Thorax divided into at least eight segments; axis convex, elevated above pleural lobe, and bearing median spines. Pygidium subtriangular with five pairs of small marginal spines directed horizontally and three pairs vertically. Surface covered by large granules and spines.

Description. — The cranidium is subtriangular in outline. The glabella is expanded forward, swollen above the fixigenae, are not marked by glabellar furrows; the dorsal furrow is deep and broad; the occipital furrow is deep, narrow, and steep-sided. No anterior border or preglabellar field are seen. The fixigenae are triangular in outline and bear a pair of long fixigenal spines; the palpebral lobes are small, rounded, prominent, and situated on, or slightly behind, the mid-line of the glabella (tr.); the posterior fixigenae are broad and have narrow posterior borders; the posterior fixigenal furrows are narrow and distinct, and turn anterior-lateral before reaching the margin. The anterior branches of the facial sutures are convergent, the posterior nodes are divergently transverse. The surface is covered by medium-sized granules and spines; there are four pairs of long vertical spines on the anterior half of the glabella; two pairs on the palpebral lobes; one on the posterior center of the fixigenae; and at least five pairs inside the lateral border and fixigenal spines.

The librigena is triangular and has a rounded lateral border; no genal spine is present; the ocular platform is narrow; the palpebral ring is blunt and vertical. The surface is covered by granules. Numerous long and short spines extend from the lateral border.

The hypostoma is quadrilateral, with a low median body; the anterior margin is slightly acute; the lateral wings bear upturned narrow and tilted margins; the posterior margin is upturned and ridged, with a median spine directed posteriorly. The posterior-lateral areas are marked by a pair of distinct elongate nodes. The anterior half of the hypostoma is covered by coarse granules.

The thorax is divided into at least eight segments; the axis is convex above the pleural lobes, and each ring has a tiny median spine. The pleural lobes are moderately wide and curve ventrally; each segment bears a pair of long and short lateral spines on the outside half of the pleural bands. The surface is granulose.

The pygidium is semicircular in outline; its axis is convex above the pleural lobes, which are flat and curve ventrally along the margin; the axis is divided into four rings and a small terminal portion; no tubercles are present; the four pleural segments each bear a pair of long posteriorly directed marginal spines and a pair of vertical spines on the margin.

Remarks. — This genus resembles the genus *Bevanopsis* Cooper, (1953), but *Libertella* has a cranidium with less expanded glabella, no spines on the posterior fixigenal borders and occipital ring, and fewer spines on the surface. *Libertella* differs from the genera *Encrinurus* Emmrich (1844), and *Encrinuroides* Reed (1931) in that *Libertella* has a spinose skeleton, whereas the other two genera have no spines; their pygidia are elongate-subtriangular. Doubtlessly, this genus is a member of the family Encrinuridae, because it has 1) proparial facial sutures, 2) a small palpebral lobe, 3) forwardly expanded glabella, 4) possesses no anterior border or preglabellar field, and 5) has a prominently ornamented skeletal surface.

Type species. — *Libertella corona,* n. gen., n. sp.

Libertella corona, n. gen., n. sp.

Plate 22, figs. 1-39, Text-fig. 52

Bevanopsis ulrichi Cooper, 1953, p. 32, pl. 13, figs. 23, 24 only. (Not figs. 21, 22, 25.)

Remarks. — This species is represented by more than 200 specimens, all etched from a few pieces of black, finely crystalline limestone. Both immature and mature forms are well preserved and a beautiful growth sequence obtained. The young skeletons resemble those of *Calliops strasburgensis* Ulrich and Delo (1940), but comparing the same-sized instars, the present species has a narrower axis and but little expanded frontal lobe, whereas *C. strasburgensis* has a wider axis and the frontal lobe is strongly expanded forward.

Cooper (1953) figured four cranidia referred to his *Bevanopsis ulrichi.* His figure 21 (the holotype U.S.N.M. 116485a) is a moderately complete cranidium, showing a well-preserved glabella and part of the fixigenae. The other four cranidia are all poorly preserved specimens, but the glabellae are well shown and there is no doubt that the specimens of his figures 22, 25 (U.S.N.M. 116485b and 116485c) are identical to his holotype. On the other hand, his figures 23, 24 (U.S.N.M. 116485c and 116485d) are alike in all characteristics but are unquestionably synonymous with the present species, *L. corona.*

Horizon and locality.— Lower Middle Ordovician, Edinberg Formation, 1.5 miles southeastern Strasburg Junction, Shenandoah Co., Virginia.

Figured specimens. — Holotype, a complete skeleton, U.C.M. 38741; paratype, cranidia, U.C.M. 38741o-q, d′; librigenae, U.C.M. 38741r-t′; thoracic segment, 38741u; hypostomata, U.C.M. 38741v, w; pygidia, U.C.M. 38741a′-c′.

Libertella corona, n. gen., n. sp., ontogeny

Paraprotaspid stage (Pl. 22, figs. 1-4, 7, 8, Text-fig. 52A-C). The subspherical shield is about 0.45 to 0.48 mm in length (sag.), with separated axial and pleural lobes. The anteriorly expanded axis is divided into five or six axial rings by faint furrows. The fixigenae are broad, convex, and approximately twice as wide as the glabella; the palpebral lobes are located at the anterior-lateral margin of the shield, and at a short distance from the lateral margin of the frontal lobe. The protopygidium is transverse, has one or two segments, and a spinose margin.

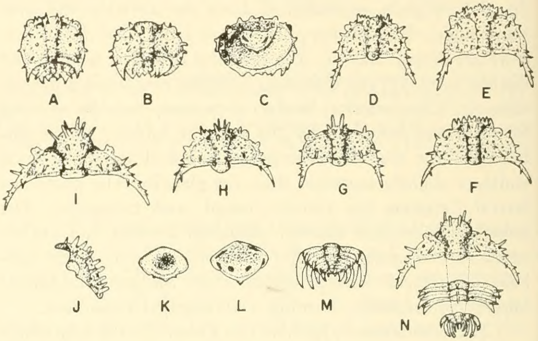

Text-fig. 52 — *Libertella corona,* n. gen., n. sp. A-C. Dorsal and ventral views of two paraprotaspids, x 38, x 35; D-F. Three early meraspids, x 26, x 25, x 25; G,H. Two late meraspids, x 18, x 16; I. Adult cranidium, x 15; J. Librigena, x 15; K,L. Ventral and top views of two hypostomata, x 10; M. Pygidium, x 33; N. Reconstration, x 13. (Drawings made from photographs.)

The surface of the skeleton is covered by granules and scattered spines; three pairs of spines are located on the frontal lobe, of which two pairs are directed forward from the anterior margin, and the other pair is on the sides of the base; seven pairs of spines occur on the fixigenae, of which three pairs are on the inner margin, additional pairs, including the large posterior fixigenal ones, extend laterally from the outer margin. A tiny median tubercle occurs on the occipital ring, and three pairs of tubercles are distributed along the posterior protopygidial margin.

The underside of the shield has a narrow doublure along the posterior margin; the hypostoma is semicircular with a few pairs of marginal spines; the librigena is subtriangular and narrow with a spinose lateral margin.

Early meraspid stage (Pl. 22, figs. 5, 6, 9-11, Text-fig. 52D-F). The trapezoidal cranidium ranges from 0.40-0.55

mm in length (sag.). The glabella is expanded anteriorly and separated into four rings by faint, transverse furrows; the dorsal furrows are distinct; the broad occipital ring is defined by a distinct occipital furrow and bears a median tubercle. The fixigenae are twice as wide as the glabella at the mid-line of the cranidium (tr.); the small palpebral lobes are located in front of the first glabellar furrow (tr.); the fixigenae are broad with rounded, gently deflected lateral margins; the posterior fixigenal border is narrow and delimited by a furrow; a pair of long fixigenal spines projects posteriorly from the hind border; the skeletal surface is covered by large granules and spines. The latter are arranged as in the previous stage but have small and shorter spines appearing among them.

There are no striking morphologic changes between the present stage and the previous one, except for the displacement of the pygidium, increase in the number of smaller spines, and the posterior-lateral migration of the palpebral lobes.

Late meraspid stage (Pl. 22, figs. 12-16, 25, 26, 28-31, Text-fig. 52G, H). The cranidium is subtrapezoidal, convex, and about 0.60-1.00 mm in length (sag.). The glabella is expanded slightly anteriorly, with two pairs of steep-sided glabellar furrows; the occipital ring is broad, elevated, and distinctly delimited by the occipital furrow. The fixigenae are more than twice as wide as the glabella at the mid-line of the cranidium (tr.); the small palpebral lobes are small, imbricated, and situated slightly behind the glabellar expansion (tr.); the posterior fixigenal furrows are narrow, distinct, and turn anteriorly before reaching the lateral borders; the posterior fixigenal borders are narrow and continue as a pair of long and posterior-laterally directed fixigenal spines.

This stage is distinguished from the previous one in that the number of smaller cranidial spines is reduced; the palpebral lobes have shifted posteriorly from the anterior-lateral margin; the hypostoma bears three pairs of posterior marginal spines; and the pygidium is possibly associated with two thoracic segments (figs. 28, 29).

Figured specimens. — Paraprotaspids, U.C.M. 38741a-c, f; early meraspids, U.C.M. 38741d-g, h, i; late meraspids, U.C.M. 38741j-n, x-z.

Family **PROETIDAE** Salter, 1864

Genus **PHASEOLOPS** Whittington, 1963

PHASEOLOPS CONUS, n. sp.

Plate 23, figs. 1-31, Text-fig. 53

Diagnosis. — Cranidium subquadrate, convex. Anterior border rounded, arching forward. Glabella conical, last pair of glabellar furrows deeply marked. Dorsal furrow deeply impressed. Occipital ring convex, bearing a tiny median tubercle. Preglabellar field broad, having a distinct anterior furrow. Fixigenae narrow. Palpebral lobe medium-sized, and located behind the mid-line of the glabella. Posterior fixigenae narrow. Librigenae elongate, having a medium-sized genal spine. Pygidium convex, widely subtriangular in outline, with three distinctly divided pygidial segments, each segment ending with a pair of short, broad, posteriorly directed spines.

Surface covered by large and small granules, parallel ridges are well elevated along the cephalic margin.

Description. — The cranidium is convex, subquadrate in outline, with a broad, flat, concave anterior brim and conical glabella. The glabella is deeply marked by two pairs of glabellar furrows; the first is faint and located posterior of the mid-line of the glabella (tr.), the second pair is deep, directed posterior laterally from the mid-line of the glabella, and terminates before reaching the occipital furrow. The dorsal furrows are deep and broad. The occipital furrow is narrow and steep-sided at the sides of the glabellar base; the crescentic occipital ring is wider than the glabellar base (tr.), and bears a median tubercle. The broad preglabellar field is about one-half as long as the glabella (sag.); it is gently convex and ventrally curved; the convex anterior border is broad and of about the same width as the preglabellar field; it is distinctly delimited by the anterior furrow. The convex fixigenae are narrow, about one-fourth as wide as the glabella; the palpebral lobes are medium-sized, semicircular and broadly flattened; the palpebral furrows distinctly marked between the fixigenae and palpebral lobes. They are acute laterally at the mid-line of the palpebral lobes; the posterior fixigenae are narrow and delimited by marginal furrows; the posterior fixigenal borders are narrow, being about two-thirds as wide as the occipital ring, and are sharply pointed laterally. The anterior branches of the facial sutures are strongly divergently convex, and the posterior branches are divergently straight or slightly sinuous. The underside of the cranidium has a narrow anterior border doublure, and the posterior margin has a broad occipital one. The occipital doublure is broad at the central axis and tapers laterally toward the ends of the posterior fixigenal borders.

The librigena is elongate, with a medium-narrow ocular platform; the lateral and posterior furrows are both shallow but distinctly impressed; they join at the genal angle and extend along the genal spine for a short distance. The underside of the librigena bears a broad lateral doublure which is sharply pointed anteriorly and curves posterior-laterally to end at the ocular base.

The pygidium is subtriangular and convex; its axial lobe is conical and tapers posteriorly, extending about two-thirds the length of the pygidium (sag.); the axial ring furrows are shallow and undulatory; the pleural lobes are divided into three pleural bands, which are impressed by pleural furrows and directed laterally and posteriorly into short spines; the posterior axial lobe is a flat, gently convex area, without any pleural or interpleural furrows. The underside of the pygidium has a broad doublure along the posterior margin and is notched post-axially.

The surface of the skeleton is covered by scattered large granules, and bears fine radial caeca at the anterior brim; the outside of the cephalic margin and the doublures bear parallel ridges along the border.

Remarks. — This species closely resembles *P. sepositus* Whittington (1963), the type species, from the Middle Ordovician of Lower Cow Head, western Newfoundland, but it differs in having a cranidium with a broader anterior border, conical glabella, and indistinct glabellar furrows; the associated pygidium has a slightly shorter axial lobe and wider, more distinct ring-furrows.

The present species is represented by more than 100 immature and mature specimens. All were etched from a few small pieces of black, finely crystalline limestone. The materials include abundant instars of many different genera, but the present forms are distinguished from others by their gently convex or nearly flat skeletons, and the unornamented surface, (excluding a pair of anterior pits).

Horizon and locality. — Middle Ordovician, Edinburg Formation. 1.5 mile, southeastern Strasburg Junction, Shenandoah Co., Virginia.

Figured specimens. — Holotype, cranidium, U.C.M. 38742; paratype, cranidia, U.C.M. 38742p-r; librigenae, U.C.M. 38742t-v; pygidia, U.C.M. 38742x-z, a′.

Phaseolops conus, n. sp., ontogeny

Anaprotaspid stage (Pl. 23, figs. 1-3, Text-fig. 53A, B). The shield is rounded, flat, gently convex, and about 0.27 mm in length (sag.). The surface lacks any striking features, except for a slight convexity along the axis; there is no distinct dorsal furrow, axis, or pleural lobe divisions. The anterior margin has two small depressions or pits. The posterior lateral border is prolonged as a pair of short, stout spines. The posterior-lateral border is deeply notched. The underside of the shield has a broad, flat doublure along the posterior margin. The surface is roughly to finely granulose.

The specimens are so small and flattened that they are easily misidentified as different animals. They were at first thought to be either trilobite hypostomata or ostracods before photographs were taken. However, photographs reveal a pair of pits on the anterior margin and a pair of short spines at the posterior-lateral border which clearly indicate that they are small trilobites.

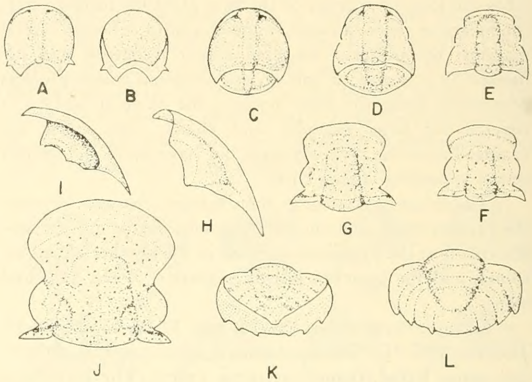

Text-fig. 53 — *Phaseolops conus,* n. sp. A,B. Top and ventral views of anaprotaspids, x 56; C,D. Two paraprotaspids, x 53, x 46; E. Early meraspis, x 30; F,G. Two late meraspids, x 31, x 28; H,I. Top and ventral views of two librigena, x 6, x 4; J. Holaspid cranidium, x 12; K,L. Ventral and dorsal views of two pygidia, x 11, x 10. (Drawings made from photographs.)

Paraprotaspid stage (Pl. 23, figs. 4-8, 22, Text-fig. 53C, D). The shield is elongate-oval, moderately convex, and varies from 0.40 to 0.55 mm in length (sag.). The axial and pleural lobes are separated dorsal furrows. The axial lobe is slenderly fusiform, without any distinct axial rings or posterior cephalic border. The pleural lobes are about the same width as the glabella; the palpebral lobes are small and located at one-third the shield length from the anterior end; the anterior facial sutures are convergent, and the posterior ones are divergently straight and terminate at two-thirds the shield length from the anterior end. The protopygidium is not definitely differentiated from the cephalon, but the facial sutures give the best clue for judging the pygidial position and shape: it is a tranversely semicircular region located behind the posterior branch of the facial sutures; the axial lobe is defined by distinct furrows; the pleural lobes are gently convex, curving ventrally to the margin, without pleural furrows or interpleural grooves. The underside of the shield has a uniformly narrow posterior doublure. The surface is covered by fine granules.

It seems that there is a growth gap between the anaprotaspid and the present stage; this gap is indicated by the fact that the anaprotaspis lacks both protopygidium and facial suture, and the paraprotaspis suddenly shows these well developed. Such an ontogenetic saltation is incompatible with other trilobite development, and it appears that the metaprotaspid stage is missing here. Probably the lack reflects the meager nature of the materials available. In comparing the morphologic features of the anaprotaspis and paraprotaspis one might expect the missing metaprotaspis to be characterized by a rounded to slightly elongate skeleton of low convexity with axial and pleural lobes obscurely differentiated; neither protopygidium or dorsal facial suture are to be expected; the posterior lateral margin of the shield would probably bear a pair of marginal spines.

Early meraspid stage (Pl. 23, figs. 9-12, Text-fig. 53E). The cranidium is subquadrate in outline, convex, and about 0.60-0.80 mm in length (sag.). The glabella is cylindrical but expands slightly anteriorly; the glabellar furrows are indistinct except for the pre-occipital ring furrow. The occipital ring, which is acute posteriorly, is defined by the occipital furrow and bears a minute median node. The dorsal furrows are well marked, parallel to the sides of the glabella, and slightly expanded laterally at the base of the last pair of glabellar furrows. The anterior border is broad and convex, curves forward, and slightly touches the anterior glabellar margin. The fixigenae are slightly narrower than, or of the same width as, the glabella; the palpebral lobes are sickle-shape, narrow, elongate, and located at the mid-line of the glabella (tr.); the posterior fixigenae are broad, triangular, and have their marginal border directed slightly posterior-laterally. The facial suture is slightly divergently convex anteriorly and divergently straight posteriorly. The surface is covered by medium-large granules.

The early meraspid specimens differ from those of the earlier stage in that the cranidium bears distinct anterior and posterior borders, and the palpebral lobes are located more posteriorly.

Late meraspid stage (Pl. 23, figs. 13-16, 23, 27, Text-fig. 53F, G). The convex cranidium is subquadrate in outline and ranges from 0.90 to 1.20 mm in length (sag.). The glabella is slenderly conical and marked by two pairs of glabellar furrows; the preoccipital furrow, or last pair of glabellar furrows, is distinct and convex; the first pair is shallow, short, and located opposite the palpebral lobes. The dorsal furrows are deep and narrow. The occipital ring is crescentic, arches posteriorly, and is defined by a distinct occipital furrow. The preglabellar field is medium-wide and gently deflected; the convex anterior border is about the same width as the preglabellar field and is distinctly defined by the anterior furrow. The convex fixigenae are about one-half as wide as the glabella, and bear flattened palpebral lobes; the broadly crescentic palpebral lobes are situated at the mid-line of the glabella (tr.), and are distinctly delimited by palpebral furrows; the posterior fixigenae are narrow, with the marginal border being of the same width as the occipital ring (tr.). The anterior branches of the facial sutures are divergently convex, and the posterior ones are divergently straight. The pygidium is semicircular or semioval and consists of five or six convex segments, and lacks marginal spines. The pygidium is possibly preceded by two or three articulating thoracic segments. The surface is covered by large granules, and caeca occur on the preglabellar field.

This stage is distinguished from the previous one by having the cranidium broader and shorter, the fixigenae narrower, and the preglabellar field present. In comparison with holaspid specimens the meraspid ones have broader fixigenae, narrower and more anterior palpebral lobes, and the pygidium is without marginal spines.

Figured specimens. — Anaprotaspids, U.C.M. 38742a, b; paraprotaspids, U.C.M. 38742c-g; early meraspids, U.C.M. 38742h-k; late meraspids, U.C.M. 38742o, s, w.

Family **PTERYGOMETOPIDAE** Reed, 1905

Genus **CALLIOPS** Delo, 1935

Calliops strasburgensis Ulrich and Delo

Plate 24, figs. 1-38, Text-fig. 54

Calliops strasburgensis Ulrich, and Delo, *in* Delo, 1940, pp. 99, 100, pl. 12, figs. 8-10.
Pterygometopus sp. Butts, 1941, pl. 82, figs. 9-13.
Calliops strasburgensis Ulrich and Delo, Cooper, 1953, p. 37, p. 17, figs. 1-15.

Diagnosis. — Cephalon highly convex. Glabella broadly expanded anteriorly and marked by three pairs of glabellar furrows. Dorsal furrow deep and narrow. Occipital ring broad, convex. No preglabellar field or anterior border. Fixigenae narrow. Palpebral lobe longitudinally sickle-shaped. Rostro-librigenae narrow without median or connective sutures. Hypostoma ovally elongated, with long posterior lateral wings. Thoracic segments convex and stout with rounded, anteriorly directed ends. Pygidium triangular in outline, strongly convex, consisting of more than ten segments. The surface is densely granulose.

Calliops strasburgensis Ulrich and Delo, male?

Plate 24, figs. 14,15,18,19,26,29,35,38, Text-figs. 54 K, O

Description. — The cephalon is semicircular in outline, highly convex, with a broad cranidium and narrow rostro-librigenae. The glabella is large and broadly expanded anteriorly; the three pairs of glabellar furrows are deeply marked; the first pair of glabellar lobes is large and transverse; the second pair is oval and small, the third is preoccipital and small. The dorsal furrows are narrow and deeply marked with the anterior ends broadly open. The broad occipital ring is curved slightly anteriorly and bears a tiny median tubercle. There is no anterior border or preglabellar field. The fixigenae are broad; the shallow posterior fixigenal furrows extend anteriorly before reaching the lateral border. A pair of short spines is directed posteriorly from the ends of the rear borders.

The arched rostro-librigenae lack median or connective sutures; the narrow ocular platform slopes steeply down from the ocular ring to the lateral margin; the lateral border is smooth and lacks a lateral furrow.

The hypostoma is elongate, ovate, and moderately convex, with a pair of short, broad lateral wings; the median body is slightly convex, with a pair of elongate lateral maculae; the posterior border is broad, concave, and U-shaped; the lateral and posterior margins are narrow and elevated; the anterior border is arched forward and bears a pair of broad, short, tilted wings.

The pygidium is triangular in outline and slightly convex. The convex and conical axial lobe tapers posteriorly with a rounded termination, and is anteriorly divided into four large rings and posteriorly into five or six smaller ones. The border lacks both furrow and spines.

The surface is covered with large granules, except for the hypostoma and pygidium which are finely granulose.

Figured specimens. — "Male" form. Cranidia, U.C.M. 38743, 38743m, q, w; pygidia, U.C.M. 38743d′, g′; rostro-librigenae, U.C.M. 38743t; hypostoma, U.C.M. 38743r.

Calliops strasburgensis Ulrich and Delo, female?

Plate 24, figs. 16,17,27,32-34,36,37, Text-figs. 54 J, N

Comparison. — The presumed female skeletons differ from those of males in that the female cephalon and the glabella are narrower and longer, the anterior cranidial margin is more acute, the rostro-librigenae lack genal spines, and the pygidium has narrower pleural lobes.

Remarks. — A few hundred well-preserved specimens were etched from several small pieces of black, finely crystalline limestone. The characters of this species conform in general to Ulrich and Delo's (1940) description, but unfortunately, their material was poorly preserved and reveal inadequate information for reliable comparison. Ulrich and Delo's types were collected from the Edinburg Limestone near Strasburg Junction, Virginia, and were refigured by Cooper (1953, p. 37, pl. 17, figs. 6, 13-15). The additional materials were collected from the same general area and formation by Cooper (1953). These are shown in a state of better preservation and characteristics. The writer's materials are identical with the latter ones. One of Cooper's adult specimens shows at least 11 thoracic segments (his pl. 17, fig. 12).

Horizon and locality. — Middle Ordovician, Chambersburg Limestone, Willow Groove, three miles southwest of Woodstock, Shenandoah Co., Virginia.

Figured specimens. — "Female" form. Cranidia, U.C.M. 38743o, p; pygidia, U.C.M. 38743a′,-f′.

Calliops strasburgensis Ulrich and Delo, ontogeny

Paraprotaspid stage (Pl. 24, figs. 1, 2, Text-fig. 54A). The rounded and convex shield with distinctly separated axial and pleural lobes, is approximately 0.57 mm in length (sag.). The convex axial lobe is strongly expanded anteriorly, without distinct ring furrows; the frontal lobe is broadly triangular, and well defined by furrows. The convex pleural lobes slope down steeply along the lateral margin; the pos-

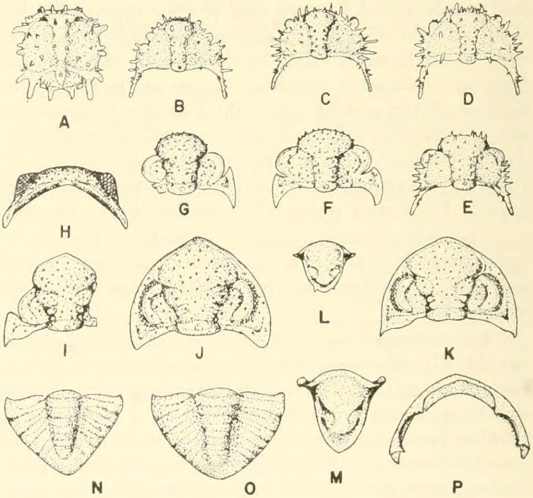

Text-fig. 54 — *Calliops strasburgensis* Ulrich and Delo. A. Paraprotaspis, x 36; B-E. Four early meraspids, x 22, x 34, x 23, x 17; F,G. Two late meraspids, x 15, x 10; H. Frontal view of a cephalon, x 3.2; I. Early holaspis, x 3; J. "Female" cephalon, x 3; K. "Male" cephalon, x 3.2; L,M. A juvenile and adult hypostoma, x 10, x 3.2; N. "Female" pygidium, x 3.8; O. A "male" pygidium, x 3.3; P. A librigeno-rostrum, x 8.7. (Drawings made from photograph.)

terior lateral borders are not clearly recognizable. The transversely subtriangular protopygidium is separated from the cephalon by a faint and anteriorly arching furrow; the axial and pleural lobes lack distinct furrows. The surface is covered by granules and spines. The anterior margin of the frontal lobe is marked by a pair of stout spines on the anterior-lateral corners and a pair of short ones at the center; the posterior lateral corners of the frontal lobe have a pair of vertically directed spines; the axial lobe, exclusive of the frontal lobe and protopygidium, is cylindrical with four pairs of tiny tubercles. The fixigenal surface has four pairs of nodes, of which two pairs are located anterior-laterally, and the other posteriorly; the fixigenal margin bears a pair of large spines behind the palpebral lobes, three short ones laterally and posteriorly, and a larger pair projecting posteriorly. The protopygidium has a spiny margin.

Early meraspid stage (Pl. 24, figs. 3-9, Text-fig. 54B-E). The convex cranidium is about 0.60-0.85 mm long (sag.) is semioval in outline and has a pair of long, posteriorly directed fixigenal spines. The glabella is distinctly defined by dorsal furrows and divided into four rings by furrows; the frontal lobe is broad and expanded anteriorly; the glabellar furrows are deep laterally but shallow across the central axis; the occipital ring is convex, crescentic, and bears a median tubercle; no anterior border or preglabellar field are seen. The fixigenae are broad posteriorly. The palpebral lobes are small and located opposite (tr.) the first glabellar furrow. The outer surface is covered by both fine and coarse granules and spines; the inner surface is finely punctate and spinose.

Late meraspid stage (Pl. 24, figs. 10-13,20,23,24,30-31, Text-fig. 54F, G). The semicircular cranidium is about 0.90-1.50 mm in length (sag.). The glabella is broadly expanded anteriorly and has a narrower (sag.) preoccipital segment; the glabellar furrows are distinctly separated and directed posterior-laterally; the large palpebral lobes are convex above the dorsal furrows. The posterior fixigenae are narrow and have a wide lateral portion; the posterior-lateral border bears a pair of short terminal spines, directed backwardly. The librigenae lack median or connective sutures and are arched; the ocular platforms are narrow and almost vertical; the anterior and later borders bear wide spines. The hypostoma is ovate, moderately convex, and with a vertically curved marginal border. A pair of short, delicate spines extends from the posterior-lateral margins. The pygidium is triangular in outline and divided into six or seven segments by distinct furrows; each segment ends in a pair of posterior-laterally directed spines. The surface is coarsely granulose and the anterior glabella and librigenal borders are spinose.

The main morphologic changes of this stage are: the supplanting of the spinosity in earlier instars by granulation; the enlargement of the palpebral lobes and their shifting from the anterior fixigenae to the rear portion; the posterior fixigena which was broad in earlier instars now becomes narrower; the fixigenal spines decrease in size; the ocular platform broadens; and the hypostoma loses its spines; the formerly spinosely fringed pygidium now has smooth margins.

Figured specimens. — Paraprotaspids, U.C.M. 38743a; early meraspids, U.C.M. 38743b-h; late meraspids, U.C.M. 38743i-l, s, u, v, y, z.

Family **CALYMENIDAE** Burmeister, 1843

Genus **FLEXICALYMENE** Shirley, 1936

Flexicalymene granulosa (Foerste)

Plate 25, figs. 1-29, Text-fig. 55

Calymene callicephala granulosa Foerste, 1909, p. 294.
C. granulosa Foerste, Bassler, 1919, p. 356, pl. 56, figs. 1, 2.
Flexicalymene granulosa (Foerste), Bucher, Caster, and Jones, 1939; Caster Pope, and Dalvé, 1945, 1961, pl. 2, figs. 9,10.

Diagnosis. — Cranidium trapezoidal in outline and convex. Glabella broadly conical, with three pairs of deeply marked glabellar furrows. Dorsal furrow very deep. Occipital ring convex. No preglabellar field. Anterior border of medium width. Fixigenae narrow anteriorly and broad posteriorly. Palpebral lobes small, located well in front of the mid-length of the glabella. Hypostoma subquadrate and slightly convex, with a pair of posterior marginal spines. Librigenae elongate, with or without genal spines. Thorax divided into 13 segments. Pygidium triangular or subtriangular in outline, convex, with five distinctly marked segments and a small terminal portion. Surface covered with medium coarse granules.

Flexicalymene granulosa (Foerste), male?

Plate 25, figs. 17,18,19B,22,23,26-28, Text-fig. 55J,K,M

Description. — The cranidium is trapezoidal in outline and convex. The glabella is broadly truncate-conical and convex above the fixigenae; the first pair of glabellar furrows is short and shallow and directed anterior-medially from the dorsal furrow; the second pair is short and deeply depressed with distinct pits; the third pair of furrows is longer, deeper, and directed slightly posteriorly with bifurcations at the ends. The glabellar lobes are rounded elongate and increase in size from the anterior to the posterior pair. The dorsal furrow is deep and broad, and curves inward behind the last pair of glabellar lobes. The occipital furrow is deep laterally but shallow and swings forward at the axial line. The anterior brim lacks a preglabellar field; the anterior furrow is deep and straight; the anterior border is narrow, convex, and arches slightly anteriorly. The subtriangular fixigenae slope anteriorly and laterally downward from the palpebral lobes, which are located between the first and second glabellar furrows (tr.). The anterior facial suture is convergent, and the posterior one is divergently convex. The posterior fixigenal furrow is shallow and broad; the marginal borders are convex and about the same width as the occipital ring (tr.).

The librigena is elongate with a short and stout genal spine; the ocular platform is moderately broad, convex, and has a small ocular ring; the lateral border is roundly convex and delimited by a shallow broad, lateral furrow.

The hypostoma is subquadrate in outline; its median body is gently convex; the posterior lobe is U-shaped, gently convex, and delimited by furrows. The marginal border is convex laterally and flattened posteriorly with a pair of posteriorly directed spines. The lateral furrow is deep and occupied by two pairs of elongate pits. The anterior lateral wings are concave, broad, and triangular, and have a pair of rounded and deeply marked pits.

The rostral plate is gently convex, narrow, and transverse, and curves slightly forward. The thorax is divided into 13 segments. The axial rings are strongly convex and associated with deeply marked furrows. The pleural lobes are narrower than the axis, gently convex, and curve ventrally. The ends of each pleural segment are rounded without spines.

The pygidium is subtriangular in outline and strongly convex. The conical lobe tapers posteriorly and is divided by distinct ring furrows into four or five rings and a triangular terminal portion. The dorsal furrow is well impressed; the terminal portion which is set off by distinct ring furrows, end before reaching the posterior margin. The pleural lobes gently curve ventrally and are separated into four or five pleural lobes by narrow interpleural grooves. No marginal border or marginal spines are present.

The surface of the skeleton is covered by fine to medium-sized granules.

Figured specimens. — "Male" form. Cranidia, U.C.M. 38744q-s; pygidia, U.C.M. 38744v, w; librigena, U.C.M. 38744b′; hypostomata, U.C.M. 38744z, a′.

Flexicalymene granulosa (Foerste), female?

Plate 25, figs. 15,19A,24,29, Text-fig. 55 L, N. Q

Comparison. — The "female" forms differ from the "male" in that the cranidium has a broader anterior furrow, broader anterior border, and more posteriorly located palpebral lobes. The librigenae have narrower ocular platforms and lack genal spines. The pygidium is quadrate or subrounded in outline.

Remarks. — According to Bassler (1919) and Dalvé (1948), two species of *Flexicalymene* are found in the Cincinnati area, *i.e., F. granulosa* and *F. meeki. F. granulosa,* which occurs in the Eden Formation, the lower part of the Cincinnatian, is characterized by a smaller skeleton and granulose surface. *F. meeki* which occurs in the Maysville and Richmond Formations, the Upper Cincinnatian, is characterized by a larger-sized skeleton and more finely granulose surface (Pl. 25, figs. 30-32). The materials here studied were collected from the Eden Shale. The material contains three other trilobite genera: *Isotelus, Cryptolithus,* and *Primaspis.*

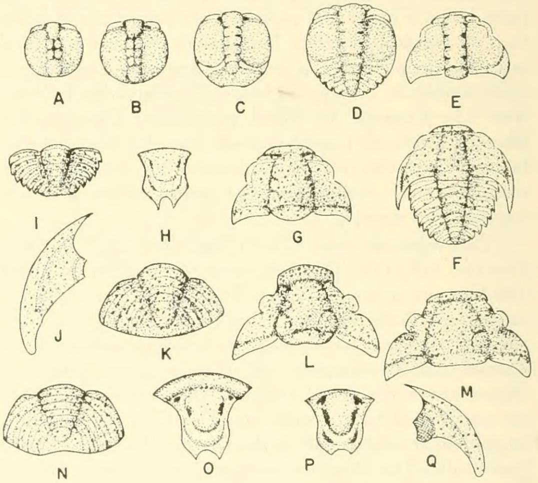

Text-fig. 55 — A growth sequence of *Flexicalymene granulosa* (Foerste). A. Anaprotaspis, x 52; B. Metaprotaspis, x 50; C,D. Two paraprotaspids, x 40, x 31; E. Early meraspis, x 26; F,G. Two late meraspids, x 14, x 13; H. Immature hypostoma, x 20; I. Small pygidium, x 24; J. "Male" librigena, x 2; K. "Male" pygidium, x 4.5; L. Medium-sized "female" cranidium, x 15; M. Large sized "male" cranidium, x 4.2; N. "Female" pygidium, x 14; O. Medium-sized hypostoma, associated with rostrum, x 14; P. Adult hypostoma, x 6; Q. "Female" librigena, x 13. (Drawings made from photographs; except for B, schematic.)

About 80 specimens, both immature and mature forms, were prepared from 50 kg of grey to yellowish-brown shale; the small instars are rare and adult fragments common; most of the specimens are slightly deformed. The "female" form here reported has not been found before, and while it may belong to a new species, and certainly would have been so designated in accord with previous taxonomic procedure, here is interpreted as a sexual difference within *F. granulosa,* comparable dimorphism occurs in other materials herein reported. The sexual ratio is about 385.

Horizon and locality. — Upper Ordovician, Cincinnatian, Eden Formation. Park Hills, western Covington, west side of Highway Route 42, Kenton Co., Kentucky.

Figured specimens. — "Female form." Cranidia, U.C.M. 38744o,s; pygidium, U.C.M. 38744x; librigena, U.C.M. 38744c′.

Flexicalymene granulosa (Foerste), ontogeny

Anaprotaspid stage (Pl. 25, figs. 1-4, Text-fig. 55A). The rounded to moderately convex shield with the axial and pleural lobes distinctly separated, ranges from 0.24 to 0.28 mm in length (sag.). The axial lobe consists of an elongate frontal lobe, two pairs of central nodes, and a large, convex terminal one. The dorsal furrows are distinct; an axial fissure extends from behind the frontal lobe to the front of the terminal tubercle. The supercilioid ridges are broadly convex, and distinctly separated from the pleural lobes by furrows. The convex pleural lobes are broadly convex, and distinctly separated from the pleural lobes by furrows. The convex pleural lobes are about one and one-half times wider than the axis. The surface is finely granulose.

Metaprotaspid stage (Text-fig. 55B). The moderately convex shield is spherical to subspherical in outline, and approximately 0.35 mm in length (sag.). The conical axial lobe tapers slightly posteriorly and is divided into five rings with a well-defined central axial fissure; the frontal lobe is rounded with a pair of narrow supercilioid ridges extending laterally; the second, third, and fourth ones are transverse and of about the same size. The dorsal furrow is distinct. The palpebral lobes are convex and about twice the width of the glabella. A broad unsegmented area is located behind the fifth axial ring. A longitudinal fissure extends along the central axis. The surface is covered by granules.

No metaprotaspid specimens have been recovered, but the morphologic differences between the anaprotaspis early forms, with four axial rings, and the early meraspis, with more than six axial rings, clearly indicate that the stage with five axial rings is lacking. The absence of the metaprotaspid instar in *F. granulose* may be due to preservation, meagerness of materials, or ecologic adaptation of planktonic larvae. In any case, the early immature specimens of the present material are rare.

Paraprotaspid stage (Pl. 25, figs. 5-10, Text-fig. 55C, D). The moderately convex, subrounded shield is composed of a protopygidium and cephalon with distinct glabella and fixigenae; it varies from 0.45 to 0.70 mm in length (sag.). The glabella is cylindrical to slightly expanded anteriorly; it is divided into four rings; the glabellar furrows are deep laterally, shallow across the axis, and straight or slightly curved posteriorly; the transverse occipital ring is delimited by the occipital furrow. The prominent eyebrow-like ridges extend posterior-laterally from the frontal lobe or first glabellar ring. The convex fixigenae slope down toward the lateral margin and are approximately one and one-half times wider than the glabella. The rear fixigenal borders extend posterior-laterally and are faintly delimited by a marginal furrow. The semicircular to subtriangular protopygidium is formed of two or four segments. The conical axial lobe tapers posteriorly with impressed ring furrows. The pleural furrows and the interpleural grooves are distinctly defined. The surface is covered by granules.

This stage differs from the previous one in having the distinct protopygidium, and the posterior fixigenae expanded laterally.

Early meraspid stage (Pl. 25, figs. 11-12, 20, Text-fig. 55E). The cranidium which is about 0.70-0.85 mm in length (sag.), and is convex and trapezoidal in outline. The glabella is cylindrical and has three pairs of minute glabellar furrows. The dorsal furrows are deep and parallel. The occipital ring is crescentic and has a tiny median node. The fixigenae are narrow between the palpebral lobes but broad and convex posteriorly; the posterior border which are directed posterior laterally before terminating laterally, are defined by marginal furrows and are approximately twice as wide as the occipital ring (tr.); the small palpebral lobes are situated at one-fourth the length of the glabella from the anterior margin. A narrow preglabellar brim arches anteriorly along the anterior margin of the glabella. The transverse oval pygidium is preceded by three articulating thoracic segments; its convex axial lobe is conical, tapers posteriorly, and is divided by ring furrows; the pleural lobes are the same width as the axis and deeply marked by three pairs of interpleural grooves. The posterior margin bears short spines. The surface of the skeleton is covered by granules.

The important characters of this stage are that the glabella is cylindrical, the eye-ridges are distinct, and the preglabellar brim first appear.

Late meraspid stage (Pl. 26, figs. 13,14,16,21,25, Text-fig. 55F, G). The cranidium is about 0.8-1.4 mm long (sag.). The conical glabella is deeply marked by three pairs of glabellar furrows; the dorsal furrow is deep and broad; the occipital ring has a tiny median tubercle. The anterior border is separated by a deeply impressed anterior furrow. The fixigenae are about one-half as wide as the glabella between the palpebral lobes and the dorsal furrows; the posterior fixigenae are broad with the posterior border projecting posteriorly before terminating. The hypostoma is subquadrate, gently convex and has a pair of spines projecting posteriorly. The semicircular pygidium is divided into five or six segments, and each segment is directed slightly posterior-laterally from the convex axis and ends in a pair of spines.

The surface of the skeleton is covered by both fine and coarse granules.

Figured specimens. — Anaprotaspids, U.C.M. 38744a-d; paraprotaspids, U.C.M. 38744e-j; early meraspids, U.C.M. 38744k, l, t; late meraspids, U.C.M. 38744m, n, p, u, y.

Family **TRINUCLEIDAE** Hawle and Corda, 1847

Genus **CRYPTOLITHUS** Green, 1832

Cryptolithus bellulus (Ulrich)

Plate 26, figs. 1-13, Text-fig. 56

Trinucleus bellulus Ulrich, 1878, pp. 99, 100, pl. 4. fig. 15.
Cryptolithus recurvus (Ulrich), Bassler, 1919, pp. 334-335, pl. 56, figs. 14-17.
Cryptolithus lorrainensis Ruedemann, 1926, pp. 107-115, pl. 21, figs. 4,5.
Cryptolithus bellulus (Ulrich), Whittington, 1941a, pp. 30-34, pl. 5, figs. 1,7-9,13,14,19,21,22,25,26,28.

Diagnosis. — Cephalon semicircular in outline and moderately convex, with a broad pitted fringe. Glabella ovate and convex above the fixigenae. Occipital ring bearing a long, stout median spine. Thorax divided into six thoracic segments with convex axial rings and flat pleural lobes. Pygidium subtriangular in outline, with slightly elevated axial lobe and flattened pleural lobes. Ridged marginal border elevated and convex, but curved ventrally.

Description. — The skeleton is rounded to subrounded in outline and has a large cephalon and a small pygidium. The cranidium is semicircular in outline and extends about one-half the body length. The glabella is ovate, elongate, and convex, above the fixigenae; the glabellar furrows are deep laterally, the posterior ones are deeper than the anterior ones; a median tubercle occurs at one-third the length of the glabella from the anterior. The dorsal furrow is shallow and broad. The occipital ring is narrow, curves backward, and is drawn out into a stout occipital spine. The fixigenae measured from the inner margin of the fringe to the dorsal furrow at the mid-line of the glabella, are approximately one and one-half times wider than the glabella. The posterior lateral fixigenae have deep and laterally widened marginal furrows; the posterior fixigenal borders are curved slightly backward before reaching the lateral ends. The fringe slopes downward, widens laterally, and narrows in front of the glabella, it is marked by concentric rows of pits; the outer margin of the fringe bears two essentially concentric rows of pits; the outer ones are elongate; the inner ones are all rounded and smaller; a few additional pits occur posterior-laterally at the rear fixigenal border, where the concentric arrangement of pits is lost. The lower lamella or rostro-librigena is broad and of the same shape as the region of the fringe, except for a pair of genal spines directed posteriorly; the inner surface of the lamella bears shallow tubercles, the arrangement of the tubercles is the same as that of the pits on the upper lamella or cranidium; the under surface of the lamella shows pits (Pl. 26, fig. 7); the shape and arrangement of which conforms to those of the cranidial fringe; a prominent ridge or girder occurs along the anterior cranidial margin; between the first and second rows of pits which extends continuously into the genal spines.

The thorax is divided into six segments; the axial lobe is convex above the pleural lobes; the dorsal furrow is shallow and marked with a pair of distinct pits on each segment.

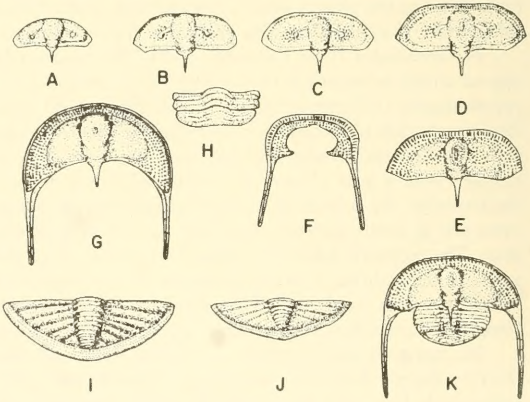

Text-fig. 56 — *Cryptolithus bellulus* (Ulrich). A. Paraprotaspis, x 23; B,C,D. Three early meraspids, x 20, x 19, x 8; E. Late meraspis, x 3.4; F. Ventral view of lower lamella, x 2.5; G. Holaspid cephalon, x 1.8; H. Early meraspid pygidium associated with two thoracic segments, x 18; I,J. Meraspis, x 5. (Drawings from photographs.)

The pleural segments are flat and directed laterally, with a pair of short terminal spines projecting posteriorly. The pleural furrows are shallow and wide.

The pygidium is transversely subtriangular in outline; the axial lobe is convex, slightly elevated above the pleural lobe, and divided into more than 10 axial rings; the first and second ring furrows are distinct, and the following are faint or almost indistinguishable; the pleural lobes are flat, separated by four pairs of ridges anteriorly, and indistinctly separated posteriorly. The broad and prominent margin has a ridge rising from the inner marginal border; the outer margin slopes steeply downward and is marked with fine, parallel, well-elevated ridges.

Remarks. — More than 100 specimens were prepared from 50 kg of yellowish-brown shale, and include immature and mature forms, both of which are moderately common, but most of the specimens are slightly deformed.

According to Bassler (1915, p. 1471) and Dalvé (1948), two species occur in the Eden Shale of the Cincinnati area, *i.e., C. tesselatus* and *C. bellulus*. The specific assignment of the present material is in accord with Whittington's (1941) criteria.

It is interesting to note that the small instars of the present species have well-developed eye tubercles which have gradually disappeared in the larger instars. It is evident that the mode of life changed during the ontogenetic development of the animal; the early larvae were apparently planktonic, whereas the mature stage was benthonic. The ontogeny suggests that the ancestor of the present species may well have possessed eyes. This suggests original existence in a photic environment from which the trilobite migrated into the dark or subsurface during which they were progressively reduced, just as in certain cave fish, polychaetes with similar life history. The animal *(C. bellulus)* was possibly a burrower in the substrata, a nocturnal animal, or, perchance, lived below light penetration on the sea-floor.

It is also noteworthy that most of the immature specimens have the upper and lower lamellae of the rostro-librigena preserved separately, whereas those of adults are fused without separation; this phenomenon suggests that possibly the suture which lies between the lamella and the cranidium facilitated ecdysis during early stages, but ecdysis took other paths or stopped in the adult stage. This feature has also been observed in *Calliops strasburgensis* (Pl. 24, figs. 1-15,16-19) and also is the situation in modern *Xiphosura.*

Horizon and locality. — Upper Ordovician, Cincinnatian, Eden Shale Formation, Park Hills, Kenton Co., western Covington, west side of Highway Route 42, Kentucky.

Figured specimens. — Cephalon, U.C.M. 38745; pygidia, U.C.M. 38745j, k.

Cryptolithus bellulus (Ulrich), ontogeny

Paraprotaspid stage (Pl. 26, fig. 1, Text-fig. 56A). The cranidium is transverse, semicircular in outline, moderately convex, and about 0.35 mm long (sag.). The glabella is elongate, oval, and expanded anteriorly; no glabellar furrows are observed except for a pair of elongate pits on the sides of the posterior portion; the narrow occipital ring is defined by the occipital furrow. No preglabellar field or anterior borders are seen. The fixigenae are triangular and gently convex with a rounded margin; the prominent eye ridges curve posterior-laterally from the distal lateral sides of the glabella, and end at a pair of eye tubercles without reaching the rear fixigenal border. The latter is prominent and turned slightly anterior-laterally. The surface is finely granulose.

Early meraspid stage (Pl. 26, figs. 2-5, 10, Text-fig. 56B-D). The moderately convex cranidium is semicircular in outline, and ranges from 0.45 to 1.00 mm in length (sag.). The glabella is elongate, convex above the fixigenae, and distinctly defined by a pair of posterior glabellar furrows. The dorsal furrow is broadly impressed, has a pair of eye ridges directed posterior laterally, and ends with a pair of eye tubercles on the center of the fixigenae. The anterior border and pitted fringe have appeared. The occipital ring curves posteriorly with a large, posteriorly directed spine. The surface is marked with fine punctation surrounding the eye tubercles.

The pygidium is transversely reniform, and consists of two or three segments which are preceded by the same number of articulated thoracic segments. The axial and pleural furrows are deep and clearly defined; the marginal border is upturned.

Late meraspid stage (Pl. 26, figs. 6-8, 11, Text-fig. 56 E). The cranidium varies from 1.50-3.30 mm in length (sag). The glabella is convex; its high-point is located anteriorly and bears a median tubercle. The occipital ring curves backwardly and bears a long posteriorly directed spine. The posterior fixigenal border turns anterior-laterally before terminating. The surface is finely granulated, except for the fringe; scattered punctation surround the eye tubercle area and the median tubercle of the glabella, but eye tubercles are absent. Five pairs of distinct pits are present on the dorsal furrow of the thorax.

Figured specimens. — Paraprotaspis, U.C.M. 38745a; early meraspids, U.C.M. 38745b-e, h; late meraspids, U.C.M. 38745f-g, i-j.

Family **ASAPHIDAE** Burmeister, 1843

Genus **ISOTELUS** Dekay, 1824

Isotelus stegops Green

Plate 26, figs. 14-31, Text-fig. 57

Isotelus stegops Green, 1832, p. 71, casts 26, 27; Bassler, 1919, p. 342, pl. 56, figs. 3, 4.
Homotelus stegops (Green), Ruedemann, 1926, p. 126, pl. 20, fig. 4, pl. 22, figs. 1-9.

Diagnosis. — The body is elongate-oval, moderately convex, with poorly defined furrow; both cephalon and pygidium are large; and thorax divided into eight segments. Cranidium flat to gently convex, without distinct glabella, anterior brim or anterior, or posterior borders. Palpebral lobe medium-sized, situated behind mid-length of cranidium. Librigena having medium-sized genal spine. Hypostoma almost parallel-sided; posterior margin with broad, deep notch. Thoracic segments with broader axial ring and shorter pleural lobes. Pygidium roundly triangular, with poorly impressed dorsal and pleural lobe furrows with flat, broad border. Both cephalon and pygidium with broad marginal doublures.

Description. — The cephalon is semicircular in outline, moderately convex, with broad, flat margins. The cranidium bears a convex axial lobe, is subquadrate in outline and slopes gently downward into a flat anterior brim. The narrow (sag.) occipital ring is defined by a pair of distinct lateral pits, which suggest the posterior ends of the glabella. The palpebral lobes are medium-sized and located behind the mid-line of the cranidium (tr.). The anterior branches of the facial suture are divergently convex and meet at the anterior margin of the cranidium; the posterior branches are divergently straight.

The convex librigenae bear ocular platforms which are broad posteriorly; the lateral borders are broad and concave, but narrower and sharply pointed anteriorly; the genal spines are moderately short; the doublures are flat and broad anteriorly and meet in front of the cranidium at a median suture.

The hypostoma is flat, subquadrate in outline, with a deep posterior notch; no median body or marginal border is present. The lateral wings are broad and short.

The thoracic axis is unusually broad, twice as wide as the pleural lobes; eight segments are present in the adult form. The dorsal furrows are shallow and broad. The pleural lobes slope gently downward and are directed posteriorly and laterally; pleural lobe furrows are shallowly impressed.

The pygidium is roundly triangular in outline, moderately convex, with a broad, flat marginal border; the axial lobe is slenderly conical, tapering posteriorly and ending at the inner marginal furrow. The axial ring and the pleural segments are not distinctly defined, but at least ten segments are estimated. The doublure is broad, convex, and expands slightly toward the front.

The surface is smooth or covered by punctation, except for a median tubercle on the posterior cranidium; parallel ridges are present along the doublures and the hypostoma. A pair of distinct, rounded pits is impressed on the central portion of the hypostoma.

Remarks. — Many beautiful Ordovician specimens have been collected from the greater Cincinnati area (southeastern Indiana, northern Kentucky, and southwestern Ohio) by students and by amateur paleontologists. Several local collectors have hundreds of *Isotelus, Flexicalymene, Cryptolithus, Acidaspis, Isorophus,* and *Glyptocrinus.* Such abundance is truly remarkable. However, materials here studied are from the writer's collection. While they are less complete than much of the material in amateur hands, they serve

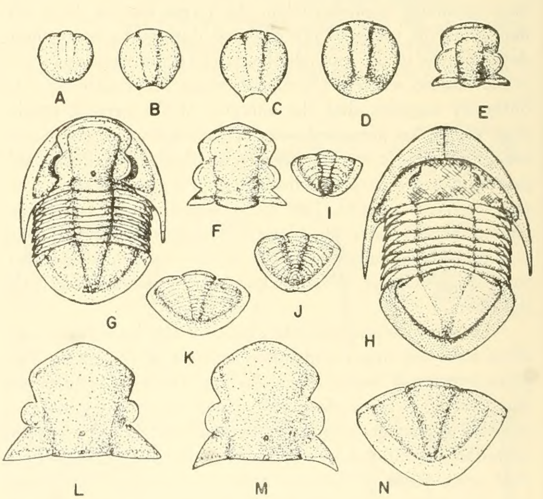

Text-fig. 57 — *Isotelus stegops* Green. A. Anaprotaspis, x 57; B,C. Two metaprotaspids, x 30, x 27; D. Paraprotaspis, x 12; E. Late early meraspis, x 13; F,G. Two late meraspids, x 12, x 3.4; H. Ventral view of a complete skeleton, x 1.7;I-K. Growth series of pygidia, x 15, x 10, x 4; L. "Male" cranidium, x 1.5; M. "Female" cranidium. (Drawings made from photographs.)

admirably to illustrate morphology. According to literature search, about eight species of *Isotelus* have been published from the greater Cincinnati region:

Isotelus maximus Locke, 1838; Liberty Formation, Richmond group, from Treber's Run, Adams County, Ohio.

I. brachycephalus Foerste, 1921; base of Liberty on top of Waynesville, Richmond group, from Dayton, Oregonia, Warren County, Ohio.

I. megistos Locke, 1842, Upper Maysville Formation, from Adams County, and Cincinnati Hill, Ohio.

I. gigas Dekay, *in* Green, 1832; Yellow argillaceous slate [upper Eden or lower Maysville Formation?], from near Cincinnati, Ohio.

I. stegops Green, 1832; Clay slate [Eden Formation?], from near Newport, Campbell Co., Kentucky.

I. planus Dekay, *in* Green, 1832; Yellow argillaceous slate [Eden Formation ?], from near Newport, Campbell Co., Kentucky.

I. covingtonenesis Ulrich, 1914; Cynthiana Formation, from 59.7 and 59.1 miles of Ludlow, near Rogers Gap, north of Cynthiana Station, Harrison Co., Kentucky.

Isotelus benjamini Ulrich, 1914; Cynthiana Formation, at 54.5 miles from Ludlow, Sadieville, Rogers Gap, north of Cynthiana Station, Harrison Co., Kentucky.

Bassler's (1915) survey of the literature on *Isotelus* listed three species as occurring in the Ordovician of the Cincinnati area: *Isotelus gigas* Dekay, *I. maximus* Locke (both from Maysville Formation), and *I. gigas* Dekay, *I. megistos* Locke (both from Richmond). Dalvé (1948) listed only two species: *I. gigas* and *I. maximus*. Cumings (1908) said that the common species in the Cincinnati region possesses the genal spine and should be referred to *I. maximus* Locke and that those fragments which do not show this critical part are indeterminable. Hall, 1847, considered *I. gigas, I. planus,* and *I. stegops* to be synonymous. Ruedemann (1926) placed *I. stegops* in the genus *Homotelus* without giving any reasons. It is assumed that Ruedemann's figures are showing the animal as possessing a broader posterior fixigenae, forwardly located palpebral lobes, and a rounder pygidium as that of *Homotelus*. It is still doubtful that these are any specific or even the generic significance because the sexual dimorphism might exist in the present genus. *Isotelus* (see below). Foerste (1921) suggested that the two forms occurring in the Richmond strata might represent sexual differences of one species: *i.e., I. maximus* Locke, about 17-21 inches long, with an elongate cephalon, no librigenal spine, and an elongate-triangular pygidium, is the male form, and *I. brachycephalus* Foerste, 14.5 inches long with librigenal spine, and with cephalon and pygidium remarkably shorter and wider, the female. Ross (1967) studied Ordovician trilobites from the Kentucky and Ohio regions, and assigned the Middle Ordovician *Isotelus* to *I. gigas*.

As listed above, there are about eight species of *Isotelus* which have been established around the greater Cincinnati area, ranging in age from Middle to Upper Ordovician (Cynthiana through Cincinnatian). It is difficult to judge the validity of these species, because the characteristics noted are ambiguous and almost none of the criteria employed can serve for species differentiation. Through the Ordovician range noted, the body length increases from three or four inches in the Cynthiana to 21 inches in the Upper Cincinnatian. Furthermore, if the sexual dimorphism existed here, as suggested by Foerste, it would be exceedingly difficult to separate species based on such criteria as length or width of cranidium and pygidium, genal spine, facial suture, or palpebral lobe position. Furthermore, both preservation and ontogenetic stage enter into the evaluation of the published "species".

One interesting observation is evident in the foregoing list of species occurring in the Middle-Upper Ordovician of the Cincinnati area: two "species" have been recognized for each horizon. To what extent, if at all, these reflect sexual dimorphism awaits further study.

Careful stratigraphic collecting and statistical analysis are imperative if the true nature of *Isotelus* speciation and variation in the Middle-Upper Ordovician of the classic Cincinnati Ordovician are to be resolved. Unfortunately most amateur collected materials, and this includes much of museum collections, lack stratigraphic precision, and routine professional collecting commonly is not rewarding. Hundreds of amateurs, seeking trilobites almost to the exclusion of all other fossils, create an erroneous impression as to trilobite, and especially *Isotelus,* abundance in these local strata. Moreover, most outcrops are stripped of trilobites before the professional collects.

The material of this report was collected from the upper part of the Eden Formation, probably from the lower part of the McMicken member. Therefore, judging from both the stratigraphic position and the morphologic (mainly dimensional) features, I have assigned the materials to *I. stegops*. The specimens show dimorphism such as Foerste indicated; one group of specimens has elongate cranidia and pygidia, and another group short and broad cranidia and pygidia. It is suggested that the broad and short forms (Pl. 26, fig. 30) are male and that the elongate ones (Pl. 26, figs. 25, 29) female. Bassler (1919, p. 343) said that what are judged as possible females lack genal spines and the males have them. This interpretation would be in keeping with sexual differences in modern arthropods.

Horizon and locality. — Upper Ordovician, Cincinnatian, Eden Formation. Park Hills, western Covington, west side of Highway Route 42, Kenton Co., Kentucky.

Figured specimens. — Cranidium ("male"), U.C.M. 38746m; cranidium ("female"), U.C.M. 38746i,e; librigena, U.C.M. 38746n; complete skeleton, U.C.M. 38746; hypostoma, U.C.M. 38746j.

Isotelus stegops Green, ontogeny

Anaprotaspid stage (Pl. 26, figs. 17, Text-fig. 57A). The shield is rounded, convex, and about 0.30 mm in length (sag); no distinct features occur on the surface except a pair of frontal pits which are present on the anterior margin and suggest the frontal lobe and the orientation of the shield. The surface is covered by fine granules.

Metaprotaspid stage (Pl. 26, figs. 18, 19, Text-fig. 57B, C). The shield is subspherical, convex, and about 0.40-0.60 mm in length. The slenderly fusiform axis is defined by distinct dorsal furrows; no axial rings are seen. The anterior pits are distinctly impressed. The fixigenae are more than one and one-half times wider than the axial lobe. A pair of short, broad spines is directed posteriorly from the posterior lateral margin. The surface is finely granulated.

This stage differs from the early one in having the shield distinctly divided into axial and pleural lobes.

Paraprotaspid stage (Pl. 26, figs. 20,21, Text-fig. 57 D). The cranidium is elongate, oval in outline, moderately convex and ranges from 0.70 to 1.00 mm in length (sag.). The glabella is hemicylindrical with a pair of distinctive anterior pits on the anterior margin; the glabellar furrows are indistinct and the dorsal furrows are shallow; the occipital ring and the posterior fixigenal border are not differentiated. There is no preglabellar field; the anterior margin is roundly convex and arches anteriorly. The convex fixigenae are more than one and one-half times wider than the glabellar and lack palpebral lobes and ridges.

Late aspect of the early meraspid stage (Pl. 26, figs. 14, 15,22, Text-fig. 57E, I, J). The cranidium is subquadrate in outline, about 1.30-1.45 mm in length (sag.), with broad palpebral lobe located behind the mid-line of the glabella (tr.). The glabella is broadly hemicylindrical and marked by three pairs of glabellar furrows. The preglabellar field and anterior border have both appeared.

The pygidium is roundly triangular and convex. The axial lobe is conical, tapers posteriorly and ends with a broad, triangular terminal portion. The axis is divided into six rings by well-defined ring-furrows; the terminal portion consists of three concentric wrinkles and a ridge directed posteriorly to the marginal border. The pleural lobes are marked by six pleural furrows, and the same number of interpleural grooves. At least one thoracic segment is associated with the pygidium. The surface is covered by fine granules.

The characteristics of this stage are different from the paraprotaspids, but closely similar to the late meraspis. Hence the specimens of this ontogenetic stage seen here adjudged as belonging to a later aspect of the early meraspid stage; considerable record between this and the paraprotaspis seems to be lacking. The gap is possibly due to the meager nature of the collections.

Late meraspid stage (Pl. 26, figs. 23, 24, 27, Text-fig. 57F, G, K). The cranidium is subquadrate in outline, moderately convex, with distinctly impressed dorsal furrows, and ranges from 1.50 to 2.00 mm in length (sag.). The glabella is hemicylindrical to strongly expanded anteriorly with three pairs of moderately impressed glabellar furrows. The occipital ring is convex and slightly expanded at the axial line. The anterior furrow is convex, and broader at the median notch; no preglabellar field is present, except in smaller specimens which show a narrow, flat area in front of the glabella; the anterior border is subtriangular, narrow, and anteriorly projecting. The fixigenae are narrower than in the previous stage, being one-half or less than one-half as wide as the glabella; they are flat to gently upturned; the palpebral lobe is medium-sized and located somewhat posterior to the mid-line of the glabella (tr.). The posterior-lateral fixigenae are narrowly triangular, being about one-third as wide as the occipital ring.

The pygidium is subtriangular, convex, without distinct axial or pleural furrows; fine, parallel ridges are marked along the pleural bands on the inner skeletal surface.

Figured specimens. — Anaprotaspis, U.C.M. 38746a; metaprotaspids, U.C.M. 38746b, c; paraprotaspids, U.C.M. 38746d, e; late-early meraspids, U.C.M. 38746o, p, f; late meraspids, U.C.M. 38746g, h, k.

DIMORPHIC TRILOBITE PROBLEMATICA

Endo and Resser (1937) reported a specimen from the southern Manchuria, Middle Cambrian, which showed two well-preserved trilobites, *Fengtienia peculiaris* Endo, lying side by side joined at the tip of the pygidium as though they are in copulation. The left individual is larger than the right one, and has a larger pygidium. The larger body may belong to the female and the smaller one to the male. If this association is rightly interpreted, it is the first example of copulation yet reported from the Trilobita and serves admirably to account for the new widely documented dimorphism in trilobite assemblages of closely similar morphology. Two similar specimens of *Flexicalymene meeki* (Foerste) and *Acidaspis cincinnatiensis* Meek in the Geology Museum at the University of Cincinnati seem to document the same act and dimorphism. Both are from older collections carrying the general label from the "Upper Cincinnatian, Cincinnati area". The following is a brief discussion of two specimens.

1. *Flexicalymene meeki* (Foerste) (Pl. 25, figs. 30-32, Text-fig. 58A, B). The two individuals are rolled into cone-in-cone form, cephalon directed to cephalon, and pygidium to pygidium. The two dorsa curve outwardly. The specimen is ovoid, about 19.6 mm in maximum, and 12.2 mm in minimum diameters. Both of the individuals have their pygidia slightly weathered and the outer individual (Text-fig. 58"b") has the cephalon broken off. Hence the close morphologic comparisons that are desirable are impossible, however, the inner, or "a" form, has the relatively larger pygidium.

There are three possible causes for the enrolled preservation of the animals: a) skeletal moulting, b) accidental preservation, and c) sexual conjugation.

Exoskeletal moulting is common to most crustaceans, xiphosurans, insects. During their ecdysial period the animals are inactive, and their new skeletons are soft and thin. This condition seems hardly to apply to this specimen, because the soft body of newly molted animal is hardly preserved as a fossil. Moreover, the specimen shows both individuals have skeletons of the same thickness, and both are apparently well calcified. The cause of possible accidental preservation may be interpreted in two ways: the animals were associated after death or perhaps represent living association. If the association occurred after death, the enrollment must have occurred before decay of the animal tissues. Otherwise, the hard skeletons should have been disarticulated, because dead animals always are attacked immediately by scavengers, and there is almost no chance for two long-dead individuals to have been rolled together. On the other hand, if the two animals were rolled together accidentally during their life period, possibly for protection, there would seem little chance that the two individuals oriented themselves thus, parallel; head-to-head and pygidium as they occur here.

The orientation of the animals suggests a volitional life association, and that the head-to-head and tail-to-tail relationship is more than a chance; if so, the easiest explanation is that they record copulation. This orientation during the sex act would correspond to that well demonstrated in modern *Xiphosura* where the smaller male lies over the larger female while depositing the milt. The enrollment of the two animals may well have been caused by fright or excitement during the mating period, and the two individuals became enrolled from their originally extended natural position into the cone-in-cone form now seen.

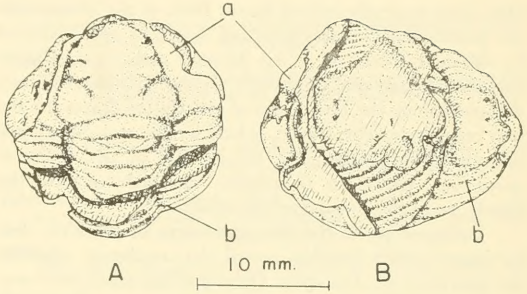

Text-fig. 58 — *Flexicalymene meeki* (Foerste). Showing two individuals lying in a "cone-in-cone" relationship; A. Dorsal view; B. Ventral view; "a" individual lying in "b". (Drawings made from a photograph.)

2. *Acidaspis cincinnatiensis* Meek (Pl. 10, figs. 24-27, Text-fig. 59A-C). The specimen is 20.1 mm in length, 13.8 mm wide at the mid-length, and 5.6 mm in thickness. It shows two different-sized individuals lying with venters opposed, head-to-head, and pygidium-to-pygidium. The articulated thorax and pygidium of the smaller individual is 14.9 mm long. The larger individual measures 15.2 mm over a comparable area (both measurements are from the first axial ring to the posterior pygidial margin). In the small individual the cephalon is present but slightly displaced; it is lost in the large one.

The venter-to-venter orientation of these two-sized individuals of the same species is highly suggestive of sexual conjugation. Perchance the digitate pygidia spines were inter-locked as clasping devices during conjugation, whether fertilization was external or internal. Such a copulatory position is common among arthropods. Which size variant correlates with which sex is problematic, although present data suggest that the male is the larger form.

The conjugation of recent arthropods is highly vari-

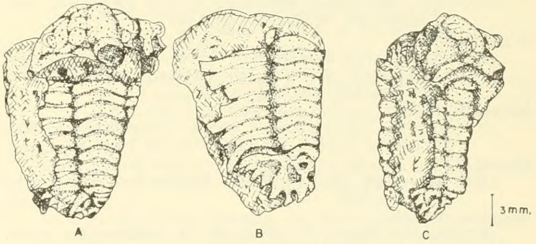

Text-fig. 59 — *Acidaspis cincinnatiensis* Meek. Two individuals lying facing each other as if they are in copulation. A. Dorsal view of small individual; B. Dorsal view of a large individual; C. Side view of both A and B individuals; note coincidence cephalon to cephalon and pygidium to pygidium. (Drawings made from photographs.)

able, even in closely related forms. Both of the inferred sex act positions of *Flexicalymene* and *Acidaspis* are illustrated by different species of living decapod crabs: *e.g.*, *Cancer borealis* Stimpson and *Callinectes sapidus* Rathbun, common decapods along the East Coast of the United States. In the first crab the smaller female, is held by the male, in a position facing each other, like the position of the *Acidaspis* specimen, whereas in *C. sapidus* the male mounts the female, as in the *Flexicalymene* example.

In any event in the three specimens of trilobites thus far known which possibly record the copulatory position, the specimens are dimorphic. Quite possibly much more material reposes in public and private hands and should be reported.

Figured specimens. — *Flexicalymene meeki* (Foerste), U.C.M. 23263; *Acidaspis cincinnatiensis* Meek, U.C.M. 38729.

REFERENCES

Akesson, B.

1961. *On the histological differentiation of the larvae of Pisione remota (Pisionidae, Polychaeta).* Acta Zoologica, Bd. 42, No. 3, pp. 177-225, 24 text-figs.

1962. *The embryology of Tomopteris helgolandica (Polychaeta).* Acta Zoologica, Bd. 43, No. 2,3, pp. 135-199, 31 text-figs.

1963. *The comparative morphology and embryology of the head in scale worms (Aphroditidae, Polychaeta).* Arkiv för Zoologi, ser. 2, Bd. 16, No. 7, pp. 125-163, 21 text-figs.

1967. *The embryology of the polychaete Eunice kobiensis.* Acta Zoologica, Bd. 48, No. 1,2, pp. 141-192, 22 text-figs.

1967a. On the biology and larval morphology of *Ophryotrocha puerilis* Claparède and Metschnikov (Polychaeta): Ophelia, vol. 4, pp. 110-119.

1697b. *On the nervous system of the Lopadorhynchus larva (Polychaeta).* Arkiv för Zoologi, Bd. 20, No. 2, pp. 55-58, 17 text-figs.

Anderson, D. T.

1959. *The embryology of the polychaete Scoloplos armiger.* Quart. Jour. Microscopic Sci., vol. 100, pp. 89-166, 22 text-figs.

1961. *The development of the polychaete Haploscoloplos fragilis.* Quart. Jour. Microscopic Sci., vol. 102, pp. 257-272, figs. 1,2.

1966. *The comparative embryology of the Polychaeta.* Acta Zoologica, Bd. 47, Nos. 1,2, pp. 1-39.

Angelin, N. P.

1878. *Palaeontologia Scandinavica, Crustacea formationis transitionis.* Repub. ed. Lindström. Holmiae. Fasc. 1, 2, (Stockholm), pp. 1-96, pls. 1-42.

Ashworth, J. H.

1904. *Arenicola* (the lug-worm) *marina.* Liverpool Marine Biol. Committee, L.M.B.C., 11, pp. 1-118, pls. 1-8.

Barnes, R. D.

1963. Invertebrate Zoology. W. B. Sanders Co., Philadelphia. Pp. 1-632, illus.

Barrande, Joachim

1852. Systême Silurien du Centre de la Bohême: Iére partie, Crustacés, Trilobites. Vol. 1, 935 pp. 51 pls. (Prague and Paris).

Bassler, R. S.

1915. *Bibliographic index of American Ordovician and Silurian fossils.* Smith. Inst., United States National Museum, Bull. 92, vol. 1, pp. viii + 718; vol. 2, pp. iv, 719-1251, pls. 1-5.

1919. *Cambrian and Ordovician Formations of Maryland.* Maryland Geol. Sur., Arthropoda, pp. 332-362, illust.

Beecher, C. E.

1895a. Further observation on the ventral structures of *Triarthrus.* Amer. Geol., vol. 15, p. 91-100, pls. 4, 5.

1895b. *The larval stages of Trilobites.* Amer. Geol., vol. 16, pp. 166-197, pls. 8-10.

1897. *Outline of a natural classification of trilobites.* Amer. Jour. Sci. ser. 4, vol. 3, No. 49, pp. 89-106, 181-207, pl. 3.

Beklemischew, W. N.

1958. *Grundlagen der vergeichenden Anatomie der Wirbellosen, Bd. 1-2.* Deutcher Verlag der Wissenschaften, Berlin.

Bell, W. C., and Ellinwood, H. L.

1962. *Upper Franconian and Lower Trempealeauan Cambrian trilobites and brachiopods, Wilberns Formation, Central Texas.* Jour. Paleont., vol. 36, No. 3, pp. 385-423, pls. 51-64.

Bernard, H. M.

1894. *The systematic position of the trilobites.* Quart. Jour. Geol. Soc. London, vol. 50, pp. 411-442, pl. 20, text-figs. 1-17.

Bookhout, C. G.

1957. *The development of Dasybranchus caducus (Grube) from the egg to the preadult.* Jour. Morph. vol. 100, No. 1, pp. 141-186, pls. 1-7.

1964. *Salinity effects on the larval development of Pagurus bernhardus (L.), reared in the laboratory.* Ophelia, vol. 1, No. 2, pp. 275-294.

Bookhout, C. G., and Costlow, T. D. Jr.

1959. *Feeding, moulting, and growth in barnacles.* In *Marine boring and fouling organisms.* Friday Harbor Symposia, University of Washington Press, pp. 212-225, (Seattle). [536 pp., illus.]

Bookhout, C. G., and Horn, E. C.

1949. *The development of Axiothella mucosa (Andrews).* Jour. Morphology, vol. 84, No. 1, pp. 145-183, pls. 1-5.

Brøgger, W. C.

1875. *Fossiler fra Øxna og Kletten.* Geol. Fören. Stockholm, Förh., Bd. 2, pp. 572-580, pl. 25.

Brooks, H. K.

1957. *Chelicerata, Trilobitomorphia, Crustacea (exclusive of Ostracoda), and Myriapoda.* Geol. Soc. America, Mem. 67, vol. 2, pp. 895-929. [Annotated bibliography.]

Butt, F. H.

1960. *Head development in the Arthropods.* Biol. Rev., (Cambridge Philos. Soc.), vol. 35, No. 1, pp. 43-91, 15 text-figs.

Butts, C.

1941. *Geology of the Appalachian Valley in Virginia.* Virginia Geol. Sur., Bull. 52, pt. 1, text, 568 pp., pt. 2, 135 pls.

Calman, W. T.

1909. *Crustacea* in E. R. Lankester (ed.), *A treatise on zoology.* Vol. 7, Appendiculata, fasc. 3, 346 pp., 194 text-figs.

1939. *Structures of trilobites.* Nature, vol. 143, p. 1077.

Carpenter, G. H.

1903. *On the relationships between the classes of Arthropoda.* Proc. Roy. Irish Acad., vol. 24 (B), pp. 320-360.

Caster, K. E.

1938. *A restudy of the tracks of Paramphibius.* Jour. Paleont., vol. 12, No. 1, pp. 3-60, pls. 1-13, 9 text-figs.

Caster, K. E., Dalvé, E. A., and Pope, J. K.

1961. *Elementary guide to the fossils and strata of the Ordovician in the vicinity of Cincinnati, Ohio.* Cincinnati Mus. of Nat. Hist., Cincinnati, Ohio, 47 pp., 8 pls.

Chaudonneret, J.

1950. *La morphologie céphalique de Thermobia domestica (Packard).* Ann. Sci. nat. Zool. (II), 12 pp. 145-302, 79 text-figs.

Clark, R. B.

1964. *Dynamics in metazoan evolution.* Clarendon Press, Oxford, Pp. x + 313, illus.

Cobbold, E. S.

1931. *Additional fossils from the Cambrian rocks of Comley, Shropshire.* Geol. Soc. London, Quart. Jour., vol. 87, pp. 459-511.

Comstock, J. H.

1924. *Introduction to Entomology.* The Comstock Pub. Co., Ithaca, N.Y. Pp. i-xix, 1-1044, illus. (1940 edition, 1228 text-figs.)

Cooper, B.

1953. *Trilobites from the Lower Champlainian Formations of the Appalachian valley.* Geol. Soc. Amer., Mem. 55, pp. 1-69, pls. 1-19.

Costello, D. P., et al.

1957. *Methods of obtaining and handling marine eggs and embryos.* Marine Biol. Lab., Woods Hole, Massachusetts. Pp. xv + 247.

Costlow, J. D., Jr., and Bookhout, C. G.

1957. *Larval development of Balanus eburneus in the laboratory.* Biol. Bull., vol. 112, No. 3, pp. 313-324, 5 text-figs.

1958a. *Moulting and respiration in Balanus amphitrite var. denticulata Broch.* Physiological Zool., vol. 31, No. 4, pp. 271-280, 5 text-figs.

1958b. *Larval development of Balanus amphitrite var. denticulata Broch, reared in the Laboratory.* Biol. Bull., vol. 114, No. 3, pp. 284-295, 2 text-figs.

1959. *The larval development of Callinectes sapidus Rathbun reared in the Laboratory.* Biol. Bull., vol. 116, No. 3, pp. 373-396, 11 text-figs.

1960. *The complete larval development of Sesarma cinereum (Bosc) reared in the Laboratory.* Biol. Bull., vol. 118, No. 2, pp. 203-214, 5 text-figs.

Costlow, J. D., Jr., Bookhout, C. G., and Monroe, R. R.

1960. *The effect of salinity and temperature on larval development of Sesarma cinereum (Bosc) reared in the Laboratory.* Biol. Bull., vol. 118, No. 2, pp. 183-202, 12 text-figs.

Cummings, E. R.

1908. *The stratigraphy and paleontology of the Cincinnati series of Indiana.* Indiana Dept. Geol. Nat, Res., 32d Ann. Rpt. (1907), pp. 605-1188.

Dahl, E.

1956. *On the differentiation of the topography of the crustacean head.* Acta Zool. vol. 37, Hft. 1, 2, pp. 123-192, 33 text-figs.

1958. *The ontogeny and comparative anatomy of some protocerebral sense organs in notostracan phyllopods.* Microscopical Sci., Quart. Jour., ser. 3, vol. 100, pp. 445-462, fig. 2 (1 pl.).

1963. *Main evolution lines among Recent Crustacea in Phylogeny and Evolution of Crustacea.* Mus. Comp. Zool., Special Publ., No. 1, pp. 1-15, 2 text-figs.

Dales, R. P.

1963. *Annelids.* Hutchinson University Library, Hutchinson & Co., London. Pp. 1-200, 19 text-figs.

Dalvé, E. A.

1948. *The fossil fauna of the Ordovician in the Cincinnati region.* Univ. Cincinnati, Geol. Museum., Publ., Cincinnati, Ohio. Pp. 1-55.

Dean, W. F.

1960. *The Ordovician trilobite faunas of the South Shropshire. I.* British Mus. Bull. Geol., vol. 4, No. 4, pp. 71-143, pls. 11-19, 2 text-figs.

Deiss, Ch.

1939. *Cambrian stratigraphy and trilobites of northwestern Montana.* Geol. Soc. America, Spec. Paper 18, pp. 1-135, pls. 1-18.

Dekay, J. E.

1824. *Observations on the structure of trilobites and description of an apparently new genus.* Lyceum Nat. Hist., New York Annals, vol. 1, pt. 1, pp. 174-189.

Deland, C. R., and Snow, A. B.

1956. *Upper Cambrian trilobites from western Wyoming.* Jour. Paleont., vol. 30, No. 3, pp. 542-562, pls. 63-67.

Dobkin, S.

1961. *Early developmental stages of pink shrimp, Penaeus duorarum from Florida water.* Fish. Bull. 190, vol. 61, pp. 321-348, 20 text-figs.

Endo, R.

1935. *The post-embryonic development of Blackwelderia quadrata* Endo. Imp. Acad. Tokyo, Proc., vol. 15.

Endo, R., and Resser, C. E.

1937. *The Sinian and Cambrian formations and fossils of southern Manchoukuo.* Manchurian Sci., Mus., Bull. 1, 474 pp., 73 pls.

Evitt, W. R.

1961. *Early ontogeny in the trilobite family Asaphidae.* Jour. Paleont., vol. 35, No. 5, pp. 986-995, pls. 117, 118, 6 text-figs.

Evitt, W. R., and Whittington, H. B.

1953. *The exoskeleton of Flexicalymene (Trilobita).* Jour. Paleont., vol. 27, No. 1, pp. 49-55, pls. 9, 10, 1 text-fig.

Fage, L.

1949. *Classe des Merostomaces.* Traite de Zoologie, Tome VI, pp. 219-262 (Paris).

Fedetov, D.

1924. *On the relations between the Crustacea, Trilobita, Merostomata and Arachnida.* Bull. d'Acad. de Sci. de Russ., 6 ser., T. 18, pp 383-408.

Foerste, A. F.

1909 *Preliminary notes on Cincinnatian and Lexington fossils.* Denison University, Sci. Lab. Bull., vol. 14, pp. 289-324, pls. 7-10.

1919-1921. *Notes on Isotelus, Acrolichas, Calymene, and Encrinurus.* Denison University, Sci. Lab. Bull., vol. 19, pp. 65-81, pls. 14-18.

Ford, S. W.

1877. *On additional embryonic forms of trilobites from the primordial rocks of Troy, N.Y.* American Jour. Sci., ser. 3, vol. 22, pp. 250-259, 12 text-figs.

Fränsemeier, L.

1939. *Zür Frage der Herkunft des metanauplialen Mesoderms und die Segmentbildung bei Artemia salina Leach.* Zeitschr. Wiss. Zool., vol. 152, pp. 439-472, 17 text-figs.

Fraser, J.

1962. *Nature Adrift.* G. T. Foulis & Co., Ltd., London. Pp. v + 178, pls. 1-36, text-figs. 1-38.

Frederickson, E. A.

1948. *Upper Cambrian trilobites from Oklahoma.* Jour. Paleont., vol. 22, No. 6, pp. 798-803, pl. 123.

1949. *Trilobite fauna of the Upper Cambrian Honey Creek Formation.* Jour. Paleont. vol. 23, pp. 431-463, pls. 68-72, 1 text-fig.

Grant, R. E.

1965. *Faunas and stratigraphy of the Snowy Range Formation (Upper Cambrian) in southwestern Montana and northeastern Wyoming.* Geol. Soc. America, Mem. 96, pp. i-ix, 1-171, pls. 1-15.

Green, J.

1832. *A monograph of the trilobites of North America.* No. 12, Joseph Brano Co., Philadelphia, Pa., pp. 1-93.

1961. *A Biology of Crustacea.* H. F. & G. Witherby, Ltd. Pp. 1-180, 58 text-figs.

Hall, J.

1847. *Paleontology of New York. Containing descriptions of the organic remains of the lower division of the New York system.* Nat. Hist. New York, Paleont., vol. 1, pp. 1-338, 33 pls.

Hanson, E. D.

1964. *Animal diversity.* (Foundation of Modern Biology Series.) Prentice-Hall, Inc., New York. Pp. viii + 118, illus.

Hanström, B.

1928. *Vergleichende, Anatomie des Nervensystems der wirbellosen Tiere, . . .* Berlin. Pp. xi + 628 pp., 650 text-figs.

Harrington, H. J.

1956. *Olenellidae with advanced cephalic spines.* Jour. Paleont., vol. 30, No. 1, pp. 56-61, pl. 15, 1 text-fig.

1959. *General description of Trilobita* in *Treatise on Invertebrate Paleontology, Arthropoda, pt. 0.* Geol. Soc. American and Univ. Kansas Press, pp. 38-117, text-figs. 27-85.

Harrington, H. J., and Kay, M.

1951. *Cambrian and Ordovician faunas of eastern Colombia.* Jour. Paleont., vol. 25, No. 5, pp. 655-668, pls. 96, 97.

Harrington, H. J., and Leanza, F.

1957. *Ordovician trilobites of Argentina.* Univ. of Kansas, Dept. of Geology, Spec. Publication 1, 276 pp., 140 text-figs.

Hartman, O.

1945. *The marine annelids of North Carolina.* Duke Univ. Marine Station, Bull. No. 2, pp. 1-54, pls. 1-10.

Heegaard, P.

1945. *Remarks on the phylogeny of arthropods.* Ark. Zool., vol. 37, pp. 1-15.

Henningsmoen, G.

1951. *Remarks on the classification of trilobites.* Norsk geol. Tidsskr., Bd. 29, pp. 174-217 (Oslo).

1957. *The trilobite family Olenidae.* Norsk Vidensk. Akad., (Oslo), Skr., 1 Kl., No. 1, pp. 1-303, pls. 1-30.

1958. *The Upper Cambrian faunas of Norway; with description of non-olenid invertebrate fossils.* Norsk geol. Tidsskr., Bd. 38, pp. 179-196 (Oslo), pls. 1-7.

1964. *Zig-Zag Evolution.* Norsk. geol. Tidsskr., Bd. 44, pp. 341-352, Text-figs. 1-9.

Henriksen, K. L.

1926. *The segmentation of the trilobite's head.* Dansk. geol. Foren., Medd., vol. 7, pp. 1-32 (København).

Herskowitz, I. H.

1962. *Genetics.* Little Brown and Co., Boston. Pp. x + 466, illus. or 7.

Hinte, L. F.

1952. *Lower Ordovician trilobites from western Utah and eastern Nevada.* Univ. Utah, Bull. 48, pp. 1-249, 28 pls.

Hofmann, T. F., and Parsley, R. L.

1966. *Antennae of Ogygopsis.* Jour. Paleont., vol. 40, No. 1, pp. 208-211, 2 Text-figs.

Holm, G., and Westergård, A. H.

1930. *A Middle Cambrian fauna from Bennett Island.* Acad. Sci., U.S.S.R., Mem. ser. 8 (Phy.-Math., Class, vol. 21, No. 8).

Holmgren, N.

1916. *Zur vergleichenden Anatomie der Gehirne von Polychaeten, Onychophoren, Xiphosuren, Arachniden, Crustaceen, Myriapoden und Insecten.* K. Svenska Vetens.-Akad. Handl., Bd. 56, pp. 1-303, 12 pls., 54 text-figs.

Horn, E. C., and Bookhout, C. G.

1950. *The early development of Haploscoloplos bustoris (Eisig).* Elisha Mitchell Sci. Soc., Jour. vol. 66, No. 1, pp. 1-9.

Howell, B. F.

1925. *The faunas of the Cambrian Paradoxides beds at Manuels, Newfoundland.* Bull. Amer. Paleont., vol. 11, No. 43, pp. 5-140, pls. 1-3.

Howell, B. F., and Duncan, D.

1939. *Middle-Upper Cambrian transition faunas in North America.* Wagner Free Inst. Sci., Philadelphia, Bull., vol. 14, No. 1, pp. 1-10, 1 pl.

Howell, B. F., et al.

1947. *Terminology for describing Cambrian trilobites.* Jour. Paleont., vol. 21, No. 1, pp. 72-76, 1 fig.

Hu, C. H.

1963. *The dimorphism and ontogeny of Norwoodella halli Resser.* Paleont., Soc. Japan, Proc. Trans., No. 52, pp. 129-132.

1964. *The ontogeny and dimorphism of Welleraspis lata Howell (Trilobita).* Jour. Paleont., vol. 38, No. 1, pp. 95-97, pl. 24.

1968. *Notes on the ontogeny and sexual dimorphism of Upper Cambrian trilobites or the Welleraspis faunule from Pennsylvania.* Jour. Nanyang Univ., vol. 2, pp. 321-357, pls. 1-5, 8 text-figs.

Hunt, A. S.

1967. *Growth, variation, and instar development of an agnostid trilobite.* Jour. Paleont., vol. 41, No. 1, pp. 203-208, pl. 22, 2 text-figs.

Hupé, P.

1950. *Étude statistique de l'évolution du cephalon chez les Trilobites, Proparia et Opistoparia.* Soc. Géol. France, Bull., 5 Sér., t. 20, fasc. 1, pp. 9-24, 4 text-figs.

1951. *Sur les affinités des Trilobites.* Soc. Géol. France, Bull., 6 Sér., vol. 1, fasc. 7, pp. 469-486.

1953a. *Classe des trilobites.* Traité de paléontologie, vol. 3, pp. 44-246 (Paris), 140 text-figs.

1953b. *Quelques rémarques sur la croissance et la segmentation des Trilobitea.* Soc. Géol. France, Bull., 6 Sér., vol. 3, fasc. 1, pp. 3-11, text-figs. 1-4.

1953c. *Contribution à l'étude du Cambrien inférieur et du Précambrien III de l'Anti-Atlas marocain.* Serv. géol. Maroc., Notes et Mém. No. 103, (1952), pp. 1-402, 24 pls., 99 figs.

1955. *Classification des Trilobites.* Ann. Paléont., vol. 41, pp. 111-325, figs. 83-247, 247 text-figs.

1960. *Reflexions sur quelques traits de la structure cephalique chez les larves de Trilobites.* Geol. Soc. France, Bull., 7th ser., v. 1, No. 7, pp. 745-788, 16 text-figs.

Ishibashi, E., et al.

1938. *General Zoology.* Kasho Book Co., Tokyo. (In Japanese).

Iwanoff, P. P.

1928. *Die Entwichelung der Larvalsegmente bei den Anneliden.* Zeitschr. Morph. Ökol, Tiere 10, pp. 62-161.

1933. *Die embryonale Entwicklung von Limulus moluccanus.* Zool Jahrb. Bd. 56, Abt. f., Anat., H. 2, pp. 163-348, 77 text-figs.

1944. *The primary and secondary metamery of the body.* Jour. Gen. Biology, Moscow, vol. 5, No. 2, pp. 61-95, (Russian with English summary).

Jaanusson, V.

1954. *Zur Morphologie und Taxonomie der Illaeniden.* K. Svenska Vet.-akad., Arkiv. für Mineral. Geol., No. 20, pp. 545-583, 3 pls., 1 fig.

Jaekel, O.

1901. *Ueber die Organisation der Trilobiten.* Zeitschr. Deutsch. geol. ges., Bd. 53, pp. 133-171, pls. 4-6, 31 text-figs.

Johansson, G.

1933. *Beiträge zur Kenntnis der Morphologie und Entwicklung des Gehirns von Limulus polyphemus.* Acta Zoologica, Bd. 14, pp. 1-100, 45 text-figs. (Stockholm).

Kiaer, J.

1916. *The Lower Cambrian Holmia fauna at Tomten in Norway.* Norske. vidensk. Selskab. Skrifter Kristiania 1, No. 10, pp. 1-140.

Kingsley, J. S.

1885. *Notes on the embryology of Limulus.* Quart. Jour. Micro. Sci., vol. 25, pp. 521-576, pls. 37-39.

1892-3. *The embryology of Limulus.* Jour. Morph., vol. 7, pp. 35-66, pls. 5, 6; vol. 8, pp. 196-260, pls. 10-13.

1897. *The systematic position of the trilobites.* Amer. Geol., vol. 20, pp. 33-40.

Kobayashi, T.

1935. *The Cambro-Ordovician Formations and faunas of South Chosen.* Imp. Univ. Tokyo, Jour. Fac. Sci., Sec. II, vol. 4, pt. 2, pp. 1-344, pls. 1-24.

1936. *On the Parabolinella fauna from province Jujuy, Argentina with a note on the Olenidae.* Japanese Jour. Geol. and Geog., vol. 13, No. 1-2, pp. 85-102, pls. 15-16.

1939a. *On the agnostids (part 1).* Imp. Univ. Tokyo, Jour. Faculty Sci., Sec. II, vol. 5, pt. 5, pp. 69-198.

1939b. *Supplementary notes on the Agnostidae.* Geol. Soc. Japan, Jour., vol. 46, No. 554, pp. 97-100.

1944. *On the Eodiscids.* Imp. Univ. Tokyo, Jour. Fac. Sci., Sec. II, vol. 7, pt. 1, pp. 1-74, pls, 1,2.

1960a. *Notes on the natural classification of Trilobita.* Geol. Soc. Japan, Jour., vol. 66, No. 776, pp. 538-546 (in Japanese).

1960b. *Studies on trilobites in last three decades (Presidential Address).* Paleont. Soc. (Japan), Trans.-Proc., No. 37, pp. 230-237.

1960c. *The Cambro-Ordovician Formations and faunas of South Korea, part 7 Palaeontology 6.* Univ. Tokyo, Jour. Fac. Sci., Sec. II, vol. 12, pt. 2, pp. 329-420, pls. 19-21.

1962. *The Cambro-Ordovician Formations and faunas of South Korea, part 9 Palaeontology 8.* Univ. Tokyo, Jour. Fac. Sci., Sec. II, vol. 14, pt. 1, pp. 1-152, pls. 1-8.

Kobayashi, T., and Kato, F.

1951. *On the ontogeny and ventral morphology of Redlichia chinensis with description of Alutella nakamurai, new gen. and sp.* Univ. Tokyo, Jour. Fac. Sci., Sec. II, vol. 8, pt. 3, pp. 99-143, pls. 1-5.

Lankester, E. R.

1904. *The structure and classification of the Arachinida.* Quart. Jour. Microscopical Sci., n.s., vol. 48, pt. 2, pp. 165-269, 78 text-figs.

Lever, W.

1966. *New criteria for ascertaining sex in Oncopeltas fasciatus (Dallus).* Turtox News, vol. 44, No. 2, pp. 62, 63.

Lillie, R. S.

1905. *The structure and development of the nephridia of Arenicola cristata Stimpson.* Zool. Station, Mitt., Neapel. vol. 17, pp. 341-405, pls. 22-25.

Lindström, G.

1901. *Researches on the visual organs of the trilobites.* K. Svenska Vetens.-Akad., Handl., Bd. 34, No. 8, p. 1-86, pls. 1-6.

Lochman, C.

1940. *Fauna of the basal Bonneterre dolomite (Upper Cambrian) of southeastern Missouri.* Jour. Paleont., vol. 14, No. 1, pp. 1-53, pls. 1-6.

1950. *Upper Cambrian faunas of the Little Rocky Mountains, Montana.* Jour. Paleont., vol. 24, No. 3, pp. 322-349, pls. 46-51.

1952. *Trilobites* in G. A. Cooper *et al. Cambrian stratigraphy and paleontology near Caborca, northwestern Sonora, Mexico.* Smith, Misc. Coll., vol. 119, No. 1, 184 pp., 31 pls. [pp. 60-61, pls. 15-31].

1956a. *The evolution of some Upper Cambrian and Lower Ordovician trilobites families.* Jour. Paleont., vol. 30, No. 3, pp. 445-462, pls. 47,48.

1956b. *Stratigraphy, paleontology, and paleogeography of the Elliptocephala, Asaphoides strata in Cambrian and Hoosick Quadrangles, New York.* Geol. Soc. Amer., Bull., vol. 67, No. 10, 1331-1396, pls. 1-10, 2 text-figs.

1964a. *Upper Cambrian faunas from the subsurface Deadwood Formation, Williston Basin, Montana.* Jour. Paleont., vol. 38, No. 1, pp. 33-60, pls. 9-15, 1 text-fig.

1964b. *Basal Ordovician faunas from the Williston Basin, Montana.* Jour. Paleont., vol. 38, No. 3, pp. 453-476, pls. 63-67.

1966. *Lower Ordovician (Arenig) faunas from the Williston Basin, Montana and North Dakota.* Jour. Paleont., vol. 40, No. 3, pp. 512-548, pls. 61-65, 2 text-figs.

Lochman, C., and Duncan, D.

1944. *Early Upper Cambrian faunas of Central Montana.* Geol. Soc. Amer., Spec. Paper No. 54, pp. 1-181, pls. 1-19.

Lochman, C., and Hu, C. H.

1959. *A Ptychaspis faunule from the Bear River Range, southeastern Idaho.* Jour. Paleont., vol. 33, No. 3, pp. 404-427, pls. 57-60, 1 text-fig.

1960. *Upper Cambrian faunas from the northwest Wind River Mountains, Wyoming, Pt. I.* Jour. Paleont., vol. 34, No. 5, pp. 793-834, pls. 95-100.

1961. *Upper Cambrian faunas from the northwest Wind River Mountains, Wyoming, Pt. II.* Jour. Paleont., vol. 35, No. 1, pp. 125-146, pls. 26-30.

1962a. *Upper Cambrian faunas from the northwest Wind River Mountains, Wyoming, Pt. III.* Jour. Paleont., vol. 36, No. 1, pp. 1-28, pls. 1-7.

1962b. *An Aphelaspis zone faunule from Logan, Montana.* Jour. Paleont., vol. 36, No. 3, pp. 431-441, pls. 68-70.

Lochman, C., and Wilson, J. L.

1958. *Cambrian biostratigraphy in North America.* Jour. Paleont., vol. 32, No. 2, pp. 312-350, 18 text-figs.

Locke, J.

1838. *Geological report on southwestern Ohio. Isotelus maximus Locke.* In Geol. Surv. Ohio, 2d Ann. Rep., vol. 2, pp. 203-286.

1842. *On a species of trilobite of very large size.* American Jour. Sci., and Arts, vol. 42, No. 2, pp. 366-368, pl. 3.

Lu, Y. H.

1957. *Trilobita. Index fossils of China. Acad-Sinica,* Inst. Paleontology, Geol. Press, pp. 249-320, pls. 137-155.

Manton, S. M.

1934. *On the embryology of the crustacean Nebalia bipes.* Roy. Soc. London, Philos. Trans., Ser. B, vol. 223, pp. 163-238, pls. 20-26.

1949. *Studies on the Onychaphora VII; The early embryonic stages of Peripatopsis and some general considerations concerning the morphology and phylogeny of the Arthropoda.* Roy. Soc. London, Philos. Trans., Ser. B, vol. 233, pp. 483-580, pls. 31-41.

1960. *Concerning head development in the arthropods.* Biol. Rev. (Cambridge Philos. Soc.), vol. 35, No. 2, pp. 265-282, 3 text-figs.

Matthew, G. F.

1896. *Faunas of the Paradoxides beds in eastern North America, No. 1.* New York Acad. Sci., Trans., vol. 15, pp. 192-247, pls. 14-17.

1898. *Studies on Cambrian faunas No. 2.* Roy. Soc. Canada, Trans.-Proc., 2d Ser., vol. 4, Sec. 4, pp. 123-150, pls. 1, 2.

Meek, F. B.

1873. *Fossils of the Cincinnati Group.* Geol. Surv. Ohio, Report, vol. 1, pt. 2, pp. 1-757, pls. 1-13.

Milne Edwards, H.

1838. *Recherches relatives au developpement des Limulus.* Ext. Proc. Verb. Soc. Philomath. Paris.

Moberg, J. C.

1899. *Sveriges älsta känka trilobiter.* Geol. fören. (Stockholm) Förh., vol. 21, Höft 4, pp. 309-348, pls. 13-15.

Moberg, J. C., and Möller, H.

1898. *Om Acerocarezonen.* Geol. Foren. (Stockholm) Forh., vol. 20, pp. 197-290, pls. 10-14.

Miner, R. W.

1950. *Field Book of seashore life.* G. P. Putnam's Sons, New York. Pp. xv + 888, 251 pls.

Nelson, C. A.

1951. *Cambrian trilobites from the St. Croix valley.* Jour. Paleont., vol. 25, No. 6, pp. 765-784, pls. 106-110.

Nickles, J. M.

1902. *The geology of Cincinnati.* Jour. Cincinnati Soc. Nat. Hist., vol. 20, No. 2, pp. 49-100.

Öpik, A. A.

1952. *The hypostoma of Pagetia.* Jour. Paleont., vol. 26, No. 2, pp. 272-274, 2 text-figs.

1958. *The Cambrian trilobite Redlichia: organization and generic concept.* Australia Dept. Nat. Develop., Bureau Min. Res. Geol. and Geog., Bull., No. 42, pp. 5-37, pls. 1-6, 9 text-figs.

Packard, A. S.

1872. *The development of Limulus polyphemus.* Boston Soc. Nat. Hist., Mem., vol. 2, No. 4, pp. 155-202, pls. 2-5.

1880a. *The anatomy, histology, and embryology of Limulus polyphemus.* Boston Soc. Nat. Hist., Anniv. Mem., pp. 1-45, pls. 1-7.

1880b. *Further studies on the brain of Limulus polyphemus with notes on its embryology.* Nat. Acad. Sci. 8th Mem., vol. 6, pp. 287-331.

Palmer, A. R.

1954. *The fauna of the Riley Formation in Central Texas.* Jour. Paleont., vol. 28, No. 6, pp. 709-786, pls. 76-92, 6 text-figs.

1955. *Upper Cambrian Agnostidae of the Eureka district, Nevada.* Jour. Paleont., vol. 29, No. 1, pp. 86-101, pls. 19, 20, 2 text-figs.

1957. *Ontogenetic development of two olenellid trilobites.* Jour. Paleont., vol. 31, No. 1, pp. 105-128, pl. 19, 9 text-figs.

1958. *Morphology and ontogeny of a Lower Cambrian ptychoparioid trilobite from Nevada.* Jour. Paleont., vol. 32, No. 1, pp. 154-170, pls. 25,26, 7 text-figs.

1960. *Trilobites of the Upper Cambrian Dunderberg Shale, Eureka district. Nevada.* United States Geol. Sur., Prof. Paper 334-C, pp. 1-109, pls. 1-11.

1962. *Comparative ontogeny of some opisthoparian, gonatoparian, and proparian, Upper Cambrian trilobites.* Jour. Paleont., vol. 36, No. 1, pp. 87-96, pl. 19.

1964. *An unusual Lower Cambrian trilobite fauna from Nevada.* United States Geol. Sur., Prof. Paper 483-F, pp. 1-12, pls. 1-3.

1965. *Trilobites of the Late Cambrian pterocephaliid Biomere in the Great Basin, United States.* United States Geol. Sur., Prof. Paper 493, pp. 1-105, pls. 1-20.

Patten, W.

1889. *Segmental sense-organs of arthropods.* Jour. Morph., vol. 2, No. 3, pp. 600-602.

1896. *Variations in the development of Limulus polyphemus.* Jour. Morph., vol. 12, No. 1, pp. 21-146, pls. 2-11.

1912. *The evolution of the vertebrates and their kin.* Philadelphia, Pa., 215-248. Pp. xxi + 486, illus.

Peach, B. N.

1894. *Additions to the fauna of the Olenellus-zone of the northwest highlands.* Quart. Jour. Geol. Soc. London, vol. 50, pp. 661-676, pls. 29-32.

Pocock, R. I.

1902. *The taxonomy of Recent species of Limulus.* Ann. Mag. Nat. Hist., Ser. 7, vol. 9, pp. 256-266.

Poulsen, C.

1923. *Bornholms Olenuslag og deres fauna.* Danm. Geol. Undersøg. ser. 2, vol. 40, pp. 1-83, pls. 1-3.

1932. *The Lower Cambrian faunas of East Greenland.* Medd. om Grønl., vol. 87, No. 6, pp. 1-16, pls. 1-14.

Poulsen, V.

1964. *Contribution to the Lower and Middle Cambrian paleontology and stratigraphy of northwest Greenland.* Medd. om Grønland, Bd. 164, No. 6, pp. 1-105, pls. 1-4, 10 text-figs.

Prantl, F., and Přibyl, A.

1949. *Studie O Trilobitech Nadčeledi Odontopleuracea nov. superfam.* Rozpravy Státuiho Geol., Ŭstavu Rep Ceskoslovenske Svazek, vol. 12, pp. 1-110 (English summary pp. 117-221) pls. 1-12.

Raasch, G. H., and Lochman, C.

1945. *Crepicephalus edwardsi* Raasch, new name for *Crepicephalus oweni Raasch, 1943.* Jour. Paleont., vol. 19, No. 1, p. 77.

Rasetti, F.

1944. *Upper Cambrian trilobites from the Lévis conglomerate.* Jour. Paleont., vol. 18, No. 3, pp. 229-258, pls. 36-39.

1945a. *New Upper Cambrian trilobites from the Lévis conglomerate.* Jour. Paleont., vol. 19, No. 5, pp. 462-478, pls. 60-62.

1945b. *Evolution of the facial sutures in the trilobites Loganopeltoides and Loganopeltis.* American Jour. Sci., vol. 243, No. 1, pp. 44-50, pl. 1.

1945c. *Fossiliferous horizons in the "Sillery Formation" near Lévis, Quebec.* American Jour. Sci., vol. 243, No. 6, pp. 305-319, pls. 1,2.

1946. *Early Upper Cambrian trilobites from Western Gaspé.* Jour. Paleont., vol. 20, No. 5, pp. 442-462, pls. 67-70.

1948a. *Lower Cambrian trilobites from the conglomerates of Quebec.* Jour. Paleont., vol. 22, No. 1, pp. 1-24, pls. 1-6.

1948b. *Cephalic structures in Loganopeltoides and the origin of "Hypoparian" trilobites.* Jour. Paleont., vol. 22, No. 1, pp. 25-29, pl. 7.

1951. *Middle Cambrian stratigraphy and faunas of the Canadian Rocky Mountains.* Smith. Misc. Coll., vol. 116, No. 5, pp. 1-271, pls. 1-34.

1952. *Ventral cephalic sutures in Cambrian trilobites.* American Jour. Sci., vol. 250, pp. 885-898, pl. 1.

1965. *Upper Cambrian trilobites fauna of Northeastern Tennessee.* Smith. Misc. Coll., vol. 148, No. 3, pp. 1-172, 21 pls., 2 text-figs.

Raw, F.

1925. *The development of Leptoplastus salteri (Callaway) and of other trilobites.* Geol. Soc. London, Quart. Jour., vol. 81, pt. 2, pp. 223-324, pls. 15-18.

1927. *The ontogenies of trilobites and their significance.* American Jour. Sci., Ser. 5, No. 14, pp. 7-35, 131-149.

1936. *Mesonacidae of Comley in Shropshire, with a discussion of classification within the family.* Quart. Jour. Geol. Soc., vol. 92, pp. 236-293.

1937. *Systematic position of the Olenellidae (Mesonacidae).* Jour. Paleont., vol. 11, No. 7, pp. 575-597, text-figs. 1-7.

1952. *A note on Ross' "ontogenies of three Garden City (Early Ordovician) trilobites".* Jour. Paleont., vol. 6, No. 5, pp. 854-858, 4 text-figs.

1953. *The external morphology of the trilobite and its significance.* Jour. Paleont., vol. 27, No. 1, pp. 82-129, 7 text-figs.

Raymond, P. E.

1917. *Beecher's classification of trilobites after twenty years.* American Jour. Sci., vol. 43, pp. 196-210, 3 text-figs.

1920a. *Phylogeny of the Arthropoda with special reference to the trilobites.* Amer. Nat., vol. 54, pp. 398-413.

1920b. *The appendages, anatomy, and relationships of trilobites.* Connecticut Acad. Arts and Sci., Mem. vol. 7, pp. 1-169, pls. 1-11, figs. 1-46.

1921. *Criteria for species, phylogenies, and faunas of trilobites.* Geol. Soc. America, Bull., vol. 32, No. 3, pp. 349-352.

1924. *New Upper Cambrian and Lower Ordovician trilobites from Vermont.* Boston Soc. Nat. Hist., Proc., vol. 37, No. 4, pp. 389-466, pls. 12-14.

1925. *Some trilobites of the lower middle Ordovician of eastern North America.* Mus. Comp. Zool., Bull., vol. 67, No. 1, pp. 1-180, pls. 1-10.

Remane, A.

1950. *Theorie d. Coelomentstehung.* Verb. dtsch. Zool. Ges., Main, 1949.

Resser, C. E.

1928. *Cambrian fossils from the Mohave desert.* Smith. Misc. Coll., vol. 81, No. 2, pp. 1-14, pls. 1-3.

1936. *Second contribution to nomenclature of Cambrian trilobites.* Smith. Misc. Coll., vol. 95, No. 4, pp. 1-29.

1937. *Third contribution to nomenclature of Cambrian trilobites.* Smith. Misc. Coll., vol. 95, No. 22, pp. 1-29.

1938. *Cambrian system (restricted) of the southern Appalachians.* Geol. Soc. America, Spec. Paper, No. 15, pp. 1-140, 16 pls.

1939. *The Ptarmigania strata of the northern Wasatch Mountains.* Smith. Misc. Coll., vol. 98, No. 24, pp. 1-72, pls. 1-14.

Resser, C. E., and Howell, B. F.

1938. *Lower Cambrian Olenellus zone of the Appalachians.* Geol. Soc. America, Bull., vol. 49, pp. 195-248, pls. 1-13.

Richter, R.

1932. *Crustacea.* Handwörterbuch der Naturw. 2d ed., pp. 840-863, Jena.

Robison, R. A.

1964. *Late Middle Cambrian faunas from western Utah.* Jour. Paleont., vol. 38, No. 3, pp. 510-566, pls. 79-92, 4 text-figs.

1967. *Ontogeny of Bathyuriscus fimbriatus and its bearing on affinitives of Corynexochid trilobites.* Jour. Paleont., vol. 41, No. 1, pp. 213-221, pl. 24, 5 text-figs.

Ross, R. J., Jr.

1951a. *Stratigraphy of the Garden City Formation in northeastern Utah and its trilobite faunas.* Peabody Mus. Nat. Hist. Yale Univ., Bull. 6, pp. 1-161, pls. 1-36.

1951b. *Ontogenies of three Garden City (Early Ordovician) trilobites.* Jour. Paleont., vol. 25, No. 5, pp. 578-586, pls. 81-84.

1953. *Additional Garden City (Early Ordovician) trilobites.* Jour. Paleont., vol. 27, No. 5, pp. 633-646, pls. 62-64.

1967. *Calymenid and other Ordovician trilobites from Kentucky and Ohio.* United States Geol. Sur., Prof. Paper 583-B., pp. 1-18, pls. 1-5.

Rozova, A. V.

1964. *Biostratigraphy and morphology of trilobites from the Lower and Middle Cambrian of the northwestern Siberia. plateau.* Acad. Sci. U.S.S.R., vol. 5, pp. 1-97.

Ruedemann, R.

1926. *Utica and Lorraine Formations of New York.* Part 2, No. 2, New York State Mus., Bull. No. 272, pp. 1-227, 28 pls.

Saito, I.

1934. *Older Cambrian Trilobita and Conchostraca from Northwestern Korea.* Japanese Jour. Geol. and Geog., vol. 11, No. 3-4, pp. 211-237, pls. 25-27.

Sanders, H. L.

1957. *Cephalocarida and crustacean phylogeny.* Systematic Zool., vol. 6, (Ser. 3), pp. 112-128, 9 text-figs.

1959. *The significance of the Cephalocarida in crustacean phylogeny.* International Cong. Zool., 15th Session, London (1958), Proc., pp. 337-340, 2 text-figs.

1963a. *Significance of the Cephalocardia.* In *Phylogeny and evolution of Crustacea.* Mus. Comp. Zool. Spec. Pub., pp. 163-177, figs. 69-77.

1963b. *The Cephalocarids; Functional morphology, larval development, comparative external anatomy.* Connecticut Acad. Arts Sci., Mem., vol. 15, pp. 1-43.

Sanders, H. L., and Hessler, R. P.

1963. *The larval development of Lightiella incisa Gooding (Cephalocarida).* Crustaceana, vol. 7, pp. 82-97, 8 text-figs.

Segrove, F.

1941. *The development of the serpulid Pomatoceros triqueter L.* Quart. Jour. Microscopic Sci., vol. 82, pp. 467-540, 25 text-figs.

Sharov, A. G.

1966. *Basic Arthropodan Stock (with special reference to insects).* Pergamon Press Ltd., Headington Hill Hall, Oxford (England), pp. 1-271, 88 text-figs.

Shaw, A. B.

1951. *The paleontology of northwestern Vermont, part I. New Late Cambrian trilobites.* Jour. Paleont., vol. 25, No. 1, pp. 97-114, pls. 21-24.

1956a. *A Cambrian Aphelaspis fauna from Steel Butte near Boulder, Wyoming.* Jour. Paleont., vol. 30, No. 1, pp. 48-52, pls. 9-13.

1956b. *Quantitive trilobite studies I. The statistical description of trilobites.* Jour. Paleont., vol. 30, No. 5, pp. 1209-1224, 2 text-figs.

1966. *Paleontology of northwestern Vermont, part XII: Fossils from the Ordovician Highgate Formation.* Jour. Paleont., vol. 40, No. 6, pp. 1312-1330. pls. 161-163, 1 text-fig.

Shiino, S. M.

1950. *Studies on the embryonic development of Panulirus japonicus (von Siebold).* Univ. Mie, Jour. Faculty of Fishery, vol. 1, No. 1, pp. 1-168, 25 pls. (Japan).

Shuster, C. N.

1950. *Observation on the natural history of the American horseshoe crab Limulus polyphemus.* Woods Hole Oceanographic Institution, Contribution No. 564, pp. 18-23, 2 text-figs.

1955. *On morphometric and serological relationships within the Limulidae with particular reference to Limulus polyphemus (L.).* Dissertation Abstracts, vol. 18, No. 2, pp. 371,372. (1958).

1960. *Xiphosura.* Encyclopedia of Science and Technology. McGraw Hill Book Co., Inc., New York. Pp. 563-567.

Siewing, R.

1963. *Studies in Malacostracan morphology: Phylogeny and evolution of Crustacea.* Mus. Comp. Zool., Spec. Pub., No. 7, pp. 85-110, text-figs. 26-44.

Slocom, A. W.

1916. *Trilobites from the Maquaketa beds Fayette County, Iowa.* Iowa Geol. Sur., Ann. Report, vol. 25, (for 1914), pp. 183-248, pls. 14-19, fig. 32.

Šnajdr, M.

1958. *Trilobiti Českého středniho kambria. Nakladatelestvi* Československé Adad., Svazek 24, pp. 1-237. (English summary, p. 237-280), pls. 1-46, text-fig. 46.

Snodgrass, R. E.

1938. *Evolution of the Annelida, Onychophora, and Arthropoda.* Smith Misc. Coll., vol. 97, No. 6, pp. 1-159, 54 Text-figs.

1952. *A text-book of arthropod anatomy.* Comstock Publishing Assoc., Cornell Univ. Press, Ithaca, New York. Pp. viii + 363, 88 text-figs.

1956. *Crustacean metmorphoses.* Smith. Misc. Coll., vol. 131, No. 10, pp. 1-78, 28 text-figs.

Sollaud, E.

1923. *Recherches sur l'embryogénie des Crustacés décapodes de la sousfamille des "Palemoninae".* Bull., Biol. France et Belgique, Suppl., vol. 5, pp. 1-234.

Storer, T. I.

1943. *General Zoology.* McGraw-Hill Book Co., Inc., New York. 798 pp.

Størmer, L.

1930. *Scandinavian Trinucleidae.* Norsk Vidensk.-Akad. (Oslo), Skr., 1 Kl., No. 4, pp. 1-105, pls. 1-14.

1939. *Studies on trilobite morphology, Part I. The thoracic appendages and their phylogenetic significance.* Norsk. geol. Tidsskr., Bd. 19, pp. 143-273, pls. 1-12. 35 text-figs.

1942. *Studies on trilobite morphology. Part II. The larval development, the segmentation, and the sutures, and their bearing on trilobite classification.* Norsk geol. Tidsskr., Bd. 21, pp. 49-164, pls. 1,2, 19 text-figs.

1944. *On the relationships and phylogeny of fossil and Recent Arachnomorpha.* Norsk Vidensk.-Akad. (Oslo), 1 Kl., Bd. 5, pp. 1-153, 30 text-figs.

1949. *Class Trilobita.* Traité de Zoologie, vol. 6, pp. 159-197 (Paris).

1951. *Studies on trilobite morphology. Part III. The ventral cephalic structures with remarks on the zoological position of the trilobites.* Norsk geol. Tidsskr., Bd. 29, pp. 108-158, pls. 1-4, 14 text-figs.

1952. *Phylogeny and taxonomy of fossil horseshoe crabs.* Jour Paleont., vol. 26, No. 4, pp. 630-636, 3 text-figs.

1955. *Merostomata. Treatise on Invertebrate Paleontology; Arthropoda 2, part P.* Geol. Soc. America and Univ. Kansas Press, pp. 4-41, text-figs. 3-30.

Strand, T.

1927. *The ontogeny of Olenus gibbosus.* Norsk geol., Tidsskr., Bd. 9, No. 3-4, pp. 320-329.

Stubblefield, C. J.

1926. *Notes on the development of a trilobite, Shumardia pusilla (Sars).* Linn. Soc. Zool. London, Jour. vol. 36, pp. 345-372, pls. 14-16.

1936. *Cephalic sutures and their bearing on current classifications of trilobites.* Biol. Rev. (Cambridge Philos. Soc.), vol. 11, pp. 407-440, 8 text-figs.

Stumm, E., and Kauffman, E. G.

1958. *Calymenid trilobites from the Ordovician rocks of Michigan.* Jour. Paleont., vol. 32, No. 5, pp. 943-960, pls. 123, 124, 2 text-figs.

Tasch, P.

1952. *Adaptive trend in eyeline development in the Olenellidae.* Jour. Paleont., vol. 26, No. 3, pp. 484-488, 1 text-fig.

Temple, J. T.

1952. *The ontogeny of the trilobite Dalmanitina olini.* Geol. Mag., vol. 89, No. 4, pp. 251-262, pls. 9,10.

Thorson, G.

1946. *Reproduction and larval development of Danish marine bottom invertebrates, with special reference to the planktonic larvae in the Soung (Øresund).* Komm. Danmarks Fiskeri-og Havunders., Medd., Ser. Plankton, 4, no. 1, pp. 1-523.

Tiegs, O. W., and Manton W.

1958. *The evolution of the arthropods.* Biol. Rev. (Cambridge Philos. Soc)., vol. 33, No. 3, pp. 255-337.

Tripp, R. P.

1958. *Stratigraphical and geographical distribution of the named species of the trilobites superfamily Lichacea.* Jour. Paleont., vol. 32, No. 3, pp. 574-582, pl. 85.

Troedsson, G. T.

1929. *On the Middle and Upper Ordovician faunas of northern Greenland.* Part II; Jubilaeum ekspeditionen nord om Grønland, 1920-1923. No. 7, Medd. om Grønl., vol. 72, Pt. 1, No. 1, pp. 1-197, pls. 1-56, 12 text-figs.

Ulrich, E. O.

1878. *Descriptions of some new species of fossils from the Cincinnati Group.* Cincinnati Soc. Nat. Hist., Jour., vol. 1, No. 2, pp. 92-100.

1914. *In* A. F. Foerste, *The Rogers Gap fauna of Central Kentucky.* Cincinnati Soc. Nat. Hist., Jour., vol. 21, pp. 109-156, pls. 1-4.

Vendel, A.

1949. *Généralité composition de L'embranchement.* Traité de Zoologie, Tome 6, pp. 79-158 (Paris).

Vernberg, F. J., and Costlow, J. D., Jr.

1966. *Handedness in fiddler crabs (genus Uca).* Crustaceana, vol. 11, pt. 1, pp. 61-64.

Wahlenberg, G.

1821. *Petrificata Telluris Svecanae examinata.* Nova Acta Soc. Regiae Soc. Sci., Upsaliae, ser. 2, vol. 8, pp. 1-116, pls. 1-4,

Walcott, C. D.

1877(1878). *Note upon the legs of trilobites.* 31st Rept. N.Y.S. Mus. Nat. Hist., p. 64; *Note upon the eggs of trilobites.* Pp. 66, 67.

1879. *Fossils of the Utica Slate.* Albany Inst. Trans., vol. 10, pp. 18-38, pl. 2.

1881. *The trilobite, new and old evidence relating to its organization.* Mus. Comp. Zool., Bull., 8, pp. 191-230, pls. 1-6.

1894. *Note of some appendages of the trilobites.* Proc. Biol. Soc. Washington, vol. 9, pp. 89-97, pl. 1.

1910. *Cambrian geology and paleontology.* No. 6, *Olenellus and other genera of the Mesonacidae.* Smith Misc. Coll., vol. 53, pp. 231-422, pls. 23-44.

1913. No. II. New Lower Cambrian subfauna. Smith. Misc. Coll., vol. 57, No. 3, pp. 309-326, pls. 50-54.

1914. *Dikelocephalus and other genera of the Dikelocephalinae.* Smith. Misc. Coll., vol. 57, No. 13, pp. 346-383, pls. 60-70.

1916. *Cambrian geology and paleontology. III, No. 3, Cambrian trilobites.* Smith. Misc. Coll., vol. 64, pp. 155-258, pls. 24-38; No. 5, pp. 301-456.

1917. *Cambrian geology and paleontology, IV, No. 3. Fauna of the Mount Whyte Formation.* Smith. Misc. Coll., vol. 67, pp. 61-114, pls. 8-13.

1918. *Cambrian geology and paleontology. IV, No. 4. Appendages of trilobites.* Smith. Misc. Coll., vol. 67, pp. 115-216, pls. 14-42.

1921. *No. 4. Notes on Structure of Neolenus.* Smith. Misc. Coll., vol. 67, No. 7, pp. 365-377, pls. 92, 94.

1924. *Cambrian geology and paleontology. No. 2; Cambrian and Lower Ozarkian trilobites.* Smith. Misc. Coll., vol. 75, pp. 51-60, pls. 9-14.

1925. *Cambrian geology and paleontology, V, No. 3. Cambrian and Ozarkian trilobites.* Smith. Misc. Coll., vol. 75, pp. 59-146, pls. 15-24.

Warburg, E.

1925. *The trilobites of the Leptaena limestone in Dalarne.* Univ. Uppsala, Geol. Inst., Bull., vol. 27, pp. 1-450, pls. 1-11, text-figs. 1-23.

Waterman, T. H.

1960. *The physiology of Crustacea.* Vol. 1 and 2. Academic Press, New York and London.

Weber, H.

1952. *Morphologie, Histologie und Entwicklungegeshichte der Articulaten.* Fortsch. Zool., Bd. 9, pp. 18-231, 24 text-figs.

Westergård, A. H.

1936. *Paradoxides oelandicus beds of Öland.* Geol. Fören. ser. C. No. 394, (Årsbok 30, No. 1), pp. 1-66, pls. 1-12.

Whittington, H. B.

1941a. *The Trinucleidae, with special reference to North American genera and species.* Jour. Paleont., vol. 15, No. 1, pp. 21-41, pls. 5, 6, 1 text-fig.

1941b. *Silicified Trenton trilobites.* Jour. Paleont., vol. 15, No. 5, pp. 492-522, pls. 72-75, 13 text-figs.

1954. *Status of invertebrate paleontology, 1953.* Mus. Comp. Zool., Bull., vol. 112, No. 3, pp. 193-200.

1956a. *Beecher's supposed odontopleurid protaspis is a phacopid.* Jour. Paleont., vol. 30, No. 1, pp. 104-109, pl. 24, 2 text-figs.

1956b. *Type and other species of Odontopleuridae (Trilobita).* Jour. Paleont., vol. 30, No. 3, pp. 504-520, pls. 57-60, 4 text-figs.

1956c. *Photographing small fossils.* Jour. Paleont., vol. 30, No. 3, pp. 756-757, 1 text-fig.

1956d. *Beecher's lichid protaspis and Acanthopyge consanguinea (Trilobita).* Jour. Paleont., vol. 30, No. 5, pp. 1200-1204, pl. 131, 1 text-fig.

1956e. *Silicified Middle Ordovician trilobites: the Odontopleuridae.* Mus. Comp. Zool., Bull., vol. 114, pp. 155-288, pls. 1-24, 25 text-figs.

1957a. *Ontogeny of Elliptocephala, Paradoxides, Sao Blainia, and Triarthrus (Trilobita).* Jour. Paleont., vol. 30, No. 5, pp. 934-946, pls. 115, 116.

1957b. *The ontogeny of trilobites.* Biol. Rev. (Cambridge Philos. Soc.), vol. 32, pp. 421-469, 29 text-figs.

1958. *Ontogeny of the trilobite Peltura scarabaeoides from Upper Cambrian, Denmark.* Paleontology, vol. 1, pt. 3, pp. 200-206, pl. 38.

1959a. *Silicified Middle Ordovician trilobites.* Mus. Comp. Zool., Bull., vol. 121, No. 8, p. 369-496, 36 pls.

1959b. *Ontogeny of Trilobita. Treatise on Invertebrate Paleontology, Part O, Arthropoda 1.* Geol. Soc. America and Univ. Kansas Press, pp. 127-145, text-figs. 86-106.

1963. *Middle Ordovician trilobites from Lower Head, western Newfoundland.* Mus. Comp. Zool., Bull., vol. 129, No. 1, pp. 1-118, pls. 1-36, 6 text-figs.

1965. *Trilobites of the Ordovician Table Head Formation, western Newfoundland.* Mus. Comp. Zool., Bull., vol. 132, No. 4, pp. 275-442, pls. 1-68, 7 text-figs.

1966. *Phylogeny and distribution of Ordovician trilobites.* Jour. Paleont., vol. 40, No. 3, pp. 696-737, 16 text-figs.

Whittington, H. B., and Bohlin, B.

1958. *New Lower Ordovician Odontopleuridae (Trilobita) from Öland.* Univ. Uppsala, Geol. Inst., Bull., vol. 38, pp. 37-45, pls. 1-3.

Whittington, H. B., and Evitt W. R.

1953. *Silicified Middle Ordovician trilobites.* Geol. Soc. American, Mem. 59, pp. 1-137, pls. 1-33.

Williams, A.

1965. *Marine decapod crustaceans of the Carolinas.* Fish. Bull., vol. 65, No. 1, pp. 1-271.

Wilson, J. L.

1951. *Franconian trilobites of the Central Appalachians.* Jour. Paleont., vol. 25, No. 5, pp. 617-654, pls. 89-95, 1 text-fig.

1956. *Revisions in nomenclature and new species of Cambro-Ordovician trilobites from the Marathon uplift, West Texas.* Jour. Paleont., vol. 30, No. 6, pp. 1341-1349, pl. 146.

1957. *Geography of olenid trilobite distribution and its influence on Cambro-Ordovician correlation.* American Jour. Sci., vol. 225, No. 5, pp. 321-340, 1 text-fig.

Winston, P., and Nicholls, H.

1967. *Late Cambrian and Early Ordovician faunas from the Wilberns Formation of Central Texas.* Jour. Paleont., vol. 41, No. 1, pp. 66-96, pls. 9-13, 4 text-figs.

PLATES

The cost of the illustrations was met by funds from the Graduate School of the University of Cincinnati.

EXPLANATION OF PLATE 7

Figure | *Page*

1-14. *Kormagnostus simplex* Resser 73,74

1,6-8. Early meraspides. 1. Smallest cephalon, showing the conical glabella and the median furrow on the preglabellar field, × 53, U.C.M. 38722a. 6,7. Two pygidia each associated with one thoracic segment; notice the conical pygidial axis. 6. U.C.M. 38722f; × 35. 7. U.C.M. 38722g; × 34. 8. A broken pygidium apparently without thoracic segment, ×25, U.C.M. 38722h.

2-4,9,10,12-14. Late meraspides. 2-4. Three cephala, showing the disappearance of the median furrow and the truncate-conical glabella. 2. U.C.M. 38722b; × 32. 3. U.C.M. 38722c; × 15. 4. U.C.M. 38722d; × 17. 9,10. Two pygidia showing the subquadrate axial lobe; 9. U.C.M. 38722i; × 30. 10. U.C.M. 38722j; ×29. 12-14. Pygidial, side, and cephalic views of an enrolled meraspis, × 17, U.C.M. 38722.

5,11. Holaspides. 5. A cephalon, note the anterior pits and the palpebral ridges on the sides of the glabella, × 8. U.C.M. 38722e. 11. A broken pygidium showing the broadly expanded posterior axis, × 13, U.C.M. 38722k.

15-32. *Pagetia clytia* Walcott 75,76

23. Paraprotaspis. A complete instar with no thoracic segments, × 50, U.C.M. 38723i.

15-17. Three early meraspid pygidia. Note the association of the thoracic segment. 15. U.C.M. 38723a; × 39. 16. U.C.M. 38723b; × 40. 17. 38723c; × 40.

24,25. Two early meraspid cranidia. Note the narrower anterior border and the paired anterior pits on the sides of the glabella. 24. U.C.M. 38723j; × 26. 25 U.C.M. 38723k; × 26.

18,19. Two late meraspid pygidia. 18. U.C.M. 38723d; × 25. 19. U.C.M. 38723e; × 28.

26,27. Two late meraspid cranidia. Note the expansion of the anterior borders. 26. U.C.M. 38723l; × 26. 27. U.C.M. 38723m; × 28.

20-22. Three holaspis pygidia, showing the median tubercles on the axial rings. 20. U.C.M. 38723f; × 13. 21. U.C.M. 38723g; × 14. 22. U.C.M. 38723h; × 15.

28-32. Holaspid cranidia. Note the broad anterior border and the distinct paraglabellar tubercles on the sides of glabellar bases. 28. U.C.M. 38723n; × 16. 29. U.C.M. 38723o; × 14. 30. U.C.M. 38723p; × 14. 31. U.C.M. 38723q; × 14. 32. U.C.M. 38723; × 13.

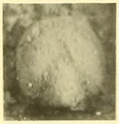
1

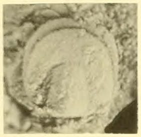
2

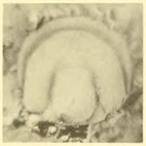
3

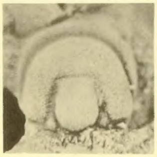
4

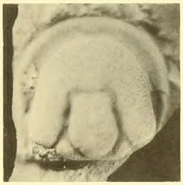
5

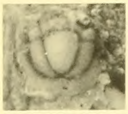
6

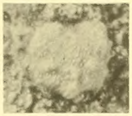
23

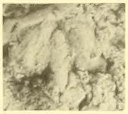
24

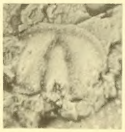
25

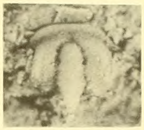
26

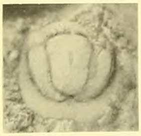
7

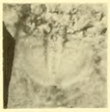
15

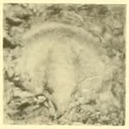
27

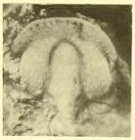
28

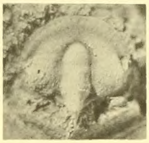
29

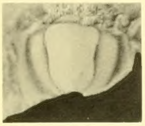
8

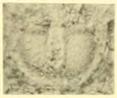
16

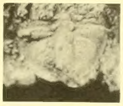
17

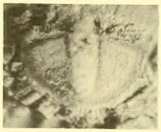
18

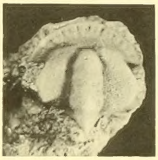
30

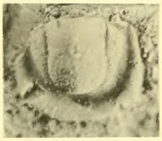
9

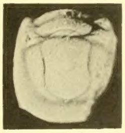
12

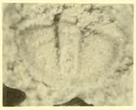
19

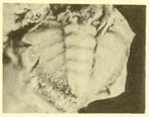
20

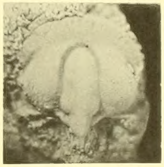
31

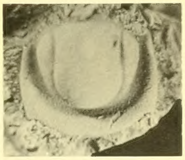
10

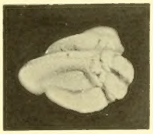
13

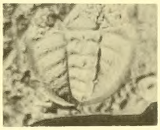
21

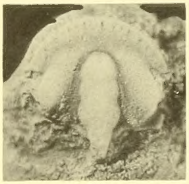
32

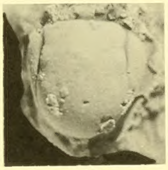
11

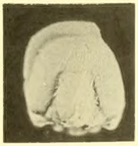
14

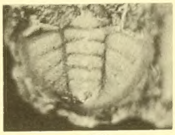
22

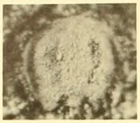
1

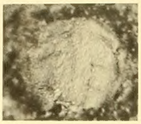
2

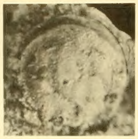
3

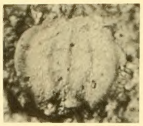
4

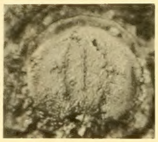
5

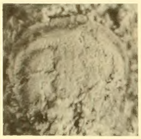
10

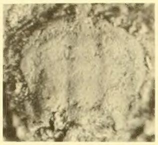
9

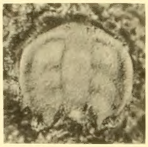
8

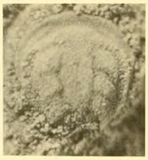
7

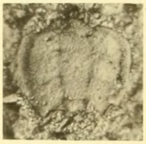
6

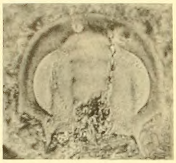
14

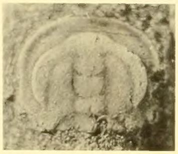
13

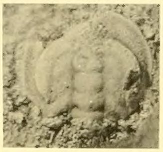
12

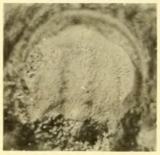
11

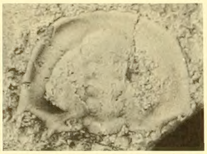
15

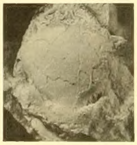
21

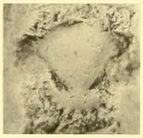
20

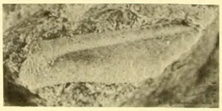
24

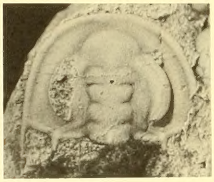
16

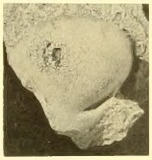
22

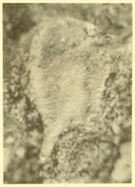
23

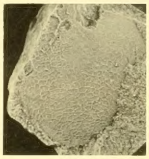
25

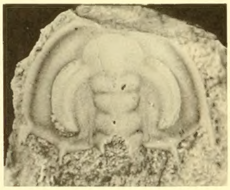
17

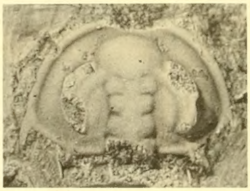
18

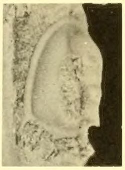
19

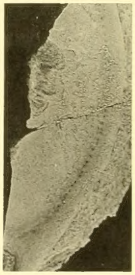
26

EXPLANATION OF PLATE 8

Figure		*Page*
1-26.	*Olenellus truemani* Walcott	76-78

1-5. Paraprotaspides. Note the longitudinal fissure along the axis, and the pleural furrows on the fixigenae. 1-3. U.C.M. 38724a-c; × 40. 4. U.C.M. 38724d; × 36. 5. U.C.M. 38724e; × 34.
6-10. Early meraspides, showing the disappearance of the longitudinal fissure, but distinct pleural furrows retained on the fixigenae. 6. A less complete shield, × 28, U.C.M. 38724f; 7. A well-preserved shield, × 30, U.C.M. 38724g. 8-10. Three less well-preserved shields. 8. U.C.M. 38724h; × 30. 9. U.C.M. 38724i; × 24. 10. U.C.M. 38724j; × 20.
20. An early meraspid hypostoma, showing the spinose posterior margin, × 9.5, U.C.M. 38724t.
23. A broken cephalon showing a long, left metagenal spine, × 25, U.C.M. 38724w.
11-14. Late meraspides, showing the disappearance of the pleural furrows and the presence of the fixigenal spines. 11. U.C.M. 3872k; × 17. 12. U.C.M. 38724n; × 14. 13. U.C.M. 38724m; × 16.
21. Hypostoma with shorter marginal spines and expanded median body, × 3, U.C.M. 38724u.
15-19. Holaspides. 15. U.C.M. 38724o; × 9. 16. U.C.M. 38724p; × 8. 17. U.C.M. 38724q; × 6.4. 18,19. U.C.M. 38724; × 6.
22. Hypostoma. Note the expanded median body, × 3, U.C.M. 38724v.
24. Part of the thoracic segment, showing the dorsal skeletal surface, × 10, U.C.M. 38724z.
25. Part of the anterior glabella, showing shrunken surface; × 10, U.C.M. 38724x.
26. Part of the cephalic marginal border, showing the pitted inner marginal furrow, × 1, U.C.M. 38724y.

EXPLANATION OF PLATE 9

Figure *Page*

1-19. *Apomodocia conica,* n. gen., n. sp. 88-90

1-19. Anaprotaspis, showing a longitudinal fissure along the axis, × 43, U.C.M. 38725a.
2,3. Metaprotaspides, showing the differentiation of the axial and pleural lobes. 2. U.C.M. 38725b; × 45. 3. U.C.M. 38725c; × 38.
4-8. Paraprotaspides. Note the segmentation of the protopygidium; 4,5. U.C.M. 38725d; × 36. 6. U.C.M. 38725f; × 37. 7. U.C.M. 38725g; × 35. 8. A cranidium without protopygidium, × 35, U.C.M. 38725h.
9,10. Early meraspides. Note that the cranidia bear no occipital spines, differing in this respect from *Cedarina cordillerae.* 9. U.C.M. 38725i; × 40. 10. U.C.M. 38725j; × 31.
11. A late meraspis, showing the well-developed preglabellar field and anterior border, × 17, U.C.M. 38725k.
12-19. Holaspides. 12. U.C.M. 38725l; × 11. 13. U.C.M. 38725m; × 10. 14. U.C.M. 38725n; × 9. 15,16. Dorsal and lateral views of a well-preserved cranidium, × 5.4, U.C.M. 38725. 18. A broken librigena, × 4.3, U.C.M. 38725o. 17,19. Top and side views of a broken pygidium, × 3.6, U.C.M. 38725p.

20-31. *Laudonia canadiensis,* n. sp. 78-81

20,21. Two early meraspides. Note the three pairs of marginal spines; 20. U.C.M. 38726a; × 14. 21. U.C.M. 38726b; × 11.
28,29. Late meraspides. Note the shortening of the anterior pair of marginal spines. 28. U.C.M. 38726g; × 10.5. 29. U.C.M. 38726h; × 6.5.
25. Late meraspid hypostoma. Note the long marginal spines, × 11, U.C.M. 38726d.
22-24,30,31. Holaspides. Note the disappearance of the anterior pair of marginal spines and the lengthening of the lateral genal spines. 22-24. Dorsal, frontal, and lateral views of an incomplete cranidium, × 4.3, U.C.M. 38726c; 30. U.C.M. 38726i; ×6.3. 31. U.C.M. 38726; × 4.6.
26. A broken holaspid hypostoma with shorter posterior marginal spines and expanded median body, × 2.5, U.C.M. 38726e.
27. Part of the thoracic segment showing the serration along the anterior lateral margin, × 3.3, U.C.M. 38726f.

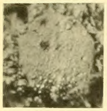
1

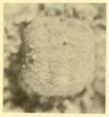
2

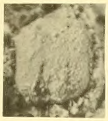
3

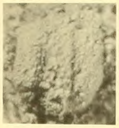
4

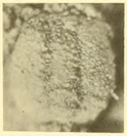
5

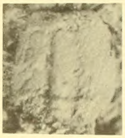
6

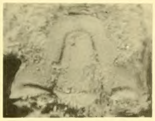
11

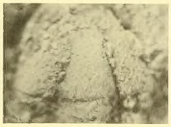
10

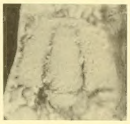
9

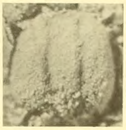
8

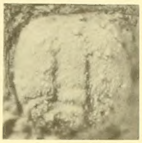
7

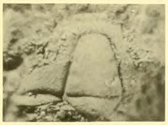
12

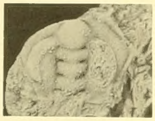
20

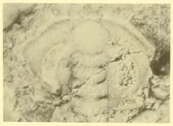
21

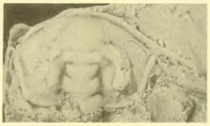
22

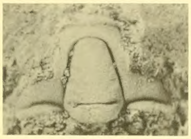
13

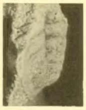
17

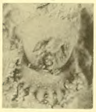
25

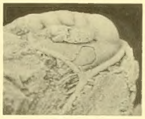
24

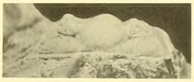
23

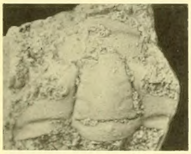
14

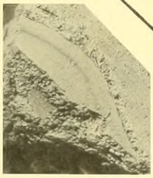
18

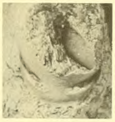
26

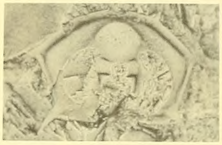
28

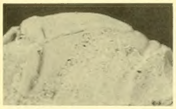
15

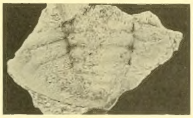
19

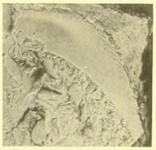
27

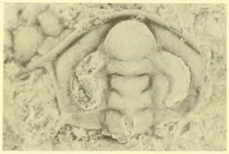
29

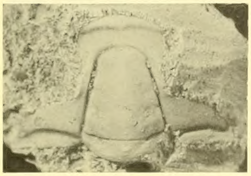
16

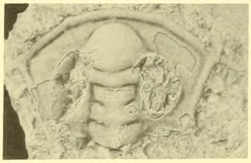
30

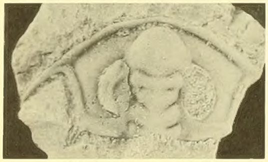
31

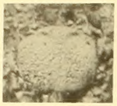
1

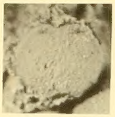
2

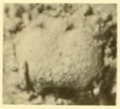
3

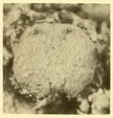
4

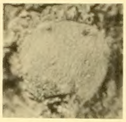
5

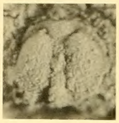
6

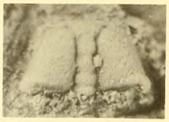
11

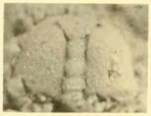
10

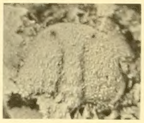
9

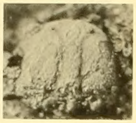
8

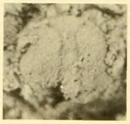
7

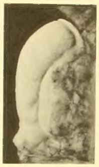
21

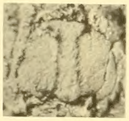
12

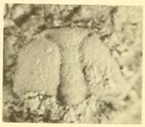
13

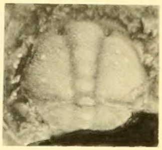
14

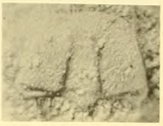
15

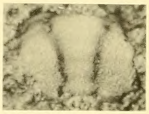
16

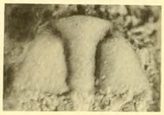
17

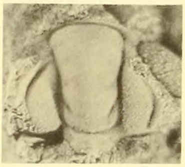
22

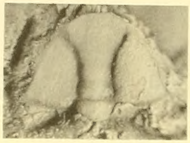
18

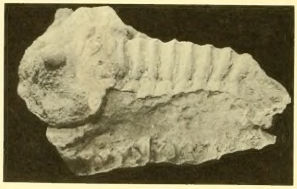
24

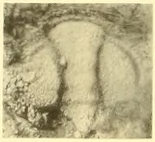
19

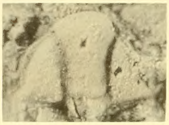
20

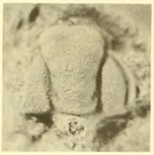
23

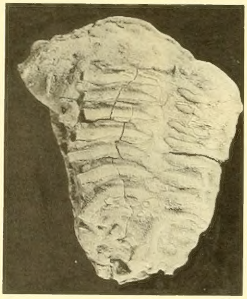
26

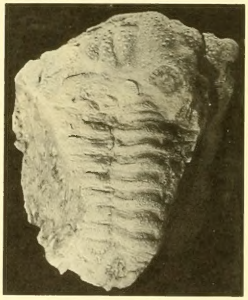
27

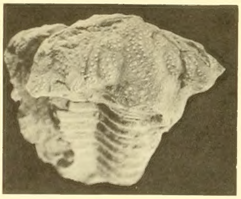
25

EXPLANATION OF PLATE 10

Figure *Page*

1-23. *Ptarmigania aurita* Resser 81-83

1-5. Anaprotaspides. 1,2. Showing the faint axis; 1. U.C.M. 38727a; × 40. 2. U.C.M. 38727b; ×43. 3. Showing the narrow depression along the axis, × 43, U.C.M. 38727c. 4,5. Showing the slightly elevated axis; note the posterior marginal median tubercle. 4. U.C.M. 38727d; × 43. 5. U.C.M. 38727e; × 38.

6,7. Metaprotaspides. Note the narrow axis and the distinct dorsal furrow. 6. U.C.M. 38727f; × 40. 7. U.C.M. 38727g; × 38.

8-13,15. Paraprotaspides. Note the glabella expanded both anterior and posteriorly. 8. U.C.M. 38727h; × 37. 9. U.C.M. 38727i; × 37. 10. U.C.M. 38727j; × 35. 11. U.C.M. 38727k; × 33. 12. U.C.M. 38727l; × 37. 13. U.C.M. 38727m; × 30. 15. U.C.M. 38727o; × 36

14,16-18. Early meraspides, showing the glabella tapering posteriorly. 14. U.C.M. 38727n; × 28. 16. U.C.M. 38727p; ×18. 17. U.C.M. 38727q; × 27. 18. U.C.M. 38727r; × 30.

19,20. Late meraspides. Note the presence of the anterior border. 19. U.C.M. 38727s; ×27. 20. U.C.M. 38727t; × 25.

21-23. Holaspides. 21,22. Top and side views of a complete cranidium; 21-22 U.C.M. 38727; × 12. 23. U.C.M. 38727u; × 17.

24-27. *Acidaspis cincinnatiensis* Meek 125

An isolated specimen showing two individuals facing each other, cephalon directed to cephalon, and pygidium. 24. Lateral view; note the upper and lower individuals. 25,27. Cephalic view and dorsal view of the smaller individual (upper one in fig. 24). 26. Dorsal view of the larger individual, the cephalon and part of pleural lobe are broken off. All × 2.3, U.C.M. 38729.

EXPLANATION OF PLATE 11

Figure *Page*

1-30. *Glyphaspis* cf. *parkensis* Rasetti 83-87

1-3. Anaprotaspides. Note that the smallest instar shows a faint fissure along the axis. 1. U.C.M. 38728a; × 53. 2. U.C.M. 38728b; × 60. 3. U.C.M. 38728c; × 53.

4,5. Metaprotaspides, showing the differentiation of the axial and pleural lobes. 4. U.C.M. 38728d; × 45. 5. U.C.M. 38728e; × 45.

6,7. Paraprotaspides, showing the presence of the protopygidium. 6. U.C.M. 38728f; × 40. 7. U.C.M. 38727g; × 29.

8-11. Early meraspides, showing the development of the anterior border and the posterior migration of the palpebral lobes. 8. U.C.M. 38728h; ×27. 9. U.C.M. 38728i; × 25. 10. U.C.M. 38728j; × 24. 11. U.C.M. 38728k; × 25.

23,24. Early meraspid pygidia, in each articulated series with three or four thoracic segments. 23. U.C.M. 38728t; × 26. 24. U.C.M. 38728u; × 21.

12,14. Late meraspid cranidia. Note the widening of the anterior brim and the truncate-conical glabella. 12. U.C.M. 38728l; × 20. 13. U.C.M. 38728m; × 16. 14. U.C.M. 38728n; × 10.

25. A late meraspid pygidium, × 12, U.C.M. 38728v.

15-18,22,27. Holaspides ("male"). 15. U.C.M. 38728o; × 7.6. 16. U.C.M. 38728p; × 16. 17,18. Top and lateral views of a cranidium; note the strongly upturned anterior brim, × 1.6, U.C.M. 38728q. 22. A small, broken librigena, × 10, U.C.M. 38728s. 27. An elongate pygidium, × 1.7, U.C.M. 38728y.

19,20,26,28-30. Holaspides ("female"). 19,20. Dorsal and side views of a larger cranidium, showing the less upturned anterior brim, × 7, U.C.M. 38728. 26,28. Two incomplete pygidia, showing the rounded outline. 26. U.C.M. 38728w; × 1.7. 28. U.C.M. 38728x; × 1.9. 29,30. Dorsal and back views of a large pygidium, × 2, U.C.M. 38728z.

21. An incomplete hypostoma, × 5.6, U.C.M. 38728r.

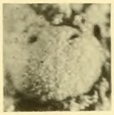

1

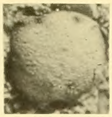

2

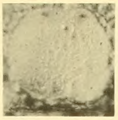

3

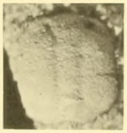

4

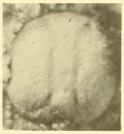

5

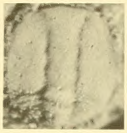

6

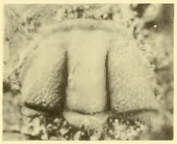

11

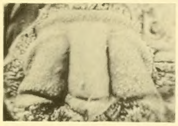

10

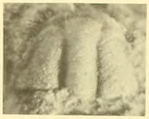

9

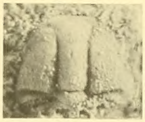

8

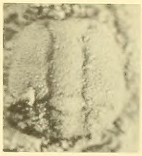

7

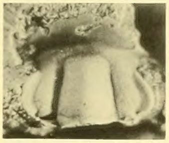

14

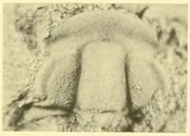

13

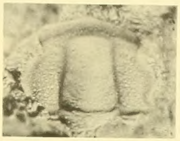

12

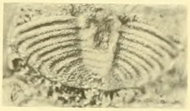

24

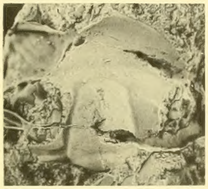

16

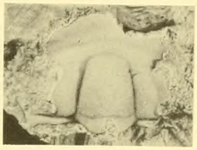

15

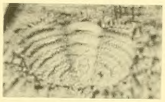

23

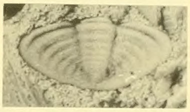

25

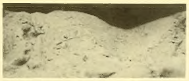

17

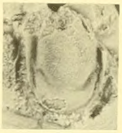

21

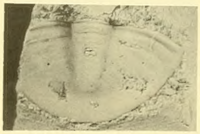

26

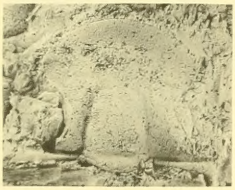

18

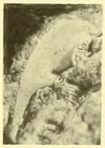

22

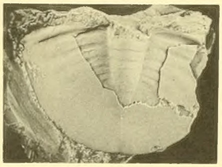

28

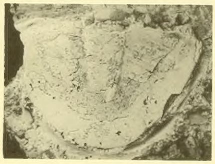

27

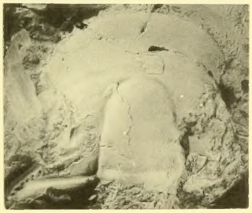

19

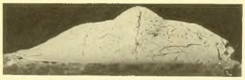

29

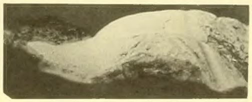

20

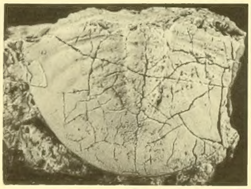

30

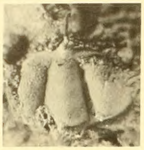
1

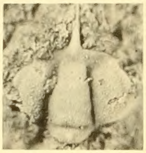
2

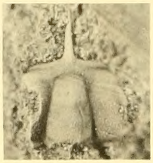
3

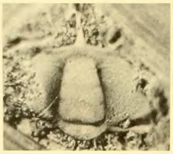
4

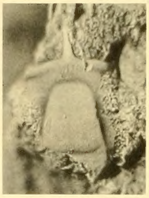
5

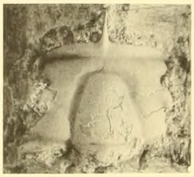
7

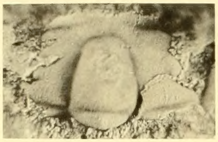
6

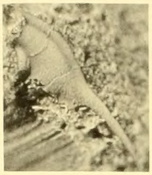
8

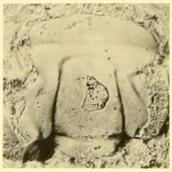
23

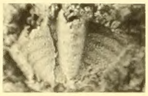
10

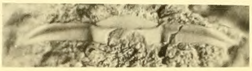
9

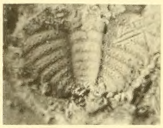
11

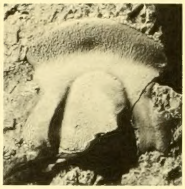
24

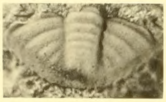
13

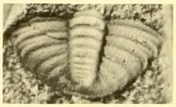
12

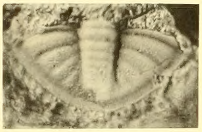
14

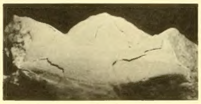
15

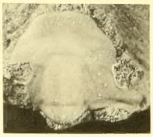
16

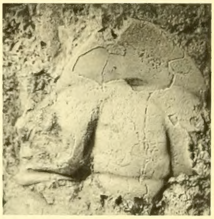
25

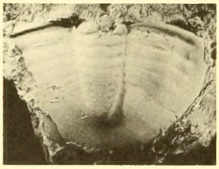
17

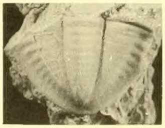
18

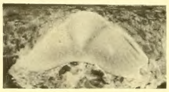
19

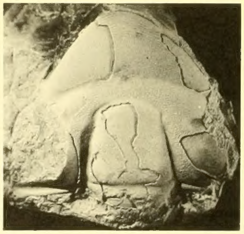
26

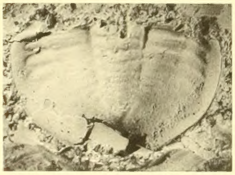
20

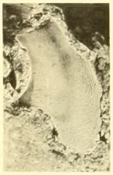
21

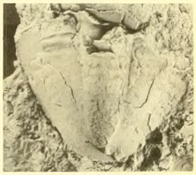
22

26

EXPLANATION OF PLATE 12

Figure *Page*

1-14. *Kepisis stenotoides* (Matthew) 108,109

1,2,10,11. Early meraspides. 1,2. Two cranidia showing the longer anterior median spines and the slender glabellar, × 17, U.C.M. 38730a,b. 10,11. Two pygidia with slender axis and spinose margins, × 25, U.C.M. 38730i,j.
3-5,12,13. Late meraspides. 3-5. Three cranidia with narrow and well-developed preglabellar field and fine palpebral ridges. 3. U.C.M. 38730c; × 11. 4. U.C.M. 38730d; × 14. 5. U.C.M. 38730e; × 13. 12,13. Two pygidia decorated with marginal spines. 12. U.C.M. 38730k; × 16. 13. U.C.M. 38730l; × 15.
6-9,14. Holaspides. 6. A less complete cranidium, × 11, U.C.M. 38730f. 7. A complete cranidium, × 5.5, U.C.M. 38730. 8. A small sized librigena, × 1.7, U.C.M. 38730g; 9. A broken thoracic segment, × 6.7, U.C.M. 38730h. 14. A well-preserved pygidium, × 11, U.C.M. 38730m.

15-26. *Iohomia sickia,* n. gen., n. sp. 87

15,18,19,21,22,25,26. Holaspides ("male"). 15,26. Frontal and dorsal views of an incomplete cranidium, × 2.5, U.C.M. 38737. 25. Top view of an incomplete cranidium, showing the well-impressed anterior median pit, × 2.5, U.C.M. 38737i. 18,19. Top and back views of a pygidium, × 4.5, U.C.M. 38737c. 22. A broken pygidium, × 3.1, U.C.M. 38737f. 21. An imperfectly preserved librigena, × 5.4, U.C.M. 38737e. 16. A meraspid cranidium, showing the large and scattered granules, × 10, U.C.M. 38737a.
17,20,23,24. Holaspides ("female"). 17,20. Two imperfectly preserved pygidia, showing the rounded outline. 17. U.C.M. 38737d; × 2.2. 20. U.C.M. 38737b; × 1.8. 23,24. Two cranidia showing the narrower anterior border. 23. U.C.M. 38737g; × 4.3. 24. U.C.M. 38737h; × 3.

EXPLANATION OF PLATE 13

Figure		*Page*
1-29.	*Cedarina cordillerae* (Howell and Duncan)	90-92

1. Anaprotaspis, × 52, U.C.M. 38731a.

2-4. Metaprotaspides, showing the well-developed axial and pleural lobes. 2. U.C.M. 38731b; × 50. 3. U.C.M. 38731c; × 40. 4. U.C.M. 38731d; × 43.

5-8. Paraprotaspides, showing the well-preserved dorsal furrow and protopygidium, but no distinct glabellar ring. 5. U.C.M. 38721e; × 42. 6. U.C.M. 38731f; × 42. 7. U.C.M. 38731g; × 35. 8. U.C.M. 38731h; × 36.

9,10,26. Early meraspides, showing the development of the anterior borders. 9. U.C.M. 38731i; × 28. 10. U.C.M. 38731j; × 24. 26. A pygidium in articulated series with one or four thoracic segments, × 26, U.C.M. 38731y.

11-13,25. Late meraspides. Note the occipital spines. 11. U.C.M. 38731k; × 23. 12. U.C.M. 38731l; × 19. 13. U.C.M. 38731m; × 14. 25. A pygidium possibly associated with one or two thoracic segments, × 8.3, U.C.M. 38731x.

14,15,17,18,20. Holaspides ("female"). Note the longer and narrower glabella. 14. U.C.M. 38731n; × 9.5. 15. U.C.M. 38731o; × 9.5. 17. U.C.M. 38731q; × 6.2 18. U.C.M. 38731r; × 4.5. 20. U.C.M. 38731t; × 4.7.

16,19,21,22. Holaspides ("male"), showing the wider and shorter glabella. 16. U.C.M. 38731p; × 5.6. 19. U.C.M. 38731s; × 4.2. 21,22. Dorsal and side views of an incomplete cranidium, × 3.7, U.C.M. 38737u.

23,24,27-29. Holaspides. 23. An isolated hypostoma, × 8, U.C.M. 38731v. 24. A librigena, × 2.4, U.C.M. 38731w. 27-29. One small and two large pygidia. 27. U.C.M. 38731z; × 11. 28. U.C.M. 38731a; × 6.5. 29. U.C.M. 38731b; × 6.5.

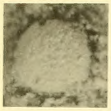
1

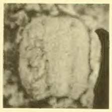
2

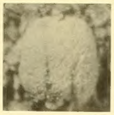
3

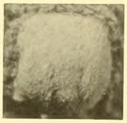
4

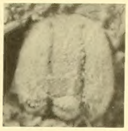
5

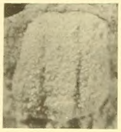
6

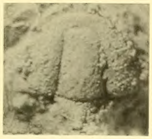
11

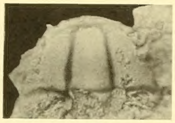
10

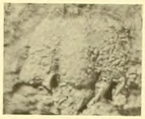
9

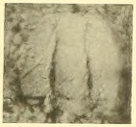
8

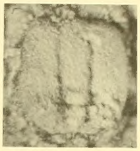
7

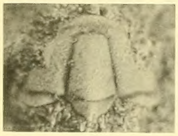
12

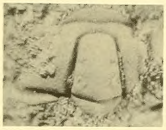
13

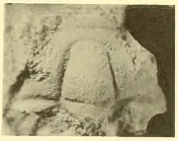
14

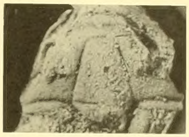
15

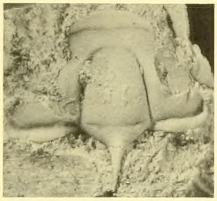
17

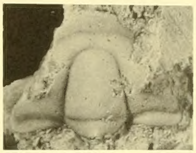
16

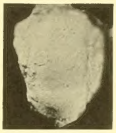
23

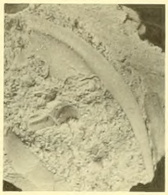
24

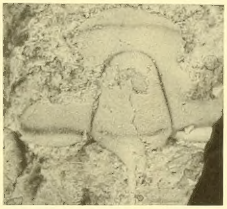
19

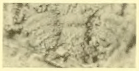
25

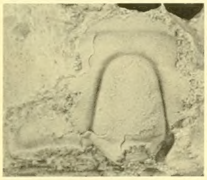
18

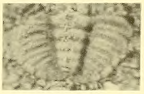
26

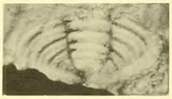
27

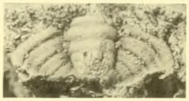
28

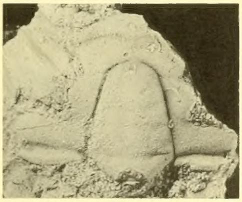
20

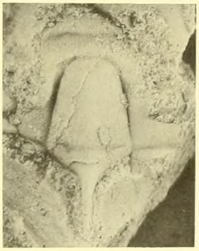
21

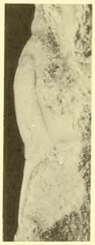
22

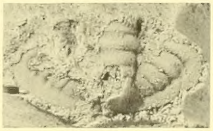
29

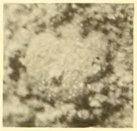
1

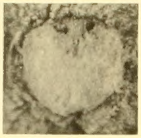
2

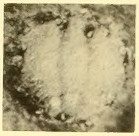
3

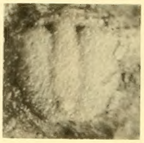
4

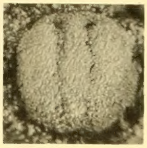
5

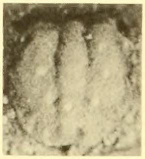
10

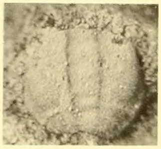
9

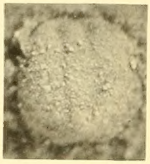
8

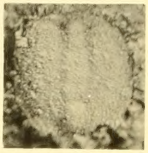
7

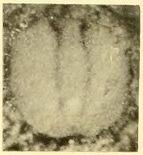
6

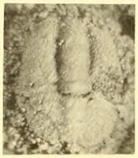
11

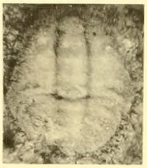
12

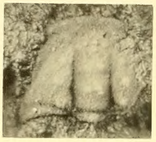
13

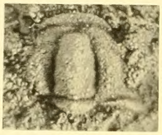
14

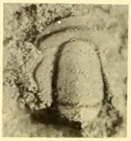
15

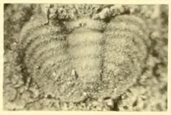
21

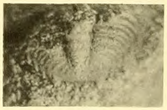
22

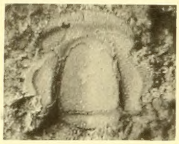
17

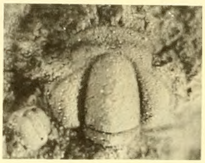
16

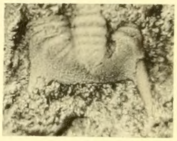
24

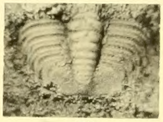
23

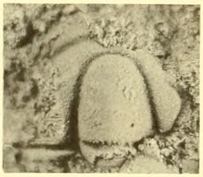
18

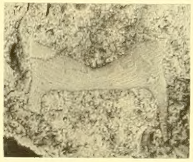
25

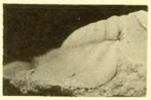
26

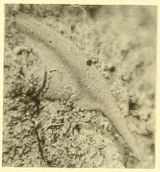
27

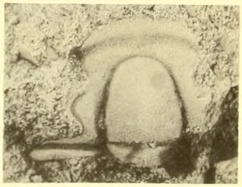
19

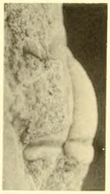
20

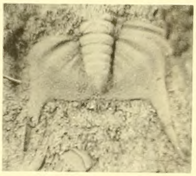
28

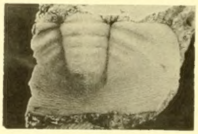
29

EXPLANATION OF PLATE 14

Figure *Page*

1-29. *Crepicephalus deadwoodiensis,* n. sp. 92-94

1,2. Anaprotaspides. 1. Smallest shield size, showing no axial lobe or dorsal furrow, × 65, U.C.M. 38732a. 2. Shield shows a narrow depression along the anterior axis and a tubercle on the posterior end, × 68, U.C.M. 38732b.
3-7. Metaprotaspides, showing the well-differentiated axial and pleural lobes. 3. U.C.M. 38732c; × 63. 4. U.C.M. 38732d; × 63. 5. U.C.M. 38732e; × 63. 6. U.CM 38732f; × 68. 7. U.C.M. 38732g; × 55.
8-10. Paraprotaspides, notice the indistinct protopygidium. 8. U.C.M. 38732h; × 49. 9. U.C.M. 38732i; × 40. 10. U.C.M. 38732j; × 33.
11-13. Early meraspides, showing the well-differentiated pygidia and the large granules on the fixigenae. 11. U.C.M. 38732k; × 21. 12. U.C.M. 387321; × 20. 13. U.C.M. 38732m; × 19
21. Early meraspid pygidium. Note the associated one or two thoracic segments, × 27, U.C.M. 38732r.
14-17. Late meraspides. Note the disappearance of the coarse granules. 14. U.C.M. 38732o; × 16. 16. U.C.M. 38732n; × 16. 16. U.C.M. 38732p; × 15. 17. U.C.M. 38732q; × 12.
22,23. Two meraspides. Pygidia articulated with four thoracic segments. 22. U.C.M. 38732s; × 30. 23. U.C.M. 38732t; × 16.
18-20,24-29. Holaspides. 18. A broken cranidium, × 14, U.C.M. 38732z. 19,20. Top and side views of a cranidium, × 5.7, U.C.M. 38732. 24,28. Two pygidia both associated with part of the thoracic segments. 24. U.C.M. 38732u; × 13. 28. U.C.M. 38732w; × 12. 25. Ventral view of a pygidium. Note the wrinkled doublure × 10, U.C.M. 38732v. 27. A small librigena, × 17, U.C.M. 38732y; 26,29. Dorsal and side views of a broken pygidium, × 5.1, U.C.M. 38732x.

EXPLANATION OF PLATE 15

Figure *Page*

1-40. *Dunderbergia ? anyta* (Hall and Whitfield) 94-97

1. Anaprotaspis. A small shield shows the axial lobe with two pairs of central nodes and a longitudinal fissure, × 58, U.C.M. 38733a.
2-5. Metaprotaspides. 2,3. Dorsal view and ventral view of an incomplete shield. Note the three pairs of marginal spines and the perrostro-hypostoma, × 50. U.C.M. 38733b. 4,5. Dorsal views of two shields. Note the appearance of three pairs of central nodes. 4. U.C.M. 38733c; × 53. 5. U.C.M. 38733d; × 55.
6. Ventral view of an incomplete shield, showing the perrostro-hypostoma slightly displaced, × 55, U.C.M. 38733e.
7-12. Paraprostaspides, showing the fusion of the central nodes and the appearance of the protopygidium. 7. U.C.M. 38733f; × 48. 8. U.C.M. 38733g; × 48. 9. U.C.M. 38733h; × 45. 10,11. Ventral view and dorsal view of a shield, note the librigenae in place, × 42, U.C.M. 38733i. 12. A complete shield, × 40, U.C.M. 38733j.
13,14,27,28,33. Early meraspides. 13,14. Dorsal view each of two well-preserved cranidia, showing the presence of the anterior borders. 13. U.C.M. 38733k; × 25. 14. U.C.M. 38733l; × 20. 27. Librigena, showing the narrower ocular platform, × 16, U.C.M. 38733y. 28. Hypostoma, showing the shorter marginal spine, × 46, U.C.M. 38733z. 33. A pygidium with spinose marginal border and in articulated series with one or 4 thoracic segments, × 24, U.C.M. 38733e.
15-17,26,29,34,35,37. Late meraspides. 15-17. Three complete cranidia showing the narrow preglabellar fields. 15. U.C.M. 38733m; × 15. 16. U.C.M. 38733n; × 14. 17. U.C.M. 38733o; × 12. 26. A librigena with wider ocular platform, × 8.2, U.C.M. 38733x. 29. A broken hypostoma, showing the expansion of the median body and shorter posterior marginal spines, × 37, U.C.M. 38733a. 34,35,37. Three pygidia each in articulated series with one or two thoracic segments, note the disappearance of the marginal spines and the presence of a median notch on the posterior margin. 34. U.C.M. 38733f; × 26. 35. U.C.M. 38733g; × 26. 37. U.C.M. 38733i; ×25.
23. A well-preserved rostral plate, × 8, U.C.M. 38733u.
19,20,21,25,36,39. Holaspides ("female"). 19. U.C.M. 38733p; × 6.5. 20. U.C.M. 38733; × 3.8. 21. U.C.M. 38733r; × 9. 25. U.C.M. 38733w; × 3.5. 36. U.C.M. 38733h; × 14. 39. U.C.M. 38733k; × 18.
18,22,24,38,40. Holaspides ("male"). 18. U.C.M. 38733o; × 6.8. 22. U.C.M. 38733t; 24. U.C.M. 38733v; × 3.8. 38. U.C.M. 38733j; × 16. 40. U.C.M. 38733l;× 4.
30. A larger hypostoma, showing the more prominent median body and the absence of marginal spines, × 9.5, U.C.M. 38733b.
31. A broken thoracic segment, showing the long right pleural spine, × 4, U.C.M. 38733c′.
32. A pair of thoracic segments with the shorter pleural spines, × 29, U.C.M. 38733d′.

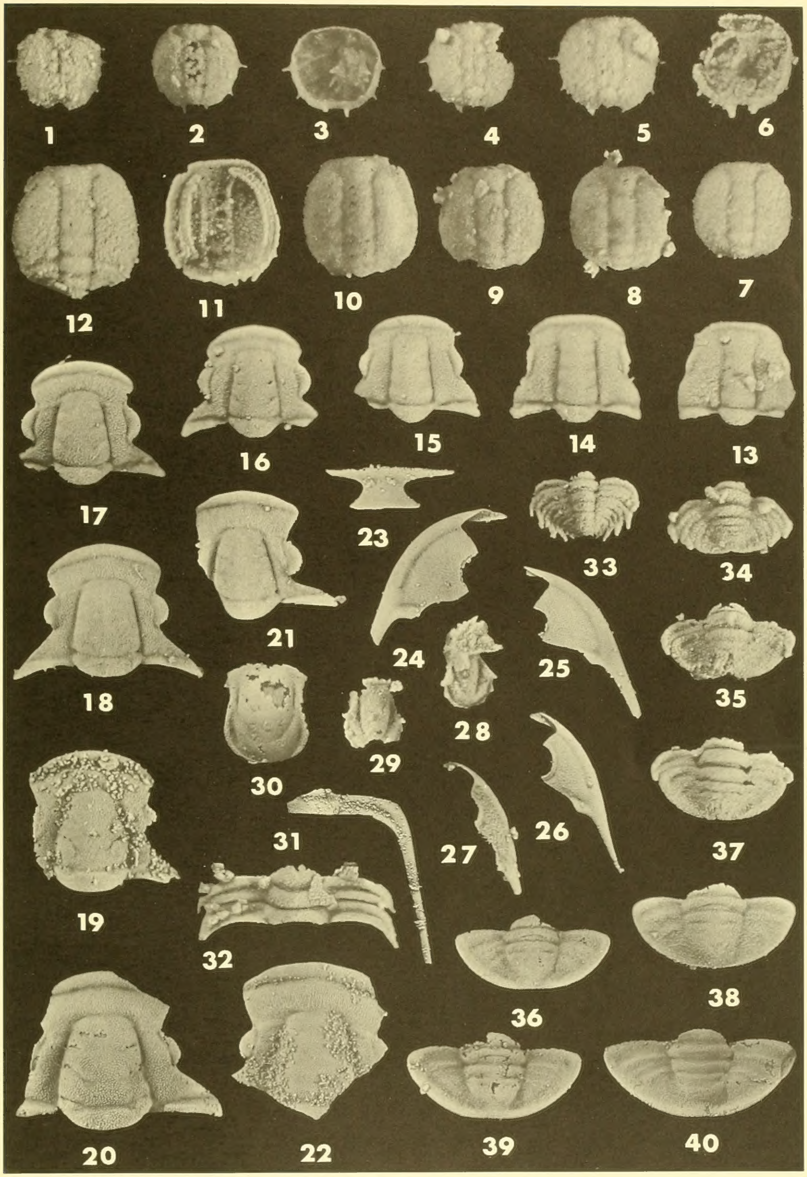
1
2
3
4
5
6
12
11
10
9
8
7
17
16
15
14
13
23
33
34
21
24
25
18
35
28
29
30
37
31
26
27
19
32
36
38
20
22
39
40

Plate 16

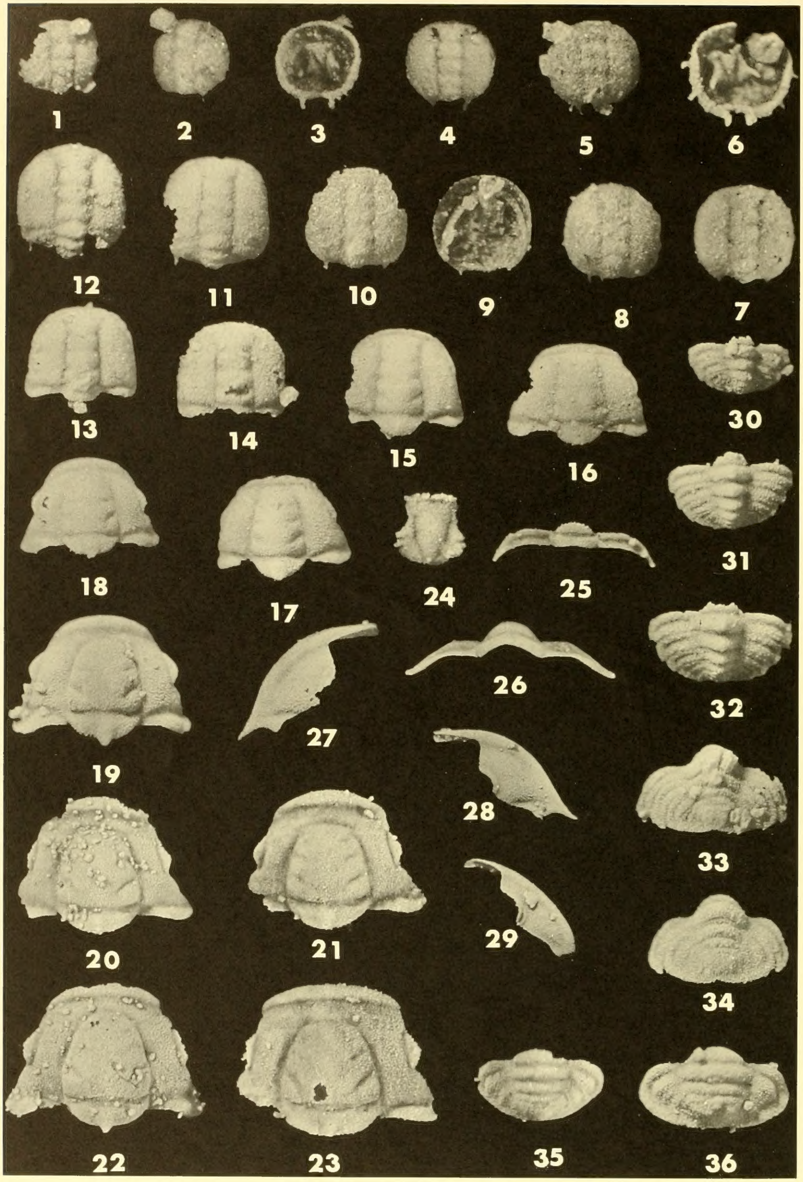
1
2
3
4
5
6
12
11
10
9
8
7
13
14
15
16
30
18
17
24
25
31
19
27
26
32
28
33
20
21
29
34
22
23
35
36

EXPLANATION OF PLATE 16

Figure *Page*

1-36. *Dytremacephalus granulosus* Palmer 97-100

1. Anaprotaspis. An incomplete shield, showing four axial rings, × 56, UC.M. 38734a.

2-6. Metaprotaspides. 2,3. Dorsal view and ventral view of a well-preserved specimen; note that the perrostro-hypostoma has a pair of large lateral spines, × 54, U.C.M. 38734b. 4,5. Two shields showing the five axial rings and faint pleural furrows, × 57, U.C.M. 38734c; × 55, U.C.M. 38734d. 6. Ventral view of an incomplete shield showing the slightly displaced hypostoma; note the large lateral spines, × 58, U.C.M. 38734e.

7-14. Paraprotaspides. 17. Well-preserved shield, × 62, U.C.M. 38734f. 8,9. Ventral view and dorsal view of a complete shield, showing the perrostro-hypostoma slightly displaced, × 62, U.C.M. 38734g. 10,11. Two broken shields, × 50, U.C.M. 38733h; × 52, U.C.M. 38734i. 12. Well-preserved shield showing the protopygidia, × 40, U.C.M. 38734j. 13,14. Two cranidia without protopygidia. 13. U.C.M. 38734k; × 42. 14. U.C.M. 38734l; × 34.

15-17, 24,29-32. Early meraspides. 15-17. Three cranidia; note the appearance of the anterior border. 15. U.C.M. 38734m; × 32. 16. U.C.M. 38734n; × 25. 17. U.C.M. 38734o; × 21. 24. Hypostoma, × 15, U.C.M. 38734u. 29. Librigena with narrower ocular platform and shorter genal spines, × 22, U.C.M. 38734a′. 30-32 Three pygidia, each in articulated series with two or three thoracic segments; note that the shorter marginal spines, and the axial ring tubercle, are different from those of *Dunderbergia*. 30. U.C.M. 38734b′; × 36. 31. U.C.M. 38734c′; × 31. 32. U.C.M. 38734d′; × 20.

18,19,33,34. Late meraspides. 18,19. Two cranidia with narrow preglabellar field. 18. U.C.M. 38734p; × 15. 19. U.C.M. 38734q; × 16. 33,34. Two pygidia each associated with one or two thoracic segments. 33. U.C.M. 38734e′; × 34. 33. U.C.M. 38734f′; × 33.

21,23,28,35. Holaspides ("male"). 21. U.C.M. 38734s; × 15. 23. U.C.M. 38734v; × 10. 28. U.C.M. 38734z; × 9.4. 35. U.C.M. 38734g′; × 13.

25,26. Top and side views of two thoracic segments. 25. U.C.M. 38734w; × 15. 26. U.C.M. 38734x; × 16.

20,22,27,36. Holaspides ("female"). 20. U.C.M. 38734r; × 10. U.C.M. 38734t; × 9. 27. U.C.M. 38734y; × 7.5. 36. U.C.M. 38723h′; × 15.

EXPLANATION OF PLATE 17

Figure *Page*

1-34. *Ptychaspis bullasus* Lochman and Hu 100,101

1. Metaprotaspis. Note the three pairs of axial nodes and the longitudinal fissure along the axis, × 45, U.C.M. 38735a.

2-4. Paraprotaspides. Note the fusion of the axial nodes and the presence of the protopygidium. 2. U.C.M. 38735b; × 46. 3. U.C.M. 38735c; × 35. 4. U.C.M. 38735d; × 29.

5-7. Early meraspides. Note the disappearance of the anterior pits and the cone-shaped glabella. 5. U.S.N.M. 137100a; × 20. 6. U.C.M. 38735e; × 15. 7. U.C.M. 38735f; × 13.

29,30. Two pygidia articulated with three or four thoracic segments. 29. U.C.M. 38735w; × 14. 30. U.C.M. 38735x; × 16.

8-13,26,27,31. Late meraspides. 8-13. Showing the broadly based glabella. 8-10. U.C.M. 38735g,h,i; × 12. 11. U.C.M. 38735k; × 13. 12. U.C.M. 38735j; × 12. 13. U.C.M 38735l; × 10. 26,27. Librigenae, showing the wider ocular platform; 26. U.C.M. 38735t; × 6. 27. U.C.M. 38735u; × 5. 31. Late meraspid pygidium, × 7.5, U.C.M. 38735q.

14-25,28,32,33,34. Holaspides. 15. U.C.M. 38735m; × 8.6. 16,17. Dorsal view and side view of a cranidium, × 6.2, U.C.M. 38735. 14,18,19. Top view of frontal view of a cranidium, × 5, U.C.M. 38735n. 20,21. U.C.M. 38735o; × 10. 22. U.C.M. 38735p; × 6. 23. U.C.M. 38735q; × 4.4. 24. U.C.M. 38735r; × 3.3. 25. U.C.M. 38735s; × 2.7. 28. Librigena, showing the narrower ocular platform, × 6.6, U.C.M. 38735v. 32-34. Three pygidia; × 8.5, U.C.M. 38735y. 32. U.C.M. 38735z; × 2.8. 34. U.S.N.M. 13700h; × 3.

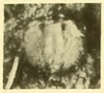
1

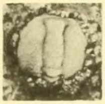
2

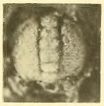
3

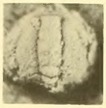
4

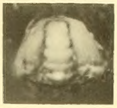
5

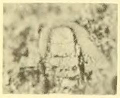
6

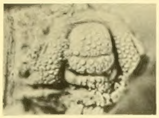
11

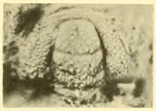
10

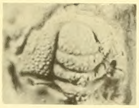
9

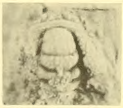
8

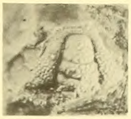
7

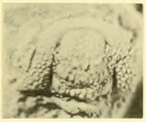
12

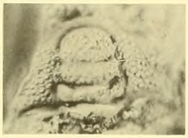
13

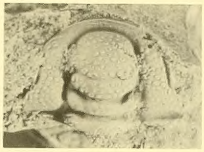
14

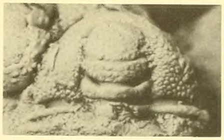
15

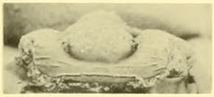
22

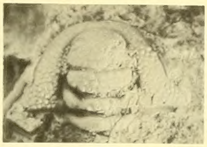
21

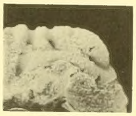
18

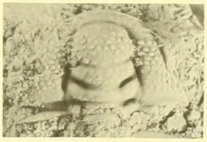
16

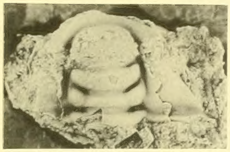
23

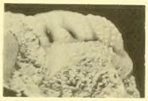
20

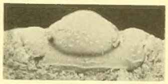
19

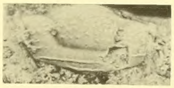
17

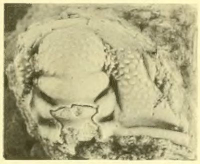
24

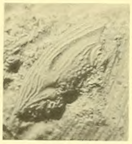
26

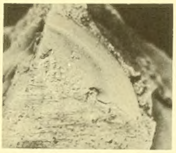
27

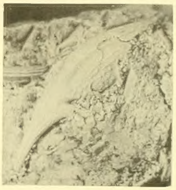
28

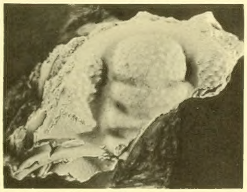
25

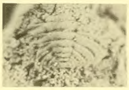
29

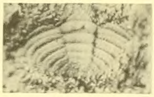
30

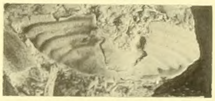
33

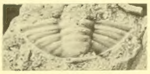
31

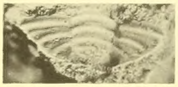
32

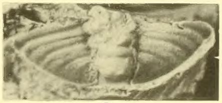
34

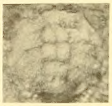
1

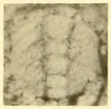
2

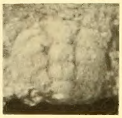
3

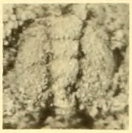
4

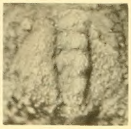
5

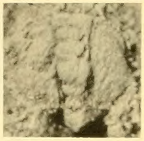
6

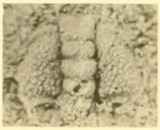
10

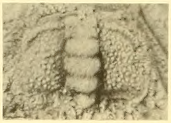
9

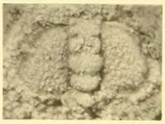
8

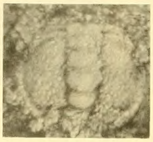
7

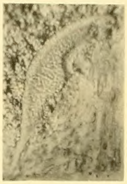
25

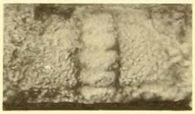
11

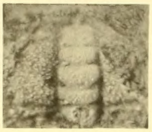
12

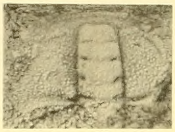
13

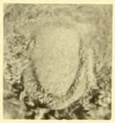
23

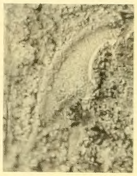
26

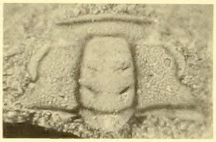
16

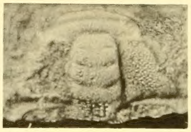
15

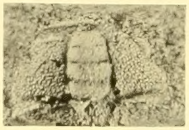
14

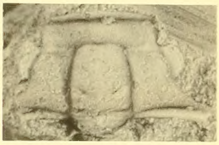
19

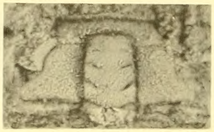
18

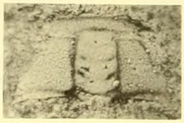
17

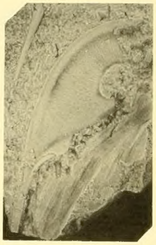
27

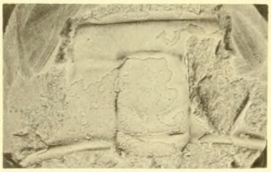
21

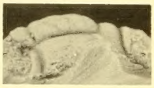
20

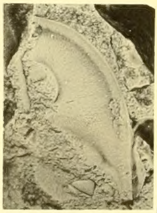
28

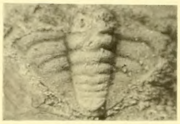
31

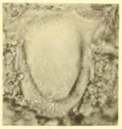
24

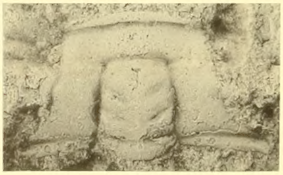
22

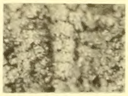
29

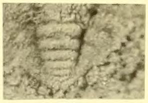
30

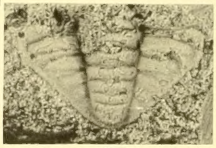
32

EXPLANATION OF PLATE 18

Figure *Page*

1-32 — *Olenus gibbosus* (Wahlenberg) 101-104

1-3. Metaprotaspides. Note the longitudinal fissure along the axis and the presence of ridges on the pleural lobes, × 55, U.C.M. 38736a-c.

4-8. Paraprotaspides, showing the fusion of the axial nodes and the appearance of the protopygidium. 4. U.C.M. 38736d; × 66. 5. U.C.M. 38736e; × 50. 6. U.C.M. 38736f; × 42. 7. U.C.M. 38736g; × 50. 8. U.C.M. 38736h; × 42.

9-12. Early meraspides, showing the development of the anterior border. 9. U.C.M. 38736i; × 45. 10. U.C.M. 38736j; × 30. 11. U.C.M. 38736k; × 23. 12. U.C.M. 38736l; × 20.

29. Early meraspid pygidium, × 27, U.C.M. 38736z.

13-18. Late meraspides, showing the development of the preglabellar field and the impression of the glabellar furrows. 13. U.C.M. 38736m; × 21. 14. U.C.M. 38736n; × 17. 15. U.C.M. 38736o; × 16. 16. U.C.M. 38736p; × 16. 17. U.C.M. 38736q; × 14. 18. U.C.M. 38736r; × 14.

25,26. Late meraspid librigenae. 25. U.C.M. 38736v; × 23. 26. U.C.M. 38736w; × 17.

30. Late meraspid pygidium, × 20, U.C.M. 38736a'.

19-22. Holaspid cranidia. 19 .U.C.M. 38736s; × 7.8 20. Lateral view of a cranidium. × 4.6, U.C.M. 38736d'. 21. U.C.M. 38736e'; × 1.3. 22. U.C.M. 38736; × 4.5.

23,24. Hypostomata. 23. U.C.M. 38736t; × 23 24. U.C.M. 38736u; × 20.

27,28. Two incomplete librigenae. 27. U.C.M. 38736x; × 8. 28. U.C.M. 38736y; × 4.2.

31,32. Two pygidia. 31. U.C.M. 38736b'; × 9. 32. U.C.M. 38736c'; ×7.

EXPLANATION OF PLATE 19

Figure *Page*

1-34. *Acerocare ecorne* Angelin 103-105

1-2. Metaprotaspides. Note the two pairs of axial nodes and the indistinct fourth and fifth axial rings. 1. U.C.M. 38738a; × 50. 2. U.C.M. 38738b; × 50.
3-6. Paraprotaspides, showing the distinct axial rings and steeply deflected protopygidium. 3,4. Note the pleural lobe furrows, × 56, U.C.M. 38738c; U.C.M. 38738d. 5. U.C.M. 38738e; × 47. 6. U.C.M. 38738f; × 48.
7-9. Early meraspides, showing the expansion of posterior fixigenal borders. 7. U.C.M. 38738g; × 35. 8. U.C.M. 38738h; × 32. 9. U.C.M. 38738i; × 25.
26. Early meraspid pygidium associated with one thoracic segment, × 22, U.C.M. 38738y.
10-12. Late meraspides, showing the dorsal facial sutures and the posteriorly expanded glabella. 10. U.C.M. 38738h; × 26. 11. U.C.M. 38738j; × 25. 12. U.C.M. 38738k; × 22.
20. Late meraspid librigena, × 11, U.C.M. 38738s.
22. Late juvenile pygidium; note the slender axis, × 18, U.C.M. 38738u.
27-29. Three juvenile pygidia. 27. U.C.M. 38738z; × 30. 28. U.C.M. 38738a'; × 24. 29. U.C.M. 38738b'; × 19.
15,17,19,24,32,34. Holaspides ("male"). 15. U.C.M. 38738n; × 13. 17. U.C.M. 38738p; × 10. 19. U.C.M. 38738r; × 8. 24. U.C.M. 38738w; × 9.2. 32. U.C.M. 38738e'; × 7.2. 34. U.C.M. 38738g'; × 6.8.
13,14,16,18. Holaspid cranidia ("female"). Note that the glabellae are narrower and longer than those of the "male" form. 13. U.C.M. 38738l; × 16. 14. U.C.M. 38738m; × 10. 16. U.C.M. 38738o; × 10. 18. U.C.M. 38738q; × 8.
23. Early holaspis, showing the cranidium associated with a few thoracic segments, × 9, U.C.M. 38738v.
25. A "female" librigena; note the narrower ocular platform, × 9, U.C.M. 38738x.
30,31,33. Holaspid pygidia ("female"). Note that they are more rounded in comparison with the pygidia of the "male" form. 30. U.C.M. 38738c'; × 11. 31. U.C.M. 38738d'; × 8.4. 33. U.C.M. 38738f; ×8.4.
21. Hypostoma. Note the expanded median body and the narrower posterior brim in comparison with figure 22, × 11, U.C.M. 38738t.

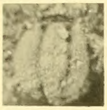
1

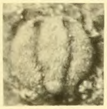
2

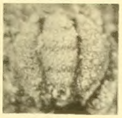
3

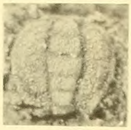
4

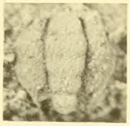
5

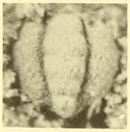
6

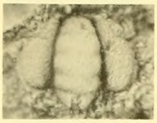
11

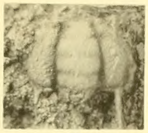
10

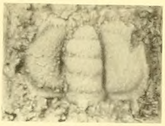
9

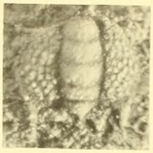
8

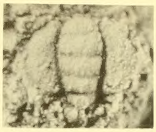
7

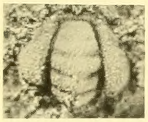
12

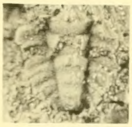
26

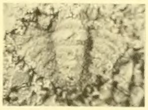
27

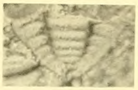
28

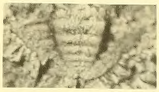
29

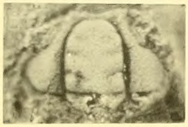
13

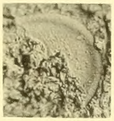
20

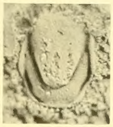
21

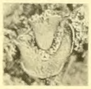
22

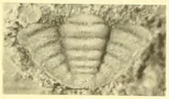
30

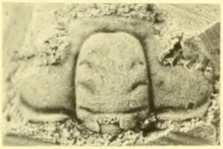
14

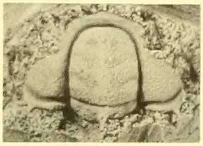
15

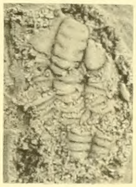
23

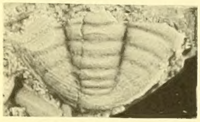
31

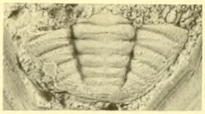
32

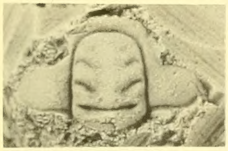
16

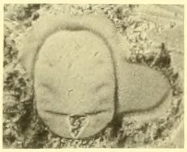
17

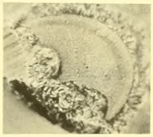
24

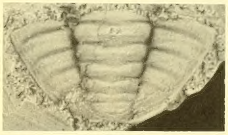
33

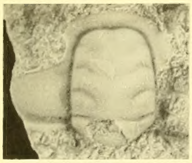
18

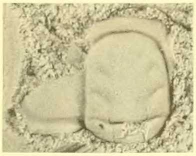
19

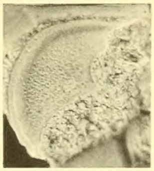
25

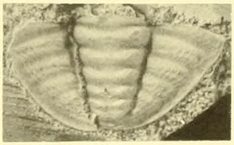
34

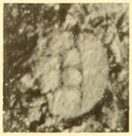
1

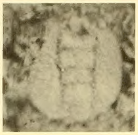
2

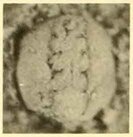
3

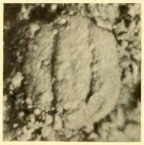
4

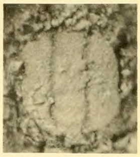
5

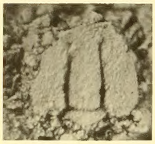
10

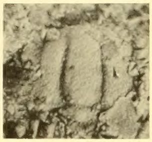
9

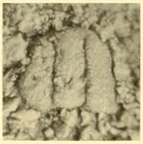
8

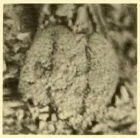
7

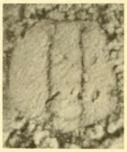
6

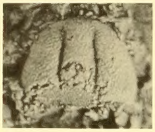
11

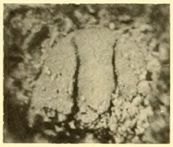
12

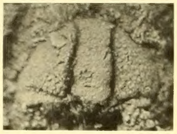
13

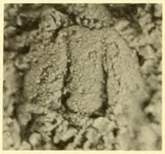
14

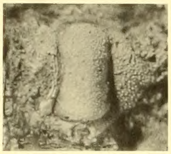
17

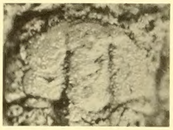
16

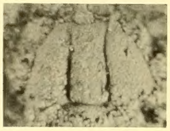
15

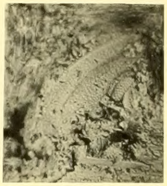
22

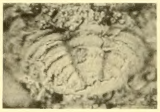
24

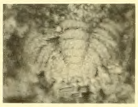
23

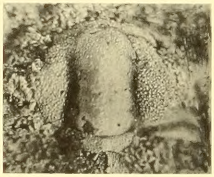
18

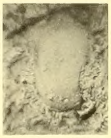
21

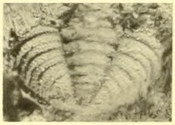
25

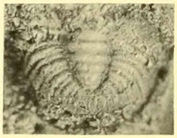
26

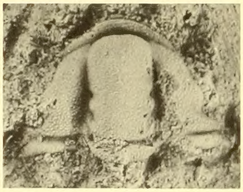
19

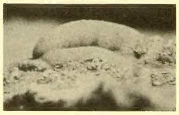
20

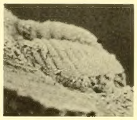
27

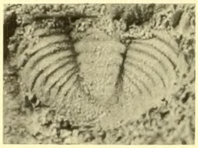
28

EXPLANATION OF PLATE 20

Figure *Page*

1-28. *Missisquoia cyclochila*, n. sp. 109-111

1. Anaprotaspis. The left side of the shield missing; note the axial lobe composed of a small frontal lobe, two pairs of axial nodes, and a large terminal lobe, × 70, U.C.M. 38749a.

2,3. Metaprotaspides, showing the fusion of the axial nodes and the distinct axial rings. 2. U.C.M. 38749b; × 70. 3. U.C.M. 38749c; × 70.

4-7. Paraprotaspides. Note the narrow, transverse protopygidium steeply deflected behind the posterior cranidial margin. 4. U.C.M. 38749d; × 10. 5. U.C.M. 38749e; × 66. 6. U.C.M. 38749f; × 60. 7. U.C.M. 38749g; × 57.

8-15,23. Early meraspides. Note the separation of the glabellar furrows. 8. U.C.M. 38749h; × 50. 9. U.C.M. 38749i; × 48. 10. U.C.M. 38749j; × 47. 11. U.C.M. 38749k; × 43. 12. U.C.M. 38749l; × 45. 13. U.C.M. 38749m; × 45. 14. U.C.M. 38749n; × 40. 15. U.C.M. 38749o; × 30. 23. Roundly triangular pygidium in articulated series with possibly three thoracic segments, × 50, U.C.M. 38749u.

16,17,24,25. Late meraspides. 16,17. Two cranidia, showing the appearance of the anterior border and shortening of the glabellar furrows. 16. U.C.M. 38749p; × 24. 17. U.C.M. 38749q; × 20. 24,25. Two pygidia having the terminal portion extended to the posterior margin. 24. U.C.M. 38749v; × 28. 25. U.C.M. 38749x; × 36.

18-22,26-28. Holaspides. 18. Party exfoliated cranidium, × 18, U.C.M. 38749r. 19,20. Dorsal and side views of a partly exfoliated cranidium, × 12, U.C.M. 38749. 21. Incomplete hypostoma, × 18, U.C.M. 38749s. 22. Broken librigena, × 20, U.C.M. 38749t. 26. Less complete pygidium; note that the axial lobe is not extended to the posterioir margin, × 10, U.C.M. 38749x. 27,28. Dorsal and side views of a complete pygidium, × 19, U.C.M. 38749y.

EXPLANATION OF PLATE 21

Figure		*Page*
1-26.	*Highgatella facila,* n. sp.	105-107

1-5. Metaprotaspides. Note the indistinct protopygidium at the posterior margin of the shield. 1-4. U.C.M. 38740a-d; × 62. 5. U.C.M. 38740e; × 53.
6. Paraprotaspis, × 53, U.C.M. 38740f.
7-9. Early meraspides. Note the presence of the anterior borders. 7. U.C.M. 38740g; × 40. 8. U.C.M. 38740h; × 38. 9. U.C.M. 38740i; × 40.
10,11. Late meraspides, showing the preglabellar fields. 10. U.C.M. 38740j; × 30. 11. U.C.M. 38740k; × 25. 13,14,17,20. Holaspides ("male" form). Note the shorter and broader glabellae. 13. U.C.M. 38740m; × 11. 14. U.C.M. 38740n; × 14. 17. U.C.M. 38740q; × 10. 20. U.C.M. 38740r; × 6.
12,15,16,18,19. Holaspides ("female"), showing preglabellar field. 12. U.C.M. 38740l; × 18. 15. U.C.M. 38740o; × 8. 16. 38740p; × 15. 18,19. Top and side views of a less complete cranidium, × 6, U.C.M. 38740.
21. A nearly complete hypostoma, × 24, U.C.M. 38740s.
22,24. Two "female" pygidia; note that each axial lobe is divided into two rings only. 22. U.C.M. 38740t; × 30. 24. U.C.M. 38740v; × 12.
23. A "male" pygidium. Note the axis is divided into three axial rings, × 25, U.C.M. 38740u.
25,26. Two librigenae. 25. U.C.M. 38740w; × 5. 26. U.C.M. 38740x; × 5.

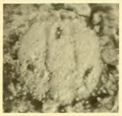
1

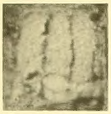
2

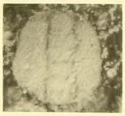
3

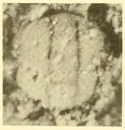
4

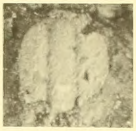
5

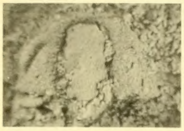
9

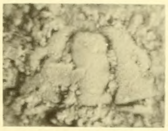
8

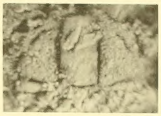
7

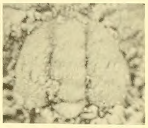
6

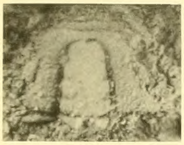
10

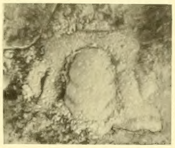
11

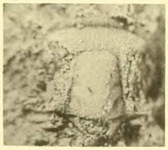
12

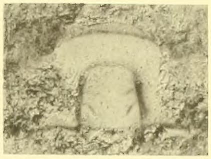
13

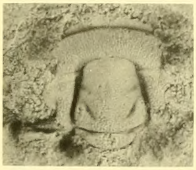
15

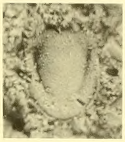
21

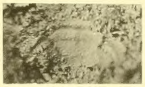
22

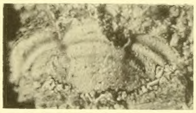
23

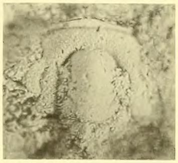
14

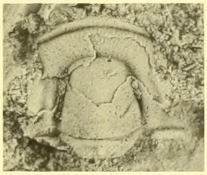
16

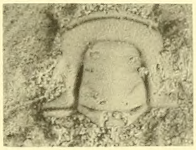
17

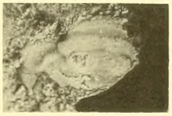
24

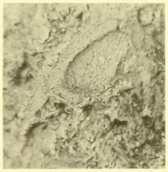
25

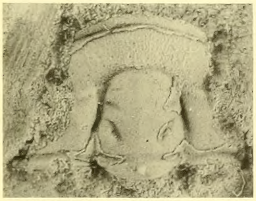
18

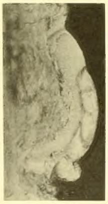
19

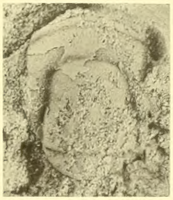
20

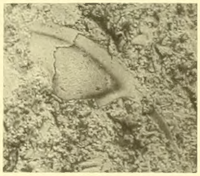
26

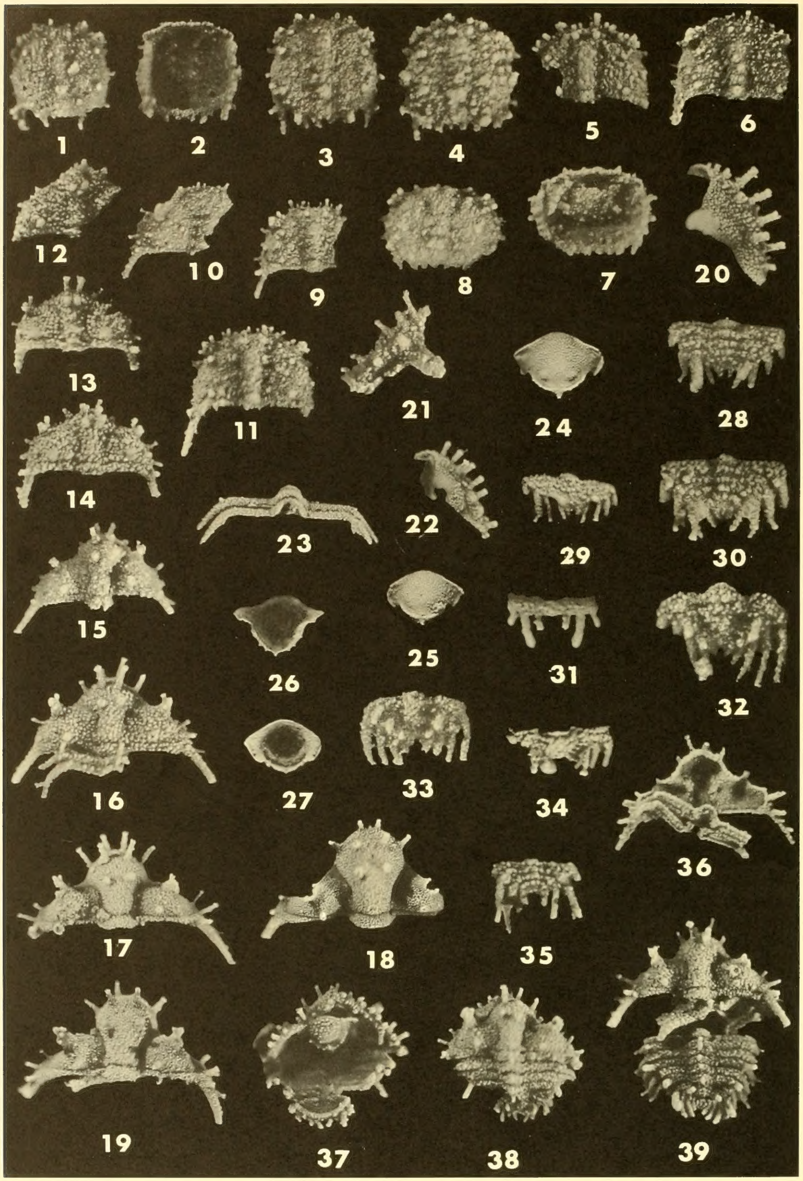
1
2
3
4
5
6
12
10
9
8
7
20
13
11
21
24
28
14
23
22
29
30
15
26
25
31
32
16
27
33
34
36
17
18
35
19
37
38
39

EXPLANATION OF PLATE 22

Figure *Page*

1-39. *Libertella corona,* n. gen., n. sp. 112-113

1-4,7,8. Paraprotaspides. 1,2. Dorsal view and ventral view of a complete shield, × 38, U.C.M. 38741a. 3,4. Two nearly complete shields, × 39, U.C.M. 38741b,c. 7,8. Dorsal view and ventral view of a slightly deformed shield, note the librigena and hypostoma in place, × 35, U.C.M. 38741f.

5,6,9-11. Early meraspides. Note the migrations of the palpebral lobes during the growth periods. 5. U.C.M. 38741d; × 30. 6. U.C.M. 38741e; × 29. 9. U.C.M. 38741g; × 26. 10. U.C.M. 38741h; × 25. 11. U.C.M. 38741i; × 26.

12-16,25,26,28-31. Late meraspides. 12-16. Showing the development of the posterior fixigenal borders and the lateral widening of the glabellae. 12. U.C.M. 38741j; × 22. 13. U.C.M. 38741k; × 18. 14. U.C.M. 38741l: × 16. 15. U.C.M. 38741m; × 18. 16. U.C.M. 38741n; × 15. 25,26. Ventral view and dorsal view of a hypostoma; note three pairs of posterior marginal spines, × 10, U.C.M. 38741w. 28-31. Dorsal view, posterior view, and horizontal view of four pygidia; note the different directions of the marginal spines. 28,29. U.C.M. 38741x;× 20. 30. U.C.M. 38741y; × 21. 31. U.C.M. 38741z; × 36.

17-27,32-39. Holaspides. 17-19. Three cranidia 17. U.C.M. 38741o; × 15. 18. U.C.M. 38741p; × 11. 19. U.C.M. 38741q; × 9.4. 20-22. Top view and lateral view of three librigenae, showing the marginal spines and the stolked eyes, × 20, U.C.M. 38741r; 21. U.C.M. 38741s; × 21. 22. U.C.M. 38741t; × 15. 23. A pair of thoracic segments, × 8.2, U.C.M. 38741u. 24,27. Ventral view and dorsal view of a hypostoma, × 10, U.C.M. 38741v. 32,34. Top view and ventral view of a pygidium, × 22, U.C.M. 38741a'. 33,35. Two pygidia. 33. U.C.M. 38741b'; × 28. 35. U.C.M. 38741c'; × 14. 36,39. Ventral view and dorsal view of a less complete skeleton in fig. 36, (the thoracic segments and pygidium were broken off by an accident after fig. 39 was taken), × 13, U.C.M. 38741d'. 37,38. Ventral view and dorsal view of a late meraspis skeleton; note that the hypostoma is in place; × 8.5, U.C.M. 38741.

EXPLANATION OF PLATE 23

Figure *Page*

1-31. *Phaseolops conus,* n. sp. 113-115

1-3. Anaprotaspides. 1. Dorsal view of an incomplete shield, × 56, U.C.M. 38742a. 2,3. Dorsal view and ventral view of a complete shield; note the posterior marginal doublure and a pair of posterior lateral spines, × 56, U.C.M. 38742b.

4-8,22. Paraprotaspides. 4-7 are four shields all with undifferentiated pygidia; note the facial suture and the palpebral lobes. 4,5. U.C.M. 38742c,d; × 53. 6. U.C.M. 38742e; × 46. 7. U.C.M. 38742f; × 42. 8,22. Dorsal view and ventral view of shield (associated with the shell of an ostracod), × 40, U.C.M. 38742g.

9-12. Early meraspides. Four cranidia without pygidia, showing the distinct anterior borders. 9. U.C.M. 38742h; × 46. 10. U.C.M. 38742i; × 34. 11. U.C.M. 38742j; × 34. 12. U.C.M. 38742k; × 30.

13-16,23,27. Late meraspides. 13-16. A few incomplete cranidia, showing the well-preserved preglabellar fields. 13. U.C.M. 38742l; × 31. 14. U.C.M. 38742m; × 27. 15. U.C.M. 38742n; × 28. 16. U.C.M. 38742o; × 20. 23. A small librigena; note the narrow ocular plate form, × 8, U.C.M. 38742s. 27. An incomplete pygidium, lacking marginal spines, × 26, U.C.M. 38742w.

17-21,24-26,28-31. Holaspides. 17-18. Top view and side view of a complete cranidium. × 13. U.C.M. 38742p. 19-21. Three nearly complete cranidia. 19. U.C.M. 38742q; × 13. 20. U.C.M. 38742r; × 12. 21. U.C.M. 38742; × 21.

24-26. Holaspid librigena. 24,26. Two complete forms; note that the lateral furrows extend to the genal spines. 24. U.C.M. 38742t; × 6. 25. U.C.M. 38742u; × 4. 26. Ventral view of a complete form, showing a broad doublure with distinct ridges along the border, × 4, U.C.M. 38742v.

28-31. Holaspid pygidia. 28,29,31. Three well-preserved forms all showing three pairs of short marginal spines. 28. U.C.M. 38742x; × 20. 29. U.C.M. 38742y; × 11. 31. U.C.M. 38742z; × 10. 30. Ventral view of a well-preserved pygidium; note the wide doublure and the ridges along the border, × 11, U.C.M. 38742a'.

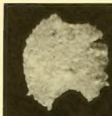
1

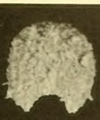
2

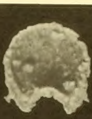
3

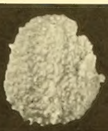
4

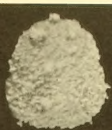
5

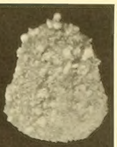
6

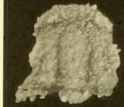
11

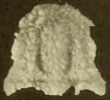
10

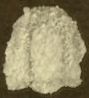
9

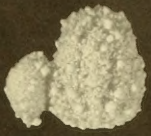
8

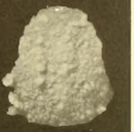
7

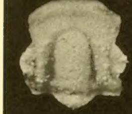
14

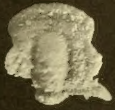
13

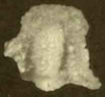
12

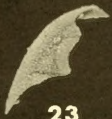
23

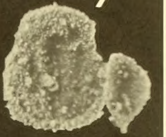
22

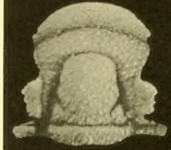
17

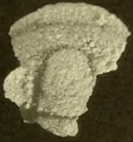
16

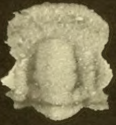
15

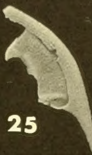
25

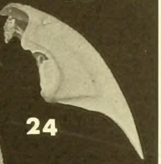
24

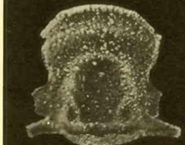
18

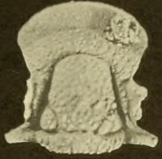
19

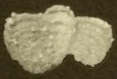
27

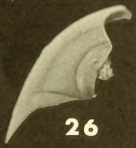
26

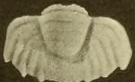
28

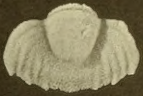
29

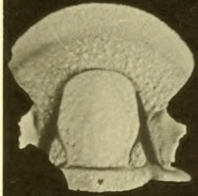
20

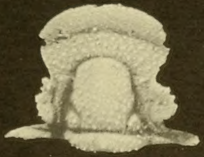
21

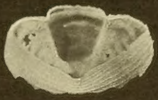
30

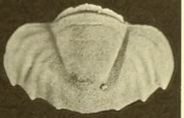
31

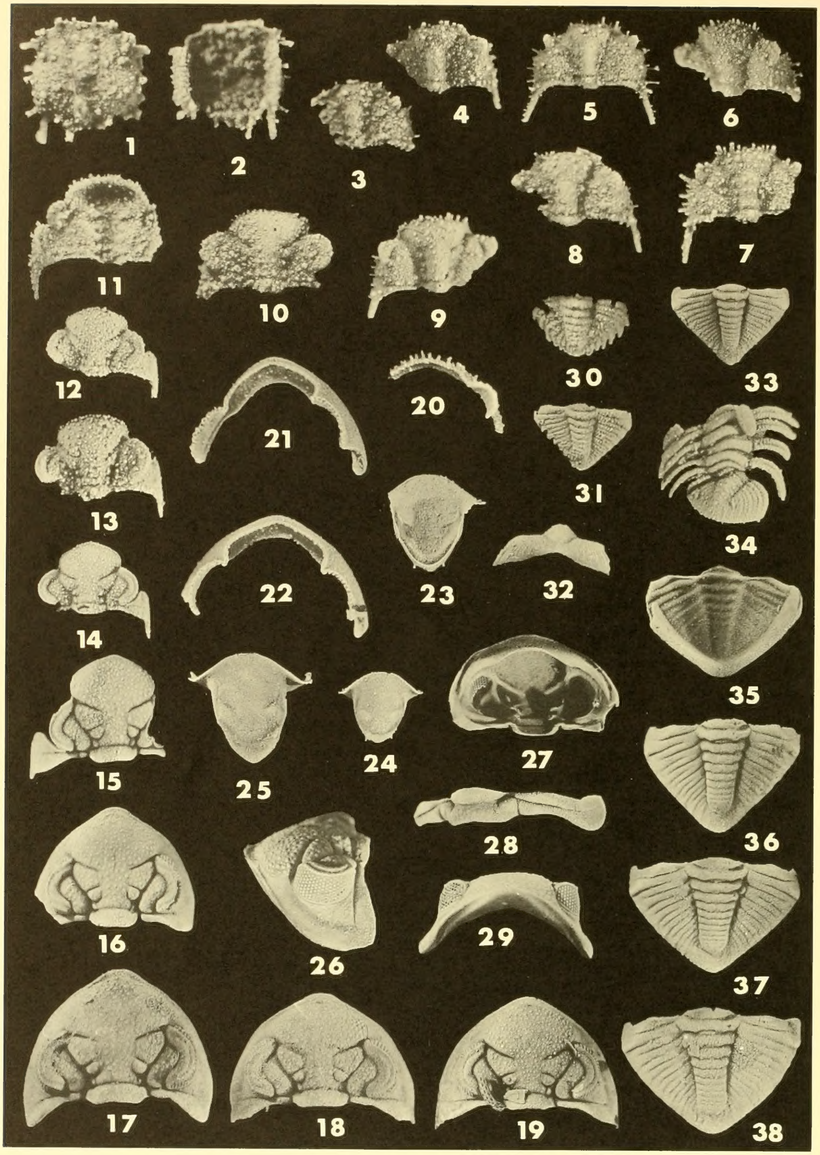
1
2
3
4
5
6
11
10
9
8
7
12
21
20
30
33
13
31
34
22
23
32
14
35
15
25
24
27
36
28
16
26
29
37
17
18
19
38

EXPLANATION OF PLATE 24

Figure *Page*

1-38. *Calliops strasburgensis* Ulrich and Delo 116,117

1,2. Paraprotaspis. Dorsal view and ventral view of a complete instar, × 36, U.C.M. 38743a.

3-9. Early meraspides. Note the change in position of the palpebral lobes in small to larger specimens. 3. U.C.M. 38743b; × 21. 4. U.C.M. 38743c; × 23. 5. U.C.M. 38743d; × 22. 6. U.C.M. 38743e; × 27. 7. U.C.M. 38743f; × 34. 8. U.C.M. 38743g; × 23. 9. U.C.M. 38743h; × 17.

10-13. Late meraspides. Note the reduction of the spines and the increase in size of the palpebral lobes. 10. U.C.M. 38743i; × 15. 11. Ventral view of a broken cranidium, × 14, U.C.M. 38743j. 12. U.C.M. 38743k; × 8. 13. U.C.M. 38743l; × 10.

20,23,24,30,31. Late meraspides. 20. A broken rostro-librigena, showing the anterior marginal spines, × 25, U.C.M. 38743s. 23,24. Ventral view and dorsal view of two hypostomata, showing the narrow marginal doublure, posterior border, and a pair of posterior spines. 23. U.C.M. 38743u; × 6. 24. U.C.M. 38743v; × 10. 30,31. Two pygidia bearing marginal spines; 30. × 20, U.C.M. 38742y. 31. U.C.M. 38743z; × 6.1.

21,22,25,28. Holaspides. 21,22. Anterior lateral view and anterior view of a rostro-librigena, × 8.7., U.C.M. 38743t. 25. Hypostoma, × 3.2, U.C.M. 38743r. 28. Lateral oblique view of a thoracic segment, × 2, U.C.M. 38743x.

14,15,18,19,26,29,35,38. Holaspides ("male"). 14,15. Two cranidia without rostro-librigenae; note the small fixigenal spines. 14. U.C.M. 38743m; × 3.5. 15. U.C.M. 38743n; × 32. 18,19. Two cephala with rostro-librigenae in place, note the small fixigenal spines. 18. U.C.M. 38743; × 3.5. 19. U.C.M. 38743q; × 3.2. 26,29. Side view and frontal view of a less complete cephalon (the genal spines were broken off) × 2.8. U.C.M. 38743w. 35. Ventral view of a less complete pygidium, × 4, U.C.M. 38743d′. 38. A complete pygidium, × 3.3, U.C.M. 38743g′

16,17,27,32-34,36,37. Holaspides ("female"). 16,27 Dorsal view and ventral view of a cephalon, × 3.1, U.C.M. 38743o. 17. A complete cephalon, showing no fixigenal spines, × 3, U.C.M. 38743p. 32. Back view of a broken pygidium, × 3, U.C.M. 38743a′. 33. A medium-sized pygidium, × 3.7, U.C.M. 38743b′. 34. A small pygidium associated with a few thoracic segments, × 11, U.C.M. 38743c′. 36,37. Two well-preserved pygidia. 36. U.C.M. 38743e′; × 3.8. 37. U.C.M. 38743f′; × 3.

EXPLANATION OF PLATE 25

Figure *Page*

1-29. *Flexicalymene granulosa* (Foerste) 117-120

1-4. Anaprotapides; showing two pairs of axial nodes and a longitudinal fissure. 1,2. U.C.M. 38744a,b; × 53. 3. An impression, × 52, U.C.M. 38744c. 4. U.C.M. 38744d; ×52.
5. Paraprotaspis; showing the fusion of the axial nodes and the origin of the axial rings; note the posterior portion of the shield without segmentation or differentiation, × 40, U.C.M. 38744e.
6-10. Paraprotaspides. Note the segmented protopygidium. 6. U.C.M. 38744f; × 35. 7. U.C.M. 38744g; × 30. 8. U.C.M. 38744h; × 31. 9. U.C.M. 38744i; × 32. U.C.M. 38744j; × 23.
11,12,20. Early meraspides. 11,12. Two cranidia showing the hemi-cylindrical glabella and absence of any pygidium; 11. U.C.M. 38744k; × 25. 12. U.C.M. 38744l; × 26. 20. Small pygidium possibly associated with three or four thoracic segments, × 30, U.C.M. 38744t.
13,14,16,21,25. Late meraspides. 13. Incomplete skeleton, showing the conical glabella, × 14, U.C.M. 38744m. 14. Incomplete cranidium, showing the conical glabella, × 19, U.C.M. 38744n. 16. Rubber mould of a cranidium, × 13, U.C.M. 38744p. 21. Broken pygidium, showing short marginal spines, × 24, U.C.M. 38744u; 25. Hypostoma; note a pair of short broad posterior spines, × 20, U.C.M. 38744y.
15,19A,24,29. Holaspides ("female"). 15,19. Two incomplete cranidia, showing the broader anterior borders. 15. U.C.M. 38744o; × 15. 19A. U.C.M. 38744s; × 6.8. 24. Well-preserved pygidium showing broader pleural lobes, × 8.4, U.C.M. 38744x. 29. A small librigena, × 13, U.C.M. 38744c'.
26,27. Two hypostomata. 26. Well-preserved specimens; note a pair of distinct pits on the anterior wings and the short posterior spines, × 5.9, U.C.M. 38744z. 27. U.C.M. 38744a'; × 14.
17,18,19B,22,23,28. Holaspides ("male"). 17,18,19B. Three cranidia; note the narrow anterior border, × 8, U.C.M. 38744q; × 30. 18. U.C.M. 38744r; × 4.2. 19B. U.C.M. 38744s; × 6.8. 22,23. Two complete pygidia with subtriangular outline, × 4.5, U.C.M. 38744v,w. 28. Librigena, ×2, U.C.M. 38744b'.

30-32. *Flexicalymene meeki* (Foerste) 119-125

Two individuals enrolled concentrically, the inner one is less incomplete, the outer one has the cephalon broken off. 30. Side view; note that the left one is complete, and the right one shows the thoracic segments and pygidium only. 31. Dorsal view; note the inner one is on top, and the outer one, on the bottom. 30. Ventral view, showing the weathered pygidia and cephalon. All × 2.1, U.C.M. 23263.

1

2

3

4

5

6

11

10

9

8

7

12

13

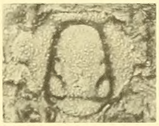
14

29

15

16

21

20

30

17

22

25

31

18

26

23

27

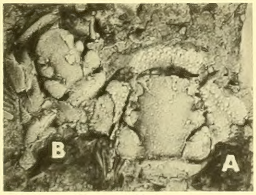

19

28

24

32

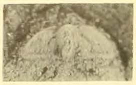
1

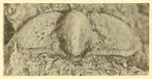
2

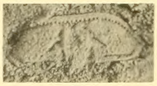
3

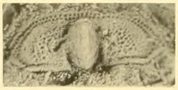
4

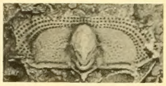
5

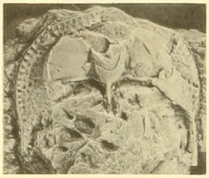
9

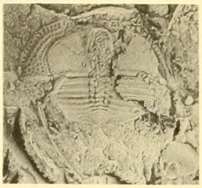
8

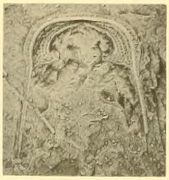
7

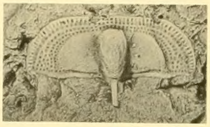
6

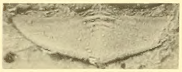
12

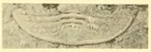
11

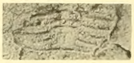
10

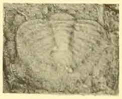
14

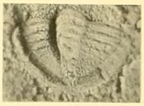
15

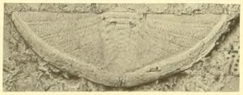
13

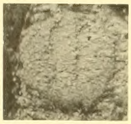
19

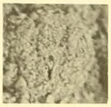
18

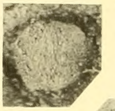
17

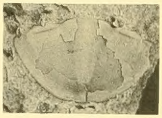
16

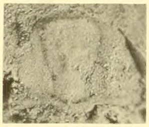
23

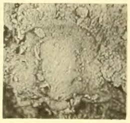
22

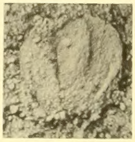
21

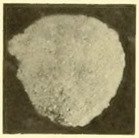
20

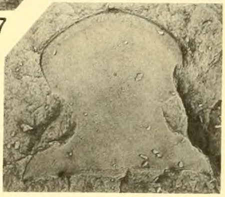
29

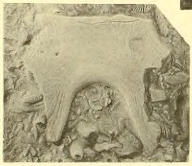
26

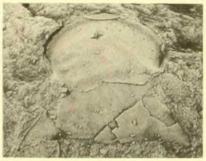
25

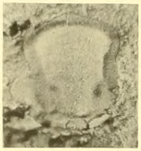
24

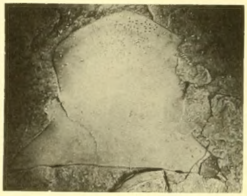
30

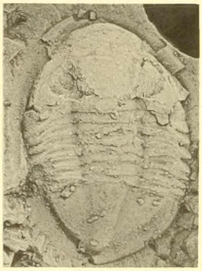
27

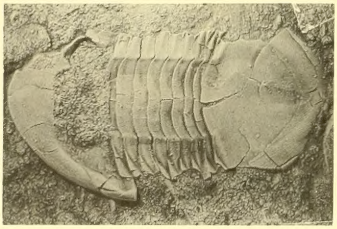
28

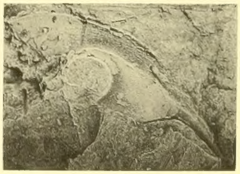
31

EXPLANATION OF PLATE 26

Figure *Page*

1-13. *Cryptolithus bellulus* (Ulrich) 120-122

1. Paraprotaspis. Cranidium, showing a pair of palpebral ridges and eye tubercles; note the anterior margin without fringe, × 23, U.C.M. 38745a.
2-5,10. Early meraspides. Note the shortening of the palpebral ridges and the expansion of the anterior fringe. 2. U.C.M. 38745b; × 20. 3. U.C.M. 38745c; × 20. 4. U.C.M. 38745e; × 19. 5. U.C.M. 38745d; × 8. 10. Small pygidium associated with two thoracic segments, × 18, U.C.M. 38745h.
6-8,11. Late meraspides. 6. Cranidium, showing the disappearance of the palpebral lobes and the tubercles, × 3.4, U.C.M. 38745f. 7. Ventral view of a lower lamella; note that the girdle extends into the genal spines, × 2.5, U.C.M. 38745g. 8. Incomplete skeleton which shows four or five thoracic segments, × 5, U.C.M. 38745i. 11. Pygidium which shows three distinct segments, × 12, U.C.M. 38745j.
9,12,13. Holaspides. 9. A poorly preserved cephalon; note the fusion of the upper and lower lamella, × 1.8, U.C.M. 38745. 12,13. Two pygidia showing the pleural lobe ridges, × 8.3, U.C.M. 38745j; × 3.7, U.C.M. 38745k.

14-31. *Isotelus stegops* Green 122-124

17. Anaprotaspis. Note the longitudinal fissure along the central axis, × 57, U.C.M. 38746a.
18,19. Metaprotaspides. Note the well-differentiated axial lobes. 18 U.C.M. 38746b × 30. 19. U.C.M. 38746c; × 27.
20,21. Two paraprotaspides. Note the elongation of the posterior portion. 20. U.C.M. 38746d; ×20. 21. U.C.M. 38746e; × 26.
14,15,22. Late early meraspides. 14. A small pygidium, showing distinct axial furrow and pleural furrow and terminal portion of the axis with elongate and concentric ridges, × 15, U.C.M. 38746o. 15. A less well-preserved pygidium, × 8.3, U.C.M. 38746p; 22. Cranidium with narrow preglabellar field and well-defined anterior border, × 13, U.C.M. 38746f.
23,24,27. Late meraspides. 23,24. Two cranidia, showing no preglabellar field. 23. U.C.M. 38746g; × 11. 24. U.C.M. 38746h; × 12. 27. Complete skeleton with seven thoracic segments only, × 3.4, U.C.M. 38746k.
16,25,26,28-31. Holaspides. 16. A pygidium. Note the disappearance of the distinct axial lobe furrow and pleural lobe furrow but presence of fine ridges, × 4, U.C.M. 38746q. 25,29. Two "female" cranidia, × 2.1, U.C.M. 38746i; U.C.M. 38746e. 26. broken hypostoma, showing a pair of lateral pits and wrinkled surface, × 7, U.C.M. 38746j. 28. Ventral view of an incomplete skeleton, × 1.7, U.C.M. 38746. 30. "male" cranidium; note that it is wider and shorter than those of the "female form," × 1.5, U.C.M. 38746m. 31. Librigena, showing the doublure and the well-preserved median suture line, × 3, U.C.M. 38746n.

INDEX

Bold face figures refer to the page of the description of the species.

A

Acanthoparypha 63
Acerocare 58
Acerocare Zone 102
Acidaspis 120,124
Acrocephalites 105,106
Adams County, Ohio 121
Akesson, B. 38,43,71
Alberta 51
Alokistocare 80
americana, Minkella 98
amiger, Scoloplos 43
amphitrite var. denticulata, Blanus 45
? anyta, Dunderbergia 51,55,59,72,92,**96**
Anderson, D. T. 39,42,43
Anomocare 82,84
Anomocarella 106
Aphelaspis 71
Apomodocia 86
Arenicola 60
armatus, Olenelloides 79
amiger, Scoloplos 42
Asiatic realm 106
aurita, Ptarmigania 52,55,60,61,**80**

B

Bälz, von 36
Barrande, J. 50,51,53,54
Bassler, R. S. 116,119,121
Bathynotus 32,71
Bathyuriscus-Elrathina Zone 75,83,85
battsi montanensis, Crepicephalus 90
Beaufort, North Carolina 34,36,40
Beaver County, Utah 93,96
Beecher, C. E. 48,49,51,53,59-61,63,65,68
Beklemischew, W. N. 43
bellulus, Cryptolithus 53,56,61,62,**118**
bellulus, Trinucleus 118
benjamini, Isotelus 121
Bernard, H. M. 59,65
Bevanapsis 110
Bird Schoals, Beaufort, North Carolina 40
bispinata, Laudonia 79
Bjerbasholmen, Norway 104
Black Hills, South Dakota 90
Blountia 86
Bohemia 53
Bonnettere Dolomite 74
Bonnettere, Missouri 74
Bookhout, C. G. 45
bootes, Pagetia 75
bovealis, Cancer 124
brachycephalus, Isotelus 121
Bretonian 106
British Columbia 65,79
Brøgger, W. C. 51
Buelina Formation 77
bullasus, Ptychaspis 51,55,60,**97**
Butt, F. H. 65-68

C

Caborca, Mexico 77
Callavia 71
Callianassa 35
callicephala granulosa, Calymene 115
Calliops 58
Calman, W. T. 68
Cambarus 69
Cambrian 31,50,51,57,58,61,65,71,79,122
Canada 106
Canadian Rockies 31
canadiensis, Laudonia 55,71,**79**
carens, Hydrocephalus 51
carinatus, Reedolithus 56
Carpenter, G. H. 65
Caster, K. E. 99,104
Cedaria 71
Cedaria Zone 86,88
Cedarian 57,71
Cephalocarida 65
Ceratopyge Limestone 104
Ceraurus 68
Chambersburg Limestone 114
Chaudonneret, J. 67
Chilopoda 68
chinensis, Redlichia 51
Chuangia 106
Cincinnati, Ohio 56,116,119,120
Cincinnati Hill, Ohio 121
Cincinnatian 117,119
cincinnatiensis, Acidaspis 122,123
clarki, Paedeumias 55
clytia, Pagetia 54,**74**
conica, Apomodocia 52,55,86,88
Conocoryphe 71
conus, Phaseolops 111
Cooper, B. 110,114
cordillerae, Cedarina 52,55,**86**-88
cordillerae, Euloma 104
cordillerae, Piemontia 87
corona, Libertella 52,**110**
Costlow, J. D. 45
covingtonensis, Isotelus 121
Crampton, G. C. 67
Crepicephalus 58
Crepicephalus Zone 90
cristata, Arenicola **40**,43,44
Crook County, Wyoming 104,108
Cryptolithus 46,48,68,116,**118**,120
Cumings, E. R. 121
cylochila, Missisquoia 52,59,**107**
Cynthiana Formation 121

D

Dahl, E. 68
Dalvé, B. 116,119,121
Dayton, Ohio 121
deadwoodiensis, Crepicephalus 51,55,60,62,**89**
Deadwood Formation 90,104,108
Delo, D. M. 114
Devonian 71
Dicellomus 88
Diceralocephalus 63
Dicranopeltis 65
Diplopoda 68
Dokimocephalus 105,106
domestica, Thermobia 67
Duke Marine Laboratory 36,40
Dunderbergia 57-71
Dunderbergia Zone 93,96

E

eatoni, Triarthrus 53,56
ecorne, Acerocare 53,56,60,61,63,**101**
Eden Formation 117,119,121
Eden Shale 116
Edinburg Formation 50,110,112,114
Edwards, M. 46
Elliptocephala 55,62,63,71
elongata, Armonia 86

INDEX

Elrathina ... 80
Elrathina-Bathyuriscus Zone ... 81
Encrinuroides ... 110
Encrinurus ... 110
Endo, R. ... 51,122
Entomaspis ... 71
Entomostraca ... 44
ephelitus, Hepatus ... 34
esterius, Kormagnostus ... 72,**73**
Evitt, W. R. ... 31,52,59,61

F

facilia, Highgatella ... 103
fasciatus, Oncopeltus ... 35
Fedotov, D. ... 65
Flexicalymene ... 58,71,120,124
Foerste, A. F. ... 121
Ford, S. W. ... 50
fragilis, Halploscoloplos ... 43
Fränsemeier, L. ... 45

G

Garstang, W. ... 68
gelasinata, Highgatella ... 104
genalunata, Menoparia ... 52,53,56
Geology Museum, University of Cincinnati ... 106,122
gibbosus, Entomostracites ... 99
gibbosus, Olenus ... 51,55,59,62,**99**
Glyphaspis ... 58,84
Glyptocrinus ... 120
Cf. granulatus, Sphaerocoryphe ... 64
granulosa, Calymene ... 115
granulosa, Flexicalymene ... 51-60,**115**
granulosus, Dytremacephalus ... 51,55,59,62,72,**93**,94
Green, J. ... 58
Greenland ... 83

H

Hall, J. ... 121
halli, Norwoodella ... 52,53,56
hanseni, Paedeumias ... 57
Hanström, B. ... 67
harlanensis, Kormagnostus ... 72,73
Heegaard, P. ... 68
helgolandica, Tomopteris ... **38**,43
Heminysis ... 45,65
Henrikson, K. L. ... 60
hercules, Dynastes ... 33
Herskowitz, I. H. ... 34
Highgatella ... 58
Hintze, L. F. ... 31,57
Hippolyte ... 34
hirsuta, Sao ... 51,58
Holanshania ... 63
Holm, G. ... 58,73
Hölmgren, N. ... 67
Holmia ... 62,63,71
Homalopyge ... 71
Homotelus ... 121
Housia ... 71
Howell, B. F. ... 51,106
Hu, C. H. ... 52,98
Hungia ... 71
Hunt, A. S. ... 50
Hupé, P. ... 58-63
Hydrocephalus ... 55

I

Idaho ... 98
incisa, Lightiella ... 64
Indiana ... 120
inflata, Missisquoia ... 108
Insecta ... 31,68
International Geological Congress, 1962 ... 99,104
Iohomia ... 84
iowensis, Crepicephalus ... 90
Ishibashi, E. ... 34
Isorophus ... 120
Isotelus ... 52,56,58,68,116
Iwanoff, P. P. ... 43,46,65,66

J

Jaekel, J. ... 60
Johansson, G. ... 67

K

Kato, F. ... 51
Kennebe River, New Brunswick ... 106
Kentucky ... 117,119,121
Kepisis ... 58,105,106
Kiaer, J. ... 62
Kingsley, J. S. ... 46
Kjerufia ... 62,71
kjerufi, Holmia ... 51
Kobayashi, T. ... 51,54,73
kobayashi, Blackwelderia ... 51
kobiensis, Eunice ... 43
Kootenia ... 68

L

Lacanus ... 33
Lanica ... 60
lata, Perioura ... 86
lata, Welleraspis ... 51,59
Lawrence County, South Dakota ... 90
Leander ... 45,46
Lever, W. ... 35
Levisella ... 71
Libertella ... 109
Liberty Member, Richmond Group ... 121
"Limulus" ... 67
Lindström, G. ... 59,63
linnarssoni, Liostracus ... 51
Lochman, Christina ... 73,77,86,88,98,104
Loganopeltis ... 71
Loimia ... 50
Lonchodomas ... 105,106
lorrainensis, Cryptolithus ... 118
Lower Cow Head, New Foundland ... 112
Ludlow, Kentucky ... 121

M

maladensis, Pagetia ... 75
maluccanus, Xiphosura ... 46
Manchuria, China ... 108,122
Manton, S. M. ... 43,45,65,67
Matthew, G. F. ... 50,106
Maustonia ... 86
maximus, Isotelus ... 121
Maysville Formation ... 116,121
McMicken Member ... 121
Meager Formation ... 83,85
meeki, Flexicalymene ... 61,116,122,**123**
megista, Isotelus ... 121
Menoparia ... 71
Mexico ... 31,51
mexicana prima, Wanneria ... 79
Millard County, Ohio ... 93,96

INDEX

Milne-Edwards, H. 67
Mink Creek, Idaho 98
minuta, Eupsalis 33
Missisquoia 58
Missisquoia Zone 104,108
Missouri 74
Moberg, J. C. 62
Modocia 86
mucosa, Axiothella 43,44

N

Nascocephalus 105,106
nasuta, Missisquoia 108
nasuta Pseudocybele 49
Nebalia 45,65
Neoconocephalus 34
Nereis 37,38,42,43
Nevada 31,51
Nevadia 71
New Brunswick 106
Newport, Kentucky 121
New York 50,53
Nicholls, H. 104
North America 31,71
North of Radium, British Columbia 79
North Sea 71
North Wales 53
Northern China 108
Northwestern Sonora, Mexico 77
Norway 51,100,104
Nye 102

O

Ogygopsis 68
Ohio 120,121
Olenelloides 63,71
Olenellus 57,58,62,68,71,77,79
olini, Dalmanitina 53,56
Onychophora 43
Ordovician 31,51-53,58,71,112,121
orientalis, Blatta 34
ornata, Onnia 53,56
ornatum, Euloma 104
Oryctocephalus 71
Oslo 100

P

Packard, A. S. 46,65
Paedeumias 63,71
Pagetia 80
Palaemonetes 34
Palmer, A. R. 31,49,50,51,54,55,57,63,92
Parabolinella 104
Parabolinoides 86
Paradoxides 55,71
Parakoldinoides 108
Cf. parkensis, Glyphaspis 52,55,60,61,**82**
Patten, W. 46,47
Peach, B. N. 79
peculiaris, Fengtienia 122
Peltura 71
Pennsylvania 51
perforata, Acanthoparypha 64
Phacops 53,68
? pinus, Paradaxides 58
Pisione 32,38,42,71
planus, Isotelus 121
Polygordius 43
polyphemus, Xiphosura 46
Poulsen, C. 51,53,83
prima, Cedarina 88
Primaspis 116
Proetus 71
Ptarmigania 57
Pterygometopus sp. 113
Ptychaspis-Prosaukia Zone 98
pusilla, Shumardia 53,56,58,64

R

Rasetti, F. 72,80,83,106
Raw, F. 49,53,54,56-60,62-64,69-71
Raymond, P. E. 59,63,65,68,73
recurvus, Cryptolithus 118
Redlichia 32,55,71
Remopleurides 32,43,52,53,56,65,71,72
remota, Pisione 38,70
Resser, C. E. 71,73,80,122
resseri, Pagetia 75
Richmond Formation 116
Richter, R. 72
Ringsaker Station, Norway 100
Robergilla 52
robiniae, Prionoxystus 34
Robison, R. A. 31,57
Ross, Jr. R. J. 31,52,57,121
Ross-Shire, Scotland 79
rossensis, Ptarmigania 80
Royal Ontario Museum 106
Ruedemann, R. 121

S

Salterella 79
salteri, Leptoplastus 52,56,58
Sanders, H. L. 65,68
Santaquin Canyon, Utah 75,81
sapidus, Callinectes 124
Scandinavia 53
Scandinavia Peninsula 31
scarabaeoides, Peltura 53,56
Scoloplos 37
Scotland 79
Scutellum 65,71
Segrove, F. 43
senaria, Flexicalymene 61
sepositus, Phaseolops 112
serratus, Olenoides 65
Shantongia 105,106
Sharov, A. G. 65
Sheep Mtn., Wyoming 104,108
Shenandoah County, Va. 110
Shumardia 50
Shuster, C. N. 36,46
sickia, Iohomia 84
simplex, Kormagnostus 72
Snajdr, M. 50
Snodgrass, R. E. 43,45,65,67
socialis, Dalmanitina 53,56
solitecti, Scinocephalus 56
Sollaud, E. 44,45
South Boulder Creek, Montana 83,85
splendens, Kormagnostus 72,73
St. Charles Formation 98
St. Francois County, Missouri 74
St. John, New Brunswick 106
stegops, Homotelus 120
stegops, Isotelus 54,56,61,**120**
stenotoides, Anomocare 106
stenotoides, Kepisis 106
Størmer, L. 43,46,49,51,53,55,57,59-69,99
Strand, T. 99
Strasburg Junction, Virginia 110,112,114

strasburgensis, Calliops 53,56,60,72,**110**,**113**,119
Stubblefield, C. J. 57,58,64,72
Sundance, Wyoming 104
Sweden 102
Symphysurina 104

T

Temple, J. T. 53
tesselatus, Cryptolithus 119
Theodenisia 71
Thysanopyge 105
Tiegs. O. W. 43,65,67
tityus, Dynostes 33
Tomopteris 38,42
Treber's Run, Ohio 121
Tremadocian 104
Tretaspis 45
Triarthrus 68,71
truemani, Olenellus 51,55,59,62,76,**77**
typicalis, Missisquoia 108

U

Ulrich, E. O. 114
ulrichi, Bevanopsis 110
University of Cincinnati 122
Utah 31,52,75,81,96
Utica Shale 53

V

Virginia 31,50,110,112,114

W

Wah Wah Range, Utah 93,96
Walcott, Chas. 53,57,59,63,68,79
walcotti, "Cassifimbra" 49
Wanneria 71
Warburg, E. 60,62,72
Wasatch Mts., Utah 75,81,86,88
Waynesville, Ohio 121
Weber, H. 67
West Madison County, Montana 83,85
Westergård, A. H. 58
Whittington, H. B. 31,49-64,119
Williston Basin 104
Willow Grove, Virginia 114
Winston, P. 104
wisconiensis, Idahoia 98
Woodstock, Virginia 114
Wyoming 104

X

Xenostegium 71
Xiphopeneus 34
Xiphosura 34,46,58,59,61-69,119,123

Y

yorkense, Paedeumias 51,53-55,64

Z

Zuninaspis 105

XLII.	(No. 193). 673 pp., 48 pls. Venezuelan Cenozoic gastropods.	18.00
XLIII.	(Nos. 194-198). 427 pp., 29 pls. Ordovician stromatoporoids, Indo-Pacific camerinids, Mississippian forams, Cuban rudists.	16.00
XLIV.	(Nos. 199-203). 365 pp., 68 pls. Puerto Rican, Antarctic, New Zealand forams, Lepidocyclina, Eumalacostraca.	16.00
XLV.	(No. 204). 564 pp., 63 pls. Venezuela Cenozoic pelecypods	18.00
XLVI.	(Nos. 205-211). 419 pp., 70 pls. Large Foraminifera, Texas Cretaceous crustacean, Antarctic Devonian terebratuloid, Osgood and Paleocene Foraminifera, Recent molluscan types.	16.00
XLVII.	(Nos. 212-217). 584 pp., 83 pls. Eocene and Devonian Foraminifera, Venezuelan fossil scaphopods and polychaetes, Alaskan Jurassic ammonites, Neogene mollusks.	18.00
XLVIII.	(No. 218). 1058 pp., 5 pls. Catalogue of the Paleocene and Eocene Mollusca of the Southern and Eastern United States.	18.00
XLIX.	(Nos. 219-224). 671 pp., 83 pls. Peneroplid and Australian forams, North American carpoids, South Dakota palynology, Venezuelan Miocene mollusks, *Voluta.*	18.00
L.	(Nos. 225-230). 518 pp., 42 pls. Venezuela and Florida cirripeds, Antarctic forams, Linnaean Olives, Camerina, Ordovician conodonts, Niagaran forams.	18.00
LI.	(Nos. 231-232). 420 pp., 10 pls. Antarctic bivalves, Bivalvia catalogue.	18.00
LII.	(Nos. 233, 236). 387 pp., 43 pls. New Zealand forams, Stromatoporoidea, Indo-Pacific, Miocene-Pliocene California forams.	18.00
LIII.	(Nos. 237-238). 488 pp., 45 pls. Venezuela Bryozoa, Kinderhookian Brachiopods.	18.00
LIV.	(Nos. 239-245). 510 pp., 50 pls. Dominican ostracodes, Texan pelecypods, Wisconsin mollusks, Siphocypraea, Lepidocyclina, Devonian gastropods, Miocene Pectens Guadaloupe.	18.00
LV.	(Nos. 246-247). 657 pp., 60 pls. Cenozoic corals, Trinidad Neogene mollusks.	18.00
LVI.	(Nos. 248-254). 572 pp., 49 pls. American Foraminifera, North Carolina fossils, coral types, Belanski types, Venezuelan Cenozoic Echinoids, Cretaceous Radiolaria, Cymatiid gastropods.	18.00
LVII.	(Nos. 255-256). 321 pp., 62 pls. Alaskan Jurassic ammonites, Pt. II, Jurassic Ammonitina New Guinea.	18.00
LVIII.	(Nos. 257-262). 305 pp., 39 pls. Cretaceous Radiolaria, Cretaceous Foraminifera, Pacific Silicoflagellates, North American Cystoidea, Cincinnatian Cyclonema, new species Vasum.	18.00
LIX.	(No. 263). 314 pp. Bibliography of Cenozoic Echinoidea.	18.00

Palaeontographica Americana

Volume I.	See Johnson Reprint Corporation, 111 Fifth Ave., New York, N. Y. 10003 Monographs of Arcas, Lutetia, rudistids and venerids.	
II.	(Nos. 6-12). 531 pp., 37 pls. Heliophyllum halli, Tertiary turrids, Neocene Spondyli, Paleozic cephalopods, Tertiary Fasciolarias and Paleozoic and Recent Hexactinellida.	23.00
III.	(Nos. 13-25). 513 pp., 61 pls. Paleozoic cephalopod structure and phylogeny, Paleozoic siphonophores, Busycon, Devonian fish studies, gastropod studies, Carboniferous crinoids, Cretaceous jellyfish, Platystrophia and Venericardia.	28.00
IV.	(Nos. 26-33). 492 pp., 72 pls. Rudist studies Busycon, Dalmanellidae, Byssonychia, Devonian lycopods, Ordovican eurypterids, Pliocene mollusks.	28.00
V.	(Nos. 34-37). 445 pp., 101 pls. Tertiary Arcacea, Mississippian pelecypods, Ambonychiidae, Cretaceous Gulf Coastal forams.	32.00
VI.	(Nos. 38-41). 444 pp., 83 pls. Lycopsids and sphenopsids of Freeport Coal, Venericardia, Carboniferous crinoids, Trace fossils.	35.00
VII.	(Nos. 42-43). 26 pp., 6 pls. Torreites Sanchezi, Cancellariid Radula.	2.50

BULLETINS OF AMERICAN PALEONTOLOGY

Vols. I-XXIII. See Kraus Reprint Corp., 16 East 46th St., New York, N. Y. 10017, U.S.A.

XXIV.	(Nos. 80-87). 334 pp., 27 pls. Mainly Paleozoic faunas and Tertiary Mollusca.	12.00
XXV.	(Nos. 88-94B). 306 pp., 30 pls. Paleozoic fossils of Ontario, Oklahoma and Colombia, Mesozoic ehinoids, California Pleistocene and Maryland Miocene mollusks.	12.00
XXVI.	(Nos. 95-100). 420 pp., 58 pls. Florida Recent marine shells, Texas Cretaceous fossils, Cuban and Peruvian Cretaceous, Peruvian Eogene corals, and geology and paleontology of Ecuador.	14.00
XXVII.	(Nos. 101-108). 376 pp., 36 pls. Tertiary Mollusca, Paleozoic cephalopods, Devonian fish and Paleozoic geology and fossils of Venezuela.	14.00
XXVIII.	(Nos. 109-114). 412 pp., 34 pls. Paleozoic cephalopods, Devonian of Idaho, Cretaceous and Eocene mollusks, Cuban and Venezuelan forams.	14.00
XXIX.	(Nos. 115-116). 738 pp., 52 pls. Bowden forams and Ordovician cephalopods.	18.00
XXX.	(No. 117). 563 pp., 65 pls. Jackson Eocene mollusks.	16.00
XXXI.	(Nos. 118-128). 458 pp., 27 pls. Venezuelan and California mollusks, Chemung and Pennsylvanian crinoids, Cypraeidae, Cretaceous, Miocene and Recent corals, Cuban and Floridian forams, and Cuban fossil localities.	16.00
XXXII.	(Nos. 129-133). 294 pp., 39 pls. Silurian cephalopods, crinoid studies, Tertiary forams, and Mytilarca.	16.00
XXXIII.	(Nos. 134-139). 448 pp., 51 pls. Devonian annelids, Tertiary mollusks, Ecuadoran stratigraphy paleontology.	16.00
XXXIV.	(Nos. 140-145). 400 pp., 19 pls. Trinidad Globigerinidae, Ordovician Enopleura, Tasmanian Ordovician cephalopods and Tennessee Ordovician ostracods and conularid bibliography.	16.00
XXXV.	(Nos. 146-154) 386 pp., 31 pls. G. D. Harris memorial, camerinid and Georgia Paleocene Foraminifera, South America Paleozoics, Australian Ordovician cephalopods, California Pleistocene Eulimidae, Volutidae, and Devonian ostracods from Iowa.	16.00
XXXVI.	(Nos. 155-160). 412 pp., 53 pls. Globotruncana in Colombia, Eocene fish, Canadian Chazyan Antillean Cretaceous rudists, Canal Zone Foraminifera, fossils, foraminiferal studies.	16.00
XXXVII.	(Nos. 161-164). 486 pp., 37 pls. Antillean Cretaceous Rudists, Canal Zone Foraminifera, Stromatoporoidea.	16.00
XXXVIII.	(Nos. 165-176). 447 pp., 53 pls. Venezuela geology, Oligocene Lepidocyclina, Miocene ostracods, and Mississippian of Kentucky, turritellid from Venezuela, larger forams, new mollusks, geology of Carriacou, Pennsylvanian plants.	18.00
XXXIX.	(Nos. 177-183). 448 pp., 36 pls. Panama Caribbean mollusks, Venezuelan Tertiary formations and forams, Trinidad Cretaceous forams, American-European species, Puerto Rico forams.	16.00
XL.	(No. 184). 996 pp., 1 pls. Type and Figured Specimens P.R.I.	18.00
XLI.	(Nos. 185-192). 381 pp., 35 pls. Australian Carpoid Echinoderms, Yap forams, Shell Bluff, Ga. forams. Newcomb mollusks, Wisconsin mollusk faunas, Camerina, Va. forams, Corry Sandstone.	16.00

P 15

PALAEONTOGRAPHICA AMERICANA

(Founded 1917)

VOL. VII

NO. 45

RUDISTS OF JAMAICA

By

L. J. CHUBB

1971

Paleontological Research Institution
Ithaca, New York, U.S.A. 14850

SMITHSONIAN
OCT 4 1971
LIBRARIES

PALEONTOLOGICAL RESEARCH INSTITUTION

1970 - 71

PRESIDENT	WILLIAM B. HEROY
VICE-PRESIDENT	DANIEL B. SASS
SECRETARY	REBECCA S. HARRIS
DIRECTOR, TREASURER	KATHERINE V. W. PALMER
COUNSEL	ARMAND L. ADAMS
REPRESENTATIVE AAAS COUNCIL	DAVID NICOL

Trustees

REBECCA S. HARRIS (Life)
AXEL A. OLSSON (Life)
KATHERINE V.W. PALMER (Life)
DANIEL B. SASS (1965-1971)
KENNETH E. CASTER (1966-1972)
DONALD W. FISHER (1967-1973)
MERRILL W. HAAS (1970-1973)
PHILIP C. WAKELEY (1970-1973)
WILLIAM B. HEROY (1968-1974)
VIRGIL D. WINKLER (1969-1975)

BULLETINS OF AMERICAN PALEONTOLOGY

and

PALAEONTOGRAPHICA AMERICANA

KATHERINE V. W. PALMER, *Editor*
MRS. FAY BRIGGS, *Secretary*

Advisory Board

KENNETH E. CASTER
A. MYRA KEEN
HANS KUGLER
JAY GLENN MARKS
AXEL A. OLSSON

Complete titles and price list of separate available numbers may be had on application.

For reprint, Vols. 1-23, Bulletins of American Paleontology see Kraus Reprint Corp., 16 East 46th St., New York, N.Y. 10017 U.S.A.

For reprint, vol. I, Palaeontographica Americana see Johnson Reprint Corporation, 111 Fifth Ave., New York, N. Y. 10003 U.S.A.

Subscription may be entered at any time by volume or year, with average price of $18.00 per volume for Bulletins. Numbers of Palaeontographica Americana invoiced per issue. Purchases in U.S.A. for professional purposes are deductible from income tax.

For sale by

Paleontological Research Institution
1259 Trumansburg Road
Ithaca, New York 14850
U.S.A.

PALAEONTOGRAPHICA AMERICANA

(Founded 1917)

VOL. VII

NO. 45

RUDISTS OF JAMAICA

By

L. J. Chubb

September 17, 1971

Paleontological Research Institution
Ithaca, New York, U.S.A. 14850

Library of Congress Card Number: 73-163637

Printed in the United States of America
Arnold Printing Corporation

CONTENTS

Page
Abstract ... 161
Introduction ... 161
Acknowledgments ... 161
Geographic and stratigraphic considerations ... 162
The rudist shell ... 163
Shell structure ... 164
Definitions ... 164
Classification ... 165
Systematic descriptions ... 166
  Monopleuridae ... 166
  Caprotinidae ... 168
  Caprinidae ... 168
    Caprininae ... 169
    Plagioptychinae ... 179
  Radiolitidae ... 183
    Radiolitinae with ligament ... 184
    Radiolitinae without ligament ... 186
    Sauvagesiinae with ligament ... 196
    Sauvagesiinae without ligament ... 198
  Hippuritidae ... 203
    Hippuritinae ... 203
    Barrettiinae ... 207
Bands, pillars, and oscules ... 217
Stratigraphic distribution ... 220
References ... 221
Plates ... 223
Index ... 256

TEXT-FIGURES

Page
1. *Sphaerucaprina seafieldensis* (left valve, commissural aspect) 170
2. *Antillocaprina occidentalis* (left valve, commissural aspect) .. 173
3. *Antillocaprina lowenstami* (right valve, section) ... 174
4. *Agriopleura falconi* (right valve, section) ... 184
5. *Praeradiolites verseyi* (reconstruction of right valve) ... 185
6. *Orbignya ceibarum* (section showing hinge) ... 205
7. *Barrettia monilifera* (longitudinal section, after Woodward) .. 209
8. *Barrettia multilirata* (structure of left valve) ... 212
9. *Barrettia multilirata* (section below commissure) ... 213
10. *Barrettia multilirata* (section at a lower level) ... 213

RUDISTS OF JAMAICA

L. J. Chubb

ABSTRACT

All species of rudists known to occur in Jamaica are described and figured. Of the 71 species, 37 were already known; these are re-described on the basis of a re-examination of the original material and, in most cases, of new material. Of the remainder, five forms are new to Jamaica but are referred to species which occur elsewhere; another five which are imperfectly preserved are described as far as possible; they are unnamed, but three of them are compared with known species. The remaining 24 species, which include one new genus and eight other genera new to Jamaica, have been briefly described elsewhere and are here fully described and figured for the first time.

INTRODUCTION

Rudists, though not the commonest, are the most characteristic fossils of the Jamaican Cretaceous rocks. The group receives scant treatment in most text books with the result that many students, even professional palaeontologists, have little basic knowledge of it. In early days there were differences of opinion as to their systematic position, various species having been assigned to the Brachiopoda, Cephalopoda, Cirripedia, and Coelenterata but, since the beginning of this century, it has been generally recognised that they were highly aberrant bivalved mollusks, *i.e.* Pelecypoda or Lamellibranchiata.

Lucas Barrett (1860) first recorded the presence of "Rudistes" in the island. Since then Jamaican rudists have been described by Woodward (1862), Whitfield (1897a and b), Trechmann (1922, 1924b, 1927, 1929), and Chubb (1955a, 1956a and b, 1967). The descriptions are scattered through several periodicals and the collections also are scattered, Woodward's and Trechmann's types being in the British Museum (Natural History), Whitfield's in the American Museum of Natural History, and Chubb's formerly in the museums of the Geological Survey of Jamaica and the Department of Geology of the University of the West Indies, Kingston, have been transferred to the Smithsonian Institution, Washington, D.C. There is a collection in the Museum of the Institute of Jamaica, Kingston; one made by G. P. Wall in the British Museum (Nat. Hist.), London, which has also acquired the Trechmann Bequest, including some hundreds of Jamaican rudists; a collection made by C. A. Matley is in the United States National Museum, Washington, D.C., and one made by P. W. Jarvis is in the Naturhistorisches Museum, Basle, Switzerland. All these collections have been studied by the writer.

In recent years several previously unknown rudistiferous horizons have been discovered and a number of new species or species new to Jamaica have come to light. New work on the stratigraphy and palaeontology of the Cretaceous has made possible a more accurate zonal subdivision and correlation with the standard succession than could previously be attempted. The older publications on the Jamaican rudists have long been out of print and are today almost unobtainable, and many of their descriptions are inadequate or inaccurate. The time seems ripe, therefore, for a new monograph in which every known Jamaican species of rudist, both old and new, will be described and figured, and placed in its correct stratigraphic and taxonomic context.

ACKNOWLEDGMENTS

This work is based upon 14 years study of Jamaican Cretaceous palaeontology and stratigraphy carried out while the author was a member of the island's Geological Survey. Many of the specimens here described were collected by past and present members of the Department, whose help and cooperation is gratefully acknowledged. Much of the writing was done between September, 1963, and June, 1964, at the University of the West Indies, Mona, and it was continued in England chiefly in the British Museum (Natural History). My gratitude is due to these institutions for the facilities they afforded me and especially for allowing me access to their collections. The Trechmann Bequest was received by the British Museum (Nat. Hist.) while I was working there; it included several new species and many specimens of known species in a better state of preservation than any previously seen.

I am indebted to the American Museum of Natural History for certain photographs, for the loan of several type specimens, and for permission to reproduce a number of illustrations from Whitfield's articles in their Bulletin; to Dr. H. G. Kugler and the Naturhistorisches Museum, Basle, for the loan of their collections; and to Professor M. G. Rutten of Utrecht University for the loan of certain Cuban specimens. Some of the figures have previously appeared in Palaeontographica Americana, volume IV, numbers 26, 27. Thanks are due to the editors of the Geological Magazine for permission to reproduce one of Woodward's figures in the Geologist for 1862 and to the Société géologique de France for permission to reproduce a figure from Douvillé's *Revision des principales espéces d'hippurites*. The majority of the photographs are new, some having been made by Dr. Tom Goreau, others by Mr. Owen Jackson, both of the University of the West Indies, and many by Mr. A. Rowe of the British Museum (Natural History).

Finally I gratefully acknowledge my debt to the late Dr. L. R. Cox for help and advice while I was working at the British Museum, (Nat. Hist.) and to the late Dr. C. T. Trechmann who first introduced me to the study of Jamaican rudists and whose criticisms kept me on the alert and compelled me to confirm every observation and reconsider every conclusion during my work in Jamaica.

GEOGRAPHIC AND STRATIGRAPHIC CONSIDERATIONS

The rudists originated late in the Jurassic Period, but were especially characteristic of the Cretaceous, reaching their acme in numbers and variety in Upper Cretaceous times, and becoming extinct at the end of that period. Their distribution was determined partly by geographic and partly by climatic factors. Their zone of maximum concentration coincides closely with that of the Tethys; they were essentially benthonic animals, able to live only in fairly clear water in the shallower parts of the geosyncline and in the seas connected with it. They could develop a full and abundant life only in the tropical seas of their time.

The rudist belt of maximum concentration runs from southern Mexico through the Greater Antilles; it is continued northeastwards in Portugal and the Pyrenees, thence eastwards across south Europe and Turkey and southeastwards through Iraq and Persia, beyond which it passes into the Indian Ocean. According to Douvillé (1900b, p. 235) the middle line of the belt departs little from a circle which would cross the equator at an angle precisely equal to the inclination of the ecliptic. Northwards and southwards of the belt rudists become scarcer and eventually disappear, their northern limit extending beyond 50°N in south Saskatchewan, southern England and Sweden, Esthonia and Moscow, to little more than 30°N in Tibet and to 17°N in the west Pacific. Their southern limit extends to 30°S in Chile, though elsewhere in the continental areas it does not reach as far south as the present equator, embracing only northwestern South America as far east as Trinidad and the coastal belt of north and northeast Africa. Only in the area of the Indian Ocean are rudists found again in the Southern Hemisphere.

No Jurassic rocks are known in Jamaica. The greater part of the island consists of Tertiary and Quarternary formations but the Cretaceous appears in many inliers, the largest being the Blue Mountains with an area of about 240 square miles, and the smallest occupying only a few acres. The total area of Cretaceous rocks is some 500 square miles, less than one-eighth of the island's surface. They consist chiefly of waterlaid tuffs and conglomerates, tuffaceous shales and limestones. Rudists occur abundantly in the limestones, rarely in the shales, and occasionally reworked in the conglomerates. An account of the Jamaican Cretaceous was recently published (Chubb, 1962-1963), but this requires modification.

A revised version of the Cretaceous succession is given in Table 1. It has been pieced together from the sequence in several of the inliers, but it is often impossible to correlate exactly the rocks in one inlier with those in another, so there may be gaps or overlaps. Twelve limestones are included in the table and every one of them yields rudists. The dating of the various series has been done mainly on the basis of their microfossils, except for the Lower Cretaceous up to and including the Albian, in which only macrofossils have been found.

The rocks of the Benbow Inlier of northeastern St. Catherine are slightly metamorphosed, with the result that the rudists are welded into the limestones and can be studied only on weathered surfaces or in sections. It is now known that the Bonnett Limestone and Copper Limestone, previously regarded as distinct, are one and the same. The Phillipsburg Limestone, formerly thought to be equivalent to the Copper, is now believed to be a local lenticle at a slightly lower horizon. A fauna similar to that of the Seafield Limestone has been found in rocks of Lower and Middle Albian age in Texas, and the fauna of the lower limestones suggests a still earlier age. It is only in this

TABLE 1

Cretaceous Succession in Jamaica

Maestrichtian (*Titanosarcolites* Series)	Upper Tuffaceous Series	Maldon Inlier St. James
	Vaughansfield Limestone	
	Shaw Castle Shale	
	Chatsworth Limestone	
	Woodland Shale	
	Maldon Limestone	
	Summerhill Shale	
	Calton Hill Limestone	
	(concealed)	
	Praebarrettia Limestone	Sunderland Inlier St. James
Campanian (*Barrettia* Series)	Shepherds Hall Series	
	Upper *Barrettia* Limestone	
	Newman Hall Shale	
	Sunderland Shale	
	Johns Hall Conglomerate	
	New Ground Conglomerate	St. Anns Great River Inlier St. Ann
	Diozoptyxis Shale	
	Lower *Barrettia* Limestone	
Turonian-Coniacian (*Inoceramus* Series)	Conglomerate	
	Inoceramus Beds	
	Peters Hill Shale	Eastern part of the Central Inlier NE Clarendon
	Peters Hill Limestone	
	Conglomerate	
Albian	Tuff and Conglomerate	Benbow Inlier NE St. Catherine
	Seafield Limestone	
	Tuff and Conglomerate	
Lower Cretaceous	Benbow Limestone	
	Magnetic Tuff	
	Jubilee Limestone	
	Tuff and Shale	
	Bonnett-Copper Limestone	
	Metamorphosed Tuff	

inlier that rocks of Lower Cretaceous age have been recognised in Jamaica.

The Peters Hill group, outcropping in the part of the Central Inlier lying in northeastern Clarendon, includes a shale member characterized by a large species of *Inoceramus*. In this shale Bronnimann found a fauna with a *Globotruncana* of the *Gl. apenninica* group, possibly *Gl. alpina*, indicating an Upper Cenomanian to Lower Turonian age. Hippuritidae have recently been found by Coates (1964, p. 10) in the limestone at the base of the shale and, as it is regarded as axiomatic that this family started in the Turonian, it appears that the possibility of a Cenomanian age must be rejected, and a Lower Turonian age accepted.

In the *Inoceramus* beds of St. Ann, Bronnimann found a fauna including *Globotruncana coronata, Gl. helvetica*, and *Guembelina globulosa*, indicating a Turonian, or possibly a Turonian-Coniacian age. The presence of Coniacian beds is confirmed by the macrofossils, including *Inoceramus* cf. *deformis*, a Lower Coniacian form, and *Nowakites* aff. *paillettei* of the Upper Coniacian.

Slightly higher in the St. Ann succession in the New Ground area, there is a limestone yielding *Barrettia*, followed by a shale containing many gastropods, including *Diozoptyxis matleyi* and Foraminifera, among which Bolli recognised *Globotruncana stuarti, Gl. fornicata*, and *Gl. lapparenti lapparenti*, indicating a Campanian age. These three species are found also in the Johns Hall Conglomerate and the Sunderland and Newman Hall Shales of the Sunderland Inlier of St. James; here they occur through a thickness of about 4,500 feet of strata which are immediately succeeded by another *Barrettia* Limestone. The *Barrettia* Limestone of St. Ann is therefore assigned to the basal Campanian, and that of St. James, which is correlated with similar formations at Green Island and Rock Spring in western Hanover, to the Upper Campanian.

At the southern end of the Sunderland Inlier, following the almost unfossiliferous Shepherds Hall Series (probably equivalent to the Lower Tuffaceous Series of the Central Inlier), a new limestone fauna appears, including the first *Titanosarcolites*, associated with *Praebarrettia*. Southwards the Cretaceous disappears beneath the overstepping Eocene Yellow Limestone, to reappear in the inliers of Calton Hill and Maldon. The *Titanosarcolites* Series here includes four limestones, all yielding a similar rudist fauna, interbedded with shales. This series is correlated with similar formations in the part of the Central Inlier lying in northern and especially northwestern Clarendon, and its upper part with the rocks of the Marchmont Inlier on the borders of St. James and Westmoreland, and the Jerusalem Mountain Inlier of western Westmoreland. The limestones yield *Orbitoides apiculata* Schlumberger and the intervening shales *Kathina jamaicensis* (Cushman and Jarvis) Maestrichtian Foraminifera.

The Cretaceous rocks of the Blue Mountain area of eastern Jamaica are thought to represent a different faunal province from those of the rest of the island (Chubb, 1960b). They are less well known, but it can be assumed that the *Barrettia* Limestones of Back Rio Grande and the Plantain Garden River are Campanian, and that the Blue Mountain Shales of the Peak, the Providence Shales of the West Town River, and the *Titanosarcolites* Limestones of the Rio Grande Valley are Maestrichtian. There are also metamorphosed rocks in which fossils are rarely preserved.

It may be noted that there appears to be no positive evidence of the presence of Cenomanian or Santonian rocks in Jamaica.

THE RUDIST SHELL

Most pelecypods are free to move over the sea floor, but several groups have adopted a sessile habit, the best known being the oysters, which fix themselves by cementing their left valve to a rock or other hard surface. This manner of life involves considerable changes, the animal losing its symmetry, the attached valve becoming larger, thicker, deeper, and in some genera twisted or distorted, while the free valve remains small and flat.

The rudists also were sessile, usually cementing themselves by one of their valves. They were a more advanced group than the oysters with a more elaborate structure, having two adductor muscles, anterior and posterior, to the oyster's one, and a hinge consisting of interlocking teeth and sockets, which the oysters do not have. The remarkable series of evolutionary changes that the rudists underwent were necessitated by their successful attempt to adapt their complex structure to a mode of life which, in the more advanced families, seems more appropriate to corals than to pelecypods.

Most of the earlier and more primitive rudists were attached by their left valves and, since this condition is usual among cemented bivalves, it is regarded as "normal." But the majority of rudists, including all the more advanced forms, fixed themselves by their right valve, a condition described as "inverse." The arrangement of the hinge teeth varies according to which valve was fixed; nearly always the fixed valve, whether left or right, has one tooth between two sockets, and the free valve, whether right or left, has a socket between two teeth.

Almost all rudists had thick and heavy shells. The more primitive forms were twisted, the beaks always curving towards the anterior. In more advanced groups the fixed valve was often conical or cylindrical; the free valve at first remained coiled or curved, but generally tended to decrease in size and, in the most specialized forms, became a low cone or even a flat or concave lid.

SHELL STRUCTURE

Some authors have described the shells of rudists as having three layers (Trechmann, 1924b, p. 407; Mullerried, 1931, p. 243; Palmer, 1933, p. 96) or have referred to a "middle layer" implying the existence of three in all (Zittel-Eastman, 1913, pp. 479-480). Others have said that the wall of some species consisted of one layer only (Douvillé, 1904, p. 525). It is here suggested that the rudist shell, like that of other pelecypods, consisted always of two calcareous layers. Presumably in life there was a third or cortical layer, the periostracum, but this, being composed of horny conchiolin, is not preserved in fossils.

The cardinal apparatus, including teeth and sockets, and the attachment areas of the adductor muscles belong to the inner layer. The ligament, however, was originally an external element, and for it to become internal required an infolding of the outer layer. The siphons are a local modification of the periphery of the mantle; for them to open through one of the valves, always the left, necessitated infolding of the mantle edge and, since this is the part that secretes the outer layer, infolding of that layer also. This involved both mantle lobes and, therefore, both valves, producing oscules in the left valve and generally pillars in the right.

Except in the more advanced rudists the outer layer is thin and laminar, the laminae forming a kind of coating over the outer surface of the thick inner layer. In the most highly specialized families, however, the outer layer is thick and the laminae forming it diverge from the inner layer to form a series of inverted cones fitting one into another; from their resemblance to funnels these are commonly called funnel plates (Palmer, 1928, p. 76). In the family Radiolitidae these plates are traversed and intersected by vertical radial plates which, in the more advanced genera, by repeated bifurcation and reunion, make a polygonal pattern. The Hippuritidae have funnel plates but no vertical radial plates.

In the Caprinidae the outer layer is thin and the inner thick, the so-called "middle layer" is part of the inner. It is composed of numerous vertical radial plates between which are longitudinal, tubular, often capillary canals, which may be subdivided by horizontal tabulae. There is a superficial resemblance between this structure and that of the Radiolitidae, but it is not correct to say that, if a caprinid had the tabulae in its adjacent canals arranged at the same levels, they would constitute funnel plates and the form would be a Radiolite (MacGillavry, 1937, p. 57), for the caprinid structure belongs to the inner layer and the Radiolite structure to the outer. The inner layer lines the body cavity and, in most species with cylindrical or elongate conical shells, forms a series of concave tabulae below it.

There has been confusion between the outer and inner layers even within one family, the Hippuritidae. Palmer, having defined the term "funnel plates" and made it clear that they belong to the outer layer (1928, p. 13, figs. 1,2, p. 76), later applied the term to the tabulae that occupy the lower part of the body cavity and which are part of the inner layer (1933, pp. 97,99). This has led to misunderstanding (see below: remarks on *Orbignya maldonensis* and *Parastroma trechmanni).*

DEFINITIONS

Tabulae and *septa.* — Two kind of plates are often found within the rudist shell: (a) horizontal or transverse plates which are normal to the long axis of the valve and, in straight conical or cylindrical forms, are parallel to the commissure; such plates are of the nature of diaphragms which cut off the lower part of a cavity; and (b) vertical plates, parallel to the long axis and, in straight shells, perpendicular to the commissure; they are of the nature of walls. Writers have differed in the nomenclature of these plates. Some *(e.g.* Whitfield, 1897a) used the term *septa* for the horizontal plates; others *(e.g.* MacGillavry, 1937) reserved this term for vertical plates, and referred to the horizontal plates as *tabulae.*

The lack of uniformity has led to some confusion; for example, in a discussion of Whitfield's description of "septa" in *Antillocaprina occidentalis* (Chubb, 1955a, p. 7), it was remarked that none of his specimens showed them. Earlier Trechmann (1924b, p. 407) stated that this species had no septum in the living chamber. Caldwell and Evans (1963, p. 616) put these two observations together, equating Whitfield's *septa* with Trechmann's *septum.* The two statements have no relevance to each other. Trechmann's *septum* would be a vertical wall standing within the body cavity; Whitfield's *septa* would be horizontal diaphragms below the body cavity. *Antillocaprina* has no vertical wall but does have horizontal diaphragms, even though Whitfield's specimens show none.

MacGillavry's terminology will be adopted here: *septum* will be used for a vertical plate, *tabula* for a horizontal one. This is the nomenclature used for corals.

Valves — The two valves of the rudist shell have been distinguished by different authors as left and right, lower and upper, fixed and free, or α and β. Many were recumbent and for them the terms *lower* and *upper* are inappropriate.

Some were unattached in which case both valves were *free* and neither can be correctly described as *fixed*. The Greek letters represent the hinge, the single loop of α symbolizing the single socket of a free valve, and the two loops of β the two sockets of a fixed valve. Such expressions as "lower, attached, right (β) valve" and "upper, free, left (α) valve" (Palmer, 1928, pp. 118,120) are tautological. Here in the systematic descriptions the valves will usually be referred to as *left* and *right*.

Orientation of valves. — The dorsal side of a valve can generally be recognised because the ligament and hinge are located there, and if the shell is curved the concave side will usually be dorsal. Normally the opposite side is regarded as ventral and, if it is known whether the valve is right or left, it is easy to deduce which side is anterior and which is posterior.

Because the rudists were sedentary it is not clear what use they could have for an extensible foot; some forms, however, seem to have had one and its presence is shown by a sinus which crosses the commissure. This is always on the anterior side. In many forms the two siphons, exhalent and inhalent, leave evidence of their existence in the form of sinuses across the commissure, below which there may be bands on the outside of the shell, comparable to the slit bands of certain gastropods, or actual infolds of the shell substance which may penetrate the body cavity as pillars.

Many authorities refer to "anterior and posterior siphons." The use of these terms is to be deprecated as in all pelecypods both siphons are on the posterior side of the shell. According to where they happen to be situated on the commissure either may be nearer to the anterior than the other. In *Sauvagesia* the inhalent siphon is usually diametrically opposite to the ligament; it is anterior to the exhalent siphon. In *Vaccinites* or *Pironaea* the exhalent siphon is near the ligament and is anterior to the inhalent. Here the siphons will always be distinguished by the terms *exhalent* and *inhalent* or by the symbols S and E (see below).

Accessory cavities. — This term is here used for cavities between the myophores and the shell wall, not for a cavity cut off from the body cavity by a vertical septum; the latter, when present, is interpreted as a muscle cavity.

Hinge line. — A line connecting the centres of the two sockets in the fixed valve or of the two teeth in the free valve.

Height. — The elevation of the apex of a valve above or below the plane of the commissure; not, as in ordinary pelecypods, the dorso-ventral diameter.

Size. — In the systematic descriptions a general indication of the size of each species will be given according to the following code:

Very small	mean	adult	diameter	below 25 mm
Small	"	"	"	25- 50 mm
Medium	"	"	"	50-100 mm
Large	"	"	"	100-200 mm
Gigantic	"	"	"	200 mm or more

A more exact statement of the dimensions will be given in a separate paragraph following the descriptive section.

Symbols. — In the systematic descriptions and the plates some of the traditional symbols will be used for certain features of the rudist shell:

L	Ligamental grooves, infolds, crests, ridges or pillars
S (sortie)	Bands, furrows, pillars or oscules attributed to the exhalent siphon
E (entree)	Bands, furrows, pillars or oscules attributed to the inhalent siphon
I	Interband between the siphonal bands
N	Single tooth of the fixed valve
B′ and B	Anterior and posterior teeth of the free valve
b′ and b	Anterior and posterior sockets of the fixed valve
n	Single socket of the free valve
D (droite)	Body cavity of the right valve
G (gauche)	Body cavity of the left valve
ma	Anterior myophore or muscle attachment area
mp	Posterior myophore or muscle attachment area
maO	Anterior accessory cavity
mpO	Posterior accessory cavity
V	A downfold or outfold believed to be pedal
PD	A posterior-dorsal fold
RV	Right valve
LV	Left valve

CLASSIFICATION

The classification of the rudists has been the subject of considerable diversity of opinion. Woodward (1851) included the normal genera and a few of the more primitive inverse genera with *Chama* in the family Chamidae, and all others in the family Hippuritidae. Later workers raised these families to superfamilies, Chamacea and Rudistacea, the former divided into several families, including the Chamidae and the Megalodontidae as well as the Diceratidae, Monopleuridae, Caprotinidae, and Caprinidae, and the latter embracing only the two most advanced families, the Radiolitidae and Hippuritidae. The term Pachydonta was coined by Neumayr to include both groups.

Most modern rudistologists exclude the Chamidae and the Megalodontidae from the group but include all the other families. This system will be adopted here, the Rudistae being regarded as a suborder of the Pelecypoda, divided into six families: Diceratidae, Monopleuridae, Caprotinidae, Caprinidae, Radiolitidae, and Hippuritidae.

Diceratidae. — This family includes all normal rudists, *i.e.* those attached by the left valve, and a few which, although attached by the right valve, have normal dentition with one tooth in the left valve and two in the right. As no representatives of this family have yet been recognized in Jamaica it will not be further considered.

All other families are inverse, *i.e.* attached by the right valve.

Monopleuridae. — The simplest inverse forms; all have inverse dentition with one tooth in the right valve and two in the left. The muscles were attached either directly to the inner surface of the shell wall or to horizontal platforms in the same plane as the hinge plate.

Caprotinidae. — Resemble the Monopleuridae, but the muscles were attached to myophores which rise from within the shell and are separated from the wall by accessory cavities.

Caprinidae. — The principal character is the development in one or both valves of a system of longitudinal canals in the thick inner layer of the shell wall. The outer layer is thin.

Radiolitidae. — Differentiated from the former families by the great development of the outer layer of the right valve which consists of funnel plates crossed by vertical radial plates. The inner layer is thin. Hinge and muscle equipment specialised to permit vertical rise of the left valve.

Hippuritidae. — The outer layer is composed of funnel plates without vertical radial plates. The distinguishing character is the presence of two, three or more infolds of the outer layer which, in the right valve, project into the body cavity to form pillars while, in the left, the two principal infolds form apertures or oscules corresponding in position with the two principal pillars. Hinge rather similar to that of the Radiolitidae.

SYSTEMATIC DESCRIPTIONS

Family **MONOPLEURIDAE** Munier-Chalmas, 1873

Shell inequivalve, fixed by right valve which is conical or curved and bears a single tooth between two sockets; left valve operculiform or capuloid and slightly curved, having two equal teeth separated by a socket; ligament external, in a groove which runs more or less normal to the commissure; outer layer thin, inner layer thick, shell substance with no canals or accessory cavities. Muscles attached either directly to wall or to horizontal myophores.

Genus **MONOPLEURA** Matheron, 1842

Shell normally conical or only slightly curved; medial tooth in right valve well developed, rising from the inner edge of the shell wall; both muscles attached directly to the internal surface of the valves.

Monopleura jamaicensis Chubb

Plate 27, figure 1-3

Monopleura jamaicensis Chubb, 1956a, p. 7, pl. 1, figs. 1-3; 1956c, p. 7.

Occurrence. — A rare fossil in the *Titanosarcolites* Limestone of Ducketts Land Settlement, Westmoreland, and Vaughansfield and Catadupa, St. James.

Description. — Right valve small, broadly conical, antero-dorsal side flattened this being the area of attachment, and only the tip of the umbo being twisted; a narrow ligamental groove runs from umbo to commissure on the dorsal side behind the attachment area; trilobed, owing to two furrows on the ventral side running from umbo to commissure. Surface ornamented with fine radiating striae. The hinge structure is unknown.

Left valve operculiform, with prominent umbo near the centre of the straight dorsal margin; from it three furrows radiate to the margin of the valve, the anterior and median furrows corresponding with the two furrows of the right valve. Ornamented with fine radial striae.

Dimensions of holotype. — Antero-posterior diameter 55 mm; dorso-ventral diameter 36 mm; height of right valve 31 mm; height of left valve 8 mm.

Monopleura diaboli Chubb

Plate 27, figures 4,5

Monopleura sp. Chubb, 1962/1963, p. 16.
Monopleura diaboli Chubb, 1967, p. 24.

Occurrence. — Abundant in the Bonnett-Copper Limestone in the Benbow Inlier of northeast St. Catherine, believed to be the oldest fossiliferous horizon in Jamaica. Being welded into the hard limestone, the fossil can be studied only in sections and on weathered surfaces.

Description. — Right valve small, elongate conical, tapering to a point, straight or curved, with a smooth surface; sections show that the shell is thick on the dorsal and thin on the ventral side, and has no accessory cavities or canals; in transverse sections the tooth is always weathered away, though a few show two sockets in the thickness of the dorsal wall, the posterior socket oblique and near to the ligamental furrow, the anterior socket smaller.

Left valve capuloid with its beak strongly curved towards the anterior. One rock surface shows several left valves face down; their upper surface has been eroded away so that they show both the body cavity and the socket, which is oblique.

Dimensions. — Maximum diameter at the commissure 30 mm, though most are smaller; maximum height of right valve 70 mm; that of left valve uncertain, but probably some 20 mm.

Remarks. — This is the small rudist mentioned by Matley and Raw (1942, p. 246) in the road section south of Guy's Hill. It resembles several species described by Mullerried (1933b, pp. 315-330) from the Barremian and Aptian of the region of Tehuacan, Puebla, Mexico. He referred these to the subgenus *Himeraelites* Di Stefano, but it may be doubted if this attribution is correct. *Himeraelites* has a character which was mentioned by Di Stefano (1888, p. 1-16), by Douvillé (1900a, pp. 215-216) and by Parona (1909, pp. 171-182), and is shown in their figures; this is a septum in the left valve that extends from the anterior tooth to the ventral margin, cutting off the posterior part of the body cavity to accommodate the posterior muscle; this cavity is in open communication with the dental socket. This character, which is seen also in many Caprotinidae and Caprinidae, is not shown in any of the ten species ascribed by Mullerried to this subgenus, nor in the species, *diaboli,* in the Bonnett-Copper Limestone, which is, therefore, ascribed to *Monopleura s.s.* The specific name refers to its abundance where the Bonnett-Copper Limestone crosses the road known as the Devil's Race Course, running between Water Works and Benbow at Mile Post 22.

Monopleura sp.

Plate 27, figure 6

Monopleura sp. Chubb, 1962/1963, p. 19.

Occurrence. — A block of limestone incorporated in a metamorphosed crushbreccia from Whitfield Hall, at an altitude of about 4000 feet on the southwestern slopes of the Blue Mountain Range, among other indeterminable fossils, shows three sections of a simple rudist. The rock is marmorized and contains white flecks of silicate material, chlorite and sericite, which grade into streaks, having been mechanically distributed in the marble during shearing. They are absent from many of the fragments in the breccia.

Description. — The species is a small one. Of the three sections one is transverse and oval, the second is oblique, and the third is a longitudinal conical section. Probably all are right valves, but the conical section contains a large fragment which may be the left valve crushed into it. The lack of accessory cavities, mural canals, funnel plates or infolds shows that it can belong to no family except the Monopleuridae, and the absence of coiling puts it in the genus *Monopleura.* None of the sections show teeth or myophores.

Dimensions. — The conical section is 37 mm long on one side which may be dorsal, and 50 mm on the other; its maximum diameter is 27 mm. The oval section is 31 mm by 24 mm. The thickness of the wall is 5-6 mm.

Remarks. — This is the first reported occurrence of fossils in the metamorphosed series of Jamaica. Its chief interest is that it proves that this series is not pre-Mesozoic or pre-Palaeozoic as believed by De la Beche (1827) and Matley (in Matley and Higham 1929) but is Cretaceous or later as suggested by Trechmann (1936), Zans (1951), and Chubb (1962-1963).

Genus **GYROPLEURA** Douvillé, 1887

Shell coiled, with a large area of attachment; hinge displaced towards the anterior; in the left valve both muscle impressions are superficial and indicated by thickenings of the test; in the right valve the anterior muscle impression is similar, but the posterior is borne on a horizontal plate resembling a cardinal plate, which extends backwards from the posterior socket and covers the umbonal cavity; the tooth rises from the antero-dorsal margin of this plate.

Gyropleura shaviensis Chubb

Plate 27, figures 7-9

Gyropleura shaviensis Chubb, 1956a, pp. 7-8, pl. 1, figs. 4-6; 1956c, p. 7.

Occurrence. — Many horizons in the *Titanosarcolites* Series in the parish of St. James and neighbouring parts of Westmoreland; especially abundant in the Shaw Castle Shale; this species is found to be commoner and to have a longer range than was formerly thought.

Description. — A small species; complete shell the size and shape of a segment of an orange; hinged on the straight edge. Surface of the right valve divided by a sharp curved carina, extending from the umbo to the ventral corner, into two areas, a flat anterior area and a curved posterior area; shell attached by the umbonal part or the whole of the flat surface; no external ornament except inconspicuous growth lines; hinge consists of a prominent tooth between two sockets, the posterior socket just below the incurved umbo, the hinge line being parallel to the straight anterior margin; tooth grooved on its anterior side, the groove descending into the corresponding socket; anterior muscle attachment a platform-like thickening of the shell wall, running parallel to the straight edge; posterior myophore a horizontal shelf which abuts anteriorly against the tooth and posterior socket, and extends diagonally across the valve to the curved wall.

Left valve a thin, flat, semicircular plate, with faint growth lines, its internal characters not exposed.

Dimensions. — Maximum dorso-ventral diameter 53 mm; antero-posterior diameter 35 mm; height of right valve on posterior side 25 mm; but most specimens are smaller.

Family **CAPROTINIDAE** Gray, 1848

Resemble conical or cylindrical Monopleuridae, but typically the muscles are attached to myophores which rise almost vertically from the interior of the shell; the chief characteristics of the family is the separation of the myophores from the shell wall by open spaces, shallow or deep, called accessory cavities. Some forms have accessory cavities in only one valve, and some have only posterior cavities. In the left valve of some genera a septum connects the anterior tooth with the ventral wall. The ligamental groove is infolded, the ligament being submerged in the thickness of the wall.

Genus **PACHYTRAGA** Paquier, 1900

Right valve cylindro-conical, more or less straight or curved, but never coiled; surface smooth, ligamental infold shown by a longitudinal groove which runs on the dorsal side from the umbo to the posterior socket; single tooth robust, upright, high, crescentic; anterior socket large, in the hollow of the crescent, posterior socket small; anterior muscle impression borne on a thickening of the shell wall; posterior myophore separated from the wall by an elongated accessory cavity. Left valve capuloid, curved or slightly coiled; anterior tooth robust and long, posterior tooth small; anterior myophore parallel to the shell margin, from which it may be separated by a shallow accessory cavity; a septum runs from the anterior tooth to the ventro-posterior margin, forming a cavity into which the posterior myophore slopes; the latter may, at its outer edge, be separated from the wall by a small accessory cavity.

Pachytraga jubilensis Chubb

Plate 27, figures 10,11

Pachytraga sp. Chubb, 1962/1963, p. 16.
Pachytraga jubilensis Chubb, 1967, p. 24.

Occurrence. — Locally abundant in the Jubilee Limestone of the Benbow Inlier. It can only be studied in sections on weathered surfaces of the hard limestone.

Description. — A small shell. Wall of the right valve thick, especially on the dorsal side, its surface smooth with a longitudinal ligamental furrow; valve cylindrical, straight or curved, tapering somewhat towards the base. It has only one accessory cavity, the posterior, which may be seen in most sections; this, and the body cavity, extend down to the base of the shell. Transverse sections in the hinge area show a massive crescentric tooth enclosing a large oval or kidney-shaped anterior socket, with a small posterior socket, near which the ligamental groove ends; this socket is separated from the accessory cavity by a septum.

Left valve small, capuloid, coiled; ligamental groove curves round to the posterior tooth, which is small; anterior tooth large, prominent and robust; the outer edge of the anterior myophore projects 5-6 mm beyond the commissure, and fits within the margin of the right valve; no positive evidence has been found of accessory cavities or of a transverse septum in the left valve.

Dimensions. — Maximum diameter of right valve 30 mm, maximum height 100 mm; probable maximum height of left valve 20 mm.

Remarks. — This species compares most closely with *P. lapparenti* Paquier (1903, pp 65-68), from the upper Urgonian (Aptian) of the south of France, which in many cases has no anterior accessory cavity in the right valve, though the posterior cavity is always present. The left valve too generally lacks an anterior cavity, while the posterior myophore, which projects 4 to 6 mm beyond the commissure, is separated from the edge of the valve only by a shallow furrow, a rudimentary accessory cavity. It would appear that *P. jubilensis* is more primitive than *P. lapparenti.*

It may be noted that the infilling of the shells is a black limestone crowded with small siliceous sponge spicules; the matrix, also a black limestone, is devoid of spicules.

Family **CAPRINIDAE** d'Orbigny, 1850

In this family the right valve is generally conical or cylindrical but may be curved, while the left valve may be small and capuloid, or large, rarely larger than the right, and curved or coiled. The shell is often said to have three layers, a thin outer layer, a thick middle layer characterised by the development within it of thin-walled longitudinal canals, and a thin inner layer. The view here adopted is that this family, like all other pelecypods, has only two calcareous layers. The outer layer is thin and smooth, marked by growth lines, which may be inconspicuous; it is often completely removed by weathering or erosion. The so-called "middle layer", with its canals, is a specialized part of the inner layer; this is proved by the fact that in some genera the tubular structure invades the myophores and hinge teeth, elements which, in all pelecypods, are formed of the material of the inner layer. At the innermost margin of this layer the walls of the canals coalesce to form a continuous smooth surface, which lines the body cavity and, in cylindrical and elongate conical forms, forms a series of saucer-shaped tabulae, which cut off and subdivide the lower unoccupied part of this cavity.

The longitudinal canals were apparently derived from caprotinid type accessory cavities, which have become subdivided by vertical radial plates. Primitive genera, such as *Amphitricoelus* Harris and Hodson (1922) of Trinidad, may have only a single row of rectangular canals, running part way around the shell, separating the myophores and teeth from the wall; in more specialized forms the vertical plates may bifurcate several times leading to a multiplication of canals, and in the most advanced genera the plates bifurcate and reunite repeatedly with the result that the whole circuit of the shell consists almost entirely of fine capillary tubes. In many genera the development of canals is more advanced in the left valve than in the right. In the left valve of some genera a vertical septum runs from the anterior tooth to the ventral wall, cutting off from the body cavity a space which accommodates the posterior muscle; in many species this muscle cavity is continuous with the neighbouring dental socket. Similarly, in the right valve, the posterior muscle may occupy a cavity opening into the posterior socket, but divided from the body cavity by a thin septum. The ligament is internal, being infolded into the thickness of the wall; generally, the infold is shown externally by a longitudinal furrow.

The Caprinidae are divided into two subfamilies, the Caprininae and the Plagioptychinae.

Subfamily **CAPRININAE** Douvillé, 1910

Generally both valves are conical. Right valve elongated conical or cylindro-conical, straight or curved or, in some forms, coiled. Left valve curved or coiled; in primitive genera it is shorter than the right, but in many advanced forms it is nearly or quite as long and in some it is longer. Canals are always present in the walls of both valves. While many forms have a posterior muscle cavity cut off by a septum from the body cavity, some of the later and more advanced genera have raised myophores in the form of platforms which are nearly at the same level as the commissure; these need no septum.

Genus **CAPRINULOIDEA** Palmer, 1928

Right valve long, cylindro-conical, curved or straight, left valve horn-shaped, curved or loosely coiled; surface smooth. The walls of both valves have vertical radial plates with intervening canals; the plates bifurcate two or three times, and branches from contiguous plates anchylose, producing rounded or polygonal canals; the inner canals may be tabulate or not; the outer canals, which are usually pyriform in cross section, are never tabulate. Single tooth in right valve robust, prominent, quadrilateral in cross section, with flanged corners from which septa radiate to the wall, separating the dental sockets and the posterior muscle cavity from the body cavity. Left valve has two strong and prominent teeth, the anterior slightly the larger and triangular in cross section; from it a septum runs to the ventroposterior wall cutting off the posterior muscular cavity, which is shallower than the body cavity.

Caprinuloidea perfecta Palmer

Plate 27, figures 12-14

Caprinuloidea perfecta Palmer, 1928, pp. 59-60; text fig. 6; pl. 8, fig. 8; pl. 9, figs. 1-2.
Caprinuloidea perfecta Thiadens, 1936b, pp. 1134-1138; text figs. 3,4.
Caprinuloidea cf. *C. perfecta* Chubb, 1962/1963, p. 16.

Occurrence. — Abundant in the Seafield Limestone, the highest limestone in the Benbow Inlier; it is welded into the rock, and can be studied only in sections on weathered surfaces.

Description. — The shell is small to medium-sized. A section of a right valve (Pl. 27, fig. 14) closely resembles Palmer's figures of *C. perfecta.* In outline it is subquadrilateral, with its anterior side flattened and a ventral angle. It shows the anterior socket, the base of the tooth between the two sockets, and the posterior socket connected by a constricted channel with the posterior muscle cavity; the latter is separated by a thin vertical septum from the body cavity which is rounded in outline. The ligament is infolded; it is shown by an external groove and a small internal cavity, with no visible connection between the two. The walls, though much weathered, show a system of canals separated by radial plates which divide and anchylose at least twice.

A section near the commissure of the left valve (Pl. 27, fig. 13) hardly differs from Palmer's figures of *C. perfecta* (1928, text fig. 6; pl. 9, fig. 1), except that the teeth have been removed by erosion. The outline is quadrilateral, the anterior wall is thin and flattened, and meets the dorsal and ventral walls in rounded angles. The vertical septum, running from the anterior tooth to the ventral wall, and cutting off the posterior muscle cavity from the body cavity, is clearly seen. The canal system in the walls is visible, except on the anterior side, and resembles that shown in Palmer's figures, but other sections (Pl. 27, fig. 12) show this better.

Dimensions. — The right valve illustrated has a dorso-ventral diameter of 56 mm, and an antero-posterior diameter of 46 mm; the corresponding measurements for the left valve shown are 54 mm by 44 mm. These figures are comparable with, though slightly less than those of Palmer's holotype of *C. perfecta;* they are substantially greater than those of his *C. perfecta gracilis.*

Remarks. — Palmer (1928), the author of the generic name *Caprinuloidea* and of the species name *C. perfecta,* collected his material from Soyatlan de Adentro, Jalisco, Mexico. He ascribed the formation in which he found them to the Cenomanian because of the resemblance of their fauna to that of the *Schiosia* Beds of Sicily, which Douvillé believed to be of that age. Thiadens (1936b) found the same species in southern Santa Clara, Cuba, in association with *Tepeyacia* and *Sabinia.* He was inclined to refer his fauna to the Cenomanian with the possibility of a Turonian age. Recently *Caprinuloidea* and *Tepeyacia* have been found in Texas in beds of Lower and Middle Albian age, and not in any higher horizon. It seems probable, therefore, that the Seafield Limestone, the provenance of *Caprinuloidea,* should be ascribed to the Albian.

Genus **SPHAERUCAPRINA** Gemmallaro, 1865

Right valve resembles that of *Caprina.* Left valve has around its posterior, ventral and anterior sides a marginal row of oval canals, within which there are several rows of polygonal canals, the innermost row the largest; several large accessory cavities lie on the dorsal and dorso-anterior sides of the body cavity; the posterior muscle cavity opens into the socket, but is separated from the body cavity by a thin septum; there is a well-marked ligamental groove.

Sphaerucaprina seafieldensis Chubb

Plate 30, figure 5; Text-figure 1

Sphaerucaprina seafieldensis Chubb, 1967, p. 25.

Occurrence. — A single incomplete left valve, considerably recrystallized, was found in a locality described by the collector as N 20°E of Seafield Manse, St. Catherine. It was learnt, however, that the direction was an estimate as a strong local magnetic anomaly rendered a compass bearing impossible. It may be assumed that the site was in a general north-northeasterly direction from the Manse and within sight of it. The shell was associated with *Sabinia totiseptata* and *Tepeyacia multicostata* described below, and near to the horizon of *Caprinuloidea perfecta.* Two transverse sections of the valve have been cut nearly parallel to the commissure.

Description. — A small to medium-sized shell. The greater part of the outer surface is concealed by tuffaceous matrix, but where exposed it is covered with inconspicuous costae about 1-1.5 mm wide. A well-marked open V-shaped ligamental groove is seen in the sections. The valve is involute with its umbo curved over so that it lies at the dorso-anterior corner of the commissural surface. Body cavity circular and exceptionally small, its diameter at the commissure being only about one quarter of the antero-posterior diameter of the valve; it curves over in a semicircle in conformity with the umbo, its diameter tapering from 16 mm to 10 mm in a distance of 75 mm; only in its deepest part, near the umbo, are there two or three thin, well-spaced, subconical tabulae. The wall is extremely thick on the dorsal, anterior, and posterior sides; the ventral wall is broken away.

The outer shell layer is thin; the thick inner layer is pierced by many longitudinal canals, a single row around the posterior margin being oval in cross section with their radially directed long axes about 1.5 mm and their short axes 0.5 mm; this band extends some distance round the dorsal side but has not been recognized on the anterior side which is much recrystallized, and the ventral side is missing. Within this band on the posterior side there is a zone of irregularly rounded or polygonal canals with an average diameter of 1 mm and within this a narrow, curved, shallow accessory cavity, about 1.5 mm wide and 15 mm long, subdivided in its deeper parts by septa; another band of larger irregular canals separates this cavity from the posterior muscle cavity. Tubular canals exist in other parts of the shell but, except where they are filled with rock matrix, they are difficult to detect owing to crystallization. There are several large and small accessory cavities in the dorsal and anterior regions.

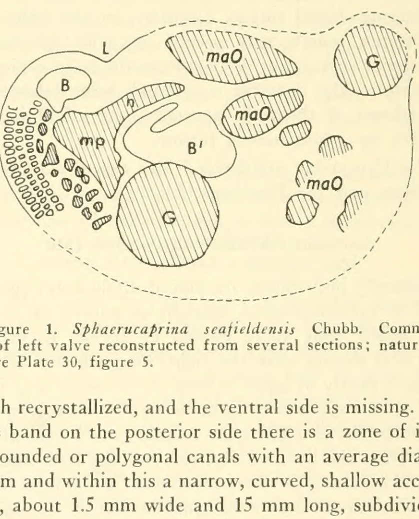

Text-figure 1. *Sphaerucaprina seafieldensis* Chubb. Commissural aspect of left valve reconstructed from several sections; natural size. Compare Plate 30, figure 5.

The anterior tooth is large and triangular and stands near the center of the valve on the dorsal side of the body cavity, it is anteriorly grooved. The posterior tooth is much smaller and is apparently conical; it lies close to the dorsal margin. The intervening socket is long and oblique, narrowing towards the dorso-anteror and widening in the opposite direction to open into the posterior muscle cavity, which is separated from the body cavity by a thin septum.

The right valve is unknown.

Dimensions. — Height of left valve 40 mm; diameter, antero-posterior 65 mm, dorso-ventral (estimated) 45-50 mm.

Remarks. — *Sphaerucaprina* differs from *Coalcomana* in its small body cavity, thick walls and the nonbifurcation of the plates separating its marginal canals. It differs from *Schiosia* in having several rows of canals within the marginal row. *Coalcomana* was found by Thiadens (1936b), associated with *Sabinia, Caprinuloidea,* and *Tepeyacia* in southern Santa Clara, Cuba, and *Schiosia* by Palmer (1928) in the Maltrata Limestone at Orizaba, Vera Cruz, Mexico. Neither *Coalcomana* nor *Schiosia* has yet been recognized in Jamaica.

Genus **SABINIA** Parona, 1908

Externally resembles *Plagioptychus* but differs from it in that both valves are canaliculate. A cross section shows many small, irregularly polygonal canals, fairly uniformly distributed throughout the whole thickness of the inner layer of the shell, including the part external to the cardinal apparatus. There are no accessory cavities external to the myophoric laminae.

Sabinia totiseptata Palmer

Plate 30, figure 6

Sabinia totiseptata Palmer, pp. 73-74, pl. 14, fig. 5.

Occurrence. — A single fragment of a right valve was found in the locality NNE of Seafield Manse, St. Catherine, which yielded *Sphaerucaprina* and *Tepeyacia.* As found the valve was split longitudinally, and the resulting flat face has been polished and two transverse sections cut.

Description. — A small shell; right valve curved cylindrical, the concave side being dorsal; the surface was probably originally smooth but the greater part is either covered with tuffaceous matrix or weathered away. The body cavity is round to subquadrangular in cross section, its diameter is about half that of the shell and it is without tabulae, being filled with matrix throughout the length of the fragment. Outer layer thin and mostly weathered away. Inner layer thick, its structure is destroyed in places by crystallization, but elsewhere it consists entirely of round to subpolygonal canals or tubules, with a mean diameter of 1-2 mm; the intervening septa are thick, attaining a maximum of 0.5 mm; even the marginal tubules are rounded, not oval, and all are tabulate, the tabulae being slightly concave and irregularly spaced, the intervals between them varying from less than 1 mm to 2.5 mm. A trace of the hinge structure may be seen at the upper end in the form of two deep rock-filled hollows, the anterior some 4 mm wide and the posterior about 9 mm; there can be little doubt that these are sockets; the wall between them representing the tooth is 6 mm thick.

The left valve is unknown.

Dimensions. — The original length of the fragment was about 90 mm; diameter near the commissure 50 mm tapering to 40 mm at the lower end; diameter of body cavity 25 mm tapering to about 18 mm.

Remarks. — This specimen, imperfect as it is, appears to resemble three Mexican species of *Sabinia* named by Palmer and to be indistinguishable from *S. totiseptata* Palmer, in which the marginal canals are rounded and tabulate.

Genus **ANTILLOCAPRINA** Trechmann, 1924

Trechmann proposed the generic name, *Antillocaprina,* for the species Whitfield named *Caprinella occidentalis;* he gave no description of the genus but only of the specimens that he had collected, which he believed to belong to the same species. He had never seen Whitfield's material and his description differs from it in one important character — the arrangement of the teeth and sockets. It would appear, therefore, that Trechmann's specimens represent a different species, here called *A. suboccidentalis,* which must be regarded as the type species. *C. occidentalis* belongs to the same genus but is less typical.

The genus *Antillocaprina* may be defined as follows; inequivalve, right valve conical, cylindro-conical or pyramidal, straight, undulating or curved, usually but not always larger than left; left valve curved or coiled; surface of both valves sometimes smooth but often longitudinally fluted, the broad shallow grooves being separated by rounded costae, which may be inconspicuous or prominent. Outer layer thin and smooth except for faint growth lines which run across grooves and costae at right angles. Inner layer of both valves thick, forming the main mass of the shell; it is composed of a tightly packed plexus of small tubules, which are polygonal or, in the marginal row, radially oval in section; the tubes invade the myophores and hinge teeth; the polygonal tubes are generally tabulate, the marginal oval tubes nontabulate; typically the myophores are large, subequal, and nearly flush with the hinge plate and the commissure in both valves.

In most species the hinge tooth of the right valve is quadrilateral, and from its inner corners two septa extend anteriorly and posteriorly, dividing the sockets from the body cavity; in the left valve the anterior tooth is conical or pyramidal, the posterior tooth crescentic or sigmoidal, presenting its convex side to the body chamber and the socket. There is no external ligamental groove but there may be a small ligamental pillar, which presumably originated as an infold but which has lost its connection with the outer layer; it is crescentic in section and occupies the hollow of the crescentic posterior tooth in the left valve (Text-figure 2) and the corresponding position relative to the crescentic posterior socket in the right. As MacGillavry observed (1937, p. 63) the ligamental pillar is often dissolved, leaving a cavity which retains its characteristic shape, and in many cases no trace of the ligament can be seen. A comparison of the valves shows that the ligamental pillar, crescentic in both, would face in opposite directions if the two valves were brought together; this seems to be the rule in all species. The innermost part of the inner layer is thin, lining the body cavity and forming a series of saucer-shaped tabulae below it.

There has been some controversy as to the systematic position of *Antillocaprina.* When first defining it Trechmann (1924b, p. 407) remarked that "the structure of the living chamber is quite unlike that of *Caprina, Plagioptychus* or *Coralliochama,* and recalls that of *Monopleura* . . . there is no septum in the living chamber, nor any accessory cavities behind the posterior tooth." To compare its body cavity to that of *Monopleura* is not to include it in the Monopleuridae, indeed the resemblance is not obvious, and it would appear from his choice of name, *Antillocaprina,* that Trechmann regarded it as belonging to the Caprinidae; he listed it between *Plagioptychus* and *Coralliochama,* both members of this family; and he described a specimen that he presented to the Institute of Jamaica as a "Caprinid Rudist."

MacGillavry (1937, pp. 26-129) grouped the Antillocaprinae with the Ichthyosarcolitinae, Trechmannellinae, Rousselinae, *Lithocalamus, Immanitas,* and the Hippuritinae, not as directly related to each other, but as following the same line of evolution which he called the Trechmannellid type. He stated (p. 67) that "the *Antillocaprina* hinge can be derived directly . . . from that of *Monopleura michaillensis* Pictet-Campeche." This would appear to involve a rotation of the hinge through an angle of 90° for, according to Douvillé's figures (1918, pl. 3, figs. 1-11), the teeth of that species are subparallel to each other and to the dorsal margin of the shell, like those of *Chama,* and are unlike those of *Antillocaprina.*

Other authorities including Kutassy (1934) and Dechaseaux (1952) recognised the Antillocaprinae and most of the other forms in MacGillavry's trechmannellid group (except the Hippuritinae) as belonging to the Caprinidae. *Antillocaprina* has many typical caprinid characters, the external shape of the valves, the structure of their inner and outer layers, and the invasion of the teeth and myophores by polygonal tubules, which can be matched in some unquestioned Caprinidae, such as *Coralliochama.*

A comparison of Trechmann's types of *A. suboccidentalis* with a plaster cast of Palmer's holotype of *Caprinuloidea perfecta* shows only such differences as could arise naturally in the course of evolution. The hinge structure is almost identical and the ligamental pillar or cavity also is similar, its cross-section being described, in *Caprinuloidea,* as "boot-shaped" by Palmer (1928, p. 56) and in *Antillocaprina* as "comma-shaped" by MacGillavry (1937, p. 63), and as "crescentic" by the writer; all three expressions imply similar shapes. In *Caprinuloidea,* as in *Antillocaprina,* the pillar has lost is connection with the outer layer, but the former genus retains the external ligamental groove which the latter has lost.

Several authors have stressed the absence from the left valve of *Antillocaprina* of a septum which they claim to be an essential character of the Caprinidae. The function of this septum is to divide the cavity occupied by the posterior muscle from the body cavity. But in *Antillocaprina* the muscle attachment areas have risen until they are nearly flush with the commissure, so the septum ceases to be of the nature of a fence between two fields and comes to resemble a retaining wall supporting a raised terrace.

There seems to be no adequate reason for excluding *Antillocaprina* from the Caprinidae.

Antillocaprina suboccidentalis Chubb

Plate 28, figures 3,4

Antillocaprina occidentalis Trechmann, 1924b, p. 407, pl. 25, figs. 1-3.
Antillocaprina suboccidentalis Chubb, 1967, p. 25.

Occurrence. — A common fossil in the *Titanosarcolites* Limestones of Logie Green, Upper Clarendon, and in the Great River Valley on the borders of St. James and Westmoreland.

Description. — This species closely resembles *A. occidentalis;* it tends to be somewhat smaller though still of medium size. The right valve is conical, more or less straight, curved or twisted, with the commissure inclined at an angle of 110° to its dorsal side; the left valve tends to be low and arched rather than coiled.

Not only the walls but also the large anterior and posterior myophores and the hinge plate in both valves are composed of fine, longitudinal, polygonal tubes, which are generally about 0.5 mm in diameter, and are divided transversely, at distances about equal to their own diameter, by horizontal tabulae, except for the marginal row which are oval and nontabulate. The two myophores and the hinge plate together form a horseshoe-shaped structure which encircles all except the ventral side of the body cavity in both valves. The only important difference between the two species is in the structure of the hinge. In the left valve of *A. suboccidentalis* the two teeth are well separated and between them lies a rectangular socket. The posterior tooth is not especially large or massive, it is a ridge elongated transversely, *i.e.* parallel to the dorsal margin, and is sigmoidal, its anterior end curving up against the socket and its posterior curving down around the dorsal side of the body cavity; the anterior tooth appears to be conical, generally oval in cross section, the long axis of the oval being normal to the shell margin. No ligamental pillar or cavity has yet been recognized in this valve.

In the right valve a rectangular tooth stands between two sockets, the anterior oval and the posterior sigmoidal; these sockets are separated from the body cavity by septa which spring from the ventral angles of the tooth. A crescentic ligamental cavity lies within the concavity of the posterior socket and both present their concave sides towards the dorso-posterior.

Dimensions. — Height of type right valve 85 mm; length of type left valve measured around curve 167 mm, height of left valve above commissure 43 mm; height of largest known right valve about 150 mm; commissure more or less circular, its diameter 55-60 mm; body cavity 30 mm by 20 mm.

Antillocaprina occidentalis (Whitfield)

Plate 28, figures 1,2; Plate 30, figure 8; Text-figure 2

Caprinella occidentalis Whitfield, 1897a, pp. 193-194, pls. 16,17.
Antillocaprina occidentalis Chubb, 1955a, p. 7; 1956c, p. 8.
not *Antillocaprina occidentalis* Trechmann, 1924b, p. 407, pl. 25, figs. 1-3.

Occurrence. — A common fossil in the *Titanosarcolites* limestones wherever they occur in Jamaica.

Description. — According to Whitfield "shell of moderate size and very inequivalve, the lower valve long, straight, slightly enrolled, twisted or loosely spiral like a corkscrew, smooth, ribbed or slightly channelled on the exterior surface, and gradually expanding from the apex outward. Upper valve coiled and generally more or less involute, often closely so and nearly symmetrical, the exterior surface being nearly smooth or with spiral ridges extending from the apex to the border of the valve; the ridges, from five to ten in number, are elevated and distinct, rounded or sub-obsolete." The body cavity is small and obliquely oval; its deeper parts in both valves are divided off by oblique curved tabulae, those in the left valve being more oblique and more delicate than those in the right.

The structure of the hinge is the distinguishing character of this species. It is clearly seen in one of Whitfield's type left valves, though his figure (1897a, pl. 16, fig. 4) fails to show it; a new photograph of this specimen is given in Plate 28, figure 2, and an interpretative drawing in Text-figure 2. The posterior tooth is large and crescentic and is in contact with the smaller anterior tooth. The socket is thus occluded and is displaced from its normal position between the teeth towards the dorsal margin; it is shallow and relatively small. A crescentic ligamental pillar stands within the crescent of the posterior tooth; it presents its concave side towards the anterior, whereas the tooth itself is concave towards the dorso-posterior.

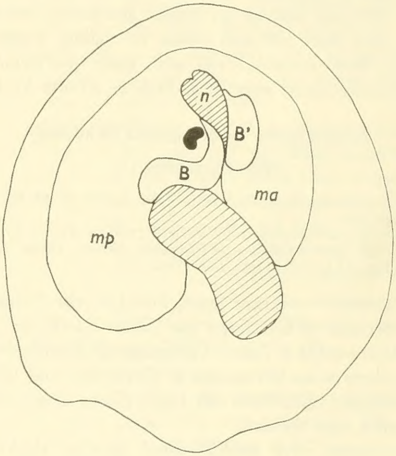

Text-figure 2. *Antillocaprina occidentalis* (Whitfield). Commissural aspect of left valve; natural size. Ligament black. Compare Plate 28, figure 2.

Another left valve in the Brit. Mus. (Nat. Hist.) No. L63259, retains both its teeth (Pl. 30, figure 8). The posterior one is extremely large and massive; its crescent is composed of compact shell substance with its concavity filled in with tubular material; no ligamental pillar is seen. It is in contact with the anterior tooth, which is small and conical and is mainly tubular, though the side facing the suture seems to have a layer of compact material; this tooth has a vertical groove on its dorsal side. The socket is small and oval; its depth is only about 6 mm measured vertically, but it burrows in horizontally below the hinge plate towards the posterior for a distance of 11 mm.

No right valve showing its hinge structure has been seen, but it would probably have a single large socket for the reception of the two teeth of the left valve, perhaps with a septum in its bottom, which would rise dorsally to support a small conical tooth.

Dimensions. — Height of adult right valve about 200 mm, length of left valve measured around the outer curve may be 350 mm, though its height above the commissure may be less than 100 mm owing to coiling; commissural diameter, dorso-ventral 75-80 mm, antero-posterior 60-70 mm; the body cavity may be as little as 30 mm by 10 mm.

Antillocaprina quadrangularis (Whitfield)

Plate 29, figures 1-6

Caprinella quadrangularis Whitfield, 1897a, p. 193, pl. 12, fig. 4; pl. 14, figs. 4,5.
Antillocaprina quadrangularis (Whitfield), Chubb, 1955a, pp. 6-7.
Antillocaprina quadrangularis (Whitfield), Chubb, 1965a, pp. 12-13, pl. 1, figs. 15,16; pl. 2, figs. 1,2; 1956c, p. 8.

Occurrence. — A rare fossil, found in the *Titanosarcolites* Limestone of Catadupa and Shaw Castle, St. James. Whitfield recorded it from "Christianna," Manchester Parish, but there is no Cretaceous at Christiana and his specimens probably came from the Logie Green area, some five or six miles east thereof.

Description. — A medium-sized species. Right valve roughly quadrangular in cross section, owing to the development of four longitudinal flanges; the height is little more than the maximum diameter, so the shape is that of an inverted pyramid; the flanges are respectively dorsal, ventral, anterior, and posterior, and the shell is slightly curved or twisted with its dorsal side concave and ventral convex; the commissure is tilted at a steep angle; the flat faces between the flanges may be smooth or have minor costae of varying widths; the tubes composing the thick inner layer are 1-2 mm in diameter. A section shows the hinge to be essentially of *Antillocaprina* type (Plate 29, figure 6).

The left valve also is quadrangular in outline, capuloid or highly arched with overhanging umbo in the dorsal corner, from which a strong, rounded ridge or flange curves up and over to the ventral corner; this is flanked by two broad and open furrows, which divide it from two lateral wings or ridges extending outwards to the anterior and posterior corners respectively. The thin outer layer is smooth except for growth lines; decorticated specimens show the capillary tubes which radiate from the umbo. The hinge structure consists of a deep rectangular socket beneath the umbo, flanked by two teeth, the posterior transversely elongate and sigmoidal, the anterior conical; the myophores appear to be arranged like those of *A. occidentalis,* but there is a projecting knob on the anterior myophore; the body cavity is transversely oval.

Dimensions. — Whitfield's larger specimen of a right valve is 144 mm high, by 108 mm in maximum diameter; the largest left valve has a dorso-ventral diameter of 93 mm and an antero-posterior diameter of 85 mm; the most highly arched left valve has a height of over 80 mm.

Antillocaprina lowenstami Chubb

Plate 28, figures 5-9; Text-figure 3

*Antillocaprina lowenstammi** Chubb, 1967, p. 25.

Occurrence. — In a marly nodular limestone about 80 feet above the *Barrettia* Limestone of Stapleton, St. James. Two specimens were found, one a weathered right valve and the other bivalved. Named for Dr. Heinz Lowenstam, who found the first specimen. The right valve was sectioned

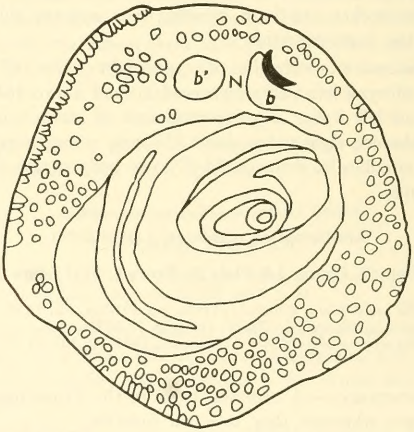

Text-figure 3. *Antillocaprina lowenstammi* Chubb. Transverse section of right valve near commissure; × 2. Ligament black. Compare Plate 28, figure 8.

---

*Spelling emended. Obvious error. Named for H. Lowenstam.

and polished; the bivalve was split apart at the commissure and both surfaces developed.

Description. — A small species, the right valve conical, slightly curved, left valve conical, strongly curved with overhanging umbo, shaped like a Phrygian cap. There is no ligamental groove. Both valves have two shell layers, the outer thin and smooth except for inconspicuous growth lines, it is largely weathered away; the inner layer thick, composed of many longitudinal canals, the outermost row radially elongate and parallel-sided, rather than oval, in cross section; other canals polygonal or rounded; marginal canals 0.5 mm wide by 0.75 to 2.5 mm radially; polygonal canals generally 1 mm in diameter with some larger especially on the posterior side of the right valve, where a few may attain a diameter of 2.5 or even 3 mm. Inner part of this layer forms thin saucer-shaped tabulae at least in the right valve and probably in both.

In the right valve the cellular structure invades only the margins of the hinge area; the polished section (Pl. 28, fig. 8; Text-fig. 3) shows that the hinge is essentially of antillocaprinid type; a rock-filled, crescent-shaped cavity represents the ligamental pillar on the concave side of the equally crescentic posterior socket; in the bivalved specimen the whole hinge area is recrystallized and shows no structure except the ligamental cavity, which is not crescentic but oblique, presumably in an intermediate stage between a crescent concave posteriorly and one concave anteriorly. Anterior muscle attached to the internal surface of the valve; posterior muscle to a surface which slopes down towards the body cavity.

The left valve has a row of large canals on the dorsal side of the hinge plate; elsewhere the canals are as in the right valve, but none are more than 1.5 mm in diameter. Hinge area recrystallized, showing oblique ligamental cavity. Anterior muscle attached to the internal surface of the valve; posterior to a myophore which slopes up to a sharp ridge, with the form of a cuesta, fitting the down sloping muscle area of the right valve.

Dimensions. — Overall length of bivalved specimen 75 mm; height of right valve, dorsal side 44 mm, ventral side 65 mm; left valve, dorsal side 15 mm, ventral side measured around curve 75 mm; diameter at commissure, dorso-ventral 39 mm, antero-posterior 44 mm.

Remarks. — *A. lowenstammi* is a rather primitive member of the genus. The ligament and hinge are typical but the muscle attachments have not developed the characteristic form, though the posterior myophore of the left valve has already risen, so as to render the septum unnecessary.

Antillocaprina stellata Chubb

Plate 30, figures 1-3

Antillocaprina aff. genus B. MacGillavry, 1937, pp. 83-85; pl. 2, figs. 8,9; pl. 8, fig. 11.
Antillocaprina stellata Chubb, 1967, p. 25.

Occurrence. — Fragments are common in the Shaw Castle Shale of the *Titanosarcolites* series of St. James.

Description. — The fragments belong to a species of medium size with a conical right valve, which is often irregularly twisted, and which has a number of prominent longitudinal flanges projecting from the wall. It appears to be similar to, perhaps identical with that described by MacGillavry from Piñar del Rio Province, Cuba, which he regarded as related to *Antillocaprina,* though probably belonging to a different genus. The Jamaican material is more fragmentary than the Cuban, but is better preserved in one respect, that some of the fragments show the thin, smooth outer layer. According to MacGillavry the Cuban forms resemble *Antillocaprina* in the absence of such a layer; the Jamaican forms resemble it by its presence, for there is no doubt that all species of this genus, like other Caprinidae, had a thin outer layer.

In the Cuban material some of the flanges extend out as far as 60 mm. In the Jamaican specimens none of those still attached to the shell project more than a quarter of this distance, but isolated broken flanges attain widths up to 33 mm, with a thickness of about 5 mm. One fragment shows exceptionally regular horizontal growth lines averaging about 18 to a centimeter. The canals forming the shell wall and flanges may be seen, but it has not been possible to ascertain if any show a cross section similar to that illustrated by MacGillavry (1937, pl. 2, fig. 9).

The left valve is unknown.

Dimensions. — Owing to the fragmentary nature of the material the exact dimensions are unknown. The largest fragment is 73 mm high by 39 mm wide.

Antillocaprina williamsi Chubb

Plate 30, figure 7

Antillocaprina sp. Trechmann, 1927, pp. 59-60, pl. 2, fig. 10; pl. 4, fig. 6; 1929, p. 488, pl. 18, fig. 6.
Antillocaprina williamsi Chubb, 1967, p. 25.

Occurrence. — Found in shales about 30 feet below a rudist limestone along the Cambridge-Catadupa railway line; also in a shale at an elevation of about 7,000 feet near the summit of Blue Mountain Peak. Named after Mr. John Williams of the Jamaica Geological Survey.

Description. — A small species. All specimens are somewhat crushed in a dorso-ventral direction. Shell free or lightly attached, nearly equivalve but has the right valve slightly larger than the left. Both valves short, they may be equally curved with the umbones anteriorly directed, or the right valve may be the straighter. Outer layer very thin and sometimes weathered away; when preserved it is smooth with growth lines which are inconspicuous except near the commissure. Inner layer composed of fine longitudinal tubules, which are about 0.8 mm in diameter and appear to be nontabulate. Internal structures, hinge apparatus, myophores unknown.

Dimensions. — The best preserved bivalved specimen, with both valves arched, has an overall length of 66 mm, each valve being 33 mm high. Measured around the outer curve the right valve has a length of about 80 mm, the left valve about 68 mm. Diameter at commissure: antero-posterior 48 mm, dorso-ventral 23 mm, but the former figure has been increased and the latter reduced by crushing.

Antillocaprina depressa Chubb

Plate 30, figure 4

Antillocaprina (?) sp. Trechmann, 1929, p. 487, pl. 18, figs. 4,5.
Antillocaprina sp. Chubb, 1961a, pp. 3-4.
Antillocaprina depressa Chubb, 1967, p. 26.

Occurrence. — Internal and external moulds of a single right valve were found by Trechmann in the Cretaceous shale near the top of Blue Mountain Peak.

Description. — The right valve is very small, depressed conical, its height being considerably less than its diameter, transversely oval at the commissure. Outer surface smooth with a few strong foliated growth lines and faint radial striae probably caused by an extremely thin outer layer being moulded onto an inner layer composed of capillaries. Umbo nearly central, slightly twisted. Body cavity apparently nontabulate, deep and acutely conical in the centre, but flaring towards the commissure; deeper part smooth, flaring part marked by strong radial striae, no doubt representing the capillaries. The hinge plate is transverse to the capillaries, being covered with mammillae which are moulds of their ends. The hinge is of *Antillocaprina* type, the two sockets being represented by projections and the tooth by a hollow; the posterior socket is transversely elongated, its anterior end curving up against the tooth, the anterior socket is round triangular, and the tooth more or less square with flanges at each free corner, which extend as septa to divide the sockets from the body cavity. The sides of the sockets are vertically striated. No ligament is seen. The anterior myophore is a ridge encircling that side of the body cavity; the posterior muscle was attached to the wall.

The left valve is unknown.

Dimensions. — Diameter: antero-posterior 25 mm, dorso-ventral 20 mm; height 10 mm.

Remarks. — A depressed conical right valve is not uncommon among medium-sized or large rudists but extremely rare among small ones. Although none of the original shell remains, the mould gives a very good idea of the structure.

Genus **TITANOSARCOLITES** Trechmann, 1924

Generic name proposed by Trechmann for the species described by Whitfield (1897a, pp. 194-196) under the name of *Caprinula gigantea.* It is subequivalve, both valves being nearly cylindrical but tapering distally. It was recumbent on its anterior side, and both valves are curved in one plane, the concave side of the curve being dorsal. Both valves have numerous longitudinal rounded costae, separated by narrow grooves, on their dorsal and anterior sides; the ventral and posterior sides show broad, roundly concave flutings, separated by angular ridges or flanges.

The shell has two layers. The outer, rarely preserved, is thin and smooth, with inconspicuous transverse growth lines, which cross all longitudinal ridges and furrows at right angles. The inner layer is thick, constituting the main mass of the shell; it consists chiefly of fine capillary tubes which are rather closely tabulated; these tubes are mostly polygonal or rounded in section, forming a network, but those in the outermost row on the fluted sides are oval, with their long axes perpendicular to the surface; these are nontabulate; on the costate sides the polygonal mosaic continues to the edge.

The chief structural character of *Titanosarcolites* is the presence, in both valves, among the polygonal capillaries, of many rounded or oval tubular canals, whose diameter may be more than ten times that of the capillaries. They are nontabulate and are confined to the costate sides. As Trechmann has shown, the tubes are formed by a repeated growing out of the costae, and their spreading "in a roof-like manner" over the intervening furrows, which thus become occluded; each of the tubes is lined with a discrete portion of the outer layer. The tubes were described by MacGillavry (1937, p. 89) as "enclosures of the world outside into the animal's shell."

The commissural surfaces show the ends of the capillaries and tubes. The body cavity, which generally lies ventrally of the centre, is small, its diameter varying between a third and a sixth of the long diameter of the shell; the thin smooth part of the inner layer lines it and forms close-set, deeply concave tabulae below it. The hinge lies between the body cavity and the dorsal zone of tubes; the teeth, which are rounded or oval, are composed of fine polygonal capillaries; the lower unoccupied parts of the sockets are filled with deep funnel-shaped tabulae, fitting into each other in a cone-in-cone structure. The myophoric areas are often shown by a different pattern in the capillary network. There is no ligamental groove and no ligamental pillar or cavity has been seen in any Jamaican specimen.

There have been differences of opinion as to the orientation of the valves of *Titanosarcolites.* The question was discussed in an earlier publication (Chubb, 1955a, pp. 8-9) and the conclusion was reached that the tubular canals were more or less confined to the dorsal and posterior sides. This view was largely based on a valve described and figured by Trechmann (1924b, p. 400, pl. 23, fig. 2) and now in the British Museum (Natural History). Trechmann stated that it had two teeth which were fused together in the body cavity but divided as they emerged; this interpretation was accepted in 1955 and it was concluded that this was a free or left valve because it had two teeth.

A re-examination of the specimen (Pl. 32, fig. 3) has led to a revision of this view and it is now thought to be a right valve with a single bifid tooth set between two sockets. If it were a left valve with two close-set teeth it would be comparable to *Antillocaprina occidentalis,* illustrated in Plate 28, figure 2 and Plate 30, figure 8, in which the teeth are near together and have occluded the socket, which has moved in a dorsal direction, no such occluded socket is present in the *Titanosarcolites* under discussion. Several specimens of the latter genus have been sectioned and show their hinge apparatus (Pl. 32, figs. 1-2; Pl. 33, fig. 2); in every right valve the two sockets and in every left valve the two teeth are set well apart, usually at a distance of 15-20 mm, not crowded together. In the specimen under discussion the bifid tooth stands between two cavities which appear to be sockets as they occupy the same relative positions as the sockets in the sectioned right valves.

The specimen is, therefore, now believed to be a right valve and the orientation proposed in 1955 is erroneous. The costate side is anterior, and this side and the dorsal have tubular canals; the fluted side with the oval nontabulate capillaries is posterior. This interpretation agrees with that of MacGillavry (1937). The other criteria proposed for the orientation of the valves are valid: the hinge teeth are on the dorsal side of the body cavity, one (which may be bifid) in the right valve, two (well spaced) in the left; both valves taper distally and curve dorsally; and the tabulae below the body cavity of each valve present their concave faces to the other valve.

There has been controversy as to the systematic position of *Titanosarcolites.* Whitfield believed it to be a *Caprinula,* a member of the family Caprinidae. Douvillé (1898, pp. 123-124) compared it with *Ichthyosarcolites* and thought that in both genera the tests were composed chiefly of *lames externes, i.e.* the plates which are today called funnel plates by many English-speaking rudistologists; the capillaries and canals would be in the outer layer and both genera would belong to the Radiolitidae.

Trechmann (1924b, p. 397) transferred *Caprinula gigantea* to the new genus, *Titanosarcolites;* he believed the tubes to be in the outer layer and expressed conviction that it was one of the Radiolitidae. Though he did not refer to him there is little doubt that his views were influenced by those of Douvillé. Two years later, however, the latter author (1926, p. 132) recognised that the canals of *Titanosarcolites* were in the inner layer.

MacGillavry (1937, p. 91) thought that the cardinal apparatus of *Titanosarcolites* resembled that of *Trechmannella* and *Hippurites.* He was the first to recognise the close relationship of the genus with *Antillocaprina,* from which he believed it to be derived. As explained above he thought that *Antillocaprina* in its turn had developed from a monopleurid ancestor.

Thus *Titanosarcolites* has been believed to have affinities with the Caprinidae, the Monopleuridae, the Radiolitidae, and even with the Hippuritidae. Kutassy (1934) and Dechaseaux (1952) included it among the Caprinidae and this view is here accepted. Its affinities with *Antillocaprina* can hardly be doubted and there seems to be no valid reason for excluding either genus from the family.

Titanosarcolites giganteus (Whitfield)

Plate 31, figures 1,3; Plate 32, figures 1,2; Plate 33, figures 1,2

Caprinula gigantea Whitfield, 1897a, pp. 194-196, pls. 18-22.
Titanosarcolites giganteus (Whitfield), Trechmann, 1924b, *pars,* pp. 397-400, text fig. 1; pl. 23, fig. 1.
Titanosarcolites giganteus (Whitfield), Chubb 1955a, pp. 7-9; 1955b, pp. 178-185; 1956c, p. 8.
Not *Titanosarcolites giganteus* (Whitfield), MacGillavry, 1937, pp. 85-92, pl. 3, figs. 1-5.

Occurrence. — One of the commonest fossils in the *Titanosarcolites* series wherever it occurs in Jamaica. This is the most widespread of all rudist horizons and is found in the Jerusalem Mountain Inlier, Westmoreland; the Marchmont Inlier on the borders of Westmoreland and St. James; the Maldon Inlier and the south side of the Sunderland Inlier, St. James; the Central Inlier of Upper Clarendon; and in the Rio Grande Valley of Portland, on the east side of the Blue Mountain Inlier.

Description. — As for the genus: the type species *T. giganteus* is characterized by its gigantic size. Both valves are subcylindrical, and oval in cross section, the long diameter being dorso-ventral. The right valve tends to be longer and broader than the left and may have lateral outgrowths to assist fixation; according to Trechmann its umbo is acutely pointed and bent upwards from the surface of attachment; probably many were unattached and relied on their weight to keep them in position. The left valve may be curved or coiled in a plane spiral. The costae on the dorsal and anterior sides have an average width of 10 mm; the flutings on the other sides are few in number, in adults are generally some 40 to 60 mm wide, and are separated by acute ridges not by projecting flanges.

The capillaries are generally less than 1 mm in diameter, and the tubes, which are rounded, oval or kidney-shaped in cross section, have a maximum diameter rarely exceeding 15 mm; there is a tendency for the larger tubes to be on the dorsal side. All costae, ridges, furrows, flutings and tubular canals are continuous across the commissure from one valve to the other. Young individuals may be difficult to distinguish from *Antillocaprina occidentalis* unless the tubes have been brought to light by weathering or fracture.

Dimensions. — The length of a bivalved specimen, measured around the curve, may be anything up to 2 metres; the maximum diameter at the commissure may exceed 300 mm. The majority are much smaller and it is uncertain whether some of these are the young *T. giganteus* or whether they belong to another species.

Remarks. — It may be doubted if the Cuban specimens attributed to *T. giganteus* (MacGillavry, 1937) actually belong to this species; they should probably be included in the species described below. The Texan species, *T. oddsensis* Stephenson (1938), differs from *T. giganteus* in the diameter of its capillaries and tubes, the former being up to 2.5 mm and the latter attaining a maximum of nearly 40 mm. The tubes are more crowded than in the Jamaican form and their zoning is different, the larger being near the myophores and body cavity and the smaller being marginal.

Titanosarcolites alatus Chubb

Plate 31, figure 2; Plate 32, figure 3

Titanosarcolites giganteus Trechmann, 1924b, *pars,* p. 400, pl. 23, fig. 2.
Titanosarcolites giganteus MacGillavry, 1937, pp. 85-92, pl. 2, figs. 1-5; pl. 9, fig. 1.
Titanosarcolites alatus Chubb, 1967, p. 26.

Occurrence. — Apparently a rather rare fossil in Jamaica, occurring in the *Titanosarcolites* Limestone of the Great River Valley on the borders of S̊t. James and Westmoreland, and neighbouring areas, but possibly many specimens that have been thought to be the young of *T. giganteus* may belong to this species.

Description. — This is a medium to large-sized species, its maximum dimensions being less than half those of *T. giganteus.* The chief characteristic of *T. alatus* is the development of projecting flanges on the posterior and ventral sides; they are considerably more numerous than the ridges on *T. giganteus.* These flanges are flat, parallel-sided, and rounded at the ends; in the specimen illustrated (Pl. 31, fig. 2) there are about seven flanges which project from 25 to 46 mm from the bottoms of the intervening flutings, and they are from 3 to 9 mm thick. A single row of oval capillaries follows the whole periphery of the flanges and flutings with the long axes of the ovals always at right angles to the surface; some of the costae towards the ventral part of the anterior side are lined with suboval capillaries, which are considerably less compressed than those in the flanges. The marginal capillaries on the posterior side are about 1.2 mm by 0.3-0.4 mm; the internal capillaries are generally 0.5-0.7 mm in diameter. The smallest of the tubular canals, which are on the anterior side, have a diameter of 3 mm, the largest, which are dorsal may be as much as 10 mm by 7.5 mm; the specimen illustrated in Plate 31, figure 2 clearly shows the formation of the tubes by the overgrowing of the costae. The interior of this shell is recrystallized so no trace of the hinge structure can be seen, but the right valve shown in Plate 32, figure 3 is the one with the bifid tooth, which is clearly seen between its two sockets.

Dimensions. — The dorso-ventral diameter is about 120 mm, the antero-posterior diameter 83 mm. The length of each valve measured around the curve is likely to be of the order of 250 or 300 mm.

Remarks. — The Cuban specimens described by MacGillavry probably belong to this species. They all appear to be smaller than a typical *T. giganteus* and all have flat, parallel-sided flanges on the posterior and ventral sides, projecting as much as 45 mm. MacGillavry regarded two of the grooves between the flanges as siphonal. Some of the Cuban specimens showed a hinge structure and ligament similar to that of *Antillocaprina.*

Genus **ANTILLOSARCOLITES** Chubb, 1967

Shell of medium size, nearly equivalve, but the right valve possibly rather larger, both strongly curved in a dorsal direction and in the same plane; shell probably recumbent on the anterior side. Both valves are characterized by a few acutely angular longitudinal carinae, separated by broad rounded flutings on the dorsal, anterior, and ventral sides, possibly also on the posterior side, but this is not known.

Outer layer thin, smooth. Inner layer extremely thick on the dorsal side, elsewhere of moderate thickness; it is mainly composed of numerous longitudinal capillary canals, usually oval in section, and 0.4 to 0.5 mm in diameter, with intervening walls relatively thick. The noncanaliculate innermost part of the inner layer is exceptionally thick, especially on the anterior side.

The body cavity is oval or subquadrilateral in section. The hinge lies in the thick dorsal side of the inner layer. In the right valve the anterior socket is almost central; the posterior socket is connected with the neighbouring myophoric cavity, which is cut off from the body cavity by a septum. The anterior muscle was attached to the thickened lining of the body cavity. The hinge of the left valve is less well known being visible only in section. There appears to be no ligamental furrow, pillar or cavity. The lower part of the body cavity is subdivided by transverse tabulae.

Antillosarcolites macgillavryi Chubb

Plate 30, figures 9-12

Antillocaprina aff. genus A. MacGillavry, 1937, pp. 83-84, pl. 1, fig. 10.
Ichthyosarcolites sp. Chubb, 1956c, p. 7.
Antillosarcolites macgillavryi Chubb, 1967, p. 26.

Occurrence. — Two specimens were found in the *Barrettia* beds of Haughton Hall, Green Island, Hanover. They are right and left valves and almost certainly belonged to one individual though they cannot be fitted together as the apertural part of both valves is broken away. Both valves were sectioned and, as far as possible, developed.

Description. — Shell of small to medium size. The two valves are equally curved in the same plane, the left valve shorter than the right; concave side of curve dorsal. Strongly carinate, the carinae being acutely angular and separated by broad, rounded flutings; they match on the two valves, and are respectively dorsal, anterior, ventral, and ventro-posterior; the posterior side is considerably eroded, and its original characters cannot be determined.

Outer layer thin, with faint growth lines, it is largely weathered away. Inner layer thicker, on the dorsal side very thick, its capillary canals rounded or oval in cross section, with an average diameter of 0.5 mm; they are not apparently tabulated. The innermost part of the inner layer, lining the body cavity, is unusually thick, attaining 3 to 4 mm on the anterior side in both valves. The body cavity is oval in the right valve, obliquely subquadrangular in the left; it is crossed by a series of oblique tabulae, which spring from the thickened anterior part of the lining and slope down at an angle of about 120° to the thinner posterior side; these tabulae have the exceptional thickness of 3 to 5 mm, and are from 6 to 9 mm apart.

It has been possible to develop the base of the tooth and the two sockets of the right valve; the anterior socket is oval and nearly central; the stump of the tooth, which is about 3 mm wide, divides it from the posterior socket; both sockets are about 6 mm dorso-ventrally by 4.5 mm antero-posteriorly, and are separated from the body cavity by a wall 2 mm thick. The posterior socket is partially separated from the neighbouring myophoric cavity by thin vertical buttresses, which bound the posterior side of the socket but fail to meet; the posterior myophoric cavity is divided from the body cavity by a septum 2 mm thick. The anterior muscle appears to have been attached to the thick inner lining of the body cavity; the attachment area is bounded on its inner margin by a slight, nearly horizontal ridge. Cardinal area of left valve seen only in sections.

Dimensions. — Length of right valve 90 mm, probably originally at least 110 mm; length of left valve 65 mm, probably originally 90 mm; approximate diameter at commissure from dorsal to ventral carina 55 mm, from furrow to furrow 42 mm; antero-posterior diameter over 30 mm; body cavity, dorso-ventral diameter 20 mm, antero-posterior about 15 mm.

Remarks. — This form seems to be similar to, probably identical with that collected by Thiadens in southern Santa Clara (Las Villas), Cuba, and described by MacGillavry under the name of *Antillocaprina* aff. genus A. He regarded it as occupying a position between *Antillocaprina* and *Titanosarcolites.* The fluted walls and the hinge do indeed resemble those of the latter genus, but in the absence of tubes it must be regarded as an independent genus. MacGillavry's figure shows a dorso-anterior carina which is absent from the Jamaican specimen, and a larger dorsal carina; the Cuban form probably had an anterior carina which is broken off; his section shows the characteristic thickening of the lining of the body cavity, but the sockets appear to be smaller than those of the Jamaican form perhaps because the section is cut lower. MacGillavry described the canals as irregularly tabulated, with the distance between the tabulae generally greater than the canal's diameter. Syntypes of the Cuban material lent by Prof. M. G. Rutten of Utrecht University have some of the canals distantly or not tabulated; others, especially in the flanges, show irregular tabulation.

Subfamily **PLAGIOPTYCHINAE** Douvillé, 1910

The right valve is not greatly elongated; it may be conical but is often cylindrical or low and exogyrate when its height is less than its diameter. Left valve low, it may be arched with its umbo overhanging the dorsal margin of the right, but in many species it is opercular, gently convex or nearly flat, without projecting umbo. In some genera canals are present only in the left valve. This valve has a septum which supports the anterior tooth and cuts off the posterior muscle cavity; the anterior muscle was borne on an undercut shelf on the dorsal side of the body cavity.

Genus **PLAGIOPTYCHUS** Matheron, 1843

Right valve variable in form according to the shape of the attachment area, conical or cylindrical, straight or more or less coiled, generally short; it has no canals or accessory cavities and often resembles the right valve of a *Gyropleura;* single tooth prominent, it is near the posterior and from it run ridges delimiting the two sockets and muscle areas; the posterior muscle is raised on a platform. The plane of the commissure is inclined, the dorsal side of the right valve being shorter than the ventral.

The left valve is usually transversely oval, arched but not coiled or twisted, with an umbo on the dorsal side which may be displaced towards the posterior. Its thin outer layer is generally brown in colour and is ornamented only with inconspicuous growth lines; the thick inner layer is penetrated by radial nontabulate canals, separated by plates which bifurcate once or more but do not reunite, with the result that there are more canals near the outer surface than near the inner; these canals are visible in the broad brim which encircles the anterior, ventral, and posterior margins of the valve. The hinge, which is solid and not invaded by the canals, is displaced towards the posterior; it consists of two prominent teeth with intervening socket; from the anterior tooth a vertical septum runs to the ventral margin separating the posterior muscle cavity from the body cavity; this posterior cavity is divided from the socket, if at all, only by a low ridge, which may be oblique; the anterior muscle is set on a deeply undercut myophoric lamina, a horizontal shelf running across the dorsal side of the body cavity. Several species of *Plagioptychus* are known in Jamaica.

Plagioptychus jamaicensis (Whitfield)

Plate 34, figure 1.

Caprina jamaicensis Whitfield, 1897a, p. 192; pl. 15; not pl. 13, figs. 1-2.
Plagioptychus jamaicensis (Whitfield), Chubb, 1955a, p. 6; 1956c, p. 7.
Not *Plagioptychus jamaicensis* Trechmann, 1924b, pp. 407-408; pl. 25, fig. 4.

Occurrence. — A rare fossil in the *Titanosarcolites* Limestone. Whitfield's specimen was found at Logie Green, Clarendon Parish; the Jamaica Geological Survey found it between Greenwich and Lambs River, near the northeastern corner of Westmoreland Parish.

Description. — A large, almost a gigantic species. According to Whitfield: shell large and ponderous, having a diameter across the lower valve of eight inches. Lower valve very oblique, broadly spreading and very much curved, shortest on the hinge side; its substance quite thick and strongly marked by irregular concentric ridges or growth lines. Upper valve thin, smooth or with microscopic lines on the exterior; beak large, incurved and overhanging the cardinal side of the lower valve. Within, the shell of this valve is marked by fine, threadlike grooves radiating from the apex.

Both specimens are badly crushed. The wall of the right valve is solid and without canals; inclination of commissure about 130°. In describing the upper (left) valve as thin Whitfield was evidently referring to its outer layer, which is thin and brown, with the horny appearance so characteristic of this genus. Below it is the thick inner layer traversed by nontabulate canals, which are separated by bifurcating plates radiating from the umbo. Whitfield saw these as "thin thread-like grooves".

Dimensions. — Height of Whitfield's right valve 190 mm on ventral side, 60 mm on dorsal; diameter at commissure 200 mm; height of left valve 90 mm. Diameter of Geological Survey specimen at commissure 150 mm; its other measurements without significance owing to crushing and erosion.

Plagioptychus toucasianus Matheron

Plate 34, figures 2-4

Plagioptychus toucasianus Matheron, 1843, p. 117, pl. 6, figs. 1,2.
Caprina coquandi d'Orbigny, 1847, p. 185.
Plagioptychus coquandi (d'Orbigny), Chaper, 1873, p. 82, pls. 11,12, text figs. 1-4.
Plagioptychus toucasi Douvillé, 1888, p. 719, text fig. 6.
Plagioptychus sp. Trechmann, 1924b, p. 408.
Plagioptychus toucasi Douvillé, Muellerried, 1933a, p. 9, text figs. 6-9, 11.
Plagioptychus toucasi Douvillé, Chubb, 1956c, p. 7; 1959, p. 45.

Occurrence. — A single left valve was found by the Jamaica Geological Survey in the *Barrettia* Limestone of Haughton Hall, Green Island, Hanover Parish. Trechmann's specimen came to the British Museum (Natural History) with his bequest (No. LL30294); it is from the same locality.

Description. — The Geological Survey specimen has been much rolled, all the outer layer has been lost, and the inner layer with its canals brought to light; the radial plates bifurcate at least twice. Trechmann's specimen is better preserved, retaining part of its brown outer layer, but its interior is filled with hard matrix. The shell is of medium size and highly arched, and the umbo, which is slightly behind the centre of the hinge line, projects well beyond it. The anterior myophore is prominent, thick, and massive; the base of the anterior tooth is preserved, it is quadrangular, its dorso-anterior side abutting against the myophore, its posterior angle projecting into the socket, and its ventral angle being extended as a septum which cuts off the posterior muscle cavity. The single tooth of the right valve, much eroded, is in the socket; it is large and anteriorly grooved, so that its fits around the posterior angle of the anterior tooth of the left valve. The ventral and lateral margins of the Geological Survey specimen have been eroded away; the Trechmann specimen shows the posterior tooth and part of the brim with its bifurcating plates.

Dimensions. — Geological Survey specimen: dorso-ventral diameter 60 mm; antero-posterior diameter 72 mm. Probably before erosion the dimensions were about 80 by 80 mm. Height 45 mm; originally probably over 50 mm. Trechmann specimen, corresponding figures: 80 mm, 88 mm, 54 mm.

Remarks. — This form is tentatively attributed to the European species *P. toucasianus* from which it shows no significant difference. Mulleried (1933a) described the same species from the Lower Senonian of a locality between La Vega del Paso Real and San Bartomolé do los Llanos in Chiapas, south Mexico, but his specimens were bivalved and did not show the structure of the hinge and myophores; he confirmed his determination by sectioning.

Plagioptychus zansi Chubb

Plate 33, figures 3-5

Caprina jamaicensis Whitfield, 1897a, *pars*, pl. 13, figs. 1,2.
Plagioptychus zansi Chubb, 1956a, pp. 9-10, pl. 1, figs. 7-9; 1956c, p. 8.

Occurrence. — Fairly common in the *Titanosarcolites* Series, chiefly in the more shaly beds of the Maldon Inlier, St. James, and the Marchmont Inlier on the borders of Westmoreland and St. James. Whitfield's specimen came from Logie Green, Upper Clarendon.

Description. — A small species, its right valve variable in form, conical and either straight, curved or twisted, in some cases becoming exogyrate or wedge-shaped; attachment area often large; internal characters unknown; inclination of commissure about 130°.

Left valve gently and evenly arched, without abrupt change of curvature, and the umbo, which is considerably displaced towards the posterior, hardly if at all projecting beyond the cardinal line; it is transversely oval, the antero-posterior diameter being about 25 per cent greater than the dorso-ventral. Outer layer brown, smooth, with fine, close-set growth lines; inner layer shows radial plates which bifurcate at least once and often twice; in a distance of 20 mm on the ventral margin there are 21 canals at the inner edge and 46 at the outer. The anterior tooth is a prominent ridge with its long axis directed postero-dorsally at an angle of 45° to the long axis of the valve; the posterior tooth is similarly directed, and both lean slightly towards the posterior; both teeth are supported by septa which converge below the socket and continue as a ridge to the ventral margin. The ligamental groove is short, running a distance of only about 8 mm from the umbo to the posterior tooth, the dorsal side of which it indents. The anterior myophore is a thin, deeply undercut lamina with, on its ventral edge, a raised rim which shows a slight thickening and projection near its middle; the posterior myophore is an oval plate occupying the whole of the cavity behind the two septa, and rising posteriorly to overhang the brim of the valve.

Dimensions. — Height of right valve variable being, in a conical shell about 55 mm on the dorsal side and 75 mm on the ventral, and in a wedge-shaped shell zero on the dorsal and 30 mm on the ventral. Other measurements much less variable, the diameter at the commissure being about 50 mm antero-posteriorly and 40 mm dorso-ventrally; height of left valve about 13 mm.

Plagioptychus trechmanni Chubb

Plate 32, figures 6,7

Plagioptychus jamaicensis (Whitfield), Trechmann, 1924b, pp. 407-408, pl. 25, fig. 4.
Plagioptychus trechmanni Chubb, 1956a, pp. 8-9, text figs. 1,2; 1956c, p. 7.

Occurrence. — Two bivalved specimens and one free left valve were collected by Trechmann from the *Titanosarcolites* Series of Logie Green, Upper Clarendon; now in the British Museum (Natural History). The Institute of Jamaica has some specimens (J67) from the Cambridge-Catadupa railway line.

Description. — Right valve small, short, straight, and cylindrical, ornamented with coarse growth lines, attached by the apex which is broad and flattened, the plane of the commissure is inclined at an angle of about 110°.

Left valve differs from *P. zansi,* in its relative ruggedness, high arching, and overhang of the umbo which is nearly central; the arching is associated with an abrupt change of curvature, the curve being moderate as far as a certain growth line, which is usually slightly dorsad of the middle of the valve, beyond which it steepens abruptly, so that this growth line often forms a carina; other growth lines are strongly developed, especially on the ventral side of the carina, making the valve more rugged than other Jamaican species of *Plagioptychus.* The anterior myophore is narrower than that of *P. zansi* and lacks the central projection. The anterior tooth is a triangular pyramid supported by a buttress which rises from the bottom of the valve. The posterior tooth is a sharp ridge 11 mm long, parallel to the dorso-posterior margin; it is supported by a low buttress as wide as the tooth at its upper end but narrowing downwards. The socket is not separated from the muscle cavity.

Dimensions. — In the bivalved specimen illustrated (Pl. 32, fig. 7) height of right valve on dorsal side is 11 mm, on ventral side 30 mm; dorso-ventral diameter at commissure 39 mm; at base, *i.e.* area of attachment, 35 mm. The free left valve has an antero-posterior diameter of 49 mm, a dorso-ventral diameter at the commissure of 29 mm, beyond which the umbo projects 10 mm; height above plane of commissure 22 mm.

Plagioptychus minor Chubb

Plate 34, figures 5-8

Plagioptychus minor Chubb, 1956a, pp. 10-11, pl. 1, figs. 10-13; 1956c, p. 8.

Occurrence. — Probably confined to one horizon near the top of the *Titanosarcolites* Series in the Ducketts Land Settlement on the borders of St. James and Hanover, and perhaps at Logie Green, Clarendon.

Description. — A small and highly gregarious species, the individuals attaching themselves in clusters to shells of *Antillocaprina,* to corals, or to each other; this habit often leads to mutual interference, and distortion of the right valve, but when unencumbered it is curved conical, with ventral side convex, attached by the whole of the antero-dorsal surface, which is flattened, so that the shape comes to resemble the toe of a slipper; inclination of the commissure about 130°. Tooth a four-sided pyramid set obliquely, with low ridges running from its three free corners around the ventral sides of the posterior socket and the two muscle scars; a groove on its antero-dorsal face descends into the adjacent anterior socket. Posterior muscle set on a small raised platform.

Left valve slightly and evenly arched, its umbo projecting little if at all beyond the cardinal margin; outer and inner layers as in *P. zansi,* but the radial plates bifurcate only once, near the inner margin. Anterior tooth grooved dorsally and ventrally; a ridge connects the two teeth, separating the intervening socket from the posterior muscle cavity; the latter is considerably shallower than the body cavity, from which it is separated by the usual septum. Anterior myophore a narrow, parallel-sided, undercut shelf, with no projection at mid-point, but a raised rim which continues round the ventral side of the body cavity.

Dimensions. — Height of a well-developed right valve on dorsal side 22 mm, on ventral side 33 mm; diameter at commissure, antero-posterior 30 mm, dorso-ventral 22 mm; dorso-ventral diameter is from 68 to 77 percent of antero-posterior. Height of left valve 10 to 12 mm.

Plagioptychus fragilis Chubb

Plate 32, figures 4,5

Plagioptychus fragilis Chubb, 1967, p. 27.

Occurrence. — Not uncommon in the Shaw Castle Shale of the *Titanosarcolites* Series of the Maldon Inlier of St. James. The specific name refers to the delicacy of the shell, especially the left valve.

Description. — A small species, apparently not gregarious. Right valve generally low, twisted and exogyrate, or possibly sometimes slipper-shaped. Hinge set far back; posterior socket, in extreme corner, is divided by a small ligamental ridge; tooth with an anterior groove descending into the neighbouring socket, which is oblique. Posterior myophore a small platform supported by a buttress rising from the interior; anterior myophore a thickening of the shell wall, running parallel to the dorsal margin.

Left valve only slightly arched, long, delicate, almond-shaped, tending to taper anteriorly; umbo inconspicuous; outer layer extremely thin, smooth; inner layer thin, its radial plates, at least in the postero-ventral area, bifurcate twice or thrice, with the results that the canals near the outer margin outnumber those near the inner by over four to one. Posterior tooth set far back and tilted so that, in extreme cases, it may overhang the posterior margin; it is grooved on the dorsal side by the ligamental furrow; socket triangular in young forms, oblique in adults, bounded by the septa that support the two teeth; anterior tooth peglike and notched in youth, oblique in maturity. Posterior myophore an oblique oval area occupying the cavity behind the septum and sloping up to overhand the postero-ventral brim; anterior myophore a thin, deeply undercut shelf, in the adult widening form 5 mm near the tooth to 11 mm near the anterior end.

Dimensions. — Height of right valve variable between 20 and 30 mm; antero-posterior diameter of an adult 40 to 50 mm; dorso-ventral diameter about 60 percent of antero-posterior; height of left valve 5 to 6 mm; thickness of left valve in base of body cavity 1.5 to 2 mm.

Remarks. — This form differs from previously known Jamaican species of *Plagioptychus* in the relative flatness, narrowness, and thinness of its left valve; it is unusual, in a small species, for the radial plates to bifurcate more than once.

Genus **MITROCAPRINA** Boehm, 1895

In its shape and many of its characters this genus resembles *Plagioptychus*. The right valve has no canals. In the left valve the hinge and muscle areas are like those of *Plagioptychus*, the chief difference between the two genera being that in *Mitrocaprina* the radial plates separating the canals in the inner layer bifurcate and anastomose again several times, producing a series of polygonal or rounded canals which are seen in the marginal brim.

Mitrocaprina multicanaliculata Chubb

Plate 34, figure 9

Mitrocaprina multicanaliculata Chubb, 1956a, pp. 11-12, pl. 1, fig. 14; 1956c, p. 8.

Occurrence. — A single left valve, considerably weathered, was found in the *Titanosarcolites* Series of Logie Green, Upper Clarendon. The Basle collection includes a specimen (G13110) from near Catadupa railway station which probably belongs to the same species.

Description. — Valve small, considerably arched, with even curvature. Outer layer thin, brown, of horny appearance, smooth with inconspicuous growth-lines. Inner layer thick, with numerous oval or polygonal canals arranged in six to eight rows; they are well preserved only on the posterior and ventral margins but probably were originally present around the anterior side; the alternate bifurcation and inosculation of the plates continue almost to the periphery. The teeth have been damaged by rainwater solution; posterior tooth quadrilateral, its long axis subparallel to the valve margin; socket large; anterior tooth much damaged, its supporting septum, which is 4 mm thick, runs obliquely in a postero-ventral direction at an angle of 45° to the long axis of the valve, cutting off only a small posterior muscle cavity which opens into the socket. Anterior myophore is much weathered but apparently resembles that of *Plagioptychus*.

Dimensions. — Antero-posterior diameter 42 mm, dorso-ventral from cardinal to ventral margin 30 mm; umbo projects 9 mm beyond cardinal margin; height above plane of commissure 17 mm.

Family **RADIOLITIDAE** Gray, 1848

In this family the right valve is typically straight and conical or cylindrical, and the left valve usually opercular, forming a lid which is flat, depressed conical, or concave, though rarely it is high and coiled. As in other rudists the shell consists of two layers but, whereas in the families already described the outer layer is normally less than one mm thick and consists merely of a series of superimposed growth rings, in the Radiolitidae this layer forms the main part of the shell-wall, at least in the right valve, and consists of a series of thin, ring-shaped plates. In the more primitive genera these plates take the form of inverted cones fitted one within another which, owing to their resemblance to funnels, are called *funnel plates*. In more advanced forms the funnel plates tend to become horizontal, and in many they are radially frilled or folded.

The funnel plates, although close-set, are usually not in contact. They are separated by vertical radial plates and, according to the pattern made by these, the family is divided into two subfamilies: the Radiolitinae, in which the vertical plates are straight and radial, so that in a section they, together with the funnel plates, make a quadrangular pattern, resembling muslin; and the Sauvagesiinae, in which the vertical plates make a polygonal pattern like a fine honeycomb, which may be seen either on the surfaces of the funnel plates or in a transverse section. The inner layer is thin and serves only to line the body cavity and form concave tabulae below it.

Both subfamilies show various types of external ornament. Many genera have longitudinal costae and, if the funnel plates are frilled, the downfolds usually correspond with the ridges and the upfolds with the intervening furrows. Most genera show, on the posterior side, two vertical bands with ornament different from that of the rest of the shell. These, which may be either ridges or grooves, are the *siphonal bands*, one near the posterior myophore representing the exhalent siphon (S) and a further one the inhalent siphon (E); they are comparable with the slit bands of certain gastropods. A few genera, in which the siphonal bands are considerably infolded, have two orifices, called *oscules*, in the left valve, immediately above the bands; these are evidently siphonal apertures. Oscules are characteristic of gregarious genera.

The structure of the left valve varies; the outer layer is thin and consists of superimposed laminae; the inner layer is thick and in some genera has a structure resembling that of a caprinid, with vertical radial plates, which may bifurcate, separating "canals" within its thickness. In most members of the families previously discussed the left valve opened like the hinged lid of a box, swinging upwards and outwards. The Radiolitidae, however, had a highly specialized hinge apparatus, contrived to allow this valve to rise vertically. The hinge is remarkably symmetrical, the left valve having two long, straight, vertical, parallel and nearly equal teeth, joined at the base by a yoke, which slide into deep sockets, or merely in channeled grooves in the wall of the body cavity of the right valve. Except in the most primitive genera the latter valve has lost its single tooth.

Anterior and posterior myophores branch from the bases of the two teeth in the left valve, curving around within the body cavity close to its walls. Their outer faces are denticulate for the attachment of the adductor muscles which, in the right valve, were attached directly to the inside of the wall. The gut must have passed close by the end of the posterior muscle (Douvillé, 1910, p. 14) and the long extension of this muscle may cause a shift of the anus, and, therefore, of the S band, towards the venter. This necessitates a shift of the E band which may come to lie diametrically opposite to the hinge area and ligament (if present), though it never lies anterior to the mid ventral point. But, while the anterior myophore is always attached for its whole length to the inside of the left valve, the posterior is commonly pedunculate, being attached only at its dorsal end either to the tooth or to the yoke, so the gut was able to pass over it to the S siphon, which is then sited alongside the muscle and not ventral to it.

The ligament, which was external in the Diceratidae and Monopleuridae, and sunk in a groove in the Caprotinidae and Caprinidae, was in the more primitive Radiolitidae submerged so deeply that it was supported by an infold of the outer layer, which projected into the body cavity to form a vertical ridge or pillar attached to the dorsal wall. The more advanced Radiolitidae have lost this ridge and presumably had no ligament, using some other method to raise the lid.

Subfamily **RADIOLITINAE** Douvillé, 1902

Vertical plates radial and generally unbranched, appearing on the surface of the funnel plates as fine close-set ridges; in section the funnel plates and the radial plates together make a pattern of small squares or quadrangles.

(a) *Radiolitinae with ligament*

Genus **AGRIOPLEURA** Kühn, 1932

This name replaces the preoccupied name of *Agria* Matheron, 1878. It is one of the most primitive genera of the Radiolitidae and some authors refer it to the Monopleuridae. But in the right valve the thin outer layer consists of upturned funnel-plates, crossed by simple radial plates; it has a ligamental ridge and also a tooth. The left valve is flat, with two long, vertical teeth, and myophores only slightly projecting.

Agriopleura falconi (Chubb)

Plate 35, figure 1; Text-figure 4

Agria falconi Chubb, 1956a, pp. 13-14; pl. 2, fig. 3, text fig. 3; 1956c, p. 8.

Occurrence. — Occurs rarely in the Shaw Castle Shale, Maldon Inlier, St. James.

Description. — A very small species, the right valve elongated conical, tending to become cylindrical, generally slightly curved towards the apex by which it is attached; more or less quadrangular or triangular in cross section. Ornamented with five or six longitudinal costae alternating with furrows, all being actual folds of the wall involving both layers; in the specimen illustrated they may have been somewhat accentuated by crushing. Outer layer generally less than one mm thick, composed of funnel plates and vertical radial plates; inner layer thin. Three of the outfolds are interpreted as the pedal fold (V), the inhalent siphon (E) and the exhalent siphon (S). It is now thought that the published section (Chubb, 1956c, text fig. 3) is inaccurate: the outer layer is involved in the ligamental infold, but it is enveloped in an infold of the inner layer (Text-fig. 4). The funnel plates, of which there are about 25 to 1 cm, are inclined upwards at an angle of 45°, they show slight downfolds at the costae and upfolds in the furrows; dorsally they are strongly downfolded at the ligamental furrow. The vertical radial plates are spaced at about 35 or 40 to 1 cm.

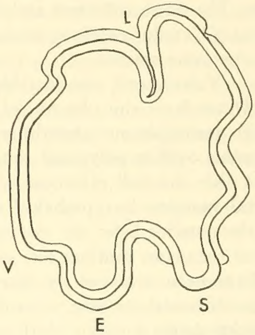

Text-figure 4. *Agriopleura falconi* Chubb. Transverse section of right valve; × 2.5. This corrects the section in Chubb 1956a, p. 13, Text-figure 3, which fails to show the outer layer entering into the ligamental infold.

The left valve is unknown.

Dimensions. — The largest specimen is 60 mm high; diameter, dorso-ventral 21 mm, antero-posterior 17 mm.

Genus **PRAERADIOLITES** Douvillé, 1902

Outer layer of right valve thick composed of funnel plates which are smooth and turned up at a steep angle, so that they show a cone-in-cone structure. They are not frilled but have several comparatively slight folds, which affect only the outer layer, not the inner layer. There are three principal costae formed by these folds corresponding to the three openings of the mantle, the two siphonal openings (S and E) and the pedal opening (V); there may also be a postero-dorsal fold. The ligamental ridge is an extremely thin infolding of the outer layer, projecting into the body cavity; it is enveloped in a thicker infold of the inner layer which may be interpreted as a tooth (N). This stands between two sockets which are separated from the body cavity by thin vertical septa. The left valve is of normal radiolite type, with two strong, parallel, vertical teeth, prominent myophores and a ligamental ridge.

Praeradiolites verseyi Chubb

Plate 35, figures 2-4; Text-figure 5

Praeradiolites verseyi Chubb, 1956a, pp. 14-15, pl. 2, figs. 4-6; 1956c, p. 7.

Occurrence. — Not uncommon in the *Barrettia* Limestone at Stapleton, Sunderland Inlier, St. James.

Description. — Shell of medium size. The right valve is conical or pyramidal and slightly curved with the ligament on the convex side, *i.e.* the direction of curvature is ventral and not, as is usual, dorsal. The shell was probably cemented to some solid object when young but was recumbent on its dorsal side in maturity. The ligamental infold forms a barely perceptible groove in the outer surface. The cross section tends to a roundly triangular form and the outer surface has three carinae corresponding with folds of the funnel plates. The outer layer is generally from 10 to 15 mm thick, widening to 20 or 25 mm at the carinae; the funnel plates rise from the inner layer at angles of 90° to 120°, and except at the carinae curve rapidly upwards; they are 0.05 mm thick and at their inner edges are about 1 mm apart, but as they curve upwards they approach each other, in an asymptotic manner, and become nearly tangential, giving a false impression of a cortical layer, at least on the dorsal surface. The folds in the funnel plates should be described as outfolds, rather than downfolds, for they slope upwards, though at a lower angle than the intervening sections. A sharp angular fold at the antero-dorsal corner, only a short distance from the ligamental ridge, is regarded as a pedal fold (V); probably this fold did not form a continuous carina, but a series of spoutlike protuberances; the lowest of these seem to have taken part in the fixation of the valve. A second fold, the so-called postero-dorsal fold (PD) is generally feebly developed; it is the third fold, representing the exhalent siphon (S), which occupies the postero-dorsal corner; the fourth fold (E) is near the middle of the posterior side. The four folds form radial sinuses in the chalice wall. Owing to the prominence of the V and S carinae the dorsal margin tends to form a nearly straight line. The vertical radial plates generally form a quadrangular pattern, but where the funnel plates are nearly horizontal polygonal cells may be seen, though the radial tendency is still obvious.

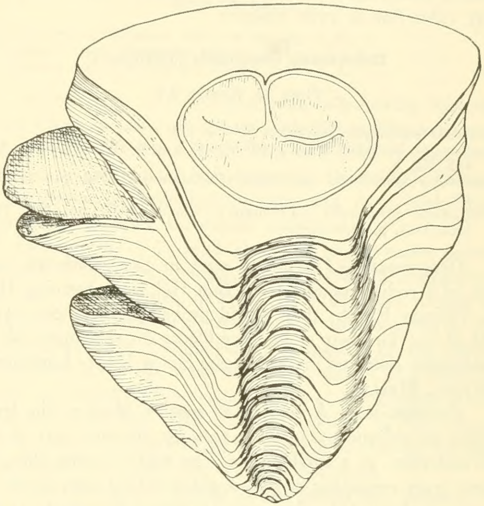

Text-figure 5. *Praeradiolites verseyi* Chubb. Right valve reconstructed from several specimens; × 0.8.

The inner layer is about 0.7 mm thick and forms a narrow rim around the inner margin of the chalice. The ligamental ridge is displaced towards the anterior; it consists of an attenuated infold of the outer layer enveloped in an infold of the inner layer; in the adult it projects from 11 to 15 mm into the body cavity, it is 1 mm thick, expanding to form a flange at least 2 mm and perhaps sometimes 5 or 6 mm wide at its inner end. It stands between the two sockets which, below the level of the commissure, are separated from the body cavity by vertical septa running obliquely from the inner flange of the infold to the dorsal wall.

The left valve is unknown.

Dimensions. — Height of right valve about 150 mm;

diameter at commissure, antero-posterior 90 mm, dorso-ventral 70-75 mm; diameter of body cavity 45-50 mm.

(b) *Radiolitinae without ligament*

Genus **DISTEFANELLA** Parona, 1901

This genus includes small, subcylindrical forms, with several acute longitudinal costae and two rather broad, smooth siphonal bands, separated by a single costa. No ligamental infold and no tooth in the right valve, but two sockets which are connected by a vertical transverse plate. Left valve flat or even concave.

Distefanella lombricalis (d'Orbigny)

Plate 35, figures 6,7

Radiolites lombricalis d'Orbigny, 1842, p. 173.
Distefanella lumbricalis [*sic*] (d'Orbigny), Douvillé, 1913, pp. 413-415, fig. 8.
Biradiolites lombricalis (d'Orbigny), Mullerried, 1932, pp. 237-242, fig. 1.
Distefanella lombricalis (d'Orbigny), Chubb, 1959, pp. 742, 748; 1962/1963, p. 18.

Occurrence. — Fragments seen in the weathered surface of a rudist coquina from Bon Hill, near Sunning Hill, St. Thomas Parish; they would probably have been overlooked but for their close resemblance to specimens of *D. lombricalis* collected in 1956 in the Sierra Madre Limestone, Chiapas, Mexico.

Description. — A very small species. Most of the fragments are obliquely transverse sections, showing part of the circumference of a small rudist. The wall is rather thin, its outer layer consisting of funnel plates which turn up at an angle of about 45°; these are traversed by simple radial plates and, in suitable sections, the two sets of plates make a quadrangular pattern. There are about twelve to fifteen acute longitudinal costae separated by rounded furrows; two flat siphonal bands, with a single small sharp costa in the interband. Inner layer thin; hinge and left valve have not been observed in Jamaican material.

Dimensions. — Diameter about 12-15 mm; maximum thickness of outer layer 3 mm, of inner layer 0.4 mm.

Remarks. — The horizon of the Bon Hill Limestone is not known, but *D. lombricalis* is characteristic of the Turonian in south Europe and Mexico.

Distefanella mooretownensis (Trechmann)

Plate 35, figure 5

Biradiolites mooretownensis Trechmann, 1924b, pp. 404-405, pl. 25, fig. 8.
Biradiolites mooretownensis Trechmann, Chubb, 1956c, p. 6.
Distefanella mooretownensis (Trechmann), Chubb, 1962/1963, p. 20.

Occurrence. — A highly gregarious species occurring in the *Titanosarcolites* Limestone in abundance near Moore Town in the Rio Grande Valley, Portland, and rarely in the Catadupa area, St. James, and the Jerusalem Mountain area, Westmoreland.

Description. — This is a smaller species than *D. lombricalis.* The right valve is elongated, cylindrical or tapering gradually, gently curved or somewhat twisted, growing in clusters of many individuals of various sizes. It has 10 to 12 sharp longitudinal costae, separated by shallow sulci; the two slightly wider sulci representing the siphonal bands are not always easy to recognise. The wall, including both layers, is not more than 1 mm thick, except at the costae, where it attains 1.5 mm. The funnel plates turn up at an angle of about 45°, and are crossed by simple vertical radial plates. The hinge structure has not been observed. The left valve is concave, showing fine concentric growth laminae.

Dimensions. — Trechmann gave the diameter of the right valve at the commissure as 15 mm, and of the left valve as 11 mm; these figures are rare, the diameter of the right valve does not generally exceed 10 mm, and a cluster may include hundreds of individuals many of which are less than 5 mm across. He gives the length as 56 mm, but this is often exceeded and probably a length of 100 mm is not uncommon.

Genus **BIRADIOLITES** d'Orbigny, 1847

Shell small or medium-sized, right valve elongate conical with longitudinal costae, and two smooth siphonal bands separated by a costa. Outer layer usually thick, with funnel plates which are more or less horizontal near the body cavity but may be marginally folded, usually with downfolds corresponding with the costae and upfolds with the furrows. No ligament, no tooth and no true sockets in the right valve, but a pair of channelled grooves for the reception of the long, vertical teeth of the left valve. The latter is opercular, flat or slightly convex or concave; springing from the base of the teeth are two projecting myophores which curve around the anterior and posterior sides, and fit closely within the wall of the body cavity of the right valve.

Biradiolites jamaicensis Trechmann

Plate 35, figures 8-12

Biradiolites jamaicensis Trechmann, 1924b, p. 404, pl. 24, figs. 5, 5a, 6, 6a, 7.
Biradiolites jamaicensis Trechmann, Chubb, 1956c, p. 8.

Occurrence. — A common fossil in the *Titanosarcolites* Limestones of the Central Inlier of Upper Clarendon, the

Maldon Inlier of St. James, and the Marchmont Inlier on the borders of St. James and Westmoreland.

Description. — Right valve small, elongated, tapering gradually, straight or slightly curved, growing singly or in clusters of several individuals in contact for their whole length. The valve has eight to eleven sharply angular costae separated by angular furrows which are irregular in depth. Many specimens have a more or less smooth surface, the growth lines, representing the edges of the funnel plates, not being obvious. The funnel plates turn up around the whole circumference, with the result that the costae form spout-like processes at the commissure. On the posterior side the two smooth siphonal bands are separated by a broadly angular costa with a sharp but narrow groove down its middle; the costa limiting the dorsal side of the S band is rounded, that limiting the ventral side of the E band is acutely angular like the normal costae. The body cavity is circular.

The left valve is more or less concave, with subcentral apex, and fine concentric growth lines; in some individuals it nearly covers the right valve, in others it fits well into it and has angular marginal projections to correspond with its costae.

Dimensions. — According to Trechmann the length is up to 140 mm and the diameter at the commissure up to 42 mm. Such dimensions are rare; the length is more often between 50 and 100 mm, and the diameter between 25 and 35 mm, but a cluster in the collection of the Institute of Jamaica (J31) includes shells over 200 mm high.

Biradiolites robinsoni Chubb

Plate 36, figures 1-3

Biradiolites robinsoni Chubb, 1967, p. 27.

Occurrence. — A single right valve was found in the *Titanosarcolites* beds of Cotton Tree Gully, Lambs River valley, Westmoreland. Named after Dr. Edward Robinson of the University of the West Indies, Jamaica.

Description. — A medium-sized species, curved conical, its maximum diameter near equal to its height. It is attached by the whole of its dorsal side to a right valve of *Biradiolites jamaicensis,* which it enwraps. Its anterior side has about four or five strong, prominent and rather rugged costae, corresponding with sharp downfolds of the funnel plates. On the posterior side the siphonal area is similar to that of *B. jamaicensis,* the two bands being smooth and separated by a broadly angular costa with a narrow groove down its middle; the S band is on the side of a rounded costa, the E band on a sharply angular one. The body cavity is oval, and the two channelled grooves for the reception of the teeth of the right valve may be seen within it. The downfolds of the funnel plates on the anterior side make grooves across the commissure, and there are similar grooves on the other sides to a total of about ten in all.

The left valve is unknown.

Dimensions. — Height of right valve 67 mm; diameter at commissure: dorso-ventral 63 mm, antero-posterior 48 mm; diameter of body cavity, dorso-ventral 32 mm, antero-posterior 24 mm.

Biradiolites rudis (Whitfield)

Plate 36, figure 4

Radiolites rudis Whitfield, 1897a, p. 189, pl. 11, fig. 4.
"Radiolites" rudis Whitfield, Chubb, 1955a, pp. 3-4.
Biradiolites rudis (Whitfield), Chubb, 1956c, p. 8.

Occurrence. — A single specimen, collected by Nicholas in the *Titanosarcolites* Series of Logie Green, Upper Clarendon, was described and figured by Whitfield. It must be a rarity as no others have been found by Trechmann, Matley, or the Jamaica Geological Survey, and none have been reported from other Caribbean countries.

Description. — A small shell, the right valve curved elongate conical, but irregular and rugose in appearance. The thin funnel plates spread horizontally and project in irregular folds, which correspond with deep notches in the commissure; it is the uneven development of the funnel plates that gives the shell its rugged shape. The siphonal bands are broadly open concave grooves, each about 9 mm wide, corresponding with rounded upfolds of the funnel plates; they are separated by a strong costa, about 5-6 mm wide, which coincides with a sharp downfold.

The left valve is domed in the centre but flattens towards the margin; it extends to the border of the commissure, its brim is upfolded over the siphonal bands and has a tongue extending down over the interband; elsewhere it fits into the notches and folds of the right valve. According to Whitfield the surface of the left valve is obscured by adhering substances, but when visible is cancellated by two sets of lines, one concentric, the other radial. A re-examination of the specimen showed that this valve is much weathered.

Dimensions. — Height of right valve on dorsal side 73 mm; maximum diameter 45 mm; height of left valve 10 mm.

Biradiolites rudissimus Trechmann

Plate 36, figures 5-8

Biradiolites rudissimus Trechmann, 1924b, p. 402, pl. 26, figs. 4, 4a, 5.
Biradiolites rudissimus Trechmann, Chubb, 1956c, p. 8.

Occurrence. — Fairly common in the *Titanosarcolites*

Series of Logie Green, the Catadupa area, and the Great River Valley.

Description. — Trechmann described this species as "the most irregularly shaped and clumsily grown Radiolite that I have seen" (in conversation he would describe it as "the rudest rudist I know."). The shell is of medium size, solitary, or occasionally growing in clusters. The right valve is exceedingly irregular in form, and may be more or less conical, cylindrical, or low and spreading. The funnel plates generally spread widely and are unevenly wavy; they show, in addition to the close-set radial striae characteristic of the subfamily, more widely spaced radial vascular impressions some of which bifurcate once or twice. The S band is a longitudinal depression, sometimes with an indefinite raised ridge running up it; the E band is the most definite feature, consisting of a nearly parallel-sided, flat band, crossed by strong horizontal growth laminae representing the edges of the funnel plates; it lies in a depression and is bounded by narrow grooves. The funnel plates are upfolded in both bands, and downfolded in the rugged interband.

The left valve does not quite cover the right; it is thin and more or less convex, with subcentral apex from which low rounded costae radiate towards the margin (Pl. 36, figs. 6,7).

Dimensions. — According to Trechmann the height is up to 105 mm, and the commissural diameter up to 109 mm. Of the specimens illustrated in Plate 36, the taller (fig. 5) is 85 mm high, maximum diameter 85 mm, diameter of body cavity 40 mm; the shorter (fig. 8) is 50 mm high, maximum diameter 100 m, diameter of body cavity 24 mm.

Remarks. — This species has considerable resemblance to *Radiolites robusta* Palmer (1928, pp. 80-81, pl. 16, fig. 1) from Huescalapa, Jalisco, Mexico, and to *Bournonia* nov. sect. sp. 4 MacGillavry (1937, pp. 40,41, text fig., pl. 8, fig. 10) from Camaguey, Cuba. The latter is a *Biradiolites,* not a *Bournonia.*

Biradiolites forbesi Chubb

Plate 37, figures 1,2

Biradiolites forbesi Chubb, 1956a, pp. 15-16, pl. 3, figs. 1-2; 1956c, p. 8.

Occurrence. — A single right valve with the upper portion of the posterior wall broken away was collected in the higher part of the *Titanosarcolites* Series in the Ducketts Land Settlement, Lot 184, one mile east of the Lands Department office on the road from Ducketts to Retrieve, St. James Parish. The body cavity is filled with large calcite crystals.

Description. — Shell of medium size, curved cylindroconical; wall thick. The outer surface cannot be seen as it is embedded in hard limestone, but it seems to have been irregularly lobed and without definite costae; the posterior wall can only be studied in sections of the lower part of the shell, from which it appears that the E and S bands were broad open furrows separated by a single costa. The funnel plates are thin and close-set, numbering about 100 to 1 cm; they show a circular upfold, about 10 mm wide, which runs around their inner margin; outside this upfold they turn out more or less horizontally and generally dip again towards their periphery. They tend to undulate irregularly but do not have definite radial folds; they are crossed by radial vascular markings which generally bifurcate once or twice. The cellular structure is extremely fine and can be seen in transverse sections, which show the cell pattern to be quadrangular. The inner layer is 0.5 mm thick. The body cavity is circular; there is no ligamental ridge and no visible hinge structure.

The left valve is unknown.

Dimensions. — The height of the specimen is about 120 mm, its maximum diameter 80 mm; thickness of wall 12 to 37 mm, the thickest part being at the anterior and the thinnest representing the E band. The diameter of the body cavity is about 36 mm.

Remarks. — When *B. forbesi* was named it was not known that *B. rudissimus* had vascular markings. It now appears that there is little, except the concentric upfold, to differentiate between the two species, which may be synonymous.

Biradiolites cf. **rudissimus** Trechmann

Plate 36, figure 9

Occurrence. — Two fragments were found in the *Barrettia* Limestone of St. Anns Great River. Both had been split longitudinally and represented the posterior half of the right valve.

Description. — Shell of medium size, low and broad, the height being half to three-quarters of the diameter. The funnel plates are wide and spreading; they are strongly upfolded at the S band and downfolded in the interband; the E band is missing; they are downfolded on the dorsal side of the S band, in one specimen excessively so, and elsewhere undulate irregularly. They have no vascular markings. Neither specimen has tabulae in its body cavity.

The left valve is unknown.

Dimensions. — First specimen: diameter 70 mm, body cavity 28 mm, height 50 mm; second specimen, diameter 77 mm, body cavity 35 mm, height 38 mm.

Remarks. — This form differs from *B. rudissimus* and

B. forbesi in its lack of radial vascular impressions, and from the latter in its lack of a concentric upfold. It is probably an independent species.

Biradiolites minhoensis Trechmann

Plate 37, figures 3,4

Biradiolites minhoensis Trechmann, 1924b, pp. 402-403, pl. 26, figs. 1, 1a.
Biradiolites minhoensis Trechmann, Chubb, 1956c, p. 8.

Occurrence. — A scarce fossil known only by the type specimens collected by Trechmann in the *Titanosarcolites* Series of Logie Green and Trout Hall in the Rio Minho Valley of Upper Clarendon.

Description. — Shell of medium size. Right valve conical, not strongly costate; funnel plates strong and irregular, directed upwards and outwards, somewhat flaring towards the top, thus making the sides of the valve concave. The type specimen shows a development resembling rejuvenation in corals; after attaining a height of about 50 mm the shell continues its upward growth with a smaller diameter, the pre-existing flaring funnel plates are left behind, forming a ledge around the dorsal side, above which the new funnel plates rise more steeply. The S band is marked by a very sharp and narrow upfolding of the funnel plates, the sides of which rise almost vertically to a peak at the commissure; the E band, which is smooth, 10 mm wide and slightly sunken, is marked by a relatively gentle flat-topped upfolding.

The left valve is thin, nearly circular, sunken, slightly concave, smooth, with fine concentric growth lines and subcentral apex. It has slight, almost imperceptible radial undulations, the sector radiating from the apex to the S band is slightly raised, that to the E band slightly sunken. The diameter of the left valve is considerably less than that of the right; it probably extends very little beyond the limits of the body cavity.

Dimensions. — According to Trechmann the height of the right valve is up to 95 mm; diameter of right valve 65 mm; diameter of left valve 40 mm. These are maximum dimensions; the figured specimen is 60 mm high, originally probably 65 mm; diameter of right valve 57 mm, of left valve 30 mm.

Remarks. — MacGillavry (1937, p. 39) thought that this species was a *Bournonia.* An examination of the type British Museum (Nat. Hist.) leaves no doubt that Trechmann was right in attributing it to *Biradiolites* as both siphonal bands are in grooves.

Biradiolites novaterrensis Chubb

Plate 37, figures 5-8

Biradiolites novaterrensis Chubb, 1967, p. 27.

Occurrence. — A single bivalved shell from the *Barrettia* Limestone of New Ground, St. Ann's Great River Valley, was included in the Trechmann Bequest. Two imperfect specimens were collected by the Geological Survey in the same locality.

Description. — A small species. Right valve conical, attached by its umbo; the antero-dorsal side, which is the highest, is smooth and flaring, with upturned, tangential funnel plates. Ventrally the smooth face ends at the costa which borders the E band; both bands are broad open grooves, the E band in the figured specimen being 18 mm wide by 9 mm deep, and the S band 11 mm by 6 mm; the interband is a prominent costa and another, nearly as prominent, stands on the dorsal side of the S band. In one of the specimens the latter costa forms the posterior margin of the smooth area, but the figured specimen has three subsidiary costae, appearing later and becoming progressively smaller. All the costae are characterized by strong downfolds of the funnel plates, while in all the grooves, notably the siphonal, these plates stand erect and become tangential; in the three major and the first of the minor costae the amplitude of the downfolds may be as much as 25 mm, but it is only about 7 mm in the two lesser costae.

The central part of the left valve is more or less flat; its outer layer is composed of laminae folded in conformity with the funnel plates; it also has vertical radial plates. It fits in against the high antero-dorsal wall of the right valve, its own margin turning up with it. From its other sides project grooved lappets which fit into the downfolds of the costae.

Dimensions. — Height 54 mm; diameter: dorso-ventral 53 mm, antero-posterior 42 mm.

Remarks. — Of known species of *Biradiolites* this seems to have most resemblance to *B. canaliculatus* d'Orbigny from the Turonian of the south of France.

Biradiolites riograndensis Chubb

Plate 37, figures 9-11

Biradiolites riograndensis Chubb, 1967, p. 27.

Occurrence. — A single bivalved specimen was found in Maestrichtian limestone south-east of Alligator Church in the Rio Grande Valley, Portland. It was associated with *Titanosarcolites* sp., *Antillocaprina* sp., *Distefanella mooretownensis,* and other fossils.

Description. — A small shell. Right valve conical, attached by its apex, which is curved antero-dorsally. A broad, flat flange projects abruptly from the ventral side, its height being about equal to that of the shell and its width to the shell's diameter. The dorsal and anterior sides, including the anterior side of the flange, are smooth, the funnel plates being erect and nearly tangential but slightly separated by vertical radial plates. On the posterior side the S band is flat and slightly sunken, nearly parallel sided, some 10 mm wide, with about five costellae, and coinciding with a broad upfold of the funnel plates; the interband and the E band are both damaged, but the interband appears to have been prominent and was marked by a downfold, as the E band was by an upfold. Between the E band and the flange there is a broad depression with downfolded funnel plates.

The left valve undulates in conformity with the contours of the funnel plates of the right, with upfolds over the bands and a downfold over the interband; a large, saddle-shaped lappet fits into the space between the E band and the flange.

Dimensions. — Height 42 mm; diameter, dorso-ventral excluding the flange 33 mm, including flange 62 mm, antero-posterior 47 mm.

Genus **THYRASTYLON** Chubb, 1956

Shell of medium size, curved cylindro-conical when free to develop, but often distorted by close adherence to foreign bodies; fixation lateral, the whole or a considerable part of the anterior face of the right valve being moulded onto the surface of attachment. The diagnostic character of the genus is in the siphonal areas of both valves. In the right valve the two siphonal bands lie in rather deeply sunken grooves, separated by a rounded interband. The E band, always the wider, is flat and is generally marked by several narrow longitudinal costellae; the S band is smooth and convex. The funnel plates, which have numerous small radial undulations, are more or less horizontal near the body cavity, but turn up sharply at the siphonal bands, forming two peaks which rise above the commissural surface, the S peak usually higher and sharper than the E peak; further out the funnel plates turn upwards on the anterior side and spread over the attachment area, and turn downwards in the dorsal and ventral regions and in the interband. In these regions the funnel plates hang down to form an imbricating series of skirts or aprons; these aprons, bordering the siphonal grooves, tend to spread laterally over them, and may meet in a structure resembling a box pleat, occluding the grooves and converting them into tubes the course of which is indicated by sutures on the surface. Although deeply sunken the siphonal grooves do not form pillars or pseudo-pillars within the body cavity, which is round or oval, with channelled grooves for the reception of the teeth.

The left valve is shaped like a broad-brimmed hat, its crown, which covers the body cavity, being domed or conical, and its brim fitting closely over the commissural surface. It turns upwards on the anterior side and downwards in the dorsal, ventral, and interband regions, in conformity with the funnel plates; it is sharply upfolded over the siphonal peaks and the sides of the upfolds tend to grow together and may join along sutures, so as to leave open oscules above. The S oscule is vertically oval, with a sharp peak above it, the E oscule is transversely oval. Since they fit closely over the peaks of the right valve, the oscules could inhale or exhale only if the left valve were raised slightly; the expulsion of water from the S oscule would be obliquely upwards at an angle of about 45° to the axis of the shell. The hinge resembles that of *Biradiolites.*

Thyrastylon adhaerens (Whitfield)

Plate 38, figures 1-6

Radiolites adhaerens Whitfield, *pars,* 1897a, pp. 188-189, pl. 10, fig. 1; pl. 12, fig. 1.
Biradiolites adhaerens (Whitfield), Trechmann, 1924b, pp. 400-401.
"Radiolites" adhaerens Chubb, 1955a, p. 3.
Thyrastylon adhaerens (Whitfield), Chubb, 1956b, pp. 36-37, pl. 6, figs. 1-3; pl. 7, figs. 5-9; 1956c, p. 8.

Occurrence. — One of the commonest fossils in the *Titanosarcolites* Series at many localities in the parishes of Westmoreland, St. James, Upper Clarendon, and Portland. Locally it is an important rock-forming organism. It is not certain if specimens from Cuba described by MacGillavry under the name of *Biradiolites adhaerens* (1937) should be assigned to this or to another species of the genus.

Description. — A highly gregarious species of small to medium size, commonly occurring in clusters of 20 or more individuals, the right valves being attached by the whole or nearly the whole of the anterior side. They are moulded onto the surface of attachment, generally primarily the shell of another rudist, and secondarily onto each other; many shells begin growth in a recumbent position but later turn upwards, so that commonly the shells have no regular form, but are rugged and irregular, though the apertural part often becomes free and more or less cylindrical. The S band is about 3-5 mm wide, slightly convex, and smooth except for occasional transverse growth lines; the E band is some 6-8 mm wide, with about four-seven fine longitudinal costae, new ones appearing at the sides or by intercalation; both bands are sunk in grooves and coincide with sharp upfolds of the funnel plates, with the result that at their summits they rise as peaks, well above the general level of the commissure. The bands are generally overlapped by the downturned funnel plates at their sides but are not always completely occluded. The interband is rounded and is about 16 mm wide. The outer layer is usually 10-15 mm thick, but may be twice this thickness in parts of the anterior side, where it has spread over the surface of attachment, while in the siphonal areas it may be no more than 4-5 mm thick. The funnel plates, of which there are some 25 in 1 cm, are marked by about 30-35 small radial undulations which often bifurcate. The vertical radial plates may sometimes be seen as fine close-set striae on the surface of a well-preserved funnel plate.

The central part of the left valve is a low rounded or conical dome, the brim has fine radial undulations corresponding with those of the underlying funnel plate. In well preserved specimens, if the siphonal bands are occluded, the corresponding peaks of the left valve will bear oscules.

Dimensions. — The height of the right valve is generally between 80 and 160 mm, though in crowded clusters the shells may attain a height of 250 mm or more, no doubt owing to keen competition for access to sea water. The diameter of the shell is usually between 40 and 60 mm, that of the body cavity between 20 and 25 mm; the height of the crown of the left valve is 5 to 8 mm.

Thyrastylon coryi (Trechmann)

Plate 38, figures 7-9; Plate 39, figures 1-3

Radiolites adhaerens Whitfield, *pars,* 1897a, pl. 10, figs. 2,3; pl. 11, figs. 1-3.
Biradiolites coryi Trechmann, 1924b, p. 401, pl. 25, fig. 5.
Biradiolites adhaerens (Whitfield), MacGillavry, 1934, pp. 236-237, pl. 1, fig. 3.
Thyrastylon coryi (Trechmann), Chubb, 1956b, pp. 37-38, pl. 1, figs. 1-3; 1956c, p. 8.

Occurrence. — Locally common in the *Titanosarcolites* Series of Logie Green, Upper Clarendon; at Shaw Castle, St. James; below Catadupa and in the Great River Valley on the borders of St. James and Westmoreland; and in the Ducketts Land Settlement, Westmoreland, where it seems to characterize a definite horizon.

Description. — This species differs from the last chiefly in that normally it grows singly and rarely in groups of two or three individuals, so that it is more free to develop its proper form. The right valve is cylindro-conical, often showing slight longitudinal costae from 5 to 8 mm wide, and is attached by the whole of its anterior side to a foreign object. The shell is shaped in conformity with the surface of attachment and if, as is usual, this is the convex surface of a shell of *Antillocaprina occidentalis,* the anterior surface of *T. coryi* is concave and the whole shell is correspondingly curved, so that the posterior side, bearing the siphonal bands, is convex (Pl. 38, fig. 7). Specimens from Shaw Castle, however, lie in the base of a shale and are attached to the surface of the underlying limestone; the anterior side is therefore flat, and the umbo curves dorsally as in typical pelecypods (Pl. 39, figs. 1,2). The bands are broader than in *T. adhaerens,* the E band occasionally attaining a width of 12 mm. In some individuals the siphonal grooves are open so that the full width of the bands is visible; in many the margins of the grooves are more or less hidden by lateral overlap of the down-folded funnel plates; occlusion of the S band is common, but the E band is rarely if ever completely occluded. Weathering may reopen grooves which were originally occluded.

The left valve of *T. coryi* differs from that of *T. adhaerens* in that the central part is much more elevated, being high rounded conical or nearly hemispherical, indeed it is sometimes higher than the right valve. The brim has from 30 to 35 radial plications, corresponding with the similar plications of the funnel plates; the siphonal upfolds form deep notches which are rarely occluded. A transverse section cut across the domed crown shows it to be hollow and thin-walled, the mean thickness of the outer layer being about 1 mm, of the inner layer 0.5 mm.

Dimensions. — The dimensions are similar to those of *T. adhaerens* except that the height of the right valve is generally less than 100 mm. The crown of the left valve may be 20 or 25 mm high.

Thyrastylon semiannulosus (Trechmann)

Plate 39, figure 4

Biradiolites semiannulosus Trechmann, 1924b, pp. 401-402, pl. 25, figs. 6,7.
Thyrastylon semiannulosus (Trechmann), Chubb, 1956b, p. 38; 1956c, p. 8.

Occurrence. — A rare fossil in the *Titanosarcolites* Limestone of Logie Green and Catadupa.

Description. — Like *T. coryi* this is a solitary form, but it is small and is attached by only the lower half of its anterior side. The right valve is straight and conical and the siphonal bands are similar to those of the preceding species; as Trechmann observed "both bands are frequently covered by the growth foliations," *i.e.* they are occluded. In such cases all that can be seen are two open V-shaped furrows with sutures in their bottom. As in other species of *Thyrastylon* the siphonal tubes rise up in peaks. The varix-like annulations shown by some of these specimens are due to the weathering of a surface similar to that of *T. coryi.*

The left valve has more resemblance to that of *T. ad-*

haerens than to that of *T. coryi,* the central part being a low cone, but the brim has only about 20 low radial plications. The figured specimen has the E oscule well developed; the S band is completely occluded but, though the brim of the left valve rises above it in a sharp peak, the two sides of the upfold do not come together, so there is no oscule.

Dimensions. — The height of the right valve is some 50-60 mm and the diameter 30-35 mm. The height of the crown of the left valve is 4-5 mm.

Thyrastylon sp.

Biradiolites sp. Chubb, 1961a, pp. 3-4.

Occurrence. — A single mould of the interior of the body cavity of a right valve was found in the shales at a height of 7,000 ft. near the summit of Blue Mountain Peak. It was associated with *Antillocaprina depressa* and *A. williamsi.*

Description. — A very small shell. The body cavity was conical, there is no tooth or ligamental ridge, but the impressions of the fluted grooves for the reception of the teeth of the left valve are well marked. The impression of the uppermost funnel plate, representing the commissural surface, clearly shows fine, simple, radial ridges, which would make a quadrangular, not a polygonal cell pattern. This funnel plate rises steeply on the anterior side as in *Thyrastylon;* most of it is broken away on the other sides but enough remains to suggest that it was turned down except at two points on the posterior side, where it was sharply turned up; these would be the siphonal upfolds.

Dimensions. — Mean diameter of body cavity 8 mm, depth 8 mm; width of commissural wall on anterior side 8 mm.

Remarks. — The simple radial plates prove that this is a Radiolitine, and the sharp upturn of the funnel plate suggests that it was attached by the whole of its anterior side as in *Thyrastylon* or *Bournonia.* The funnel plates do not seem to be sufficiently frilled for the latter genus. The small dimensions of this species and of the associated species of *Antillocaprina* suggest stunting due to an environment unfavourable to rudists.

Genus **BOURNONIA** Fischer, 1887

Bournonia differs from *Biradiolites* in that the siphonal bands take the form of projecting longitudinal costae, separated by a single furrow or by a few minor costae and furrows. The right valve was generally attached by the whole of its anterior or, in species that favoured a muddy environment, lay recumbent, with the result that the anterior side was flattened and the valve typically assumed the form of the toe of a slipper. The dorsal, posterior and ventral sides are costate. The funnel plates turn up steeply and become nearly tangential on the flat anterior side but on the other sides are radially folded and, as in *Biradiolites,* the downfolds correspond with the costae and the upfolds with the intervening furrows. The commissure is more or less semicircular in outline, with its anterior side straight; the body cavity is oval. The left valve is opercular, usually with its umbo near the middle of the straight side, from which costae radiate to the margin where they coincide with the folds of the right valve. In the previously described species with semicircular commissures, *Praeradiolites verseyi, Monopleura jamaicensis,* the straight edge was the hinged side. This is not so with *Bournonia* which has a typical radiolite hinge with two long teeth in the left valve which slide into furrowed grooves inside the body cavity of the right; from near the base of the teeth the two myophores project, running in a ventral direction, respectively within the anterior or flat side and the posterior or curved side; the anterior myophore is attached for nearly or all its length to the inside of the left valve but the posterior myophore is pedunculate, being attached only by a relatively narrow stem to the posterior teeth or to the yoke connecting the teeth. The space thus left between the myophore and the inner surface of the left valve may have served to permit the passage of the S or exhalent siphon. This interpretation would seem to be implicit in Rutten's placing of the S band in his figures of certain species (1936, fig. 3, fig. 4k) in such a position that the corresponding siphon would have to cross the myophore; to pass below would involve piercing the muscle, but the space above it was unimpeded. It is generally difficult to distinguish the siphonal from the other costae, which they closely resemble, though they tend to be somewhat wider and more prominent.

Bournonia cancellata (Whitfield)

Plate 39, figures 5-8

Radiolites cancellatus Whitfield, 1897a, p. 190, pl. 12, fig. 4, pl. 13, figs. 3-7.
Biradiolites cancellatus (Whitfield), Trechmann, 1924b, p. 403; not pl. 24, fig. 4.
Bournonia cancellata (Whitfield), MacGillavry, 1937, p. 39.
Bournonia cancellata (Whitfield), Chubb, 1955a, p. 4; 1956c, pp. 8, 13.

Occurrence. — A common fossil in the more shaly parts of the *Titanosarcolites* Series: at Logie Green and Trout Hall in Upper Clarendon, Catadupa and the Great River Valley on the borders of St. James and Westmoreland, and elsewhere. The specimens collected by Trechmann in the St. Anns Great River Valley are believed to belong to another species described below.

Description. — A small species, the right valve either tapering towards the base or parallel-sided. It was probably recumbent. The anterior side is flat and is crossed by numerous growth lines representing the edges of the funnel plates; one or sometimes two narrow, shallow grooves run longitudinally. The convex dorsal, posterior and ventral sides have five or six rounded costae alternating with rather shallow, subangular furrows; as usual these correspond with folds in the funnel plates. A broad costa nearly in the middle of the posterior side is probably the S band; it is separated by a narrow costa between two furrows from the E band.

The left valve is moderately convex, with its umbo near the centre of the anterior side. It has low radial costae marked by plications in the thin laminae of the outer layer corresponding with those of the funnel plates; its scalloped edge fits that of the lower valve. Its cardinal apparatus is well shown in the section illustrated (Pl. 39, fig. 7). The two teeth fit into the channelled grooves of the right valve; the anterior myophore runs from the corresponding tooth in a ventral direction within the flattened anterior wall; the pedunculate posterior myophore springs from the yoke connecting the teeth, and at its ventral end there is a slight inflexion of the wall.

Dimensions. — Whitfield's largest specimen was 60 mm high; dorso-ventral diameter 50 mm, antero-posterior diameter 33 mm. The specimen figured in Plate 39 is slightly taller, its height being 70 mm; dorso-ventral diameter 45 mm, antero-posterior diameter 28 mm.

Bournonia subcancellata (Trechmann)

Plate 40, figures 1-3

Biradiolites subcancellatus Trechmann, 1924b, *pars,* p. 403, pl. 26, fig. 3.
Bournonia cancellata Chubb, 1955a, *pars,* p. 4.

Occurrence. — An uncommon fossil found in the *Titanosarcolites* Series of Logie Green, Upper Clarendon.

Description. — The shell is small to medium in size and relatively short, the height being less than the dorso-ventral diameter. From its base the right valve increases rapidly in breadth; its anterior side is flattened with steeply upturned funnel plates, these have a small sharp downfold in their middle which may express itself as a narrow longitudinal groove or ridge. The other sides are curved and bear about seven strong subangular costae; the funnel plates turn up all round at a low angle and are upfolded at the furrows and relatively downfolded at the costae. The small, simple, radial ridges, characteristic of the subfamily, are seen on the surfaces of the funnel plates. The position of the siphonal bands cannot be definitely determined.

The left valve is slightly convex with its umbo near the anterior margin; it does not appear to have radial undulations; it covered the body cavity but it is uncertain whether it extended out over the folded parts of the funnel plates.

Dimensions. — The largest specimen has a height of 42 mm; diameter, dorso-ventral 65 mm, antero-posterior 45 mm. Trechmann gave the height as 52 mm, but this figure must have been obtained by measuring around the curved posterior side.

Remarks. — In a previous publication (Chubb, 1955a, p. 4) the opinion was expressed that this species was based on short, stumpy individuals of *B. cancellata.* Recently, however, as a result of study of specimens included in the Trechmann Bequest to the British Museum (Nat. Hist.) the conclusion has been reached that it is a distinct species. It is still thought that Trechmann's specimen from St. Ann's Great River should be excluded.

Bournonia sanctannae Chubb

Plate 39, figures 9-12

Biradiolites cancellatus Trechmann, 1924b, p. 403, *pars;* pl. 24, fig. 4.
Biradiolites subcancellatus Trechmann, 1924b, pp. 403-404, *pars.*
Bournonia sanctannae Chubb, 1967, p. 28.

Occurrence. — A fairly common fossil in the *Barrettia* Limestone of St. Anns Great River Valley.

Description. — A species of medium size. It somewhat resembles *B. cancellata* but is larger, has seven or eight angular costae, and generally no incised line on the anterior side, though a trace of this may occasionally be seen. The right valve is conical and is usually curved, the dorsal side being concave, but it may be straight or even curve ventrally. On the flattened anterior side the funnel plates turn up, becoming tangential; around the dorsal, posterior, and ventral sides the funnel plates are strongly inflected, the acutely angular downfolds corresponding with the costae; the amplitude of the folds may be as much as 10 mm. The two extreme costae, the dorsal and ventral, which bound the anterior face, are usually stronger and more projecting than the others; the ventral may be a pedal fold, but it is impossible to be sure which bands were siphonal.

The left valve is convex with its umbo near the middle of the anterior side. Radial costae are poorly developed; the strong and rather rugged growth lines are only slightly undulose near the umbo, but farther out the inflexions become more marked and, at the commissure, angular projections from the margin of the left valve fit into the grooves formed by the downfolds of the funnel plates of the right. Sections show that the hinge resembles that of *B. cancellata.*

Dimensions. — Maximum height 90-95 mm; diameter: dorso-ventral 65-70 mm, antero-posterior 35-45 mm.

Remarks. — Trechmann did not differentiate between this species and *B. cancellata,* but there are considerable differences between the two species, and also in their horizon, *B. sanctannae* being found in the lowest *Barrettia* Limestone and *B. cancellata* in the *Titanosarcolites* beds.

Bournonia thiadensi Vermunt

Plate 40, figures 6-8

Bournonia sp. Rutten, 1936, p. 138, text fig. 4k.
Bournonia thiadensi Vermunt, 1937, pp. 271-272, pl. 36, figs. 4,5; text figs. 3 e-g.
Bournonia thiadensis [*sic*] MacGillavry, 1937, p. 39.
Bournonia thiadensi Vermunt, Chubb, 1956c, p. 13; 1961b, p. 421.

Occurrence. — A uncommon fossil in the outcrops of *Titanosarcolites* Limestone at the 14th mile post on the Point-Flamstead road, St. James, and in the Ducketts Land Settlement, Westmoreland, seems to belong to the Cuban species described by Rutten and Vermunt.

Description. — Rutten, who gave a transverse section showing the two teeth fitting into their grooves, their yoke, and the posterior myophore, described it as "a neat little form with strong ribs." According to Vermunt the two siphonal bands are pronounced costae, coinciding with downfolds of the funnel plates, 4 to 6 mm wide, separated by a sharp groove. Dorsally of S there are two sharp costae and ventrally of E there is another one, making five costae in all. The anterior side is flat or moulded onto the attachment surface.

The left valve entirely covers the right, it is depressed, with the apex anterior to the centre and somewhat raised; at its margin the strong ribs correspond with the grooves of the lower valve; the S and E are said to be developed as grooves, but are more probably on two of the costae.

Additionally it may be noted that the costae of the right valve are not necessarily limited to five, as there may be one or two adventitious ones, which are usually small. The shell is generally attached by its antero-dorsal side which tends to be concave as it preferred to fix itself to the convex surface of another rudist; the anterior side is nevertheless flat.

Dimensions. — Vermunt's type specimen has a height of 47 mm, dorso-ventral diameter 37 mm, antero-posterior diameter 25 mm. The largest of the Jamaican specimens illustrated in Plate 40 has a height of 40 mm, dorso-ventral diameter 45 mm, antero-posterior diameter 30 mm.

Bournonia barretti Trechmann

Plate 40, figures 4,5

Bournonia barretti Trechmann, 1924b, p. 405, pl. 26, figs. 2,2a.
Bournonia barretti Trechmann, Chubb, 1956c, p. 8.

Occurrence. — A rare fossil found in the *Titanosarcolites* Limestone of Logie Green, Upper Clarendon, and in the Great River Valley and the railway cuttings near Catadupa, St. James.

Description. — Shell of medium size, growing singly; right valve curved conical, its maximum diameter about equal to its height, attached only by the apical portion of its anterior side. It bears 14 or 15 strong angular costae, including two or three less prominent on the anterior side, alternating with angular furrows; the funnel plates are strongly downfolded at the costae and upfolded at the furrows, the downfolds forming grooves across the commissure; the costae may appear as vertical series of spoutlike processes. In some individuals the funnel plates are greatly extended on the anterior side. Body cavity oval or kidney-shaped in outline, the anterior side straight or bulging slightly inwards; dorso-ventral diameter greater than antero-posterior.

Left valve slightly convex with subcentral umbo, concentric growth lines and marginal projections fitting into the grooves in the commissure of the right valve which it nearly covers.

Dimensions. — Height of the figured specimen 60 mm; diameter: dorso-ventral 59 mm, antero-posterior 40 mm; body cavity 35 by 24 mm. The largest specimen known has a diameter at the commissure of 100 by 82 mm; height of the right valve was probably about 90 or 100 mm, of left valve 25 mm.

Bournonia baileyi Chubb

Plate 40, figures 9,10

Bournonia baileyi Chubb, 1967, p. 28.

Occurrence. — Two specimens were found in the *Barrettia* Limestone of Haughton Hall, Green Island by Mr. B. V. Bailey of the Geological Survey of Jamaica, for whom it is named. It has also been found in the *Barrettia* Limestone of St. Anns Great River.

Description. — A small to medium-sized shell, right valve conical, expanding rapidly with the result that the dorso-ventral diameter is greater than the height; it is curved with the dorsal side concave. On the smooth rounded anterior side the funnel plates turn up steeply and become tangential. The apical part of the posterior side also is nearly smooth, the costae becoming prominent nearly half way up; there are about five broadly rounded costae separated by relatively narrow and deep furrows; as might be expected the funnel plates show broad downfolds at the costae and sharp upfolds in the furrows. A characteristic feature is a strong, narrow, nearly parallel-sided ventral outfold, a spoutlike process which projects, as a flange, about 20 mm, and is only some 3 mm wide; it is separated from the next adjacent costa by a narrow, acutely angular furrow, 5 mm deep. It may be a pedal fold.

The left valve is only slightly convex, its apex seems to be but little displaced towards the anterior. Radial costae are hardly developed, but such as there are can be seen to correspond with the furrows of the right valve, while the intervening grooves extend as lappets over the sinuses in the commissure at the costae. A narrow grooved process fits into the ventral outfold of the right valve.

Dimensions. — Height of right valve 53 mm; dorso-ventral diameter 72 mm, antero-posterior 39 mm; height of left valve 9 mm.

Bournonia sanctmariae Chubb

Plate 40, figure 13

Radiolites cf. *cancellatus* Trechmann, 1924a, pp. 9,19; pl. 1, fig. 3.
Bournonia sanctmariae Chubb, 1967, p. 28.

Occurrence. — A conglomerate interbedded in the Richmond Beds or Carbonaceous Shale, near Port Maria, St. Mary, has yielded a number of rudists and Cretaceous gastropods; both the shale and the conglomerate contain an Eocene molluscan and foraminiferal fauna, and it is obvious that the Cretaceous fossils are reworked. Most of the rudists have been reduced to the condition of pebbles by rolling; these include *Thyrastylon* spp., *Bournoni cancellata* and probably other Maestrichtian fossils. But a *Barrettia monolifera* collected by the Geological Survey, and a *Bournonia* sp. collected and figured by Trechmann show little if any rolling, so there is presumptive evidence that these two specimens derive from the same nearby outcrop and are of the same age, *i.e.* Campanian. Probably the conglomerate was supplied with material from a near Campanian outcrop and a distant Maestrichtian one. The *Bournonia* (BMNH No. L63255) differs somewhat from any known species.

Description. — A small to medium-sized shell, apparently attached by the whole of its anterior side, which is flattened and rough, with its funnel plates vertical and tangential. The dorsal side also is flat with upstanding tangential funnel plates. The posterior and ventral sides have seven longitudinal costae, that nearest the dorsum being small and succeeding ones becoming progressively larger and more prominent; they are separated by narrow angular furrows; the funnel plates are sharply downfolded at the costae, the amplitude of the folds attaining or exceeding 10 mm. The sixth costa divides into two near the commissure and the seventh, which is separated from it by an angular furrow some 15 mm wide by 15 mm deep, is the most prominent and consists of a series of downturned spouts; it is probably a pedal fold.

The marginal parts of the left valve are preserved although the central part has been crushed into the body cavity. It seems to have been more or less flat, its outer layer is laminar, the laminae being folded in conformity with the folding of the funnel plates; as a result of this it has a strong radial costae, the intervening furrows corresponding with the costae of the right valve.

Dimensions. — The height is 60 mm; diameter, dorso-ventral 65 mm, antero-posterior 45 mm.

Bournonia tetrahedron Chubb

Plate 40, figures 11,12

Bournonia tetrahedron Chubb, 1967, pp. 28-29.

Occurrence. — Three individuals, of which two are immature, are attached to a left valve of *Antillocaprina occidentalis* (Whitfield), from the Maestrichtian of Logie Green, Upper Clarendon, which was included in the Trechmann Bequest.

Description. — A very small shell, tetrahedral, right valve attached by the whole of its triangular anterior face, the dorsal and ventral corners of which are prolonged as narrow, tapering, hornlike processes, closely adherent to the surface of attachment; the umbo curves ventrally. The dorsal and ventral faces are both triangular, their funnel plates turn up parallel to the surface and are mutually tangential, with the result that only the outermost funnel plate is visible and the surface is smooth; each of these faces has a slight downfold at the commissural margin, close to the nearby siphonal band. The bands are represented by two prominent costae, 3 mm wide, and the interband by a slightly broader subangular furrow; the funnel plates rise parallel to the surface in the interband but are downfolded in the bands, where they are rather widely spaced at 14 in 1 cm; here also the vertical radial plates may be seen to the number of about six in a breadth of 3 mm.

The left valve is triangular, nearly flat, not extending over the horns of the right valve, but with grooved lappets covering the siphonal costae. It has a structure similar to that of the right valve of the Radiolitinae, with parallel laminae, not in contact, resembling funnel plates, crossed by vertical radial plates, making a pattern of quadrangular cells. The outermost lamina, forming the surface of the valve, is present in the two immature shells, but is largely lost in the adult; however, some is preserved showing a low, nearly flat umbo in the middle and about 5 mm from the anterior margin; it is also preserved in the rounded groove which runs out on the lappet over the E costa; probably the S lappet had a similar groove. The hinge structure and myophores are unknown.

Dimensions. — The adult shell has a height of 23 mm; diameter, antero-posterior 16 mm, dorso-ventral, left valve 29 mm, right valve including horns 44 mm.

Bournonia coxi Chubb

Plate 44, figures 2-4

Bournonia coxi Chubb, 1967, p. 29.

Occurrence. — A single specimen consisting of two mutually adherent bivalve shells was found in the *Barrettia* Limestone of St. Ann's Great River, St. Ann. Named for the late Dr. L. R. Cox of the British Museum (Natural History).

Description. — A small or very small species. Right valve smooth, conical, height considerably greater than diameter, cross-section quadrilateral. The shell is smooth with the funnel plates turned up and becoming tangential except at the siphonal folds where they are downfolded. The bands are two smooth, rounded costae, separated by a narrow, acute furrow. There is a small outfold, probably pedal, near the E band. The siphonal area resembles that of *B. tetrahedron,* but the two right valves are attached to each other, not by their anterior sides as is usual, but by their dorsal sides. Perhaps their relationship is accidental and due to both having originally attached themselves to the same small shell.

The left valves are flat or concave with lappets extending over the siphonal and pedal folds. Their structure is similar to that of *B. tetrahedron,* with horizontal laminae separated by vertical radial plates, making a quadrangular reticulate pattern. Each left valve bears a small adherent *Ostrea* sp.

Dimensions. — The smaller shell is 35 mm high, its antero-posterior diameter is 24 mm, its dorso-ventral 22 mm; the corresponding figures for the larger are 45 mm, 32 mm, 24 mm.

Subfamily **SAUVAGESIINAE** Douvillé, 1910

Radiolitidae in which the vertical radial plates of the outer layer, by repeated bifurcation and inosculation, make a polygonal cell pattern resembling a fine honeycomb; this may be seen either on the surface of the funnel plates or in a transverse section.

(a) Sauvagesiinae with ligament

Genus **SAUVAGESIA** Bayle, 1887

Right valve cylindro-conical with numerous longitudinal costae; funnel plates show strong radial plications, the downfolds corresponding with the costae and the upfolds with the intervening furrows. The ligamental infold (L) is well developed in Jamaican species; it is shown externally by a furrow, not noticeably different from the others, but a transverse section may show a line of crowded cells extending from this furrow across the funnel plates into the infold; the latter projects several millimetres into the body cavity and may have a flange at its inner end. The siphonal bands are represented by two broadly concave sulci, the interband (I) consisting of two costae separated by a narrow furrow; the inhalent band (E) is diametrically opposite to the ligament. The inner layer is thin, lining the body cavity and forming concave tabulae below it. The left valve is depressed conical, with thin outer layer and well-developed inner layer. The hinge is of normal radiolite type.

Sauvagesia macroplicata (Whitfield)

Plate 41, figures 1-4

Radiolites macroplicatus Whitfield, 1897a, pp. 190-191, pl. 13, fig. 8; pl. 14, figs. 1,2; not pl. 12, figs. 2,3.
Sauvagesia macroplicata (Whitfield), Chubb, 1955a, pp. 4-5; 1956a, pp. 16-17, pl. 3, fig. 5; pl. 4, figs. 1,2; 1956c, p. 8.
Not *Radiolites macroplicatus* Thiadens, 1936a, pp. 1013-1014.

Occurrence. — A rare species in the *Titanosarcolites* Limestone; Whitfield's and Matley's specimens are from the Logie Green section of Upper Clarendon, and a Jamaican Geological Survey specimen from the Shortwood parochial road, St. James. Whitfield included three species under the name *R. macroplicatus,* so a lectotype was selected (Chubb, 1955a) of which Whitfield's original figure is reproduced in Plate 41, figure 1.

Description. — Shell of medium size. Right valve elongate conical, its maximum diameter being attained some distance below the commissure; above this level the outer layer becomes progressively thinner by decrease in width of the funnel plates, while the body cavity, bounded by the inner layer, continues to increase in diameter to a maximum at the commissure. The outer layer may fail to reach the commissure on the dorsal side, where the uppermost part of the shell wall may consist of inner layer only; on the ventro-posterior side, with its siphonal bands, the outer layer must necessarily reach the commissure. The valve has 14 or 15 sharp longitudinal costae, corresponding to downfolds of the funnel plates. The excessive plication of these plates is the chief specific character; the amplitude of the folds may exceed 25 mm; both the upfolds and the downfolds are sharply angular and the two limbs of a fold may be almost parallel in the middle part of their length and meet in an angle as low as 30°. The siphonal bands are deep rounded grooves and the interband consists of two costae with a relatively shallow furrow between. There are from 35 to 40 funnel plates in 1 cm; the cells forming the polygonal mosaic are between 0.25 and 0.50 mm in diameter. The maximum thickness of the outer layer is at least 25 mm, that of the inner layer only some 0.3 to 0.5 mm. The body cavity is circular; the ligamental ridge, which projects into it about 5 mm, is flat and planklike, being about 1 mm thick; it is formed by an infold of the outer layer covered by a thin envelope of inner layer.

The left valve is a low cone with central apex. The Survey specimen had two young shells of the same species growing upon it and when these were broken away a horizontal section of the left valve was obtained (Pl. 41, fig. 3). It resembles that of a caprinid; its outer layer is laminar, about 2.5 mm thick, and ornamented with concentric growth lines and low radial plications; its inner layer is thick and is penetrated by "canals" separated by a series of thin vertical plates, some of which bifurcate when traced outwards; at their internal edges these plates spread and coalesce to form the smooth inner surface of the valve. The left valve of one of the young individuals has been eroded away showing part of the hinge structure, including the teeth and the myophoric processes with denticulated outer faces, forming a horseshoe within the right valve.

Dimensions. — The lectotype in the American Museum of Natural History has lost the apical part of its right valve, which was probably originally some 90 mm high; it has a maximum diameter, about 35 mm below the commissure, of 64 mm, and a commissural diameter of 45 mm. The Survey specimen also has lost its apical part; it is 115 mm high (perhaps originally 180), and has a diameter at the lowest part preserved of 65 mm, at its widest part at least 85 mm, and at its commissure some 60-65 mm, the widest part being about 60 mm below the commissure; the diameter of the body cavity at the same levels is at lowest point 41 mm, at widest part 46 mm, and at commissure 55 mm. The small Matley specimen in the United States National Museum is 75 mm long, with a maximum diameter of 45 mm, and a commissural diameter of 35 mm.

Sauvagesia mcgrathi Chubb

Plate 42, figures 1-3

Radiolites macroplicatus Whitfield, *pars*, 1897a, pl. 12, fig. 2.
Sauvagesia mcgrathi Chubb, 1956a, pp. 17-18, pl. 3, figs. 3,4; 1956c, p. 8.

Occurrence. — Found in float and river gravel derived from the lowest limestones of the *Titanosarcolites* Series near the southern margin of the Sunderland Inlier, St. James, where it is associated with *Praebarrettia sparcilirata* (Whitfield). Whitfield's specimen came from Logie Green, Upper Clarendon.

Description. — Right valve straight cylindro-conical with nearly circular cross section, ornamented with about 14 longitudinal costae. It is of medium size with its maximum diameter at the commissure. The siphonal bands are broadly concave each attaining a maximum width of about 20-22 mm; they were originally finely costate with seven or eight low rounded longitudinal ridges; the interband is parallel-sided, about 20 mm wide, and consists of two costae separated by an angular furrow. The funnel plates are plicated, the downfolds corresponding with the costae, the amplitude of the folds being about 10 mm, and the angle between the limbs of each fold being 50° to 60°. The thickness of the outer layer varies from a maximum of about 25 mm on the ligamental side to a minimum of some 12 mm in the siphonal bands. The polygonal cell pattern is fine. The inner shell layer is about 0.5 mm thick; the body cavity is nearly circular. In one of the sections illustrated in Plate 42 the ligamental ridge is broken and its end displaced; in the other it is intact, projecting about 6 mm into the body cavity; its breadth is 0.8 mm, expanding abruptly at its inner end to 2.5 mm.

The left valve of Whitfield's specimen is the best preserved; it is depressed conical with eccentric apex, and marked by radial corrugations and concentric growth lines. That of the specimen illustrated in Plate 42, figures 1,2 has been badly eroded, but the section shows within the right valve the posterior myophore of the left valve in position attached to the posterior tooth which has been hollowed by solution; the anterior myophore and tooth are present, but are broken and displaced.

Dimensions. — The specimen illustrated is about 150 mm high, the diameter of the smaller end being about 50 mm and that of the larger or commissural end about 90 mm. The mean diameter of the body cavity is about 50 mm.

Sauvagesia fluminisagni Chubb

Plate 42, figures 4,5

Sauvagesia fluminisagni Chubb, 1956a, p. 18, pl. 4, figs. 3,7; 1956c, p. 8.

Occurrence. — A single right valve considerably eroded on its ventral and anterior sides, and with its upper part crushed, was collected in the *Titanosarcolites* Limestone of Cotton Tree Gully, Lambs River Valley, Westmoreland, near the St. James border.

Description. — This small to medium species is slenderer and more cylindrical than the two preceding. It has about 16 narrow angular costae corresponding with downfolds of the funnel plates; the amplitude of the folds is generally about 5 mm but in a few places reaches 8 mm.

and the angle between the limbs of the folds is about 60° to 70°. The inhalent siphonal band (E) is not clear owing to erosion, but it is indicated by a broad rounded upfold of the funnel plates which evidently correspond with a sunken band about 10 mm wide, diametrically opposite to the ligament. The interband is about 15 mm wide, and consists of two sharp costae with an angular furrow between. The exhalent band (S) is a flat-bottomed channel about 10 mm wide, with the funnel plates making sharp upfolds in its two corners joined by a slight broad downfold across its floor; there are indications that it had five or six small longitudinal costellae. The thickness of the outer layer is 13-15 mm except at the siphonal bands where it is only 10 mm; the cell pattern is polygonal with traces of radial structure in places. The inner layer is about 0.5 mm thick. The ligamental crest is 0.7 mm wide and projects some 3-4 mm into the body cavity.

Dimensions. — The specimen is about 150 mm high and 50-55 mm in diameter. The mean diameter of the body cavity is about 30 mm.

Sauvagesia annulosa (Whitfield)

Plate 41, figures 5-7

Radiolites annulosus Whitfield, 1897a, pp. 191-192, pl. 14, fig. 3.
Radiolites annulosus Whitfield, Chubb, 1955a, pp. 5-6; 1956c, p. 8.

Occurrence. — Only a single specimen, the holotype, is known. It is stated to have been found in the Cretaceous limestones near "Christianna," Manchester Parish; probably from the Logie Green area, Upper Clarendon Parish.

Description. — Shell of medium size, right valve straight, acutely conical, left valve depressed conical. Right valve has numerous regular varix-like rings, of which there are about seven or eight in 25 mm. The varices, each of which consists of about eight to ten funnel plates, run around the shell almost without inflections, but two broad shallow upfolds occur on the ventral side, separated by a slightly sharper downfold; the funnel plates are grouped into bands of finer and coarser sets to form the varix-like annulations. As Douvillé observed (1898, p. 123) this specimen has been much eroded; the present thickness of the outer layer is only about 1 mm on the dorsal side and 2-3 mm on the ventral, and its original thickness, and whether the funnel plates were marginally frilled or folded cannot be guessed. The cell pattern is not obvious, but a re-examination of the specimen has led to a revision of the opinion that it is radial and quadrangular (Chubb, 1955a, p. 6); it is now thought to be polygonal. A ligamental infold projects about 5 mm into the body cavity, and can be traced down the outside of the shell to the apex by a slight narrow downfold of the funnel plates.

The umbo of the left valve is near the dorsal side. The valve is much eroded and most, if not all, of the outer layer has disappeared. The inner layer thus revealed resembles that of a caprinid or of *S. macroplicata,* with vertical radial plates which, at their inner edges, spread out and unite to form a smooth lining for the valve. The hinge structure is unknown.

Dimensions. — Height of right valve 95 mm, of left valve 20 mm; maximum diameter at commissure 60 mm.

Remarks. — It is regrettable that a new species was created for such a poorly preserved specimen, and that its specific name was based on a character produced by weathering. It is here transferred from the genus *Radiolites* to *Sauvagesia* because of its apparently polygonal cell pattern.

(b) Sauvagesiinae without ligament

Genus **TEPEYACIA** Palmer, 1928

Only the right valve is known. Shell conical, nearly straight, dorso-ventral diameter less than antero-posterior; outer shell layer thin, with numerous strong, acute, longitudinal costae, corresponding with sharp downfolds of the funnel plates. The siphonal bands are smooth and lie in deep grooves which are actual infolds of both outer and inner layers, the latter thinning and bulging into the body cavity to form incipient pseudopillars; the E infold is more pronounced than the S. Inner layer generally thicker than outer; hinge located in the inner layer. Palmer described a ligamental infold but there is no such structure in the Jamaican material. No myophores seen; presumably the muscles were attached directly to the inside of the right valve as in other members of the family.

Tepeyacia multicostata Chubb

Plate 43, figures 1-4

Tepeyacia multicostata Chubb, 1967, p. 29.

Occurrence. — In Cretaceous tuffaceous shaly material, NNE of Seafield Manse, where it is associated with *Sabinia totiseptata* Palmer and *Sphaerucaprina seafieldensis* Chubb. The matrix attached to and infilling the shells is mainly a finely conglomeratic tuff. One specimen (Pl. 43, fig. 2) shows graded bedding in its interior; evidently when buried it was lying on its posterior side, and it contains coarse tuff on this side which grades into a fine material on its anterior side.

Description. — A small species, obviously closely related to, though not identical with *T. corrugata* Palmer. Right valve conical, the height somewhat greater than the diameter, and the antero-posterior diameter slightly greater than the dorso-ventral. It is ornamented with numerous sharp costae, at least 50, and in the larger shells perhaps as many as 90; these correspond with acutely angular downfolds of the funnel plates comparable with those of *Sauvagesia macroplicata* (Whitfield) though on a much smaller scale. The siphonal bands lie in deep rounded grooves and the interband is marked by several angular costae.

Sections show that the outer layer is relatively thin and the inner thick, in places thicker than the outer. A fine polygonal cellular pattern may be seen in the siphonal areas of the outer layer where the funnel plates are nearly horizontal. There is no ligamental infold but the hinge is well developed, the tooth N, nearly square in section, having flanges at its two free corners; it is flanked by two long transversely oval sockets which, in the higher parts of the body cavity, are mere vertically striated grooves between the tooth and anterior and posterior buttresses which curve inwards from the wall. In the deeper parts these buttresses are connected with the flanged corners of the tooth by extremely thin laminae which separate the sockets from the body cavity. The S and E grooves are sharp infolds of both shell layers, but the inner layer is much attenuated at the infolds, reducing though not eliminating the bulges into the body cavity, which form slight pseudopillars. The E band is diametrically opposite the tooth. The ventro-posterior (*i.e.* the siphonal side) is slightly flattened, with the result that the body cavity is oval. The inner layer forms tabulae only in the deeper parts of the shell, the body cavity being open nearly to the bottom.

The left valve is unknown except that the end of its two teeth may be seen in the deeper parts of the sockets of the right valve; they are transversely oval and fluted on their outer faces to correspond with the flutings of the sockets.

Dimensions. — There are two specimens: (a) antero-posterior diameter 38 mm, dorso-ventral 34 mm, height 35 mm: corresponding figures for (b) 48 mm, 41 mm, 45 mm.

Remarks. — The Jamaican material is superior to the specimens of *Tepeyacia corrugata* found by Palmer (1928, pp. 46-47) in the Tepeyac Mountains, south of Puebla, Mexico, and by Thiadens (1936b, pp. 1133-1134) in the Provincial Limestones of southern Las Villas, Cuba. The latter author found no trace of a ligamental infold and rightly thought that Palmer's figure, which purported to show one, was far from convincing. He, however, believed that he had found traces of myophores, but his own figure fails to carry conviction. Owing to the alleged absence of vertical radial plates Palmer included *Tepeyacia* in the Monopleuridae, but Thiadens, although he did not find such plates, thought the Cuban form more closely related to the Radiolitidae. Kühn (1932, p. 178) included it in the Radiolitidae. The discovery of a polygonal cellular structure in the Jamaican specimens leaves no doubt that they belong to the family Radiolitidae, subfamily Sauvagesiinae; the difficulty in recognising this structure is due to the intense folding of the funnel plates which, in a cross cut, are seen in almost vertical section except in the siphonal areas.

T. multicostata differs from *T. corrugata* in having twice or thrice as many costae and in being less flattened, though it may be suspected that the flattening of Palmer's specimen has been accentuated by crushing. One of Thiadens' specimens is not much more flattened than the Jamaican material.

Tepeyacia multicostata is one of the earliest and most primitive of the ligamentless Sauvagesinae. As noted above *Tepeyacia* and *Caprinuloidea* have been found by Bob Perkins in Texas rocks of Albian age, so it is probable that the Seafield Series, including limestone and tuff, belongs to this period.

Genus **DURANIA** Douvillé, 1908

Durania typically has a polygonal cell pattern and is generally defined as being essentially like *Sauvagesia* except for the absence of the ligamental ridge. But there seems to be less tendency to plication of the funnel plates, which are often more or less flat and horizontal; this is especially true of Jamaican species. The siphonal bands are represented by two grooves or furrows, which may be sharply angular or broadly concave; in the latter case they may be smooth or finely costate. The interband consists of one or two costae, rounded or angular.

Durania nicholasi (Whitfield)

Plate 43, figure 6; Plate 44, figure 1; Plates 45,46

Radiolites (Lapeirousia) nicholasi Whitfield, 1897a, pp. 186-188, pls. 6-9.
Lapeirousia nicholasi (Whitfield), Trechmann, 1924b, pp. 405-406.
Durania nicholasi (Whitfield), Kühn, 1932, p. 108.
Durania nicholasi (Whitfield), Chubb, 1955a, pp. 2-3; 1956c, pp. 7-8.
Durania cf. *nicholasi* Chubb, 1959, pp. 743-746, fig. 10.

Occurrence. — This is the only rudist species that has been found in Jamaica in association with both *Barrettia* and *Titanosarcolites*. It occurs in the limestones of the *Barrettia* Series at New Ground in the St. Ann's Great River Valley, St. Ann; in the Stapleton Limestone of the Sunderland Inlier, St. James; and in the Haughton Hall Limestone of the Green Island Inlier, Hanover. It is found also in the lowest beds of the *Titanosarcolites* Series in the Logie Green area of Upper Clarendon, where it is associated with *Praebar-*

rettia sparcilirata. Right valves, generally incomplete, are common in all these localities, but only one free left valve has been found.

Description. — This is a gigantic species having the largest diameter, though not the greatest height, of any Jamaican rudist, the adult right valve commonly having a diameter of 450 mm or even more. The height may be as great but is usually less the characteristic form being turbinate or depressed conical with a large apical angle. The external surface is rugged with annular ridges running around it, but it is generally badly weathered or eroded and the posterior wall, being the thinnest, is rarely preserved. A specimen figured by Whitfield (1897a, pl. 7, fig. 2) and reproduced here in Plate 43, figure 6, retains this wall, which shows two grooves about 40 mm apart at the base, diverging to 140 mm at the commissure; the intervening area is convex. No doubt these grooves are siphonal.

A specimen in the museum of the Institute of Jamaica, Kingston, figured in Plates 44 and 45, shows a broad rounded furrow extending from the base to the commissure, increasing in width from about 40 mm at the lowest part preserved to 70 mm at the commissure; its depth is a little less than half its width. This is certainly the E band; the S band is broken away.

The diameter of the body cavity is generally about one third of that of the valve, varying between one quarter and two fifths. The wall, except on the posterior side, is extremely thick, usually wider than the body cavity, while that on the siphonal side is much less. Whitfield, who believed this to be the cardinal side, gave its thickness as 25 or 50 mm, but in the Institute specimen the thickness in the E band is only 15 mm, and this band bulges into the body cavity to form an incipient pseudopillar as in *Tepeyacia.* The S band does not form a pseudopillar.

The body cavity is conical extending to the base of the shell. In low broad individuals it is generally open to the bottom, and the inner layer which lines it does not form tabulae. But in the Institute specimen, which is nearly as high as it is broad, the deeper parts of the cavity are filled with vesicular tissue resembling that described below under *Chiapasella radiolitiformis.*

The funnel plates of the outer layer are extremely thin and close set so that there may be as many as 100 in one cm. Usually they are in contact, when no cell pattern is visible, but exceptional specimens show a fine polygonal pattern. The great thickness of the wall is due to the enormous width of the funnel plates which may attain 180 mm or more around the dorsal, anterior, and ventral sides. They show radial vascular grooves which branch dichotomously or laterally several times. The plates are smooth or gently undulating and have no sharp folds except at the siphonal bands. The downfold at the E band may have an amplitude of 70 mm, steep even precipitous at the sides, but levelling to a gentle curve across the bottom of the groove; there is a sharp upfold at the S band, well shown in Whitfield's figure (see Plate 43, figure 6).

The only known free left valve is that described and figured by Whitfield (1897a, pls. 8,9). It is a thick and massive shell, convex, with a diameter much less than that of the right valve, though somewhat greater than that of the body cavity, which it overlaps by some 12-20 mm. It is transversely oval, its antero-posterior diameter being the greater. The teeth are oblique, relatively short and thick, the anterior the longer, united by a yoke in the form of a vertical plate which is nearly as tall as the posterior tooth. The anterior myophore is a strong vertical process, separated by a notch from the anterior tooth, and curving around within the margin of the right valve; the posterior myophore is a horizontal triangular plate, attached by a relatively narrow neck, and spreading out towards its abutment against the greatly thickened inner layer of the body cavity of the right valve, where it ends in numerous denticulations.

Dimensions. — The principal dimensions are given above; the average diameter of the right valve is some 400 mm and the maximum 600 mm. According to Whitfield the height is "probably somewhat greater"; Trechmann described it as "sometimes two feet in height and over a foot in diameter." In both these estimates the height is exaggerated; it may equal the diameter but is usually less. The body cavity is generally some 120 to 150 mm in diameter. The thickness of the wall, corresponding to the breadth of the funnel plates, on the dorsal, anterior and ventral sides, is from 150 to 200 mm; on the posterior side perhaps about 25 to 50 mm, and in the E band 15 mm. The diameter of the left valve is antero-posteriorly 155 mm, dorso-ventrally 120 mm; height above commissure 50 mm.

Remarks. — Whitfield ascribed this species to Bayle's genus *Lapeirousia,* but it lacks the true pseudopillars in the right valve and the oscules in the left that characterize that genus. He described a plate and ridge, which are attached to the left valve, as a fragment of the right. In an earlier publication (Chubb, 1955a, p. 2) this statement was discredited and the view was expressed that the plate and ridge were an integral part of the left valve. It is now believed that Whitfield was right and the plate and ridge are part of a thickened inner layer of the right valve. The doubt was partly due to the fact that no such thickened inner layer has been seen in any of the many right valves that have been examined. The ridge is a process which penetrates between the posterior tooth and the posterior myophore; such a process is common in the Radiolitidae, it is seen for example in the figured section of *Bournonia cancellata* (Plate 39, fig. 7).

MacGillavry (1937, pp. 40-42) included several species, among them *Radiolites (Lapeirousia) nicholasi,* in a group which he called *Bournonia* new section, "characterized by the nature of the siphonal region. E is a broad, flat-bottomed downfold of the funnel-plates. At the posterior side of E the funnel-plates slope suddenly and dizzily upwards. The highest point is reached at the exhalent siphonal band, S, where they form a flat, narrow, slightly depressed top, to slope downward, but not as steeply again, on the other side of S."

MacGillavry's "new section" appears to be a natural group, but it cannot be ascribed to *Bournonia,* which has a quadrangular cell pattern, a flattened anterior side, and siphonal bands in the form of costae not grooves.

Durania cf. **aguilae** Adkins

Plate 43, figure 5

Durania sp. cf. *D. aguilae* Chubb, 1956a, pp. 18-19, pl. 4, figs. 5,6; 1956c, p. 7.

Occurrence. — A simple incomplete right valve was found in the *Barrettia* Limestone near mile post 9 on the Kensington-Amity Hall road, St. James. This is a continuation of the Stapleton Limestone outcrop.

Description. — Right valve large, broadly conical at the base with apical angle of about 60°, turning up rather abruptly and becoming more cylindrical, with a mean diameter at the commissure of 160 mm. A slight inward inflection of the wall, some 30 mm wide, resembling one of the rudimentary pseudopillars of *Tepeyacia,* represents the E siphonal band; the part of the wall where the S band would be expected is missing. The maximum thickness of the wall is 25 mm, the minimum thickness is 9 mm at the E band. The funnel plates, of which there are about 40 in 1 cm, are crossed by radial vascular grooves, many of which branch once. The plates turn up slightly from the inner shell layer but soon become horizontal except at the E band, where they continue the upward slope to their outer margin; they are uninflected except at their peripheral edge which is sharply folded, the downfolds being about 5-8 mm wide around most of the circumference, but only 2 mm wide in the E band. The outer surface is nearly everywhere covered with rock material, but where small areas are visible rounded costae may be seen corresponding with the downfolds and rising about 1 mm above the intervening furrows; in the E band the costellae are some 2 mm wide. The cell pattern is polygonal, the diameter of the cells being 0.3-0.5 mm. The inner layer is 0.7-1 mm thick; it is not known whether it forms tabulae.

The left valve is unknown.

Dimensions. — Height of the specimen 92 mm; diameter at the lowest part preserved 135 by 90 mm; commissural diameter 175 by 140 mm.

Remarks. — This form resembles *D. aguilae* Adkins which, though smaller, has similar proportions and similar slight inward inflexions of the S and E bands. Adkins' species, however, is more strongly ribbed and increases in diameter much more gradually than the Jamaican form.

Genus **CHIAPASELLA** Mullerried, 1931

Shell of medium to large size, right valve conical or cylindro-conical; left valve depressed conical in youth, becoming high conical and arched or coiled, and overhanging the dorsal margin of the right valve in maturity.

The right valve is usually costate, the costae being rounded and intervening furrows angular. The siphonal bands are probably on two of the costae but are difficult to distinguish. The outer layer is thick and is composed of funnel plates which are more or less horizontal, not generally being downfolded at the costae and hardly upfolded at the furrows. Some of the furrows mark the position of infolds which penetrate the outer layer to about the middle of its thickness; they are club-shaped in cross section and the margins of the funnel plates are turned up against them. Inner layer thin, lining the body cavity and filling its lower part with irregular tabulae or vesicular tissue.

The left valve has a smooth surface, sometimes with a few broad, shallow, rounded furrows, separated by low rounded ridges, which converge towards the umbo; this is nearly centrally located on the patelliform valve of young individuals, and arched and overhanging on that of adults. The outer layer is thin and laminar; its commissural edge is turned out and scalloped, with rounded lappets which fit over the costae of the right valve. The inner layer is thick and in youth resembles that of *Sauvagesia macroplicata (q.v),* being composed of vertical radial plates or septa, some of which bifurcate when traced outwards, separated by empty spaces; at their internal edges these septa spread and unite to form a smooth lining for the valve. In the long curved adult valve these septa extend to the umbo, and the innermost part of the inner layer fills the deeper part of body cavity with vesicular tissue as in the right valve.

The cardinal apparatus is of normal radiolite type, with two externally channelled teeth united by a yoke, sliding in channelled grooves in the body cavity of the right valve which has no tooth or ligament. The myophores run around within the anterior and posterior margins of the body cavity; the posterior myophore is comparatively short; the anterior is exceptionally long extending at least to the ventral point or even beyond it.

Chiapasella radiolitiformis (Trechmann)

Plate 47, figures 1-4; Plate 48, figures 1-4

Coralliochama radiolitiformis Trechmann, 1924b, pp. 406-407, pl. 24, figs. 1,2,2a,3.
Chiapasella radiolitiformis (Trechmann), Mullerried, 1931, pp. 244-252, figs. 1-11.
Chiapasella radiolitiformis (Trechmann), Chubb, 1956c, p. 8; 1959, p. 746.
Not *Chiapasella radiolitiformis* Boissevain and MacGillavry, 1932, pp. 1308-1312.

Occurrence. — A common fossil in the *Titanosarcolites* beds wherever they occur in Jamaica, especially in the Logie Green area of Upper Clarendon, the Chatsworth, Vaughansfield, and Catadupa areas of St. James, and Lambs River and Ducketts areas of Westmoreland.

Description. — A large species though not, by Jamaican standards, gigantic. It is usually solitary though clusters of half a dozen shells have been found.

An adult right valve is normally cylindro-conical; it has from 16 to 20 low rounded longitudinal costae, separated by angular furrows; in well-preserved specimens fine longitudinal costellae, less than 1 mm wide, are superimposed on the costae. In some individuals the right valve was broadly turbinate in youth but, after attaining a maximum breadth, the walls turned up abruptly and the diameter became somewhat reduced; at the horizon where the direction of growth changed the costae project as "thumb-like outward or downwardly directed prolongations" (Trechmann, 1924b, p. 406). Two of the costae, which have a number of longitudinal grooves, represent the siphonal bands; between them the interband consists of two normal costae. In the outer layer the funnel plates are unfolded except for a small but sharp upturn at the club-shaped infolds. The cellular pattern is sometimes radial close to the body cavity, but is normally polygonal, the mean diameter of the cells being about 1 mm. The inner layer does not form the concave tabulae which are usually found in elongated rudists, but an irregular and complex system of small domed plates, convex towards the body cavity, forming a vesicular tissue, resembling that of certain Palaeozoic corals such as *Michelinia.*

The left valve in young individuals is a low, broad cone, with its umbo eccentric towards the dorsal side; in older forms high and strongly arched with its umbo incurved and overhanging the dorsal margin of the right valve, so that it resembles the left valve of a caprinid. The smooth outer layer is from 0.5 to 1 mm thick; it is often partly or wholly removed by weathering or erosion, when the underlying vertical septa of the inner layer may be seen. In adults, within the septate zone, the inner layer forms a vesicular tissue of small domed plates convex towards the body cavity, similar to those of the right valve. A section shows that the septate zone merges into the vesicular zone, with no plane of demarcation between them, proving that they belong to the same shell layer. The outer layer is clearly demarcated from the septate zone.

The hinge and myophores have not been seen but there is no reason to suppose that they differ from those of the closely related species *C. pauciplicata* Mullerried which has been described (under the name of *C. radiolitiformis*) by Boissevain and MacGillavry (1932, p. 1311, fig. 6) and *C. cubensis* Rutten, described by its author (1936, p. 140, fig. 4h). See generic description above.

Dimensions. — According to Trechmann his largest specimen was about 206 mm high and 117 mm in maximum diameter; the height of the left valve was generally about half that of the right. The largest specimen shown in Plate 48 is 260 mm high, but before the loss of the apical part of its right valve it was probably well over 300; its commissural diameter is: antero-posterior 150 mm, dorso-ventral 130 mm; the left valve is perhaps half the original height of the right but, measured around the outside of the curve, it would be considerably longer. The outer layer of the right valve is up to 25 mm thick, the inner layer 0.5 mm. The specimens found by Mullerried in Mexico were all considerably smaller.

Remarks. — There has been much confused thinking about this species. It was first described by Trechmann who, misled by the left valve, believed it to be a caprinid and ascribed it to the Mexican and Californian genus *Coralliochama;* he thought that the resemblance of the right valve to a radiolite was deceptive and perpetuated this opinion in the specific name, *radiolitiformis.* Mullerried (1931) found the same species in Mexico, and created the new genus, *Chiapasella,* for it; he believed it to be between the Caprinidae and the Radiolitidae to be related somewhat to the Hippuritidae and to the Chamidae. His description is diffcult to follow owing to his unusual use of terms, *e.g.* anterior and posterior for ventral and dorsal, right and left for posterior and anterior; the siphonal zones are described (p. 250) as concave, and later in the same paragraph as convex; probably he meant to convey that the bands are concave in the left valve and convex in the right, but this is not stated. Mullerried also claimed that there were three layers in each valve; in the right a cortical layer in addition to outer and inner, while in the left the actual outer layer was regarded as cortical and the septal zone as the outer layer. The so-called "cortical layer" of the left valve was stated to be up to 1 cm thick; in Jamaican material the thickness of this outer layer is generally less than 1 mm.

Mullerried (pp. 252-253) described another Mexican species, *C. pauciplicata*. This and other species have also been found in Cuba (Boissevain and MacGillavry, 1932, pp. 1308-1311; Palmer, 1933, pp. 101-102; Rutten, 1936, p. 140; Vermunt, 1937, pp. 274-275; MacGillavry, 1937, pp. 44-45). The Utrecht geologists discussed the structure of *Chiapasella* and, in his last-mentioned publication, MacGillavry correctly placed the genus in the family Radiolitidae and clarified the problem of the shell layers. He explained that the "cortex" of the right valve is only a compact outer part of the outer shell layer, present in some specimens but not in others; in the left valve the "cortex" is the outer layer, and the canal-bearing zone belongs to the inner layer. It follows that there are only two layers in each valve.

Kühn (1932, p. 97) too, included *Chiapasella* in the Radiolitidae; there can be no question that this is its correct taxonomic position because its hinge is of radiolite type and other members of the family have caprinid-like left valves. Its polygonal cell pattern puts it in the sub-family Sauvagesiinae. Thus there is nothing remarkable about the internal structure of *Chiapasella*. The genus is exceptional, perhaps unique among the Radiolitidae, only in the height and curvature of the left valve. This valve would seem to have been unduly large, clumsy and heavy, although its weight was kept as low as possible by economy in the use of calcareous material. Such a valve seems unsuited to the radiolite hinge with its vertical uplift yet, judging by its abundance, *Chiapasella radiolitiformis* was a highly successful species.

Family **HIPPURITIDAE** Gray, 1848

The right valve is conical or cylindrical, fixed by its apex and its anterior side, often being in contact with others of the same species for its whole length. Its surface may be ornamented with longitudinal costae or may be smooth. The outer layer consists of funnel plates without vertical radial plates, and the inner layer is smooth, lining the body cavity and forming concave tabulae below it.

There are normally three principal longitudinal furrows indicating infolds of the outer layer. These project into the body cavity where they are enveloped in thin infolds of the inner layer. They form vertical pillars: the first, dorsal in position, evidently supported the ligament; the second, close to the posterior myophore, shows the position of the exhalent siphon(S); and the third that of the inhalent siphon (E).

The left valve is opercular, flat, slightly convex, or rarely concave; its surface is porous. Its margin shows infolds coinciding with the infolds of the right valve. The S and E infolds open up at their inner ends to form round or oval apertures or *oscules*, and it was obviously through these oscules that the animal's siphons communicated with the surrounding water. The withdrawal of the siphons away from the margins seems to have been an adaptation to crowded conditions, for the Hippuritidae might live in clusters of scores or even hundreds of shells.

The hinge structure somewhat resembles that of the Radiolitidae, and uplift of the left valve was vertical. But the right valve retains its single tooth; it rests against the ligamental ridge, is vertically grooved on both sides, and stands between two deep sockets. The two long vertical teeth of the left valve fit into the grooves and occupy the sockets. These two teeth are generally unequal, the anterior is the larger and the corresponding myophore curves around within the anterior side of the body cavity as in the Radiolitidae; the posterior myophore, however, is small, peglike, and fits into a cavity in the right valve between the posterior socket and the S pillar. In some forms the hinge is oblique to the line of the ligamental infold, leaving room for an accessory cavity in front of the anterior socket.

For the purposes of this monograph the Hippuritidae of the Western Hemisphere are divided into two subfamilies: the Hippuritinae[1], with not more than three infolds, and the Barrettiinae, with multiple infolds. This leaves undecided the position of *Pironaea,* an Old World genus with multiple infolds which some regard as an ancestor of the *Barrettiinae,* but which is probably an independent though parallel development.

Subfamily **HIPPURITINAE,** n. subfam.

Hippuritidae with only three infolds of which one, the ligamental, may be small or rudimentary. The two siphonal folds are generally well developed, forming pillars in the body cavity. There are always two oscules in the left valve; they were formed by infolds of the margin, starting as notches which, as growth proceeded, became occluded, their development keeping pace with the infolding of the S and E pillars of the right valve. Stages in the process may be seen in immature shells. The pillars of the right valve completely blocked the oscules when the shell was closed making it necessary for the hippurites, like most other pelecypods, to separate their valves slightly to gain access to sea water. The mantle lobes were probably united around the periphery, preventing the inflow or outflow of fluid except through the siphons, like the leather of a bellows.

---

[1] The term Hippuritinae was used by MacGillavry (1935) to include all the Hippuritidae, which he regarded as a subfamily of his family, Gyropleuridae. This view is unacceptable. Hippuritinae is here used in a new sense and is treated as a new subfamily.

In this subfamily the left valve is penetrated by a great number of thin-walled, branching canals, which radiate from the umbo in its centre. The pattern is more complex than that seen in the corresponding valve of the Caprinidae and certain of the Radiolitidae, from which it also differs in that the canals open to the exterior by means of a network of small pores, whose shape, whether linear, polygonal or reticulated was used by Douvillé (1890) for classification. But the left valves of the Jamaican Hippuritinae are rarely preserved and here the classification of Toucas (1903), which depends mainly on the development of the ligamental ridge, is adopted. Hippuritinae are rather rare in Jamaica and only three genera are known.

Genus **ORBIGNYA** Woodward, 1862

Hippuritinae in which the ligamental pillar is represented only by a slight angular inflexion of the shell wall, but the two siphonal pillars are well developed. The hinge line is nearly or quite parallel to the dorsal margin, *i.e.* at right angles to the line of the ligamental infold. Most species were gregarious.

Orbignya mullerriedi Vermunt

Plate 49, figures 1,2

Hippurites (Orbignya) sp., Trechmann, 1924b, pp. 396-397, pl. 23, fig. 5.
Orbignya mullerriedi Vermunt, 1937, pp. 261-264, pl. 36, figs. 1-2, text figs. 3a-d.
Hippurites mullerriedi (Vermunt), MacGillavry, 1937, p. 110-111, 123, fig. 2.
Hippurites (Orbignya) mullerriedi (Vermunt), Chubb, 1956a, p. 19, pl. 4, figs. 4,8; 1956c, p. 8.

Occurrence. — A rare fossil in the *Titanosarcolites* Limestone of the Logie Green section, Upper Clarendon; in the Great River Valley opposite Catadupa, on the borders of St. James and Westmoreland; and in the Ducketts Land Settlement, Westmoreland.

Description. — A small gregarious species, the right valves taper gradually and form clusters by mutual adherence for their whole length. Shell smooth with occasional growth lines, several slight longitudinal folds, and three longitudinal furrows corresponding with the pillars. As MacGillavry (1937, p. 111) showed, the upturned funnel plates have a series of narrow, radial upfolds which extend from one funnel plate to the next. These resemble the radial plates of the Radiolitinae but have a different origin and structure. The ligamental infold is an open one, forming an inconspicuous pillar triangular in section, broad at the wall and obtusely angular at the inner end; deeper in the cavity it appears to widen and develop a broad open groove on its inner face and relatively deeper and narrower grooves on its two flanks; this extension constitutes the tooth (N), it is part of the inner layer, but is closely moulded onto the L pillar and hardly protrudes beyond it; the hinge line is parallel to the valve margin. In the largest shell the S pillar projects 6 mm into the body cavity. It is 2 mm thick near the base and 3 mm near the end; the E pillar projects 8 mm, with a width of 1.5 mm near the base and 3 mm at the end. The angular distance between L and E is 140° to 150° with S about midway between them.

The left valve is unknown.

Dimensions. — Maximum length of right valve 135 mm; diameter at the commissure 22-37 mm; thickness of wall 2.5 to 4 mm.

Orbignya ceibarum (Chubb)

Plate 49, figure 3; Text-figure 6

Hippurites cf. *incisus* Mullerried, 1930, pp. 165-168, figs. 1,2.
Hippurites mullerriedi MacGillavry, *pars,* 1937, p. 111, lines 35-39, pl. 5, fig. 6.
Hippurites (Orbignya) ceibarum Chubb, 1956a, pp. 19-21, pl. 4, figs. 9,10, text fig. 4; 1956c, p. 8.

Occurrence. — A single specimen from the *Titanosarcolites* Limestone of Cotton Tree Gull, Lambs River, Westmoreland.

Description. — A very small gregarious species, the specimen including at least ten mutually adherent right valves, some of them showing fragments of the left valve. It is smaller and shorter than *O. mullerriedi.* Right valve subcylindrical, slightly curved or straight, with rounded longitudinal costae about 4 to 5 mm wide, except on the anterior side where there are three or four angular costae separated by broad rounded grooves. The S and E furrows are definite angular infolds, the L furrow a shallow open inflexion. The outer layer, about 2.5 to 5 mm thick, seems to have a structure similar to that of *O. mullerriedi.* Internally the L pillar is low and broad, and rounded rather than angular; the S pillar is hardly if at all constricted and projects about 4 mm with a width of 3 mm; the E pillar is constricted at the base, projects 4 to 6 mm, and widens from 2 to 3 mm. The approximate angular distances between the pillars are L:S 60°, S:E 60°. The inner layer is 0.5 to 0.8 mm thick, but in the depths of the valve it thickens in the recesses between the pillars, reducing their protuberance; it also thickens to form low vertical ridges in the antero-dorsal corner of the body cavity, and between the L and S pillars;

these ridges, presumably forming the outer margins of the sockets, do not appear in sections near the commissure. The inner layer also forms the single tooth (N), which extends inwards from the L pillar a distance of 2.5 mm; it is 2 mm wide and has two vertical lateral grooves and a terminal groove, the three grooves being delimited by four acutely angular vertical flanges; the tooth is less prominent deeper in the valve. The hinge line is parallel to the dorsal margin.

Surviving fragments of the left valve show that the pores were reticulate. The largest shell in the group shows a swastika-like process (Pl. 49, fig. 3) with four bent arms that penetrate between the pillars, and two teeth that fit into the lateral grooves of the tooth N. A section lower down (Text-fig. 6) shows the process somewhat broken and displaced, but the interlocking teeth can be seen and, of the four arms, only two survive; these are the myophores, the posterior fitting between the L and S pillars, and the anterior curving around within the wall, as in other hippurites. The other arms of the swastika were no doubt mere ridges on the under side of the left valve, serving to strengthen it and to help it lock in the correct position when closed.

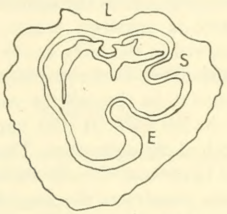

Text-figure 6. *Orbignya ceibarum* Chubb. Transverse section of right valve a few mm below the commissure; × 2. Compare with the section at the commissure shown in the right centre of Plate 49, figure 3.

Dimensions. — Length of right valve 60 to 80 mm; diameter at the commissure 15 to 20 mm; thickness of wall 2.5 to 6 mm.

Orbignya maldonensis (Chubb)

Plate 50, figures 4-6

Parastroma maldonensis Chubb, 1956a, pp. 21-23, pl. 5, figs. 1-6; 1956c, p. 8.

Occurrence. — A single specimen, a fragment of a cluster that included at least three right valves, was found in the *Titanosarcolites* Limestone south of Maldon cross roads, St. James.

Description. — Shell of medium size; it is the largest species of *Orbignya* known in Jamaica, having at least twice the diameter of *O. mullerriedi.* Right valve cylindrical, tapering gently, its smooth surface showing three furrows, the ligamental furrow hardly perceptible, the S and E furrows narrow, shallow, and sharp angular infolds. In the deep body cavity the L pillar protrudes 3-5 mm, it is broad based and obtusely angular with rounded summit; the S pillar protrudes some 13 mm; it is almost parallel sided and is 5-8 mm wide; the E pillar protrudes 17-18 mm, it is constricted near the wall to 2 mm and widens near the inner end to 6-7 mm. The angular distance between L and E is 150°, with S midway between them. In one of the incomplete shells the E pillar is anomalous, a secondary pillar grows beside it and increases in size while the original pillar becomes thinner and less protuberant; at a higher level the new pillar probably replaced the old.

The outer layer consists of horizontal or slightly upturned funnel plates, which are penetrated by numerous fine vertical capillary tubes, oval, kidney-shaped or vermicular in cross section; the tubes consist of upturned collars, surrounding perforations in the funnel plates, which extend up to the corresponding perforation in the next funnel plate; thus each tube comprises a continuous succession of short tapering rings fitting one into another. The average diameter of the tubes is 0.25 mm and their distance apart about the same; near the inner and outer margins the tubes are radially extended. As a result of this structure a cross section of the outer layer has a superficial resemblance to the corresponding layer of one of the Sauvagesiinae.

The inner layer is about 0.6 mm thick. It forms a series of inverted conical tabulae below the body cavity, with infolds around the pillars and the minor ridges of the outer layer. The hinge tooth is not obvious.

The left valve is unknown.

Dimensions. — Only a fragment 93 mm long is preserved, its original length was probably at least 150-200 mm; maximum diameter 65 mm dorso-ventrally by 85 mm antero-posteriorly; thickness of wall 10-15 mm; depth of body cavity over 75 mm.

Remarks. — This species was originally attributed to *Parastroma,* as it was believed to belong to the same genus as *P. sanchezi* Douvillé (1926, pp. 133-134). This was first recognised as a rudist by Palmer (1933, p. 97), who described it under the name of *Orbignya sanchezi* as "compuesta de placas en forma de embudo (funnel plates) . . . . la porcion central de la concha (funnel plates) se encuentra perforada por finos tubos capillares verticales (Lam. 3, fig. 2)." The latter figure shows a structure apparently identical with that of the outer wall of *O. maldonensis.* Subsequently *O. sanchezi* was transferred back to *Parastroma* by MacGillavry (1935, pp. 559-560). Palmer had previously

(1928, p. 13) made it clear that the funnel plates belonged to the outer layer, so it appeared that these were the plates perforated by the fine tubes, especially as, in a paper written in Spanish, he twice inserted the English term (funnel plates) in an apparent attempt at clarification. Actually in *Parastroma sanchezi* it is not the funnel plates but the tabulae below the body cavity that are penetrated by the tubes; *maldonensis* is, therefore, transferred to the genus *Orbignya.*

Genus **VACCINITES** Fischer, 1887

Hippuritinae in which the ligamental ridge is well developed, generally thin and extending far into the body cavity. Siphonal pillars unequal, the S pillar variable, the E pillar always longer and usually constricted near the wall, expanding towards the interior of the body cavity. The hinge line is always inclined at a high angle to the dorsal margin and usually at a lower, sometimes a very low angle to the ligamental ridge; this leaves room for a large anterior accessory cavity. The three pillars are generally relatively nearer together than in *Orbignya.*

Vaccinites eyrei Chubb

Plate 50, figures 1-3

Vaccinites sp. Chubb, 1962/1963, p. 12.
Vaccinites eyrei Chubb, 1967, p. 29.

Occurrence. — Three right valves were collected from the Clifton Limestone, some three miles southeast of Lucea, Hanover, where they were associated with *Barrettia.* Named for Mr. L. A. Eyre, who first found it during a field-class of senior students from Rusea's High School, Lucea, Hanover.

Description. — Two of the shells (a and b) are depressed conical or even discoidal, the height being only one half or one third of the diameter; the umbo is eccentric, towards the dorsal side. The third, incomplete specimen (c) apparently grew in an irregular discoidal form to a diameter of about 80 mm, beyond which its walls turned abruptly upwards diverging somewhat so that the form is a curved, inverted, truncated cone highest on the ventral side. Shell of medium size, smooth or with slight costae about 2 mm wide; the vertical part of the wall has the usual three infolds and irregularly spaced incremental corrugations. Funnel plates show slight, irregular radial wrinkling. The ligamental pillar is thin and tapering, curving gradually and, at its inner end, sharply, to the anterior; it extends up to half way across the body cavity. Both the S and E pillars are constricted near the wall to a width of about 2 mm and expand inwards to 6 or 8 mm; the E pillar of specimen (b) swells to 15 mm. The spacing of the pillars differs in different specimens; in a depressed conical form (a) with a circumference of 250 mm, the distance L:S is 40 mm, S:E 30 mm; in a discoidal form (b) with circumference 283 mm, L:S is 31 mm, S:E 35 mm; in the third specimen (c) with vertical walls, L:S is 35 mm, S:E 40 mm; the circumference of the last is unknown but was probably about 330 mm. In the first, the distance L:E is some 28 per cent of the circumference, in the second 23.2 per cent, and in the third about 22.7 per cent. The discrepancy is chiefly in the distance L:S which varies between 10.6 and 16 percent; the distance S:E remains fairly constant at 12 to 12.5 percent of the circumference. The approximate angular distances between L and E are (a) 90°, (b) 60° and (c) 55°. The discoidal specimen (b) shows the H-shaped tooth N attached to the convex posterior side of the ligamental pillar.

The left valve is unknown except that its cardinal apparatus is preserved in the body cavity of the first specimen (a) mentioned above. The teeth cannot be distinguished as the section seems to be through the yoke which connects the two teeth of the left valve at their upper ends and overlies the single tooth of the right valve. The inclination of the hinge line to the ligamental ridge is about 20° to 30° The posterior myophore penetrates the space between L and S; the anterior is a thin plate springing from the anterior tooth, curving anteriorly and then ventrally, running parallel to the ventral margin and penetrating the space below E; immediately before entering this space it widens abruptly from less than 1 mm to 9 mm, beyond which it tapers gradually to a point.

Dimensions. — Antero-posterior diameter of (a) 85 mm, dorso-ventral about 73 mm, height about 40 mm; corresponding figures for (b) 95 mm, 83 mm, 30 mm; for (c) antero-posterior diameter unknown, dorso-ventral 110 mm, height over 50 mm on dorsal side, over 110 mm on postero-ventral side.

Remarks. — *Vaccinites eyrei* resembles *V. macgillavryi* (Palmer) of the *Durania* beds of Loma Yucatan, Cuba, in the spacing of its pillars, but differs in the inclination of the hinge line which, in the latter species, is usually between 35° and 50°; it also differs in shape, the Cuban form being elongate conical to cylindrical. It differs from *V. vermunti* MacGillavry, of the *Barrettia* beds of Cuba, in which the pillars are more widely spaced and the inclination of the hinge line is 40° to 50°. In both Cuban species the L pillar is shorter and straighter than in the Jamaican species.

Genus **TORREITES** Palmer, 1933

Generic name created by Palmer for a Cuban species which had been described by Douvillé under the name of

Hippurites (Vaccinites) sanchezi. Torreites differs from *Vaccinites* chiefly in the development of its three major infolds. The ligamental ridge is lamelliform, rounded at its end, thick and exceptionally long, extending more than halfway across the body cavity. The S and E pillars are also lamelliform and of uniform thickness, they are neither swollen at their ends nor contracted at their base; the S pillar has a length about 80 percent of that of L; the E pillar has the exceptional character of being shorter than the S, little more than half as long. The outer layer has many short narrow infolds, which do not reach to the inner margin. Palmer described the left valve as having slots through which the three pillars came through to the surface; and as being composed of numerous radial, semicapillary tubes which do not open to the surface; consequently there are no pores.

Torreites cf. **sanchezi** (Douvillé)

Plate 49, figure 4

Hippurites (Vaccinites) sanchezi Douvillé, 1927, pp. 54-55, pl. 4, fig. 1.
Torreites sanchezi (Douvillé), Palmer, 1933, p. 100, pl. 7, figs. 1,2; pl. 8, figs. 1,2.
Torreites sanchezi (Douvillé), Rutten, 1936, p. 135, text fig. 4g.
Torreites sanchezi (Douvillé), Vermunt, 1937, p. 269.
Torreites sanchezi (Douvillé), MacGillavry, 1937, pp. 128-129, pl. 5, figs. 4e-h.

Occurrence. — A single fragment was found in the Peters Hill Limestone, where it is associated with *Praebarrettia coatesi* Chubb.

Description. — The fragment is a portion of a right valve, welded into a hard limestone. A weathered surface shows the dorso-posterior arc of the shell viewed from below; this has been sectioned. It is not possible to determine the shape of the valve, whether conical or cylindrical. It is large, its diameter being at least 110 mm, or rather more. The outer wall has been largely destroyed by boring organisms, and it is not clear whether it had the typical short narrow infolds, but judging by Douvillé's figure it is possible that these were confined to the antero-ventral margin, which is not preserved in the Jamaican specimen. The three principal infolds are preserved, and they seem to have been indicated by furrows in the outer wall. The ligamental ridge is about 55 mm long, 12 mm wide at the wall, thinning to about 6 mm it its inner end; the S pillar is about 40 mm long by 5 mm wide; the E pillar is some 25 mm long by 8 mm wide. These figures are a little higher but compare reasonably well with those of Douvillé's type. The chief difference is in the spacing of the pillars; in the type these are widely separated, the internal measurement between the base of L and the base of S is 38 mm, between S and E 22 mm. In the weathered surface of the Jamaican specimen the corresponding distances are 30 mm and 15 mm, but the distance from L to S seems to become greater higher in the shell. Palmer's figures also (1933, pls. 7,8) show a wide separation of pillars.

The left valve of the Jamaican form is unknown.

Dimensions. — All known dimensions are given above.

Remarks. — Since the above was written *Torreites sanchezi* has been found by Dr. Peter Jung of the Naturhistorisches Museum, Basel, (1970) in the *Barrettia* Limestone of the Green Island Inlier, Hanover (Jung, 1970).

Subfamily **BARRETTIINAE**, n. subfam.

Hippuritidae whose right valve is characterized by multiple infolds of the outer layer, two of which can be recognised as corresponding to the siphonal infolds of the Hippuritinae. The ligamental infold can generally be distinguished only by its relationship to the tooth N. The latter stands between two deep sockets, and there is a cavity between the posterior socket and the S pillar for the reception of the corresponding myophore of the left valve. The hinge line is parallel to the dorsal margin.

The diameter of the body cavity is about one-third or one-quarter of that of the shell. The wall is extremely thick and both layers enter into its structure. The outer layer is exceptionally thin, usually only one or two millimetres, and its multiple infolds penetrate the wall, the longer reaching almost to the edge of the body cavity, though only the S and E pillars enter into it. The inner layer is greatly developed; its central part is concave, lining the body cavity and forming a series of close set tabulae below it. Each of these tabulae has a broad horizontal brim, which gives it the form of an inverted hat, and these superimposed brims constitute the major part of the wall. The intruding infolds cut the brims into a series of radial strips, each of which has a number of sharp transverse upfolds alternating with rounded downfolds which form cavities between the infolds well shown in Plate 52, figure 1. Thus the outer and inner layers mutually interpenetrate, together forming the wall.

The left valve is flat or slightly convex, often with a central boss over the body cavity. It has infolds corresponding with those of the right valve, the longer of which reach nearly to the boss. It thus consists essentially of a solid boss from which radiate numerous flat bars in lateral contact one with another, the intervening sutures representing the infolds. There are many perforations through the shell along the sutures, and the S infold opens up at its inner end to form an oscule over the corresponding pillar.

The presence of an E oscule has not been proved and it is absent from the best known species.

There are two long, parallel, more or less equal teeth, which slide into the sockets of the right valve, gripping its tooth between them; the posterior myophore is small and peg-shaped, fitting into the cavity provided for it; the anterior myophore is crescentic and, from the corresponding tooth, it runs around within the anterior margin of the body cavity to the ventral side; it is attached to the under side of the left valve for its whole length.

The chief difference between the Barrettiinae of the Caribbean Region and Mexican Region and the *Pironaeae* of the Mediterranean countries and the Near East is seen in the distance between the principal pillars. In *Pironaea* the distance between L and E is generally less than one-fifth of the circumference of the shell; the angular distance is not more than 70°. In the Barrettiinae the distance is at least one-third of the circumference, equivalent to 120°, and is often considerably more.

Genus **BARRETTIA** Woodward, 1862

The distinguishing character of this genus is that the infolds or rays, seen in cross section, are *moniliform* or necklace-like, *i.e.* they resemble a string of beads on a thin thread. Actually each ray is a row of vertical parallel tubes, connected by a thin wall. Though only a small fraction of a millimetre thick, the connecting wall consists of two vertical laminae, and the tubes are formed by these laminae diverging, curving around, and rejoining; thus the tube consists of two hemicylinders, each of which is closely tabulate, the tabulae being dome-shaped, *i.e.* convex upwards; the tabulae in the two hemicylinders are not continuous with each other though, since there is no dividing wall, they are contiguous; they are disjunct portions of the funnel plates which form the outer layer. At the commissure the summits of the tubes project as rounded knobs along the radial walls formed by the infolds; there appears to be no relationship between the position of these knobs and of the upfolds of the intervening strips of the inner layer. The innermost tube of each ray is always the largest and is generally pear-shaped in section. The rays vary in length, some penetrating nearly to the body cavity and others falling far short of it; some of the latter may have only one or two beads. The ligamental infold has no distinguishing features; the S infold has a large cylindrical column at its inner end, which has domed tabulae like the small tubes, and is connected with the outer layer by a moniliform ray; the E infold has a radially elongated, laterally flattened column with flat tabulae, at the end of a relatively short moniliform ray.

A right valve will generally split easily along the median line of any of the infolds, especially S and E; the longitudinal sections thus produced show that the vertical tubes on all sides are parallel to each other and to the vertical axis of the valve for their whole length. The innermost tube of each infold is the first to appear, and young shells not exceeding 25 to 30 mm in diameter have only one tube to each ray; this tube grows vertically upwards and other tubes are inserted, one by one, between it and the outer wall, which grows upwards and outwards; if the valve becomes cylindrical no more tubes are added. Meanwhile, as the shell increases in diameter, so does the body cavity, with the result that the first-formed tubes, except on the dorsal side, are either cut off or else diverted obliquely outwards, in contact with the lining of the body cavity; they coalesce with and absorb the neighbouring tubes. The S and E pillars are not cut off but may be somewhat diverted so that they absorb some of the lesser tubes; the E pillar, which increases greatly in size, usually absorbs several minor tubes.

The radial bars of the left valve overlie the interrays and the sutures overlie the infolds. The bars are laterally notched, the notches being symmetrically arranged on the two sides of each rod, and opposed to the notches on the adjacent rods. Thus each suture opens up to form a row of small apertures which fit over the knobs on the infolds of the right valve as the larger S oscule fits over the S pillar. In view of the absence of an E oscule it seems probable that the function of these apertures was to admit sea water into the mantle cavity, in fact they were all little E oscules.

Barrettia monilifera Woodward

Plate 51, figures 1-3; Plate 52, figures 2,3; Text-figure 7

Hippurites sp. Barrett, 1860, pp. 324-326.
Barrettia monilifera Woodward, 1862, pp. 372-377, pls. 20,21.
Barrettia monilifera Woodward, Douvillé, 1890, pp. 110-112, pl. 17, fig. 6.
Barrettia monilifera Woodward, Chubb, 1956c, p. 6; 1962/1963, p. 19.
Not *Barrettia monilifera* Whitfield, 1897b, pp. 233-244, pls. 27-32.
Not *Barrettia* cf. *monilifera* Trechmann, 1922, pp. 510-511, pl. 19, fig. 2; pl. 20, figs. 1,2.

Occurrence. — This species occurs in limestone bands from a few inches to three feet in thickness subordinate to many hundreds of feet of shale, in Back River, a tributary of Rio Grande, about half a mile below the confluence of Catalina River, Portland Parish; also in Clarke's River, a tributary of the Plantain Garden River about one and a half miles southwest of Sunning Hill, St. Thomas Parish. The following description is based on Woodward's types, collected by Lucas Barrett in January, 1861, which are now in the British Museum (Natural History) and on a number of topotypes collected in Back River by the late V. A. Zans in June, 1958, specimens formerly in the Geology Department of the University of the West Indies, Kingston, Jamaica; now in the Smithsonian Institution, Washington, D.C.

Description. — A large but not gigantic species, tending to be gregarious. Right valve conical; when free to develop it is usually cornute, with a circular cross section; when forming part of a cluster it is generally polygonal; diameter at commissure about one third or one quarter of length. The infolds are indicated by slight longitudinal furrows in the outer surface. Outer wall thin, rarely more than 1 mm thick; this thickness is not exceeded even in the double walls separating the individuals in a cluster, which consist of two walls, each 0.5 mm thick.

The number of infolds varies according to the size of the shell; Woodward's type specimen, with a diameter of about 120 mm has 65 infolds, the average distance apart, measured around the circumference, being about 5.8 mm. In cross section the L infold is 29 mm long and has eight beads, including the terminal one; between it and the S pillar there are 17 infolds; the latter pillar is 34 mm long, the tabulate column at its inner end is 9 mm in diameter, its stem having six beads; eight infolds lie between it and the E pillar, whose length is 39 mm, its tabulate column 27 mm by 3 mm, and its stem having three beads. The other infolds vary in length, like the septa of a coral; ten of them, the longest, penetrate some 32 mm and have from eight to ten beads; in the sectors between the longer infolds there are other minor infolds, longer and shorter alternating, the shortest having only one or two beads. The individual beads are oval in cross section, averaging 1.5 by 1 mm, and are generally about 1.5 mm apart, though the distance varies somewhat; the innermost bead is larger and may be as much as 4 by 2.5 mm. The angular distance between the L and S pillars is 100°, between S and E about 45°.

A topotype with a diameter of 110 mm has 57 infolds; a pentagonal member of a cluster (Pl. 51) with dorso-ventral diameter 73 mm, and antero-posterior 63 mm has 37; a rounded member of the same cluster with an average diameter of 60 mm has 32. There seems to be a fairly close relationship between the size and the number of infolds, which are set at mean intervals of between 5.8 and 6 mm around the circumference. The angular distances between L, S and E vary little from those given above. The transverse section of Woodward's type specimen (Pl. 51, fig. 3) shows the form of the tooth N, and of the posterior muscle cavity *mp*.

The inner layer shows sharp wrinkling, which appears to be irregularly concentric, below the body cavity, the structure resembling that of *Parastroma guitarti* (MacGillavry, 1937, pl. 10, figs. 8,9), and the folding of the strips between the infolds also appears to be irregular; in fact this layer may be said to have a vesicular, rather than a tabular structure, resembling that of certain Palaeozoic corals such as *Michelinia* or *Cystiphyllum*.

The left valve is known only from Woodward's type specimens; it is depressed conical in form; its surface features are concealed by hard black matrix. The transverse section (Plate 51, fig. 3) shows its two teeth (B′ and B) fitting into the sockets and clasping the tooth (N) between them; the hinge is at right angles to the ligamental infold (L), the posterior myophore *(mp)* is seen fitting into its cavity. The longitudinal section figured by Woodward (Text-figure 7) is cut through the posterior myophore *(mp)* which is seen to be peglike and to fit into its cavity in the right valve; a similar process, on the other side, is almost certainly the crescentic anterior myophore *(ma)* which appears to be attached for its whole length to the left valve, and which curves around within the anterior margin of the body cavity; part of the S pillar is seen on the right. The original of Woodwards' figure is lost, but the counterpart is preserved in the British Museum (Natural History), (Plate 52, fig. 2). It is parallel to Woodward's section but is separated by a distance of some 4 or 5 mm, the thickness of the cut. It shows the continuation of the anterior myophore, but misses the posterior one; the S pillar of the right valve is shown to

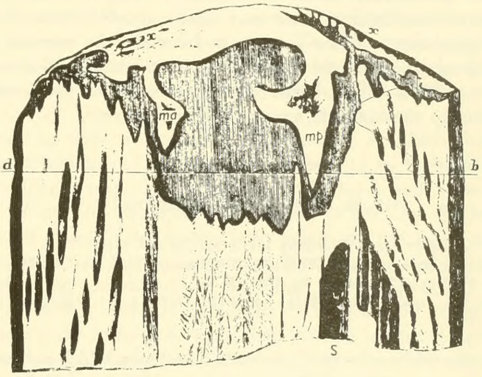

Text-figure 7. *Barrettia monilifera* Woodward. Longitudinal section of bivalved specimen after Woodward, 1862; × 0.66. This is the counterpart of the specimen illustrated in Plate 52, figure 2. Courtesy Geological Magazine.

a greater height though not to its summit; it seems probable that the corresponding oscule ran obliquely through the thickness of the left valve from the top of the pillar, and opened at a point nearer to the centre. Other smaller but similar perforations run obliquely through the left valve; their inner ends probably fitted onto the knobs at the tops of the vertical tubes.

Dimensions. — Woodward described his type specimen as 5 inches (125 mm) in diameter and probably originally 18 inches to 2 feet (450-600 mm) in length. Another of his illustrated specimens (his pl. 20, fig. 1) which is cornute, has a maximum diameter of 110 mm, and a length of 375 mm, perhaps originally 400 mm. It seems probable that *B. monilifera* does not normally greatly exceed 125 mm in diameter.

Remarks. — Many specimens of *Barrettia* found in Cuba, Puerto Rico, the Virgin Islands, and elsewhere have been determined as *B. monilifera.* It may be doubted whether the determination was correct in every case. Few of them appear to be gregarious. In many the number of rays, relatively to the diameter is fewer than in the true *B. monilifera* and the beads on each ray are fewer and larger. Probably they include one or two new species.

Barrettia gigas Chubb

Plate 52, figure 1; Plate 53, figures 1-3

Barrettia monilifera Whitfield, 1897b, pp. 233-244, pls. 27-32.
Barrettia cf. *monilifera* Whitfield, Trechmann, 1922, pp. 510-511, pl. 20, figs. 1,2; not pl. 19, figs. 2a,2b.
Barrettia gigas Chubb, 1955a, pp. 9-12; 1956c, p. 7; 1962/1963, pp. 6-15.

Occurrence. — In Cretaceous limestones, which are usually between 10 and 25 feet thick, at Haughton Hall and Rock Spring, Hanover Parish; near Grange, Westmoreland Parish; at Stapleton and Whitechapel Spring, St. James Parish; and at New Ground, St. Ann's Great River Valley, St. Ann Parish.

Description. — The most obvious character of *B. gigas* is its size. It is a gigantic form, the adult commonly having a diameter of 250 or 300 mm. In youth the right valve was generally broadly turbinate or even saucer-shaped and young individuals may have a diameter of twice their height. On attaining the adult diameter the shell continued its upward growth but became cylindrical sometimes with a slight curvature, and usually grew to a height of 300-400 mm. But the form is variable, some individuals continuing a gradual increase in diameter throughout their life so that the shell may be bowl-shaped, broadly turbinate, or even, rarely, cornute.

The outer wall is hardly ever preserved, and it is doubtful if it was more than 2 or 3 mm thick; as might be expected, in view of its greater diameter, *B. gigas* has more moniliform rays than *B. monilifera.* The holotype in the American Museum of Natural History (No. 9665/1) with a diameter of 250 mm has 78 rays, and among other adults the figures are as follows: diameter 250 mm, rays 84; diameter 250 mm, rays 100; diameter 290 mm, rays 102; diameter 300 mm, rays 90; diameter 350 mm, rays 140. Measured around the circumference the distance between rays averages 8-10 mm. They are closer in young individuals.

In cross section the tubes appear as oval beads with a maximum diameter of 2 to 3 mm, and they are separated by a similar distance. The longer rays may have up to 24 beads; the S pillar is a cylinder about 16 mm in diameter, with about 18-20 beads on its stem; the E pillar may be 60 mm by 5 mm, horizontally tabulate, with 8 to 12 beads on its stem. The angular distance L:E is at least 120° and may be as much as 140°; S is variable in position; it is nearer to E than to L.

The diameter of the body cavity is about one-third of the diameter of the shell. The inner layer below it does not show any wrinkling of the tabulae, though the strips extending outwards between the infolds have regular sharp, transverse upfolds, producing a pattern of rectangular cavities over the whole surface of the commissure.

The left valve is not well known except for its cardinal apparatus. One of the specimens believed by Trechmann (1922, p. 510, pl. 19, figs. 2a, 2b) to be a *B. gigas* (his *B.* cf. *monilifera*), with its upper valve, is a *Parastroma,* described below. Another of his specimens (his pl. 20, fig. 2) is said to show part of its left valve much crushed; it shows nothing but some shells of *Ostrea* sp. adhering to the commissural surface of the right valve. The specimen, illustrated in Plate 52, figure 1, shows the teeth and myophores of the left valve within the body cavity of the right. The posterior myophore *mp* fits snugly into the special cavity provided for it on the dorsal side of the S pillar; it is connected by a yoke with the posterior tooth B. The anterior tooth B′ is nearby, and from its springs the anterior myophore *ma,* a crescentic process that lies close within the wall of the body cavity; about halfway along its length there is a slight infold of the inner layer and beyond its end there is a stronger infold; these appear as vertical ridges in the wall of the body cavity. The anterior myophore was seen by Whitfield, who believed it to be a thickening of the inner shell layer of the right valve, and this view was accepted in an earlier publication (Chubb, 1955a, p. 11). But in the specimen illustrated it has been developed and has been found to have no connection with the right valve, but to be attached to the anterior tooth which is in position in the socket; probably it was also attached by its whole length to the underside of the left valve. A split specimen (Plate 53, figure 1) shows the *mp* cavity beside the deep B socket, which extends nearly to the bottom of the shell.

A right valve was collected in many fragments from Stapleton, St. James, by the late Dr. V. A. Zans. Among the fragments were found the greater part of the two teeth of the left valve, which have been assembled in their correct relative position (Pl. 53, fig. 2). The shell from which they came was a young adult, 300 mm in diameter, but probably not more than 200 mm high. The teeth must have been originally over 150 mm long, penetrating far into the right valve; they are parallel, both about 15 mm in diameter and 12 mm apart; they are curved, the dorsal side being convex, and they are longitudinally striated, at least on the dorsal side.

Dimensions. — The principal dimensions have been mentioned above. The usual adult diameter is 250 to 300 mm; the largest known specimen, found in a road cutting east of Bath Mountain in the Grange Inlier of Westmoreland has a diameter of 350 mm; it was not possible to extract the whole, but it was probably 1,000 mm long. Trechmann (1922, p. 511) recorded that the largest example seen by him was 1 foot (300 mm) in diameter at the top, and 2½ feet (750 mm) in length. A very young individual may be 100 mm or less in diameter and only 50 mm high.

Remarks. — *B. gigas* has so far been reported only from Jamaica, west of the Wagwater fault, but Mullerried (1934) stated that specimens of *B. "monilifera"* found in Chiapas, Mexico, attained a diameter of 33 cm and a height of 1 metre. The writer has also been informed that gigantic forms of *Barrettia*, of comparable size, are found in south-eastern Puerto Rico. All these could be *B. gigas*.

Barrettia multilirata Whitfield

Plate 54, figures 1-4; Plate 55, figure 2; Text-figures 8-10

Barrettia multilirata Whitfield, 1897b, p. 244, pls. 33,34,35.
Barrettia cf. *multilirata* Whitfield, Trechmann, 1922, pp. 511-512, pl. 18; pl. 19, fig. 1; pl. 20, fig. 3.
Barrettia multilirata Whitfield, Chubb, 1955a, pp. 12-13; 1955b, pp. 180-189; 1956c, p. 7.

Occurrence. — Occurs in abundance in association with *B. gigas* at Haughton Hall, Green Island, Hanover. It has not yet been found elsewhere in Jamaica.

Description. — This species is large, though not gigantic, being approximately the size of *B. monilifera* or a little larger. Typically the form is conical at the base, soon becoming cylindrical, and is often slightly curved. However, the form is variable and Trechmann (1922, p. 511) erected three varieties: var. *typica*, var. *cyclindrica (sic cylindrica)*, and var. *conica*. It may be doubted if this subdivision is justified; there seems to be little difference between *typica* and *cylindrica*, while *conica* represents young forms. Among adults the diameter is approximately half the height.

The outer layer of the right valve is about 1 mm thick; its surface is marked by longitudinal furrows representing the infolds, at average intervals of 3.5 to 5.0 mm; the intervening ridges may be flattened or rounded, with longitudinal striae separating low rounded costae averaging 1.5 mm wide; the growth lines, representing funnel plates, run straight across all ridges, costae, furrows.

The chief difference between *B. multilirata* and the species described above is in the multiplication of its infolds. For any given diameter this species may have from one and a half times to nearly twice as many rays as either *B. monilifera* or *B. gigas*. Whitfield's type, with a mean diameter of 155 mm, has 125 rays; one of Trechmann's, with a diameter of 127 mm has about 90; a Geological Survey specimen with a diameter of 175 mm has over 100; a conical form with mean diameter 150 mm has 91; another with diameter 130 mm has 87. Cross sections show that the beads on each ray are narrower than in *B. monilifera*, being about 0.75 by 1.5 mm; there are about 14 to 16 beads on the longer rays. The S pillar is cylindrical and some 10 or 11 mm in diameter; the E pillar is laterally flattened and is about 25 by 4 mm; both pillars are connected with the outer wall by moniliform rays. Not only the two siphonal pillars but also several of the longer rays project into the body cavity, about 22 in Whitfield's type and 18 in Trechmann's, the recesses between them serving for the reception of ridges on the under side of the left valve. The angular distances between the three main pillars are large. If Whitfield's interpretation of the figure in his plate 34 is correct the angle L:E would be nearly 180°. But he is probably mistaken in his identification of the teeth and, therefore, of the position of L. The angle L:S is usually 72°, and S:E 72°, the total angular distance L:E averaging 145°.

The body cavity is relatively wider than in *B. monilifera* or *B. gigas*. The inner layer forms close-set concave tabulae which are not wrinkled; they turn up and coalesce on the anterior side, presumably to provide a firm basis for the attachment of the anterior adductor. The parts of the inner layer extending into the interrays form small cavities, quadrangular or sometimes triangular, which are crowded and contracted especially at the points where intercalated rays appear, and towards the outer margin.

Several bivalved specimens of *B. multilirata* were included in the Trechmann Bequest to the British Museum

(Natural History). The left valves are depressed conical or nearly flat, slightly undulating to conform with the shape of the commissure of the right valve. Generally they have a low boss in the centre, though in one of the specimens illustrated (Plate 54, fig. 4), Trechmann's var. *cylindrica,* this is missing, its place being taken by an aperture some 14 by 7 mm, which seems to have been due to an injury inflicted during life. However this specimen has the advantage that, in the dorso-posterior quadrant, the left valve is partly broken away, revealing the commissural surface of the right valve and its relationship to the left.

Trechmann (1922, p. 512) thus described the left valve: "the decoration of the top valve . . . consists of irregular rounded ribs radiating from the central apex, often breaking up into two or three divergent ribs, and between these cross ribs arranged parallel with the margin of the valve. Between these again, more smaller ribs diverge, forming a reticulate or honeycomb design . . . the two apertures or foramina of the lid, corresponding to the first and second pillars in the living chamber, are more or less well shown".

The specimens have been re-examined. The left valves are typically some 10 to 15 mm thick in the central boss, thinning to 5 mm halfway to the margin, and 2 mm at the edge. There is no system of branching radial canals opening to the exterior by pores, as in the Hippuritinae. The central boss is from 15 to 25 mm across and is covered with small polygonal cells some 0.5 to 2 mm in diameter. Trechmann's "irregular rounded ribs" which radiate from it and branch dichotomously once or twice are the interrays, and they are separated by sutures representing the infolds.

Along each infold there are numerous perforations which notch the sides of the two adjacent ribs or costae. Between the perforations of each costa little processes extend to abut against those of its neighbour and at the abutment, they spread centripetally and centrifugally, giving the appearance of intercalary radial "smaller ribs" as noted by Trechmann. Thus each perforation consists of two rounded halves partially or completely separated, giving it the form of a figure 8. Trechmann's "cross ribs arranged parallel with the margin" are not continuous, but consist of the processes between the perforations, which are more or less in line from costa to costa.

The radial costae overlie the interrays of the right valve; the infolds with their rows of apertures overlie the moniliform rays. The apertures penetrate right through the valve; they have the figure of 8 only at the upper surface, downwards they become cylindrical and they fit over the knobs at the tops of the moniliform tubes. On the outer surface the infolds of the left valve extend farther in than those of the right; but the apertures in the central and thicker parts of the left valve slope downwards and outwards at an angle approaching 45° to bring their inner ends into apposition with the moniliform knobs; farther from the centre the slope of the tubes becomes less and near the margin they are vertical. Evidently the boss represents the juvenile left valve; after infolding had begun, as both valves grew larger and the body cavity grew wider, it became necessary for the first formed apertures of the left valve to develop into outwardly sloping tubes if they were to retain their connection with the moniliform bodies of the right valve.

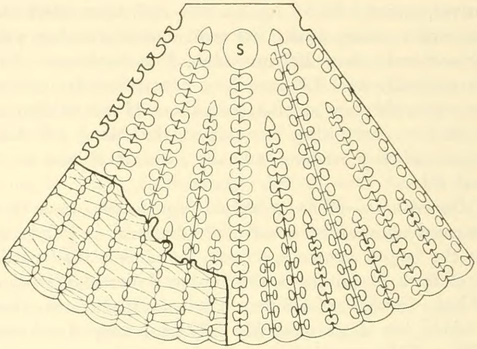

Text-figure 8. *Barrettia multilirata* Whitfield. Diagrammatic sketch of a sector of a left valve resting in position on the right; × 1.0. The left valve is represented as being partly broken away to show the relationship of the two valves. Compare Plate 54, figures 1-4.

Trechmann referred to "the two apertures or foramina of the lid". The S oscule is present; it is oval and overlies the S pillar, but it is smaller, being only 6 by 5 mm while the pillar is 11 by 9 mm. A careful examination of all available left valves has failed to confirm the presence of an E oscule. But the numerous perforations through the valve fit over the little pillars of the moniliform rays exactly as the oscules of any hippurite fit over the S and E pillars. It is, therefore, suggested that they are all little E oscules and served to admit sea water to the mantle cavity.

Whitfield's section (1897b, pl. 34) was cut 50 mm below the commissure, too low to show any of the characters of the underside of the left valve. A section was cut of the specimen shown in Plate 54, figure 4, at about 8 to 15 mm below the commissure (Text-figures 9,10). The underside of the top slice shows the teeth (apparently hollow) connected by a yoke; the posterior myophore fits into its usual place on the dorsal side of the S pillar; a long, narrow, curved process runs from the anterior tooth around, within the margin of the body cavity for about 180°; this should be interpreted as a ridge supporting the anterior myophore rather than the myophore itself.

From the outer side of the ridge a number of short branches extend into recesses in the wall of the right valve. There is a small central boss from which three ridges extend towards the posterior, each ridge bifurcates and its branches fit into recesses between the S and E pillars and ventrally to the latter. On its anterior side the central boss is surrounded by a kidney-shaped, radially striated body, resembling that observed by Whitfield in the body cavity of *B. gigas* (his *B. monilifera*), marked d in his plates 27 and 28. Most of the processes described are mere ridges on the underside of the left valve, serving to strengthen it and lock it firmly in position when closed. The counterpart of the slice (Text-figure 10), representing a section a few mm lower, shows only the two myophores, the anterior one considerably wider than the ridge which supports it.

Dimensions. — The maximum diameter recorded is about 175 mm, but the more usual is about 125 to 150 mm. In adults the height is about twice the diameter, though in young conical forms it may be less than half the diameter.

Remarks. — The left valve of *B. multilirata* has been described in considerable detail as it is thought to be typical of the Barrettiinae and no full description has previously been published.

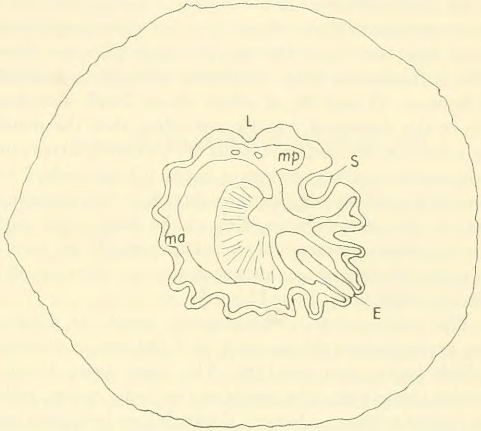

Text-figure 9. *Barrettia multilirata* Whitfield. Transverse section of right valve about 8 mm below commissure; × 0.62. The structural details of the wall are omitted, being shown in Plate 55, figure 2. The specimen is that illustrated in Plate 54, figure 4. Within the body cavity the processes attached to the under side of the left valve may be seen fitting into the recesses in the wall of the right.

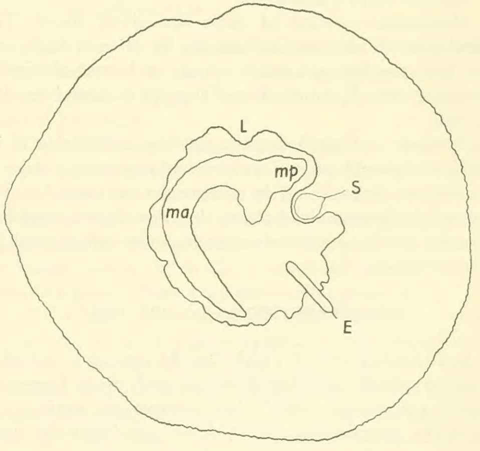

Text-figure 10. *Barrettia multilirata* Whitfield. Transverse section of right valve about 15 mm below commissure; × 0.62. Same specimen as Text figure 9. At this level only the two myophores of the left valve are seen.

Barrettia ruseae Chubb

Plate 55, figure 1

Barrettia sp. Dixon, 1960, pp. 109-110.
Barrettia sp. Chubb, 1960a, p. 89; 1962/1963, p. 12.
Barrettia ruseae Chubb, 1967, p. 30.

Occurrence. — Common in the Clifton Limestone, about three miles southeast of Lucea, Hanover. Named in honour of Rusea's High School, Lucea, whose 6A Geology Group first found it during a field exercise in July 1960 and recognised it as a species of *Barrettia.*

Description. — The typical form is large, discoidal or saucer-shaped with a flat base; the height is generally less than half the diameter and may be as low as 60 mm for a diameter of 140 mm, though a fragment shows that the height may attain 130 mm. Outer layer about 1 mm thick.

The number of infolds varies according to the diameter, their average distance apart, measured around the circumference, being about 5.5 mm. The following description will be based chiefly on the best specimen from Clifton, which is a low discoidal form but is incomplete having lost part of its ventral side; its mean diameter is 140 mm so its circumference must have been 440 mm, of which 300 mm remain; in this circumference it has 53 infolds; probably it originally had between 75 and 80, of which about 26-28 were long. Even in this depressed, rapidly expanding shell the moniliform tubes are vertical; the infolds are extremely attenuated and in section appear as strings of beads, 0.5 mm wide, 2 mm apart, each bead tapering into the threadlike line connecting them; in some cases the swelling of the beads is so slight as to be almost imperceptible when the infolds are seen as thin lines; the longest infolds penetrate to a distance of 50 or 55 mm, with about 10 or 12 beads.

The body cavity is exceptionally small, its diameter being approximately 30 mm in a shell 140 mm in diameter, *i.e.* little more than one-fifth. The inner layer forms a vesicular tissue lining the inside of the body cavity, rather than regular tabulae; it forms a similar highly irregular tissue in the interradial areas, showing no trace of the usual quadrangular cells.

Both the S and E pillars penetrate the wall of the body cavity. The former is diamond-shaped in cross section, its dimensions being about 12 mm by 7 mm; it is connected with the outer wall by a moniliform ray. The E pillar is 3 mm wide, and it is seen to a length of 17 mm but its outer part and moniliform ray are broken away. It is not certain which is the L infold, but a probable interpretation would make the angle L:S 75°, S:E 60°.

The left valve is unknown.

Dimensions. — Most of these are given above. The typical form is 140 mm in diameter by 60 mm high, and other less complete specimens appear to have had similar dimensions though, as noted, one appears to have been 130 mm high.

Remarks. — Considering the extreme attenuation of its infolds, it is possible that *B. ruseae* may represent a stage in the evolution from *Barrettia* to *Parastroma;* indeed in the taller specimen mentioned above the rays show a tendency to wander and loose themselves amongst the cells formed by the inner layer.

Genus **PARASTROMA** Douvillé, 1926

Includes large forms which may be conical or cylindrical and externally resemble *Barrettia,* with many longitudinal sulci representing infolds, but a transverse section or a view of the commissural surface shows that internally these infolds are largely or completely effaced, and the concentric wrinklings of the inner layer become much more prominent. The ligamental infold has generally disappeared, and the moniliform stems of the S and E pillars are lost, although the pillars themselves survive. In some species remnants of the rays are visible near the outer wall, and in some a few can be traced nearly to the body cavity, but they meander among the concentrically elongated cells formed by the foldings of the inner layer. This layer takes an even larger part in the formation of the commissure than in other Barrettiinae.

Parastroma trechmanni Chubb

Plate 56, figures 1-3

Barrettia cf. *monilifera* Trechmann, 1922 *pars,* p. 510, lines 27-30, pl. 19, figs. 2a-b.
Parastroma trechmanni Chubb, 1967, p. 30.

Occurrence. — Among the material collected by Trechmann from the *Barrettia* Beds of Green Island, Hanover, was a specimen which he believed to be a *Barrettia gigas* (his *B.* cf. *monilifera*) with its upper (left) valve. A reexamination of his type (L44200) in the British Museum (Natural History) led to the conclusion that it is a *Parastroma* without the left valve. A young shell from the same locality (L63237) seems to belong to the same species.

Description. — A gigantic species, the right valve broadly conical; the outer surface shows numerous sulci which radiate from the central apex to the commissural margin; as these diverge others are intercalated between them; the intervening costae, which are some 4-6 mm wide, are generally flat and crossed by growth lines representing funnel plates.

The commissural surface closely resembles Palmer's figure of *Orbignya (Parastroma) guitarti* (1933, pl. 2, fig. 2). The rays are discernible near the outer margin, but most of them become less definite when traced inwards, though they are not so completely effaced as in *P. guitarti;* some, especially round the anterior side, run more or less straight towards the body cavity, but elsewhere they become lost, apparently zigzagging amongst the cavities formed by the concentric wrinkling of the inner shell layer. Measured radially the concentric wrinkles are generally 2-3 mm from crest to crest, rarely 4-5 mm; the cells they form are up to 30 mm long measured tangentially; the radial distances from crest to crest compare closely with those in MacGillavry's thin section (1937, pl. 10, fig. 9) of *P. guitarti,* but in that species the cells are much longer, measured tangentially. In *P. trechmanni,* as in *P. guitarti,* the wrinkles become smaller and closer towards the periphery.

When Trechmann studied the larger specimen its principal features were concealed by matrix; it has been possible to remove this and to clean out the body and posterior myophoric cavities. It can now be seen that the body cavity is small, its diameter being one-quarter of the commissural diameter. The cardinal apparatus and siphonal pillars are essentially like those of *Barrettia.* The tooth is quadrangular, with grooved sides and flanged corners, the flanges extending outwards and obliquely downwards as septa which divide the sockets from the cavity; the teeth of the left valve are still present in the sockets. The posterior myophoric cavity is roundly conical; it is separated from the neighbouring socket by a low septum and is bounded on its ventral side by the stem of the S pillar. This pillar is a cylindrical column, 13 mm in diameter, standing beside the posterior socket; the E pillar is a ridge 8 mm wide, extending 25 mm into the body cavity. The stem of the S pillar, when traced outwards, soon becomes unrecognisable; the E pillar, however, extends almost to the outer wall. The trend of the wrinkling of the commissural surface is not concentric near the E pillar but turns outwards, parallel to the stem of the pillar.

The left valve is unknown.

Dimensions. — Diameter of adult shell: antero-posterior 205 mm, dorso-ventral 195 mm; height 112 mm; diameter of body cavity, antero-posterior 55 mm, dorso-ventral 50 mm; depth of body cavity 35 mm; width of commissure 60-70 mm; diameter of posterior myophoric cavity 20 mm, depth 16 mm. The young shell has a diameter of 85 mm; height 30 mm.

Remarks. — *Parastroma* was first named by Douvillé (1926, pp. 133-134, pl. 8, figs. 1-4) from material collected by Sanchez Roig in the province of Camaguey, Cuba. It consisted of fragments showing a succession of thin parallel plates, more or less close together, united by pillars which penetrated through the plates; the latter rose to form conical projections at their junction with the pillars. Douvillé regarded it as a stromatoporoid, which he called *Parastroma sanchezi.* Palmer (1933, pp. 96-97, pls. 1-3) first recognised that Douvillé's material consisted of rolled fragments of the right valve of two rudist species, which he called *Orbignya guitarti* and *O. sanchezi.* He observed that the so-called pillars were in fact capillary tubes but, as noted above *(Orbignya maldonensis:* Remarks), stated that the tubes perforated the funnel plates, when in fact they perforate the tabulae below the cavity. MacGillavry (1935, pp. 559-560) restored both species to *Parastroma,* which he agreed was a hippurite. It is not known whether the tabulae below the body cavity of *P. trechmanni* are perforated by tubes.

Parastroma seems to be not uncommon in Cuba in both the *Barrettia* and the *Titanosarcolites* Series and it occurs also in Puerto Rico. This is the first record of a true *Parastroma* in Jamaica, because the species formerly described under the name of *P. maldonensis* (Chubb, 1956a, pp. 21-23) is now ascribed to *Orbignya.* Since the above was written several specimens of *Parastroma* have been found by Dr. Peter Jung in the *Barrettia* beds of the Grange Inlier, Westmoreland.

Genus **PRAEBARRETTIA** Trechmann, 1924

This name was proposed by Trechmann for the species which had been described by Whitfield (1897b, pp. 245-246) under the name of *Barrettia sparcilirata.* Other species have since been referred to it. The right valve is conical or cylindrical and the distinguishing characters of the genus are seen in the infolds. These may be parallel-sided, when they are non-moniliform; or the sides of the rays may undulate and, if the undulations are symmetrically arranged on either side, a ray will show an alternate thickening and thinning, a structure which may be described as submoniliform; if the undulations do not match on the two sides, a swelling on one side being opposed to a sinus on the other, a result is a sinuous or vermicular ray (Boissevain and MacGillavry, 1932, p. 1304).

Praebarrettia sparcilirata (Whitfield)

Plate 57, figures 1,2; Plate 58, figure 1

Barrettia sparcilirata Whitfield, 1897b, pp. 245-246, pls. 36,37.
Barrettia sparcilirata Whitfield, Trechmann, 1922, p. 512.
Praebarrettia sparcilirata (Whitfield), Trechmann, 1924b, pp. 395-396, pl. 23, figs. 3,4.
Praebarrettia sparcilirata (Whitfield), Chubb, 1955a, pp. 13-14; 1956c, p. 8; 1962/1963, pp. 12,14.

Occurrence. — *P. sparcilirata* occurs in the lowest beds of the *Titanosarcolites* Series in the Logie Green area of the Central Inlier of Upper Clarendon, and in the Sunderland Inlier of St. James.

Description. — A large but not gigantic species; it is conical, becoming cylindrical; the height of an adult is probably at least twice the diameter. The outer layer is some 1 or 2 mm thick; its surface shows widely spaced sulci indicating the infolds; between these are low, rounded or nearly flat ridges which, in the best preserved specimens, show horizontal growth lines representing the funnel plates.

The infolds are comparatively few; Whitfield's type has 23, several of which extend inwards hardly enough to be detected on the cut surface. Other specimens show from 20 to 30 rays, and the distances between the infolds measured around the circumference are variable, the maximum being about 25 mm. The internal structure is usually not clear owing to crystallization but it appears that about half the infolds reach the neighbourhood of the body cavity; the L, S and E pillars are often unrecognisable, but in the specimen illustrated in Plate 57, fig. 2, the L inflexion extends well into the body cavity and at its end is bent anteriorly, and the three pillars, which resemble those of other Barrettiinae occupy an arc of over a third of the circumference.

The inner layer forms tabulae with interradial extensions which are well shown when the outer layer is weathered away (see Pl. 57, fig. 1); there are about eight in a vertical distance of 50 mm, *i.e.* they come at mean intervals of about 6 mm. They form large quadrangular cells between the rays.

No Jamaican specimen has been found with the left valve well preserved but the right valve shown in Plate 57, figure 2 contains its cardinal apparatus. The section is immediately below the commissure, through the yoke connecting the teeth, so the individual teeth are not seen. However, it is clear that the hinge line is parallel to the dorsal margin of the shell as in *Barrettia,* not inclined as in *Vaccinites* or *Pironaea.* The anterior myophore curves around within the margin of the body cavity, and the posterior penetrates between L and S.

Some Cuban specimens of *P. sparcilirata* have their left valve. It is of normal barrettine type with such modifications as might be expected in a form with few infolds. The radial bars broaden towards the periphery to fit over the wide interrays of the right valve, and thus assume a petalloid shape; a longitudinal section shows that they thicken to a maximum of some 16 mm in the middle of their length. Laterally they have numerous grooves separating processes which abut against those of the next radial bar. Where they overlie a submoniliform infold the processes expand at the line of abutment to form minor radial rods between the major ones; where the underlying infold is sinuous they meet in an irregular manner, the processes on one side abutting against the grooves on the other.

Dimensions. — Whitfield's type specimen from Logie Green is about 125 by 150 mm in diameter; its height is not mentioned; he described another specimen as abruptly turbinate, about 200 mm high, with a diameter of 125 by 175 mm. Another from near Shepherd's Hall, St. James, is 110 by 175 mm in diameter; it has a height of some 215 mm and is more or less cylindrical but has lost both ends. The conical specimen illustrated in Plate 57, fig. 1 has a height of 140 mm and a diameter of 130 mm.

Praebarrettia coatesi Chubb

Plate 58, figures 2-4

Praebarrettia sp. Coates, 1964, p. 10.
Praebarrettia coatesi Chubb, 1967, p. 30.

Occurrence. — Abundant in the Peter's Hill Limestone at the base of the *Inoceramus* shales in the eastern part of the Central Inlier, Clarendon Parish. Many specimens are largely crystallized and interpretation of the structure is difficult. Named after Dr. A. G. Coates who first discovered it.

Description. — The size is small to medium, making this the smallest of the Barrettiinae known as yet in Jamaica. Right valve typically conical, varying from cylindro-conical to turbinate, sometimes slightly curved; the diameter at the commissure may be half or one-third the height, or may be equal to it. There is a tendency to gregariousness and clusters of up to four or five individuals are not uncommon, though many are isolated. The outer layer is usually weathered away but when preserved is about 0.5 mm thick; infolds fairly numerous, spaced at distances of 5 or 6 mm around the circumference; a small shell with a mean diameter of 45 mm has 23 infolds; other specimens show diameter 52 mm, infolds 30; diameter 55 mm, infolds 31; diameter 73, infolds 40. The infolds are generally parallel-sided, straight or slightly vermicular, rarely submoniliform, 0.4 mm wide, expanding at the inner end to 1.5 or 2 mm, but some of the longest rays bend to the right or left just short of the body cavity and expand less; these in section resemble golf clubs.

The L, S, and E infolds can generally be recognised. The L infold may be long or only of moderate length; it is golf-club-shaped, and curves anteriorly; the S and E pillars penetrate to the body cavity; they are of the typical barrettine pattern; the S pillar is connected with the outer layer by a normal infold, it is oval in cross section and varies from 8 by 6 mm in a large shell to 4 by 3 mm in a small one; the E pillar is from 1.5 to 2 mm wide and extends from the body cavity to the outer layer, with only a slight constriction. The angular distance from L to S is about 90°, S to E some 50°. The hinge is essentially similar to that of other Barrettiinae, the hinge line being parallel to the dorsal margin.

The inner layer forms tabulae rather irregularly spaced at an average interval of 0.5 to 1 mm; sometimes they anastomose, making an irregular tissue between the infolds; in some cases the body cavity too is lined with a vesicular tissue. The diameter of the body cavity is about one-third of that of the shell at the commissure.

The left valve is unknown.

Dimensions. — Two of the largest specimens have diameters at the commissure of antero-posterior 80 mm, dorso-ventral 65 mm; one of these has a height on the dorsal side of 75 mm, ventral side 110 mm; the other has a height of about 115 mm but it is considerably eroded and may originally have been 130 mm or more in height. Another elongate conical specimen has a commissural diameter of 65 by 50 mm and a height of 110 mm. The best preserved is a small one, with a nearly circular commissure, diameter 45 mm, height about 50 mm.

Remarks. — *Praebarrettia coatesi* appears to be the earliest of the Barrettiinae so far found in the Caribbean area. It most closely resembles *P. porosa* Palmer (1933, p. 99, pl. 6, figs. 3-6) from the Maestrichtian of Cuba. The latter species differs in the wider spacing of its tabulae (miscalled funnel plates by Palmer), which are 1 to 2 mm apart, and in the structure of its rays which are described as beaded and similar to those of *Barrettia;* probably they are submoniliform; if truly moniliform the Cuban species should be referred to *Barrettia.*

Affinities of the Barrettiinae. — According to Trechmann (1924b p. 395) *Praebarretia* "occupies an intermediate position between *Pironaea* and *Barrettia,* and the stages of evolution of the Hippuritidae may be illustrated by the genera *Vaccinites* — *Orbignya* — *Batolites* — *Pironaea* — *Praebarrettia* — *Barrettia.*" Of these six genera the first two and the last two are described above; the others are European genera with multiple infolds. *Batolites* closely resembles *Orbignya* but in addition to the three main infolds it has many small ones, affecting only the outer layer. In *Pironaea* the multiple infolds are pronounced, involving both layers and projecting into the body cavity to form pillars; thus it has a superficial resemblance to *Praebarrettia* though its infolds are non-moniliform.

A few New World species have been ascribed to *Pironaea* and Milovanovic (1936, p. 30) regarded one of these, *P. peruviana,* as intermediate between the European forms and *Praebarrettia.* MacGillavry (1937, p. 122), however, noted that the distance L:E is always much greater in the Antillean and American forms with multiple infolds than the European forms, and he suggested that all New World species that have been attributed to *Pironaea* should be removed to *Praebarrettia.* These would include *P. peruviana* Gerth, *P.* cf. *peruviana* Vermunt, *P. corrali* Palmer, and *P. pacifica* (Olsson).

Until recently the only known Jamaican species of the unhappily named *Praebarrettia* was the post-barrettian form, *P. sparcilirata.* Obviously this could not be accepted as an ancestor of *Barrettia.* Its cardinal apparatus had never been adequately described or illustrated, but a re-examination of one of Trechmann's specimens has thrown light on it (see Plate 57, fig. 2), and it can be seen that this specimen does somewhat resemble *Pironaea polystylus* of south Europe in having a long, curved ligamental pillar, with the tooth N on its convex posterior side.

The newly discovered *Praebarrettia coatesi* occurs in rocks that are probably Turonian so it could possibly be an ancestor of the Campanian *Barrettia.* It also has a long ligamental ridge, anteriorly bent at its inner end, but both *coatesi* and *sparcilirata* differ from *Pironaea* in that (a) the three principal pillars are widely spaced, the angular distance between L and E being at least 120° and sometimes as much as 160° or more, while in *Pironaea* the distance is 70° or less; (b) the hinge line is at right angles to the proximal, uncurved part of the ligamental ridge and is parallel to the cardinal margin, whereas in *Pironaea* it is inclined.

Thus Trechmann's view of the evolutionary stages leading to *Barrettia* ignores certain important characters, notably (a) the distance between the L, S and E pillars, which is small in *Vaccinites* and *Pironaea* and large in *Orbignya, Batolites, Praebarrettia,* and *Barrettia;* (b) the ligamental ridge, which is long and anteriorly curved in *Vaccinites, Pironaea,* and *Praebarrettia,* and short and straight in *Orbignya, Batolites,* and *Barrettia,* and (c) the hinge line, which is inclined in *Vaccinites* and *Pironaea,* but not in *Orbignya, Batolites, Praebarrettia,* or *Barrettia.*

Pironaea seems to be more closely related to *Vaccinites,* the Barrettiinae to *Orbignya* and *Batolites,* from which they may be descended, though not by way of *Pironaea.* It seems reasonable to accept MacGillavry's suggestion that the Barrettiinae are an independent, parallel group, which developed from a centre of their own.

BANDS, PILLARS, AND OSCULES

In this memoir an hypothesis put forward many years ago (Chubb, 1956b, pp. 39-44) has, with minor modifications, been taken for granted. It was suggested that most of the characters that distinguish the Hippuritidae and to a lesser extent the Radiolitidae were adaptations to life in crowded conditions with a minimum of mutual interference. These characters include the elongate-conical or cylindrical form of the right valve, which made possible the growth of large fasciculate clusters, and the reduction of the left valve to an operculum, without projecting umbo and with vertical uplift, which involved the withdrawal of the hinge teeth, sockets and ligament away from the margin. The problem of water pollution was met by a similar withdrawal of the siphons, with the formation of open oscules in the free valve, which in turn necessitated the development of pillars in the fixed one. Some osculiferous genera, such as *Lapeirousia* and *Barrettia,* had excessively thick walls, and the infolding brought the siphons from the distant shell edge to the margin of the relatively small body of the animal.

The belief that the function of the oscules was to give the siphons access to sea water has been held by nearly all rudistologists since Douvillé first propounded it in the 1880's. It is not accepted by Dechaseaux (1947) who claims that the oscules are often closed, at least partially, in old individuals. An examination of many hippurites has failed to confirm this. She brought forward evidence that the rudists did not have long siphons but left open the question of whether they had "a mantle widely open, or one closed except in the two regions of entry and exit of water".

An inspection of Plate 51, figure 1, a cluster of *Barrettia monilifera,* may help to decide this question. The left valves of *Barrettia* completely covered the right, so in this cluster they must have fitted closely together like the pieces in a mosaic, with no room between. If the mantles were open each animal would discharge its faeces directly into the mantle cavity of its neighbours, and there would be no possibility of inhaling clean water.

Recently Sir Maurice Yonge (1967) published an important monograph on form, habit, and evolution in the Chamidae with reference to conditions in the rudists. His knowledge of the Chamidae is based on many years study of living animals, but for the rudists he relied on certain publications: Palmer (1928), Cox's (1933) account of a demonstration he gave to the amateurs of the Geologists' Association, Chubb (1956b), and especially Dechaseaux (1947, 1952, 1960), the last two being text books. Yonge also had discussions with the late Dr. L. R. Cox of the British Museum (Natural History), who would no doubt have shown him some specimens.

On Cox's advice Yonge separated the Hippuritacea (including all rudists) from the Chamacea, though he thought their relationship to be "obviously close" (1967, p. 86). Thirty or forty years ago many palaeontologists might have agreed, but few would today. Yet Yonge's analysis of the Chamidae does throw light on at least the more primitive of the rudists, the Diceratidae, the Monopleuridae, even the Caprinidae, for, though not closely related, they have adapted a similar hinged, isomyarian shell to similar living conditions, which has resulted in the development of similar form and habit.

But with the Hippuritidae and the Radiolitidae Yonge is on less certain ground. He did not accept Dechaseaux's view that the mantle cavity may have been open; he supposed two short siphons like those of *Chama* which he placed, not at the oscules, but at the outer margin.

He summarized the writer's 1956 suggestions and continued (p. 94):

> The immediate criticism of these ingenious views is that the oscules were *outside* the animal; they could not have communicated with the mantle cavity . . . From consideration of the position of the posterior adductor and so of the anus, the exhalent opening must have been dorsal to the 'S' pillar and the inhalent aperture *between* the pillars . . . The effect of the mantle foldings which create the pillars is to create a deep canal between them which would lead to the inhalent opening. The corresponding folding of the mantle on the upper valve would produce the oscules. Any attempt to bring siphons upward through these openings would involve an upward and a *sideways* bending. Since the oscules would close down on top of the pillars when the adductors contracted the siphons would be in constant danger of being crushed. In any case there is the fact that oscules often close or greatly diminish with age . . .

Thus Yonge believed that the function of the two infolds was to create a canal. This was for the disposal of waste, silt, and other suspended and inedible material which would accumulate in the mantle cavity, and be conveyed posteriorly by currents to collect as masses of pseudofaeces at the base of the inhalent aperture, as in the Chamidae. From time to time this material would be expelled, by sudden contractions of the adductor muscles, through this aperture, situated not at an oscule but between the two.

Yonge's description of the oscules as being outside the animal recalls MacGillavry's reference to the tubes in *Titanosarcolites* as "enclosures of the outside world into the animal's shell". But the function of the siphons was to communicate with the outside world, and here were two small enclosures of it brought conveniently near to the animal.

For the siting of the exhalent opening and the anus he referred to his Figure 28B. This is a cross section of "*Hippurites*" in which the sockets, the adductors (really the myophores), the mouth, a ctenidium, and the anus are inserted. The anus is placed between the posterior adductor and the 'S' pillar. It is immediately noticeable that only the outer shell layer is shown, the much thicker inner layer being omitted. If it were sketched in there would be no room for the anus where it is placed.

This may be confirmed by an inspection of the figure of *Barrettia gigas* in Plate 52, figure 1. Yonge would put the anus between *mp* and S. These two shelly processes are in contact and in the living animal would move against each other as the upper valve rose and fell. The faeces emitted by this infinitesimal anus would have to travel some 90 mm to reach a siphon at the outer margin. It is hard to understand the objection to the siphon being at the S oscule, a nearby part of the margin. In this respect *Barrettia* is not unusual; in hippurites the S pillar commonly forms the side of the cavity which receives the posterior myophore.

As regards the suggestion that the formation of oscules was an incidental consequence of the formation of pillars, how would he explain *Thyrastylon,* which has oscules but no pillars? It is of course true that any infold in the lower valve would be reflected as an infold in the upper. But the latter would not open up at its inner end to form an oscule unless there were a reason. Most hippurites have a third pillar, the ligamental, but while this involves infolds in both valves, there is no ligamental oscule.

It is difficult to understand Yonge's objection to a sideways bending of a siphon. Does he expect bilateral symmetry in a hippurite? And why would the contraction of the adductors crush the siphons? It does not crush them in *Chama* whose valves fit together as closely as the hippurite oscules fit onto their pillars. As for the "fact" that oscules close with age, no statement, however often repeated, should be accepted as fact without evidence.

Yonge's figure 25 is a vertical section of *"Hippurites"* based on a woodcut by Woodward (1854, fig. 2). Yonge shows the left valve as raised and has inserted an adductor muscle, the mantle, including the fused fold, and a siphon. The latter projects laterally and would be crushed if another shell grew alongside. Referring again to the illustration of a *Barrettia* cluster (Plate 51, fig. 1.) it is obvious that these animals had no lateral siphons for there is no room for them; their only possible means of access to sea water would be through the oscules.

Many of the above observations on Yonge's views on the hippurites apply also to his views on the radiolites, but here some additional comments are necessary. He wrote (p. 94) "The Radiolitidae possess siphonal bands, in some forming more pronounced pseudopillars symmetrically situated mid-ventrally," and he referred to his figure 28C.

This figure is a cross section of *"Radiolites."* As in 28B only the outer layer is shown but in this case it matters little as the inner layer would be thin. It shows the position of the sockets, the adductors, and the suggested position of some internal organs, the mouth, a ctenidium, and the anus. Also it indicates by arrows the position of the inhalent and exhalent currents. There can be no criticism so far.

But at two points, respectively some 15 mm anterior and 15 mm posterior to the mid-ventral point, the letters PP appear, and the key shows that these stand for pseudopillars. Here two criticisms are called for. The figure shows no trace of pseudopillars; and pseudopillars or bands are never found at the sites indicated.

A pseudopillar is a definite structure. It is found in few genera of which the best known is *Lapeirousia*. No known Jamaican species have them fully developed though two, *Tepeyacia multicostata* and *Durania nicholasi*, have incipient pseudopillars (Plate 43, figures 2-4; Plate 45, figure 1). The two siphonal bands in the former species and the E band in the latter are so deeply infolded that they bulge slightly into the body cavity. For these to become true pseudopillars it would be necessary for the two sides of each infold to come together in a cicatrix and the inward bulge to become accentuated. Yonge's figure 28C shows no pseudopillars but only a slight flattening at the points indicated, such as might be produced by pressure of neighbouring shells.

The position of the bands or pseudopillars in the Radiolitidae is fixed within definite limits. They are never situated, as Yonge claimed, "symmetrically mid-ventrally" but both always lie on the posterior side, the S band near the posterior myophore and the E band between it and the mid-ventral point. It often lies at the mid-ventral point but never anterior to it. This is shown in many figures in the publications consulted by Yonge such as that of *Thyrastylon adhaerens* (Chubb, 1956b, pl. 7, fig. 6) which shows the two teeth, their connecting yoke, a trace of the myophores, and the S and E bands. This figure is reproduced here on a smaller scale in Plate 38, figure 6. Other figures that show the position of the bands relative to the myophores, hinge or ligament are Plate 35, figure 3; Plate 39, figure 7; Plate 41, figure 2; Plate 42, figure 4; and Plate 43, figure 2.

Perhaps the most interesting point about Yonge's figure 28C is the position of the arrows he drew to indicate the exhalent and inhalent currents, the former by the ventral end of the posterior adductor and the latter mid-ventral. These are precisely the points where the siphonal bands or, if present, the pseudopillars and oscules would be expected. Thus unintentionally Yonge gave strong support to the belief of most rudistologists that these mark the positions of the two siphons.

It must be emphasized that all these criticisms of Sir Maurice Yonge's views apply to only two pages of a valuable memoir of nearly 60 pages. Also that in 1968 he visited Jamaica, when the writer had the benefit of a long discussion with him and was able to show him many specimens including those illustrated here. Perhaps our mutual differences were largely resolved.

STRATIGRAPHIC DISTRIBUTION

Maestrichtian
Monopleura jamaicensis Chubb
Gyropleura shaviensis Chubb
Antillocaprina suboccidentalis Chubb
A. occidentalis (Whit.)
A. quadrangularis (Whit.)
A. stellata Chubb
A. williamsi Chubb
A. depressa Chubb
Titanosarcolites giganteus (Whit.)
T. alatus Chubb
Plagioptychus jamaicensis (Whit.)
P. zansi Chubb
P. trechmanni Chubb
P. minor Chubb
P. fragilis Chubb
Mitrocaprina multicanaliculata Chubb
Agriopleura falconi (Chubb)
Distefanella mooretownensis (Trech.)
Biradiolites jamaicensis Trech.
B. robinsoni Chubb
B. rudis (Whit.)
Biradiolites rudissimus Trech.
B. forbesi Chubb
B. minhoensis Trech.
B. riograndensis Chubb
Thyrastylon adhaerens (Whit.)
T. coryi (Trech.)
T. semiannulosus (Trech.)
T. sp.
Bournonia cancellata (Whit.)
B. subcancellata (Trech.)
B. thiadensi Vermunt
B. barretti Trech.
B. tetrahedron Chubb
Sauvagesia macroplicata (Whit.)
S. mcgrathi Chubb
S. fluminisagni Chubb
S. annulosa (Whit.)
Chiapasella radiolitiformis (Trech.)
Orbignya mullerriedi Vermunt
O. ceibarum (Chubb)
O. maldonensis (Chubb)

Basal Maestrichtian
Durania nicholasi (Whit.)
Praebarrettia sparcilirata (Whit.)

Campanian
Antillocaprina lowenstami Chubb
Antillosarcolites macgillavryi Chubb
Plagioptychus toucasianus Matheron
Praeradiolites verseyi Chubb
Biradiolites cf. rudissimus Trech.
B. novaterrensis Chubb
Bournonia sanctannae Chubb
B. baileyi Chubb
B. coxi Chubb
Durania nicholasi (Whit.)
D. cf. aguilae Adkins
Vaccinites eyrei Chubb
Barrettia monilifera Woodward
B. gigas Chubb
B. multilirata Whit.
B. ruseae Chubb
Parastroma trechmanni Chubb

Turonian
Torreites cf. sanchezi (Douvillé)
Praebarrettia coatesi Chubb

Albian
Caprinuloidea perfecta Palmer
Sphaerucaprina seafieldensis Chubb
Sabinia totiseptata Palmer
Tepeyacia multicostata Chubb

Pre-Albian
Pachytraga jubilensis Chubb
Monopleura diaboli Chubb

Age uncertain	*Horizon*
Monopleura sp	Whitfield Breccia
Distefanella lombricalis (d'Orbigny)	Bon Hill Limestone
Bournonia sanctmariae Chubb	Reworked in Eocene shale

REFERENCES

Adkins, W. S.

1930. *New rudistids from the Texas and Mexico Cretaceous.* Univ. Texas Bull. 3001, pp. 77-100, pls. 4-9.

Barrett, Lucas

1860. *On some Cretaceous rocks in the South-Eastern Portion of Jamaica.* Quart. J. Geol. Soc. London, vol. 16, pp. 324-326.

Boehm, G.

1892. *Ein beitrag zur Kenntniss der Kreide in den Venetianer Alpen.* Ber. Naturforschenden Gesellschaft, Freiburg, vol. 6, pp. 134-149, pls. 6-9.

Boissevain, H., and MacGillavry, H. J.

1932. *Some remarks on Barrettia sparcilirata Whitfield and Chiapasella radiolitiformis (Trechmann).* Proc. K. Akad. Wetensch., Amsterdam, vol. 35, pp. 1303-1312.

Caldwell, W. G. E., and Evans, J. K.

1963. *A Cretaceous rudist from Canada, and a redescription of the holotype of Ichthyosarcolites coraloidea (Hall & Meek).* Jour. Paleont., vol. 37, pp. 615-620, pl. 75.

Chaper, M.

1873. *Observations sur une espèce du genre Plagioptychus.* Études faites dans la Coll. de l'École des Mines, . . . , Paris, vol. 2, pp. 82-90, pl. 11,12.

Chubb, L. J.

1955a. *A revision of Whitfield's type specimens of the rudist mollusks from the Cretaceous of Jamaica, B.W.I.* Amer. Mus. Novitates, No. 1713, pp. 1-15.

1955b. *The Cretaceous succession in Jamaica.* Geol. Mag., vol. 92, pp. 177-195.

1956a. *Some rarer rudists from Jamaica, B.W.I.* Palaeontographica Americana, vol. 4, pp. 1-30, pls. 1-5.

1956b. *Thyrastylon, a new rudist genus from the Upper Cretaceous of Guatemala, the Antilles and Persia, with a discussion of the functions of rudist oscules and pillars. Ibid.*, pp. 31-48, pls. 6-7.

1956c. *Rudist assemblages of the Antillean Upper Cretaceous* Bull. Amer. Paleont., vol. 37, pp. 1-23.

1959. *Upper Cretaceous of Central Chiapas, Mexico.* Bull. Amer. Ass. Petrol. Geol., vol. 43, pp. 725-56.

1960a. *Correlation of the Jamaican Cretaceous.* Geonotes, Jamaica, vol. 3, pp. 85-97.

1960b. *The Antillean Cretaceous geosyncline.* Trans. Second Carib. geol. Conference, Puerto Rico, pp. 17-26.

1961a. *Blue Mountain Shale.* Geonotes, Jamaica, vol. 4, pp. 1-7.

1961b. *Rudist assemblages in Cuba.* Bull. Amer. Paleont., vol. 43, pp. 409-422.

1962/1963. *Cretaceous formations, in Synopsis of the Geology of Jamaica.* Geol. Survey, Jamaica, Bull. 4, pp. 6-20.

1967. *New rudist species from the Cretaceous rocks of Jamaica.* Jour. Geol. Soc. Jamaica, vol. 9, pp. 24-31.

Coates, A. G.

1964. *Geology of the area around Crawle River, Arthurs Seat, Crofts Hill and British, Clarendon.* Geol. Survey, Jamaica, Annual Rept. for 1962/1963, Appendix A, pp. 6-10.

Dechaseaux, Colette

1947. *Bandes siphonales, piliers et siphons des Rudistes.* Bull. Soc. Géol. France, ser. 5, vol. 17, pp. 425-435.

1949. *Le genre Bournonia.* Ann. de Paléontologie, vol. 35, pp. 121-138, pls. 14-17.

1952. *Rudistes, in* Piveteau, Traité de Paléontologie, vol. 2, pp. 323-364.

1960. *Bivalves fossiles, in* Grassé, Traité de Zoologie, vol. 5, pp. 2134-2164.

De la Beche, H. T.

1827. *Remarks on the Geology of Jamaica.* Trans. Geol. Soc. London, ser. 2, vol. 2, pp. 143-194.

Di Stefano, G.

1888. *Studii stratigraphici e paleontologici sul systema cretaceo della Sicilia. I Gli Strati con Caprotina de Termini Imerese.* Atti R. Accad. Sci., Lett. ed Arti, Palermo, vol. 10, pp. 1-16, pls. 1-11.

Dixon, Inez

1960. *Research at Rusea's.* Geonotes, Jamaica, vol. 3, pp. 109-110, text-fig.

Douvillé, Henri

1887. *Sur quelques formes peu connues de la famille des Chamidés.* Bull. Soc. Géol. France, ser. 3, vol. 15, pp. 756-802, pls. 28-31.

1888. *Études sur les Caprines. Ibid.*, vol. 16, pp. 699-730, pls. 22-25.

1890-7. *Revision des principales espéces d'hippurites.* Mem. Soc. Géol. France, No. 6, pp. 1-236, pls. 1-34.

1898. *Les rudistes de la Jamaique, par R. P. Whitfield.* Rev. Crit. Paléozool., year 1, No. 3, pp. 122-125.

1900a. *Sur quelques rudistes Américains.* Bull. Soc. Géol. France, ser. 3, vol. 28, pp. 205-221.

1900b. *Sur la distribution géographique des Rudistes, des Orbitolines et d'Orbitoides. Ibid.* vol. 1, pp. 222-235.

1902. *Classification des Radiolites. Ibid.*, ser. 4, vol. 2, pp. 461-477. pl. 15.

1904. *Sur quelques rudistes à canaux. Ibid.*, ser. 4, vol. 4, pp. 519-538, pls. 13-14.

1908. *Sur la classification des Radiolités* C.R. Soc. Géol. France, No. 12, pp. 114-116.

1910. *Rudistes de Sicile, d'Algérie, d'Égypte, du Liban et de la Perse.* Mem. Soc. Géol. France, Paléontologie, vol. 18, fasc. 1, No. 41, pp. 1-84, pls. 1-7.

1913. *Sur quelques rudistes du Liban et sur l'évolution des Biradiolitines.* Bull. Soc. Géol. France, ser. 4, vol. 13, pp. 409-421, pl. 9.

1918. *Le Barrémien supérieur de Brouzet,* Partie III: *Les rudistes.* Mem. Soc. Géol. France, Paléontologie, No. 52, pp. 1-20, pls. 1-4.

1926. *Quelques fossiles du Crétacé supérieur de Cuba.* Bull. Soc. Géol. France, ser. 4, vol. 26, pp. 127-138, pls. 7-8.

1927. *Noveaux rudistes du Crétacé de Cuba. Ibid.*, ser. 4, vol. 27, pp. 49-56, pl. 4.

Fischer, P.

1887. *Manuel de Conchyliologie et de Paléontologie conchyliologique,* pp. 1-1041.

Harris, G. D., and Hodson, F.

1922. *Rudistids of Trinidad.* Palaeontographica Americana, vol. 1, pp. 119-162, pls. 18-28.

Jung, P.

1970. *Torreites sanchezi (Douville) from Jamaica.* Palaeontographica Americana, vol. 7, No. 42, pp. 1-3, pls. 1-3.

Kühn, O.

1932. *Rudistae.* Fossilium Catalogus I. Animalia, pars 54, pp. 1-200.

Kutassy, A.

1934. *Pachydonta mesozoica (Rudistes exclusis). Ibid.*, Pars 68, pp. 1-202.

MacGillavry, H. J.

1932. *The rudist fauna of the Seroe Teintje Limestone (Northern Curaçao).* Proc. K. Akad. Wetensch., Amsterdam, vol. 35, pp. 381-392, pl. 1,2.

1934. *Some rudists from the Alta Verapaz, Guatemala. Ibid.*, vol. 37, pp. 232-238.

1935. *Remarks on rudists. Ibid.*, vol. 38, pp. 558-565.

1937. *Geology of the province of Camaguey, Cuba, with revisional studies of rudist paleontology.* Geogr. Geol. Meded., Utrecht, No. 14, pp. 1-168, pls. 1-10.

Matheron, P.

1843. *Catalogue methodique et descriptif des corps organisés fossiles du Départment des Bouches-du-Rhone et lieux circonvoisins, Marseilles,* pp. 1-269, pls. 1-41.

Matley, C. A., and Higham, F.

1929. *The Basal Complex of Jamaica with special reference to the Kingston District.* Quart. J. Geol. Soc. London, vol. 85, pp. 440-492, pls. 23-25.

Matley, C. A., and Raw, F.

1942. *A road section near Guy's Hill, Jamaica.* Geol. Mag., vol. 79, pp. 241-252, pl. 7.

Milovanovic, B.

1936. *Yvania maestrichtiensis n. sp. et son importance pour la question de la formation brusque des formes nouvelles.* Ann. Geol. Peninsule Balk., vol. 13, pp. 28-41.

Mullerried, F. K. G.
1930. *Un hippurites de la region de Cardenas.* Ann. Inst. Biol., Mexico, vol. 1, pp. 165-168.
1931. *Chiapasella, un paquiodonto extrañisimo de la America. Ibid.*, vol. 2, pp. 243-254.
1932. *El Biradiolites lombricalis D'Orb sp. de Ejutla, Edo. de Oaxaca. Ibid.*, vol. 3, pp. 237-242.
1933a. *El genero Plagioptychus en Mexico. Ibid.*, vol. 4, pp. 1-14.
1933b. *Estudios paleontologicos y stratigraphicos en la region de Tehuacan, Puebla. Ibid.*, vol. 4, pp. 309-330.
1934. *Sobre el hallazgo de paqiodontos gigantescos en el Cretácico de Chiapas. Ibid.*, vol. 5, pp. 81-82.

Orbigny, A. d'
1842. *Quelques considérations zoologiques et géologiques sur les Rudistes.* Ann. Sci. Nat., ser. 2, vol. 17, pp. 173-192.
1847. *Paléontologie francaise.* Terr. Crét., vol. 4, Brachiopodes, pp. 157-373, pls. 528-99.

Palmer, R. H.
1928. *The rudistids of southern Mexico.* California Acad. Sci., Occ. Pap. 14, pp. 1-137, pls. 1-18.
1933. *Nuevos rudistes de Cuba.* Revista Agricultura, vol. 14, pp. 95-125, pls. 1-10.

Paquier, V.
1903-5. *Les Rudistes urgoniens.* Mem. Soc. Géol. France, Paléontologie, vol. 29, pp. 1-95, pls. 1-12.

Parona, C. F.
1908. *Notizie sulla fauna a Rudiste della pietra di Subiaco nella valle dell'Aniene.* Boll. Soc. Geol. Ital., vol. 27, pp. 299-310, pl. 9.
1909. *La Fauna coralligena dei Monti d'Ocre nelle Abruzzo Aquilano.* Mem. Carta. Geol. d'Italia, vol. 5, pp. 1-242, pls. 1-28.

Rutten, M. G.
1936. *Rudistids from the Cretaceous of northern Santa Clara Province, Cuba.* Jour. Pal., vol. 10, pp. 134-142.

Stephenson, Ll. W.
1938. *A new Upper Cretaceous rudistid from the Kemp Clay of Texas.* U.S. Geol. Surv. Prof. Paper 193-A, pp. 1-15, pls. 1-5.

Thiadens, A. A.
1936a. *Rudistids from southern Santa Clara, Cuba.* Proc. K. Akad. Wetensch., Amsterdam, vol. 39, pp. 1010-1019.
1936b. *On some Caprinids and a Monopleurid from southern Santa Clara, Cuba. Ibid.*, pp. 1131-1141.

Tobler, A.
1928. *Demonstration einiger mittelamerikanischer Rudistenfaunen.* Ecl. Geol. Helvet., vol. 21, pp. 216-217.

Torre, Alfredo de la
1960. *Notas sobre rudistas.* Mem. Soc. Cubana de Hist. Nat., vol. 25, pp. 51-64.

Toucas, A.
1903. *Études sur la classification et l'évolution des hippurites.* Mem. Soc. Géol. France, Paléontologie, vol. 30, pp. 1-128, pls. 1-17.
1909. *Études sur la classification et l'évolution des radiolitides. Ibid.*, vol. 36, pp. 1-132, pls. 1-24.

Trechmann, C. T.
1922. *The Barrettia beds of Jamaica.* Geol. Mag., vol. 59, pp. 501-514, pls. 18-20.
1924a. *The Carbonaceous Shale or Richmond Formation of Jamaica. Ibid.*, vol. 61, pp. 2-19, pls. 1,2.
1924b. *The Cretaceous limestones of Jamaica and their Mollusca. Ibid.*, vol. 61, pp. 385-410, pls. 22-26.
1927. *The Cretaceous shales of Jamaica. Ibid.*, vol. 64, pp. 27-42, 49-65, pls. 1-4.
1929. *Fossils from the Blue Mountains of Jamaica. Ibid.*, vol. 66, pp. 481-491, pl. 18.
1936. *The basal complex in Jamaica. Ibid.*, vol. 73, pp. 251-267; 382-3.

Vermunt, L. W. J.
1937. *Cretaceous rudistids of Pinar del Rio Province, Cuba.* Jour. Paleont., vol. 11, pp. 261-275, pls. 36-7.

Whitfield, R. P.
1897a. *Descriptions of species of Rudistae from the Cretaceous rocks of Jamaica, W. I., collected and presented by Mr. F. C. Nicholas.* Bull. Amer. Mus. Nat. Hist., vol. 9, pp. 185-196, pls. 6-22.
1897b. *Observations on the genus Barrettia Woodward, with descriptions of two new species. Ibid.*, vol. 9. pp. 233-246, pls. 27-38.

Woodward, S. P.
1851-1856. *Manual of the Mollusca.* Pp. XVI, 486, 25 pls. map.
1855. *On the structure and affinities of the hippurites.* Quart. Jour. Geol. Soc. London, vol. 11, pp. 40-61, pls. 3-5.
1862. *Some account of Barrettia, a new and remarkable fossil shell from the Hippurite Limestone of Jamaica.* Geologist, vol. 5, pp. 372-377.

Yonge, C. M.
1967. *Form, habit and evolution in the Chamidae (Bivalvia) with reference to conditions in the rudists (Hippuritacea).* Phil. Trans. Roy. Soc., Ser. B, vol. 252, pp. 49-105.

Zans, V. A.
1951. *Geology and mineral deposits of Jamaica.* Govt. Printer, Jamaica, pp. 1-11.

———— **(and others)**
1962/1963. *Synopsis of the geology of Jamaica.* Geol. Survey Dept., Jamaica, Bull. 4, pp. 1-72.

Zittel, K. A. von, and Eastman, C. R.
1913. *Text-book of Paleontology,* pp. 476-484.

PLATES

Location of the Figured Specimens

The location and identity of the specimens illustrated in the following plates are indicated by letters and numbers:

AMNH — American Museum of Natural History, New York. These are Whitfield's types. The Catalogue Numbers are quoted.

BMNH — British Museum (Natural History), London. These include Woodward's types whose numbers have no prefix, specimens presented by the late Dr. C. T. Trechmann during his lifetime whose numbers are prefixed by the letter L, and those in the Trechmann Bequest which are prefixed by LL.

Inst — Institute of Jamaica, Kingston. The collection includes, among others, specimens presented by F. C. Nicholas which are topotypes of Whitfield's species; and by C. T. Trechmann, including paratypes of his species.

Smith — Smithsonian Institution, Washington. Nearly all the types of new species and many older ones have been transferred to the Smithsonian.

USNM — United States National Museum. Specimens collected by the late Dr. C. A. Matley in 1939-40.

UWI — University of the West Indies, Department of Geology. Includes specimens collected by the Jamaica Geological Survey. With few exceptions the types formerly at U.W.I. have been transferred to the Smithsonian.

EXPLANATION OF PLATE 27

All illustrations natural size. Figures 1-3 and 7-9 are free specimens; all others are sections on weathered surfaces of limestone.

Figure *Page*

1-3. *Monopleura jamaicensis* Chubb 166

Bivalve, ventral view. (Chubb, 1956a, pl. 1, fig. 1). Smith, Maestrichtian, Ducketts, Westmoreland. 2. Same specimen. Anterior view. (Chubb, 1956a, pl. 1, fig. 2). 3. Same specimen. Left valve. (Chubb, 1956a, pl. 1, fig. 3).

4,5. *Monopleura diaboli* Chubb 166

Right valve, transverse section near commissure, showing two sockets (b' and b) and body cavity (D) containing a fragment of left valve within its ventral margin. UWI 4161 — Bonnett-Copper Limestone, Benbow Inlier, St. Catherine. 5. Same species. Left valve lying with its commissural side down; outer surface weathered away to show socket (n) and body cavity (G). Same number, horizon and locality.

6. *Monopleura* sp. 167

Sections. UWI 6176. Whitfield Hall crush-breccia, Blue Mountains.

7-9. *Gyropleura shaviensis* Chubb 167

Right valve somewhat broken, showing hinge structure and both myophores (ma and mp). (Chubb, 1956a, pl. 1, fig. 5). Smith. Shaw Castle Shale, Shaw Castle, St. James. 8. Same species. Right valve unbroken, but umbonal area eroded. Smith. Same horizon and locality. 9. Same species. Bivalve. (Chubb, 1956a, pl. 1, fig. 4). Smith. Maestrichtian, Ducketts, Westmoreland.

10,11. *Pachytraga jubilensis* Chubb 168

Bivalve, longitudinal section. Right valve showing body cavity, accessory cavity (mp0), and tooth (N) fitting into socket of left valve. Smith. Jubilee Limestone, Benbow Inlier, St. Catherine. 11. Same species. Transverse section of right valve, showing ligamental infold (L), small posterior socket (b), accessory cavity (mp0), large crescentic tooth (N) embracing anterior socket (b') which contains broken off tooth of left valve. Smith. Same horizon and locality.

12-14. *Caprinuloidea perfecta* Palmer 169

Left valve, oblique section, showing curvature, ligamental infold (L), longitudinal canals etc. Smith. Seafield Limestone, Benbow Inlier, St. Catherine. 13. Same species. Left valve, transverse section near commissure, showing canaliculate walls, body cavity (G), septum, and posterior muscle cavity (mp). Smith. Same horizon and locality. 14. Same species. Right valve, transverse section near commissure, showing canaliculate walls, ligamental groove (L) and cavity, anterior (b') and posterior (b) sockets the latter connected with muscle cavity (mp), which is divided from body cavity (D) by a septum. Smith. Same horizon and locality.

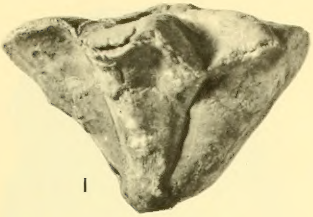
1

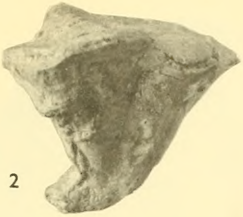
2

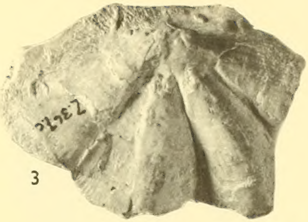
3

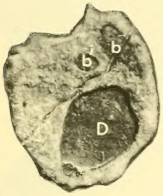

4

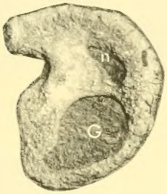

5

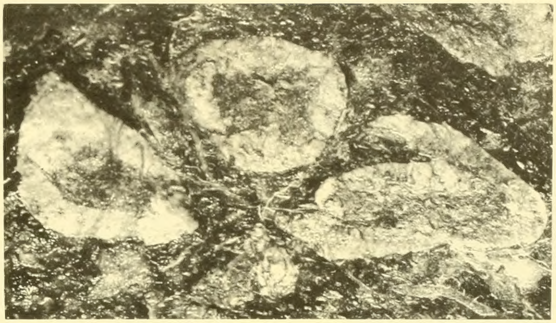
6

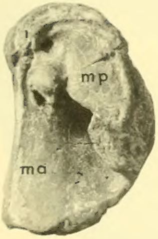

7

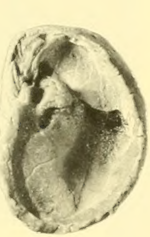
8

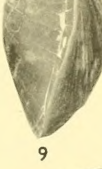
9

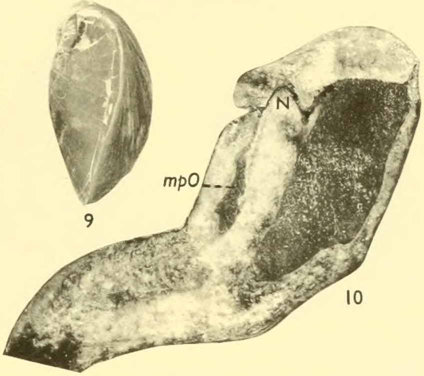

10

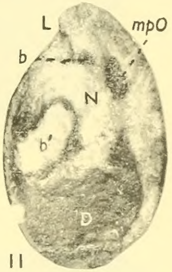

11

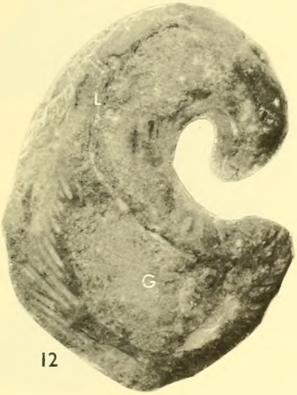

12

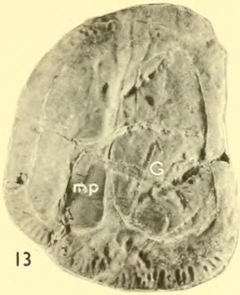

13

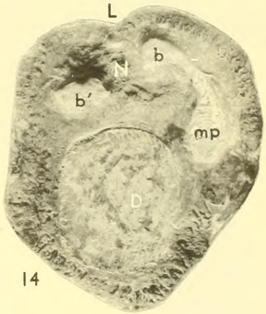

14

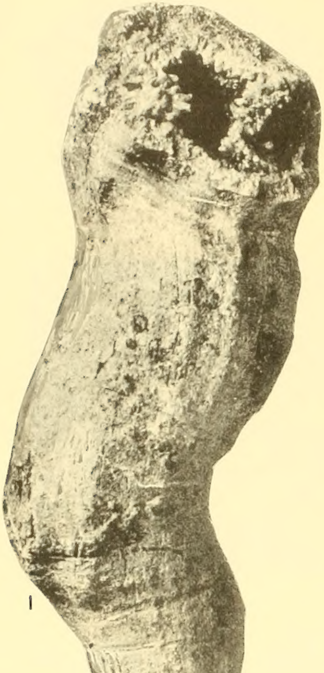

1

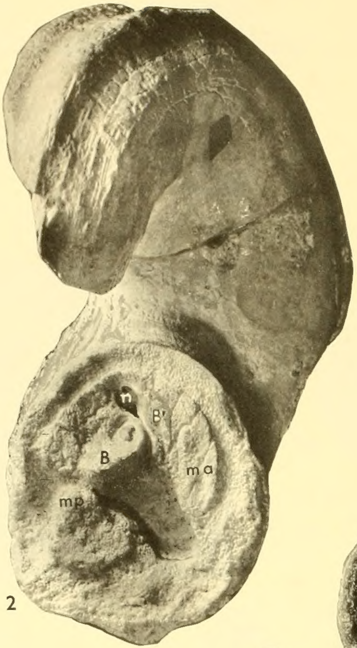

2

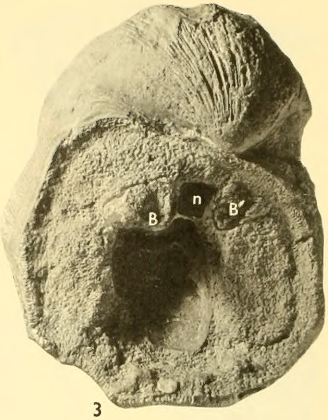

3

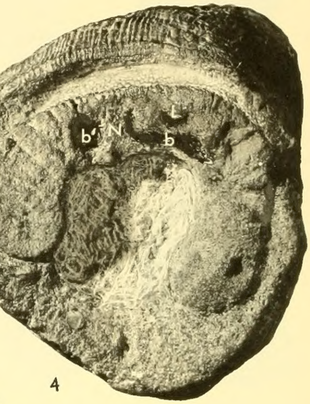

4

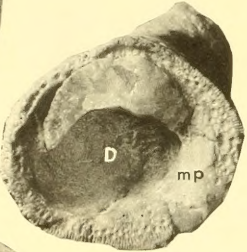

5

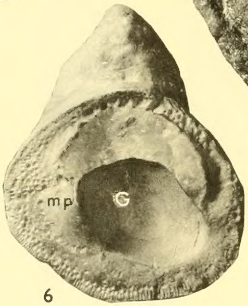

6

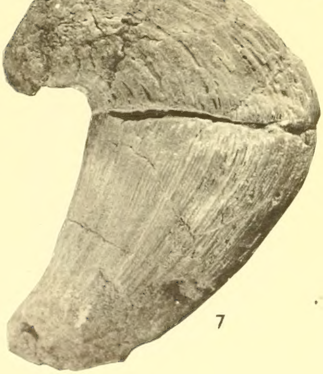

7

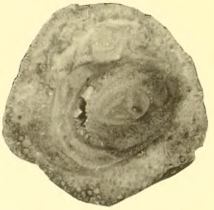

8

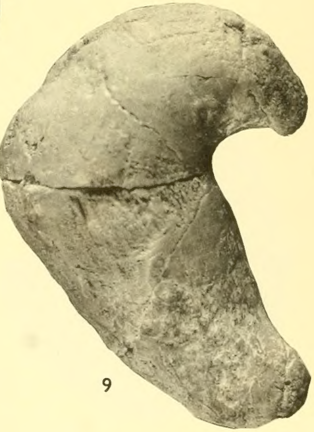

9

EXPLANATION OF PLATE 28

All illustrations natural size except figure 2
Figure 1 courtesy American Museum of Natural History

Figure		*Page*
1,2.	*Antillocaprina occidentalis* (Whitfield)	173

Right valve, reproduced from Whitfield's figure (1897a, pl. 17, fig. 3). A more or less corkscrew-like specimen. AMNH 9673/1. Maestrichtian, Logie Green, Upper Clarendon. 2. Same species. Left valve X 0.67. A new photograph of one of Whitfield's syntypes (1897a, pl. 16, fig. 4). A coiled but not closely involute form, showing body cavity, commissural surface, anterior and posterior myophores, the former (ma) fissured and the latter (mp) having its middle part broken away, anterior tooth (B′) abutting against large crescentic posterior tooth (B); the latter embraces a small ligamental pillar which is crescentic in the opposite sense; socket (n) small, occluded; walls, myophores and teeth canaliculate. Compare Text figure 2. Same museum number. Same horizon and locality.

3,4. *Antillocaprina suboccidentalis* Chubb 172

Left valve. A new photograph of one of Trechmann's types (1924b, pl. 25, fig. 3). A more involute form; both myophores complete and undamaged, showing stump of anterior tooth (B′), socket (n) large and not occluded, and crescentic posterior tooth (B); no ligamental pillar seen. BMNH L63211. Maestrichtian, lower part of Logie Green section. 4. Same species. Right valve. A new photograph of another of Trechmann's types (1924b, pl. 25, fig. 2). It shows both myophores, a single tooth (N) between two sockets, the anterior (b′) oval, the posterior (b) transversely sigmoidal, and a ligamental cavity (L) crescentic in the same sense as the socket. BMNH L63210. Maestrichtian, Great River Valley below Catadupa, St. James.

5-9. *Antillocaprina lowenstami* Chubb 174

Right valve, showing body cavity (D), canaliculate wall, and smooth downsloping posterior muscle attachment area (mp); the whole hinge plate recrystallized and showing no structures other than the oblique rock-filled ligament cavity. Smith. Campanian, marly limestone 80 ft. above the *Barrettia* Limestone, Stapleton, St. James. 6. Same specimen. Left valve; body cavity (G), walls, hinge plate similar to those of right valve; posterior muscle attachment a smooth up-sloping myophore (mp). 7. Same specimen, before separation of the valves, anterior view; on this side nearly all the outer layer has been removed by weathering, revealing the canals in the walls. 8. Same species. Transverse section of the right valve of another specimen, showing canaliculate walls, concave tabulae in body cavity, and hinge plate with narrow tooth between two sockets and crescentic rock-filled ligament cavity. Compare Text figure 3. Smith. Same horizon and locality. 9. Same specimen as figures 5-7. Posterior view of bivalve; on this side most of the smooth outer layer is preserved.

EXPLANATION OF PLATE 29

All illustrations natural size except Figure 2
Figure 2 courtesy American Museum of Natural History

Figure		*Page*
1-6.	*Antillocaprina quadrangularis* (Whitfield)	174

Highly arched left valve, dorsal aspect. Two minor costae are seen between the central flange and the anterior wing. The sigmoidal posterior tooth (B) and the conical anterior one (B') project below the commissure. BMNH LL30298. Maestrichtian, locality unknown. 2. Same species, right valve, ventral aspect X 0.67. A copy of Whitfield's plate 14, figure 4. Anterior flange seen on left, ventral flange in centre, posterior flange on right broken away. AMNH 9681/1. Said to be from Cretaceous limestones at Christianna; perhaps Logie Green, Clarendon. 3. Same species Left valve, commissural aspect; showing central socket (n), long sigmoidal posterior tooth (B), stump of oval anterior tooth (B'). (Chubb, 1956a, pl. 2, fig. 2). BMNH L88064. Maestrichtian, Catadupa, St. James. 4. Same specimen, external aspect. Outer layer weathered away, inner layer shows tubular structure. (Chubb, 1956a, pl. 2, fig. 1). 5. Same species, left valve of a bivalved specimen. Outer layer preserved, showing growth lines (Chubb, 1956a, pl. 1, fig. 16). BMNH L88065. Same horizon and locality. 6. Same specimen, transverse section of right valve near to commissure. Shows single tooth (N), hourglass-shaped in section, slightly displaced, flanked by sockets (b' and b) containing the teeth of the left valve, the anterior one round, the posterior crescentic.

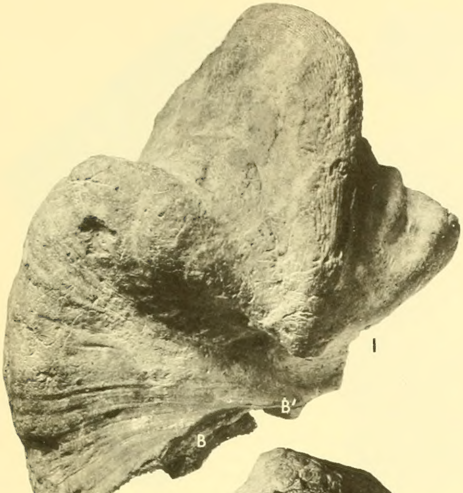

1

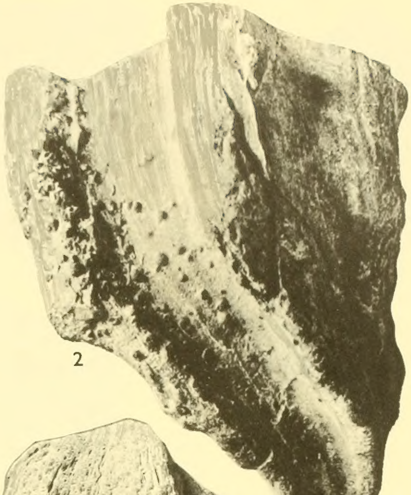

2

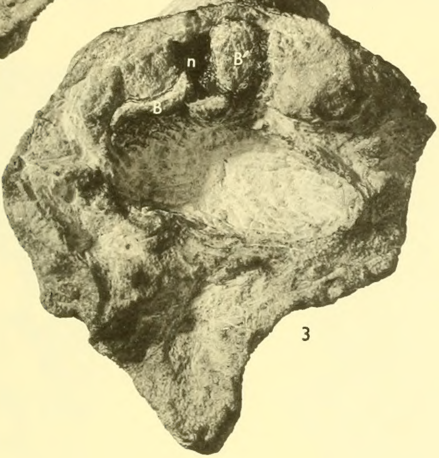

3

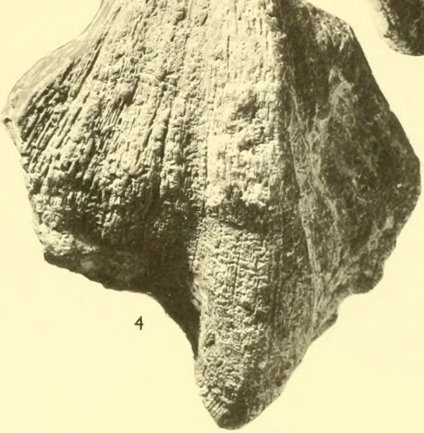

4

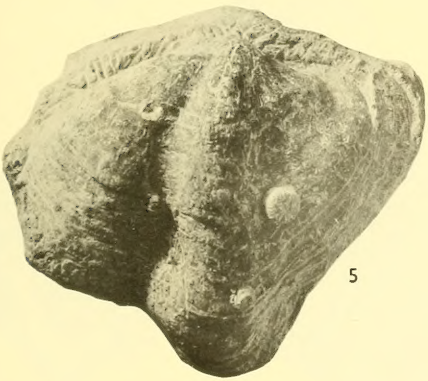

5

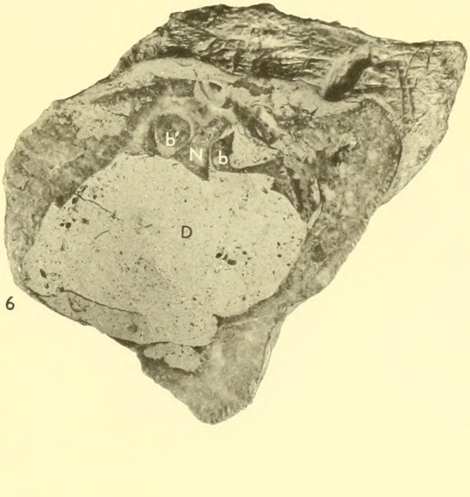

6

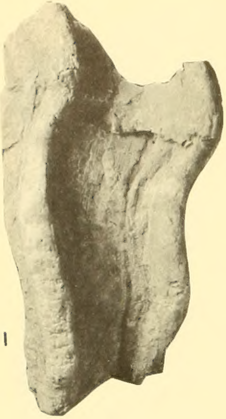
1

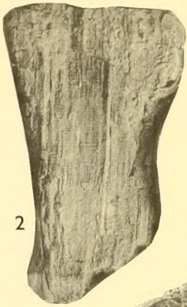
2

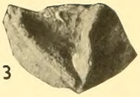
3

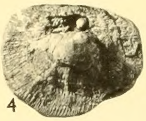
4

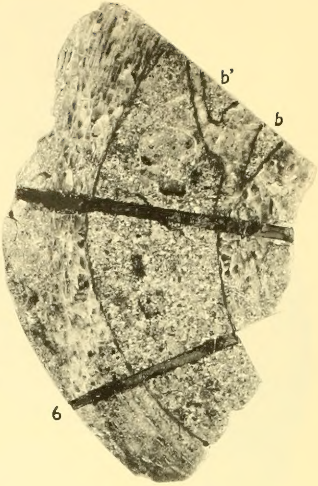

6

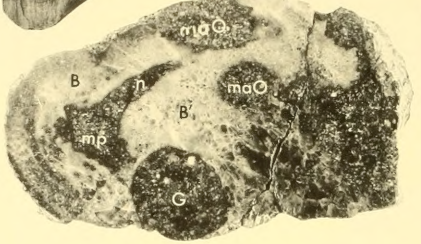

5

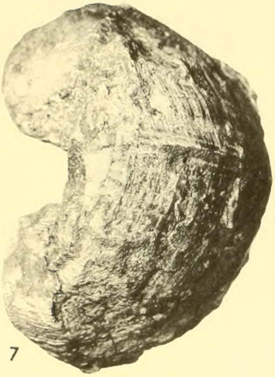
7

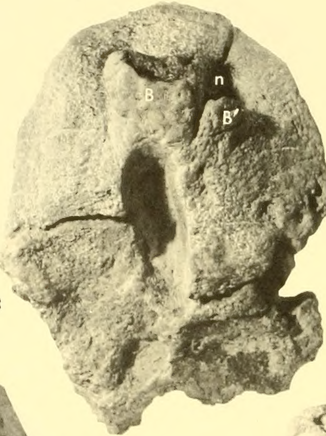

8

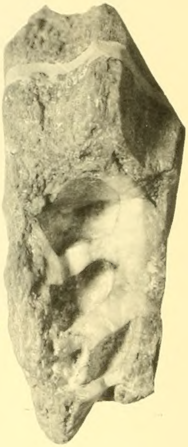
9

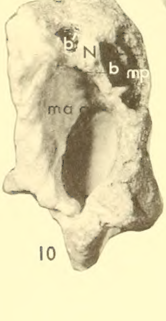

10

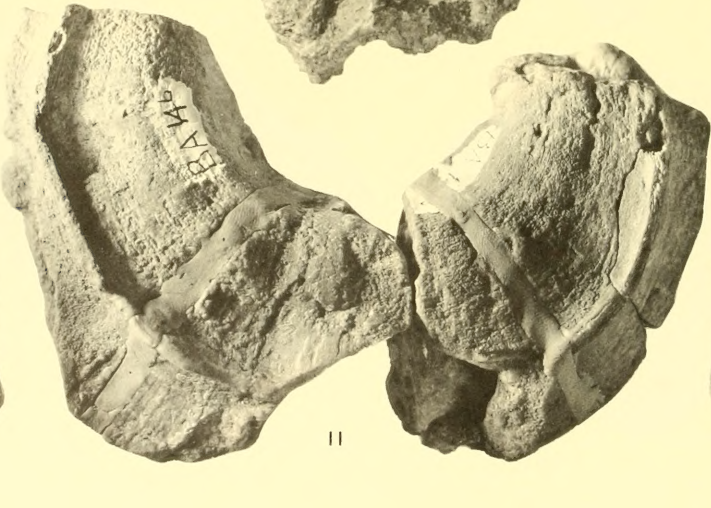

11

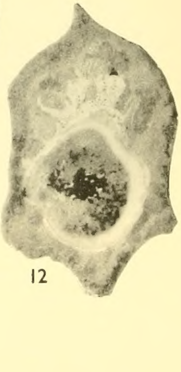
12

EXPLANATION OF PLATE 30

All illustrations natural size

Figure *Page*

1-3. *Antillocaprina stellata* Chubb 175

Fragment of right valve showing two flanges. Smith. Shaw Castle Shale, Maestrichtian, Shaw Castle, St. James. 2. Same species. Isolated flange showing close-set horizontal growth-lines crossing longitudinal tubes. Smith. Same horizon and locality. 3. Same species, apical end of a young individual. Smith. Same horizon and locality.

4. *Antillocaprina depressa* Chubb 176

Mould of interior of right valve. Shows a clear impression of a hinge of *Antillocaprina* type with tooth represented by quadrangular hollow, anterior socket by conical projection, and posterior socket by transversely elongated sigmoidal projection. A new photograph of Trechmann's type (1929, pl. 18, figs. 4,5). BMNH LL30290. Maestrichtian, Blue Mountain Shale, Blue Mountain Peak, St. Thomas.

5. *Sphaerucaprina seafieldensis* Chubb 170

Left valve, transverse section. Shows small round body cavity (G); long oblique socket (n) opening into posterior muscle cavity (mp); anterior (ma0) accessory cavities etc. Cellular structure not well shown. Compare Text Figure 1. Smith. Probably Albian, near Seafield Manse, St. Catherine.

6. *Sabinia totiseptata* Palmer 171

Right valve, longitudinal section. Shows tabulate tubules in walls, nontabulate body cavity, two sockets (b′ and b). Smith. Same horizon and locality.

7. *Antillocaprina williamsi* Chubb 175

Bivalved specimen, anterior aspect. Figured by Trechmann as *Antillocaprina* sp. (1927, pl. 2, fig. 10). BMNH L63262. Maestrichtian shale, Cambridge-Catadupa railway cutting, St. James.

8. *Antillocaprina occidentalis* (Whitfield) 173

Left valve, commissural aspect. Shows large crescentic posterior tooth (B) abutting against small conical anterior tooth (B′), small socket (n) displaced dorsally. BMNH L63259. Maestrichtian, Great River Valley, below Catadupa, St. James.

9-12. *Antillosarcolites macgillavryi* Chubb 179

Left valve broken to show thick oblique tabulae. Smith. Campanian *Barrettia* Series Haughton Hall, Green Island, Hanover. 10. Same specimen, right valve, commissural aspect. Shows anterior socket (b′) separated by base of tooth (N) from posterior socket (b) which opens into posterior muscle cavity (mp); attachment area of anterior muscle (ma) seen in left of body cavity. 11. Same specimen; the two valves seen in anterior aspect, right valve on left, left valve on right. 12. Same specimen; transverse section of left valve.

EXPLANATION OF PLATE 31

Figures 1 and 3 reduced, figure 2 natural size
Figure 3 courtesy American Museum of Natural History

Figure		*Page*
1.	*Titanosarcolites giganteus* (Whitfield)	177
	Bivalved specimen × 0.67. Anterior aspect with commissure in middle, right valve on left, left valve on right. A new photograph of one of Trechmanns' types (1924b, pl. 23, fig. 1). BMNH L44205. Maestrichtian, Great River Valley, below Catadupa, St. James.	
2.	*Titanosarcolites alatus* Chubb	178
	Transverse section of a right valve. BMNH LL30292. Maestrichtian, Great River Valley, borders of St. James and Westmoreland.	
3.	*Titanosarcolites giganteus* (Whitfield)	177
	Transverse section of a left valve × 0.90. One of Whitfield's types (1897a, pl. 19, fig. 1; pl. 20), shown also in posterior aspect in Plate 33, figure 1. Compare the angular ridges and few broad flutings on the posterior side with the more numerous projecting flanges and narrow furrows of *T. alatus*. Crypt of a boring organism seen at × on left. AMNH 9685/2. Maestrichtian, Logie Green, Clarendon.	

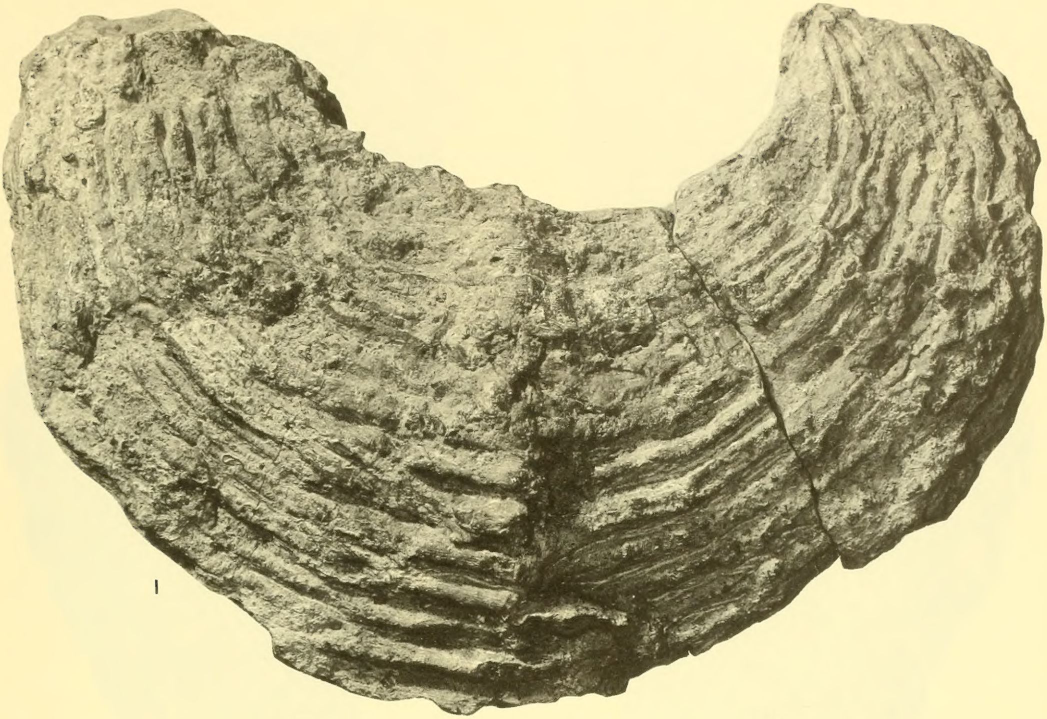

1

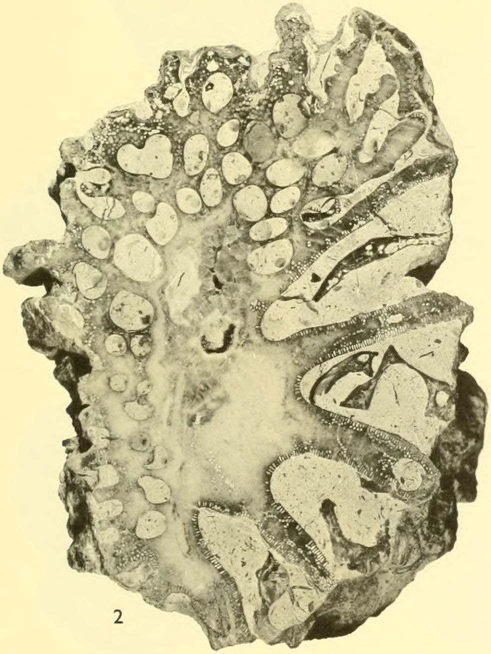

2

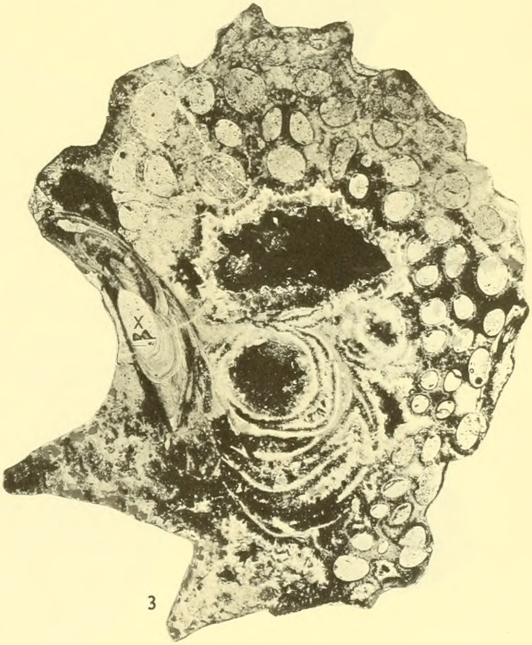

3

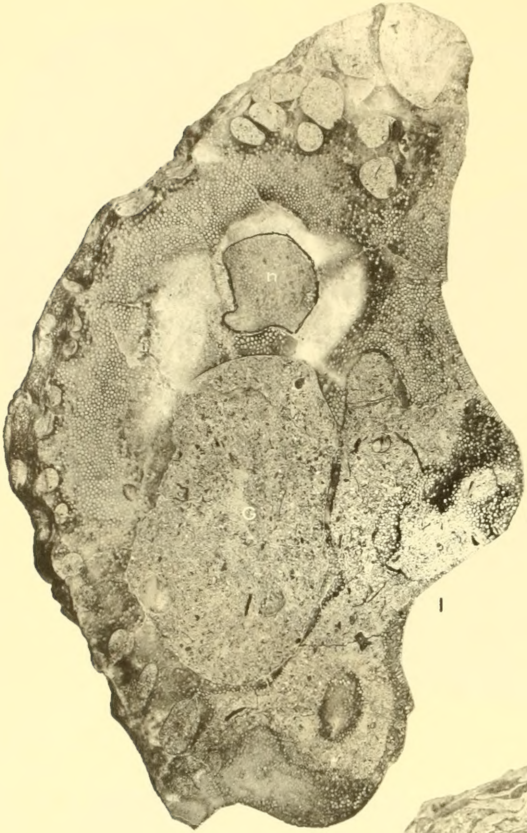

1

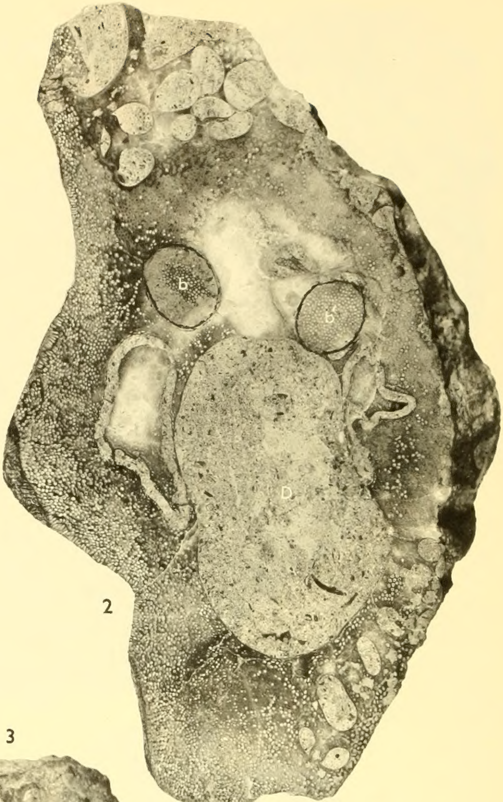

2

3

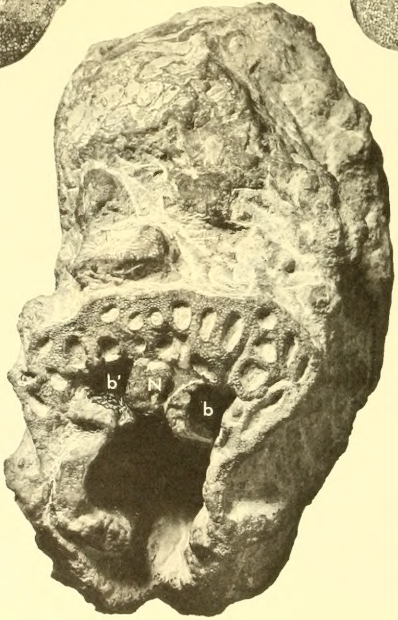

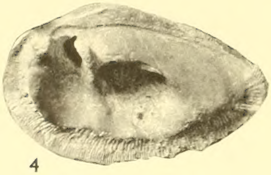

4

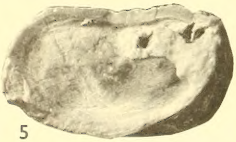

5

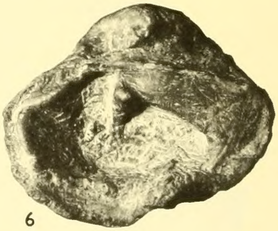

6

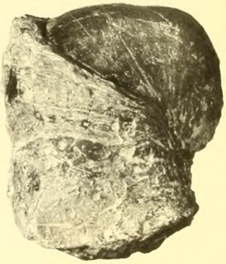

7

EXPLANATION OF PLATE 32

All illustrations natural size

Figure *Page*

1, 2. *Titanosarcolites giganteus* (Whitfield) 177

Transverse section of left valve cut about 16 mm from commissure. Anterior on left. Partly crystallized but showing many capillaries and large tubular canals; also, above the rock-filled body cavity (G), the large socket (n) containing the tooth of the right valve. BMNH L63230. Maestrichtian, Catadupa, St. James. 2. Same specimen, transverse section of right valve cut about 16 mm from commissure. Anterior on right. Shows many of the same characters as figue 1. Note that the tubular canals correspond in position, shape and size, indicating that they were continuous from one valve into the other. The two oval sockets (b′ and b) contain the teeth of the left valve. Compare Plate 33, figure 2, a similar section of a right valve cut farther from the commissure.

3. *Titanosarcolites alatus* Chubb 178

Right valve, commissural aspect. A new photograph of one of Trechmann's types (1924b, pl. 23, fig. 2) described by him as *T. giganteus.* It shows a single bifid tooth (N) between two deep sockets (b′ and b). BMNH L63232. Maestrichtian, below Catadupa, St. James.

4, 5. *Plagioptychus fragilis* Chubb 182

Left valve, commissural aspect. Smith. Maestrichtian, Shaw Castle Shale, St. James. 5. Same species, right valve. Shows posterior socket divided by ligamental ridge. Smith. Same horizon and locality.

6, 7. *Plagioptychus trechmanni* Chubb 181

Left valve, commissural aspect. This and the next figure are new photographs of Trechmanns' types (1924b, pl. 25, fig. 4) called by him *P. jamaicensis.* BMNH L63220. Maestrichtian, Logie Green, Clarendon. 7. Same species, bivalved specimen, posterior aspect. Compare Chubb 1956a, text figure 1. BMNH L 63221. Same horizon and locality.

EXPLANATION OF PLATE 33

Illustrations natural size except figures 1 and 2
Figures 1 and 2 courtesy American Museum of Natural History

Figure		*Page*
1, 2.	*Titanosarcolites giganteus* (Whitfield)	177

Left valve, posterior aspect × 0.67. A copy of Whitfield's plate 20; shown also in transverse section in Plate 31, figure 3. This side shows a few broad, rounded flutings, separated by angular ridges; compare with the anterior side shown in Plate 31, figure 1, AMNH 9685/2. Maestrichtian, Logie Green, Clarendon. 2. Same species, right valve × 0.85. A transverse section of another of Whitfield's types (1897a, pl. 21). Compare with Plate 32, figure 2; this section, being cut farther from the commissure, shows concave tabulae in the body cavity and conical tabulae in the sockets. AMNH 9685/3. Same horizon and locality.

3-5.	*Plagioptychus zansi* Chubb	181

Left valve, apertural aspect. (Chubb, 1956a, pl. 1, fig. 7). Smith. Maestrichtian, road bank facing Lot 67, Ducketts Land Settlement, Westmoreland. 4. Same species, bivalve, posterior aspect; right valve low and exogyrate (Chubb, 1956a, pl. 1, fig. 8). A *Bournonia thiadensi* is attached to the left valve (for other views of this specimen see Plate 40, figures 7 and 8). Smith. Maestrichtian, mile post 14 between Point and Flamstead, St. James. 5. Same species, bivalve with conical right valve (Chubb, 1956a, pl. 1, fig. 9). Smith. Same horizon and locality.

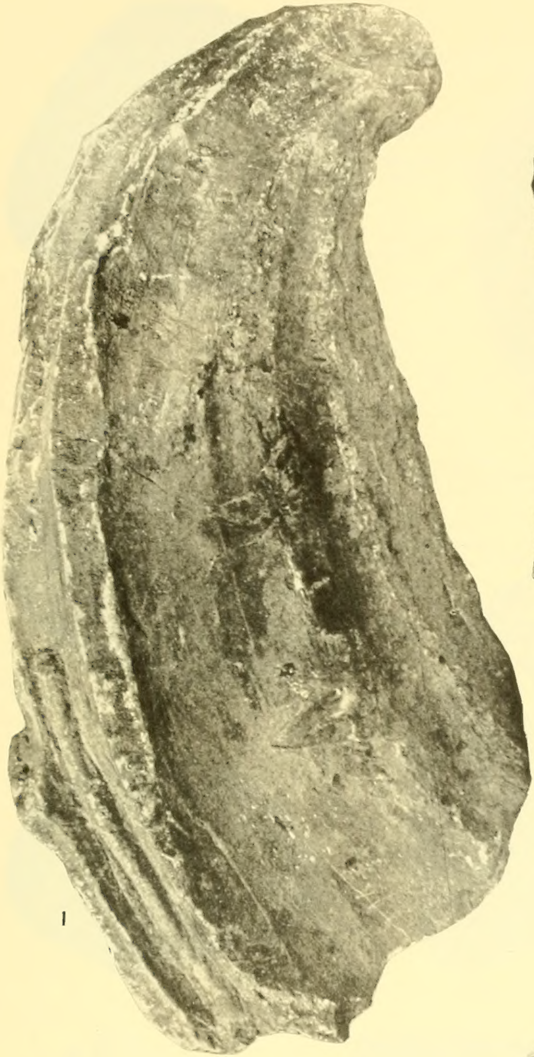

1

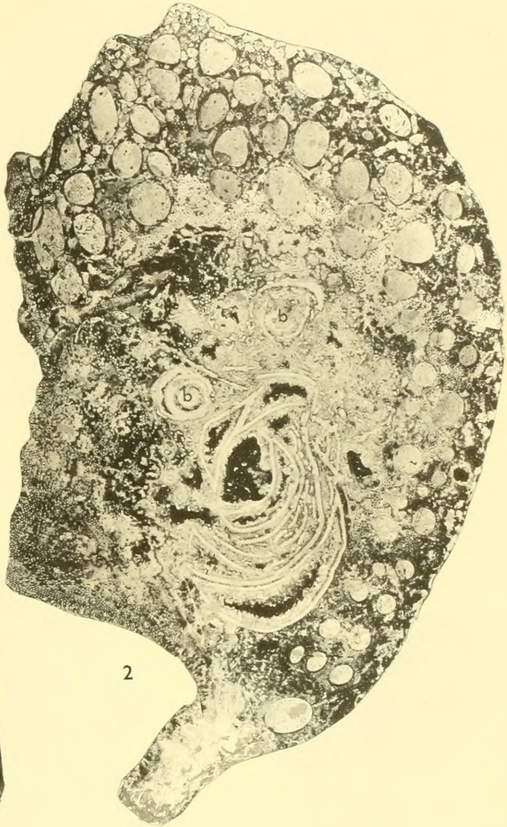

2

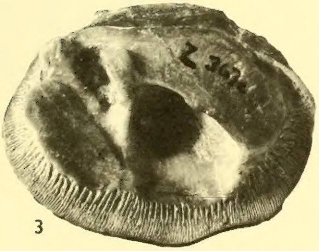

3

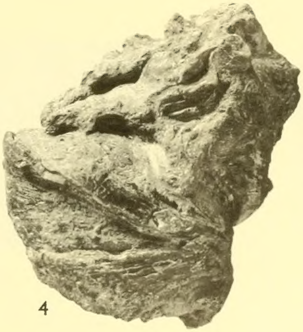

4

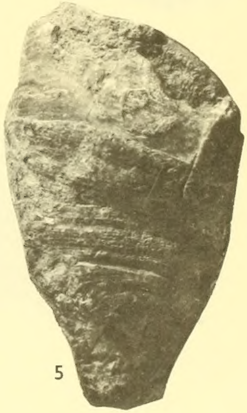

5

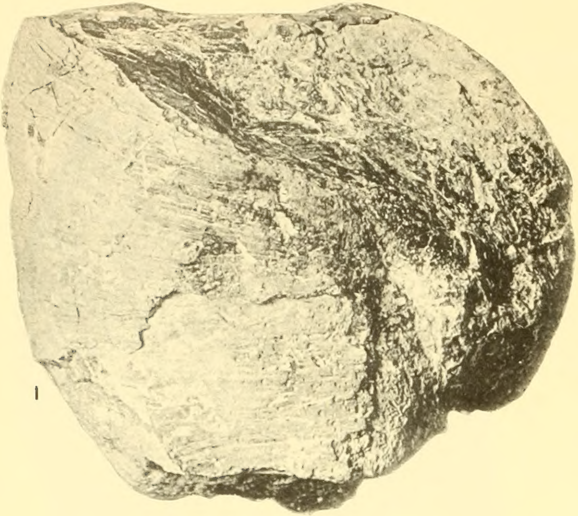

1

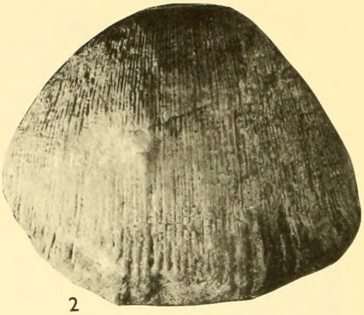

2

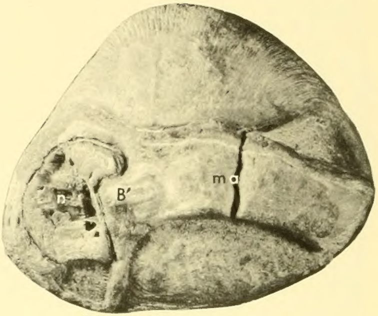

3

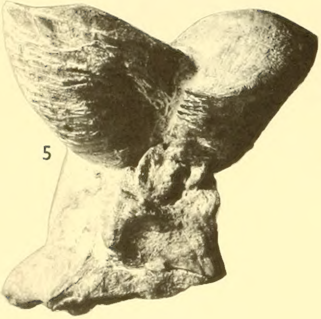

5

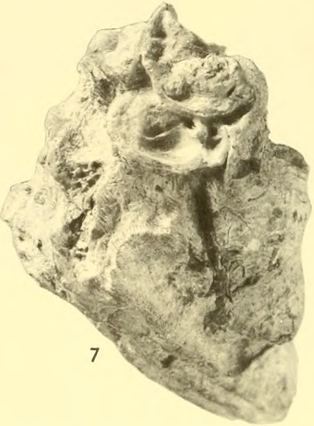

7

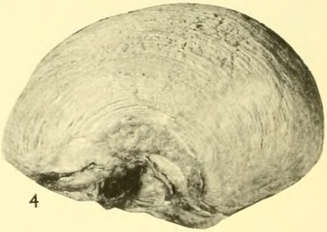

4

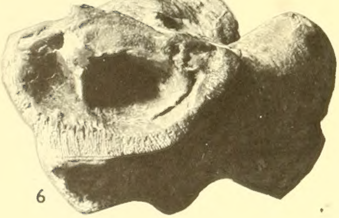

6

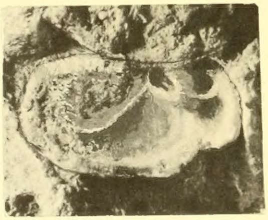

8

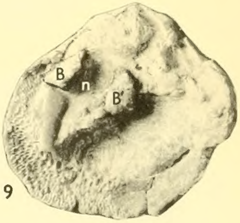

9

EXPLANATION OF PLATE 34

All illustrations natural size except figures 1 and 8
Figure 1 courtesy American Museum of Natural History

Figure *Page*

1. *Plagioptychus jamaicensis* (Whitfield) 180

Bivalve, posterior aspect × 0.45. The diameter of the right valve at the commissure is 200 mm. A copy of Whitfield's plate 15, figure 2. AMNH 9670/1. Maestrichtian, Logie Green, Clarendon.

2-4. *Plagioptychus toucasianus* Matheron 180

Left valve, outer aspect. Outer layer removed by weathering to reveal the bifurcating plates of the inner layer. Smith. Campanian, *Barrettia* bed, Haughton Hall, Green Island, Hanover. 3. Same specimen, commissural aspect. Shows the massive anterior myophore (ma), the anterior tooth (B′) and its septum, and the large socket (n) occupied by the tooth of the right valve. 4. Same specimen, posterior aspect, showing the incurving of the umbo.

5-8. *Plagioptychus minor* Chubb 182

Cluster of bivalved shells attached to a left valve of the same species (Chubb, 1956a, pl. 1, fig. 10). Smith. Maestrichtian, Ducketts Land Settlement, Westmoreland. 6. Same specimen, viewed from below, showing commissural aspect of the left valve (Chubb, 1956a, pl. 1, fig. 13). 7. Same species. Cluster of right valves attached to a shell of *Antillocaprina occidentalis* (Chubb, 1956a, pl. 1, fig. 11). Smith. Same horizon and locality. 8. Same specimen. Right valve, commissural aspect × 1.8 (Chubb, 1956a, pl. 1, fig. 12).

9. *Mitrocaprina multicanaliculata* Chubb 183

Left valve, commissural aspect (Chubb, 1956a, pl. 1, fig. 14). Smith. Maestrichtian, Logie Green, Clarendon.

EXPLANATION OF PLATE 35

All illustrations natural size

Figure		*Page*
1.	*Agriopleura falconi* (Chubb)	184
2-4.	*Praeradiolites verseyi* Chubb	185
5.	*Distefanella mooretownensis* (Trechmann)	186
6, 7.	*Distefanella lombricalis* (d'Orbigny)	186
8-12.	*Biradiolites jamaicensis* Trechmann	186

1. *Agriopleura falconi* (Chubb) 184

Right valve, ventral aspect (Chubb, 1956a, pl. 2, fig. 3). Smith. Maestrichtian, Shaw Castle Shale, Shaw Castle, St. James.

2-4. *Praeradiolites verseyi* Chubb 185

Right valve, anterior aspect. The anterior side has been broken away revealing, in the upper part, a section of the upturned funnel plates and the side of the ligamental ridge (L) and, in the lower part, the body cavity (D) with funnel plates on both sides, Chubb, 1956a, pl. 2, fig. 4). Smith. Campanian, *Barrettia* Limestone, Stapleton, St. James. 3. Same species. Transverse section of a right valve, showing the cell pattern and the ligamental ridge (L) ; the pedal fold (V) is at the top left and the S fold at the top right (Chubb, 1956a, pl. 2, fig. 6). Smith. Same horizon and locality. 4. Same specimen as Figure 2. Transverse section at the lower cut (Chubb, 1956a, pl. 2, fig. 5).

5. *Distefanella mooretownensis* (Trechmann) 186

Part of a cluster of right valves. The shell next to the left shows the siphonal bands, that on the right the antisiphonal side. Smith. Maestrichtian, near Moore Town, Rio Grande Valley, Portland.

6, 7. *Distefanella lombricalis* (d'Orbigny) 186

Fragment of right valve. Smith. Upper Cretaceous limestone. Bon Hill, near Sunning Hill, St. Thomas. 7. Same species. On the right is a longitudinal section of the wall showing funnel plates tilted at 45°. Smith. Same horizon and locality.

8-12. *Biradiolites jamaicensis* Trechmann 186

Transverse section of right valve, showing cell pattern in outer layer and, on the right, the siphonal bands and interband. BMNH LL30301. Maestrichtian, locality unknown. 9. Same species, bivalve, with siphonal area on right, left valve in position. BMNH L63127. Maestrichtian, Great River Valley, opposite Catadupa. 10. Same species. Right valve, antisiphonal side. This and figure 11 are new photographs of one of Trechmann's types (1924b, pl. 24, fig. 6). BMNH L63128. Same horizon and locality. 11. Same specimen, siphonal side. 12. Same species, siphonal side. A *Biradiolites robinsoni* is attached to the antisiphonal side; its commissure and body cavity may be seen on the right and its umbo on the left. For other views of this specimen see Plate 36, figures 1-3. Smith. Maestrichtian, Cotton Tree Gully, Lambs River, Westmoreland.

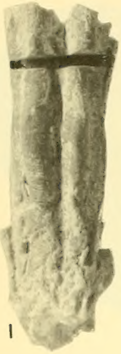

1

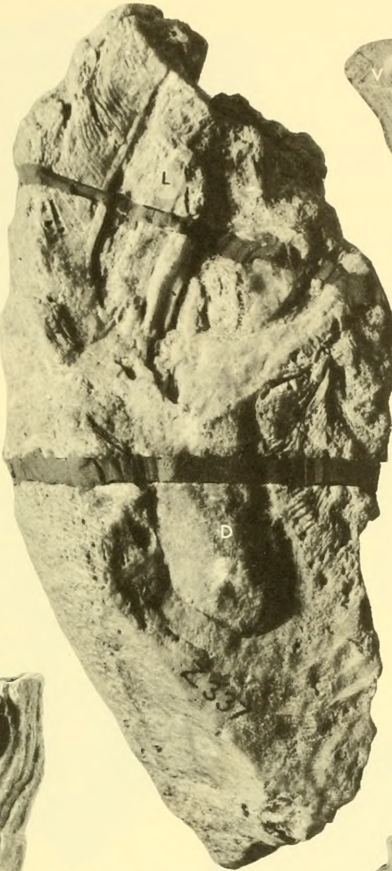

2

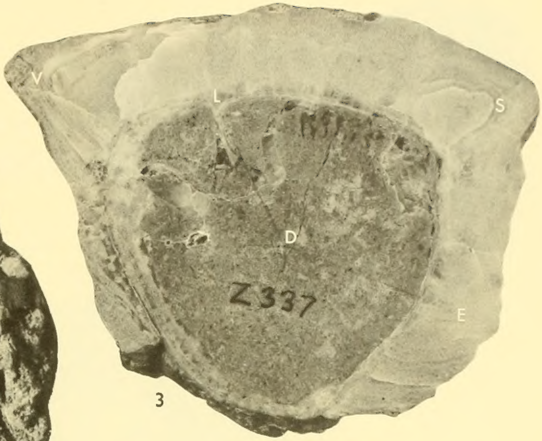

3

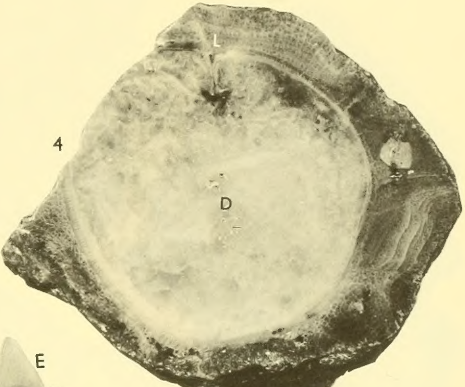

4

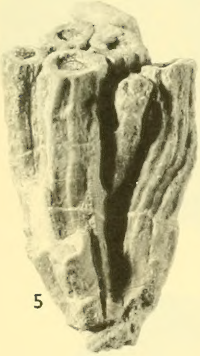

5

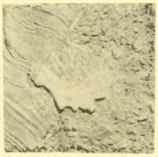

6

7

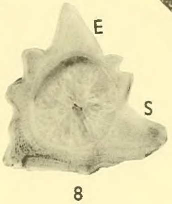

8

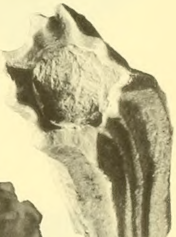

9

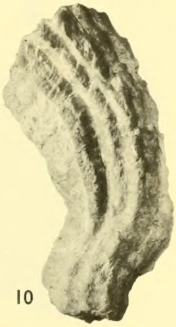

10

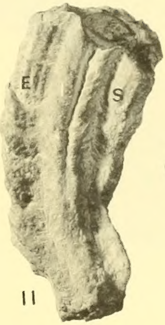

11

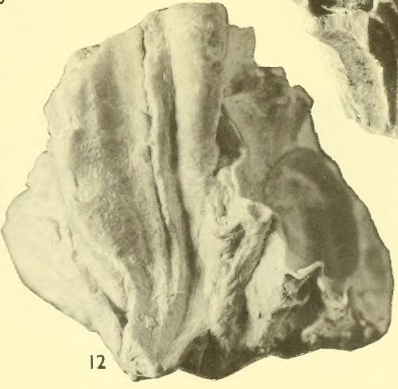

12

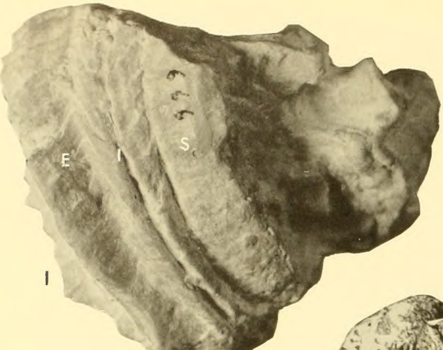

1

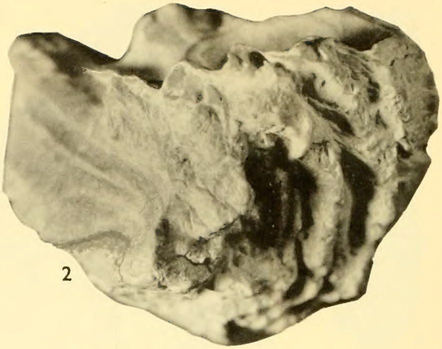

2

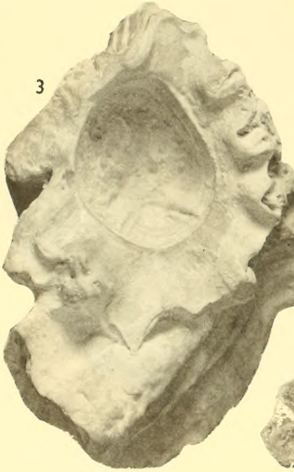

3

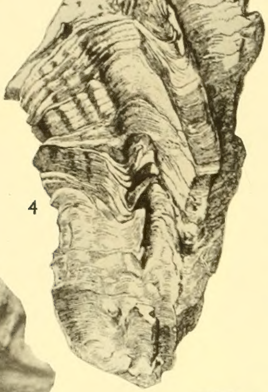

4

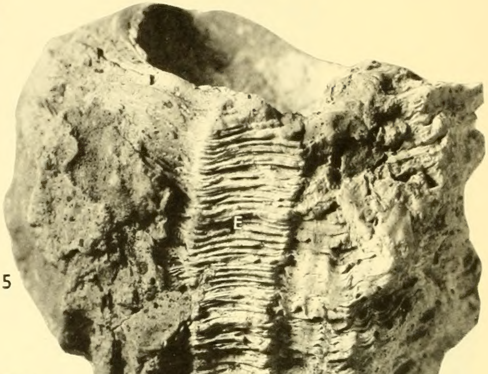

5

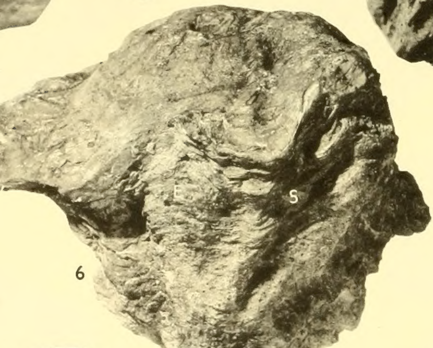

6

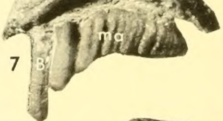

7

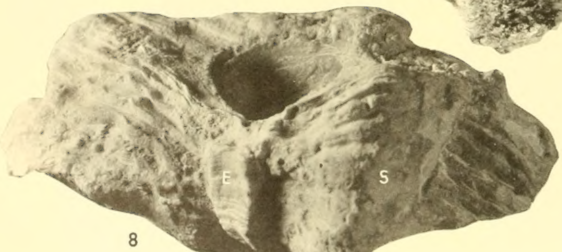

8

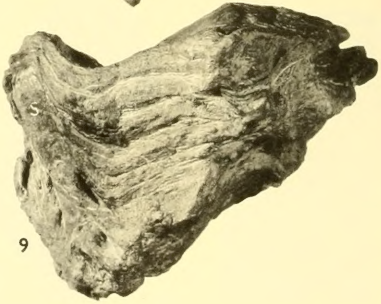

9

EXPLANATION OF PLATE 36

All illustrations natural size
Figure 4 courtesy American Museum of Natural History

Figure *Page*

1-3. *Biradiolites robinsoni* Chubb 187

Right valve, siphonal side. Same specimen as Plate 35, figure 12. The attached *B. jamaicensis* is seen on the right. Smith. Maestrichtian, Cotton Tree Gully, Lambs River, Westmoreland. 2. Same specimen, antisiphonal side. *B. jamaicensis* on left. 3. Same specimen, apertural aspect. In the body cavity may be seen the grooves for the reception of the teeth of the left valve. *B. jamaicensis* below.

4. *Biradiolites rudis* (Whitfield) 187

Bivalve, showing siphonal bands and interband. A copy of Whitfield's plate 11, figure 4. AMNH 9680/1. Maestrichtian, Logie Green, Clarendon.

5-8. *Biradiolites rudissimus* Trechmann 188

Right valve, a fairly tall individual. Smith. Maestrichtian, St. James. 6. Same species. Bivalve. BMNH L63136. Maestrichtian, Catadupa, St. James. 7. Same species. Part of left valve showing anterior myophore (ma) and tooth (B′) BMNH LL30295. Maestrichtian, Logie Green, Clarendon. 8. Same species. Right valve of a low spreading individual. Part of the specimen figured in Plate 38, figure 1. Smith. Maestrichtian, bridge half-a-mile north-west of Catadupa on the Cambridge road, St. James.

9. *Biradiolites* cf. *rudissimus* Trechmann 188

Part of right valve showing the S band on the left. Smith. Campanian, *Barrettia* Limestone, St. Ann's Great River, St. Ann.

EXPLANATION OF PLATE 37

All illustrations natural size

Figure		Page
1, 2.	*Biradiolites forbesi* Chubb Right valve, posterior aspect, showing section of calcitefilled body cavity and funnel plates (Chubb, 1956a, pl. 3, fig. 1). Smith. Maestrichtian, Lot 184, Ducketts Land Settlement, St. James. 2. Same specimen, apertural aspect, showing concentric upfold and radial, bifurcating, vascular marking (Chubb, 1956a, pl. 3, fig. 2).	188
3, 4.	*Biradiolites minhoensis* Trechmann Bivalve, commissural view of right valve with left valve in place. This and figure 4 are new photographs of Trechmann's type (1924b, pl. 26, figs. 1-1a). BMNH L63252. Maestrichtian, Logie Green, Clarendon. 4. Same specimen, siphonal aspect.	189
5-8.	*Biradiolites novaterrensis* Chubb Bivalve, anterior aspect; the upstanding funnel plates form a smooth concave wall. In this aspect the left valve is not seen. BMNH LL30296. Campanian, *Barrettia* Limestone, New Ground, St. Ann's Great River, St. Ann. 6. Same specimen, ventral aspect, showing the siphonal grooves (E and S) and interband (I). 7. Same specimen, posterior aspect, showing the subsidiary downfolds. 8. Same specimen, left valve in position on the right.	189
9-11.	*Biradiolites riograndensis* Chubb Bivalve, posterior aspect, showing on the left, the flange, in the centre the intermand with the E upfold on its left and the costellate S band on its right, and on the extreme right the smooth, concave dorsal side. Smith. Maestrichtian, Alligator Church, Rio Grande Valley, Portland. 10. Same specimen. Left valve in position on right valve. 11. Same specimen. Ventral aspect.	189

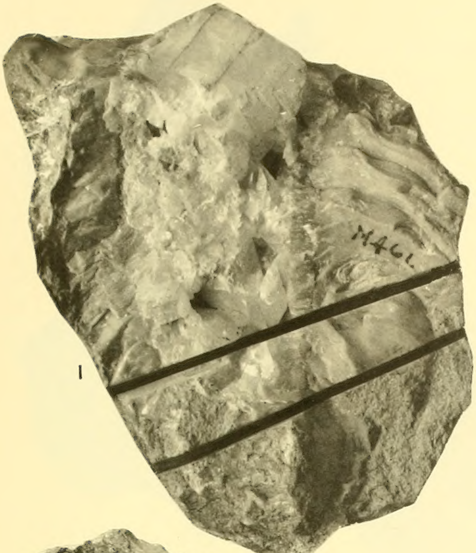

1

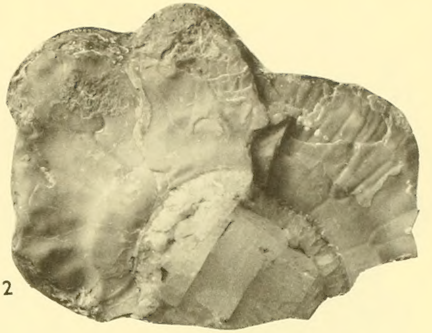

2

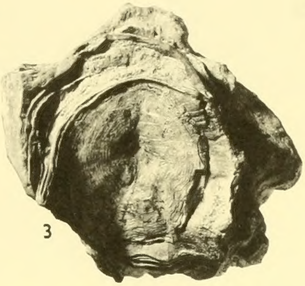

3

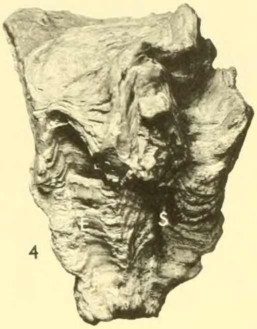

4

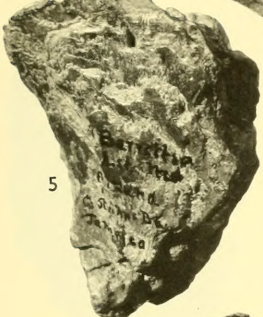

5

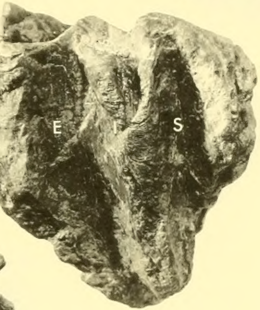

6

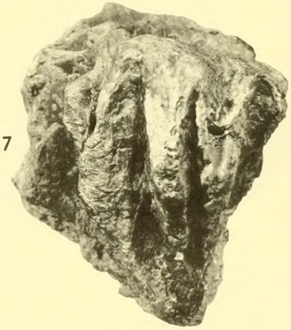

7

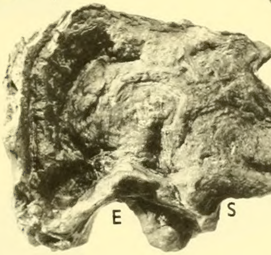

8

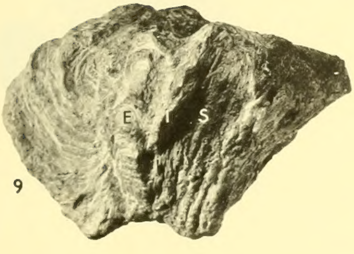

9

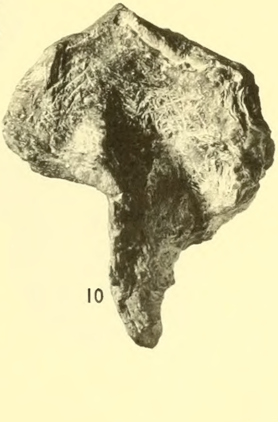

10

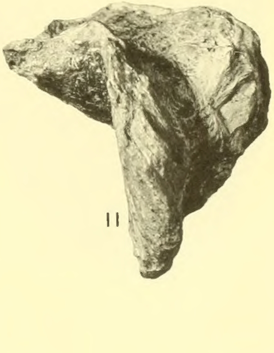

11

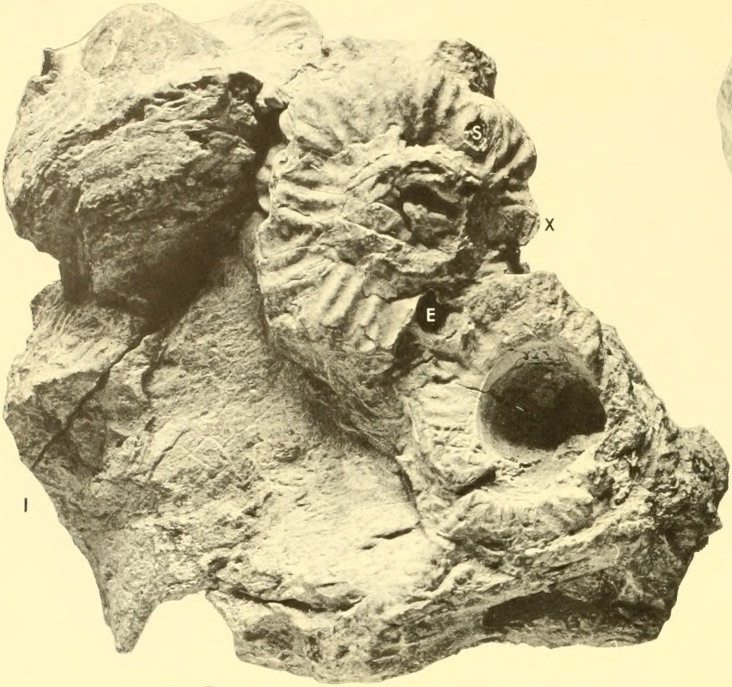
1

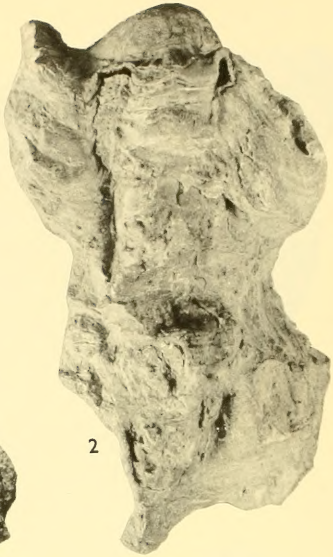
2

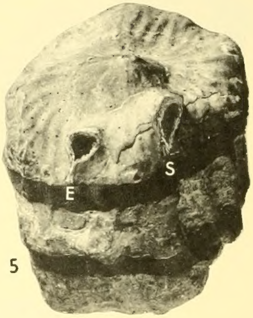
5

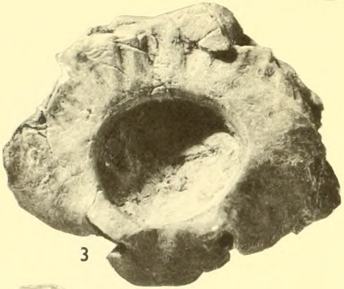
3

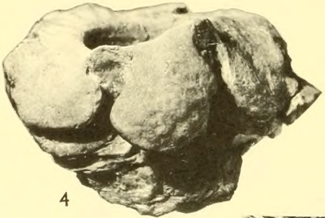
4

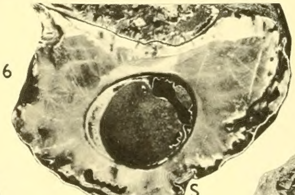
6

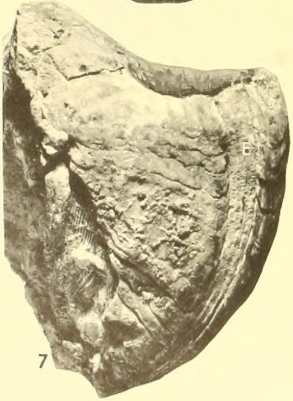
7

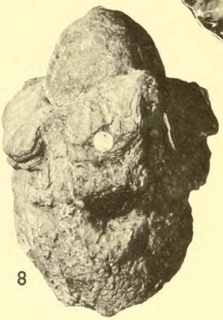
8

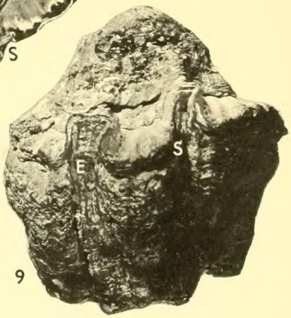
9

EXPLANATION OF PLATE 38

All illustrations natural size

Figure		*Page*
1-6.	*Thyrastylon adhaerens* (Whitfield)	190

Three shells, two of them bivalved, forming part of a cluster; they are attached to a shell of *Biradiolites rudissimus* whose aperture may be seen facing downwards at lower right (see Plate 36, fig. 8). The left hand shell shows the peak of the S oscule in silhouette; in the centre shell the S oscule is seen at the top, but the E oscule is displaced from its normal position, which would be on the projection x at the right centre of the valve, to a point about 25 mm away (Chubb, 1956b, pl. 7, fig. 8). Smith. Maestrichtian, bridge half-a-mile northwest of Catadupa on the Cambridge road, St. James. 2. Same specimen. Left hand shell viewed from the posterior; S. band occluded with peaked oscule below; E band occluded below, becoming open above, the oscule not occluded. (Chubb, 1956b, pl. 7, fig. 9). 3. Same species. Right valve, apertural view, showing partial occlusion of the two siphonal bands. (Chubb, 1956b, pl. 6, fig. 2). USNM 18011. Maestrichtian, Logie Green road, Clarendon. 4. Same specimen, posterior view, showing the funnel plates upfolded at the siphonal bands and downfolded and spreading laterally in the interband and at the sides (Chubb, 1956b, pl. 6, fig. 3). 5. Same species. Bivalve, posterior view, showing both bands occluded in the right valve and two oscules in the left (Chubb, 1956b, pl. 7, fig. 5). Smith. Maestrichtian, Catadupa, St. James. 6. Same specimen. Section at upper cut seen in Figure 5. Shows cardinal apparatus and S and E bands (Chubb, 1956b, pl. 7, fig. 6).

7-9.	*Thyrastylon coryi* (Trechmann)	191

Right valve, ventral aspect; it is attached by the whole of its anterior side to a fragment of *Antillocaprina occidentalis;* it shows curvature and costulate E band (Chubb, 1956b, pl. 7, fig. 2). Smith. Maestrichtian, Ducketts Land Settlement, one mile east of Lands Department office, St. James. 8. Same species. A new photograph of Trechmann's type (1924b, pl. 25, fig. 5). Bivalve, posterior aspect, showing high-crowned left valve, occluded S band, and open, costulate E band, BHNH L63213. Maestrichtian, near Catadupa, St. James. 9. Same species. Bivalve, posterior aspect, shows the same characters as the last, but the crown of the left valve passes smoothly into the brim (Chubb, 1956b, pl. 7, fig.1). Smith. Maestrichtian, Ducketts Land Settlement, same locality as Fig. 7.

EXPLANATION OF PLATE 39

All illustrations natural size

Figure		*Page*
1-3.	*Thyrastylon coryi* (Trechmann) ..... Right valve, ventral aspect. This shell was found in a shale but was attached to the surface of an underlying limestone; it therefore has an exceptionally flat anterior side. Smith. Maestrichtian, Shaw Castle Shale, Shaw Castle, St. James. 2. Same specimen, posterior aspect. 3. Same species. Posterior aspect, showing S band nearly occluded, E band costulate, unusually wide and partially overlapped by funnel plates (Chubb, 1956b, pl. 7, fig. 3). BMNH L63123. Maestrichtian, Catadupa, St. James.	191
4.	*Thyrastylon semiannulasus* (Trechmann) ..... Bivalve. A new photograph of one of Trechmann's types (1924b, pl. 25, fig. 6). Both bands are occluded but only the E band has an oscule. BMNH L63247. Maestrichtian, Logie Green, Clarendon.	191
5-8.	*Bournonia cancellata* (Whitfield) ..... Bivalve, posterior aspect. Smith. Maestrichtian, Logie Green, Clarendon. 6. Same specimen, left valve. 7. Same specimen, transverse section below commissure, shows cardinal apparatus of left valve including two teeth connected by a yoke and fitting into grooves in the right valve, anterior myophore and pedunculate posterior myophore. 8. Same specimen, anterior aspect, showing longitudinal groove.	192
9-12.	*Bournonia sanctannae* Chubb ..... Bivalve, posterior aspect. This specimen was figured by Trechmann (1924b, pl. 24, fig. 4) as *Biradiolites* (?) *cancellatus.* BMNH L63244. Campanian, *Barrettia* Limestone, St. Ann's Great River, St. Ann. 10. Same specimen, left valve. 11. Same specimen, transverse section below commissure. 12. Same specimen, anterior aspect.	193

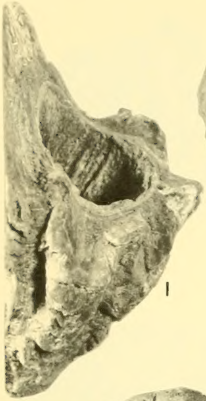
1

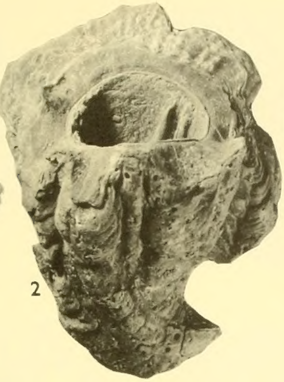
2

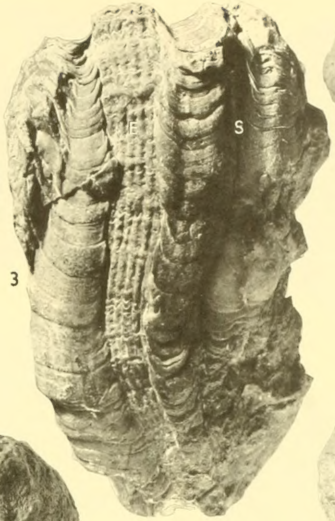

3

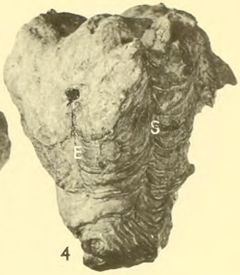

4

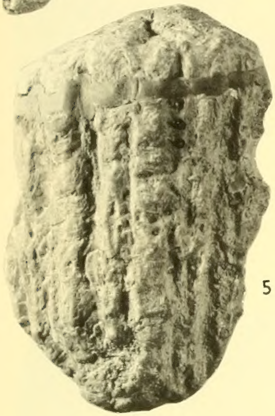
5

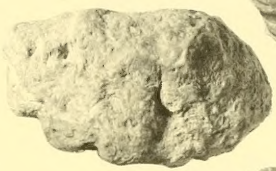
6

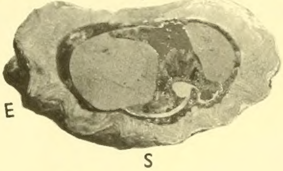

7

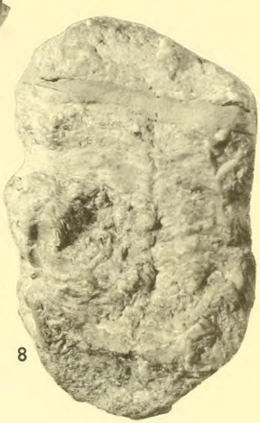
8

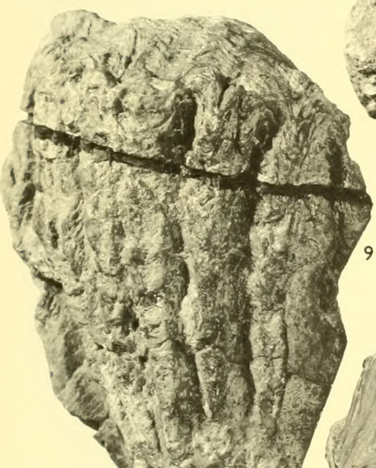
9

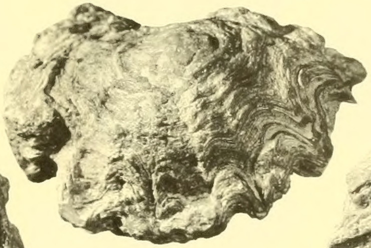
10

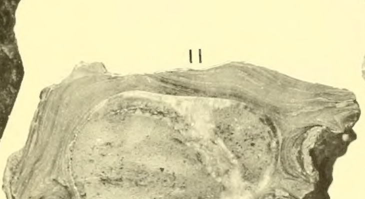
11

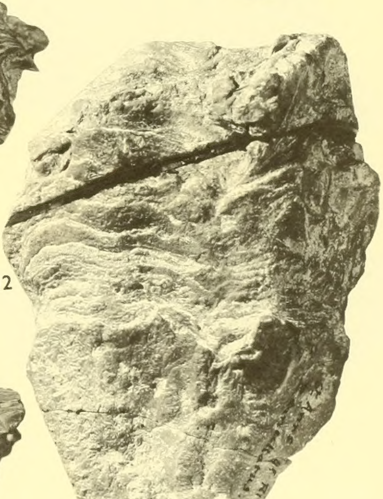
12

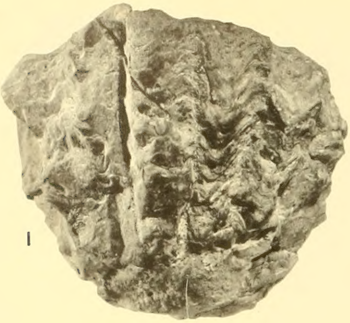
1

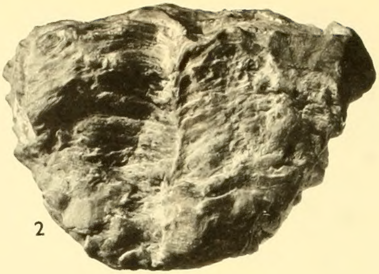
2

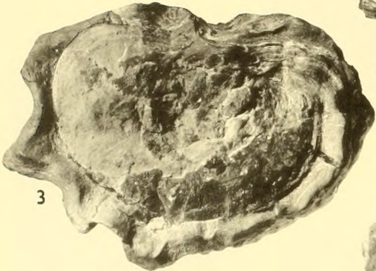
3

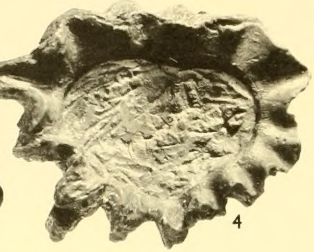
4

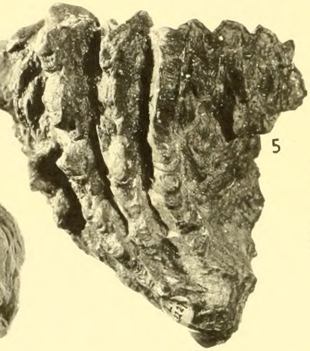
5

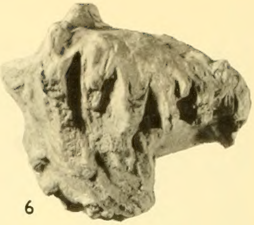
6

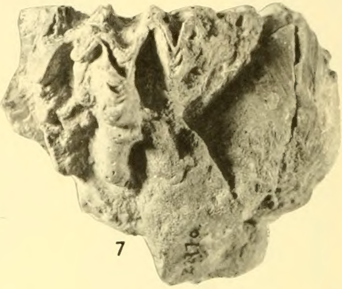
7

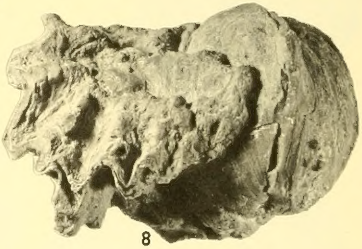
8

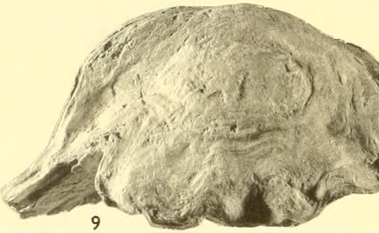
9

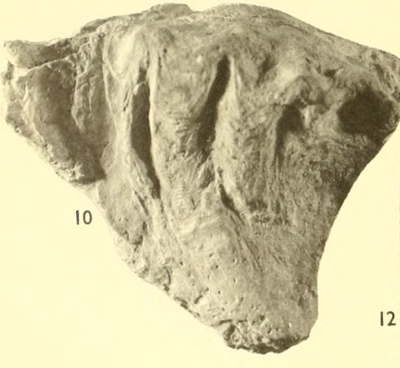
10

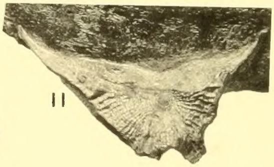
11

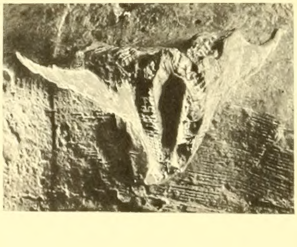
12

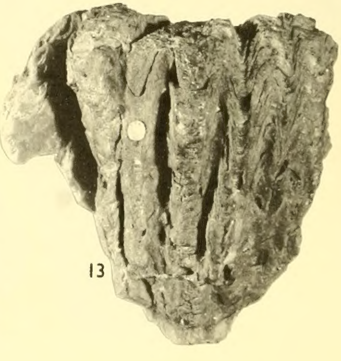
13

EXPLANATION OF PLATE 40

All illustrations natural size

Figure *Page*

1-3. *Bournonia subcancellata* (Trechmann) 193
Bivalve, posterior aspect. BMNH LL30299. Maestrichtian, Logie Green, Clarendon. 2. Same specimen, anterior aspect. 3. Same specimen, left valve in position on the right.

4, 5. *Bournonia barretti* Trechmann 194
Right valve, apertural aspect. This and the next figure are new photographs of Trechmann's type (1924b, pl. 26, figs. 2, 2a). BMNH L63227. Maestrichtian, Great River Valley, opposite Catadupa, St. James. 5. Same specimen, posterior aspect.

6-8. *Bournonia thiadensi* Vermunt 194
Posterior aspect. Smith. Maestrichtian, road facing Lot 67, Ducketts Land Settlement, Westmoreland. 7. Same species, posterior aspect. Attached to the left valve of ***Plagioptychus zansi;*** for another view of this specimen see Plate 33, figure 4. Smith. Maestrichtian, mile post 14 between Point and Flamstead, St. James. 8. 8. Same specimen, left valve.

9, 10. *Bournonia baileyi* Chubb 194
Left valve. Smith. Campanian, ***Barrettia*** Limestone, Haughton Hall, Green Island, Hanover. 10. Same specimen, posterior aspect.

11,12. *Bournonia tetrahedron* Chubb 195
Left valve. BMNH LL30287. Maestrichtian, Logie Green, Clarendon. 12. Same specimen, right valve, posterior aspect.

13. *Bournonia sanctmariae* Chubb 195
Right valve, posterior aspect. This specimen was figured by Trechmann as *Radiolites* cf. *cancellatus* (1924a, pl. 1, fig. 3). BMNH L63255. Reworked in Eocene shale, Port Maria, St. Mary.

EXPLANATION OF PLATE 41

All illustrations natural size
Figures 1 and 5 courtesy American Museum of Natural History

Figure		*Page*
1-4.	*Sauvagesia macroplicata* (Whitfield)	196
	Bivalve. A copy of Whitfield's figure of his type (1897a, pl. 13, fig. 8). AMNH 9679/1. Maestrichtian, Logie Green, Clarendon. 2. Same species. Transverse section of a right valve, showing the strong folding of the funnel plates, the polygonal cell pattern and the ligamental infold (Chubb, 1956a, pl. 3, fig. 5). Smith. Maestrichtian, Shortwood Parochial road, St. James. 3. Same specimen. Transverse section of left valve, showing radial plates in the inner layer (Chubb, 1956a, pl. 4, fig. 1). 4. Same species. Young right valve, showing siphonal bands and interband (Chubb, 1956a, pl. 4, fig. 2). USNM 18013. Maestrichtian, Logie Green, Clarendon.	
5-7.	*Sauvagesia annulosa* (Whitfield)	198
	Bivalve, anterior aspect. A copy of Whitfield's figure of his type (1897a, pl. 14, fig. 3). The ligament is at the left of the figure and a slight upfold at the right probably represents the E band. The left valve shows radial plates like those of *S. macroplicate.* AMNH 9676/1. Maestrichtian, said to be from Christianna, probably Logie Green, Clarendon. 6. Same specimen. Left valve showing ligamental infold and radial plates. This and the next figure are new photographs of Whitfield's type. 7. Same specimen, ventral aspect. The slight upfold seen in the centre is thought to be the E band, that on its right the S band.	

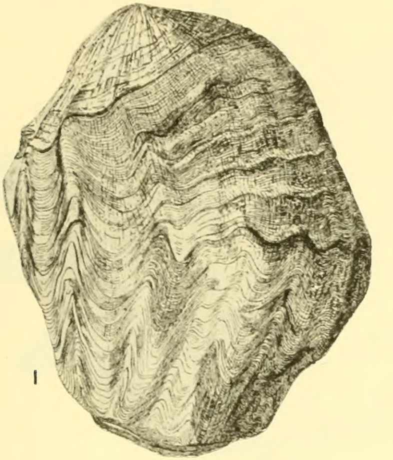
1

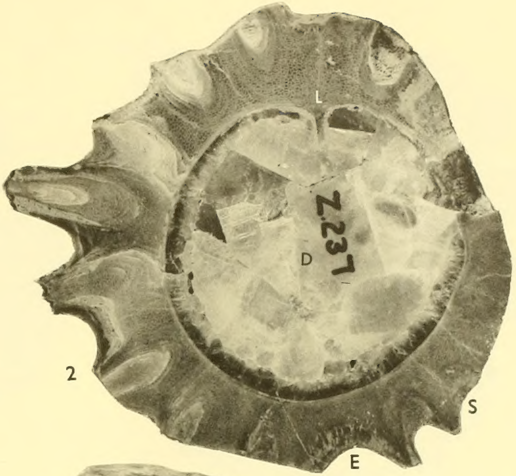

2

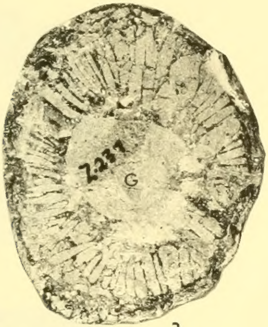

3

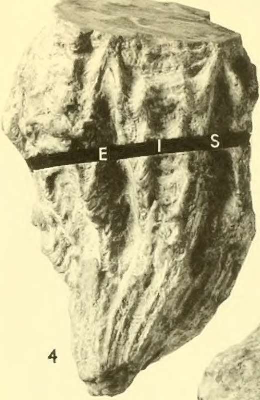

4

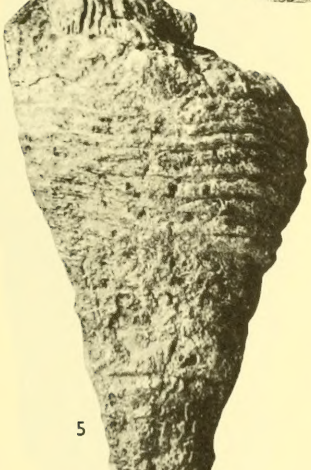
5

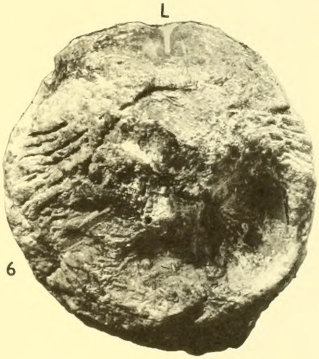

6

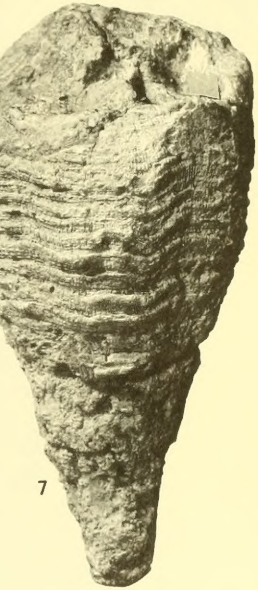
7

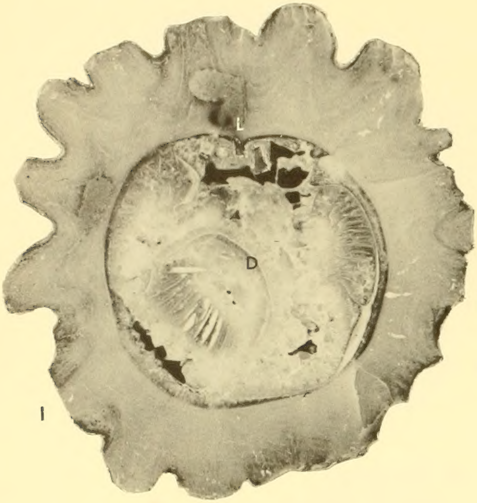
1

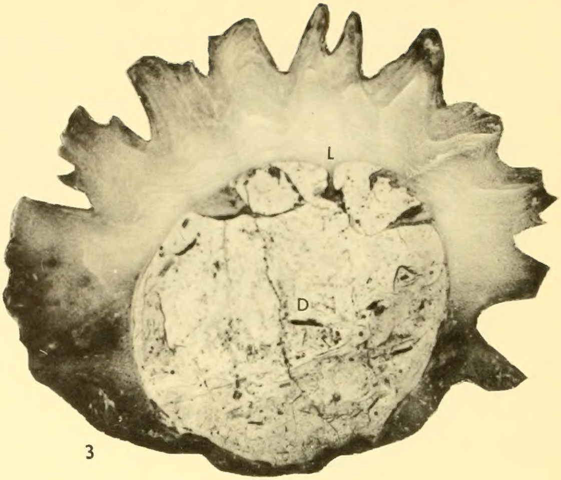
3

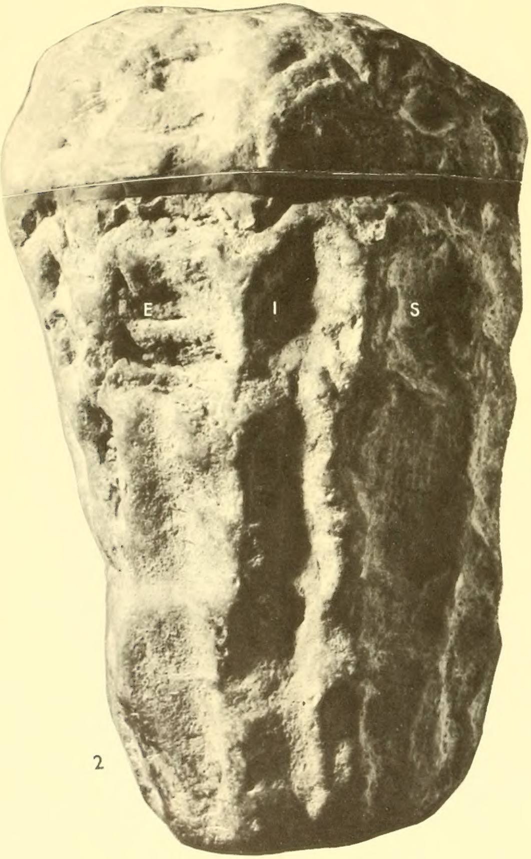
2

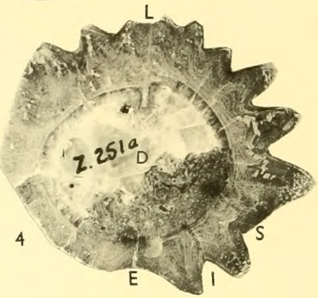
4

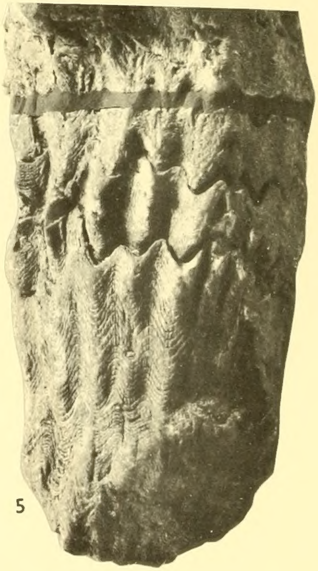
5

EXPLANATION OF PLATE 42

All illustrations natural size

Figure		*Page*
1-3.	*Sauvagesia mcgrathi* Chubb Transverse section of right valve, showing ligamental ridge broken and dislodged, posterior myophore of left valve in position, anterior myophore displaced (Chubb, 1956a, pl. 3, fig. 4). Smith. River gravel in the Orange River at Stapleton, St. James, derived from Basal Maestrichtian limestone in the headwaters of the river below Kensington. 2. Same specimen, bivalve, much waterworn. Ventro-posterior aspect, showing in the centre the interband consisting of two costae with a furrow between, on its left the E band and on its right the S band, which has costellae (Chubb, 1956a, pl. 3, fig. 3). 3. Same species. Transverse section of right valve clearly showing the ligamental infold. Loose in soil of banana fields at the head of the Orange River, St. James.	197
4,5.	*Sauvagesia fluminisagni* Chubb Transverse section of right valve. (Chubb, 1956a, pl. 4, fig. 3). Smith. Maestrichtian, Cotton Tree Gully, Lambs River, Westmoreland. 5. Same specimen. Right valve, posterior aspect. The upper part, which is crushed, is cut away (Chubb, 1956a, pl. 4, fig. 7).	197

EXPLANATION OF PLATE 43

All illustrations natural size except figures 5 and 6
Figure 6 courtesy American Museum of Natural History

Figure		*Page*
1-4.	*Tepeyacia multicostata* Chubb	198
	Right valve lateral aspect. Smith. Cretaceous tuffaceous shale, probably Albian, north-north-east of Seafield Manse, St. Catherine. 2. Same specimen. Transverse section showing tooth (N) between two oval sockets (b′ and b) which are separated from the body cavity by thin laminae and are occupied by the ends of the teeth of the left valve; also siphonal infolds (S and E) forming slight pseudopillars. The E infold is diametrically opposite to the tooth N, i.e. it is mid ventral. 3. Same specimen. Transverse section a few millimetres higher than the last. The sockets are not separated from the body cavity but appear as grooves between the tooth and the outer buttresses. 4. Same species. Transverse section of another specimen cut at a higher level; tooth and buttresses have disappeared. Smith. Same horizon and locality.	
5.	*Durania* cf. *aguilae* Adkins	201
	Right valve, apertural aspect × 0.7 (Chubb, 1956a, pl. 4, fig. 6). Smith. Campanian, *Barrettia* Limestone mile post 9 on the Kensington-Amity Hall road, St. James.	
6.	*Durania nicholasi* (Whitfield)	199
	Right valve, posterior aspect × 0.28, the original being about 450 mm in diameter. A reproduction of one of Whitfield's figures (1897a, pl. 7, fig. 2). It shows the two siphonal grooves, the rounded interband, and the angular upfold of the funnel plates at the S band. AMNH 9675/1. Stated to be from the Cretaceous of Orange Cove, Hanover; probably from the Campanian, *Barrettia* Limestone, Haughton Hall, Green Island, Hanover.	

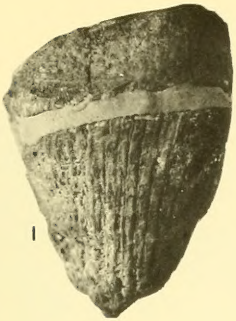
1

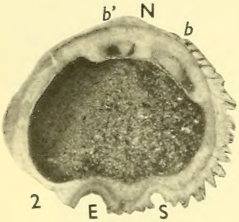

2

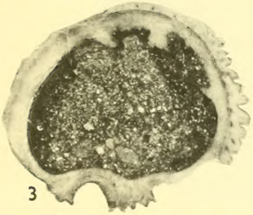
3

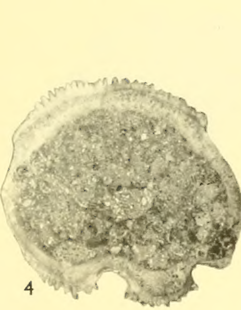
4

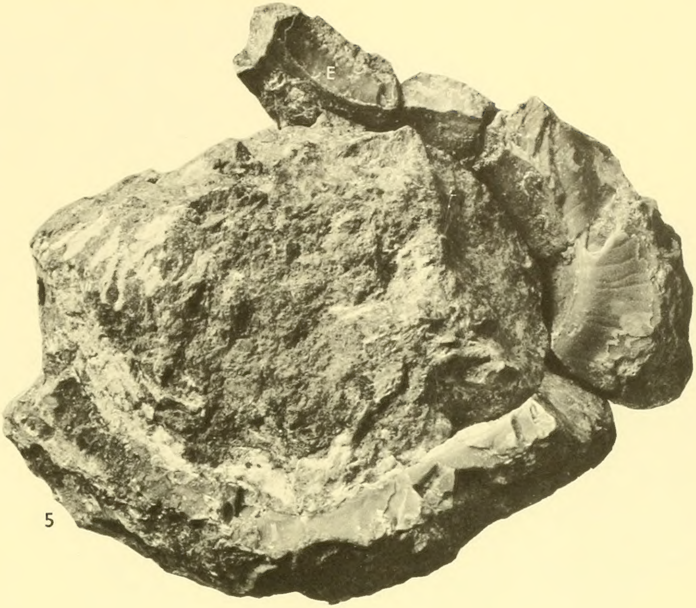

5

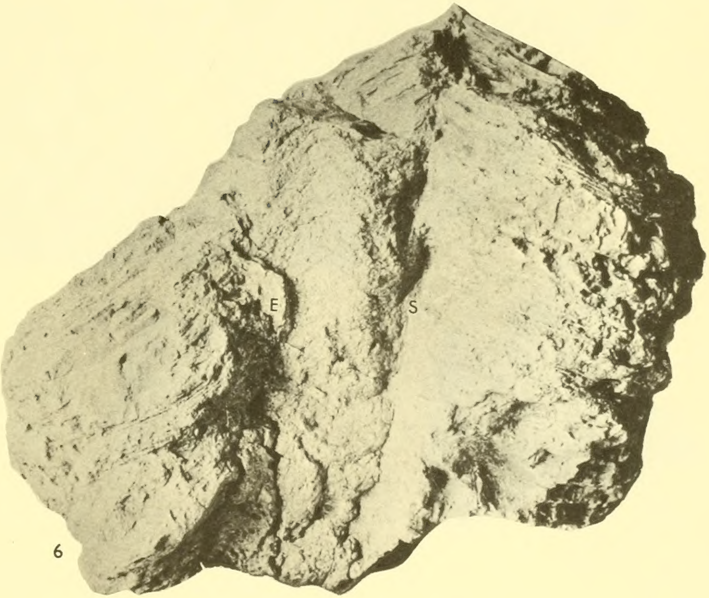

6

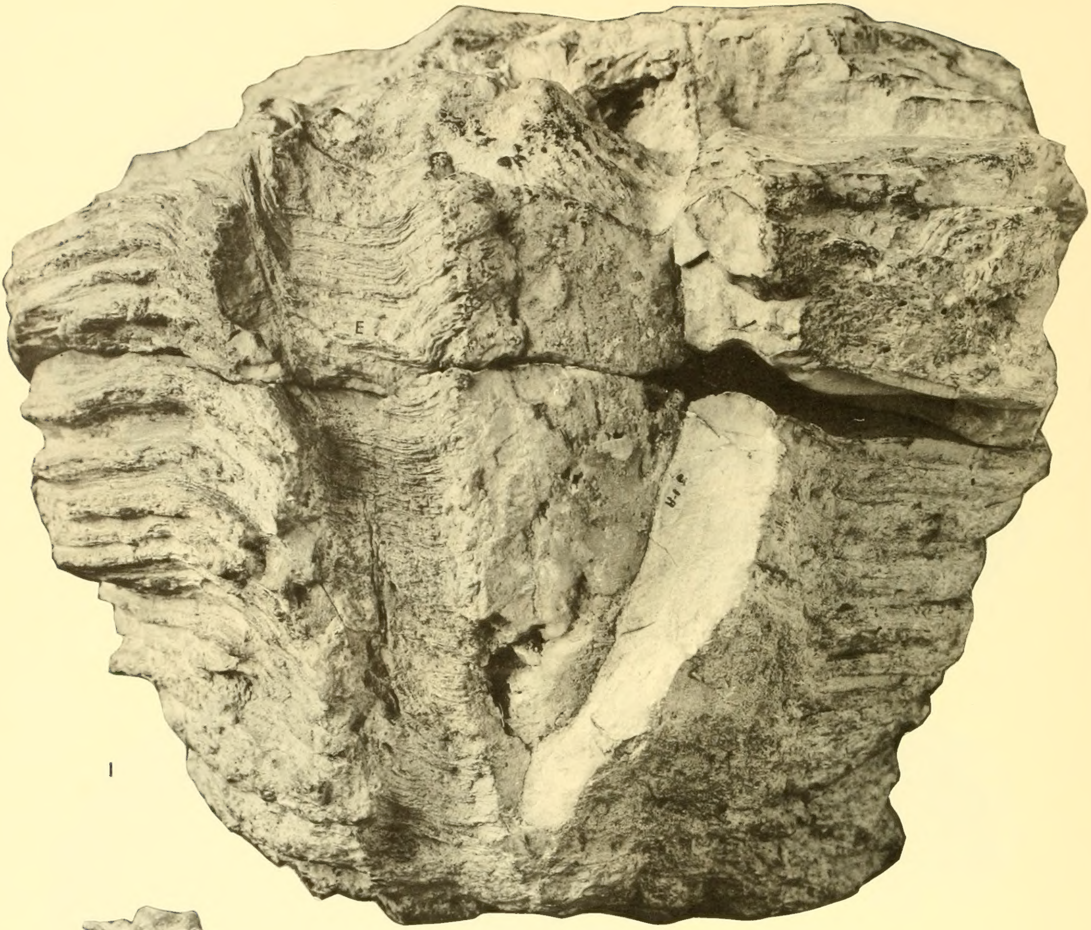

1

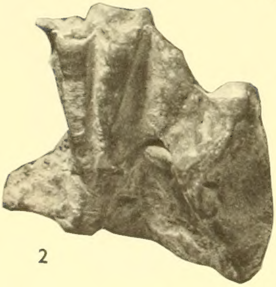

2

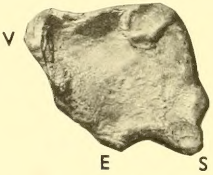

3

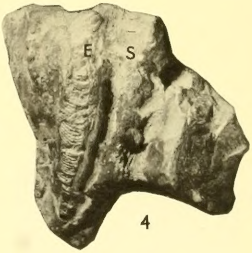

4

EXPLANATION OF PLATE 44

Figure 1 reduced; figures 2-4 natural size

Figure		*Page*
1.	*Durania nicholasi* (Whitfield) Right valve, posterior aspect, × 0.4. The deeply sunken E band and the corresponding downfold of the funnel plates are clearly seen. The outer layer is broken away at the S band. Inst J1A-B. Probably *Barrettia* Limestone, Haughton Hall, Green Island, Hanover.	199
2-4.	*Bournonia coxi* Chubb The smaller shell upright with the larger shell lying transversely behind it. The two rounded siphonal bands are well shown. Smith. *Barrettia* Limestone. New Ground, St. Ann's Great River, St. Ann. 3. Same specimen, left valve of larger shell. The lappet covering the E band is broken off short, but the S lappet is complete. Small *Ostrea* on dorsal side. 4. Same specimen, the larger shell upright with the smaller lying behind it.	196

EXPLANATION OF PLATE 45

The illustration is reduced

Figure	*Page*
1. *Durania nicholasi* (Whitfield)	199

Right valve, apertural aspect, × 0.5; the lower part of the specimen figured in Plate 44, figure 1. Shows the broad flat funnel plates crossed by branching vascular impressions. The vesicular structure of the inner layer may be seen in the body cavity. The deeply impressed E band bulges into the cavity to form an incipient pseudopillar. Though the outer layer is broken away at the S band it can be seen that it did not form a pseudopillar. Inst J1A.

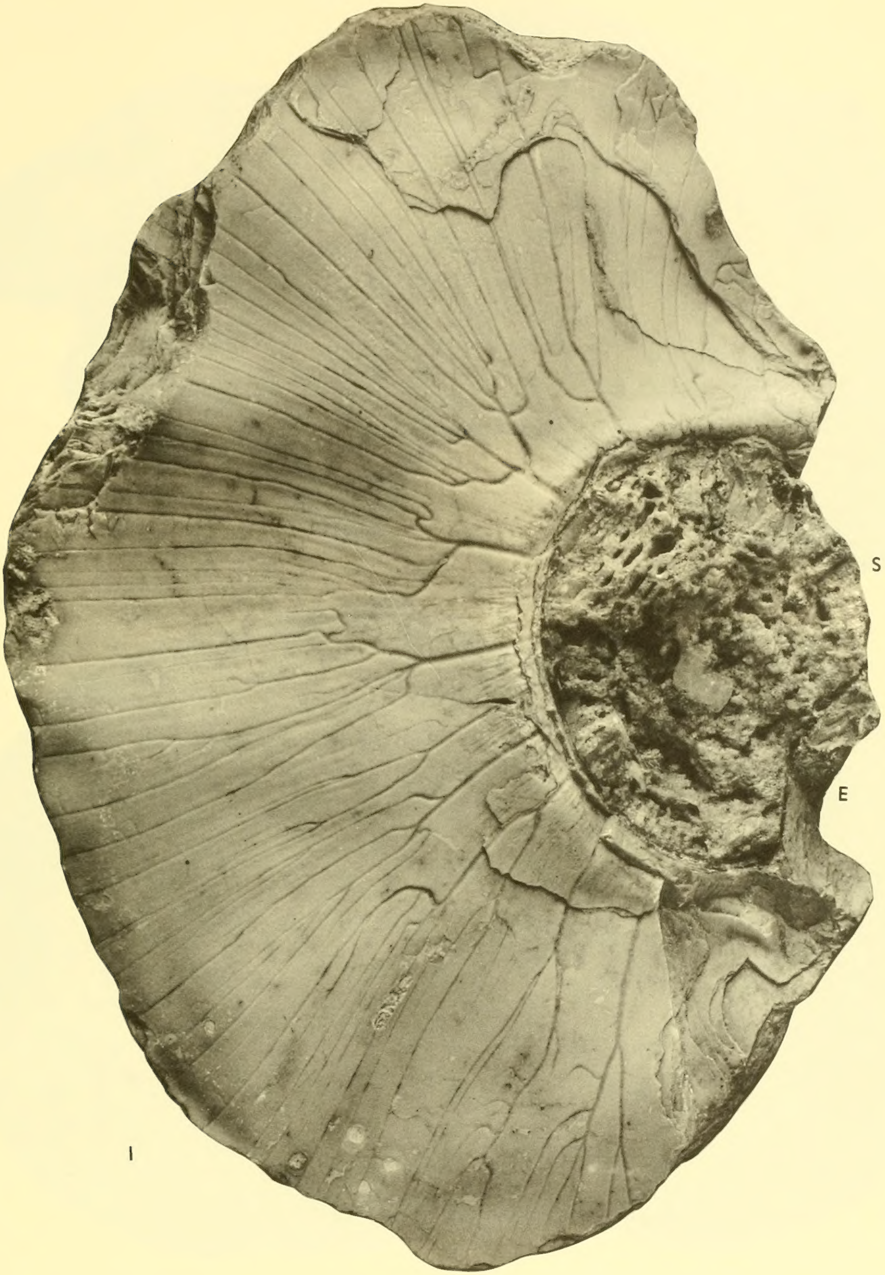
S
E
I

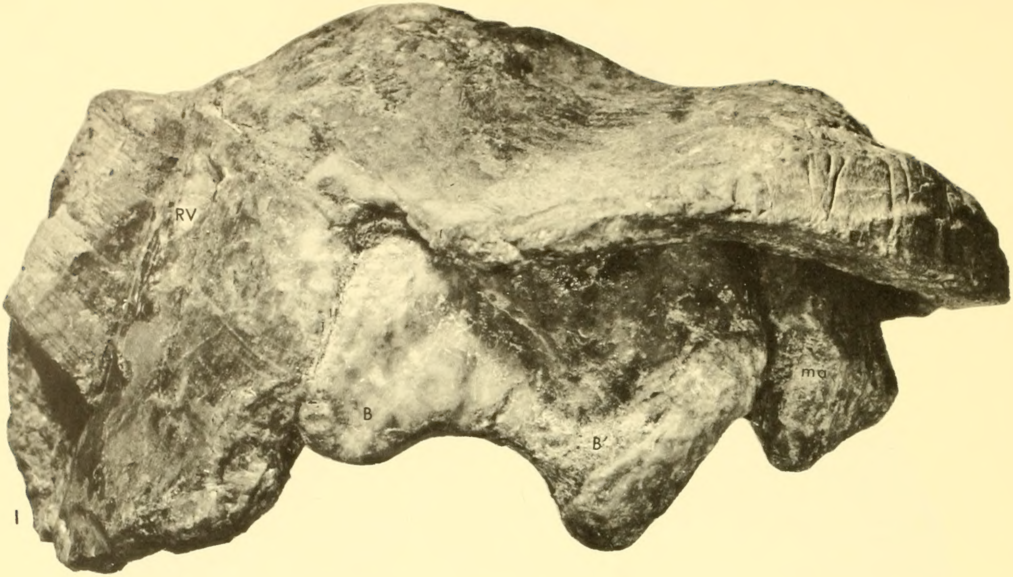

1

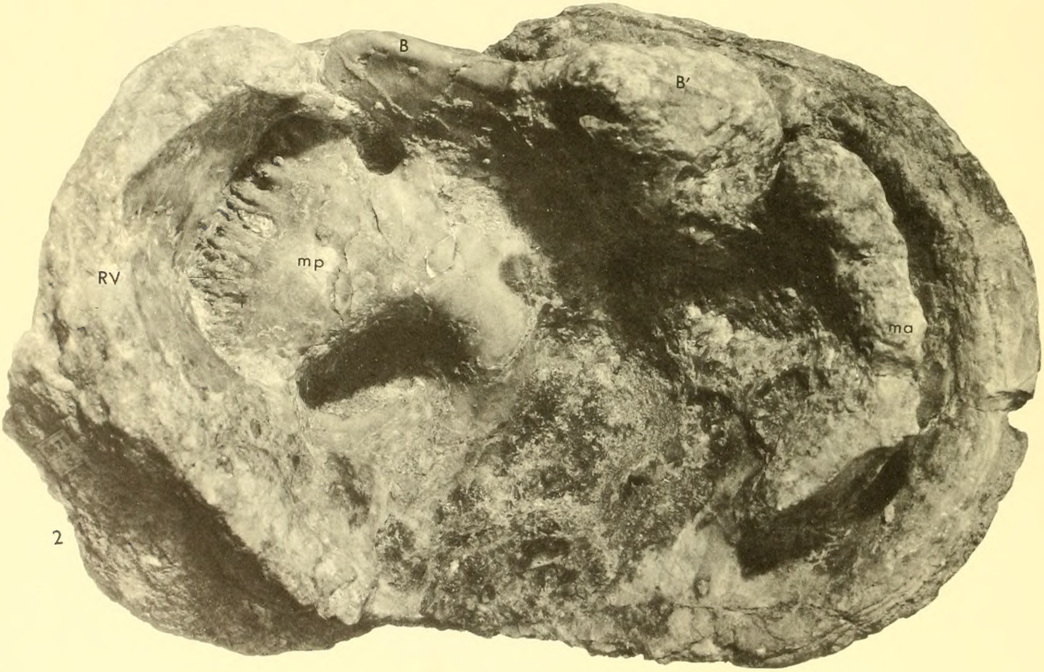

2

EXPLANATION OF PLATE 46

Illustrations natural size

Figure *Page*

1,2. *Durania nicholasi* (Whitfield) 199

Left valve, dorsal aspect. The two oblique teeth (B′ and B) and their connecting saddle are seen in the centre of the figure, with the anterior myophore (ma) on their right and an attached fragment of the right valve (RV) on their left. This and the next figure are new photographs of Whitfield's type (1897a, pl. 9, figs. 1-2). AMNH 9675/3. Campanian, *Barrettia* Limestone, Haughton Hall, Green Island, Hanover. 2. Same specimen, internal aspect. On the left the pedunculate posterior myophore (mp) abuts against the attached fragment of the right valve (RV) from which a process projects into the gap between this myophore and the adjacent posterior tooth (B). This tooth is connected by a saddle with the longer anterior tooth (B′), beyond which the anterior myophore (ma) curves around within the margin of the valve; its ventral end is broken away.

EXPLANATION OF PLATE 47

All illustrations natural size

Figure		*Page*
1-4.	*Chiapasella radiolitiformis* (Trechmann)	202

Bivalve. A new photograph of one of Trechmann's syntypes (1924b, pl. 24, figs. 2 and 2a). The left valve is seen in position upon the right; lappets from its margin overlie the costae with the invaginations rising between them. In places the polygonal pattern of the right valve may be seen. BMNH L63118. Maestrichtian, Logie Green, Upper Clarendon. 2. Same specimen, posterior view. The surface is unweathered and shows the costellae, also the costae projecting downwards and outwards as thumblike processes. 3. Same species, young individual, somewhat weathered; the left valve is depressed conical. Smith. Same horizon and locality. 4. Same species, adult right valve split longitudinally and showing the vesicular structure formed by the inner layer. Smith. St. James, exact locality unknown.

Plate 47

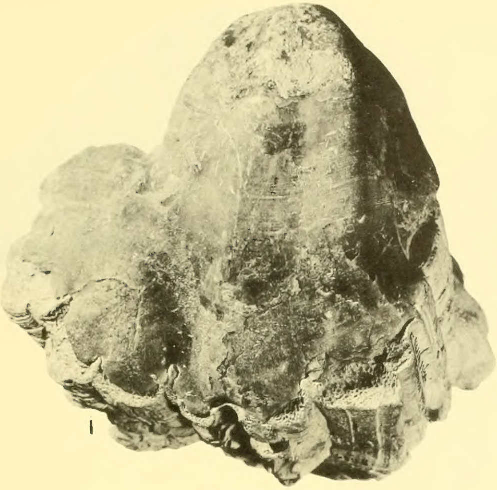

1

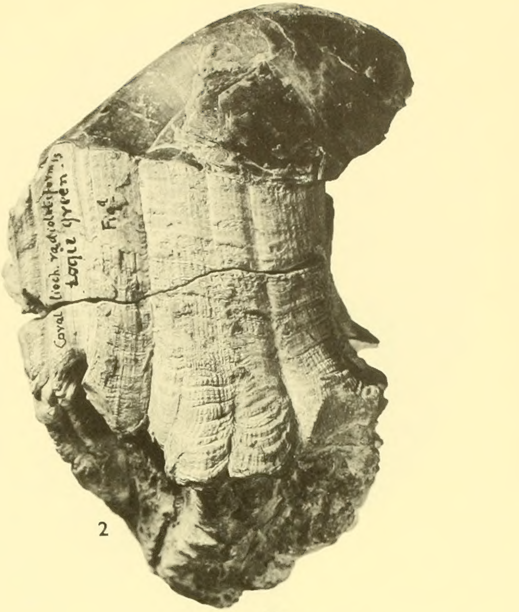

2

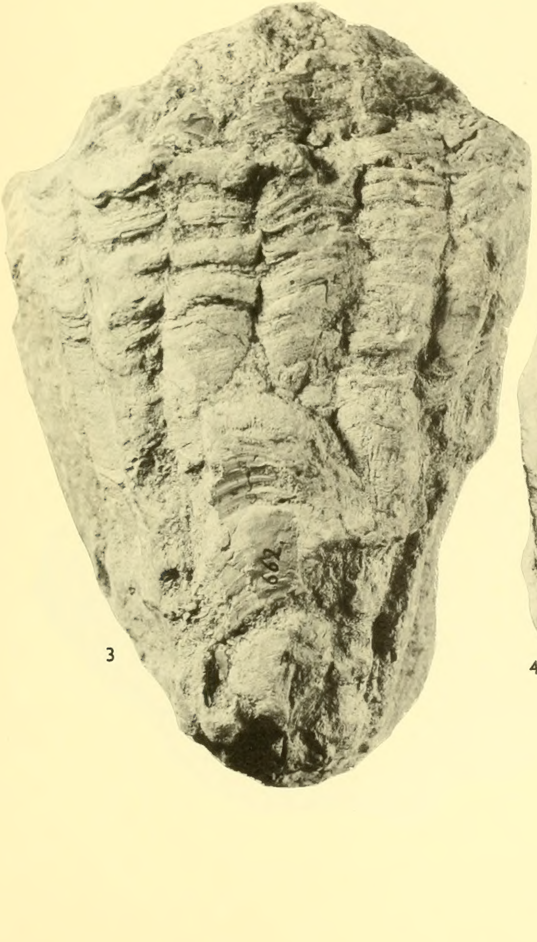

3

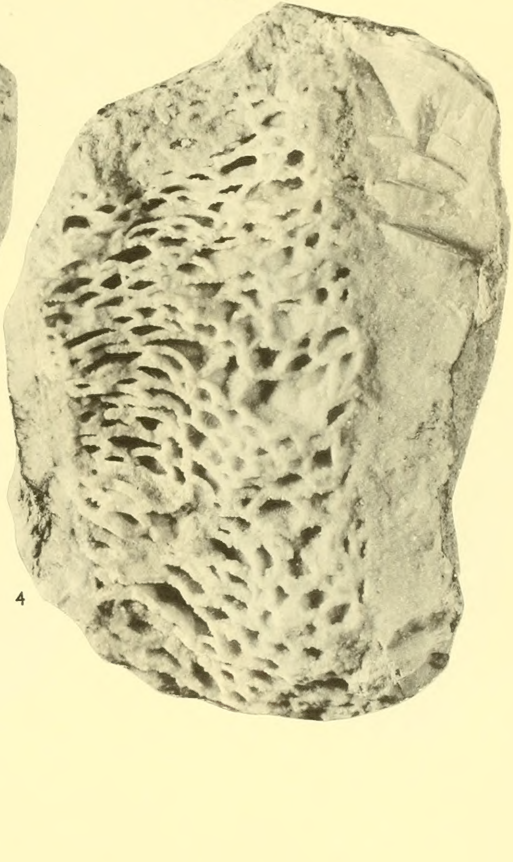

4

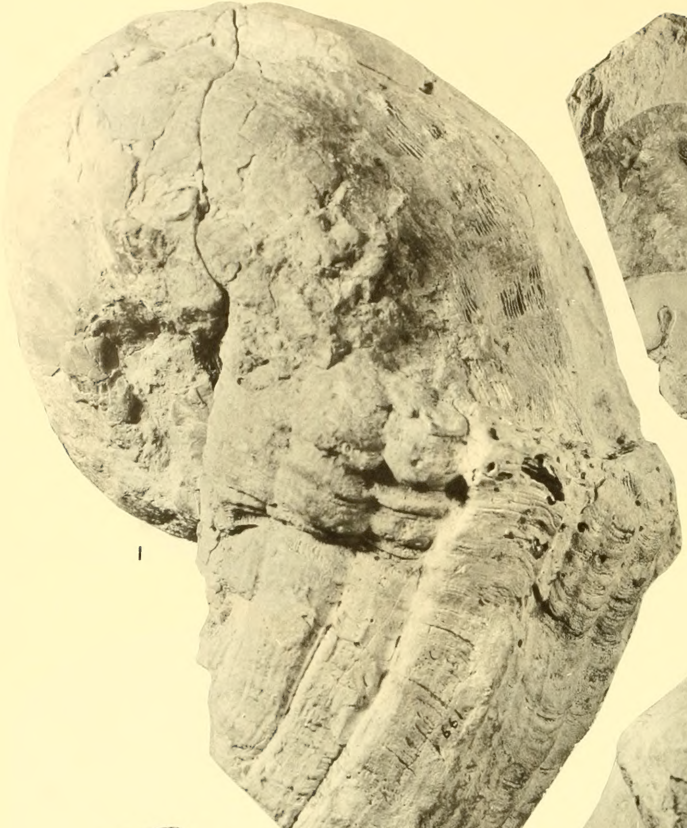
1

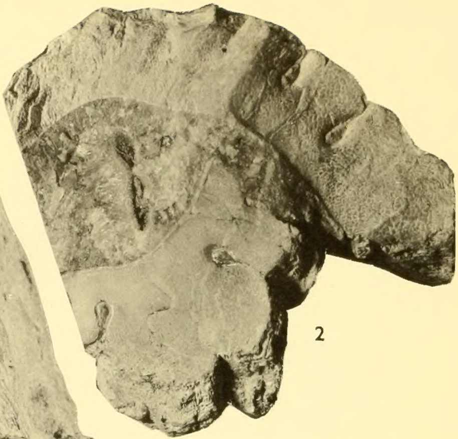
2

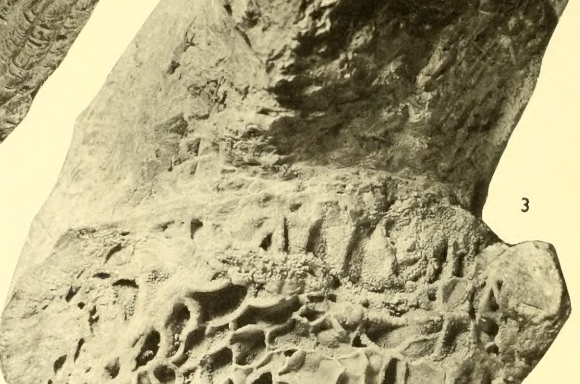
3

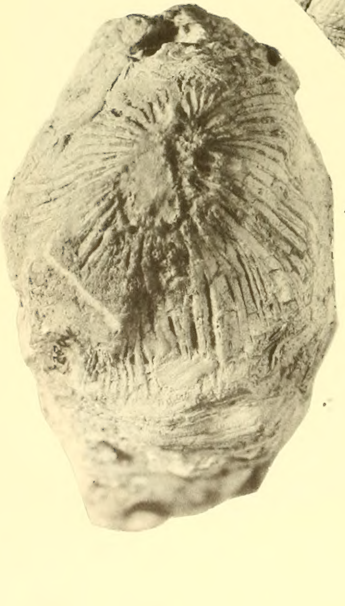
4

EXPLANATION OF PLATE 48

All illustrations natural size except figure 1

Figure		*Page*
1-4.	*Chiapasella radiolitiformis* (Trechmann)	202

Adult bivalved specimen × 0.67. Left valve (above) retains most of its outer layer but where this is weathered away the underlying vertical plates can be seen. Right valve shows rounded costae, slight longitudinal costellae and, on the right, the E band; its apical part is broken away. Smith. Maestrichtian, Lambs River bridge, Westmoreland. 2. Same specimen, natural size. Part of broken lower surface of right valve, with a portion of the wall crushed in. It shows the surface of the funnel plates with polygonal cell pattern and invaginations. 3. Same specimen, natural size. Part of left valve. The broken surface shows the extremely thin outer layer; within this the inner layer shows in its marginal part a system of radially elongated "canals" separated by vertical plates; this border merges into the central part which has a vesicular structure, different from the tabular structure shown by most advanced rudists. 4. Same species. Young individual, natural size. The left valve is a low cone which, having lost its outer layer, shows a system of radial vertical plates, most of them bifurcating, similar to those of certain other Radiolitidae. Smith. Maestrichtian, Ducketts Cross Roads, Westmoreland.

EXPLANATION OF PLATE 49

All illustrations natural size

Figure		Page
1,2.	*Orbignya mullerriedi* Vermunt A cluster of right valves closely associated with several species of coral notably *Multicolumnastrea cyathiformis* Duncan (Chubb, 1956a, pl. 4, fig. 4). Smith. Maestrichtian, at base of a *Titanosarcolites* limestone near its junction with underlying purple shale, sinkhole on Lot 45, Ducketts Land Settlement, Westmoreland. 2. Same specimen, apertural aspect. (Chubb, 1956a, pl. 4, fig. 8).	204
3.	*Orbignya ceibarum* Chubb Apertural view of a cluster of shells, the top right-hand one showing part of its left valve, and the middle one showing the tooth of the right valve and the cardinal apparatus of the left (Chubb, 1956a, pl. 4, fig. 10). Compare Text-figure 6. Maestrichtian, Cotton Tree Gully, Lambs River Valley, Westmoreland.	204
4.	*Torreites* cf. *sanchezi* (Douvillé) Part of right valve, transverse section showing the three pillars. Smith. Probably Turonian, Peters Hill Limestone, Peters Hill, northeast Clarendon.	207

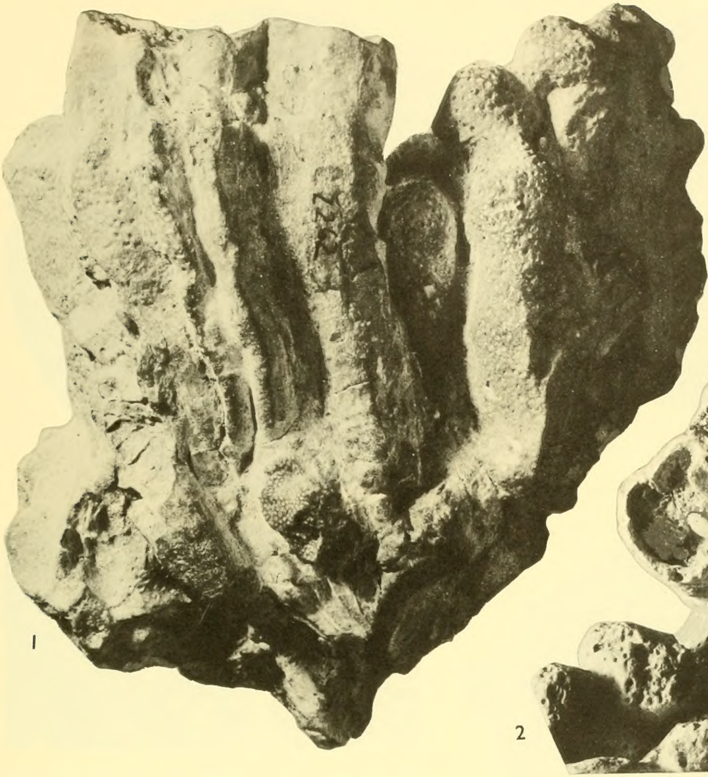

1

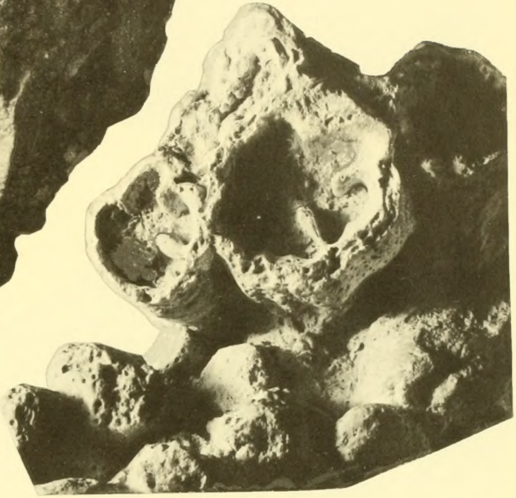

2

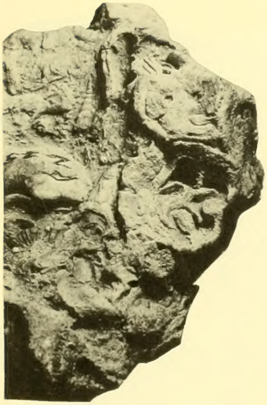

3

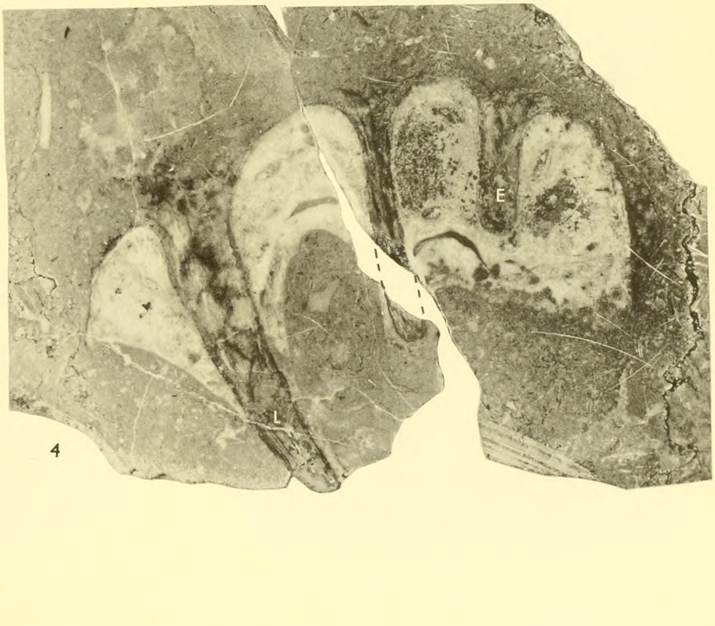

4

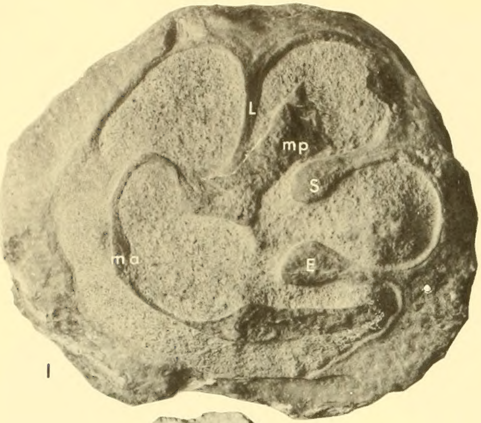

1

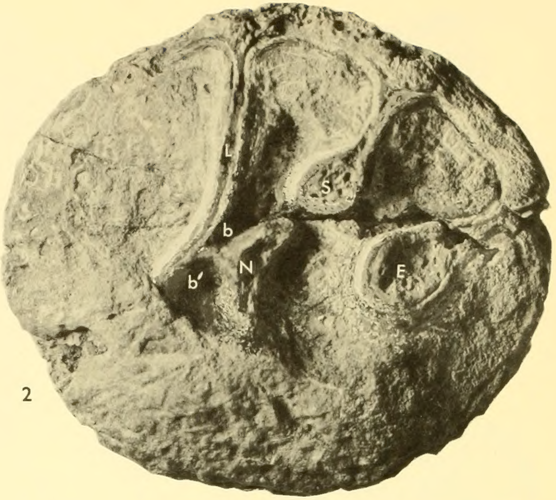

2

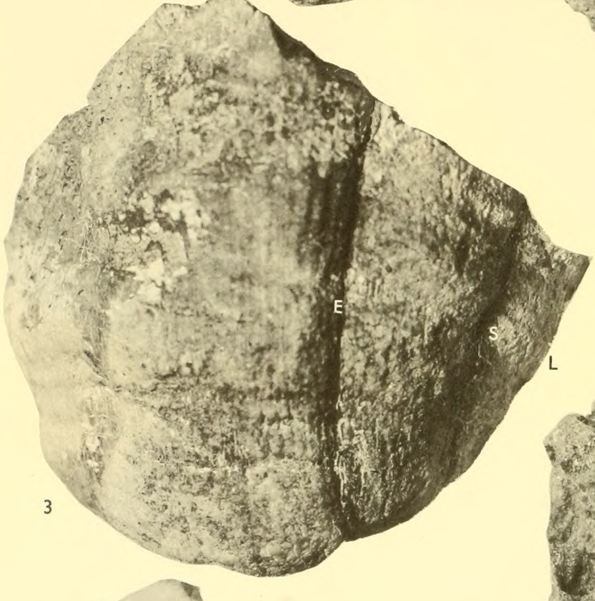

3

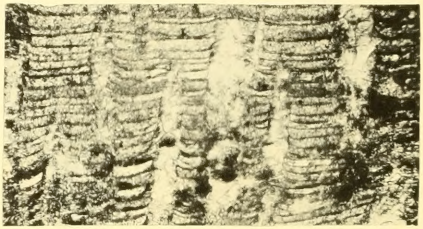

4

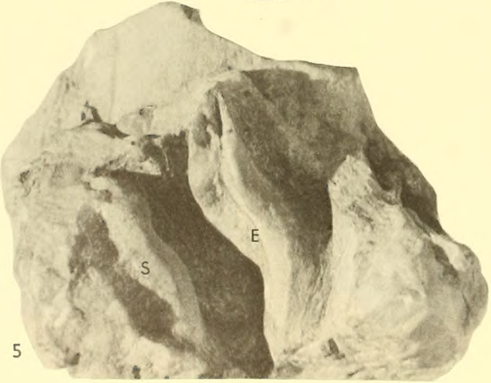

5

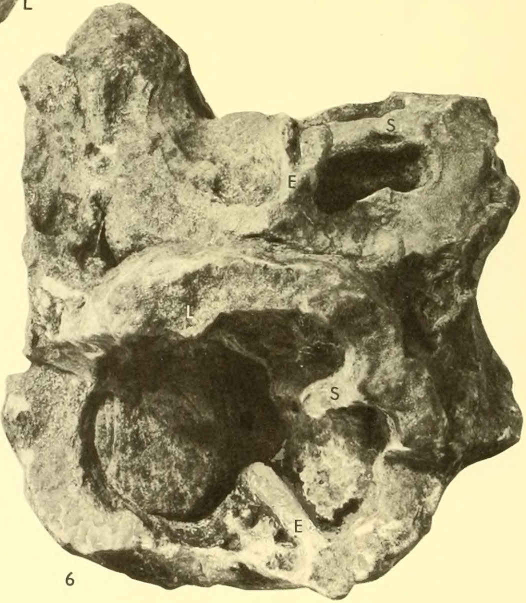

6

EXPLANATION OF PLATE 50

All illustrations natural size except figure 4

Figure		*Page*
1-3.	*Vaccinites eyrei* Chubb	206

Right valve (specimen a), apertural aspect, containing the cardinal apparatus of the left valve. Smith. *Barrettia* Limestone, Clifton, Hanover. 2. Same species (specimen b), showing tooth (N). Smith. Same horizon and locality. 3. Same species (specimen c), posterior aspect; it is split in the ligamental plane and posed so that L is at the right hand margin; the S and E furrows may be seen. Smith. Same horizon and locality.

4-6.	*Orbignya maldonensis* Chubb	205

Right valve, vertical radial section of the outer layer × 20 (Chubb, 1956a, pl. 5, fig. 5). Smith. Maestrichtian, south of Maldon cross, St. James. 5. Same specimen, interior of the body cavity of an incomplete right valve showing, on the left, the S pillar and in the centre, the E pillar becoming bilobed. The smooth surface of another shell is seen above, showing the S furrow (Chubb 1956a, pl. 5, fig. 3). 6. Same specimen, apertural view of two right valves, the incomplete one showing bilobed E pillar above, the complete normal one below, and a fragment of a third on the right. (Chubb, 1956a, pl. 5, fig. 1).

EXPLANATION OF PLATE 51

All illustrations natural size except Figure 1
Figure 3 courtesy Société géologique de France

Figure		*Page*
1-3.	*Barrettia monilifera* Woodward	208

Topotype. Transverse section of a cluster of eight right valves × 0.8, its marginal parts considerably damaged by a boring organism. Since rudists normally attached themselves by their anterior or dorso-anterior, *i.e.* their antisiphonal sides, no doubt in order to keep their siphons clear, it is obvious that the first member of the group was the rounded shell in the upper row second from the left. This is largely surrounded by a circle of shells which attached themselves by their own anterior sides to its dorsal, posterior and ventral sides; these in turn are partially surrounded by a second circle of shells attached by their anterior sides. Smith. Cretaceous, probably Campanian, Back River, Portland. 2. Same species. Topotype. Cornute specimen with adherent young shells of the same species, natural size. Smith. Same horizon and locality. 3. Same species. One of Woodward's syntypes. A copy of a photograph by Douvillé of a slice of a right valve lent to him by the British Museum (Natural History) (Douvillé, 1890-7, pl. 17, fig. 6). It shows the moniliform infolds, including L, S and E, the tooth N between the sockets *b'* and *b*, and the cavity between *b* and S which accommodates the posterior myophore *mp* of the left valve. BMNH42861. Same horizon and locality.

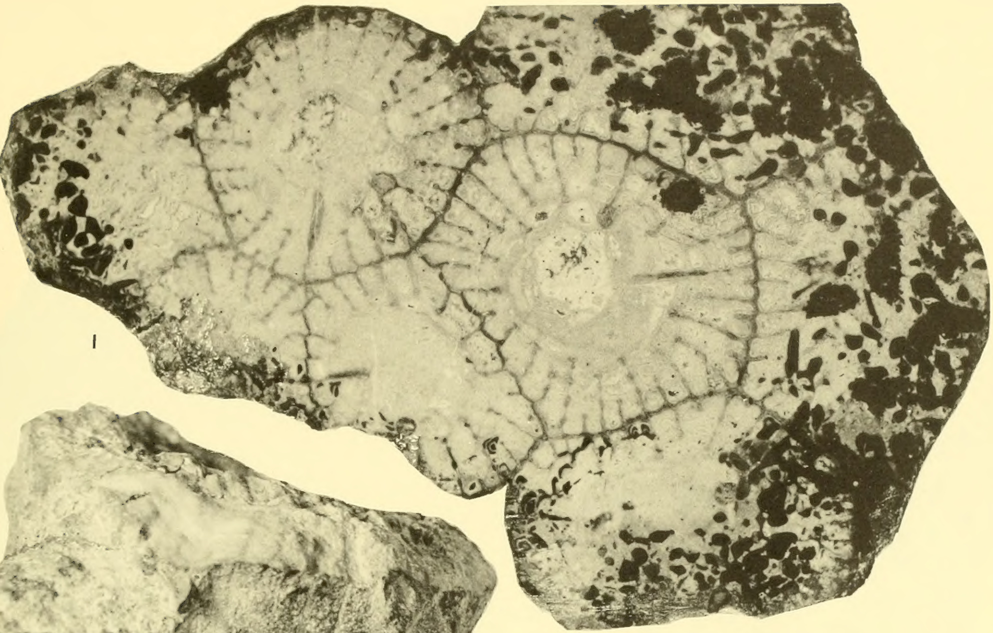

1

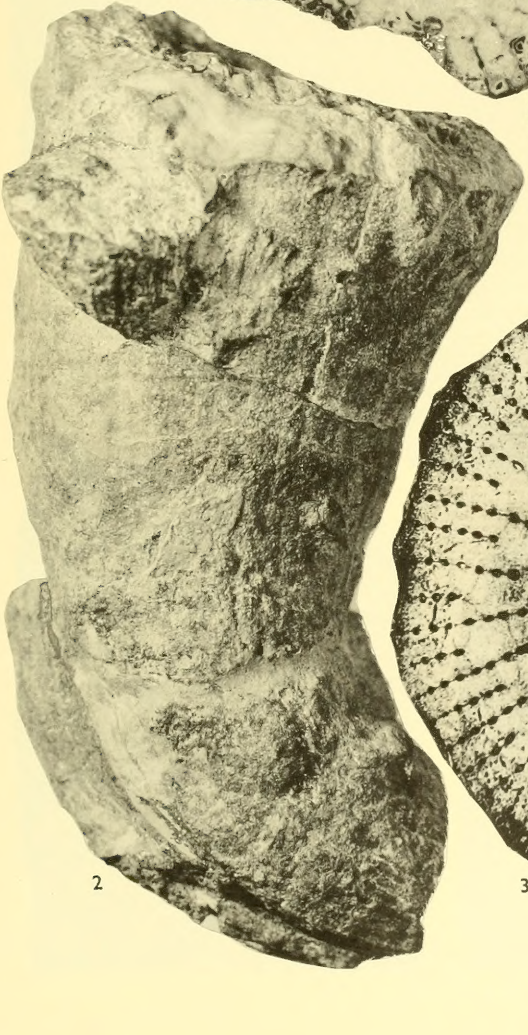

2

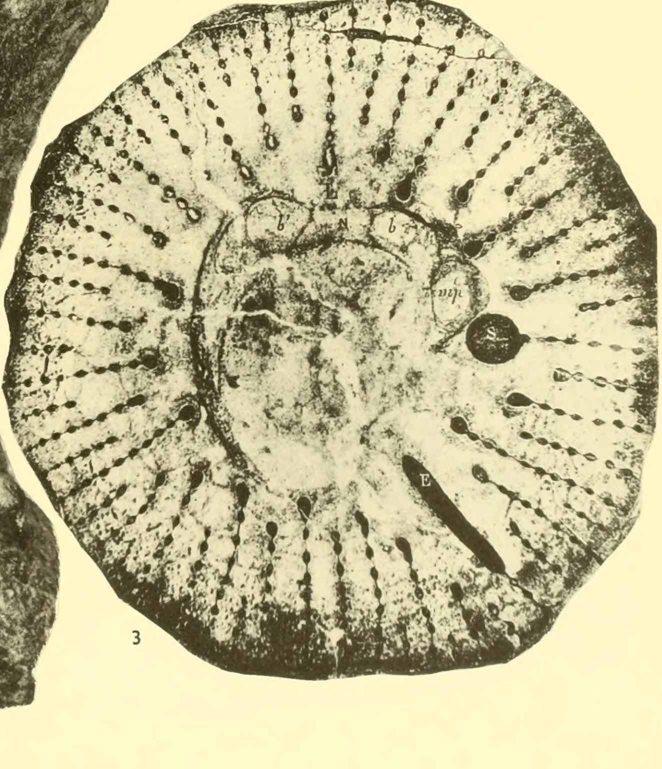

3

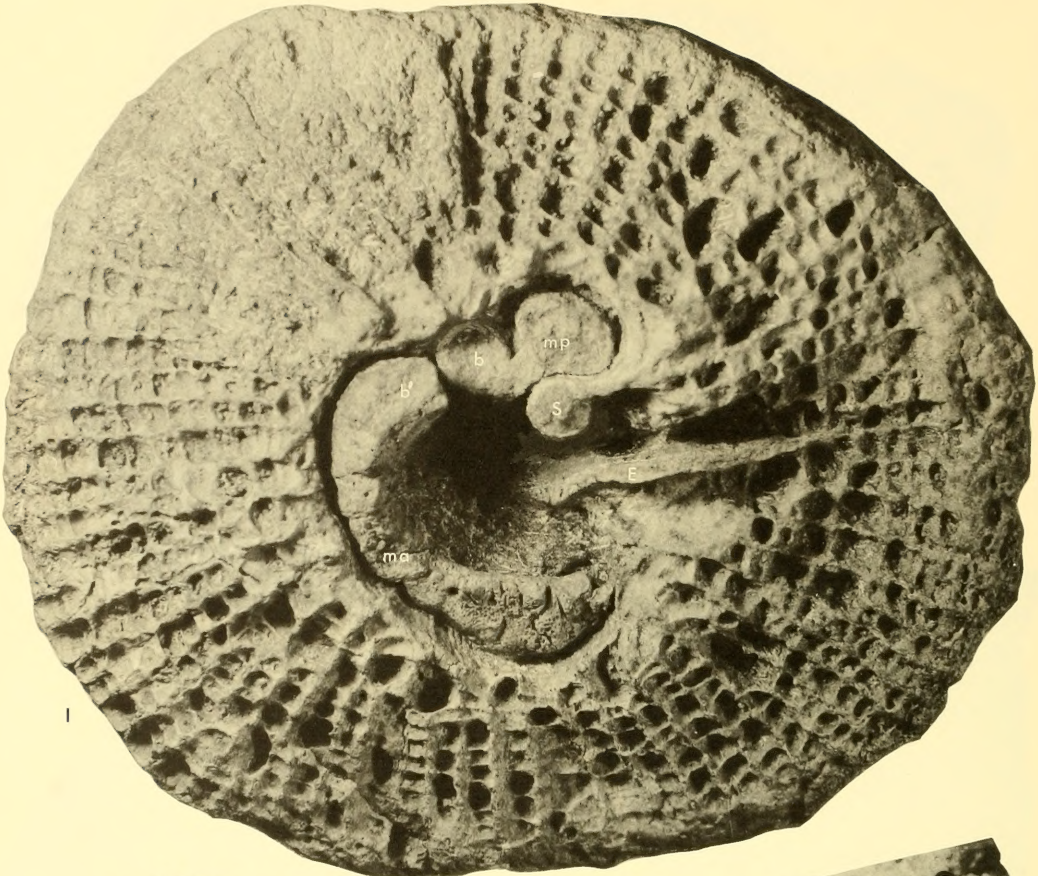

1

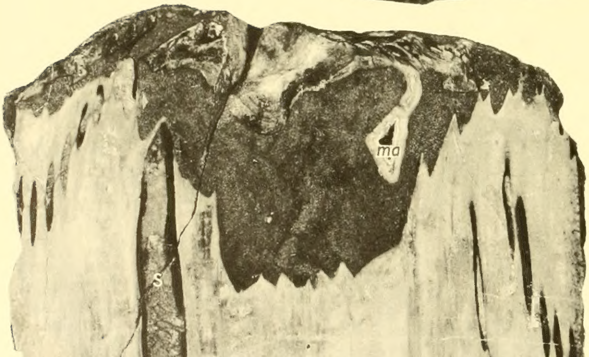

2

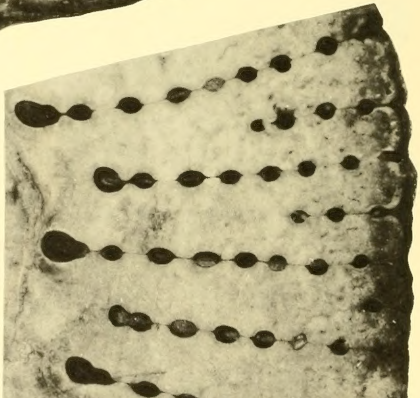

3

EXPLANATION OF PLATE 52

Figures 1 and 2 reduced, figure 3 enlarged

Figure *Page*

1 *Barrettia gigas* Chubb 210

Adult right valve × 0.67. Commissural view showing moniliform infolds with intervening quadrangular cells; L not clear, S with cylindrical column and E with radially extended flat column, its inner end deflected ventrally. Body cavity contains cardinal apparatus of left valve, including crescentic anterior myophore *(ma)*, springing from anterior tooth *(B')*, and posterior myophore *(mp)* fitting into its cavity and connected by a yoke with posterior tooth (B). Smith. Campanian, *Barrettia* limestone, Haughton Hall, Green Island, Hanover.

2,3. *Barrettia monilifera* Woodward 208

Longitudinal section of bivalve × 0.8. This is the counterpart of Woodward's section reproduced in Text-figure 7. It shows the corrugated floor of the body cavity, the S pillar on the left and above it an oblique perforation through the left valve, probably the S oscule; the anterior myophore *(ma)* is suspended from the upper valve on the right. BMNH 42863. *Barrettia* Limestone, Back River Portland. 3. Same specimen. Transverse section of part of base × 2, showing details of structure.

EXPLANATION OF PLATE 53

Figures 1 and 3 reduced; figure 2 natural size

Figure		*Page*
1-3.	*Barrettia gigas* Chubb	210

Young adult right valve × 0.84 (the original being 215 mm across). It is split in half in the plane of two opposite infolds, that on the left being near to, but not, the ligamental. Dorsum on left, venter on right, conical body cavity in centre, lined with thin inner layer, which also forms concave tabulae that slope down evenly towards the dorsal side; the E pillar, which at its inner end is deflected ventrally, penetrates the body cavity and cuts through the tabulae; further to the left is the S pillar and beyond it the cavity for the reception of the posterior myophore *(mp)*; below the latter is the posterior socket *(b)*, which extends almost to the base of the shell. On the ventral side of the vertical tubes of the infold are deflected or absorbed by the increase in width of the body cavity; on the dorsal side the tubes adjacent to the socket run parallel to it. Smith. *Barrettia* Limestone, Haughton Hall, Green Island, Hanover. 2. Same species. Parts of the two hinge teeth of a left valve, natural size; the shell was broadly conical, about 300 mm in diameter at the commissure, and not less than 190 mm high. The teeth were at least 150 mm long. The convex side of their curve is dorsal, and this side is fluted to fit the flutings in the socket; the nearer tooth is the posterior one. The direction of curvature may not be typical; obviously the tooth fitting in the socket seen in figure 1, above, was nearly straight. UW16177. *Barrettia* Limestone, Stapleton, St. James. 3. Same species. Segment of a bowl-shaped valve × 0.75. It is split in the plane of the E infold; it shows the rapid widening of the flattened tabulate pillar, and the deflection and absorption of adjacent tubes. Smith. *Barrettia* Limestone, Haughton Hall, Green Island, Hanover.

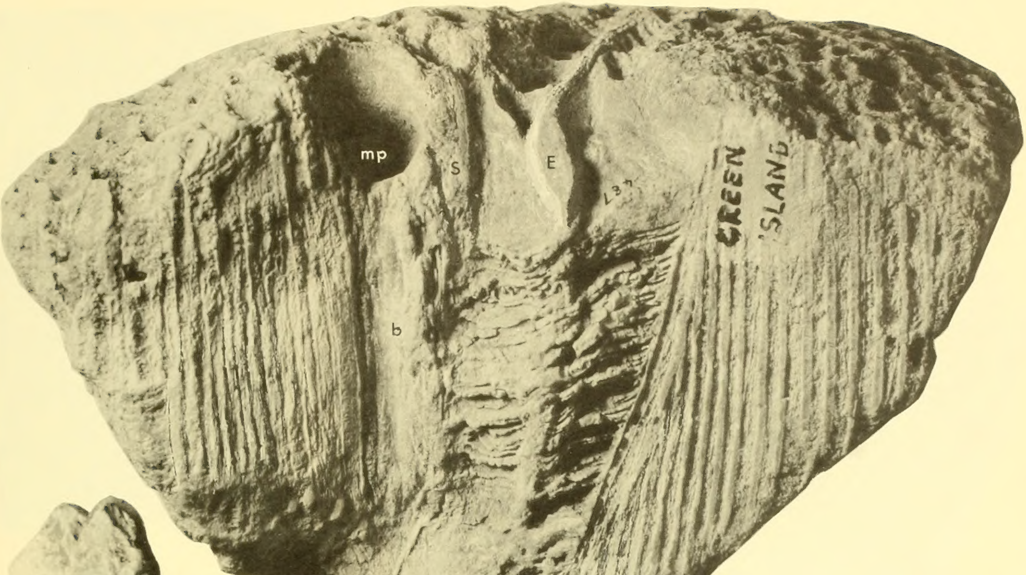

1

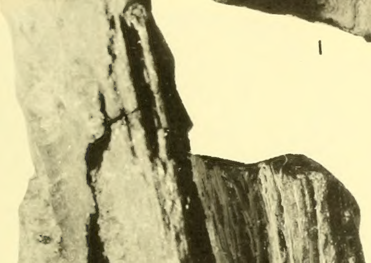

2

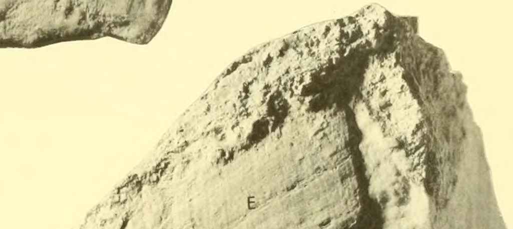

3

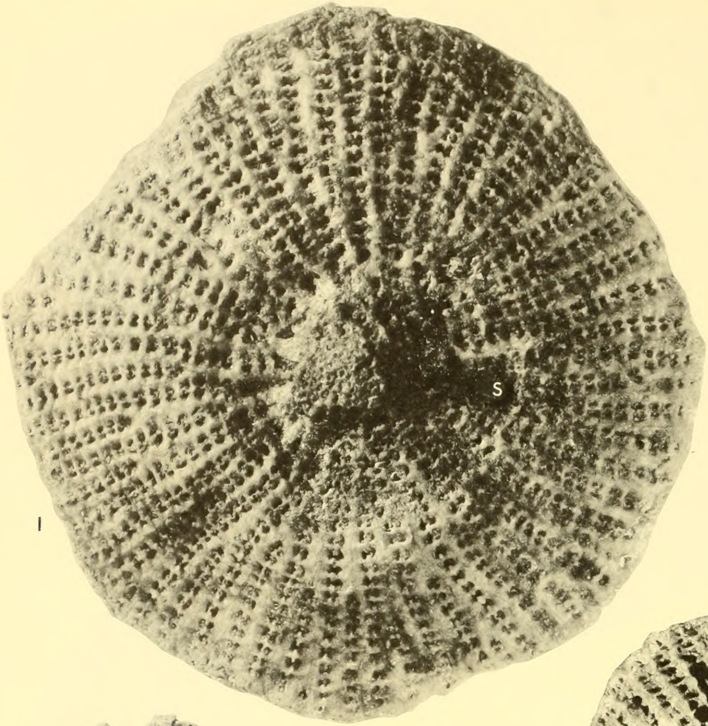

1

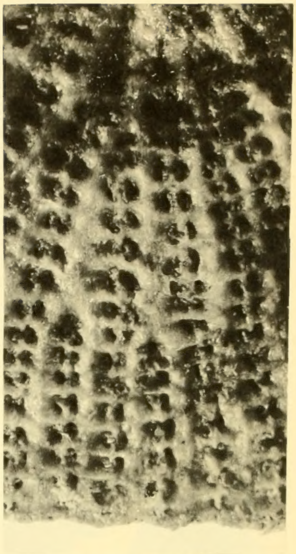

2

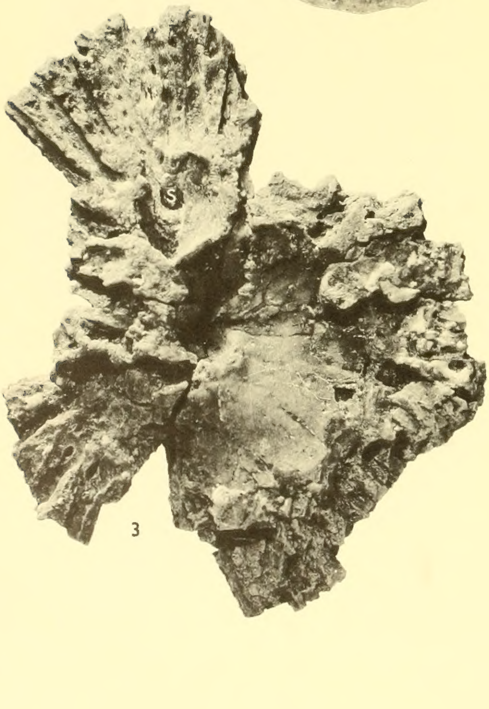

3

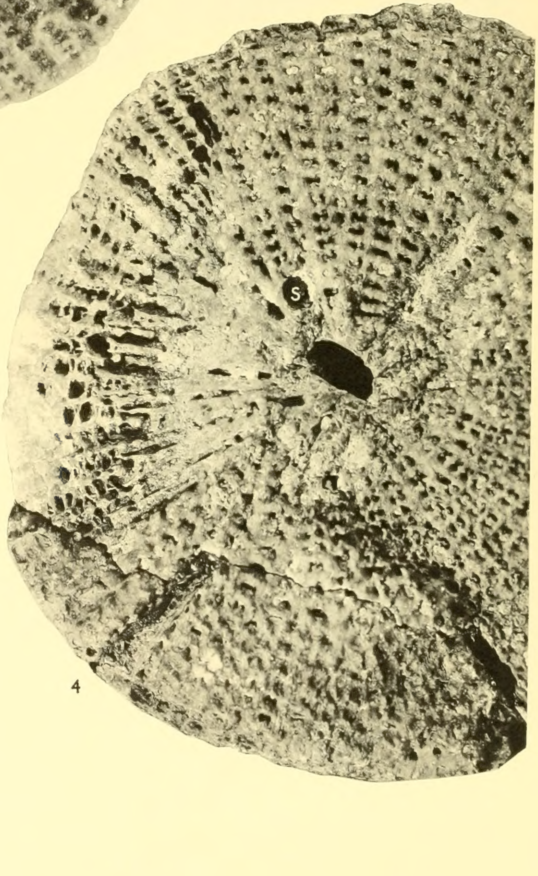

4

EXPLANATION OF PLATE 54

All figures natural size except Figure 2

Figure		*Page*
1-4.	*Barrettia multilirata* Whitfield	211

Left valve, outer aspect. The S oscule may be seen on the right of the central boss; note the absence of an E oscule. BMNH LL30293. *Barrettia* Limestone, Haughton Hall, Green Island, Hanover. 2. Same specimen, a portion of the surface × 2 to show details of structure. Compare with Text-figure 8. 3. Same species. Incomplete left valve, inner aspect. BMNH LL7136. Same horizon and locality. 4. Same species. Bivalve. In the middle quadrant on the left of the figure the left valve is broken away exposing the commissural surface of the right valve. The central boss is missing, its place being taken by an oval aperture, possibly due to an injury sustained during life. The S oscule is seen above and to the left of this aperture. A new photograph of one of Trechmann's types (1922, pl. 20, fig. 3). BMNH L44198. Same horizon and locality.

EXPLANATION OF PLATE 55

Illustrations natural size

Figure *Page*

1. *Barrettia ruseae* Chubb 213
Right valve, incomplete; transverse section. Smith. *Barrettia* Limestone, Clifton, Hanover.

2. *Barrettia multilirata* Whitfield 211
Right valve; transverse section of an exceptionally large shell. Smith. Campanian, *Barrettia* Limestone, Haughton Hall, Green Island, Hanover.

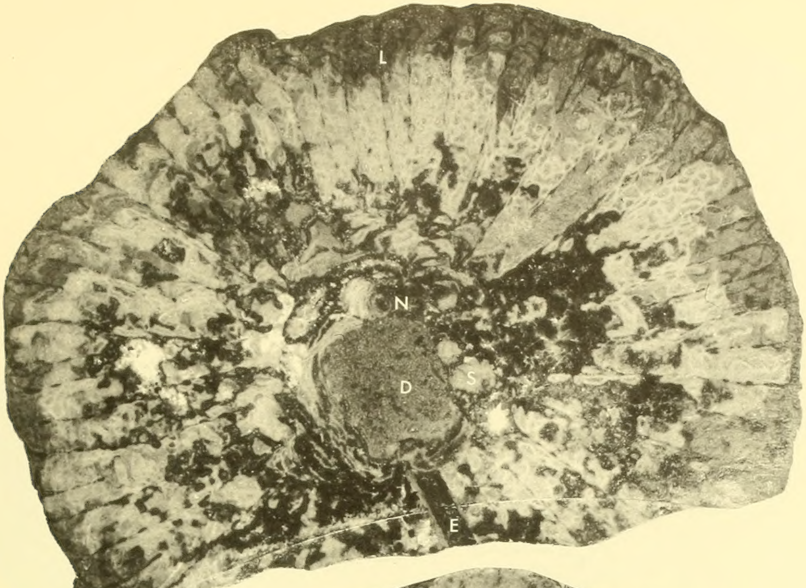

1

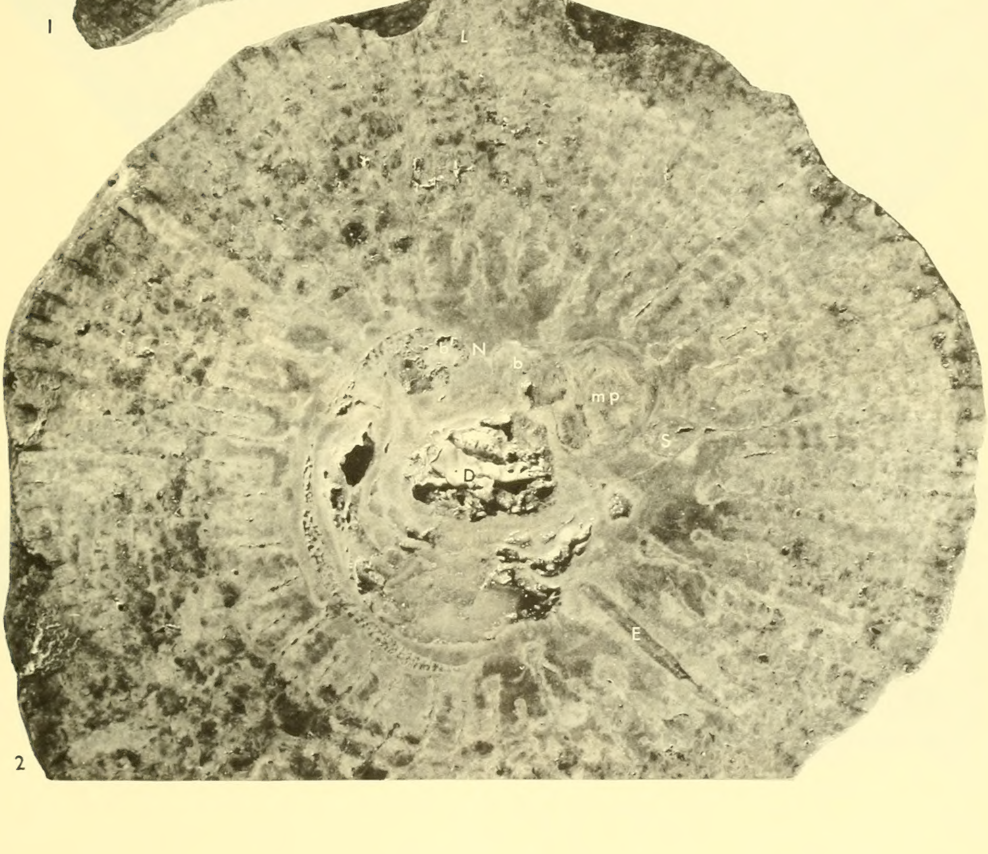

2

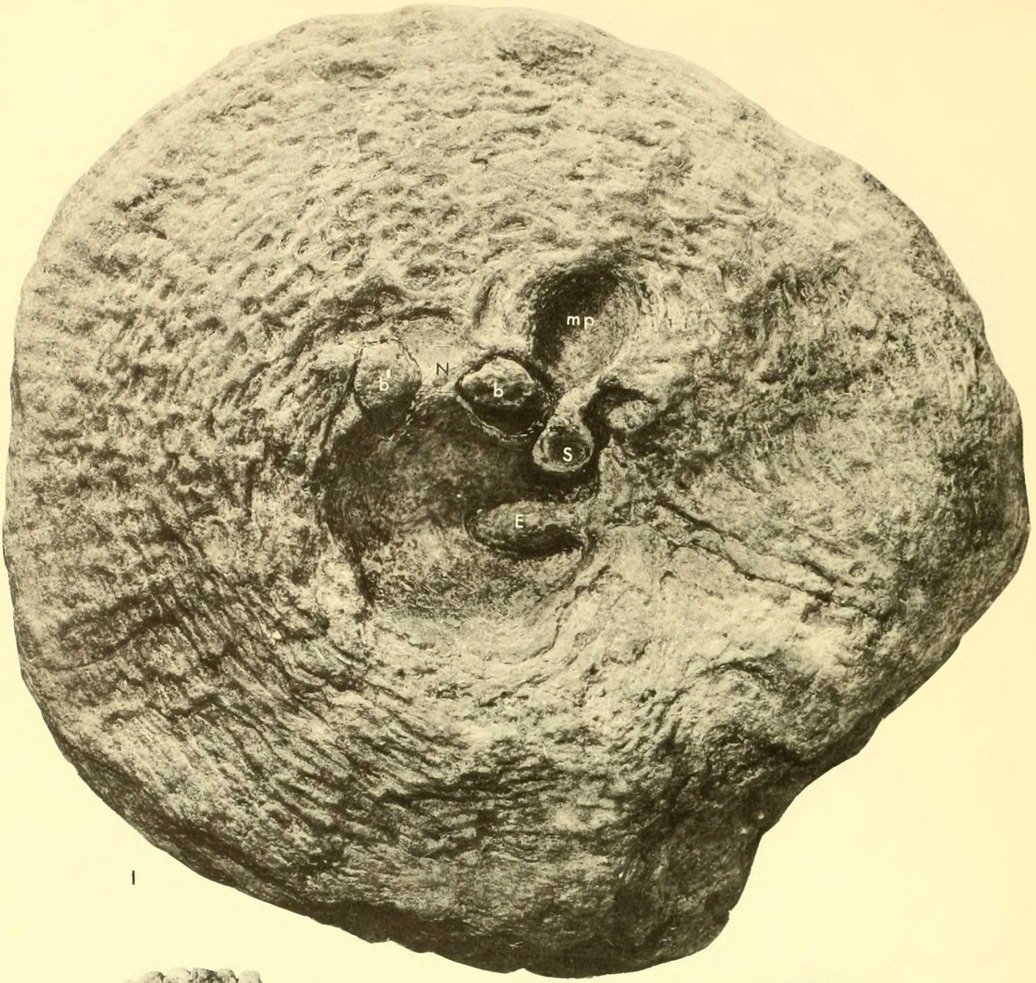

1

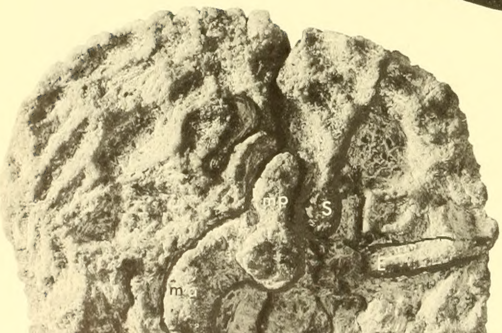

2

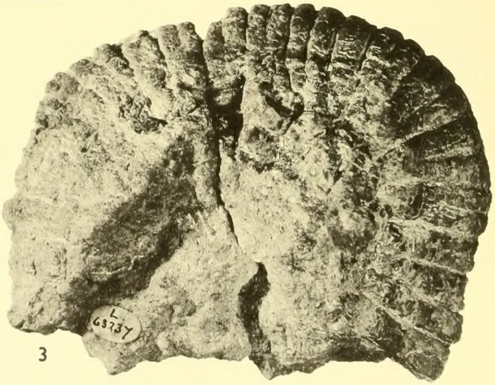

3

EXPLANATION OF PLATE 56

Figure 1 reduced, others natural size

Figure *Page*

1-3. *Parastroma trechmanni* Chubb 214

Commissural surface of young adult valve × 0.9. It shows the body cavity, tooth (N) between the two sockets (b′ and b) in which are the broken off teeth of the left valve; the posterior myophoric cavity and the S and E pillars. This specimen was figured by Trechmann as *Barrettia* cf. *monilifera* (1922, pl. 19, figs. 2a, 2b). BMNH L44200. *Barrettia* Limestone, Haughton Hall, Green Island, Hanover. 2. Same species, commissural surface of young right valve. Both the myophores of the left valve may be seen within it. BMNH L63237. Same horizon and locality. 3. Same specimen, lower surface, showing radial sulci between flat costae.

EXPLANATION OF PLATE 57

Figure 1 natural size, figure 2 reduced

Figure		*Page*
1,2.	*Praebarrettia sparcilirata* (Whitfield)	215

Right valve, lateral aspect. Part of the outer layer is preserved; where it is weathered away the outer edges of the infolds and of the tabulae may be seen. Smith. Loose in soil of banana fields at head of Orange River; derived from basal Maestrichtian limestone. 2. Same species, right valve × 0.75. Weathered specimen showing a section of the body cavity near the commissure with the three principal pillars and the cardinal apparatus of the left valve. A new photograph of one of Trechmann's types (1924b, pl. 23, fig. 4). BMNH L44204. Lower part of Logie Green section, *i.e.* basal Maestrichtian.

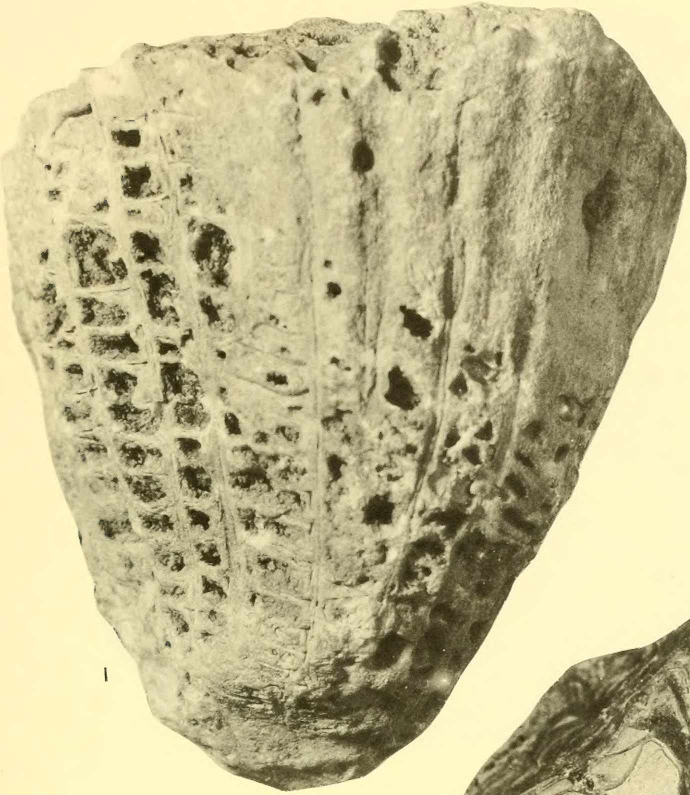

1

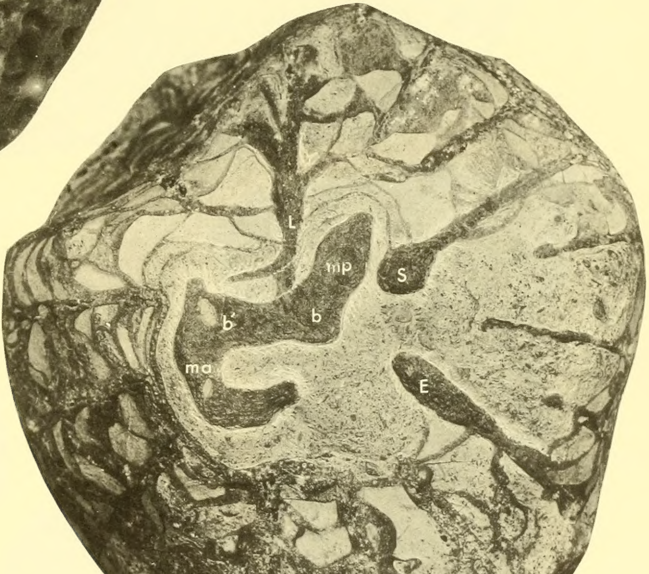

2

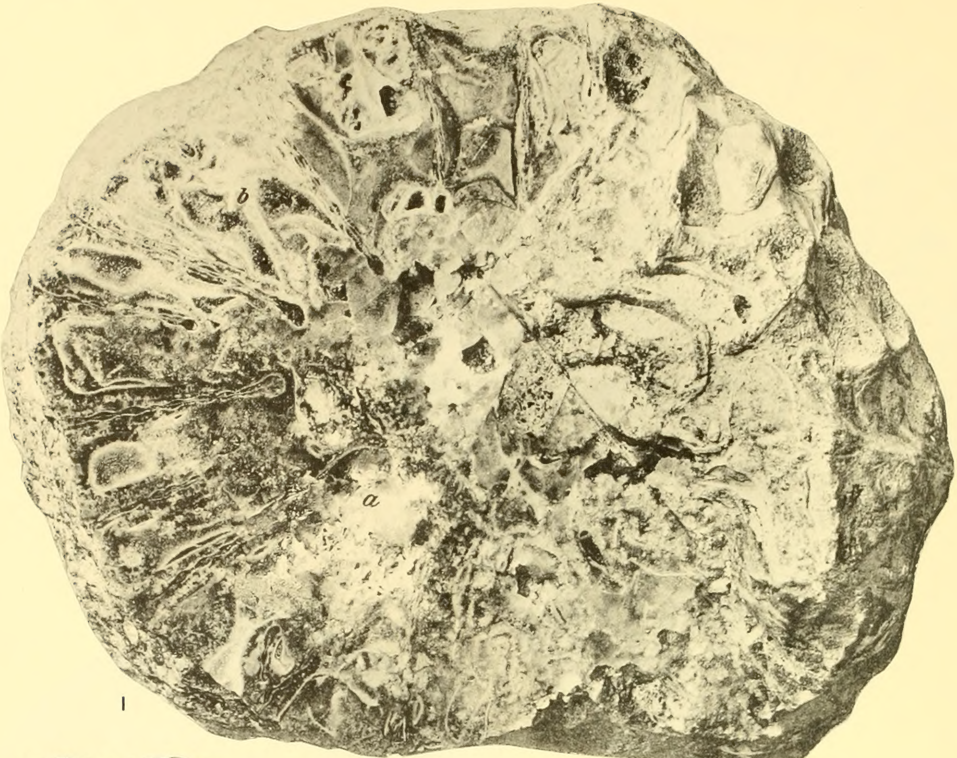

1

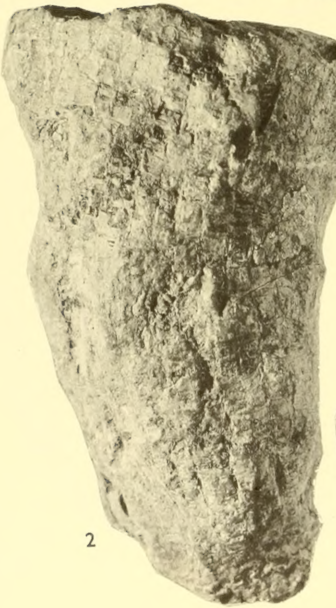

2

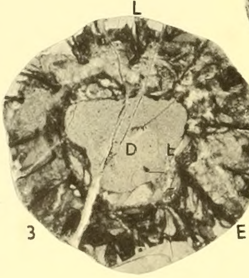

3

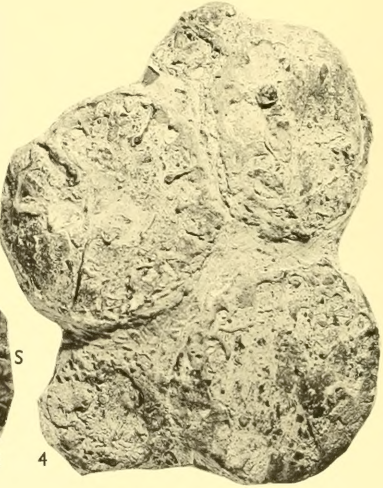

4

EXPLANATION OF PLATE 58

All illustrations natural size
Figure 1 courtesy American Museum of Natural History

Figure		*Page*
1.	*Praebarrettia sparcilirata* (Whitfield)	215
	Right valve, transverse section. A reproduction of one of Whitfield's illustrations (1897b, pl. 37). He believed that he had found the S pillar at *a* and, more doubtfully, the E pillar at *b*. AMNH 9667. Maestrichtian, Logie Green, Clarendon.	
2-4.	*Praebarrettia coatesi* Chubb	216
	Right valve, posterior lateral aspect. Shows the infolds as faint striae. UWI 4162. Peters Hill Limestone, probably Turonian, Peters Hill, north-east Clarendon. 3. Same species. Transverse section of a right valve, showing the L, S and E pillars. UWI 4163. Same horizon and locality. 4. Same species. A cluster of right valves. UWI 4164. Same horizon and locality.	

INDEX

NOTE: Light face type refers to page numbers. Bold face type refers to plate numbers.

A

- adhaerens, Biradiolites 190, 191
  - Radiolites 190, 191
  - Thyrastylon **38,** 190, 219, 220
- Agriopleura **35,** 184, 220
- aguilae, Durania cf. **43,** 201, 220
- alatus, Titanosarcolites **31, 32,** 178, 220
- Amphitricoelus 169
- annulosa, Sauvagesia **41,** 198, 220
- annulosus, Radiolites 198
- Antillocaprina **28-30,** 164, 172-179, 191, 192, 195, 220
- Antillocarpina sp. 175, 176
- Antillosarcolites **30,** 179, 220

B

- baileyi, Bournonia **40,** 194, 220
- barretti, Bournonia **40,** 194, 220
- Barrettia **51-55,** 163, 195, 208-211, 213, 217, 218, 220
- Barrettia beds 179, 214
- Barrettia Limestone 163, 174, 180, 185, 194, 196, 201
- Barrettia sp. 213
- Biradiolites **35-37,** 186-190, 192, 193, 220
- Biradiolites sp. 192
- Blue Mountains 162, 163, 176
- Bonnett Limestone 162, 166, 167
- Bournonia **39, 40, 44,** 192-196, 220
- Bournonia sp. 194, 195
- British Museum (Natural History) 209

C

- Caldwell, W.G.E. 164
- canaliculatus, Biradiolites 189
- cancellata, Bournonia **39,** 192-195, 201, 220
- cancellatus, Biradiolites 192, 193
  - Radiolites 192, 195
- Caprina 170, 172, 180, 181
- Caprinella 171, 174
- Caprinula 176, 177
- Caprinuloidea **27,** 169, 170, 171, 220
- ceibarum, Hippurites 204
  - Orbignya **49,** 204, 205, 220
- Chiapasella **47, 48,** 200, 202, 203, 220
- Clifton Limestone 206, 213
- Coalcomana 171
- coatesi, Praebarrettia **58,** 207, 216, 217, 220
- Copper Limestone 162, 166, 167
- coquandi, Caprina 180
  - Plagioptychus 180
- Coralliochama 202
- corrugata, Tepeyacia 198, 199
- corvi, Biradiolites 191
  - Thyrastylon **38, 39,** 191, 192, 220
- Cox, L. R. 218
- coxi, Bournonia **44,** 196, 220
- cubensis, Chiapasella 202
- Cystiphyllum 209

D

- De la Beche, H. T. 167
- depressa, Antillocaprina **30,** 176, 192, 220
- diaboli, Monopleura **27,** 166, 220
- Diozoptyxis 163
- Di Stefano, G. 167
- Distefanella **35,** 186, 220
- Douville, Henri 162, 167
- Ducketts Land Settlement 182, 188, 191, 194
- Durania **43-46,** 199, 201, 219, 220

E

- eyrei, Vaccinites **50,** 206, 220

F

- falconi, Agriopleura **35,** 184, 220
- fluminisagni, Sauvagesia **42,** 197, 220
- forbesi, Biradiolites **37,** 188, 220
- fragilis, Plagioptychus **32,** 182, 220

G

- gigantea, Caprinula 176, 177
- giganteus, Titanosarcolites **31-33,** 177, 178, 220
- gigas, Barrettia **52, 53,** 210, 211, 214, 218, 220
- Globotruncana 163
- Guembelina 163
- guitarti, Orbignya 214
  - Parastroma 209, 214
- Guy's Hill 167
- Gyropleura **27,** 167, 180, 220

H

- Hippurites 204, 209

I

- Ichthyosarcolites 177, 179
- incisus, Hippurites cf. 204
- Indian Ocean 162
- Inoceramus beds 162
- Institute of Jamaica 181, 200

J

- jamaicensis, Biradiolites **35,** 186, 220
  - Caprina 180, 181
  - Monopleura **27,** 166, 220
  - Plagioptychus **34,** 180, 181, 220
- Jubilee Limestone 168
- jubilensis, Pachytraga **27,** 168, 220

L

- Lapeirousia 199, 200, 201, 217, 219
- lapparenti, Pachytraga 168
- lombricalis, Biradiolites 186
  - Distefanella **35,** 186, 220
  - Radiolites 186
- lowenstami, Antillocaprina **28,** 174, 175, 220

M

- MacGillavry, H. J. 164, 176
- macgillavryi, Antillosarcolites **30,** 179, 220
  - Vaccinites 206
- macroplicata, Sauvagesia **41,** 196, 198, 220
- macroplicatus, Radiolites 196, 197
- maldonensis, Orbignya **50,** 164, 205, 220
  - Parastroma 205
- Matley, C. A. 167
- mcgrathi, Sauvagesia **42,** 197, 220
- Michelina 209
- minhoensis, Biradiolites **37,** 189, 220
- minor, Plagioptychus **34,** 182, 220
- Mitrocaprina **34,** 183, 220
- monilifera, Barrettia **51, 52,** 195, 208-211, 218, 220
- Monopleura **27,** 166, 167, 220
- Monopleura sp. 166, 167, 220

INDEX

mooretownensis, Biradiolites 186
  Distefanella **35,** 186, 220
mullerriedi, Hippurites 204
  Orbignya **49,** 204, 220
multicanaliculata, Mitrocaprina **34,** 183, 220
multicostata, Tepeyacia **43,** 170, 198, 199, 219, 220
multilirata, Barrettia **54, 55,** 211-213, 220

N

Newman Hall Shale 163
nicholasi, Durania **43-46,** 199, 219, 220
  Lapeirousia 199
  Radiolites 199, 201
novaterrensis, Biradiolites **37,** 189, 220

O

occidentalis, Antillocaprina **28, 30,** 164, 172, 173, 177, 191, 195, 220
  Caprinella 171, 173
Orbignya **49, 50,** 164, 204, 205, 217, 220
Ostrea sp. 196

P

Pachytraga 168, 220
Pachytraga, n. sp. 168
Parastroma **56,** 164, 209, 214, 220
pauciplicata, Chiapsella 202, 203
perfecta, Caprinuloidea **27,** 169, 170, 220
peruviana, Praebarrettia 217
Peters Hill Limestone 207
Phillipsburg Limestone 162
Pironaea 165, 203, 217
Plagioptychus **32-34,** 171, 180-183, 220
Plagioptychus sp. 180
porosa, Praebarrettia 217
Praebarrettia **57, 58,** 197, 199, 200, 207, 215-217, 220
Praebarrettia sp. 216
Praeradiolites **35,** 185, 220

Q

quadrangularis, Antillocaprina **29,** 174, 220
  Caprinella 174

R

Radiolites 186, 187, 190, 192, 195-199, 201
radiolitiformis, Chiapasella **47, 48,** 200, 202, 203, 220
  Coralliochama 202
riograndensis, Biradiolites **37,** 189, 220
robinsoni, Biradiolites **36,** 187, 220
rudis, Biradiolites **36,** 187, 220
  Radiolites 187
rudissimus, Biradiolites **36,** 187, 220
rudissimus, Biradiolites, cf. **36,** 188, 220
ruseae, Barrettia **55,** 213, 214, 220

S

Sabinia **30,** 170, 171, 198, 220
sanchezi, Hippurites 207
  Orbignya 205, 215
  Parastroma 205, 215
  Torreites cf. **49,** 207, 220
sanctannae, Bournonia **39,** 193, 194, 220
sanctmariae, Bournonia **40,** 195, 220
Sauvagesia **41, 42,** 165, 196-198, 220
Schiosia 171
seafieldensis, Sphaerucaprina **30,** 170, 198, 220
Seafield Limestone 162, 169, 170
semiannulosus, Biradiolites 191
  Thyrastylon **39,** 191, 220
semiannulosus, Biradiolites 191
  Thyrastylon **39,** 191, 220
shaviensis, Gyropleura **27,** 167, 220
Shaw Castle Shale 182, 184
Sierra Madre Limestone 186
sparcilirata, Barrettia 215
  Praebarrettia **57,58,** 197, 199, 200, 215, 217, 220
Sphaerucaprina **30,** 170, 171, 198, 220
Stapleton Limestone 199, 201
St. Anns Great River 194, 199
St. Catherine 166, 170
St. James 166,174, 175, 182, 190,194, 197, 199, 201
stellata, Antillocaprina **30,** 175, 220
sanctmariae, Bournonia **40,** 195, 220
subcancellatus, Biradiolites 193
suboccidentalis, Antillocaprina **28,** 171-173, 220

T

Tepeyacia **43,** 170, 171, 198-200, 219, 220
tetrahedron, Bournonia **40,** 195, 196, 220
Thyrastylon **38, 39,** 190-192,195, 218, 220
Thyrastylon sp. 192, 220
thiadensi, Bournonia **40,** 194, 220
Titanosarcolites **31-33,** 175-178, 218, 220
Titanoscarlites Limestone 166, 180, 186, 194, 196, 204, 205
Torreites **49,** 207, 220
totiseptata, Sabinia **30,** 170, 171, 198, 220
toucasi, Plagioptychus 180
toucasianus, Plagioptychus **34,** 180, 181, 220

V

Vaccinites **50,** 165, 206, 207, 217, 220
Vaccinites sp. 206
vermunti, Vaccinites 206
verseyi, Praeradiolites 185, 220

W

Westmoreland 166, 190, 191, 197
Whitfield Hall 167, 173
williamsi, Antillocaprina **30,** 175, 192, 220

Z

zansi, Plagioptychus **33,** 181, 182, 220

XLV.	(No. 204). 564 pp., 63 pls. Venezuela Cenozoic pelecypods	18.00
XLVI.	(Nos. 205-211). 419 pp., 70 pls. Large Foraminifera, Texas Cretaceous crustacean, Antarctic Devonian terebratuloid, Osgood and Paleocene Foraminifera, Recent molluscan types.	16.00
XLVII.	(Nos. 212-217). 584 pp., 83 pls. Eocene and Devonian Foraminifera, Venezuelan fossil scaphopods and polychaetes, Alaskan Jurassic ammonites, Neogene mollusks.	18.00
XLVIII.	(No. 218). 1058 pp., 5 pls. Catalogue of the Paleocene and Eocene Mollusca of the Southern and Eastern United States.	18.00
XLIX.	(Nos. 219-224). 671 pp., 83 pls. Peneroplid and Australian forams, North American carpoids, South Dakota palynology, Venezuelan Miocene mollusks, *Voluta*.	18.00
L.	(Nos. 225-230). 518 pp., 42 pls. Venezuela and Florida cirripeds, Antarctic forams, Linnaean Olives, Camerina, Ordovician conodonts, Niagaran forams.	18.00
LI.	(Nos. 231-232). 420 pp., 10 pls. Antarctic bivalves, Bivalvia catalogue.	18.00
LII.	(Nos. 233, 236). 387 pp., 43 pls. New Zealand forams, Stromatoporoidea, Indo-Pacific, Miocene-Pliocene California forams.	18.00
LIII.	(Nos. 237-238). 488 pp., 45 pls. Venezuela Bryozoa, Kinderhookian Brachiopods.	18.00
LIV.	(Nos. 239-245). 510 pp., 50 pls. Dominican ostracodes, Texan pelecypods, Wisconsin mollusks, Siphocypraea, Lepidocyclina, Devonian gastropods, Miocene Pectens Guadaloupe.	18.00
LV.	(Nos. 246-247). 657 pp., 60 pls. Cenozoic corals, Trinidad Neogene mollusks.	18.00
LVI.	(Nos. 248-254). 572 pp., 49 pls. American Foraminifera, North Carolina fossils, coral types, Belanski types, Venezuelan Cenozoic Echinoids, Cretaceous Radiolaria, Cymatiid gastropods.	18.00
LVII.	(Nos. 255-256). 321 pp., 62 pls. Alaskan Jurassic ammonites, Pt. II, Jurassic Ammonitina New Guinea.	18.00
LVIII.	(Nos. 257-262). 305 pp., 39 pls. Cretaceous Radiolaria, Cretaceous Foraminifera, Pacific Silicoflagellates, North American Cystoidea, Cincinnatian Cyclonema, new species Vasum.	18.00
LIX.	(No. 263). 314 pp. Bibliography of Cenozoic Echinoidea.	18.00
LX.	(Nos. 264-266). 190 pp., 45 pls. Jurassic-Cretaceaus Hagiastridae, Venezuela cirriped, palynology Iowa	11.55

PALAEONTOGRAPHICA AMERICANA

Volume I.	See Johnson Reprint Corporation, 111 Fifth Ave., New York, N. Y. 10003 Monographs of Arcas, Lutetia, rudistids and venerids.	
II.	(Nos. 6-12). 531 pp., 37 pls. Heliophyllum halli, Tertiary turrids, Neocene Spondyli, Paleozic cephalopods, Tertiary Fasciolarias and Paleozoic and Recent Hexactinellida.	23.00
III.	(Nos. 13-25). 513 pp., 61 pls. Paleozoic cephalopod structure and phylogeny, Paleozoic siphonophores, Busycon, Devonian fish studies, gastropod studies, Carboniferous crinoids, Cretaceous jellyfish, Platystrophia and Venericardia.	28.00
IV.	(Nos. 26-33). 492 pp., 72 pls. Rudist studies Busycon, Dalmanellidae, Byssonychia, Devonian lycopods, Ordovican eurypterids, Pliocene mollusks.	28.00
V.	(Nos. 34-37). 445 pp., 101 pls. Tertiary Arcacea, Mississippian pelecypods, Ambonychiidae, Cretaceous Gulf Coastal forams.	32.00
VI.	(Nos. 38-41). 444 pp., 83 pls. Lycopsids and sphenopsids of Freeport Coal, Venericardia, Carboniferous crinoids, Trace fossils.	35.00
VII.	(Nos. 42-44). 153 pp., 26 pls. Torreites Sanchezi, Cancellariid Radula, Ontogeny, sexual dimorphism trilobites.	15.00

BULLETINS OF AMERICAN PALEONTOLOGY

Vols. I-XXIII.	See Kraus Reprint Corp., 16 East 46th St., New York, N. Y. 10017, U.S.A.	
XXIV.	(Nos. 80-87). 334 pp., 27 pls. Mainly Paleozoic faunas and Tertiary Mollusca.	12.00
XXV.	(Nos. 88-94B). 306 pp., 30 pls. Paleozoic fossils of Ontario, Oklahoma and Colombia, Mesozoic ehinoids, California Pleistocene and Maryland Miocene mollusks.	12.00
XXVI.	(Nos. 95-100). 420 pp., 58 pls. Florida Recent marine shells, Texas Cretaceous fossils, Cuban and Peruvian Cretaceous, Peruvian Eogene corals, and geology and paleontology of Ecuador.	14.00
XXVII.	(Nos. 101-108). 376 pp., 36 pls. Tertiary Mollusca, Paleozoic cephalopods, Devonian fish and Paleozoic geology and fossils of Venezuela.	14.00
XXVIII.	(Nos. 109-114). 412 pp., 34 pls. Paleozoic cephalopods, Devonian of Idaho, Cretaceous and Eocene mollusks, Cuban and Venezuelan forams.	14.00
XXIX.	(Nos. 115-116). 738 pp., 52 pls. Bowden forams and Ordovician cephalopods.	18.00
XXX.	(No. 117). 563 pp., 65 pls. Jackson Eocene mollusks.	16.00
XXXI.	(Nos. 118-128). 458 pp., 27 pls. Venezuelan and California mollusks, Chemung and Pennsylvanian crinoids, Cypraeidae, Cretaceous, Miocene and Recent corals, Cuban and Floridian forams, and Cuban fossil localities.	16.00
XXXII.	(Nos. 129-133). 294 pp., 39 pls. Silurian cephalopods, crinoid studies, Tertiary forams, and Mytilarca.	16.00
XXXIII.	(Nos. 134-139). 448 pp., 51 pls. Devonian annelids, Tertiary mollusks, Ecuadoran stratigraphy paleontology.	16.00
XXXIV.	(Nos. 140-145). 400 pp., 19 pls. Trinidad Globigerinidae, Ordovician Enopleura, Tasmanian Ordovician cephalopods and Tennessee Ordovician ostracods and conularid bibliography.	16.00
XXXV.	(Nos. 146-154) 386 pp., 31 pls. G. D. Harris memorial, camerinid and Georgia Paleocene Foraminifera, South America Paleozoics, Australian Ordovician cephalopods, California Pleistocene Eulimidae, Volutidae, and Devonian ostracods from Iowa.	16.00
XXXVI.	(Nos. 155-160). 412 pp., 53 pls. Globotruncana in Colombia, Eocene fish, Canadian Chazyan Antillean Cretaceous rudists, Canal Zone Foraminifera, fossils, foraminiferal studies.	16.00
XXXVII.	(Nos. 161-164). 486 pp., 37 pls. Antillean Cretaceous Rudists, Canal Zone Foraminifera, Stromatoporoidea.	16.00
XXXVIII.	(Nos. 165-176). 447 pp., 53 pls. Venezuela geology, Oligocene Lepidocyclina, Miocene ostracods, and Mississippian of Kentucky, turritellid from Venezuela, larger forams, new mollusks, geology of Carriacou, Pennsylvanian plants.	18.00
XXXIX.	(Nos. 177-183). 448 pp., 36 pls. Panama Caribbean mollusks, Venezuelan Tertiary formations and forams, Trinidad Cretaceous forams, American-European species, Puerto Rico forams.	16.00
XL.	(No. 184). 996 pp., 1 pls. Type and Figured Specimens P.R.I.	18.00
XLI.	(Nos. 185-192). 381 pp., 35 pls. Australian Carpoid Echinoderms, Yap forams, Shell Bluff, Ga. forams. Newcomb mollusks, Wisconsin mollusk faunas, Camerina, Va. forams, Corry Sandstone.	16.00
XLII.	(No. 193). 673 pp., 48 pls. Venezuelan Cenozoic gastropods.	18.00
XLIII.	(Nos. 194-198). 427 pp., 29 pls. Ordovician stromatoporoids, Indo-Pacific camerinids, Mississippian forams, Cuban rudists.	16.00
XLIV.	(Nos. 199-203). 365 pp., 68 pls. Puerto Rican, Antarctic, New Zealand forams, Lepidocyclina, Eumalacostraca.	16.00

P15

PALAEONTOGRAPHICA AMERICANA

(Founded 1917)

VOL. VII

No. 46

CRINOIDS FROM THE GIRARDEAU LIMESTONE (ORDOVICIAN)

By

James C. Brower

1973

Paleontological Research Institution
Ithaca, New York, U.S.A. 14850

SMITHSONIAN
SEP 27 1973
LIBRARIES

PALEONTOLOGICAL RESEARCH INSTITUTION

1972 - 73

PRESIDENT	DANIEL B. SASS
VICE-PRESIDENT	MERRILL W. HAAS
SECRETARY	PHILIP C. WAKELEY
ASSISTANT SECRETARY	REBECCA S. HARRIS
DIRECTOR, TREASURER	KATHERINE V. W. PALMER
COUNSEL	ARMAND L. ADAMS
REPRESENTATIVE AAAS COUNCIL	JOHN POJETA, JR.

Trustees

REBECCA S. HARRIS (Life)
AXEL A. OLSSON (Life)
KATHERINE V. W. PALMER (Life)
DONALD W. FISHER (1967-1973)
MERRILL W. HAAS (1970-1973)
PHILIP C. WAKELEY (1970-1973)
CECIL H. KINDLE (1971-1974)
HARRY S. LADD (1971-1974)
DANIEL B. SASS (1971-1974)
VIRGIL D. WINKLER (1969-1975)
KENNETH E. CASTER (1972-1975)
HAROLD E. VOKES (1973-1975)

BULLETINS OF AMERICAN PALEONTOLOGY
and
PALAEONTOGRAPHICA AMERICANA

KATHERINE V. W. PALMER, *Editor*
MRS. FAY BRIGGS, *Secretary*

Advisory Board

KENNETH E. CASTER
A. MYRA KEEN
HANS KUGLER
JAY GLENN MARKS
AXEL A. OLSSON

Complete titles and price list of separate available numbers may be had on application.

For reprint, Vols. 1-23, Bulletins of American Paleontology see Kraus Reprint Corp., 16 East 46th St., New York, N.Y. 10017 U.S.A.

For reprint, vol. I, Palaeontographica Americana see Johnson Reprint Corporation, 111 Fifth Ave., New York, N.Y. 10003 U.S.A.

Subscription may be entered at any time by volume or year, with average price of $18.00 per volume for Bulletins. Numbers of Palaeontographica Americana invoiced per issue. Purchases in U.S.A. for professional purposes are deductible from income tax.

For sale by

Paleontological Research Institution
1259 Trumansburg Road
Ithaca, New York 14850
U.S.A.

PALAEONTOGRAPHICA AMERICANA

(Founded 1917)

VOL. VII

No. 46

CRINOIDS FROM THE GIRARDEAU LIMESTONE (ORDOVICIAN)

By

JAMES C. BROWER

August 30, 1973

Paleontological Research Institution
Ithaca, New York, U.S.A. 14850

Library of Congress Card Number: 72-83697

Printed in the United States of America
Arnold Printing Corporation

CONTENTS

Page

- Abstract 263
- Introduction 263
- Faunal composition 263
  - Previous and present work 263
- Correlation 264
- Localities 265
- Acknowledgment 265
- Paleoecology 266
  - Burial of crinoids 269
  - Crinoid "size" and frequency distribution 271
  - Crinoid gardens 273
  - Mortality rates 275
  - Population size and structure 277
  - Crinoid attachment 281
- Bulk density, stem leverage, and arm waving 283
- Terminology and measurements 290
- Statistical treatment of ontogeny 291
- General statement of ontogeny 292
  - Girardeau camerate dorsal cup plate growth model 293
  - Girardeau camerate brachial growth model 294
  - Tegmen plate growth model 298
  - Columnal growth model 298
  - Integration and coordination 299
  - Plate growth sequence in modern crinoids 301
  - Time growth in Recent crinoids 304
  - Comparison of ontogeny: Girardeau camerates and living crinoids 305
  - Summary of Girardeau camerate ontogeny 310
  - Calyx growth 310
  - Girardeau camerate brachials 314
  - Food gathering system ontogeny 318
  - Growth of supporting structures 325
  - Column ontogeny 327
- Phylogeny — General statement 328
  - Summary of evolutionary trends 329
  - Paleography and evolution 330
  - Paleobiogeography 331
- Systematic paleontology 331
  - Subclass Camerata Wachsmuth and Springer 331
    - Order Monobathrida Moore and Laudon 331
      - Suborder Glyptocrinina Moore 331
- Relationship of intraspecific variation in Girardeau patelliocrinids to taxonomic hierachy 396
- Phylogeny of Girardeau patelliocrinids and allies 401
  - Previous work 401
  - Sources of data and limitations 401
  - Discussion of dendrogram 401
  - Evolutionary trends 403
  - Relations between characters 406
  - Origin of the Hapalocrinidae 407
  - Paleobiogeography 407
- Phylogeny of Girardeau alisocrinids and allies 432
  - Previous work, source of data and limitations 432
  - Discussion of dendrogram 432
  - Evolutionary trends and mechanisms thereof 434
  - Relations between evolutionary trends 436
  - Paleogeography and evolution 436
      - Suborder Tanaocrinina Moore 443
    - Order Diplobathrida Moore and Laudon 445
  - Ptychocrinid phylogeny 450
  - Subclass Inadunata Wachsmuth and Springer 451
    - Order Disparida Moore and Laudon 451
    - Order Cladida Moore and Laudon 451
  - Subclass Flexibilia Zittell 460
    - Order Taxocrininida Springer 460
    - Order Sagenocrinida Springer 462
- Evolution of *Clidochirus* and its allies 464
- References 467
- Plates 473
- Index 495

TABLES

Page
1. Taxonomic and ecological diversity . . . horizons with Girardeau transgression sequence 267
2. Population size and allied data for common Girardeau camerate species 278
3. Evolution of adaptation in crinoids ....Fold in 289-290
4. Microcrinoid values for various living crinoids and Girardeau camerates ... 308
5. Comparative features of Patelliocrinidae genera ....Fold in 332-333
6. Changes in "size" components . . . R edge 343
7. Ontogeny of "size"/calyx . . . involved 344
8. . . . Relations of correlation coefficients . . . *Alisocrinus tetrarmatus*, n. sp. 352
9. Variation of food gathering system components in *Eopatelliocrinus scyphogracilis*, n. gen., n. sp. 357
10. Change in "size" components during the ontogeny of *Macrostylocrinus pristinus*, n. sp. and *Eopatelliocrinus scyphogracilis*, n. gen., n. sp. 376
11. Ontogeny of the "size"/dorsal cup width in *M. pristinus*, n. sp. and *E. scyphogracilis*, n. gen., n. sp. . . . involved 377
12. Comparative Brr dimensions growth rates . . . patelliocrinids ....Fold in 384-385
13a,b,c. Data for Girardeau patelliocrinids 402
14. Changes in "size" components during the ontogeny of *Alisocrinus tetrarmatus*, n. sp. 415
15. Ontogeny of the "size"/dorsal cup width in *A. tetrarmatus*, n. sp. . . . plates involved 415
16. Summary and comparison of food gathering . . . Girardeau patelliocrinids and *A. tetrarmatus*, n. sp. ....Fold in 426-427
17a. Original data matrix . . . *Alisocrinus* and its allies 433
b. Taxonomic distance matrix . . . Girardeau alisocrinids . . . forms 435
c. Dendrogram for *Alisocrinus tetrarmatus*, n. sp. . . . vice versa 435

TEXT-FIGURES

Page
1. Life table analysis of Girardeau Limestone camerates 276
2. Sketches illustrating Brr terminology 291
3. Drawings illustrating development of Brr and columnals 295
4. Graphs . . . "size" versus plate circlet growth patterns in various Recent crinoids 303
5. Graphs . . . Time-"size" and Time-plate . . . crinoids 306
6. Restorations . . . calyx growth in *Eopatelliocrinus*, n. gen. 335
7. *E. scyphogracilis*, n. gen., n. sp., Girardeau Limestone 336
8. *E. latibrachiatus*, n. gen., n. sp., Girardeau Limestone 336
9. Graphs . . . calyx growth in *E. scyphogracilis*, n. gen., n. sp. 337
10. Graphs . . . calyx growth in *E. latibrachiatus*, n. gen., n. sp. 338
11. Graphs and restoration . . . standard Brr . . . *E. scyphogracilis*, n. gen., n. sp. 347
12. Graphs and restoration . . . standard Brr growth in *E. latibrachiatus*, n. gen., n. sp. 348
13. Graphs . . . food gathering system growth in *E. scyphogracilis*, n. gen., n. sp. 354
14. Graphs . . . food gathering system growth in *E. latibrachiatus*, n. gen., n. sp. 355
15. Graphs . . . supporting structure growth in *E. scyphogracilis*, n. gen., n. sp. 359
16. *Macrostylocrinus cirrifer* Ramsbottom 365
17. Superpositions of major calyx plates for *M. cirrifer* Ramsbottom 368
18. Graphs . . . percentage height and width points in *M. cirrifer* Ramsbottom 369
19. Column and arms of *M. cirrifer* Ramsbottom 371
20. Superpositions of major calyx plates for *Macrostylocrinus pristinus*, n. sp. . 373
21. *M. pristinus*, n. sp., Girardeau Limestone 374
22. Graphs . . . calyx growth of *M. pristinus*, n. sp. 375
23. Graphs of standard Brr growth in *M. pristinus*, n. sp. 381
24. Brr superpositions showing ontogeny in *M. pristinus*. n. sp. and allied data. 383
25. Graphs . . . food gathering system growth in *M. pristinus*, n. sp. 389
26. Graphs . . . supporting structure growth in *M. pristinus*, n. sp. 392
27. *Culicocrinus ? girardeauensis*, n. sp. . . . exposure 400
28. Phylogeny of Girardeau patelliocrinids 403
29. *Alisocrinus tetrarmatus*, n. sp. . . . "assemblage" animals 409
30. Superpositions of major calyx plates for *A. tetrarmatus*, n. sp. 410
31. Graphs . . . percentage height and width . . . *A. tetrarmatus*, n. sp. 410
32. Graphs . . . calyx growth of *A. tetrarmatus*, n. sp. 413
33. Graphs and restoration Brr growth in *A. tetrarmatus*, n. sp. 421
34. Graphs . . . food gathering . . . in *A. tetrarmatus*, n. sp. 426
35. Graphs . . . supporting structure in *A. tetrarmatus*, n. sp. 429
36. Phylogeny of *A. tetrarmatus* . . . allies 436
37. *Alisocrinus ? heterodactylus*, n. sp. 437
38. Superpositions of . . . plates for *A. ? heterodactylus* 438
39. Graphs . . . calyx growth in *A. ? heterodactylus*, n. sp. 439
40. Graphs . . . standard Brr growth in *A. ? heterodactylus*, n. sp. 440
41. *Compsocrinus nodosus*, n. sp. 444
42. *Ptychocrinus fimbriatus* (Shumard) 447
43. *Ptychocrinus splendens* (Miller) . . . Girardeau Limestone 450
44. Holotype of *Clidochirus serrulatus*, n. sp. 463
45. Evolution of *Clidochirus* and its allies 465

CRINOIDS FROM THE GIRARDEAU LIMESTONE (ORDOVICIAN)

James C. Brower
Department of Geology
Syracuse University

ABSTRACT

The Girardeau Limestone crinoids comprise: Camerata: *Ptychocrinus splendens* (Miller), *P. fimbriatus* (Shumard), unidentified archaeocrinid, ***Compsocrinus nodosus,*** n. sp., *Alisocrinus tetrarmatus,* n. sp., *A. ? heterodactylus,* n. sp., *Eopatelliocrinus scyphogracilis,* n. gen., n. sp., *E. latibrachiatus,* n. gen., n. sp., *Macrostylocrinus pristinus,* n. sp., *Culicocrinus ? girardeauensis,* n. sp. Inadunata: *Dendrocrinus casei* (Meek), *D.* ? n. sp. aff. *D. ? navigiolum* Miller, *D. curvijunctus,* n. sp., three unidentified species. Flexibilia: *Protaxocrinus girardeau* Springer and *Clidochirus serrulatus,* n. sp. The Girardeau fauna is most consistent with an Upper Ordovician age assignment.

In addition, *Dendrocrinus constrictus,* n. sp. from the Cape Limestone is described, and the Orchard Creek Shale species, *Calceocrinus constrictus* Brower, discussed.

The Girardeau crinoids were rooted and stalked types occurring in optimum environments that developed near the end of a transgressive overlap sequence. High and low density gardens were inhabited, and these exhibited different population dynamics with respect to age structure, taxonomic composition, levels exploited, competition and reproduction. Size-frequency diagrams of the abundant crinoids reflect time-size growth vectors, differential mortality, and seasonal breeding. Certain species formed small populations while others maintained large panmictic types ranging over 1,000,000 individuals. Reproductive structure was dictated by population density and the presence or absence of currents. Preservation of the crinoids yields information about burial rates and living positions.

Relatively complete growth sequences are known for various Girardeau camerates. Living and camerate crinoids show the same plate development sequence except for the iBrl which appears later in extant forms. Contrasts in calyx and arm plate ontogeny are related to differential placement of the aboral nerve cords. Columnal growth and nerve cord position are uniform in all crinoids.

Phylogenies are presented for one flexible and three camerate groups. All evolutionary trends are best interpreted as progressive adaptations. This in conjunction with the large populations involved denotes that natural selection was the principal evolutionary vector. Evolution occurred through "mutations" which affected the ontogenies of young crinoids by inducing growth divergences.

INTRODUCTION

Although crinoids have been known from the Girardeau Limestone (Late Ordovician) since at least 1855, a detailed systematic study of the fauna has never been presented. Only three crinoid species have been described: *Ptychocrinus fimbriatus* (Shumard) (1855), *P. splendens* (Miller) (1883), and *Protaxocrinus girardeau* Springer (1920).

Considering the abundance and diversity (18 species) of Girardeau crinoids, this is highly anomalous. Over the years about 500 crinoids have been assembled by various workers of which the most important follow: A. H. Worthen, latter part of nineteenth century, Illinois Geological Survey; E. O. Ulrich, around 1890 to 1920, United States National Museum; G. A. Cooper and J. Bridge, 1936, United States National Museum; J. M. Weller, during the 1930's, Illinois Geological Survey; T. E. Savage, roughly 1905 to 1920, University of Illinois; and J. C. Brower, 1964 and 1967, Illinois Geological Survey.

The anomaly becomes even more striking because the Girardeau fauna is critical to knowledge of Early Paleozoic crinoids for three reasons: 1. Crinoids are well known from two localities, the Cape Rock exposure near Cape Rock, Missouri, and the bed of Orchard Creek, near Thebes, Illinois. These two occurrences afford an unparalleled opportunity to study Early Paleozoic crinoid paleoecology and population dynamics. 2. Six Girardeau camerate species are represented by relatively complete growth sequences. These range from immature animals about 1.0 mm in "size" (*i.e.*, height from cup base to distal margin of IAx) with from four to eight IIBrr per arm to mature adults which attained "sizes" up to 15 mm and had several hundred Brr per arm. The only comparable Early Paleozoic camerate ontogeny sequences known to the writer occur in the Late Ordovician of the Cincinnati area. The most familiar are *Glyptocrinus decadactylus* Hall and *G. dyeri* Meek; the smallest individuals of these species are larger and were probably older than the youngest Girardeau animals. However, the Cincinnatian crinoids are better preserved than the Girardeau specimens and detailed study is planned. 3. The Girardeau crinoid genera include forms which elsewhere are — Ordovician and Silurian, Ordovician, and Silurian or later. One genus is endemic to the Girardeau. The Girardeau Silurian or later types constitute the earliest occurrence in North America or in the world for these crinoids. Such suggests that the Silurian elements were in the initial phase of an adaptative radiation during which they coexisted with Ordovician forms. By the end of the Ordovician period the Ordovician genera became extinct, and the Silurian elements fully occupied the available habitats by Middle Silurian time.

FAUNAL COMPOSITION

The Girardeau occurs at the top of a transgressive overlap sequence consisting of the Thebes Sandstone, Orchard Creek Shale and Girardeau Limestone. In Illinois, the sequence unconformably overlies various Early and Middle Ordovician units. This unconformity pinches out in Missouri and the contact between the Thebes and older Maquoketa strata is gradational. Another unconformity is generally found above the Girardeau where the unit is overlain by the Edgewood or Sexton Creek Limestones. The unconformity is not observed at the Orchard Creek exposure and the Girardeau grades upward into the Sexton Creek.

PREVIOUS AND PRESENT WORK

Most early workers considered the Thebes and Orchard Creek as Late Ordovician (*e.g.*, Worthen, 1866, p. 139). T. E. Savage spent numerous years working on the paleontology and stratigraphy of the Girardeau transgressive sequence. In 1908 (p. 433), he believed the Thebes and Orchard Creek to be of Richmond (Late Ordovician) age. Later Savage (1917b, p. 265) transferred the Orchard Creek to the Silurian because of faunal similarity. Ulrich (1926, pp. 329, 342-344) agreed with Savage and placed the Orchard Creek in the Silurian. Ross (*in* Pryor and Ross, 1962, p. 9) reported the presence of the characteristic Cincinnatian graptolite, *Climacograptus putillus* Hall, in the Orchard Creek. R. M. Liebe (personal communication) also found Ordovician conodonts in the unit. Thus paleontological evidence clearly indicates an Ordovician age for the Thebes and Orchard Creek. Lithologically, the two units have greater affinity with Ordovician rocks than with Silurian ones. Present practice of the Missouri Geological and Illinois Geological Survey assigns both formations to the Late Ordovician (Templeton and Willman, 1963, pp. 131-136; Martin, Knight, and Hayes, 1961, pp. 31, 32).

Some early workers placed the Girardeau in the Silurian (*e.g.,* Shumard, 1855, p. 154) whereas others grouped the unit with the Late Ordovician (Worthen, 1866, pp. 139, 140). In 1917, Savage (1917a) published a comprehensive report on Girardeau stratigraphy and paleontology. Crinoids were not treated in detail and only three species (identified by Frank Springer) were listed: *Ptychocrinus splendens* S. A. Miller; *Tanaocrinus* cf. *T. typus* Wachsmuth and Springer (*Compsocrinus nodosus*, n. sp. of this report); *Archaeocrinus sp.* (this specimen has not been found). In all publications, Savage considered the Girardeau as Early Silurian, stating (1917a, p. 75):

> The decidedly Silurian aspect of the fauna of the Girardeau limestone appears in the lists presented above. The post-Richmond age of the Girardeau limestone is shown by the total absence of a single characteristic Richmond species in the formation, and also by the presence of such Silurian genera as *Schuchertella, Homoeспira,* *Camarotechia?, Diaphorostoma, Protozeuga,* and *Proetus.* The only species in the Girardeau fauna that are listed by Cumings from the Richmond strata of Indiana, or that are known to occur in the Maquoketa (Richmond) strata of Iowa and Illinois, are *Leptaena rhomboidalis* and *Cornulites tenuistriata,* neither of which possesses any stratigraphic significance.

Ulrich (1926, pp. 329, 342-344) followed Savage and assigned the Girardeau to the Silurian. Ulrich also published a faunal list including some crinoids. These are listed below; the names used in this report are given in parentheses:

Ptychocrinus splendens (*P. splendens*)
Ptychocrinus, five n. spp. (*P. splendens* and *P. fimbriatus*)
Canistrocrinus, four n. spp. (*P. splendens*)
Mariacrinus ?, five n. spp. (*Alisocrinus tetrarmatus,* n. sp. and *A. ? heterodactylus,* n. sp.)
Xenocrinus, n. sp. (*Compsocrinus nodosus,* n. sp.)
Macrostylocrinus ?, five n. spp. (*M. pristinus,* n. sp.)
Macrostylocrinus, (subgen. with uniserial arms), four n. spp. (*Eopatelliocrinus scyphogracilis,* n. gen., n. sp. and *E. latibrachiatus,* n. gen., n. sp.)
Haplocrinus ?, n. sp. (*Culicocrinus ? girardeauensis,* n. sp.)
Carpocrinus ?, n. sp. (specimens not located)
Dendrocrinus, n. sp. (*D. casei*)
Protaxocrinus girardeau (*P. girardeau*)
Girardeaucrinus suberectus, n. gen., n. sp. (This manuscript name was proposed for an unidentifiable inadunate crinoid with questionable calceocrinid affinities.)
Eucheirocrinus, n. sp. (indeterminate calceocrinid)

It should be realized that Ulrich only presented a faunal list and the crinoids were not formally described. The differences between his identifications and those of the writer reflect the following: 1. Ulrich subdivided growth sequences into a series of species whereas the writer considers these as one form, *e.g.,* most camerates; 2. Changes in crinoid generic diagnoses since 1926, *i.e., Compsocrinus nodosus,* n. sp. and *Culicocrinus ? girardeauensis,* n. sp.; 3. Contrasts in Ulrich's species concept relative to that of the writer, *i.e., Dendrocrinus casei* Meek; 4. Disagreements as to what constitutes an identifiable specimen, *i.e., Girardeaucrinus suberectus,* n. gen., n. sp. and *Eucheirocrinus,* n. sp. of Ulrich.

Later authors have been skeptical about a Silurian age for the Girardeau. Weller and Ekblaw (1940, pp. 8, 9) suggested a Late Ordovician assignment on lithological grounds. At present, the Illinois Geological Survey tentatively places the unit in the Silurian with the reservation that detailed restudy of the fauna is necessary (Templeton and Willman, 1963, p. 133). The Missouri Geological Survey retains the Girardeau in the Silurian (Martin, Larsen and Muilenburg, 1961, p. 34). As later discussed, the crinoid evidence is most consistent with an Ordovician age. R. Parkinson (personal communication) is restudying the brachiopod fauna and is inclined toward a latest Ordovician grouping (Gamachian stage).

Recently Satterfield (1971) examined conodonts from the Girardeau Limestone. These strongly suggest a latest Ordovician age.

CORRELATION

The crinoid fauna of the Girardeau is listed below:

Camerata
  Ptychocrinus splendens (Miller)
  P. fimbriatus (Shumard)
  Unidentified archaeocrinid
  Compsocrinus nodosus, n. sp.
  Alisocrinus tetrarmatus, n. sp.
  A. ? heterodactylus, n. sp.
  Eopatelliocrinus scyphogracilis, n. gen., n. sp.
  E. latibrachiatus, n. gen., n. sp.
  Macrostylocrinus pristinus, n. sp.
  Culicocrinus ? girardeauensis, n. sp.

Inadunata
  Dendrocrinus casei (Meek)
  D. ?, n. sp. aff. *D. ? navigiolum* Miller
  D. curvijunctus, n. sp.
  Three unidentified species

Flexibilia

Protaxocrinus girardeau Springer
Clidochirus serrulatus, n. sp.

The Girardeau genera exhibit mixed stratigraphic ranges as indicated by the following: Ordovician elements; *Ptychocrinus* and *Compsocrinus.* Ordovician and Silurian, sometimes Devonian forms; *Macrostylocrinus, Dendrocrinus* and *Protaxocrinus.* Silurian and later; *Alisocrinus, Clidochirus,* and the questionable *Culicocrinus. Eopatelliocrinus,* n. gen. is endemic to the Girardeau.

Of the 14 definitely identified Girardeau species, only *Dendrocrinus casei* is known elsewhere. This crinoid is common in the Richmond (Late Ordovician) of the Cincinnati, Ohio, and Indiana areas and also occurs in the Maquoketa of the Iowa-Illinois outcrop belt.

The species affinities of the undescribed Girardeau forms also yield mixed results (see systematic paleontology and phylogeny for more details): most closely related to Ordovician species, both Girardeau *Ptychocrinus, Compsocrinus nodosus,* n. sp., *Dendrocrinus curvijunctus,* n. sp. *D.* ?, n. sp. aff. *D.* ? *navigiolum* Miller, and *Protaxocrinus girardeau* Springer; Silurian affinities, *Macrostylocrinus pristinus,* n. sp. and *Clidochirus serrulatus,* n. sp.; equal relationships with Ordovician and Silurian species, *Alisocrinus tetrarmatus,* n. sp., and the two *Eopatelliocrinus,* n. gen.; no close relatives, *Culicocrinus* ? *girardeauensis,* n. sp. and *Alisocrinus heterodactylus,* n. sp. Although the above listings are not conclusive, Ordovician affinities seem to predominate at the species level.

Tabulation of the ranges of Mississippian crinoid genera and species shows virtually all nonmonotypic genera have ranges which exceed those of the individual species. Most species were short-lived in time (see Brower, 1969 for summary). Such suggests that in crinoid correlation, maximum reliance should be placed at the species rather than the generic level. Consequently, it is believed that the Girardeau is Late Ordovician, probably Richmond or slightly younger (Gamachian stage). An Early Silurian age is possible but seems less probable. Savage's conclusions about the paleontology of groups other than crinoids are not strongly weighted as the material should be restudied. A Late Ordovician age is also supported by the lithological evidence. The phylogenies presented in this paper are consistent with a Late Ordovician or Early Silurian assignment.

LOCALITIES

Girardeau crinoids occur at various outcrops in the vicinity of Cape Girardeau, Missouri, and Thebes, Illinois. Virtually all well-preserved crinoids have been taken from two exposures: 1. Orchard Creek exposure, bed of Orchard Creek, SW 1/4, SE 1/4, sec. 21, T. 15S., R. 3W., Thebes Quadrangle, Alexander County, Illinois; 2. Cape Rock exposure; bank of Mississippi River by power house along Cape Rock Drive about one-quarter mile north of Cape Rock and two miles north of Cape Girardeau, NE 1/4, sec. 28, T. 30N., R. 14E., Cape Girardeau Quadrangle, Cape Girardeau County, Missouri. Other Girardeau localities are listed under Systematic Paleontology.

In addition to the Girardeau, several detailed paleoecological samples have been taken from the Thebes and Orchard Creek Formations: 1. Upper Thebes Sandstone, from highway cut near Gale, NE 1/4, NW 1/4, sec. 4, T. 15S., R. 3W., Thebes Quadrangle, Alexander County, Illinois; 2. Lower Orchard Creek, shale bed from Salamans Creek, center of sec. 10, T. 15S., R 3W., Thebes Quadrangle, Alexander County, Illinois; 3. Upper Orchard Creek, limestone bed along side of Mississippi River, SE 1/4, sec. 5, T. 15S., R. 3W., Thebes Quadrangle, Alexander County, Illinois.

Details of the Illinois stratigraphic sections may be found in Pryor and Ross (1962). The Missouri sections have not been published; however, these are on file at the Department of Geology, Missouri State College at Cape Girardeau.

ACKNOWLEDGMENT

The writer is grateful to the following individuals for loan of materials: Charles Collinson, Lois S. Kent and Charles Ross, Illinois Geological Survey (IGS.); Porter M. Kier and Thomas Phelan, United States National Museum (USNM., also Springer Collection, S.); R. Parkinson, Missouri State College at Cape Girardeau; Richard Leary, Illinois State Museum (Ill. St. Mus.); Matthew Nitecki, Field Museum of Natural History (UC.); John Carter and R. H. Hansman, University of Illinois (Univ. Ill.); Copeland MacClintock, Yale Peabody Museum (YPM.); W. D. Ian Rolfe, Hunterian Museum (HM.) Glasgow, Scotland; C. D. Waterston, Royal Scottish Museum (RSM.). Charles Collinson, Charles Ross, R. Parkinson, and Louis Unfer (Missouri State College at Cape Girardeau) provided information about collecting localities and correlation of the Girardeau and allied units. R. P. S. Jefferies and P. M. Kier respectively, have graciously allowed the writer access to the British Museum of Natural History and the Smithsonian Institution collections examined in conjunction with this study. R. C. Moore, Georges Ubaghs, N. G. Lane, D. L. Meyer, and James Sprinkle kindly read portions of the manuscript, and the writer thanks these individuals for their criticisms and editorial comments.

Thanks are due to J. R. Kramer, McMaster University;

T. D. Kurtz, University of Michigan; Don S. Thompson and James Wilson of Syracuse University; and Beverly Deflores and John Zwierzynski of the Syracuse University Research Corporation for much needed computer programming. Bryce Hand of Syracuse University kindly calculated the Girardeau current velocities.

The photographs were taken by James Wilson and processed by the writer's wife. Text-figures were drawn by John Fonda of Syracuse University.

The initial stages of the work were supported by a Grant-in-aid from the Illinois Geological Survey while later phases and illustrations were financed by NSF Grant GB-4115 and Syracuse University. Without these, the project would not have been possible. Gratefully I thank my wife for editorial help, typing, proof reading, and making of the index.

PALEOECOLOGY

The Girardeau "sequence" represents a transgressive overlap consisting of three units, listed from bottom to top: Thebes Sandstone; Orchard Creek Shale; and Girardeau Limestone (Illinois nomenclature used). The base of the "sequence" rests unconformably on rocks of Early and Middle Ordovician age in Illinois. Across the Mississippi River in Missouri, the equivalent unit to the Thebes Sandstone is conformable with older Maquoketa Group strata. The Girardeau Limestone is generally unconformably overlain by the Edgewood or Sexton Creek Limestones; the unconformity seems to be absent at the Orchard Creek exposure (Illinois).

The Thebes Sandstone is principally composed of well-sorted angular quartz sandstone with a minor quartz silt and iron-stained clay matrix fraction. The most common sedimentary structures are cross bedding, cut and fill and allied types which indicate some degree of current agitation. A low diversity fauna (four species) is present, including a linguloid brachiopod, one graptolite and two types of feeding trails and burrows. The density of bottom dwelling individuals equals .28/ft^2. Table 1 summarizes the density, diversity, and ecological categories in the entire Girardeau transgressive sequence; the high density crinoid gardens are omitted from the Girardeau Limestone figures as these are rare and only low density occurrences are included. The environment probably represented an agitated intertidal or inner subtidal situation. Salinity may have been normal marine or somewhat brackish. Presumably the graptolites were not endemic to the area but simply drifted in and were buried in the shifting sand.

Dark grey silty clay shale predominates in the lower Orchard Creek beds. Typically, the sediments are finely laminated and have not been disrupted by burrowing organisms. When unweathered, the shale has a dark grey or almost black color, indicative of appreciable organic detritus. The fauna exhibits low diversity (three species) and density. Groups present include linguloid brachiopods, orthocone cephalopods, and graptolites. The latter two were pelagic and do not represent native (to the bottom) faunal elements. The brachiopods may have lived on the bottom during times of moderate dissolved oxygen. The lack of linguloid brachiopod burrows in the finely laminated shale may denote that the brachiopods were epiplanktonic. The fine-grained texture and thin laminations of the sediment are proof of quiet water and low agitation. The organic carbon content suggests marginal dissolved oxygen or reducing conditions on the sea bed. Lack of dissolved oxygen would account for the fine lamination and absence of burrowing of the sediment. Salinity cannot be determined but was probably normal marine or slightly brackish.

The upper Orchard Creek strata consist of alternating shale and limestone beds with the latter increasing in thickness and frequency toward the top of the unit. The shales are poorly exposed but seem similar to those of the lower Orchard Creek where observed. The limestone occurs in two to three inches (5.1 to 7.6 cm) thick beds which are composed of massive unstratified lithographic silt-sized and clay-sized calcite and clay minerals. The organic detritus cannot be ascertained as the rocks are highly weathered. The fauna is characterized by high diversity (16 species tabulated in field work) and moderate density (.27 bottom dwellers/ft^2) and mainly consists of strophomenid and orthid brachiopods, trilobites, gastropods, a few crinoids, and cyclocystoids. Virtually all fossils are found on the upper surfaces of bedding planes; the distribution seems random and not strongly aggregated as in the Girardeau. All in all, the species are similar to those in the overlying "crinoid beds" of the Girardeau. The Orchard Creek Limestones were probably deposited in quiet water and under low sedimentation rates. The bedding planes may represent scour surfaces and times of relatively high agitation; the exposure are too poorly preserved to determine this critical point. Certainly the groups present and their diversity denote normal marine salinity. The substrate must have been suitable for the rooting of various brachiopod species (orthids) and calceocrinids. When found in fine-grained sediments, calceocrinids probably required a firm substrate because of the recumbent stem and short roots (Brower, 1966).

The Girardeau is composed of two alternating lithologies which are cyclically interbedded in units ranging from two to four inches (5.1 to 10.2 cm) thick. The predominant rock in a single cycle (about 75 to 80%) is a dark green massive and unlaminated lithographic limestone. Most of

Table 1

Stratigraphic horizon	Total species	Reclining filter feeding species	Rooted filter feeding species	Cemented filter feeding species	Attached to crinoid tegmen — feed on crinoid excrement	Detritus feeding species	Questionable detritus feeding species	Unknown bottom dwelling niches	Pelagic and epiplanktonic species	Bottom dweller population density/ft^2
Girardeau limestone 25-30′	14	2	11	1	0	0	0	0	0	3.5
Girardeau limestone 20-25′	14	2	11	1	0	0	0	0	0	3.8
Girardeau limestone 15-20′	32	1	25	1	1	0	3	1	0	7.2
Girardeau limestone 10-15′	11	1	8	1	0	0	0	0	1	2.4
Upper Orchard Creek limestone bed	16	5	6	1	0	0	1	3	0	.27
Lower Orchard Creek shale bed	3	0	0	0	0	0	0	0	3	0
Upper Thebes sandstone	4	0	1	0	0	2	0	0	1	.28

Table showing the taxonomic and ecological diversity and the bottom dweller population density at various horizons within the Girardeau transgressive sequence.

All Girardeau Limestone samples from the Orchard Creek exposure. Thickness quoted are above the base of the unit. The basal Girardeau is not exposed at Orchard Creek but the formation is estimated to be about 40 feet thick (Pryor and Ross, 1962, pp. 8-10).

Upper Orchard Creek Limestone bed from the Mississippi River exposure.

Lower Orchard Creek Shale bed from the Salamans Creek exposure.

Upper Thebes Sandstone sample from the highway cut near Gale.

The Girardeau population densities represent low density calcareous shale crinoid garden values, not the total population densities. The Girardeau fauna occurs in clumps and patches which are separated by barren intervals; the latter is not included in the calculations. The Girardeau lithographic limestone beds are largely barren and have not been sampled. The bottom dwelling faunas of the Thebes Sandstone and the Upper Orchard Creek Limestone beds are randomly distributed on the bedding planes. Consequently, these densities are not comparable to the Girardeau figures. The Orchard Creek Shale linguloid brachiopods are considered epiplanktonic as discussed in the text.

this material represents clay-sized and silt-sized calcite, although clay minerals are present. When broken, a fetid odor composed of hydrogen sulfide (perhaps with some other gases) is commonly released; such is probably indicative of high original organic detritus. Typically, the beds are massive and show few traces of lamination. Fossils are rare and only a little crinoid debris is present. The fine-grained material, organic detritus, and general lack of fossils seem to denote a lack of or a marginal amount of dissolved oxygen. Alternatively, the substrate might have been unsuitable for faunal colonization. The fine-grained sediment and general lack of lamination imply continuous deposition in quiet water, and the few crinoids provide proof of normal marine conditions.

Some of the green limestones contain fine laminations, small scale cross bedding and ripple marks, and minor scour surfaces. Fossil debris, mostly crinoidal, is common. These sedimentary structures closely resemble those of the Girardeau shaly partings and they suggest episodic oxidizing and moderately agitated intervals.

The green lithographic limestone of a single cycle grades upward and downward into light brown shaly partings. The most common mineralogic and size fractions are: calcite, quartz, and dolomite ? silt- and sand-sized material; clay-sized calcite; and clay minerals. The shale partings always show fine laminations and commonly have small scale cross bedding, cut and fill structure, and a few ripple marks. Large scale (up to six inches or 15 cm wave length) symmetrical or asymmetrical ripples are abundant. Many of the laminae within the shale partings seem to represent scour surfaces and small scale "unconformities". The shale partings (especially the scour surfaces) bear a dense and highly diversified suite of fossils. Usually the faunal distribution is patchy and clumps of abundant specimens are interspaced with barren or nearly barren areas. Where large ripples are found, their crests are devoid of fossils. Diversity ranges from 11 to 32 species and the clump or patch density varies from 2.4 to 175 bottom dwellers per square foot (930 cm^2). Maximum density and diversity occur in the middle part of the Girardeau (about 15 to 25 feet or 4.6 to 7.7 m above base of the unit). The upper and lower portions of the formation show lower density and diversity. Ecologically, the total assemblage is almost entirely epifaunal suspension feeder and consists principally of highly diversified (up to 18 species) and abundant crinoids and crinoidal debris, strophomenid, orthid and small atrypid ? brachiopods, fragile twiglike bryozoans, trilobites, filter feeding calcareous worm tubes, platyceratid gastropods, and a few rhombiferan cystoids and starfishes.

The most common Girardeau shaly parting sedimentary structures are laminations, small ripple marks, and ripple cross bedding. These denote transportation of coarse silt and, sometimes, fine sand-sized particles of quartz, calcite, and dolomite. The morphology of the structures shows that current velocities were only slightly above the critical level required for grain transport. The current velocity profile which prevailed during formation of these structures was calculated by Bryce Hand of Syracuse University as follows: Shields friction criterion (Θ) for the threshold of grain motion was estimated from figure 2.32 in Allen (1968, p. 27). Following this, the shear stress (τc) required to initiate movement of a coarse slit-sized particle was determined by (see Allen 1968, p. 26):

$$\Theta = \tau c \cdot (\rho \text{ grain } - \rho \text{ sea water}) \cdot g \cdot D$$

ρ = density in gm/cm^3

g = acceleration of gravity in cm/sec^2

D = grain diameter in cm

The shear velocity (V^*) provides a measure of the velocity change with increasing height above the substrate and it is defined as:

$$V^* = \sqrt{\tau c/\rho \text{ sea water}}$$

The approximate velocity profile was then computed by analogy with water flow in smooth pipes (see discussion of Nikuradse diagram in Rouse, 1961, pp. 236-245). The analysis seems justified inasmuch as the fine grains of the Girardeau shaly partings should have been completely contained within the laminar boundary sublayer of current flow. This is hydrodynamically equivalent to a smooth boundary. At a short distance (.07 cm) above the bed, the flow must have been fully turbulent. The velocity profile for flow past a smooth boundary can be calculated by the following equations:

Laminar flow:

$$\frac{V}{V^*} = V^* \cdot \left(\frac{y}{Y}\right)$$

Y = kenematic viscosity

V^* = shear velocity

V = current velocity in cm/sec

y = height above the sea bed in cm

Turbulent flow:

$$\frac{V}{V^*} = 5.5 + 5.75 \cdot \log_{10} \left[V^* \cdot \left(\frac{y}{Y}\right) \right]$$

The boundary between the laminar and turbulent flow layers was approximated by the intersection between the velocities determined from the above two equations. The below listed current velocities were estimated for the Girardeau shaly partings:

Table listing Girardeau Current Velocities

Flow type	Height above substrate	Current velocity
Laminar	.01 cm	2.5 cm/sec
Top of laminar boundary sublayer	.07 cm	16 cm/sec
Turbulent	.7 cm	24 cm/sec
Turbulent	1.0 cm	25 cm/sec
Turbulent	7 cm	32 cm/sec
Turbulent	10 cm	33 cm/sec

It must be realized that the above moderate current velocities only occurred during sediment transportation and formation of the laminations, ripple cross bedding and small scale ripple marks. Higher velocities most likely developed during the erosional intervals, when the large scale ripple marks formed and while coarse fossil debris was transported. The rare submarine mudflows also were produced by high current velocities. Relatively quiet water periods doubtless prevailed when fine suspended sediment settled on the sea floor. Thus the Girardeau crinoid habitats should be visualized as variable; they ranged from almost still water to highly agitated areas. The faunal distribution suggests that the animals were able to live during intervals of quiet water and during times of higher agitation. The greater diversity along scour surfaces implies that the latter intervals were preferred.

Despite the above current velocities, the Girardeau fauna is not considered a rough water assemblage. The Girardeau species are dominated by small, fragile and pinnulate forms. Typical rough water Ordovician crinoid faunas are represented by the Benbolt Limestone of Virginia and Tennessee and the Decorah Shales of the Twin Cities area in Minnesota. These habitats were characterized by strikingly different crinoids as follows: 1. Numerous short-armed nonpinnulate inadunates such as *Carabocrinus, Palaeocrinus* and *Hybocrinus;* 2. Thick-plated forms like *Diabolocrinus* and *Hybocrinus.* These faunal elements are conspicuously absent from the Girardeau communities.

The abundant and diversified epifauna is proof of an oxidizing environment and favorable substrate (see later discussion of crinoid attachment). Normal marine salinity is evidenced by both the groups present and their high diversity. Sedimentation rates and the suspended sediment content appear to have been low with the exception of a few catastrophic mud flows (see later discussion).

Survey of the overall faunal diversity and abundance and the postulated environmental conditions indicates that the most optimum to least favorable Girardeau "sequence" habitats were Girardeau shale partings, upper Orchard Creek Limestone beds, Girardeau green lithographic limestones, Thebes Sandstone, and Orchard Creek Shale beds.

The general paleogeographic interpretation follows. The Thebes Sandstone was deposited under agitated conditions in the intertidal zone or inner subtidal area. All other lithologies probably developed in deeper water. The Orchard Creek Shales and the Girardeau green lithographic limestones constituted hydrographically restricted and quiet water environments. Possibly these formed in blocked embayments such as silled estuaries or lagoons with prominent barriers. The shales represent clastic sedimentation and the limestones largely carbonate. Both optimum habitats, the Orchard Creek Limestones and the Girardeau shale partings, were deposited under strongly oxidizing, open water conditions which varied in the amount of wave or current agitation, or both. Such might imply that these developed in shallower water than the Orchard Creek Shales and Girardeau green limestones. However, no evidence supports this theory. All four sediments could have occurred at the same depth. When barriers were present, restricted quiet water conditions would have prevailed. In the absence of barriers, water interchange, an oxidizing sea floor and intermittent agitation would be expected.

BURIAL OF CRINOIDS

Girardeau crinoid preservation types generally fall into three categories: 1. Disarticulated crinoid debris usually consisting of a few stem segments, isolated columnals, Brr, pinnulars and calyx plates. Rarely, the columnals and stem segments occur without associated calyx and stem plates; 2. Calyces with disarticulated arm plates, columnals and stem segments. In some instances, the calyces may bear long or short column segments but arms are invariably lacking; 3. Crowns associated with isolated columnals and stem segments. Commonly long or short portions of the columns are attached to the dorsal cup.

The calyces, crowns, and crinoidal debris in the Girardeau shaly partings show no traces of abrasion, which indicates that these were buried near or at the living habitat. Also, the nature of preservation is suggestive of the relative rate of burial. The Girardeau preservation types illustrate this point.

During the life of living and fossil crinoids, the component plates are held together by the epidermis, ligaments, muscles, and articular surfaces of various types. According to H. L. Clark (1915), when Recent comatulid crinoids are exposed to certain toxic conditions the arms begin to fragment. This process is initiated at the tips of the arms and proceeds toward the calyx, plate by plate. Culmination would have resulted in decomposition of the calyx, if Clark had completed the experiments. The calyx breaks up last because it represents the most compact and tightly sutured part of the animal.

Direct stem comparison cannot be presented because adult comatulids lack columns. Many fossil crinoids suggest that a similar process operated. After death the arms and possibly the stem apparently began to decompose, plate by plate, in a proximal direction, with the calyx being the last to break up. This plate by plate decomposition seems reasonably certain for the arms; however, post-mortem breakage was probably as important, or more so, than plate by plate decomposition in the column.

Decomposition and breakage would then have freed the various plates, which might have been stirred by waves and transported by the available currents. Plates of different sizes and shapes would have received hydraulic sorting from currents of even moderate intensity so that relative rates of burial could be recognized. Under conditions of rapid burial, a crinoid would have been covered by debris before decomposition and current action could have fragmented and separated the various components. The result would be preservation of a relatively complete specimen, with calyx, arms, and column, or portions thereof, included. In slow burial, decomposition might have been completed, so that only scattered columnals, Brr, and calyx plates would have remained. With moderate rates of burial, preservation of calyces, isolated columnals, and Brr would be expected.

Variable burial rates of the Girardeau crinoids are indicated by several lines of evidence. On single crinoid patches or gardens of large slabs (about 18 by 18 inches or .21 m^2), two or three types of preservation may be observed at different places. For example, complete crowns may be associated with calyces which lack arms and crinoidal debris. Tracing the crinoid assemblages along a single bedding plane shows that all three burial types may occur within a single crinoid clump or along a series of gardens.

Rapid burial rates are denoted for at least some of the crowns with or without attached columns. A layer of contorted sediment immediately overlies these individuals. This is believed to represent a submarine mudflow which literally "mowed down" and buried these crinoids.

In several cases complete crowns (with or without attached stems) and calyces are located on top of a debris layer consisting of stem segments, isolated columnals, arm and calyx plates. Some of the debris probably represents portions of the crowns and calyces (some stem segments, isolated columnals, and arm plates). However, the bulk of the arm and calyx plates and most of the stem parts cannot be accounted for in this way. Probably the largest part of the "debris individuals" constitutes crinoids which died prior to the animals which are represented by the calyces and crowns. These decomposed and were disarticulated by wave or current action, or both (*i.e.*, slow burial). Later the "calyx" and the "crown individuals" died in that order and were buried more rapidly. Evidence for this death sequence is discussed in more detail in the section on crinoid gardens.

The Girardeau "crown individuals" were buried in three positions: 1. Arms spread out at angles ranging from 45 to 90° relative to the stem-crown axis. The two pinnule fans of a single arm are separated at angles of 90 to 180° in some cases. The covering plates have not been observed; consequently, it is unknown whether these are open or closed. By analogy with living forms, these crinoids are believed to have been buried in the act of feeding. The ecology of living crinoids has recently been discussed by Fell (1966) and Breimer (1969). Food gathering is not continuous in Recent comatulids. These animals only feed when at rest and attached to the substrate or some other object. A considerable amount of the life span is occupied by food gathering; Breimer estimated that living species spend about half their entire life time in this activity.

Two feeding orientations are known. Under still water conditions, the arms are spread roughly horizontally with upraised tips to form a collecting bowl (rheophobes of Breimer, 1969). The pinnules are extended at right angles to the arms and all covering plates are open so that the tube feet have access to the food supply. This orientation is basically designed to trap a down-falling rain of food particles; consequently, it is restricted to quiet water. The quiet water feeding orientation is most commonly reported in aquaria specimens of *Antedon* (*e.g.*, Nichols 1960; Hyman, 1955). According to Breimer (1969, p. 141), Porter Kier has observed a living quiet water comatulid feeding in the same position.

Where appreciable currents are present (Breimer, 1969, Magnus, 1967, Fell, 1966), the crinoids climb to higher places, such as rock ledges, sea grass and sea fans and adopt a fishing posture. The arms are held more or less vertical, relative to the sea floor. The aboral sides of the arms face into the current. As before, the pinnules are extended and the covering plates opened. *Heterometra savignyi* (J. Müller) assumes this feeding posture at current velocities ranging from two to five cm per second (Magnus, 1967). Magnus failed to state how or exactly where the current velocities were measured and his figures are considered suspect. Two to five cm per second seems a low current velocity to the writer. At times, the Girardeau crinoids lived in much faster currents, *e.g.*, 24 cm per second at seven cm above the sea bed. This orientation is a direct response to the current and is only fully efficient at trapping food particles carried by a current which parallels the sea bed. If the current direction changes, the crinoid folds up the arms and reorients them to face the current in the proper way. The expanded arms of *H. savignyi* are not strong enough to withstand faster currents (Magnus, 1967). Presumably, the comatulids vacate such areas when the need arises. Breimer (1969) termed crinoids of this type rheophiles. Both Breimer (1969) and the writer believe that these two feeding orientations can probably be extrapolated to fossil stalked crinoids. As previously mentioned, the Girardeau habitat alternated between almost quiet water and agitated conditions although the latter predominated. This suggests that the Girardeau crinoids assumed both feeding positions with the orientation depending on current velocity. D. L. Meyer (personal communication) reported a similar phenomena in Recent comatulid crinoids. In quiet water, the Girardeau crinoid food supply consisted of a down-falling rain of plankton and, possibly, organic detritus. At such time, the animals most likely fed in the stalked rheophobe fashion with the stem vertical and the arms spread horizontally to trap the food particles. During agitated intervals, the currents (see previous calculations) were rapid enough to transport food parallel to the sea floor. Here the animals must have assumed the rheophile orientation. The stem was flexed down current with the calyx long axis more or less parallel to the substrate; when feeding, the arms would have been vertical with their aboral sides facing into the current.

When not collecting food, the arms of 10-armed species are typically directed more or less vertically above the calyx with the pinnules closed together over the food groove (H. L. Clark, 1915, p. 144). *H. savignyi*, a 20-armed comatulid, has the arms coiled spirally inward over the tegmen (Magnus, 1967). In Recent multibrachiate forms (many more than 10 arms) the arms are more or less widespread when not feeding (H. L. Clark, 1915, p. 114), and presumably, the pinnules are held in the closed position. Most or all (depending on the species) of the arms of the abundant Girardeau camerates rise directly from the calyx; the arms are close spaced and do not spread distally to any great extent. Therefore, these species are analogous to the 10-armed comatulids rather than the multibrachiate forms. The arm flexibility of the Girardeau camerates is estimated from the curvature shown by the preserved arms. Clearly, these were not flexible enough to have allowed the arms to have been rolled inward over the tegmen as in *H. savignyi*. However, many flexible crinoids probably assumed the nonfeeding orientation of *H. savignyi* (see numerous illustrations in Springer, 1920). Recent comatulids do not gather food when swimming or crawling from place to place.

2. A few Girardeau camerates (*e.g.*, holotype of *Eopatelliocrinus scyphogracilis*, n. gen., n. sp., and a crown of *Ptychocrinus splendens*) were buried with one or two arms spread and the others vertical. Typically the stem is bent with its distal end curved toward the outspread arms. These animals probably died while threshing one or two arms downward or with the arm on the upward or return stroke. At any rate, the movements involved are believed to be related to balance. All specimens seen have the pinnules folded over the food groove and not in the extended position. This may be due to the nature of burial or perhaps indicates the return stroke (see discussion of arm leverage). Some evidence from living crinoids may denote that the balance hypothesis is incorrect. Dropping food onto one arm of tank dwelling comatulids shows that the animal will feed with only the arm or arms closest to the food source (Kier, personal communication). Magnus (1967) reported *Heterometra savignyi* first unrolled a few arms when preparing to feed. Later, all arms were extended. However, this phenomena is rarely reported from the natural habitat; when seen, it appears to be of short duration. As far as known to the writer, all naturally living crinoids extend all arms during almost all of the time spent feeding. Consequently the balance hypothesis is preferred here.

3. Most Girardeau crowns are preserved with the arms directed upward and parallel to the stem-crown axis. The two pinnule fans of the same arm are close together. When determined, the covering plates are closed. Presumably, these individuals were not gathering food at the time of death. In this resting position the fragile food grooves with their covering plates and the tegmen would have been protected by the stronger parts of the arms and pinnules.

The relative frequency of the two most common crown orientations changes with age. Most of the individuals buried in the act of feeding were young animals whereas almost all mature crinoids were buried in the resting position. This suggests that young crinoids spent more time feeding than the older individuals.

CRINOID "SIZE" FREQUENCY DISTRIBUTIONS

The smallest Girardeau camerates are about 1.0 to 1.3 mm in "size", possess four to nine IIBrr in each arm and pinnules are well developed. IBr1 and sometimes IAx are incorporated into the calyx. Microcrinoid and the earliest arm bearing growth stages are conspicuously absent although these have been searched for during several field seasons. The reason for this remains uncertain and several alternatives exist. Possibly, the plates had not come into vertical and lateral contact during these growth stages. Consequently, on death of these crinoids, the plates could have been scattered over the sea floor by wave or current action, or both. Such does not seem unduly probable as no isolated calyx plates, within the microcrinoid and early arm bearing growth "size" ranges, have been found. Study of crinoids and their plates in thin section discloses numerous etched and blurred margins. Commonly, isolated plate edges completely blend into the surrounding matrix. Within a single thin section, the etched and blurred plates are most commonly small although some larger plates also show traces of these phenomena. Apparently, specimens of this type are in the earlier stages of diagenetic (solution) attack; continuation of the process could eventually obliterate the crinoid.

The environment was highly favorable for the growth of the youngest crinoids and their initial mortality rates after settling on the substrate were low. Higher death rates did not occur until "sizes" of about 1 mm were attained. This hypothesis does not provide a satisfactory answer. By analogy with life-table analysis of living marine invertebrates with pelagic larvae, the highest mortality rates should have occurred in the youngest stages. The Girardeau camerates probably had pelagic larvae, because brood pouches are lacking in the arms. All modern crinoids which lack pelagic larval stages, known to the writer, are characterized by these structures (see Hyman, 1955, pp. 71-75, for summary of brood pouches).

Thus, in view of the above evidence and by process of elimination, diagenesis is concluded to be the main factor responsible for the lack of Girardeau camerate microcrinids. Mature Girardeau camerates range from 5 to 15 mm in "size", possess from 50 to 200 Brr in each arm, and are characterized by varying numbers of fixed IIBrr and sometimes IIIBrr.

With the exception of *Ptychocrinus splendens*, each abundant Girardeau species (*i.e.*, 10 or more individuals in growth sequence) shows a bimodal "size" frequency curve (Text-fig. 1, p. 276). One mode occurs in the young crinoid interval and the second characterizes the adults (detailed figures given under the various species). For purposes of discussion, crowns associated with the immature specimen mode are termed "young assemblages" and those grouped with the larger mode "adult assemblages". The two "assemblages" are always separated by a low frequency "size" group. "Young assemblage" crinoids typically range from about 1.0 to 3.5 mm in "size" whereas "adult assemblage" types occur over approximately the 4.0 to 9.0 mm or more interval. Within a single form, "adult" and "young assemblage" crinoids may be found on the same bedding plane. The two "assemblages" of a single species are not observed together in high density gardens (see later discussion). On the other hand, both "young" and "adult assemblage" individuals are commonly preserved in low density gardens (*i.e,* small number of crinoids per unit area).

The "young" and "adult assemblage" crinoids of any one species most likely represent strong seasonal breeding relative to the life time acting in conjunction with the time-size growth rates. If the spawning intervals were closely spaced relative to the life span, a continuous "size" frequency diagram would be observed as in *P. splendens*. Therefore, the discontinuity between the "young" and "adult assemblage" individuals is probably caused partly by seasonal breeding. A. H. Clark (1921, pp. 369-375) and Boolootian (1966, pp. 562-564) tabulated the little known data on spawning intervals of living crinoids; conclusive figures are available for about half-a-dozen species. Some [*e.g., Antedon mediterranea* (Lamarck)] breed continuously and ripe eggs may be found throughout the year, although most of the larvae are produced in February, April, November, and December. Other forms show discontinuous spawning; for example *Hathrometra sarsii* (Düben and Koren) breeds in June, *Antedon bifida* (Pennant) in June and July, and *Comanthus japonicus* (J. Müller) in early October. The data are insufficient to warrant general deductions on paleogeography. Inasmuch as a crinoid life span probably ranges from 10 to 20 years (see introductory statement on ontogeny), reproduction once a year would be sufficient to introduce a significant discontinuity into the "size"-frequency distribution.

Time-size growth rates are poorly known in crinoids. The available information (see introductory statement on ontogeny) suggests that living and fossil crinoids fit the common marine invertebrate slow-fast-slow model. Probably the slow time-size growth phase ends about when the arms begin to develop. Approximately 67 to 90% of the total size is attained at roughly 50% of the life span. The mature crinoid slow time-size growth rates mainly postdate the 50% terminal age point (see also Hallam, 1967, pp. 31-35 for representative time-size curves of this type in molluscs). By analogy with living crinoids, the Girardeau "young assemblage" crinoids were undergoing rapid time-size growth. "Adult assemblage" crinoids occurred in the later part of the fast time-size growth phase and throughout the slow time-size growth interval. Probably the "young assemblage" animals of most species represented one spatfall. Here the discontinuous breeding and the rapid time-size growth rates operated to produce the narrow young crinoid "size" range and the discontinuity between "young" and "adult assemblages". Most "adult assemblages" constituted more than one spatfall. Discontinuities within the "adult assemblage" animals are not recognized because of: 1. Small sample size—the largest growth sequences (ptychocrinids) are composed of about 50 crinoids distributed over "size" ranges of about 1.5 to 15 mm; 2. The lower time-size growth rates obscured and blurred the discontinuities. Thus, two crinoids separated by one generation (*i.e.*, one spatfall apart) would be nearly identical in "size" if they were subject to slow time-size growth vectors.

CRINOID GARDENS

As used here, the term "crinoid garden" refers to one clump or patch of crinoids which was isolated from adjacent habitats by a more or less barren area. Such gardens were observed ranging from several inches (five cm) across up to about three feet (.92 m) in diameter. Judging from the crowns and calyces preserved in them, most patches were inhabited by from three to 60 individuals and contained one to five species. Girardeau crinoid patches are subdivided into two basic types:

1. Low density clumps invariably have less than 20 crinoids per square foot (930 cm^2) of bedding plane surface. Generally the maximum crinoid density ranges about five to 10 individuals/ft^2 (930 cm^2). Commonly "young" and "adult assemblage" crinoids occur together; these may or may not be conspecific. Taxonomic diversity is variable and from one to five species can be counted. Only small amounts of crinoidal debris are observed in the garden; clearly these individuals were not established on previously populated areas.

2. High density patches exhibit crinoid densities greatly in excess of 20 individuals/ft^2 (930 cm^2). In some instances up to 60 well-preserved crowns may be collected from less than one square foot. "Young" and "adult assemblage" animals are never associated, regardless of species; the two seem to be mutually exclusive. About 10 high density gardens are well known.

The population density for "young assemblage" clumps ranges from roughly 100 to 175 individuals/ft^2 (930 cm^2). In these, each animal possessed 9.3 to 5.3 cm^2 of living space with linear dimensions of 3.05 and 2.3 cm respectively on a side. The arms of "young assemblage" animals are 10 mm or less in length. Thus, the living space was large enough for each crinoid to spread its arms during rheophobe and rheophile feeding.

"Adult assemblage" population densities vary from almost 35 to 70 individuals/ft^2 (930 cm^2). Each animal had 26.6 to 13.3 cm^2 of area; the linear dimensions equalled 5.2 and 3.6 cm, respectively. Inasmuch as the adult Girardeau camerate arms are about 30 mm long, the animals in the 70 individuals/ft^2 garden would have barely had room to spread their arms for rheophobe feeding if they all lived at the same level. Clearly, such was not true. Adult animals of different species may have lived at various heights above the sea bed depending on stem length. Unfortunately, stem length data usually are not available on Girardeau crinoids. During ontogeny, stem length was progressively augmented. The "sizes" of the 43 specimens of *Ptychocrinus fimbriatus* Shumard in the 70 crinoids/ft^2 garden range from 4.9 to 11.1 mm. Thus, all of these animals were not at the same elevation relative to the substrate. When feeding in the rheophile position, all individuals probably possessed adequate living space.

Generally, three or more species are found in high density gardens. "Adult assemblage" patches were always dominated by one form, although two or more species commonly shared dominance in "young assemblage" areas; this is listed below for two examples.

TABLE SHOWING SPECIES COMPOSITION FOR TWO HIGH DENSITY GARDENS

Garden	Species	Percentage of total identifiable calyces and crowns Percent
"Adult Assemblage" USNM large slab	*Ptychocrinus fimbriatus*	74
	P. splendens	12
	Macrostylocrinus pristinus, n. sp.	12
	unidentified cystoid	2
"Young Assemblage" IGS slab	*Ptychocrinus fimbriatus*	11
	Alisocrinus tetrarmatus, n. sp.	33
	A? heterodactylus, n. sp.	11
	Macrostylocrinus pristinus, n. sp.	33
	Eopatelliocrinus latibrachiatus, n. gen., n. sp.	11

Comparison of the population density and taxonomic composition of "adult" and "young assemblage" gardens suggests that: 1. Natural selection eliminated about 60 to 65% of the "young assemblage" individuals prior to maturity. 2. The various species had different competitive abilities under high density conditions. In the "adult assemblage" USNM slab, *Ptychocrinus fimbriatus* was able to outcompete *Macrostylocrinus pristinus*, n. sp. and *Ptycho-*

crinus splendens (see above tabulation). Crowns and calyces of the latter two are subordinate to *P. fimbriatus.* However, *Macrostylocrinus pristinus,* n. sp. and *Ptychocrinus splendens* are relatively more abundant in the crinoidal debris layer than *P. fimbriatus,* judging from the number of isolated calyx plates observed. As later mentioned, the "debris animals" seem to have died prior to the individuals preserved as calyces and crowns. *Macrostylocrinus pristinus,* n. sp. and *Ptychocrinus splendens* are never abundant in high density "adult assemblage" gardens with *P. fimbriatus.* Consequently, it is concluded that *P. fimbriatus* consistently outcompeted the other two forms under high density conditions. This may be caused by differential mortality rates (see later discussion); *P. fimbriatus* was characterized by low juvenile mortality, whereas *P. splendens* and *Macrostylocrinus pristinus,* n sp. had higher young crinoid death rates. Conclusive competitive data are not available for the eopatelliocrinids and *Alisocrinus tetrarmatus,* n. sp. Although "young assemblage" crinoids of these species may be associated in high density stands, "adult assemblage" gardens are dominated by one species. Consistent patterns are unknown and on the average, the three forms probably exhibited roughly equal high density competitive ability.

Crinoidal debris is low when the gardens were populated by young crinoids. Adult crinoid clumps are characterized by much crinoidal debris; this material mostly represents the plate components of individuals which died previous to most of the animals preserved as crowns (see section on crinoid burial). This is supported by two lines of evidence: In considering one species within a single garden, the mean "size" of calyces (arms and stem not preserved) ranges less than the crowns. For example on the large "adult assemblage" USNM slab, 43 *Ptychocrinus fimbriatus* are identifible. The mean "size" of the crowns and calyces equals 8.6 and 6.3 mm respectively. Most of the conspecific isolated RR (when identifiable) are smaller than those of the calyces and crowns. Clearly, the average life spans of the animals represented in the crinoidal debris layer were the shortest whereas those of the individuals preserved as crowns were the longest. This, in conjunction with the general nature of crinoid preservation (see section on burial), suggests that the "debris individuals" died first, than the "calyx animals" and lastly the "crown individuals". The superposition of the different preservation types also outlines the death sequence to some extent. Where found in the same garden, the crowns and calyces always overlie the crinoidal debris. This shows that the "debris individuals" died first. Superposition of the crowns and calyces has not been observed.

The mutual exclusiveness of high density "adult" and "young assemblages" is highly significant. Actually, this term fails to express the true situation. Properly speaking, "young assemblage" crinoids never occur with older individuals. The relationship suggests that the presence of a certain critical population density (about 20 crowns/ft^2) of older crinoids inhibited the settling of the larvae. Under low density conditions, the reaction failed to operate and the larvae clearly settled on the substrate. It is postulated that each resident crinoid secreted some type of biochemical compound, the content of which per unit volume of sea water was a function of crinoid population density. When the material reached a certain critical level, the crinoid pelagic larvae were repelled; if necessary metamorphosis was postponed and larval settling occurred elsewhere. Larvae of various living marine invertebrates are known to be affected by the presence or absence of conspecific adults (see Johnson, 1964, pp. 110-116 for summary).

This type of larval reaction would be strongly adaptative to crinoid population structure because: 1. Time-size growth rates. The minimum amount of living space required by a crinoid is a function of arm length (which was augmented throughout growth) and the arm spreading angle when feeding. Actually, judging from the most dense Girardeau gardens, one individual occupied at least the minimum area. During ontogeny, the Girardeau crinoid stem length increased due to formation of new columnals and height augmentation of old ones. Thus, young crinoids lived close to the substrate whereas older individuals were elevated higher above the sea floor. Presumably the stem length-time growth vectors paralleled those of time-size. If young and older crinoids occurred together in high density stands, the larger animals must have formed an overstory and the smaller crowns an understory regardless of feeding orientation. The difference in elevation between the two levels would have been controlled by the chronological or spatfall age gap and the time-size growth rates operating on over- versus understory crinoids. The mean stem length-time growth rates of understory crinoids would have exceeded those of the overstory. Consequently the understory crinoids could have reached the adult crinoid level prior to the death of its inhabitants in many cases. Such would have resulted in overcrowding at the mature crinoid level. High mortality rates would have occurred which may have been detrimental to the species. This problem was eliminated by forcing the crinoid pelagic larvae to settle outside the high density stand.

2. The food problem. Again consider an overstory of older animals and understory of younger animals in a high density stand. At times, the Girardeau habitat was char-

acterized by quiet or almost quiet water with the crinoids feeding in the rheophobe orientation. Under such conditions, the crinoid food supply would have consisted largely of a down falling rain of plankton or organic detritus (probably mostly plankton as the crinoids lived in shallow water). When feeding, the overstory animals would have removed food from the water, thus depleting the plankton and organic detritus content prior to its reaching the young crinoid understory. As in the previous case, the problem was negated by the prevention of larval settling and the consequent lack of an understory. During the agitated intervals, some of the crinoid food probably traveled parallel to the substrate; here the food supply problem would not have applied.

At first glance, the Girardeau high density situation conflicts greatly with that postulated by Lane (1963b) for the Crawfordsville adult crinoids. Lane showed the presence of two levels of adult crinoids, a higher level composed mostly of flexibles which lived 60 to 100 cm above the sea bed, and an understory principally composed of camerates and inadunates at 20 to 25 cm elevations. Unlike the Girardeau, quiet water conditions predominated or prevailed throughout the Crawfordsville deposition. However, the population densities (46 crinoids/m^2, about five crowns/ft^2 or 930 cm^2) reported by Lane indicate that the Crawfordsville actually represents a low density garden in this writer's terminology (Girardeau high density gardens exceed 20 crinoids/ft^2). Also the Crawfordsville over and understories involved mature animals of several species, whereas the Girardeau situation basically represented segregation of different age classes of a series of single species. Despite the differences in size the crinoid biomass of the two habitats may have been comparable because the Crawfordsville crinoids are larger than the Girardeau forms.

MORTALITY RATES

"Size" frequency diagrams and survivorship analyses of the six abundant Girardeau camerates are presented in Text-figure 1. Mortality rates are inferred from the slope of the survivorship curve; steep slopes denote high death rates and vice versa. The mortality rates discussed here are relative to the survivorship; this relative mortality was calculated by the number of crinoids dying in a certain "size" interval/number of crinoids alive at the beginning of the interval. Absolute mortality rates can also be inferred from the data; this is number of crinoids dying within a selected size range/total number of crinoids in sample. However, absolute mortality rates are not considered here. Survivorship is depicted rather than mortality as larger numbers are involved; consequently smoother curves result which are easier to interpret.

The data should be viewed with caution. As stated under ontogeny, the youngest crinoids were obliterated due to diagensis. The "size" frequency graphs only include the observed data over "size" ranges from 1.0 to 2.0 mm up to the terminal value. To be significant, the survivorship graphs should show normal mortality rates. Some Girardeau camerates were buried by rare catastrophic mud flows, which were probably not normal causes of death. Whenever possible, these crinoids were eliminated from the calculations although some individuals may not have been recognized. The mud flows may not have represented the only agents of catastrophic mortality in the Girardeau. For example, most individuals in high density "young assemblage" gardens might have suffered instant death due to unknown causes other than the mud flows. The animals are retained in the survivorship graphs and such deaths are considered normal to the habitat. The remaining crinoids used in the mortality studies were not subject to catastrophic death and they are presumed to have died of normal causes. Nothing is known of the reproductive rates involved; the survivorship of the pelagic larvae and the earliest bottom dwelling stages is also conjectural. Lacking such data, total survivorship analyses cannot be obtained. Thus the analyses here simply yield information on Darwinian survival for part of the life span.

Assuming that the data are significant, there are two end-member mortality types. A first group was characterized by low juvenile mortality rates which occurred within the first "size" and relative age class; these death rates were 11 and 14%. This resulted in a long mean "size" life span with respect to the terminal "size" (52 and 63%). The maximum mortality rates tended to be located in intermediate and larger "size" classes. *Ptychocrinus fimbriatus* and *Alisocrinus tetrarmatus*, n. sp. are assigned here. The second group exhibited high juvenile mortality rates which ranged from 26 to 35% in the first relative age class. Lower death rates were seen in larger animals although these increased somewhat in the largest crinoids. *Ptychocrinus splendens, Macrostylocrinus pristinus,* n. sp. and the two eopatelliocrinids are grouped in this category.

The significance of the two groups is not entirely clear. 1. As previously implied, the low juvenile mortality of *Ptychocrinus fimbriatus* constituted a direct or indirect adaptation to living under high density garden conditions where the species outcompeted the associated high juvenile mortality species, *P. splendens* and *Macrostylocrinus pristinus*, n. sp. However, the high density competitive abilities

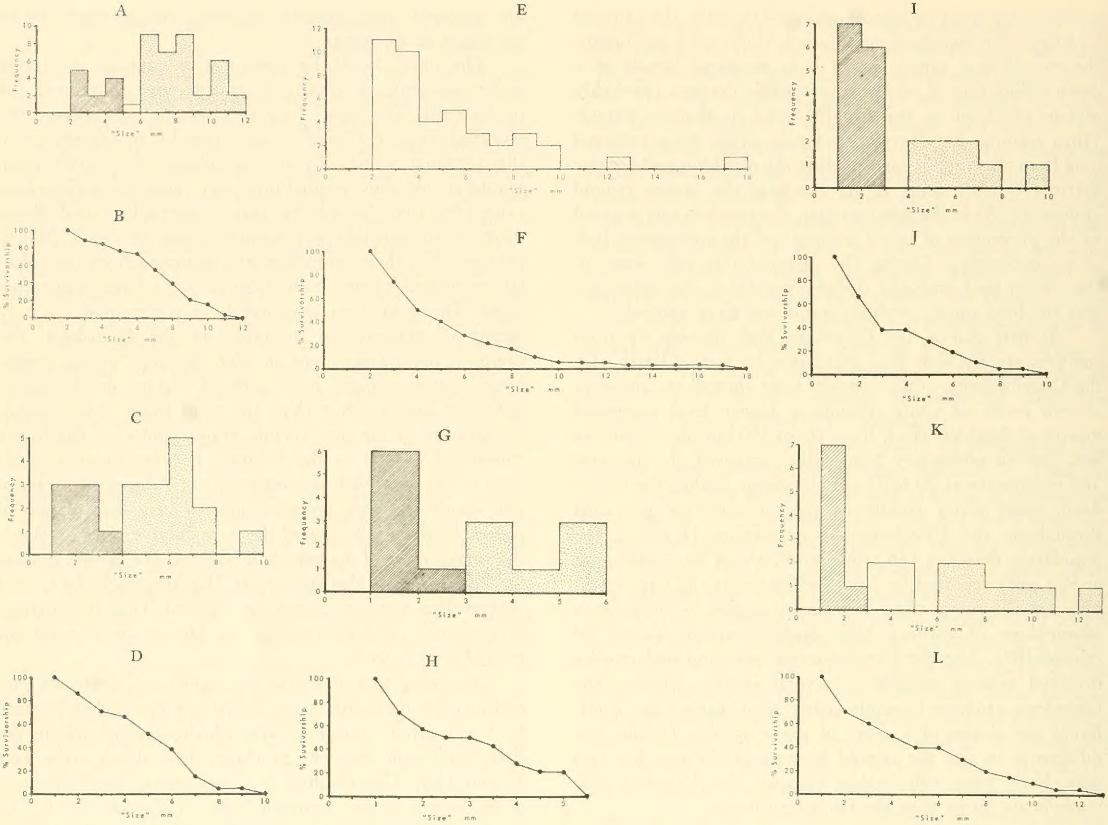

Text-figure 1. — Life table analysis of Girardeau Limestone camerates. Graphs of "size" versus frequency which is expressed as number of individuals. "Young assemblage" animals are obliquely ruled; "adult assemblage" stippled; for *Macrostylocrinus pristinus*, n. sp., "transitional" crowns are blank; *Ptychocrinus splendens* does not show a discontinuous distribution and the entire graph is blank. Plots of "size" versus percentage survivorship; the latter equals number of survivors at the beginning of a "size" class divided by the total number of individuals. Mortality rates are proportional to the slopes of the survivorship curves; steep slopes denote high percentage mortality rates and vice versa. Percentage survivorship is graphed rather than percentage mortality because smoother curves result. Mean "size" life span equals: Sum of all "sizes"/number of crinoids; this figure is expressed as a percentage of the maximum observed "size". Initial mortality is the number of animals dying in the first "size" class interval/total number of crinoids. The species are arranged in order of increasing juvenile mortality. A,B. *Ptychocrinus fimbriatus*. "Young assemblage" "size" range, 2.0 to 4.3 mm. Transitional crinoid "size", 5.4 mm. "Adult assemblage" interval, 6.0 to 11.1 mm. Mean "size" life span, 63%. First "size" class mortality, 11%. Number of crinoids, 47. C,D. *Alisocrinus tetrarmatus*, n. sp. "Young assemblage" "sizes", 1.1 to 3.4 mm. "Adult assemblage", 4.2 to 9.0 mm. Mean "size" life span, 52%. Initial mortality, 14%. Number in sample, 21. E,F. *Ptychocrinus splendens*. "Size" range, 2.0 to 17.0 mm. Mean "size" life span, 30%. Initial mortality, 26%. Number of specimens, 42. G,H. *Eopatelliocrinus latibrachiatus*, n. gen., n. sp. "Young assemblage" "size" interval, 1.15 to 2.15 mm. "Adult assemblage", 3.1 to 5.0 mm. Mean "size" life span, 58%. First "size" class mortality, 29%. Number of animals, 14. I,J. *E. scyphogracilis*, n. gen., n. sp. "Young assemblage" "size" interval, 1.15 to 2.7 mm. "Adult assemblage", 4.2 to 9.6 mm. Mean "size" life span, 37%. Initial mortality, 33%. Number of crinoids, 21. K,L. *Macrostylocrinus pristinus*, n. sp. "Young assemblage" "size" range, 1.0 to 2.4 mm. Transitional crinoids, 3.0 to 4.4 mm. "Adult assemblage," 6.5 to 12.6 mm. Mean "size" life span, 38%. Initial mortality, 35%. Number of crinoids, 20.

of *Alisocrinus tetrarmatus,* n. sp., a low juvenile mortality form, and the two eopatelliocrinids, both high juvenile death rate types, were probably about equal. The relations between standing crop, effective breeding population and juvenile mortality rates are discussed in the following section.

2. Mortality type is not closely related to total abundance in the fauna. The two ubiquitous Girardeau camerates, *Ptychocrinus fimbriatus* and *P. splendens* had low and high juvenile mortality. Apparently, the high juvenile death rates did not prevent the success of *P. splendens.*

3. Mortality rates are not reflected in the survival or extinction of a lineage. *P. splendens* and *Eopatelliocrinus latibrachiatus,* n. gen., n. sp. left no descendants; both possessed high juvenile death rates. The other four abundant camerates constituted important ancestral stocks. Two, *E. scyphogracilis,* n. gen., n. sp. and *Macrostylocrinus pristinus,* n. sp., were characterized by high juvenile mortality whereas *Alisocrinus tetrarmatus,* n. sp. and *Ptychocrinus fimbriatus* had lower juvenile death figures. The Girardeau camerates are all known from an "instant" in time and a continuous record of populations is not available. Thus, the exact stage of evolution (*e.g.,* just becoming established or on the verge of extinction) of any species is uncertain. Perhaps if such data were available, the mortality rates could be closely related to phylogeny and the evolution of or loss of adaptation.

4. The mortality rates are not correlated with breeding type. Strong seasonal breeders showed both mortality types. The only nonseasonal breeder, *P. splendens,* had high juvenile death rates. However, the seasonal breeding "size" discontinuity introduces a low mortality interval into the survivorship curves.

5. Turning to morphological criteria, the death rates were obviously not controlled by calyx type. The two eopatelliocrinids and the macrostylocrinid all had few-FBrr calyces and high juvenile mortality. The primitive many-FBrr species showed high (*P. splendens*) or low juvenile mortality rates as in *P. fimbriatus* and *Alisocrinus tetrarmatus,* n. sp. The best morphological relationship lies with the food gathering efficiency (*i.e.,* length of food gathering system/calyx volume) of adult crinoids. Species with high food gathering efficiency, *A. tetrarmatus,* n. sp. (4800) and *Ptychocrinus fimbriatus* (3400) had low juvenile mortality. Food gathering efficiency of the high juvenile death rate forms ranged from 1400 to about 3700, although most taxa averaged 2500 or less.

Admittedly, the above discussion is inconclusive and perhaps the causative factors involve a combination of the above. Many further data are required prior to the development of a meaningful hypothesis.

POPULATION SIZE AND STRUCTURE

The total standing crop of a single abundant Girardeau species can be estimated; rare forms were not computed, because the sample significance relative to the total distribution is unknown. A minimum number of collected crinoids is available. This represents a least value because only identifiable specimens were tabulated and although diligent search was made, perhaps some examples were not located. The exposed area, intensively collected, was measured. Essentially this equals the combined areas of the Cape Rock and Orchard Creek exposures which comprise roughly 25500 ft^2 (.0009 $mile^2$) or 2400 m^2. The total area occupied by crinoid bearing Girardeau strata is about 24.5 $mile^2$ (64 km^2) most of which does not outcrop owing to vegetation and soil cover, overlain by younger rocks or removal by post-Girardeau erosion. Using these values the standing crop of any one taxon equals:

$$\text{Number in each species} \cdot \frac{\text{Total Area}}{\text{Exposed Area}}$$

The standing crops computed in this way range from 1,400,000 to 190,000 (Table 2). Obviously this procedure assumes that the crinoid distribution within the Cape Rock and Orchard Creek exposures approximates the total distribution within the Girardeau. Field work at several other smaller localities with poorly preserved and unidentifiable crinoids indicated that such is a reasonable estimate for total crinoids. Unfortunately, the species composition cannot be verified because of poor preservation.

Inasmuch as the computed standing crops include prereproductive, reproductive, and post-reproductive individuals which lived under high and low density conditions, these values greatly exceed the original effective breeding populations. Actually, the effective breeding population cannot be derived for any fossil species, as this represents the number of reproducing animals. However, the number of crinoids in the reproductive phase and close enough to reproduce can be estimated. In later discussion these individuals are termed potential effective breeding population; clearly its values are somewhat greater than true effective breeding population. The following calculations are crude and rule of thumb and much critical data on living crinoids are conspicuously absent. Consequently, the computed potential effective breeding populations are only designed to yield approximate figures.

Table 2

Species	Number in sample	Sexually mature crinoids in sample	Sexually immature crinoids in sample	Senile crinoids in sample	Approximate standing crop	Potential effective breeding population	
						Still water	Unidirectional current
Ptychocrinus fimbriatus	52	38	7	7	1,400,000	880,000	620,000
P. splendens	45	14	30	1	1,200,000	320,000	230,000
Alisocrinus tetrarmatus, n.sp.	23	14	6	1	630,000	320,000	230,000
Eopatelliocrinus scyphogracilis, n.gen., n.sp.	21	7	13	1	570,000	160,000	110,000
Macrostylocrinus pristinus, n.sp	20	7	12	1	540,000	160,000	110,000
E. latibrachiatus, n.gen., n.sp.	14	7	4	3	380,000	160,000	110,000
A.? heterodactylus, n.sp.	7	—	—	—	190,000	—	—

Population size and allied data for common Girardeau camerate species.

The times at which living crinoids attain sexual maturity are not exactly known but comatulids do not seem to reach the reproductive phase until after the pentacrinid growth stages are ended and the larval column is released. In *Hathrometra sarsii* (Duben and Koren), careful inspection of the pinnules discloses no traces of gonads in the oldest known pentacrinids; these animals are about 10 to 12 months old and have more than 20 IIBrr per arm (A. H. Clark, 1921, pp. 564-574). Thus by vague analogy with comatulids, the "young assemblage" Girardeau camerates were almost certainly sexually immature and have been eliminated from the potential effective breeding populations.

Further insight into the problem is yielded by the echinoid, *Strongylocentrotus purpureatus* A. Agassiz, which is reasonably well known with respect to time-size growth rates and time of maturity (see data in Swan, 1966, pp. 400-402; Boolootian, 1966, pp. 578-590; H. B. Moore, 1966; unpublished data by James Sprinkle). The animal shows slow-fast-slow time-size growth rates similar to those postulated by the writer for crinoids (see introductory statement on ontogeny). The largest known individual has a test diameter of 114 mm. Extrapolation of the best known time-size growth rates (six to 38 months) suggests that this specimen is about 105 to 140 months old (approximately nine to 12 years). *S. purpureatus* attains sexual maturity at a test diameter of roughly 40 mm and age of two years. This corresponds to a pre-reproductive period of 17 to 23% of the terminal age and 35% of the largest known size. These figures also seem reasonable for *Hathrometra sarsii* (Düben and Koren) which could not breed before the second year. The pentacrinid growth stages of *Antedon bifida* (Pennant) and *Promachocrinus kerguelensis* (P. H. Carpenter) occupy 3½ months and 1½ to two years, respectively (see introductory statement on ontogeny). Thus *Antedon bifida* may reproduce at the end of the first year and *Promachocrinus kerguelensis* at the end of the third year.

At least some echinoderms exhibit a post-reproductive or senile phase as reported by Swan (1966, p. 417) for a starfish and an echinoid. The duration of this interval relative to the life span is not known for any echinoderm. However, Allee, *et al.* (1949, p. 286) tabulated such values for numerous terrestrial animals ranging from fruit flies to man. The average senile phase is 13% of the time life span or roughly 9% of the terminal size in *Strongylocentrotus purpureatus*.

In order to determine the number of reproductive phase animals belonging to a Girardeau crinoid, the presumed sexually immature and senile individuals are subtracted from the total known crinoids. The two subtracted values were approximated from the *S. purpureatus* data. All values computed for the abundant Girardeau camerates (Table 2) appear plausible and closely agree with the "size" frequency distributions with the exception of *Ptychocrinus splendens* which probably had an unduly large number of sexually immature individuals.

Living crinoids bear the gonads in the genital pinnules of the arms. Fertilization is external. The male sheds the sperm into the water which stimulates release of eggs from the female. The eggs are fertilized immediately after extrusion through the pinnule wall of the female (Hyman, 1955, pp. 72-75). Although not verified, it would seem that sperm from several males could fertilize different eggs of a single female and one male could service several females. Reproduction in the Girardeau camerates is believed to have followed the same pattern because pinnules are present. Proximity clearly has a major influence on the reproductive pattern. In general, sexually mature animals living under high density conditions would have higher chances of reproducing than low density individuals. To compute the potential effective breeding population, the crinoids which were too far away from conspecific individuals of the opposite sex to breed must be subtracted from the sexually mature animals. Two end-member models are defined as quiet water and unidirectional current. Other situations would be intermediate between these two types.

Knowledge concerning the reproductive radius of living marine invertebrates is scanty. Grave (1934) experimented with sperm of the echinoid *Arbacia* in absolutely still water under reasonably natural conditions. The sperm swim by means of flagella with the following velocities and distances:

Table listing swimming velocities for *Arbacia* sperm

Duration mins.	Distance cm	Mean Velocity cm/min.
55	First 7	.13
65	2nd 5	.077
30	3rd 3	.10
330	last 3	.009
	Total 18	

The sperm exhibited maximum swimming velocity for roughly two to 2½ hours, after which the swimming intervals became interspaced with quiescent conditions. The sperm essentially ceased swimming after nine to 12 hours. Grave reported up to 100% fertilization for sperm up to three hours. At nine to 12 hours, some were still alive and capable of fertilization but few sperm retained fertilization ability past 12 hours. Grave also documented similar results for other aquatic invertebrates, namely *Cumingia* and *Hydroides*. At any rate, the *Arbacia* still water figure is applied to the Girardeau camerates. Crinoid functional morphology and geometry dictate that the sperm must be shed with the arms spread out. A three cm arm spread is estimated for the genital (gonad bearing) pinnules of a Girardeau camerate; rheophobe orientations are assumed (see discussion of burial). Thus the male crinoid is visualized as the center of a circular ring of outwardly migrating sperm with a radius of 19.5 cm (*i.e.*, 18 cm sperm travel, 1.5 cm arm spread on each side of the crown). This simple picture would be complicated by two factors, both of which tend to reduce the sperm cloud density (*i.e.*, number of sperm per unit volume of water) with progressive distance away from the crinoid. Individual sperm swim with different velocities. Because of simple geometry, sperm cloud density decreases rapidly as the radius of the cloud is augmented. Such indicates that a male crinoid has the best chance of fertilizing the closest female; farther away the odds decline with falling sperm cloud density. These effects are not considered in the following calculations because no data are available on the number of sperm produced by living crinoids.

With these figures and a 1:1 sex ratio, the still water potential breeding populations can be estimated. The 1:1 sex ratio is supposed; it cannot be verified for living or fossil crinoids. The procedure is as follows: an eight by eight grid with 64 squares is defined and labelled in terms of columns and rows; this allows any square to be located. The sides of the squares are proportional to the living space occupied by a single animal. For example, in a Girardeau 35 individual/ft^2 (930 cm^2) garden the sides of each square would be 2.03 inches or 5.2 cm long. Each crinoid is rooted at the center of the square. Random numbers are generated and 32 males located on the grid. Random distribution of the sexes is assumed. For high density gardens, the total grid is used and a population of 64 conspecific sexually mature animals is considered. The grid is broken up into a series of gardens in low density conditions; for example, in five crinoid/ft^2 (930 cm^2) gardens, the grid is divided into 12 gardens with four squares left over. The 19.5 cm (7.7 inch) radius reproductive circles are superimposed on the simulated gardens after which the individuals which are too far away from those of the opposite sex to reproduce are eliminated. The following results are obtained for the Girardeau camerates: under high density conditions, all individuals could have reproduced; the potential effective breeding population decreased with falling population density in low density gardens.

Table showing relation between potential effective breeding population and population density under Girardeau still water conditions.

Population Density	Potential effective breeding population (expressed as percentage of total sexually mature crinoids)
10 crinoids/ft^2 (930 cm^2)	98%
5 crinoids/ft^2 (930 cm^2)	91%
3 crinoids/ft^2 (930 cm^2)	63%
1 or 2 crinoids/ft^2 (930 cm^2)	0%

Thus in still water conditions, all the high density garden sexually mature crinoids could have interbred whereas only 71% of the low density garden individuals could have done so. Roughly half of the mature animals of each Girardeau species lived under high density conditions, whereas the other 50% existed in low density gardens. The still water potential effective breeding populations are listed in Table 2. There are two main features of this model. High potential effective breeding population occurs relative to the total number of sexually mature crinoids. For all practical purposes, the Girardeau breeding was restricted to a single garden. The 19.5 cm reproductive radius was too small for sperm to travel from one garden to the next.

The second model involves a unidirectional current of 30 cm/sec (see previous discussion for derivation of the figure). The current velocity is not especially critical to the model proposed here. Almost any straight-line figure which exceeds sperm swimming velocity could have been taken. A straight-line current is used and eddies which would diffuse the sperm laterally are not treated. With such a current, sperm moving up-current would have to combat the flow; actually current velocity would be greater than the sperm swimming velocity and the sperm would travel down-current. Sperm swimming down-current would be aided by the water movement. A rheophile crinoid was assumed with the arms spread at right angles to the sea bed; the arms were located in the center of each grid square. The current effects would transform the reproductive area of the crinoid into a three dimensional surface. The basic shape comprises a trapezoid with slightly curved sides which is rotated 180° about its long axis. The rheophile crinoid is placed at the narrow end of the area with the long axis of the rotated trapezoid oriented down-current and parallel to the sea bed. The long axis would be a function of current velocity plus still water swimming distance of the sperm over nine to 12 hours. The width of the narrow end of the trapezoid corresponds to the three cm genital pinnule arm spread of the crinoid. The distance between the long axis of the rotated trapezoid and its sides is controlled by swimming distance of the sperm in the elapsed time plus the genital pinnule arm spread/2. The model is simulated as before except that each garden is subjected to several currents. Field study indicates that high density gardens are generally circular, whereas low density ones tend to be elongate. Unfortunately, the orientations of the long axes of the low density gardens with respect to the current directions were not recorded in the field. Relative to the simulated 64 square grid, the high density gardens are subjected to diagonal water flow and currents directed at 90° angles to the grid sides. In low density gardens, the currents are oriented parallel to and at 90° to the long axes. Compared to the still water model, the unidirectional current introduces two effects.

1. Intra-garden effect. Basically, this deprives females at the up-current end of the garden of sperm and removes the sperm of down-current males from the garden. As shown below, the current effect tends to lower the potential effective breeding population (see same data for still water model).

Table showing relationships between Girardeau population density, current direction and potential effective breeding population for the unidirectional current model.

Population density of reproductive stage crinoids	Potential effective breeding population under indicated current direction			
	Against sides	Diagonal	Parallel to long axis	Perpindicular to long axis
35 to 70 crinoids/ft^2 (930 cm^2)	78%	62%	—	—
10 crinoids/ft^2 (930 cm^2)	—	—	59%	32%
5 crinoids/ft^2 (930 cm^2)	—	—	49%	16%
3 crinoids/ft^2 (930 cm^2)	—	—	38%	—
2 crinoids/ft^2 (930 cm^2)	—	—	32%	—

The above figures suggest some generalizations about the critical nature of garden shape, orientation, and crinoid spacing. In high density gardens, diagonal unidirectional currents somewhat reduce the potential effective breeding population relative to the other current. The low density potential effective breeding populations are much higher with current flow parallel to the long axis of the garden. Also the spacing of males and females affects the value as the potential effective breeding population within a single garden would reach a maximum value with the males at the up-current and the females at the down-current end of the garden. In the quiet water model, garden shape (*e.g.*, circular versus elliptical) makes little difference. Random rather than preferential distribution of the sexes yields the largest potential effective breeding populations in quiet water. The models also suggest that moderately high population densities are required to ensure marine invertebrates which shed sperm into the water reasonable chances of reproduction. Probably, this is one of the major factors which causes groups with this reproductive structure to live in patches and clumps separated by barren areas.

2. Inter-garden effect. The 30 cm/sec current travels about 13 km in 12 hours (life of *Arbacia* sperm). Obviously, this transport was easily able to carry sperm from one garden to the next and also between some of the localities. Consequently, the introduction of a current allowed inter-garden reproduction, whereas only intra-garden reproduction existed in quiet water. However, the field data do not permit any estimation of this effect; the data in Table 2 only take account of the intra-garden effect.

Summarizing, the two models have both advantages and disadvantages. The advantages: Quiet water model — high potential effective breeding population; current model — inter-garden reproduction and more rapid genetic interchange. Due to the rotated trapezoidal shape of the sperm cloud, the decrease in sperm density away from the crinoid is less than that of the quiet water model. Consequently, a current model male has better chances of fertilizing a distant female than a quiet water male. The disadvantages: Quiet water — confined to intra-garden reproduction. To some extent, this would be offset by pelagic larval migration (see later discussion). The rapid decrease in sperm cloud density away from the crinoid also limits the quiet water model to intra-garden reproduction; current model — low potential effective breeding population.

The above models are clearly end-member oversimplifications. The actual Girardeau situation was probably much more complex due to turbulent currents flowing in more than one direction and at various velocities and eddies superimposed on the currents which would cause increased lateral migration of the sperm. These variables would have produced an intermediate effect between the quiet water and unidirectional current models which could have represented the optimum for this type of reproduction.

In general, the potential effective breeding populations are directly proportional to the total species abundance in the fauna, inversely proportional to the young crinoid mortality rates, and directly proportional to the population density within individual gardens.

The minimum effective selection coefficient (s) is a function of the size of the effective breeding population (N) and can be computed by formulas from Grant (1963, pp. 195-198, 280).

$$\mathrm{N} = \frac{1}{2s} \qquad \text{where}$$

$$s = 1 - \frac{(\text{effective rate of reproduction of allele } a_1)}{(\text{effective rate of reproduction of allele } a_2)}$$

In the following calculations, the potential effective breeding populations of the Girardeau camerates were substituted for the effective breeding populations. The computed minimum effective selection coefficients for the Girardeau forms range from: Quiet water model — .0000031 to .00000057; unidirection current — .0000045 to .00000081. The computations clearly indicate that the Girardeau camerate populations were large enough, so small selection coefficients would have operated effectively. It is concluded that these species were evolving under the impetus of natural selection.

All abundant camerates are well known from the Orchard Creek and Cape Rock exposures which are separated by about 10 miles (16 km). Also most taxa occur at other localities, although these are not well enough preserved for detailed study. Statistical analysis of conspecific crinoids discloses no significant differences between the two localities. Therefore, it is believed that the species formed panmictic populations which were subject to free genetic interchange between the two localities and the same selection pressures (or nearly so) at both areas.

Clearly, most genetic interchange did not occur during the breeding periods but was due to larval migration and settling. The pelagic larvae of living *Antedon* last from a few hours up to 108 hours (A. H. Clark, 1921, p. 450). The absence of brood pouches in the Girardeau camerate arms indicates that a pelagic larval stage was present. Assuming that these fossil larvae had comparable durations to those of *Antedon* and assigning a current plus larval swimming velocity of .50 knots/hour, a 100 hour larva could easily have traversed the distance between the Orchard Creek and Cape Rock exposures with time to spare. The original Girardeau outcrop belt was probably continuous and the larvae could have covered the distance in a series of larval generations with shorter pelagic time periods.

CRINOID ATTACHMENT

Introduction. — The Girardeau crinoid attachment or rooting devices are grouped into a series of morphological categories. Stem segment-cirrus roots are comprised of short column lengths with a series of cirrus whorls each of which consists of about four cirri. The cirri are generally broken and only "stumps" are observed. In one specimen, complete unbranched cirri are preserved in which the length equals roughly three times the stem diameter. All stem segments are straight and were probably rigid during life of the crinoid. The complete stem segment length is unknown. The stem segment-cirrus roots could have been attached in two ways: 1. Cirrus bearing part of stem buried in the substrate, as in Recent *Rhizocrinus* or *Bathycrinus* (see Hyman, 1955, text-figs. 12b, 38f). 2. This portion of the stem elevated above sea floor with the cirri utilized to grasp, like living *Isocrinus* or *Metacrinus* (see Hyman, 1955, text-fig. 12a). In living species, both the stem segments and their grasping cirri show much flexibility. Column segments associated with rooting cirri tend to be more rigid; the cirri may be stiff or somewhat flexible. The Girardeau stem segment-cirrus roots were probably rooted types, which is suggested by the rigid stem segments and most likely stiff cirri. These Girardeau roots have not been observed in the presumed living position; always, the stem segments lie parallel to the bedding plane. Presumably, the crinoids were up-rooted at the time of death or burial.

Stem segment-rootlets represent the most common Girardeau holdfast. These resemble the above root type except that the rootlets lack axial canals; cirri always possess axial canals. Possibly, the rootlets either lacked nerve cords or if these were present, the axial canals were later filled with calcite. Rootlet preservation is poor and the two possibilities cannot be differentiated. Like cirri, the rootlets are usually broken and only the stumps remain. From four to about 10 stumps occur on a single columnal. When observed, the rootlets are straight, unbranched and have lengths about 1.5 to two times the column diameter. The associated stem segments range up to roughly 25 mm long. Curved rootlets are unknown and all rootlets are believed to have been stiff. Almost always, the stem segments are straight and probably rigid. During the life of the crinoid, the stem segment-rootlets of this type most likely were buried in the substrate with the stem segment length axis approximately perpendicular to the sea floor, as in similar stem segment-cirrus roots.

A few coiled stem segments with rootlets were collected. These could have been coiled around some object such as an erect bryozoan colony or another crinoid stem. If so, prehensile or grasping rootlets would be expected. Perhaps they were coiled on or slightly below the sea bed with the rootlets penetrating the substrate. The probable lack of rootlet flexibility indicates a substrate root form rather than a grasping device.

Several examples of tree stump roots are known in which the distal end of the stem developed about four cirrus roots. The roots are heavy and their diameter ranges up to about 50% that of the column. Commonly the roots branch at least once. Cirri lengths cannot be determined because the distal parts of the roots penetrate the sediment. All observed specimens are preserved in the living position. These root forms closely resemble tree stumps in gross geometry. Middle Silurian *Eucalyptocrinites* possess the same root type (see Macurda, 1968, text-figs. 8g, 10i).

One bulbous tuber type root occurs on a small slab with *Dendrocrinus casei.* Basically, the tuber consists of a series of rigid columnals which have been widened and thickened. Cirri are lacking. The long axis of the root parallels the bedding plane of the slab. During life the tuber most likely was buried, with the long axis at a right angle to the sea bed. Lane (1963b, pl. 128, fig. 2) illustrated a similar root form in living position from the Mississippian Crawfordsville locality.

The two lump type holdfasts found were collected from a peculiar hard grey silty shale. Crinoids are rare in this lithology and only three species are known, an undetermined camerate, probably an archaeocrinid, *Dendrocrinus* ?, n. sp. aff. *D. ? navigiolum* Miller, and *D. curvijunctus,* n. sp. The poorly preserved massive attachment device has a column facet and was probably cemented to the sea floor. Other structural details cannot be ascertained. The massive structure suggests that the holdfast is referable to the camerate rather than the smaller dendrocrinids.

Species assignments of holdfasts. — The attachment devices may be grouped with crowns on the basis of two lines of evidence: holdfast observed at the distal stem end of the calyx or crown of a particular species and consistent association of one species with a certain rooting device. In theory this line of reasoning should yield adequate results. However practice is complicated by the fact that rigid stem segment-rootlet and rigid stem segment-cirrus devices cannot always be distinguished because the axial canal area is not commonly seen.

One young individual of *Ptychocrinus fimbriatus* has the complete stem preserved with a rigid stem segment-rootlet device at the end. All coiled stem segment-rootlets are associated with this species and stem segment-cirrus roots commonly occur with *P. fimbriatus.* Such suggests two possibilities: different conspecific individuals developed different root forms. This explanation may apply to the coiled and straight stem segment-rootlet structures; alternatively, the same animal had two or more root types along various parts of the column. For example one rigid stem segment-rootlet is known with a small lump holdfast at the distal end. Possibly this belongs to *P. fimbriatus.* Perhaps, the straight stem segment-rootlet and stem segment-cirrus roots also fall into this category.

The calceocrinid-like recumbent stem of *Protaxocrinus girardeau* Springer bears a straight stem segment-rootlet holdfast whereas the proximal part of the column was elevated above the substrate. The recumbent and elevated stem regions are separated by several wedge-shaped columnals.

Several short upward directed cirri are located on the distal part of the column of one individual of *Dendrocrinus* ?, n. sp. aff. *D. ? navigolum*. Possibly, the cirri were used for grasping upright objects such as other crinoid stems. However, the orientations are not suggestive of clinging cirri; in living forms, these are either horizontal or they hang down. The dendrocrinid cirri are not long enough to have enveloped and protected the crown, and their function remains unknown.

The following species root assignments are postulated on the basis of consistency and frequency of association.

Table listing root types of Girardeau species

Macrostylocrinus pristinus, n. sp. — Tree stump.
Ptychocrinus splendens — Stem segment—cirrus or straight stem segment—rootlet or both.
Alisocrinus tetrarmatus, n. sp. — Stem segment—cirrus or rigid stem segment—rootlet or both.
A. ? heterodactylus, n. sp. — Rigid stem segment—rootlet.
Eopatelliocrinus scyphogracilis, n. gen., n. sp. and
E. latibrachiatus, n. gen., n. sp. — Stem segment—cirrus or rigid stem segment—rootlet or both.
Dendrocrinus casei — Tuber.
Unknown archaeocrinid — Lump holdfast.
Compsocrinus nodosus, n. sp. — Tree stump.

Root types are unknown for the following forms

Clidochirus serrulatus, n. sp.
Dendrocrinus curvijunctus, n. sp. and *D.* ?, n. sp. aff. *D. ? navigiolum*
Culicocrinus ? girardeauensis, n. sp.

Root assemblages. — Four of the holdfast types are restricted to the normal Girardeau crinoid bearing soft brown shale partings which consists of calcite, quartz, and dolomite silt-sized and sand-sized grains, clay-sized calcite, and clay minerals. Root types confined to this lithology are: stem segment-cirrus, rigid or flexible stem segment-rootlet, tree stump, and tuber. Assuming the curved stem segment-rootlets were coiled on or slightly below the substrate, the main common denominator was moderate to deep vertical or lateral penetration (or both) of sediment. Such denotes an originally soft substrate and is consistent with observations on Recent crinoids. Soft sediment dwelling isocrinids, are characterized by branching roots of various types (for example, see Hyman 1955, text-fig. 12b, *Rhizocrinus;* text-fig. 38f, *Bathycrinus*; discussion in Fell, 1966, pp. 55, 56). Adult comatulids taken from soft muddy sediments exhibit long slender cirri suitable for grasping such material (A. H. Clark 1915, pp. 258-266).

The few lump holdfasts were found in a peculiar hard, blue shale which is usually devoid of fossils except for a few crinoids. Most likely, this attachment device indicates a hard substrate. Young pentacrinid growth stages (possess stem) of living comatulids cement their disks to hard objects such as shells or crinoid stems (see A. H. Clark, 1915, pl. 3; discussion in A. H. Clark, 1921, pp. 513-590). According to Fell (1966, pp. 55, 56), hard substrate stalked Recent isocrinids have flat or lump type holdfasts which are cemented to the sea bed.

BULK DENSITY, STEM LEVERAGE, AND ARM WAVING

Recently, Lane (1968) summarized the evolution of adaptation in fossil crinoids considering arm leverage, arm articulations, center of gravity, and indirectly stem leverage. Breimer (1969) discussed the paleoecology of fossil crinoids also, disagreeing with Lane on some basic points. The views expressed here represent a partial compromise although the writer's thoughts most closely parallel those of Lane. The principal disagreements with Breimer are with respect to the amount of stem and arm leverage exerted by fossil camerates. In addition to the comments of Lane and Breimer, the evolution of bulk density is added as another variable.

Most crinoid specialists (*e.g.*, Lane, Breimer, and the writer) believe the most successful Paleozoic crinoid niche was an attached filter feeder with the crown elevated above the sea floor. In almost all Paleozoic forms and in living isocrinids elevation is progressive and continues throughout ontogeny. Recently settled larvae are essentially at the sea bed level. During development, new columnals are added to the stem, and the heights of previously formed plates are increased; both processess result in continuous augmentation of stem length although the time-size growth vector varies with growth phase. At any rate the stem allows the juvenile and adult crinoids to tap a food supply and living area which is not exploited by most sedentary epifaunal filter feeders, such as brachiopods. However, some workers have postulated a semi-eleutherozoic existence for certain stalked echinoderms (*e.g.*, Kirk, 1911; Paul, 1968; see later discussion also).

The previous remarks show that all or most Girardeau crinoids were attached to the sea bed. Lane (1968) determined the geometrical center of gravity (assuming constant bulk density through stem and crown) for various Paleozoic crinoids; these occur at the base of the calyx or proximal column region. As later discussed, the density gradient within the crinoid indicates that the true center of gravity (c.g.)

occurs below the geometrical center of gravity, at least in the Girardeau camerates.

Crinoid bulk densities are poorly known. They have been computed by Gislén (1924, p. 285) for 16 living comatulids, which show bulk densities ranging from 1.11 to 1.39 gm/cm^3 with a mean of 1.26 gm/cm^3. The crinoid is partially supported by the surrounding sea water. Thus, the effective density which must be supported by the crinoid equals: bulk crinoid density minus that of sea water (1.03 gm/cm^3). These effective densities cover the .08 to .36 gm/cm^3 interval (mean .23 gm/cm^3). Similarly, Cain (1968, pp. 196-198) measured a bulk density of 1.2 gm/cm^3 for skeletal remains of *Antedon bifida* at the time of death. This is comparable to Gislén's 1.15 gm/cm^3 figure for *A. petasus,* These comatulid bulk densities (stems are lacking) correspond to the crown values of the Girardeau camerates.

The bulk density of a thin-plated Girardeau camerate was roughly computed on the basis of the following assumptions. The plate porosity equals 60% of the external plate volume. Stem, calyx and arm plates of *Metacrinus* sp. and several unidentified comatulids were examined. These possess approximately 80 to 90% pore space along a linear dimension (straight line traverse). Cubing the mean (about 85%) yields roughly 60% pore volume per unit of external volume. Although thin sections have been prepared for several Girardeau crinoids, the plate porosity cannot be ascertained owing to the poor state of preservation. Consequently, the above modern crinoid values were extrapolated to the Girardeau forms. The soft part density consists of 1.07 gm/cm^3 for all components, for example the viscera, organic matrix filling the plate pore system and ligaments which hold adjacent plates together. Calcite density is 2.72 gm/cm^3. Using the above figures yields a solid plate bulk density of 1.73 gm/cm^3. The epidermis thickness is unknown in the Girardeau camerates. In living crinoids, this layer is thin relative to the other dimensions. Consequently, the epidermis was omitted from the density computations. The connective tissue, ligaments, and muscles which bind the adjacent mature camerate Brr (Br width about 1.0 mm), was less than .10 mm thick. Like the epidermis, the connective tissue was ignored in the derivation of density for these forms although a certain amount of connective tissue would be included in the 60% porosity value. Conversely, the extensive connective tissue observed in living crinoids constitutes a significant component of the bulk density. The Girardeau camerate partial densities were estimated as follows.

The column bulk density was approached through analysis of the individual columnals. These consist of three elements: the solid plate (bulk density 1.73 gm/cm^3), the axial canal which housed the axial nerve cord (bulk density 1.07 gm/cm^3) was approximated by a cylinder; and the central parts of the proximal and distal articular surfaces are depressed (spatium), these are separated from those of the adjacent columnals by gaps. The outer parts of these areas bore most of the ligaments which held the columnals together; these surrounded the proximal or distal parts of the axial nerve cord and associated organs. Each columnal has two of these areas, one located proximally, the other distally. Each area was estimated by half of a flattened ellipse of rotation (bulk density 1.07 gm/cm^3). The total external volume of a columnal comprises the sum of the three components; this was calculated in terms of a cylinder. Averaging values from about 30 Girardeau camerate plates indicates that the solid plate occupies 91.5% of the total external volume (density 1.73 gm/cm^3). The soft parts, ligaments and axial nerve cord, equalled 8.5% of the external volume (bulk density 1.07 gm/cm^3). Using these figures, the bulk density of the column was calculated at 1.67 gm/cm^3. Although the bulk densities of the holdfasts have not been determined, these were probably roughly equal to that of the column.

The Brr and pinnular soft parts included the nerve cords, feeding tissue, associated coelomic cavities and sinuses, and other tissues. The covering plates were ignored, because their dimensions are poorly known, and the bulk density of the whole food groove is assigned a value of 1.07 gm/cm^3. This component was estimated to have occupied about 45% of the total Br and food groove volume, whereas the Br plate and the contained organic matrix (density 1.73 gm/cm^3) represented 55% of the volume. The arm and pinnule computed bulk density amounts to 1.43 gm/cm^3.

The calyx enclosed the viscera (density 1.07 gm/cm^3). In a mature thin plated Girardeau camerate, the outer shell consisting of calyx plates (density 1.73 gm/cm^3) equals approximately 21% of the total external calyx volume, whereas the viscera comprised the remaining 79%. The computed calyx bulk density is only 1.21 gm/cm^3.

Crown bulk density represents the weighted volume average of the calyx and arm-pinnule components. Crude estimates indicate that the mature Girardeau camerate arms comprised 92 to 93% of the total crown volume. The computed bulk crown density equals 1.41 gm/cm^3. Actually, most camerates probably were more dense than the Girardeau crinoids because of the relatively thicker calyx plates and smaller food grooves.

In similar fashion the total bulk density for a stemmed crinoid could be computed if both the crown and complete column volumes were known. Unfortunately, not enough fully preserved stems are available to allow estimates of meaningful values. The previous tabulations clearly indicate that a density gradient existed within a single animal. This was from the highest to lowest density, the stem, arms and pinnules, and calyx. The stem density exceeded that of the crown by about .3 gm/cm^3.

One would expect a decrease of bulk density in crinoids or crinoid-like echinoderms which adapted to an eleutherozoic or semi-eleutherozoic mode of life. From the previous discussion, it follows that the bulk density may be decreased in numerous ways: casting off the stem; shortening the column; increasing the axial canal diameter relative to the total stem volume or evolving more strongly depressed articular surfaces with extensive ligaments between the adjacent columnals; developing a thin plated calyx, perhaps with pores in the plates; augmenting the food groove size relative to the Brr size; decreasing the arm volume relative to the calyx volume which could occur in several fashions (*e.g.*, simplification of the arm branching, loss of pinnules, and shortening or reducing the diameter of the arms and pinnules); increasing the amount of connective tissue between the arm and calyx plates; and augmenting the plate porosity.

Recent young comatulids possess a stem which is attached to the substrate or some other object during the pentacrinid growth stages; basically these are rooted filter feeders, as were the Girardeau crinoids. When maturity is attained, the comatulid casts off its stem and assumes a semi-eleutherozoic existence. Most of the time, the crinoid is attached to the substrate or some object by means of the cirri located on the base of the calyx. Periodically, the comatulids move from place to place. Some, such as *Antedon,* swim whereas others crawl along the sea bed like the Comasteridae (see Fell, 1966 for summary of Recent crinoid ecology). A few articulate crinoids (*e.g., Unitacrinus, Saccocoma,* see R. C. Moore and Jeffords, 1968, p. 18) seem to have been fully pelagic.

The average thin-plated Girardeau camerate crown bulk density (about 1.41 gm/cm^3) was significantly higher than that of adult comatulids. The average in the true comatulids equals 1.26 gm/cm^3 and that of the crawling comasterids is 1.27 gm/cm^3 (latter two values computed from Gislén, 1924, p. 285). The basic difference lies in the amount of connective tissue which is extensively developed in the comatulids (especially the arms) but was minor in Girardeau camerates. Rough computations indicate that all or nearly all of the density gap can be accounted for in this fashion; the differences in calyx versus arm geometry are not important. Thus, adult comatulids show two low density adaptations to the semi-eleutherozoic mode of life relative to the Girardeau camerates. The stem is lost, which is by far the most dense part of the animal (bulk density unknown but it must exceed that of the crown). Extensive connective tissue is developed (bulk density roughly 1.07 gm/cm^3). Both adaptations result in decreased crinoid density. Possibly noteworthy is the fact that the mean density of crawling comasterids (1.27 gm/cm^3) slightly exceeds that of the true free swimming comatulids (1.26 gm/cm^3).

The bulk densities of living stalked crinoids (isocrinids) were not examined. Judging from the writer's observations on the morphology of *Metacrinus* and *Isocrinus decorus,* the crown bulk density lies within the comatulid interval. The isocrinid column would increase the total crinoid bulk density, although its exact density is unknown.

Macrocystella was a free living column bearing Ordovician cystoid which recently has been studied in detail by Paul (1968). Apparently, the animal drifted along, perhaps waving its brachioles to stay above the sea floor. Like the Girardeau camerates, the bulk density of *Macrocystella* clearly exceeded that of sea water and the cystoid had negative buoyancy. The distal end of the stem was either dragged along the substrate, as suggested by Paul, or periodically wrapped around some object to temporarily fix the cystoid as illustrated by Bather (1900, text-fig. 18; see also later annotation of *Woodocrinus*). *Macrocystella* shows several morphological features which would have reduced its bulk density below that of a Girardeau camerate. The proximal columnals have large lumens which occupy approximately 50% of the stem diameter. The calyx plates are thin and strongly corrugated. The brachioles are nonpinnulate and the brachiole volume is small relative to calyx volume.

As previously mentioned, the stalked crinoid center of gravity lies in the proximal part of the calyx or stem region and the bulk density of all parts exceeds that of sea water. Clearly, a quiet water-rooted stalked crinoid (rheophobe of Breimer, 1969) is only statically stable when the stem and crown are vertical and gravity acts straight down the stem. If the animal becomes inclined due to bending of the stem or crown, the center of gravity would be shifted toward the leaning direction. Gravity no longer would act down the stem. Rather a gravitational torque would tend to lever the crown down on to the sea floor. The situation is roughly the same for a rheophile crinoid (see Breimer 1969). In the feeding position, the arms are expanded and oriented vertically with their dorsal sides facing into the current. The proximal-distal axis of the calyx probably would be roughly horizontal and parallel to the sea bed. The stem would be bent with the proximal end oriented down current. Consequently, the center of gravity does not act straight down the stem; rather this would be offset down current from the rooting device. Basically, the crinoid would lean with the current. To some extent, the crown would be supported by the current; however, the crown is mainly held aloft by the stem. If the current velocity is more rapid than the normal ecological limits of the species, the current and gravity could exceed the strength limits of the expanded arms, or tend to flex the stem and lever the expanded crown down on the substrate, or break the column. Rooted rheophile crinoids have several mechanisms to combat the current and gravity. The arms might be closed. This would decrease the crown surface area exposed to the current which would allow the stem to hold the crown aloft. Living comatulids can swim or crawl to avoid excessive currents. Obviously, this alternative is not available to a rooted form. Both stalked rheophiles and rheophobes have two types of leverage which counteract gravity and currents.

Arm leverage. — Adult comatulids are able to swim or crawl along the substrate by means of "arm flapping". In crawling, the arms are used to grasp, pull, and lever the animal along. When swimming, the pinnules are extended outward to provide a large surface area in contact with the water, on the down or propulsion strokes. During the slower upward or return movements the pinnules of a single arm are brought together over the food groove to ensure less water resistence. Generally, the arms work in two alternate groups, half at a time. Variations in the strokes performed by different rays result in directed swimming (see Fell, 1966, pp. 56-58 for summary of locomotion of Recent crinoids).

The Brr of modern crinoids are held together and flexed by ligaments (dorsal and central fossae) and muscles (ventral fossae). The distinction between crinoid ligaments and muscles is obscure. Both possess contractile power which can be activated by the nervous system (Gislén, 1924, pp. 56, 57, 62-64). In living crinoids, purely ligamental articulations (*e.g.*, cirri) react more slowly than muscular articulations which have both ligaments and muscles (*e.g.*, most Brr), *i.e.* about half ? the speed (Gislén, 1924, pp. 56, 57, 62-64). Swimming forms have better developed muscular articulations and larger muscles and ligaments than crawling species (Gislén, 1924, pp. 56, 57, 62-64). The ligaments and muscles of Recent stalked crinoids seem to roughly parallel the crawling comasterids in this respect.

Breimer (1969, pp. 144-147) considered that most typical camerates were rheophiles; this excludes atypical forms, such as platycrinitids, but the Girardeau camerates would probably be deemed typical in the morphological sense. He correctly interpreted the Mississippian Burlington Limestone fauna as a rheophile assemblage. Breimer, largely based his rheophile camerate crinoid arm flexing hypothesis on this fauna. He believed that contraction of the Brr ligaments served mainly to open the arms. Arm closure was largely caused by the currents; this extended the ligaments. The writer postulates that most camerate crinoids had ability to both open and close the arms. The Girardeau camerates, when living in the rheophobe orientation, were clearly able to open and close the arms and pinnules. This is evidenced by the burial positions and the lack of currents which would have closed the arms. The primitive Brr articular surfaces of the Girardeau camerates are roughly the same as many of those of the Burlington crinoids. Consequently, the question becomes one of rate and strength of extending and closing the arms. In a rheophile crinoid, the current probably would have aided in arm closure, but currents certainly were not the only agents of arm closure. Living crinoids actively flex the arms into both open and closed positions.

In the Girardeau camerates, the adjacent Brr and pinnulars were joined by ligaments; muscles were probably lacking (see Van Sant and Lane, 1964, pp. 34-67 for summary of articulations in Paleozoic crinoids). Also, the ligaments were short relative to the Br height. All Girardeau camerates possess primitive Brr articular surfaces; basically, the proximal and distal Brr surfaces are slightly concave with ill-defined transverse bulges in some cases. The ligaments were probably not clearly differentiated into dorsal and ventral ones. Therefore, contraction of the dorsal part of the ligaments must have opened the arms; shortening the ventral parts of the same ligaments served to close the arms. Obviously, the articular surfaces and short ligaments severely limited movements of the adjacent Brr and pinnulars relative to one another. However, the short ligaments and primitive articular surfaces of the Girardeau camerates would have resulted in slow "arm waving". Probably, an attached Paleozoic camerate was able to exert some leverage against gravity and currents (when present) by threshing its arms on the leaning side down; this would have tended to right and rebalance the crinoid. The arm orientations observed in the Girardeau camerates are consistent with this hypothesis (see discussion of burial positions). Certainly, the amount of leverage was less than that of living crinoids owing to the less efficient arm articulations.

Many post-Ordovician inadunates and flexible crinoids have much more sophisticated arm articulations than those of the Girardeau camerates. Typically, these exhibited differentiated dorsal and ventral ligaments with more or less prominent transverse ridges (see later annotation on *Woodocrinus* for an example). These inadunate and flexible arm articulations were probably less efficient than the muscular arm articulations of Recent crinoids for two reasons. Muscles were usually lacking, although numerous Devonian and later Paleozoic inadunates developed muscular articulations between the RR and IBrr. Compared to modern forms, the ligaments of most Paleozoic species were short. The muscular articulations, typical of living crinoids, possess the highest efficiency, both with respect to rate and amount of movement. These have two types of ligaments, dorsal and interarticular, in conjunction with ventral muscles. The ligaments and muscles are large relative to the size of the Brr.

The arm articulations of almost all Paleozoic forms were definitely less efficient than the muscular articulations of Recent species. Nevertheless, some stalked Paleozoic and later crinoids were most likely able to move from place to place (see later discussion on *Woodocrinus*).

As previously mentioned, pinnulate arms increased the bulk density of the crown whereas the nonpinnulate crowns had lower bulk densities. Lane (1968) noted that pinnulate arms (camerates, advanced inadunates) provided more surface area on the down (righting or leverage) stroke. Nonpinnulate (flexibles, primitive inadunates) arms possessed less surface area and correspondingly less leverage. Thus, the increased bulk density due to pinnules was compensated for by the large surface area.

Stem leverage. — The Girardeau camerate columnals are united by crenulate sutures which provided rigid joints relative to most other columnal articular types. However, curved stem segments are commonly seen, indicating a certain measure of flexibility and power of movement. Seilacher, *et al.* (1968; see also Linck, 1954, 1965) showed that column flexibility gradients can be correlated with mode of life, at least to some extent. Most Girardeau crinoids correspond to their *Encrinus* model. Stem flexibility was measured by the amount of curvature observed, high curvature denoting high flexibility and vice versa for low curvature.

Breimer (1969, p. 144) believed that crinoid columns can bend to avoid breaking although the stem probably is not able to change its position actively by muscular activities. Although definitive proof is not known, much circumstancial evidence suggests that living and fossil crinoids do possess the ability to actively bend the column. The cirri of living crinoids are capable of movement; they can grasp and release (see A. H. Clark, 1915, pp. 258-312 for details of the cirri in Recent comatulids). In fact, A. H. Clark (1915, p. 266) reported that young *Iridometra nana* were observed to swim through the water with motionless arms, propelled by rapid movements of the cirri. The geometry of the cirrals and their articular surfaces are reasonably similar to those of columnals. At least in some living crinoids extentions of the axial nerve cord can be traced up to the ligaments which hold the adjacent columnals together (see P. H. Carpenter, 1884, pp. 111-127, pl. 7a, fig. 1). This suggests that the nervous system can stimulate contraction of the inter-columnal ligaments (see also earlier comments under arm leverage). The observed orientations of many fossil crinoid stems are consistent with this hypothesis. For example, the S-shaped bend in the stem of *Mespilocrinus konincki* Hall, the helical coil of *Acanthocrinus rex* (see Ubaghs, 1953, figs. 97, 122), and the coiled parts of many *Ctenocrinus paucidactylus* (Hall) columns (see Goldring, 1923, pls. 9-11) are unlikely to have been induced by external agents such as currents. Also some of the older observations on Recent crinoids seem to denote that the crinoid has some ability to activate movement of the stem. On the *BLAKE* cruises (1877-1879), numerous isocrinids were dredged. Captain Sigsbee and A. Agassiz placed some living animals in a tank of still ice water and the specimens survived for several hours. Agassiz reported that the cirri moved more rapidly than the arms and that the columns slowly passed from a vertical to a curved or even drooping position (Agassiz is quoted *in* P. H. Carpenter, 1884, pp. 332-333). In 1893, Nutting noted the same movements in *Isocrinus decorus* (see Gislén, 1924, pp. 56, 57, 203). A. H. Clark (1921, p. 525) quoted J. V. Thompson's observations on *Antedon bifida* pentacrinids stating (Thompson's observations date about 1820):

> J. V. Thompson says that they possess the power of bending or inclining the column freely in every direction, and, what is more remarkable, of twisting it up into a short spiral, and that with a considerable degree of vivacity.

W. B. Carpenter (1866, pp. 736, 737) and Chadwick (1907, p. 37) saw the same column movements in *Antedon bifida* pentacrinids. Admittedly, the few data on living species are not definitive because the environmental conditions under which they were made have not been outlined. Full documentation must await properly controlled experiments on live specimens. D. L. Meyer (personal communication) obtained morphological evidence from living stalked forms which indicates that the animals can actively flex the stem and maintain the column in a selected orientation for a certain period of time. However, in view of the present uncertainty, both possibilities with respect to column bending are entertained in this paper.

Whether or not the crinoid can or cannot flex the column is not especially critical to the rooted species. If the stem becomes bent, the normal restoring movement, caused by the columnals and their ligaments, tends to return the stem to a vertical orientation. However, the nature of stem flexing probably governs the method of locomotion for a semi-eleutherozoic stalked crinoid (see annotation on *Woodocrinus*).

Moderately long column segments attached to crowns are known in numerous Girardeau crinoids, especially camerates. The proximal-most parts of the columns are straight and were presumably rigid during life, whereas the mid-length part of the stem was flexible. The mid-length stem segment comprises at least 67 to 75% of the total column length in a Girardeau camerate. Most column segments associated with the attachment devices were rigid, although a few curved (possibly flexible) ones are known, namely the curved stem segment-rootlet type. Thus, the normal Girardeau crinoid stem flexibility gradient (*i.e.*, *Encrinus* type) equalled: A. Proximal-rigid. B. Mid-length-flexible. C. Attachment device and associated column-rigid. Leverage could have been exerted by this type of crinoid through bending or flexing the middle area of the column against the rigid rooting system. In effect the rigid holdfast and associated stem served as a strong rigid brace against which the column was flexed.

The curved stem segment-rooting device flexibility distribution follows: A. Proximal-rigid. B. Middle stem-flexible. C. The strong curvature of the rootlet bearing stem segment suggests some flexibility. However, this flexibility may have been wholly or partially counteracted by rootlet penetration into the sediment. Presumably crinoids of this type possessed some degree of stem leverage and uprighting movements due to column flexing. Seemingly, a nonrigid stem segment with and immediately above the holdfast would have afforded much less mechanical leverage. All in all, substrate roots of this type are uncommon in Paleozoic crinoids, although the Crawfordsville *Gilbertsocrinus* shows a similar stem coil which lacks rootlets (Lane, personal communication). Most Paleozoic species with highly flexible distal column regions probably stabilized themselves by wrapping the distal stem around some object such as a rock, or an erect crinoid stem (*e.g., Heterocrinus*, Thomas Weaver, personal communication, apparently coiled around a *Glyptocrinus* column).

The pseudoplanktonic stalked echinoderm column flexibility differed markedly from the *Encrinus* type. For example, *Seirocrinus*, a Jurassic pentacrinid, was pseudoplanktonic and joined (cemented ?) the holdfast to a floating log (Seilacher, *et al.*, 1968). Although the crown was less dense than the stem, nevertheless it hung down because the crown density exceeded that of the surrounding sea water. In this form, maximum column flexibility occurred around where the stem joined and was wrapped around the log.

Various authors have cited many living mature isocrinids which probably lived semi-eleutherozoic existences (see P. H. Carpenter, 1884, pp. 12-32, 315-346; Kirk, 1911, pp. 33-64; Ehrenberg, 1929, pp. 34-39). For example, one adult *Isocrinus decorus* has a stem which terminates in a worn and rounded nodal (P. H. Carpenter, 1884, p. 18). Clearly, this specimen and many others lost the distal part of the column and rooting device. Young individuals are generally visualized as being attached with the stem detachment occurring in later life (P. H. Carpenter, 1884, p. 18; Kirk, 1911, pp. 35-38). The column breakage may represent a normal growth process (P. H. Carpenter, 1884, p. 21) or it may be involuntary (Kirk, 1911, p. 35), perhaps caused by external environmental factors such as currents. The two mechanisms may be combined with ontogeny producing a zone of structural weakness in the stem which is particularly susceptible to breakage. Regardless of the cause, the adults of certain species are consistently found detached. The examples cited by P. H. Carpenter and Kirk are *Isocrinus decorus, I. wyville-thompsoni, I. parrae* (*maclearanus* of P. H. Carpenter), *I. alternicirrus*, and *Metacrinus angulatus*. These semi-eleutherozoic species are considered as being usually attached to various objects, for example, other crinoid stems and cirri, by the grasping cirri. During locomotion, the stem is dragged or carried along with propulsion provided by swimming movements of the arms (P. H. Carpenter, 1884, p. 19; Kirk, 1911, pp. 41-43, 58-64). P. H. Carpenter (1884, p. 319) also suggested a correlation between environment and life habits. Crinoids living in deep water muds are believed to spend more time in the detached state whereas those found in different habitats (presumably harder substrates) are more commonly attached. This was applied to different individuals of *Isocrinus decorus*, although it is probably valid at the species level also. It should be realized that the writer does not postulate these living habits for all isocrinids. For example, *Rhizocrinus* and *Bathycrinus* are two common rooted forms (see P. H. Carpenter, 1884, pls. 7-10).

Many stalked Paleozoic crinoids probably exploited the same semi-eleutherozoic mode of life (see Kirk, 1911, pp. 30-64, for many examples; however, some of these are probably incorrect).

The common Carboniferous inadunate *Woodocrinus* is most familiar to the writer (Brower, in preparation; see Wright, 1950-54, pp. 47-59, pls. 21-29, for taxonomy and illustrations). A rooting device is lacking and the distal stem tapers to a point. Except for the proximal part, the entire column was moderately flexible. The distal 33% of the column bears long slender unbranched cirri. The observed orientations of these indicate much flexibility during life of the animal; all in all, the woodocrinid cirri are similar to the grasping cirri of living crinoids. The tapering distal column obviously denotes that *Woodocrinus* was not rooted in the usual Paleozoic crinoid fashion. Most likely, the crinoids were temporarily or permanently attached to various objects, such as other crinoid stems or submarine plants, by means of the long cirri. Observation of numerous large slabs discloses little evidence of grasping other crinoid columns, and submarine plants are postulated as the main basis of attachment. This may have been permanent or temporary. Permanent fixation does not seem likely because of the reduced stem leverage which would have been caused by the lack of a rigid rooting device. Thus, attachment was probably only temporary and the crinoid is believed to have been capable of some movement.

Woodocrinus also most likely possessed much arm leverage which is at least consistent with movement. In species with simple arm structure, such as *W. macrodactylus,* the arms are wide and massive with long pinnules. Complexly branched forms like *W. extensus* have more slender arms and many more pinnules. Both types show large arm and pinnule surface area. Sophisticated ligamental or muscular articulations with well-developed transverse ridges occur between the RR and IBrr1 (IAxx) and between the IIAxx and IIIBrr1; some specimens show five fossae and muscles may have been present. The observed arm orientations indicate much power of movement along these articulations. The other Brr have ligamental articulations with shallow fossae and small transverse ridges. Only limited movement existed on these articular surfaces.

Two methods of progression are outlined. The first assumes the crinoid had no ability to actively bend and flex the stem; this is the classic hypothesis discussed by P. H. Carpenter (1884, pp. 12-32, 315-346) and Kirk (1911, pp. 33-64). Most of the movement was probably affected by arm waving. This may have been augmented by grasping and pulling actions of the cirri. However, the cirri are short compared to the overall size of the crinoid. This type of locomotion most likely was limited. Lacking the ability to flex the column, the crinoid would have had to drag the stem, at least to some extent. The second method of movement invokes the ability of the crinoid to actively bend and flex the stem. Locomotion is believed to have utilized both the arms and column. Most likely, the crown was held aloft by arm threshing which was similar to the swimming strokes of living comatulids. Lateral movement is postulated to have occurred by means of the stem and cirri. Probably these were extended, a suitable object grasped by the cirri, following which the crinoid pulled itself along. A single cycle of this type would have obviously resulted in more distance covered than in the first method of movement. Repetitions would have allowed considerable travel. Basically, a combination of swimming and crawling is proposed. Mechanically, this type of locomotion seems much more feasible than the first, especially for Paleozoic forms which had less arm leverage than the Recent isocrinids.

At present, the *Woodocrinus* bulk density has not been computed and only one comment will be presented. The woodocrinid columnals below the proximal region have strongly depressed articular surfaces, and extensive ligaments must have been present. Consequently, the *Woodocrinus* stem was obviously less dense than that of a Girardeau camerate.

Not all semi-eleutherozoic stalked Paleozoic crinoids had cirri on the stem. *Ctenocrinus paucidactylus* (Kirk, 1911, p. 43; see Goldring, 1923, p. 122, pls. 9-11) and *Dendrocrinus oswegoensis* Meek and Worthen (complete specimen never illustrated) provide two examples.

The advantages of a semi-eleutherozoic mode of life to a stalked crinoid seem numerous. During attached periods, the crown was elevated above the substrate, as in rooted types (see previous discussion); however, an attached semi-eleutherozoic individual probably suffered reduced stem leverage relative to most permanently rooted types. Owing to its powers of movement, the animal could have moved to an optimum place for feeding or reproduction, and could have vacated local areas which were unfavorable due to excessive current velocities. Essentially, this mode of life was probably an adaptative compromise between crown elevation and movement. Mechanically, the crown elevation was most likely more efficient in the rooted forms. Crinoids which lack stems are better adapted for locomotion (*e.g.,* Recent comatulids, possibly some agassizocrinids and certain edriocrinids in the Paleozoic (Kirk, 1911, pp. 106, 111-114). A brief survey of stalked crinoids suggests that this way of life was less common in Paleozoic species (camerates, inadunates, and flexibles) than in stem bearing articulate crinoids (isocrinids). This is attributed to the less efficient Brr and perhaps columnal articulations which characterized the Paleozoic groups. Much of the previous discussion is tabulated in Table 3 in a brief, somewhat incomplete and highly tentative summary on the evolution of the major adaptations in crinoids. Minor adaptations, such as the planktonic scyphocrinids, pseudo-planktonic *Seirocrinus,* the peculiar stemless edriocrinids, agassizocrinids, and other Late Paleozic inadunates, are omitted. Many of these were discussed by Kirk (1911). However, the writer has not examined any of these forms in detail and cannot comment on Kirk's conclusions. In the following text, the term "Grade" is used in the context of an adaptative grade or zone.

The following general conclusions are drawn from the adaptation table and the previous comments. In the transition from Grade I to II, pinnule development represented the main evolutionary breakthrough. Probably the main adaptative rationale for pinnule initiation was the increased food gathering capacity, rather than arm leverage. The additional arm leverage conferred by the pinnules was at least partially counteracted by the resultant rise in crown bulk density.

During the evolution of Grade II to III, the crown bulk density was decreased, whereas arm leverage was augmented because of the greater amount and higher efficiency of the connective tissue, especially in the arms. Clearly, this adaptation occurred in and benefited bottom dwelling rooted animals. The higher arm leverage probably allowed the more rapid spread of all arms for feeding and arm closure and the more rapid threshing of isolated arm groups to retain the crown in the stable position.

Semi-eleutherozoic stalked forms were repeatedly developed in Grades I, II, and III. These involved unrelated groups and clearly constituted convergent evolution. Among crinoids, stalked semi-eleutherozoic living habits were and are probably most common in isocrinids (Grade III).

In the change from Grade III to IV, the comatulid transition to a new semi-eleutherozoic or pelagic mode of life was made possible by casting off the high density column. However, the development of the highly sophisticated arm leverage which occurred within Grade III was prerequisite to and preadaptative to Grade IV. Basically relative to Paleozoic pinnulate crinoids, the comatulid semi-eleutherozoic adaptations are low mean crown density, loss of the column, and the well-developed connective tissue and arm articulations.

TERMINOLOGY AND MEASUREMENTS

Generally the terminology follows R. C. Moore (1952a, text-fig. 18-2). The proximal plate of the camerate CD (posterior) interray is designated the primanal following Jaekel (1918, p. 28). Brachials rigidly incorporated into the dorsal cup are termed fixed-brachials (FBr, plural FBrr). These terms respectively replace the "tergal" and "cup-brachial" of Moore.

The ray orientation system used is that of P. H. Carpenter (1884, text-fig. 2). The Carpenter A and C rays correspond to the anterior and right-posterior rays of most authors, respectively. The interray areas are designated by the flanking rays; for example, the posterior interray which lies between the C and D rays becomes the CD interray. In this paper, most of the other camerate interrays (*e.g.,* AB, BC) are not differentiated but are merely referred to as lateral interrays.

The camerate crinoids examined here have two to four arms per ray. Two-armed species show two half-rays; the area between these and the equivalent position in four-armed crinoids is termed an inter-half-ray, the dorsal cup plates of which are inter-half-ray iBrr. In four-armed taxa, two half-rays are present, each consisting of two arms called quarter-rays. The space between two quarter-rays is designated the inter-quarter-ray and its plates are the inter-quarter-ray iBrr.

The camerate plate sequence directly overlying the primanal is the anal series, the elements of which are anal series plates. The anal series is generally separated from the C and D rays by CD interray iBrr.

One of the major problems in relative growth studies is the determination of a standard relative age parameter. Obviously, this character must be well known to enable measurements to be made on all individuals in the growth sequence. Such restricts the Girardeau camerate relative age character to the dorsal cup. Preservation of the crinoids further limits the possibilities to: height of the B, R, IBr1 or IAx; height from the base of the dorsal cup to the distal margin of the IAx (hereafter termed "size"); calyx volume. If used as an independent variable (x), the most satisfactory character should minimize variation of the other dorsal cup parameters (*e.g.,* dorsal cup height, width, IBr1 height). Consequently, a series of regression lines for the calyx dimensions were computed for roughly seven to 10 individuals of most species with these independent variables. The smallest percentage standard deviations were found when "size" or the R height constituted the independent variable; the latter percentage standard deviations were slightly smaller. Intra-specimen variability was determined for the calyx characters of representative specimens (except calyx volume, a single animal has only one volume). Again the "size" and R height showed minimum scatter, although "size" was slightly more constant. Because of this and ease of visualization, "size" was selected as the standard relative age measure. It must be noted that the growth rate of "size"

f life	Examples
to substrate.	Undescribed dendrocrinid from Middle Ordovician of Ottawa. *Dendrocrinus casei* from the Girardeau. *Onychocrinus exsculptus* (Springer, 1920, pl. 71) and numerous other flexibles illustrated by the same author.
wrapped around ssibly moved e.	*Heterocrinus* (T. Weaver, personal communication).
Distal end rapped around times.	*Macrocystella* (Paul, 1968). *Dendrocrinus oswegoensis* Meek and Worthen (complete specimen never illustrated).
ed to substrate.	Most Girardeau species. *Platycrinites regalis* (Wachsmuth and Springer, 1897, pl. 72, fig. 1). *Eucalyptocrinites ovalis* (Wachsmuth and Springer, 1897, pl. 82, figs. 1-6). Numerous other forms figured by Wachsmuth and Springer (1897).
istal end of stem ight object. Prob- ace to place.	*Glyptocrinus dyeri* (Miller, 1880, pl. 7, figs. 2, 3). *Alisocrinus warreni* (Wachsmuth and Springer, 1897, pl. 22, fig. 1). *Ctenocrinus paucidactylus* (Goldring, 1923, pls. 9-11).
cirri used t least ved from place	*Woodocrinus* (see text). *Aorocrinus iola* (Laudon, 1933, pl. 2, fig. 8; also various other Gilmore City species). *A. immaturus* (Laudon and Beane, 1937, pl. 17, fig. 1; also numerous other LeGrand forms).
ed on or the substrate.	*Gilbertsocrinus* from the Crawfordsville (Lane, personal communication). Girardeau species with coiled stem segment-rootlet device.
ed to substrate.	*Rhizocrinus* and *Bathycrinus* (P.H. Carpenter, 1884, pls. 7-10).
cirri used for from place to	Various species of *Isocrinus* and *Metacrinus* cited by P.H. Carpenter (1884) and Kirk (1911).
. A few pelagic	Swimming: true adult comatulids, *e.g.*, *Antedon*. Crawling: adult comasterids. Pelagic: *Unitacrinus* and *Saccocoma* (Moore and Jeffords, 1968, p. 19).

Table 3

Adaptative Grade	Time duration	Total bulk density	Crown bulk density	Arm leverage	Stem flexibility gradient			Mode of life	Examples
					Proximal	Central	Distal		
I. Non-pinnulate stem bearing crinoid, cystoid or eocrinoid.	Cambrian to Permian	Uncertain, but average is less than II.	Average is less than II because of lack of pinnules.	Low because of short ligaments and lack of muscles.	Rigid	Flexible	Rigid	Rooted or cemented to substrate.	Undescribed dendrocrinid from Middle Ordovician of Ottawa. *Dendrocrinus casei* from the Girardeau. *Onychocrinus exsculptus* (Springer, 1920, pl. 71) and numerous other flexibles illustrated by the same author.
					Rigid	Flexible	Probably flexible	Distal end of stem wrapped around upright object. Possibly moved from place to place.	*Heterocrinus* (T. Weaver, personal communication).
					Rigid	Flexible	Flexible	Semi-eleutherozoic. Distal end of stem possibly wrapped around various objects at times.	*Macrocystella* (Paul, 1968). *Dendrocrinus oswegoensis* Meek and Worthen (complete specimen never illustrated).
II. Pinnulate stem bearing inadunate and camerate crinoids.	Ordovician to Triassic	Maximum value, must be between 1.41 and 1.67 gm/cm^3.	Ranges from minimum value of 1.41 gm/cm^3 to unknown higher figure.	Low, but higher than I due to presence of pinnules.	Rigid	Flexible	Rigid	Permanently attached to substrate.	Most Girardeau species. *Platycrinites regalis* (Wachsmuth and Springer, 1897, pl. 72, fig. 1). *Eucalyptocrinites ovalis* (Wachsmuth and Springer, 1897, pl. 82, figs. 1-6). Numerous other forms figured by Wachsmuth and Springer (1897).
					Rigid	Flexible	Probably or definitely flexible	Stem lacks cirri, distal end of stem wrapped around upright object. Probably moved from place to place.	*Glyptocrinus dyeri* (Miller, 1880, pl. 7, figs. 2, 3). *Alisocrinus warreni* (Wachsmuth and Springer, 1897, pl. 22, fig. 1). *Ctenocrinus paucidactylus* (Goldring, 1923, pls. 9-11).
					Rigid	Flexible	Flexible	Stem with grasping cirri used for attachment. At least some definitely moved from place to place.	*Woodocrinus* (see text). *Aorocrinus iola* (Laudon, 1933, pl. 2, fig. 8; also various other Gilmore City species). *A. immaturus* (Laudon and Beane, 1937, pl. 17, fig. 1; also numerous other LeGrand forms).
					Rigid	Flexible	Unknown	End of column coiled on or immediately below the substrate.	*Gilbertsocrinus* from the Crawfordsville (Lane, personal communication). Girardeau species with coiled stem segment-rootlet device.
III. Stalked isocrinids and pentacrinid growth stages of comatulids.	Triassic to Recent	Greater than 1.26 gm/cm^3 but less than II due to extensive connective tissue.	Average about 1.26 gm/cm^3.	Higher than II due to development of muscles and extensive connective tissue.	Rigid	Flexible	Rigid	Permanently attached to substrate.	*Rhizocrinus* and *Bathycrinus* (P.H. Carpenter, 1884, pls. 7-10).
					Rigid	Flexible	Absent	Stem with grasping cirri used for attachment. Move from place to place.	Various species of *Isocrinus* and *Metacrinus* cited by P.H. Carpenter (1884) and Kirk (1911).
IV. Adult comatulids.	Jurassic to Recent	Minimum value due to loss of stem.	Mean about 1.26 gm/cm^3.	Slightly higher than III.	—	—	—	Semi-eleutherozoic. A few pelagic forms.	Swimming: true adult comatulids, *e.g.*, *Antedon*. Crawling: adult comasterids. Pelagic: *Unitacrinus* and *Saccocoma* (Moore and Jeffords, 1968, p. 19).

Evolution of adaptation in crinoids.

is not constant with respect to time. Living and fossil crinoids are characterized by slow-fast-slow time-size growth rates (see paleoecology and introductory statement on ontogeny). Consequently, "size" only measures the relative growth, not the absolute chronological age.

Heights of dorsal cup ray plates were measured along the ray axis and the interray plates were determined parallel to the interray axis. Width was taken at right angles to the height; the maximum values were used. The percentage height and width points locate the position of the aboral nerve cord knots on the inside of the plates; externally these are defined by the median-ray and stellate ridge ornamentation (see later discussion). The height point equals height of the nerve cord knot above proximal plate margin/total plate height. The width point consists of plate width to nerve cord knot/total width. Both points are expressed as percentages. Generally, the orientation of the rays is unknown, consequently, the width points are conventionally expressed as 50% or less.

For computation of regression lines, the various FBrr were coded in terms of a numerical scale. Two digits were assigned to each plate, the first to the proximal and the second to the distal margin as follows: Proximal IAx, 6.0; Distal IAx, 7.0; Proximal IIBr1, 8.0; Proximal IIBr2, 10.0; Proximal IIBr3 or IIIBr1 (IIBr2 is axillary in species with four arms per ray), 12.0.

The standard lateral interray calyx width (hereafter termed dorsal cup width or calyx width) includes one ray plus one interray at the IAxx mid-level of the adjacent rays. Width of a lateral interray (iBrr width) was measured at the same level. CD interray width is defined in the same fashion. Dorsal cup height or calyx height ranges from the base of the calyx to the distal margin of a lateral interray area.

The standard brachials (Br, plural Brr) usually consist of IIBrr 8 to 13 in 10 armed species or the equivalent IIIBrr 6 to 11 in 20 armed crinoids. All measurements were taken at right angles to the dorsal-ventral plane. Due to the nature of preservation, it has not been possible to present meaningful dorsal-ventral data. Consequently, the Brr growth models presented here are essentially two rather than three dimensional. The food grooves of a Br are subdivided into "brachial food grooves" and "pinnule facet food grooves". These and the standard measurements are illustrated in Text-figure 2 for uniserial and biserial Brr.

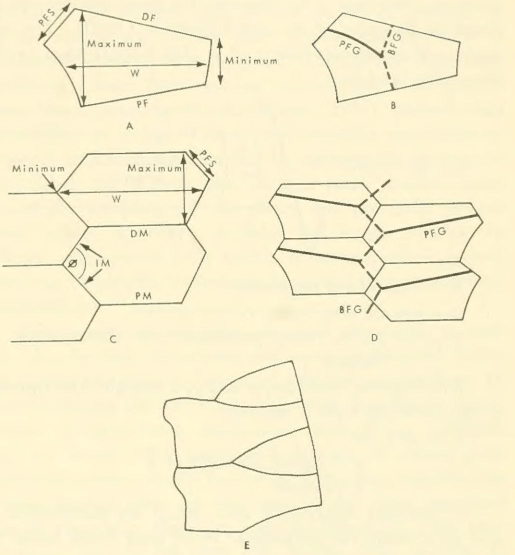

Text-figure 2. — Sketches illustrating Brr terminology. A. Uniserial Br, dorsal view showing measurements and terms. PF and DF are proximal and distal faces, respectively. W denotes width; maximum indicates maximum height; minimum represents minimum height; average height is mean of previous heights; PFS indicates pinnule facet size. Convergence angle is measured between proximal and distal faces. B. Uniserial Br, ventral view with food groove designations. BFG is "brachial food groove"; PFG denotes "pinnule facet food groove". C. Mature biserial Brr, dorsal view. Symbols as in A except: IM represents inner margin; DM and PM are distal and proximal margins. Note differentiation of inner from proximal and distal margins. ø indicates convergence angle, always measured between inner margins or equivalent thereof. Minimum height of biserial Brr is always zero. D. Mature biserial Brr, ventral view. Food grove legend as in B. E. Oblique sketch of immature biserial Brr. Pinnule facets only shown on left side. Note lack of differentiation of inner versus proximal and distal margins.

Discussion of supporting structures emphasizes the relations between the proximal columnal area and calyx volume and between the supporting Br (distal FBr) and food gathering system lengths. The columnals are circular; the diameter of the stem axial canal was ignored because this is small relative to overall columnal size. Supporting Brr area is most closely approximated by a half-circle or half-ellipse where the depth slightly exceeds width of the distal face. The food groove is not considered as its dimensions are generally unknown.

The rationale underlying the food gathering system measurements is treated under the summary statement on Girardeau camerate ontogeny.

STATISTICAL TREATMENT OF ONTOGENY

The basic data were derived from regression and correlation analysis of *y* (dependent variable) and *x* (independent variable). The formulas for most parameters are listed in Simpson, Roe, and Lewontin (1960). The percentage standard deviations of y with respect to x ($\sigma y\%$) were calculated by:

$$\sigma y\% = 100 \cdot \sqrt{\frac{\sum \left(\frac{y_{eqn} - y_{act}}{y_{eqn}} \right)^2}{N - 1}}$$

N = number of specimens

y_{act} are the observed y values whereas

y_{eqn} are the y values predicted from the equation involved

Utilizing the variables, x and y, a straight line equation of the following form is defined:

$y = a + bx$

a = initial intercept of y

b = slope

If common logarithims (*i.e.*, $\log_{10}$) are substituted for x or y, or both, the curvilinear trend lines listed below are computed:

$\log y = \log a + bx$

$y = a + b \log x$

$\log y = \log a + b \log x$

In cases where several equation forms were determined for a single pair of variables, the best fit was almost always characterized by the lowest percentage standard deviation.

The principal emphasis in discussion of the regression lines is placed on the growth rates of y with respect to x and the relationship of these to the ontogeny of the various species. These growth rates were derived directly from the equations. For example, changes in calyx shapes during the development sequences are discussed in context of the differential plate growth rates which produced them. When values of x and y are given, the former generally consist of actual specimen values whereas the latter are equation figures. Theoretically, such should indicate the ontogeny of the mean or average individual. In some instances, the equations failed to yield wholly satisfactory fits to the data and actual values of x and y are presented. This is most common in the food gathering system ontogeny where two or more equation forms invariably were tried for a single pair of variables; apparently, the true relations are intermediate between two regression line types. The initial intercepts of certain equations were used to predict "microcrinoid sizes" or when a certain plate developed in the growth sequence. This procedure assumes that the regression trend line constituted a good fit to the available data and that the y growth rates could be extrapolated backward in terms of x.

Unfortunately, it is impractical to build a complete correlation matrix for a single species owing to two reasons. The number of different measurements reaches 100 in certain forms. Inasmuch as $\log_{10}$ of x or y or both, were commonly used as variables, the total matrix dimensions could have exceeded 200 by 200 for a growth sequence. The writer does not have access to a computer which could process such a large block of data. A total matrix could be constructed from several partial ones; however, this was deemed impractical due to the cost, time involved and the frustration factor; also many of the data sets are incomplete, especially those involving calyx growth.

Two correlation matrices were derived for most species, namely the standard Brr, and the food gathering system. Calyx growth matrices were not attempted for most forms; many of the data sets are incomplete because not all measures could be taken from a single crinoid. Basically the correlation coefficients express the amount of integration and coordination shown by x and y during ontogeny (see introductory statement on growth).

In the univariate statistics, all standard deviations are expressed as percentages of the applicable means, so that the various values can be easily compared. The calculation of the univariate parameters followed Simpson, Roe, and Lewontin (1960, pp. 65-95).

GENERAL STATEMENT OF ONTOGENY

Two basic approaches exist to the growth study of crinoids: measurement of parameters on a series of individuals of different "sizes" and ages and determination of the ontogeny of a single individual through tracing the development of a single plate or series thereof by means of successive growth lines.

The former approach is applied to calyx growth because the dorsal cup plate growth lines occur on the inside of the plates. Consequently, these are not available for direct measurement in the Girardeau crinoids, although such growth lines may be examined in isolated plates and internal molds from other stratigraphic units such as the Mississippian Burlington Limestone of the mid-continent. Thus, preservation determines the approach to Girardeau camerate calyx growth.

Both approaches have been utilized in arm and Br growth. The basic quantitative data are derived from measurement of a set of standard Brr in crinoids of different "sizes" and ages; because of practicality and preservation the standard Brr usually consist of IIBrr 8 to 13 or the equivalent IIIBrr where the half-rays branch near the calyx. Also, free Br growth stages within the arms of single crinoids have been investigated qualitatively and in some cases quantitatively. Inasmuch as crinoids add new Brr at the tips of the arms, the least mature Brr will be found at these areas; proceeding proximally, more and more mature and older Brr are encountered. Despite some difficulties owing to the nature of preservation, the growth trends derived from the two approaches are basically the same.

A Recent crinoid consists of an internal skeleton composed of a series of adjacent plates. Basically, the endoskeleton is mesodermal and occupies the major part of this layer; the outer plate surfaces are covered by a thin epidermal layer which is not always completely developed. In the calyx, the plates represent the bulk of the body wall and encloses the viscera of the animal (see Hyman, 1955, pp. 47-61, for summary).

GIRARDEAU CAMERATE DORSAL CUP PLATE GROWTH MODEL

The camerate dorsal cup plate (tegmen plates are excluded from this discussion) growth model is based on that of J. S. Miller (1821), Lane (1963a, p. 929), Meyer (1965), Macurda (1968), and the writer's personal observations.

Maximum growth rates usually occurred in the lateral directions (*i.e.*, width and height); such is clearly denoted by growth lines where these can be observed and also by changes in lateral versus thickness components during ontogeny.

Growth lines are not visible on external surfaces of crinoid plates, because these were obliterated by subsequent deposition of external laminae of calcite.

When growth lines developed on crinoid plates, they invariably were present on the insides of the plates and recorded growth of the plate lateral margins. In such examples, no material was deposited on the inside of the plate. As noted by Lane, this pattern is related to the original placement of the aboral nerve cords which can be traced as grooves on the insides of the ray plates and BB of many crinoids (*e.g.*, *Macrostylocrinus cirrifer* and the Girardeau camerates). Some Paleozoic forms, such as platycrinitids (see Meyer, 1965, text-fig. 1), lacked these grooves and the aboral nerve cords were probably located on the inner surfaces of the plates. Immature RR of *Antedon bifida* have the same configuration (see later discussion). In either case, subsequent internal deposition of calcite could have interferred with these nerve cords by disruption or burial. In the ray plates which became fixed in the calyx during ontogeny (IBrr and proximal IIBrr in most Girardeau camerates), the internal grooves also record the position of the ambulacral tract when these plates were free Brr. If the growth lines represent periodic phenomena (*i.e.*, nondeposition), then their spacing reveals the time growth rates. Data given by H. B. Moore (1935) showed that growth lines on living echinoid plate exteriors were seasonal. However, this cannot be verified for crinoids. In the writer's observation, the growth lines become more closely spaced toward the periphery of the plate; this probably denotes slower calcite deposition in older and larger crinoids. In addition, the growth lines testify to discontinuous growth consisting of periodic increments of calcite interspaced with nondeposition.

Examination of the plate interiors of certain crinoids (*e.g.*, *Ptychocrinus fimbriatus* and some unidentified Paleozoic forms) discloses no traces of internal growth lines. In a few instances, complete sets of growth lines are probably present. Judging from comparison with living echinoids (*e.g.*, see Moore, 1935, text-figs. 5, 6), not all crinoid plate growth lines were usually preserved. Typically, crinoid plate internal growth lines are not seen on the most immature parts of the plate; these can only be detected on the later developed parts of the plate (see Meyer, 1965, text-fig. 1; Wanner, 1916, pl. 99, figs. 6a, b; Wachsmuth and Springer, 1897, pl. 4, fig. 6). There are three possible explanations for the complete or partial absence of growth lines on crinoid plates. 1. Calcite deposition was continuous. 2. The growth lines were obliterated by deposition of internal calcite laminae; this is known in *Antedon* and Recent echinoids (Moore, 1935). However, there is no evidence that such occurs in Paleozoic crinoids. 3. Nonpreservation due to recrystallization, solution or some other mechanism. Because of the placement of the aboral nerve cords, the first or third explanation is preferred.

In general, the following growth gradients existed. The lateral growth exceeded the external growth which was greater than the internal growth (as postulated here this growth component equalled zero).

As previously mentioned, traces of the aboral nervous system are commonly shown by the presence of grooves on the inside of the plates. These correspond to ridges on internal molds (see *Macrostylocrinus cirrifer* for detailed discussion). Examination of growth lines on a single plate and study of a series of adjacent plates in crinoids of different "sizes" and ages indicate that the plate accretion simply extended the previously established grooves and the nerve cords therein. These grooves did not migrate during ontogeny; consequently, these previously established grooves form constant reference axes for the ontogeny of a single plate. During growth, the internal grooves and presumably the nerve cords therein became wider. This denotes that resorption occurred along the sides of the grooves and the aboral nerve cords. Nevertheless, the axes of these nerve cords clearly comprise constant topographic reference points (see *M. cirrifer* for more details).

Study of internal and external molds of *M. cirrifer* indicates that the external ornamentation (median-ray ridges and stellate ridges) developed directly over the internal aboral nervous system. This is also seen in numerous other camerates with thin plates and well-developed external median-ray and stellate ridge type ornamentation. Readily available published examples are: *Reteocrinus onealli* (Wachsmuth and Springer, 1897, pl. 9, fig. 1e), *Xenocrinus baeri* (Wachsmuth and Springer, 1897, pl. 9, fig. 5c), *Glyptocrinus decadactylus* (Wachsmuth and Springer, 1897, pl. 21, fig. 4a), and *Periechocrinites* spp. (Wachsmuth and Springer, 1897, pl. 50, figs. 2a, 3b, and 7b). Thus, the approximate location of the original aboral nervous system may be ascertained by inspection of the external ornamentation. However, precise determination of the nervous system position is not possible because the external median-ray ridges and other external ridges which reflect the nervous system are much wider than the internal grooves which housed the aboral nerve level.

The relationship between the aboral nerve cords and the external ornamentation for the BB of monocyclic camerates and for the IBB of dicyclic forms is somewhat uncertain. As discussed under *Macrostylocrinus cirrifer* Ramsbottom, most of the chambered organ was probably located at the BB level in monocyclic forms. Some of the external ridges on the BB seem to have corresponded to the chambered organ lobes whereas others may have been associated with its interlobes. An analogous situation probably existed with the dicyclic camerate IBB, although these are not studied here.

In modern crinoids, the relation of dorsal cup plates and the aboral nervous system is more complex. The axial nerve cords of *Antedon* (*i.e.*, armward extensions of the aboral nerve level) are separated from the food grooves by solid calcite throughout the free arms. When these join the calyx at the RR level, they penetrate and pass through the R and then join the chambered organ. The main aboral nerve plexus of *Antedon* is located under the BB rosette, partly under and beside the RR circlet and partly inside and above the centro-dorsal (see Nichols, 1962, fig. 2 where this is clearly shown). The aboral nerves within the cirri of *Antedon* and within the stem of living isocrinids originate at the base of the chambered organ. Consequent to these differences, the plate growth of modern crinoids (especially for BB and RR) is much different from the above Girardeau camerate type. During the early development of *Antedon*, the aboral nerve cords lie on the internal sides of the RR. Due to subsequent internal calcite deposition, the nerve cords are gradually buried within the plate (W. B. Carpenter, 1866, pp. 738, 739; 1876, p. 454). Also calyx plate resorption is much more common in Recent crinoids than in the Paleozoic camerates examined here (A. H. Clark, 1915, pp. 322-340). The individual plate growth of living forms is far more complex than that of most Paleozoic species (see later comparison of development of living forms with the Girardeau camerates).

GIRARDEAU CAMERATE BRACHIAL GROWTH MODEL

Little is known of Br growth in living or fossil crinoids. The writer postulates the following based largely on personal observations and Bather's studies on *Gissocrinus goniodactylus* (1893, p. 167, pl. 9, figs. 328-333; 1900, p. 101, fig. 8; see also other crinoids in 1893 paper; see text-figs. 3m-o, in this paper) and *Cyathocrinus acinotubus* (1892, pp. 216-220, text-figs. 4, 5, 5a). In these cyathocrinids, immature Brr had the axial nerve cord and the food gathering structures located in a single ventral groove, with the former below the latter. During growth, the food gathering and associated structures migrated ventrally; eventually the axial nerve cord became separated from the food gathering tissues due to calcite deposition. As Br size increased, the axial canal (during growth stages when this was separated from the food groove) became higher and wider owing to resorption of calcite along its margins. Consideration of the axial canal shape and position convinces the writer that resorption probably occurred along all sides. Thus, it appears that the center (axis) of the axial nerve cord remained constant during Br growth.

In an attempt to further evaluate the pattern, a Brr growth sequence of a single individual of a Recent unidentified species of *Metacrinus* was examined. Serial grinding in the dorsal-ventral and proximal-distal planes was used to determine growth of the Brr with respect to the axial canals (Text-fig. 3). The Brr of this crinoid consist of simple uniserial pinnulate types which show moderate proximal and distal face convergence. The overall Br shape is reasonably similar to the uniserial armed Ordovician camerates studied here. As in all modern crinoids, the axial nerve cords are separated from the food gathering tissue by solid calcite. In this respect, the *Metacrinus* Brr resemble Bather's mature cyathocrinids and differ from the Girardeau camerates.

In the ventral view (Text-figs. 3a-d), the main axial

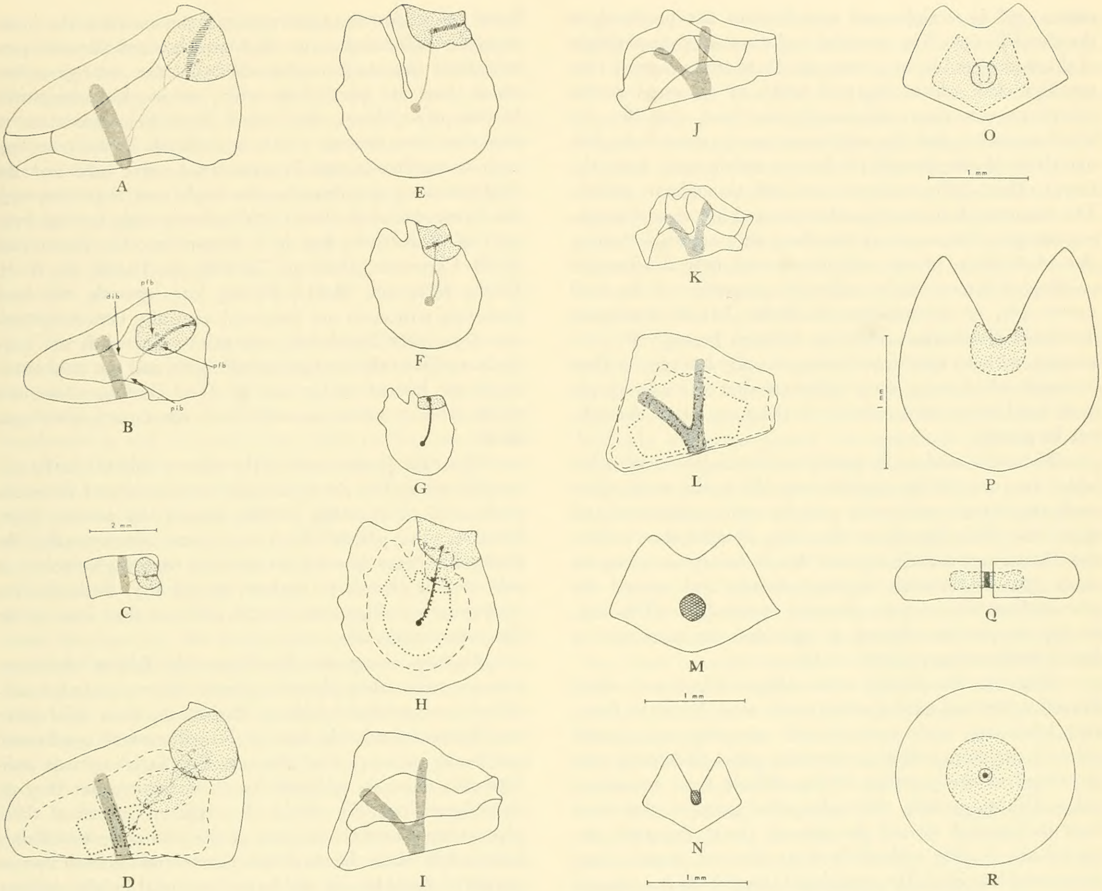

Text-figure 3. — Drawings illustrating development of Brr and columnals. A-L. Sketches showing growth of Brr dimensions relative to axial nerve cords in *Metacrinus* sp. All Brr were taken from the same individual. Smaller and less mature Brr occur near the distal arm tips; larger and more mature Brr are located closer to the calyx. For clarity, details of the articular surfaces and food grooves are omitted. A-L all drawn to same scale. A-C. Dorsal-ventral plane views. Axial nerve cords grey. On B, dib points out the distal inner branch; pib denotes proximal inner branch; pfb indicates pinnule facet branch. Pinnule facet is stippled and its transverse ridge is ruled. D. Superposition of A-C. Smallest Br outline and its nerve cords dotted; middle sized Br is dashed and the biggest is shown by a solid line. Pinnule facets stippled. Main axial nerve cords grey. E-G. Proximal-distal plane views. Symbols as in A-C. The proximal and distal inner branches directly overlie each other; the same is true of the pinnule facet branches. Consequently, these are seen as a single line. H. Superposition of A-C. Symbols as in D. I-K. Dorsal-ventral plane views of axillary Brr. Only the main axial nerve cords occur; these are shaded. L. Superposition of I-K. Symbols as in D. M-O. Proximal-distal plane views showing growth of *Gissocrinus goniodactylus* Brr. After Bather (1893, pl. 9, figs. 328-333). Modern crinoid Brr show the same type development. M-O drawn to same scale. M,N. Mature and immature Brr, respectively. Location of axial nerve cords indicated by cross-hatching. O. Superposition of M and N to show growth of Br relative to axial nerve cord. Smaller Br outline is dashed. Larger Br outline shown by the solid line. Small Br stippled. P. Proximal-distal plane views of schematic Girardeau camerate uniserial Brr, superimposed to show postulated growth of food groove. The diagram allows for some resorption of the base and sides of the food groove which was caused by increase in size of the axial nerve cord. Smaller Br is stippled with dashed outline. Larger Br shown by the continuous line. The drawing is schematic and is not designed to show the growth of any particular species. The scale indicates the approximate size. Q,R. Schematic superpositions of two columnals to illustrate postulated growth patterns. The sketches are not to any scale, and are not intended to depict any one form. Smaller plate stippled with dashed outline. Axial canal is black. Large columnal shown by solid line. Q. Side view section through axial canal. R. Plan view.

nerve cord is straight and travels from the proximal to the distal Br face. The proximal and distal Br face positions of this nerve cord lie at or near the Br width mid-point (see text-figs. 3e-h which illustrate width as measured in the Girardeau camerates; in text-figures 3a-d, the Brr are tilted somewhat and the width component toward the pinnule facet is exaggerated relative to width away from the facet). This configuration is retained throughout growth. The diameter of the main axial nerve cord increases throughout ontogeny due to resorption along all margins. Examination of the sides of the axial nerve cord tube discloses no evidence of lateral calcite resorption, migration of the axial nerve cord, or redeposition of calcite. Lateral resorption in crinoid plates can usually be detected because the pore stucture without resorbed areas is generally less regular than in nonresorbed areas. Such indicates that the axis of the main axial nerve cord remains in the same place throughout Br growth.

The main axial nerve cord gives rise to lateral branches which run toward the pinnule facet. Near the main nerve cord, two inner nerve cords may be seen, a proximal and distal one (Text-figs. 3a-c). Scrutiny of these shows that: the distal inner branch expands due to resorption along its sides. Also this branch migrates distally and toward the pinnule facet due to resorption and redeposition (Text-figs. 3a-d); the proximal branch is expanded due to resorption but it does not migrate on the Br.

Closer to the pinnule facet, the proximal and distal branches join and form a single nerve cord. Near the facet, this bifurcates, with each branch emerging on opposite sides of the pinnule facet transverse ridge. Obviously, this is related to the presence of the pinnule facet transverse ridge. During growth, the unbranched part of the nerve cord is extended toward the pinnule facet; the path traversed lies roughly midway between the two pinnule facet nerve cord branches. The two pinnule facet branches migrate outward toward the pinnule facet due to lateral resorption and redeposition. It is clear that the proximal inner branch, the unbranched part and the mean position of the two pinnule facet nerve cord branches form constant topographic reference points for the growth of a single Br (Text-fig. 3d). Thus, growth basically extends the most important elements of the previously established nervous system. In this orientation, the growth vectors (Text-fig. 3d) from maximum to minimum equal: width toward pinnule facet; width away from pinnule facet; distal height; and proximal height.

In the proximal-distal plane (Text-figs. 3e-h), the same growth model can be observed where the above axial nerve cords form the same reference points. Both the inner proximal and distal nerve cord branches and the two pinnule facet branches are not visible in the text-figures because these are parallel or nearly so in this orientation. In this plane, the growth vectors listed from maximum to minimum are: ventral, width, and dorsal. In the most immature modern crinoid Brr, the axial nerve cord and the food gathering apparatus lie in a single ventral groove, with the former below the latter (this growth stage has not been seen in *Metacrinus*, but it is known in other forms (see W. B. Carpenter, 1866, pp. 738-741, pls. 36, 41, 42; A. H. Clark, 1921, pls. 18-20). During later growth, the food gathering structures are displaced ventrally because of calcite deposition. Eventually, the axial nerve cords are fully separated from the food gathering tissue, and the axial nerve cords are housed within the Br (see Text-figs. 3m-o for cyathocrinids; modern crinoids have the same growth pattern).

The food groove axes on the ventral side of the Br run roughly parallel to the main axial nerve cord and the mean position of its branches tending toward the pinnule facet. However, the parallelism is not exact; consequently, the food groove axes do not form constant topographic points of reference in growth of modern crinoid Brr. Basically, the food groove configuration is the same as that seen in the Girardeau camerates.

Axillary ontogeny (Text-figs. 3i-l) follows the same pattern except that pinnules, pinnule facets, and the associated nerve cords are lacking. Rather, the main axial nerve cord bifurcates near the base of the axillary with one branch continuing on to each of the next Brr. Serial sections indicate that these are widened due to resorption, but they do not migrate laterally within the axillary. Growth of these plates simply extends the axes of the previously established nerve cords. Here, the maximum to minimum growth vectors consist of distal height, width, and proximal height. Axillary food groove axes directly overlie the axial nerve cord axes or nearly so.

The Br growth model applied to the Girardeau camerates is an extrapolation of that of the cyathocrinids and modern crinoids. In these camerates, the axial nerve cord was not separated from the food groove. By analogy with modern crinoids and immature cyathocrinids, this structure lay at the base of the food groove of a camerate Br.

Examination of the young and adult uniserial Brr of *Ptychocrinus splendens* (Miller), *Glyptocrinus dyeri* (Meek), *Eopatelliocrinus latibrachiatus*, n. gen., n. sp. (see Text-fig. 8h) and other species discloses basically Y-shaped food grooves in ventral view. The proximal leg of the Y continues from the previous Br; one of the distal legs proceeds to the next Br. Hereafter, these are designated "brachial food grooves". The other distal leg leads to the pinnule facet ("pinnule facet food groove"). In uniserial armed crinoids, this food groove is somewhat curved (convex distally) where it branches from the "brachial food groove". The "brachial food grooves" are always straight and lie at angles to each other. In the camerates examined, presumably the axial nerve cords were housed at the base (axis) of these food grooves. The food groove axis always underlies the center of the whole food groove as seen in ventral view.

The following axial nerve cord homologies are postulated between the living *Metacrinus*, cyathocrinids, and the camerates studied: 1. The metacrinid main axial nerve cord is clearly homologous with the axial nerve cord of the cyathocrinids and the axial nerve cord at the base of the "brachial food grooves" in the camerates. 2. The camerate "pinnule facet food groove" axial nerve cord is homologous with several of the metacrinoid nerve cords, *i.e.*, partly with the proximal inner nerve cord branch, partly with the unbranched portion of the metacrinid nerve cords and partly with the mean position of the two metacrinid pinnule facet nerve cord branches. The latter homology is not critical because this branch in the metacrinids is clearly related to and correlated with the presence of a transverse articular ridge on the pinnule facet. The camerates studied lack this transverse ridge and consequently the problem does not arise. The homology between the metacrinid proximal inner branch and the inner part of the camerate "pinnule facet food groove" nerve cord is most critical to the growth model. This homology is suggested by: A. Comparison of topographic position of the two structures. Clearly the orientation of the proximal inner branch of the metacrinid is more comparable to the inner part of the camerate "pinnule facet food groove" nerve cord than is the metacrinid distal inner branch (compare Text-figs. 3a-d with 8h). B. In the metacrinids, the proximal inner branch remains in a constant topographic reference point throughout ontogeny, whereas the distal inner branch migrates laterally on the Br. C. In the metacrinids when one of the inner nerve cord branches is absent, invariably this is the distal one and never the proximal branch. Missing distal inner nerve cord branches occur in about 10% of the metacrinid Brr studied, suggesting that the proximal inner nerve cord branch is functionally more important and perhaps phylogenetically older than the distal branch. Pinnules and pinnule facets are lacking in the cyathocrinids previously discussed. Consequently, these crinoids lack structures homologous with the "pinnule facet food groove" nerve cords of the camerates.

In view of the above geometry and homologies, the bases of the camerate "brachial food grooves" and the "pinnule facet food grooves" which housed the axial nerve cords are believed to have constituted constant topographic points of reference during ontogeny of a single Br. Probably Br accretion simply extended these structures. Significant lateral resorption did not occur, although some dorsal and marginal resorption associated with the increase in diameter of the axial nerve cords was probably present at the base of the food grooves (Text-fig. 3p). Clearly, this was not significant relative to the overall Br dimensions.

This growth model is applied to uniserial camerate Brr with a relatively high degree of certainity (see ontogeny of *Eopatelliocrinus scyphogracilis*, n. gen., n. sp. for discussion of the method of application of the model to uniserial Brr). Probably the same general developmental pattern existed throughout most of the biserial Br growth (*i.e.*, during both the uniserial and biserial stages). If the writer's hypothesis for biserial Br ontogeny is correct, widespread resorption of one of the Br sides and lateral migration and resorption of the "pinnule facet" axial nerve cord occurred when the Br changed from the uniserial to biserial configuration (see *Macrostylocrinus pristinus*, n. sp. for details).

In the camerates the above growth model seems to have been basically designed to limit the Br growth rates toward articular surfaces (*i.e.*, proximal and distal Br surfaces and pinnule facets) as much as possible within the limits imposed by the basic geometry (see later discussion) and to minimize migration of the axial nerve cords. In the camerates examined here, the food groove became wider and deeper during ontogeny. This was largely caused by ventral extension of the sides of the Br flanking the food groove and not resorption (Text-fig. 3p). As previously mentioned, some calcite resorption, associated with increase in diameter of the axial nerve cords, probably occurred at the base (axis) of the uniserial Br food grooves and in the transitional (uniserial to biserial) stage of biserial Br growth. However, this was minor relative to the overall pattern. Thus, the growth model for Brr resulted in the minimum possible interference with the axial nerve cords.

In many cyathocrinids and Recent crinoids, the main parts of the axial nerve cords remain constant, although some plate resorption takes place due to progressive increase of the axial nerve cord diameter. Basically, the food grooves migrate ventrally with respect to the axial nerves (Text-figs. 3m-o).

This relationship between the growth of all crinoid plates and the nervous system cannot be overstressed. Living and presumably fossil crinoids possess a three-level nervous system. For a summary of the nervous system of modern crinoids, the reader is referred to Nichols (1962, pp. 22-29), Hyman (1955, pp. 61-63), Cuénot (1948, pp. 40-44), W. B. Carpenter (1884), and P. H. Carpenter (1884, pp. 111-127). The lowest (most proximal) level is the aboral nervous system. This comprises the predominant level and apparently controls posture (bending the stem and flexing the arms) and other basic reactions (Nichols, 1962, p. 29; A. R. Moore, 1924). The two surficial nerve nets consist of the surficial oral or ectoneural net and the hyponeural or deeper oral nervous system. These are rarely preserved in fossil material. Apparently, these determine movement of the tube feet and covering plates. Also the three crinoid nervous systems are interconnected. Essentially, a single three-tiered complex is present in which the aboral level predominates.

Growth of the camerate calyx and Br plates was adjusted to cause minimum interference with the aboral nervous system within the available geometrical limits of the structure. For example, deposition of calcite on the inside of a dorsal cup plate or the base of a camerate Br food groove could have disrupted and interfered with the fragile aboral nerve cords. The adaptative significance of this pattern to a Paleozoic echinoderm where the aboral nervous system was the predominant level is obvious. Perhaps, this was one of the major factors which contributed to the success of crinoids relative to other contemporary stem bearing echinoderms.

The development of modern crinoid calyx plates and Brr poses special problems of regulation, integration and coordination of growth. These are discussed briefly under comparison of the Girardeau camerates and Recent crinoids.

TEGMEN PLATE GROWTH MODEL

Little is known of the development of these plates which are critical to crinoid ontogeny. The available information is summarized under *Macrostylocrinus cirrifer*. Basically, the growth model is the same as that postulated for dorsal cup plates except that most of the tegmen plate insides were not in contact with any of the crinoid nerve levels. Resorption of tegmen plate margins does not appear to have been common. If such occurs, it is probably confined to the tegmen plates in the vicinity of the arm bases and perhaps the OO.

COLUMNAL GROWTH MODEL

During development of most living and fossil crinoids, new plates form in the stem. Typically some of these are initiated immediately below the calyx whereas others grow between previously present columnals. In a few crinoids (*e.g., Pisocrinus*), all columnals developed just distal to the calyx. Although the writer has not studied the columns of Recent or fossil crinoids in any great detail, a general pattern of ontogeny can be presented.

The basic columnal growth model (see Text-figs. 3q, r) follows that of Brr and calyx plates. The axial nerve cord penetrates the center of the columnals and passes through the axial canal. As in other plates, the axis of this structure forms a constant topographic reference point. During ontogeny, the axial canal diameter is augmented by marginal resorption. After formation, the height and width of individual columnals typically increase. This can be documented for living forms, such as *Antedon bifida* pentacrinids (Sir Wyville Thompson, 1865, pp. 538, 539), and for fossil species, like *Pisocrinus* cf. *campana* from the Pentland Hills, near Edinburgh, Scotland, and the Girardeau camerates. The principal calcite accretion direction is outward (*i.e.,* peripheral width). This growth vector greatly exceeds those of proximal and distal height. This is clearly shown by the growth lines in the transverse and longitudional columnal sections illustrated by Moore, Jeffords, and Miller (1968, pl. 2, figs. 1, 2; see also pl. 3; various illustrations in Moore and Jeffords, 1968, and Jeffords and Miller, 1968). Brief study of cirrus bearing columnals (branches of the column axial nerve cord extend into the cirri) indicates that the proximal and distal height growth rates are equal or nearly so. The above mentioned illustrations seem to denote symmetrical proximal and distal height growth rates in columnals which lack cirri. For more detail on column and columnal growth, the reader is referred to Moore and Jeffords (1968), Jeffords and Miller (1968), Seilacher, *et al.* (1968), Termier and Termier (1949), Biese (1927), Bather (1900, pp. 105-108, 131-136), and Wachsmuth and Springer (1897, pp. 39-52).

As previously mentioned, large parts of the Girardeau camerate stems were flexible. The amount of flexibility is measured by the radius of curvature shown by the column at various places; Seilacher, *et al.* (1968) have used the same procedure in their comparative studies on *Seirocrinus* and *Encrinus liliiformis* Miller (see section on paleoecology and Seilacher, *et al.,* 1968, for functional significance). In the conventional attached Girardeau camerates and living isocrinids (*e.g.,* some *Isocrinus decorus* and various others) examined by the writer, the maximum flexibility generally occurs in the middle 67 to 75% of the column. Relatively rigid stem segments are associated with the rooting device (not present in the isocrinids seen) and immediately below the calyx. The same was true of *Encrinus liliiformis* (see

Linck, 1954, 1965; Seilacher, *et al.,* 1968). With a certain articular type, column flexibility is mainly a function of the ligament volume relative to the external columnal volume; it increases as the ligament volume/external columnal volume ratio rises. Crinoids possess three basic ways of retaining a flexible stem.

1. As recently pointed out by Seilacher, *et al.* (1968) the width growth vector of the columnals tends to decrease the column flexibility; conversely, the intercalation of new columnals increases flexibility. In the Girardeau camerates and isocrinids mentioned above, flexibility of the middle part of the stem is largely maintained by intercalation; the decrease in flexibility of the distal area of the column (associated with rooting device) is mainly caused by the columnal width growth vectors and lack of intercalation of new columnals. The relatively rigid proximal stem area (immediately below the calyx) is due to wide columnals and a low rate of new columnal initiation. As usual in crinoids, some of the Girardeau camerate columnals formed just below the calyx whereas others developed between previously formed columnals. Most of the Girardeau camerate columnals, 50% or more, were initiated by intercalation. Although this has not been examined in the living isocrinids, a similar growth pattern probably exists. In the Girardeau camerates, the adjacent columnals are united by crenulate sutures; the columnal articular surfaces are relatively flat and not strongly depressed. The volume of the ligaments and axial canal of an immature Girardeau camerate columnal ranged approximately 10% of the external columnal volume. The equivalent value for a mature plate equalled only about seven percent. Clearly, the ligament volume/external columnal volume ratio was larger for the immature columnals of the Girardeau camerates. Probably this also holds true for most crinoids with similar stems.

2. All columnals of *Pisocrinus* cf. *campana* S. A. Miller from the Silurian, near Edinburgh, Scotland, (Brower, in preparation) formed just below the calyx. Immature columnals are thin and disk-shaped. The volume of the ligaments relative to external columnal volume is uncertain, but it clearly did not exceed seven percent. During later growth, height and width of the columnals were augmented and the mature columnals are barrel-shaped. The height growth allowed the development of strongly depressed articular surfaces with large ligaments which occupied roughly 8.5% of the external columnal volume. The observed bends in the stem indicate that the maximum flexibility was associated with the barrel-shaped columnals. The distal part of the *P.* cf. *campana* stem is unknown. The growth of these depressed articular surfaces was not due to resorption. Rather, the height augmentation vectors increased toward the outsides of the columnals; consequently, depressed articular surfaces were formed.

3. Most species of *Woodocrinus* seem to have combined the two mechanisms. Intercalated columnals are common and the mature columnals developed depressed articular surfaces (Brower, in preparation; isolated *Woodocrinus* columnals have never been illustrated; see Wright, 1950-1954, pls. 20-29 for external views of stems).

INTEGRATION AND COORDINATION

In simple minded fashion, three processes are seen in Recent and fossil crinoid ontogeny: 1. Development of new plates (see later section on the sequence of plate initiation); 2. Calcite accretion and increase in size of the previously formed plates; 3. Resorption of plates or parts thereof. Examples are the resorption of the *Antedon bifida* iRR (discussed later) and resorption along the axial canal margins of Brr as previously mentioned.

When the BB, RR, and OO first develop in a young Recent crinoid, these are isolated from one another and not in lateral contact. At this time, the plates of a single circlet are commonly somewhat irregularly arranged and the individual plates show wide variation in size and shape (see for example, the BB and OO in *Antedon bifida* illustrated by A. H. Clark, 1921, figs. 1181, 1189). This suggests that the growth of a certain plate is poorly coordinated and integrated with the other plates in the same or adjacent circlets during this growth stage.

Calcite accretion eventually brings all of the adjacent, subadjacent and superadjacent calyx plates and Brr together. For example, in *Comactina meridionalis,* the major calyx plates are largely joined together by the time the proximal IIBrr appear (see Springer, 1920, pl. B, figs. 7-10). Presumably, the Girardeau camerates developed in the same general fashion. These earliest growth stages are not preserved; the youngest Girardeau crinoids examined have all calyx plates and Brr in lateral contact. Once the plate lateral margins of living and fossil species join, the plate growth becomes better coordinated and integrated.

At this time, the camerate crinoid calyx was composed of a series of adjacent plates which enclosed the viscera. "Holes" were located at strategic points where the food grooves entered the tegmen, where the axial nerve cords penetrated the stem, and for the anal opening. Growth of the individual plates must have been adjusted so that this configuration was maintained. Otherwise, gaps would have developed between adjacent plates and the skeleton would no longer have supported the soft tissues. Thus if one plate increased in size, its neighbors must have done the same.

Growth gradients were complex and probably varied in time (see previous remarks on growth lines).

Nevertheless, the geometric requirements necessary to prevent gaps from developing between adjacent plates present an approach to growth. A correlation matrix provides data as to the degree of integration and coordination between the adjacent, subadjacent, and superadjacent plates necessary to have retained the plates' surfaces in opposition to each other. Macurda (1968) applied this approach to *Eucalyptocrinities*. Possibly a scaled covariance matrix (*i.e.*, each variable adjusted to a range of 1.0) might serve a similar purpose although this was not attempted here. Unfortunately, the Girardeau camerate data are not sufficient for this purpose, because complete measurement sets on the calyx plates cannot be obtained from all individuals in the growth sequences. Study of a more complete data matrix in *Hybocrinus punctatus* (Miller and Gurley) shows correlation (*i.e.*, integration and coordination) gradients. In this form, the dimensions of a given dorsal cup plate correlate best with those of the directly adjacent, subadjacent and superadjacent plates and less well with the plates which are farther away. These integration requirements apparently require or are simplified by linear growth relations. For example, in the Girardeau crinoids, the development of almost all of the calyx plate dimensions relative to "size" followed linear patterns. Similarly, the growth of width of a certain plate with respect to its height was always linear. Exponential regression lines are never observed for the major calyx plates (*i.e.*, RR, IBrr, proximal iBrr and anals); however, the column facet and possibly the fixed IIBrr exhibited exponential growth in several forms. Blastoids were also mainly characterized by linear development, although a few examples of exponential growth of different parts of a single plate are known (Macurda, 1966).

In the Girardeau camerates, FBrr were added to the dorsal cup throughout ontogeny. Prior to fixation, these functioned as free Brr. Once incorporated, they behaved as calyx elements and their growth was highly integrated and coordinated with the adjacent calyx plates.

A growth sequence of internal molds of *Macrostylocrinus cirrifer* Ramsbottom (see ontogeny of this species for more detail) allows the relationship between dorsal cup plate growth and the aboral nervous system, which may be traced by means of ridges on the internal molds, to be determined. Throughout ontogeny, the nerve cords became wider and deeper due to marginal resorption. Accretion of the adjacent calyx plates was arranged so that plate growth simply extended the previously established aboral nervous system. Any other configuration would have resulted in the development of gaps between the adjacent dorsal cup plates; clearly, these gaps did not develop. Such suggests that the aboral nervous system was indirectly responsible for the integration and coordination of dorsal cup plate ontogeny and thus, prevented the formation of gaps. The ultimate control is believed to have been mesenchymal. Most tegmen plates were not in direct contact with any of the crinoid nerve levels. Yet the growth of crinoid tegmens seems to have been highly integrated and coordinated. Probably, integration and coordination of the tegmen and tegmen plate growth was completely regulated by the mesenchyme.

In Recent *Antedon*, the surficial oral or ectoneural nervous system first appears in the fourth week of growth and is more advanced in the next week (A. H. Clark, 1921, p. 485). Although few data are available, this level may give rise to the deeper oral or hyponeural nervous system. The aboral nervous system seems to form a little later where it may be determined around the chambered organ during the sixth week (A. H. Clark, 1921, p. 499). At any rate, the endoskeleton is well developed and consists of BB + OO + IBB + columnals + RR at this time. Thus, the aboral nervous system develops prior to the appearance of arms. Obviously, the initial growth stages of the above plates which first form about 100 hours after birth cannot be controlled, directly or indirectly, by the aboral nervous system which does not appear until five weeks or so later. Raup (1966, p. 393) suggested that echinoderm plate geometry (*i.e.*, shape and position) is controlled by the configuration of the mesenchyme cells which, in turn, is controlled by its physical relation to the overlying epidermis.

This conclusion seems valid for the youngest crinoids. In adult Recent crinoids, the ectoderm is poorly developed, consisting of a thin syncytial layer which is almost absent in some forms. In addition, this layer is not sharply differentiated from the underlying mesenchyme and the two layers grade into each other (Hyman, 1955, p. 48). The degeneration of the epidermis may be traced back in the larval development of *Antedon* to the fifth day and perhaps earlier (see A. H. Clark, 1921, pp. 464, 483). Such indicates to the writer that the ectoderm of *Antedon* is unable to control skeletal development after the early larval development, although the exact point of no return is not evident. Inasmuch as growth of modern crinoids and the camerates follows the same basic pattern, these findings are extrapolated to the fossil forms.

Consequently, the following conclusions are made. 1. Plate geometry and growth of the youngest crinoids is basically determined by the physical relationship of the mesenchyme to the ectoderm as suggested by Raup. 2. In older animals the aboral nervous system indirectly integrates and coordinates the arm and dorsal cup plate growth. The control is probably indirect and operates by means of the physical relationship of the aboral nervous system to the surrounding mesenchyme. When the transition from ectodermal to mesenchyme and aboral nervous system control occurs is not known. Possibly the transition occurs before or during the appearance of IBrr. As later mentioned, the embryonic IBrr1 possess an axial nerve cord (*i.e.*, armward extention of aboral nerve cord). Certainly the transition would be expected prior to the development of IIBrr. 3. Growth of tegmen plates is most likely controlled by means of their relations with the surrounding mesenchyme. 4. The hypothesis should be considered highly tentative. Far more work on the physiologic aspects of modern crinoid ontogeny is required before a definitive model can be presented.

Intuitively, one would expect the Br ontogeny to be somewhat less well integrated and coordinated than that of the calyx plates. In the case of most calyx plates (BB, RR, FBrr, iBrr and anals), all margins are in contact with those of adjacent plates and only the inner and outer sides are not opposed by other plates. The Brr situation is greatly different. In dorsal view a pinnulate uniserial Br possesses five sides. Two of these are free while the other three, proximal and distal Br faces and pinnule facet, are bounded by other plates. The dorsal side of the plate is free while the ventral face bears the food and axial canal grooves (in camerates), the sides of which are in contact with two rows of covering plates. A biserial Br (see Text-fig. 2 for diagram and terminology) exhibits six sides in dorsal view, of which only one side (outer side below pinnule facet) is not bounded by adjacent plates. In ventral view, the Br only bears half of a food groove; the other half of the food groove is shared by the two adjacent Brr on the opposite side of the arm. Consequently, the Br only has one row of covering plates along the food groove margin. As with uniserial Brr, the dorsal side is free.

Comparison of the degree of integration and coordination of the Brr versus the calyx plate dimensions and "size" is difficult owing to the nature of the data. Generally complete sets of Brr measurements can be derived from all arm bearing individuals in the ontogeny sequences. However, this is not possible for the calyx plate dimensions because of the state of preservation. Thus, when comparing correlation coefficients, different degrees of freedom are generally encountered in the arms versus the calyx. Although definitive conclusions cannot be presented, the following generalizations are observed for Girardeau camerates.

1. Probably the best way to compare the Brr versus the calyx plate degree of integration and coordination with the available data is by means of correlation coefficients with respect to "size". If this reasoning is valid, then the Br dimensions were marginally less well integrated and coordinated with "size" than were the calyx plates. Nevertheless the overall Brr ontogeny was well integrated with "size" growth (see regression and correlation data for the various species).

2. In the ontogeny of the dorsal cup plate dimensions verus each other and "size", the equation growth rates relative to the plate dimensions or "size" are generally large. Consequently, high correlation coefficients are observed where adequate data are available. On the other hand, the Br growth rates with respect to the other Br dimensions and "size" were variable. For example, the highest Brr growth rate invariably consisted of width; high correlations are seen where this variable is involved. Conversely the small minimum height growth rate always results in much lower correlations. Thus, the general Brr trend is for high correlation coefficients to be associated with high growth rates (see discussion of the various species for more details). With the exception of minimum height, the Br dimensions are highly correlated with each other; on an average basis these correlations are only slightly less than those of the height and width of a single calyx plate.

3. Commonly, the development of one Br dimension versus another or "size" followed an exponential pattern. For example, the maximum and minimum height growth rates in some species showed an exponential decrease with respect to constant Br width increments throughout ontogeny. Apparently, this developmental geometry was possible because the Brr are not bounded by adjacent plates on all sides as are the calyx plates.

4. The mechanism of Br integration and coordination was the same as that for dorsal cup plates.

Ontogeny of the column and pinnulars of the Girardeau crinoids has not been investigated quantitatively in all species. Consequently, conclusions on integration and coordination cannot be presented. Probably the general pattern was similar to the large growth rate (relative to dimension concerned) Brr dimensions.

PLATE GROWTH SEQUENCE IN MODERN CRINOIDS

Plate growth sequences are well known in numerous living crinoids, for example, *Antedon bifida*, *A. mediterranea* *A. adriatica* A. H. Clark, *Comactina meridionalis*, *Promachocrinus kerguelensis*, *Hathrometra sarsii*, and various others. Most knowledge of the early larval development is derived from *Antedon adriatica* and *A. mediterranea,* whereas the later growth stages are best seen in *A. bifida, Comactina meridionalis, Promachocrinus kerguelensis,* and *Hathrometra sarsii.*

The following discussion emphasizes the plate development and the sequence thereof. This is principally summarized from A. H. Clark (1921, pp. 431-590 and cited illustrations) and Springer (1920, pp. 79-87, pls. B, C on *Comactina meridionalis*). Details of the individual plates growth are found in A. H. Clark (1915, pp. 194-382; 1921, pp. 1-368). For *Antedon bifida,* Sir Wyville Thompson (1865) and W. B. Carpenter (1866, 1876) should be consulted. For discussion of soft part development, the reader is referred to A. H. Clark (1921, pp. 431-590) for detailed treatment and to Hyman (1955, pp. 75-87) for an excellent summary. Text-figures 4 and 5 present data on the development of plate circlets versus "size", time-size growth rates, and time-size plate circlet development.

In the youngest skeleton bearing larvae, the BB, OO and several columnals occur; these are initially seen in individuals of *A. mediterranea* early in the sixth day of growth. At first, the plates consist of small reticulate or spicular networks of calcite arranged in rather erratic fashion. During later growth, calcite accretion occurs and the BB and OO become organized into more regular circlets. Great variation in plate size and shape is observed in this growth stage, especially in the earlier phases.

In *A. mediterranea,* the IBB appear next at the beginning of the seventh day. Generally three IBB are found but individuals with four or five are known. The time-plate circlet growth rates of *A. adriatica* are more rapid and 100 hour larvae possess BB + OO + IBB and about 11 stem plates. Larvae with only BB + OO + stem plates are unknown; apparently all these plates develop rapidly. The IBB may or may not be present in comatulids; for example, five IBB occur in *A. adriatica* and *Promachocrinus kerguelensis,* three in *Antedon mediterranea,* and none in *A. bifida* and *Comactina meridionalis.* The IBB may or may not be found in *Hathrometra sarsii.* In modern crinoids with IBB, the fate of these plates differs greatly from that seen in the Girardeau camerates. During growth, the Recent crinoid IBB become arranged in a circle around the chambered organ, after which the IBB fuse with each other and the proximal columnal to form the centrodorsal. In *Antedon adriatica,* this process is well underway in 110 hour larvae.

Growth of the RR circlet (RA + RR) constitutes the next stage. Here various sequences may be observed. Prior to the appearance of this circlet, rhomboidal gaps occur between the BB and OO in radial orientation; the RR circlet develops within these gaps. At first, the adjacent RR are isolated from each other; during later growth, accretion occurs and these plates eventually come into lateral contact in most modern crinoids. The RA is the first RR circlet plate to form in *Comactina meridionalis* and *Promachocrinus kerguelensis* and is followed by the RR (Text-figs. 4a, c, 5d). In *Hathrometra sarsii,* the RR appear first and are nearly in lateral contact prior to formation of the RA. The RA of *Antedon bifida, A. mediterranea,* and *A. adriatica* is not seen until the IBr2 begins to develop, although the RR are not yet in contact.

Homology of the living crinoid RA with the posterior interray plates of fossil crinoids is somewhat uncertain. As noted by Springer, the RA of *Comactina meridionalis* is attached to or closely associated with the gut. He concluded that the modern crinoid RA is homologous with the flexible crinoid RA based on recapitulation and phylogeny of flexibles.

The writer suggests that the modern crinoid RA is homologous with the camerate primanal; this is largely evidenced by ontogeny, phylogeny, and functional morphology. Comparison of the ontogeny of *Comactina* and other living crinoids and presumed camerate phylogeny is considered first. One might question the citation of evidence based on recapitulation in support of homology. As discussed later (see sections on phylogeny), crinoids, at least those examined by the writer, seem to have evolved by means of changes affecting the ontogeny of the ancestral stocks; these changes involved the acceleration or deceleration of growth rates of certain parts of a plate or series thereof, the displacement of plates relative to other plates, the addition or loss of plates, and various other changes. Consequently, "recapitulation" is believed to constitute valid evidence for homology in crinoids. In *Comactina* when the RA is first observed, it lies between the distal margins of the CD and BC interray BB (Springer, 1920, pl. B, figs. 1-3). A similarly located primanal is unknown in camerates. Later in comactiniid growth, the RA rests on the truncated CD interray B and between the C and D ray RR (Springer, 1920, pl. B, fig. 7). The primitive camerate primanal is found in this position. Eventually, the comactiniid RA is displaced out of the RR circlet. At this time the RA is found in a notch between the distal margins of the C and D ray RR (Springer 1920, pl. B, figs. 8-10, pl. C). This position corresponds to the primanal orientation of more advanced camerates. In numerous primitive camerates, the CD interray is protuberant and wider than the other interrays. This, in conjunction with the anal opening position (*i.e.,* at top of anal series leading from primanal), suggests that the

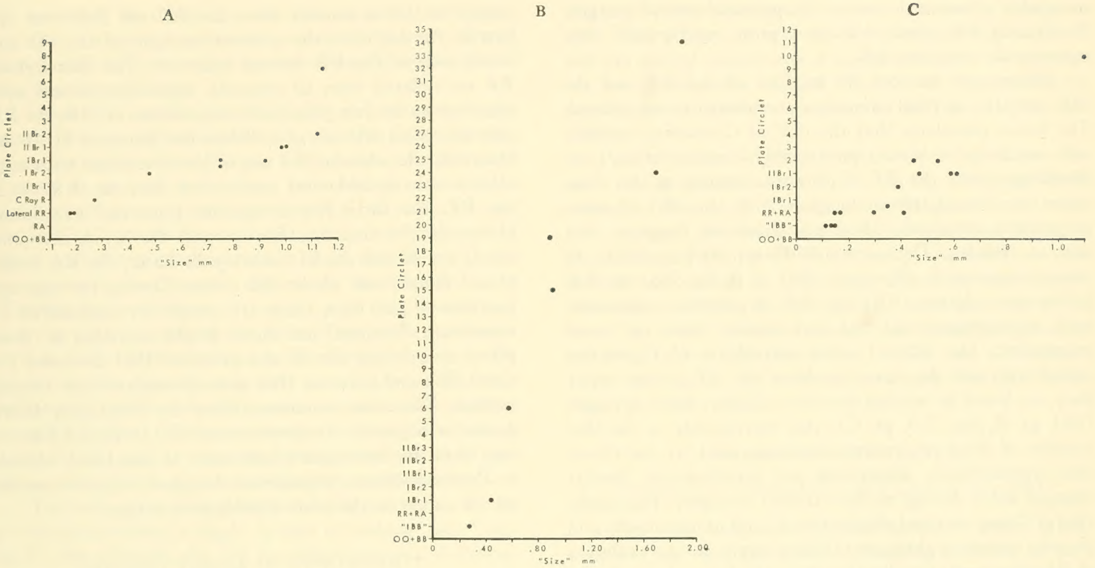

Text-figure 4. — Graphs showing "size" versus plate circlet growth patterns in various Recent crinoids. Horizontal axis is "size". Vertical axis gives plate circlets in order of appearance. RA grouped with RR in A and B. A. *Comactina meridionalis.* Data from Springer (1920, pp. 79-82, pls. B and C). B. *Hathrometra sarsii.* Data from Clark (1921, pp. 564-574, figs. 407, 413, 530, 534, 536, 537, 539-542, 1216-1225). C. *Promachocrinus kerguelensis.* Data from Clark (1921, pp. 530-557, figs. 881-937).

gut was either attached to the primanal or was in contact with the proximal CD interray plate. Protuberant CD interrays of this type are observed in all Girardeau camerates except *Culicocrinus* ?. Admittedly this homology is highly suggestive and speculative. At any rate, the homology is not unduly important to the observed Girardeau camerate ontogenies and will not be further discussed.

The first arm plates to appear are the IBrr1; these are followed by the IAxx and the proximal IIBrr, IIBrr1, then IIBrr2, and so on. New Brr always develop at the distal arm tips, never between previously formed arm plates. This process continues throughout life of the crinoid, although at various rates. New Brr are added rapidly (relative to time) until the adult stage is reached. In comatulids, the rapid phase seems to begin fairly late in the pentacrinid stage and continues for an uncertain period after the stem is cast off. In the adult stage the time-Brr addition rates decrease to almost nil (A. H. Clark, 1915, pp. 197, 198); here most arm growth involves calcite accretion of the previously developed Brr.

In modern crinoids, calcified pinnules do not form until after the arms are well developed. The first pinnule of *Hathrometra sarsii* is seen when about IIBr14 is present; in *Antedon bifida,* pinnules occur along with the IIBrr12. The first formed pinnules are on the arm tips; these are followed by the proximal (oral) pinnules on IIBr2. After these, the intervening ones appear. Pinnule calcification occurred earlier in the Girardeau camerates. The smallest Girardeau individuals are about 1.0 to 1.3 mm in "size", possess four to nine IIBrr per arm, and show a full complement of calcified pinnules.

Development of the modern crinoid iRR is highly variable. These form after IBr2 is well developed, when they appear in gaps between the adjacent RR of *Comactina meridionalis.* By the time the proximal IIBrr are observed and the RR are in lateral contact, the iRR have been displaced to an iBr1 position above the RR circlet and in the proximal part of the tegmen. In *Antedon bifida,* the iRR develop at about the same time relative to plate structure but are soon rsorbed. The iRR of *Promachocrinus kerguelensis* are not seen until after the RR are in lateral contact and about five IIBrr are present. These are initiated as small triangular elements between the proximal-lateral margins of adjacent RR, after which they grow rapidly until they separate the adjacent RR.

Homologies between the modern crinoid iRR and the iRR and iBrr of fossil camerates are somewhat conjectural. The writer postulates that the iRR of *Comactina meridionalis* and *Antedon bifida* (questionably *Promachocrinus*) are homologous with the iRR of primitive camerates; also these plates are considered homologous with the iBrl of more progressive camerates. These postulates are based on two lines of evidence. The topographic positions are similar. In young comactiniids (Springer, 1920, pl B, fig. 5b), the iRR lie between adjacent RR; the iRR of primitive camerates, such as archaeocrinids and xenocrinids, show the same orientation. The iRR of older individuals of *Comactina meridionalis* are displaced to above the RR circlet where they are found in notches between adjacent RR (Springer, 1920, pl. B, figs. 7-9, pl. C); this corresponds to the iBrl position of more progressive camerates, such as the Girardeau ptychocrinids, alisocrinids and patelliocrinids. Similar changes occur during modern crinoid ontogeny (especially that of *Comactina* and similar forms) and in monocyclic and dicyclic camerate phylogeny. For example, in the evolution of *Rhaphanocrinus* to *Ptychocrinus*, the basic change is the displacement of the iR to an iBrl position (see discussion of ptychocrinid phylogeny for more details); the same occurs in comactinid growth.

During ontogeny, new plates continue to develop in the stem. These form just below the calyx and between previously present columnals.

Three main processes may be observed in the growth of living crinoids: development of new plates; calcite accretion and increase in size of the previously formed plates; and resorption of plates or their parts. Examples are the resorption of the *Antedon bifida* iRR and resorption along the axial canal margins of Brr and columnals as previously mentioned.

When the living crinoid plates first appear, these are separated from the adjacent plates and are not in lateral contact. Throughout later ontogeny, the previously formed plates increase in size due to calcite accretion and new ones are formed. Eventually all of the plates come into lateral, vertical-lateral and vertical (*i.e.,* proximal-distal axis) contact, although the time of this event varies from crinoid to crinoid and plate to plate. Generally, in any one species or individual, the earliest formed plates are the first to come into contact. *Comactina meridionalis* (see Springer, 1920, pls. B, C) is chosen as the prime example because the writer has seen most of the material; similar sequences occur in most other forms. The BB and OO (if closed) are largely in lateral contact when the RR and RA have appeared. At this time, the proximal margins of the OO and distal ends of the BB remain separated. The first formed RR are isolated from all adjacent, superadjacent and subadjacent plates. Just prior to the appearance of iRR, the RR join the distal BB margins. When the proximal IIBrr are observed, the adjacent RR are in lateral contact with each other and in distal-lateral conjunction with the iRR. As in the RR, the early RA is separate from the neighboring plates. By the time the IBrr are well developed, this joins the C ray R and the CD interray B. Later, the RA is displaced distally out of the RR circlet. During the first appearance of the IBrr, these are completely surrounded by mesoderm. Proximal and distal height accretion of these plates soon brings the R and proximal IBrl face and the distal IBrl and proximal IBr2 articular surfaces into vertical contact. The same situation affects the developing IIBrr. A similar sequence of contacts occurs in *Antedon bifida* except that the individual plates seem to join later, whereas in *Promachocrinus kerguelensis* the plate contacts are observed earlier in the plate development stages.

TIME-GROWTH OF RECENT CRINOIDS

Little is known of time-size and time-plate circlet growth rates in living forms. Text-figure 5 summarizes some of the available data; these are largely self-explanatory and only a few comments will be made here.

A. H. Clark (1921, pp. 530-537) studied a growth sequence of 43 individuals assigned to *Promachocrinus kerguelensis* of varying sizes and ages collected at all times of the year around Gaussberg, Antarctica, in 1902 and 1903. He concluded the following time-growth rates. Spawning occurs in mid-September or early October. At the end of the first five months (February), the RR appear and show considerable growth by April. When the crinoids are about one year old (November), the IBrr have formed. In the following September to January (about two years), the RR are in lateral contact and the proximal IIBrr are present. The crinoids have about 30 IIBrr and are ready to cast off the stem when about two and one half to three years old.

For several reasons these growth rates seem far too slow; by analogy with the time-growth rates of other cold water marine invertebrates which have pelagic larval stages, and by analogy with the time-plate circlet growth rates in other crinoids (see later discussion). Consequently, the time-growth rates shown for *Promachocrinus kerguelensis* in Text-figures 5b and d are adjusted so the IIBrr30 crinoid is about one and one half to two years old. Fell (1966, p.

49) estimated the life span of the species at about 20 years and that maturity is attained at roughly 10 years. Based on the amended pentacrinid growth rates, the writer postulates roughly a 15 year life span.

Time-plate circlet and time-size growth rates vary greatly between different species. In *Antedon bifida*, spawning occurs at the end of May or early June and the crinoid is ready to cast off the column and terminate the pentacrinid growth stage in mid-September (Sir Wyville Thompson, 1865). Thus the microcrinoid (prior to development of arms) and the pentacrinid (with arms and stem) stages occupy about three months. Apparently *Hathrometra sarsii* (Text-fig. 5c) reproduces in June as eggs have been found in the genital pinnules at this time. The pentacrinid stage is terminated by March through May of the next year. By far the slowest growth rates are seen in *Promachocrinus kerguelensis* which probably spawns around mid-September or early October. Individuals ready to discard the column are found in June. As postulated here, the microcrinoid and pentacrinid growth stages encompass about 20 months.

The wide variation of time-size and time-plate circlet growth rates within a single species is striking (see Text-fig. 5). For example, the 130 day old individuals of *Promachocrinus kerguelensis* range in crown height from .3 to 1.0 mm and in plate circlet from the BB + OO + IBB to young pentacrinids with the IIBr2 developed. Similar variability characterized *Hathrometra sarsii* where the 30 day old crinoids may have only the OO + BB up to IIBrr6 pentacrinids with the "size" interval consisting of .27 to .58 mm.

The few available data suggest that time-size growth rates in modern crinoids fit the common marine invertebrate "slow-fast-slow" model. "Slow" growth rates seem to occur throughout the microcrinoid growth phase and well into the pentacrinid stage. Apparently, the "fast" growth is initiated just prior to loss of the column. When these growth rates are terminated is uncertain, but probably these end at or immediately prior to maturity. Older crinoids are characterized by "slow" time-size growth rates. The transition from the initial "slow" to the "fast" growth rates is illustrated in Text-figure 5. The change from the "fast" to the mature crinoid "slow" growth rates is indicated by two lines of evidence: The spacing of growth lines on calyx plate interiors was previously mentioned. For some unknown reason, the initial "slow" phase growth lines are not preserved; only the "fast" and mature "slow" growth lines have been observed. Data given by H. B. Moore (1935) denote that growth rings form seasonally in living echinoids. According to A. H. Clark (1915, pp. 197-198), after the modern crinoid adult stage is reached, the rate of Brr formation at the arm tips takes place at a constantly decreasing rate. During later growth, the Brr addition rate is "slow" and the general proportions of the arms relative to the calyx are not substantially changed. Most adult size increase occurs by means of calcite accretion to the previously formed plates.

Similar time-size growth rate curves are known for other living echinoderms (H. B. Moore, 1966, pp. 73-75, echinoids; Feder and Christensen, 1966, pp. 107-110, starfish; previous discussion of population size and structure; also Hallam, 1967, pp. 31-35, for easily visualized time-size growth rate curves in mollusks). Many of these fit the "slow-fast-slow" growth rate model. Sometimes the initial "slow" growth rates are lacking; this probably represents sampling in some instances (*e.g.*, Feder and Christensen, 1966, text-fig. 4, the earliest larvae are lacking) rather than the true situation.

COMPARISON OF ONTOGENY:

GIRARDEAU CAMERATES AND LIVING CRINOIDS

With the exception of *Cyttarocrinus eriensis* (Hall) (see Koenig, 1965, pp. 406-412), nothing is known of early camerate growth stages. The cyttarocrinid is assigned to the Hapalocrinidae and the arms are free above the RR as in most platycrinitids. The youngest crinoids are about .4 mm high and possess the BB, OO, and RR. The RR are in lateral contact and all other plates are joined together; the arm facets are lacking. The largest cyttarocrinids (1.85 mm high) retain the same plate structure as the young crinoids except that all five arm facets are seen and the proportions of the various plates relative to each other have changed. Although a complete growth sequence is not available for this species, the observed changes are similar to modern crinoids except that the arm facets appeared in a different order and the calyx plates joined earlier.

The smallest Girardeau camerates are about 1.0 to 1.3 mm in "size", possess four to nine IIBrr in each arm, and pinnules are well developed. The IBr1 and sometimes IAx are incorporated into the calyx. The microcrinoid and the early arm bearing growth stages are conspicuously absent, although these have been searched for during several field seasons. The reason for this is not fully understood. The most plausible explanation seems to be obliteration during diagenesis (see paleoecology). Mature Girardeau camerates range from 5 to 15 mm in "size", have 50 to 200 Brr in each arm, and are characterized by varying numbers of fixed IIBrr and sometimes IIIBrr.

Comparable growth sequences to those of the Girardeau forms are available for various Paleozoic camerates, al-

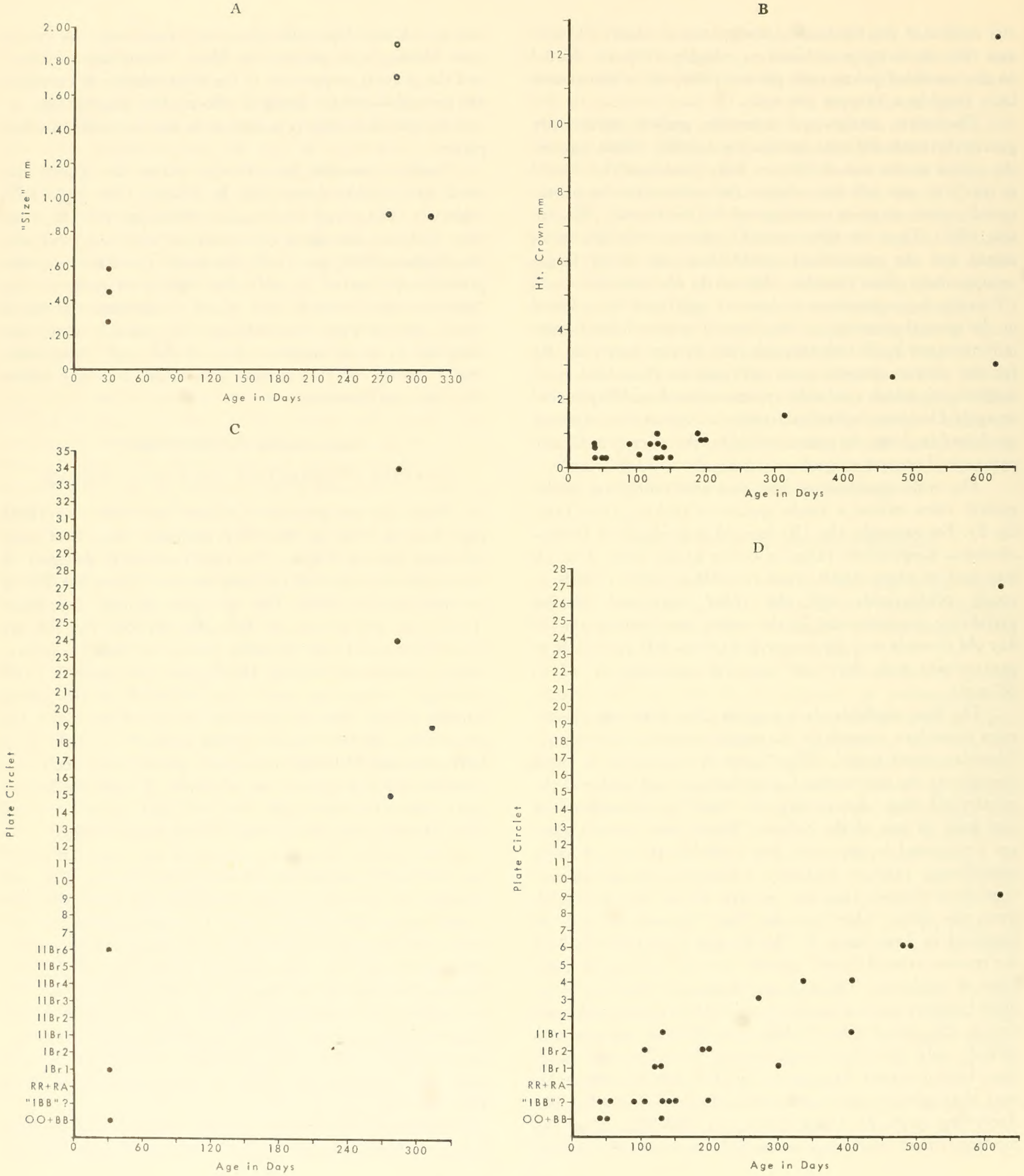

(See caption page 307)

Text-figure 5. — Graphs showing Time-"size" and Time-plate circlet growth rates in various living crinoids. Horizontal axes give age in days. Vertical axis gives "size" or plate circlet; RA grouped with RR. Data sources same as Text-fig. 4. *Promachocrius keguelensis* data adjusted as stated in text. A,B. Time-"size" growth. A. *Hathrometra sarsii;* B. *Promachocrinus kerguelensis.* C,D. Time-plate circlet growth. C. *Hathrometra sarsii;* D. *Promachocrinus kerguelensis.*

though most of these have not been treated in detail. For example: *Rhodocrinites douglassi* "var." *serpens* (Laudon) (growth sequence never illustrated); *Ptychocrinus parvus* (Hall) (not in literature); *Megistocrinus depressus* (Hall) (see Goldring, 1923, p. 226, pl. 23); *Glyptocrinus decadactylus* Hall (not illustrated); *G. dyeri* Meek (see Wachsmuth and Springer, 1897, p. 274, pl. 20, figs. 1a-c; pl. 21, figs. 3a-f); *Ctenocrinus paucidactylus* (Hall) (see Goldring, 1923, p. 122, pl. 8, fig. 5; pls. 9-11); *Platycrinites americanus* (Owen and Shumard) (see Wachsmuth and Springer, 1897, p. 686, pl. 75, figs. 10-13); *P. bozemanensis* (Miller and Gurley) (see Laudon, 1967); *P. burlingtonensis* (Owen and Shumard) (see Wachsmuth and Springer, 1897, p. 653, pl. 69, figs. 3a-i); *P. huntsvillae* Troost (see Wachsmuth and Springer, 1897, p. 678, pl. 73, figs. 6-12); *P. ornigranulatus* (McChesney) (see Wachsmuth and Springer, 1897, p. 701, pl. 68, figs. 10-12).

Comparison of the Girardeau camerates and Recent crinoids will be presented under two categories: the plate growth sequence and the development of individual plates. During the observed Girardeau camerate growth sequences, free Brr were incorporated into the calyx, although the rates varied from species to species. This does not occur in modern crinoids and in some camerates, such as platycrinitids and dichocrinids, where the arms remained free above the RR throughout life. Making allowance for the development of FBrr and allied differences (see later discussion), the Girardeau camerate and modern crinoid plate development sequences are almost the same, especially with respect to the arms and column. In many living crinoids, the animal discards the column at the end of the pentacrinid growth stage (comatulids) and assumes a more or less free living existence. Such does not occur in the Girardeau camerates and Recent isocrinids, where barring traumatic accidents, all or part of the column is retained until death. Despite this difference, growth of the comatulid larval column and the camerate and isocrinid stem follows the same pattern.

"Theoretical microcrinoid" sizes for the Girardeau camerates also yield some information on comparison. By analogy with the plate development sequence in living crinoids, monocyclic camerates possessed two of these growth stages: 1. BB + OO "microcrinoid" and 2. BB + RR + OO "microcrinoid". In similar fashion, three "microcrinoids" could be predicted for dicyclic forms: 1. BB + OO; 2. BB + OO + IBB; and 3. BB + OO + IBB + RR.

Computation of these "microcrinoids" basically involved prediction by means of the extrapolation of certain Girardeau camerate regression lines backward in relative age and "size". The process assumes: 1. The regression lines yield good fits to the available data. 2. The "microcrinoids" grew according to the same "size"-FBrr relationships that are observed in older animals. Clearly, this hypothesis cannot be verified for the camerates as the "microcrinoids" are not known. However, inspection of Text-figure 4 seems to denote that such holds true for the Recent crinoids studied. 3. Plate development sequences of the camerates and modern crinoids are basically the same (with the probable exception of the iBrr). As above, this assumption cannot be proven by direct observation. However, all the available facts support or are at least consistent with such a growth model.

The "microcrinoids" for monocyclic camerates were estimated as follows: 1. BB + OO + RR. The maximum possible "size" for this "microcrinoid" equals the height of the BB and the RR in the smallest individual of any one species. Actually, the maximum "size" of the BB + OO + RR stage would be smaller because some accretionary height growth of the BB and RR must have taken place after this phase. Another value was obtained from the "size" (x) versus FBrr (y) curve by computing "size" when the highest "FBrr" was the distal margin of the R (*i.e.*, FBr equals 3.0 in the numerical scale). 2. BB + OO. One "size" has been determined by the previous method when the highest "FBr" consisted of the top of the BB (1.0 in the numerical FBrr scale). The height R (x) versus "size" (y) initial intercept also approximates this "microcrinoid size".

At worst, these "microcrinoids" constitute an interesting statistical exercise. At best, they have biological significance and outline the rough "sizes" of these growth stages for the Girardeau camerates. The writer favors the latter view. At any rate, comparisons of the Girardeau camerate and Recent comatulid "microcrinoid" values are given in Table 4 and inspection thereof indicates that all are similar. In the writer's opinion, the data denote or are at least consistent with the hypothesis that the basic plate development sequence in the camerates (except for the iBr1) and living crinoids is the same. Similar conclusions are derived from the knowledge of plate growth sequences in Paleozoic microcrinoids (see Koenig, 1965, for brief summary).

Typically, the proximal iBrr (iR or iBr1 depending on topographic position) of Recent crinoids develop late in

Microcrinoid values

Monocyclic crinoids

Comatulids	BB + OO "size" mm	BB + RR + OO "size" mm	First appearance of IIBrr "size" mm
Comactina meridionalis	--	.17 to .27 mm	.98 mm
Hathrometra sarsii	.27 mm	--	IIBr6 present at .58 mm
Antedon bifida	.26 to .32 mm	--	--
Hathrometra prolixa	.22 to .27 mm	.42 to .48 mm	about 1.4 mm
Camerates *Eopatelliocrinus scyphogracilis*, n. gen., n. sp.	.11 to .17 mm	.22 to .63 mm	.29 to .56 mm
E. latibrachiatus, n. gen., n. sp.	.16 to .33 mm	.39 to .63 mm	.34 to .77 mm
Macrostylocrinus pristinus, n. sp.	.10 mm	.23 to .63 mm	.28 to .83 mm
Alisocrinus tetrarmatus, n. sp.	anomalous	.50 mm	.22 to .57 mm

Microcrinoid values

Dicyclic crinoids

Comatulids	BB + OO "size"mm	BB + OO + IBB "size" mm	BB + OO + IBB + RR "size" mm	First appearance of IIBrr "size" mm
Antedon adriatica	--	.10 mm	.25 mm	--
Promachocrinus kergnelensis	--	.12 to .15 mm	.15 to .41 mm	.80 mm

Table 4

Microcrinoid values for various living crinoids and Girardeau camerates.

ontogeny. For example, these are first seen after IBr2 is well defined in *Comactina meridionalis;* the iRR of *Promachocrinus kerguelensis* do not appear until after about five IIBrr are present. Generally, the living crinoid proximal CD interray plate (RA) forms earlier than the iR or iBrl, ranging from just prior to soon after the RR.

Initial intercepts derived from equations of "size" (x) versus calyx plate dimensions (y) in the Girardeau *Alisocrinus tetrarmatus,* n. sp. suggest that some or all camerates were characterized by a different sequence. The *A. tetrarmatus,* n. sp. iBrl was probably initiated along with or immediately after the RR. Most likely, the alisocrinid primanal (believed homologous with the RA of living species) formed at about the same time. Relative to modern crinoids, the *A. tetrarmatus,* n. sp. iBrrl are postulated to have appeared earlier, whereas the proximal CD interray plates of both the camerate and Recent forms began at roughly the same time. Whether or not this pattern was typical of FBrr bearing camerates cannot be determined at present. Data matrices are not complete enough for the other Girardeau camerates to calculate the necessary initial intercepts. However the geometry of all FBrr bearing camerates is consistent with early iBrl development. If so, the different iBrl plate sequence between the FBrr bearing camerates and living crinoids is clearly related to and correlated with the presence or absence of FBrr. The camerate FBrr are incorporated into the calyx by iBrr; Recent crinoids lack FBrr and the arms are free above the RR.

Some Paleozoic camerates did not develop FBrr (*e.g.*, platycrinitids and dichocrinids). These may or may not have retained the *A. tetrarmatus,* n. sp. type of early iBrl formation. However, the earliest growth stages of *Platycrinites bozemanensis* (Miller and Gurley) illustrated by Laudon (1967, text-figs 1, 2) are suggestive of early iBrl development.

The developmental sequence of the stem and arm plates of living species and the camerates follows the same order. Columnals typically form immediately distal to the calyx, below the centrodorsal in pentacrinid growth stages of comatulids and below the IBB or BB of camerates. Also new columnals are generally intercalated between the previously present plates. All Brr and pinnulars first appear at the distal tips of the arms or pinnules. As previously mentioned, the proximal calcified pinnules of the camerates developed earlier than those of Recent species.

Growth of the camerate and modern crinoid dorsal cup plates follows strikingly different paths. In the camerates examined, the base of the calyx is floored by the IBB in dicyclic and the BB in monocyclic forms. The calyx walls are composed of the upright BB (wholly or partially), RR, FBrr, iBrr and anals. In dicyclic crinoids, the upper margins of the IBB commonly form the basal cup walls, whereas the distal parts of the BB serve this purpose in monocyclic forms. The food grooves and the distal part of the viscera were roofed by the camerate tegmen plates. At least one Girardeau species, *Ptychocrinus fimbriatus,* had a calcite convoluted organ located inside the calyx. This structure is believed to have both supported the gut and separated the gut from the chambered organ and the aboral nerve cords (see *P. fimbriatus* for more detail). If so, the camerate convoluted organ served roughly the same purpose as the BB rosette in comatulids (see later discussion). Whether or not all camerate crinoids possessed convoluted organs is unknown; however, these occur in many Mississippian forms (see Wachsmuth and Springer, 1897, pp. 142, 143; Ubaghs, 1953, pp. 687-690). At any rate, the basic camerate calyx functions were to enclose, protect and support the viscera, and to bear the free arms. The free arms were supported by the distal FBrr; in turn these were maintained by the more proximal FBrr, RR, BB, IBB (if present), and the iBrr. All camerate calyx plates performed more or less the same functions.

Consequent to this functional morphology, major resorption did not occur in the dorsal cup plates of the camerates examined here. Probably this was true for all camerates. However, a few exceptions may have existed where dorsal cup plate resorption took place during ontogeny. Examples are the IAx of some platycrinitids and IBr1 of certain batocrinids, although these have not been examined by the writer. Most camerate tegmen plates probably also had a non-resorption mode of growth. If resorption occurred in tegmen plates, the author believes it was confined to plates associated with the arm bases and perhaps the OO.

As aptly pointed out by A. H. Clark (1915, pp. 316-354, especially pp. 344-348), comatulids depart greatly from the camerate model. In the modern crinoids, the principal specializations are related to the reduction of the calyx plates and increase in the calyx strength (see Nichols, 1962, fig. 2 for clear diagrammatic cross-section through a comatulid calyx). Different parts of the comatulid calyx serve different functions. The comatulid IBB, if present, are reduced. Early in ontogeny they fuse with the proximal columnal to form the centrodorsal; this gives rise to the cirri which the crinoid uses to grasp the substrate after the column is discarded. The comatulid BB are also insignificant calyx elements; during growth these are metamorphosed and shifted upward (distally) to form the BB rosette. In a mature animal, the chambered organ is almost completely enclosed within the centrodorsal on the base and sides, RR on the sides, and BB rosette on the top. The bulk of the viscera proper (*i.e.*, inner and outer coelom of Nichols, gut, and so forth) rests on the distal margin of the BB rosette and the RR. Thus, the BB rosette serves as a "septum" which largely separates the chambered organ from the viscera proper. The principal function of the comatulid RR seems to be merely to support the arms which are free above the RR. Lateral protection and support for the comatulid viscera proper are provided by the IBrr. Thus in the comatulids and isocrinids to a lesser extent, the IBB, BB and RR do not serve to support and protect the sides of the viscera as in the camerates. Consequent to this, the calyx plate growth patterns of the modern crinoids and the less complex camerates have diverged. As mentioned above, resorption does not occur in camerate calyx plates, or if so this was not common. On the other hand, in comatulids (isocrinid ontogeny is not well known), resorption during calyx plate growth is common and can be documented for the BB, centrodorsals, RA, OO and other tegmen plates (A. H. Clark, 1915, pp. 322-340). The initially formed comatulid RR have flat inner and outer surfaces with the axial nerve cords located on the inside of the plates. Throughout ontogeny, calcite is deposited on the inside of the comatulid RR; this contrasts greatly with the camerate mode of growth. In the next comatulid RR growth stage, calcite deposition builds up the plate internal margins and the axial nerve cords occur in a groove on the inside of the plate. Continued inward calcite deposition completely buries the axial nerve cords within the RR in the last developmental phase (W. B. Carpenter, 1866, pp. 738-741).

Growth of the comatulid Brr exhibits the same pattern (see Text-figs. 3m-o for cyathocrinids; comatulids have the same general growth type). At first, the axial nerve cords are housed in a single ventral groove where they underlie the food gathering and associated tissues. Subsequent ventral calcite deposition displaces the feeding tissue ventrally. Eventually, the axial nerve cords are completely separated and housed in axial canals inside the Br (W. B. Carpenter, 1866, pp. 739-741). In the Girardeau camerates, the uniserial Br ventral food groove remained deep in all growth stages; throughout life, the axial nerve cords occupied the base (axis) of this food groove. Ventral calcite deposition simply extended the sides of the camerate food grooves (see Text-fig. 3p).

The camerate type uniserial Br growth pattern predominated in the Paleozoic whereas all living forms known to the writer are characterized by the comatulid type. This suggests progressive evolution and adaptation. Obviously the Recent crinoid axial nerve cords are better protected. Damage to the food groove tissue need not harm the axial nerves. Such seems important because the aboral nerve level which includes the axial nerve cords in the arms is the major level in crinoids; it controls posture and other basic reactions (see previous discussion). Conversely in the camerate type, many food gathering structure injuries probably also affected the axial nerve cords.

Geometrically, the comatulid growth pattern is far more complex than the camerate one. This implies that the comatulid Brr require a higher degree of developmental integration and coordination than camerate Brr. At present, this can only be postulated because the writer has no correlation matrices for comatulid Brr ontogeny to compare with those of the Girardeau camerates. If true, this may partially explain why camerates retained their type of growth, despite the vulnerability of their axial nerve cords.

Some Paleozoic crinoids (*e.g.*, many cyathocrinids) had the axial nerve cords housed within the Brr like living forms. Most of these were non-pinnulate types. Judging from their diversity and abundance, they were not so successful as the contemporary camerates and other crinoids with camerate type Brr growth patterns. Apparently the disadvantages of not having pinnules (*e.g.*, less food gathering capacity, lower arm leverage) outweighed the advantages of superior axial nerve cord protection.

In crinoid morphology and taxonomy, the R is considered the base of a ray. This plate receives paramount importance in taxonomy. It is also notable, that the growth models of the RR and Brr are basically the same for any one crinoid. For example in comatulids, calcite is deposited on the inside of the RR and on the ventral sides of the Brr. In the camerates, no deposition occurred on the insides of the RR. This also characterized the Brr food groove axes. The RR develop before the Brr in both living crinoids and camerates. The implication is that the RR growth type dictates the mode of Brr ontogeny. Clearly this reinforces the morphological and taxonomic significance of the RR.

In the arms, the growth vectors of uniserial Brr in the camerates and comatulids are almost identical, if one allows for the difference in axial canal geometry. Recent crinoids with biserial arms are unknown, although forms with strongly wedge-shaped Brr are not uncommon (*e.g.*, *Antedon petasus*, *A. bifida*, *A. mediterranea*, and *A. adriatica*, see A. H. Clark, 1915, figs. 103-107). Consequently, no biserial Brr growth model is available from living animals. However, as already discussed, biserial Brr ontogeny most likely followed the same general "ground rules" as the uniserial type with respect to the axial canal, except for the transitional uniserial to biserial growth stage (see also summary of Girardeau camerate growth and *Macrostylocrinus pristinus*, n. sp., for more detail).

Compared to the Brr and calyx plates, the main columnal growth patterns are highly conservative. As far as can be determined, these are uniform in living crinoids and all fossil forms examined by the writer.

SUMMARY OF GIRARDEAU CAMERATE ONTOGENY

Ontogeny sequences are well known in the following Girardeau Limestone camerates: *Eopatelliocrinus scyphogracilis*, n. gen., n. sp., *E. latibrachiatus*, n. gen., n. sp., *Macrostylocrinus pristinus*, n. sp., *Alisocrinus tetrarmatus*, n. sp., *A. ? heterodactylus*, n. sp., *Ptychocrinus splendens*, and *P. fimbriatus*. In addition, certain developmental aspects of *Macrostylocrinus cirrifer* Ramsbottom from the Late Ordovician of Scotland were investigated. The smallest Girardeau camerates are roughly 1.0 to 1.5 mm in "size" and bear four to eight Brr per arm. The oldest crinoids range from 5.0 to about 15 mm in "size", depending on species, and over 100 Brr may be found in a single arm. The growth sequences of the two ptychocrinids are not presented here. The writer plans on restudying these forms, utilizing techniques involving more direct use of the growth rates than those applied to the other five taxa.

CALYX GROWTH

All crinoids studied possessed predominantly linear calyx development with constant growth rates throughout ontogeny. With the exception of the column facet, the plots of calyx plate dimensions versus "size" and versus one another are linear. However, any one plate may have shown differential growth along the various axes. Consequently, the plate shapes changed during ontogeny. Most Girardeau camerates were characterized by calyx plate height/width ratios which generally increased with progressive "size" and age. This is caused by the initial intercepts and the plate height growth rates which typically exceeded those of width. Because of differential growth of the component plates, the Girardeau camerate calyx shape underwent a series of correlated changes during ontogeny. Macurda (1968) reported a similar pattern in two species of *Eucalyptocrinites*. Blastoids were also characterized by largely linear relations, although a few examples of exponential development of different parts of a single plate are known (Macurda, 1966). Apparently, linear growth facilitated the integration and coordination of the calyx ontogeny.

The development of "size" versus the various types of FBrr had either linear or logarithmic growth in the Girardeau forms. Free Brr were fixed into the dorsal cup throughout growth, although the fixation rate commonly varied with "size" and age. Prior to incorporation, the FBrr resembled typical free Brr. During and soon after fixation, these plates developed angular margins along which the fixing iBrr joined them into the dorsal cup. The formation of these angular margins involved relative changes of the various width growth rates of the new FBrr. Such could be considered as "metamorphosis" of the plate although the "size" — change rate was much less marked than the "metamorphosis" that occurred during biserial Brr ontogeny. The pinnulars were joined into the calyx in similar fashion.

The overall degree of integration and coordination of the Girardeau camerate calyx geometry was high. Reliable correlation coefficients of the various plate dimensions versus each other, the calyx plate dimensions versus "size" and the other dorsal cup shape parameters, and the calyx shape measures versus one another range from .77 to .997; the correlation coefficient significance levels almost always exceed .999 (two-sided test). Considerable difficulties were encountered in comparison of the various correlation coefficients and their significance levels within a single form and between different species because of the variation in degrees of freedom. The only comprehensive intra-species data was derived from *Alisocrinus tetrarmatus*, n. sp. Here, the ray plates, RR, IBr1, IAx and IIBr1, were most closely integrated and coordinated with each other and with the calyx size measures. The IIIBrr2 (ray plate), the interray plates (iBr1 and primanal) and the BB, all of which are peripheral to the main ray plate sequence, show lower correlations and significance levels and a correspondingly less sophisticated degree of integration and coordination. In *A. tetrarmatus*, n. sp., the height and width of the individual plates have equal correlation coefficients with the calyx height and width measures. Conversely, the plate heights are generally best correlated with "size" and were less well integrated with the calyx width growth in most Girardeau patelliocrinids. The same situation is observed with the plate widths of these crinoids.

The correlation coefficients and their significance levels for "size" versus the various FBrr vary with the FBrr type and species. For FBrr in the lateral interrays, the correlations range from .92 to .97; all significance levels exceed .999. When the inter-half-ray FBrr are involved, a lower degree of integration and coordination was present. These correlation coefficients cover an interval of zero (no FBrr added) to .92 and the significance levels may be greater than .999.

The original aboral nerve cord knot positions can generally be located for most major calyx plates (*i.e.*, RR, IBr1, IAx, iBr1, and primanal). The percentage width points equal roughly 50% and indicate symmetrical or nearly so width growth vectors on each side of the ray axis for ray plates and the interray axis for the iBr1 and primanal. The percentage height points are more variable and usually range more or less than 50%. This denotes asymmetrical proximal and distal height growth rates. During ontogeny, some of the percentage height points remained constant, whereas others migrated with increasing "size" and age. In the former case the proximal and distal height growth vectors were constant relative to each other for a single plate. These growth rates changed with respect to one another in the latter instance.

In this discussion, camerate crinoid calyces are subdivided into five basic types depending on the extent of the FBrr, nature of the iBrr, and to some extent the number of arms. It must be stressed that the five groups comprise a continuous spectrum. Overlap is common and assignment to a single type is commonly somewhat subjective and arbitrary. The five categories follow; these will be referred to by number in the remaining text.

Type 1. Many FBrr; iBrr small and irregular; iRR may or may not be present; few arms per ray. Examples: Reteocrinidae, Xenocrinidae and some Tanaocrinidae. The calyx growth is partially known in *Xenocrinus multiramus* Ramsbottom (1961, p. 21, pl. 6, figs. 1-4). This species will be discussed at a later date.

Type 2. Many FBrr; iBrr large and regular; iRR present or absent; few arms per ray. Examples: most Archaeocrinidae, some Rhodocrinitidae, some Dimerocrinitidae, some Tanaocrinidae, some Periechocrinitidae, Glyptocrinidae, Scyphocrinitidae, Melocrinitidae. Numerous camerate growth sequences fall into this category; of the Girardeau fauna, *Alisocrinus tetrarmatus*, n. sp., *A. ? heterodactylus*, n. sp., *Ptychocrinus splendens*, and *P. fimbriatus* are included.

Type 3. Many FBrr; iBrr large and regular; iRR rarely present; numerous arms per ray. Examples: a few Rhodocrinitidae, some Periechocrinitidae, most Actinocrinitidae, and Batocrinidae. None of the Girardeau crinoids are assigned to this group. Various Mississippian crinoids of which the ontogenies are partially known are placed here; the example alluded to in this paper is *Teleiocrinus umbrosus* (Hall) (see Wachsmuth and Springer, 1897, p. 628, pl. 60, figs. 2a-d).

Type 4. Few FBrr; iBrr large and regular; iRR rarely present; few arms per ray. Examples: Gazacrinidae, some Dimerocrinitidae, Desmidocrinitidae, Coelocrinidae, Eucalyptocrinitidae, Patelliocrinidae, certain Hapalocrinidae. The ontogenies are best known in the three Girardeau patelliocrinids.

Type 5. No FBrr; arms free above RR. Examples: Nyctocrinidae, some Hexacrinitidae, Dichocrinidae, some Hapalocrinidae, Platycrinitidae. Adequate growth sequences are available from numerous platycrinitids; the example emphasized here is *Platycrinites bozemanensis* (Miller and Gurley) (see Laudon, 1967).

COMPARISON OF TYPE 2 AND TYPE 4 CAMERATES

Both young patelliocrinids (Type 4, few-FBrr, see Text-fig. 7 for representative growth sequence) and alisocrinids (Type 2, many-FBrr, see Text-fig. 29) have various parts of the IAx fixed into the calyx. Divergences between the two groups occurred during later ontogeny. All few-FBrr crinoids examined show an exponential "size" versus lateral interray FBrr regression line in which the FBrr incorporation rates declined with increasing "size" and age; the mean FBrr fixation rates ranged smaller than those of the many-FBrr types. Most Type 2 crinoids examined were characterized by linear patterns (*i.e., Alisocrinus tetrarmatus,* n. sp., *A. ? heterodactylus,* n. sp., *Glyptocrinus decadactylus, Ptychocrinus splendens*); however, a few crinoids possessed an exponential pattern (*e.g., Ptychocrinus fimbriatus*). The linear FBrr or mean FBrr fixation rate somewhat exceeded that of the few-FBrr crinoids.

Another striking difference between the many- versus the few-FBrr types is the more extensive formation of the inter-half-ray and inter-quarter-ray (if more than two arms per ray occur) iBrr in the former group. Young crinoids of both categories have the IIBr1 proximal parts joined together along the ray axis. Some patelliocrinids retained this juvenile configuration (normal individuals of *Eopatelliocrinus,* n. gen.) but others developed inter-half-ray FBrr at low fixation rates (*Macrostylocrinus pristinus,* n. sp.). The Girardeau patelliocrinids have only two arms per ray; consequently, the inter-quarter-ray iBrr are not observed. The many-FBrr species incorporated inter-half-ray FBrr at rapid growth rates relative to "size". In crinoids with two arms per ray such as *Glyptocrinus dyeri,* the inter-quarter-ray iBrr are lacking. Forms with three or four arms per ray developed these iBrr and the associated FBrr (*e.g., Alisocrinus tetrarmatus,* n. sp., some rays in *A. ? heterodactylus,* n. sp., *Glyptocrinus decadactylus*). Generally, the inter-quarter-ray FBrr fixation was not initiated until after the inter-half-ray FBrr incorporation was well underway. Despite these FBrr development rate differentials between the few- and many-FBrr crinoids, the mechanism of Brr and pinnule fixation remained constant.

The variation in FBrr incorporation rates between the Type 2 and Type 4 crinoids caused a series of correlated mean growth divergences.

1. Because of the extensive development of inter-half-ray iBrr in Type 2 species, the adjacent half-rays (belong to same ray) were spread apart. Young crinoids which lack the inter-half-ray iBrr have closely spaced half-rays within a single ray; the different rays are separated by wide lateral and CD interray areas. The formation of the inter-half-ray iBrr and the consequent Brr fixation spread the half-rays of a single ray apart so these became more widely spaced relative to calyx width; consequently, the lateral and CD interray iBrr areas were constricted with respect to "size." When the development of inter-quarter-ray iBrr occurred, the quarter-rays were spread apart and the adjacent inter-half-ray, lateral interray, and CD interray iBrr were constricted relative to dorsal cup width. Most of this ray spreading was caused by the insertion of the proximal one or two ranges of inter-half-ray and inter-quarter-ray iBrr. Above these levels, the adjacent arms of a single ray tend to come together.

The formation of these iBrr changed the arm distribution around the calyx during the ontogeny of Type 2 many-FBrr species. Young crinoids have the arms of a single ray closely spaced; the iBrr areas are wide relative to size. In mature animals the arms are more evenly located around the dorsal cup. Such probably prevented the pinnules of adjacent arms from becoming entangled or twisted together. Even arm spacing also enabled each arm to filter a separate water area, which allowed wider and more complete coverage of the water surrounding the arms. This adaptation was unnecessary for the youngest crinoids which have short pinnules. Ray spreading of this type is unknown in the few-FBrr Girardeau patelliocrinoids (Type 4). These forms retained the juvenile condition with closely spaced half-rays (of single ray) throughout growth because of the low "size"-inter-half-ray FBrr fixation rates.

2. A high FBrr incorporation rate resulted in rapid distal extension of the dorsal cup and viscera. Thus, given many- and few-FBrr species with equal calyx shapes, the viscera volume was augmented at a faster rate (relative to "size") in the former type.

3. The inter-half-ray and inter-quarter-ray (when present) iBrr generally extend higher than the lateral and CD interray iBrr in the Type 2 crinoids. Consequently, a strongly lobate tegmen was formed with elevated Ambb areas and depressed iAmbb regions. This configuration is less marked in the few-FBrr species and a smoother tegmen is observed.

4. The formation of numerous FBrr may have provided a stronger support for the growing arms; the available data are insufficient to accept or reject this hypothesis (see later discussion of supporting structures and food gathering system).

The "size" component geometry of the Type 2 and Type 4 camerates shows a significant mean difference. Young crowns of both groups have similar configurations in which the RR comprise the dominant ray plates; the IBrr are subordinate elements relative to the RR and "size" (compare young crinoids in Text-figs. 7 and 29). Divergence occurred in the later development. The mature few-FBrr animals more or less retained or accentuated this juvenile RR-IBrr arrangement throughout ontogeny. Partly, such was caused by the growth rate differentials: the IBrr height-"size" growth vectors were exceeded by those of the RR. Conversely, the Type 2 forms possessed similar RR and IBrr-"size" growth rates. This resulted in an adult calyx with the IBrr and RR roughly equal in height and percentage height contributions to "size."

For the Girardeau crinoids, phylogeny provides a partial answer. Both the patelliocrinids (few-FBrr) and the alisocrinids (Type 2) shared a common many-FBrr glyptocrinid ancestor. The patelliocrinids were evolving toward a hapalocrinid configuration with the arms free above the RR. In this lineage the decrease in the IBrl and IAx height and width with respect to the calyx "size" was somewhat correlated with the reduction in number of FBrr. Although, a character correlation existed in this instance, such was not always the case and functional morphology probably did not dictate the relationship. For example, *Cyphocrinus* (see Springer, 1926, p. 15, pl. 1, figs. 15-18) has numerous FBrr and small IBrr. This suggests that natural selection acted independently on the two characters.

TYPE 3 CAMERATES

The basic morphological and developmental features of these crinoids parallel the more primitive Type 2 many-FBrr group with one exception. The Type 2 forms have few arms per ray (usually two to four) whereas six or more arms generally occur in Type 3 rays. The evolution of more arms was a general theme; for example, some *Teleiocrinus* range around 80 arms. The development of numerous arms and the associated axillaries tended to spread the arms apart, because the axillaries are roughly pentagonal and expand distally. Probably due to the many axillaries, the inter-half-ray, inter-quarter-ray, and higher iBrr were less well developed than in the more primitive Type 2 many-FBrr camerates (for example, compare growth of *Teleiocrinus umbrosus* in Wachsmuth and Springer, 1897, p. 628, pl. 60, figs. 2a-d with *Alisocrinus tetrarmatus,* n. sp. in Text-fig. 29 of this paper).

TYPE 5 CAMERATES

Camerates with the arms free above the RR (*i.e.*, no FBrr) are most similar to and were derived from the Type 4 few-FBrr forms. Primitive groups, such as hapalocrinids, retain both the IBrl and IAx. More advanced types (*e.g.*, platycrinitids) tended to lose the IBrl (mechanism unknown to the writer) and the IAx rests directly on the RR.

The ontogenies are reasonably well known in various species. *Platycrinites bozemanensis* (described by Laudon, 1967, see especially text-figs. 1-4) is most familiar to the writer and is taken as a typical example. The most striking growth differentials between the platycrinitid and the few-FBrr camerates were: 1. The arms remained free above the RR throughout Type 5 crinoid ontogeny. The few-FBrr species incorporated FBrr into the calyx throughout development and the proximal IIBrr usually comprise the distal FBrr in mature individuals. Therefore, given Type 4 and Type 5 crinoids with indentical dorsal cup shapes, the calyx volume per unit of "size" increment was augmented more rapidly in the former group.

2. The *P. bozemanensis* IAx (IBrl is lacking) width and height growth rates with respect to "size" ranged much smaller than in the Girardeau patelliocrinids. Thus, the platycrinitid IAx became progressively much smaller in relation to the total dorsal cup dimensions throughout growth. In young animals, a pentagonal IAx completely supports the IIBrrl. Mature animals have a triangular IAx which only partially serves this function; the outer IIBrl margins rest on the RR. Although advanced crinoids, like *P. bozemanensis,* comprise extreme cases, the IBrl and IAx width and height growth vectors of Type 5 camerates were generally exceeded by the equivalent few-FBrr crinoid figures.

GEOLOGICAL HISTORY OF THE FIVE CAMERATE CALYX TYPES

It should be emphasized that the following presents a generalized summary which is only designed to illustrate a large scale pattern of successions and replacements. Detailed lineages are not proposed and all dorsal cup types were polyphyletic. For example, Type 5 hexacrinitids probably had desmidocrinitid ancestors, whereas hapalocrinids were descended from patelliocrinids (see phylogeny section for glyptocrinid - alisocrinid and glyptocrinid - patelliocrinid-hapalocrinid evolution).

Ordovician camerate faunas consisted principally of Types 1 and 2, although subordinate members of the other three groups are known. Type 1 species are generally considered ancestral to Type 2 forms (Moore and Laudon, 1943, pp. 76-101); stratigraphic position suggests that this hypothesis may be incorrect even though accepted by most crinoid specialists. Types 2 and 3 dominated the Silurian. Types 4 and 5 were common and diversified but were less abundant than the previous ones. Only rare Type 1 calyces are encountered. The Early Paleozoic Types 3 and 4 clearly evolved from Type 2 groups and Type 5 lineages were derived from Type 4 stocks. The overall Devonian fauna resembled the Silurian assemblage except that Types 2, 3, 4 and 5 showed more equal diversity. Mississippian camerates were mainly composed of Types 3 and 5. Only subordinate

Types 2 and 4 genera are seen and Type 1 was extinct. With the exception of a few actinocrinitids, the last Permian camerates are assigned to Type 5. This general pattern suggests that during the Early and Middle Paleozoic: Type 2 may have replaced Type 1 if Moore and Laudon (1943, pp. 76-101) are correct; extinct Type 2 groups were succeeded by Types 3 and 4; Type 5 species supplanted Type 4 and perhaps some others. Late Paleozoic camerates (especially Pennsylvanian, to some extent Permian and Latest Mississippian) were characterized by low diversity and were not successful except for one "last stand" in the Permian of Timor; soon after, the camerates became extinct. Probably during this late Paleozoic interval, the camerates were replaced by inadunates and flexibles, (no FBrr, arms free above the RR in most forms) if they were supplanted by crinoids. All Mesozoic (except *Encrinites*-inadunate, Type 5) are assigned to the Articulata and have the arms free above the RR. Such apparently indicates that the Type 5 calyx was most successful in the long run.

GIRARDEAU CAMERATE BRACHIALS

The pinnulate Brr of camerates are divided into two types. Uniserial plates have been examined in four taxa, *Eopatelliocrinus scyphogracilis,* n. gen., n. sp., *E. latibrachiatus,* n. gen., n. sp., *Alisocrinus tetrarmatus,* n. sp., and *A. ? heterodactylus,* n. sp. Cuneiform or wedge-shaped Brr are regarded as uniserial types because of growth pattern similarities. Biserial Brr were only studied in *Macrostylocrinus pristinus,* n. sp. It must be realized that the Brr ontogeny models presented here are two- rather than three-dimensional. All measurements were made at right angles to the dorsal-ventral plane. Unfortunately, it has not been possible to derive measurements in the dorsal-ventral plane because the total Brr thickness cannot be determined consistently in view of the variation in arm orientation. The food groove depths, Brr thickness underneath the food grooves, and similar dimensions were not observed often enough to compile a meaningful development sequence.

GENERAL PATTERN OF STANDARD UNISERIAL BRACHIAL ONTOGENY

Two representative examples are illustrated in Text-figures 11g and 12g. As previously mentioned, the "brachial" and "pinnule facet food groove" axes constituted constant topographic reference points throughout life. The Br accretion simply extended these and lateral migration and calcite resorption did not occur along the axes. Probably, some resorption existed; if so, it was confined to the base of the food grooves and was caused by the increased diameter of the axial nerve cord in older animals. This did not result in movement of the food groove axes.

Uniserial Brr retained the same basic geometry throughout development. Regardless of growth stage, these are clearly recognized as uniserial, although the height/width and the other dimensions varied with Brr age. All ontogenetic changes were gradual and incremental. Conversely, biserial Brr showed major metamorphosis at a certain phase.

The development of "size" versus the various Brr parameters and the combinations of the Brr measurements versus each other followed either linear patterns with constant growth vectors or exponential regression lines in which the growth rate changed with age. On the other hand, the ontogeny of "size" versus the calyx plate dimensions and the calyx plate parameters versus one another almost always exhibited linear relations with unchanging growth vectors.

The total growth rates, listed from largest to smallest were: A. Brr width. B. Maximum height. C. The pinnule facet size vector either exceeded or was less than that of minimum height depending on the species. The width was divided into two accretionary growth rates, toward the pinnule facet and opposite the pinnule facet. Invariably, the two components were equal or nearly so. Similarly, the maximum and minimum height developmental vectors were broken down into the proximal and distal categories. The latter predominated by two times or more. The pinnule facet accretion was controlled by both the width (toward the facet) and maximum height increments.

The growth rate distribution indicates that the basic plan of Br ontogeny was designed to minimize the calcite accretion across the critical articular surfaces, as much as possible within the geometrical limits of the plate. Minimizing these vectors caused the least possible amount of interference with the ligaments and muscles which hinged and flexed the adjacent articular surfaces. The relative growth rates toward the articular surfaces, listed from greatest to least were: A. Pinnule facet. B. Distal Br. C. Proximal Br. The calcite accretion differentials closely correlated with the mechanics for support of the developing arms. The rapid width developmental vectors provided increased supporting area for the growing arms and pinnules. The predominance of the distal height growth rates over the proximally orientated ones is not fully understood. Geometrically, such was dictated by the angular relationship of the "pinnule facet food groove" with the "brachial food groove". Perhaps, this was related to the need for support of the developing arms. Consider IIBr10 in a crinoid with 50 IIBrr per arm. The distal IIBr9 face bears 41 IIBrr and associated pinnules, whereas the distal IIBr10 facet supports only 40 IIBrr and associated pinnules. Thus the lowest height accretion vector was directed toward the facet which supported the most Brr. The largest growth rate to an articular surface was toward the pinnule facet which only held the corresponding pinnule.

The immature Brr present a relatively high and angular appearance with prominent and roughly horizontal pinnule facets. The mature plates are wider with respect to height and possess a smoother outline with steeply inclined pinnule facets which are less obvious than in the younger Brr. This progressive obliteration of angularity was caused by the large width growth vectors relative to those of height and the change in pinnule facet inclination.

The total convergence angle (between proximal and distal faces) decreased throughout ontogeny. Usually, the angle dropped most rapidly in the youngest Brr and more slowly in mature plates. Progressively smaller convergence angles were due to changes in the maximum and minimum height growth rates relative to each other and the large width accretion vectors with respect to those of height.

In young crinoids and in juvenile Brr of adults (near distal arm tips), the height axes of succeeding plates are not parallel; rather these are set at angles to one another. The height axis is always inclined toward the pinnule bearing side. The height axes of successive Brr intersect at angles ranging from 20° to 40° in the youngest plates. This imparts a crooked or bent appearance to the adjacent plates (*e.g.*, Text-figs. 7a-c, g). The inclination angle with respect to the arm length axis is about 10° to 20° for such Brr. This configuration is produced by unequal angular convergence of the proximal and distal faces relative to the Br width axis (line along which width was measured). The distal face convergence angle exceeds that of the proximal one. Due to the alternation of the pinnules from one side of the arm to the other, the arm length axis remains straight.

During later growth, the height axes became more or less parallel because equal or nearly equal proximal and distal Brr face convergence angles were formed (*e.g.*, compare Text-figs. 7a-c, g with proximal Brr of 7f; see also plates in Text-fig. 11g). This was caused by adjustments in the proximal and distal maximum and minimum height growth rates: *i.e.*, decreasing the distal maximum height developmental rate relative to that of proximal maximum height, or increasing the distal minimum height accretion vector with respect to that of proximal minimum height, or combining the two mechanisms. Different patterns are observed in the various species studied.

The inclination of the juvenile Brr height axes may have had functional significance. Inclination offsets the pinnules of successive plates more so than if the height axes were parallel. This probably allowed these offset pinnules to filter more water than if they were not offset. Inclination of the immature Brr height axes is geometrically dictated by the large size and orientation of the pinnule facet relative to the width. In more mature Brr, when additional Brr had developed at the arm tips, support became more important. Hence, the height axes of successive Brr grew more or less parallel to provide a more stable support for the arms.

The ontogenetic changes in the Brr inclination angles and in the pinnule facets dictated corresponding changes in the food gathering system pattern. The young crinoid pinnules are relatively wide-spaced whereas those of adults are almost in contact with each other (*e.g.*, compare Text-figs. 7a-c with 7f). Probably the mature animal food gathering system completely filtered the water covered when the arms were extended. Conversely, the juvenile crinoid was most likely unable to fully drain the water immediately surrounding the arms and pinnules.

The dorsal-ventral Brr ontogeny cannot be discussed quantitatively although several qualitative generalizations can be presented (see Text-fig. 3p for schematic sketch). The ventral calcite accretion rates were probably small or nil at the axes of the various food grooves. The deepening of the food grooves was principally produced by ventral extention of the areas flanking the food grooves. Some resorption most likely occurred along the base and sides of the food grooves. This is believed to have been due to the increase in diameter of the axial nerve cords. The average dorsal developmental vectors probably exceeded the ventral ones.

REGULATION OF UNISERIAL BRACHIAL GROWTH

As already outlined, the degree of integration and coordination was measured by correlation coefficients. The Brr data were taken from the plots of "size" versus the Brr dimensions and the various Brr parameters versus each other. The correlation coefficients and their significance levels are directly proportional to the Br dimension growth rate involved. The high correlation coefficients and significance levels are associated with large developmental vectors and vice versa (*e.g.*, Table 8).

Within one taxon, lower correlations and significance levels are seen for "size" versus the Brr parameters than for the Brr measurements versus one another. This shows that the Brr ontogeny was less well integrated and coordinated with the calyx "size" development than with that of the adjacent Brr and Brr dimensions.

The correlation coefficient significance levels vary greatly and these may range from above .999 (two-sided test) to less than .900 in any one form. Generally, when the width and maximum height are considered, the significance levels exceed .999. Lower significance levels are found with minimum height and sometimes pinnule facet size.

The overall degree of Brr ontogeny integration and coordination changed from species to species. *Eopatelliocrinus scyphogracilis,* n. gen., n. sp. exhibited the most sophisticated and highly regulated pattern whereas *E. latibrachiatus,* n. gen., n. sp. was least well integrated and coordinated. *Alisocrinus tetrarmatus,* n. sp., and possibly *A. ? heterodactylus,* n. sp. were intermediate between the two eopatelliocrinids.

Considering the low Brr parameter growth rates with respect to "size" and each other, all species showed highly correlated Brr development.

UNISERIAL CRINOID ARM TIPS

Like living crinoids, the Girardeau camerates formed new Brr throughout ontogeny, although the time-"size"-additional Brr growth vectors varied with age and species. All new Brr developed at the distal arm tip, and these were never inserted between older Brr.

The distal arm tip bears one or rarely two uniserial Brr which lack pinnules. These terminal Brr exhibit parallel proximal and distal faces. The least mature and most recently formed ones have rounded distal margins but slightly older terminal plates are characterized by angular distal margins (*e.g.,* Text-figs. 7,8). The highest pinnulate Brr occur immediately below the terminal one or two Brr. Small pinnule facets are present with a short pinnule consisting of one or two joints. The proximal and distal faces converge on each other. Apparently the maximum and minimum heights became differentiated as soon as the pinnule facet and the associated pinnule appeared.

GENERAL PATTERN OF STANDARD BISERIAL BRACHIAL ONTOGENY

The food groove configurations of biserial armed crinoids resemble those of uniserial forms except that the "pinnule facet food groove" is straight, rather than curved as in uniserial Brr. To facilitate description, the biserial Brr development is divided into five phases. 1. Throughout the early uniserial stage, the biserial Brr growth patterns essentially paralleled those of a uniserial armed species in which the pinnule facet ontogenetic vector exceeded that of minimum height (Text-figs. 24a-d). During this phase, the proximal and distal Br face convergence angle increased from roughly 25° to about 40° unlike the invariable convergence angle decrease of uniserial armed crinoids. The convergence angle development contrasts were related to two fundamentally different growth rates. Uniserial armed forms possessed large Brr width growth vectors relative to "size" and maximum height, whereas the reverse characterized biserial Brr. The early minimum height developmental rates with respect to "size", Brr width and maximum height were large in the uniserial species but these were small in the biserial crinoids. These two growth differentials constituted one of the major causes of the biserial Brr divergence from the uniserial type.

2. The late uniserial stage largely represented a continuation of the previous phase except that the minimum height began to decrease and showed a negative growth rate (Text-figs. 24e, f). Owing to this and the change in the width development vector relative to that of maximum height, the convergence angle rose from approximately 30° to 45°.

3. Transitional uniserial to Immature biserial stage (Text-figs. 24g-i). Apparently, the Brr underwent a major metamorphosis during this phase. The minimum height growth rate became more strongly negative and the relations between the maximum and minimum heights were less equal than in the previous stage. This partly accounted for the further rapid increase in the convergence angle from about 40°to 65°. Eventually, the Brr inner margins joined and the minimum height remained at O mm throughout the later ontogeny. These immature biserial plates have wedge-shapes with curved proximal and distal faces. The inner margins were not yet differentiated from the proximal and distal ones, although the inner area of the plate is in contact with two Brr on the opposite side of the arm (compare uniserial and immature biserial Brr of Text-fig. 21g). As indicated in Text-figures 24g-i, especially the latter, the development of the immature biserial Br involved resorption of the Brr inner sides (*i.e.,* opposite the pinnule facet) and the associated proximal and distal Brr faces. Virtually all resorption was confined to the Br half opposite the pinnule facet. This resorption did not affect the "brachial food groove" axes. However, the resorption caused most of the convergence angle increase. The large scale resorption was dictated by the relations between the Brr width, maximum height and minimum height developmental vectors.

Within this growth phase, the Girardeau macrostylocrinid pinnule facets became more steeply inclined. For example, the biserial Brr facets of paratype USNM 164 574 dip roughly 30° more than the uniserial plate pinnule facets of the same individual. This required lateral migration and probably major resorption of the "pinnule facet food groove" axis while the Brr changed from the uniserial to the immature biserial configuration. The "pinnule facet food groove" axis migration was the second factor which caused the macrostylocrinid biserial Brr ontogeny to diverge from the uniserial type. In the latter crinoids, the pinnule facet inclination change was more gradual and less abrupt. Therefore, the "pinnule facet food groove" axis lateral migration did not occur.*

4. Immature biserial to mature biserial stage (Text-figs. 24j, k). The resorption continued on the inner Br side (opposite the pinnule facet) which increased the convergence angle from about 65° in the immature biserial Br to approximately 105° in the mature biserial one. The width growth was completely asymmetrical, with all accretion directed toward the pinnule facet. About 75% of the Br exhibited some height growth, although the symmetry of the proximal and distal vectors is uncertain. Because of these developmental patterns, the Brr inner margins became strongly differentiated from the proximal and distal ones. The lateral migration of the "pinnule facet food groove" axis ended and the pinnule facet accretion simply extended the axis established in the immature biserial stage.

5. Mature biserial phase (Text-figs. 24l, m). The resorption ceased and the growth was adjusted so that the Brr faces remained parallel or nearly so. The developmental vectors, listed from highest to lowest, equalled: width, height at 90° angles to the proximal and distal margins and "height" at 90° to the inner margins. Although width accretion occurred toward and away from the pinnule facet, the two vectors were unequal. The former growth rate was two to three times the latter. Probably, this resulted in the minimum interference with the various food grooves and their axial nerve cords. The convergence angle between the inner margins either remained constant or increased depending on the species.

Owing to the nature of preservation, the dorsal-ventral biserial Brr development is unknown, although several suggestions can be outlined. Some of the biserial Brr examined by the writer have shallow food grooves (depth roughly 20% of Br depth) whereas others show deep food grooves like these of the Girardeau uniserial armed camerates. During the transition from the uniserial to the immature biserial Brr, one or a combination of two possibilities must have occurred in species where "pinnule facet food groove" axis migration took place. The "pinnule facet food groove" and the "brachial food groove" axial nerve cords may have been displaced ventrally by calcite deposition underneath them. If so, the "brachial food groove" nerve cord migrated ventrally and the "pinnule facet food groove" nerve cord moved ventrally and laterally. If calcite deposition did not take place below the "pinnule facet food groove" axis, then the lateral migration of this axis required some resorption of the ventral part of the plate. A combination of the two mechanisms can be visualized. Perhaps, forms with deep food grooves were mainly characterized by resorption, whereas those with shallow food grooves tended to deposit calcite underneath the axial and nerve cords.

INTEGRATION AND COORDINATION OF BISERIAL BRACHIAL GROWTH

The biserial Brr correlation coefficients have proven difficult to evaluate because of the curve fitting problems encountered where the minimum height represents one of the variables. Undoubtedly, the true measures of "correlation" are higher than those derived from the equations used here. The correlation coefficient magnitudes range from .59 to .97 with most being above .85. All correlation signs are positive except for the minimum height signs which are negative. The significance level interval comprises about .980 to well above .999; most exceed .999 (two-sided test). The main difference between the uniserial and biserial forms consists of the correlation coefficients involving the minimum height. In the biserial species, these vary from –.79 to –.92 with significance levels around .999. The uniserial armed crinoid minimum height correlations are lower and significance levels of less than .900 are not uncommon. Thus, the minimum height was better integrated and coordinated with the development of "size" and the adjacent Brr dimensions in the biserial armed taxa than in the uniserial armed forms.

BISERIAL ARM TIPS

The distal ends of the arms are unknown in adult specimens with numerous biserial Brr. The few available data suggest that the biserial crinoid arm tips resemble those of uniserial species and that the Brr only become biserial below the distal end of the arms.

COMPARISON OF UNISERIAL AND BISERIAL BRACHIALS

The non-resorption development of the uniserial type was relatively simple and straight-forward. On the other hand, resorption represented a major growth factor in the biserial Brr. Consequently, the ontogeny was more complex

---

*Since the Girardeau monograph text was written, the writer examined the transitional uniserial to immature biserial Br development stage in several species of *Woodocrinus* (Brower, in preparation). The woodocrinid ontogenetic changes paralleled those of the Girardeau macrostylocrinid except that the "pinnule facet food groove" axis shows no evidence of lateral migration. Thus, the woodocrinid biserial Brr development was less complex and underwent less metamorphosis than in the Girardeau form.

and a higher degree of integration and coordination of the various Brr dimensions was required to prevent gaps from developing between the adjacent Brr, especially during the transitional and early biserial stages. Study of the uniserial and biserial armed patelliocrinids shows that the pinnules are more densely packed along biserial arms owing to the presence of two rows of pinnulate Br which alternate from side to side of the arm. Thus, given uniserial and biserial individuals with comparable arm lengths and Brr heights, the latter possessed roughly twice as many pinnules. Also judging from the amount of curvature shown by arms of both types the biserial ones were more flexible, at least in the species where sophisticated muscular or ligamental articulations were not developed.

In Paleozoic camerates and pinnulate inadunates, the usual evolutionary sequence was from uniserial to biserial arms. The ubiquity of this trend suggests that it was strongly adaptive to most forms. It is notable that virtually all Paleozoic pinnulate forms lacked sophisticated muscular articulations within the arms. Most Paleozoic pinnulate crinoids had strictly ligamental articulations. In camerates, distinct transverse ridges are not generally present, although these occur in numerous inadunates. Usually, the ligaments were short with respect to the Brr heights. Therefore, the arms were relatively rigid and not especially flexible. However, some late Paleozoic inadunates developed muscular articulations within the proximal portions of the arms, although the distal Brr retained the ligamental type (see Van Sant and Lane, 1964, pp. 34-67, for summary of Paleozoic crinoid articulations; Gislén, 1924, for living taxa).

All modern species have uniserial or wedge-shaped pinnulate Brr; none are biserial. In addition, sophisticated and well-developed large-scale muscular articulations are present which allow a high degree of arm flexibility. Apparently, natural selection places a premium on uniserial, not biserial, arms in living forms. Thus, the present selection pressure is reversed from that which prevailed throughout the Paleozoic.

The writer presents the following hypothesis. The adaptive significance of the change from uniserial to biserial arms was twofold: development of moderate flexibility which augmented the arm leverage and increase in number of pinnules per unit arm length. This clearly resulted in a larger food gathering system, both in terms of the number of food catching tube feet and in the area of water covered, and most likely in a higher degree of arm leverage owing to the rise in the arm and pinnule surface area. In Paleozoic crinoids, these advantages usually out-weighed the disadvantages of the more complex biserial Br ontogeny.

In modern species, a higher degree of arm flexibility is achieved by the sophisticated muscular Brr articulations. The adaptive significance of the increased pinnule number in a biserial arm may be less in extant taxa than in Paleozoic forms. This is because the viscera volume relative to arm length seems less in the average living crinoid than in the average Paleozoic one. Here, the potential advantages of the biserial over uniserial arms may be over-balanced by the disadvantages of the more complex biserial Brr growth mechanism. Also, it is difficult to visualize the development of the modern crinoid arm muscular articulations in biserial Brr. In the long run, the uniserial pinnulate Brr have proved more successful than the biserial ones.

FOOD GATHERING SYSTEM ONTOGENY

The food gathering efficiency of any crinoid is a function of two components. First is the tissue mass or volume which must be supplied with food and its metabolic rates. This determines the amount of food ingested over a given time interval. Essentially, nothing is known about Recent crinoid metabolic rates. However, the time-size growth rate variation within one species and between different forms probably indicates that these vary within the life of one animal and that different species are characterized by different metabolic rates. Breimer (1969) suggested that deeper water crinoids show lower metabolic rates and slower time-size growth rates than those dwelling in shallower water. He believed that this is related to a more abundant food supply in shallow water habitats.

The tissue volume was estimated as follows. The Girardeau crowns are invariably in matrix. Because of this and the complex geometry involved, the total endoskeleton and soft part volume cannot be measured. Inspection of the crowns will convince the investigator that about 15% of the tissue, except for the organic matrix within the plates, lay inside the calyx. Most of the tissue within the porous plates occurred in the arms (97% of the total crown value) and stem with only a subordinate amount housed in the calyx plates. By analogy with living crinoids, the epidermis (outside the plates) was thin relative to the other layers and it was ignored in computation. Due to the geometry, the tissue volume can only be approximated by calyx volume. Completely preserved stems are rare and the food gathering system volume is too complex to measure. In the Girardeau individuals, the internal calyx volume, (viscera volume) cannot be calculated as the plate thickness is not known in all cases. Inasmuch as most species studied are thin-plated types, the internal volume nearly equals the external figure. Experimentation shows that this involves relatively little change in volume. Also the plates are porous and the pores were permeated by organic matrix; the porosity figure (taken from living crinoids) comprises 60% of the external plate volume. Although the total volume was not determined, both the calyx volume and total volume are (linear dimension)^3 functions; in this context, the approximation is somewhat justified. The calyx volume was calculated assuming that the calyx is a prolate ellipse of rotation.

Secondly is the rate of food gathering per unit time multiplied by the total feeding time. These two parameters cannot be determined for any fossil crinoid, and they have not been fully measured for any extant form. Breimer (1969, p. 140) estimated that living crinoids probably spend at least half their lives obtaining food. Magnus (1967) calculated the amount of water filtered by *Heterometra savignyi,* a shallow-water Recent rheophile. The water area drained by the food gathering system ranges around 500 cm^2 with a current velocity of 2 cm per second. During a 12 hour feeding interval, the crinoid processes 40,000 liters of water. Feeding is not continuous in living forms nor was it continuous in the Girardeau camerates (see burial orientations). Only those Girardeau animals preserved in the food gathering position were feeding at the time of death. The Girardeau camerate feeding specimens are less abundant in the collections than the non-feeding ones. This implies to the writer that the feeding intervals were shorter than the non-feeding ones. The frequencies of the food gathering burial orientations also suggest that the "young assemblage" Girardeau camerates spent more time feeding than did the "adult assemblage" crinoids.

The food gathering rate is a function of many variables such as: A. Mean amount of food per unit volume of water surrounding the crinoid food gathering system and the variation thereof in time and space during the feeding interval; B. The type of food taken (see later discussion); C. Number and kinds of tube feet. Most Girardeau camerate species possess roughly four or five covering plate pairs per Br and pinnular. The number remained constant through ontogeny except for the terminal Brr and pinnulars in forms where this can be determined (*e.g., Ptychocrinus splendens, P. fimbriatus*). This denotes a constant number of tube feet per Br and pinnular for the Girardeau camerates. The total number and tube feet types cannot be directly ascertained (see later discussion); D. Rate of reaction and food catching efficiency of the tube feet; E. Movement speed of the food particles down the food grooves once trapped and the subsequent number of particles lost or rejected; F. Total amount of water drained by the food gathering system.

Of all these variables, only the last can be approached directly, although C and the food gathering time are discussed in an indirect and speculative context. The food gathering system area cannot be measured because the food grooves are almost always buried by matrix, and due to the complex geometry. Consequently, the food gathering system is determined in terms of lengths. Obviously, the two are related, the greater the length, the greater the area. The free ambulacral tract length per arm equals: the number of pinnule bearing Brr in each arm, multiplied by the average pinnule length, plus the free arm length. To obtain the total length, the previous value is multiplied by the arm number. Most of the food gathering system is represented by the Brr number and the mean pinnule length product (90 to 97% in mature animals). The young crinoid average pinnule length can generally be defined by the mean, as most or all pinnules are visible. In the adult crinoids, all pinnules are observed in some but not all individuals. The mean is applied to the former case. In the latter crowns, the average pinnule is located by analogy with roughly equivalent "sized" conspecific crinoids. Usually, this pinnule is about 75% above the arm base. The food gathering efficiency of the Girardeau camerates is total length of free ambulacral tracts in cm/calyx volume in cc.

ONTOGENY OF THE ENTIRE FOOD GATHERING SYSTEM

The development of calyx volume and "size" always followed an exponential pattern. The youngest crinoids have calyx volumes ranging from about .001 to .01 cc and "sizes" of 1.0 to 1.5 mm. Most adults are distributed over the 5 to 10 mm "size" interval; the corresponding calyx volumes vary from roughly .1 to 1.0 cc. During the early development, 1 mm "size" increments resulted in small volume growth rates (.008 cc in *Eopatelliocrinus scyphogracilis,* n. gen., n. sp.), whereas in mature individuals, the same "size" increments caused much more rapid calyx volume augmentation (.08 cc in the above species).

All regression line types are observed in the "size" versus length of food gathering system. The relation may have been linear with a constant free ambulacral tract length growth rate per 1 mm "size" increment or exponential with an increasing or decreasing growth rate in the older and larger crinoids.

Two patterns were shown by the food gathering system development relative to calyx volume, both of which were curvilinear. Type 1. Most Girardeau forms were characterized by free ambulacral tract length per calyx volume increment growth vectors which dropped with increasing volume and age (*i.e.,* all patelliocrinids, *Alisocrinus tetrarmatus,* n. sp. and *Ptychocrinus splendens*). Type 2. In *P. fim-*

briatus, the food gathering system length growth rate per additional unit of calyx volume rose in larger crinoids. Although not seen in the Girardeau camerates, linear relations presumably existed.

The significance of the different developmental patterns remains unknown. The Type 2 crinoid has a primitive many-FBrr calyx (calyx Type 2 of previous discussion). Type 1 species include both few-FBrr dorsal cups (patelliocrinids) and primitive many-FBrr calyces (*Alisocrinus tetrarmatus,* n. sp. and *Ptychocrinus splendens*). Thus no apparent relationship is discerned between the calyx geometry and the food gathering system and calyx volume development. However, further data are required prior to the formulation of a meaningful hypothesis.

The Girardeau camerate food gathering efficiencies were computed from the equations of calyx volume versus length of free ambulacral tracts or calculated from single specimens depending on the species. These are listed below for the largest and smallest crinoids of all species with the means and percentage standard deviations for the youngest and oldest crowns of all taxa (one of the youngest *Ptychocrinus splendens* individuals was omitted from the computations because the calyx volume is about 10 times those of the other species):

Table of Food Gathering Efficiencies for Girardeau Camerates

Species	Food Gathering Efficiencies cm/cc	
	Youngest crinoids	Oldest crinoids
Eopatelliocrinus scyphogracilis, n. gen., n. sp.	8600	3100, 1900
E. latibrachiatus, n. gen., n. sp.	9700, 5500	1800
Macrostylocrinus pristinus, n. sp.	6000, 6200	3700
Ptychocrinus splendens	8900, 3080	1400
P. fimbriatus	11,200, 4500	3400
Alisocrinus tetrarmatus, n. sp.	7800	4800
Mean — all species	7800	2900
Percentage standard deviation — all species	13%	43%

Invariably, the food gathering efficiency declined during progressive development of a single species. The initial change was most rapid and 50% or more of the total drop occurred over the lower 15% of the calyx volume interval, whereas the remaining decrease was distributed over the latter 85% volume range.

Gislén (1924, p. 285) investigated the food gathering efficiency in 16 species of adult living crinoids. His values range from 126 to 1002 cm/cc. These food gathering efficiencies are not comparable to those of the Girardeau forms, because Gislén's ratio equalled the length of food gathering system/total endoskeleton volume where the Girardeau values are defined by the length of free ambulacral tracts/calyx volume. Gislén tentatively concluded that the food gathering efficiency increased with greater depths of water. The correlation coefficient for Gislén's data comprises –.28, which indicates no significant relationship. The Girardeau camerates also provide a useful test of this hypothesis. According to Gislén's theory, the adult crinoids of all species should be characterized by similar food gathering efficiencies because they occurred in the same habitat. The Girardeau form mean food gathering efficiency equals 2900, with a range of 1400 to 4800; the percentage standard deviation consists of 43%. Clearly, the wide variation shows that the ratio was not strongly subject to depth control.

The average food gathering efficiency of the youngest Girardeau camerates is 7800, the range from 6100 to 8900 (excludes the smallest *Ptychocrinus splendens*), and the percentage standard deviation 13%. Perhaps, the more narrow variation was related to more intense selection of the young individuals. Unfortunately, comparable data are not available from other stratigraphic units.

As previously discussed, the abundant Girardeau camerates maintained large populations where small selection coefficients comprised effective agents of evolution. This suggests that any consistent trend toward differential elimination of certain morphological types during ontogeny was produced by natural selection which operated over the life of the crinoid (*i.e.,* Darwinian selection). If this reasoning is valid, then the differential trends should be interpreted in terms of adaptation. Although this view is followed here, a slight doubt remains because nothing concrete can be inferred about reproductive survival. For example a character with no adaptive significance to a mature animal could have or be linked to some attribute which confers reproductive advantage. In fossils where the entire life cycle is not known, the reproductive survival must be approached indirectly. The camerates maintained their large population through an appreciable time, *i.e.,* 10 or more feet of Girardeau Limestone. This denotes some measure of reproductive survival.

To facilitate interpretation of the amount of variation shown by the Girardeau camerates, the most convenient method is to reduce the variability of calyx volume (x) and food gathering system length (y) to variation in the latter character only. Consequently y was regressed on x (see previous discussion of statistical techniques). The percentage standard deviation of y with respect to x was calculated in the usual manner.

The "young assemblage" crinoids represent deaths in that interval. The "adult assemblage" animals constitute those which survived the "young assemblage" period and died later during the life cycle. The percentage standard deviations are tabulated below for the three Girardeau camerates in which these have been determined:

Table Showing Percentage Standard Deviations of Food Gathering System Length with Respect to Calyx Volume for some Girardeau Camerates

Species	Number of Specimens	Percentage standard deviation. Food gathering system length with respect to calyx volume
Eopatelliocrinus scyphogracilis, n. gen., n. sp.		
"Young Assemblage"	11	13%
"Adult Assemblage"	5	2.6%
E. latibrachiatus, n. gen., n. sp.		
"Young Assemblage"	6	18%
"Adult Assemblage"	4	2.2%
Alisocrinus tetrarmatus, n. sp.		
"Young Assemblage"	6	5.2%
"Adult Assemblage"	6	2.4%

The above figures clearly indicate a decline in variation from the "young" to the "adult assemblage" crinoids in all three species. Expressed somewhat differently, the survivors (*i.e.*, "adult assemblage") showed much less variability than the animals which died earlier in the life cycle (*i.e.*, "young assemblage"). The large population sizes suggest that this was caused by natural selection which operated during the life span of the species. Unfortunately, the Girardeau camerate data are not abundant enough to define more than two age groups per species. However, the same general type of selection can be documented for a large sample of *Woodocrinus macrodactylus* (Brower, in preparation); the sample comprises about 60 crinoids, divided into six mortality and survivorship classes. The woodocrinid number of Brr per arm variation is analysed relative to size; the woodocrinid size equals the height plus width of the RR. Over the woodocrinid life span, the number of Brr per arm percentage standard deviations declined from 21% in the youngest animals to 4.7% in the oldest ones.

It must be realized that the above figures do not indicate the direction of selection. In the Girardeau camerates this is inferred from the distribution of abnormal individuals. Three "young assemblage" crowns of *Alisocrinus tetrarmatus,* n. sp. have only three arms in one or more rays rather than the normal four. These had lower food gathering efficiency than the equivalent "sized" normal specimens. Only one such "adult assemblage" crown abnormal is known. "Young assemblage" individuals of *Ptychocrinus splendens* and *P. fimbriatus* with aborted arms or rays are fairly common. Generally, the abnormal arm or ray is shorter than a normal arm or ray and does not seem to have developed fully. These do not represent regeneration. Like the alisocrinid, the abnormal ptychocrinids had low food gathering efficiency with respect to normal specimens of the same "size". None of the "adult assemblage" ptychocrinids show these aborted arms or rays. The higher frequencies of the abnormal youngsters suggest that these were eliminated by natural selection prior to maturity. Basically, it appears that the selection acted against the individuals with low food gathering efficiency. This is also supported by the fact that the "young assemblage" Girardeau camerates probably spent more time feeding that did the older animals. Similar selection can be documented for *Woodocrinus macrodactylus* (Brower, in preparation). The normal variants bear 20 arms; about 15% of the specimens possess more than 20 arms, up to 35 arms. The size life spans of the animals with more than 20 arms are significantly longer than those of the typical 20 armed variants.

The food gathering system of a crinoid serves four functions. Food gathering and arm leverage have already been discussed. Gaseous interchange for respiration of living and presumably fossil crinoids is a surface area process. In a Girardeau camerate, over 80% of the crown surface area was contained in the arms and pinnules. The gonads of living and probably fossil pinnulate crinoids occur on the proximal pinnules. Most Recent crinoids have 10 to 20 pairs of genital pinnules in each arm (A. H. Clark, 1921, pp. 149-154).

Relative to an equivalent "sized" crinoid with average or high food gathering efficiency, the low food gathering efficiency Girardeau camerate exhibited: A. Lesser food gathering and respiratory capacity owing to the shorter food gathering system with fewer tube feet. B. Reduced arm leverage because of the shorter food gathering system with smaller surface area. C. For normal specimens with the usual number of arms, the number of genital pinnules was probably not affected. However, the fewer pinnulars probably decreased the number of gonads present in the low food gathering efficiency animals. Certainly, the abnormal individuals (*i.e.*, aborted rays or less than the usual number of arms) bore fewer gonads than normal crinoids. Which character or combination of characters was (were) selected for and against cannot be determined for the Girardeau camerates.

The available information on the Girardeau camerates indicates the following conclusions. Natural selection reduced the food gathering system length variation relative to calyx volume throughout growth. The direction of selection favored the animals with high food gathering efficiencies and operated against the individuals with low food gathering efficiencies. The large decrease in the percentage standard deviations from the "young" to "adult assemblage" conspecific crinoids implies that the food gathering efficiency selection was most intense during the earlier growth stages. Regardless of species, the youngest Girardeau camerate food gathering efficiencies range about the same. The mean for the six species tabulated is 7800 with a range of 8900 to 6100 and a percentage standard deviation of 13%. Possibly, this was related to the intense food gathering efficiency selection previously postulated for the "young assemblage" animals. Also, the relatively uniform food gathering efficiencies may denote a low number of niches for the young animals. Perhaps, the youngest crinoids of all forms lived at roughly the same elevation above the sea bed (*i.e.*, all stems were about the same length). If so one would expect that similar food gathering efficiency selection operated on the youngest animals of all species. The mature animal food gathering efficiencies of the different species vary greatly. These cover the 1400 to 4800 interval with a 2900 mean and 43% standard deviation. This may imply more diversified adaptations for the adult crinoids. Possibly, the adults of the various camerates lived at different elevations above the sea floor. This cannot be verified for the Girardeau forms because the complete stem lengths are unknown. However, Lane (1963b) showed that the different Crawfordsville crinoid species formed a multi-layered community.

The high food gathering efficiencies and the postulated intense selection, due to food gathering efficiency, of the youngsters may have been related partly to two factors.

1. Time-size growth rates. By analogy with modern crinoids (see the introductory statement on ontogeny), the Girardeau "young assemblage" camerates were undergoing rapid time-size growth rates. The "adult assemblage" animals probably fall into the latter portion of the rapid time-size growth vectors and the slower time-size growth rates characteristic of mature forms which have attained 50% or more of the life span (see previous discussion, Hallam, 1967, pp. 31-35 for representative curves of this type). Thus, the "young assemblage" crinoids most likely expended more energy on growth than the older individuals.

2. Elevation above the substrate at which the crinoids lived. The growth of "size" and stem length cannot be determined as the complete columns are rarely preserved. Nevertheless, it is known that new columnals formed throughout ontogeny and that the height of at least some previously formed stem plates was augmented during growth. Consequently, the Girardeau camerate stem lengths increased with progressive age. Thus, the young crinoids lived close to the substrate whereas the older ones were elevated higher above the sea bed.

Perhaps, the food supply differed from the young to the adult crinoid levels — possibly less abundant or of a different type nearest the sea floor. The stomach contents have been examined for various living forms; these mostly consist of phytoplankton, zooplankton and organic detritus. Most common are diatoms, unicellular and filamentous green algae, foraminifers, dinoflagellates, other protozoans, small pelagic crustaceans, crustacean larvae, other planktonic animals, and organic detritus. Within these components, the food supply varies greatly for different species (see Hyman, 1955, p. 106; Gislén, 1924, pp. 276-279). Fell's tabulation (1966, p. 52, table 2-1) suggests that organic detritus is principally consumed by deep water forms. The phytoplankton are restricted to the euphotic zone. The organic detritus reaches a maximum near the surface (50 to 800 μg Carbon/liter) and then declines rapidly to a depth of about 100 m (10 to 100 μg C/liter). A gradual drop is observed down to 200 m, below which the detritus content remains constant at roughly 5 to 10 μg C/liter (Menzel, 1967; Menzel and Goering, 1966). The zooplankton biomass generally falls with greater depths (Banse, 1964, p. 82, fig. 4). Little is known about zooplankton near the sea bed; the data are conflicting (summary in Banse, 1964, pp. 75-77). Sometimes, the biomass increases in the lowest 3 to 4 m above the substrate; in other cases the reverse is observed (*e.g.*, Banse, Kiel Bay data, p. 75). Near Toulon in the last few meters above the sea floor, the amount of "snow" (Radiolaria, organic detritus) decreases. The few decimeters of water immediately over the sea bed are crystal clear and almost devoid of "snow." Off Villefranche-sur-Mer, abundant animal plankton is observed immediately over the substrate. Possibly, the zooplankton biomass generally rises near the substrate in agitated environments and vice versa in quiet water habitats.

Under the quiet water conditions, which sometimes occurred during Girardeau deposition, the crinoid food supply probably consisted of a down-falling rain of particles. If the "young" and "adult assemblages" occurred together in dense stands, one would expect that the mature individuals depleted the food supply somewhat before it reached the young animal understory. The Girardeau camerate populations avoided this problem because the "young" and "adult assemblage" crowns were not located together in high density gardens. The "young" and "adult assemblage" crowns were associated in low density stands where the above problem did not apply. In an agitated habitat, most of the food supply probably traveled roughly parallel to the substrate. The high density "young" and "adult assemblage" crinoids would not necessarily have been mutually exclusive under these conditions (see discussion of paleoecology).

Also, the "young assemblage" individuals probably lived in water with a higher suspended sediment content than the older crowns. Thus, the youngsters may have expended more energy in "combatting the sedimentation" (*e.g.*, expelling sediment particles from the food gathering system). Predation does not seem to have constituted a significant factor in Girardeau crinoid paleoecology.

The energy expended on growth and the level at which the animals lived can be combined into a single explanation to some extent. For example, consider conspecific young individuals of equivalent "size" and age which existed together in a high density stand, and assume that one had high food gathering efficiency whereas the others were characterized by low values. Possibly, the high food gathering efficiency crinoid was able to expend more energy on ontogeny. Presumably this resulted in more rapid time-"size" and time-stem length augmentation for the high food gathering efficiency animal than for the low food gathering efficiency ones. If so, the former individual lived at progressively higher elevations above the sea bed than did the latter ones. Consequently, the high food gathering efficiency specimen would have had a distinct competitive advantage over the low food gathering efficiency crinoids under either quiet or agitated water conditions in a high density garden. Regardless of agitation, the high food gathering efficiency animal would have had more available living space. During quiet water intervals, the longer-stemmed crinoid could have filtered food before it reached the lower level individuals. In more agitated times, the food supply probably traveled parallel to the sea floor and the crinoids fed in the rheophile orientation; here, the high food gathering efficiency specimen would have exploited a food source which could not have been reached by the shorter-stemmed animals.

The above hypothesis must be considered tentative because the stem length "size" growth rates are not available. Many variables cannot be evaluated, such as the tube feet ontogeny and similar data on crinoids from other stratigraphic units and environments are lacking.

The explanation of the highly variable food gathering efficiencies of the mature crinoids is unknown. The above discussion suggests an inverse correlation with stem length; the longer columns were associated with low food gathering efficiency and vice versa. This is not intended because the stem lengths cannot be determined. Data pertinent to such a hypothesis must be gathered from faunas with complete columns, such as found in the Rochester Shale of New York or the Keokuk of Indiana.

In an attempt to further evaluate the food gathering efficiency, the approximate number of tube feet was computed for several crowns of *Aliosocrinus tetrarmatus*, n. sp. The tube feet of *Antedon bifida* were recently studied by Nichols (1960). The pinnular tube feet occur in groups of three. Each group is associated with a lappet and consists of one long, one short, and one intermediate length tube foot. The long tube feet catch most of the food; the shorter ones mainly transfer particles to the food groove. The Br groups also have three tube feet, each of which corresponds to a middle-sized pinnular tube foot. All are active in feeding and each group is found with a single lappet. One lappet of *Antedon* rests on a single adambulacral or covering plate. The Girardeau crinoid covering plates are probably homologous with the *Antedon* adambulacrals, although these may also have functioned as lappets. For calculation, the *Antedon* arrangement is extrapolated to the camerates; actually, the tube foot order is not important as long as it was constant throughout growth. All Girardeau camerates have four to five pairs of covering plates per Br and pinnular (except terminal Br and terminal pinnulars for which the number is unknown). This distribution was retained during ontogeny where observed (*Ptychocrinus splendens*, *P. fimbriatus*). The computations are listed below.

Table Showing Number of Tube Feet for
Alisocrinus tetrarmatus, n. sp.

"Size" mm	Calyx volume cc	Feeding tube feet per arm	Feeding tube feet in pinnules of single arm	Total feeding tube feet	Total feeding tube feet/ calyx volume
1.1	.001	150	60	4,200	4,200,000
1.4	.002	180	150	6,600	3,300,000
4.2	.20	1710	5700	148,000	740,000
5.5	.20	1950	4550	130,000	650,000

Scrutiny of the above table shows that the food gathering efficiency, as measured by the number of feeding tube feet/calyx volume, decreased throughout ontogeny. As in the length of free ambulacral tracts/calyx volume, the initial down-trend of the ratio was most rapid and over half of the total decline occurred over roughly 5 to 10% of the calyx volume interval. At any rate, the growth patterns of food gathering efficiency, as determined by both methods, were essentially the same.

GROWTH OF FOOD GATHERING SYSTEM COMPONENTS

New Brr were added to the arms throughout ontogeny. As in living species, these formed at the arm tips; the Brr were never intercalated between previously formed plates.

Generally most plates within a free arm bear pinnules except for one or two terminal Brr and several proximal plates.

Additional pinnules developed as new Brr were incorporated into the growing arm. The previously formed pinnule lengths were increased by two mechanisms. New pinnulars grew at the distal pinnule tip. In most species examined the young crinoid standard Brr pinnules have only two or three joints whereas 10 or more pinnulars occur in those of mature individuals. The previously present pinnular lengths were augmented throughout ontogeny.

Inspection of any camerate growth sequence shows that the length of a single free arm increased with progressive "size" and age. Two factors controlled this pattern: the addition of new Brr and the height growth of the previously formed plates.

Because of the growth relationship between the "size," the food gathering system, and its components, the percentage of ambulacral tracts represented by the pinnules, rose rapidly during development. The pinnule component percentage was determined as follows:

$$\frac{\begin{pmatrix}\text{Number of}\\ \text{pinnule bearing}\\ \text{Brr per arm}\end{pmatrix} \times \begin{pmatrix}\text{Average}\\ \text{pinnule}\\ \text{length}\end{pmatrix} \times \begin{pmatrix}\text{Total}\\ \text{number}\\ \text{of arms}\end{pmatrix}}{\text{Total length of food gathering system}}$$

The minimum pinnule component percentages vary from 60 to 80% in the smallest crinoids depending on "size" and species. The mature specimen values equal about 94 to 96% for all Girardeau camerates.

INTEGRATION AND COORDINATION OF FOOD GATHERING SYSTEM DEVELOPMENT

The correlation coefficient ranges involving the food gathering system length and its components, the calyx volume, and "size" are tabulated below for the four species studied in detail (the food gathering system growth is not known in *Alisocrinus ? heterodactylus,* n. sp.):

Table Listing Correlation Coefficient Ranges for Some Girardeau Camerates

Species	Usual Number of Individuals	Correlation Coefficient Range
Eopatelliocrinus scyphogracilis, n. gen., n. sp.	16	.90 — .994
E. latibrachiatus, n. gen., n. sp.	10	.88 — .989
Macrostylocrinus pristinus, n. sp.	11	.94 — .994
Alisocrinus tetrarmatus, n. sp.	12	.96 — .996

The significance levels of the correlation coefficients always equal or exceed .999. The high correlation coefficients and significance levels thereof indicate that the food gathering system ontogeny of all forms was subject to a high degree of integration and coordination. Thus, the larger crinoids had longer food gathering systems, greater calyx volumes, more pinnules and pinnulars, and longer arms. The data also show that an integration and coordination gradient existed among the various species; listed from maximum to minimum regulation, these were: *A. tetrarmatus,* n. sp., *Eopatelliocrinus scyphogracilis,* n. gen., n. sp., *Macrostylocrinus pristinus,* n. sp. and *Eopatelliocrinus latibrachiatus,* n. gen., n. sp. At present, the food gathering system growth data are not available from enough species to draw any general conclusions or relationships.

Assuming that adequate support was provided by the FBrr (see discussion of supporting structures), the explanation of the high degree of integration and coordination of the camerate food gathering system is easily visualized from the following relationships:

1. The arm length and number of Brr are positively correlated. In turn, these were both partially controlled by the growth of several free Br dimensions. First, the average height and width. Arms of roughly a given length, composed of relatively high plates, have fewer Brr (compare *Eopatelliocrinus scyphogracilis,* n. gen., n sp. and *E. latibrachiatus,* n. gen., n. sp.). Second, the convergence angle of the lateral Brr sides which is determined by the proximal and distal Br widths and the average height. Clearly, the lateral convergence defines the rate of arm taper, and other factors being equal, large angles dictate short arms with small numbers of Brr. Although this convergence was not investigated quantitatively, several generalizations are presented. The lateral convergence always increases from small angles in the proximal Brr to larger values in the distal regions, although the rate of convergence increase varies from species to species. Basically, the problem involves simple mechanics: how many cylinders (Brr bound together by ligaments in the camerates) can be arranged from top to bottom before the structure became statically unstable?

2. The pinnule length and the pinnule facet size and area are clearly related as the facet supported the pinnule. In turn, the pinnule facet area and its rate of increase was controlled by the growth rates of three Br parameters: First, the average width which partly extended the facet proximally, distally and outward. Second, the maximum height which partially caused the distal facet extension. Third, the dorsal-ventral growth rates (probably largely dorsal) dictated the facet enlargement along this axis. As previously indicated, these free Br growth rates were at least reasonably well integrated and coordinated with the "size" ontogeny.

Also, the half-ray food gathering system length was highly coordinated and integrated with the supporting Brr area. In turn, the development of these plates can be related to the calyx "size" growth. The calyx "size" and volume showed a high degree of integration because the growth of "size" and the component calyx plates caused increased calyx volume and viscera mass augmentation. Functionally, the food gathering system supplied the viscera with food and to some extent oxygen. Because of these complex geometrical and functional interrelationships, the food gathering system development comprised a highly integrated and coordinated package.

Examination of the correlation coefficients and percentage standard deviations indicates that the food gathering system growth was more highly integrated and less variable with respect to the calyx volume than "size" in four of the six Girardeau camerates (data are available for the two ptychocrinids in addition to the four species studied in detail). A similar situation is observed in comparing the correlation coefficients of the "size" and calyx volume versus the various food gathering system components. Obviously, this is due to the fact that the volume more closely reflects the amount of tissue which must have been supplied with food than does "size".

GROWTH OF SUPPORTING STRUCTURES

The supporting element ontogeny is only known in three species, *Eopatelliocrinus scyphogracilis*, n. gen., n. sp., *Macrostylocrinus pristinus*, n. sp., and *Alisocrinus tetrarmatus*, n. sp. A crinoid endoskeleton is a complex of supporting relationships. Essentially, each plate bears all the higher ones. For example, the proximal columnal supports the crown, the BB underlie the RR and all higher plates, the distal FBrr elevate the arms, and the pinnule facet holds the pinnule. The following information is required to evaluate all relations properly, the cross section areas of all plates, articular surface type together with the size and strength of all ligaments and muscles, and the effective masses of all components (*i.e.,* mass less weight of the equivalent volume of sea water). The limitations of time and preservation preclude this approach. Therefore, attention is focused on two oversimplified relationships, namely the proximal columnal area and the area of the Br which supports the free arm.

In the first case, a valid approximation consists of development of the crown effective mass versus proximal column area. Unfortunately, the former has not been determined although the calyx volume is known for most crinoids. Both the calyx volume and the crown effective mass comprise (linear dimension)^3 functions; however, their growth rates must have differed with respect to any one linear dimension. If the stem area growth vector per .01 cc calyx volume increment declined throughout ontogeny, the same situation must have occurred in the proximal columnal area development rate per unit of additional crown effective mass. The rates of decrease would have varied depending on whether calyx volume or crown effective mass was used. The supporting ratios, proximal stem area/calyx volume and proximal columnal area/crown effective mass, must have been affected in the same fashion. The development of the calyx volume and proximal columnal area is summarized below for the three taxa (*e* denotes equation value; *o* indicates minimum observed specimen ratio):

Table Showing Proximal Supporting Structure
Ontogeny in Three Girardeau Camerates

Species	Proximal columnal area growth vector in mm^2 per .01 cc calyx volume increase			Columnal area/calyx volume		
	Young	Adult	Mean	Young	Adult	Lowest "adult" assemblage ratio
Eopatelliocrinus scyphogracilis, n. gen., n. sp.	.17	.17	.17	140*e*	18*e*	13*o*
Macrostylocrinus pristinus, n. sp.	.14	.046	.067	51*e*	6.9*e*	3.4*o*
Alisocrinus tetrarmatus, n. sp.	.32	.0044	.030	42*o*	2.7*e*	3.8*o*

Regardless of the growth pattern, the columnal area relative to the calyx volume decreased during the ontogeny of all species. Two forms, *Macrostylocrinus pristinus*, n. sp. and *Alisocrinus tetrarmatus*, n. sp., showed proximal columnal area growth rates per calyx volume increment which fell throughout development. These taxa were characterized by: negative allometry; small mean columnal area growth vectors; and low adult crinoid stem area/calyx volume ratios, 3.4 and 3.8. Conversely, *Eopatelliocrinus scyphogracilis*, n. gen., n. sp. had a large and constant area growth rate which resulted in a high mature animal columnal area/calyx volume ratio of 13.

Seemingly, continuation of the proximal columnal area/calyx volume decline could have eventually produced a stem which was too small to have elevated and supported the crown. Actually, the undefined stem area/crown effective mass must have represented the important variable. Perhaps, some critical ratio served as a limit which prevented further "size" growth. Whether or not any of the Girardeau camerates reached this limit is speculative. The crown bulk densities of the three species were most likely comparable (ranged about 1.43 gm/cm^3). The observed adult proximal columnal area/calyx volume ratios suggest that *Macrostylocrinus pristinus,* n. sp. and *Alisocrinus tetrarmatus,* n. sp., might have approached this limit. Clearly, *Eopatelliocrinus scyphogracilis,* n. gen., n. sp. was well above the critical ratio.

Basically, the arms are borne by the distal FBrr. Plotting the supporting Br distal face area versus the food gathering system effective mass would illustrate the necessary relationship. The latter parameter cannot be measured, mainly due to lack of data about the food gathering system depth. Consequently, the supporting Br area is discussed relative to the half-ray or quarter-ray ambulacral tract length. *Eopatelliocrinus scyphogracilis,* n. gen., n. sp. and *Macrostylocrinus pristinus,* n. sp. have two arms per ray which are supported by the IIBrr, and the half-ray food gathering system length is used for these taxa. Four arms are found in an *Alisocrinus tetrarmatus,* n. sp. ray with each arm borne by a IIIBr. The supporting Br development is analysed with respect to the quarter-ray length in this form. The ontogenies of the three crinoids are outlined below (*e* denotes equation value; *o* indicates observed specimen highest ratios).

Table Summarizing Supporting Br Growth of Three Girardeau Limestone camerates

Species	Supporting Br area growth rate (mm^2) per 10 mm additional food gathering system length. Quarter-ray length for alisocrinids. Half-ray length for patelliocrinids.			Half-ray or quarter-ray food gathering system length/supporting Br area		
	Young	Adult	Mean	Young	Adult	Largest "adult assemblage" ratio
Eopatelliocrinus scyphogracilis, n. gen., n. sp.	.006	.008	.006 and .008	500*e*	1400*e*	2400*o*
Macrostylocrinus pristinus, n. sp.	.014	.0033	.0058	95*e*	1700*e*	2100*o*
Alisocrinus tetrarmatus, n. sp.	.038	.011	.017	74*e*	620*e*	1000*o*

One species, *Eopatelliocrinus scyphogracilis,* n. gen., n. sp. exhibited a constant supporting Br area growth rate per 10 mm of additional half-ray ambulacral tract length. The other crinoids were characterized by supporting Br area growth vectors which declined with progressive "size". Invariably, the half-ray or quarter-ray food gathering system length/supporting Br area ratio rose throughout ontogeny. This indicates that the relative supporting Br area dropped in the older and larger animals.

The highest half-ray ambulacral tract length/supporting Br area ratios for the adult patelliocrinids are 2400 and 2100. The maximum alisocrinid quarter-ray food gathering system length/supporting Br area, 1000, is only about half the patelliocrinid values. These figures were not related to the growth vector pattern (*i.e.,* linear or declining). The adult crinoid largest ratios are inversely correlated with the arm number: *Alisocrinus tetrarmatus,* n. sp., 20 arms, 1000 is maximum ratio; *Macrostylocrinus pristinus,* n. sp. and *Eopatelliocrinus scyphogracilis,* n. gen., n. sp., 10 arms, highest ratios comprise 2100 and 2400; the alisocrinid supporting Br area mean growth rate per standard half-ray or quarter-ray ambulacral tract length increment ranged over twice those of the two patelliocrinids. This was probably dictated by the number of arms.

As previously indicated, the half-ray or quarter-ray food gathering system length/supporting Br area increased in the larger animals of all taxa. Obviously the development of the food gathering system mass, a (linear dimension)^3 function, must have been exponential with respect to its length which is a linear dimension. Therefore, the half-ray or quarter-ray food gathering system effective mass/supporting Br area also must have been augmented during the observed ontogeny. Probably, continuation of this pattern would have eventually resulted in arms which were too long and heavy for the crinoid to support. Possibly, a critical ratio provided a mechanical limit, beyond which further size growth could not have taken place. Whether or not any of the Girardeau taxa approached or reached this limit is not known. However, two statements are presented. The two adult patelliocrinids were closer to the limit than was the alisocrinid. Increase in the number of arms per ray may have resulted in a larger camerate crinoid size growth limit. This is consistent with the writer's observations on Mississippian platycrinitids and dichocrinids where the larger forms tend to have more arms than the smaller species in any one fauna (Brower, 1969). However, the largest adult "sizes" of the Girardeau patelliocrinids and alisocrinid are all comparable (9.0 to 12.6 mm). Perhaps, such arm number augmentation was prerequisite and preadaptive to the larger size limit.

Comparison of the overall supporting structure data suggests that the alisocrinid terminal size may have been dictated by the proximal stem area whereas the supporting Br served this purpose in *Eopatelliocrinus scyphogracilis,* n. gen., n. sp. The *Macrostylocrinus pristinus,* n. sp. final "size" was apparently limited by both the stem and supporting Br areas.

All three taxa showed a highly integrated and coordinated pattern of supporting structure development. The correlation coefficients range from .91 to .98 and their significance levels always exceed .999 (two-sided test).

COLUMN ONTOGENY

Growth of the stem is not well known because the complete columns of mature and immature crinoids are not preserved. Generally, only the proximal portion is seen. The individual columnal articular surfaces usually cannot be examined, and few "young assemblage" crinoid stems are available for study, most of which are weathered.

The detailed mode of development for a columnal cannot be determined directly in the Girardeau camerates. The stem plate growth model formulated on the basis of living and other crinoids is discussed in the introductory statement on ontogeny.

The best known Girardeau camerate stem ontogeny sequences are those of the two ptychocrinids which are not treated statistically in this paper. The species examined here are *Eopatelliocrinus scyphogracilis*, n. gen., n. sp., *Culicocrinus ? girardeauensis*, n. sp., and *Compsocrinus nodosus*, n. sp.

The adult Girardeau camerate columns consist of four or five orders of plates (numbering of orders follows Bather, 1900, text-fig. 17; the highest orders being the thickest, the lowest the thinnest). Near the calyx, roughly two or three orders are present. All columnal orders occur three to four or more order cycles below the calyx. The order distribution suggests the developmental sequence. The highest two orders were initiated immediately below the calyx. Seemingly, these plates appeared and grew rapidly as incompletely formed ones are rare. Usually, these possess somewhat nodose margins when first observed. The lowest one or two orders were intercalated between the previously formed columnals. Immature columnals are common. When first seen, these range thin and may be discontinuous as viewed from the outside of the stem. After appearance, the initial height and width growth rates were moderately rapid and the columnal soon assumed the mature morphology. The fact that highly immature lowest order plates can be identified probably denotes that their early height and width growth rates with respect to time were slower than those of the highest order columnals. In *Eopatelliocrinus scyphogracilis*, n. gen., n. sp. and *Compsocrinus nodosus*, n. sp. one or two intermediate columnal orders may have developed by initiation below the calyx, by intercalation, or by a combination of both mechanisms. The columnal order formulas are not definitive on this point. The morphology of these plates is intermediate between that of the highest and lowest order plates. Each *Culicocrinus ? girardeauensis*, n. sp. columnal order exhibited only one mode of growth. All adult crinoid stem plates had a crenulate suture (characteristic of all Girardeau camerates) when the plates first appeared.

The mature columns typically taper distally, although the rate varies with the species. This suggests that the mean growth rates decreased distally. Expressed somewhat differently, the columnals which formed later during the ontogeny of a single individual had larger average width growth vectors and larger terminal width values than the earlier plates.

The heights of the highest orders rise down the stem, showing that these plates continued to grow in height throughout the observed column ontogeny. The distal tapering indicates that the columnal width ceased to be augmented rapidly after the earliest developmental stages. Thus, the writer visualizes two growth phases for a single highest order columnal. During the early or formation stage, the time-growth vectors were most rapid; the width growth greatly exceeded that of height. Slow time-height augmentation was present in the later ontogenic phases. In addition, slow width growth may have occurred. In the lowest one or two orders, the columnal heights either remain constant or increase slightly in the distal direction. The widths decline distally. The formation stage is believed to have consisted of moderately rapid time-size growth rates (slower than higher orders) during which the height growth was exceeded by that of width. Throughout later ontogeny, either constant heights were retained or the heights were augmented slowly.

Comparison of comparable stem regions (in terms of number of order cycles below the calyx) for conspecific "young" and "adult assemblage" ptychocrinids discloses that the former have one or two fewer columnal orders. Always the highest order columnals are present whereas the lowest order ones are lacking. Thus, the young crinoid columnals mainly formed below the calyx, and probably less than 50% of the plates were initiated by intercalation. For the adult specimens, intercalation was more common, and from 40 to 70% of the columnals most likely grew by this mechanism. Also, only the highest "young assemblage" crinoid order generally has nodose margins; the other stem plates exhibit smooth sides. Preservation is insufficient to determine whether or not crenulate sutures exist in all cases.

The "size"-stem length growth rates cannot be ascertained for the Girardeau camerates because the complete columns are not available. Nevertheless, three processes operated to augment the stem length throughout ontogeny:

continuous development of new higher order plates immediately below the calyx; intercalation of lower orders between the previously present columnals; and height growth of the columnals after their first appearance.

GIRARDEAU CAMERATE ORNAMENTATION

All Girardeau camerates of which the ontogeny is known possess similar ornamentation. The predominant plate sculpture consists of the median-ray ridges and the associated ridges on the BB. In addition, various types of ornamentation such as stellate ridges with or without nodes generally occur on the iBrr of which the stellate ridges may cross onto the subadjacent, superadjacent, and adjacent ray plates. All Girardeau camerates followed all or part of the same ornamentation sequence. The first formed elements were the median-ray and probably the anal-interray ridges. The earliest median-ray ridges developed on the IBrr. During later ontogeny, these were extended proximally and eventually reached the lower margins of the BB. The early stages of the anal-interray ridge growth are unclear. The second ornamentation components comprised the lateral RR ridges and the lateral-oblique ridges. The latter connect the anal-interray ridge on the primanal to the C and D ray RR. Apparently, the lateral RR ridges were initiated on the C and D ray RR and thereafter spread to the other RR. During the last phase, the iBrr stellate ridges, sometimes with nodes, appeared in most species. The exact development sequence is unknown because these elements formed rapidly. The iBrr stellate ridges are lacking in *Eopatelliocrinus latibrachiatus*, n. gen., n. sp.

As previously mentioned, the median-ray and other ridges grew directly over the aboral nerve cords within the calyx. By analogy with Recent crinoids, the aboral nervous system was fully developed in the youngest Girardeau camerates. The various external ridges did not begin to form until after the aboral nervous system was present. Clearly, the time of development of a particular external ridge type did not correspond to when the underlying aboral nerve cord originated.

PHYLOGENY — GENERAL STATEMENT

The statistical technique followed is that of Sokal and Sneath (1963, see their appendix for the outline of computations). The similarity matrix (*i.e.*, correlation coefficient matrix between species) was not used because the significance levels of most individual coefficients are below .950. Rather in both lineages examined statistically, the taxonomic distance method was selected. Essentially, this constitutes a morphological distance matrix as the characters are coded herein. The clustering is by simple averages.

The method has yielded satisfactory results in the two lineages studied quantitatively. Satisfactory should be translated as the lineages and evolutionary trends deduced therefrom largely fit the writer's preconceived notions. The phylogenies will probably be accepted by most crinoid specialists, at least in general outline. Nevertheless, three disadvantages to the Sokal and Sneath method have become apparent during this study:

1. The taxonomic distance does not directly weight the characters. However, this can be accomplished to some extent in the original data matrix, by duplicating the character or by redundant coding where the same character is coded in two ways. Conversely, both evolution through natural selection and taxonomists by various methods do weight characters. Taxonomic weighting is easily seen in the melocrinitid original data matrix (Table 17a). The BB number is a family level character, Melocrinitidae with four and Glyptocrinidae with five. The other characters are either species or genus level. Although the weight differentials between these characters due to natural selection remain unknown, a few generalizations can be presented. The basic calyx structure is more or less constant for large groups of crinoids, such as families. Within a single family, a great diversity of arm structures can be observed. The Melocrinitidae provides a classic example. This suggests to the writer that the main calyx structures evolved rapidly and were stabilized quickly in camerate crinoids. Calyx evolution of this type occurred in the patelliocrinid lineage. After stabilization the basic calyx remained constant, presumably due to stabilizing selection. In the post calyx stabilization phase, the arm structure continued to evolve, usually toward more complexity through addition of more arms or formation of ray trunks, or both. This implies to the writer that the calyx structure should be weighted more heavily than the arm morphology in camerate taxonomy and phylogeny. Essentially, the calyx and arms of camerates probably developed in two different phases. Evolution of a new calyx type seems to have constituted an adaptative breakthrough which later became more fully or better exploited by means of arm evolution. In some cases, the two phases were more or less separated in time; in other lineages, much overlap existed. Of the groups studied here, the patelliocrinids were largely characterized by calyx evolution, melocrinitids by arm evolution, and ptychocrinids by both arm and calyx evolution in which the latter mostly pre-dated the former.

2. The taxonomic distance method ignores the relationships between characters. Character relations can be of various types of which only two are known to occur in the

Girardeau lineages. Two or more characters may be functionally linked by natural selection, like in patelliocrinid evolution. One character may be prerequisite to another, as exemplified by melocrinitid arm evolution.

3. The taxonomic distances omit stratigraphic position and paleobiogeography. Any proposed lineage must be consistent with both criteria. Such is easily visualized by comparison of the dendrograms (Tables 13c, 17c), which are direct derivatives from the taxonomic distance matrices (Tables 13b, 17b), with the phylogeny diagrams (Text-figs. 28, 36). Basically, the latter are dendrograms which are modified to conform to stratigraphic relationships.

SUMMARY OF EVOLUTIONARY TRENDS

The two most intensively studied lineages are the patelliocrinids and melocrinitids which are followed from the Middle Ordovician (Trenton) to Middle Silurian (Late Llandovery and Wenlock). The evolutionary trends within both groups are most logically interpreted in an adaptative context as having benefited the crinoids concerned. This does not prove the adaptative significance of the trends; only a certain probability of such is indicated. Functional significance is also suggested by the probable population sizes of the forms involved. In both lineages, the population sizes of almost all species were large enough for small selection coefficients to have been effective agents of evolution (see paleoecology for discussion of the population size and structure of the Girardeau crinoids). Of 17 species in the two lineages, only two populations, *Culicocrinus ? girardeauensis*, n. sp. and *Alisocrinus warreni*, could have been small enough for genetic drift to have been important. Although the dimerocrinitid and clidochirid lineages have not been examined as intensively as the others, their evolutionary trends were also most likely beneficial to the crinoids.

Throughout the patelliocrinid lineage, the arms were stabilized at two per ray although the Brr evolved from the uniserial to biserial geometry. The main theme was calyx evolution during which a primitive many-FBrr calyx (Calyx Type 2 of previous discussion) was transformed into a few-FBrr configuration. The calyx eventually produced was intermediate between the typical few-FBrr patelliocrinid dorsal cup and the no FBrr type of the Platycrinitidae. The change from one extreme to the other occurred within the Middle Ordovician (Trenton) to Late Ordovician (Girardeau time, probably Richmond) interval. The principal calyx evolutionary trends were: A. Reduction of the BB from five to three. B. Loss of FBrr. C. Fixed ray-plate simplification during which the IBr1 was changed from hexagonal to rectangular, and the IAx was altered from pentagonal to septagonal to pentagonal. Because of this, the height of the adjacent iBr1 relative to "size" was augmented. D. Decrease in the number of plates following the primanal from three to two; apparently, the proximal anal series plate was displaced distally during this process. E. Decline of the IBrr heights relative to "size"; this was correlated with increasing RR height with respect to "size".

During the studied portion of the lineage, certain sets of characters were correlated, positively or negatively, and tended to evolve together. Relative to the above list, characters A and B formed one group and C, D and perhaps E constituted another character complex. Clearly natural selection was operating on a series of characters, some of which were correlated, at any one time. Inasmuch as the correlated characters were selected together, presumably they were functionally related. The general line of evolution was:

Glyptocrinus (two arms per ray) → *Eopatelliocrinus*, n. gen., →

Macrostylocrinus → {*Culicocrinus ? girardeauensis*, n. sp.
Patelliocrinus

In the melocrinitid line, the calyx was fixed at a primitive many-FBrr type throughout evolution and the only consistent calyx change was reduction of the BB from five to four. Almost all primitive melocrinitid evolution affected the arms, and the principal steps were, listed in order of appearance in the fossil record: A. Development of four arms per ray from two arms per ray. This change was affected by converting the IIBrr2 pinnules into pinnulate arms. B. Formation of the first inner quarter-ray arm branches. C. Loss of pinnules proximal to the above arm branches. At this time, the inner quarter-rays constituted primitive ray trunks. D. Initiation of more ray trunk branches along the inner quarter-rays. In this stage of evolution, the new ray trunk branches appeared and the ray trunk pinnules proximal to these were lost simultaneously. E. Development of biserial Brr on the outer quarter-rays and ray trunk branches.

Correlated characters are also known in the melocrinitid evolution, although the correlations were of a different type than seen in the patelliocrinids. All melocrinitid correlations were of the prerequisite rather than the functionally linked type. For example, the acquisition of four arms per ray occurred prior to and as seemingly prerequisite to any ray trunk evolution. This prerequisite did not hold true for all phylogenies; *Steganocrinus*, a Mississippian actinocrinitid, developed ray trunks from only two arms per ray. In similar fashion, the primitive melocrinitids initiated the first inner quarter-ray arm branch prior to the loss of any inner quarter-ray pinnules. As a consequence of the type of char-

acter correlations in the studied melocrinitid species, natural selection operated on one character at a time throughout the lineage. The general succession of taxa was:
Glyptocrinus (two arms per ray) → *Glyptocrinus* (four arms per ray) → *Alisocrinus* → *Promelocrinus.*

The dimerocrinitid and clidochirid sequences have not been treated in as much detail as the other two groups. Both were only examined at the genus rather than the species level and important details of the lines remain unknown.

The main dimerocrinitid phylogeny consisted of:
Rhaphanocrinus → *Ptychocrinus* → *Dimerocrinites* and possibly *Eudimerocrinus*

Dimerocrinitid evolution represented calyx change which was followed by arm developments. The principal trends listed in order of appearance in the fossil record were: A. Displacement of the iR to an iBrl position. B. Primitive forms have two unbranched arms per ray and this geometry was retained by some crinoids (*e.g.*, certain species of *Dimerocrinites*). The other crinoids with two arms per ray evolved more or less numerous arm branches (*Ptychocrinus splendens* and *Eudimerocrinus*). Various forms attained four unbranched arms per ray with the IIBr2 being axillary (*Ptychocrinus* and some *Dimerocrinites*). C. Formation of biserial from uniserial Brr. The evolution of the arm branching formula and Brr type overlapped to some extent although the arm branching changes appeared prior to biserial Brr in the whole line. The evolutionary trends were probably not correlated.

Both *Clidochirus* and *Anisocrinus* are known from Late Ordovician rocks. The two genera are basically the same except that the iBrrl are present in the anisocrinids and are lacking in the clidochirids. Both taxa are believed to constitute important flexible crinoid ancestral stocks. Later Ichthyocrinidae and Lecanocrinidae were probably descended from a primitive species of *Clidochirus,* such as the Girardeau form. *Anisocrinus* most likely represented the ancestral homalocrinid. The close resemblence of the early *Anisocrinus* and *Clidochirus* is suggestive of a common origin. The later evolution of the anisocrinids and clidochirids involved the CD interray, crown habit, and arm structure in various ways.

Both growth and phylogeny sequences are available in all lineages, except the flexible crinoids. The evolutionary trends probably occurred through "mutations" (used in the most general sense, includes gene changes, chromosome inversions, and so forth) which affected the young crinoids at various growth stages and caused divergences during the later ontogeny. This is supported by comparing the young versus the adult crinoids of two different species. In all cases examined here, the young crinoids are much more similar than the adults (see comparisons within the ontogeny sections on the Girardeau species). The responsible "mutations" can be catalogued with reasonable certainty relative to the known ontogenies. In this context, any phylogeny can be visualized as a sequence of successive ontogenies. In two lines, the melocrinitids and dimerocrinitids, the stratigraphically younger "mutations" tended to occur later during ontogeny, except for the transition from uniserial to biserial Brr. The other groups were not characterized by this feature. On an average basis, the calyx "mutations" generally appeared earlier during growth than those which affected the arms. The "mutations" involved: A. Addition of new plates or loss of old ones, *i.e.*, changes in the plate supply rate. B. Variation in the plate development sequence. Only two examples are documented. In the primitive patelliocrinids, the first anal series plate probably developed before the proximal CD interray iBrr; this plate sequence was reversed in the advanced species. It is also suggested that the camerate crinoid iBrl formed earlier than the equivalent plate in living comatulids (see calyx ontogeny of *Alisocrinus tetrarmatus,* n. sp.). C. Changes in the developmental vectors of one or a series of plates, relative to time, "size", or growth of the adjacent plates.

One of the most spectacular aspects of the Girardeau crinoid phylogenies is they indicate that certain bursts of evolution, which were previously believed to be largely Silurian, were well underway during the Late Ordovician. The glyptocrinid - patelliocrinid - hapalocrinid evolution was mostly completed in the Ordovician. The later Silurian phases largely filled the morphological gaps between the previously present Late Ordovician types. Prior to this study, primitive melocrinitids (*Alisocrinus*) were not known from pre-Silurian rocks and the early stages of melocrinitid evolution are now assigned to the Ordovician. The clidochirid and anisocrinid ancestral stocks were also initiated in the Late Ordovician.

PALEOGEOGRAPHY AND EVOLUTION

In recent years, R. C. Moore (1948, 1952b) noted a strong correlation between crinoid taxonomic evolution (families and genera) and paleogeography. During the favorable intervals when suitable habitats were numerous and widespread, crinoids showed high taxonomic diversity and great abundance as a group. Not all species were abundant; some maintained large populations whereas others were small. In unfavorable times, suitable habitats were rare, at least on the present continents, and crinoids were restricted geographically and exhibited low taxonomic diversity. In the Early and Middle Paleozoic, the favorable intervals corresponded with widespread epicontinental seas and the unfavorable times mostly represented regressive phases when the epicontinental seas were restricted. During the Late Paleozoic, this relationship no longer held true. For example, the Permian basically constituted a regressive phase. Yet highly diversified crinoids occurred on the island of Timor and a moderate diversity fauna is known from Nevada. Throughout the Paleozoic, crinoid genera usually became extinct during the unfavorable times. Within the next favorable phase, the extinct taxa were replaced by new groups. In the studied lineages, the favorable intervals were Middle Ordovician, most of the Trenton; most of the Late Ordovician; and Middle Silurian. The unfavorable times consisted of: uppermost Middle Ordovician and lowermost Late Ordovician, *i.e.* top of the Trenton and basal Eden; Early Silurian; and Late Silurian.

The Girardeau quantitative lineage data provide a useful test of this theory. If correct, the taxonomic or morphological distances between adjacent taxa within one line of evolution should follow a pattern in which the mean taxonomic distances across a paleogeographic break (unfavorable interval) exceed those for crinoids within a single favorable interval. Both quantitatively examined lineages, patelliocrinids and melocrinitids, fit this model to some extent, especially the latter. Most of the melocrinitid large morphological distances were located across the unfavorable intervals. For the patelliocrinids, the mean distances across the paleogeographic breaks slightly exceed the within values (1.059 and .952) although the difference between the two figures is not striking. The Girardeau data are interpreted as follows. The morphological rates of evolution showed a certain correlation with paleogeography in the two Girardeau phylogenies. This correlation could represent a casual relationship or a meaningful phenomena. Further data are required prior to the formulation of a meaningful hypothesis. The boundaries between genera provide a poor measure of any relationship between paleogeography and evolution because these are all more or less arbitrary. The morphological data between adjacent stages in a lineage or series of lineages should furnish a more useful "yardstick". The term stage is considered independent of taxonomy, indicating only two adjacent populations in an evolutionary sequence. Integrating the morphological distances along with the diversity and the population size and structure data is the only approach to an understanding of the relations between paleogeography and evolution.

PALEOBIOGEOGRAPHY

The Ordovician phases of the Girardeau phylogenies were restricted to North America with two exceptions. *Rhaphanocrinus* (dimerocrinitid) occurred in the Middle Ordovician of Great Britain. However, the dimerocrinitid lineage was not complete in Europe. The next known European phase was *Dimerocrinities* of the Middle Silurian of Great Britain and Gotland. The intermediate link *Ptychocrinus* was conspicuously absent and was only found in North America. Therefore, it is concluded that *Rhaphanocrinus* was ancestral to *Ptychocrinus* in North America. The British *Rhaphanocrinus* (Bala beds) postdates the oldest North American rhaphanocrinid of the Chazyan and is believed to have represented an immigrant from North America. *Macrostylocrinus cirrifer* (patelliocrinid) is recorded from the Late Ordovician of Scotland. Clearly, the species had North American affinities. *M. cirrifer* was ancestral to an undescribed Scottish macrostylocrinid from the Pentland Hills, near Edinburgh, after which the line became extinct.

By the Middle Silurian, all the studied Girardeau lineages were well-diversified in both Europe and North America. Clearly, the intervening time between the known Late Ordovician and Middle Silurian occurrences was one of considerable crinoid interchange, mainly from North America to Europe.

SYSTEMATIC PALEONTOLOGY

Subclass CAMERATA Wachsmuth and Springer, 1885

Order MONOBATHRIDA Moore and Laudon, 1943

Suborder GLYPTOCRININA Moore, 1952a

Diagnosis. — Monocyclic camerates with primanal in iBr1 position; all RR in lateral contact.

Superfamily **PATELLIOCRINACEA** Ubaghs, 1953

Amended Diagnosis. — Glyptocrinina with few-FBrr calyx; iBrr composed of a small number of plates; RR large relative to IBrr; arms uniserial, biserial, or consisting of compound Brr.

Remarks. — The above diagnosis largely follows that of Ubaghs except that the superfamily limits are expanded to include *Eopatelliocrinus,* n. gen. which has uniserial arms. The previous diagnosis was restricted to forms with biserial or compound Brr.

Family **PATELLIOCRINIDAE** Angelin, 1878

Diagnosis. — Patelliocrinacea with BB circlet usually consisting of three plates, two large and one small; one genus with all BB fused together; tegmen consists of numerous plates which are differentiated into Ambb and iAmbb; arms uniserial, biserial, or made of compound Brr; arms two to four per ray.

Remarks. — This family is most closely allied to the Stelidiocrinidae (Angelin, 1878) but it differs in having a numerous plated tegmen and one B or three BB rather than a five plated circlet. The stelidiocrinid tegmen consists of a small number of large plates and is dominated by the OO and inter-half-ray iAmbb. *Stelidiocrinus* (Angelin, 1878, p. 21), the only genus in the family, has two biserial arms per ray whereas the arm structures of the Patelliocrinidae show much greater diversity.

Genus **EOPATELLIOCRINUS**, n. gen.

Type species. — By designation herein, *E. scyphogracilis*, n. gen., n. sp.

Diagnosis. — Patelliocrinidae with conical calyx; BB erect, forming part of cup walls. Primanal followed by three plates; anal interray ridge present; CD interray wider and composed of more numerous plates than lateral interrays. IBr1 ranges from rectangular to hexagonal; IAx varies from five to seven sides; structure of IBr1 and IAx correlated to some extent; hexagonal IBr1 usually associated with pentagonal IAx, these have small iBr1; rectangular IBr1 generally occurs with septagonal IAx, if so, the iBr1 is large; BB three, two large and one small; arms uniserial, two per ray.

Description of mature crinoid. — Dorsal cup conical, with steep and straight or rounded walls; BB erect with distal portions forming part of cup walls; CD interray wider than lateral interrays. Ornamentation always shows some traces of median-ray and anal interray ridges; iBrr ornamentation sometimes present.

BB three, unequal; two large and one small; sutures located in A, C and E ray positions.

RR five, generally hexagonal, largest dorsal cup plates. IBrr1 hexagonal, five sided, or rectangular. IAx ranges from pentagonal to septagonal. IBrr smaller than RR. IBr1 and IAx shapes generally correlated; hexagonal IBr1 occurs with pentagonal IAx; rectangular IBr1 with septagonal IAx. IAx bears two IIBrr1 in each ray. Distal FBr in lateral interrays ranges from IIBr2 to IIBr3. Distal inter-half-ray FBrr varies from proximal IIBr1 to IIBr4.

The iBr1 is largest iBrr; when associated with hexagonal IBr1, the iBr1 is "small" and terminates at IBr1 level; if IBr1 is rectangular, a "large" iBr1 occurs which reaches IAx level. The iBrr2 range consists of two or three plates.

Primanal located in iBr1 position (*i.e.*, C and D ray RR in lateral contact with primanal above these plates); primanal followed by three plates; the central one comprises an anal series plate; the two flanking ones are proximal CD interray iBrr. Anal series plates continue distally to tegmen, these larger than adjacent CD interray iBrr. CD interray iBrr begin with single small plate; higher ranges consist of one or perhaps two plates each.

Tegmen poorly known; lobate with upraised Ambb areas and depressed iAmbb; tegmen plates numerous; Ambb small, arranged in biserial rows of two plates each; iAmbb larger than Ambb; anal opening position uncertain, probably on tegmen surface.

Arms two per ray, erect, long or moderately long, uniserial; most Brr pinnulate with each Br bearing a single pinule; pinnules alternate from side to side of arm; terminal Br, IIBr1 and IIBr3 typically lack pinules; proximal pinnule generally located on interray side of IIBr2. Pinnules long or moderately long, straight.

Standard Brr (*i.e.*, IIBrr 8 to 13) uniserial; wide or moderately wide; width/average height ranges from 2.0 to 2.3; proximal and distal face convergence angle is 16 to 18°; pinnule facets more or less protuberant. Distal pinnulate Brr are less mature than standard Brr. Proximal IIBrr are higher relative to width than standard Brr.

Column round or pentagonal.

Remarks. — At present, two species *E. scyphogracilis*, n. gen., n. sp. and *E. latibrachiatus*, n. gen., n. sp. are definitely referred to the genus. Both are from the Girardeau. In 1904, Rowley described several crinoids from the Lower Silurian Edgewood Limestone which he assigned to *Glyptocrinus*. Two of these, *G. insperatus* Rowley (1904, p. 275, pl. 16, figs. 34, 42, 43) and *G. insperatus* "var." *pentagonus* Rowley (1904, p. 276, pl. 16, figs. 35, 36), are closely related. The type of the "variety" is clearly a monocyclic camerate with the primanal resting between the C and D ray RR (*i.e.*, tanaocrinid position). Both of these forms should be referred to the Periechocrinitidae although the exact generic assignment is uncertain to the writer. *G. insperatus* "var." *carinatus* Rowley (1904, p. 278, pl. 16, fig. 56) is divergent from the other two crinoids. Possibly, this form could be placed in *Eopatelliocrinus*, n. gen. Unfortunately, the holotype is poorly preserved and its generic or family affinities cannot be established.

Of the North American patelliocrinid genera, *Eopatelliocrinus*, n. gen. is most closely related to *Macrostylocrinus* and *Patelliocrinus*. Comparison of the new genus with all other patelliocrinid genera is tabulated on Table 5 in diagnosis form.

The data on *Briarocrinus* and its synonym *Angelinocrinus* (Jaekel, 1918, p. 38) have not been fully published. The information quoted in Table 5 is courtesy of G. Ubaghs (personal communication). For more details, the reader should consult the forthcoming "Treatise" crinoid volume.

Bassler and Moodey (1943, pp. 594, 595) assigned 12

	er of Arms per ray	Type of Brr	Range
Eopa	Two	Uniserial	Upper Ordovician, North America.
Macr p.	"	Biserial	Upper Ordovician, North America and Europe; Middle Silurian, North America and Europe; perhaps Lower Devonian, North America.
Love p.	Four	"	Middle Silurian, Europe; possibly Lower Devonian, North America.
Pate p.	Two	"	Middle Silurian, North America and Europe.
Laur p.	Probably four	Unknown	Middle Silurian, North America.
All Sp	Two	Compound	Middle Silurian, North America.
Bri p.	"	"	Middle Silurian, Europe.
Cent p.	Unknown.	"	Lower Devonian, North America.

Partial description of adult. — The bulk of the description is listed under growth, variation, and comparison of the Girardeau eopatelliocrinids.

The iBr1 range always consists of one plate; iBrr2 composed of two, rarely three plates; iBrr3 are smallest proximal iBrr, made up of two or three plates. Distal iBrr smaller and less regular than proximal iBrr; plates with four to seven sides; single range usually composed of three or four plates. Inter-half-ray plates consist of one plus two plates in only specimen where known.

Only proximal portion of CD interray preserved; primanal located in iBr1 position, followed by prominent and strongly convex series of anal plates; these plates usually hexagonal; distal margin of primanal flanked by single CD interray iBr1 on each side; CD interray iBr1 followed by one plate in next range where observed; higher structure not seen.

Articular surfaces of calyx plates smooth.

Tegmen poorly known; composed of small irregular plates with somewhat lobate Ambb areas, depressed iAmbb; IAmbb composed of series of ranges, each with two small plates; iAmbb larger than IAmbb.

Depth (*i.e.*, dorsal to ventral) of free Br exceeds width by about 20% where this can be determined. Articular surfaces poorly known; in some Brr, food groove is narder dorsal cup.

Types. — Holotype — USNM 165 541. Paratypes — USNM 164 542 — 164 555; IGS. 35P-13 — 35P-16, 35P-18, 35P-19.

Occurrence. — Girardeau Limestone, Cape Rock and Orchard Creek exposures.

EOPATELLIOCRINUS LATIBRACHIATUS, n. gen., n. sp.

Plate 61; Text-figures 6c, d, 8, 12g

Diagnosis of adult. — A small species of *Eopatelliocrinus*, n. gen. characterized by moderately wide dorsal cup with rounded walls and distal constriction at level of proximal IIBrr; median-ray ridges present but iBrr are smooth; free Brr with gently converging proximal and distal faces, Brr wide; arms moderately long with taper angle increasing sharply in distal one-third of arm; proximal part of column probably weakly pentagonal.

Partial description of adult. — Most of the description is given under the following section on ontogeny, variation, and comparison of the Girardeau eopatelliocrinids.

CD interray not completely known; primanal in iBr1 position, large, higher and wider than iBrr1 in lateral interrays, all observed primanals have "small" iBr1-type geometry; primanal followed by three plates with central plate belonging to anal series and the other two plates comprising

Table 5

Genus and Reference	Calyx Shape	Shape of IBrl	Shape of IAx	Distal level of iBrl	CD interray structure	Width of CD interray	Number of BB	Number of Arms per ray	Type of Brr	Range
Eopatelliocrinus, n. gen.	Conical with BB forming part of cup wall.	Rectangular to hexagonal.	Pentagonal to septagonal.	Mid-IBrl or IAx	Primanal plus three plates. Anal interray ridge present.	Wider than lateral interrays.	Three	Two	Uniserial	Upper Ordovician, North America.
Macrostylocrinus Hall (1852, p. 203)	"	"	"	"	Generally primanal plus three plates with or without anal interray ridge. Sometimes primanal plus two or more plates with or without anal interray ridge.	"	"	"	Biserial	Upper Ordovician, North America and Europe; Middle Silurian, North America and Europe; perhaps Lower Devonian, North America.
Loveniocrinus Jaekel (1918, p. 37)	"	Rectangular	Pentagonal	Proximal IIBrr.	Has extra plates (*i.e.*, primanal plus four). No anal interray ridge.	"	"	Four	"	Middle Silurian, Europe; possibly Lower Devonian, North America.
Patelliocrinus Angelin (1878, p. 1)	"	"	"	"	No significant extra plates. No anal interray ridge.	Like lateral interrays.	"	Two	"	Middle Silurian, North America and Europe.
Laurelocrinus Springer (1926, p. 32)	High with flat base. BB confined to base.	"	"	"	"	"	"	Probably four	Unknown	Middle Silurian, North America.
Allocrinus Wachsmuth and Springer (1889, p. 227)	Low, flat with BB confined to base.	"	"	"	"	"	"	Two	Compound	Middle Silurian, North America.
Briarocrinus Angelin (1878, p. 1)	Conical with BB forming part of cup wall.	Lateral interray IBrr joined together.	Lateral interray IAxx sometimes joined together.	"	"	"	"	"	"	Middle Silurian, Europe.
Centriocrinus Bather (1899a, p. 127)	Low, rounded with BB confined to base.	Hexagonal	Pentagonal	Mid-IBrl level.	"	"	One	Unknown.	"	Lower Devonian, North America.

Table showing comparative features of Patelliocrinidae genera.

to
p.
a-
ly
lic
D
ns
ne
n-
g.
is
r-
or

y-
s
ll
n

-
.
s
r

species to *Patelliocrinus*. Three forms, all described by Angelin, are clearly not congeneric judging from the original figures. *P. chiastodactylus* Angelin (1878, p. 1, pl. 19, fig. 12) has a hexagonal IBr1. *P. duplicatus* Angelin (1878, p. 1, pl. 19, fig. 5) shows four arms per ray and the iBr1 truncates the BB. *P. fulminatus* Angelin (1878, p. 2, pl. 26, figs. 14, 14a, b) is now assigned to *Promelocrinus* (Ubaghs, 1958, p. 272). Although these are not *Patelliocrinus*, the writer is not familiar enough with the first two crinoids to present definite generic assignments. At any rate, the three taxa do not lie within the writer's diagnosis of the genus.

Occurrence. — Upper Ordovician, North America; possibly Lower Silurian, North America.

EOPATELLIOCRINUS SCYPHOGRACILIS, n. gen., n. sp.

Plates 59, 60; Text-figures 6a, b, 7, 11g

Diagnosis of adult. — A large species of *Eopatelliocrinus*, n. gen. characterized by slender dorsal cup with straight walls which lack distal constriction; strong median-ray ridges and BB flange; calyx plates, especially iBrr with weakly developed stellate ornamentation; free Brr with gently converging proximal and distal faces, Brr slender; arms slender with slight and gradual distal taper; column round.

Partial description of adult. — The bulk of the description is listed under growth, variation, and comparison of the Girardeau eopatelliocrinids.

The iBr1 range always consists of one plate; iBrr2 composed of two, rarely three plates; iBrr3 are smallest proximal iBrr, made up of two or three plates. Distal iBrr smaller and less regular than proximal iBrr; plates with four to seven sides; single range usually composed of three or four plates. Inter-half-ray plates consist of one plus two plates in only specimen where known.

Only proximal portion of CD interray preserved; primanal located in iBr1 position, followed by prominent and strongly convex series of anal plates; these plates usually hexagonal; distal margin of primanal flanked by single CD interray iBr1 on each side; CD interray iBr1 followed by one plate in next range where observed; higher structure not seen.

Articular surfaces of calyx plates smooth.

Tegmen poorly known; composed of small irregular plates with somewhat lobate Ambb areas, depressed iAmbb; IAmbb composed of series of ranges, each with two small plates; iAmbb larger than IAmbb.

Depth (*i.e.*, dorsal to ventral) of free Br exceeds width by about 20% where this can be determined. Articular surfaces poorly known; in some Brr, food groove is narrow with rounded and slightly expanded base, depth of food groove about 45% of Br depth; in other Brr, food grooves wider and somewhat deeper although this may represent weathering. Articular surface bordered by faint dorsal and lateral marginal rim; articular surface proper smooth; faint transverse ridge may be present in some although this is not certain. Pinnule facet poorly known, only observed on one Br; apparently with marginal rim and concave articular face proper.

Pinnular food groove narrow, deep with depth equal to about 50% of pinnular height; food groove sometimes with rounded, slightly expanded base and expanded ventral area; in other pinnulars, food grooves are wider and deeper with triangular cross sections. Distal articular surface with marginal rim and gently concave articular face. Outer side covering plates massive, thick; inner side covering plates either not present or not seen.

Column round with columnals united by crenulate sutures; articular surfaces poorly known; axial canal apparently pentagonal.

Remarks. — The discussion of growth, variation, and comparison for the two Girardeau eopatelliocrinids is presented together in a single section following *E. latibrachiatus*.

Specific name. — *scyphogracilis* in allusion to the slender dorsal cup.

Types. — Holotype — USNM 165 541. Paratypes — USNM 164 542 — 164 555; IGS. 35P-13 — 35P-16, 35P-18, 35P-19.

Occurrence. — Girardeau Limestone, Cape Rock and Orchard Creek exposures.

EOPATELLIOCRINUS LATIBRACHIATUS, n. gen., n. sp.

Plate 61; Text-figures 6c, d, 8, 12g

Diagnosis of adult. — A small species of *Eopatelliocrinus*, n. gen. characterized by moderately wide dorsal cup with rounded walls and distal constriction at level of proximal IIBrr; median-ray ridges present but iBrr are smooth; free Brr with gently converging proximal and distal faces, Brr wide; arms moderately long with taper angle increasing sharply in distal one-third of arm; proximal part of column probably weakly pentagonal.

Partial description of adult. — Most of the description is given under the following section on ontogeny, variation, and comparison of the Girardeau eopatelliocrinids.

CD interray not completely known; primanal in iBr1 position, large, higher and wider than iBrr1 in lateral interrays, all observed primanals have "small" iBr1-type geometry; primanal followed by three plates with central plate belonging to anal series and the other two plates comprising

CD interray iBrr1; anal series plates wider and higher than adjacent CD interray iBrr; CD interray iBrr1 high, slender, terminating at IIBrr1 level, followed by one slender CD interray iBr2; higher structure unknown.

Calyx plate articular surfaces known in RR and IBrr of one crinoid, smooth. Tegmen unknown.

Depth of free Brr exceeds width by roughly 10%. Articular surfaces unknown. Outer side covering plates large, mostly arranged in irregular rows of two plates; where proximal "brachial food groove" branches, additional plates are present and three or four plates are seen in a row.

Pinnular food grooves wide. Covering plates more regular than those of Brr; basic arrangement is four to five biserial rows of two plates each; sometimes a row consists of three plates.

Proximal column poorly known in mature crinoid, apparently pentagonal and composed of two columnal orders: Order 2, nodose, thickness about .17 mm; Order 1, non-nodose, thickness roughly .10 mm. Articular surfaces not seen.

Remarks. — The treatment of growth, variation, and comparison is discussed in the section following this species.

Specific name. — *latibrachiatus* in allusion to the relatively wide Brr and arms.

Types. — Holotype — USNM 164 556. Paratypes — USNM 164 557 — 164 564; IGS. 35P-21 — 35P-24.

Occurrence. — Girardeau Limestone, Cape Rock and Orchard Creek exposures.

ONTOGENY, VARIATION, AND COMPARISON OF *EOPATELLIOCRINUS*, n. gen.

Ontogeny. — *Eopatelliocrinus scyphogracilis*, n. gen., n. sp. is a moderately abundant Girardeau crinoid, being represented by about 35 whole or partly preserved crowns. Of these, 21 have proved suitable for a complete or partial set of measurements. The 13 individuals assigned to the "young assemblage" range from 1.15 to 2.70 mm in "size" while the eight "adult assemblage" crinoids fall in the 4.2 to 9.6 mm "size" group (see Text-fig. 1).

E. latibrachiatus is less abundant than the type species of the genus and averages smaller in "size." The seven "young assemblage" crinoids have "sizes" from 1.15 to 2.15 mm. Seven animals are referred to the "adult assemblage"; these cover the 3.1 to 5.0 mm "size" interval (see Text-fig. 1).

The "young assemblages" of the two forms are believed to have been of equivalent "chronological ages" in terms of the number of spatfalls. Thus, the 1.15 mm "size" crinoids of both species represented the youngest individuals of the first breeding season spatfall. Similarly, the 2.15 mm *E. latibrachiatus* and the 2.70 mm *E. scyphogracilis* crinoids constituted the largest and oldest animals of this breeding season for each form. It is realized that the time duration of and the time interval between adjacent breeding seasons possibly varied between the two taxa. The same reasoning is applied to the "adult assemblages." However, less certainty is involved, because with increasing age, the Girardeau crinoid skeletal growth rates decreased. Therefore, the degree of "size" distinction between individuals produced during adjacent breeding seasons declined as the animals grew older. Consequently, the "adult assemblage" of each species could easily include specimens produced in more than one breeding season. Nevertheless, the comparison clearly denotes that the size and associated growth rates relative to spatfalls were significantly higher in the type species than in *E. latibrachiatus*.

The purpose of the growth discussions of the individual genera and species is two-fold. First is to outline the ontogeny of the taxon considered. Secondly is to compare and contrast the various developmental sequences and to illustrate the mechanisms by which one morphological type can be derived from another through progressive ontogenetic divergences. It is desired to present the growth of the average or mean crinoids. Consequently, this procedure is usually followed. The growth rates are calculated directly from the equations. Where dimensions are quoted, the independent variables (x) constitute specimen values. The dependent variable figures (y) are derived from the equations, and these correspond to the x values used. In some instances, the equations do not yield satisfactory fits to the observed data. If so, specimen figures are used in conjunction with equation growth rates, and annotations indicate the sections where this treatment is adopted. Unfortunately, complete data sets cannot be obtained for most of the crinoids in the developmental sequences. Consequently each section lists values for the largest and smallest animals for which accurate measurements were obtained.

CALYX GROWTH

Text-figure 6 presents restorations which illustrate the major features of dorsal cup plate growth for *Eopatelliocrinus*. Representative crinoids are shown in Text-figures 7 and 8 whereas the graphs and equation data are given in Text-figures 9 and 10.

As mentioned in the introduction and under *Macrostylocrinus cirrifer*, dorsal cup plate growth was adjusted so that the internal plate grooves which housed the aboral nervous system were extended; these did not migrate on the plate interiors except for minor resorption along the sides

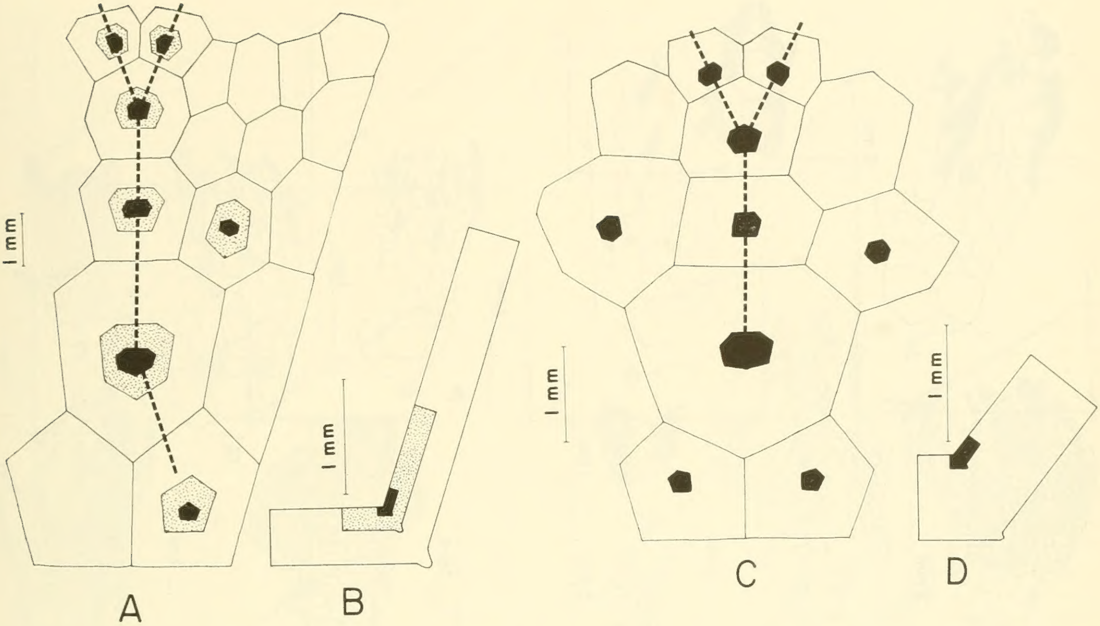

Text-figure 6. — Restorations showing calyx growth in *Eopatelliocrinus*, n. gen. A,B. *E. scyphogracilis*, n. gen., n. sp. "Sizes" 1.3, 4.0, and 9.6 mm. C,D. *E. latibrachiatus*, n. gen., n. sp. "Sizes" 1.15 and 5.0 mm.
Symbols: Smallest plates solid black; middle-sized stippled; largest blank. Axes of median-ray ridges outlined in heavy black dashed lines; as mentioned in the text, these correspond to the internal main aboral nerve grooves. In the IBrr and proximal IIBrr, these also reveal the food groove positions prior to their fixation in the dorsal cup.
Construction: Plate dimensions were computed from the equations of "size" versus the applicable plate constant. Shapes of plates not located on the ray axis are somewhat distorted because these are planar projections of surfaces which are curved in relation to the rays. Relative position of plates is based on the observations and assumptions discussed in the text. The IBrr and iBrr shapes are designed to depict the most common variant or variants in the species. Changes in side to side outline of a single plate illustrate this variation. A and C show growth of the calyx plates as seen from the exterior. Only a small B is illustrated. B and D present cross-sections of small BB for the two species. BB thickness were assumed at 17% of the R height in *E. scyphogracilis*, n. gen., n. sp., and 50% of the B height in *E. latibrachiatus*, n. gen., n. sp.

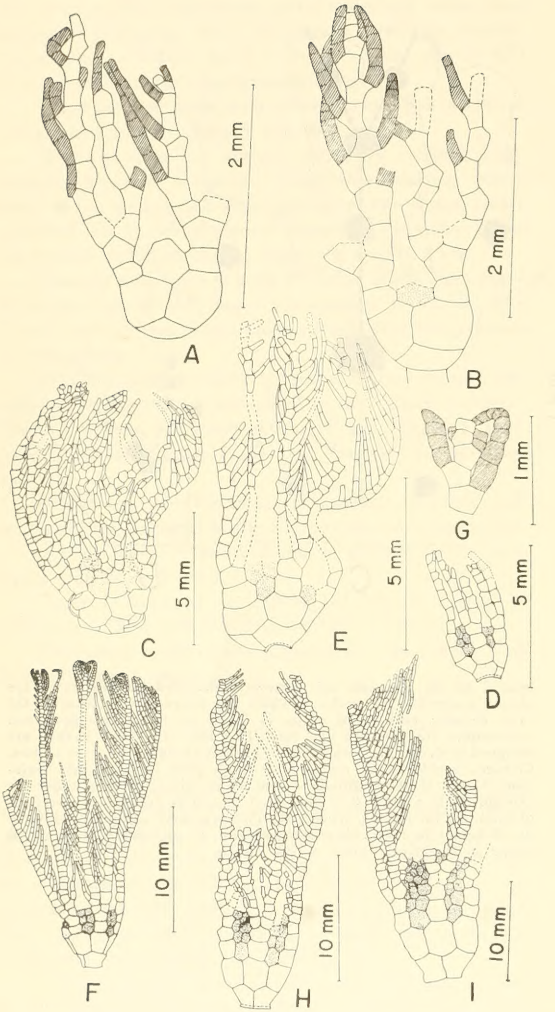

Text-figure 7. — *Eopatelliocrinus scyphogracilis*, n. gen., n. sp., Girardeau limestone. A-E are "young assemblage" crinoids whereas F-I comprise "adult assemblage" animals. A. Paratype, IGS. 35P-19, CD interray, "size" 1.15 mm, Orchard Creek exposure. B. Paratype, IGS. 35P-18, probably B and C rays, "size" 1.3 mm, Orchard Creek exposure. C. Paratype, USNM 164 550, E ray, "size" 2.5 mm, Orchard Creek exposure. D. Paratype, USNM 164 548, lateral view, "size" 2.6 mm, Cape Rock exposure. E. Paratype, USNM 164 549, lateral view, "size" 2.6 mm, Orchard Creek exposure. F,G. Holotype, USNM 164 541, "size" 4.8 mm, Cape Rock exposure. F. Lateral view of crown. G. Distal arm fragment. H. Paratype, USNM 164 544, lateral view, "size" 6.6 mm, Cape Rock exposure. I. Paratype, USNM 164 542, lateral view, "size" 9.6 mm, Cape Rock exposure.
Symbols: All iBrr stippled. Pinnules ruled on G and small crowns.

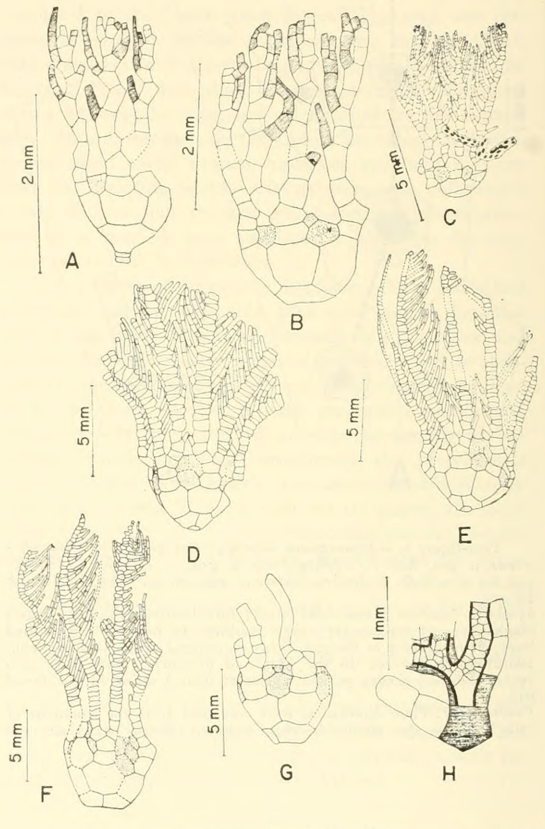

Text-figure 8. — *Eopatelliocrinus latibrachiatus*, n. gen., n. sp., Girardeau limestone. A-C represent "young assemblage" specimens; D-H are "adult assemblage" crowns. A. Paratype, IGS. 35P-23, D ray, "size" 1.15 mm, Orchard Creek exposure. B. Paratype. USNM 164 564, lateral view, "size" 1.4 mm, Orchard Creek exposure. C. Paratype, IGS. 35P-21, lateral view, "size" 1.8 mm, Orchard Creek exposure. D. Paratype, USNM 164 560, probably E ray, "size" 3.8 mm, Cape Rock exposure. E. Holotype, USNM 164 556, C ray, "size" 4.0 mm, Cape Rock exposure. F. Paratype, USNM 164 558, C ray, "size" 5.0 mm, Cape Rock exposure. G. Paratype, USNM 164 557, lateral view, "size" 5.0 mm, Cape Rock exposure. H. Sketch of immature Brr from arm fragment associated with F and G. Food grooves outlined in heavy black. Covering plates poorly preserved, diagramatic, stippled. Brr ruled. Pinnulars blank. The food groove pattern is somewhat distorted due to inclination. However, the food groove axis curvature is evident.
Symbols, A-G: All iBrr stippled. Pinnules obliquely ruled in young crinoids.

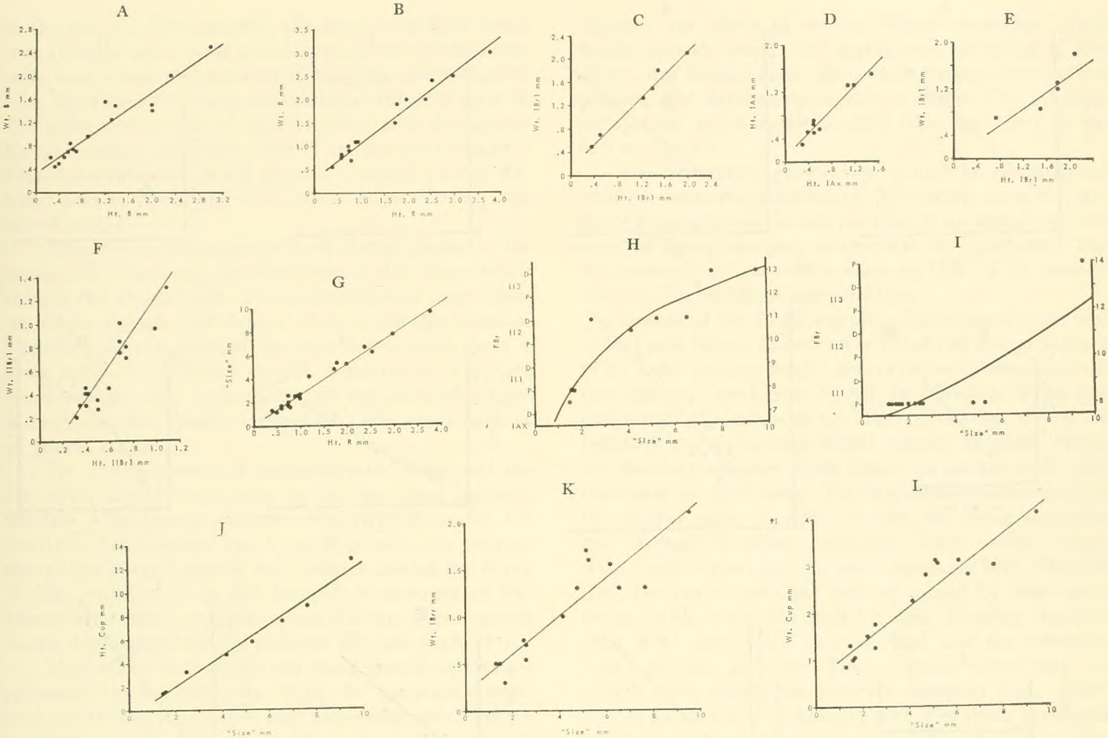

Text-figure 9. — Graphs showing calyx growth in *Eopatelliocrinus scyphogracilis*, n. gen., n. sp. FBrr scales are given in both the numerical scale used for statistical computations and the plate scale (*i.e.*, IAx, IIBr1 = II1, etc., P denotes proximal margin, D indicates distal margin). H gives the FBrr in lateral interrays. I shows the same for inter-half-rays. "*a*" designates the "initial intercept" or "pseudointercept".

Equation data:

A — $y = .327 + .692x$. $r = .958$.
$\sigma y\% = 15.6$. N = 16.

B — $y = .358 + .731x$. $r = .984$.
$\sigma y\% = 10.8$. N = 15.

C — $y = .182 + .979x$. $r = .992$.
$\sigma y\% = 5.5$. N = 6.

D — $y = .0764 + 1.00x$. $r = .975$.
$\sigma y\% = 15.0$. N = 9.

E — $y = .00445 + .733x$. $r = .879$.
$\sigma y\% = 19.9$. N = 5.

F — $y = -.172 + 1.28x$. $r = .921$.
$\sigma y\% = 22.9$. N = 15.

G — $y = .167 + 2.54x$. $r = .988$.
$\sigma y\% = 13.9$. N = 20.

H — $y = 6.89 + 6.15\log x$. $r = .931$.
$\sigma y\% = 7.7$. N = 9. "a" = .74 ($x = .1$).

I — $\mathrm{Log}\, y = .850 + .0241x$. $r = .844$.
$\sigma y\% = 3.8$. N = 12.

J — $y = -.535 + 1.28x$. $r = .991$.
$\sigma y\% = 9.8$. N = 8.

K — $y = .211 + .197x$. $r = .914$.
$\sigma y\% = 20.6$. N = 15.

L — $y = .592 + .379x$. $r = .953$.
$\sigma y\% = 14.7$. N = 15.

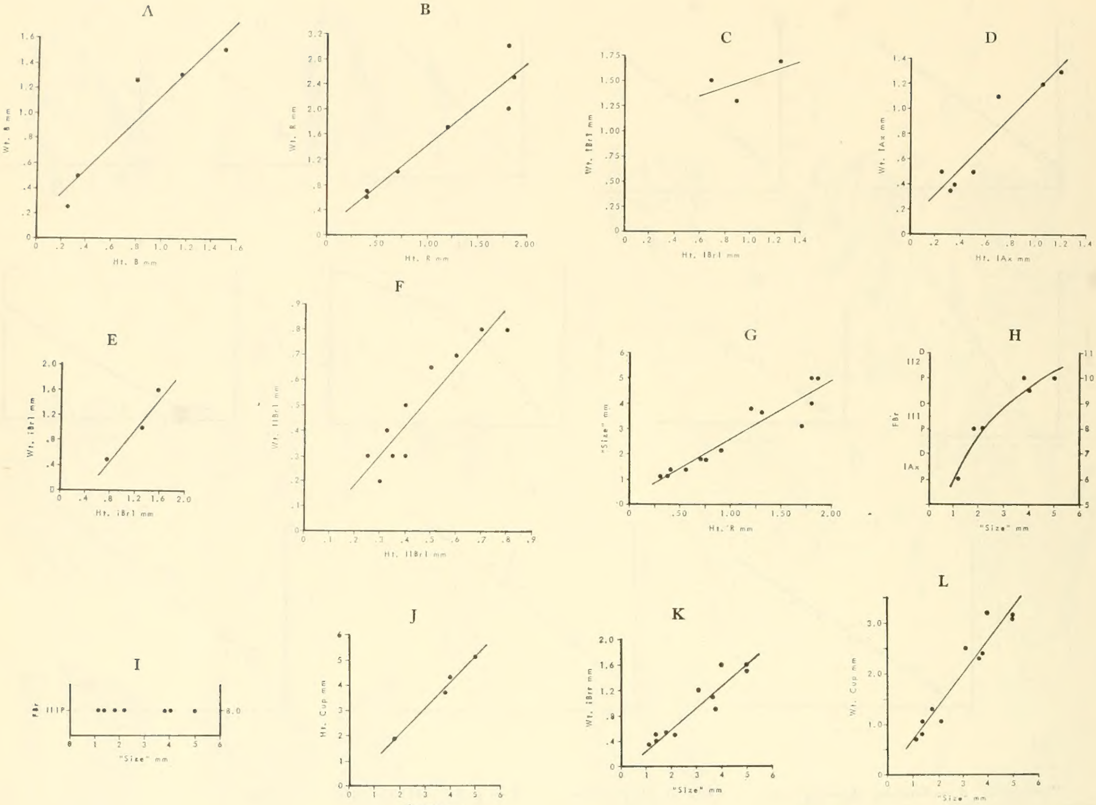

Text-figure 10. — Graphs showing calyx growth in *Eopatelliocrinus latibrachiatus*, n. gen., n. sp. FBrr are lister in both the numerical scale used for statistical computations and the plate scale (*i.e.*, IAx, IIBr1 = II1, etc., P denotes proximal margin, D refers to distal margin). H gives the FBrr in lateral interrays. I is the same for inter-half-rays. "*a*" designates the "initial intercept" or "pseudointercept".

Equation data:

A — $y = .177 + .972x$. $r = .943$.
$\sigma y\% = 25.8$. N = 5.
B — $y = .127 + 1.30x$. $r = .949$.
$\sigma y\% = 13.3$. N = 7.
C — $y = 1.071 + .452x$. $r = .629$.
$\sigma y\% = 10.6$. N = 3.
D — $y = .114 + 1.04x$. $r = .940$.
$\sigma y\% = 23.4$. N = 7.
E — $y = -.525 + 1.30x$. $r = .965$.
$\sigma y\% = 13.8$. N = 3.
F — $y = -.0456 + 1.16x$. $r = .929$.
$\sigma y\% = 20.7$. N = 10.
G — $y = .330 + 2.28x$. $r = .941$.
$\sigma y\% = 14.4$. N = 13.
H — $y = 5.97 + 6.20 \log x$. $r = .973$.
$\sigma y\% = 4.4$. N = 6. "a" = -2.37 ($x = .1$).
I — $y = 8.0$. $r = 0$.
$\sigma y\% = 0$.
J — $y = .0729 + 10.1x$. $r = .993$.
$\sigma y\% = 4.1$. N = 4.
K — $y = -.0283 + .323x$. $r = .936$.
$\sigma y\% = 17.5$. N = 11.
L — $y = .0164 + .657x$. $r = .958$.
$\sigma y\% = 15.0$. N = 11.

of the grooves. Consequently, the nerve cord knot where several aboral nerve cords joined on the plate and the nerve cords axes constituted constant topographic points of reference; plate accretion simply extended the nerve cord grooves. The nerve cord grooves are directly overlain by the median-ray and stellate ridges (if present) on the plate exteriors. This allows the position and shape of a certain plate at different sizes to be defined with respect to previous or later growth stages.

The main ornamentation of both species consists of the median-ray ridges and horizontal-lateral RR ridges which connect the adjacent RR. The *Eopatelliocrinus latibrachiatus* ridges are less well defined than in the type species. Therefore, the placement of the calyx aboral nerve cords is more precise in the latter crinoid. Some traces of stellate ornamentation occur on the iBrr and ray plates of mature *E. scyphogracilis*. The *E. latibrachiatus* iBrr are smooth at all growth stages.

The central position of the median-ray ridges and the underlying aboral nerve cords on the ray plates indicates that the width growth rates were symmetrical for the RR and IBrr. For example, the A ray R growth rate directed toward the B ray R equals that oriented toward the E ray R. This condition in the RR dictated the same for all BB. Symmetrical width accretion in the RR and IBrr required similar development for the proximal iBrr and anals.

The vertical or proximal and distal growth vectors are approached in the same way. Here, the topographic reference points comprised nerve cord branchings which can be ascertained on the RR and the IAxx. The RR branch was located where the median-ray ridge bifurcates toward the BB and for the horizontal-lateral RR ridges. The IAx branch underlay the point where the median-ray ridges split below the IIBrr1. In *E. scyphogracilis* these bifurcations were placed roughly at the plate midpoints for all crinoids in which the median-ray ridges are well developed ("sizes" over 2.5 mm), and the proximal and distal height growth vectors were approximately equal. The RR and IAxx nerve cord branches were not symmetrically located in *E. latibrachiatus*. The IAx point occurred 55% below the distal edge of the plate, and the distal height growth rate exceeded the proximal one. The R nerve cord knot lay 45% below the upper plate margin which denotes that the distal height accretion vector was less than the corresponding proximal one.

The proximal and distal IBr1 growth rates are not certain because the main aboral nerve cords were unbranched on this plate. Traces of the calyx nerve cords on the iBrr are lacking in all *E. latibrachiatus* and most *E. scyphogracilis*. Incompletely formed stellate ridges on the iBrr and adjacent ray plates of several "adult assemblage" type species crinoids permit the approximate definition of the nerve cord knots. These show that roughly symmetrical proximal and distal accretion vectors existed. This has been extrapolated to all eopatelliocrinid IBrr1 and iBrr1 shown in Text-figure 6.

The BB vertical growth rates cannot be reconstructed from the external ornamentation. The growth rates in Text-figure 6 are adjusted so that the base of the circlet was not resorbed during ontogeny except near the axial canal. The placement of the axial nerve cords on IIBr1 is by analogy with free Brr which are discussed later.

Growth of the dorsal cup plate dimensions (height and width) with respect to each other and dorsal cup parameters (*e.g.*, "size" and cup width) always followed linear patterns (see legends, Text-figures. 9, 10). In individual dorsal cup plates with the exception of IIBr1 (Text-figs. 6-10) the tendency was to increase height relative to width during the observed ontogeny. With respect to the equations, this represents two phenomena. The height growth rates generally exceeded those of width. Usually, the initial intercepts are strongly positive, indicating finite width values when height equals zero. In some instances, IBr1, IAx and iBr1, the initial intercepts may be caused by poor curve fitting owing to the few available data. In other examples (BB, RR), more data were obtained and the regression lines constitute good fits. The equations reflect only the growth rates during the observed ontogeny (*e.g.*, "size" 1.15 to 9.6 mm in *E. scyphogracilis*). The initial intercepts represent these growth rates projected backward in time and morphology. Consequently, the writer postulates rapid initial (pre-"size" equals 1.15 mm) width growth rates relative to those of height when the plates first developed. Such growth rates would not be seen in the equations. This hypothesis is supported by another line of reasoning. Assuming the ontogeny of the Girardeau eopatelliocrinids was similar to that of modern crinoids, the major calyx plates appeared in the following order: BB, RR, IBrr1, and IAxx. The sequence of iBr1 is variable in living crinoids (see introductory statement on ontogeny; consequently, it is uncertain exactly when this developed in the eopatelliocrinids. The initial intercepts of these plates decline in nearly the same order with the exception of iBr1 (see legends to Text-figs. 9, 10). Declining width intercepts for individual plates should correlate with the order of development in the calyx, because the initial width growth rates relative to height would probably have been smaller for later formed plates. A similar order is seen in the initial intercepts of "size" versus height of the various plates.

The main dorsal cup growth patterns of the two species were essentially the same with three exceptions. The *E. latibrachiatus* BB, RR, and IAx height growth rates relative to width were smaller than *E. scyphogracilis*. The reverse occurred in IIBrr1 where the relative height growth rate was larger in the former crinoid. The contrasts in calyx shape between the two forms were related to these and FBrr growth differentials. The distribution of initial intercepts (*i.e.*, width when height equals zero) of BB, RR, IAx and IIBr1 are similar in both taxa. However, the magnitudes are distinctly different, and those of *E. latibrachiatus* range about half as large as equivalent intercepts in the type species. This is believed to denote that the initial width growth rates relative to height were smaller in *E. latibrachiatus*. The calyx plates of *E. latibrachiatus* are much thicker. In paratype USNM 164 560, the R and IAx thickness is approximately .65 mm whereas the heights of these plates equal 1.2 and .75 mm, respectively. In mature *E. scyphogracilis*, the average plate thickness comprises only about 17% of the plate height. Thus, the outward (thickness) growth vectors of the type species were greatly exceeded by those of the other crinoid.

The RR width growth rate per 1 mm height increment comprised .73 mm in the type species; this contrasts greatly with the much larger 1.3 mm value of *E. latibrachiatus*. The RR dimensions are tabulated below (Text-figs. 9b, 10b):

Species	Initial height	Initial width	Initial height/ width	Maximum height	Maximum width	Maximum height/ width
E. scyphogracilis	.60 mm	.80 mm	.75	3.8 mm	3.1 mm	1.2
E. latibrachiatus	.38 mm	.62 mm	.61	1.85 mm	2.5 mm	.74

Lateral accretion occurred in all directions and maintained a seven-sided plate. However, the RR shape changed somewhat because the distal margins of the RR sutures migrated upward and the central part of the RR-BB suture moved toward the B with increasing "size" and relative age. Consequently, the proximal edges of the R became more angular.

Comparison of RR growth in the Girardeau eopatelliocrinids with the platycrinitid pattern discussed by Meyer (1965) shows a major contrast. In the latter crinoids, where the IBrr are free-Brr, the distal height growth rates were much smaller than proximal ones. Conversely, the IBrr were fixed into the eopatelliocrinid calyx and the distal and proximal RR height growth components were roughly equalized. This RR growth pattern was probably typical for camerates which have the FBrr rigidly incorporated into the calyx. The differences in RR growth are believed to have been caused by the presence or absence of FBrr. The mechanics of the FBrr bearing camerate RR growth perhaps constituted a functional disadvantage. This is suggested by the fact that platycrinitids and dichocrinids, both with the arms free above the RR, were the end products of camerate evolution.

Growth of the IBrr1 is not fully known in either form. The growth rate of width per 1 mm additional height consisted of .98 mm in the type species; this growth vector is unknown for *E. latibrachiatus* because of the small sample (three crinoids). The IBr1 data are listed below (see Text-figs. 9c, 10c; all figures given for the latter species are specimen values):

Species	Initial height	Initial width	Initial height/ width	Maximum height	Maximum width	Maximum height/ width
E. scyphogracilis	.35 mm	.53 mm	.66	2.0 mm	2.1 mm	.95
E. latibrachiatus	.27 mm	.30 mm	.90	1.25 mm	1.7 mm	.74

Two end IBr1 morphological types, hexagonal and rectangular, are observed. In individuals with both types (*e.g.*, *E. latibrachiatus*, Text-fig. 8c), the hexagonal plates tend to be slightly higher and wider than rectangular ones. This is especially marked when the IBr1-distal iBr1 junction is located near the middle of the plate. In other individuals, this junction is near the IBr1 distal margin and the height approaches that of a rectangular plate (*e.g.*, *E. latibrachiatus*, Text-figs. 8e, g). All crinoids examined have the IBr1 fixed into the calyx. Probably, the number of IBr1 sides remained constant throughout the observed growth of one individual plate, because hexagonal and rectangular IBrr1 are exhibited by crinoids of all growth stages (Text-figs. 7, 8). During ontogeny, the IBr1 height/width of the type species increased whereas the reverse characterized *E. latibrachiatus*. In hexagonal IBr1 of *E. scyphogracilis*, the IBr1-iBr1-iBr2 junction migrated distally relative to the IBr1 mid-point in older and larger crinoids.

The IAxx width growth rates per 1 mm height increments equalled about 1.0 mm in both taxa. The IAxx measurements are presented below (see Text-figs. 9d, 10d):

Species	Initial height	Initial width	Initial height/ width	Maximum height	Maximum width	Maximum height/ width
E. scyphogracilis	.30 mm	.38 mm	.79	1.5 mm	1.6 mm	.94
E. latibrachiatus	.30 mm	.37 mm	.81	1.2 mm	1.4 mm	.86

As in the IBrr, two end member plate shapes are found, one being pentagonal and the other septagonal. In *E. latibrachiatus*, septagonal IAxx are associated with rectangular IBrr1 and pentagonal IAxx occur with hexagonal IBrr1 (Text-fig. 8). When both IAxx types are seen in one animal, the septagonal ones are slightly higher and wider (*e.g.*, Text-fig. 8d). Thus, the higher septagonal IAxx compensate for the underlying shorter rectangular IBrr1 and vice versa. Consequently, the overall dorsal cup shape is constant for individuals of equal "size", regardless of the IBrr geometry. The smallest animals possess a IAxx which is fixed into the calyx by iBr1 or iBr2 and the IAxx shape was stabilized throughout development.

E. scyphogracilis exhibits mostly septagonal IAxx (Text-fig. 7). The hexagonal IBrr1 have either pentagonal or septagonal IAxx in the same ray, but the rectangular IBrr1 occur with septagonal IAx. In the youngest individual ("size" 1.15 mm), the highest FBr apparently consists of IBr1 (Text-fig. 7a), and the IAx is pentagonal. In the usual septagonal IAx specimen, this plate was fixed into the calyx when a "size" of about 1.5 mm was reached (Text-fig. 7c). Evidently, the seven-sided outline developed during or just prior to incorporation; most likely, this configuration was due to acceleration of the mid-IAx width growth rates. The iBrr2 incorporated the septagonal IAx into the dorsal cup along the lateral, angular margins. Mature crinoids with a pentagonal IAx fixed in the calyx retained the juvenile condition.

The available iBr1 data are not complete enough to accurately depict growth of this plate. The smallest crinoids in which this plate is fully known range slightly over 2.0 mm in "size"; the iBr1 heights and widths are approximately .75 and .55 mm, respectively. The width growth rate per 1 mm of additional height constituted .73 mm in *E. scyphogracilis*, but this growth rate is obscure for *E. latibrachiatus*. The other iBrr1 data are given below for the type species (see Text-figs. 9e, 10e):

Species	Approximate Initial height/width	Maximum height	Maximum width	Maximum height/width
E. scyphogracilis	1.4	2.1 mm	1.5 mm	1.4

Six and seven-sided plates have been seen with the former followed by two and the latter by three iBrr2. Both types are divided into "small" and "large" categories. The heights of the two categories are roughly comparable within a single crinoid, but the lateral margins of "small" plates end at the IBr1 level whereas those of "large" plates reach the IAx level (*e.g.*, *E. latibrachiatus*, Text-figs. 8d, e). The "large" plates are associated with rectangular IBrr1 and "small" ones with hexagonal IBrr1. Consequently, the angle between the distal-lateral margins is greater for "large" iBrr1 than for "small" types, and the area of the former exceeds that of the latter. In the youngest *E. scyphogracilis* and *E. latibrachiatus* (Text-figs. 7, 8), the iBrr2 were not fully incorporated into the calyx, and the distal iBr1 margin is somewhat flat or rounded. Probably, the angular distal iBr1 edge formed during or immediately prior to the fixation of the iBrr2 into the dorsal cup. This was probably caused by an increase in the iBr1 height growth vector parallel to the interray axis. The number of iBr1 sides remained constant throughout the later ontogeny.

The BB growth model is not certain for the two eopatelliocrinids. In monocyclic camerates with thin BB (*e.g.*, *Glyptocrinus decadactylus*), calcite deposition did not take place on the inside of the plate circlet, and this growth type is extrapolated to *Eopatelliocrinus scyphogracilis* with little doubt in Text-figure 6. The pattern for species with thick BB has not been fully investigated, but it probably paralleled that of thin BB types. Although *E. latibrachiatus* has thick BB, the thin plate growth model is applied (Text-fig. 6).

Two BB types occur in the eopatelliocrinids, small and large. The large BB widths range about twice those of small ones, but the other dimensions are comparable. The small BB width growth rates per 1 mm height increase comprised .69 mm in the type species and .97 mm in *E. latibrachiatus*. The other data are listed below for the small BB (Text-figs. 9a, 10a):

Species	Initial height	Initial width	Initial height/ width	Maximum height	Maximum width	Maximum height/ width
E. scyphogracilis	.25 mm	.50 mm	.50	3.0 mm	2.4 mm	1.2
E. latibrachiatus	.25 mm	.42 mm	.60	1.5 mm	1.6 mm	.94

Throughout ontogeny, the outlines of the small and large BB remained pentagonal and six-sided, respectively. In addition, the BB circlet column facet expanded during the known growth sequences, with expansion rates around .50 mm per 1 mm of BB height increase in both forms. The column expansion was controlled by two growth vectors. 1. Inward calcite accretion toward the axial canal, during which the axial canal diameter was augmented due to marginal resorption around the nerve cords. 2. Outward expansion caused by the thickness growth component. All deposition took place on the outside of the plates. This vector also increased the thickness of the entire plate. The type species small BB growth rates, listed from maximum to minimum, comprised: height, width, inward expansion, and thickness. The same gradient for *E. latibrachiatus* was: height and width almost equal, thickness, and lastly inward expansion.

The IIBr1 width growth rate per .1 mm of height increase constituted .13 in *E. scyphogracilis* and .12 mm in

E. latibrachiatus. The plate dimensions are tabulated below (see Text-figs. 9f, 10f):

Species	Initial height	Initial width	Initial height/ width	Maximum height	Maximum width	Maximum height/ width
E. scyphogracilis	.32 mm	.24 mm	1.3	1.1 mm	1.2 mm	.92
E. latibrachiatus	.25 mm	.24 mm	1.0	.80 mm	.88 mm	.91

In both species, the width with respect to height increased in older and larger animals. This contrasts with most calyx plates where the relative width declined during growth. In young crinoids with IIBr1 forming a free Br, the plate shows five sides (*e.g., E. scyphogracilis,* Text-fig. 7a). Older animals with "sizes" exceeding 1.5 to 2.0 mm have the IIBr1 wholly or partially fixed into the calyx by iBrr (*e.g.,* Text-fig. 7c). Along with or immediately before this process, the interray side of the plate developed an angular margin along which the iBrr joined the IIBr1 into the calyx. The formation of this was probably due to an acceleration of the interray mid-plate width growth vector. The overall IIBr1 growth pattern paralleled that of free Brr prior to fixation in the calyx after which, the plate behaved like a dorsal cup element.

Due to the differential growth patterns of the individual calyx plates, the dorsal cup shape underwent a sequence of correlated changes. These are divided into three broad categories; variation in plate contributions to "size", change in calyx width relative to height, and adjustments in the ray and interray width components.

The development of "size" in relation to RR height followed the characteristic linear pattern in which the "size" growth rates per 1 mm RR height increments were 2.5 and 2.3 mm in the type species of the genus and *E. latibrachiatus,* respectively. The measurements are presented below (Text-figs. 9g, 10g):

Species	Initial R height	Initial "size"	Maximum R height	Maximum "size"
E. scyphogracilis	.42 mm	1.2 mm	3.8 mm	9.8 mm
E. latibrachiatus	.30 mm	1.15 mm	1.85 mm	5.0 mm

Tables 6 and 10 illustrate the changes in "size" components during ontogeny for *E. latibrachiatus* and *E. scyphogracilis,* listed in the same order. The totals exceed 100% because the distal margins of the BB overlap the proximal edges of the RR. The dorsal cup of young crinoids is largely dominated by the RR and the other plates are subordinate (*e.g., E. latibrachiatus,* Text-figs. 8a-c). When maturity was attained, the predominant calyx plates comprised the RR and BB, and the IBrr were relatively small (*e.g.,* Text-fig. 8g). Clearly, the explanation lies in the height growth rates of the individual plates with respect to "size" and the size of the plates concerned. For example, the BB are relatively small but their height growth vectors in relation to "size" were large; consequently, the contribution of these plates to "size" increased during ontogeny. Table 6 indicates that the *E. latibrachiatus* B largely augmented its percentage at the expense of the IBrr because of the relatively small size and growth rates of the latter plates with respect to "size". In the type species, the percentage height increase of the BB occurred at the expense of IAxx and RR (Table 10, Text-fig. 7).

The RR comprised the most stable calyx plates throughout growth of the two taxa, both in terms of shape and general proportions in the dorsal cup. Such indicates that where a single plate is selected as a measure of relative crinoid age, the R is the most suitable and biologically meaningful.

In the case of "size" and calyx width (Text-figs. 9l, 10l), the width growth vectors per 1 mm "size" increments equalled .38 mm in the type species and .66 mm in *E. latibrachiatus*. The dimensions are listed below:

Species	Initial "size"	Initial calyx width	Initial "size"/ width	Maximum "size"	Maximum calyx width	Maximum "size"/ width
E. scyphogracilis	1.3 mm	1.1 mm	1.2	9.6 mm	4.25 mm	2.25
E. latibrachiatus	1.15 mm	.75 mm	1.5	5.0 mm	3.3 mm	1.5

In the type species, the calyx width relative to "size" decreased markedly throughout development; this is attributed to the low calyx width growth rate with respect to "size" (.38 mm) and the previously mentioned increases in individual calyx plate height/width. Conversely, the "size"/calyx width of *E. latibrachiatus* was stabilized at 1.5, because of the larger calyx width growth vector (.66 mm) and the smaller height/width changes of the component plates.

Calyx width is a composite of two elements, width of the iBrr areas and the rays at the IAx level. The iBrr width growth rates per 1 mm of additional "size" consisted of .20 mm in *E. scyphogracilis* and .32 mm in *E. latibrachiatus*. The iBrr width and "size"/iBrr width values are given below (the "sizes" correspond to the above listed crinoids; see Text-figs. 9k, 10k):

Species	Initial iBrr width	Initial "size"/iBrr width	Maximum iBrr width	Maximum "size"/iBrr width
E. scyphogracilis	.47 mm	2.8	2.1 mm	4.6
E. latibrachiatus	.35 mm	3.0	1.6 mm	3.1

Table 6

Youngest Crinoid ("size", 1.15 mm) Equation % of "size" represented by plate height		Plate height	Oldest Crinoid ("size", 5.0 mm) Equation % of "size" represented by plate height	Plate height	Plate height growth rate per 1 mm "size" increase
B	19%	.22 mm	28%	1.4 mm	.30 mm
R	38%	.44 mm	39%	2.0 mm	.39 mm
IBr1	23%	.22 mm	19%	.95 mm	.19 mm
IAx	24%	.28 mm	22%	1.1 mm	.21 mm
Total	104%		108%		

Table illustrating changes in the "size" components during the ontogeny of *Eopatelliocrinus latibrachiatus*, n. gen., n. sp. The total percentages slightly exceed 100% because the distal B margin overlaps the proximal R edge.

The rapid increase of "size"/iBrr width seen in larger type species animals contrasts with the more stable proportions of *E. latibrachiatus*. However, the individual iBrr growth vectors are not well enough known in either species to present meaningful comparison. The growth rates of iBrr area width per 1 mm calyx width increments were .50 mm and .53 mm in *E. latibrachiatus*, and *E. scyphogracilis*, respectively. The calyx width/iBrr width remained at about 2.0 in the former species, regardless of age. In the type species, the ratio ranged from 2.3 in the smallest animals to 2.1 in the largest ones, and the rays became progressively more narrow relative to the iBrr areas.

The previous discussion indicates that the youngest individuals of both species are similar with respect to dorsal cup proportions, such as "size"/calyx width, and calyx outline. During ontogeny, the dorsal cup of *E. latibrachiatus* diverged from that of the type species in two major respects, both of which were related to growth rate differentials (compare Text-figs. 7 and 8; see summary in Table 7).

1. Proximal calyx shape (*i.e.*, up to IAxx level). The young *E. latibrachiatus* individuals are slightly more slender than the type species, but the discontinuity is smaller than implied in the Table 7 (see Text-figs. 7, 8, 91, 101). During development, the *E. scyphogracilis* dorsal cup underwent a major increase in "size"/calyx width while that of the other form retained the young crinoid geometry. The proximal sides of the *E. latibrachiatus* calyx expand more widely than in the type species. A partial explanation consists of the RR and IBrr width growth vectors with respect to "size" which were smaller in *E. scyphogracilis* (Table 7). Also, the plate shapes are involved; the *E. latibrachiatus* BB and RR expand more rapidly in the distal direction. The RR width growth rates relative to "size" exceeded those of the small BB in both taxa. However, the proximal to distal growth vector rate of increase was greater in *E. latibrachiatus* than in the type species.

The *E. scyphogracilis* rays (at IAx level) became more narrow in relation to the adjacent iBrr whereas the *E. latibrachiatus* ray and iBrr components were equal throughout ontogeny. Unfortunately, the data do not provide a solution, mainly due to lack of knowledge about the iBrr dimensions. Probably, the true IBrr and adjacent iBrr width growth rates relative to "size" were roughly equalized in *E. latibrachiatus* but were subequal in the type species.

At the IBrr level, the *E. latibrachiatus* cup walls are roughly vertical, and the calyx expansion angle approaches that of *E. scyphogracilis*. Despite some ambiguities in the data, two factors were most likely responsible. The total IBrr and adjacent iBrr width growth vectors relative to "size" of the two taxa were more similar than the equivalent

Table 7

	Eopatelliocrinus latibrachiatus, n. gen., n. sp.	*E. scyphogracilis*, n. gen., n. sp.
"Size"/calyx width of youngest crinoid	1.5	1.2
"Size"/calyx width of oldest crinoid	1.5	2.2
"Size"/iBrr width of youngest crinoid	3.0	2.8
"Size"/iBrr width of oldest crinoid	3.1	4.6
Growth rate of plate width per 1 mm "size" increment		
BB	.32 mm	.23 mm
RR	.54 mm	.29 mm
IBr1	.30 mm?	.20 mm
IAx	.23 mm	.18 mm
iBr1	–	.13 mm
IIBr1	.14 mm	.13 mm

Table illustrating the ontogeny of the "size"/calyx width and the "size"/iBrr width in *Eopatelliocrinus*, n. gen., and the relationships to the width growth rates at the plates involved.

RR growth rates. At this level, the *E. latibrachiatus* proximal to distal IBrr and adjacent iBrr width growth vector gradient was smaller than the BB and RR gradient.

2. Distal constriction. Immature individuals of both taxa exhibit a slight distal constriction at the IIBr1 level. With increasing "size" and age, this was almost obliterated by the type species but was retained and accentuated by *E. latibrachiatus*. The *E. latibrachiatus* IBrr calyx level is wider than in *E. scyphogracilis* because of the larger IBrr and probably adjacent iBrr width growth rates. The IIBr1 width growth vectors per 1 mm "size" increments equalled .14 mm and .13 mm for *E. latibrachiatus* and the generic type species, respectively. However, the IIBr1 width growth rate relative to that of the underlying IAx was smaller in

E. latibrachiatus. The mature animal IIBrr1 are fixed into the dorsal cup by the iBrr2 or iBrr3. Although the growth vectors of these iBrr have not been determined, inspection of Text-figures 7 and 8 suggests that *E. latibrachiatus* was characterized by the smaller iBrr growth rates relative to "size" and with respect to the underlying iBr1.

Both species exhibited curvilinear development of the lateral interray FBrr in relation to "size" (Text-figs. 9h, 10h). The initial FBrr incorporation rates were the most rapid and these decreased in older and larger animals. The maximum and minimum numerical scale (see graphs) fixation vectors are listed below:

Species	Initial growth rate	Maximum growth rate
E. scyphogracilis	1.8 over "size" 1.5 to 2.5 mm	.28 over "size" 9.0 to 10.0 mm
E. latibrachiatus	1.9 over "size" 1.15 to 2.15 mm	.60 over "size" 4.0 to 5.0 mm

The distal portion of IAx or the lower part of IIBr1 forms the highest FBrr in the youngest type species individuals for which conclusive data are available ("size" 1.5 mm, Text-fig. 7). From this growth stage to the 3.0 mm "size" range, new FBrr developed rapidly; by the end of this period, the distal FBrr generally consisted of the IIBrr2 lower edges. After this "size" the FBrr incorporation rate dropped markedly and when the crinoids reached the 6.0 mm "size," the proximal portion of IIBr3 just began to be fixed into the calyx. In the largest individual studied ("size" 9.6 mm), the distal IIBr3 margin is solidly incorporated into the dorsal cup.

The mechanism of pinnule fixation into the interrays is illustrated in *E. scyphogracilis*. The proximal IIBr2 one, usually located on the outside of the half-ray, is free in young ly located on the outside of the half-ray, is free in young crinoids (Text-figs. 7a-d). This pinnule was not joined into the calyx until after the upper margin of IIBr2 was incorporated (Text-fig. 7c). At this time, the proximal part of the first pinnular became angular; soon after, the pinnular was fixed by an iBr (Text-fig. 7h, right and left center rays). During later development, several more IIBr2 pinnulars were taken into the dorsal cup in the same fashion, although most of the pinnulars remained free (Text-fig. 7i). Typically, the pinnulars were first fixed into the interrays, after which the iBrr joined the pinnulars to the adjacent IIBrr.

The smallest *E. latibrachiatus* has the IAx lower edge joined into the calyx ("size" 1.15 mm, Text-fig. 8b). At "sizes" around 2.0 mm, the iBrr had started to fix the IIBrr1 into the dorsal cup. The distal FBrr of the largest crinoids comprise the proximal parts of IIBrr2 ("size" 5.0 mm, Text-fig. 8f).

The *E. scyphogracilis* relation between size and inter-half-ray FBrr is questionable, and the best fit equation is concave upward (*i.e.*, log *y* type, Text-fig. 9i). The regression line is mainly controlled by the largest crinoid in which the distal FBrr consist of IIBrr4 ("size" 9.6 mm, Text-fig. 7i). The highest FBr in all other specimens equals the lower IIBr1 margin. Possibly the largest animal is abnormal.

In *E. latibrachiatus* the distal inter-half-ray FBrr constituted the proximal IIBr1 edges regardless of age, and inter-half-ray iBrr were not developed (Text-fig. 10i).

The ontogeny of "size" and dorsal cup height was linear and the dorsal cup height growth vectors per 1 mm "size" increments equalled 1.3 mm in the type species and 1.0 mm in *E. latibrachiatus*. The dimensions are tabulated below (Text-figs. 9j 10j):

Species	Initial "size"	Initial calyx height	Initial height/ "size"	Maximum "size"	Maximum calyx height	Maximum height/ "size"
E. scyphogracilis	1.5 mm	1.4 mm	.93	9.6 mm	11.8 mm	1.2
E. latibrachiatus	1.4 mm	1.2 mm	.86	5.0 mm	5.1 to 5.5 mm	1.0 to 1.1

The dorsal cup height/"size" increased in both species throughout development, because of two factors: 1. Formation of new FBrr. In the youngest crinoids, the IAx is not fully incorporated into the calyx and dorsal cup height/ "size" is less than 1.0. As the IIBrr were joined into the calyx, the ratio increased. 2. The height relative to "size" of the new FBrr and the subsequent ontogeny of these plates. The *E. latibrachiatus* calyx height growth rate with respect to "size" was smaller than that of the type species (1.0 versus 1.3 mm). This was dictated by two opposing ontogenetic differentials. At equivalent "sizes," *E. latibrachiatus* averages roughly .5 FBrr (numerical scale) less than *E. scyphogracilis*. The FBrr height growth vectors of the former crinoid exceeded those of the latter. For example, the IIBrr1 height growth rate of the type species consisted of .089 mm per 1 mm of additional "size", whereas the same *E. latibrachiatus* value was .11 mm.

As previously outlined, several initial intercepts were used to estimate the "theoretical microcrinoid sizes" and "size" ranges; these are tabulated below for the Girardeau eopatelliocrinids:

Species	BB + 00 "microcrinoid"	BB + OO + RR "microcrinoid"
E. scyphogracilis	.11 mm .17 mm	.22 mm, minimum .63 mm, maximum
E. latibrachiatus	.16 mm .33 mm	.39 mm, minimum .63 mm, maximum

Interpretation of the correlation coefficients is difficult because complete data sets for all crinoids in the growth sequences are not available (see legends, Text-figs. 9, 10). The *E. scyphogracilis* dorsal cup plate and calyx shape correlations are typically high, and most of these are significant at probability levels above .999 (two sided test). The iBr1 correlations range lower; the significance levels vary from .900 to .995. This is attributed to the incomplete sample which comprises only five crinoids. In *E. latibrachiatus* lower correlation coefficients are generally observed and most of the significance levels vary from .990 to greater than .999 (correlations involving IBr1 and iBr1 are omitted due to lack of data). All in all, the correlation coefficients denote that the dorsal cup shape parameters and individual calyx plates were subject to a high degree of integration and coordination throughout the observed growth of the two taxa. However, the development of the *E. latibrachiatus* calyx was slightly less well regulated than that of the type species. As later discussed, the same was true for the Brr and the food gathering system.

Usually, the eopatelliocrinid dorsal cup height measures are better correlated with the height dimensions of the component plates than with the plate widths. The same situation exists for the calyx width parameters which show higher correlations with the dorsal cup plate widths than with their heights.

The correlation coefficients between "size" and lateral interray FBrr consist of .97 and .93 in *E. latibrachiatus* and the generic type species, respectively. The equivalent figures for the inter-half-rays are zero and .88. The lack of correlation in *E. latibrachiatus* is because IIBr1 remained the distal FBr throughout development.

BRACHIAL DEVELOPMENT

The standard Brr selected for statistical treatment consist of IIBrr8 to 13. In addition, the proximal to distal Brr maturity gradients are discussed. The standard Brr superpositions are illustrated in Text-figures 11g and 12g. Examination of *Ptychocrinus splendens, Glyptocrinus dyeri, Eopatelliocrinus latibrachiatus* (Text-fig. 8h) and numerous other uniserial armed forms indicates that the free Brr food grooves are basically Y-shaped in ventral view. This configuration is seen in young and adult individuals of the first two taxa. The proximal leg of the Y continues from the previous Br; one of the distal legs of the Y proceeds to the next Br ("brachial food grooves"). The other distal branch leads to the pinnule facet ("pinnule facet food groove"). This is curved and slightly convex distally, especially near where it branches from the "brachial food groove." The "brachial food grooves" are straight and lie at angles to each other. The "brachial food groove" axes are located in the middle of the Br where they cross from one plate to the next. The "pinnule facet food groove" axis occurs in the middle of the ventral side of the facet. Consequently, the various food groove axes can be outlined approximately for a Br in which these are not visible.

In cross section (proximal or distal face), the food grooves are roughly V-shaped. The axial nerve cord lay along the apex of the V whereas the feeding tissue was in the open ventral part of the V. The basic assumption involved in the restorations (Text-figs. 11g, 12g) is that the food groove axes represented constant topographic reference points on the Brr. If so, the Br ontogeny was adjusted so that the food groove axes and the axial nerve cord axes were simply extended during subsequent development. In other words, the food grooves did not migrate laterally on the Brr with increasing age. Consequently, major axial resorption of calcite was not necessary. By analogy with the previously discussed modern crinoids and cyathocrinids, some calcite resorption occurred along the base and sides of the food grooves; this was associated with the augmented axial nerve cord diameter in larger animals. The morphology of the Girardeau camerate food grooves implies that such marginal resorption was common. Nevertheless, the ventral food groove growth was largely produced by ventral calcite deposition on the Br areas flanking the food grooves. Despite the marginal resorption along the axial nerve cord, the food groove axes remained constant on the Brr.

Preparation of the Brr restorations involved several stages. First, the Brr were defined. In some taxa, the Brr were taken from the equations whereas mean standard specimen Brr were used for other forms. Following this, the food groove axes were derived for the individual plates. Lastly, the Brr were superimposed so that the food groove axes were parallel.

The development of "size" and standard Brr width was linear in both species. The *E. scyphogracilis* Brr width growth vector per 1 mm "size" increase consisted of .095 mm. The same *E. latibrachiatus* value equalled .13 mm. The dimensions are tabulated below (Text-figs. 11a, 12a):

Species	Initial "size"	Initial Brr width	Initial "size"/ Brr width	Maximum "size"	Maximum Brr width	Maximum "size"/ Brr width
E. scyphogracilis	1.3 mm	.15 mm	8.7	9.6 mm	.94 mm	10
E. latibrachiatus	1.15 mm	.18 mm	6.4	5.0 mm	.64 mm	7.8

During progressive ontogeny, the "size"/Brr width of both forms was augmented despite the Brr width growth rate differentials. The relationship between "size" and Brr

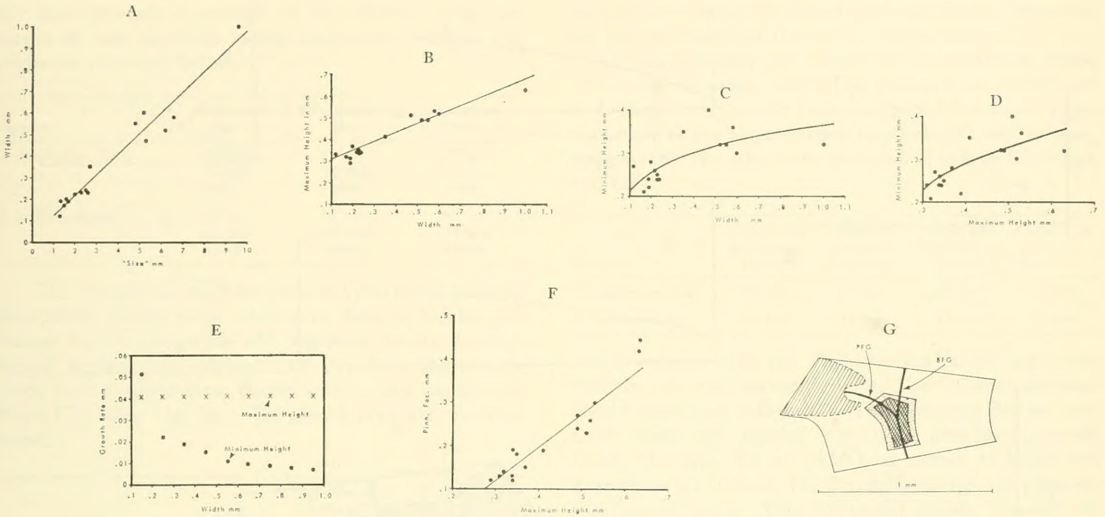

Text-figure 11. — Graphs and restoration showing standard Brr growth in ***Eopatelliocrinus scyphogracilis***, n. gen., n. sp. All dimensions on graphs except "size" refer to the Brr measurements shown on Text-figure 2. "*a*" indicates the "initial intercept" or "pseudointercept" where the *x* axis is logarithmic.
A — F — Graphs. Equation data.
A — $y = .0257 + .0954x$. $r = .974$.
$\sigma y\% = 14.1$. N = 16.
B — $y = .259 + .413x$. $r = .961$.
$\sigma y\% = 6.8$. N = 16.
C — $y = .364 + .153 \log x$. $r = .720$.
$\sigma y\% = 13.2$. N = 16. "a" = .059 ($x = .01$).
D — $y = .458 + .432 \log x$. $r = .818$.
$\sigma y\% = 10.2$. N = 16. "a" = −.416 ($x = .01$).
E — Equation not applicable.
F — $y = -.115 + .768x$. $r = .946$.
$\sigma y\% = 13.7$. N = 15.
G — Three Brr superimposed to show growth patterns. Food groove axes in heavy black. BFG and PFG are "brachial" and "pinnule facet food groove" axes, respectively. Smallest Br cross-hatched. Middle one stippled. Pinnule facet of largest Br schematic, ruled. The Brr dimensions were derived from equations; the closest specimen was then used to sketch in the details of shape and the pinnule facet.

maximum height was linear in the type species but curvilinear in *E. latibrachiatus*. Both crinoids exhibited logarithmic regression lines for "size" versus Brr minimum height. Where exponential development was observed, the Brr maximum or minimum height development vector decreased with progressive age. The average figures follow:

Species	Mean maximum height growth rate per 1 mm additional "size"	Mean minimum height growth rate per 1 mm additional "size"
E. scyphogracilis	.040 mm	.015 mm
E. latibrachiatus	.025 mm	.0062 mm

The Brr width ontogenetic vectors relative to "size" greatly exceeded those of height, especially in *E. latibrachiatus* where the width growth rate equalled 5.2 times that of average maximum height and 21 times that of the mean minimum height. The same *E. syphogracilis* values comprised 2.4 times and 6.3 times, respectively.

The type species growth of Brr width versus Brr maximum height was linear with a constant maximum height growth rate of .041 mm per .1 mm width augmentation (Text-fig. 11e). Curvilinear development characterized *E. latibrachiatus* during which the maximum height development vector fell from .039 to .011 mm with an .020 mm average (Text-fig. 12e). The other pertinent data are listed below (Text-fig. 11b, 12b):

Species	Initial Brr width	Initial Brr maximum height	Latest Brr width	Latest maximum height
E. scyphogracilis	.12 mm	.31 mm	1.0 mm	.68 mm
E. latibrachiatus	.15 mm	.24 mm	.63 mm	.34 mm

Exponential development of Brr width versus Brr minimum height was seen in both taxa. The *E. scyphogracilis* youngest, oldest and mean Brr maximum height ontogenetic rates per .1 mm Brr width increment constituted .051, .007, and .017 mm, listed in the same order (Text-fig. 11e). The equivalent *E. latibrachiatus* figures consisted of .014, .0042 and .0074 mm, respectively (Text-fig. 12e). The type species

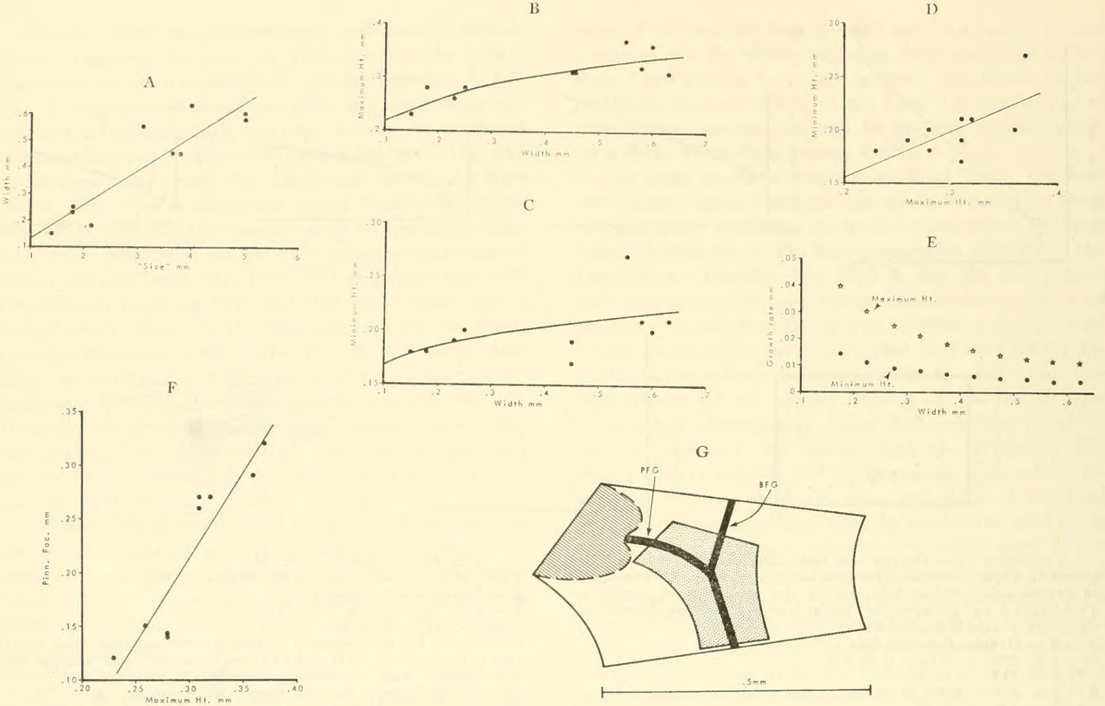

Text-figure 12. — Graphs and restoration showing standard Brr growth in *Eopatelliocrinus latibrachiatus*, n. gen., n. sp. All dimensions except "size" are the standard Brr measurements shown in Text-figure 2. "*a*" denotes the "initial intercept" or "pseudointercept" where the x axis is logarithmic.

A — F — Graphs. Equation data.

A — $y = .00213 + .128x$. $r = .909$.
$\sigma y\% = 20.4$. N = 10.

B — $y = .372 + .156 \log x$. $r = .862$.
$\sigma y\% = 7.0$. N = 10. "a" = .0601 ($x = .01$).

C — $y = .226 + .0579 \log x$. $r = .491$.
$\sigma y\% = 11.6$. N = 10. "a" = .110 ($x = .01$).

D — $y = .0708 + .427x$. $r = .653$.
$\sigma y\% = 9.9$. N = 10.

E — Equation not applicable.

F — $y = -.265 + 1.60x$. $r = .922$.
$\sigma y\% = 15.7$. N = 9.

G — Two Brr superimposed to illustrate growth patterns. Food groove axes in heavy black. BFG and PFG are "brachial" and "pinnule facet food grooves", respectively. Smallest Br stippled. Pinnule facet of larger Br schematic, ruled. The Brr dimensions were derived from equations of width versus the applicable dimensions. Widths are .15 and .63 mm. The closest specimen was then used to fill in the exact shape and pinnule facet.

average minimum height growth vector ranged roughly 41% of the maximum height value. The comparable *E. latibrachiatus* percentage equalled 37%. The dimensions follow (Text-figs. 11c, 12c):

Species	Initial Brr width	Initial Brr minimum height	Latest Brr width	Latest Brr minimum height
E. scyphogracilis	.12 mm	.22 mm	1.0 mm	.36 mm
E. latibrachiatus	.15 mm	.18 mm	.63 mm	.21 mm

The Brr maximum height versus Brr minimum height ontogeny followed a straight line in *E. latibrachiatus* with a minimum height growth vector of .043 mm per .1 mm additional maximum height. The same *E. scyphogracilis* developmental rate decreased from .054 to .034 mm over the ontogeny sequence. The other values follow (Text-figs. 11d, 12d):

Species	Initial Brr maximum height	Initial Brr minimum height	Latest Brr maximum height	Latest Brr minimum height
E. scyphogracilis	.29 mm	.23 mm	.63 mm	.37 mm
E. latibrachiatus	.23 mm	.17 mm	.37 mm	.23 mm

The convergence angle between the proximal and distal

Brr faces presents a measure of the relative width and maximum and minimum height ontogenetic vectors. The angles are tabulated below:

Species	Smallest Brr	Intermediate Brr	Largest Brr
E. scyphogracilis	41° at .12 mm width	22° at .20 mm width	18° at 1.0 mm width
E. latibrachiatus	25° at .15 mm width	18° at .25 mm width	16° at .63 mm width

The convergence angle decrease was due to two factors: large width growth rates relative to those of height, and changes in the maximum and minimum height developmental vectors with respect to one another. The convergence angle dropped most rapidly in the early ontogenetic stages (Text-figs. 11g, 12g). The growth rates are tabulated below:

Species	Brr width growth vector per 1 mm "size" increment	Brr maximum height growth rate per 1 mm "size" increment	Brr minimum height growth rate per 1 mm "size" increment
E. scyphogracilis	.095 mm regardless of age.	.040 mm regardless of age	.043 mm in youngest. .0066 mm in oldest.
E. latibrachiatus	.13 mm regardless of age.	.043 mm in youngest. .016 mm in oldest.	.0086 mm in youngest. .0032 mm in oldest.

The initial type species convergence angle decline largely reflected the youngest crinoid maximum and minimum height developmental vectors. The 1.3 mm "sized" crown bears 9 or 10 IIBrr per arm. Probably, the standard Brr appeared just prior to death. At this time, the Brr minimum heights were small relative to the maximum heights (.22 and .31 mm), but the initial maximum height growth rate was exceeded by that of minimum height. This in conjunction with the width developmental vector caused a rapid early convergence angle decrease. During subsequent ontogeny, the convergence angle fell slightly which was dictated by two constrasting growth differentials. The maximum height augmentation vectors were much larger than the minimum height figures. In the absence of other variables, this would have resulted in greater convergence angles. However, the interaction between the maximum and minimum height growth vectors and the much larger width developmental rates produced a slight convergence angle drop.

In *E. latibrachiatus*, a slower early convergence angle change is seen because the initial maximum height growth rate predominated over that of minimum height. Otherwise, the pattern resembled that of *E. scyphogracilis*.

Linear ontogeny was shown by Brr maximum height versus pinnule facet "size." The generic type species and *E. latibrachiatus* pinnule facet size growth rates per .1 mm maximum height augmentation equalled .077 and .16 mm, respectively. The other data are listed as follows (Text-figs. 11f, 12f):

Species	Initial Brr maximum height	Initial Brr pinnule facet size	Latest Brr maximum height	Latest Brr pinnule facet size
E. scyphogracilis	.29 mm	.11 mm	.63 mm	.37 mm
E. latibrachiatus	.23 mm	.10 mm	.37 mm	.33 mm

Text-figures 11g and 12g illustrate the Brr superpositions for the two eopatelliocrinids. The following developmental trends are indicated. 1. The immature Brr are relatively high and angular with large prominent pinnule facets. The adult Brr are wider with respect to height and have smoother outlines. The Brr width growth rates exceeded those of height. This differential mainly dictated the decrease in angularity. The .63 mm wide *E. latibrachiatus* Br and the 1.0 mm wide type species Br show comparable maturity stages. The *E. latibrachiatus* Brr width growth vector relative to "size" equalled eight times that of the mean average height. The equivalent type species value ranged about four times. Essentially, the relatively large *E. latibrachiatus* width growth rate produced Brr maturity much faster with respect to "size" or Br width.

2. Assuming the restorations are correct, the *E. latibrachiatus* width growth vector toward the pinnule facet was slightly larger than that directed away from the facet. The reverse characterized *E. scyphogracilis*. This was probably related to the relatively wider Brr and smaller height developmental rates in the former crinoid. These may have caused increased curvature of the "pinnule facet food groove" which in turn may have controlled the width growth vector toward the pinnule facet and the facet orientation. The *E. latibrachiatus* proximal pinnule facet margin is roughly straight but that of *E. scyphogracilis* is strongly curved.

3. In young crinoids and in immature adult crinoid Brr, the height axes of the succeeding Brr are not parallel. The Br height axis is inclined toward the pinnule facet. The axes of successive Brr intersect at around 20° in the youngest plates. This imparts a bent or crooked appearance to these Brr (*e.g., E. scyphogracilis*, Text-figs. 7a-c, g). The inclination angle with respect to the arm length axis ranges about 10° for the immature plates. This configuration is due to unequal angular convergence of the proximal and distal Br

faces relative to the Br width axis, along which width was measured. The distal face convergence angle exceeds the proximal one. Inasmuch as the pinnules alternate from one side of the arm to the other, the arm length axis remains straight.

During later development, the Brr height axes became parallel because the proximal and distal convergence angles attained approximately equal values (compare Text-figs. 7a-c, g with proximal Brr in 7f; see also 11g, 12g). This was caused by one or a combination of two growth rate adjustments: decrease in the distal maximum height growth vector and increase in the proximal maximum height developmental rate; and vice versa with the proximal and distal minimum height growth vectors. The functional significance is discussed in the summary on Girardeau camerate ontogeny.

4. The distal height growth vectors equalled roughly eight times those of proximal height in *E. latibrachiatus*. The corresponding *E. scyphogracilis* figure consisted of 2.3 times. In the former crinoid, equal proximal and distal Br face convergence angles were mainly developed by decreasing the distal maximum height growth rate relative to the distal minimum height vector. The formation of symmetrical convergence angles in the type species involved adjustments of both the proximal and distal height growth rates.

5. The proximal-lateral expansion of the *E. scyphogracilis* pinnule facet was largely caused by the width growth vector which was directed toward the facet. The distal extention of the pinnule facet was a function of the width and maximum height growth rates. This is reflected by the correlation coefficients of Brr width and maximum height versus pinnule facet size; these are .97 and .95 respectively. The immature pinnule facet is oriented almost parallel to the Br width. The adult Brr ventral part of the pinnule facet is inclined toward the "brachial food groove" and the outer margin of the facet dips more steeply in the proximal direction.

The dorsal-ventral orientation of the *E. latibrachiatus* pinnule facet is not sufficiently known to present meaningful comparison with the type species.

The above discussion shows that Brr development minimized the growth vectors across the articular surfaces as much as possible within the geometrical limits of the structure. The Brr growth rates, listed from maximum to minimum, comprised width toward or away from the pinnule facet, distal height and proximal height. The growth rates toward the articular surfaces, listed from greatest to least, equalled: toward pinnule facet; toward distal face; and toward proximal face. Geometrically, the predominance of the distal height growth vectors over the proximal ones was dictated by the angular relationship between the "pinnule facet" and "brachial food grooves." As indicated in the summary of Girardeau camerate ontogeny, the distribution of the growth rates was closely correlated with the problem of supporting the growing arms.

The quantitative picture of Brr ontogeny is incomplete because of the lack of dorsal-ventral data. The dorsal-ventral dimensions cannot be consistently determined due to the orientation of the arms in the enclosing matrix. These measurements must be made on isolated Brr. The general dorsal-ventral growth model for uniserial Brr is outlined in the summary of Girardeau camerate ontogeny.

The eopatelliocrinid terminal Brr are divided into two types. Type-1 plates are only known in *E. scyphogracilis*. These probably formed just prior to death, and they have rounded distal margins (Text-fig. 7a, right ray). Type-2 terminal Brr can be examined in both taxa. In this developmental phase, the distal margins became angular and the proximal and distal faces were approximately parallel (*e.g.*, *E. scyphogracilis*, left ray Text-fig. 7a, also 7b, g). Type-2 Brr are consistently larger than Type-1. For example, the type species immature crinoid Type-1 and 2 terminal Brr possess average heights of .08 mm and .11 to .12 mm, listed in the same order. Consequently, angular distal margins are believed indicative of slightly older Brr. The *E. scyphogracilis* Type-2 terminal Brr heights remained roughly constant regardless of the age and "size" of the individual. Wider terminal Brr are seen in the larger animals. For example, the Type-2 terminal Brr widths constitute .12 and .19 mm in the 1.3 and 4.8 mm "sized" crowns, respectively. The *E. latibrachiatus* Type-2 terminal Brr widths and heights increased during progressive growth as listed below:

"Size"	Type-2 terminal Brr height	Type-2 terminal Brr width
1.15 mm	.11 mm	.08 mm
1.4 mm	.14 to .16 mm	.12 to .15 mm
5.0 mm	about .20 mm	roughly .20 mm

Comparison of the Type-2 terminal Brr widths and heights of *E. latibrachiatus* and *E. scyphogracilis* indicates that these are relatively more slender in the former taxon.

During the next Br growth stage, the pinnule and its facet developed. These Brr occur immediately distal to the non-pinnulate terminal Brr (*e.g.*, Text-figs. 7a, b g). The smallest type species pinnulate Brr are about .15 mm high. Those of *E. latibrachiatus* range around .14 mm in height. These heights agree closely with the y equals 0 values obtained from the equations of standard Brr maximum height

(x) versus pinnule facet size (y). Most likely, the initial pinnules grew rapidly. The immature pinnules are composed of one or two short pinnulars. The proximal and distal Br face convergence only began after the pinnule appeared; before this, the two faces were parallel (compare two distal Brr in Text-fig. 7g).

In all crinoids, the most immature free Brr are encountered at the distal arm margins; proceeding proximally, the Brr become more mature (see Text-figs. 7, 8). In the larger specimens with fixed IIBrr, the proximal IIBrr are relatively high, angular, and have juvenile outlines. The free Brr immediately above the FBrr are wide and mature, like the more distal plates. Although, the younger crowns have free Brr maturity gradients, these are more obvious in the larger individuals because a greater range of Brr age classes can be seen (*e.g.*, compare Text-figs. 7a, b with 7f, g). The maturity gradients of the two eopatelliocrinids contrast somewhat. As previously documented, the *E. scyphogracilis,* terminal Brr are wider relative to height than those of *E. latibrachiatus.* The reverse characterizes the mature Brr. This is controlled by differences in the arm taper rates. The *E. latibrachiatus* taper angle increases rapidly near the distal arm tips (*e.g.,* Text-fig. 8f). The type species retains a slight and relatively constant taper angle throughout the arms (*e.g.,* Text-fig. 7f). Consequently, the proximal-distal Brr maturity gradient in the distal 33% of the arms is steeper in *E. latibrachiatus* than in *E. scyphogracilis.*

Interpretation of the initial intercepts and "pseudo-intercepts" remains conjectural (partially listed in Text-figs. 11 and 12 legends). The eopatelliocrinid standard Brr, IIBrr8 to 13, appeared rapidly over the 1.15 to 1.5 mm "size" interval. One would expect this to be reflected in the intercepts derived from the equations of "size" (x) versus the various standard Brr dimensions (y). Most of these values are positive and they range from –.005 to .27 mm. Inasmuch as the standard Brr developed quickly, the initial Brr shape parameter growth vectors with respect to time or "size" were probably faster than were the subsequent growth rates. The regression lines only show the growth vectors which postdated the origin of the Brr. The initial intercepts and "pseudo-intercepts" represent the equation growth rates projected backward in time and "size". Thus, the true initial developmental vectors cannot be determined from the regression lines.

The eopatelliocrinid correlation coefficients and their significance levels exhibit two major patterns (legends, Text-figs. 11, 12, Table 8). The lowest values are seen where minimum height comprises one of the variables. The *E. scyphogracilis* correlations and significance levels range higher than those of *E. latibrachiatus.* This is tabulated below:

Species	Correlation coefficient and significance level range (two sided test)	
	Excluding Brr minimum height	Involving minimum height only
E. scyphogracilis	$r = .95$ to .97 significance level—all above .999	$r = .72$ to .82 significance level—slightly above or below .999
E. latibrachiatus	$r = .80$ to .92 significance level—almost .999 to above .999	$r = .24$ to .65 significance level—less than .900 to about .950

Within either taxon, the lowest Brr dimension growth rates caused the smallest correlation coefficients. The correlations and their significance levels denote that the *E. latibrachiatus* standard Brr development was less well integrated and coordinated than that of the type species. This was not related to the growth rate differentials between the two forms. The *E. latibrachiatus* Brr width and pinnule facet size growth vectors exceeded those of *E. scyphogracilis;* yet the lower correlation coefficients and significance levels are associated with the former crinoid. Allowing for the small growth rates involved, the standard Brr ontogeny was reasonably well correlated with the development of calyx "size" and the adjacent Brr dimensions.

The type species Brr percentage standard deviations range lower than those of *E. latibrachiatus* (ranges, 6.8 to 14% versus 7.0 to 20%; see legends, Text-figs. 11, 12). The largest standard deviations are found where Brr width is the dependent variable. The lowest percentage standard deviations occur when maximum height equals the dependent variable (7.0 to 8.3% in *E. latibrachiatus,* 6.8 to 7.1% in *E. scyphogracilis*). This suggests that maximum height may have regulated the growth of the other Brr parameters with the exception of the pinnule facet. This is consistent with the fact that the lowest percentage standard deviations for Brr width and minimum height are seen when maximum height is taken as the independent variable. The pinnule facet size does not follow the above pattern, mainly because development of the facet was largely determined by Brr width.

FOOD GATHERING SYSTEM GROWTH

Considerable difficulty was encountered in fitting regression lines to the *Eopatelliocrinus* food gathering system data; generally, the lines or curves represent the best of several tested equations. As seen in Text-figures 13 and 14, the regression lines approximate the young crinoids more closely than the adults. The largest individuals typically deviate significantly from the comparable equation values. Probably, the underlying cause is the relative numbers of young versus adult specimens; the former are more common than the latter. Thus, the record of the *Eopatelliocrinus* food gathering system is largely based on young crinoids. To some extent, this is due to the mortality rates, but differential preservation is also involved as the adults were less liable to have been buried with the food gathering system intact.

Because of the adult crinoid deviations from the equations, the actual specimen values are discussed here rather than equation values. As done previously, the growth rates are computed from the regression lines. However, these should be regarded as approximate, and the growth rates are mainly included to illustrate the general developmental patterns.

In *E. scyphogracilis*, whole or partial measurement sets are available for 11 youngsters, "size" less than 3.0 mm, whereas only five adults are known ("size" exceeds 4.5 mm). Seven *E. latibrachiatus* are assigned to the "young assemblage", "size" 1.15 to 2.15 mm, and five specimens to the "adult assemblage", "size" 3.7 to 5.0 mm. Complete data were obtained from 10 crinoids and partial measurements from two individuals.

The ontogeny of "size" and food gathering system length was linear in the type species and exponential in *E. latibrachiatus*. The former developmental vector was constant at 71 cm of additional food gathering system length per 1 mm "size" increase. The *E. latibrachiatus* growth rates rose from 24 to 140 cm during the ontogeny sequence; the average comprised 80 cm. The dimensions are tabulated below (Text-figs. 13a, 14a):

Species	Initial "size"	Initial food gathering system length	Maximum "size"	Maximum food gathering system length
E. scyphogracilis	1.15 and 1.3 mm	6.0 and 7.0 cm	6.2 and 7.7 mm	420 and 480 cm
E. latibrachiatus	1.15 mm	5.8 and 6.0 cm	5.0 mm	240 cm

The development of calyx volume and "size" followed the usual curvilinear pattern in which the "size" ontogenetic vectors declined with increasing age. The type species maximum and minimum "size" augmentation rates per .01 cc

Table 8

Independent variable	Dependent variable (all are Brr dimensions)	Growth rate or mean growth rate per 1 mm "size" increase	Correlation coefficient	Significance level (two sided test)	Species
"Size"	Width	.095 mm	.97	above .999	*E. scyphogracilis*, n. gen., n. sp.
"Size"	Maximum height	.040 mm	.96	above .999	*E. scyphogracilis*, n. gen., n. sp.
Log."size"	Minimum height	.015 mm	.73	about .999	*E. scyphogracilis*, n. gen., n. sp.
"Size"	Pinnule facet size	.034 mm	.98	above .999	*E. scyphogracilis*, n. gen., n. sp.
"Size"	Width	.13 mm	.91	above .999	*E. latibrachiatus*, n. gen., n. sp.
Log."size"	Maximum height	.025 mm	.80	.990 to .999	*E. latibrachiatus*, n. gen., n. sp.
Log."size"	Minimum height	.0062 mm	.24	less than .900	*E. latibrachiatus*, n. gen., n. sp.
Log."size"	Pinnule facet size	.050 mm	.88	about .999	*E. latibrachiatus*, n. gen., n. sp.
"Size"	Width	.073 mm	.88	above .999	*A. tetrarmatus*, n. sp.
Log."size"	Maximum height	.049 mm	.74	above .999	*A. tetrarmatus*, n. sp.
Log."size"	Minimum height	.027 mm	.64	between .990 and .999	*A. tetrarmatus*, n. sp.
"Size"	Pinnule facet size	.019 mm	.48	about .950	*A. tetrarmatus*, n. sp.

Table showing relations of the correlation coefficients and their significance levels to the Brr dimension growth rates in *Eopatelliocrinus*, n. gen. and *Alisocrinus tetrarmatus*, n. sp.

calyx volume change were 1.0 and .08 mm, respectively; the same *E. latibrachiatus* values consisted of .83 and .11 mm. The mean *E. latibrachiatus* vector equalled .27 mm whereas that of *E. scyphogracilis* constituted .23 mm. The growth rate differentials were controlled by contrasts in the calyx shape. The former taxon exhibits a relatively short and stout dorsal cup, but that of the type species is more slender. Unfortunately, the *E. latibrachiatus* calyx volume provides a poor approximation of the viscera size (*i.e.*, internal volume) because of the thick calyx plates. For example, the R and IAx thickness ranges about .65 mm in the 3.8 mm "sized" crown (paratype USNM 164 560). The type species plates are much thinner and the calyx and viscera volumes were roughly the same. The other data follow (Text-figs. 13e, 14e):

Species	Initial "size"	Initial calyx volume	Maximum "size"	Maximum calyx volume
E. scyphogracilis	1.15 and 1.3 mm	.0007 and .0008 cc	7.7 and 9.6 mm	.22 and .32 cc
E. latibrachiatus	1.15 mm	.0006 and .0011 cc	5.0 mm	.13 cc

The relations between calyx volume and free ambulacral tract length were exponential in which the food gathering system length augmentation vectors per .01 cc caylx volume increment fell in the older and larger crinoids. Both forms showed roughly similar growth at comparable ages. The initial, latest, and mean ontogenetic rates for the type species equalled 40, 23, and 26 cm, listed in the same order. The equivalent *E. latibrachiatus,* figures were 36, 17, and 23 cm, respectively. The developmental vectors declined most rapidly in the youngest animals. Over the initial 15% of the volume interval, the ambulacral tract growth rates dropped from 50 to 60%. The remaining 40 to 50% decrease occurred during the later 85% volume range. The measurements are listed below (Text-figs. 13f, 14f):

Species	Initial "size"	Initial calyx volume	Initial food gathering system length	Maximum "size"	Maximum calyx volume	Maximum food gathering system length
E. scyphogracilis	1.15 mm	.0007 cc	6.0 cm	6.2 and 7.7 mm	.15 and .22 cc	480 and 420 cm
E. latibrachiatus	1.15 mm	.0006 and .0011 cc	5.8 and 6.0 cm	5.0 mm	.13 cc	240 cm

The above pattern dictated the development of the food gathering efficiency (*i.e.*, free ambulacral tract length/calyx volume). The type species food gathering efficiency is about 8600 in the smallest individual and 3100 and 1900 in the largest two specimens. The young *E. latibrachiatus* food gathering efficiency ranges from 9700 to 5500 whereas that of the oldest crown is only 1800. Roughly 70 to 80% of the food gathering efficiency decline developed over the first 15% of the volume interval, and the remainder was observed during the subsequent 85% of the volume range.

During growth, new Brr were continually added to the arms. As in all crinoids, these formed at the distal arm tips. The ontogeny of "size" and IIBrr per arm was curvilinear in both species and the Brr addition rates per 1 mm "size" increment rose in the larger animals. The type species initial, maximum, and average Brr addition rates constituted 8.1, 10, and 9.3 Brr, respectively. *E. latibrachiatus* was characterized by higher vectors which were 11, 17, and 15 Brr, listed in the same order. Most IIBrr bear pinnules with the exception of IIBrr1 and the terminal Brr; in addition, the *E. scyphogracilis* IIBr2 also lacks a pinnule. The other data are tabulated below (Text-figs. 13d, 14b):

Species	Initial "size"	Initial Brr per arm (*i.e.*, half-ray)	Maximum "size"	Maximum Brr per arm
E. scyphogracilis	1.15 to 1.7 mm	four to nine IIBrr	6.2 and 7.7 mm	57 and 59 IIBrr
E. latibrachiatus	1.15 mm	seven or eight IIBrr	5.0 mm	55 IIBrr

The development of the half-ray food gathering system and number of IIBrr in each arm was logarithmic in which the half-ray ambulacral tract length augmentation rates per new Br increased during ontogeny. The maximum and minimum type species developmental vectors comprised .9 and 45 mm, a 50-fold increase from the youngest to the oldest individual. The young *E. latibrachiatus* growth rate was 1.5 mm whereas an 8.2 mm figure was found in the adults. The *E. scyphogracilis* mean developmental vector, 12 mm, ranged over twice that of the other taxon (5.0 mm), which was due to the more rapid Brr addition rate relative to "size" in *E. latibrachiatus.* The measurements follow (Text-figs. 13g, 14g):

Species	Initial Brr per arm (*i.e.*, half-ray)	Initial half-ray food gathering system length	Maximum Brr per arm	Maximum half-ray food gathering system length
E. scyphogracilis	four to nine IIBrr	5.0 to 7.0 mm	57 and 59 IIBrr	480 and 420 mm
E. latibrachiatus	seven or eight IIBrr	5.8 and 6.0 mm	55 IIBrr	240 mm

Throughout ontogeny, more pinnules developed as new Brr were added to the growing arm, while the previously formed pinnules increased their lengths by two mechanisms:

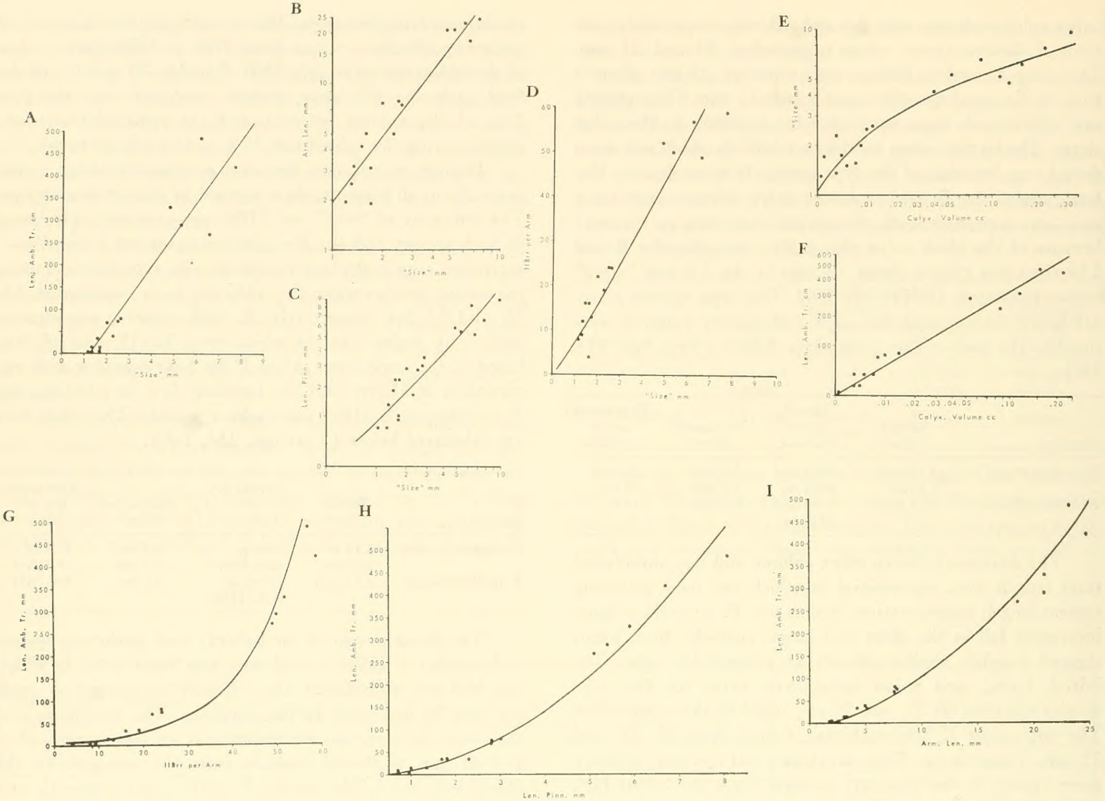

Text-figure 13. — Graphs showing food gathering system growth in *Eopatelliocrinus scyphogracilis*, n. gen., n. sp. Food gathering system length is given as Len. Amb. Tr. If the value is listed in cm, the total length is intended. Where in mm, the half-ray length is intended because each animal has ten half-rays. "*a*" refers to the "initial intercept" or "pseudointercept" where the *x* axis is logarithmic. Equation data:

A — $y = -87.6 + 71.0x$. $r = .948$.
$\sigma y\% = 17.5$. $N = 16$.
B — $\log y = .868 + 1.02 \log x$. $r = .900$.
$\sigma y\% = 13.6$. $N = 16$. "a" $= .570$ $(x = .1)$.
C — $\log y = -.0796 + 1.12 \log x$. $r = .922$.
$N = 16$. "a" $= .063$ $(x = .1)$.
D — $\log y = .281 + 1.35 \log x$. $r = .945$.
$\sigma y\% = 20.8$. $N = 16$. "a" $= .00385$ $(x = .01)$.
E — $\log y = 1.07 + .331 \log x$. $r = .957$.
$N = 20$. "a" $= .558$ $(x = .0001)$.
F — $\log y = 3.33 + .807 \log x$. $r = .976$.
$\sigma y\% = 11.0$. $N = 16$. "a" $= 1.26$ $(x = .0001)$.
G — $\log y = .804 + .0339x$. $r = .958$.
$\sigma y\% = 15.1$. $N = 16$.
H — $\log y = 1.01 + 1.90 \log x$. $r = .985$.
$\sigma y\% = 11.4$. $N = 16$. "a" $= .129$ $(x = .1)$.
I — $\log y = .316 + 1.69 \log x$. $r = .994$.
$\sigma y\% = 5.5$. $N = 16$. "a" $= .042$ $(x = .1)$.

1. Addition of new pinnulars at the pinnule distal tips. For example, the smallest *E. scyphogracilis* has a IIBr7 pinnule with only two or three joints ("size" 1.2 mm, Text-fig. 7a). At least seven pinnulars are seen in the same pinnule of the 2.5 mm "sized" crown (Text-fig. 7c). 2. Lengthening of the previously present pinnulars. The two eopatelliocrinids possessed curvilinear development of "size" and average pinnule length. The type species pinnule length growth rates per 1 mm "size" increment rose from .98 to 1.2 mm during progressive development. On the other hand, the same *E. latibrachiatus* ontogenetic vector was 1.6 mm in the young crinoids and .44 in the adults. The *E. scyphogracilis* and *E. latibrachiatus* average augmentation rates comprised 1.1 and .80 mm, respectively. This caused divergences in the mean pinnule lengths of the mature animals, as outlined below (Text-figs. 13c, 14c):

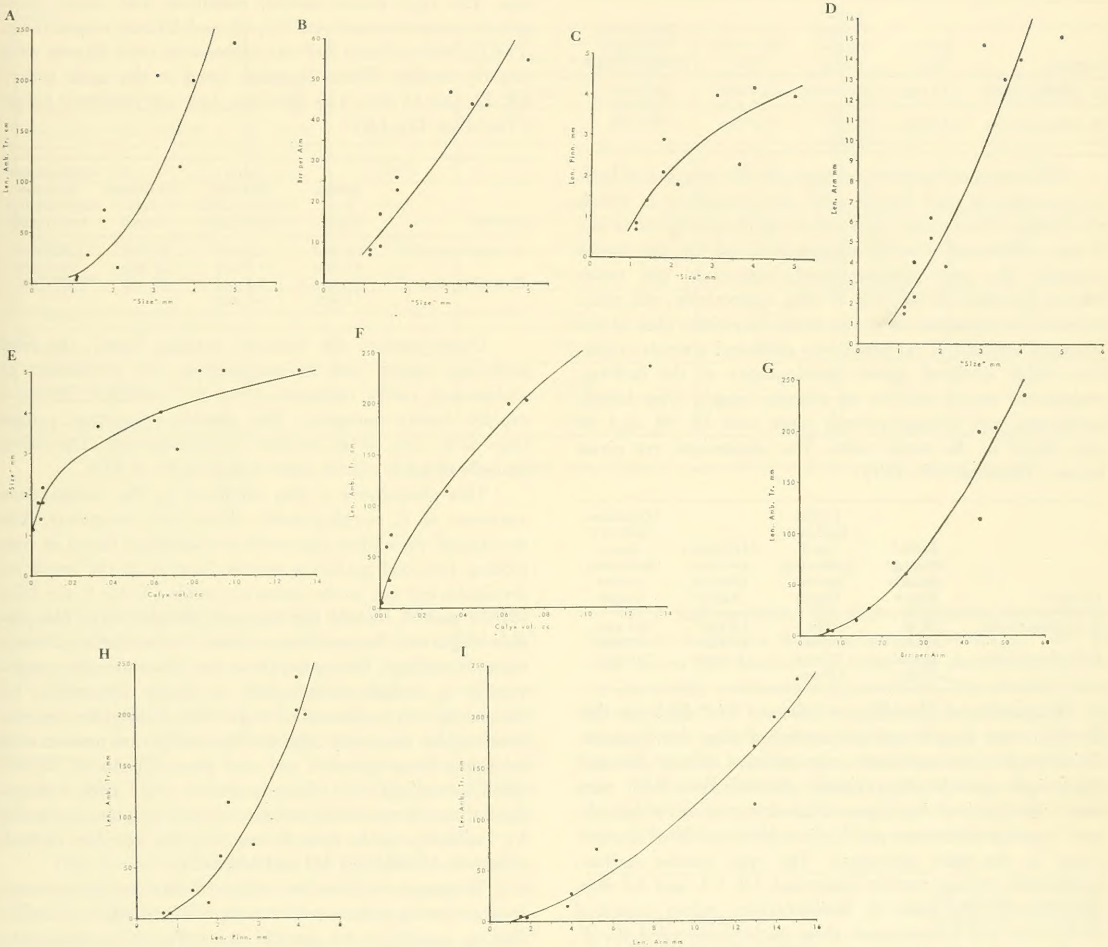

Text-figure 14. — Graphs showing food gathering system growth of *Eopatelliocrinus latibrachiatus*, n. gen., n. sp. Food gathering system length is given as Len. Amb. Tr. If in cm, the total value is denoted. Where in mm, it refers to the half-ray figure. "*a*" is the "pseudo-intercept" or "initial intercept" where the *x* axis is logarithmic. Equation data:

A — $\text{Log}y = .874 + 2.35\log x$. $r = .885$.
$\sigma y\% = 20.1$. $N = 10$. "a" $= .0298$ ($x = .1$).
B — $\text{Log}y = .884 + 1.34\log x$. $r = .919$.
$\sigma y\% = 10.8$. $N = 11$. "a" $= .350$ ($x = .1$).
C — $y = .715 + 4.94\log x$. $r = .880$.
$\sigma y\% = 24.8$. $N = 11$. "a" $= -4.22$ ($x = .1$).
D — $\text{Log}y = .222 + 1.56\log x$. $r = .939$.
$\sigma y\% = 24.0$. $N = 11$. "a" $= .0458$ ($x = .1$).
E — $\text{Log}y = .297 + .952\log x$. $r = .966$.
$N = 13$. "a" $= .341$ ($x = .00001$).
F — $\text{Log}y = 3.13 + .720\log x$. $r = .936$.
$\sigma y\% = 15.5$. $N = 10$. "a" $= .296$ ($x = .00001$).
G — $\text{Log}y = 1.87 + .854\log x$. $r = .989$.
$\sigma y\% = 5.5$. $N = 10$. "a" $= .0104$ ($x = .1$).
H — $\text{Log}y = 2.13 + 1.02\log x$. $r = .960$.
$\sigma y\% = 11.6$. $N = 10$. "a" $= .0128$ ($x = .1$).
I — $\text{Log}y = 1.59 + .457\log x$. $r = .979$.
$\sigma y\% = 8.2$. $N = 10$. "a" $= .0137$ ($x = .1$).

Species	Initial "size"	Initial average pinnule length	Maximum "size"	Maximum average pinnule length
E. scyphogracilis	1.15 mm	.70 mm to .95 mm	6.2 and 7.7 mm	6.7 and 8.1 mm
E. latibrachiatus	1.15 mm	.70 and .85 mm	5.0 mm	4.0 mm

The relations between average pinnule length and half-ray ambulacral tract length were also curvilinear in which the half-ray food gathering system length growth rates per 1 mm additional pinnule length increased in the larger crinoids. The type species initial, maximum, and mean vectors equalled 28, 110, and 75 mm, respectively; the adult crinoid developmental rate was about four times that of the youngest animals. *E. latibrachiatus* exhibited a similar situation which involved slower development of the half-ray ambulacral tracts relative to pinnule length. The initial, maximum, and average growth rates were 16, 98, and 56 mm, listed in the same order. The dimensions are given below (Text-figs. 13h, 14h):

Species	Initial average pinnule length	Initial half-ray food gathering system length	Maximum average pinnule length	Maximum half-ray food gathering system length
E. scyphogracilis	.70 to .95 mm	6.0 to 7.0 mm	6.2 and 6.7 mm	420 and 480 mm
E. latibrachiatus	.70 and .85 mm	5.8 and 6.0 mm	5.0 mm	240 mm

Inspection of Text-figures 13b and 14d discloses that the free arm length was augmented during development. This was due to two factors, the addition of new Brr and the height growth of previously formed Brr. Both taxa were characterized by exponential ontogeny in which the arm length growth rates per 1 mm additional "size" became larger in the older specimens. The type species earliest, latest, and average vectors comprised 3.0, 5.2, and 4.2 mm, respectively. The same *E. latibrachiatus* values consisted of 3.1, 6.4, and 4.9 mm, and these slightly exceeded the *E. scyphogracilis* development rates. The measurements are tabulated as follows:

Species	Initial "size"	Initial arm length	Maximum "size"	Maximum arm length
E. scyphogracilis	1.15 and 1.3 mm	1.8 and 2.5 mm	6.2 and 7.7 mm	19 to 25 mm
E. latibrachiatus	1.15 mm	1.5 and 1.8 mm	5.0 mm	15 mm

The arm length and half-ray ambulacral tract length followed the typical curvilinear pattern in which the food gathering system length growth rates rose with progressive age. The type species initial, maximum and mean ontogenetic vectors constituted 7.5, 36, and 20 mm, respectively. The *E. latibrachiatus* half-ray ambulacral tract figures were slightly smaller. These equalled, listed in the same order: 6.8, 22, and 15 mm. The specimen data are presented below (Text-figs. 13i, 14i):

Species	Initial arm length	Initial half-ray ambulacral tract length	Maximum arm length	Maximum half-ray ambulacral tract length
E. scyphogracilis	1.8 and 2.5 mm	6.0 and 7.0 mm	19 and 25 mm	480 and 420 mm
E. latibrachiatus	1.5 and 1.8 mm	5.8 and 6.0 mm	15 mm	240 mm

Consequent to the relations between "size", the food gathering system and its components, the percentage of ambulacral tracts represented by the pinnules increased rapidly during ontogeny. The pinnule percentage ranges from 62 to 70% in the smallest eopatelliocrinids. The oldest animals of both species show values of 94 or 95%.

This phenomena is also exhibited by the comparative variation of *E. scyphogracilis* adults and youngsters. The arm length variability represents an important factor in controlling the food gathering system lengths of the small individuals, but not in the mature crinoids (Table 9, see IGS. 35P-18 and 19, USNM 164 544, and IGS. 35P-13). The pinnule length and Brr per arm variation is of major importance regardless of age. Generally, these two characters change inversely to a slight extent. Such is readily determined by comparing two specimens with the same food gathering system lengths; unusually high numbers of Brr are present with relatively short pinnules and vice versa (Table 9, USNM 164 552 and 164 555). The significant adult crinoid deviations from the predicted ambulacral tract lengths are caused by variability in the pinnule length or Brr number, or both (Table 9, USNM 164 543 and 164 545).

The previous discussion indicates that the young crown food gathering systems of both eopatelliocrinids are similar. During ontogeny, the growth rate differentials caused the food gathering systems of the two species to diverge, and several major differences are observed between the adults: 1. In a mature *E. latibrachiatus* the arms are about 15 mm long whereas 25 mm arms are found in roughly equivalent aged *E. scyphogracilis*. Nevertheless, similar numbers of IIBrr occur in the adult arms of both taxa (*i.e.*, 55 in *E. latibrachiatus* and 57 to 59 in the other form). Basically, *E. latibrachiatus* has more IIBrr per unit arm length. This is related to contrasts in the IIBrr heights between the mature specimens. In *E. latibrachiatus* the adult standard IIBrr average height equals .28 mm but the same type

Table 9

Specimen	"Size" (mm)	Calyx volume (cc)	Length of free ambulacral tracts (cm) or length of free ambulacral tracts per half-ray (mm)	Arm length per half-ray (mm)	IIBrr per half-ray	Average pinnule length (mm)
Paratype IGS. 35P-19	1.15	.0007	6.2	2.0	8 or 9	.70
Paratype IGS. 35P-18	1.3	.0008	7.4	2.5	9	.70
Paratype USNM. 164 555	1.4	.0028	14.0	3.2	12	1.4
Paratype USNM. 164 552	1.7	.0039	14.0	3.1	12	1.0
Paratype IGS. 35P-13	5.3	.052	290.0	21.0	50	5.4
Paratype USNM. 164 545	6.2	.16	480.0	23.0	57	8.1
Paratype USNM. 164 544	6.6	.087	270.0	19.0	49	5.1
Paratype USNM. 164 543	7.7	.22	420.0	25.0	59	6.7
Holotype USNM. 164 541	4.8	.12	330.0	21.0	52	5.9

Table illustrating variation of the food gathering system components in *Eopatelliocrinus scyphogracilis*, n. gen., n. sp.

species value consists of about .40 mm. 2. The *E. scyphogracilis* adult crown pinnule lengths range from 6.7 to 8.1 mm compared to 4.0 mm in the largest *E. latibrachiatus*.

The type species of the genus correlation coefficients range from .90 to .99 (legend, Text-fig. 13). The *E. latibrachiatus* correlations are slightly lower and cover the .88 to .99 interval (legend, Text-fig. 14). All significance levels exceed .999. These denote that the food gathering system development was highly integrated and coordinated in both forms, although slightly more so in *E. scyphogracilis*.

This is also documented by the distribution of the individual crinoids with respect to selected regression lines. The *E. scyphogracilis* adults almost always occur on the same sides (*i.e.*, above or below) the equations of "size" versus the food gathering system length and its components. For example in "size" versus food gathering system length, USNM 164 545, 164 555, and the holotype lie above the trend line and USNM 164 552 and 164 544 are below the equation. The same pattern characterizes the plots of "size" versus arm length, number of IIBrr and average pinnule length. The two youngest specimens, IGS. 35P-18 and 35P-19, "sizes" 1.15 and 1.3 mm, have more variable positions relative to these regression lines. This suggests that the young crinoid food gathering system ontogeny was slightly less well regulated than in older individuals.

In *E. latibrachiatus*, the adults commonly changed positions with respect to the equations. The holotype, "size" 4.0 mm, shows low numbers of IIBrr and short arms in conjunction with relatively long pinnules. The reverse occurs in the "size" 3.7 mm crown. This clearly illustrates the slightly less well correlated food gathering system growth pattern of this taxon compared to that of the type species.

The food gathering system ontogeny was more highly integrated and coordinated and less variable with respect to calyx volume than to "size" as outlined below:

Species and equation	Correlation coefficient	Percentage standard deviation
E. scyphogracilis "Size" versus food gathering system length	.95	18%
E. scyphogracilis Calyx volume versus food gathering system length	.98	11%
E. latibrachiatus "Size" versus food gathering system length	.88	20%
E. latibrachiatus Calyx volume versus food gathering system length	.94	16%

A similar situation is found in comparison of the correlations of "size" and calyx volume versus the food gathering system components; such is because the calyx volume more closely represents the amount of tissue which was supplied with food than does "size".

The initial intercepts and y equals O values are self-explanatory. The y equals near O and the "initial intercepts" or "pseudo-intercepts" comprise unity (*i.e.*, 1.0, .01, .001 and so forth) to the nearest order of magnitude below the smallest observed specimen figure; this is necessary because there is no common logarithm of O. For the equations of food gathering system components (x) versus half-ray ambulacral tract length (y), the y equals near O values are small, and most of these range from .002 to .52 mm.

The y equals O and y equals near O figures from certain equations, such as "size" (x) versus Brr per arm (y), provide direct estimates of the "sizes" when the IIBrr and food gathering system initially developed. An indirect procedure was involved in dealing with calyx volume. An "initial volume" was calculated from the applicable regression line, for example, calyx volume (x) versus food gathering system length (y). The corresponding "size" was then determined from the calyx volume (x) versus "size" (y) trend line. The ranges of the remotely plausible "sizes" follow (unusually high or low estimates were eliminated):

Species	"Size" range at which food gathering system developed	"Size" range for BB + OO + RR "microcrinoid"
E. scyphogracilis	.29 mm to .56 mm	.22 mm, minimum .63 mm, maximum
E. latibrachiatus	.34 mm to .77 mm	.39 mm, minimum .63 mm, maximum

Comparison of the above figures with each other and with similar values for living crinoids and monocyclic Paleozoic "microcrinoids" shows that the eopatelliocrinid lower calculated "sizes" are probably too small. It is postulated that the *Eopatelliocrinus,* free ambulacral tracts were initiated at "sizes" ranging from approximately .50 to .75 mm.

SUPPORTING STRUCTURE ONTOGENY

Growth of the supporting structures is only known in *Eopatelliocrinus scyphogracilis.* The development of the proximal column width and "size" followed a linear pattern in which the stem diameter width growth vector equalled .30 mm per 1 mm "size" increment (Text-fig. 15a). The maximum and minimum available "sizes" consist of 9.6 and 1.7 mm with equation column widths of 2.7 and .31 mm, respectively. During ontogeny, the "size"/stem diameter decreased from 5.5 to 3.6.

Linear relations also characterized calyx volume and proximal column area. The stem area growth rate per .01 cc calyx volume increase comprised .17 mm^2 (Text-fig. 15b). The smallest and largest volumes constitute .001 and .32 cc ("sizes" 1.7 and 9.6 mm); these correspond to .14 and 5.5 mm^2 column areas, respectively. The stem area/calyx volume ranged from 140 in the youngest animals to 18 in the oldest. Consequently, the proximal columnal area fell with respect to calyx volume in the larger specimens.

Additional FBrr were incorporated into the dorsal cup during development. Prior to IIBr2 fixation, the free arms were supported by the IIBrr1 over the 1.2 to 4.7 mm "size" interval. Once the IIBr2 joined into the calyx, the distal margin of this plate served as the supporting Br. This continued until the IIBr3 was fully fixed at a 9.6 mm "size".

The development of "size" and IIBr1 width was linear with a width developmental vector of .13 mm per 1 mm "size" change (Text-fig. 15c). The smallest and largest individuals have 1.15 and 9.6 mm "sizes" with equivalent IIBrr1 widths of .24 and 1.3 mm, listed in the same order. The "size"/IIBr1 width rose from 4.8 to 7.4 during growth.

The IIBr1 width and half-ray ambulacral tract length showed curvilinear ontogeny in which the supporting Br width growth rate per 1 mm half-ray food gathering system increment dropped from .0066 to .00075 mm (Text-fig. 15d). Consequently, the half-ray ambulacral tract length/IIBr1 width changed from 36 in the youngest animal to 530 in the 6.2 mm "sized" crown.

Similar patterns are seen in the development of IIBr2 with respect to "size" and the half-ray food gathering system.

The growth of half-ray food gathering system length and supporting IIBrr area followed a linear pattern regardless of "size" and age (Text-figs. 15e, f).

The correlation coefficients for half-ray ambulacral tract length versus supporting Brr area range from .99 in young crinoids where the IIBr1 bears the arms to .93 for the mature animals in which the IIBr2 performed this function. In addition, low variation and similar developmental vectors were observed. The immature individual supporting Br area growth rate equalled .006 mm^2 per 10 mm additional half-ray food gathering system length; the adult crown value was .008 mm^2. During ontogeny the half-ray ambulacral tract length/supporting Br area rose from 500 to 1400 (equation values of y used). The highest "adult assemblage" specimen value comprised 2400. The change in the ratio denotes that the supporting Br area declined relative to the half-ray food gathering system length.

Full evaluation of the small crinoid IIBrr2 data is difficult due to equation problems (Text-fig. 15f). This plate forms the proximal free Br in the young animals. Compared to the IIBr1 data, the correlation coefficient, .63, is much lower as is the calculated growth vector which constituted

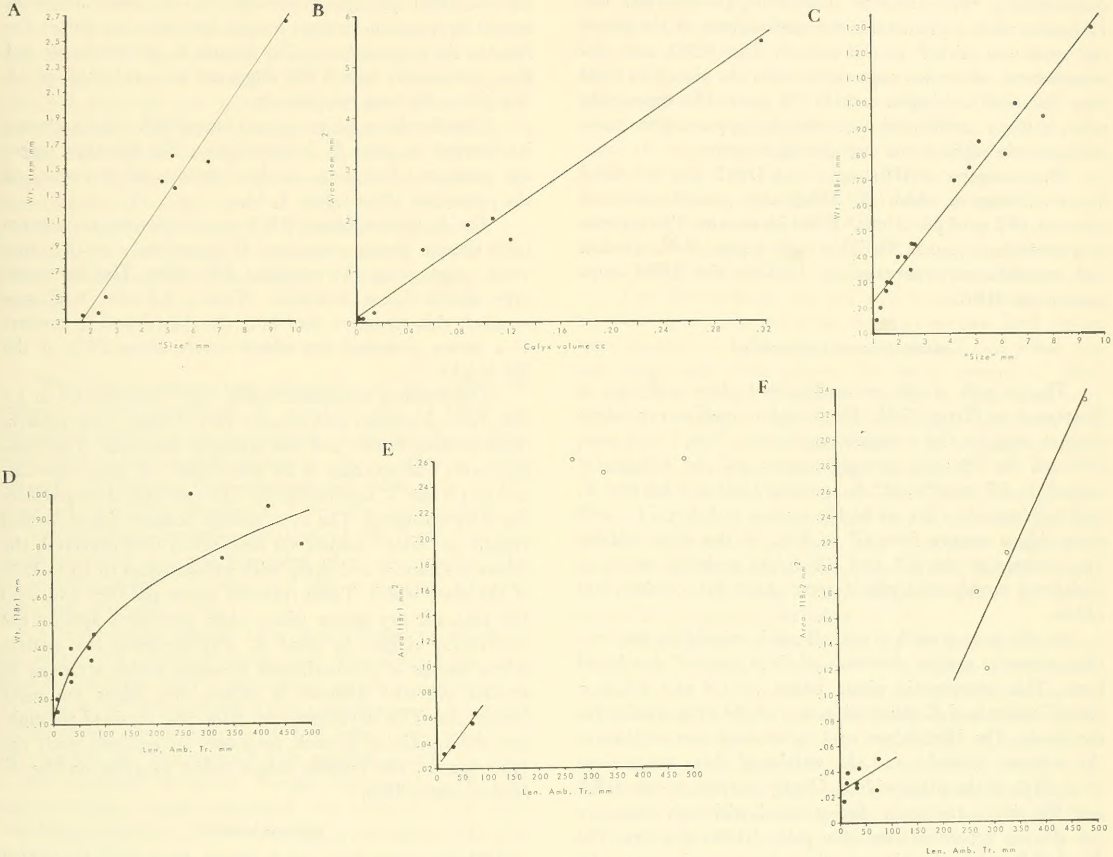

Text-figure 15. — Graphs showing supporting structure growth in *Eopatelliocrinus scyphogracilis*, n. gen., n. sp. Stem width and area refer to the proximal columnal. Supporting Br width and area are those of the distal FBr. In E and F, the young crinoids are indicated by solid dots; mature crinoids by open circles. "*a*" gives the "initial intercept" or "pseudointercept" where the *x* axis is logarithmic. Equation data:
A — $y = -.194 + .297x$. $r = .981$.
$\sigma y\% = 15.2$. N = 8.
B — $y = .124 + 16.9x$. $r = .987$.
N = 8.
C — $y = .0916 + .127x$. $r = .982$.
$\sigma y\% = 13.8$. N = 17.
D — $\text{Log}\,y = -1.076 + .387 \log x$. $r = .958$.
$\sigma y\% = 11.3$. N = 13. "a" = .119 ($x = .1$).
E — Young crinoids. $y = .0206 + .000613x$. $r = .988$.
N = 4. Equation not fitted to adults.
F — Young crinoids. $y = .0263 + .000193x$. $r = .626$.
N = 8. Adult crinoids. $y = -.0776 + .000838x$.
$r = .926$. N = 4.

only .002 mm² IIBr2 area increase per 10 mm additional half-ray ambulacral tract length. Both the growth rate and correlation coefficient seem too small because of the nature of the regression line. The mature specimen IIBrr1 measurements preclude the determination of a meaningful equation.

Although the data are scanty, several tentative conclusions are formulated. At any one developmental stage, the half-ray food gathering system length was more closely integrated and coordinated with the supporting Br area than with the area of the proximal free Br. This is shown by comparison of the correlation coefficients, growth rates and variation; such is predictable because support of the growing arms was critical to the crinoid. The IIBr2 area developmental vector was augmented when the plate was fixed into the calyx and began to bear the arms. The supporting ratio, half-ray ambulacral tract length/supporting Br area, increased throughout the ontogenetic sequence.

The ontogeny of IIBr1 area and IIBr2 area exhibited linear relations in which the IIBr2 area growth rate consisted of .097 mm^2 per .1 mm^2 IIBr1 increment. The correlation coefficient equals .93. This high degree of integration and coordination was required because the IIBr1 supported the IIBr2.

ORNAMENTATION DEVELOPMENT

The growth of the eopatelliocrinid plate sculpture is illustrated on Plates 59-61. The complete median-ray ridges are not seen in the youngest specimens, "size" 1.15 mm, although the IBrr are strongly convex and the RR gently arched. In 1.7 mm "sized" *E. scyphogracilis* and 1.4 mm *E. latibrachiatus* the IBrr are highly convex with flat sides, and these ridges occupy from 67 to 80% of the plate widths. The outlines of the RR and BB ridges probably occur as ill-defined tumid areas which cover about half of the plate widths.

In the next growth stage, all adult crinoid median-ray ridge elements can be observed, albeit in less well developed form. This ontogenetic phase began in 1.8 and 2.3 mm "sized" animals of *E. latibrachiatus,* and the type species, respectively. The IBrr ridges tend to be more narrow than in the younger crinoids, and the widths of these range from 50 to 75% of the plate widths. Gently convex proximal RR and BB ridges are easily distinguished, although these are not sharply separated from the plate lateral margins. The distal RR ridges are intermediate between those on the proximal RR and IBrr.

The median-ray ridges of the two taxa diverged slightly during subsequent growth. In the older *E. scyphogracilis*, the IBrr ridges became higher and relatively more narrow; these only occupy 40 to 50% of the plate widths. The distal RR ridges showed the same trend but this was less striking. The largest specimen, "size" 9.6 mm, retained proximal RR and BB ridges which are like those of 2.5 mm "size" individuals. *E. latibrachiatus* slightly decreased the convexity of the IBrr and distal RR ridges whereas the other ridges were accentuated. Completely developed median-ray ridges are found in 3.1 mm "size" and larger crowns.

The lateral RR ridges, which connect the adjacent RR, initially developed in 1.8 mm "sized" *E. latibrachiatus,* and 2.5 to 2.7 mm type species animals. At first, these are represented by vague horizontal bulges, but they are better defined in the larger calyces. The mature *E. latibrachiatus* and *E. scyphogracilis* lateral RR ridges are seen at "sizes" of 3.1 and 4.0 to 5.0 mm, respectively.

Considerable median-ray and lateral RR ridge variation is observed in adult *E. latibrachiatus*. The holotype ridges are prominent but these are less pronounced in several of the paratypes (Pl. 61, figs. 1, 3).

The *E. latibrachiatus* BB flange underwent no appreciable change during ontogeny. It comprises a small transverse bulge along the proximal BB edges. The immature type species flange is similar. When a 4.2 mm "size" was reached, this structure was fully developed and it consists of a strong proximal rim which covers about 20% of the BB height.

The smallest eopatelliocrinids, "size" interval 1.2 to 1.7 mm, have depressed and concave iBrr. During later growth, these became flatter and less strongly depressed. This configuration was attained in 2.5 mm "sized" *E. scyphogracilis,* and in 1.8 mm *E. latibrachiatus*. The two taxa diverged during later ontogeny. The type species stellate ridges formed rapidly at "sizes" around 4.0 mm. When first observed, the ridges are narrow and sharp with widths equal to 10 to 15% of the plate width. These traverse across the iBrr and onto the adjacent ray plates where they terminate against the median-ray ridges. In some *E. scyphogracilis,* the stellate ridges consist of discontinuous elongate nodes arranged in stellate patterns whereas in others, the ridges are more continuous. This developmental stage was retained throughout the remaining growth sequence. In contrast with the type species, the stellate ridges failed to grow on the *E. latibrachiatus* iBrr.

COLUMN GROWTH

The stem ontogeny can be inferred for adult *E. scyphogracilis*. Although complete columns with rooting devices are unknown, reasonably long stem segments are attached to several mature individuals. A total of five columnal orders occur. The heights of these are distributed as follows in the largest crown, "size" 9.6 mm (numbering of orders after Bather, 1900, text-fig. 17): Order 5, .50 mm, Order 4, .33 mm, Order 3, .25 mm, and Order 2, .18 mm. Order 1 is not seen in this specimen but where present, these plates range slightly thinner than those of the previous order.

Comparison of the proximal and distal order sequences shows that some columnals formed by intercalation whereas others grew immediately below the calyx. A typical distal order formula comprises 5-1-2-1-3-2-4-2-3-2-5. All orders are complete except for Order 1. The proximal columnal sequences exhibit more variability and are more difficult to determine; the approximate mean, compiled from several examples, consists of 5-3-2-4-2-2-5. Order 1 is absent and Orders 2 and 3 are not fully developed. All Orders 4 and 5 were initiated just below the calyx whereas the entire Order 1 was intercalated between previously present plates. At least some Order 2 and 3 columnals must have grown by intercalation. Possibly some of these were inserted immediately below the calyx. The columnal sequences are not definitive on this point. At least 40 to 50% of the stem plates developed by intercalation in the various adult crinoids.

VARIATION

The IBrr geometry has been examined in roughly 10 crinoids of both species. In *E. scyphogracilis*, 11 IBrr1 are hexagonal while four are rectangular. Assigning these plates numerical values corresponding to the number of sides present, the average IBr1 possesses 5.5 sides with a 14% standard deviation. Hexagonal IBrr1 also predominate in *E. latibrachiatus*, occurring in seven of the rays. Two rectangular plates and one five-sided plate are present. The mean IBr1 shows 5.5 sides and the percentage standard deviation comprises 15%.

Fourteen type species IAxx were studied of which 10 are septagonal and four pentagonal. The mean value consists of 6.4 sides with a percentage standard deviation of 11%. Seven *E. latibrachiatus* IAxx are well enough preserved to determine the structure with five being pentagonal and two septagonal. The average side number equals 5.6 with a 16% standard deviation. Similar variation can be observed within a single individual. For example, in *E. latibrachiatus* paratype USNM 164 560, a pentagonal IAx and hexagonal IBr1 occur beside a ray with rectangular IBr1 and septagonal IAx.

Generally, the IBr1 and IAx shapes are closely related. In *E. scyphogracilis*, the hexagonal IBrr1 are always associated with pentagonal or septagonal IAxx whereas the rectangular IBrr1 occur with septagonal IAxx. The shapes of the two plates were better integrated in *E. latibrachiatus*. With one exception the hexagonal IBrr1 are found with pentagonal IAxx and rectangular IBrr1 with septagonal IAx. In the exceptional ray, a five-sided IBr1 is observed with a pentagonal IAx (paratype USNM 164 557). The correlation between the number of IBrr1 sides versus number of IAxx sides equals –.923 which is significant at a probability level between .990 and .999.

The size of the adjacent iBrr is largely controlled by the IBrr geometry. With hexagonal IBr1 and septagonal IAx, the adjacent iBrr are small; the iBr1 terminates at the IBr1 mid-level and the iBrr2 end at the IAx level (most iBrr areas in Text-fig. 7). Where hexagonal IBrr1 are associated with pentagonal IAxx, a small iBr1 is seen, but the iBrr2 are relatively high and end at the IIBr1 level (right side of B ray, Text-fig. 7f; many rays in Text-fig. 8). In *E. latibrachiatus*, rectangular IBr1 and septagonal IAx are moderately common. Here, the iBr1 is large and attains the mid-IAx level; typically, the iBrr2 are small, terminating at the IIBr1 height (Text-fig. 7c; some rays in Text-fig. 8).

The iBrr formulae are not well known although some variation can be documented. Six type species iBrr2 ranges were counted with five ranges composed of two plates and one range with three plates. The mean number of iBrr2 equals 2.2 with a 17% standard deviation. The iBrr3 vary from two to three plates. An iBr2 row with two plates may be followed by two or three iBrr3. The number of iBrr3 is unknown in the specimen with three iBrr2.

E. latibrachiatus is more variable. Three interrays show three iBrr2; two plates are found in five interrays and one interray apparently possesses only one iBr2. Usually, all determinable interrays of one animal exhibit the same number of iBrr2. The mean iBrr2 range comprises 2.2 plates with a 28% standard deviation.

Variation in the important species and generic level characters is listed as follows: 1. Br shape. As definitive at the species level, this is a composite of "size"/width and width/average height. Although total shape variation has not been investigated, data on variability of single shape parameters with respect to each other are available (*e.g.*, width in relation to "size" and average height relative to width). These percentage standard deviations range from 6.8 to 14% for *E. scyphogracilis* and from 7.0 to 20% for *E. latibrachiatus* (see legends for Text-figs. 11 and 12). 2. Calyx shape. As used to separate species of *Eopatelliocrinus*, this is a combination of outline and relative height and width. Relative height and width variation is best approximated by "size" versus calyx width; both forms have percentage standard deviations of 15%. 3. Mature individuals of the two species show some variation in strength of the median-ray and lateral RR ridges. However, stellate ridges or nodes are never found on the iBrr of *E. latibrachiatus*. Some of these elements always occur on adults of the type species. 4. FBrr structure. Variability is most closely indicated by the curves of "size" versus FBrr in lateral interrays and "size" versus FBrr in inter-half-rays. These standard deviations consist of 7.7 and 3.8%, respectively for

E. scyphogracilis. The *E. latibrachiatus,* lateral interray FBrr standard deviation equals 4.4% whereas the inter-half-ray percentage standard deviation comprises 0%.

The following are invariant: 1. Number and orientation of BB. This can only be determined, wholly or partially, for about six specimens of the type species. 2. Number of plates following primanal for the type species, not known for *E. latibrachiatus.* 3. Calyx outline in adults of both eopatelliocrinids. 4. Inter-half-ray FBrr for *E. latibrachiatus.* 5. General nature of calyx ornamentation in mature specimens of both taxa. 6. Presence of two arms per ray in the two eopatelliocrinids. 7. Both forms always have uniserial Brr, regardless of growth stage.

COMPARISON

Young individuals of *E. latibrachiatus, E. scyphogracilis,* and *Macrostylocrinus pristinus* are similar and difficult to separate. During ontogeny, the three forms diverged due to differential growth, and distinction of adult crinoids presents little difficulty. The problems of separating the eopatelliocrinids from the macrostylocrinid will be discussed under *M. pristinus;* the following remarks only treat the Girardeau eopatelliocrinids.

Inasmuch as the eopatelliocrinids showed gradual divergence during ontogeny, the writer has first separated mature individuals after which progressively younger crinoids were considered. Distinction of adults is compounded by the fact that for many characters no clearcut morphological discontinuity is observed between the two forms although the "mean" (*i.e.,* equation value) crinoids may differ sharply. For example, "size" equals 5.0 mm individuals of *Eopatelliocrinus latibrachiatus* and the type species have "size"/dorsal cup width values of 1.5 and roughly 2.0, respectively. Inspection of Text-figures 9l and 10l shows no overlap of the two forms, but a discontinuous distribution is lacking. A similar situation is seen in "size" versus FBrr in lateral interrays (Text-figs. 9h and 10h) in which "average" type species crinoids possess more FBrr than similar "sized" crowns of *E. latibrachiatus.* In Br width and "size", *E. latibrachiatus* mature individuals exhibit wider "average" Brr; at a "size" of 5.0 mm, the Br width equation values equal .64 mm in this crinoid but only .50 mm in the type species. Scrutiny of Text-figures 11a and 12a, indicates wide variation and a small amount of overlap between the two crinoids. Similar situations are found in many other differences which have been treated under ontogeny.

On the other hand, some characters show discontinuities and these are emphasized in separation of adult forms. These are:

1. "Size" range of "adult assemblages". In *E. scyphogracilis,* the adult assemblage interval equals 4.2 to 9.6 mm in "size" while the equivalent figure for the other taxon is only 3.1 to 5.0 mm.

2. Calyx outline. In the type species, the cup walls extend straight upward and a distal constriction is lacking whereas rounded calyx walls and a more or less prominent distal constriction at the proximal IIBrr are seen in *E. latibrachiatus.*

3. Ornamentation. The type species is characterized by sharp median-ray and lateral RR ridges in conjunction with more or less continuous stellate ridges on the iBrr. In *E. latibrachiatus,* the median-ray and lateral RR ridges are less well developed and the iBrr lack ornament.

4. Shape of standard free Brr (*i.e.,* IIBrr 8 to 13). At equivalent "sizes", those of *E. latibrachiatus* tend to be wider relative to height as shown by the following:

	"Size"	Brachial width	Brachial average height	Width/ average height
E. latibrachiatus	5.0 mm	.63 mm	.28 mm	2.25
E. scyphogracilis	5.0 mm	.50 mm	.40 mm	1.25
E. scyphogracilis	9.6 mm	1.01 mm	.48 mm	2.10

Scrutiny of the appropriate graphs (see Text-figs. 11 b, c, 12b, c) shows a marked morphological discontinuity between the two crinoids.

5. Arm taper. In the type species, the taper angle is slight and even throughout the arm which gives the arms a relatively slender and graceful appearance. An *E. latibrachiatus* arm shows strongly uneven taper which is very slight in the proximal area but increases rapidly in the distal one-third of the arm. Consequently, the arms appear heavy and cumbersome.

In younger crinoids ("size" 1.15 to 2.70 mm), distinction is more difficult because some of the adult morphological discontinuities were not developed at these growth stages. For example, ornamentation of the two crinoids is identical and if there is any difference in the nature of the distal constriction, such is not apparent to the writer. Br width relative to height has proven the most useful diagnostic character at this growth stage, for example at "size" equals 2.0 mm:

	Brachial width	Brachial average height	Width/ average height
E. latibrachiatus	.26 mm	.24 mm	1.1
E. scyphogracilis	.22 mm	.31 mm	.75

Inspection of the scatterplots (Text-figs. 11b, c, 12b, c) indicates the presence of a morphological discontinuity between the two crinoids although this is not as marked as the "adult assemblage" break.

In some of the youngest animals ("size" about 1.15 to 1.30 mm), the standard Brr had just begun to develop prior to death; commonly, these are poorly preserved. Consequently, securing the measurements necessary to separate the two species with certainty is difficult. In such cases, arm taper usually proves diagnostic as the youngest *E. latibrachiatus* possess more rapidly tapering arms than the type species.

As previously mentioned, the Lower Silurian *Glyptocrinus insperatus* ? "var." *carinatus* Rowley may be referable to *Eopatelliocrinus*. Rowley's form is easily separated from the Girardeau eopatelliocrinids as follows: 1. Br shape. In the Silurian crinoid, the proximal and distal face convergence angles are large; consequently, the free Brr are distinctly wedge-shaped (cuneiform). This differs from the true uniserial configuration of the Girardeau eopatelliocrinids where the convergence angles are small. 2. The BB circlets of the Girardeau taxa are higher and lack nodes. *Glyptocrinus insperatus* ? "var." *carinatus* is characterized by a flat BB circlet with long proximally directed nodes.

Genus **MACROSTYLOCRINUS** Hall, 1852

Type species. — By monotypy, *Macrostylocrinus ornatus* Hall, 1852, p. 204, pl. 46, figs. 4a-g.

Diagnosis. — Patelliocrinidae with conical calyx; BB forming part of cup walls. Primanal typically followed by three plates, the central one comprises an anal series plate, the two flanking ones form CD interray iBrr; anal interray ridge present or absent. Rarely the primanal is followed by two, four, or five plates with or without an anal interray ridge. CD interray always wider than lateral interrays. IBr1 rectangular to hexagonal; IAx pentagonal to septagonal; the IBr1 and IAx shapes may or may not be correlated. BB three, unequal, two large and one small. Arms, two per ray, composed of mature or immature biserial Brr.

Remarks. — The comparison of *Macrostylocrinus* with the other patelliocrinid genera is presented in Table 5 under *Eopatelliocrinus, n. gen.* Ubaghs (personal communication) believes that *Loveniocrinus* (Jaekel, 1918, p. 37; see type species, *L. gotlandicus* Jaekel, 1918, text-fig. 27) is congeneric with *Macrostylocrinus*. This view is not followed here because loveniocrinids show four erect arms per ray whereas macrostylocrinids have only two arms per ray, both of which are erect. The Devonian species *M. recumbens* Springer which is generally assigned to *Macrostylocrinus* has 23 to 25 arms with four or five in each ray. The arms are pendent and envelop the calyx and part of the stem. The reason for this adaptation remains uncertain; the recumbent arms could have been related to feeding or disguise, or both. At any rate it is tentatively suggested that *M. recumbens* is more closely allied to *Loveniocrinus* than to *Macrostylocrinus*.

Occurrence. — Upper Ordovician, North America, and Europe; Middle Silurian, North America, and Europe; Lower Devonian, North America.

MACROSTYLOCRINUS CIRRIFER Ramsbottom

Plates 64, 65; Text-figures 16, 17, 19

1961. *Macrostylocrinus cirrifer* Ramsbottom, British Ord. Crinoidea, Palaeont. Soc. Mono., p. 20, pl. 6, figs. 6-13.

Diagnosis. — A species of *Macrostylocrinus* with median-ray ridges and numerous well-developed nodes on calyx; column bears cirri arranged in whorls of four, five, or six.

Ontogeny. — *M. cirrifer* is known from 13 internal and external molds from the Ashgillian "Starfish Bed" near Girvan, Scotland. In "size", the crinoids range from about 2.5 mm up to 6.8 mm. The "size" distribution is continuous with roughly two crinoids in each 1 mm "size" class. Relative to the Girardeau patelliocrinid assemblages, these crinoids fall into the upper limits of the "young" assemblage and all or most of the "adult" assemblage range.

Due to the nature of preservation, data cannot be obtained from all material. Most of the following discussion is based on five individuals within the 3.9 to 6.8 mm "size" interval. In view of the small sample and available "size" range, the treatment emphasizes the qualitative rather than the quantitative aspects of growth.

The most important growth features shown by this crinoid are that the relationship between the external ornamentation and the internal calyx aboral nervous system can be ascertained; and that growth of the dorsal cup and its component plates can be related to the aboral nervous system.

As previously mentioned, traces of the aboral nervous system are commonly shown by the presence of grooves on the inside of the dorsal cup plates or the corresponding ridges on internal molds. Consideration of the anatomy and the size and location of the aboral nerve cords (*i.e.*, extention into the calyx of the axial nerve cords within the free arms) of modern crinoids convinces the writer that these ridges on the Girvan internal molds represent traces of the aboral nervous system. For a summary of the nervous system in living crinoids the reader is referred to Nichols (1962, pp.

22-29), Hyman (1955, pp. 61-63), Cuénot (1948, pp. 40-44), P. H. Carpenter (1884), and W. B. Carpenter (1884).

In all modern crinoids examined by the writer, the axial nerve cord is separated from the base of the food groove by solid calcite throughout the free arms. In *Antedon*, where the arms join the calyx, the axial nerve cord penetrates and passes through the radial at the base of the arms and then joins the chambered organ (see Nichols, 1962, figure 2). In *Antedon*, the nerve cords within the cirri are derived from the base of the chambered organ. In stem bearing forms, the nerve cords within the stem originate at the proximal end of the chambered organ. These nerve cords form the aboral nervous system which is the predominant nerve level in crinoids; apparently, this is responsible for posture and movement of the arms and stem (Nichols, 1962, p. 29; A. R. Moore, 1924). In addition, living crinoids possess two surficial nervous systems, the surficial oral or ectoneural net and the hyponeural or deeper oral nervous system; these are not preserved in fossil material and will not be further discussed. The three crinoid nerve systems are all interconnected. Basically, a single three level complex seems to be present with the aboral level dominating the other two.

In the camerates examined, the axial nerve cord was not separated from the Br food groove as in modern crinoids and the mature cyathocrinids studied by Bather; rather, this nerve cord lay at the base of the food groove like the immature cyathocrinid Brr. Although this cannot be directly observed in the Girvan crinoid, such is true of other macrostylocrinids and, therefore, it is extrapolated to *Macrostylocrinus cirrifer*. This configuration was maintained throughout the free arms and where the food grooves and the axial nerve cord entered the calyx at the IIBrr2 to 4 level. Consequently, the calyx extensions of the axial nerve cord (*i.e.*, aboral nervous system) are recorded, if at all, by grooves or other traces on the inside of the dorsal cup plates. In the Girvan crinoids, these correspond to ridges on the internal molds. Numerous crinoid specialists have reached the same conclusion with respect to similar structures in fossil forms (*e.g.*, Lane 1963a, p. 929; Ubaghs, 1953, pp. 663-667; Bather, 1900, pp. 100-105).

Teichert (1949, pp. 13-18) and Sieverts (1927) documented the more intricate intra-plate nervous systems of *Calceolispongia* and *Marsupites*. However, the calceolispongid and the complexly ornamented marsupitid nerve systems are far more complicated than that of this crinoid. The Girvan macrostylocrinid pattern is most similar to that of the simply ornamented species of *Marsupites*. It must be noted that these structures are strikingly different from those illustrated and discussed by Schmidt (1930) for *Hallocrinus ? inagilis* (p. 28, pl. 3, figs. 9-13), *Lophocrinus minutus* (p. 31, pl. 2, figs. 13-15, pl. 3, fig. 1), and *Culmicrinus regularis* (p. 40, pl. 1, figs. 1-4, pl. 3, figs. 2-8, 22). The structures in Schmidt's crinoids can be followed from the inside to the outside of the plates. All in all, these canals or grooves are similar to those of palaeocrinids (see Hudson, 1911) and are probably respiratory as suggested by Schmidt.

Description of nervous system. — The internal mold ridges, representing the nervous system, are most extensively developed in HM.E.3602 (Text-fig. 16a) although the sharpest ridges occur on HM.E.3584 (Text-figs. 16g, h).

The main aboral (axial) nerve cords entered the calyx at the IIBrr2 through IIBrr4 level. If the growth of the Girvan macrostylocrinid were similar to the Girardeau form, the proximal IIBrr were originally free Brr which were gradually incorporated into the calyx during ontogeny. Consequently, the internal mold ridges at this level represent the original food grooves when these plates were free Brr. It is presumed that the axial nerve cord lay at the base (axis) of this food groove (this corresponds to the high point of a ridge on an internal mold).

This seems correct for two reasons. In modern crinoids (see A. H. Clark, 1921, pls. 18-21) and in Bather's mature cyathocrinids (best seen in Bather, 1893, pls. 8, 9 on *Cyathocrinus* and *Gissocrinus*), when the axial nerve cord tube within the Br is separate from the food groove, this structure more or less directly underlies the food groove axis. The immature cyathocrinid axial nerve cord tube is not separate from the food groove, and this nerve cord must have rested at the base (axis) of the food groove. The axis is symmetrical with respect to the whole food groove (see Bather 1893, especially pl. 9, figs. 300, 310d, 311, 319a, 332, 333).

The two half-ray main aboral nerve cords tended down the IIBrr and joined on the IAx of the same ray. The detailed pattern of the IIBrr ridges and nerve cords is difficult to reconstruct because the ridges are wide relative to the IIBrr widths. Apparently, it is similar to that of the free uniserial Brr of the eopatelliocrinids: 1. Fixed-pinnules present. Here, the ridges are basically Y-shaped. The proximal leg of the Y represents part of the "brachial food groove" with the axial nerve cord at its center. One of the distal legs tends toward the pinnule facet and then along the pinnule; this represents the "pinnule facet food groove" and its associated nerve cord. The third leg of the Y continues to the succeeding Br and traces the distal portion of the "brachial food groove". As in the Girardeau forms, the

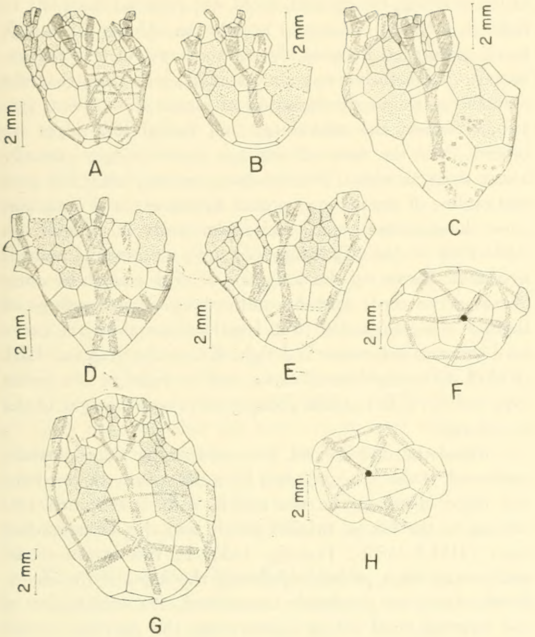

Text-figure 16.—*Macrostylocrinus cirrifer* Ramsbottom. Drawings of calyces. Ashgill; Upper Drummock Group, "Starfish Bed"; Thraive Glen, near Girvan, Scotland.

A — Figured specimen, HM. E. 3602, internal mold, C ray, "size" 3.9 mm.
B — Paratype, HM. E. 3599a, external mold, lateral view, "size" 3.4 mm.
C — Paratype, RSM. 1958.1.244, rubber cast of external mold, lateral view, "size" 5.8 mm.
D — Holotype, HM. E. 3585b, external mold, C ray in center, D ray on right, "size" 6.1 mm.
E — Holotype, HM. E. 3585a, internal mold, C ray, "size" 6.1 mm.
F — Paratype, HM. E. 3588, internal mold, calyx base.
G, H — Paratype, HM. E. 3584, internal mold, "size" 6.8 mm.
G — Lateral view of calyx.
H — Calyx base.

Symbols: All iBrr stippled. Traces of aboral nervous system ruled.

proximal and distal parts of the ridge, corresponding to the "brachial food groove", are not straight but are set at angles to one another (see IIBrr2 in Text-fig. 16g, IIBrr2 and IIBrr4 in Text-fig. 16a). 2. Fixed pinnules lacking. In this case, a ridge tending toward a pinnule facet is absent, and the proximal and distal parts of the ridge seem straight.

The Br nerve cords were not symmetrically placed with respect to the Br face. In the distal IIBrr1 and IIBrr3 faces, the nerve cord lay slightly closer to the intra-ray side of the plate. On the distal IIBrr2 and IIBrr4 faces, the nerve cord occurred closer to the interray Br side (33 to 47% of the width toward the pinnule facet). The pinnule facet nerve cord was apparently located in the center of the facet. The IAx-IIBr1 facets also possessed asymmetrical nerve cords; here, the nerve cords were closer to the intra-ray axis (39 to 45% of the facet width). In the free eopatelliocrinid Brr, the food groove axes seem to have been located symmetrically with respect to the proximal and distal faces.

The main branch of the aboral nerve cord within a single ray continued proximally down the remainder of the IAx and traversed from the IBr1 to the R mid-level. Below this, the ridges become faint and difficult to reconstruct; these are shown as accurately as possible in Text-figure 16. Usually, the ridges continue straight down the ray axis from the proximal part of the R and onto the B (see HM.E.3584, 3588 and 3602 in Text-figs. 16a, f-h). In HM.E.3585a (Text-fig. 16e), the ridges may branch at the R mid-point with one branch tending right and the other left; however, this is not certain. The decrease in ridge strength below the R mid-level may denote passage into the chambered organ. If so, the chambered organ was large, ranging in height from the cup base to the R mid-level, and most of the ridges below this level represent the original interlobe areas between the five chambers of the chambered organ. The lobes (chambers) of the chambered organ were interradial in orientation. Basically, the pattern shown by the Girvan crinoid is similar to that postulated by Bather for monocyclic crinoids (1900, see fig. 12) except that the distal extent of the chambered organ was greater.

The main aboral nerve cords were connected by horizontal-lateral branches which linked the main nerve cords of adjacent rays. Generally, the corresponding horizontal-lateral ridges are weaker than the main ridges. These fall into three types: A. RR level, connecting the adjacent RR. B. IBr1 level, which traverses from the IBr1 to iBr1 to IBr1 in the next ray. C. IAx level, traversing from the IAx to iBrr2 (usually have two iBrr2 within a single range) to IAx of the next ray. Of the horizontal-lateral nerve cord levels, the proximal one is best developed and always present to some extent, whereas the distal level is weakest and commonly absent.

The third order aboral nerve cords consisted of the lateral-oblique types which were located at oblique angles to the previous ones. These are divided into two levels and three groups, listed from proximal to distal: A. RR to iBr1. B. IBr1 to iBr2 and iBr1 to iBr2. Of the three main ridge orders, this is most poorly developed and most commonly absent. As in the horizontal-lateral ridges, the proximal ridges tend to be better developed and more frequently observed than the distal ridges.

Consequent to this pattern, nerve cord knots were located on all plates where the various aboral nerve cords joined. These may be observed on the RR, IBrr1, IAxx, iBrr1 and iBrr2 when the aboral nervous system was fully developed (see Text-fig. 16a). Generally, all orders intersected at the same point on a single plate although some exceptions exist (see iBr1, Text-fig. 16g and IAx of 16a). The locations of these nerve knots with respect to the various plate dimensions are discussed later because systematic change occurred during ontogeny.

The CD interray pattern is largely unknown although a vague ridge is seen on the primanal of HM.E.3585a (Text-fig. 16e).

Similar ridge patterns and presumably nervous systems occur on Middle Silurian Racine internal dolomite molds of other *Macrostylocrinus* species (see Weller, 1900, p. 95, pl. 4, fig. 6 for *M. obconicus;* p. 96, pl. 4, fig. 8 for *M. subglobosus*).

Considerable variation is observed in both the strength of the nerve cord ridges and the level to which they are developed in the Girvan crinoid. The strongest ridges are seen in HM.E. 3584 (Text-figs. 16g, h) whereas weaker ones occur in the other crinoids. All crinoids possess well-developed main ridges on the rays. The maximum variation exists within the horizontal-lateral and lateral-oblique ridges and the associated nerve cords. For example in HM.E.3602 (Text-fig. 16a), these orders reach the mid-iBrr2 level while these terminate at the mid-iBr1 level in HM.E.3584 (Text-fig. 16g). The RR level horizontal-lateral ridges are the highest in HM.E.3585a (Text-fig. 16e).

Correlation between internal nervous system and external ornament. This is clearest in HM.E.3585 where both internal and external molds, showing the same rays and interrays (Text-figs. 16d, e), are available. Text-figure 17a illustrates the median-ray and lateral ridges of E. 3585b (external mold) superimposed on the plate structure and nervous system of the internal mold, E.3585a; in preparation of the drawing, the external mold was reversed from left to right to maintain consistent orientation. Above the mid-R level, correlation between the nervous system and the external ornamentation was almost exact, indicating that the median-ray ridges developed directly over the nervous system. However, the median-ray and lateral RR ridges are coarser than the internal nervous system ridges (usually about twice as wide). Nevertheless, one may trace the general outline of the nervous system by the external ornament even though exact and precise placement is difficult. In RSM.1958 .1 .244 (Text-fig. 16c), only an external mold is available. However, the following second and third order aboral nerve cords may be outlined by aligned groups of slightly elongate nodes: RR level horizontal-lateral nerve cord between the center and right RR in the diagram; IBr1 to iBr1 horizontal-lateral nerve cord to right of the center ray; and R to iBr1 lateral-oblique nerve cord to right of the center ray.

Below the mid-R level, two median-ray ridge patterns are found. If the R is underlain by a BB suture, the median-ray ridge bifurcates at the mid-R with one branch traversing to the left of the BB suture and the other tending right (HM.E.3585b, Text-fig. 16d). In this instance, the median-ray ridge probably followed the lobes of the chambered organ; as previously mentioned, the orientation of the internal mold ridges representing the nervous system is uncertain in this crinoid. When the R lies distal to a large B, both the median-ray and the internal ridges continue straight down (all other internal molds in Text-fig. 16; RSM.1958.1.244 of the external molds). Here, both internal and external features paralleled the interlobes of the chambered organ.

Plate ontogeny model. — (See discussion under the introductory statement on ontogeny). Faint traces of the dorsal cup plate growth lines are visible on a few plates of two internal molds (HM.E.3585a, E.3584). These are poorly preserved and only partly developed. Evidently, this is related to the size of the internal mold forming sediment relative to the growth line thickness. The matrix is mostly fine sand or silt and the diameter of these particles is much larger than the growth line width. Therefore, the growth lines are not preserved although these are believed to have occurred on all plates. This is reasonable; usually, internal crinoid molds showing well-preserved growth lines are composed of fine-grained chert. The general growth rate (calcite accretion) gradient listed from maximum to minimum equalled: lateral growth (height and width), outward growth (thickness), and inward growth vector which was zero (no inward plate growth).

For an animal with no internal plate growth and the aboral nervous system located in grooves along the dorsal cup plate interiors, the most likely and simplest ontogeny model consists of accretionary augmentation which simply extended the previously established nervous system. If so, the nerve cord knots (junctions of several nerve cords) remained at the same topographic position on the plate (*i.e.,* RR, IBrr1, IAxx, proximal iBrr) and the plate accretion took place outward from this position. In this case, the lateral accretion merely lengthened existing nervous systems at the plate edges. Lateral migration of the nervous system did not occur. Consequently, major calcite resorption along the nerve cords was not necessary.

Some minor resorption occurred because the internal ridges which represent the aboral nervous system tend to be wider and higher in larger crinoids (compare HM.E.3602, Text-figure 16a with the larger E.3585a and E.3584 in 16e, g). Such indicates that the nerve cords were widened and thickened during ontogeny; if so, resorption along their sides and base was the only possible mechanism. Assuming the above postulates are correct, the dorsal cup plate growth was adjusted to cause the minimum interference with the fragile aboral nerve cords.

This plate growth hypothesis can be verified, at least to some extent, in three ways: 1. Study of a series of growth lines relative to the nerve cord branches in a group of adjacent plates of the same crinoid. This has not been investigated quantitatively but qualitative studies were performed on internal chert molds of *Agaricocrinus* from the Mississippian Burlington Limestone at Louisiana, Missouri. On the RR, IBrr1, IAxx and iBrr1, the nerve cord knots are well preserved. The main nerve cord (ray) ridges and the horizontal-lateral ridges are somewhat less distinct although these may be traced. The positions of the growth lines with respect to the nerve knots and the nerve ridges confirm the growth model. 2. Superimpose a series of homologous plates from different specimens of various ages and "sizes" to determine whether or not the plate growth resulted in simple extention of the nerve cords. Some results of this are shown for the RR, IBrr1, IAxx, iBr1 and IIBrr2 in Text-figures 17b-k. The procedure followed was to superimpose the plates and their nervous systems of the larger crinoids on those of smaller individuals. In some cases, the plates were reversed from left to right to obtain better fits in plate outline; for example, the RR are superimposed so that the longest R-iBr1 suture is on the left. Almost all of the plate and nervous system fits are good considering the wide amount of plate shape variation. In the iBr1 for HM.E.3584/E.3602 (Text-fig. 17h), the horizontal-lateral ridges yield a poor fit because the IBr1-iBr1-IBr1 ridge of E.3584 lies well above the junction of the lateral-oblique R-iBr1 ridges. This configuration is unusual; generally, the horizontal-lateral and lateral-oblique ridges join at or near the same place as in HM.E.3602 (Text-fig. 16a) and RSM. 1958.1.244 (Text-fig. 16c). Consequently, HM.E.3584 is believed abnormal in this respect; apparently, this is caused by the unusually high IBr1 and iBr1 of this crinoid. All in all, the "superposition" results are clearly consistent with the nerve cord extention mode of growth. In the writer's opinion these data indicate that the postulated growth model is certain for these crinoids. 3. "Geometrical doodling" is discussed later.

Ontogeny of the plates. — The dorsal cup of the Girvan macrostylocrinid was essentially stabilized throughout the observed development. No FBrr were incorporated into the calyx and single plates retained constant shapes (*e.g.,* IBr1, hexagonal in normal crinoids) although their proportions may have changed during the growth sequence.

Text-figure 18a illustrates the percentage width (*i.e.,* percentage of total plate width at the level involved) positions of the nervous system knots plotted versus "size" for the various plates; the smaller percentages are graphed because the ray orientation is uncertain for some individuals. These figures show no systematic change during growth. The percentages range from 43% (nerve knot slightly offset from center of plate) to 50% (central location) with most falling into the nearly symmetrical 45 to 50% interval. This indicates that the width growth rates in both directions (*e.g.,* for the A ray R, width growth rates toward both the B and E ray RR were present) were equal or nearly so (see also superimposed plates in Text-fig. 17).

The plots of the nerve cord knots, in terms of the percentage of the total plate height above the proximal margin, are presented in Text-figure 18b. These points clearly "migrated" in relation to the plate height during growth. Actually, the reverse occurred because the plate margins were extended with respect to the nerve net; however, the graphs are shown in the above form because this represents the manner in which the data were derived. In the RR and IBrr1, the percentage height point "migrated" distally in relation to the total plate height. The reverse characterized the IAxx and iBrr1.

Clearly, the above RR-IBrr1-iBr1 height and width growth pattern was necessary to maintain the junctions of the three nerve cord orders together on these plates. In addition, the pattern adjusted growth so that the nervous

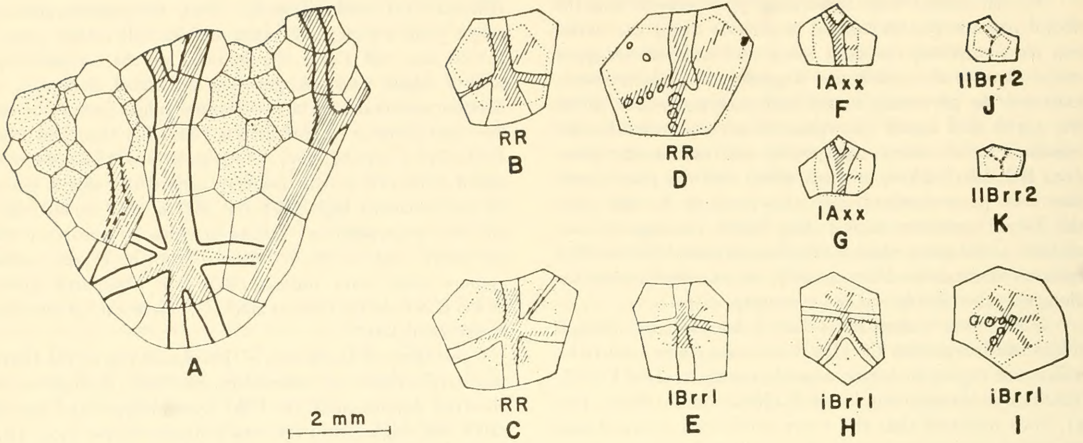

Text-figure 17. — Superpositions of major calyx plates for *Macrostylocrinus cirrifer* Ramsbottom.

A — Holotype HM. E. 3585 a,b, superimposed internal and external molds to show correspondence of internal mold ridges and external ornamentation. External mold reversed from left to right. All iBrr stippled. Internal mold ridges ruled. External ornamentation outlined with heavy black lines.

B-K — Superpositions of individual plates.

B-D — RR plates. B — HM. E. 3585/ HM. E. 3602. "Sizes" 6.1 and 3.9 mm, respectively. C — HM. E. 3584/ HM. E. 3602. Sizes 6.8 and 3.9 mm, respectively. D — HM. E. 3584/ RSM. 1958.1.244. Sizes 6.8 and 5.8 mm, respectively.

E — IBrrl. Same crinoids as C.

F, G — IAxx. F — Same crinoids as C. G — Same crinoids as B.

H, I — iBrrl. H — Same crinoids as C. I — Same crinoids as D.

J, K — IIBrr2. J — Same crinoids as D. K — Same crinoids as C.

Symbols: Smaller plate outlined by dots with ruled ornamentation or internal mold ridges. Larger plate with black outline of both ornamentation and plate.

All drawings to same scale.

system was simply lengthened and did not migrate within the plate.

The typical configuration was not maintained on the iBrl of HM.E.3584 (Text-figs. 16g, 17h) because the horizontal-lateral IBrl-iBrl-IBrl nerve cord failed to join the two lateral-oblique R-iBrl nerve cords; this may indicate that the distal height growth rates of the IBrl and iBrl were much greater than the distal R height growth rates sometime early in the ontogeny of HM.E.3584. Such is suggested by comparison of the IBrl and iBrl in E.3584 with the other crinoids (see Text-fig. 16); these are much higher relative to their widths and to the R size in E.3584.

The Girvan macrostylocrinid dorsal cup plate growth pattern was probably more complicated than that of the Girardeau eopatelliocrinids where the nerve cord knots (when ascertained from the external ornament) apparently remained at the same topographic point on the plates during ontogeny. Possibly, this is only apparent for the Girar-

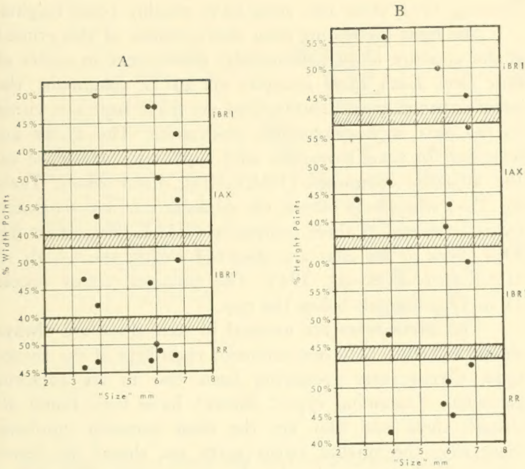

Text-figure 18. — Graphs showing percentage height and width points in *Macrostylocrinus cirrifer* Ramsbottom. Horizontal axes are "size"; vertical axes give percentage height or width point. These points were located by: A. Ridges on the internal molds; these correspond to grooves on the plates which housed the aboral nerve cords. B. External ornamentation on the external molds; this overlies the ridges mentioned in A. Percentage width is expressed as a percentage of the total plate width; the smaller point is always shown (50% or less). Percentage height is the percentage of total height from the proximal edge of the plate.
A. — Percentage width; plates annotated on graphs. B. — Percentage height points.

deau crinoids because the nerve patterns have been reconstructed from the external ornamentation. As previously mentioned, the external sculpture is much coarser than the internal mold ridges, and the location of the nervous system based on external features is less precise.

The most interesting feature of ontogeny stems from "geometrical doodling" with HM.E.3602, E.3584 E.3585 and RSM.1958.1.244. If the dorsal cup plates of a single crinoid are shifted so the nervous systems are not aligned, gaps develop between the adjacent plates. The same may be observed by comparison of individuals of different "sizes" (*e.g.* HM.E.3602 and E.3584) where if the nervous systems are shifted on the plates, gaps are observed. Clearly, the plates only joined when the nervous system knots and the nerve cords were continuous; any other configuration would have resulted in the formation of gaps between the component plates. The skeptical reader is invited to experiment with the drawings of the crinoids and their plates. Observation of the growth of *M. cirrifer* and numerous other crinoids shows that such did not occur and a high degree of coordination and integration was maintained throughout the ontogeny.

The logical interpretation is that the aboral nervous system directly or indirectly controlled the plate lateral growth rates (perhaps also the thickness although no evidence is available) and integrated and coordinated the dorsal cup growth so that the plates remained in lateral contact during ontogeny. However, as discussed in the introductory statement on growth, the ultimate control is believed to have been the mesenchyme.

The tegmen plate ontogeny has not been studied in detail for camerate crinoids. The writer's qualitative observations on internal molds of Mississippian species denote the following. The presence of growth lines on the iAmbb interiors indicates no inward calcite accretion. The Ambb which are associated with the food grooves may have undergone secondary calcite deposition on the plate interiors; this is uncertain because of preservation problems. All tegmen plates exhibited outward (thickness) and lateral (length and width) increments. The predominant growth vectors were functions of the external plate size. In small plates, the maximum vector equalled thickness, but the lateral dimensions predominated in larger plates. The resorption of tegmen plates was either non-existent or was not common. The camerate tegmen plates were not in contact with the aboral nervous system; by analogy with Recent crinoids, this passed from the dorsal cup to the free arms (see Nichols, 1962, fig. 2 for living comatulid). Some camerate Ambb interiors may have been close to the surfical oral nervous system which immediately underlies the feeding tissue of extant and presumably fossil forms, (see internal molds of *Teleiocrinus, Strotocrinus regalis* and *Physetocrinus ornatus* figured by Wachsmuth and Springer, 1897, pl. 4, figs. 1, 3, 4). In other camerates, the calyx ambulacral tracts lay well below the tegmen interior, and the tegmen plates were probably not in contact with the surficial oral nerve level (*e.g., Cactocrinus proboscidalis* Wachsmuth and Springer, 1897, pl. 5, fig. 10). At any rate, the fact that many camerate tegmen plates were not closely associated with the nervous system suggests that the tegmen plate ontogeny was regulated by the mesenchyme. If this can be extrapolated to the dorsal cup plates, columnals and Brr, then the development of these and the growth and placement of the aboral nervous system was most likely controlled by the mesenchyme (see also introductory statement on ontogeny).

Remarks. — The Br shape is only known in one crinoid (HM.E.3586, "size" about 4 to 4.5 mm, Text-fig. 19a). Despite the fact that arms and pinnules are visible in several of the crinoids, (*e.g.*, RSM.1958.1.244, HM.E.3599), the orientations do not allow the configuration to be completely determined. Although the arms are biserial, the geometry is decidedly primitive. In more advanced species, such as *Macrostylocrinus laevis* Springer (1926, p. 26, pl. 4, figs. 14-19), *M. ornatus* Hall (see Springer, 1926, pl. 4, fig. 24) and *M. pristinus*, n. sp., the proximal and distal Br margins (see Text-fig. 2 for terminology) are parallel and straight; the inner margins are also straight and converge on each other at steep angles. The proximal or distal margin width/total width ranges from about .8 to .9 in mature crinoids.

In *M. cirrifer*, the inner margins are curved and meet at relatively small angles; consequently the proximal and distal margins are not sharply separated from the inner ones. The proximal or distal margin width/total width equals only .63. All in all, these Brr are much "less biserial" than those of more advanced forms.

The Brr of *M. meeki* (Lyon) (see Springer, 1926, pl. 4, fig. 23) are even more primitive. The arms are narrow and the Brr are high relative to width; the plates range from wedge-shaped (cuneiform) to weakly biserial in which the proximal and distal margins are narrow relative to the inner margins. Evidently, the primitive aspect of the *M. meeki* Brr is related to the narrow arms which dictated small Br width growth rates relative to "size". Rapid or moderately rapid width growth rates were most likely one of the prerequisites for biserial arm development in primitive crinoids (see Br growth of *M. pristinus*, n. sp.).

The column is preserved in about five individuals. Due to the coarse-grained nature of the mold forming matrix (mostly silt and sand sized quartz) relative to the suture thickness, the sutures cannot be located. Basically the appearance of the stems is that of a series of ridged (nodose) and non-ridged segments. The original sutures may have occurred in two patterns: 1. In the middle of the non-ridged areas. If so, the ridges formed epifacets (see Moore and Jeffords, 1968; Jeffords and Miller, 1968 for terminology). The type-1 sutures are indicated by *s′* in Text-figures 19b-e. 2. Sutures located along the proximal and distal margins of the ridged areas (*s* in Text-figs. 19b-e). In this case, the ridged areas represent nodose columnals whereas the nonridged segments constitute smooth plates; both types may have or lack cirri. This suture model seems most probable because it occurs in the most closely related crinoids with which the writer is familiar (*e.g.*, Girardeau patelliocrinids).

In the smaller specimens (HM.E.3600, E.3492 a, b, E.3599 a, "sizes" from 2.5 to 4.0 mm, Text-figs. 19b-d), the ridge bearing areas are higher than those lacking ridges whereas in the larger RSM.1958.1.244 ("size" 5.8 mm, Text-fig. 19e), these two areas have roughly equal heights.

The most interesting stem characteristic of this crinoid is the presence of cirri. Generally, these occur in cycles of four cirri. Each cycle occupies six to 17 columnals; the counts assume type-2 sutures and are made from one cirrus to the next with comparable orientation. The cycles are irregular. In some cases, the cirri apparently developed on the adjacent columnals (HM.E.3600, distal whorl, Text-fig. 19b) whereas in others, the adjacent cirri are separated by at least two or three columnals (HM.E.3599a, Text-fig. 19c). Five or six cirri are observed within the whorls of HM.E.3492 (Text-fig. 19d). The proximal cirrus occurs 11 to 17 columnals below the cup.

The cirrus scars are unusual in that these are always shared by more than one columnal regardless of the suture type. Cirrus scars occupying from two to six adjacent columnals (assuming type-2 suture) have been found although three and four are the most common numbers. Generally, the smaller cirrus scars are shared by fewer columnals. In most crinoids, the cirrus scars are confined to one columnal (see Moore and Jeffords, 1968). In *M. cirrifer*, the axial canal extension from the column into the cirrus was presumably located on the columnal in the center of the cirrus scar. Most often, this is a ridge bearer although a few may lack ridges (see HM.E.3600, Text-fig. 19b).

The column ontogeny of this species is poorly known because the sutures cannot be precisely located. In addition, the only possible approach to the stem growth in this crinoid is to study the columnals of different "sized" crinoids at comparable positions below the calyx. Inasmuch as new columnals developed just below the calyx and also between the previously existing columnals, this procedure does not result in comparison of the "same" plates. Clearly, the columnal width at comparable positions relative to the dorsal cup base increased during ontogeny (compare Text-figs. 19b-d with 19e). If the drawings are correct, the nodose columnal thickness remained roughly constant at all observed sizes. The non-ridged columnals of the younger crinoids are actually higher than those of the largest crinoid. At comparable stem positions the smallest cirri are found on the youngest individual (Text-fig 19b).

The *M. cirrifer* calyces are easily distinguished from all congeneric forms by the ornamentation which consists of median-ray ridges and numerous nodes covering the entire calyx. Several other species of *Macrostylocrinus*, *M. fusibrachiatus* Ringueberg (1882, p. 119, pl. 5, fig. 4; see Wachsmuth and Springer, 1897, p. 291, pl. 23, figs 9, 10 for better illustrations), *M. ornatus* Hall (1852, p. 204, pl. 46, figs. 4a-g) and *M. ? pustulosus* Springer (1926, p. 26, pl. 4, figs.

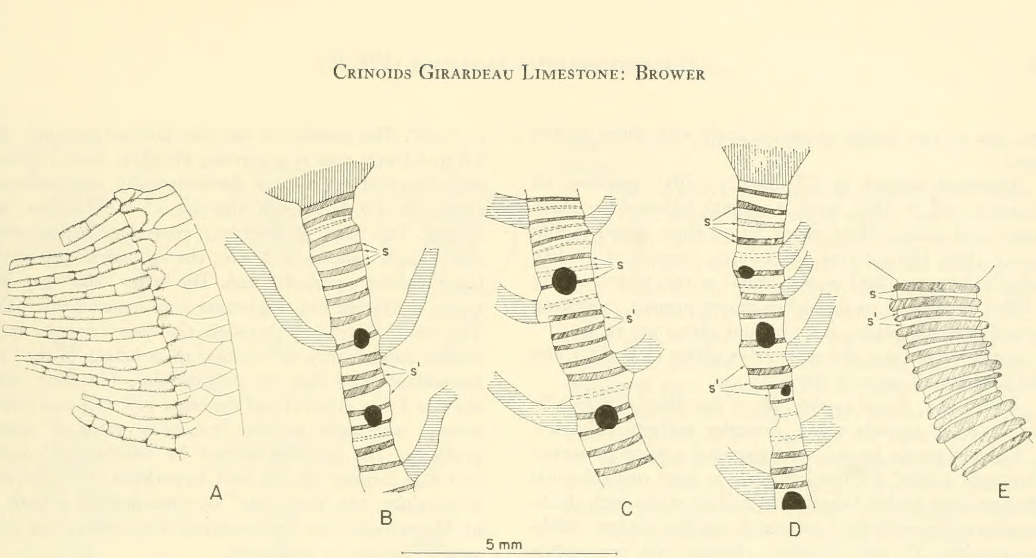

Text-figure 19. — Column and arms of *Macrostylocrinus cirrifer* Ramsbottom. Ashgill; Upper Drummock Group, "Starfish Bed"; Thraive Glen, near Girvan, Scotland.

A. — Paratype, HM. E. 3586, external mold of arm fragment, lowest Brr shown are roughly IIBrr10 or 12, "size" about 4.0-4.5 mm. Note that the distal pinnules are displaced somewhat from their facets.

B.-E. — External molds of stem. Symbols: Ridges obliquely ruled. Finer ridges stippled. Cirrus "holes" in bottom of mold, black. Cirri horizontally ruled. S and S' show possible suture locations as discussed in the text. B. — Figured specimen, HM. E. 3600, "size" about 2.5 mm. C. — Paratype, HM. E. 3599a, "size" 3.4 mm. D. — Figured specimen, HM. E. 3492a. E. — Paratype, RSM. 1951.1.244, "size" 5.8 mm.

All drawings to same scale.

25, 25a), are characterized by or sometimes possess nodes. In *M. ? pustulosus,* the nodes are fewer in number and much heavier; in addition, the calyx shape of this form with its flat base and small IBrr is strikingly different from the Girvan crinoid. In the other two taxa, the nodes (where present) are much finer than those of *M. cirrifer.*

As previously mentioned, the Brr of this crinoid contrast with those of all other macrostylocrinids in which these are observed. In *M. ornatus,* the only other macrostylocrinid where the stem is well known (see Springer, 1926, pl. 4, fig. 24), the cirri are lacking.

Types. — Holotype — HM.E.3585 a, b, (counterparts). Paratypes — RSM.1958.1.244; HM.E.3584, E.3586, E.3587, E.3588, E.3599a,b,. Figured specimens — HM.E.3492a,b, E.3600, E.3602. Additional material — HM.E.3502, E.3511, E.3577/1 and 2 (counterparts).

Occurrence. — Upper Ordovician, Ashgill; Upper Drummock Group, "Starfish Bed"; Thraive Glen, near Girvan, Scotland.

MACROSTYLOCRINUS PRISTINUS, n. sp.

Plates 62, 63; Text-figures 20, 21, 24 a-n

Diagnosis of adult. — A large species of *Macrostylocrinus* characterized by moderately high (relative to width) dorsal cup, cup base narrow, expanding rapidly up to BB circlet distal margin, higher level expansion more gradual, calyx distal constriction lacking; ornamentation consists of well developed median-ray ridges, lateral RR ridges and generally anal-interray ridge, iBrr typically with some traces of stellate ridges or nodes; arms dominated by mature biserial Brr; arms slender relative to most other species; observed part of column lacks cirri.

Partial description of adult. — Most of the description is presented under the following sections on ontogeny and variation.

The iBr1 range composed of one plate; iBrr2 consists of two or rarely three plates; iBrr3 generally with three plates. Distal iBrr smaller and less regular than proximal ones; one or two ranges observed, each with three to five plates.

Primanal located in CD interray iBr1 position, all primanals end at IBr1 level; primanal followed by three plates; anal series plates much larger than adjacent CD interray iBrr; CD interray iBrr1 large, terminates at IAx level; CD interray iBrr2 consist of one or two plates, ending at IIBr1 level; four to six higher ranges present, consisting of small irregular plates, three or four plates per range.

Articular surfaces of known calyx plates (RR, IBrr and iBrr1) smooth. Tegmen unknown.

Depth (*i.e.*, dorsal to ventral) of free biserial Brr probably equals or exceeds width. Articular surfaces unknown.

Column poorly known, only proximal portion preserved in holotype ("size" 7.3 mm); round; at least two columnal orders present: Order 2 consists of nodose plates with thickness about .3 mm. Order 1 columnals smaller, nodose, thickness roughly .15 mm. Another thinner and non-nodose columnal order may be present. Definitely known sutures crenulate. Articular surfaces not seen.

Ontogeny. — With the exception of the Brr, growth of the macrostylocrinid is comparable to that of *Eopatelliocrinus scyphogracilis* and the discussion of the dorsal cup, food gathering system, supporting structures and ornamentation emphasizes comparison with this form. *Macrostylocrinus pristinus* is the only Girardeau biserial armed camerate in which the ontogeny is known. Biserial Brr development is treated on its own merits and only general comparison with uniserial types is presented.

The ontogeny is based on 19 crinoids ranging from 1.0 to 12.6 mm in "size". Growth is fairly well known except that precise iBr1 data are only available from three individuals, the terminal and near terminal Brr have not been seen in crinoids above 4.4 mm in "size", and there is some uncertainty about the details of the biserial Brr growth.

The macrostylocrinid "size" distribution data poses a problem in interpretation. The eopatelliocrinid "size"-frequency graphs (Text-figs. 1g-j) are bimodal with one mode defining the "young assemblage" spatfall and the other indicating the "adult assemblage" which probably included several spatfalls. Conversely, the macrostylocrinid distribution (Text-fig 1k, l) is trimodal with one mode in the 1 to 2 mm "size" range, the second in the 3 to 5 mm interval and the third at 6 to 7 mm. Clearly, the eight individuals ranging from 1.0 to 2.4 mm in "size" are comparable, wholly or partially, with the single spatfall "young assemblage" of *Eopatelliocrinus scyphogracilis* ("size" range 1.15 to 2.7 mm). Also, the seven macrostylocrinids within the 6.5 to 12.6 mm interval represent all or part of the eopatelliocrinid "adult assemblage" which ranges from 4.2 to 9.6 mm in "size". The position of the four macrostylocrinids in the 3.0 to 4.4 mm area is uncertain. Possibly, these represent a single spatfall which was chronologically intermediate between the 1.0 to 2.4 mm and the 6.5 to 12.6 mm "sized" crowns. The "size" gap between these four individuals and the younger crinoids is .6 mm; the equivalent gap with the larger crowns equals 2.1 mm. The latter "size" gap is certainly significant but the former is of questionable validity. The small "size" gap between the four crinoids and the smaller animals may denote that these belong to the "young assemblage" and that the polymodality (*i.e.*, one mode in the 1 to 2 mm interval and the other in 3 to 5 mm interval) merely represents peculiar mortality rates or sampling problems. The problem cannot be resolved although the writer is inclined to the first hypothesis. In view of this uncertainty, the time-"size" or time-spatfall growth rates of *Macrostylocrinus pristinus* and *Eopatelliocrinus scyphogracilis* cannot be compared.

Dorsal cup growth. — (Tables 10, 11; Text-figs 20-22). Text-figure 20 shows the calyx plate superpositions for this species. The method of construction follows that previously discussed under *Eopatelliocrinus scyphogracilis* and *Macrostylocrinus cirrifer.* The youngest *M. pristinus* ("size" 1.0 mm) lack median-ray and stellate ridges, and the relative plate positions are presumed the same as in slightly older crinoids. The median-ray and lateral RR ridges were first consistently developed in the 2.4 mm "sized" crown. The stellate ridge elements are observed in individuals with "sizes" of 4.4 mm and above. Both the horizontal and vertical nerve cord knot orientations can be ascertained in these crinoids.

As usual the percentage width points for the major dorsal cup plates (*i.e.*, RR, IBrr, iBrr1 and primanal) average nearly 50% with a range of ±6%. This indicates symmetrical width growth rates in both directions. Somewhat variable percentage height points are observed although most occur near the plate midpoint and denote roughly symmetrical proximal and distal height growth vectors. With the exception of the IAxx, these percentages remained constant throughout ontogeny. In the IAx, this point "migrated" distally in older crinoids.

The macrostylocrinid dorsal cup plate growth was almost identical to that of *Eopatelliocrinus scyphogracilis* with several exceptions. The macrostylocrinid IAx percentage height point moved distally. In young animals ("size" 1.95 to 2.4 mm), the point lies about 30% above the proximal plate margin; this occurs at roughly 40% in mature crowns ranging from 7.3 to 12.6 mm in "size".

As in the eopatelliocrinid, the main dorsal cup plate development pattern consisted of increase in height/width

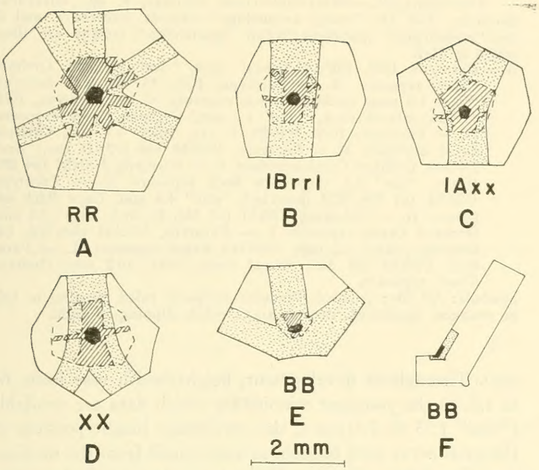

Text-figure 20. — Superpositions of major calyx plates for *Macrostylocrinus pristinus*, n. sp.
A. — RR plates. Paratypes USNM 146 566/ USNM 164 574/ IGS. 35P-28. "Sizes" are 12.6, 4.4 and 1.3 mm, respectively. B. — IBrrl. Same crinoids as A. C. — IAxx. Same crinoids as A. D. — Primanal. As in A except USNM 164 568, "sizes" 9.2 mm, is largest crinoid. E, F. — Large BB. Paratypes USNM 164 566/ USNM 164 577/ IGS. 35P-28. "Sizes" are 12.6, 2.4 and 1.3 mm, respectively. E. — Lateral view. F. — Cross-section view. The BB thickness was assumed at 28% of its height. Symbols: Smallest plate shown in black. Middle plate outline is dashed; extent of stellate ridges obliquely ruled. Large plate outline is solid line with extent of stellate ridges stippled. All drawings to same scale.

throughout ontogeny. However, the degree of this in various plates ranged from nearly equal to that of *E. scyphogracilis* to intermediate between that of *E. scyphogracilis* and *E. latibrachiatus*. Such is related to the width growth; the macrostylocrinid width growth rates relative to "size" were intermediate between those of the two eopatelliocrinids (*i.e.*, larger than the type species but smaller than the other form).

As later discussed, the BB ontogeny differed markedly between the macrostylocrinid and *E. scyphogracilis*.

The plate thicknesses are intermediate between those of *E. scyphogracilis* (average 17% of plate height) and *E. latibrachiatus*, where the thickness comprises up to 55% of the plate height. In *Macrostylocrinus pristinus*, the plate thickness varies from 6% on the R margin to about 30% where the nerve cord was overlain by the median-ray ridge. As in *Eopatelliocrinus scyphogracilis*, the typical plate growth rates listed from maximum to minimum, were height, width and thickness in which all accretion was external.

The reliable macrostylocrinid calyx plate initial intercepts (*i.e.*, width when height equals zero) decline in the same order as those of *E. scyphogracilis;* the available iBrrl data are inadequate to provide a reliable intercept and the –.013 value for the BB is clearly anomalous. The RR initial intercepts are comparable for both crinoids (*i.e.*, .292 versus .358), but the IBrr intercepts decline more slowly in *Macrostylocrinus pristinus* (legend, Text-fig. 22). Possibly such represents poor curve fitting, but inspection of the graphs (Text-figs. 22b-d) eliminates this explanation. Inasmuch as smaller intercepts are expected for later appearing plates, the intercepts may indicate that the macrostylocrinid IBrr developed more rapidly. The hypothesis is tentative and, if applicable, is not shown by the "microcrinoid" values.

The maximum and minimum RR height values equal 3.2 and .32 mm which correspond to equation widths of 3.0 and .59 mm, respectively (Text-figs. 20a, 22b). The width growth rate consisted of .94 mm per 1 mm of height increase which is similar to that of *Eopatelliocrinus scyphogracilis*. During the observed ontogeny (*i.e.*, "size" 1.0 to 10.2 mm), the height/width increased from .54 to .94. Throughout growth, the plate geometry underwent essentially no change except for the height/width ratio and the proximal margin where the plate is underlain by a BB suture. This margin is relatively angular in young animals whereas the mature outline is smoother (compare Text-figs. 21a, c-e with 21f, i, j; see also 20a). In *E. scyphogracilis*, more striking changes were observed in RR development. The macrostylocrinid height point lies 54% above the proximal edge indicating that the distal height growth rates were slightly less than the proximal ones; the eopatelliocrinid height point occurs at 50%.

The smallest and largest IBrl heights consist of .40 and 3.0 mm; these correspond to predicted widths of .59 and 3.0 mm, listed in the same order (Text-figs. 20b, 22c). The width growth rate equalled .94 mm per 1 mm height increment which is almost the same as the .98 mm figure of *E. scyphogracilis*. The height/width's of both forms are almost identical in which the ratio ranged from .68 to 1.0 during macrostylocrinid ontogeny. Three IBrrl types occur in this species. The ontogeny of hexagonal plates is best known (Text-figs. 21b, g, i, j). When first observed, the iBrl is present and fixes the plate into the calyx along the IBrl lateral margins. The earliest lateral IBrl margins were relatively smooth (Text-fig. 21a), but during later development, these became more angular (Text-figs. 21g, i); this was caused by accelerating the mid-level width growth vectors relative to the proximal and distal ones. Comparison of

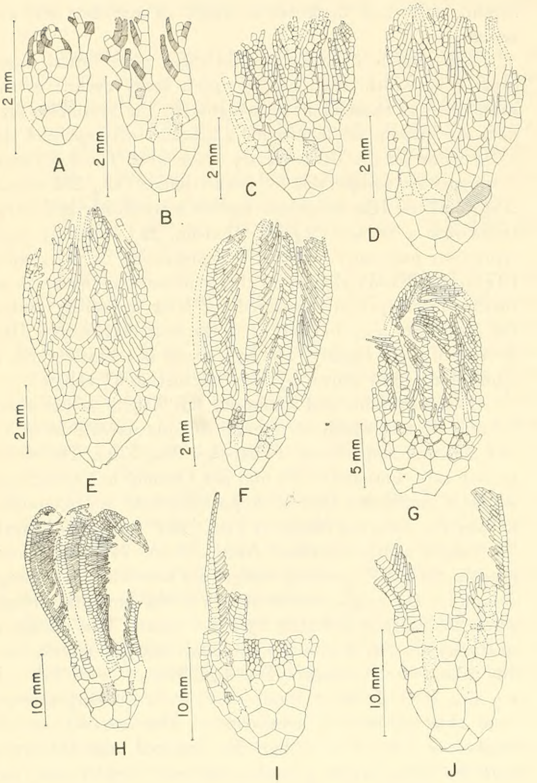

Text-figure 21. — *Macrostylocrinus pristinus,* n. sp., Girardeau limestone. A-E are "young assemblage" crinoids whereas F and G are "transitional" specimens. Adult "assemblage" crowns are illustrated by H-J.

A. — Paratype, IGS. 35P-30, lateral view, "size" 1.0 mm, Orchard Creek exposure. B. — Paratype, IGS. 35P-28, CD interray, "size" 1.3 mm, Orchard Creek exposure. C. — Paratype, IGS. 35P-26, lateral view, "size" 1.7 mm, Orchard Creek exposure. D. — Paratype, IGS. 35P-25, C ray, "size" 1.7 mm, Orchard Creek exposure. E. — Paratype, USNM 164 577, D ray, "size" 2.4 mm, Orchard Creek exposure. F. — Paratype, USNM 164 575, B ray, "size" 3.4 mm, Cape Rock exposure. G. — Paratype, USNM 164 574, CD interray?, "size" 4.4 mm, Cape Rock exposure. H. — Holotype, USNM 164 565, E ray?, "size" 7.3 mm, Orchard Creek exposure. I. — Paratype, USNM 164 568, CD interray, "size" 9.2 mm, Orchard Creek exposure. J. — Paratype, USNM 164 567, lateral view, "size" 10.2 mm, Orchard Creek exposure.

Symbols: All iBrr stippled. Pinnules obliquely ruled, dipping to left, in youngest specimens. Broken areas ruled, dipping to right.

Text-figures 21a and 21b (the latter is at a slightly more advanced FBrr stage) indicates that the plate margin change took place rapidly.

The development of five-sided and rectangular plates is poorly documented (Text-figs. 21f, 21h). Apparently the number of sides on a single IBr1 was stabilized throughout ontogeny. At a given age and "size", the heights of hexagonal, five-sided and rectangular IBrr1 seem equal, but the hexagonal plates are wider than five-sided ones which are, in turn, wider than rectangular types. The IBr1 height point occurs 48% above the proximal plate margin denoting nearly symmetrical height growth vectors.

The IAxx heights range from .30 to 3.0 mm which correspond to equation widths of .47 and 3.0 mm (Text-figs. 20c, 22d). The width growth rate was .94 mm per 1 mm height augmentation which is exceeded by the 1.0 mm figure for *E. scyphogracilis* and the 1.04 mm value of *E. latibrachiatus.* Throughout development, height/width rose from .64 to 1.0. In the youngest crinoids for which data are available ("size" 1.95 to 2.4 mm), the percentage height position of the axial nerve cord branch, as ascertained from the median-ray ridge bifurcation, lies 30% above the proximal margin. When a 4.4 mm "size" was attained, a 33% position is observed whereas in the largest crowns ("size" 7.3 to 12.6 mm), the point is located at roughly 40%. In the youngest specimens, the distal height growth rate greatly exceeded the proximal one, but in older animals, these ontogenetic vectors were more equal. The most obvious IAx shape change was to augment the apex angle between the distal sides (Text-fig. 20c, see also 21); probably, this provided progressively more firm support for the growing arms in older crinoids. Three IAxx types are seen in this species. The septagonal ones (Text-figs. 21b, h, i, j) are best known and occur with rectangular or hexagonal IBrr1. The lateral margins of seven-sided IAxx are usually incorporated into the cup by iBrr1 and iBrr3, if present (Text-figs. 21b, i, j). In the younger specimens, the lateral margins are relatively smooth but greater angularity characterizes larger animals. This represents an increase in the mid-level width growth rates relative to the proximal and distal ones as in the IBrr1. The six-sided IAxx are associated with hexagonal IBrr1 (Text-fig. 21g), and the pentagonal ones are found with hexagonal IBrr1 (Text-fig. 21e). As indicated above, the IBr1-IAx-iBr1 relations were less stable than in *E. scyphogracilis* and *E. latibrachiatus.* As far as can be determined, the number of IAxx sides remained constant during ontogeny of a single plate; certainly, this was true after the plate was fixed into the calyx.

The iBr1 data (only two or three crinoids) are inadequate to characterize quantitative development of the plate. In the younger crinoids ("size" 1.30 mm), the iBr1 is roughly .36 mm high and .25 mm wide; the same values

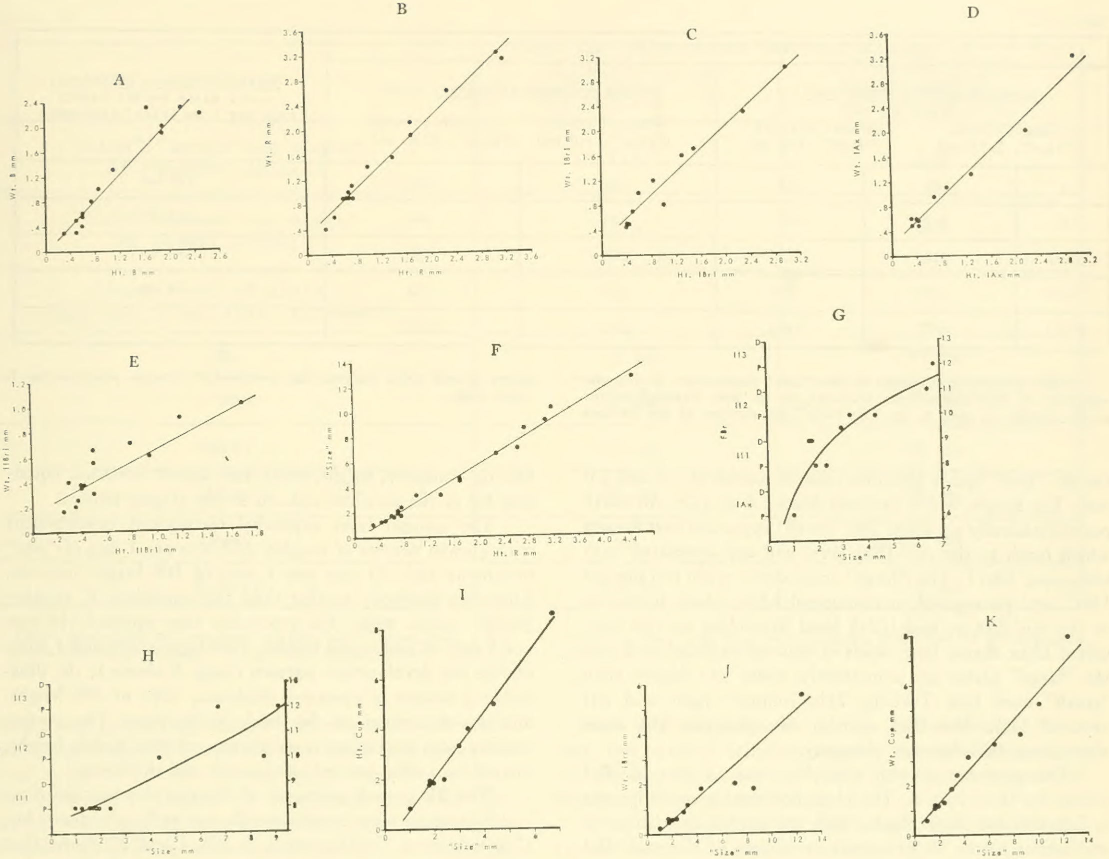

Text-figure 22. — Graphs showing calyx growth of *Macrostylocrinus pristinus*, n. sp. FBrr scales are given in both the numerical scale used for computer purposes and the plate scale (*i.e.*, IAx, IIBr1 = III, etc., P indicates proximal margin, D denotes distal margin). G gives the FBrr in lateral interrays. H gives the same for inter-half-rays. "a" refers to the "initial intercept" or "pseudointercept" if the x axis is logarithmic.

Equation data:

A — $y = -.0126 + 1.04x$. $r = .960$.
$\sigma y\% = 19.4$. N = 14.
B — $y = .292 + .942x$. $r = .990$.
$\sigma y\% = 12.1$. N = 15.
C — $y = .213 + .935x$. $r = .979$.
$\sigma y\% = 17.8$. N = 11.
D — $y = .189 + .938x$. $r = .988$.
$\sigma y\% = 13.4$. N = 10.
E — $y = .140 + .560x$. $r = .895$.
$\sigma y\% = 29.0$. N = 14.
F — $y = -.149 + 2.93x$. $r = .993$.
$\sigma y\% = 11.1$. N = 19.
G — $y = 6.70 + 5.76\log x$. $r = .919$.
$\sigma y\% = 8.0$. N = 10. "a" = .944 ($x = .1$).
H — $\log y = .871 + .0219x$. $r = .919$.
$\sigma y\% = 2.7$. N = 13.
I — $y = -.629 + 1.33x$. $r = .994$.
$\sigma y\% = 12.1$. N = 9.
J — $y = .235 + .387x$. $r = .937$.
$\sigma y\% = 29.7$. N = 11.
K — $y = .183 + .545x$. $r = .977$.
$\sigma y\% = 13.1$. N = 12.

Table 10

	Equation % of "size" represented by plate height				Macrostylocrinus pristinus, n.sp. plate height growth rate per 1 mm "size" increment
	Eopatelliocrinus scyphogracilis, n.gen., n.sp.		Macrostylocrinus pristinus, n.sp.		
	Young Crinoid ("size", 1.15 mm)	Largest Crinoid ("size", 9.6 mm)	Young Crinoid ("size", 1.0 mm)	Largest Crinoid ("size", 12.6 mm)	
B	18%	30%	33%	21%	.19 mm
R	36%	28%	37%	34%	.34 mm
IBrl	22%	20%	20%	23%	.24 mm
IAx	29%	19%	16%	23%	.24 mm
Total	105%	107%	106%	101%	

Table illustrating changes in the "size" components during the ontogeny of *Macrostylocrinus pristinus*, n. sp. and *Eopatelliocrinus scyphogracilis*, n. gen., n. sp. The "size" percentages of the various plates exceed 100% because the proximal R margin overlaps the B upper edge.

for the "size" equals 10.2 mm crinoid consist of 2.5 and 2.0 mm. The height/width declined from 1.4 to 1.25. All iBrrl possess basically six sides. The "small" types are best known which reach to the mid-IBrl level and are associated with hexagonal IBrrl. The "large" ones occur with rectangular IBrrl and pentagonal to septagonal IAxx; these terminate at the mid-IAx or mid-IIBrl level depending on the associated IAxx shape. In crinoids of equivalent "size" and age, the "large" plates are consistently wider and higher than "small" ones (see Text-fig. 21h, compare right and left rays of 21f). The iBrl number of sides was the same throughout the observed ontogeny.

The primanal growth was the same as that of iBrl except for three factors. The plate possesses seven sides and is followed by three plates, with the center one being an anal series plate. All primanals terminate at the mid-IBrl level, and the plate is always higher and wider than the "small" iBrrl in adjacent interrays. The height and width equal .39 and .35 mm, respectively, in the smallest animal ("size" 1.0 mm); the equivalent values for the "size" equals 9.2 mm crown consist of 3.1 and 2.8 mm, listed in the same order. The number of sides and height/width (1.1) were stabilized throughout the observed growth. The percentage height point of the iBrrl and primanals lies a constant 51% above the proximal margin, and the proximal and distal height developmental rates were nearly equal.

The maximum and minimum small BB heights consist of 2.5 and .30 mm which correspond to equation widths of 2.6 and .30 mm, respectively (Text-fig. 22a). The width growth vector was 1.0 mm per 1 mm height augmentation which exceeds the equivalent .70 mm of *E. scyphogracilis*. During ontogeny, height/width was almost constant, equalling 1.0 in the smallest and .96 in the largest crinoid.

The column facet expanded throughout development with growth vectors of roughly .095 mm per 1 mm of "size" increment and .40 mm per 1 mm of BB height increase. These are distinctly smaller than the equivalent *E. scyphogracilis* values where the expansion rate equalled .48 mm per 1 mm of additional height. Text-figures 20e and f summarize the development pattern (large B shown); the illustrations assume a constant thickness, 30% of BB height, and non-deposition on the inside of the plate. The growth vectors from maximum to minimum equalled width, height, inward expansion toward axial canal, and thickness.

The BB growth geometry of *Macrostylocrinus pristinus* and *Eopatelliocrinus scyphogracilis* was strikingly dissimilar. Comparison of Text-figures 6, 7, 20e, f and 21 shows that the BB of young individuals are similar in both species. During later ontogeny, divergence occurred. The mature macrostylocrinid BB and BB circlets have relatively wide and rapidly expanding distal margins in conjunction with narrow bases and column facets. Conversely, the adult eopatelliocrinid shows a wide base, a larger height/width, and more nearly vertical sides. All three differences were caused by the column facet expansion and width growth vector differentials between the two species.

The relationship between IIBrrl height and width is questionable. The best fit equation consists of a straight line. However, inspection of Text-figure 22e indicates a poor visual fit; this is also suggested by the large 29% standard deviation and the low correlation coefficient (.90) relative to those of the other calyx plates. Perhaps, the true rela-

Table 11

	Macrostylocrinus pristinus, n. sp.	Eopatelliocrinus scyphogracilis, n. gen., n. sp.
"Size"/"dorsal cup width" of youngest crinoid	1.4	1.2
"Size"/"dorsal cup width" of oldest crinoid	1.8	2.2
Growth rate of plate width per 1 mm "size" increment	—	—
BB	.19 mm	.23 mm
RR	.30 mm	.29 mm
IBrr1	.23 mm	.20 mm
IAxx	.23 mm	.18 mm
iBrr1	—	.13 mm
IIBrr1	.11 mm	.13 mm

Table illustrating the ontogeny of the "size"/dorsal cup width in *Macrostylocrinus pristinus*, n. sp. and *Eopatelliocrinus scyphogracilis*, n. gen., n. sp. and the relationship thereof to the width growth rates of the plates involved.

tionship was partly logarithmic. The maximum and minimum heights equal 1.7 and .25 mm which correspond to actual widths of 1.0 and .15 mm, respectively. The height/width remained at roughly 1.7 throughout ontogeny. The equation width growth rate is .056 mm per 1 mm height increment, which seems anomalously low compared with the .13 and .12 mm values of the two eopatelliocrinids. The youngest crinoids ("size" 1.0 to 1.3 mm) possess five-sided IIBrr1 which were not incorporated into the calyx by iBrr (Text-figs. 21a, b); a relatively smooth margin is present on the interray side. Just prior to and during fixation of IIBrr1 into the calyx, the interray side developed an angular margin due to acceleration of the plate mid-level growth vector. The iBrr incorporated the plate into the calyx along this angular margin. The C ray IIBr1 of paratype IGS. 35P-28 (Text-fig. 21b) illustrates angular margin development prior to fixation; during incorporation, angularity became more pronounced as seen in Text-figures 21e, f and g.

Throughout ontogeny, the dorsal cup shape changed because of differential growth of the component plates. Most macrostylocrinid calyx ontogenetic variations were similar to those of *E. scyphogracilis* in type and magnitude. However, two marked contrasts existed, namely differences in the plate contributions to "size" and a lesser amount of dorsal cup height/width increase.

The development of RR height and "size" followed the typical linear relationship (Text-fig. 22f) with a "size" growth rate of 2.9 mm per 1 mm RR height augmentation which is slightly more than the 2.5 mm eopatelliocrinid figure. The macrostylocrinid growth rate is unusually high due to the initial intercept of –.149. The maximum and minimum RR heights consist of 4.5 and .32 mm, corresponding to actual "sizes" of 12.6 and 1.0 mm.

The changes in the individual plate "size" components are illustrated in Table 10; the totals exceed 100% as the distal BB margins overlap the proximal ends of the RR. The young macrostylocrinid dorsal cup is dominated by the BB and RR whereas the IBrr are minor elements (see also Text-figs. 21a-e). The RR and IBrr predominate in the adult calyx and the BB are subordinate. The IBr1 and IAx contributions to "size" were augmented largely at the "expense" of the BB. These relations are functions of the initial observed size of the plate in the youngest crinoid, and the plate height growth vectors relative to "size". Both the smallest R and its height growth rate were relatively large, and the percentage "size" contribution was maintained. The earliest IBrr1 and IAxx are small with respect to "size", but the height growth vectors of these plates were large relative to their original size. Therefore, the percentage "size" contribution of these plates increased. When first observed, the BB are large with respect to "size", but the "size"-height growth rates of these were the least of all the calyx plates. Accordingly, the relative BB height declined as a "size" element.

The eopatelliocrinid "size" development pattern was significantly different; young calyces exhibit relatively large RR with the BB, IBrr1 and IAxx as subordinate elements. Throughout ontogeny, the calyx became dominated by the BB and RR, both of which showed large height growth vectors relative to "size".

In "size" versus dorsal cup width (Text-fig. 22k), linear relations are observed in which the width growth rate equalled .54 mm per 1 mm "size" increase; this is intermediate between the .38 mm value of *E. scyphogracilis* and the .66 mm figure of *E. latibrachiatus*. The maximum and minimum "sizes" consist of 12.6 and 1.0 mm which correspond to predicted dorsal cup widths of 7.2 and .73 mm respectively. During ontogeny, "size"/dorsal cup width increased from 1.4 to 1.8. A greater change in the ratio is observed in growth of *E. scyphogracilis*, during which "size"/dorsal cup width rose from 1.2 to 2.2 (Table 11). The explanation is the differential calyx plate width growth rates relative to "size" in the two crinoids (Table 11); these ranged higher in the macrostylocrinid. For example, in the RR, IBrr1 and IAxx, the plate width-"size" growth rates averaged roughly 15% less in *E. scyphogracilis*. The macrostylocrinid IIBr1 value seems anomalous, probably due to poor curve fitting.

In "size" versus iBrr width (Text-fig. 22j) and dorsal cup width versus iBrr width, considerable difficulty was experienced with the equations. Generally, the best regression lines yield poor fits to the youngest and oldest crinoids; in both instances, the predicted growth rates are anomalous with the first being too small and the latter too large (Text-fig. 22j and legend). Poor fits are also implied by the high percentage standard deviations which consist of 30% and 130%. Despite the equation difficulties, the true relations were probably linear. The maximum and minimum "sizes" equal 12.6 and 1.0 mm; these correspond to iBrr widths of 5.5 and .24 mm, respectively. The "size"/iBrr width declined from 4.2 to 2.3 throughout ontogeny, and dorsal cup width/iBrr width ranged from 2.4 to 1.8. These indicate that the iBrr areas at the IAx level expanded relative to "size" and dorsal cup width during the observed growth. A similar pattern is seen in *E. scyphogracilis*, although detailed comparison is impractical due to the curve fitting problems.

The ontogeny of the lateral interray FBrr and "size" (Text-fig. 22g) followed the typical patelliocrinid exponential pattern with a declining FBrr incorporation vector. In the smallest crinoids, "size" range 1 to 2 mm, the numerical scale FBrr growth rate equalled 1.7, whereas the mature crinoid value declined to .38 mm over the 5.8 to 6.8 mm "size" interval (*i.e.*, the largest for which exact data are available). The mean fixation rate consisted of .81 per 1 mm "size" augmentation. The smallest crinoids, "size" 1.0 to 1.3 mm, have the mid-level of IBr1 or IAx fixed into the calyx (Text-figs. 21a, b). When a 1.7 to 2.4 mm "size" was attained, the IIBr1 began incorporation or was joined into the dorsal cup (Text-figs. 21c-e). The lower half of the IIBr2 was fixed into the calyx over the 3.35 to 4.4 mm "size" range. The mature crinoids have the IIBr3 proximal edge forming the highest FBrr ("size" 6.8 mm).

The macrostylocrinid lateral FBrr development rates were almost identical to those of *E. scyphogracilis*. Generally, the young crowns possess the same FBrr. When "sizes" of roughly 4 mm were reached, the two forms diverged slightly and the macrostylocrinids averaged .5 fewer FBrr (numerical scale); this continued throughout growth. For example, when IIBr1 was completely fixed in the macrostylocrinid calyx, the IIBr2 was just beginning incorporation into the *E. scyphogracilis* dorsal cup.

The relation between "size" and inter-half-ray FBrr (Text-fig. 22h) was logarithmic in which the FBrr incorporation vector increased throughout ontogeny. The initial numerical scale growth rate equalled only .40 over the 1 to 2 mm "size" interval, but over the 8.2 to 9.2 mm range, the vector rose to .58. Normal *E. scyphogracilis* individuals did not add inter-half-ray FBrr during development. In the smallest macrostylocrinids (Text-fig. 21a), the IIBr1 inner sides are joined. At a "size" of 4 to 5 mm, the proximal parts of the IIBr2 were fixed by inter-half-ray iBr1 or iBrr2 (Text-fig. 21g). The largest crinoids for which data are available ("size" 9.2 mm, Text-fig. 21i) possess the lower part of IIBr3 as the highest FBrr. During fixation of the inter-half-ray iBr1, the inner IIBr2 sides developed angular margins along which the iBr was joined (Text-fig. 21f). This was repeated when the IIBrr2 distal parts or the IIBrr3 proximal margins were incorporated (Text-fig. 21g). The IIBr3 bears the proximal pinnule on the inter-half-ray side. In the later growth stages, the proximal part of the first pinnular shows an angular margin along which the inter-half-ray iBrr2 or iBrr3 fixed the plate into the dorsal cup (Text-fig. 21i). This angular margin is not observed before the pinnular was joined into the calyx (Text-fig. 21f) and presumably, it formed during or immediately prior to this process.

The development of "size" and dorsal cup height (Text-fig. 22i) followed a linear pattern in which the dorsal cup height growth rate per 1 mm "size" increase was 1.3 mm which is the same as that of *E. scyphogracilis*. The maximum and minimum "sizes" for which measurements are available consist of 6.8 and 1.0 mm; the corresponding cup heights are 8.4 and .70 mm. During growth, dorsal cup height/"size" increased from .70 to 1.2, and similar values characterize the eopatelliocrinid.

The following "microcrinoid" values have been computed: 1. BB + OO + RR "microcrinoid". Maximum possible "size" (*i.e.,* height of the BB and RR in smallest crinoid), .63 mm. "Size" from equation of "size" versus lateral interray FBrr where the distal "FBr" is the top of the RR circlet, .23 mm. 2. BB + OO "microcrinoid". "Size" from "size" versus lateral interray. FBrr where the distal "FBr" equals the BB upper margin, .10 mm. "Size" from the initial intercept of R height versus "size" equation, –.15 mm. This last figure is anomalous, and inspection of Text-figure 22f indicates the equation yields a poor fit to the smallest specimens. Aside from this, the "theoretical microcrinoids" closely approximate those of *E. scyphogracilis.*

The distribution and magnitude of the correlation coefficients (see legends for Text-figs. 9, 22) of *Macrostylocrinus pristinus* and *Eopatelliocrinus scyphogracilis* are similar with the following exceptions:

1. Like the eopatelliocrinid, the plate height measures show higher correlations with "size" than with calyx width. Strangely, the macrostylocrinid plate widths are equally correlated with both "size" and calyx width. In *E. scyphogracilis,* the plate widths have higher correlation coefficients with calyx width than with "size".

2. The macrostylocrinid "size" versus inter-half-ray FBrr exhibits a higher correlation (.92, N = 13 versus .88, N = 12). The explanation is found in the two contrasting growth patterns. Normal *E. scyphogracilis* individuals did not add inter-half-ray FBrr during development; the .88 correlation coefficient is caused by the abnormal largest crinoid which has fixed-IIBrr4. Conversely, the development of new inter-half-ray FBrr was the normal ontogenetic trend in the macrostylocrinid. The "size" and lateral interray FBrr are almost equally correlated in the two crinoids (.93, N = 9; .92, N = 10).

3. The correlation coefficient range of the macrostylocrinid equals .77 to .997; all correlation coefficients have significance levels (two sided test) equal to or exceeding .999. The *E. scyphogracilis* correlation coefficient interval is .80 to .996 with significance levels ranging from .900 to greater than .999. Apparently, the macrostylocrinid degree of calyx growth integration and coordination was slightly higher and more sophisticated than that of the eopatelliocrinid.

Free brachial ontogeny. — (Table 12; Text-figs. 23, 24). The development of the standard Brr (*i.e.,* IIBrr8 to 13) is reasonably well known, and quantitative data are available from 13 to 16 specimens ranging from 1.2 to 12.6 mm in "size". The standard Brr either had not formed or were not well preserved in the 1.0 mm "sized" crown and several slightly older crinoids. Nevertheless, the qualitative development of the older standard Brr is discussed relative to the IIBr6 of a 1.3 mm "sized" individual. In the "size", Brr width, and maximum height versus the minimum height, considerable curve fitting problems were encountered. The best fit equations are of the $\log y = \log a + bx$ form.

Inspection of Text-figures 23c, e, and g discloses poor visual fits. This is confirmed by the high minimum height percentage standard deviations which vary from 19 to 33%; the other standard deviations are consistently lower (legend, Text-fig. 23). The true relations seem sigmoidal. The biserial Brr growth model is less well documented than that of the uniserial types, and the conclusions are more generalized. The standard measurements were developed for uniserial Brr, but these have not proved completely satisfactory in depicting biserial Brr ontogeny. In discussion of the biserial Brr growth rates, the following development stages are recognized:

1. Uniserial. The minimum height is large relative to the maximum height and Br size. "Size" range, 1.0 to 3.0 mm.

2. The transitional phase includes the largest uniserial Brr where the minimum height is small with respect to the width. Also, the immature biserial Brr are assigned here (see Text-fig. 2 for terminology). The immature biserial Brr inner margins are not strongly differentiated from the proximal and distal margins. The minimum height equals 0 mm and the inner Br sides adjoin two Brr on the opposite side of the arm. Both types can be seen in the standard Brr of one specimen. "Sizes", 3.4 to 4.4 mm.

3. Mature or true biserial. The proximal and distal margins are parallel and the inner margins converge on each other. The minimum height comprises 0 mm, and the proximal and distal margins are sharply separated from one another. "Size" interval, 6.6 to 12.6 mm.

In "size" versus Brr width, exponential development occurred during which the width growth rate declined from .11 to .016 mm per 1 mm "size" increment (Text-fig. 23a). The mean constituted .039 mm. The average was much smaller than the constant width developmental vectors of the uniserial armed eopatelliocrinids which ranged from .095 to .13 mm (Table 12). The largest and smallest "sizes" consist of 12.6 and 1.2 mm; these correspond to .57 and .14 mm equation widths. Throughout ontogeny, the "size"/width changed from 8.6 to 22 indicating a decrease in width relative to "size". The mean width growth rates per 1 mm additional "size" were highest in the uniserial stage and lowest for the mature biserial stage: uniserial stage, .090 mm; transitional stage, .050 mm; and mature biserial phase, .025 mm.

The ontogeny of "size" and Brr maximum height followed a logarithmic pattern in which the maximum height developmental vector dropped from .085 to .012 mm per 1 mm "size" augmentation (Text-fig. 23b). The mean growth rates for the three ontogenetic stages were: uniserial phase, .069 mm; transitional crinoids, .039 mm; and mature biserial specimens, .019 mm. The average vector for all stages comprised .030 mm. The mean width growth rate exceeded that of maximum height by 1.3 times. The uniserial armed eopatelliocrinid width developmental vectors were more predominant, and the width growth vector/average maximum height growth vector ratios equalled 2.4 and 5.2. The youngest and oldest macrostylocrinid crown "sizes" are 1.2 and 12.6 mm, and the equivalent predicted maximum heights are .23 and .56 mm, respectively.

The best fit equation for "size" versus minimum height is a curvilinear type with a decreasing minimum height developmental rate (unbroken line in Text-fig. 23c). For computer purposes, a 0 mm minimum height was equated to .01 mm because there is no common logarithm of 0. Inspection of the graph discloses a poor fit, and the regression line deviates widely from the two transitional crinoids, "sizes" 3.4 and 4.4 mm. An unsatisfactory equation is also indicated by the large 33% standard deviation. The "size" versus the other Brr parameter figures only vary from 9.3 to 20%. The true relationship is believed to be sigmoidal as shown by the hand drawn dashed curve in Text-figure 23c. Although not fully apparent here, sigmoidal curves are clearly applicable for the width versus minimum height and the maximum height versus minimum height (Text-figs. 23e, g). Hand sketched rather than mathematically derived sigmoidal curves are presented because the writer did not have access to the appropriate computer program. The youngest crinoid "sizes" range from 1.2 to 1.7 mm and they possess minimum heights of .19 to .21 mm. The largest "size" interval consists of 6.6 to 12.6 mm, all crinoids of which show mature biserial Brr and 0 mm minimum heights. The early macrostylocrinid minimum height developmental vectors were negative, and the minimum height declined. During the uniserial stage, the minimum height fell about .025 mm per 1 mm "size" increment. The largest negative growth rate was .065 mm. This occurred in the transitional phase when the Brr proximal and distal faces converged to produce an immature biserial plate. After this, the proximal and distal margins became differentiated from the inner margins and a mature biserial Br was formed with a 0 mm minimum height. This pattern contrasted greatly with the positive eopatelliocrinid minimum height growth vectors.

Linear development characterized Brr width and maximum height (Text-fig. 23d). The maximum height ontogenetic rate comprised .064 mm per .1 mm additional width. The smallest and largest Brr widths are .11 and .58 mm; the corresponding maximum heights equal .22 and .52 mm.

Sigmoidal ontogeny was seen in Brr width versus minimum height (Text-fig. 23e). The young uniserial crinoids exhibit widths from .11 to .21 mm which correspond to a .19 to .21 mm minimum height interval. In the two transitional animals, the widths vary from .45 to .51 mm and the minimum height ranges from .12 to .20 mm. All standard Brr of the 3.4 mm "sized" paratype (Text-fig. 21f) are uniserial with strongly converging sides and finite minimum heights. In the 4.4 mm "sized" crown (Text-fig. 21g), most Brr are uniserial although a few immature biserial plates are observed. The mature biserial Brr width interval consists of .48 to .58 mm with a 0 mm minimum height. During the uniserial stage, the minimum height declined at .005 mm per .1 mm width increase; the transitional specimen value represented roughly .09 mm or 18 times the uniserial rate. The mature biserial Brr minimum height was stabilized at 0 mm.

The growth of minimum height and maximum height followed the familiar sigmoidal pattern (Text-fig. 23g). The uniserial Brr maximum heights vary from .24 to .27 mm and the equivalent minimum heights are .19 to .21 mm. The two transitional crowns have .43 and .47 mm maximum heights and minimum heights of .12 and .20 mm, listed in the same order. The mature biserial Brr show maximum heights ranging from .48 to .57 mm and 0 mm minimum heights. The unserial minimum height growth vector equalled –.009 mm per .1 mm maximum height increment while the same transitional figure consisted of –.16 mm. The two vectors differed by almost 16 times.

Because of the above relations, the proximal and distal Br face convergence angle underwent a major change during ontogeny (Text-fig. 23i). The uniserial crinoid angle, "sizes" from 1.0 to 2.4 mm, rose from about 25° to 40°. In the 4.4 mm "sized" transitional crinoid, the uniserial Br value is

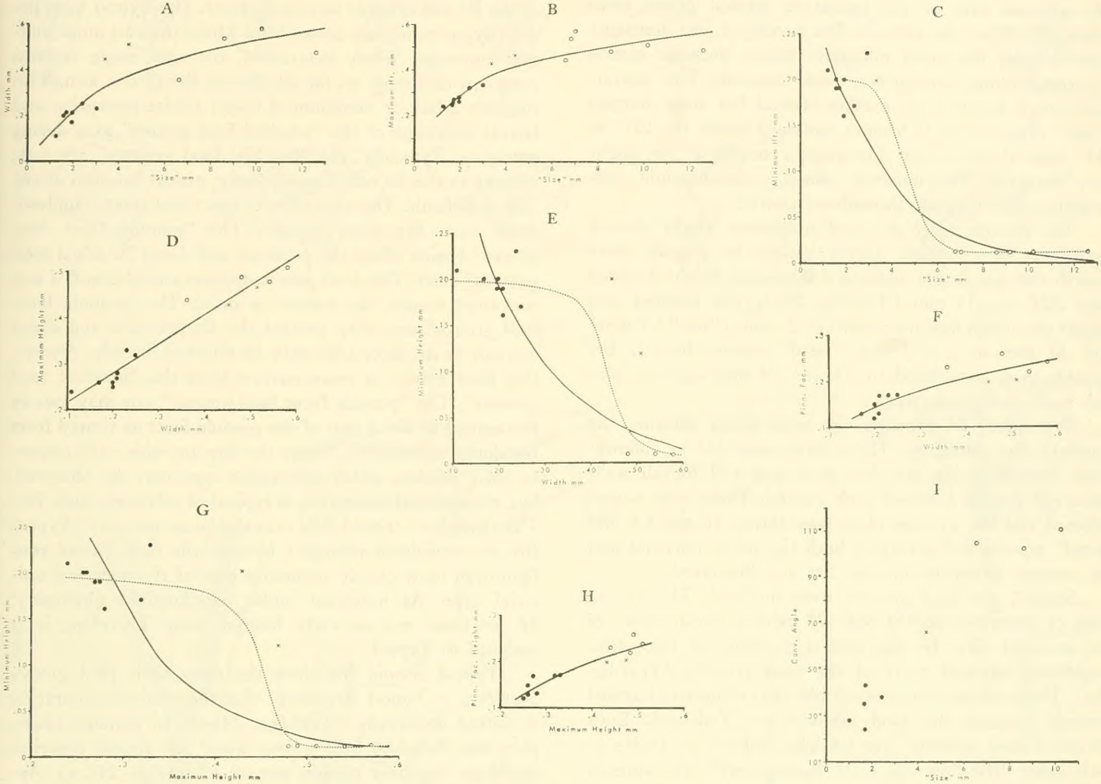

Text-figure 23. — Graphs of standard Brr growth in *Macrostylocrinus pristinus*, n. sp. All dimensions except "size" refer to the Brr measures defined on Text-figure 2. "Young assemblage" crinoids, solid dots. "Transitional", x's. "Adult assemblage" animals, open circles. On C, E and G, the best fit equations are of the $\log y = a + bx$ form (solid line). The true relations believed sigmoidal (dashed line). "a" refers to the "pseudointercept" or "initial intercept".

Equation data:

A — $y = .0977 + .432 \log x$. $r = .898$.
$\sigma y\% = 20.2$. $N = 14$. "a" $= -.335$ ($x = .1$).
B — $y = .197 + .334 \log x$. $r = .926$.
$\sigma y\% = 10.2$. $N = 16$. "a" $= -.137$ ($x = .1$).
C — $\operatorname{Log} y = -.435 + (-.158)x$. $r = -.915$.
$\sigma y\% = 33.1$. $N = 15$.
D — $y = .155 + .633x$. $r = .972$.
$\sigma y\% = 7.2$. $N = 14$.
E — $\operatorname{Log} y = -.179 + (-2.66)x$. $r = -.786$.
$\sigma y\% = 38.8$. $N = 13$.
F — $y = .288 + .202 \log x$. $r = .884$.
$\sigma y\% = 11.3$. $N = 13$. "a" $= -.117$ ($x = .01$).
G — $\operatorname{Log} y = .522 + (-4.42)x$. $r = -.860$.
$\sigma y\% = 18.9$. $N = 15$.
H — $y = .338 + .344 \log x$. $r = .930$.
$\sigma y\% = 9.5$. $N = 13$. "a" $= -349$ ($x = .01$).
I — Equation was not fitted.

37° whereas that of the immature biserial plates comprises 66°. When the uniserial Brr developed into immature biserial ones, the rapid minimum height decrease caused a corresponding convergence angle increase. The convergence angle between the mature biserial Brr inner margins ("size" range 6.6 to 12.6 mm) remained inside the 103° to 111° interval, but within this range, a roughly 5° rise might have occurred. The uniserial armed eopatelliocrinid convergence angle dropped throughout growth.

The pinnule facet size and maximum height showed curvilinear development during which the pinnule facet growth rate per .1 mm additional maximum height declined from .027 to .015 mm (Text-fig. 23h). The smallest and largest maximum heights constitute .25 mm ("size" 1.7 mm) and .51 mm in a 10.2 mm "sized" mature biserial Brr crinoid; these correspond to .13 and .24 mm equation pinnule facet sizes, respectively.

Text-figure 24 presents the restorations showing the standard Brr ontogeny. These were compiled as follows: First, camera lucida sketches were prepared for all well-preserved standard Brr of each crinoid. These were superimposed and the average plate was drawn. In the 4.4 mm "sized" transitional paratype, both the mean uniserial and the average immature biserial Brr are illustrated.

Second, the food grooves were outlined. The D ray arms of paratype USNM 164 577 exhibit dorsal views of the uniserial Brr. In the central portions of the arms, weathering exposed parts of the food grooves (Text-fig. 24n). The configuration is much like that of uniserial armed crinoids because the food grooves are Y-shaped. Both "brachial food grooves" are straight and set at angles to each other. The "pinnule facet food groove" also appears straight and not distinctly curved as in uniserial armed species. Both "brachial food grooves" emerge in the center of the proximal and distal Br faces, as seen in dorsal view. The "pinnule facet food groove" is symmetrical relative to the pinnule facet. All food grooves are at or near 90° angles to the facet concerned. These orientations are somewhat distorted in Text-figure 24n because the Brr are tilted.

The mature biserial Brr food groove patterns are not known in *M. pristinus*. Examination of the biserial Brr food grooves in numerous other forms discloses three general types. Type-1 plates are shown in Text-figures 24o-q. The "brachial food grooves" may be wide or narrow. Doubtless, their axes housed the axial nerve cords. The "brachial food groove" axes lie at angles to one another. One set of two "brachial food grooves" is shared by a single biserial Br and the two neighboring Brr on the other side of the arm. The junction of the proximal and distal "brachial food grooves" forms an angle, the apex of which points towards the outside of the Br and toward the pinnule facet. The Type-1 apex lies directly, or nearly so, across from where the two inner margins converge. When ascertained, the apex angle remains constant, or almost so, for all biserial Brr of one arm. This suggests a lack or minimum of major calcite resorption and lateral migration of the "brachial food groove" axes during ontogeny. Typically, the "brachial food grooves" are wide relative to the Br size. Consequently, precise location of the axes is difficult. The axes seem to enter and emerge midway along each Brr inner margin. The "pinnule facet food groove" begins where the proximal and distal "brachial food grooves" meet. This food groove appears straight, and if any curvature occurs, the amount is small. The "pinnule facet food groove" axis may parallel the Br proximal and distal margins or its outer edge may be directed distally. Always, this food groove is more narrow than the "brachial food grooves". The "pinnule facet food groove" axis may exit in the central or distal part of the pinnule facet as viewed from the dorsal orientation. Where the Brr are wide with respect to their heights, either emergence type may be observed, but symmetrical emergence is typical of relatively high Brr. The Girardeau crinoid falls into the latter category. Type-1 Brr are considered primitive because the food groove configuration most closely resembles that of the ancestral uniserial type. As indicated under patelliocrinid phylogeny, *M. pristinus* was an early biserial form. Therefore, it is assigned to Type-1.

Type-2 crinoid Brr show the same basic food groove geometry as Type-1 Brr except that the whole configuration is shifted proximally (Text-figs. 24r-t). In extreme examples, the "brachial food groove axes" are almost superimposed on the inner margin sutures (Text-figs. 24s, t). Apparently, Types-1 and 2 crinoids form a gradational spectrum and a transitional species is pictured in Text-figure 24r. The overall Type-2 geometry was probably designed to minimize the proximal height growth rates. This configuration is believed to have been derived from Type-1. It is thought to be a progressive character because of further departure from the uniserial condition.

Only one species is referred to Type-3 (Text-fig. 24u). Although the "brachial food groove" axes are not well preserved, they appear to be straight and parallel to the arm length axis. The Type-3 "brachial food groove" axes are most similar to the straight axial canals of Recent crinoids. Although Type-3 seems to represent an advanced character, its relations with the other two types are uncertain.

The transitional Brr food grooves are unknown in the Girardeau macrostylocrinid. The transitional uniserial Brr food grooves are believed to follow the previously discussed uniserial model. The immature biserial Brr food grooves

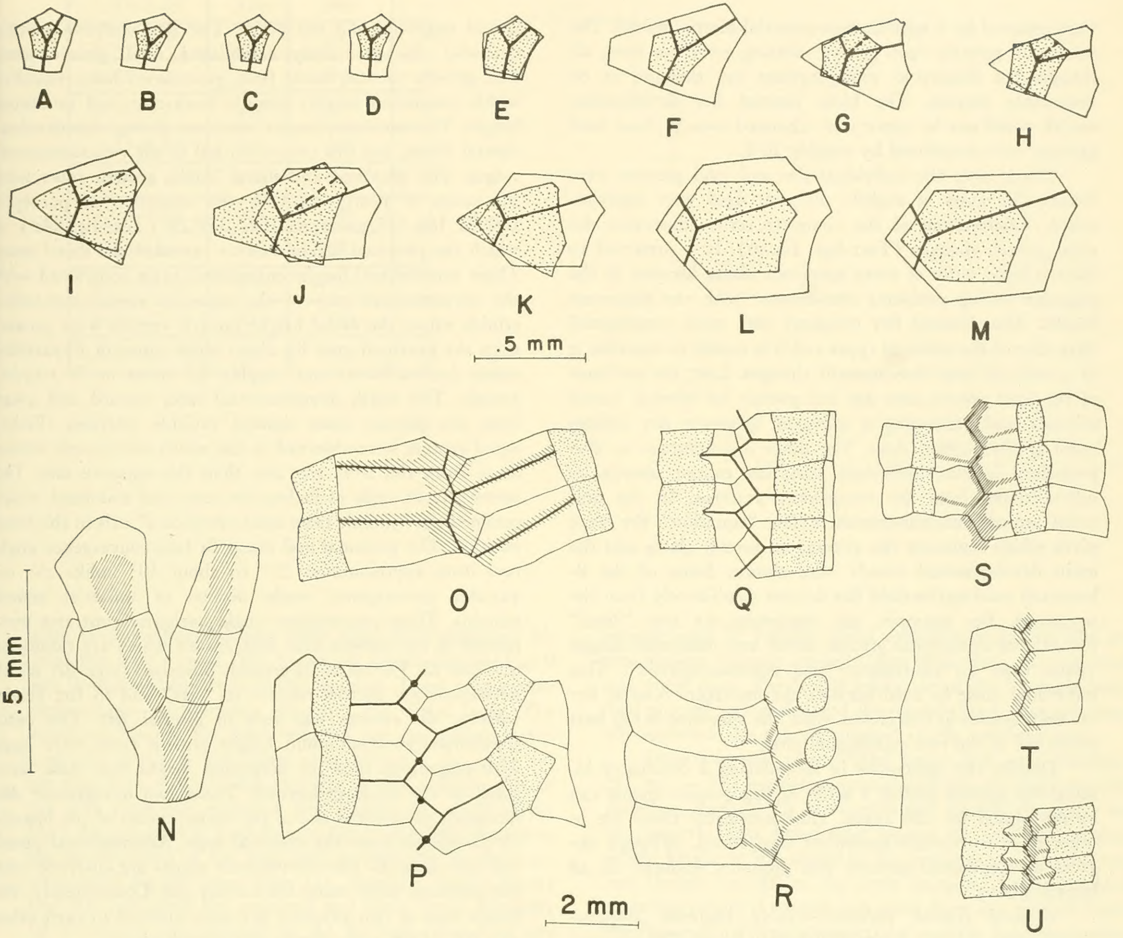

Text-figure 24. — Brr superpositions showing ontogeny in *Macrostylocrinus pristinus*, n. sp. and allied data.

A.-M. — Brr superpositions for *M. pristinus*, n. sp. Food groove axes heavy black. Smaller Br stippled, larger is blank. If resorption and lateral migration of the "pinnule facet food groove" axis was involved, that of the less mature Br is shown in the heavy dashed line. All drawings are mean specimen Brr from the paratypes listed below. A-M to same scale. A. — IGS. 35P-27/ IGS. 35P-28. "Sizes" 1.6 and 1.3 mm, respectively. B. — IGS. 35P-25/ IGS. 35P-28. "Sizes" 1.7 and 1.3 mm, respectively. C. — IGS. 35P-26/ IGS. 35P-28. "Sizes" 1.7 and 1.3 mm, respectively. D. — USNM 164 577/ IGS. 35P-28. "Sizes" 2.4 and 1.3 mm, respectively. E. — USNM 164 577/ IGS. 35P-26. "Sizes" 2.4 and 1.3 mm, respectively. F. — Uniserial Br USNM 164 574/ IGS. 35P-26. "Sizes" 4.4 and 1.7 mm, respectively. G. — Immature biserial Br USNM 164 574/ IGS. 35P-26. "Sizes" same as F. H. — Immature biserial Br USNM 164 574/ USNM 164 577. "Sizes" 4.4 and 2.4 mm, respectively. I. — Immature biserial Br/ Uniserial Br USNM 164 574. "Size" 4.4 mm. J. — USNM 164 572/ Uniserial Br USNM 164 574. "Sizes" 6.6 and 4.4 mm, respectively. K — USNM 164 572/ Immature biserial Br USNM 164 547. "Sizes" as J. L. — USNM 164 569/ USNM 164 572. "Sizes" 8.6 and 6.6 mm, respectively. M. — USNM 164 567/ USNM 164 572. "Sizes" 10.2 and 6.6 mm, respectively.

N. — Paratype, USNM 164 577, sketch of IIBrr 9-11, where weathering exposed the food grooves of uniserial Brr, "size" 2.4 mm. The Brr are tilted so that the food grooves do not appear symmetrical relative to the pinnule facets. Food grooves ruled. Size is measured by the scale.

O.-U. — Sketches showing food groove configurations of various adult biserial armed crinoids. O-Q are Primitive Type 1. R-T are Type 2. U is Type 3. Brr sutures shown by fine lines. Food groove axes by heavy black lines or oblique ruling. In O, the food groove is ruled with the axis black. Pinnule facets stippled. All drawings to same scale. O. — *Encrinites lilliformis*. P. — *Graffhamicrinus stullensis* (Strimple). Q. — Unidentified Knobstone group form. R. — *Eretmocrinus* sp., proximal to paddle part of arm. S. — *Eretmocrinus*? sp., proximal to paddle part of arm. T. — *Dorycrinus unicornis* (Owen and Shumard). U. — *Platycrinites discoideus* (Owen and Shumard).

were restored by a combination uniserial-biserial model. The maximum possible food groove plotting error lies here, although the illustrated configurations are thought to be reasonably correct. The basic biserial Brr development model would not be appreciably changed even if these food grooves were misplotted by roughly 20%.

Third, after the individual Brr and food grooves were drawn, Brr pairs of slightly different ages were superimposed. Examination of the complete series illustrates the total growth changes (Text-figs. 24a-m). It is preferred to show a large series of mean specimen plates because of the equation fitting problems encountered with the minimum height. Also, biserial Brr ontogeny was more complicated than that of the uniserial types and it is easiest to visualize it as a series of small development changes. Last, the positions of the food groove axes are less precise for biserial armed crinoids and presenting a series of specimen Brr utilizes more of the factual data. The main disadvantage to this procedure is that individual variation cannot always be differentiated from the ontogenetic patterns. In the uniserial armed eopatelliocrinids, a few "equation" Brr were given which represent the average or normal plates and the main developmental trends were shown. Some of the illustrated macrostylocrinid Brr deviate significantly from the equations. For example, the important 4.4 mm "sized" transitional crinoid has greater width and maximum height values than an equivalent "size equation-crinoid". This individual must be used because the immature biserial Brr are only known in this crown. Also, the specimen is the best preserved of the two transitional ones.

Despite the difficulties in formulating a conclusive biserial Brr growth model, a series of ontogenetic trends can be postulated for this taxon. How applicable these are to other crinoids remains somewhat conjectural, although the gross developmental pattern was probably uniform for all biserial plates.

General growth patterns — early uniserial stage. — "Size" range, 1.0 to 1.7 mm and slightly larger. The pictured Brr are the IIBrr6 of the 1.3 mm "sized" crinoid which are compared with the standard Brr of slightly older crowns (Text-figs. 24a-d). Due to the preservation, quantitative data are not available for the 1.3 mm "sized" specimen standard Brr. These formed just prior to death of the animal (Text-fig. 21b). Because of the lack of these standard Brr data, the early uniserial ontogenetic stage is not reflected by the equations which only define the later uniserial and subsequent stages.

Throughout the early uniserial stage, all food groove axes comprised constant topographic reference points and lateral migration did not occur. The Brr accretion merely extended the previously established food groove axes. The growth vectors, listed from greatest to least, equalled width, maximum height, pinnule facet size, and minimum height. The minimum height increased during this developmental phase, but this parameter fell in the two subsequent stages. The proximal and distal height growth rates were the same, or nearly so, with the exception of paratype USNM 164 577/paratype IGS. 35P-28 (Text-fig. 24d) in which the proximal height vectors exceeded the distal ones. These symmetrical height ontogenetic rates contrasted with the asymmetrical ones of the uniserial armed eopatelliocrinids where the distal height growth vectors were greater than the proximal ones by about eight times in *Eopatelliocrinus latibrachiatus* and roughly 2.3 times in *E. scyphogracilis*. The width developmental rates toward and away from the pinnule facet showed variable relations. Either equal vectors were observed or the width ontogenetic vector away from the facet was less than the opposite one. The pinnule facet angle of inclination remained stabilized which retained the "pinnule facet axial nerve cord" axis in the same position. The proximal and distal Br face convergence angle rose from approximately 25° to about 40° unlike the invariable convergence angle decline of uniserial armed crinoids. These convergence angle ontogeny contrasts were related to two growth rate differentials which are tabulated in Table 12. The uniserial crinoids possessed large Brr width developmental vectors relative to "size" and to Brr height whereas the reverse was seen in biserial Brr. The early eopatelliocrinoid minimum height growth rates were large with respect to those of maximum height but these were small in the macrostylocrinid. These two ontogenetic differentials constituted one of the major causes of the biserial Br divergence from the uniserial type. Asymmetrical proximal and distal Br face convergence angles are observed with the proximal angle being the smaller one. Consequently, the height axes of two adjacent Brr were inclined to each other at a 20° to 30° angle during this growth phase.

Late uniserial stage. — The "size" varies from 1.3 mm through the transitional animal uniserial Brr, "sizes" 3.4 and 4.4 mm (Text-figs. 24e, f). Essentially, the observed developmental patterns represented continuations of the previously established trends except that: 1. The minimum height began to decline and showed a negative growth rate for the first time. The width ontogenetic vector per 1 mm "size" increment fell from .11 to .050 mm during this phase. Consequently, the convergence angle increased from about 28° to 43°. 2. Near the end of this stage, "size" range 3.0 to 4.4 mm, the proximal and distal Br face convergence

Macrostylocrinus pristinu

"Size" interval mm	Width mm	Maximum height mm	Mi he
1.25-2.25	.110	.085	–
2.25-3.25	.069	.053	–
3.25-4.25	.050	.040	–
4.25-5.25	.040	.031	–
5.25-6.25	.033	.025	
6.25-7.25	.028	.022	
7.25-8.25	.024	.019	
8.25-9.25	.022	.017	
9.25-10.25	.019	.015	
10.25-11.25	.018	.014	
11.25-12.25	.016	.012	

mum height equalled 0 mm when these first immature biserial Brr were formed. The minimum height remained at 0 mm throughout subsequent development. These plates have wedge-shapes with convex proximal and distal faces. The immature biserial Brr inner margins are not differentiated from the proximal and distal ones although the plate inner area is in contact with two Brr on the opposite side of the arm (compare uniserial and biserial Brr of Text-fig. 21g). As indicated in Text-figures 24g-i, especially the latter, the development of the immature biserial Brr involved resorption of the Brr inner sides (*i.e.*, opposite pinnule facet) and the associated Brr proximal and distal faces. Virtually all resorption was confined to the Br half away from the pinnule facet. The resorption did not affect the "brachial food groove" axes. Most of the convergence angle increase was caused by this resorption. The data on the relative proximal and distal height growth and resorption rates are not conclusive. Text-figures 24g and h denote symmetrical or equal rates whereas strong asymmetry is implied by 24i.

Within this developmental phase, the pinnule facet became more steeply inclined. The immature biserial Brr facets of paratype USNM 164 574 dip about 30° more than the uniserial Brr facets of the same crinoid. Consequently, lateral migration and probably major resorption growth rates. In 24k the distal vectors were larger. The inner margins became strongly separated from the proximal and distal ones. The lateral migration of the "pinnule facet food groove" axis ended and the pinnule facet accretion simply extended the axis established in the previous stage.

Mature biserial stage ("size" 6.6 to 12.6 mm; Text-figs. 24l, m). — The resorption ceased and the ontogeny was adjusted so that the Br faces remained parallel or nearly so. The growth rates, listed from largest to smallest, equalled width; height at 90° angles to the proximal and distal faces; and "height" at 90° to the inner margins. Although width accretion occurred toward and away from the pinnule facet, the two vectors were asymmetrical and the former was two to three times the latter. Probably, this resulted in the minimum interference with the "brachial food groove" axes and their axial nerve cords. The proximal and distal height developmental rates were nearly the same although the proximal one might have been slightly larger. The convergence angle between the inner margins either stayed constant or showed a light increase; if so, it ranged from about 105 to 110° over the 6.6 to 10.2 mm "size" interval (Text-fig. 23i). In other biserial armed crinoids, such as *Dimerocrinites planus*, a striking increase can be documented. A convergence angle increase during the macro-

Table 12

Macrostylocrinus pristinus, n. sp.				
"Size" interval mm	Width mm	Maximum height mm	Minimum height mm	Pinnule facet size mm
1.25-2.25	.110	.085	-.025	.050
2.25-3.25	.069	.053	-.025	.018
3.25-4.25	.050	.040	-.065	.014
4.25-5.25	.040	.031	-.065	.011
5.25-6.25	.033	.025	0	.0094
6.25-7.25	.028	.022	0	.0081
7.25-8.25	.024	.019	0	.0071
8.25-9.25	.022	.017	0	.0063
9.25-10.25	.019	.015	0	.0057
10.25-11.25	.018	.014	0	.0052
11.25-12.25	.016	.012	0	.0047

Eopatelliocrinus scyphogracilis, n. gen., n. sp.				
"Size" interval mm	Width mm	Maximum height mm	Minimum height mm	Pinnule facet size mm
1.0-2.0	.095	.040	.043	.033
2.0-3.0	.095	.040	.025	.033
3.0-4.0	.095	.040	.018	.033
4.0-5.0	.095	.040	.014	.033
5.0-6.0	.095	.040	.011	.033
6.0-7.0	.095	.040	.0096	.033
7.0-8.0	.095	.040	.0083	.033
8.0-9.0	.095	.040	.0074	.033
9.0-10.0	.095	.040	.0066	.033

Eopatelliocrinus latibrachiatus, n. gen., n. sp.				
"Size" interval mm	Width mm	Maximum height mm	Minimum height mm	Pinnule facet size mm
1.5-2.0	.13	.043	.0086	.083
2.0-2.5	.13	.033	.0066	.064
2.5-3.0	.13	.025	.0054	.053
3.0-3.5	.13	.023	.0046	.045
3.5-4.0	.13	.020	.0040	.039
4.0-4.5	.13	.018	.0034	.034
4.5-5.0	.13	.016	.0032	.030

Table 12

Table showing the comparative Brr dimension growth rates per 1 mm "size" increment in Girardeau patelliocrinids. All growth rates computed from the equations of "size" versus the listed Brr dimension except for the minimum height in Macrostylocrinus pristinus, n. sp.; these vectors were estimated from the hand-sketched sigmoidal curve in Text-fig. 23c.

pre-
num
rate
mm
ase.
out
3.0
nce

angles were equal and the height axes of successive Brr became parallel (compare Text-figs. 21 a-e with 21 f, g). The exact mechanism is unknown because of the crinoid "size" distribution. The 2.4 mm crown possesses unequal convergence and the Brr height axes are inclined at nearly 30° to one another; the next crinoid in the ontogenetic sequence, "size" 3.0 mm, exhibits equal proximal and distal face convergence. The symmetrical proximal and distal height developmental rates suggest that adjustments of both vectors were involved. 3. During growth, the pinnule facet most likely became inclined more steeply.

Transitional uniserial to immature biserial stage (Text-figs. 24 g-i). — The "size" interval consists of 3.4 to 4.4 mm. If the restorations are correct or even reasonably accurate, the Brr underwent a major metamorphosis during this phase. The minimum height growth rate was more strongly negative and the maximum and minimum heights were less equal than in the previous stage (Table 12). Also, the width growth rate relative to 1 mm "size" increments decreased from .050 to .040 mm. These changes partly accounted for the rapid convergence angle increase. For example, the uniserial Brr of paratype USNM 164 574, "size" 4.4 mm, show only 37° convergence whereas the equivalent figure for the immature biserial Brr of the same individual is 66°. Eventually, the inner margins joined and the minimum height equalled 0 mm when these first immature biserial Brr were formed. The minimum height remained at 0 mm throughout subsequent development. These plates have wedge-shapes with convex proximal and distal faces. The immature biserial Brr inner margins are not differentiated from the proximal and distal ones although the plate inner area is in contact with two Brr on the opposite side of the arm (compare uniserial and biserial Brr of Text-fig. 21g). As indicated in Text-figures 24g-i, especially the latter, the development of the immature biserial Brr involved resorption of the Brr inner sides (*i.e.*, opposite pinnule facet) and the associated Brr proximal and distal faces. Virtually all resorption was confined to the Br half away from the pinnule facet. The resorption did not affect the "brachial food groove" axes. Most of the convergence angle increase was caused by this resorption. The data on the relative proximal and distal height growth and resorption rates are not conclusive. Text-figures 24g and h denote symmetrical or equal rates whereas strong asymmetry is implied by 24i.

Within this developmental phase, the pinnule facet became more steeply inclined. The immature biserial Brr facets of paratype USNM 164 574 dip about 30° more than the uniserial Brr facets of the same crinoid. Consequently, lateral migration and probably major resorption of the "pinnule facet food groove" axis and its axial nerve cord must have occurred during this ontogenetic stage. The amount of lateral migration shown in the drawings might be exaggerated because the immature biserial Br is illustrated with the "pinnule facet food groove axis" emerging from the facet center. This axis is located along the pinnule facet distal area in some biserial armed species. However, the macrostylocrinid Brr width/maximum height suggests a central or near central orientation. This "pinnule facet food groove" axis lateral migration was the second major factor which forced the biserial Br development to diverge from that of the uniserial type. In the latter forms, the pinnule facet inclination change was more gradual and less abrupt. Therefore, the migration of the "pinnule facet food groove" did not take place.

Immature biserial to mature biserial stage (Text-figs. 24j, k; "size" range, 4.4 to 6.6 mm). — The resorption continued along the inner Br side (opposite the pinnule facet) which increased the convergence angle from 66° in the immature biserial Br to about 105° in the mature biserial one. The width development was completely asymmetrical and all growth was directed toward the pinnule facet. Approximately three-fourths of the Br exhibited some height accretion although the relative proximal and distal vectors are uncertain. Text-figure 24j implies approximately equal growth rates. In 24k the distal vectors were larger. The inner margins became strongly separated from the proximal and distal ones. The lateral migration of the "pinnule facet food groove" axis ended and the pinnule facet accretion simply extended the axis established in the previous stage.

Mature biserial stage ("size" 6.6 to 12.6 mm; Text-figs. 24l, m). — The resorption ceased and the ontogeny was adjusted so that the Br faces remained parallel or nearly so. The growth rates, listed from largest to smallest, equalled width; height at 90° angles to the proximal and distal faces; and "height" at 90° to the inner margins. Although width accretion occurred toward and away from the pinnule facet, the two vectors were asymmetrical and the former was two to three times the latter. Probably, this resulted in the minimum interference with the "brachial food groove" axes and their axial nerve cords. The proximal and distal height developmental rates were nearly the same although the proximal one might have been slightly larger. The convergence angle between the inner margins either stayed constant or showed a light increase; if so, it ranged from about 105 to 110° over the 6.6 to 10.2 mm "size" interval (Text-fig. 23i). In other biserial armed crinoids, such as *Dimerocrinites planus*, a striking increase can be documented. A convergence angle increase during the macrostylocrinid ontogeny is suggested by the distal Brr maturity gradient. The pinnule facet size was augmented but the facets remained almost parallel during this growth phase.

The biserial Brr ontogeny began with a uniserial stage which was similar to the early uniserial armed crinoid Brr. The uniserial condition was retained throughout the development of uniserial armed forms because (see Table 12): 1. The Brr width growth vectors were large relative to "size" and Brr maximum height. 2. Large Brr minimum height growth rates were observed with respect to those of maximum height. 3. Due to the above ontogenetic vectors, the convergence angle decreased and the geometry remained uniserial. 4. The pinnule facet inclination angle changed gradually. Because of this and the curvature of the "pinnule facet food groove" axis, lateral migration of this axis did not occur; the accretion simply lengthened the previously established "pinnule facet food groove" axis.

On the other hand, the biserial Brr underwent a radically different pattern because of the following (see Table 12): 1. The Br width growth vectors were small compared to those of "size" and maximum height. 2. The initial positive minimum height developmental rate was low relative to those of "size", Brr width and maximum height. Following this, a negative vector was attained, whereas in the latest ontogenetic phases, the minimum height was stabilized at 0 mm. 3. Due to these growth rates, the convergence angle increased throughout development. This eventually resulted in resorption of the Brr inner side (*i.e.*, opposite the pinnule facet) and the associated proximal and distal margins when the immature and early mature biserial Brr formed. This resorption was not observed in uniserial Brr development. Despite the large scale resorption, the "brachial food groove" axes were not affected and these were simply extended during ontogeny. 4. Because of the striking change in the pinnule facet inclination during the early biserial stage in conjunction with the straight "pinnule facet food groove" axis, this food groove axis was subject to lateral migration and probably major resorption as the Brr became biserial. This migration is unknown in uniserial Brr.

The Brr maturity gradients are poorly known. Those of the adult animals are best seen in the holotype ("size" 7.3 mm, Text-fig. 21h) and in one of the paratypes ("size" 10.2 mm, Text-fig. 21j). The proximal IIBrr are composed of "early" uniserial plates which are high relative to width and the minimum heights are large with respect to the maximum heights. Upward, these grade into wedge-shaped plates (IIBrr3 to 5 in the paratype, variable in the holotype). One to three immature biserial Brr follow the cuneiform Brr in each arm. These are succeeded by mature biserial plates. The distal Brr maturity gradient is not visible in the paratype but it can be examined in the holotype. Distally, the Brr became more juvenile and "less biserial". This is evidenced in two ways. The convergence angle between the Brr inner margins declines. The inner margin width/total width increases. The immature biserial Brr ratio is almost 1.0, but the mature biserial plate figure ranges between .37 and .42. The adult crinoid arm tips are not preserved but the observed parts of the maturity gradients suggest that the Brr are uniserial.

The transitional specimen maturity gradients are shown by the 3.4 and 4.4 mm "sized" paratypes (Text-figs. 21f, g).

The proximal three to six IIBrr are "early" uniserial types as in the older individuals. Next, a series of strongly wedge-shaped uniserial Brr is present. In the 4.4 mm "sized" paratype, some immature biserial plates occur in the central arm region. The distal-most 10 or so IIBrr are uniserial and have large minimum heights with respect to the maximum heights. Uniserial terminal and near terminal Brr are observed in the smaller transitional crown.

The general pattern consists of two maturity gradients: 1. A proximal one which culminates with the most mature plates in the proximal-central arm region. 2. The distal gradient with the least mature Brr located in the distal arm tips. The same two gradients characterize all uniserial crinoids.

After the first appearance of the immature biserial Brr, the proximal biserial plate "marched" down the arm. In the largest transitional crown, "size" 4.4 mm, the first biserial plate ranges from IIBr12 to IIBr21 depending on the arm. The mature crinoids, 6.6 to 12.6 mm "size" interval, possess IIBrr4 to 7 as the proximal biserial Br. The adult individuals exhibit wide variation and no appreciable change occurred during this growth phase. The entire change took place during the transitional Brr-mature biserial Brr interval which corresponds to the Brr metamorphosis.

The terminal Brr are only known in the young uniserial crinoids and the smaller transitional animal (Text-figs. 21a, b, f). These cannot be examined in the larger biserial armed crowns. The terminal Brr have angular distal margins, and nearly equal maximum and minimum heights. The pinnules and their facets are lacking. One or rarely two terminal plates may be counted in a single arm. All observed macrostylocrinid terminal Brr are equivalent to the eopatelliocrinid Type-2 plates. The eopatelliocrinid terminal Brr widths increased in the larger animals. As tabulated below, the macrostylocrinid terminal Brr widths remained constant regardless of "size". The heights are variable and a definite trend is not obvious.

"Size"	Terminal Br width	Terminal Br height
1.0 mm	.10 mm	.08 mm
1.3 mm	.10 mm	.14 mm
3.4 mm	.11 mm	.12 mm

The earliest pinnulate Brr are located below the terminal Brr (Text-figs. 21a, b, f). These range slightly larger than the terminal Brr and the maximum and minimum heights are differentiated. Small sub-horizontal pinnule facets are present which support immature pinnules composed of one or two joints. As seen below, the larger widths are associated with the older individuals whereas the heights seem constant irrespective of "size".

"Size"	Width	Maximum height	Minimum height	Pinnule facet size
1.0 mm	.12 mm	.13 mm	.13 mm	.07 mm
1.3 mm	.16 mm	.15 mm	.14 mm	.06 mm
3.4 mm	.20 mm	.14 mm	.14 mm	.10 mm

The initial intercepts, correlation coefficients and percentage standard deviations are difficult to interpret because of the curve-fitting problems encountered with the minimum height. Reliable data are not available for this variable. Inasmuch as the average height equals (maximum height plus minimum height)/2, these figures are also suspect.

Judging by the youngest crinoid morphology, (Text-figs. 21a, b) the standard Brr began to appear within the 1.0 and 1.3 mm "size" interval. This should be reflected by the y equals 0 values from the equations of "size" versus the various Brr dimensions. Like the eopatelliocrinids, the y equals 0 figures are too small; these vary from .15 to .60 mm "sizes" (the equations involving average and minimum height were omitted). The initial Brr dimension growth rates relative to "size" are not shown by the regression lines which only treat the "size" interval after the standard Brr developed. The writer postulates initially rapid Brr dimension developmental vectors to explain the anomalies.

The correlation coefficient magnitudes range from .59 to .97 with most being above .85 (partially listed in Text-fig. 23 legend). All correlations are positive except where the minimum height comprises one of the variables. The minimum height growth rates were positive, negative or nil, depending on the Brr age. All minimum height correlation coefficient signs are negative. The minimum height correlations were derived from the $\log y = \log a + bx$ type equations. However, these regression lines yield poor fits to the data and the true relations are sigmoidal. Presumably, if measures of "correlation" were available from the sigmoidal equations, these would be higher. The significance levels vary from about .980 to well above .999 (two sided test); most exceed .999. The lowest correlations are seen when the average height is one of the variables. Larger values occur if the minimum height is involved. The highest correlations are associated with the width or maximum height.

The macrostylocrinid correlation coefficient distribution pattern contrasts with that of the uniserial armed taxa. In the eopatelliocrinids, small positive minimum height developmental vectors are observed in conjunction with low positive correlations and low significance levels. The correlations range from .24 to .82 and the significance level interval consists of less than .900 to above .999. Conversely, the macrostylocrinid minimum height growth rates were positive, negative, or zero. The correlation coefficients vary from –.79 to –.92 and the significance levels are almost equal to or exceed .999. Such denotes that the minimum height was more closely integrated and coordinated with the growth of "size" and the other Br dimensions in the biserial armed macrostylocrinid than in the uniserial armed eopatelliocrinids. This high degree of minimum height regulation was required by the complex accretion-resorption mode of development. Otherwise, gaps would have formed between the adjacent Brr during the transitional and perhaps the later ontogenetic stages. If such gaps appeared, the proximal Brr would not have been able to support the higher part of the arm.

The eopatelliocrinid pinnule facet size shows larger correlation coefficients with the Br width than with the maximum height. The reverse characterizes the macrostylocrinid. The difference between the correlations is probably partially controlled by the pinnule facet inclination. That of the macrostylocrinid lies more nearly parallel to the maximum height axis, especially during the transitional and biserial ontogenetic stages.

The smallest percentage standard deviations are observed when the maximum or average height constitutes one of the variables whereas the largest occur when the minimum height is involved; the latter represents poor curve fitting, not the true distribution. The typical order of reliable standard deviations, listed from minimum to maximum, equals: maximum height, average height, pinnule facet size, and width. The same general sequence is seen in the eopatelliocrinids. As in the uniserial armed forms, the standard deviations suggest that the maximum height dictated the growth of the other external Brr parameters.

Food gathering system growth. — (Text-fig. 25). Complete data sets are available from 11 crinoids. Eight crowns are referable to the "young assemblage", "size" ranging from 1.0 to 2.4 mm, two are transitional crinoids ("sizes" 3.4 and 4.4 mm) and only one is an adult, "size" 7.0 mm. Partial measurements have been secured from five other individuals, most of which belong to the "adult assemblage".

The "size" 1.0 mm macrostylocrinid is slightly smaller than the youngest eopatelliocrinid and shows a less well developed food gathering system. When a 1.2 to 1.3 mm "size" was attained, the *Macrostylocrinus pristinus* and *Eopatelliocrinus scyphogracilis* food gathering systems were almost identical. During later ontogeny, differential growth caused the food gathering systems of the two species to diverge. The principal factor involved in the food gathering system differences consisted of the IIBrr addition rates relative to "size".

The relationship between "size" and food gathering system length was curvilinear in which the ambulacral tract length growth rate per 1 mm "size" increments increased from 30 to 540 cm during development (Text-fig. 25a). The mean ontogenetic vector equaled 240 cm. The youngest crinoids have "sizes" of 1.0 and 1.3 mm which correspond to 1.8 and 5.6 cm food gathering systems. The largest macrostylocrinid is a 7.0 mm "size" crown with an 890 cm ambulacral tract system. The *E. scyphogracilis* developmental rate was constant and smaller at 71 cm. Consequently, the adult eopatelliocrinids possess much shorter food gathering systems; the largest crinoids are 6.2 and 7.7 mm in "size" and exhibit 420 and 480 cm long ambulacral tracts.

The usual exponential pattern was observed in calyx volume versus "size" in which the "size" growth vector per .01 cc volume augmentation declined from 1.1 mm in the smallest crinoids to .07 mm in the oldest (Text-fig. 25b). The mean developmental rate consisted of .21 mm; almost identical figures characterized the eopatelliocrinid where the mean constituted .23 mm. The youngest macrostylocrinids have "sizes" of 1.0 and 1.3 mm and .0003 and .0009 cc calyx volumes, respectively. The largest "sizes" comprise 9.2 and 10.2 mm, both with .35 cc calyx volumes. The largest eopatelliocrinid is a "size" 9.6 mm calyx with a .32 cc volume.

The development of calyx volume and food gathering system length was logarithmic in which the food gathering system length growth rate per .01 cc volume increase dropped throughout ontogeny (Text-fig. 25c). The predicted vector is anomalously low because the best equation yields a poor fit to the largest individual, and the equation value is almost 300 cm below the actual 890 cm figure. The true growth rate probably decreased from about 60 cm food gathering system length per .01 cc volume increase in the youngest animals to approximately 40 cm in the largest crinoids; these were estimated from two equations, one being fitted to the seven youngest crowns and the other to the three largest individuals. The equivalent eopatelliocrinid developmental rate fell from 40 to 23 cm. The smallest macrostylocrinids show calyx volumes of .0003 and .0009 cc which correspond to ambulacral tract length of 1.8 and 5.6 cm, respectively. The largest consists of a 7.0 mm "sized" crown with .24 cc volume and an 890 cm food gathering system length. The mature eopatelliocrinids possess .15 and .22 cc volumes and 420 and 480 cm food gathering systems.

The food gathering efficiencies of the two smallest crinoids equal 6000 and 6200. During ontogeny, the food gathering efficiency declined exponentially to 3700 in the largest crinoid for which data are available ("size" 7.0 mm). The initial drop was most rapid. An 80% decrease occurred over the .0003 to .030 cc volume interval; the remaining 20% was distributed over the .030 to .24 cc range. The young eopatelliocrinid and macrostylocrinid food gathering efficiencies are comparable; on the other hand, large eopatelliocrinids have lower values (1900 versus 3700 in the oldest macrostylocrinid).

The "initial intercept" (*i.e.*, calyx volume .00001 cc) corresponds to a .16 cm food gathering system length. Substituting the "initial volume" in the calyx volume versus "size" equation yields a .026 mm "size". As indicated later, the .026 mm figure is roughly an order of magnitude below the approximate "size" at which the food gathering system first developed.

The growth of IIBrr number per arm and "size" followed a curvilinear pattern in which the IIBrr addition rate per 1 mm "size" increment ranged from 12 Brr in the youngest crinoids to 23 in the largest (Text-fig. 25d). The mean consisted of 18 Brr. The eopatelliocrinid exhibited similar ontogeny with a much smaller developmental vector which varied from 8.1 to 10 and averaged 9.3. The youngest macrostylocrinids are 1.0 and 1.3 mm in "size"; the equivalent numbers of IIBrr equal four or five and eight or nine per arm, listed in the same order. The largest macrostylocrinid, "size" 7.0 mm, bears 91 IIBrr per arm, whereas 57 or 59 IIBrr are found in the mature eopatelliocrinids ("sizes" 6.2 and 7.7 mm).

A curvilinear regression line is seen in IIBrr per arm versus the half-ray food gathering system length in which the ambulacral tract length augmentation rate per additional IIBr increased from 1.2 to 18 mm with a 9.4 mm mean (Text-fig. 25e). Comparable figures characterized *E. scyphogracilis* where the range was .9 to 45 mm with a 12 mm average. The explanation lies in the growth differentials between the two taxa. The macrostylocrinid food

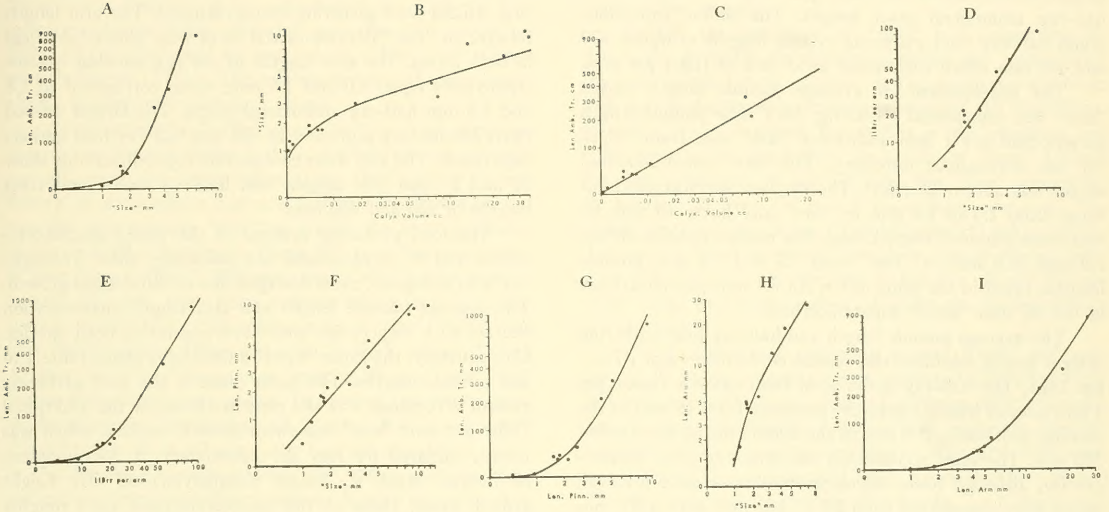

Text-figure 25. — Graphs showing food gathering system growth in *Macrostylocrinus pristinus*, n. sp. Food gathering system length is indicated by Len. Amb. Tr. When listed in cm, the total value is denoted. If in mm, the half-ray figure is referred to. "a" designates the "initial intercept" or "pseudointercept" where the x axis is logarithmic.

Equation data:

A — $\text{Log}y = .646 + 2.98\log x$. $r = .958$.
$\sigma y\% = 23.4$. $N = 11$. "a" $= .00469$ $(x = .1)$.
B — $\text{Log}y = 1.02 + .322\log x$. $r = .936$.
$N = 16$. "a" $= .0261$ $(x = .00001)$.
C — $\text{Log}y = 3.30 + .821\log x$. $r = .952$.
$\sigma y\% = 17.0$. $N = 11$. "a" $= .156$ $(x = .00001)$
D — $\text{Log}y = .823 + 1.47\log x$. $r = .952$.
$\sigma y\% = 11.3$. $N = 11$. "a" $= .226$ $(x = .1)$.
E — $\text{Log}y = -.986 + 2.00\log x$. $r = .994$.
$\sigma y\% = 9.1$. $N = 11$. "a" $= .0966$ $(x = .1)$.
F — $\text{Log}y = -.0834 + 1.13\log x$. $r = .954$.
$N = 15$. "a" $= .0613$ $(x = .1)$.
G — $\text{Log}y = .985 + 2.04\log x$. $r = .988$.
$\sigma y\% = 17.2$. $N = 11$. "a" $= .000811$ $(x = .01)$.
H — $y = -3.84 + 4.61x$. $r = .990$.
$\sigma y\% = 22.6$. $N = 11$.
I — $\text{Log}y = .356 + 1.80\log x$. $r = .994$.
$\sigma y\% = 11.9$. $N = 11$. "a" $= .0358$ $(x = .1)$.

gathering system length and IIBrr addition developmental vectors per unit "size" increase were roughly twice those of the eopatelliocrinid; consequently, similar half-ray ambulacral tract length growth rates per additional IIBrr occurred in both forms. The smallest macrostylocrinids show four or five and eight or nine IIBrr per arm and half-ray food gathering system lengths of 1.8 and 5.6 mm. The largest crinoid shows 91 IIBrr per arm and an 890 mm half-ray ambulacral tract length. The oldest eopatelliocrinid half-ray food gathering system lengths comprise 420 and 480 mm which correspond to 57 and 59 IIBrr per arm.

The development of average pinnule length versus "size" was exponential (Text-fig. 25f). The pinnule length growth rate per 1 mm additional "size" rose from .98 to 1.3 mm throughout ontogeny. The same eopatelliocrinid vector was almost identical. The smallest macrostylocrinids range from 1.0 to 1.3 mm in "size" and have .40 and .95 mm mean pinnules, respectively. The mature individuals are 7.0 and 12.6 mm in "size" with 9.5 and 9.8 mm pinnule lengths, listed in the same order. An 8.1 mm pinnule is seen in the 6.7 mm "sized" eopatelliocrinid.

The average pinnule length and half-ray food gathering system length exhibited the typical curvilinear form (Text-fig. 25g). The half-ray ambulacral tract growth vector per 1 mm pinnule length increment increased from 18 mm in the smallest crinoids to 200 mm in the oldest; the mean equalled 100 mm. The same relationship was observed in *E. scyphogracilis,* although lower developmental rates were involved which were augmented from 28 to 110 mm with a 75 mm mean. This was caused by the shorter food gathering systems of the adult crinoids. The pinnule length growth vectors relative to "size" were nearly the same in both species. The average pinnule lengths of the two smallest macrostylocrinids comprise .40 and .95 mm which are equivalent to 1.8 and 5.6 mm half-ray ambulacral tract lengths. The oldest animal bears a 9.5 mm pinnule and a 890 mm half-ray food gathering system. The largest eopatelliocrinids possess 6.7 and 8.1 mm average pinnules and 420 and 480 mm long half-ray ambulacral tracts.

The relation between "size" and arm length was linear in which the arm length growth rate constituted 4.6 mm per 1 mm "size" increment (Text-fig. 25h). The same *E. scyphogracilis* vector rose from 3.0 to 5.2 mm, but the 4.2 mm mean is similar to that of the macrostylocrinid. The smallest crinoids have arm lengths of 1.0 and 1.6 mm and "sizes" of 1.0 and 1.3 mm, respectively. The largest crown "size" consists of 7.0 mm with a 28 mm arm length. The oldest eopatelliocrinids range from 6.2 to 7.7 mm in "size" and possess 19 and 25 mm arms.

The growth of arm length and half-ray food gathering system length followed an exponential pattern in which the half-ray ambulacral tract growth vector per 1 mm additional arm length was augmented from 26 to 170 mm with a 100 mm average (Text-fig. 25i). The same relation was observed in the eopatelliocrinid although a smaller growth rate was found which varied from 7.5 to 36 mm with a 20 mm average. These contrasts reflect the differences in the mature crinoid food gathering system lengths. The arm length relative to "size" developmental rates were almost identical in both forms. The arm lengths of the two smallest macrostylocrinids equal 1.0 and 1.6 mm; these correspond to 1.8 and 5.6 mm half-ray ambulacral tracts. The largest animal bears 28 mm long arms and an 892 mm half-ray food gathering system. The two most comparable eopatelliocrinids show 19 and 25 mm arm lengths and half-ray ambulacral tract lengths of 420 and 480 mm.

The food gathering systems of the young macrostylocrinids and *E. scyphogracilis* are essentially alike. Throughout later ontogeny, these diverged due to differential growth. The average pinnule length and arm length augmentation vectors with respect to "size" were similar in both species. Consequently, the same "sized" adults have comparable arm and pinnule lengths. The main cause of the food gathering system divergence was the contrast between the additional IIBrr per unit "size" increment growth vectors, which was mainly dictated by two Brr parameters: 1. Development of biserial arms. 2. Lesser macrostylocrinid Brr height growth rates; those of the macrostylocrinid were roughly 50% of the eopatelliocrinid values. Both allowed more Brr and pinnules per unit arm length in the macrostylocrinid. Consequently, the adult macrostylocrinids exhibit food gathering systems which are about twice as long as those of the equivalent aged eopatelliocrinids.

The food gathering system correlation coefficients (legend, Text-fig. 25) range high. These vary from .94 to .99; all have significance levels well in excess of .999. The *E. scyphogracilis* correlation coefficients are roughly the same (.90 to .99). Thus the food gathering system ontogeny was subject to a high degree of integration and coordination in both species.

In the eopatelliocrinid the free ambulacral tract length is better correlated with calyx volume than with "size", .98 versus .95. Almost equal correlations are observed in the macrostylocrinid (.95 and .96). The macrostylocrinid correlations between the half-ray food gathering system length and its three components are the same, with all consisting of .99. A correlation coefficient gradient is seen in the eopatelliocrinid: with arm length .99, pinnule length .98, and number of IIBrr .96. The significance of this remains unclear, although the contrasts in number of IIBrr versus half-ray food gathering system length are probably related to the previously discussed growth rate differentials between the two taxa.

The percentage standard deviations (legend, Text-fig. 25) indicate that the food gathering system length is less variable with respect to calyx volume, 17%, than with "size", 23%. Relative to its components, the half-ray food gathering system shows minimum variation with number of IIBrr (9.1%), followed by arm length (12%) and average pinnule length (17%). The minimum eopatelliocrinid variability is associated with arm length.

As expected the "initial intercepts" for food gathering system components versus half-ray ambulacral tract lengths are all small and these range from .00081 to .097 mm. Several of the y equals 0 or near 0 figures were used to outline the approximate "size" at which the food gathering system initially developed. These fall into two categories: 1. Low figures. "Size", .020 mm, from "size" versus pinnule length; .026 mm, from calyx volume versus food gathering system length and calyx volume versus "size"; .0574 mm, from "size" versus IIBrr per arm. 2. High values. "Size", .83 mm, from "size" versus arm length; .28 mm, from "size" versus ambulacral tract length. In view of the previous remarks about the "theoretical BB + 00 + RR microcrinoid" ("size" range .23 to .63 mm), the first set of values is clearly "under-sized"; consequently, the IIBrr and the food gathering system are believed to have formed sometime during the .28 to .83 mm "size" interval. The equivalent eopatelliocrinid figures are from .29 to about .77 mm.

Supporting structures ontogeny. — (Text-fig. 26). The "size" versus proximal columnal diameter followed a curvilinear pattern (Text-fig. 26a). The stem width per 1 mm "size" increment growth vector decreased from .44 to .086 mm throughout development (mean .19 mm). The maximum and minimum "sizes" comprise 10.2 and 1.3 mm, and these correspond to equation column diameters of 1.8 and .20 mm, respectively. The "size"/proximal columnal diameter ranges from 6.5 in the smallest to 5.7 in the largest animal.

The development of proximal columnal area relative to calyx volume also exhibited an exponential relationship in which the columnal area growth rate per .01 cc volume augmentation decreased from .14 to .046 mm; the average vector consisted of .067 mm (Text-fig. 26b). The youngest crinoid has a .0009 cc calyx volume and a predicted columnal area of .046 mm^2; the equivalent figures for the largest animal are .35 cc and 2.4 mm^2. The columnal area/calyx volume equals 51 in the smallest and 6.9 in the oldest individual.

The supporting Brr varied with "size" and age due to the formation of FBrr. Prior to IIBr2 fixation, the arms are borne on IIBr1. During the 3.4 to 4.4 mm "size" interval, the IIBr2 was incorporated into the calyx, and thereafter, supported the growing arms. The IIBr3 forms the arm base in the older crinoids.

During the ontogeny of "size" and supporting Br width, the Br width developmental vector per 1 mm "size" increase changed from .22 mm in the smallest animals to .049 mm in the largest; the mean comprised .10 mm (Text-fig. 26c). The calculated Brr widths in the youngest and oldest crowns for which data are available, "sizes" 1.0 and 7.0 mm, constitute .15 and .76 mm. The "size"/supporting Br width rose from 6.7 to 9.2 throughout ontogeny. The young specimen supporting Br width equals 0 value roughly denotes the "size" at which this plate formed during ontogeny. This "size", .62 mm, lies within the .28 to .83 mm "size" range previously computed under the food gathering system growth.

The half-ray food gathering system length and supporting Br width ontogeny was exponential (Text-fig. 26d). The initial growth vector equalled .028 mm width increase per 10 mm of additional half-ray food gathering system; the final and mean values consisted of .0024 and .0072 mm, respectively. The smallest and largest animals have .16 and .75 mm equation supporting Br widths, and these correspond to half-ray food gathering system lengths of 1.8 and 890 mm. The half-ray food gathering system length/supporting Br width comprises 11 in the youngest and 1200 in the oldest crown.

The development of supporting Br area and half-ray ambulacral tract length followed a curvilinear regression line in which the supporting Br area growth rate per 10 mm of food gathering system increment declined from .014 to .0033 mm^2 during ontogeny; the average vector was .0058 mm^2 (Text-fig. 26e). The smallest individual bears a 1.8 mm long half-ray ambulacral tract and a .019 mm^2 predicted supporting Br area; the same values for the largest specimen are 890 mm and .51 mm^2, respectively. The half-ray food gathering system length/supporting Br area varied from 95 to 1700 during progressive development.

The correlation coefficients, involving the various combinations of "size", calyx volume, proximal columnal area, half-ray food gathering system length and supporting Br area, range from .97 to .92; all significance levels exceed

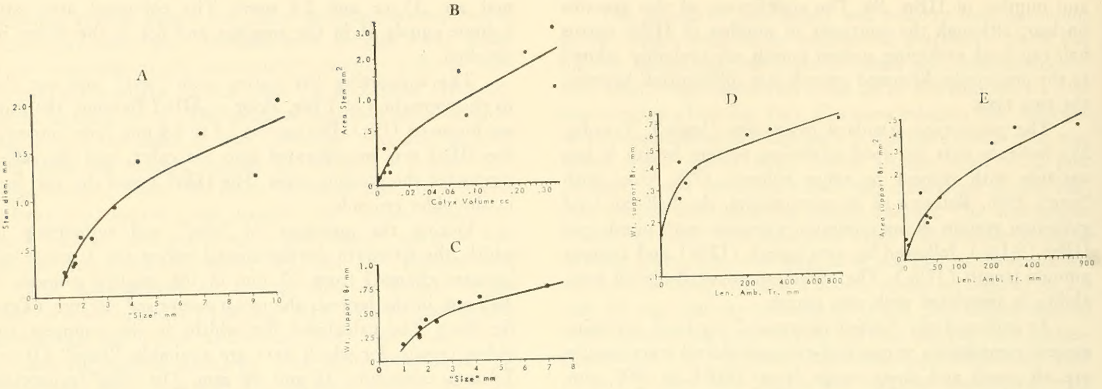

Text-figure 26. — Graphs showing supporting structure growth in *Macrostylocrinus pristinus*, n. sp. Stem area and diameter refer to the proximal columnal. Supporting Brr width and area are those of the distal FBr. "*a*" gives the "initial intercept" or "pseudo-intercept".

Equation data:

A — $y = .0345 + 1.74\log x$. $r = .949$.
$\sigma y\% = 17.2$. N = 12. "a" = -1.71 ($x = .1$).

B — $\log y = .672 + .660\log x$. $r = .950$.
N = 12. "a" = $.0107$ ($x = .0001$).

C — $y = .150 + .727\log x$. $r = .967$.
$\sigma y\% = 17.7$. N = 10. "a" = $-.577$ ($x = .1$).

D — $\log y = -.857 + .249\log x$. $r = .924$.
N = 10. "a" = $.0784$ ($x = .1$).

E — $\log y = -.0187 + .534\log x$. $r = .948$.
N = 9. "a" = $.00397$ ($x = .1$).

.999. A highly integrated and coordinated pattern of development is indicated. Both supporting relationships are characterized by almost equal correlations.

Ornamentation ontogeny. — (Plates 62,63). The development of the *Macrostylocrinus pristinus* plate sculpture closely paralleled that of *Eopatelliocrinus scyphogracilis*. The median-ray ridges were not fully formed in the youngest animals, "size" 1.0 to 1.3 mm, although the IBrr are strongly convex with flat sides. These ridges cover about 50% of the plate width. The RR are arched, especially the distal parts, but the RR ridges are not defined. Smooth BB are observed.

The smallest crinoid with well-formed median-ray ridges is 1.7 mm in "size." Sharp ridges occur on the IBrr, and these can be followed onto the RR distal edges where they are represented by bulges which occupy roughly 30% of the plate width. The median-ray ridges cannot be detected below this point. Apparently, the RR ridges grew at various "sizes" because these are absent in two other 1.7 mm "sized" individuals.

Complete median-ray ridges were initiated in the "size" 2.4 mm crown. Distinct IBrr ridges extend over approximately 60% of the plate widths. These continue on the distal RR margins in the form of convex areas on roughly half of the plates. Ill-defined median-ray ridges are found on the BB and the lower parts of the RR. During later ontogeny, the ridges became sharper and relatively more narrow. In the two transitional crinoids, "sizes" 3.4 and 4.4 mm, the IBrr and the distal RR ridges cover 40% and 30 to 50% of the plate widths, respectively. The same figures for the 9.2 and 10.2 "sized" crowns are 30% and 33%, listed in the same order. In addition, the BB and the proximal RR ridges are less obvious in the two transitional animals.

The lateral RR ridges first developed in the 2.4 mm "sized" specimen where they are seen as convex areas on the D ray R and probably the C ray R. A full set of ridges is exhibited by the transitional crinoids, and strong lateral RR ridges characterize the adults.

The primanal of the 1.3 mm "sized" calyx is gently convex whereas the CD interray iBrr are flat. A marked anal interray ridge appeared on the distal half of the primanal and the first anal series plate in the "size" 2.4 mm animal. This occupies about 40% of the primanal width. Possibly, vague lateral-oblique ridges, which cross from the primanal to the C ray and D ray RR, occur. Throughout subsequent growth, the anal interray and the associated lateral-oblique ridges became higher, relatively sharper and more strongly differentiated from the other parts of the plates. One transitional crinoid, paratype USNM 164 574, "size" 4.4 mm, seems to lack all traces of the anal interray ridges.

The earliest BB flange is observed in the 1.7 mm "sized" crowns as a slight bulge along the proximal circlet margin. The adults show a larger and more prominent flange which is easier to distinguish from the higher portions of the BB.

The iBrr stellate ridges initially formed at "sizes" ranging from 3.4 to 4.4 mm. Prior to this stage the iBrr are flat and featureless. The mature animals, "sizes" 6.5 to 12.6 mm, have sharper ridges which are characterized by great variability in number and pattern. Some calyces bear single stellate ridges; these and the median-ray ridges may or may not be striate (*e.g.*, paratype, USNM 164 567). Multiple stellate ridges are present on the iBrr and IBrr of paratype USNM 164 566, but the median-ray ridges are single. The iBrr stellate ornamentation is replaced by single or multiple nodes in paratype USNM 164 568. The holotype exhibits no evidence of stellate ridges on the iBrr.

All three Girardeau patelliocrinids followed all or part of the same ornamentation development sequence. The median-ray ridges and possibly the anal interray ridges formed first. The median-ray ridges were initiated on the IBrr, and thereafter, these were extended proximally. The second ornamentation components comprised the lateral RR and probably the CD interray lateral-oblique ridges. Lastly, the iBrr stellate ridges and nodes grew in *Macrostylocrinus pristinus* and *Eopatelliocrinus scyphogracilis.* The stellate ridge phase was absent in *Eopatelliocrinus latibrachiatus.*

Variation. — The IBrr shapes were observed in 14 to 18 rays. The IBrr1 include 12 hexagonal types, four rectangular and two five-sided plates. The mean IBr1 value equals 5.4 sides with a 12% standard deviation. Fourteen IAxx were tabulated with the following distribution: one with eight sides, seven septagonal plates, three six-sided plates, and three pentagonal types. The average IAx possesses 6.4 sides with a percentage standard deviation of 14%.

The macrostylocrinid IBr1 and IAx shapes are not closely related. The hexagonal IBrr1 may occur with pentagonal, six-sided, or septagonal IAxx. Five-sided IBrr1 are associated with six or eight-sided IAxx whereas septagonal IAxx are observed with rectangular IBrr1. The correlation coefficient between number of IBrr1 and IAxx sides equals only –.37 of which the significance level is much less than .900. Thus, the IAx and IBr1 shapes were not well integrated and coordinated. This differs markedly from the situation seen in the two eopatelliocrinids where the shapes of the two plates are strongly correlated.

Consequent to this, highly variable iBrr1 and iBrr2 geometry is observed in the macrostylocrinid. For example, when a rectangular IBr1 occurs with a septagonal IAx, the adjacent iBr1 is large and reaches to the mid-level of IAx. In the case of hexagonal IBr1 and septagonal IAx, a small iBr1 is observed which terminates at the IBr1 level; the iBrr2 are also small and reach only to the IAx level. The various combinations are summarized below:

IBr1 Shape	IAx Shape	Distal Level of iBr1	Distal Level of iBrr2
Rectangular	Septagonal	Mid-IAx	Mid-IIBr1
Five sides	Six sides	Mid-IBr1 or Mid-IAx	Mid-IAx or Mid-IIBr1
Five sides	Eight sides	Mid-IBr1 or Mid-IAx	Mid-IAx
Hexagonal	Pentagonal	Mid-IBr1	Mid-IIBr1
Hexagonal	Six sides	Mid-IBr1	Mid-IAx or Mid-IIBr1
Hexagonal	Septagonal	Mid-IBr1	Mid-IAx

Comparing these combinations with those previously presented for the eopatelliocrinids discloses about twice as many permutations in this species which is a direct result of the low correlation between the macrostylocrinid IBr1 and IAx shapes. In general, patelliocrinids evolved toward more highly integrated IBr1 and IAx shapes (see later discussion of phylogeny), and the Girardeau macrostylocrinid is considered primitive in this respect.

Variation in the IBr1-IAx-iBrr shapes within a single crinoid is poorly known because usually only one interray can be determined in most individuals. In all crinoids where two or more interrays are tabulated, two or more structural types are observed (Text-figs. 21e, f, g, h and i).

The IBrr formula variation has been studied at the iBrr2 level in seven or eight interrays. Seven interrays show two iBrr2. In one crinoid (Text-fig. 21g), a plate in the iBr1 position is followed by three plates in the next range of one interray. It is not known if this is the CD or a lateral interray; the lack of an anal-interray ridge suggests the latter. If so, the mean number of iBrr2 equals 2.1 with a percentage standard deviation of 16%; comparable variation characterizes the eopatelliocrinids.

Comparison of the iBrr formula variability and IBr1-

IAx-iBr1 shape variation in the three Girardeau patelliocrinids denotes that the two are separate and uncorrelated characters.

The Br shape variation is difficult to evaluate in this form because of curve fitting problems where minimum height constitutes one of the variables. All mature crinoids possess true biserial Brr. Total variation cannot be measured at present. The percentage standard deviations of the various Br parameters versus each other range from 7.2 to 19% (equations involving minimum height are omitted); these indicate variation which is intermediate between that of the two eopatelliocrinids.

Calyx width with respect to "size" shows moderate scatter; the percentage standard deviation consists of 13%. However, the calyx outline as considered diagnostic of the species is conservative. As previously indicated, the iBrr stellate ornamentation varies greatly in mature crinoids; however, the median-ray and lateral RR ridge patterns are invariant in adults. The "size" versus FBrr in lateral and inter-half-rays variability of this species is almost identical to that of *Eopatelliocrinus scyphogracilis;* these percentage standard deviations respectively consist of 8.0% and 2.7% in the macrostylocrinid and 7.7% and 3.8% in the eopatelliocrinid.

The following are invariant: 1. Number of plates (three) following primanal. This can be ascertained in six crinoids. 2. Number and orientation of BB (full data from four crinoids; partial measurements from 10 additional specimens). 3. Calyx outline in mature crowns. 4. Basic adult ornamentation type consisting of well-developed median-ray and lateral RR ridges with or without iBrr sculpture. 5. Number of arms per ray. 6. Presence of mature biserial Brr in adult specimens.

Comparison.—Young crinoids referred to all three Girardeau patelliocrinids are similar and difficult to distinguish. Throughout ontogeny, the three forms diverged, and adult animals are easily separated. Consequently, the writer first segregated and categorized the mature individuals, after which progressively younger specimens were considered.

The diagnostic features between mature crinoids fall into two categories: 1. Discontinuous characters in which no morphological overlap is observed between *M. pristinus* and the two eopatelliocrinids *(e.g.,* uniserial or biserial arms); 2. The mean macrostylocrinid differs from the eopatelliocrinids although end members of two or all of the taxa exhibit some morphological intergradation *(e.g.,* ornamentation). The former characters are emphasized in species taxonomy.

Adults of *M. pristinus* are most easily segregated from the eopatelliocrinids by the arms; all large macrostylocrinids show mature biserial Brr whereas these are uniserial in *Eopatelliocrinus.* This discontinuity is distinct and morphological overlap does not exist.

Also, adult calyces of the three taxa can be segregated. The dorsal cups of the macrostylocrinid and *E. scyphogracilis* show much similarity in shape, ornamentation, and adult "size" range. Both possess a slender calyx although the average *Macrostylocrinus pristinus* is slightly wider; the mean adult "size"/dorsal cup width equals about 1.8 for the macrostylocrinid and 2.2 for the eopatelliocrinid. However, plots of "size" versus cup width disclose a certain amount of morphological overlap between the two forms (Text-figs. 9l, 22k). The most striking and discontinuous calyx shape differential consists of the BB circlet. *Eopatelliocrinus scyphogracilis* is characterized by a wide base with straight and nearly vertical sides whereas the macrostylocrinid BB circlet is lower, more narrow at the base and has rapidly expanding sides (compare Text-figs. 7 and 21). The calyces of the two species differ in other ways *(e.g.,* FBrr, IBr1-IAx-iBr1 structure and ornamentation) but the differences between the means are not large enough to separate the two forms. For example, at equivalent "sizes" the macrostylocrinids average .5 fewer FBrr (numerical scale) than does *E. scyphogracilis* (compare Text-figs. 9h and 22g).

The food gathering systems of mature crinoids of the two taxa differ markedly (see ontogeny of *Macrostylocrinus pristinus.*) Adult macrostylocrinids possess longer food gathering systems because of the greater number of IIBrr per arm. A 7.0 mm "sized" macrostylocrinid arm has about 91 IIBrr whereas an equivalent *Eopatelliocrinus scyphogracilis* arm shows only 57 or 59 IIBrr (compare Text-figs. 13a, b with 25a, d). Unfortunately, these differences are of little practical taxonomic value as the mature food gathering systems are generally not preserved.

Mature *Macrostylocrinus pristinus* and adult *Eopatelliocrinus latibrachiatus* calyces are strikingly different and can be separated by the following: 1. Calyx size. Adult eopatelliocrinids range from 3.1 to 5.0 mm in "size". Mature macrostylocrinids are much larger and cover a 6.5 to 12.6 mm "size" interval. 2. Calyx outline. The eopatelliocrinid is characterized by a semi-globose calyx with narrow base, maximum width at the RR-IBr1 level and a distal constriction at the proximal IIBrr height. Fully developed *Macrostylocrinus pristinus* lack such a distal constriction. Morphological overlap is unknown. The mean adult "size"/dorsal cup width consists of 1.8 for the macrostylocrinid and 1.5 in *Eopatelliocrinus latibrachiatus;* however, plots of the two variables show moderate intergradation between the two forms (compare Text-figs. 10l, 22k). 3. Ornamentation. Virtually all adult macrostylocrinids possess some ornamentation (stellate ridges and nodes) on the iBrr, but this does not occur in the eopatelliocrinid. 4. The mean crinoids differ somewhat in other respects (*e.g.*, IBr1-IAx shapes) but morphological overlap renders these characters useless in taxonomy.

Transitional macrostylocrinids ("sizes" 3.4 and 4.2 mm) are distinguished from equivalent "sized" *Eopatelliocrinus* by the standard Brr. These possess either uniserial Brr with strongly converging proximal and distal faces (convergence angles equals 35° or more) or immature biserial Brr. All eopatelliocrinid Brr are uniserial. The eopatelliocrinid uniserial Brr may be separated from transitional macrostylocrinid uniserial Brr by the proximal and distal face convergence angles (35° or more for *Macrostylocrinus pristinus,* 16 to 22° in the eopatelliocrinids). Although this morphological break is not as large and conspicuous as that of mature crinoids, the distribution between *M. pristinus* and the eopatelliocrinids is still discontinuous and not intergradational.

Also, transitional macrostylocrinids can be separated from equal-"sized" *Eopatelliocrinus scyphogracilis* and *E. latibrachiatus* by calyx characters which are similar to those previously listed for larger crinoids although greater morphological overlap is observed and distinction is less certain.

Young macrostylocrinids ("size" range 1.0 to 3.0 mm) are difficult to separate from immature eopatelliocrinids in the same "size" interval because the Brr, food gathering system, calyx shape, and ornamentation morphological differences had not fully developed when this growth stage was attained. For example, with the exception of the 3.0 mm macrostylocrinid, the ornamentation and calyx shapes of all three taxa are almost identical. Maximum emphasis is placed on the following Brr characters in species distinction: 1. Average height relative to width; 2. Proximal and distal face convergence angle; 3. Maximum height relative to minimum height.

The young crinoids were first sorted into two groups by scatter plots of standard Br width versus average height and maximum height versus minimum height (compare Text-figs. 11, 12, 23). Identical specimen groupings were obtained in both cases although the morphological discontinuity is most apparent in the Br width versus average height graphs. On the maximum versus minimum height plots, the two groups grade into one another in the smaller "size" ranges. The animals characterized by wide Brr relative to height and high maximum height/minimum height ratios are referred to *Macrostylocrinus pristinus* and *Eopatelliocrinus latibrachiatus.* This group also possesses rapidly tapering arms. Crinoids with low width/average height and low maximum height/minimum height ratios and gently tapering arms are placed in *E. scyphogracilis.* Typical values for 2.0 mm "sized" individuals are shown below:

	Brachial width	Average height	Width/ Average height	Maximum height	Minimum height	Maximum height Minimum height
E. scyphogracilis	.22 mm	.31 mm	.75	.35 mm	.26 mm	1.4
E. latibrachiatus	.26 mm	.24 mm	1.1	.28 mm	.19 mm	1.5
Macrostylocrinus pristinus	.25 mm	.24 mm	1.0	.30 mm	.20 mm	1.5

Following this, *Eopatelliocrinus latibrachiatus* and *Macrostylocrinus pristinus* were separated by the proximal and distal face convergence angles. The macrostylocrinid convergence angle over the 1.7 to 2.4 mm "size" range varies from 24 to 43°; the equivalent "sized" *Eopatelliocrinus latibrachiatus* interval equals 18 to 20°. Although the discontinuity is small in number of degrees, it seems significant.

Standard Brr data are not available for many of the smallest crinoids due to several reasons: 1. In some animals these had not developed prior to death and burial. 2. The proximal standard Brr (IIBr8) occur as terminal Brr in several individuals, but measurements on these nonpinnulate Brr are not comparable to the pinnule bearing Brr data. 3. Pinnulate proximal standard Brr are observed in a few crowns but these are too poorly preserved for meaningful measurement.

The above specimens were first segregated into two groups: rapidly tapering arms which included *E. latibrachiatus* and *Macrostylocrinus pristinus* while gently tapering arms are assigned to *Eopatelliocrinus scyphogracilis.* The former group is broken down on minor differences of convergence angles and width relative to average height of IIBrr 4 to 6. The macrostylocrinids have slightly lower width/average height and somewhat larger convergence angles. Possibly, several of these youngest animals were placed in the wrong species. If so, the previously discussed growth trends of the several taxa would remain the same or nearly so because the young specimens are so similar.

Most previously described macrostylocrinids are only known from adult examples. Consequently, these are only compared with mature growth stages of the Girardeau form. Aside from *Macrostylocrinus pristinus,* the only other Ordovician species is *M. cirrifer* Ramsbottom (1961, p. 20, pl. 6, figs. 6-13; see also discussion in this paper) from the Ashgillian of the Girvan district in Scotland which differs from the Girardeau form in the following. 1. The Scottish crinoids (as far as known) possess immature biserial Brr in contrast to the adult biserial plates of *M. pristinus;* 2. The Girvan taxon has well developed cirri along most of the stem. Although the column is not well known in mature Girardeau individuals, cirri are apparently lacking; 3. *M. cirrifer* shows a wider calyx relative to height and different ornamentation consisting of median-ray ridges with numerous small nodes on the rest of the ray plates and iBrr. In a few *M. pristinus,* nodes are observed on the iBrr; however, these are always larger and fewer in number than those of the Girvan crinoid. The Girardeau form never has nodes on the ray plates.

The closest relative of the Girardeau macrostylocrinid is *M. ornatus* Hall (1852, p. 204, pl. 46, figs. 4a-g; best figure in Springer, 1926, pl. 4, fig. 24) from the Middle Silurian Rochester Shale of New York. Both species have similar calyx shapes and similar variability in IBr1-IAx-iBr1 structure and ornamentation. The mean *M. pristinus* shows heavier median-ray ridges and more iBrr sculpture although the ornamentation of the two forms overlaps somewhat. The most diagnostic features are the arms and Brr. The Rochester taxon is characterized by wider and heavier arms and much wider (relative to maximum height) Brr.

M. fasciatus (Hall) (see 1879, p. 130, pl. 13, figs. 5, 6; see also Springer, 1926, p. 25, pl. 4, figs. 9, 9a, b) from the Middle Silurian Waldron Shale also possesses a similar calyx shape. The Waldron species may be separated by the more slender calyx shape and the different ornamentation. *M. fasciatus* lacks iBrr ornamentation and the median-ray ridges on the RR and BB are represented by a series of fine parallel ridges in contrast to the typically single solid ridges of the Girardeau animal.

The crinoid described as *M. obconicus* by Weller (1900, p. 95, pl. 4, figs. 6, 7) may be a junior synonym of *M. semiradiatus* (Hall) (see 1868, p. 370, pl. 10, fig. 1). Both occur in the Niagaran Racine Dolomite at Bridgeport, Illinois; if not conspecific, these are closely related. The Bridgeport specimens show calyx shapes which are similar to *M. pristinus* but differ in having smooth plates.

All other described macrostylocrinids are easily separated from *M. pristinus* by differences in calyx shape, ornamentation and nature of Brr, if known.

Specific name. — *pristinus* in allusion to the Upper Ordovician stratigraphic occurrence. Only one other species, *M. cirrifer,* is known from Ordovician rocks; all other forms are Middle Silurian, Upper Silurian or Lower Devonian in age.

Types. — Holotype — USNM 164 565. Paratypes — USNM 164 566 — 164 578; IGS. 35P-25 — 35P-30.

Occurrence. — Girardeau Limestone, Cape Rock and Orchard Creek exposures.

RELATIONSHIP OF INTRASPECIFIC VARIATION IN GIRARDEAU PATELLIOCRINIDS TO TAXONOMIC HEIRARCHY

Although some knowledge exists about intraspecific variation in crinoids, few attempts have been made to document the relationship between such variation and the characters used to define the various taxonomic levels. Some of the rare studies which directly or indirectly involve this approach are Lane (1963a) and Brower (1965, 1967).

Intraspecific variation within the three Girardeau patelliocrinids relative to the main characters used at the various taxonomic levels is outlined below. Certain features which are peculiar to small numbers of taxa (one or two species or a single genus) are omitted. Growth sequences are well known in the Girardeau species. However, most patelliocrinids are known from a few mature specimens. Consequently the discussion treats only the adult crinoid characters. Thus, the survey only relates to the major adult structures which are commonly applied to large numbers of taxa. The details of the intraspecific variation are given under the individual species.

Suborder characters: A. All lateral RR margins in contact. B. Primanal in the iBr1 position. Both are invariant within all three Girardeau species.

Superfamily: A. Presence of few-FBrr calyx with the resultant small number of iBrr. Within the Girardeau species, this is most closely approximated by the percentage standard deviations of "size" versus the FBrr in lateral interrays and "size" versus inter-half-ray FBrr. These values range from 0 (*i.e.,* invariant) to 8.0%. Although low variation exists, the Girardeau calyces are all few-FBrr types. B. IBrr heights small relative to those of the RR. Intraspecific variability is approached rather indirectly in the Girardeau forms, namely by the percentage standard deviations of "size" versus heights of RR, IBrr1, and IAxx. These figures cover an interval of 10% to 24%. Usually, the RR show smaller percentage standard deviations than the IBrr. In some specimens the relative RR-IBrr heights approach the glyptocrinid or melocrinid configuration. The wide variation is surprising considering the taxonomic level involved and renders this character suspect. Possibly the variation shown by the Girardeau patelliocrinids is related to their stage of evolution. The three species were all recently derived from the Glyptocrinidae. Possibly, more advanced patelliocrinids, such as *Patelliocrinus,* exhibit less variation of this type. C. Gross structure of Brr. Invariant in all species.

Family: A. Number of BB range from one to three. B.

Gross Brr structure. C. Presence of two to four arms per ray. All three are invariant. D. Tegmen structure. Inadequately known in the Girardeau species to evaluate.

Genera (see remarks under *Eopatelliocrinus* for generic diagnoses): A. Gross calyx shape. B. Nature of CD interray, such as number of plates after primanal, CD interray width relative to that of lateral interrays, and presence or absence of anal interray ridge. C. Exact number of BB. D. Number of arms, such as two per ray. E. Specific Brr types, uniserial, biserial, or compound. All five features are invariant. F. IBr1 and IAx shapes, also includes level reached by iBr1. The IBrr shapes exhibit moderate variation in the Girardeau eopatelliocrinids and the macrostylocrinid; the percentage standard deviations range from 11 to 16%. However, the IBrr shapes are not diagnostic of *Eopatelliocrinus* and *Macrostylocrinus*. These structures are only definitive in more advanced patelliocrinids. For example, *Patelliocrinus* shows a rectangular IBr1 and usually a pentagonal IAx; consequently, the iBr1 is large and generally attains the proximal IIBrr level. Examination of *P. rugosus* Springer (1926, p. 32, pl. 6, figs. 16-18) and *P. ornatus* Springer (1926, p. 31, figs. 13-15, 15a) indicates that these characters are invariant. As far as can be determined, the IBrr shapes (and the correlated iBr1 size) are used appropriately in the taxonomy.

Species: A. Various calyx shape parameters are diagnostic, especially relative height and width and general outline (*e.g.*, globose versus conical). As defined in this paper, the calyx outline is invariant (see comparison and variation under *Eopatelliocrinus latibrachiatus*. The relative height and width are subject to more fluctuation, and the percentage standard deviations range from 13 to 15% (taken from "size" versus calyx width). Also, the different species show some overlap although the mean calyx shapes differ. B. Size of IBrr relative to the RR or "size". This serves to separate the Girardeau macrostylocrinid from some later species. The applicable percentage standard deviations of *Macrostylocrinus pristinus* vary from 11% to 24%; these were not investigated in the Middle Silurian forms. Perhaps, some end member overlap does occur although the typical Middle Silurian individuals show smaller IBrr relative to the RR size than the Girardeau species. C. The qualitative nature of the ornamentation is considered definitive of the species, for example, well-developed median-ray ridges with accessory iBrr sculpture versus poorly formed median-ray ridges with smooth iBrr. As used at the species level, the character shows no variation in the Girardeau forms. D. The approximate "size" of the largest individuals differs between the various species. Large forms attain "sizes" of 8.0 mm or more whereas small ones are 5.0 mm or less in "size". The adult "size" is clearly diagnostic of the three Girardeau patelliocrinids where adequate growth sequences are available. Most other forms are based on small numbers of specimens, all of which are about the same "size". Consequently, this character cannot be fully evaluated. E. Br shapes. Uniserial plates are mainly separated on the average height relative to width (see comparison under *Eopatelliocrinus latibrachiatus*). These percentage standard deviations are 7.5 and 9.4%; the adult individuals show no overlap. Biserial Brr are characterized by the type (*i.e.*, mature versus immature biserial) and by the relative height and width. The Br type is invariant in adults. The relative maximum height and width have a 7.2% standard deviation in *Macrostylocrinus pristinus*. Despite some variation, no overlap seems to occur between the taxa examined. F. Arm shape (*e.g.*, width relative to "size", distal taper rate) distinguishes several species. Although these variables were not treated quantitatively in the Girardeau forms, a certain amount of variation is present. Where definitive, no overlap is known.

The above data indicate three general considerations. If the relative heights of the IBrr and RR are omitted, the amount of intraspecific character variation increases from higher to lower level characters, and the variation suggests that the general patelliocrinid character heirarchy is valid with the possible exception of the IBrr sizes relative to the RR. The magnitude of the intraspecific character variation changes with stage of evolution. For example, the IBrr shapes are variable in the primitive eopatelliocrinids and macrostylocrinids but invariant in the more advanced *Patelliocrinus*. This character is not diagnostic of the primitive species but it can be used to rigidly define the more advanced genera. The same situation may characterize the IBrr size relative to the RR size although this has not been studied in the phyletically advanced taxa.

Superfamily **PLATYCRINITACEA** Ubaghs, 1953

Family **HAPALOCRINIDAE** Jaekel, 1895

Genus **CULICOCRINUS** Müller, 1855, p. 23

Type species. — *Platycrinus nodosus* Müller *in* Wirtgen and Zeiler, 1855, p. 15, pl. 6, figs. 2, 3.

Diagnosis. — A genus of Hapalocrinidae characterized by iBrr which incorporate IBrr and proximal IIBrr into the dorsal cup; arms biserial, branch once or more near dorsal cup; tegmen dominated by five large OO; anal opening on tegmen surface; remaining tegmen structure uncertain.

Remarks. — Breimer (1962, pp. 134-144) questionably assigned *Culicocrinus* to the Hapalocrinidae largely because two IBrr occur in each ray. He noted that two IBrr per ray are associated with hapalocrinid tegmens whereas only one small IBr (IAx) per ray occurs with the tegmen of Platycrinitidae. The *Culicocrinus* tegmen is poorly known but it basically consists of five large OO with several other plates. First axillar ambulacrals (see Breimer, 1962, pp. 134-144 for terminology) may or may not be present. Inspection of Schmidt's Text-figure 5g (1941) shows a plate in this position in the A ray. If this represents a first axillar ambulacral, then *Culicocrinus* may be transitional between the Hapalocrinidae and the Platycrinitidae.

Occurrence. — Lower and Middle Devonian, Europe; perhaps Upper Ordovician, North America.

CULICOCRINUS ? GIRARDEAUENSIS, n. sp.

Plate 68, figure 1; Text-figure 27

Diagnosis. — A species of Hapalocrinidae characterized by wide column facet; straight and steep walled dorsal cup with prominent BB rim; arms biserial, probably two per ray, unbranched as far as known; three iBrr most likely present consisting of one iBr1 and two iBrr2 in only known interray, the supposed iBrr reach to proximal IIBr1 level; IBrr and IIBr1 not rigidly incorporated into calyx.

Description. — Species only known from one immature specimen; "size" 2.2 mm in one ray, 2.8 mm in the other; dorsal cup wide, "size"/dorsal cup width is .9; cup base wide; cup walls straight, expanding upward at roughly 70° angle; width of IAx level interray areas is 50% of cup width.

BB circlet with prominent rim. IBrr strongly convex; distal half of R with ill-defined median-ray ridge. Remainder of plates smooth.

Number of BB unknown; only one small B seen, pentagonal, low, height/width roughly .6.

RR largest dorsal cup plates; septagonal; height/width equals .8; RR facets narrow, occupy about 67% of plate width; facet curved, concave distally; facet surface inclined outward; articular surface not observed. IAx consists of IBr1 in one ray, IBr2 in other; IBrr much smaller than RR. Non-axillary IBr1 hexagonal; height/width .67. IAxx pentagonal; height/widths are .63 and .75; IAxx support half-ray IIBrr1. IIBrr1 hexagonal; plates of adjacent half-rays with inner sides joined together; pinnules lacking; mean IIBr1 height/width is .8. Highest inter-half-ray FBr is proximal part of IIBr1; distal FBrr of interrays uncertain.

Questionable iBrr present; iBr1?, large, hexagonal, reaching mid-IBr1 level; iBrr2? smaller, shapes unknown, reaching mid-IIBr1 height; orientation of iBrr? bearing area unknown.

Articular surfaces of calyx plates and tegmen not observed.

Arms incompletely known; biserial; apparently two per ray although one arm may branch above IIBr12; arms heavy, tapering gently. Pinnules unknown except for several pinnulars.

IIBr2 composes first free Br; uniserial; in some half-rays bears pinnule on interray side, in other cases lacking pinnule; roughly equidimensional. IIBrr3 wedge-shaped; generally bears pinnule on interray side; width/average height roughly 1.5. IIBrr4 and IIBrr5 strongly wedge shaped with minimum height almost zero or immature biserial with minimum height equalling zero; pinnules present. IIBr6 always immature biserial. IIBrr7 and higher Brr mature biserial with inner margins sharply separated from proximal and distal margins; always pinnulate; width of proximal or distal margin/total width is 63%. Pinnule facets strongly necked and protuberant, inclined from horizontal by roughly 45°. Articular surfaces of Brr and pinnule facets and food groove configurations not seen.

Only proximal pinnulars preserved; length exceeds height by about 2:1; pinnular tapers rapidly in distal direction; other details unknown.

Proximal portion of column observed; distal stem and attachment device not present; column round; tapers slightly in distal direction; width of proximal column about 1.1 mm; distal diameter roughly 1.0 mm; sutures crenulate in external view; articular surfaces not preserved.

Remarks. — This species is based on one partially preserved young specimen in matrix. Although the arms are not fully preserved and the tegmen is unknown, the crinoid is definitely placed in the Hapalocrinidae. The two well-developed IBrr in one ray and the large IAx in the other ray indicate that *Culococrinus*? *girardeauensis* is not referable to the Platycrinitidae. As pointed out by Breimer (1962, pp. 134-144), the presence of two well-developed IBrr is never associated with the platycrinitid tegmen but is invariably found with the hapalocrinid tegmen. The Platycrinitidae are almost always characterized by one small IBr (IAx) per ray in combination with large proximal IIBrr (Breimer, 1962, pp. 134-144). Perhaps, the Girardeau crinoid might be assigned to the Hexacrinitidae; however, normal hexacrinitids always show three large equal-sized BB. The presence of a small B in the holotype of *C.* ? *girardeauensis* denotes placement in the Hapalocrinidae.

Three iBrr are believed to occur in the Girardeau hapalocrinid. These supposed iBrr are clearly loosely incorporated into the dorsal cup. Similar iBrr are found in other hapalocrinids, for example *Hapalocrinus* Jaekel (1895, p. 95; see species illustrated by Springer 1926, pl. 11, figs. 30-32, pl. 12, figs. 1-8). Possibly, the supposed iBrr of the Girardeau crinoid represent tegmen plates which were crushed against the IBrr and IIBrr1 during burial. However, the regular nature of the plates suggests iBrr rather than tegmen elements.

Although the family is definite, the generic assignment is questionable and has been determined largely by process of elimination. In the author's opinion, this confusion is general for hapalocrinid genera due to the nature of the material. Certain genera, for example *Hapalocrinus* Jaekel (1895, p. 95), *Thallocrinus* Jaekel (1895, p. 106), and *Bogatacrinus* Schmidt (1937, p. 5), are diagnosed on the dorsal cup and arms whereas the tegmen structure is undetermined. In a second group, *Amblacrinus* d'Orbigny (1849, pp. 102, 156) and *Cantharocrinus* Breimer (1962, p. 117), the dorsal cup and tegmen are well known but the arm structure is not preserved. In the third group, *Culicocrinus* Müller (1855, p. 23), *Cyttarocrinus* Goldring (1923, p. 265), *Cordylocrinus* Angelin (1878, p. 3), and *Lyonicrinus* Springer (1926, p. 48), both the arm and tegmen structure are known. Thus, defining the various hapalocrinid genera on different characters, with the characters being at least partially a function of preservation, has contributed to considerable confusion in diagnosing the genera and their relationships. Much restudy of the family is necessary to clarify the present state of knowledge.

Culicocrinus? *girardeauensis* cannot be referred to *Hapalocrinus, Thallocrinus, Lyonicrinus,* or *Cordylocrinus* because the latter genera all have narrow column facets and uniserial or cuneiform arms. The narrow column facet and heterotomous arm branching of *Bogatacrinus* preclude the assignment of the Girardeau form to this genus.

Cyttarocrinus, Amblacrinus, and *Cantharocrinus* are characterized by wide column facets with the arms free above the RR and these resemble the Girardeau taxon in the first feature. The *Cyttarocrinus* arms are uniserial and composed of elongate Brr; accordingly, the new species is not assigned to this genus. The arm structures of *Amblacrinus* and *Cantharocrinus* are unknown. Both genera lack iBrr and possess similar tegmen structures. These tegmens consist of five 00 and one suboral in all interrays except the CD interray which may have one or more plates. The suborals are tegmen plates rather than iBrr. Regardless of whether the three iBrr? of the Girardeau form represent iBrr or tegmen elements, the presence of three plates indicates that this crinoid is not referable to *Amblacrinus* or *Cantharocrinus.*

The Girardeau species is questionably placed in *Culicocrinus* for several reasons: 1. Presence of biserial arms. However, the arms of typical *Culicocrinus* always branch one or more times near the calyx; as far as can be determined, the Girardeau crinoid arms remain unbranched; 2. Similar iBrr structure. *Culicocrinus* is characterized by well developed iBrr1 and in some examples iBrr2; the IBrr and proximal IIBrr are firmly incorporated into the dorsal cup by these iBrr. The Girardeau form probably shows an iBr1 followed by two iBrr2 with the latter reaching the IIBr1 level. However, the supposed *C.* ? *girardeauensis* iBrr are not rigidly fixed into the dorsal cup; 3. Occurrence of wide column facet in the new species and moderately wide to wide stem attachment are in *Culicocrinus.*

C. ? *girardeauensis* is separated from European Lower and Middle Devonian species of *Culicocrinus* (for easily available discussion of these forms see Schmidt, 1934, p. 47, pl. 5, figs. 1a, b; 1941, pp. 37-45, text-figs. 5, 6, pl. 7, figs. 1-4, 8) by the calyx ornamentation, arm branching structure, and the column facet width relative to the dorsal cup width. The European crinoids have heavily nodose calyces, arm bifurcations near the cup, and relatively narrow stem attachment areas. *C.* ? *girardeauensis* shows a smooth dorsal cup, apparently unbranched arms and a wide column facet. The Girardeau form differs from the crinoid described as *C. spinosus* by Springer (1926, p. 51, pl. 11, figs. 4, 4a-c) in its straight and steep-walled dorsal cup; Breimer (1962, p. 138) refers *C. spinosus* to *Pleurocrinus. C.* ? *girardeauensis* may be distinguished from all other known Hapalocrinidae by the characters listed in the diagnosis.

In defining the generic placement of *C.* ? *girardeauensis,* the width of the column facet has been used as a diagnostic factor. Because the holotype represents a young individual, the variation of this feature during growth of related crinoids is important. The developmental stages of hapalocrinids are poorly known but the ontogeny of *Platycrinities bozemanensis* (Miller and Gurley) (1897, p. 42, pl. 3, fig. 5) has been described by Laudon (1967). The young specimens figured by the author on plate 193, figures 12-17 are characterized by relatively steep dorsal cups with wide column facets. Comparison of the immature platycrinitids with the holotype of *Culicocrinus*? *girardeauensis* shows that the crinoids are at comparable growth stages. During the development of *Platycrinites bozemanensis,* the dorsal cup became wider while the relative width of the column facet decreased (see the adults figured by Laudon on pl. 194). Although the relative width of the column facet clearly declined during the ontogeny of *P. bozemanensis,* the amount of decrease was not sufficient to categorize the species as a narrow column faceted member of the Platycrinitacea, such as *Thallocrinus* or *Hapalocrinus.* Therefore, by analogy with the growth stages of *Platycrinites boze-*

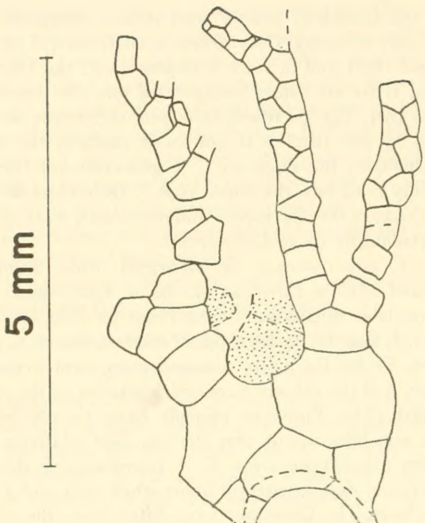

Text-figure 27. — *Culicocrinus*? *girardeauensis*, n. sp., holotype, IGS. 8258, A and E rays?, "size" 2.5 mm, Orchard Creek exposure. The iBrr are stippled.

manensis, it is believed that classification of the young holotype of *Culicocrinus*? *girardeauensis* as a wide column faceted hapalocrinid is valid, despite probable variation of this character with growth.

The Lower Silurian Brassfield Limestone specimen described by Foerste (1919, pl. 3, fig. 3) as "A Platycrinid (?)" is similar to *C.* ? *girardeauensis*. Both crinoids have two biserial arms per ray and IBrr which are loosely fixed into the calyx. The Brassfield species is easily separated by its wider dorsal cup which lacks a BB rim.

The occurrence of *C.* ? *girardeauensis* in the Upper Ordovician Girardeau Limestone extends the stratigraphic range of the family downward. Previously, the oldest known hapalocrinids were of Middle Silurian age.

The *C.* ? *girardeauensis* biserial arms indicate that this crinoid was at an advanced hapalocrinid stage of evolution. While a few hapalocrinids, *Culicocrinus* and *Oenochoacrinus*, have biserial arms, most are characterized by uniserial or cuneiform arms. Thus, the presence of biserial arms in the Upper Ordovician Girardeau form denotes the early and precocious development of this character.

The appearance of the primitive patelliocrinids, *Eopatelliocrinus* and *Macrostylocrinus*, and the hapalocrinid, *Culicocrinus*?, in the Upper Ordovician Girardeau Limestone indicates that the initial adaptative radiation of this branch of the glyptocrinid ancestral stock occurred much earlier than previously believed. Formerly, this adaptative radiation was placed in the Middle Silurian. Nevertheless, this patelliocrinid-hapalocrinid lineage is not complete because many important links (in the morphological sense, probably also in the line of evolution), such as *Chytrocrinus* (Jackel, 1918, p. 33) and *Patelliocrinus*, are not present in Upper Ordovician rocks.

Column growth. — The holotype stem segment illustrates certain aspects of development. A total of four columnal orders are found (numbering of orders follows Bather, 1900, text-fig. 17). Orders 3 and 4 are nodose whereas the Order 1 plates are non-nodose. Near the calyx, the Order 2 is non-nodose but it becomes nodose distally. The order sequence just below the calyx comprises: 4-3-2 (only partly formed) -4. Slightly further down the stem, the following is observed: 4-2-3-2-4. This resembles the proximal formula except that the complete Order 2 is present. The distal formula equals: 4-1-2-1-3-1-2-1-4. Comparison of these sequences shows that Orders 3 and 4 developed just below the calyx whereas Orders 1 and 2 were intercalated between the previously formed plates. Thus, roughly 75% of the plates were intercalated, but only about 25% initiated below the calyx.

The thickness of most orders was augmented after their development as tabulated below:

	Columnal thickness			
	Order 4	Order 3	Order 2	Order 1
Proximal column	.18 mm	.12 mm	.07 mm	absent
25% below calyx	.18 mm	.15 mm	.12 mm	absent
Distal column	.43 mm	.33 mm	.27 mm	.15 mm

Specific name. — *girardeauensis* in allusion to the occurrence.

Holotype. — Worthen Collection, IGS. 8528.

Occurrence. — The holotype of *Culicocrinus* ? *girardeauensis* occurs on a small slab with *Apiocystites*? sp., *Dendrocrinus*? n. sp. aff *D.* ? *navigiolum* Miller, and five young specimens of *Eopatelliocrinus*. It was evidently collected by Worthen although the original label has since been lost. The oldest label found with the specimen was prepared by Wachsmuth in 1892 when he reviewed the Illinois State Museum Worthen collection. This reads "Cincinnati group, Alexander County Illinois" and probably duplicates Worthen's original label. The lithology of the slab is characteristic of the Girardeau. At present, the only place in Alexander County, Illinois, from which the specimen could have been collected is the Orchard Creek exposure, and this is believed to represent the original locality.

PHYLOGENY OF GIRARDEAU PATELLIOCRINIDS AND ALLIES

PREVIOUS WORK

Little has been done on the phylogeny of patelliocrinids and related forms. The reader is referred to Moore and Laudon (1943, pp. 88-90, 96-101) for a summary of the available work. With some exceptions, their views are borne out here. Moore and Laudon believed that the Patelliocrinidae were offshoots from the early Melocrinitidae. This view is not accepted for the forms examined by the writer, because all early melocrinitids (see section on alisocrinid phylogeny) possessed four or more arms per ray whereas primitive patelliocrinids had the arms stabilized at two per ray. Based on comparative morphology and stratigraphic position, the writer believes that the early Patelliocrinidae were derived from Glyptocrinidae with two arms per ray, such as *Glyptocrinus ornatus* Billings.

SOURCES OF DATA AND LIMITATIONS

The following species which are referred to three families are treated in detail:

Glyptocrinidae

Glyptocrinus ornatus Billings. Middle Ordovician; Trenton; Canada. Five USNM and Springer Collection specimens examined by the writer.

Patelliocrinidae

Eopatelliocrinus scyphogracilis, *E. latibrachiatus*, and *Macrostylocrinus pristinus*. All Late Ordovician, Girardeau Limestone.

M. ornatus Hall. Middle Silurian; Rochester Shale, New York. Four USNM and Springer collection specimens seen by the writer, including the crinoid figured by Springer (1926, pl. 4, fig. 24).

M. laevis Springer. Middle Silurian; Beach River Formation, Tennessee. Seven Springer collection specimens studied by the writer including the primary types.

M. cirrifer Ramsbottom. Late Ordovician; Ashgill; Scotland. Not included in data matrix.

Patelliocrinus ornatus Springer. Middle Silurian; Laurel Limestone; Indiana. Seven Springer collection crinoids measured by the writer including the primary types.

Hapalocrinidae

Culicocrinus ? girardeauensis. Late Ordovician; Girardeau Limestone.

"Platycrinid." Early Silurian; Brassfield Limestone; Ohio. This form was figured by Foerste 1919 (pl. 3, fig. 3) as "A Platycrinid" (?). The crinoid should be assigned to the Hapalocrinidae not the Platycrinitidae.

In addition, collections of most other Middle Silurian North American species of *Macrostylocrinus* and *Patelliocrinus* have been examined. However, these are not included in the quantitative studies because the arms are unknown. Quantitative data on *M. cirrifer* are not considered due to uncertainty about the Brr. These have only been seen in one young crinoid where they consist of immature biserial Brr; the mature individuals may or may not show this configuration.

Essentially, all the known Ordovician material and most North American Middle Silurian species have been studied. The bizarre forms, like *Laurelocrinus*, and compound Brr bearing genera, such as *Allocrinus*, are intentionally omitted. Conversely, the European Silurian crinoids are almost completely ignored. Most of these were described by Angelin (1878) and Jaekel (*e.g.* 1918). Angelin's figures are commonly composites of several specimens and are thus unreliable. Jaekel's descriptions and illustrations are generally inadequate to compile all the characters. Nevertheless, the Ordovician part of the lineage is believed to be complete with respect to the presently known species. Also, the general evolutionary trends are considered correct for all "normal" patelliocrinids. The Middle Silurian lineage is obviously incomplete because of the lack of European forms. With the exception of the Girardeau species and one allied crinoid, the Hapalocrinidae is omitted from detailed treatment.

DISCUSSION OF DENDROGRAM

The original data matrix, the taxonomic or morphological distance matrix, and the dendrogram are presented in Tables 13a-c. Text-figure 28 illustrates the inferred phylogeny. Unlike the alisocrinids and melocrinitids, the patelliocrinid clustering order closely parallels the generic level taxonomy.

The first cycle clusters (mutually exclusive) consist of *Eopatelliocrinus scyphogracilis* plus *E. latibrachiatus* and *Macrostylocrinus pristinus* plus *M. ornatus*. In the second cycle, *M. laevis* joins the *Macrostylocrinus* cluster following which the third cluster unites the *Eopatelliocrinus* and *Macrostylocrinus* groups. The fourth, fifth, and sixth additions comprise *Culicocrinus ? girardeauensis*, *Patelliocrinus ornatus* and *Glyptocrinus ornatus*, respectively.

The phylogeny diagram (Text-fig. 28) largely represents the taxonomic distance matrix and dendrogram which are adjusted for stratigraphic position. The lineage breaks down into two basic parts: A. *G. ornatus* — *Eopatelliocrinus* — *Macrostylocrinus* — *Patelliocrinus;* B. *Culicocrinus*

Table 13a

	Glyptocrinus ornatus	*Eopatelliocrinus scyphogracilis*, n. gen., n. sp.	*E. latibrachiatus*, n. gen., n. sp.	*Macrostylocrinus pristinus*, n. sp.	*M. ornatus*	*M. laevis*	*Patelliocrinus ornatus*	*Culicocrinus? girardeauensis*, n. sp.
1. Distal FBr	18.0	13.0	10.0	12.0	9.4	10.0	9.5	3.0
2. IBrl shape	5.8	5.5	5.5	5.4	5.5	4.3	4.0	5.0
3. IAx shape	5.2	6.4	5.6	6.4	5.7	5.7	5.0	5.0
4. % Ht. RR	39.0	28.0	39.0	34.0	40.0	41.0	59.0	41.0
5. % Ht. IBrl	32.0	20.0	19.0	23.0	19.0	17.0	14.0	22.0
6. % Ht. IAx	29.0	19.0	22.0	23.0	22.0	17.0	13.0	28.0
7. CD iR str.	3.0	3.0	3.0	3.0	3.0	2.7	2.0	2.0
8. Brr type	1.0	1.0	1.0	4.0	4.0	4.0	4.0	4.0
9. First biserial Br	50.0	50.0	50.0	5.5	7.2	4.5	6.4	4.5
10. Number of BB	5.0	3.0	3.0	3.0	3.0	3.0	3.0	3.0

Raw data for the patelliocrinid phylogeny matrix. The coding follows:
1. Distal FBrr: numerical scale used on graphs.
2. and 3. IBrr shapes: average number of plate sides.
4. - 6. Percentage of total "size" occupied by the listed plate.
7. CD interray structure: number of plates following primanal.
8. Type of Brr: 1 — Uniserial. 2 — Cuneiform. 3 — Immature biserial. 4 — Mature biserial.
9. Proximal biserial IIBrr: arbitrarily coded as 50 for uniserial species.
10. Number of BB.

All data entered are for mature crinoids with the exception of *Culicocrinus? girardeauensis*, n. sp., which is only known from one specimen.

Table 13b

G. ornatus	*E. scyphogracilis*, n. gen., n. sp.	*E. latibrachiatus*, n. gen., n. sp.	*M. pristinus*, n. sp.	*M. ornatus*	*M. laevis*	*P. ornatus*	*C.? girardeauensis*, n. sp.
0	1.5663	1.4140	1.6331	1.6752	1.9688	2.3976	1.9624
1.5633	0	0.6706	0.9471	1.0833	1.2502	1.9667	1.7333
1.4140	0.6706	0	1.0348	0.8524	1.1204	1.6586	1.3673
1.6331	0.9471	1.0348	0	0.5521	0.9667	1.7864	1.3482
1.6752	1.0833	0.8524	0.5521	0	0.6975	1.4171	1.0480
1.9688	1.2502	1.1204	0.9667	0.6975	0	0.9616	1.1407
2.3976	1.9667	1.6586	1.7864	1.4171	0.9616	0	1.3792
1.9624	1.7333	1.3673	1.3482	1.0480	1.1407	1.3792	0

Taxonomic distance matrix for the Girardeau patelliocrinids and allied forms. Low numbers denote close morphological resemblance, high numbers vice versa.

Table 13c

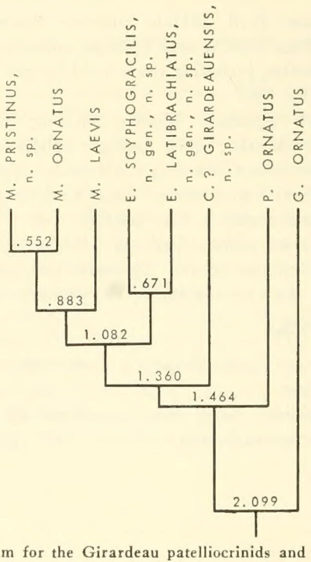
M. PRISTINUS, n. sp.
M. ORNATUS
M. LAEVIS
E. SCYPHOGRACILIS, n. gen., n. sp.
E. LATIBRACHIATUS, n. gen., n. sp.
C. ? GIRARDEAUENSIS, n. sp.
P. ORNATUS
G. ORNATUS
.552
.883
.671
1.082
1.360
1.464
2.099

Dendrogram for the Girardeau patelliocrinids and allied species. Low numbers denote close morphological resemblance, high numbers vice versa.

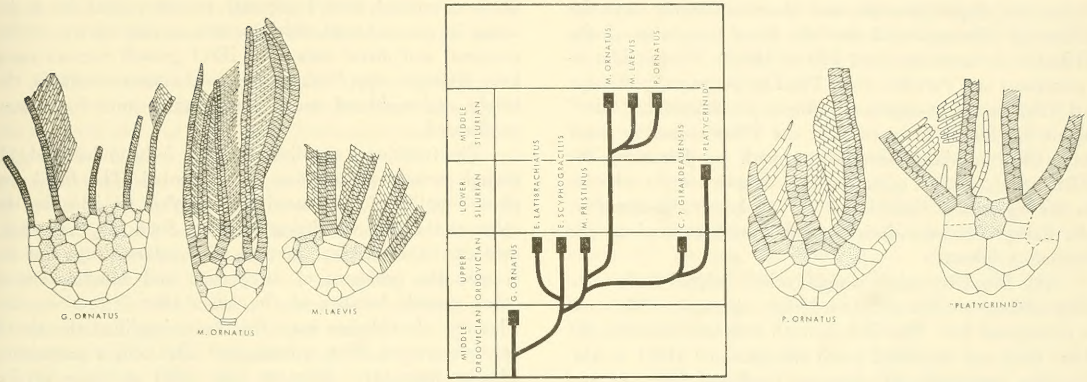

Text-figure 28. — Phylogeny of Girardeau patelliocrinids and related forms. Solid bars indicate approximate occurrence of species; finer lines show inferred lineage. Only drawings of non-Girardeau forms are given here. Sources: *Glyptocrinus ornatus* Billings (Wachsmuth and Springer, 1897, pl. 20, fig. 6a). *Macrostylocrinus ornatus* Hall (Springer, 1926, pl. 4, fig. 24). *M. laevis* Springer (composite diagram from 1926, pl. 4, figs. 14-19). *Patelliocrinus ornatus* Springer (1926, pl. 6, fig. 15a). "Platycrinid" was figured by Foerste (1919, pl. 3, fig. 3) as A. Platycrinid (?); the diagram was prepared from his illustration. This species was omitted from the taxonomic distances; however, it shows post-Girardeau survival of this type of hapalocrinid. The iBrr are stippled. Arms are ruled obliquely. Pinnules shown in highly schematic fashion. For illustrations of the Girardeau species, see the previous Text-figures.

? *girardeauensis* and "Platycrinid". Group A will be discussed first, following which the origins of Haplocrinidae will be treated.

EVOLUTIONARY TRENDS

In the entire lineage, including the hapalocrinids, the arm formula was stabilized at two per ray (total of 10), although the arms changed from the uniserial to biserial type. The principal trends involved the calyx which evolved from a complex many-FBrr type to a few-FBrr type composed of a small number of plates. The calyx eventually produced in the hapalocrinids studied was intermediate between the typical few-FBrr and the no FBrr type as seen in some Hapalocrinidae and virtually all Platycrinitidae.

All evolutionary trends probably occurred through "mutations" (most general sense, includes gene changes, chromosome abberations, and so forth) which caused growth divergences. Comparison of the taxonomic distances between the adult and young crinoids of two different species always discloses lesser distances for the youngsters (*i.e.*, more morphological similarity). This strongly suggests that evolution was by means of progressive growth divergences. The products of these "mutations" can be outlined relative to the forms in which the ontogenies are available. In this case, *Eopatelliocrinus scyphogracilis*, *E. latibrachiatus*, and *Macrostylocrinus pristinus* are included.

Glyptocrinus ornatus — *Eopatelliocrinus* — *Macrostylocrinus* — *Patelliocrinus*

The trends are listed below in the order of appearance (*i.e.*, from oldest to youngest):

I. Reduction of the BB from five to three occurred in the transition from *Glyptocrinus ornatus* (Middle Ordovician) to the late Ordovician *Eopatelliocrinus*. The applicable "mutation" involved the fusion of two pairs of single BB to produce two large and one small B. The youngest *Eopatelliocrinus* and *Macrostylocrinus* ("size" about 1.0 mm) all possess three BB. Thus, the change took place early in ontogeny, probably soon after the BB and 00 formed, by analogy with living crinoids. The functional significance was probably three-fold.

The base of the calyx was strengthened against lateral shear which could have been exerted upon strong flexing of the column. The fusion of some BB most likely provided better protection for the chambered organ which was housed at the BB and proximal RR levels (see *M. cirrifer*). Reduction of the number of plate elements may have simplified some of the problems of integration and coordination during growth.

The next group of three trends was progressive and characterized all species within the lineage to some extent.

II. Reduction of FBrr. In *Glyptocrinus ornatus* (Middle Ordovician), the IIBr6 comprises the highest FBr. Late

Ordovician *Eopatelliocrinus* and *Macrostylocrinus* have the IIBrr2 or 3 incorporated into the dorsal cup, whereas the IIBrr1 or 2 forms the distal FBr in Middle Silurian *Macrostylocrinus* and *Patelliocrinus*. The IAx is generally the distal FBrr in the youngest Girardeau patelliocrinids ("size" about 1.0 mm). Consequently, the FBrr reduction must have occurred throughout later growth by decreasing the FBrr incorporation rate. Further details remain obscure as the tegmens of these forms are not known. Presumably, the fixing iBrr were derived from iAmbb located on the tegmen periphery.

III. Fixed ray plate simplification. Middle Ordovician *Glyptocrinus ornatus* mostly exhibits a hexagonal IBr1 and a pentagonal IAx. The iBr1 is small and terminates at the IBr1 level and the iBrr2 reach the proximal IIBr1 height. Variable structures are observed in *Eopatelliocrinus* and *Macrostylocrinus*. The most common configurations, listed from primitive to advanced, are: hexagonal IBr1 and pentagonal IAx, like *Glyptocrinus ornatus;* rectangular IBr1 and septagonal IAx with a large iBr1 which reaches the IAx level; and rectangular IBr1 and pentagonal IAx with the iBr1 attaining the proximal IIBrr level. The last configuration first appeared frequently in the Middle Silurian *Macrostylocrinus laevis*. Intermediate geometry is often observed, for example, a five-sided IBr1 and a six-sided IAx. Within *Eopatelliocrinus* and *Macrostylocrinus,* the general tendency was to reduce the mean number of IBrr1 sides and to some extent the IAx sides with time as indicated below:

Table Showing IBrr Evolution in Patelliocrinids

	Mean Sides	
	IBr1	IAx
Eopatelliocrinus scyphogracilis Late Ordovician	5.4	6.4
Macrostylocrinus laevis Middle Silurian	4.3	5.7

The most advanced configuration was achieved by Middle Silurian *Patelliocrinus* with a rectangular IBr1 and a pentagonal IAx. The iBr1 is large and reaches the proximal IIBrr level. No variation has been seen and the character was stabilized.

The responsible "mutations" must have affected the development soon after the IBrr1 and IAxx appeared. The smallest Girardeau eopatelliocrinids and macrostylocrinids ("size" roughly 1.0 mm) have the IAxx fixed into the calyx, and the number of IBrr sides remained constant throughout later development. Therefore, the growth divergences must have been initiated prior to the IBrr incorporation. Two characters were involved: Change in the IBrr shapes early during their ontogeny. For example, the IBr1 were most likely converted from hexagonal to rectangular by a decrease in the mid-level width growth vectors relative to the proximal and distal ones. The iBrr1 growth vectors must have diverged also. With respect to the above example, the height and mid-level width growth rates must have been accelerated.

The functional significance is not fully understood, although several possibilities are presented. The fixed ray plate simplification reduced the number of iBrr in the calyx as the iBr1 was being enlarged. Such may have augmented the mechanical strength of the dorsal cup, and decreased the problems of integration and coordination of calyx growth because of the lower iBrr formation rate. This line of evolution may also have simplified the aboral nervous system. With a hexagonal IBr1 and a pentagonal IAx, at least three iBrr are seen (iBr1 and two iBrr2). Probably, three iBrr aboral nerve cord knots existed, all of which were connected to the other iBrr and adjacent ray plates; *Macrostylocrinus cirrifer* is characterized by this configuration. With a rectangular IBr1 and a pentagonal IAx, only the iBr1 is observed, and only one iBr nerve knot may have occurred in each lateral interray. This cannot be fully verified as the aboral nervous system grooves are not known in *Patelliocrinus*. However, *Callicrinus pentangularis* Weller (1900, p. 120, pl. 8, fig. 6) has similar IBrr-iBrr geometry and only one iBr1 nerve knot was present. If this configuration is applicable to *Patelliocrinus,* two iBrr nerve knots were lost thus shortening the aboral nerve complex.

IV. The heights of the IBr1 and IAx relative to calyx "size" gradually declined throughout the evolutionary sequence. In *Glyptocrinus ornatus* (Middle Ordovician), these occupy 32 and 29% of "size" but only 14 and 13% in Middle Silurian *Patelliocrinus*. Study of Table 13a, shows that the RR augmented their height percentages as the IBrr1 percentages decreased. As previously mentioned, the youngest Girardeau patelliocrinids ("size" about 1.0 mm) are all similar with respect to the percentage contributions to "size". Consequently, the divergence most likely postdated this growth phase. Basically the changes involved decrease in the height growth rates for the IBr1 and IAx relative to "size". The functional significance of this trend was probably closely related to the fixed ray plate simplification.

Summarizing, three morphological directions of evolution combined to convert the many-FBrr calyx of *Glyptocrinus ornatus* into the few-FBrr type of *Patelliocrinus*. These were: reduction of FBrr; fixed ray plate simplification; and decrease in the relative heights of the IBrr with respect to "size". For the general advantages and disadvantages of many-FBrr versus few-FBrr calyces, the reader is referred to the summary of Girardeau camerate ontogeny.

V. The formation of biserial arms happened during the transition between Late Ordovician *Eopatelliocrinus scyphogracilis,* with uniserial arms, and *Macrostylocrinus pristinus,* with mature biserial Brr in adults. All later North American species retained this configuration with one exception, *M. meeki,* which is annotated below. If mature *M. cirrifer* (Late Ordovician) have immature biserial Brr, then this species was somewhat transitional between *M. pristinus* and *Eopatelliocrinus.* Relative to ontogeny, three basic changes were involved in the "mutation": changes in the Brr dimension growth rates; lateral migration and probably resorption of the "pinnule facet food groove"; and resorption of the inner side of the Brr (opposite pinnule facet). The youngest Girardeau *Eopatelliocrinus* and *Macrostylocrinus* (about 1.0 mm "size") have similar uniserial Brr and the "mutation" clearly mainly affected the later growth phases. See *M. pristinus* for more details on the growth rate divergences and the summary of Girardeau camerate ontogeny for discussion of the adaptative significance of the change.

VI. The primanal is followed by three plates in the primitive species, *i.e.* two CD interray iBrr with an anal series plate in the center. This geometry was invariant from Middle Ordovician *Glyptocrinus ornatus* to Middle Silurian *Macrostylocrinus ornatus.* The more advanced configuration, primanal plus two CD interray iBrr, first appeared in the Middle Silurian *M. laevis,* although most specimens were characterized by the primitive geometry. Apparently, the advanced CD interray was derived from the primitive one by upward displacement of the first anal series plate. Consequently, the CD interray was no longer strongly differentiated from the lateral interrays. The advanced geometry was stabilized in the Middle Silurian *Patelliocrinus ornatus.*

Exactly when the change took place during growth cannot be determined due to uncertainty about the origin of the proximal anal series plate. Certainly, the "mutation" must have exerted its effect before the CD interray iBrr formed at the IAx and lower IIBrr levels around "sizes" of 1.0 to 1.5 mm. Also, the "mutation" caused a change in the plate development sequence. The most likely sequences seem to be, listed first to last formed plates: primitive, primanal — proximal anal series plate — proximal CD interray iBrr; and advanced, primanal (CD interray iBr1 of most authors) — two CD interray iBrr — proximal anal series plate. The functional morphology is not fully appreciated although the structure of the calyx was clearly simplified. Like other similar trends, the calyx mechanical stability may have been increased while the integration and coordination trials and tribulations were lessened.

Some Middle Silurian *Macrostylocrinus* specimens have the primanal followed by four or more plates, for example, *M. meeki* (Lyon) (see Springer, 1926, pl. 4, fig. 20) and *M. laevis* Springer (see 1926, pl. 4, fig. 19). The extra plates represent additional CD interray iBrr. This is probably a variant of the above mentioned primitive type where additional CD interray iBrr formed soon after the proximalmost plates. Typically, the extra CD interray iBrr occur in specimens with large primanals and either unusually wide CD interrays or small anal series plates.

Species Annotations

Glyptocrinus ornatus — Patelliocrinus

Eopatelliocrinus scyphogracilis is believed to more closely represent the ancestral stock of *Macrostylocrinus pristinus* than *Eopatelliocrinus latibrachiatus.* This is suggested by the taxonomic distances (Table 13b) which equal (low numbers indicate greater morphological similarity):

Taxonomic Distances for Girardeau Patelliocrinids

Species	Taxonomic Distance
Eopatelliocrinus latibrachiatus versus *Macrostylocrinus pristinus*	1.035
Eopatelliocrinus scyphogracilis versus *Macrostylocrinus pristinus*	.947

This view is also consistent with the study of species level characters, such as cup shape and ornamentation, which were omitted from the phylogeny data matrix (see comparisons of species). Thus, *Eopatelliocrinus latibrachiatus* is deemed a blind end offshoot from *E. scyphogracilis* which left no descendants.

Most likely, *Macrostylocrinus pristinus* constituted the ancestral stock of Middle Silurian North American *Macrostylocrinus* rather than the contemporary *M. cirrifer.* This hypothesis is supported by three lines of evidence. Paleogeography. *M. pristinus* was a North American form whereas *M. cirrifer* lived in Scotland. Mature *M. cirrifer* may have immature biserial Brr whereas mature biserial Brr occur in *M. pristinus.* The dorsal cup ornamentation and cirri bearing stem of *M. cirrifer* are strikingly different from the North American species. *M. cirrifer* was ancestral to an undescribed Middle Silurian macrostylocrinid from the Pentland Hills of Scotland, after which this line became extinct. *M. anglicus* Jaekel (1918, p. 36, text-fig. 26) from the Wenlock of Britain was most closely related to the North American Middle Silurian species (Brower, in preparation).

The Middle Silurian *M. meeki* (see Springer, 1926, pl. 4, figs. 20-23) is seemingly primitive in the possession of wedge shaped or immature biserial Brr. However, the crinoid was probably a product of regressive evolution, having been derived from a macrostylocrinid with mature biserial Brr in the adults. The Brr and arms of *M. meeki* are narrow which implies small width growth rates relative to "size". Depending on personal philosophy, this is either consistent with or suggestive of retarded ontogeny and phylogeny.

Patelliocrinus (Middle Silurian) probably evolved from an advanced macrostylocrinid which had a tendency to develop a rectangular IBr1, pentagonal IAx, the resultant iBr1 type, and the primanal plus two configuration. Of the forms examined here, *Macrostylocrinus laevis* provides the most likely ancestral stock although some species with unknown arms are also possible.

RELATIONS BETWEEN CHARACTERS

A character correlation matrix was prepared from the original data matrix (Table 13a). Inasmuch as only one of the 10 characters was arbitrarily coded, the original data were used and standardization was omitted. Correlation coefficients (r) with significance levels above .950 are deemed meaningful; lower values were rejected. The critical r equals .71 with six degrees of freedom (eight species less 2.0). Three character complexes emerge: 1. Number of the IBr1 and IAx sides and the R, IBr1 and IAx percentage heights. The correlations range from .72 to .85 (the signs were ignored). The number of plates following the primanal may also belong to this complex (r range, .72 to .74). 2. The distal FBrr and the number of BB are also correlated, although at a lower level (.71). 3. As expected, the Brr type (*i.e.,* uniserial versus biserial) and the proximal biserial IIBrr number show strong correlation (.999).

Inspection of the original data (Table 13a) indicates that the correlations represent the progressive evolution of different characters. For example, as the IBr1 evolved from a hexagonal to a rectangular plate, the percentage IBrr height contributions declined while that of the RR was augmented.

All of the evolutionary trends can be logically interpreted as having provided adaptative significance and benefit to the crinoids concerned. This suggests that the lineage largely evolved under natural selection and that genetic drift was nil or negligible. Judging from the abundance of specimens, the population sizes of most species were probably large enough so that small selection coefficients would have comprised effective agents of evolution (see paleoecology for Girardeau species population sizes). Inasmuch as selection most likely was the driving force in this lineage, the existence of character complexes implies that the selection acted on each complex as a unit. Genetic linkage (highly general sense) is eliminated by the following reasoning. Crinoid genetics are wholly unknown and thus, provide fertile field for speculation. Assuming these are at least as complex as those of fruit flies (this seems reasonable to a crinoid specialist), probability indicates that none of the characters (*e.g.,* uniserial or biserial Brr) were single units in the genetic sense (*i.e.,* controlled by alleles at one gene locus). The diversity of the morphological characters appears too great for genetic linkage. The interpretation of each character complex as a single unit with respect to natural selection is consistent also with the adaptative significance previously postulated for the individual characters within a single complex (best seen with complex A).

ORIGIN OF THE HAPALOCRINIDAE

Culicocrinus ? girardeauensis is believed to have constituted a descendent of the *Macrostylocrinus pristinus* ancestral stock. This is supported by several strong similarities. The only known Girardeau culicocrinid has one ray with two IBrr and one with only a single plate. The crinoid is probably abnormal in this respect and the usual number of IBrr is probably two like most Hapalocrinidae. The culicocrinid IBr1 has five sides and the IAx is pentagonal. This configuration is commonly found in macrostylocrinids, but not in *Patelliocrinus* which always exhibits a rectangular IBr1 and a pentagonal IAxx. Both *Macrostylocrinus pristinus* and *Culicocrinus ? girardeauensis* possess 10 biserial arms. The overall minimum taxonomic or morphological distances are seen between *Macrostylocrinus* and *Culicocrinus ? girardeauensis.* These are with *Macrostylocrinus ornatus,* 1.048; with *M. laevis,* 1.141; and with *M. pristinus* 1.348. The Middle Silurian forms postdated the Girardeau culicocrinid; consequently, *M. pristinus* is thought to have been closest to the ancestral stock.

The principal difference between the two Girardeau crinoids is the nature of the FBrr. The mature *M. pristinus* have the IIBrr3 firmly fixed into the calyx by the adjacent iBrr. One iBr1 and two iBrr2 occur in *Culicocrinus ? girardeauensis* and these plates reach the IIBr1 mid-level. However, the iBrr do not firmly incorporate the IBrr into the dorsal cup. The responsible "mutation" was probably two-fold. The iBrr formation rates were decreased relative to *Macrostylocrinus pristinus.* Although some iBrr were formed these failed to rigidly fix the culicocrinid IBrr into the cup. The *Culicocrinus ? girardeauensis* cup was intermediate between the typical few-FBrr cup of patelliocrinids and the no FBrr calyx of most Platycrinitidae, such as *Platycrinites*. In the latter crinoids, there are no iBrr between the IBrr; these are incorporated into the tegmen as iAmbb. Also, it might be noted that the compromise type calyx achieved by *Culicocrinus ? girardeauensis* and many other Hapalocrinidae failed to achieve great success. This did not occur until the true no FBrr calyx evolved.

The Girardeau culicocrinid is only known from one specimen; clearly, the species was not successful at this time and only a small population existed. Genetic drift may have constituted a factor in its evolution. If so, this lineage survived to Early Silurian time, at least.

The Early Silurian Brassfield Limestone "Platycrinid" obviously was a direct lineal descendant of the Girardeau species. The principal evolutionary advance of the Early Silurian form constituted formation of a rectangular IBr1 and a septagonal IAx. In this, the hapalocrinid line paralleled the *Glyptocrinus ornatus* — *Patelliocrinus* group. The responsible "mutations" and adaptative significance were the same as those previously enumerated.

In general Brassfield crinoid calyces and crowns are rare. "Platycrinid" proves no exception, being known from only one specimen. Such implies a small standing crop. This may be misleading because crinoidal debris is abundant in parts of the unit. Consequently, moderate or large sized populations may have existed; these were not preserved as the environment was not suitable for rapid burial and preservation of the crowns. Thus, the "Platycrinid" population size remains unknown.

The further history of this hapalocrinid lineage was not examined in detail. The first undoubted *Culicocrinus* occur in the Early Devonian of Europe; these may or may not have evolved from *C. ? girardeauensis*. With the exception of *Culicocrinus*, all Hapalocrinidae with known arms exhibit uniserial or wedge shaped Brr. See for example, *Lyonicrinus bacca* and *Hapalocrinus* spp. in Springer (1926, pl. 11, figs. 6-23, 30-32, pl. 12, figs. 1-8). The typical hapalocrinids could have had two different origins; being either derived from the Girardeau culicocrinid line by means of regressive arm evolution or descended from uniserial armed patelliocrinids through progressive arm change.

PALEOGEOGRAPHY AND EVOLUTION

The two largest morphological breaks and associated taxonomic distances in the entire lineage are: Middle Ordovician *Glyptocrinus ornatus* — Late Ordovician *Eopatelliocrinus scyphogracilis*, 1.566; and Late Ordovician *Macrostylocrinus pristinus*, — *Culicocrinus ? girardeauensis*, 1.348. The former occurred across an unfavorable paleogeographic interval and the latter during a favorable period. One of the lowest taxonomic distances crosses the Early Silurian unfavorable time; *Macrostylocrinus pristinus*, Late Ordovician — *M. ornatus*, Middle Silurian, .552. However, the mean taxonomic distances across the paleogeographic breaks slightly exceeds the within favorable intervals figure (1.059 versus .952).

PALEOBIOGEOGRAPHY

The Middle Ordovician glyptocrinid ancestral stock was restricted to North America. *Eopatelliocrinus* is only known from the Girardeau, but late Ordovician *Macrostylocrinus* was represented in North America by *M. pristinus* and in Scotland by *M. cirrifer*. Clearly, this part of the phylogeny migrated to Europe sometime during the early part of the Late Ordovician. The only known Early Silurian element, "Platycrinid", lived in North America. The Middle Silurian Patelliocrinidae and Hapalocrinidae were diversified in both North America and Europe. At least two lines extended into the Middle Silurian. The *M. cirrifer* group was confined to Scotland and became extinct without leaving any known descendants. The more important *M. pristinus* — *Patelliocrinus* lineage inhabited both North America and Europe. Possibly, the *Patelliocrinus* stage of the latter lineage was subdivided into several parts; this remains uncertain because the European species have not been studied in detail.

Superfamily **MELOCRINITACEA** Ubaghs, 1953

Diagnosis. — Glyptocrinina with four BB; primitive many-FBrr, more or less conical calyx; primanal followed by three plates.

Family **MELOCRINITIDAE** Zittel, 1879

Diagnosis. — Melocrinitacea with variable arm structure. Primitive forms usually with four arms per ray all of which are pinnulate; IIBr2 generally axillary. In later genera, inner quarter-rays become hypertrophied into massive ray trunks which bear numerous branches; pinnulation of ray trunk is lost but ray trunk branches usually retain pinnules; outer quarter-rays remain pinnulate, if present.

Genus **ALISOCRINUS** Kirk, 1929

Type species. — By designation of Kirk, 1929, p. 343, *Mariacrinus warreni* Ringueberg, 1888, p. 133, pl. 7, figs. 4, 4a.

Diagnosis. — Melocrinitidae with generally four arms per ray; IIBr2 or rarely IIBr3 axillary; all arms fully pinnulate; some individuals lack IIAx in one half-ray; consequently these rays only bear three arms; inner quarter-rays branch in one questionably assigned species.

Remarks. — The above diagnosis follows that of Kirk except that allowance is made for individuals with three armed rays, and new knowledge about *A. carleyi.* At present, only three species can be reasonably well assigned to the genus; *A. warreni* Ringueberg, the type species, *A. tetrarmatus,* and probably *A. laevis* Kirk (1929, p. 344). The latter is only known from a single dorsal cup, the holotype (S. 249); the highest preserved plates consist of IIIBrr3 (see Springer, 1926, p. 29, pl. 5, figs. 9, 10; listed as *Mariacrinus carleyi*). Consequent to the absence of well-preserved arms, the placement of this specimen in *Alisocrinus* remains uncertain.

Two species which were referred to *Alisocrinus* by Kirk are questionably assigned: 1. *A. carleyi* (Hall) (see 1879, p. 132, pl. 14, figs. 7-10). Most specimens consist of calyces which lack arms. Examination of one partial crown (S. 251) indicates that the inner quarter-rays branch on IIIBrr8 whereas the outer quarter-rays are unbranched. Most of the IIIBrr of S. 251 are incorporated into the dorsal cup but some of the inner quarter-ray fixed-IIIBrr appear to have fixed pinnules. However, the specimen is not well preserved and the interpretation of the fixed pinnules could be incorrect. Because of the probable inner quarter-ray pinnules and despite the IIIBrr8 branches, the species is tentatively retained in *Alisocrinus* rather than being placed in *Promelocrinus.* 2. *A. aureatus* (Miller) (1891-1892, p. 644, pl. 6, fig. 36). The holotype (Springer collection) shows that the proximal part of the arms and the inner quarter-ray IIIBr2 is clearly axillary. Only a few higher Brr are seen. The IIIBrr1 lack pinnules; however, this characterizes all primitive monocyclic camerates with axillary IIIBrr2. This form is clearly not congeneric with the species definitely grouped in *Alisocrinus.* Nevertheless, the crinoid is retained in the genus with much reservation because there is no evidence to place the species elsewhere.

Alisocrinus is closely related to 20 uniserial armed species of *Glyptocrinus* (Hall, 1847, p. 281), such as *G. decadactylus* Hall (1847, p. 281, pl. 77, figs. 1a-f, pl. 78, figs. 1a-u; see also Wachsmuth and Springer, 1897, p. 270, pl. 6, fig. 12, pl. 20, figs. 4a-e, pl. 21, figs. 4a, b). These glyptocrinids are easily separated from *Alisocrinus* by the presence of five rather than four BB.

Alisocrinids are also similar to primitive species of *Promelocrinus,* namely *P. fulminatus* (Angelin) (1878, p. 2, pl. 26, fig. 14; see Ubaghs, 1958, pl. 1, figs. 2-4, text-figs. 3, 4) and *P. radiatus* (Angelin) (1878, p. 7, pl. 10, figs. 1, 2, pl. 27, fig. 7; see Ubaghs, 1958, pl. 2, text-figs. 5-7). In these forms the inner quarter-rays generally branch once (*P. fulminatus*) or twice (*P. radiatus*). Pinnules are lost along the proximal parts of these quarter-rays. The outer quarter-rays remain unbranched and retain all pinnules. All arms are uniserial. The primitive promelocrinid inner quarter-ray branching pattern and loss of pinnules distinguishes them from alisocrinids.

The type species of *Promelocrinus, P. anglicus* Jaekel (1902, p. 1068, fig. 8; see also Springer, 1926, p. 27, pl. 5, figs. 2, 3, listed as *Melocrinus ? spectabilis*), shows much more specialization. The inner quarter-rays are modified into non-pinnulate ray trunks which bear numerous biserial pinnulate branches. The outer quarter-rays are biserial, pinnulate, unbranched and small relative to the ray trunks.

Occurrence. — Upper Ordovician and Middle Silurian, North America.

ALISOCRINUS TETRARMATUS, n. sp.

Plates 66, 67; Plate 68, fig. 3; Text-figures 29, 30, 33i

Diagnosis of adult. — A species of *Alisocrinus* with moderately widely expanding dorsal cup; mature crinoids with single nodes on iBrr; sometimes stellate ridges or elements thereof occur on iBrr and adjacent ray plates. Arms unbranched, four per ray; Brr moderately high relative to width.

Partial description of adult. — Most of the description follows in the sections on ontogeny and variation.

BB four, three small BB and one large B in normal specimens; large B with sutures in B and E ray positions.

Proximal iBrr large and regular; iBr1 range with one plate; iBr2 range consists of two or three plates; iBrr3 composed of two to four plates; proximal iBrr generally terminate at IIBr1 level. Distal iBrr small and irregular; each range with three to five plates; up to 10 ranges known.

Proximal inter-half-ray iBrr1 large and regular; iBr1 inserted between IIBrr1 of same ray, followed by two or three plates in next two ranges; third range at level of IIAx. Higher iBrr made up of small, irregular plates, in seven to 10 ranges; each range has three or four plates.

Inter-quarter-ray iBrr begin with single plate between adjacent IIIBrr1; followed by five to seven ranges, each consisting of two to four small irregular plates.

Primanal followed by three plates; anal series plates large; CD interray iBrr smaller than anal series plates; one plate at primanal level; higher ranges comprise one or two plates; CD interray iBrr2 usually located at IAx level.

Articular surfaces of dorsal cup plates smooth; tegmen unknown.

Depth of free Br equals or exceeds width by up to 20%. Articular surfaces probably smooth. Cross section of food groove roughly V-shaped with rounded base; ventral margins reflexed outward; food groove depth is about 55%

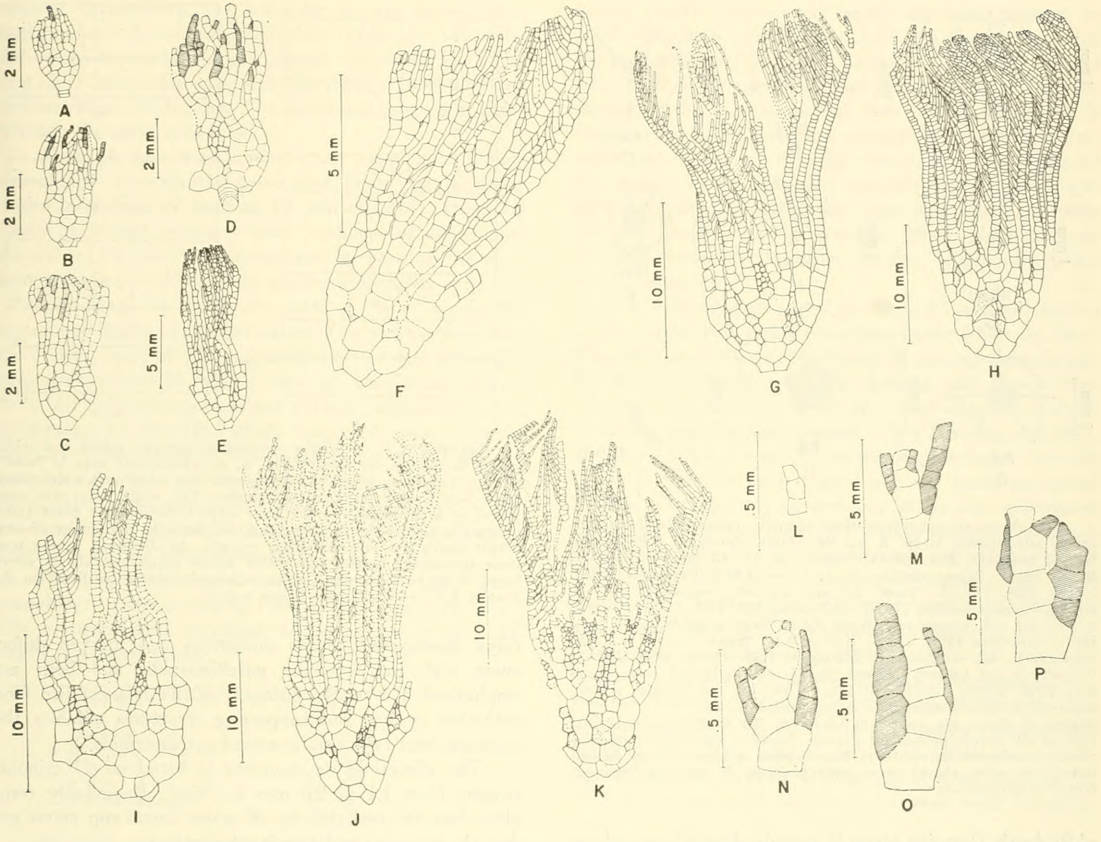

Text-figure 29. — *Alisocrinus tetrarmatus*, n. sp., Girardeau Limestone. A-F and L-N are "young assemblage" crinoids; G-K, O and P depict adult "assemblage" animals. Figures C and D show "young assemblage" animals with three arms in one ray. H illustrates the only known mature crinoid of this type. All other figures are of normal variants with four arms in all rays.

A.-K.— Crowns.

A. — Paratype, IGS. 35P-35, lateral or CD interray view of smallest crinoid, "size" 1.1 mm, Orchard Creek exposure. B. — Paratype, USNM 164 586, lateral view, "size" 1.4 mm, Cape Rock exposure. C. — Paratype, IGS. 35P-34, D ray, "size" 1.8 mm, Orchard Creek exposure. D. — Paratype, IGS. 35P-36, C and D rays?, "size" 2.0 mm, Orchard Creek exposure. E. — Paratype, Univ. Ill. X-4672, lateral view, "size" 2.4 mm, Cape Rock exposure. F. — Paratype, UNSM 164 587, lateral view, "size" 3.4 mm, Cape Rock exposure. G. — Paratype, USNM 164 580, C ray, "size" 4.2 mm, Orchard Creek exposure. H. — Paratype, YPM. 27029, CD interray, "size" 5.5 mm, Cape Rock exposure. I. — Paratype, USNM 164 581, D ray, "size" 5.9 mm, Cape Rock exposure. J. — Paratype, YPM. 27028, lateral view, "size" 6.4 mm, Cape Rock exposure. K. — Holotype, USNM 164 579, lateral view, "size" 9.0 mm, Cape Rock exposure.

L.-P. — Distal arm fragments.

L. — From paratype USNM 164 586. M. — From E ray of paratype IGS. 35P-34. N. — From center ray of paratype Univ. Ill. X-4672. O. — From B ray of paratype USNM 164 580. P. — From C ray of paratype YPM. 27029.

Symbols: Pinnules ruled on arm fragments and smallest crowns. The iBrr are stippled.

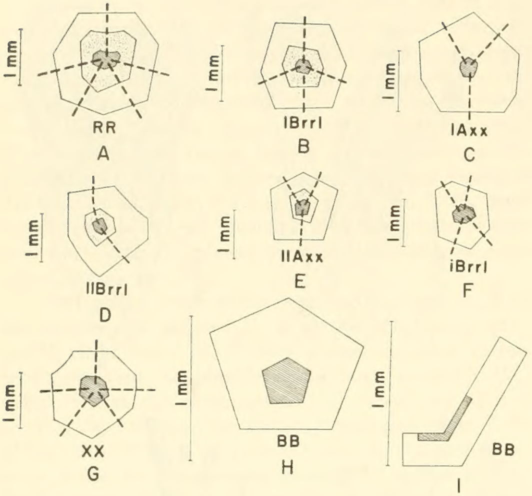

Text-figure 30. — Superpositions of major calyx plates for *Alisocrinus tetrarmatus*, n. sp. A. — RR plates. Paratypes IGS. 10486/ USNM 164 587/ IGS. 35P-35. "Sizes" 6.6, 3.4, 1.1 mm, respectively. B. — IBrrl. Same crinoids as A. C. — IAxx. Paratypes YPM. 27028/ IGS. 35P-35. "Sizes" 6.4 and 1.1 mm, respectively. D. — IIBrrl. Paratypes YPM. 27028/ USNM 164 587/ IGS. 35P-35. "Sizes" 6.4, 3.4, 1.1 mm, respectively. E. — IIAxx. Same crinoids as D. F. — iBrrl. Paratypes YPM. 27028/ IGS. 35P-35. "Sizes" 6.4 and 1.1 mm, respectively. G. — Primanal. Paratypes IGS. 10486/ IGS. 35P-34. "Sizes" 6.4 and 1.8 mm, respectively. H. — BB, lateral view. Paratype YPM. 27028/ USNM 164 586. "Sizes" 6.6 and 1.4 mm, respectively. I. — BB, cross-section. Same crinoids as H.
Shapes of plates are somewhat idealized. BB thickness assumed at 12% of RR height throughout growth. Smallest plate ruled; middle-sized one stippled (if present); biggest plate is blank. Heavy dashed lines show main aboral nerve cord positions as deduced from external ornamentation.

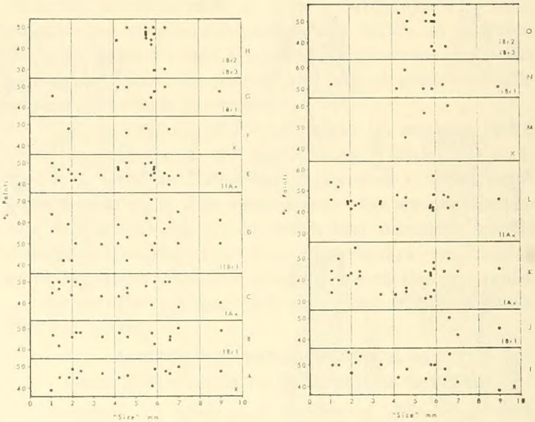

Text-figure 31. — Graphs showing percentage height and width points in *Alisocrinus tetrarmatus*, n. sp. Horizontal axis is "size"; vertical axis gives height or width point. The height and width points were located by external ornamentation. The width point was computed as a percentage of the total width; the smaller point (50% or less) is always shown. Percentage height is the percentage of total height above the proximal plate margin. As discussed in the text, these percentage height and width points locate the aboral nerve knots. A.-H. — Percentage width points; the plates are listed on the graphs. I.-O. — Percentage height points.

of Br depth. Covering plates in irregular biserial rows, about four or five rows per Br.

Pinnular articular surfaces probably smooth; food groove cross section as in mature Br; covering plates biserial, roughly four or five pairs per pinnular.

Proximal column observed, round; columnals united by crenulate suture; articular surfaces not seen. Columnals consisting of at least two orders: Order 2 thickness about .23 mm in 6.4 mm "sized" animal, nodose; Order 1 thickness .13 mm in same specimen, columnals less nodose. Order formula variable; for example, listed from proximal to distal: 2-1-1-2 and 2-1-1-1-2; such suggests a third order is present which cannot be separated from the other Order 1 types.

Ontogeny. — *Alisocrinus tetrarmatus* is the only many-FBrr camerate of which the ontogeny is fully treated. The alisocrinid growth seems typical for such crinoids. The calyx development shows similarities and marked differences with the few-FBrr patelliocrinids, and both are emphasized. Conversely, ontogeny of the uniserial Brr, food gathering system and supporting structures exhibits the same patterns as in similar-armed patelliocrinids.

The alisocrinid development is based on 23 crinoids ranging from 1.1 to 9.0 mm in "size". Reasonably complete data are available for all major dorsal cup plates except the primanal and associated elements.

The alisocrinid "size" distribution follows the usual bimodal pattern (Text-figs. 1c, d). The seven young crinoids range from 1.1 to 3.4 mm in "size" whereas the 14 adults fall into the 4.2 to 9.0 mm interval. Presumably the *A. tetrarmatus* "young" and "adult assemblages" correspond to those of the patelliocrinids "spatfall" ages.

Unlike the Girardeau eopatelliocrinids, the two alisocrinids are not discussed together because the two species are not closely related and the data are not comparable.

Dorsal cup growth. — (Tables 14, 15; Text-figs. 29-32). Text-figure 30 illustrates the plate superpositions for this species. The constructions parallel those of *Eopatelliocrinus scyphogracilis* and *Macrostylocrinus cirrifer.* The mature alisocrinids possess well developed median-ray and lateral RR ridges with traces of stellate ridges. These locate the original aboral nerve cord knots for the ray plates, iBrr1 and primanal. In addition, the iBrr1 have nodes which occur where the stellate ridges join on the plate. The iBrr2 and iBrr3 bear nodes on or near the plate centers, although stellate ridges are lacking. The nodes are believed to have overlain the nerve cord knots.

Although the ornamentation is not complete in "young assemblage" crinoids, the nerve cord knots can be determined in crinoids as small as 1.1 mm in "size". These are found by similar means to those outlined for adults over the 2.0 to 3.4 mm "size" range and by plotting the most convex areas of the plates in smaller individuals.

Text-figure 31 shows the plots of "size" versus the percentage height and width points. The width points vary more than those of the patelliocrinids and the alisocrinid points range from 38 to 50% although most equal 45% or more. All width points remained constant throughout ontogeny except for the IIBr1 which "migrated" away from the ray axis in older crinoids. The width points denote roughly symmetrical width growth rates away from the ray axis for all plates except the IIBr1. The percentage height points were constant, "migrated" distally, or "moved" proximally, depending on the plate involved.

The plate thickness is only known in three "adult assemblage" crinoids ranging from 5.8 to 6.6 mm in "size". The measurements, expressed as percentages of the RR height, are listed below:

IIBr1 side	7.5%
IIBr1 center	21 %
IAx side	13 %
IBr1 side	11 %
IBr1 center	24 %
R side	24 %
B distal margin	12 %

Although the data are incomplete, they stamp *A. tetrarmatus* as a thin plated crinoid like most Girardeau camerates.

The most striking contrasts between dorsal cup development of the many-FBrr alisocrinid and the few-FBrr patelliocrinids are treated later in detail. In outline form, these were: differences in the FBrr incorporation rates and correlated characters; and divergences in the "size" growth vectors relative to RR height.

The maximum and minimum RR heights equal 2.5 and .40 mm which correspond to predicted widths of 2.7 and .61 mm, respectively (Text-fig. 32b). The width growth rate consisted of 1.0 mm per 1 mm height increment. The percentage height points ranged from 51% in the smaller crinoids ("size" 1 to 2 mm) to 47% over the 6 to 7 mm "size" interval. The young crinoid proximal and distal height growth vectors were nearly the same whereas in older individuals, the distal growth rate slightly exceeded the proximal one (Text-figs. 30a, 31a, i). The RR retained hexagonal or septagonal shapes throughout ontogeny although height/width increased from .66 to .93. The R-R suture distal margin migrated proximally on the CD interray of older crinoids (Text-figs. 29a, c, g-i); this is related to changes in the primanal proximal and distal height growth vectors. In lateral interrays, this suture probably did not change position (Text-figs. 29b-d, j, k). Also the RR-IBr1 suture became wider relative to the plate width during ontogeny.

The IBr1 heights range from .25 to 2.5 mm with widths of .43 and 2.4 mm, listed in the same order (Text-fig. 32c). The width growth rate constituted .88 mm per 1 mm height increase. The percentage height point is only known from three crinoids in the 6.6 to 9.0 mm "size" range over which the points was stabilized at about 45% (Text-figs. 30b, 31j). The distal height growth vector was slightly larger than the proximal one. The IBr1 is fixed into the dorsal cup of all crinoids. Consequently, a constant shape was maintained throughout growth of each plate, usually hexagonal although several pentagonal or rectangular ones are present (Text-figs. 29b-d). All "adult assemblage" crinoids have hexagonal IBrr1; the non-hexagonal ones are confined to "young assemblage" animals. The height/width rose from .58 to 1.0. The young crinoid lateral IBr1 margins are relatively straight or rounded; in mature crinoids, more angular margins are observed and the IBr1-iBr2 junction projects into the interray. This was caused by augmenting the mid-IBr1 width growth rates relative to the proximal ones (Text-figs. 29a-d, i-k). Because of this, the adjacent parts of the iBr1 or the primanal became constricted with increasing "size".

The minimum and maximum IAx heights consist of .30 and 2.6 mm which correspond to widths of .45 and 2.45 mm, respectively (Text-fig. 32d). The width growth vector equalled .88 mm per 1 mm additional height. The percentage height point most likely fell slightly, being about 43% in young crinoids and roughly 41% in the larger individuals (Text-figs. 30c, 31k). The distal height growth vectors greatly exceeded the proximal ones. The IAx is partly or wholly fixed into the calyx of all crinoids, and the number of sides was the same throughout ontogeny. Normal crinoids possess septagonal plates although a few five or six-sided one occur in young crinoids. The immature specimen IAx lateral margins are angular, and this configuration underwent little change during ontogeny (Text-figs. 29a-d, i-k; 30c). The plate height/width rose from .67 to 1.1. The angle between the IAx-IIBr1 sutures is relatively small in young crowns but was augmented with increasing "size". Evidently this is related to the problem of supporting the growing food gathering system as in the patelliocrinids.

The iBr1 height range equals .30 to 2.0 mm and the widths are .34 and 1.6 mm (Text-fig. 32g). The width growth rate comprised .75 mm per 1 mm height increment. The usual iBr1 has six sides and incorporates the young crinoid IBr1 or the IAx lower margin into the calyx (Text-figs. 29a-c). Generally, the plate terminates at the mid-IBr1 level and the hexagonal shape was maintained throughout life. The height/width increased from .88 to 1.2 over the growth sequence. The iBr1 mid-level width was progressively constricted relative to the proximal width due to expansion of the adjacent IBr1-iBr1-iBr2 junctions (Text-figs. 29a-d, i-k). The iBr1 percentage height points were constant at 50 to 52% indicating equal or nearly equal proximal and distal height growth vectors (Text-figs. 30f, 31n). The RR percentage height point "migrated" proximally and the IBr1 data denotes a constant point. These relations occurred because the RR-iBr1 intersections were stabilized relative to the RR center and the IBr1-iBr1-iBr2 junction "moved" downward on the IBr1 with increasing "size" (Text-figs. 29a-d, i-k).

The iBrr2 growth is less well documented than that of the iBr1 (Text-fig. 32h). The smallest and largest plate heights equal .28 and 1.6 mm which correspond to .17 and 1.5 mm widths, respectively. The width growth rate per 1 mm of height increase was larger than that of the iBr1 and comprised 1.0 mm. The known percentage height points show great variability and range from 36 to 54%; no consistent developmental trend is apparent. The plate shapes are not stable and five to seven-sided plates are seen; the number of sides remained the same after the iBrr2 fixed the IIBr1 lower margins into the calyx. During ontogeny, the height/width decreased from 1.6 to 1.1, in contrast to the augmented ratio of the adjacent ray plates.

Primanal data are available from six crinoids (Text-fig. 32f). The greatest and least heights equal 2.0 to 2.2 mm and .60 mm which correspond to widths of roughly 1.8 and .48 mm. The width growth rate was .91 mm per 1 mm of additional height. The percentage height point showed major "migration" throughout ontogeny, ranging from 37% in the 1.85 mm "sized" crown to 60% in the 6.6 mm individual (Text-figs. 30g, 31m). The distal height growth rate greatly exceeded the proximally oriented vector in immature animals whereas the reverse occurred in adults. At least part of this change is related to ontogenetic changes in the surrounding plates. During the RR development, the percentage height point "moved" proximally. This dictated an increment in the primanal proximal height growth rate. Also, elongation and proximal migration of the C and D ray RR-primanal sutures aided in causing the primanal height growth rate changes (Text-figs. 29c, g, h, i). The few IBr1 percentage height point data obscure the relations between this plate and the primanal. However, the slight proximal shift of the IBr1-primanal-CD interray iBr1 junction decreased the primanal distal height growth rate relative to the proximal one.

The IIBr1 minimum and maximum heights consist of .25 and 2.1 mm whereas the equivalent widths are .24 and 2.0 mm (Text-fig. 32e). The width growth vector was .97 mm per 1 mm height increment. The height/width remained at 1.0. The percentage height points cannot be located. The 1.1 to 2.4 mm "size" crinoid percentage width point is roughly 53% (measured away from the ray axis) and the same figure for 5 to 7 mm "sized" crinoids equals 56% (Text-figs. 30d, 31d). The width growth rate toward the ray axes exceeded the interray width component, and this partly accounts for the gradual interray constriction which culminated in adult crinoids (Text-figs. 29a-d, i, k). The lateral interray IIBr1 was fixed into the cup at "sizes" ranging from 2.0 to 3.0 mm (Text-fig. 29e). Before incorporation, the IIBrr1 sides are joined together along the ray axis; the interray sides are free and straight or curved. When first fixed into the calyx by the iBrr3 and iBrr4, the juvenile configuration was retained. Soon after, the IIBr1 interray side became more angular because the mid-level plate growth vectors were accelerated with respect to the proximal and distal ones (Text-figs. 29a-c, d, e, i, k). Also, the IIBr1-IIBr1 suture distal margin migrated proximally with increasing age, which was correlated with the insertion of inter-half-ray iBrr.

The IIAx development was similar to that of the IAx. The percentage height point was stabilized at 45% indicating that the distal height growth rates were larger than the proximal ones throughout ontogeny. Prior to interray fixation at about a 5 mm "size" and inter-half-ray incorporation at roughly 4 mm, the plate was pentagonal. During or soon after fixation, angular lateral margins formed, and seven or more sides developed (Text-figs. 29a-d, i, k). Like all axillaries, the angle between the IIAx-IIBr1 sutures flattened out with increasing age.

The maximum and minimum IIIBrr2 heights comprise 1.2 and .30 mm with corresponding widths of 1.1 and .27 mm, listed in the same order; the width growth rate equalled .90 mm per 1 mm height increase. The height/width was 1.1 throughout growth. Before fixation, the plate has

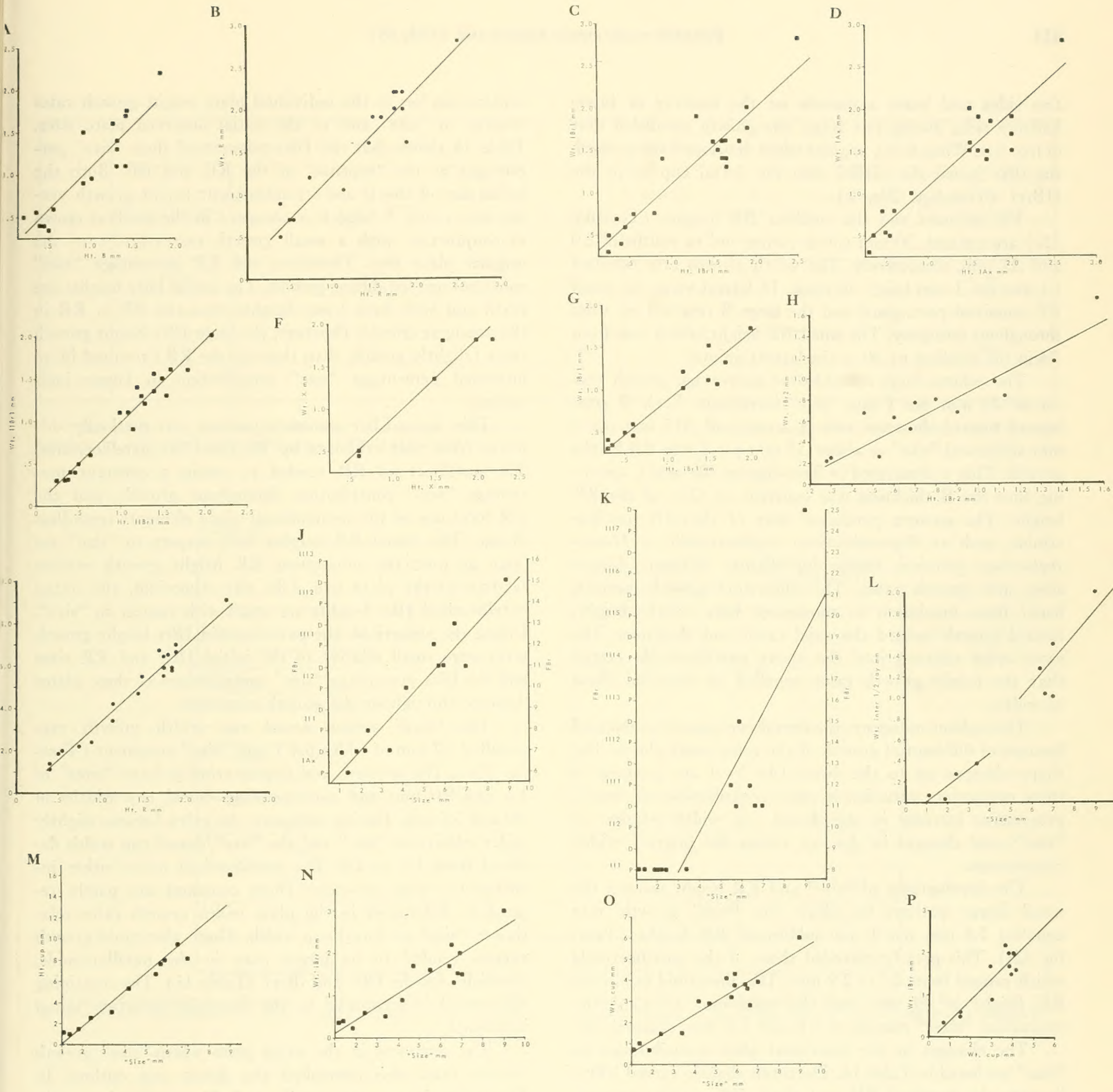

Text-figure 32. — Graphs showing calyx growth of *Alisocrinus tetrarmatus*, n. sp. X denotes primanal. FBrr scales are given in both the numerical scale used for computer purposes and the plate scale (*i.e.*, IAx, IIBr1 — II1, etc., P refers to proximal margin, D represents distal margin). J gives the FBrr in lateral interrays. K shows the FBrr in inter-half rays.

Equation data:
A — $y = .0494 + 1.06x$. $r = .903$.
$\sigma y\% = 32.1$. $N = 17$.
B — $y = .207 + 1.00x$. $r = .954$.
$\sigma y\% = 15.8$. $N = 18$.
C — $y = .209 + .882x$. $r = .937$.
$\sigma y\% = 20.0$. $N = 20$.
D — $y = .191 + .879x$. $r = .933$.
$\sigma y\% = 18.9$. $N = 19$.
E — $y = -.000765 + .966x$. $r = .976$.
$\sigma y\% = 12.7$. $N = 20$.
F — $y = -.016 + .913x$. $r = .959$.
$\sigma y\% = 14.1$. $N = 6$.
G — $y = .113 + .748x$. $r = .957$.
$\sigma y\% = 14.0$. $N = 13$.
H — $y = -.117 + 1.02x$. $r = .938$.
$N = 12$.
I — $y = -.327 + 3.62x$. $r = .982$.
$\sigma y\% = 12.4$. $N = 20$.
J — $y = 4.95 + 1.08x$. $r = .952$.
$\sigma y\% = 9.3$. $N = 13$.
K — $y = 2.30 + 1.88x$. $r = .542$.
$\sigma y\% = 30.0$. $N = 8$.
L — Young crinoids: $y = -.141 + .149x$. $r = .890$.
$N = 4$. Mature animals: $y = -.257 + .231x$. $r = .705$. $N = 6$.
M — $y = -.179 + 1.70x$. $r = .970$.
$\sigma y\% = 43.9$. $N = 13$.
N — $y = -.188 + .311x$. $r = .914$.
$\sigma y\% = 43.9$. $N = 15$.
O — $y = -.0770 + .618x$. $r = .940$.
$\sigma y\% = 19.0$. $N = 16$.
P — $y = -.118 + .503x$. $r = .945$.
$\sigma y\% = 21.2$. $N = 16$.

five sides and bears a pinnule on the interray or inter-half-ray side; during this stage, the growth paralleled that of free Brr. When fixed, angular edges developed along which the iBrr joined the IIIBr2 into the dorsal cup as in the IIBrr1 (Text-figs. 29g, k).

The greatest and the smallest BB heights (Text-fig. 32a) are 1.8 and .20 mm which correspond to widths of 2.0 and .27 mm, respectively. The width growth rate equalled 1.1 mm per 1 mm height increase. In lateral view, the small BB remained pentagonal and the large B retained six sides throughout ontogeny. The small BB height/width rose from .74 in the smallest to .90 in the largest animal.

The column facet expanded at an average growth vector of .23 mm per 1 mm "size" increment. Each B grew inward toward the stem axis at a mean of .115 mm per 1 mm additional "size" or about .55 mm per 1 mm BB height growth. This is illustrated in Text-figures 30h and i, assuming that the B thickness was constant at 12% of the RR height. The pattern paralleled that of thin-BB patelliocrinids, such as *Eopatelliocrinus scyphogracilis* or *Macrostylocrinus pristinus* except for slightly different dimensions and growth rates. The alisocrinid growth vectors, listed from maximum to minimum, were width, height, inward growth toward the axial canal and thickness. The same order characterized the above patelliocrinids except that the height growth rates equalled or exceeded those of width.

Throughout ontogeny, the dorsal cup geometry changed because of differential growth of the component plates. The shape changes up to the distal IAx level are grouped in three categories: variation in plate contributions to "size"; progressive increase in the dorsal cup width relative to "size"; and changes in the ray versus the interray width components.

The development of "size" and RR height showed the usual linear pattern in which the "size" growth rate equalled 3.6 mm per 1 mm additional RR height (Text-fig. 32i). This greatly exceeded those of the patelliocrinids which ranged from 2.3 to 2.9 mm. The alisocrinid minimum RR height is .40 mm and the maximum 2.5 mm; the equivalent "sizes" consist of 1.1 and 8.7 mm, respectively.

The changes in the individual plate contributions to "size" are listed in Table 14. The totals slightly exceed 100% because the proximal RR and distal BB margins overlap. The young alisocrinid dorsal cup geometry is largely dominated by the BB and RR as in immature patelliocrinids. The mature alisocrinids have a calyx in which the RR and IBrr comprise equal percentage elements and the BB are subordinate (Table 14; Text-figs. 29a-d, i-k). The explanation lies in the individual plate height growth rates relative to "size" and to the initial observed plate sizes. Table 14 shows that the IBrr augmented their "size" percentages at the "expense" of the RR and BB. Both the initial size of the B and its subsequent height growth vector were small. A large R is observed in the smallest crown in conjunction with a small growth rate relative to the original plate size. Therefore, the RR percentage "size" contributions fell during growth. The initial IBrr heights are small and both have lesser heights than the BB or RR in the youngest crinoid. However, the large IBrr height growth rates (slightly greater than those of the RR) resulted in an increased percentage "size" contribution in larger individuals.

This many-FBrr camerate pattern was markedly different from that exhibited by the few-FBrr patelliocrinids. The patelliocrinid RR tended to retain a constant percentage "size" contribution throughout growth, and the RR form one of the predominant plate elements regardless of age. The initial RR heights with respect to "size" are large as were the subsequent RR height growth vectors relative to the plate size. Like the alisocrinid, the initial patelliocrinid IBrr heights are small with respect to "size". Unlike the alisocrinid, the patelliocrinid IBrr height growth rates were small relative to the initial IBrr and RR sizes and the IBrr percentage "size" contributions of these plates declined throughout the growth sequences.

The "size" versus dorsal cup width growth rate equalled .62 mm of width per 1 mm "size" increment (Text-fig. 32o). The smallest and largest crinoids have "sizes" of 1.1 and 9.0 mm and corresponding dorsal cup widths of .60 and 5.5 mm. During ontogeny, the calyx became slightly wider relative to "size" and the "size"/dorsal cup width declined from 1.8 to 1.6. The patelliocrinid ratios either increased or were constant. These contrasts are partly related to differences in the plate width growth rates relative to "size" or dorsal cup width. These alisocrinid growth vectors tended to be larger than in the patelliocrinids, especially for the IBrr and iBrr1 (Table 15). The remaining differential is attributed to the dissimilar equation initial intercepts.

The contrasts in the calyx plate width-"size" growth vectors rates also controlled the dorsal cup outline. In *Eopatelliocrinus scyphogracilis* and *Macrostylocrinus pristinus*, the young crinoids possess dorsal cups which expand rapidly in the distal direction whereas the adults show steeper walled calyces, especially at the distal RR and IBrr levels. The alisocrinid dorsal cup expansion angles were wide throughout ontogeny (Text-figs. 7, 21, 29). The aliso-

Table 14

	Youngest Crinoid ("size", 1.1 mm)		Oldest crinoid (size, 9.0 mm)		
	Plate height	Equation % of "size" represented by plate height	Plate height	Equation % of "size" represented by plate height	Plate height growth rate per 1 mm "size" increase
B	.33 mm	30%	1.7 mm	19%	.18 mm
R	.43 mm	39%	2.5 mm	28%	.27 mm
IBr1	.17 mm	15%	2.4 mm	27%	.28 mm
IAx	.27 mm	25%	2.5 mm	28%	.28 mm
Totals	1.20 mm	109%	9.1 mm	102%	

Table illustrating changes in the "size" components during the ontogeny of *Alisocrinus tetrarmatus*, n. sp. The totals slightly exceed 100% because the distal B margin overlaps the proximal R margin.

Table 15

	Alisocrinus tetraramatus, n. sp.	Macrostylocrinus pristinus, n. sp.	Eopatelliocrinus scyphogracilis, n. gen., n. sp.
"Size"/dorsal cup width of youngest crinoid	1.8	1.4	1.2
"Size"/dorsal cup width of oldest crinoid	1.6	1.8	2.2
Growth rate of plate width per 1 mm "size" increment			
BB	.22 mm	.19 mm	.23 mm
RR	.28 mm	.30 mm	.29 mm
IBr1	.26 mm	.23 mm	.20 mm
IAx	.27 mm	.23 mm	.18 mm
iBr1	.17 mm	–	.13 mm

Table illustrating the ontogeny of the "size"/dorsal cup width in *Alisocrinus tetrarmatus*, n. sp., *Eopatelliocrinus scyphogracilis*, n. gen., n. sp. and *Macrostylocrinus pristinus*, n. sp. and the relationship thereof to the width growth rates of the plates involved.

crinid BB and iBr1 width growth rates per 1 mm "size" increase were the smallest whereas the equivalent figures for the RR and IBrr ranged larger and roughly equal to each other. The patelliocrinids showed small BB, IBrr and iBr1 width-"size" growth vectors in conjunction with a large RR width value (Table 15). Consequently, the distal part of the patelliocrinid calyx was steepened during ontogeny whereas the alisocrinid retained a wider and more constant expansion angle.

"Size" and iBrr width had a .31 mm width growth rate per 1 mm of additional "size" (Text-fig. 32n). The smallest and largest crowns are 1.1 and 9.0 mm in "size" with iBrr widths of .35 and 3.4 mm, respectively. Linear relations characterized dorsal cup width versus iBrr width with a .50 mm iBrr width growth vector per 1 mm cup width (Text-fig. 32p). The maximum and minimum dorsal cup widths equal 6.0 and .70 mm which correspond to iBrr widths of 2.9 and .24 mm. During ontogeny, the dorsal cup width/iBrr width dropped from 2.9 to 2.1 denoting that the iBrr areas expanded relative to the total width. This is related to the differential development of the IAx and the adjacent iBrr2. The IAx width growth rate equalled .88 mm per 1 mm height increment whereas the iBr2 vector was 1.0 mm. Consequently, the iBrr areas spread at the expense of the IAx level rays. Below the IAx, the growth vectors were reversed and the IBr1 width growth rate comprised .88 mm per 1 mm additional height whereas the same iBr1 value was only .75 mm.

The development of "size" versus lateral interray FBrr followed a straight line in which the numerical scale FBrr growth rate equalled 1.1 per 1 mm "size" increment (Text-fig. 32j). The youngest crinoids, "size" 1.1 to 1.85 mm, have the IAx fixed into the dorsal cup (Text-figs. 29a-c). When a 2.4 mm "size" was attained, the IIBr1 lower margin comprised part of the calyx (Text-fig. 29e). The highest FBr of individuals in the 5.9 to 7.0 mm "size" interval ranges from the IIBr2 distal edge to the upper part of IIIBr1. The IIIBr2 distal margin forms the highest FBr in the 9.0 mm "sized" animal.

This was strikingly different from that of the few-FBrr patelliocrinids. Both young alisocrinids and patelliocrinids, "size" range about 1.0 to 1.5 mm, show various parts of the IAxx incorporated into the dorsal cup. The divergences between the two types occurred during later development. In all few-FBrr types examined, the ontogeny of "size" versus lateral interray FBrr followed a curvilinear pattern in which the highest FBrr incorporation rates were found in young crinoids and the vectors declined with progressive age. The patelliocrinid initial FBrr fixation rates ranged from 1.7 to 1.9 (numerical scale), and the mature crown FBrr fixation vectors varied from .30 to .60 per 1 mm "size" increment. The many-FBrr alisocrinid had a constant 1.1 FBrr growth rate per 1 mm of additional "size". Most many-FBrr camerates were characterized by linear patterns (*e.g., Alisocrinus tetrarmatus, A. ? heterodactylus, Glyptocrinus decadactylus*, and *Ptychocrinus splendens*), although a few many-FBrr types possessed exponential development like the patelliocrinids (*e.g., Ptychocrinus fimbriatus*). Regardless of the "size" versus FBrr pattern, many-FBrr crinoids always exhibited somewhat higher average FBrr incorporation vectors than few-FBrr ones. However, the basic difference between the few and many-FBrr types is the more extensive development of the inter-half-ray iBrr and higher order iBrr, if present, in many-FBrr camerates.

The ontogeny of "size" versus CD interray FBrr is known from seven individuals. An exponential regression line is observed which is intermediate between the few-FBrr patelliocrinids and the typical many-FBrr camerates. The earliest numerical scale FBrr development rate equalled 2.3 whereas the adult crinoid figure was .43 per 1 mm "size" increment; the mean consisted of .82. The smallest crinoid, "size" 1.85 mm, has the IAx distal margin fixed into the CD interray. The IIBr2 upper edge forms the distal FBr of the 6.6 mm crinoid. The FBrr were incorporated less rapidly along the CD interray than in the lateral interrays. This may indicate that the FBrr reduction during evolution of some camerates first occurred flanking the CD interray. In other camerates, FBrr were added and perhaps this began in the lateral interrays.

Although the FBrr incorporation rates and patterns differ in many versus few-FBrr crinoids, the mechanisms of plate fixation were the same. The angular Brr sides first appeared when the plate was being incorporated into the calyx. After fixation, the FBrr became more angular for a short period (Text-figs. 29d, i-k).

Also the pinnules were joined into the dorsal cup in similar fashions. Where the many-FBr pinnular incorporation proceeded to its ultimate end, the fixed pinnulars sometimes lost their identity and cannot be distinguished from the iBrr (*e.g.*, IIIBr3 pinnules in Text-fig. 29k; most scyphocrinitid fixed pinnules, Springer, 1917). In others, the fixed pinnule retained its identity and can be traced by a longitudinal ridge along the pinnule (*e.g.*, IIBr2 pinnules of *Alisocrinus ? heterodactylus* and *Glyptocrinus dyeri*, see Wachsmuth and Springer, 1897, pl. 20, figs. 1a-c, pl. 21, figs. 3a-f). The partly fixed pinnules of the few-FBrr camerates examined here remained identifiable throughout growth and were not submerged in the iBrr.

The proximal IIBrr1 inner margins were joined and higher Brr were not fixed in the inter-half-rays over the "size" range of 1.1 to 3.4 mm (Text-fig. 32k). Later, FBrr were incorporated rapidly into the inter-half-rays at a constant numerical scale fixation rate of 1.9 per 1 mm "size" increment. This exceeded the equivalent 1.1 lateral interray FBrr figure. Wide variation exists and the percentage standard deviation equals 30% compared to 9.3% for the lateral interray FBrr. The development of the inter-half-ray FBrr was poorly integrated and coordinated with the calyx "size" growth (correlation $= .54$, $N = 8$). A larger value is observed for "size" versus the lateral interray FBrr ($r = .95$, $N = 13$) which denotes a much more sophisticated degree of integration and coordination. The crowns ranging from 5.5 to 7.0 mm in "size" have distal FBrr ranging from the IIBr2 upper edge to the IIIBr2 distal margin. The inter-half-ray IIBr7 and the lateral interray IIIBr2 form the highest FBr in the 9.0 mm "size" crinoid.

Due to the development of the inter-half-ray iBrr, the adjacent half-rays (belong to the same ray) were spread apart. The smaller crinoids, "size" range 1.1 to 3.4 mm, lack inter-half-ray iBrr, and the adjacent half-rays lie close together (Text-figs. 29a-e). The 1.1 mm crown has the adjacent half-rays separated by .023 mm whereas the same for the 3.4 mm "size" crinoid equals .37 mm (Text-fig. 32l). The rate of ray spreading was only .15 mm per 1 mm "size" increment. The inter-half-ray iBrr began to appear in larger individuals, "size" range 4.2 to 9.0 mm, and the adjacent half-ray spreading rate increased to .23 mm per 1 mm additional "size", a 60% augmentation (Text-figs. 29, 32l). The 5.75 mm crown adjacent half-rays are spread by 1.1 mm; the equivalent figure for the 9.0 mm animal consists of 1.8 mm.

Most half-ray spreading was caused by the formation of the inter-half-ray iBr1 and iBrr2 at the IIBr1 and IIBr2 levels because these are the largest inter-half-ray iBrr. The higher inter-half-ray iBrr are smaller and the adjacent half-rays tend to come together (Text-figs. 29i-k). The inter-half-ray iBrr and the correlated expansion of the adjacent half-rays constricted the associated interray iBrr areas relative to calyx "size".

The inter-quarter-ray iBrr developed in some crinoids. These first appeared in the "size" equals 4.2 mm crown where they are represented by the inter-quarter-ray iBr1 (Text-fig. 29g). These were fully formed in the "size" equals 5.9 and 9.0 mm crinoids with the former possessing four and the latter six or seven plate ranges (Text-figs. 29i, k). The growth of these plates was variable as no inter-quarter-ray iBrr are seen in the 5.5 and 6.4 mm "sized" calyces (Text-figs. 29h, j). These plates separated the adjacent quarter-rays. Most expansion occurs at the IIIBrr1 and 2 levels and is due to the proximal two ranges of inter-quarter-ray iBrr. The higher adjacent quarter-rays spread less rapidly (Text-fig. 29k). The expansion results in the constriction of the associated inter-half-ray and lateral interray iBrr areas (compare Text-figs. 29g, i, k with the remainder).

Because of the development of inter-half-ray and inter-quarter-ray iBrr, the arm distribution around the calyx changed throughout ontogeny. The immature crinoid arms are strongly grouped and separated by wide lateral iBrr areas relative to "size" (Text-figs. 29a-f). Adult individuals with well-formed inter-half and inter-quarter-ray iBrr have arms which are more evenly spaced around the calyx due to this ray spreading. Ray spreading is common among primitive many-FBrr camerates with few arms, two to four, per ray (other examples are *Glyptocrinus dyeri*, see Wachsmuth and Springer, 1897, pl. 20, figs. 1a-c, pl. 21, figs. 3a-f, *Ptychocrinus splendens* and *P. fimbriatus*).

The immature few-FBrr patelliocrinids exhibit strongly grouped arms like those of young alisocrinids (Text-figs. 7, 8, 21, 29). The IIBr1 proximal margins are joined along the ray axis. Normal specimens of *Eopatelliocrinus* retained this juvenile condition throughout ontogeny, but *Macrostylocrinus pristinus* formed relatively small inter-half-ray iBrr and FBrr at low fixation rates (numerical scale mean FBrr growth rate about .49 per 1 mm "size" increment, compared to 1.9 for the alisocrinid). The mature patelliocrinid arms remained strongly grouped at all growth stages, except for a small amount of ray spreading associated with the axillaries. This is directly attributed to the low inter-half-ray FBrr incorporation rates.

The FBrr development of many and few-FBrr camerates is summarized. The various FBrr incorporation rates are correlated. A high lateral interray fixation vector dictated the same for the CD interray, inter-half-rays, and inter-quarter-rays, if the latter were present, and vice versa. The main differentials comprised the various FBrr growth rates which caused a series of consequences: 1. In crinoids with equal calyx shapes, the dorsal cup and viscera volume was augmented more rapidly in many-FBrr than in few-FBrr types. 2. The presence or absence of ray spreading. 3. The inter-half-ray and inter-quarter-ray, if present, iBrr typically extend higher than the lateral interray and CD interray iBrr of many-FBrr species. This results in a lobate tegment with upraised Ambb and depressed iAmbb. The few-FBrr types have less lobate and smoother tegmens. 4. Perhaps, the development of numerous FBrr provided stronger support for the growing arms.

The "size" and dorsal cup height growth vector was 1.7

mm of height per 1 mm "size" increment (Text-fig. 32m). The minimum and maximum "sizes" equal 1.1 and 9.0 mm and correspond to dorsal cup heights of 1.15 and 15.0 mm, respectively. Dorsal cup height/"size" ranges from .71 to 1.1 in the smaller animals and consists of 1.7 in the largest. The "size" declined relative to dorsal cup height with increasing age. This was caused by the development of new FBrr and the FBrr heights when incorporated and their subsequent height growth rates with respect to "size". The patelliocrinid dorsal cup height growth rates ranged from 1.0 to 1.3 mm per 1 mm "size" increment which are much smaller than that of the alisocrinid, mainly due to the differential FBrr development vectors.

Only one reasonable *Alisocrinus tetrarmatus* "theoretical microcrinoid" value has been calculated. This is the maximum possible "size" (.50 mm) of the BB + OO + RR "microcrinoid" which was derived from the heights of the RR and BB of the smallest specimen. All the other "microcrinoid" figures are negative and range from –.33 mm to –3.7 mm; these are clearly meaningless. The reasons for this remain unknown although reasonable "microcrinoid" "sizes" have not been obtained from the equations in any many-FBrr camerate studied (*i.e., A. tetrarmatus, Ptychocrinus splendens*, and *P. fimbriatus*).

Nevertheless, consideration of some alisocrinid initial intercepts and y equals zero values throws some light on the developmental sequence of the dorsal cup plates. The following are the "size" values when the plate height equals zero; these are taken from the equations of "size" (x) versus the listed plate height (y) (*i.e.*, y equals 0 figures):

Plate	"Size" when plate height equals zero
B	–.77 mm
R	–.52 mm
IBr1	.48 mm
IAx	.15 mm
iBr1	–.36 mm
primanal	insufficient data

The reader should realize that these "sizes" do not represent the ages at which the plates appeared during ontogeny. However, the order of increase or decrease of these figures should denote the approximate order of plate development.

The following generalized sequence occurs in modern monocyclic crinoids (listed from first to last appearance): BB and OO; RR and RA; IBr1; IAx; and the iBr1 or iR develops at various stages. In *Comactina meridionalis* and *Antedon bifida*, this forms after the IBr2 (IAx) is present. The iBr1 is not seen in *Promachocrinus kerguelensis* until about five IIBrr are seen in each arm. The alisocrinid data, except for the iBr1, are consistent with this sequence even though the equation "sizes" are anomalous. The "size" computed from "size" versus BB height is the smallest; this is followed by the RR value. The IBrr1 "sizes" are much larger suggesting that these plates appeared well after the BB and RR as in living crinoids. The .48 mm IBr1 figure exceeds the .15 mm IAx "size" and is out of order. This seems to represent poor equation fits; the "size" versus IBr1 and IAx equations poorly approximate the smallest crown, especially the IBr1 trend line. Regardless, the IBrr probably formed within the .15 to .48 mm "size" interval.

The –.36 mm "size" for the iBr1 is surprising. By analogy with the iBr1 or iR of living crinoids, one would expect a much larger value. The equation of "size" versus iBr1 height is based on 13 individuals and yields a satisfactory fit to the data. The –.36 mm "size" is believed to show that the Paleozoic camerate iBrr1 were initiated much earlier than the iBrr1 (iRR) of modern articulates. This "size" probably indicates that the camerate iBr1 formed roughly in the same plate order as when the RA first appears in some living crinoids. The sequence of RA development is variable in extant forms: *Hathrometra sarsii*, after formation of the IBr1 when the RR are in lateral contact; species of *Antedon*, following the IBrr; and *Comactina meridionalis* and *Promachocrinus kerguelensis*, prior to formation of the RR. The alisocrinid data suggest that the iBr1 appeared soon after the RR and before the IBr1, a situation intermediate between those of the comactinid-promachocrinid and the hathrometrid. Probably the alisocrinid primanal formed at roughly the same time as the iBr1.

The patelliocrinid "size" values, obtained from equations of "size" versus height of the various plates, denote the following sequence: BB, RR, IBr1, and IAx. The iBr1 data are too incomplete to draw conclusions. Consequently the alisocrinid iBr1 hypothesis cannot be confirmed by patelliocrinid information and should be considered tentative.

The camerate data are somewhat consistent with the ontogenies of monocyclic inadunate microcrinoids (see Koenig, 1965, Regnéll, 1959, Moore, 1940a, b, Moore and Ewers, 1942, Strimple and Koenig, 1956, Koenig and Meyer, 1965). Review of these denotes the following plate initiation order: BB and OO, RR, IBrr, and the proximal anal appeared at various times. Generally the anal is not observed in place until after the RR are in lateral contact and arm facets are present. At least some microcrinoids possess a RA which probably formed before all of the RR (*e.g.,* *Streblocrinus,* see Koenig and Meyer, 1965; the writer believes that the RA developed first because it is larger than the three immature RR present).

The alisocrinid correlation coefficients provide more information on the integration and coordination of calyx growth than those of the patelliocrinids because more complete data sets are available, and the degrees of freedom are subject to less variation. Most patelliocrinid measurement sets are incomplete. The degrees of freedom vary greatly, depending on the variables, and meaningful comparison of the correlation coefficients is difficult.

The alisocrinid dorsal cup, except for the primanal and FBrr, correlation coefficients range from .83 to .98 (partially listed in Text-fig. 32). All have significance levels (two-sided test) exceeding .999 which indicates that the dorsal cup growth was highly integrated and coordinated.

The CD interray and its component plates correlation interval equals .70 to .97, and the significance levels vary from less than .900 to almost .999. Both the correlation coefficients and their significance levels are less than those tabulated above, for three reasons: incomplete nature of the CD interray data (N ranges from four to seven); inherent variation of the CD interray plate shapes which makes it difficult to secure consistent measurements; and the CD interray and its plate elements were less well integrated and coordinated with calyx size growth than were the lateral interrays. For example, the correlation of "size" versus CD interray width equals .93 (significance level almost .999) whereas the equivalent values for "size" versus lateral iBrr width are: $r = .91$; significance level, above .999.

The different calyx plate dimensions exhibited various degrees of integration and coordination with "size" and dorsal cup width. The highest correlations involve the ray plates, RR, IBr1, IAx, and IIBr1. These range from .98 to .93 with significance levels exceeding .999. Within this plate sequence the correlation coefficients tend to decrease distally. The mean correlation of the plate dimensions versus calyx size measures consists of .96 for the RR and .95 for the IIBrr1. Lower values characterize the BB, iBr1, IIIBr2 and CD interray plates. These are distributed over the .70 to .97 interval although most are well below .95; the associated significance levels are about .900 to almost .999. Within this plate group, the CD interray plates exhibit the lowest correlations and significance levels. The correlations of height versus width of the individual plates follow the previous pattern. This correlation coefficient differential clearly indicates the presence of an integration and coordination gradient throughout the calyx. The RR through IIBr1 ray plate series showed the highest and most sophisticated degree of regulation with each other and with calyx size measures. The IIIBr2, the interray plates and the BB, all of which are peripheral to the main ray plate sequence, were less well integrated and coordinated with the calyx size ontogeny.

The height and width of the individual plates possess equal correlations with "size"; the average correlation coefficients of "size" versus height and width of all plates are both .94. A similar situation exists for plate dimension versus calyx width measures.

Comparison of the alisocrinid and patelliocrinid correlations is difficult because of the incomplete few-FBrr crinoid data sets. Nevertheless, two differences are tentatively proposed: 1. The patelliocrinid plate heights are generally best correlated with "size" and were less well integrated with the calyx width growth; the same is observed for the patelliocrinid plate widths and measures of calyx width. These alisocrinid correlations are roughly equalized; 2. The correlation coefficients and their significance levels denote that the alisocrinid calyx exhibited a slightly higher amount of ontogenetic integration and coordination than that of the few-FBrr crinoids. Perhaps this was related to differences in the FBrr incorporation rates. These patterns are only postulated for *Alisocrinus tetrarmatus* and the three patelliocrinids examined. General extrapolation to few versus many-FBrr camerates is not warranted at this time.

The standard deviation distribution is inversely related to that of the correlation coefficients. Typically, low percentage standard deviations are associated with high correlations and vice versa. The main exception comprises the IIIBr2; this plate is characterized by relatively high percentage standard deviations and relatively low correlation coefficients. The reason for the standard deviation distribution pattern remains unclear. High correlation coefficients do not require low variation or vice versa. Perhaps the minimization of variation facilitated the integration and coordination of the dorsal cup ontogeny.

Brachial ontogeny. — (Text-fig. 33). The standard Brr consist of IIIBrr6 to 11. These are equivalent to the patelliocrinid IIBrr8 to 13 because the alisocrinid IIBr2 is axillary.

The "size" and Brr width showed a linear relationship in which the width growth rate equalled .073 mm per 1 mm additional "size" (Text-fig. 33a). This was the smallest uniserial Brr width developmental vector observed; the same values of the other uniserial armed species ranged from .095 to .13 mm. As usual, the alisocrinid width growth rates exceeded those of height. The mean Brr maximum and minimum height vectors were .049 and .027 mm per 1 mm "size" increment, respectively (Text-figs. 33b, c). Thus, the width growth rate comprised 1.5 times that of the mean maximum height and 2.7 times the average minimum height figure. In the other uniserial armed crinoids, the width-"size" vectors were more predominant and these varied from 2.4 times to 5.6 times that of maximum height and from 6.3 times to 21 times that of minimum height. Because of the relatively large height growth rates in *A. tetrarmatus,* the Brr width with respect to height increased more slowly than in the other uniserial armed forms. Consequently, the alisocrinid Brr retained a high, angular, and immature appearance longer, in terms of "size" or Brr width, than those of the other uniserial crinoids examined (compare Text-figs. 11g, 12g, 33i, 37c). The largest and smallest "sizes" consist of 9.0 and 1.4 mm (the standard Brr are not present in the 1.1 mm crinoid) and the corresponding widths are .79 and .23 mm, listed in the same order. Throughout ontogeny, the "size"/Brr width rose from 6.1 to 11. This was caused by the low Br width-"size" ontogentic vector. The other uniserial armed taxa had larger Brr width-"size" growth rates, and the ratio either decreased more slowly or remained constant.

In the plots of Brr width versus maximum and minimum height, logarithmic relations were observed in which the height growth vector dropped exponentially with increasing Brr width and "size" (Text-figs. 33d, e). Over the .21 to .77 mm width interval, the maximum height growth rate per .1 mm width augmentation changed from .11 to .036 mm, and that of minimum height ranged from .051 to .017 mm. The average maximum and minimum height growth vectors equalled about .070 and .030 mm per .1 mm width increment, respectively. Over the .21 to .77 mm width range, the maximum height values comprise .29 and .64 mm and the same minimum heights are .21 and .42 mm.

The maximum and minimum height exhibited curvilinear ontogeny during which the minimum height developmental vector declined from .097 to .037 mm per .1 mm of maximum height increment (Text-fig. 33g). The mean constituted .060 mm. The least and greatest maximum heights are .24 and .68 mm and the corresponding minimum heights comprise .18 and .43 mm, listed in the same order.

The total convergence angle (*i.e.,* proximal and distal Brr faces) is 36° in the 1.8 mm "sized" crinoid (Text-fig. 29c, small Br in 33i). The angle dropped with increasing "size". The initial decline was slow and the angle consisted of 34° in the 3.4 mm "size" individual. The mature animals are variable and the "adult assemblage" figures range from about 30° to 22°. The largest specimen, "size" 9.0 mm, possesses a 23° convergence angle. Compared to the other uniserial forms, *A. tetrarmatus* showed two differences:

1. Slow initial convergence angle change. In the other uniserial species, the convergence angle decreased most rapidly in young crinoids as indicated below:

	Br widths and convergence angles		
Eopatelliocrinus scyphogracilis	.12 mm 41°	.20 mm 22°	1.0 mm 18°
E. latibrachiatus	.15 mm 25°	.25 mm 22°	.63 mm 16°
Alisocrinus ? heterodactylus	.27 mm 22°	.60 mm 17°	1.7 mm 12°

The underlying reasons are not fully understood. The *A. tetrarmatus* pattern was partially due to the large initial maximum and minimum height growth rates relative to that of width. These tended to retain constant Br geometry and resulted in a slow decline of the early convergence angles. In subsequent ontogeny, the maximum and minimum height developmental vectors fell with respect to that of width and the convergence angle dropped more rapidly. The larger initial width growth rates with respect to those of height dictated a more marked angle decrease in the other uniserial armed taxa.

2. The mature *A. tetrarmatus* individuals exhibit greater convergence angle variation than adults of the other forms. Because of the slow and variable convergence angle decline, the alisocrinid Brr retained an angular and immature appearance well into the "adult assemblage" interval whereas the other uniserial species usually lost this immature appearance by the end of the "young assemblage" "size" range.

The maximum height and pinnule facet size had a straight trend line in which the pinnule facet developmental vector equalled .042 mm per .1 mm height increment (Text-fig. 33h). The extreme maximum heights are .26 and .68 mm and the equivalent pinnule facet sizes constitute .14 and .32 mm. Inspection of Text-figures 33f and h discloses two apparent groups of crinoids — one characterized by large pinnule facets relative to width and maximum height and the other by small facets. The *t*-tests indicated that the discontinuity was significant at levels above 95%. Originally, this was attributed to sexual dimorphism with the large pinnule facet bearing individuals being the females and the other group representing the males. Later examination showed that single specimens may possess large, intermediate, and small pinnule facet bearing Brr. Therefore, the sexual dimorphism hypothesis is not applicable because the sexes are separate in living crinoids. The causes of this

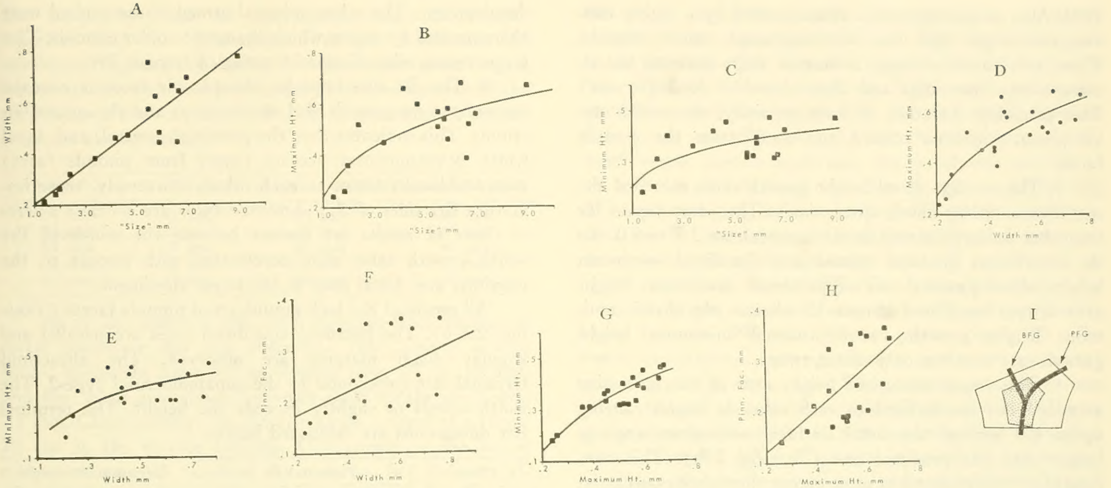

Text-figure 33. — Graphs and restoration showing Brr growth in *Alisocrinus tetrarmatus*, n. sp. All dimensions on the graphs with the exception of "size" refer to the Brr measurements defined on Text-figure 2. "a" refers to the "initial intercept" or "pseudointercept" where the x axis is logarithmic.

A-H. Graphs. Equation data:

A — $y = .0733 + .131x$. $r = .877$.
$\sigma y\% = 15.6$. $N = 17$.
B — $y = .239 + .412\log x$. $r = .738$.
$\sigma y\% = 18.3$. $N = 17$. "a" $= -.174$ ($x = .1$).
C — $y = .211 + .223\log x$. $r = .638$.
$\sigma y\% = 19.0$. $N = 17$. "a" $= -.0115$ ($x = .1$).
D — $y = .713 + .621\log x$. $r = .818$.
$\sigma y\% = 15.3$. $N = 19$. "a" $= -.529$ ($x = .01$).
E — $y = .453 + .295\log x$. $r = .630$.
$\sigma y\% = 17.8$. $N = 19$. "a" $= -.138$ ($x = .01$).
F — $y = .127 + .240x$. $r = .486$.
$\sigma y\% = 27.4$. $N = 18$.
G — $y = .526 + .552\log x$. $r = .898$.
$\sigma y\% = 9.1$. $N = 19$. "a" $= -.577$ ($x = .01$).
H — $y = .0306 + .420x$. $r = .597$.
$\sigma y\% = 25.0$. $N = 18$.

I — Two Brr superimposed to show growth patterns. The smaller Br is the mean standard plate from paratype IGS. 35P-34, "size" 1.85 mm. The larger plate is the mean Br from the holotype, "size" 9.0 mm. Food groove axes in heavy lines. BFG and PFG are "brachial" and "pinnule facet food groove" axes, respectively. Smaller Br stippled.

variation seem two-fold. It is partially controlled by the inclination angle of the Brr and partly by the thickness of the matrix which commonly covers the Brr and pinnules. The pinnule facet size variability may be related to the camerate symmetry plane which bisects the A ray and CD interray. This cannot be verified because all rays cannot be measured in a single crown.

Text-figure 33i shows the Brr growth restoration. The young Br food groove configuration is observed in paratype IGS. 35P-34, "size" 1.85 mm, where weathering exposed the food groove axes of a few distal Brr. This geometry was extrapolated to the illustrated immature plate. The adult alisocrinid food groove axes were restored like those of the other uniserial armed crinoids. The main ontogenetic patterns follow.

1. The width growth rates did not greatly exceed those of height. The alisocrinid Brr width-"size" growth rate is only 1.9 times the mean average height value. The equivalent eopatelliocrinid figures are about four and eight times. Consequently, Br angularity was retained much longer in *A. tetrarmatus* and angular and immature appearing standard Brr are seen in the 4.2 mm "sized" crinoid (Text-fig. 29g). Owing to the relatively larger width developmental vectors, the eopatelliocrinids developed smooth and mature appearing Brr by the end of the "young assemblage" stage ("sizes" 2.15 and 2.7 mm).

2. Assuming the restoration is correct, the alisocrinid Brr width growth rate toward the pinnule facet equalled that directed away from the facet. The large maximum and minimum height ontogenetic vectors with respect to that of width resulted in comparatively slight curvature of the "pinnule facet food groove", especially near its junction with the "brachial food grooves". The eopatelliocrinids and *A. ? heterodactylus* possessed relatively larger width growth rates; therefore, the "pinnule facet food groove" exhibits stronger curvature (compare Text-figs. 11g, 12g, 33i and

37c). Also *A. tetrarmatus* is characterized by a higher convergence angle than the other uniserial armed crinoids. These two variables cause a sharper angle between the *A. tetrarmatus* "proximal and distal brachial food grooves". This probably dictated, at least partially, the width developmental vectors toward and away from the pinnule facet.

3. The average distal height growth rates exceeded the proximal ones by about three times. The same figure for the other uniserial armed forms ranged from 2.3 to 8.0. An *A. tetrarmatus* gradient existed and the distal maximum height developmental vector/proximal maximum height growth rate comprised almost 10 whereas the distal minimum height growth vector/proximal minimum height growth rate one was only about two.

4. The young alisocrinid height axes of the successive standard Brr are inclined to each other at angles ranging up to 40° because the distal Br face convergence angle is larger than the proximal one (Text-fig. 29b). This configuration was retained to some extent throughout ontogeny, although it is less obvious in the larger crinoids because the Brr are relatively wider. In adults, the height axis offset varies from about 4° in the holotype ("size" 9.0 mm, Text-fig. 29k) to roughly 15° in paratype YPM. 27029 ("size" 5.5 mm, Text-fig. 29h). Thus, the proximal and distal face convergence angles became more nearly equal in older animals. Presumably, this was due to adjustments in both the proximal and distal height growth vectors. In *A. ? heterodactylus* and the two eopatelliocrinids, the standard Brr height axes were parallel when a 2.7 mm "size" was reached. As previously mentioned, the formation of equal proximal and distal convergence angles is believed to have been related to the support of the growing arms and pinnules. Firmer and more stable support was probably provided if the height axes of successive Brr were parallel. The alisocrinid has four arms per ray whereas the eopatelliocrinids bear only two arms per ray. However, the pinnule lengths and number of Brr per arm are roughly comparable for similar "sized" eopatelliocrinids and *A. tetrarmatus*. Consequently, the arm number fails to supply an explanation. Perhaps the more numerous alisocrinid FBrr constituted a more stable arm support and partly compensated for the inclined standard Brr height axes of mature animals. The few-FBrr eopatelliocrinids developed parallel Brr height axes in adult crowns. At present, this hypothesis cannot be corroborated with data from other many-FBrr camerates and it must be considered tentative.

5. The alisocrinid pinnule facet inclination angle (relative to arm length axis) remained almost constant during development. The other uniserial armed forms studied were characterized by angles which changed in older crinoids. This is one reason why alisocrinids retained angular Brr.

6. The Br side opposite the pinnule facet is concave throughout the growth of *A. tetrarmatus* and the eopatelliocrinids. This indicates that the proximal, central, and distal width developmental vectors (away from pinnule facet) were stablized relative to each other. Conversely, these immature Brr sides of *A. ? heterodactylus* are concave whereas those of adults are convex because the mid-level Brr width growth rates were accelerated with respect to the proximal and distal ones in the larger specimens.

All terminal Brr lack pinnules and pinnule facets (Text-figs. 29l-p). The proximal and distal faces are parallel and angular distal margins are observed. The alisocrinid terminal Brr correspond to the eopatelliocrinid type-2. The width equals or slightly exceeds the height. The terminal Brr dimensions are tabulated below:

"Size"	Terminal Br width	Terminal Br height
1.4 mm	.06 mm	.06 mm
1.8 mm	.07 mm	.07 mm
2.4 mm	.05 mm	.04 mm
4.2 mm	.13 mm	.12 mm
5.5 mm	.11 mm	.10 mm

The data suggest that "young assemblage" crinoids, "size" interval 1.4 to 2.4 mm, have roughly constant sized terminal Brr with widths and heights ranging around .06 mm. The two "adult assemblage" crowns ("sizes" 4.2 and 5.5 mm) exhibit approximately constant sized terminal Brr which are roughly twice as large as those of the younger animals; the adult terminal Brr widths and heights equal about .12 and .11 mm, respectively. This contrasts with the eopatelliocrinids where the terminal Br width and sometimes the height increased continuously in older crinoids.

The Br immediately below the terminal one possesses a pinnule facet and an immature pinnule consisting of one or two pinnulars. The proximal and distal faces no longer parallel each other but converge toward the Br side opposite the pinnule. Asymmetrical convergence angles are seen with the distal one being the largest. The total convergence angles vary from 8 to 19°, except for one Br which seems abnormal (Text-fig. 29n). The total convergence of these plates is less than that of Brr further down the arm. The adult individual largest convergence angle occurs in the distal third or quarter of the arm and the angle decreases below this point (Text-figs. 29g, h, j). Due to the Brr shape variation, the exact young crinoid position is uncertain although the maximum convergence probably lies one or several Brr below the distal pinnule bearer (Text-fig. 29b). The terminal

Brr morphology and the convergence angle distribution indicates that the differentiation of the maximum and minimum heights (this determined the convergence angle) was associated with and produced by the development of the pinnule facet and its pinnule. The distal pinnulate Br dimensions are shown below:

"Size"	Brr width	Maximum height	Minimum height
1.4 mm	.08 mm	.09 mm	.07 mm
1.8 mm	.10 mm	.08 mm	.07 mm
2.4 mm	.07 mm	.07 mm	.04 mm
4.2 mm	.18 mm	.18 mm	.12 mm
5.5 mm	.15 mm	.18 mm	.16 mm

As in the terminal Brr, two constant-sized groups of distal pinnulate Brr are observed. The "young assemblage" specimens have widths ranging from .07 to .10 mm, and the "adult assemblage" animals show widths of .15 and .18 mm. Consequently, the initial pinnule formed at a larger Br size in the mature crinoids. Comparison of the above measurements with those of the terminal Brr discloses almost perfect correlation. Thus, the large distal pinnule bearing Brr are found with the bigger terminal Brr and vice versa.

An adult alisocrinid arm possesses two Brr maturity gradients (Text-figs. 29g, h, j). The mature Brr are considered less angular and wider relative to height than the immature ones. In the distal to proximal gradient, the average angularity and mean height/width drops proximally and the most mature plates are encountered at the IIIBrr10 to 24 interval. In the proximal to distal gradient, the maximum angularity and height/width are located at the IIIBrr1 to 4 level and the maturity indices rise up to the mature Brr range.

The smallest crinoid has only four or five IIIBrr per arm ("size" 1.1 mm, Text-fig. 29a). The standard Brr, IIIBrr6 to 11, did not begin to appear until a 1.4 to 1.8 mm "size" was attained; these animals show up to eight or nine IIIBrr per arm (Text-figs. 29b, c). These "sizes" should be reflected in the y equals 0 values for the equations of "size" (x) versus standard Brr dimensions (y). These figures range from "sizes" of 1.8 mm down to negative numbers. Most of the values are less than 1.0 mm and are far too small. Apparently, the standard Brr developed rapidly. Therefore, most initial Brr dimension growth rates are not indicated by the equations. Similar situations are found in the other uniserial armed taxa examined here.

The correlation coefficient distribution parallels that of the eopatelliocrinids (partially listed in Text-fig. 33 legend). The alisocrinid correlations vary from .48 to .90 with significance levels ranging from about .950 to greater than .999. As in the other crinoids, the coefficients are closely related to the original growth rates. High correlations are caused by large Brr dimension growth vectors and vice versa (Table 8). For example, in "size" versus width, the correlation coefficient equals .88 and the width developmental rate was .073 mm per 1 mm "size" increment. For "size" versus pinnule facet size, the correlation consists of .48 and the pinnule facet equation growth vector is only .019 mm per 1 mm additional "size". When the Brr dimensions, width, maximum and average height, are involved, the correlation coefficients range from .72 to .88 and all significance levels exceed .999. The equivalent figures for minimum height are correlation, .63 to .90 and significance levels, between .990 and .999 to greater than .999. The lowest correlations and significance levels are associated with the pinnule facet size. These correlations vary from .48 to .60 and the significance levels are distributed over approximately the .950 to .990 interval. The eopatelliocrinids showed a different pattern in which the lowest correlations and growth vectors were those of minimum height. Larger pinnule facet size growth rates were observed in conjunction with higher correlation coefficients and significance levels (Table 8).

Comparison of the correlation coefficients of the different forms is difficult due to variation in the number of individuals (N) and the degrees of freedom (DF) as listed below:

Species	Range of N	DF interval
A. tetrarmatus	16 to 19	14 to 17
Eopatelliocrinus scyphogracilis	15 or 16	13 or 14
E. latibrachiatus	9 or 10	7 or 8

Consequently, the comparison is best exhibited by the correlation coefficient significance levels. The *E. scyphogracilis* correlations range from .97 to .72 with most being well above .90. The significance levels of all Brr dimensions are greater than .999 except for minimum height; these are slightly above or below .999. The *E. latibrachiatus* correlation coefficients cover the .92 to .24 interval and the significance levels are distributed over the above .999 level to less than .900. Thus, the overall degree of integration and coordination of Brr ontogeny shown by *Alisocrinus tetrarmatus* was less than that of *Eopatelliocrinus scyphogracilis*. The alisocrinid growth pattern was most comparable to the less well regulated one of *E. latibrachiatus*. The significance levels denote that the alisocrinid Brr were slightly better integrated and coordinated than those of the latter eopatelliocrinid (Table 8).

The alisocrinid percentage standard deviations range from 9.1 to 29% (partially listed in Text-fig. 33 legend). The Brr dimensions are more variable with respect to "size" than relative to the other Brr parameters. Where "size" is involved, the Brr standard deviation interval comprises 16% to 29%. A 9.1 to 27% range is seen in the various Brr measurements versus one another. The overall alisocrinid variation pattern is tabulated below:

Equation	Percentage standard deviation
"Size" (x) versus Brr width (y)	16%
Log. "size" (x) versus Brr maximum height (y)	18%
Log. "size" (x) versus Brr minimum height (y)	19%
"Size" (x) versus pinnule facet size (y)	29%

The greatest scatter occurs when the pinnule facet constitutes the dependent variable. The lowest percentage standard deviations are associated with Brr width. Next are maximum and minimum height, listed in order of increasing variability. The alisocrinid variation is inversely correlated with the growth vectors; small developmental rates are seen with high percentage standard deviations and vice versa. The greatest and least eopatelliocrinid variability is found with Brr width and maximum height, respectively. The variation does not appear to be closely related to the growth rates. The reasons underlying the two patterns remain unknown.

Alisocrinus tetrarmatus represents the most variable uniserial armed species studied. The equivalent eopatelliocrinid percentage standard deviations are about 33 to 67% less than those of the alisocrinid. For example, the "size" (x) versus Brr dimensions (y) percentage standard deviation ranges equal: *A. tetrarmatus*, 16 to 29%; *Eopatelliocrinus scyphogracilis*, 7.1 to 14%; and *E. latibrachiatus*, 8.3 to 20%.

Food gathering system growth. — (Table 16, Text-fig. 34). Complete data sets are available for 12 individuals of which six are assigned to the "young assemblage", "size" range 1.1 to 3.4 mm, and six grouped within the "adult assemblage" ("sizes" 4.2 to 9.0 mm). In addition, partial measurements were derived from seven other crowns, distributed about equally between the two "assemblages".

Unlike the other Girardeau camerates, the *Alisocrinus tetrarmatus* equations yield good fits to the data for individuals of all "sizes" and ages. Consequently the discussion emphasizes equation figures rather than specimen values.

A curvilinear regression line is observed in "size" versus food gathering system length in which the ambulacral tract length growth rate increased from 15 cm to 280 cm per 1 mm additional "size" throughout ontogeny (Text-fig. 34a). The mean vector consisted of 120 cm. The smallest animal, "size" 1.1 mm, has a 7.7 cm equation food gathering system whereas that of the largest available crown, "size" 6.7 mm, is 1420 cm long.

The relation between calyx volume and "size" was exponential (Text-fig. 34e). The "size" growth rate per .01 cc volume increment declined from .19 mm to .033 mm over the observed development (average .066 mm). The volume was augmented more rapidly in the many-FBrr alisocrinid than in the few-FBrr patelliocrinids; for example, the same mean developmental vectors of *Eopatelliocrinus scyphogracilis* and *E. latibrachiatus* comprised .23 mm and .27 mm, respectively. The differences were principally produced by the FBrr growth rate contrasts rather than calyx shape variations. The youngest alisocrinid possesses a predicted 1.2 mm "size" and an .001 cc calyx volume; the equivalent figures for the mature animal constitute 10.0 mm and .95 cc.

The growth of food gathering system length and calyx volume was slightly curvilinear in which the free ambulacral tract length ontogeny vector fell with increasing "size" and age (Text-fig. 34f). The initial food gathering system length growth rate equalled 52 cm per .01 cc calyx volume increase; that of the oldest animals and the mean were 46 and 48 cm, respectively. The "sizes", calyx volume and ambulacral tract lengths for the smallest and largest specimens are listed below:

"Size"	Calyx volume	Equation food gathering system length
1.1 mm	.001 cc	7.8 cm
6.4 mm	.22 cc	1060 cm

Because of the above relationship, the food gathering efficiency (*i.e.*, ambulacral tract length/calyx volume) declined from 7800 in the youngest crinoids to 4800 in the oldest individuals. The initial drop was most striking and 68% of the food gathering efficiency decrease occurred over the first 14% of the calyx volume interval.

The "initial intercept" (*i.e.*, calyx volume .0001 cc) corresponds to an equation food gathering system length of .94 cm. In turn, the calculated "size" associated with the .0001 cc calyx volume is .57 mm. This value roughly indicates the "size" at which the food gathering system first developed.

The development of "size" versus number of Brr per arm followed an exponential curve in which the additional Brr per 1 mm "size" increment rose from 8.4 to 15 Brr during growth with a 12 Brr average (Text-fig. 34b). The smallest individual, "size" 1.1 mm, bears 5.6 equation Brr whereas the 7.0 mm "sized" crinoid has 77 plates per arm.

The alisocrinid is characterized by four unbranched arms per ray; the IIBr2 or rarely IIBr3 comprises the axillary. The IIBrr lack pinnules and are ignored in the Brr number per arm; only the IIIBrr are included. Usually all IIIBrr show pinnules except for the proximal one or two plates and the terminal Brr; thus, the pinnulate IIIBrr equals the total IIIBrr less two or three plates.

The number of Brr per arm versus half-ray food gathering system length exhibited the usual curvilinear relationship in which the half-ray free ambulacral tract length per additional Br growth vector increased from 3.9 to 29 mm with a 16 mm mean (Text-fig. 34g). If the reader wishes to visualize these growth rates in terms of the quarter-rays rather than half-rays, the half-ray values should be divided by two. The half-ray tabulations are quoted here because this procedure is consistent with that previously used for the patelliocrinids. The youngest alisocrinid possesses five Brr per arm and a 6.8 mm predicted half-ray food gathering system length; the same largest crinoid figures are 70 Brr and 1080 mm.

The growth of "size" and pinnule length was exponential with a gradually rising pinnule length growth rate (Text-fig. 34c). The initial and final values consisted of .93 and 1.7 mm pinnule length increase per 1 mm "size" augmentation (average 1.4 mm). The minimum and maximum "sizes" are 1.1 and 9.0 mm and the corresponding computed pinnule lengths are .50 and 7.9 mm, listed in the same order.

The development of half-ray ambulacral tract length and pinnule length has a curved regression line in which the half-ray food gathering system length per 1 mm additional pinnule length ontogenetic vector was augmented throughout ontogeny (Text-fig. 34h). The initial, last, and mean developmental rates comprised 41, 300, and 170 mm, respectively. The smallest and largest animals have .50 and 8.8 mm pinnules and equation half-ray ambulacral tract lengths of 5.5 and 1460 mm.

The "size" and arm length (Text-fig. 34d) showed an exponential relationship in which the arm length growth rate per 1 mm "size" increase ranged from 2.4 mm in the youngest to 6.1 mm in the oldest animals. The average was 4.4 mm. The maximum and minimum crown "sizes" comprise 7.0 and 1.1 mm with 27 and 1.3 mm calculated arm lengths, respectively.

The ontogeny of arm length and half-ray free ambulacral tract length was characterized by a curvilinear pattern in which the half-ray food gathering system length growth vector per 1 mm arm length augmentation rose from 14 to 72 mm during the observed developmental sequence (Text-fig. 34i). The mean growth rate consisted of 47 mm. The smallest and largest crinoids show arm lengths of 1.0 and 20 mm; the corresponding predicted half-ray ambulacral tract lengths equal 5.7 and 1120 mm, respectively.

The percentage of the food gathering system length represented by the pinnules was augmented throughout growth. This is only about 67% in the "size" 1.1 mm individual but it ranges from 94 to 96% in the largest animals, "size" interval 5.5 to 6.7 mm. The initial increase was the most rapid and the 3.4 mm "sized" crown has an 89% value.

The food gathering system ontogenies of the three Girardeau patelliocrinids and *Alisocrinus tetrarmatus* are compared in Table 16. The calyx volume and "size" were characterized by exponential development in all species. However, the calyx volume per "size" increment growth rates of the few-FBrr patelliocrinids ranged smaller than those of the many-FBrr alisocrinid. *Eopatelliocrinus scyphogracilis* and *Alisocrinus tetrarmatus* possess similar calyx shapes up to the proximal IIBrr levels. These calyx volume differentials largely represent contrasts in the FBrr incorporation rates. Basically the development of numerous alisocrinid FBrr dictated rapid calyx and viscera expansion.

All taxa showed curvilinear ontogeny of the food gathering system length with respect to calyx volume, in which the ambulacral tract length growth vector per calyx volume increment declined in the older and larger animals. The food gathering efficiency followed the same decreasing pattern. The mean growth rates varied; those of the two eopatelliocrinids equalled 23 and 26 cm additional food gathering system length per .01 cc volume increment. The equivalent vectors for *A. tetrarmatus* and *Macrostylocrinus pristinus* consisted of 48 and about 50 cm, respectively, both of which were roughly twice the eopatelliocrinid values.

The contrast between the two *Eopatelliocrinus* species and the alisocrinid was largely related to the number of arms. All Girardeau patelliocrinids have two arms per ray and a total of 10 arms whereas the alisocrinids exhibit four arms per ray for a total of 20. The average growth rates of additional Brr per arm were similar for all three crinoids; these ranged from 9.3 to 15 new Brr per arm for each 1 mm of "size" augmentation. The mean growth vectors of arm and pinnule length per 1 mm "size" increment also yielded comparable values for all three taxa; the former varied from 4.2 to 4.9 mm and the latter covered the .80 to 1.4 mm interval. In effect the larger number of alisocrinid arms doubled

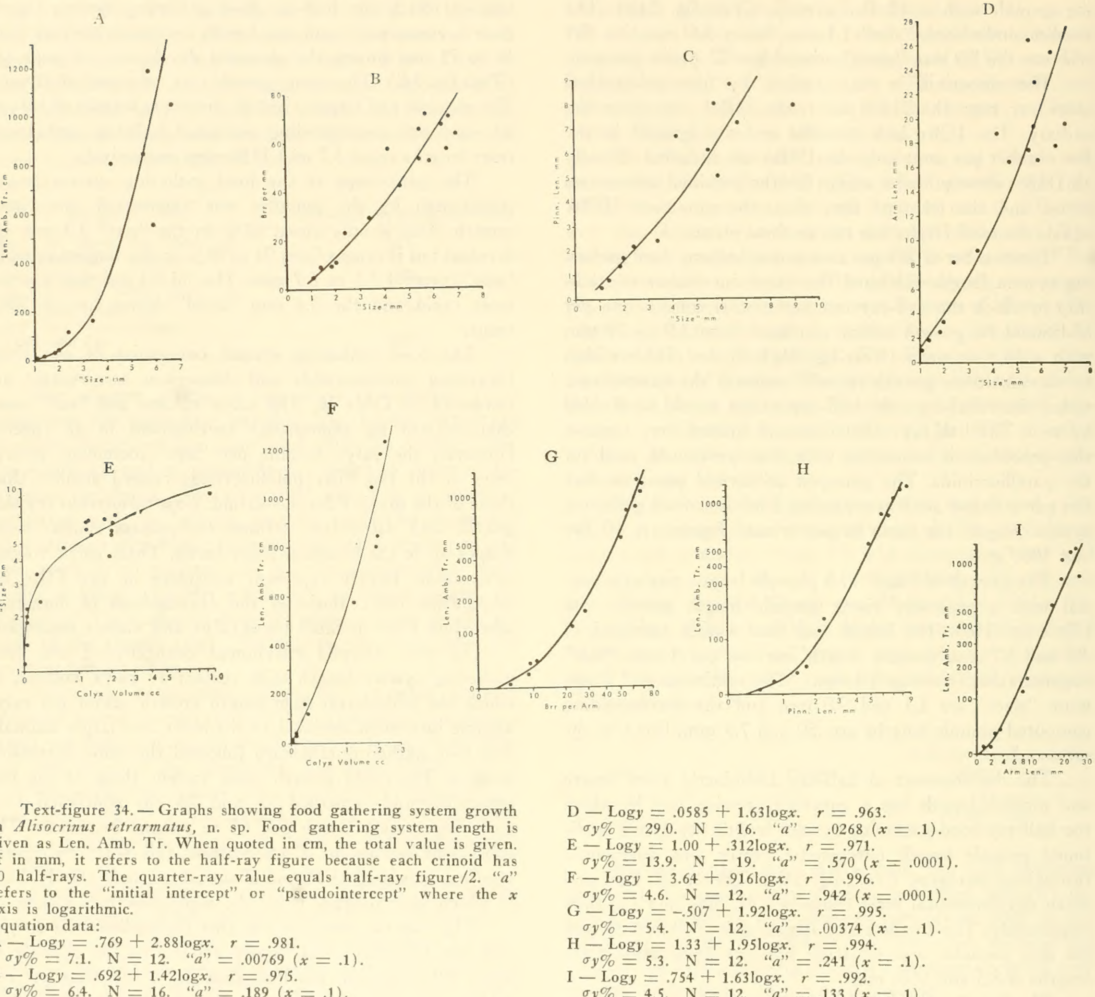

Text-figure 34. — Graphs showing food gathering system growth in *Alisocrinus tetrarmatus*, n. sp. Food gathering system length is given as Len. Amb. Tr. When quoted in cm, the total value is given. If in mm, it refers to the half-ray figure because each crinoid has 10 half-rays. The quarter-ray value equals half-ray figure/2. "a" refers to the "initial intercept" or "pseudointercept" where the x axis is logarithmic.

Equation data:

A — Log$y$ = .769 + 2.88log$x$. r = .981.
$\sigma y\%$ = 7.1. N = 12. "a" = .00769 (x = .1).
B — Log$y$ = .692 + 1.42log$x$. r = .975.
$\sigma y\%$ = 6.4. N = 16. "a" = .189 (x = .1).
C — Log$y$ = –.245 + 1.37log$x$. r = .966.
N = 13. "a" = .0241 (x = .1).
D — Log$y$ = .0585 + 1.63log$x$. r = .963.
$\sigma y\%$ = 29.0. N = 16. "a" = .0268 (x = .1).
E — Log$y$ = 1.00 + .312log$x$. r = .971.
$\sigma y\%$ = 13.9. N = 19. "a" = .570 (x = .0001).
F — Log$y$ = 3.64 + .916log$x$. r = .996.
$\sigma y\%$ = 4.6. N = 12. "a" = .942 (x = .0001).
G — Log$y$ = –.507 + 1.92log$x$. r = .995.
$\sigma y\%$ = 5.4. N = 12. "a" = .00374 (x = .1).
H — Log$y$ = 1.33 + 1.95log$x$. r = .994.
$\sigma y\%$ = 5.3. N = 12. "a" = .241 (x = .1).
I — Log$y$ = .754 + 1.63log$x$. r = .992.
$\sigma y\%$ = 4.5. N = 12. "a" = .133 (x = .1).

Species	"S
	Younge
Eopatelliocrinus scyphogracilis, n. gen., n. sp.	1.15 and 1.3
E. latibrachiatus, n. gen., n. sp.	1.15
Macrostylocrinus pristinus, n. sp.	1.0 and 1.3
Alisocrinus tetrarmatus, n. sp.	1.2

bined differentials caused a slightly shorter adult food gathering system in *Macrostylocrinus pristinus.*

The food gathering efficiency declined with increasing "size" and age. The rate of decrease is mainly determined by the food gathering system length growth vector per unit volume augmentation. The eopatelliocrinids possessed low growth rates and the adult crinoids show low food gathering efficiency (1900, 1800). Larger ambulacral tract length growth vectors were observed in *Macrostylocrinus pristinus* and *Alisocrinus tetrarmatus;* these are associated with higher mature animal food gathering efficiency (3700, 4800).

The growth patterns of the food gathering system length relative to the food gathering system components (*i.e.,* number of Brr per arm, average pinnule length and arm length) were always characterized by curvilinear relationships in which the ambulacral tract length growth rate per unit of food gathering system component increase rose throughout development, although the augmentation rates varied from species to species. In most cases, the development of food gathering components with respect to "size" followed an exponential form; generally, the food gathering system component growth vector increased in the older and larger animals.

The youngest crinoids of all taxa possess similar food gathering systems and food gathering efficiencies; the calyx volumes and "sizes" range from .0003 to .001 cc and from

food gathering system development was highly integrated and coordinated.

Comparison of the correlation coefficients and their significance levels between the alisocrinid and the three patelliocrinids is difficult because of the variation in the number of specimens among the four taxa. Nevertheless, the overall ranges suggest a general pattern:

Species	Usual number of specimens	Range of correlation coefficients	Significance level range
Eopatelliocrinus scyphogracilis	16	.90 - .994	above .999
E. latibrachiatus	10	.88 - .989	.999 to higher
Macrostylocrinus pristinus	11	.94 - .994	well above .999
Alisocrinus tetrarmatus	12	.96 - .996	well above .999

The data indicate the following integration and coordination gradient, listed from maximum to minimum regulation: *A. tetrarmatus, Eopatelliocrinus scyphogracilis* and *Macrostylocrinus pristinus, Eopatelliocrinus latibrachiatus.* The available information does not warrant any general conclusions for all crinoids.

As usual the alisocrinid correlation coefficient for calyx

Table 16

Species	Calyx volume versus "size"					Calyx volume versus Len. food gath. system							"Size" versus Brr per arm					"Size" versus Pinnule length					"Size" versus Arm Length				
	"Size" mm		Volume cc		Initial, latest and mean growth rates of "size" (mm) per .01 cc volume increase	Volume cc		Len. food gath. syst. cm		Initial, latest and mean growth rates of food gath. syst. (mm) per .01 cc volume increase.	Food gath. eff.		"Size" mm		Brr per arm		Initial, latest and mean number of additional Brr per 1 mm "size" increase	"Size" mm		Pinn. len. mm		Initial, latest and mean pinn. len. growth rates per 1 mm "size" increase	"Size" mm		Arm len. mm		Initial, latest and mean arm len. growth rates per 1 mm "size" increase
	Youngest	Oldest	Youngest			Youngest	Oldest	Youngest	Oldest		Youngest	Oldest	Youngest	Oldest	Youngest	Oldest		Youngest	Oldest	Youngest	Oldest		Youngest	Oldest	Youngest	Oldest	
Eopatelliocrinus scyphogracilis, n. gen., n. sp.	1.15 and 1.3	7.7 and 9.6	.0007 and .0008	.22 and .32	1.0 to .08, .23 mm	.0007	.15 and .22	6.0	485 and 420	40 to 23, 26 cm	8600	3100 and 1900	1.15	6.2 and 7.7	8 or 9	57 and 59	8.1 to 10, 9.3	1.15	6.2 and 6.7	.70	6.7 and 8.1	.98 to 1.2, 1.1 mm	1.15 and 1.3	6.2 and 7.7	1.8 and 2.5	19 and 25	3.0 to 5.2, 4.2 mm
E. latibrachiatus, n. gen., n. sp.	1.15	5.0	.0006 and .0011	.132	.83 to .11, .27 mm	.0006 and .0011	.13	5.8 and 6.0	235	36 to 17, 23 cm	9700 and 5500	1800	1.15	5.0	7 or 8	55	11 to 17, 15	1.15	5.0	.70 and .85	4.0	1.6 to .44, .80 mm	1.15	5.0	1.5 and 1.8	15	3.1 to 6.4, 4.9 mm
Macrostylocrinus pristinus, n. sp.	1.0 and 1.3	9.2 and 10.2	.0003 and .0009	.35	1.1 to .07, .21 mm	.0003 and .0009	.24	1.8 and 5.6	890	60 to 40 cm, mean uncertain	6000 and 6200	3700	1.0 and 1.3	7.0	4 to 5 and 8 to 9	91	12 to 23, 18	1.0 and 1.3	7.0 and 12.6	.40 and .95	9.5 and 9.8	.98 to 1.3, about 1.2 mm	1.0 and 1.3	7.0	1.0 and 1.6	28	constant 4.6 mm
Alisocrinus tetrarmatus, n. sp.	1.2	10.0	.001	.95	.19 to .033, .066 mm	.001	.22	7.8	1060	52 to 46, 48 cm	7800	4800	1.1	7.0	5.6	77	8.4 to 15, 12	1.1	9.0	.50	7.9	.93 to 1.7, 1.4 mm	1.1	7.0	1.3	27	2.4 to 6.1 4.4 mm

Summary and comparison of the food gathering system development of the Girardeau patelliocrinids and *Alisocrinus tetrarmatus* n. sp. The calyx volume per "size" unit growth rate is the inverse of the "size" per calyx volume increment vector listed in the table.

the mature crinoid food gathering system length over that of the adult eopatelliocrinids with roughly equivalent calyx volumes. The two large *E. scyphogracilis*, .15 and .22 cc calyx volumes, possess 420 and 480 cm food gathering systems whereas that of the .22 cc alisocrinid is 1060 cm in length.

In *Macrostylocrinus pristinus* and *Alisocrinus tetrarmatus*, a different situation is observed and the mature crinoids are characterized by similar food gathering system lengths: macrostylocrinid, volume .24 cc, food gathering system length 890 cm; and alisocrinid, volume .22 cc, 1060 cm ambulacral tract length. The alisocrinids have 20 arms whereas only 10 occur in the macrostylocrinids. The mean additional Brr per arm growth rates per 1 mm "size" increment comprised 18 Brr for *Macrostylocrinus pristinus* and 12 Brr for *Alisocrinus tetrarmatus*. This largely reflected the presence of biserial arms in the former versus the uniserial arms of the latter; the biserial arms allowed more Brr and pinnules per unit arm length. Essentially, the macrostylocrinid biserial Brr somewhat compensated for the smaller number of arms. The macrostylocrinid exhibited a slightly smaller average pinnule length per 1 mm "size" increment growth vector (1.2 versus 1.4 mm). These combined differentials caused a slightly shorter adult food gathering system in *Macrostylocrinus pristinus*.

The food gathering efficiency declined with increasing "size" and age. The rate of decrease is mainly determined by the food gathering system length growth vector per unit volume augmentation. The eopatelliocrinids possessed low growth rates and the adult crinoids show low food gathering efficiency (1900, 1800). Larger ambulacral tract length growth vectors were observed in *Macrostylocrinus pristinus* and *Alisocrinus tetrarmatus;* these are associated with higher mature animal food gathering efficiency (3700, 4800).

The growth patterns of the food gathering system length relative to the food gathering system components (*i.e.*, number of Brr per arm, average pinnule length and arm length) were always characterized by curvilinear relationships in which the ambulacral tract length growth rate per unit of food gathering system component increase rose throughout development, although the augmentation rates varied from species to species. In most cases, the development of food gathering components with respect to "size" followed an exponential form; generally, the food gathering system component growth vector increased in the older and larger animals.

The youngest crinoids of all taxa possess similar food gathering systems and food gathering efficiencies; the calyx volumes and "sizes" range from .0003 to .001 cc and from 1.1 to 1.3 mm, respectively. The total food gathering system lengths equal about 6 cm and the food gathering efficiency varies from 5500 to 9700. The principal difference is the presence of 20 arms in young alisocrinids and 10 arms in the three patelliocrinids; the immature alisocrinids also tend to have shorter pinnules. Consequently, comparable food gathering system lengths are observed in all four species. Because of these similarities, the young individuals are difficult to identify. The presence of four arms per ray can be determined only after three or more Brr occur in each arm; previous to this, the extra arms cannot be distinguished from pinnules. The characters which are diagnostic between the three patelliocrinids appeared later during ontogeny than those which differentiate the 20 armed alisocrinid from the 10 armed patelliocrinids. Phylogenetically the alisocrinid ancestors split from the 10 armed glyptocrinid stock in the Middle Ordovician whereas the Girardeau patelliocrinids originated in the Late Ordovician.

The alisocrinid correlation coefficients involving "size", calyx volume, food gathering system length and its components (legend, Text-fig. 34) range from .996 to .96. The number of specimens varies from 12 to 19 of which the former is most common. The significance levels of these correlations greatly exceed .999 which denotes that the food gathering system development was highly integrated and coordinated.

Comparison of the correlation coefficients and their significance levels between the alisocrinid and the three patelliocrinids is difficult because of the variation in the number of specimens among the four taxa. Nevertheless, the overall ranges suggest a general pattern:

Species	Usual number of specimens	Range of correlation coefficients	Significance level range
Eopatelliocrinus scyphogracilis	16	.90 - .994	above .999
E. latibrachiatus	10	.88 - .989	.999 to higher
Macrostylocrinus pristinus	11	.94 - .994	well above .999
Alisocrinus tetrarmatus	12	.96 - .996	well above .999

The data indicate the following integration and coordination gradient, listed from maximum to minimum regulation: *A. tetrarmatus, Eopatelliocrinus scyphogracilis* and *Macrostylocrinus pristinus, Eopatelliocrinus latibrachiatus*. The available information does not warrant any general conclusions for all crinoids.

As usual the alisocrinid correlation coefficient for calyx volume versus food gathering system length ($r = .996$, $N = 12$) exceeds that of "size" versus the ambulacral tract length ($r = .98$, $N = 12$).

Comparison of the correlations for the food gathering system components (*i.e.*, number of Brr per arm, average pinnule length and arm length) versus the half-ray food gathering system length discloses almost equal values (r ranges from .992 to .995). The patelliocrinids commonly show correlation coefficient gradients. For example, in *E. scyphogracilis*, the food gathering system growth was less well integrated with the number of Brr per arm ($r = .96$) than with the pinnule and arm length ($r = .98$ and .994, respectively). The significance of the different patterns remains unknown.

The alisocrinid percentage standard deviations for the various combinations of "size", calyx volume, food gathering system length and its components (legend, Text-fig. 34) range from 4.5 to 29% but most are below 7.1%. The highest values (14%, calyx volume versus "size", $r = .97$; "size" versus arm length, 29%, $r = .96$) are associated with two of the lowest correlation coefficients.

The equivalent patelliocrinid standard deviations are generally well above 10%. This may represent meaningful biological phenomena or problems of curve fitting. The alisocrinid equations provide satisfactory fits to crinoids of all "sizes" and ages, but the patelliocrinid regression lines yield better fits to the smallest animals.

The maximum "size" of the BB + RR + OO "theoretical microcrinoid" is .50 mm. The "initial intercepts" for the food gathering system components versus half-ray ambulacral tract length are near 0 (*i.e.*, range from .0037 to .24 mm). Some of the y equals near 0 values were used to estimate the approximate "size" when the IIIBrr first appeared:

Equation	y equals near 0 value	Predicted "size"
"Size" versus food gathering system length	.1 cm	.24 mm
Calyx volume versus "size" and calyx volume versus length of free ambulacral tracts	volume .0001 cc	.57 mm
"Size" versus Brr per arm	.1 Brr	.064 mm
"Size" versus pinnule length	.1 mm	.28 mm
"Size" versus arm length	.1 mm.	.22 mm

Except for the .064 and .57 mm figures, the calculated "sizes" are from .22 to .28 mm. These may suggest that the proximal IIIBrr appeared during this "size" interval. Conversely the .57 mm value may represent the "size" when the IIIBrr formed. At present the alisocrinid figures are inconclusive except to denote arm initiation within the .22 to .57 mm "size" interval. The patelliocrinids probably developed the proximal IIBrr around "sizes" of .3 to .8 mm.

Supporting structure ontogeny. — (Text-fig. 35). The "size" versus proximal column diameter was characterized by exponential development during which the columnal area width growth vector per 1 mm additional "size" declined from .25 mm to .22 mm with a .23 mm mean (Text-fig. 35a). The minimum and maximum "sizes" comprise 1.1 and 9.0 mm which correspond to predicted columnal widths of .29 and 2.1 mm, respectively. During growth, the "size"/proximal stem diameter increased from 3.8 to 4.3.

The relationship between calyx volume and proximal columnal area was also curvilinear (Text-fig. 35b). The initial, final and average growth rates equalled .32, .0044, and .030 mm^2 of additional stem area per .01 cc calyx volume increment, listed in the same order. The calyx volumes of the youngest and oldest crowns consist of .001 and .95 cc with equivalent proximal column areas of .042 mm^2 (observed figure, the equation value is –.38 mm^2) and 2.6 mm^2 (calculated). The proximal stem area/calyx volume ranges from 42 in the smallest specimen to 2.7 in the largest.

The FBrr were rapidly incorporated into the dorsal cup throughout ontogeny. The quarter-rays are supported, wholly or partially, by the IIIBr1 distal face over the 1.0 to 7.0 mm "size" interval. In larger animals, the IIIBr1 was completely fixed into the calyx and the IIIBr2, at least partly, bears the arms.

The ontogeny of "size" versus supporting Br width followed a curvilinear pattern over which the supporting Br growth vector per 1 mm "size" augmentation decreased from .12 to .086 mm; the mean constituted .099 mm (Text-fig. 35c). The oldest and youngest alisocrinids possess 9.0 and 1.1 mm "sizes"; the equivalent predicted supporting Br widths are .95 and .18 mm. The "size"/supporting Br width rose from 6.1 to 9.5 with progressive development.

The quarter-ray ambulacral tract length and supporting Br width had exponential development (Text-fig. 35d). The supporting Br width growth rate per 10 mm food gathering system length increase dropped from .044 to .0044 mm with a .011 mm average. The maximum and minimum quarter-ray food gathering system lengths comprise 620 and 3.1 mm which correspond to .81 and .16 mm calculated supporting Br widths. During the observed growth, the quarter-ray food gathering system length/sup-

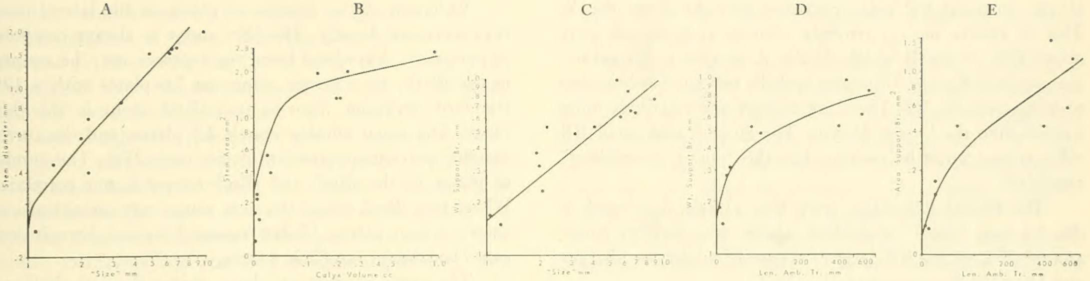

Text-figure 35. — Graphs showing supporting structure growth in *Alisocrinus tetrarmatus*, n. sp. Stem area and diameter refer to the proximal columnal. Supporting Br width and area are those of the distal FBr. "*a*" gives "initial intercept" or "pseudointercept".

Equation data:

A — Log$y$ = –.571 + .942log$x$. r = .960.
N = 12. "a" = .0307 (x = .1).
B — y = 2.46 + .942log$x$. r = .955.
N = 12. "a" = –1.31 (x = .001).
C — Log$y$ = .805 + .788log$x$. r = .907.
N = 14. "a" = .0255 (x = .1).
D — Log$y$ = –1.02 + .303log$x$. r = .926.
N = 10. "a" = .047 (x = .1).
E — Log$y$ = –1.86 + .607log$x$. r = .926.
N = 10. "a" = .00344 (x = .1).

porting Br width changed from 19 in the smallest to 770 in the largest individual.

A curved regression line is seen in the ontogeny of supporting Br area relative to quarter-ray ambulacral tract length (Text-fig. 35e). The initial, terminal, and mean supporting Br area growth vectors per 10 mm of quarter-ray food gathering system length augmentation consist of .038, .011, and .017 mm^2, respectively. The longest and shortest ambulacral tracts are 620 and 3.1 mm with equivalent equation supporting Br areas of 1.0 and .042 mm^2. The quarter-ray food gathering system length/supporting Br area ranged from a youngest animal value of 74 to 620 in the oldest crinoid.

The alisocrinid supporting structure correlation coefficients are distributed from .91 to .98 (see examples in Text-fig. 35 legend). All significance levels are greater than .999. The proximal column diameter and area correlations vary from .96 to .98. These are considerably higher than those for the supporting Br (.91 to .93). This implies that the proximal columnal development was subject to a higher degree of integration and coordination than was the supporting Brr. Perhaps the alisocrinid pattern was related to the presence of 20 arms or many FBrr or both. The patelliocrinids exhibit roughly equal correlation coefficients for both supporting relationships; these taxa have 10 arms in conjunction with a few-FBrr calyx.

Ornamentation development. — (Pls. 66, 67, Pl. 68, fig. 3). The surface sculpture ontogeny paralleled that of *Eopatelliocrinus scyphogracilis* and *Macrostylocrinus pristinus* except that the alisocrinid median-ray ridges formed earlier during ontogeny. The ridges are obscure in the smallest animals, "sizes" 1.1 to 1.4 mm. The IBrr are highly convex and arched with flat sides, and the IBrr median-ray ridges cover about 75% of the plate widths. These are represented on the distal RR margins by ill-defined vertical bulges. The gently convex distal RR ridges are not clearly separated from the plate margins, and these occupy approximately 50 to 60% of the RR widths. The 1.1 mm "sized" crown shows no evidence of the other median-ray ridge elements.

When a 1.4 mm "size" was attained, the lateral RR, proximal RR and BB ridges began to appear. All are gently convex and blend into the plate margins. The distal RR and BB ridges extend over most of the plate surfaces.

The main subsequent growth trend was to accentuate the previously formed median-ray ridges in two ways. Their convexity was augmented and they became more narrow relative to the plate widths. In the 3.4 mm "sized" individual, all ridges are defined, although the proximal RR and BB ridges continued to cover most of the plate widths. However, sharper distal RR ridges are seen, the widths of which equal roughly 50% of the RR widths.

The "adult assemblage" crinoids, "sizes" 4.2 to 9.0 mm, exhibit the mature stages of median-ray ridge differentiation. The 9.0 mm "sized" calyx has ridge widths which are distributed as follows: 40 to 50% of the IBrr widths, 40% of the distal R width, and 60% of the proximal R width. The mature crown proximal RR and BB ridges are arranged in two ways. Where the R is underlain by a large

B, the proximal RR ridge continues straight down the B. This is always heavy, strongly convex and extends over about 70% of the B width. If the R overlies a BB suture, the proximal R ridge bifurcates and the two smaller branches traverse onto the BB. These are sharper and relatively more narrow than the largest B type. The large B and small BB ridge types cannot be separated in the "young assemblage" animals.

The lateral RR ridges were first clearly developed in the 3.4 mm "sized" individual where their heights range around 30% of the RR heights. Those of adults are sharper and have similar percentage heights.

The "young assemblage" specimens, 1.1 to 3.4 mm "size" range, possess gently convex primanals and overlying anal series plates which contrast with the adjacent flat CD interray iBrr. Traces of the lateral-oblique ridges, which connect the anal interray ridge with the C ray and D ray RR, have not been seen. The adult calyces show strongly convex anal interray ridges which are more narrow with respect to the plate widths. Distinct lateral-oblique ridges are always present, and these probably formed at the same time as the iBrr sculpture.

The young crinoid iBrr are flat and featureless, up to a 3.4 mm "size". The iBrr sculpture was rapidly initiated in the smallest "adult assemblage" crown, "size" 4.2 mm. The typical mature dorsal cup ornamentation consists of a single sharp node, located at or near the plate center. Some animals have traces of stellate ridges on the proximal iBrr which comprise fine continuous or discontinuous ridges on the iBrr and adjacent ray plates. The stellate elements are not found above the IIBrr level.

Variation. — The alisocrinid IBrr shapes have been determined in 18 rays. The IBrr1 have from four to seven sides although hexagonal plates are by far the most common (15 rays). The mean side number equals 5.9 and the percentage standard deviation consists of 9.6%. The IAxx show six to eight sides; septagonal ones are observed in two-thirds of the studied rays. The average plate bears 7.0 sides with an 8.2% standard deviation.

The correlation coefficient between number of IBr1 and IAx sides equals .34, the significance level of which is less than .900. Such indicates the IAx geometry was poorly integrated and coordinated with that of the underlying IBr1. Because of this low correlation, highly variable IBrr-adjacent iBrr geometry is observed. A similar situation characterizes *Macrostylocrinus pristinus* and the various IBrr-iBrr geometries for the alisocrinid parallel those previously enumerated under the macrostylocrinid.

Variation of the number of plates in the lateral interrays increases distally. The iBr1 range is always composed of one plate. Anywhere from one to three may be counted in the iBrr2; the average comprises 2.0 plates with a 19% standard deviation. Two to four iBrr3 occur in the third range. The mean number equals 2.7 plates, and the corresponding percentage standard deviation is 25%. The number of plates in the iBrr2 and iBrr3 ranges is not correlated. Where two iBrr2 occur, the next range may consist of two, three, or four plates. Higher ranges have not been investigated because of insufficient data.

The same phenomena characterizes the inter-half-rays where the proximal range is only made up of one plate. The second level bears two or three plates, and the mean consists of 2.5 with a 20% standard deviation. As above, more distal plate groups were not measured due to the lack of available data.

The primanal position variation is surprisingly high. Five crinoids possess the normal glyptocrinid primanal where the C ray and D ray RR are in lateral contact with the primanal in the iBr1 position. In two individuals, the primanal rests directly on the CD interray B and separates the C and D ray RR. These two primanals occur in the tanaocrinid rather than the glyptocrinid position. One of these primanals (Text-fig. 29d) is small and clearly abnormal. The other (Text-fig. 29h) shows no malformation except that it is much larger than the primanals of normal individuals within the same "size" range. The percentage standard deviation for primanal position equals 35% (the normal position and the tanaocrinid positions are assigned arbitrary values of 1.0 and 2.0, respectively). This extreme variability is not completely understood. As discussed under phylogeny, *Alisocrinus tetrarmatus* is believed to have been derived from the ancestral stock of *Glyptocrinus decadactylus*. This glyptocrinid exhibits only low frequency primanal position changes and abnormal calyces are rare. Because of phyletic considerations, low variation would be expected in the alisocrinid. Thus, the large range of scatter is perplexing. Two hypotheses are presented: 1. Inadequate sample size. Perhaps if more alisocrinid calyces were available for study, the frequency of abnormal individuals would decrease. 2. The wide variability of alisocrinid primanal position may be significant and indicate genetic instability with respect to this character. If so, the Girardeau alisocrinid may have been ancestral to certain periechocrinitids. Admittedly, this hypothesis has not been adequately investigated. On the other hand, most crinoid specialists (*e.g.*, Moore and Laudon, 1943) believe that periechocrinitids were descended from tanaocrinids and not alisocrinids or glyptocrinids.

The number of plates following the primanal ranges from one to three with the latter being the general case. Quantitative data are not presented because of the small number of available measurements (only five).

Calyx width with respect to "size" is moderately variable with a percentage standard deviation of 19%. However, relative width and "size", as considered diagnostic of the species, are invariant. As previously mentioned under calyx ontogeny, the different FBrr types show marked correlation coefficient and standard deviation gradients. The correlations and percentage standard deviations for "size" versus FBrr in lateral interrays equal .95 and 9.3% whereas those for "size" versus inter-half-ray iBrr consist of .54 and 30%. Both the correlation coefficients and percentage standard deviations reflect the more poorly integrated and coordinated growth pattern of the inter-half-ray FBrr.

The total number of BB cannot be determined in any single calyx because all specimens are partly buried in matrix. The number reconstructed from the various crowns equals four. The large lateral interray B probably has sutures located in B and E ray orientation. A small CD interray B is observed where the primanal lies in the normal position; a large B occurs in conjunction with the tanaocrinid-type primanal. Aside from these two variants, the BB circlet appears to be conservative.

The number of arms per ray (34 rays counted in 20 crowns) varies from three to four. The mean equals 3.9 arms with a percentage standard deviation of 7.3%. The normal number consists of four. Only one or two rays can be determined in a single individual; the remaining rays are wholly or partially obscured by the enclosing rock. As far as known, a crown never has more than one three armed ray. The "size" distribution of animals with abnormal rays is deemed significant. Three are "young assemblage" crinoids whereas only one survived to adulthood. This suggests that differential natural selection eliminated three armed variants more rapidly than normal four armed types (see also summary statement on food gathering system growth).

In crinoids with two arms per half-ray, two or three IIBrr occur with the former being the common case (56 versus three half-rays). The mean equals 2.05 and the percentage standard deviation 11%.

As usual in Girardeau camerates, the total Br shape variation has not been investigated. However, percentage standard deviations for one parameter with respect to another are available; these range from 9.1 to 27% (see legend, Text-fig. 33).

Intraspecific variability within *Alisocrinus tetrarmatus* is related to the overall taxonomic character heirarchy as outlined below:

Suborder characters: A. RR in lateral contact. Invariant. B. Primanal in iBr1 position. Intraspecific variation is surprisingly high within the Girardeau form (percentage standard deviation consists of 35%). However, most other species of Glyptocrinina show much lower variation and *A. tetrarmatus* is considered peculiar in this respect. The character is accepted as valid at the suborder level.

Superfamily: A. Number of BB. B. Presence of conical, primitive, many-FBrr calyx in adult specimens. Both are conservative within the Girardeau crinoid. C. Number of plates following primanal (three). From one to three plates succeed the primanal of *A. tetrarmatus*. Apparently, this is abnormal because most species studied almost always have three plates above the primanal.

Family: Gross nature of arms. No variation.

Genus: Further details of arm structure (*i.e.*, subdivision of family level character). The Girardeau crinoid is conservative if the writer's generic diagnosis is followed.

Species: A. Calyx shape, principally relative height and width, is subject to a 19% standard deviation in the Girardeau crinoid. The mean calyx shapes of all three species of *Alisocrinus* are different although end-member variants probably overlap to a slight extent. B. Ornamentation. Invariant as considered diagnostic. C. Brr shapes, especially relative height and width. The applicable percentage standard deviations of *A. tetrarmatus* range from 15 to 18% (legend, Text-fig. 33). The *A. warreni* arms are only observed in one specimen and these are not preserved in *A. laevis*. Consequently, the possible amount of interspecies overlap is unknown.

Two conclusions are drawn: 1. If the wide amount of *A. tetrarmatus* primanal variation is ignored, the available information on intraspecific variability indicates the general character heirarchy is valid; 2. Intraspecific character variation increases from higher to lower taxonomic level characters.

Comparison. — Adult individuals of the Girardeau form are most similar to the Middle Silurian *A. warreni* (Ringueberg) (1888, p. 133, pl. 7, figs. 4, 4a; see Wachsmuth and Springer, 1897, p. 283, pl. 22, fig. 1 for better figure). The Silurian taxon differs from *A. tetrarmatus* in having wider Brr relative to their heights, more rapidly expanding dorsal cup, and numerous fine stellate markings on the ray plates.

A. tetrarmatus may be separated from *A. laevis* Kirk (1929, p. 344; illustrated by Springer, 1926, p. 29, pl. 5, figs. 9, 10 as *Mariacrinus carleyi*) by the stellate ridges and nodes on the iBrr and somewhat wider calyx with respect to height.

Specific name. — *tetrarmatus* in allusion to the presence of four arms per ray.

Types. — Holotype — USNM 164 579. Paratypes — USNM 164 580-164 588; Univ. Ill. X-4672; YPM. 27028-27030; IGS. 10486, 35P-31 — 35P-37.

Occurrence. — Girardeau Limestone, Cape Rock and Orchard Creek exposures.

PHYLOGENY OF GIRARDEAU ALISOCRINIDS AND ALLIES

PREVIOUS WORK, SOURCES OF DATA AND LIMITATIONS

The most notable contributions are those of Kirk (1929), Moore and Laudon (1943, pp. 89, 96-98), and Ubaghs (1953, pp. 710-712, text-fig. 82; 1958). The Ubaghs 1958 paper is the most comprehensive, and his views are largely supported by this study. The evolution of all Melocrinitidae will not be considered here. Only early and primitive forms are discussed, namely *Glyptocrinus* through *Promelocrinus*. The species involved, their geologic occurrences, and sources of the measured samples are listed below:

Glyptocrinidae

Glyptocrinus ornatus Billings. Middle Ordovician; Trenton; Canada. Five USNM and Springer Collection specimens examined by the writer.

G. decadactylus Hall. Late Ordovician; Richmond; Cincinnati area, Ohio. Fifteen USNM and Springer Collection crinoids measured by the author including those figured by Wachsmuth and Springer (1897, p. 270, pl. 6, fig. 12, pl. 20, figs. 4a-e, pl. 21, figs. 4a, b).

Melocrinitidae

Alisocrinus tetrarmatus. Late Ordovician; Girardeau Limestone.

A. warreni (Ringueberg). Type species. Middle Silurian; Rochester Shale; New York. Type and only known specimen in United States National Museum.

A. carleyi (Hall). Middle Silurian; Waldron Shale; Indiana and Tennessee. Eight USNM and Springer Collection crinoids including calyces figured by Wachsmuth and Springer (1897, p. 282, pl. 22, figs. 2a-c).

Promelocrinus fulminatus (Angelin) and *P. radiatus* (Angelin). Middle Silurian; Gotland. Data from descriptions and photographs in Ubaghs (1958).

P. anglicus Jaekel. Type species. Middle Silurian; Dudley, England. Data from seven Springer Collection crinoids including those figured by Springer (1926, p. 27, pl. 5, figs. 2, 3) as *Melocrinus* (?) *spectabilis* Angelin.

In addition, several species which were referred to *Alisocrinus* by Kirk have been examined; these are *A. laevis* Kirk and *Mariacrinus aureatus* Miller. As already mentioned under *Alisocrinus,* the latter is not referable to the genus. These forms are omitted from the numerical treatment because the arms are unknown. Basically, at least some specimens of all known applicable species within the scope of the project have been examined.

DISCUSSION OF DENDROGRAM

Study of the dendrogram (Table 17c) and the taxonomic or morphological distance matrix (Table 17b) indicates the morphological distances and generic level taxonomy do not invariably follow parallel paths, at least not as the original data matrix is coded (Table 17a). The first order or mutually exclusive taxonomic distances are four arms per ray alisocrinids, *Alisocrinus tetrarmatus* plus *A. warreni,* and *Promelocrinus fulminatus* plus *P. radiatus.* The higher orders begin to truncate the generic taxonomy. *Alisocrinus carleyi* joins the previous *Promelocrinus* cluster largely because the arm branching similarity over-rides the presence of pinnules on the ray trunks of *Alisocrinus carleyi;* these are absent in *Promelocrinus fulminatus* and *P. radiatus.* In similar fashion *Glyptocrinus decadactylus* is more similar to four arms per ray *Alisocrinus* than to *Glyptocrinus ornatus,* with two arms per ray. Here, the presence of four arms per ray outweighs the difference in BB number; *Glyptocrinus* has five BB, *Alisocrinus* only four. In the fourth clustering cycle, *Glyptocrinus ornatus* is assigned to the previous *G. decadactylus, Alisocrinus tetrarmatus,* and *A. warreni* group. Inspection of the taxonomic distance matrix (Table 17b) discloses moderately large distances in all cases. *Glyptocrinus ornatus* with two arms per ray is strikingly different from the other species, all of which have four arms per ray. The last species to cluster is *Promelocrinus anglicus* which exhibits much larger taxonomic distances than any other form. Although the lowest distances are with *P. fulminatus* and *P. radiatus,* the values are still large and impressive. The unique characters of *P. anglicus* consist of the biserial armlets and large number of ray trunk branches.

As implied in the introduction, these cross cutting relationships do not necessarily invalidate the generic taxonomy. However, the above data suggest that *P. anglicus* is not congeneric with *P. fulminatus* and *P. radiatus.* Perhaps, *Alisocrinus carleyi* should be grouped with *Promelocrinus fulminatus* and *P. radiatus* rather than with *Alisocrinus.*

Table 17a

	Glyptocrinus ornatus	G. decadactylus	Alisocrinus tetrarmatus, n. sp	A. warreni	A. carlyei	Promelocrinus fulminatus	P. radiatus	P. anglicus
1. Number of Arms per ray	2.0	4.0	3.9	4.0	6.0	6.0	8.0	24.0
2. Number of IIBrr	50.0	2.08	2.05	2.25	2.29	2.30	2.0	2.12
3. Branched or unbranched quarter rays	1	1	1	1	4	4	4	4
4. Number of branches on the inner quarter rays	0	0	0	0	1	1	2	11
5. Number of Brr between the above branches	50.0	50.0	50.0	50.0	8.0	6.0	6.75	5.24
6. Type of Brr on the inner quarter-rays	1	1	1	1	1	1	1	4
7. Type of Brr on the outer quarter-rays	1	1	1	1	1	1	1	4
8. Pinnules present or absent on the inner quarter-rays	1	1	1	1	1	4	4	4
9. Distal FBr	18.0	29.7	15.0	12.0	25.7	13.0	17.0	29.9
10. Number of BB	5	5	4	4	4	4	4	4

Original data matrix for the phylogeny of *Alisocrinus* and its allies. All data from mature crinoids. The data are coded as follows:

1. Number of arms per ray: The *Promelocrinus* figures may be too low as the arms are not fully known.
2. Number of IIBrr: Arbitrarily coded as 50.0 for species with two arms per ray.
3. Branched inner quarter-rays-4. Unbranched inner quarter-rays-1.
4. Number of branches on the inner quarter-rays. The numbers for *Promelocrinus* may be too small.
5. Mean number of Brr between the above branches.
6. Type of Brr on the inner quarter-rays: Uniserial-1. Biserial-4.
7. Same as the above for the outer quarter-rays.
8. Pinnules absent on the inner quarter-ray ray trunks-4. Pinnules present-1.
9. Distal FBr coded in the ontogenetic numerical scale.
10. Number of BB.

The lineage shown in Text-figure 36 was compiled from the taxonomic distance matrix and the dendrogram (Tables 17b, c) with adjustments made for stratigraphic relationships. Comparison of the dendrogram and the phylogeny diagram discloses obvious differences. All in all, the phylogeny diagram more closely approximates the generic taxonomy than the dendrogram. The lineage is mainly self-explanatory with one exception. The Late Ordovocian *A. tetrarmatus* is thought to represent the ancestral stock of the Middle Silurian *A. carleyi* rather than *A. warreni* also of the Middle Silurian. This is indicated by comparison of the taxonomic or morphological distances, *A. tetrarmatus* versus *A. carleyi*, .951, *A. warreni* versus *A. carleyi*, 1.02, and by comparison of species characters, such as calyx shape and ornamentation, which are not included in the original data matrix (Table 17a). Consequently, *A. warreni* probably constituted a primitive derivative of *A. tetrarmatus* which survived "past its time". Clearly, *A. warreni* was not a successful Rochester Shale species as only one specimen is known. Apparently, this form only survived because of peculiar ecological conditions or absence of more advanced melocrinitids.

EVOLUTIONARY TRENDS AND MECHANISMS THEREOF

Throughout phylogeny of the Girardeau alisocrinid and its allies, the calyx was largely stabilized at a primitive many-FBrr type although the number of BB was reduced from five to four. The major part of the sequence constituted arm evolution which proceeded from a simple to a complex configuration, and eventually, a highly ramified ray trunk was produced. Basically, the primitive melocrinitids retained a stable calyx structure while the food gathering capacity was progressively augmented. Consequently, these evolutionary trends were probably adaptative and beneficial to the crinoids. In this general theme of evolution, the melocrinitids paralleled the usual camerate crinoid model; this provides a striking contrast to the patelliocrinid evolution in which a primitive many-FBrr calyx evolved into an almost no FBrr type.

All of these evolutionary trends most likely occurred through "mutations" (most general context) which affected the ontogeny of young crinoids. Comparison of taxonomic distances between the immature and mature crinoids of two related species shows lesser taxonomic distances for the youngsters. Relative to the alisocrinoid phylogeny, growth sequences are available for three forms, and the reader is invited to compare these. *Glyptocrinus decadactylus* Hall. Late Ordovician. "Size" range about 3.0 to 20 mm. Unfortunately, the young crinoids have never been illustrated. *Alisocrinus tetrarmatus*. Girardeau Limestone. "Size" range 1.1 to 9.0 mm. *Ctenocrinus paucidactylus* (Hall). Early Devonian. This species is a melocrinitid, although more advanced than those considered here (see Goldring, 1923, p. 122, pl. 8, fig. 5, pls. 9-11 for growth sequence). The effects of these "mutations" can be catalogued with reasonable certainty even though the ontogenies are not known in all forms. The evolutionary trends and the "mutations" concerned are listed below in order of appearance in the fossil record.

I. The development of four arms per ray from two arms per ray occurred during the transition from *Glyptocrinus ornatus* (Middle Ordovician) to *G. decadactylus* of the Late Ordovician. In four armed species, the IIBr2, rarely IIBr3, is axillary. The proximal pinnule of two armed forms is most commonly located on the interray side of IIBr2. Generally, this pinnule is differentiated from the others by a prominent ridge on the fixed pinnulars (see *Alisocrinus ? heterodactylus*). This suggests the responsible "mutation" converted the IIBr2 pinnule into a pinnulate arm. Two basic changes were required. Most of the former pinnulars developed pinnules (*i.e.*, were converted into pinnulate uniserial Brr). The *Glyptocrinus ornatus* IIBr2 pinnule is not fully known, but it probably contained no more than 15 pinnulars. One of the four arms per ray of a mature *G. decadactylus* bears over 100 Brr. Consequently, the additional Brr per arm growth rate must have been greatly accelerated with respect to time and "size". The growth stage where these changes occurred may be estimated from *Alisocrinus tetrarmatus*, where the youngest animal ("size" 1.1 mm) possessed about four IIIBrr per arm. The divergence in growth pattern was most likely induced prior to this phase, roughly when the IIIBr1 appeared. Numerous abnormalities known in living crinoids indicate that pinnulars develop into pinnulate Brr and that pinnulate Brr may evolve into axillary Brr. For example, Gislén (1924, pp. 11, 12, text-fig. 4) reported branched pinnules in various comatulids. In one specimen of *Antedon petasus*, the first and third pinnulate Brr bear large pinnulate arms in several rays, in place of the normal pinnules (Gislén, 1924, pp. 20, 21).

II. Reduction of the number of BB from five to four happened during the Late Ordovician *Glyptocrinus decadactylus* to *Alisocrinus tetrarmatus* stage of evolution. The "mutation" involved, the growth stage affected, and the adaptive significance of the change were probably the same as those previously postulated for the patelliocrinids. The only difference consisted of the number of BB

Table 17b

G. ornatus	G. decadactylus	A. tetrarmatus, n. sp.	A. warreni	A. carleyi	P. fulminatus	P. radiatus	P. anglicus
0	1.0324	1.1377	1.1570	1.4450	1.5585	1.5634	2.4630
1.0324	0	0.9324	1.0250	1.0898	1.4432	1.3773	2.1978
1.1377	0.9324	0	0.1297	0.9515	1.0510	1.0672	2.1876
1.1570	1.0250	0.1297	0	1.0203	1.0479	1.0846	2.2273
1.4450	1.0898	0.9515	1.0203	0	0.8214	0.7280	1.8370
1.5585	1.4432	1.0510	1.0479	0.8214	0	0.2125	1.8707
1.5634	1.3773	1.0672	1.0846	0.7280	0.2125	0	1.7334
2.4630	2.1978	2.1876	2.2273	1.8370	1.8707	1.7334	0

Taxonomic distance matrix for the Girardeau alisocrinids and allied forms. Low numbers denote close morphological resemblance, high numbers vice versa.

Table 17c

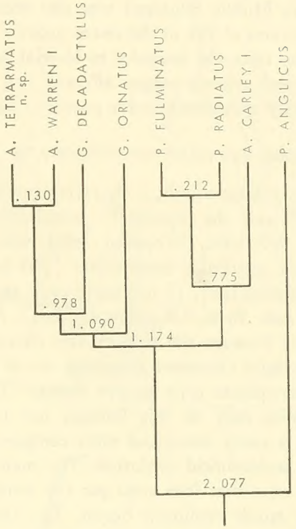

Dendrogram for *Alisocrinus tetrarmatus,* n. sp. and its allies. Low numbers indicate close morphological resemblance; high numbers vice versa.

concerned, patelliocrinids, five BB reduced to three and melocrinitids, five BB fused to four.

III. Formation of the inner quarter-ray arm branch (proximal ray trunk branch) took place during the change from *A. tetrarmatus.* (Late Ordovician) and *A. warreni* to *A. carleyi* (latter two species both Middle Silurian). A full complement of pinnules was retained. In *A. carleyi,* this arm branching is located on IIIBrr8. Thus, the "mutation" converted this plate from a pinnulate Br in *A. warreni* and *A. tetrarmatus* to an axillary Br in *A. carleyi.* Basically, the mechanism paralleled that involved in the evolution from two to four arms per ray. With respect to the ontogeny of *A. tetrarmatus,* young animals within the 1.4 to 1.8 mm "size" range have eight or nine IIIBrr per arm and the divergence must have been initiated at about this time.

IV. The change from Middle Silurian *A. carleyi* to *Promelocrinus fulminatus* (also Middle Silurian) was marked by the loss of pinnules on the proximal part of the inner quarter-rays below the IIIBrr arm branch. In terms of ontogeny, the Brr simply failed to form pinnules as they were added at the arm tips, and these Brr retained the nonpinnulate configuration of terminal Brr. Once the pinnules were lost, the proximal part of the inner quarter-rays became a ray trunk. Relative to the *Alisocrinus tetrarmatus* ontogeny, a "size" range of less than 1.1 mm to about 1.4 mm was involved. *A. carleyi* has this branch on IIIBr8 whereas IIIBr6 is axillary in *Promelocrinus fulminatus,* and the axillary migrated proximally due to accelerated ontogeny.

V. Evolution of more ray trunk branches occurred steadily in the Middle Silurian species, *P. fulminatus* (one) to *P. radiatus* (at least two) to *P. anglicus* (more than 11). Always, two growth divergences took place; the formation of the new branch or branches and the loss of ray trunk pinnules proximal to the new branches. The known fossil record and the ontogeny of *Ctenocrinus paucidactylus* suggest that both changes were simultaneous. The exact mechanisms were discussed previously.

VI. The transition from *Promelocrinus radiatus* to *P. anglicus* (both Middle Silurian) was also characterized by the transformation of Brr in the outer quarter-rays and ray trunk branches from the uniserial to biserial geometry. The "mutations" and growth stages affected are the same as those previously annotated under patelliocrinid evolution.

RELATIONS BETWEEN EVOLUTIONARY TRENDS

As in the patelliocrinids, a character correlation matrix was prepared and the significant correlation coefficients (above the .950 level, two-sided test) were noted and studied. Of 45 applicable coefficients [(10 by 10 matrix, minus 10 diagonals)/2], 15 are significant and exceed .71; these range from .78 to 1.0 (signs ignored). All significant relations occur between the various arm characters.

All meaningful character groupings are of the prior and seemingly prerequisite type in this lineage. The term prerequisite applies only to this lineage, not to crinoids in general; this is easily visualized after comparing the patelliocrinid and melocrinitid evolution. The main melocrinitid prerequisites were that four arms per ray were required before the ray trunk evolution began. The formation of a IIIBrr inner quarter-ray branch was prior to the loss of proximal ray trunk pinnules and the evolution of more ray trunk branches. A certain level of ray trunk evolution developed previous to the acquisition of biserial Brr.

Essentially, all the alisocrinid — melocrinitid lineage character correlation coefficients signify is that each step in the arm evolution (as far as examined) was consistent with the geometry of previous crinoids. Each stage of evolution represented a small change from the previous phase, and the changes in the total line were cumulative. The trends proceeded in the same general direction, namely toward more highly ramified arm branching. Thus, these correlation coefficients are merely a profound statement of the obvious.

All primitive melocrinitid evolutionary trends are most logically interpreted as having adaptive benefit to the lineage. Evolution of the ray trunks provided the animals with a progressively larger and more complex food gathering system which drained greater amounts of water. Reduction of the number of BB may have increased the mechanical strength of the calyx, better protected the chambered organ, and simplified the problems of integration and coordination of calyx growth. This suggests that natural selection constituted the evolutionary vector and that genetic drift was negligible or totally absent. The time distribution of characters and the relations between these indicate that natural selection acted on one character at a time. This was in marked contrast to the patelliocrinid evolution where several characters were selected at once. The interpretation of natural selection as the driving force is also consistent with the available data pertinent to population sizes. The writer has no knowledge of the population sizes of *Promelocrinus radiatus* and *P. fulminatus*. Judging from the abundance of specimens, all other species, with the exception of *Alisocrinus warreni*, clearly established large enough populations so that small selection coefficients would have exerted efficient evolutionary leverage (see paleoecology for population size of *A. tetrarmatus*). The largest populations were probably those of *Glyptocrinus decadactylus, Alisocrinus tetrarmatus*, and perhaps *Promelocrinus anglicus*. The smallest was *Alisocrinus warreni* which is only known from one specimen. This form may have been subject to genetic drift although this cannot be proved.

PALEOGEOGRAPHY AND EVOLUTION

Generally, the primitive melocrinitid evolutionary "jumps" as indicated by the larger taxonomic or morphological distances were correlated with paleogeography. Two of the largest taxonomic distances occur across paleogeographic breaks: *Glyptocrinus ornatus* (Middle Ordovician, Trenton) — *Glyptocrinus decadactylus* (Late Ordovician, Richmond), 1.032. *Alisocrinus tetrarmatus* (Late Ordo-

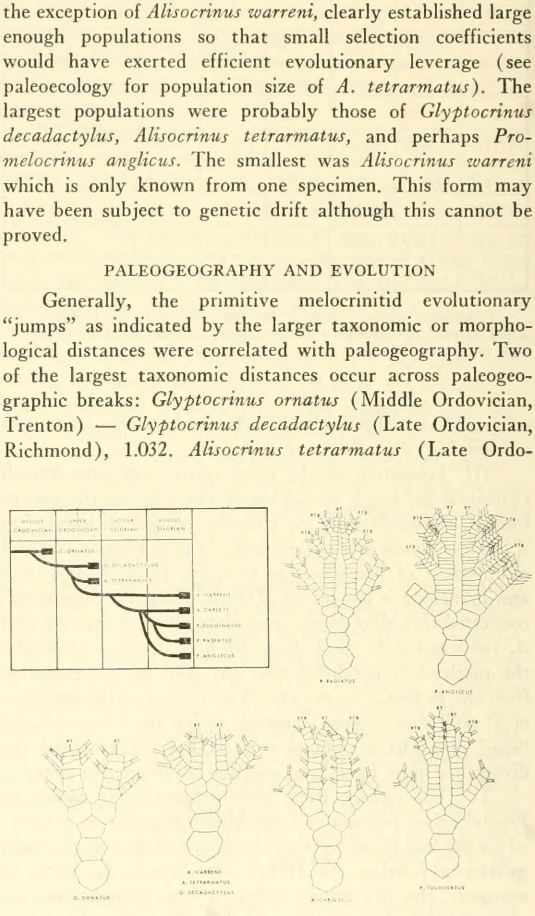

Text-figure 36. — Phylogeny of *Alisocrinus tetrarmatus*, n. sp. and its allies. Solid bars denote approximate known occurrence of species; finer lines show inferred lines of ancestry and descent. The drawings showing ray structure are schematic and not to scale. The location of pinnules on the diagrams is generalized. The sketches are not taken from specific specimens; rather these are intended to roughly illustrate the mean crinoids as far as known. The crinoids were compiled from the data and specimens mentioned in the text. RT denotes the ray trunk or arm branch from which it was derived. RTB indicates the ray trunk branch. Pinnules stippled.

vician, probably Richmond) — *A. carleyi* (Middle Silurian), .951. The greatest taxonomic distance is found within a single favorable interval: *Promelocrinus radiatus* — *P. anglicus* (both Middle Silurian), 1.733. Actually, this is somewhat misleading because *P. anglicus* was a precocious form which developed some characters much earlier than most allied crinoids. Had Middle Silurian species of *Ctenocrinus* (see for example, Ubaghs, 1958) been considered, the Middle Silurian taxonomic distances would most likely decline. Consequently, primitive melocrinitid evolution largely supports R. C. Moore's hypothesis (1948, 1952b) on the relationship of paleogeography and evolution.

PALEOBIOGEOGRAPHY

The Middle and Late Ordovician stages of evolution were confined to North America; these crinoids are unknown in Europe, and apparently, melocrinitids failed to migrate to Europe along with the Late Ordovician patelliocrinid lineage. Lower Silurian melocrinitids have not been reported. During Middle Silurian time, the lineage lived in North America and Europe as follows. North America. *Alisocrinus warreni* and *A. carleyi;* Europe. *Promelocrinus fulminatus, P. radiatus,* and *P. anglicus.* Comparison of the species distribution and evolutionary trends shows that neither continent had a complete lineage. Consequently, intermigration must have taken place between North America and Europe when the crinoids were evolving.

ALISOCRINUS? HETERODACTYLUS, n. sp

Plate 68, figures 2, 4; Text-figures 37, 38

Diagnosis of adult. — A species questionably assigned to *Alisocrinus* characterized by many FBrr; stellate dorsal cup plates; prominent median-ray ridges; BB circlet with strong proximal flange. Arm branching structure of two types: IIBr2 axillary; roughly IIIBr23 axillary. IIBr2 nonaxillary with half-ray first branching on about IIBr27. Both types common, apparently with random distribution.

Partial description of adult. — The rest of the description follows in the sections on ontogeny and variation.

Proximal iBrr large and regular; ranges consist of one, two, and three plates, listed from proximal to distal; proximal iBrr end at IIBr1 level. Intermediate iBrr with three to five ranges, each with two to four plates; last range terminates at IIBrr3 or IIIBrr1 level. About six distal ranges present with two to seven plates per range, plates small and irregular.

Proximal four inter-half-ray iBrr ranges regular; one plate in first range, usually two in higher ranges. Highest ranges composed of four or five small irregular plates.

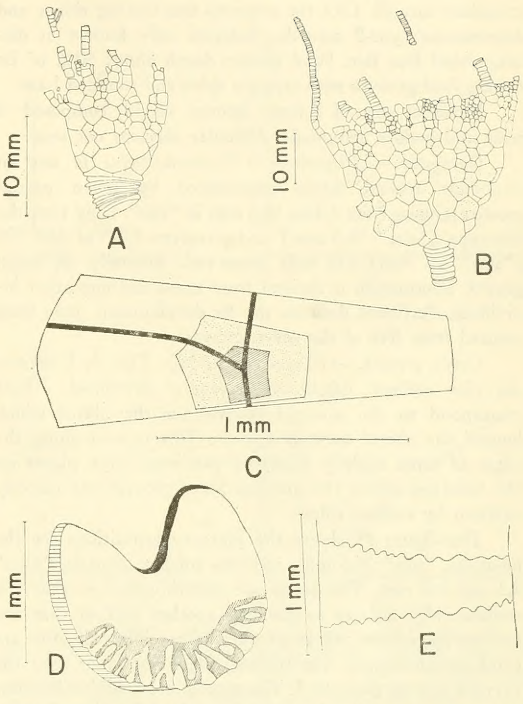

Text-figure 37. — *Alisocrinus? heterodactylus,* n. sp., Girardeau Limestone.
A. — Paratype, USNM 164 590, D ray, "size" 4.2 mm, Cape Rock exposure. The iBrr are stippled.
B,D,E. — Holotype, USNM 164 589, "size" 16.6 mm, Cape Rock exposure.
B. — Lateral view. The iBrr stippled. D. — Articular surface of free Br showing distribution of ridges and depressions on dorsal side of Br; ventral part of distal surface is weathered and these are not seen. Depressions indicated by oblique ruling. Ridges are unshaded. E. — Sketch of free IIIBr showing crenulate suture.
C. — Superimposed Brr of holotype/paratype USNM 164 590/IGS. 35P-38. "Sizes" 16.6, 4.2 and 2.5 mm, respectively. The Brr shown are mean standard Brr for the specimen concerned. Smallest is ruled; middle one stippled; largest blank. Food groove axes represented by heavy black lines.

Primanal in iBr1 position, followed by three plates. Anal series plates large. CD interray iBrr smaller; one plate in proximal range; two plates in higher ranges.

Tegmen unknown.

Free Brr with two types of articular surfaces. Dorsal and lateral margins with small sinuous ridges which alternate with depressions; long axes of ridges at right angles to Brr margins; surface of facet flat or slightly concave; when in place, the ridges and depressions interlock, forming crenulate sutures. Like the previous but lacking ridges and depressions; type-2 articular surfaces only known in disarticulated free Brr. Food groove depth about 50% of Br depth; food grooves with straight sides and rounded base.

Proximal part of column known; round, composed of wide and nodose columnals. Articular surfaces not seen.

Ontogeny. — *Alisocrinus ? heterodactylus* is not an abundant crinoid, being represented by seven partial crowns ranging from 2.5 to 16.6 mm in "size". Only two, the holotype ("size" 16.6 mm) and paratype USNM 164 590 ("size" 4.2 mm) are well preserved. Virtually all calyx growth information is derived from these and one other individual. Pertinent data on the Br development have been secured from five of the seven crowns.

Calyx growth. — (Text-figs. 37-39). The *A. ? heterodactylus* stellate ridges are strongly developed. These correspond to the internal grooves on the plates which housed the aboral nervous system. This is seen along the edges of some slightly displaced proximal calyx plates on the holotype where the internal plate grooves are directly overlain by stellate ridges.

Text-figure 38 shows the plate superpositions for the holotype, "size" 16.6 mm, and two smaller animals, "sizes" 4.2 and 6.7 mm. The plates are superimposed so that the stellate ridge centers overlie one another and so that the stellate ridge axes are as parallel as possible. The fits are good considering: 1. The stellate ridges are wider than the nervous system grooves. 2. The same plate exhibits different shapes in the various crinoids (*e.g.,* IAxx, Text-fig. 38c where one is septagonal and the other pentagonal). Consequently, the stellate ridge patterns differ and exact plate superposition is difficult.

As in most Girardeau patelliocrinids, the percentage height and width points remained constant on the BB, RR, IBrr1, IAxx, iBrr1 and iBrr2 throughout ontogeny. The percentage width points range from about 45% to 53%; the average width is nearly at the midpoint (50%) for all plates. The percentage height points vary from 46% to 55% depending on the plate; these denote unequal proximal and distal height growth rates. The proximal fixed-IIBrr and higher iBrr data are inadequate because the stellate ridges are not defined in the smaller crinoids. Also, the BB are not discussed as these are not well known.

As usual, the ontogeny of all plates was linear. The major calyx plates retained a constant number of sides during development of a single individual. The predominant growth trend consisted of height/width augmentation which proceeded more rapidly in the ray plates than in the interrays.

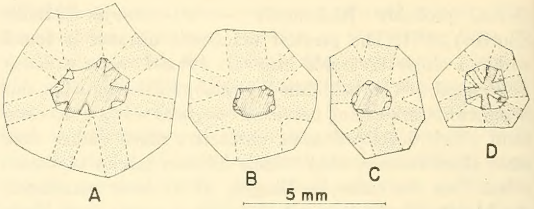

Text-figure 38. — Superpositions of major calyx plates for *Alisocrinus? heterodactylus,* n. sp. A. — RR plates. Holotype/Paratype USNM 164 590. "Sizes" 16.6 and 4.2 mm, respectively. B. — IBrr1. Same crinoids in A. C. — IAxx. Same crinoids in A. D. — iBrr2. Holotype/Paratype USNM 164 591. "Sizes" 16.6 and 6.7 mm, respectively.

Stellate ridges on small plates obliquely ruled, outlined with continuous line; larger plate ridges stippled, outlines are dashed. All drawings to same scale.

The RR percentage height point is 53%, indicating that the proximal height growth rate slightly exceeded the distal one (Text-figs. 38a, 39a). The total width growth rate equalled 1.0 mm per 1 mm height increment. The height/width ranged from .60 in the 4.2 mm "sized" crinoid to .90 in the 16.6 mm specimen. The R-B-B intersection migrated proximally relative to the plate midpoint during growth; consequently, the plate lower margins became more angular. In larger crinoids, the R-iBr1 suture is more steeply inclined relative to the ray axis due to the progressive height/width increase.

Text-figure 38b illustrates the IBr1 growth; the percentage height point consists of 51%, denoting nearly equal proximal and distal height growth vectors. The height/width rose from .72 to .97. The IBr1-IAx and IBr1-R sutures become relatively more narrow during ontogeny. The inclination of the IBr1-iBr1 and IBr1-iBr2 sutures is more pronounced in older animals. Both changes were caused by the increase in height with respect to width of the RR, IBrr1, iBrr1 and IAxx.

During IAx ontogeny, the height/width ranged from .85 to 1.3 (Text-fig. 38c). The percentage height point remained at 46%. Like the other ray plates, the IAx-iBrr sutures showed increased angles of inclination in larger specimens.

The iBr1 height/width of the smaller crinoid equals .80 whereas in the largest the same figure is 1.2. In the iBrr2 (Text-fig. 38d), the height/width was augmented from .87 in the 6.7 mm "sized" calyx to 1.0 in the largest crinoid. The percentage height points are located at 53% for the iBr1 and 55% for the iBr2. In both iBrr, the proximal height growth vectors were larger than the distally oriented ones.

The development of "size" and RR height (Text-fig. 39b) followed the characteristic linear pattern in which the relative RR height declined with respect to "size". Over the 4.2 to 16.6 mm "size" range, the "size"/height R rose from about 2.5 to 3.2.

The FBrr and iBrr incorporation rates in the lateral interrays and the inter-half-rays were linear and rapid as in most many-FBrr camerates (Text-figs. 39c, 37a, b). In the paratype, USNM 164 590 ("size" 4.2 mm), the highest lateral interray and inter-half-ray FBrr comprise IIIBrr1 and IIIBrr2, respectively. The distal FBrr of the holotype, "size" 16.6 mm, are IIBrr8 in both areas (equivalent to IIIBrr6 of half-rays with axillary IIBr2).

Major changes occurred in the Brr as they were incorporated into the dorsal cup. Prior to fixation, the free Brr sides are smooth or slightly nodose; the overall outline of these is like that of the higher free Brr. When incorporated into the calyx, the sides developed angular margins; the iBrr then joined along these margins and fixed the Br. Although these marginal growth vectors have not been examined, they must have been complex in the proximal IIBrr and IIIBrr because these Brr commonly join two or sometimes three iBrr into the dorsal cup. The higher Brr marginal growth rates, at the time of incorporation, were somewhat less complex as these plates usually only adjoin one or two iBrr (see Text-figs. 37a, b).

The development of fixed pinnules is best observed on the IIBrr2 interray sides, but can also be examined in higher pinnules, such as those of IIBrr5. Previous to fixation, the pinnulars have smooth sides and the pinnules are not differentiated from the higher free pinnules except for slightly larger size. As the pinnulars were incorporated into the calyx, two major changes occurred (compare the IIIBrr2 pinnule of Text-fig. 37a with the IIBrr2 and IIBrr5 pinnules on 37b). The pinnulars developed angular sides. Generally, the pinnular margin joins two or three iBrr. The pinnular underwent an increase in size, especially width, during or just prior to fixation. Concommittantly, the proximal pinnular inner side joined the lateral margin of the Br distal to the pinnule.

The nature of the fixing iBrr varies with their age of incorporation into the calyx. The iBrr which compose the dorsal cup walls during the early phases of calyx growth are relatively few, large and regularly aranged (see iBrr ranges up to level of IIBrr2 or 3 in the holotype). The higher iBrr ranges which were fixed later during ontogeny are much smaller, more numerous and less regular. The contact between the two iBrr types forms a discontinuity in the calyx. A similar discontinuity occurs in the inter-half-rays at a higher level (approximately IIBrr5 in the holotype) although this is less marked and consistent.

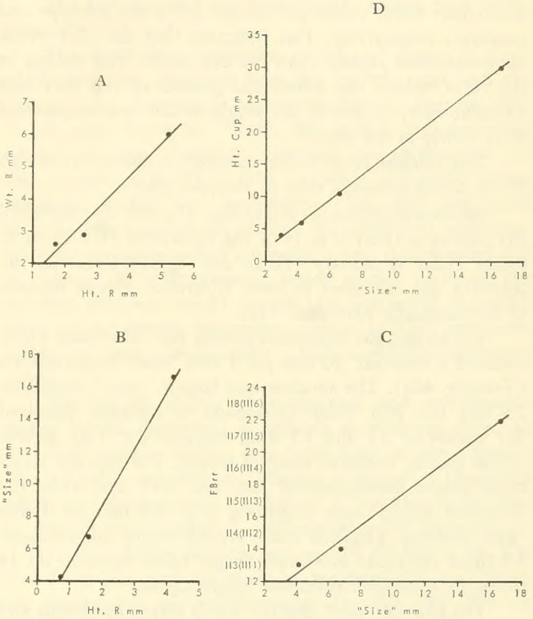

Text-figure 39. — Graphs showing calyx growth in *Alisocrinus? heterodactylus*, n. sp. FBrr are given in both the numerical scale used for statistics and the plate scale (*i.e.*, IAx, IIBr1 = II1, IIIBr2 = III2, etc.). The plate scale is listed in terms of IIBrr and IIIBrr. The former is applicable when IIBr2 is non-axillary, the latter if IIBr2 is axillary. C gives the FBrr in lateral interrays.
Equation data:
A — $y = .601 + 1.02x$. $r = .986$.
$\sigma y\% = 11.2$. N = 3.
B — $y = 2.24 + .360x$. $r = .998$.
$\sigma y\% = 7.2$. N = 3.
C — $y = 9.47 + .749x$. $r = .996$.
$\sigma y\% = 3.2$. N = 3.
D — $y = -1.49 + 1.87x$. $r = .998$.
$\sigma y\% = 16.6$. N = 4.

The growth of total calyx height and "size" was linear with a calyx height growth vector of 1.9 mm per 1 mm "size" increment (Text-fig. 39d). The calyx height/"size" increased from about 1.5 to 1.8, which was caused by the development of additional FBrr.

Comparison of the holotype and paratype (USNM 164 590) (Text-figs. 37a, b) shows several trends in calyx width and iBrr width. 1. "Size"/cup width underwent a slight increase (*i.e.*, 1.3 versus 1.4), and the calyx became slightly more slender with progressive growth. 2. The calyx width/iBrr width values are 1.6 and 2.7 in the holotype and paratype, respectively. This indicates that the iBrr width increased more rapidly than the ray width. The change in the ratio reflects the differential growth of the IBrr and adjacent iBrr, in which the height/width was augmented more slowly in the iBrr.

The column facet width relative to dorsal cup width is less in the holotype than in the paratype.

Brachial ontogeny. — (Text-figs. 37c, 40). The standard Brr consist of IIBrr10 to 15 or the equivalent IIIBrr8 to 13 where IIBr2 is axillary. These are slightly distal to the standard Brr examined in most Girardeau species because of the unusually numerous FBrr.

The largest Brr dimension growth rate was width which equalled a constant .10 mm per 1 mm "size" augmentation (Text-fig. 40a). The smallest and largest "sizes" constitute 2.5 and 16.6 mm which correspond to equation standard Brr widths of .35 and 1.7 mm, respectively. This growth vector greatly exceeded those of height. The average maximum height developmental rate was .018 mm while the minimum height figure comprised only .007 mm per 1 mm "size" increase. Thus the width growth vector ranged about 5.6 times the mean maximum height value and roughly 14 times the equivalent minimum height figure.

The plots of "size" and Brr width versus maximum and minimum height are logarithmic in which the height growth rates decreased exponentially (Text-figs. 40b, c). This pattern was most striking when maximum height was involved. The lowest width value equals .27 mm which corresponds to a .34 mm maximum height; the oldest crinoid has a 1.7 mm width and a .61 mm maximum height. Throughout ontogeny, the maximum height developmental vector per .1 mm width augmentation declined from .038 to .009 mm. In minimum height, the initial value is much lower (.31 mm minimum height at .27 mm width). The growth increments were much smaller and dropped at a slower rate; these changed from .014 to .004 mm per .1 mm additional width. The .007 mm mean minimum height growth vector was roughly one-third that of maximum height (.018 mm).

The ontogeny of Brr maximum height versus minimum height was exponential in which the minimum height growth rate fell from .051 to .030 mm per .1 mm of maximum height increase (Text-fig. 40d). The greatest and least maximum height values comprise .63 and .33 mm; the equivalent minimum heights consist of .42 and .30 mm, listed in the same order.

The convergence angle in the smallest brachial is 22° (Br width .27 mm, "size" 2.5 mm). When a 4.2 mm "size" was attained, the convergence was reduced to 17° whereas the largest crinoid possesses only a 12° angle ("size" 16.6 mm, Br width 1.7 mm). As usual, the convergence angle decrease was most rapid in the young crinoids and 50% of the convergence angle decline occurred during about 10% of the "size" interval.

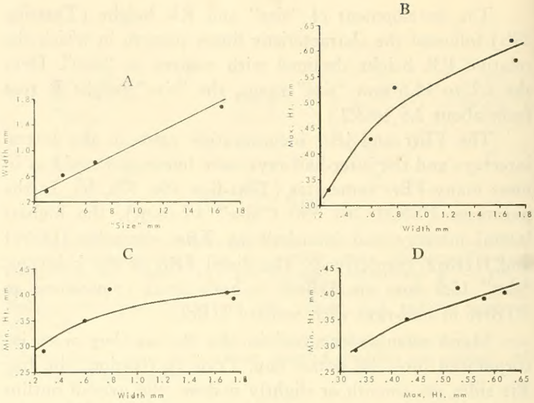

Text-figure 40. — Graphs showing standard Brr growth in *Alisocrinus? heterodactylus*, n. sp. Standard Brr are IIBrr10-15 in half-rays with non-axillary IIBrr2; IIIBrr8-13 in half-rays with axillary IIBrr2. All dimensions except "size" are the standard Brr measures shown on Text-figure 2.
Equation data:
A — $y = .0990 + .102x$. $r = .995$.
$\sigma y\% = 15.5$. $N = 4$.
B — $y = .527 + .339\log x$. $r = .974$.
$\sigma y\% = 5.1$. $N = 5$.
C — $y = .379 + .124\log x$. $r = .852$.
$\sigma y\% = 7.1$. $N = 5$.
D — $y = .499 + .418\log x$. $r = .946$.
$\sigma y\% = 4.2$. $N = 5$.

Text-figure 37c shows the standard Brr superpositions. The diagram was constructed in the same fashion as those given for the eopatelliocrinids, and the plates illustrated are mean Brr for each of the three crinoids. The pinnule facets are poorly preserved, and the outlines of these may be somewhat inaccurate. Consequently, the "pinnule facet food groove" axis may be distorted, especially in the largest specimen.

The Brr development patterns were most similar to those of *Eopatelliocrinus latibrachiatus*. These are as follows: 1. The alisocrinid width growth vectors greatly exceeded those of height. As previously discussed, the width growth rate ranged roughly 14 times that of minimum height and about 5.6 times the maximum height value. The equivalent eopatelliocrinid figures consist of 21 times and 5.2 times, respectively. Eventually the large alisocrinid width growth increments produced a low and wide Br with relatively smooth outlines. The overall mature Br geometry is that of a wider, lower and smoother *E. latibrachiatus* plate because of the different "size" intervals in the two ontogeny sequences. The eopatelliocrinid "size" range equals 1.15 to 5.0 mm whereas the equivalent alisocrinid figure constitutes 2.5 to 16.6 mm. Both forms possessed comparable Brr width developmental rates per 1 mm "size" increment; these comprised .13 mm for the eopatelliocrinid and .10 mm in this form.

2. If the restoration is correct, the alisocrinid width growth vectors toward and away from the pinnule facet were symmetrical. In *E. latibrachiatus,* the former were slightly larger than the latter. Apparently, the equal width growth components represented at least one of the factors which allowed this species to develop a relatively smooth pinnule facet. The eopatelliocrinid asymmetrical width growth rates probably dictated curvature of the Br side immediately below the pinnule facet which retarded the formation of a straight outline.

3. As in *E. latibrachiatus,* the distal height developmental vectors exceeded the proximal ones by approximately eight times.

4. In the youngest crinoid, "size" 2.5 mm, the height axes of the successive standard Brr are inclined relative to each other because of the unequal proximal and distal Br face convergence angles. Although the exact angle is unknown, the probable value ranges from 10 to 20°. By the time a 4.2 mm "size" was reached, the standard Brr height axes were parallel or nearly so, and the proximal and distal Brr face convergence angles were the same. Like the eopatelliocrinid, this was almost completely caused by adjustments of the distal height growth vectors. This involved acceleration of the distal minimum height developmental rate relative to the corresponding distal maximum height value.

5. In dorsal view, the immature Brr pinnule facets are directed sub-horizontally; the prominent facet is underlain by a somewhat curved Br side. The adult Brr pinnule facet is more steeply inclined and less striking; the underlying side shows less curvature than in the youngest Brr. The "smoothing" effect was principally due to the large width growth rate relative to those of height. The postulated orientation of the "pinnule facet food groove" axis appears to have controlled the pinnule facet orientation and inclination. The ventral orientation of the facet cannot be determined.

6. The immature Br margin opposite the pinnule facet is concave outward. When maturity was attained, this curvature was reversed because of the width growth vectors.

The terminal Brr are insufficiently known to warrant discussion.

The correlation coefficients correspond closely to those which could be predicted from the growth rates and the values of the parameters concerned (legend, Text-fig. 40). In all cases involving "size", Brr width and maximum height, the developmental rates and the correlations are high, ranging from .97 to .998. In "size" and width versus minimum height, low correlations (.79, .85) and small growth vectors are observed. The .95 correlation coefficient between maximum versus minimum height is high compared to those of the other uniserial armed species. Although the absolute minimum height growth rate was small, the minimum height growth increment relative to that maximum height was large; consequently, a high correlation coefficient occurs.

The overall degree of integration and coordination shown by the alisocrinid is difficult to evaluate owing to the small number of data sets (only four or five crowns). The available information indicates a degree of regulation which was more similar to that of *E. scyphogracilis* than to the less sophisticated *E. latibrachiatus* Brr ontogeny.

Ornamentation development. — (Pl. 68, figs. 2, 4). The dorsal cup plates of the youngest specimen, 2.5 mm "size", are convex with depressed sutures. The RR and IBrr are more strongly arched than the adjacent iBrr; this is interpreted as incipient median-ray ridge development.

The 4.2 mm "sized" calyx retained similar median-ray ridges which occupy virtually the entire widths of the ray plates. In addition, the lateral RR ridges are seen along the plate margins. The stellate ridges had just began to form on the IBrr sides and on the proximal CD interray iBrr. Some of the higher iBrr bear elongate nodes, but there is no evidence of stellate ridges.

In adult individuals (*e.g.,* holotype, "size" 16.6 mm), the median-ray ridges are narrow relative to the plate sizes, highly convex and sharply differentiated from the plate sides. The RR and IBrr ridges cover from 33 to 50% of the plate widths, but those of the fixed IIBrr and IIIBrr are wider and may extend over almost the entire width of the plates. The IIBr2 fixed pinnule has a strong longitudinal ridge which probably developed when the pinnule was incorporated into the calyx. Prominent stellate ridges are found on the iBrr and ray plates up to the IIBrr2 level. The iBrr ridges extend across the whole plate, but the ray plate ridges terminate against the median-ray ridges. Above the IIBrr2, most iBrr bear narrow elongate nodes. The larger iBrr nodes may be arranged into stellate patterns. The smaller iBrr show only one or two nodes which are typically elongated parallel to the interray axis.

The stellate ridges first appeared on the proximal iBrr and ray plates, and with increasing "size" and age, higher plates formed these ridges. The iBrr ridges grew from elongate nodes until they covered the entire plate. The ray plate stellate ridges either originated from the median-ray ridges or were initiated at the plate margins.

Variation. — The IBrr1 are invariably hexagonal. Examination of the IAxx in five specimens shows 10 septagonal plates and one six-sided one. The mean plate possesses 6.9 sides with a 4.2% standard deviation.

In seven half-rays, the arms first bifurcate on IIBr2 (hereafter termed branched half-rays). In nine cases, the proximal branch most often occurs on IIBr27 (unbranched half-rays). The former and latter configurations were assigned arbitrary values of 2.0 and 1.0, respectively. The average comprises 1.44 with a 35% standard deviation. Although the numerical values are artificial, the distribution denotes wide variability. Both branching types can be found within a single ray or between different rays of the same individual.

The IIBr2 is always axillary in the branched half-rays. The next bifurcation varies from IIIBrr20 to 25 with a IIIBr23 mean and 7.8% standard deviation.

For the unbranched half-rays, the proximal bifurcation ranges from IIBrr25 to 29. The average consists of IIBr27.2 in conjunction with a 6.2% standard deviation. Here, the IIBr2 invariably bears a pinnule on the interray side. The mature crinoid pinnule is incorporated into the dorsal cup. This is longer, composed of larger and more numerous pinnulars, and has a stronger longitudional ridge than the higher pinnules. Essentially, the IIBr2 pinnule is sharply differentiated from the higher ones. This suggests that the IIBr2 pinnule of the unbranched half-rays is homologous with the outside half-ray arm branch where an axillary IIBr2 is found. If so, the evolution of an axillary IIBr2 from a pinnulate IIBr2 probably occurred through a "mutation" which affected the IIBr2 pinnule ontogeny by converting it into an arm branch (see phylogeny of *A. tetramatus*). There is no reason to doubt that axillary IIBrr2 could have developed into pinnulate IIBrr2 by a reverse of the previous "mutation".

Remarks. — *A.* ? *heterodactylus* is based on about five partial crowns. Two arm articulation types are known. In the first type, the dorsal and lateral margins of the Br articular face bear small sinuous ridges which are roughly at right angles to the Br margins (Text-figs. 37 d, e). These alternate with depressed areas. The facet surfaces are slightly concave or convex. When the Brr are joined together, the ridges and depressions of the adjacent Brr interlock and form a crenulate suture. These articulations resemble those of the Girardeau camerate columnals. Clearly, the adjacent Brr had little power of movement. The crenulate sutures are observed on the fixed and free IIBrr and IIIBrr of unweathered specimens, such as the holotype. Supposedly, these sutures are not found in crinoid arms, but they are certainly present in this species. The second articular type has only been seen in isolated Brr. These are like the previous ones except that the ridges and depressions are absent. Probably, these Brr were capable of more movement than the crenulate types.

The generic placement of this crinoid remains uncertain for two reasons. At present, the BB number cannot be ascertained in any of the material. According to an undated note in E. O. Ulrich's handwriting found with the holotype, the BB were lost in preparation of the crown. The note states that four BB were originally found, one large and three small ones. Lacking evidence to the contrary, the form is presumed to possess four BB.

The second problem is the *A.* ? *heterodactylus* arm branching structure and variation. Exact or close counterparts of these are not known in any related species familiar to the writer. The most comparable glyptocrinids are *Glyptocrinus dyeri* Meek (see Meek, 1873, p. 32, pl. 2, figs. 2a, b; see also Wachsmuth and Springer, 1897, p. 271, pl. 20, figs. 1a-c, pl. 21, figs. 3a-f, 6) and its close allies, such as *G. subglobosus* Meek (1873, p. 34, pl. 2, fig. 2c). The arms of these glyptocrinids resemble the unbranched types of the Girardeau taxon. The glyptocrinid IIAx ranges from IIBrr9 to 15 in contrast to the IIBrr25 to 29 of *Alisocrinus* ? *heterodactylus*. The IIBr2 pinnules are similar in all three crinoids. However, branched half-rays (with axillary IIBr2) are unknown in the glyptocrinids although these are common in the Girardeau animal. Also, the calyx shapes, plate formulae, and ornamentation of *Glyptocrinus dyeri* and *Alisocrinus* ? *heterodactylus* are nearly the same except for the number of BB.

The Girardeau form unbranched half-rays exhibit some common features with species of *Scyphocrinites*, for example *S. elegans* Zenker (1833, p. 26, pl. 4, figs. a-f; see Springer 1917, pp. 30-46, pls. 1-3, pl. 4, figs. 1-4, pl. 5, figs. 1-5). The proximal scyphocrinitid branch is located on IIBrr 15 to 20 which agrees reasonably well with the IIBrr25 to 29 of the Girardeau taxon. Typically, the *S. elegans* IIBr2 pinnule is differentiated somewhat like that of *Alisocrinus* ? *heterodactylus*. However, the Girardeau crinoid unbranched half-rays only bifurcate once to form two arms per half-ray, but scyphocrinitids show eight to 12 arms per half-ray. Axillary

IIBrr2 are not seen in *Scyphocrinites* in contrast to the Girardeau taxon. Lastly, scyphocrinitids are characterized by many more FBrr than are observed in *Alisocrinus ? heterodactylus.*

The *A. ? heterodactylus* arm structure does not remotely compare with typical alisocrinids. The latter always bear an axillary IIBr2 except for a few abnormal individuals. Over 50% of the *A. ? heterodactylus* half-rays lack an axillary IIBr2.

The presumed presence of four BB indicates that the Girardeau crinoid must be placed in the Melocrinitidae or Scyphocrinitidae rather than the Glyptocrinidae which has five BB. The previous comparison shows that *A. ? heterodactylus* is not referable to the Scyphocrinitidae, but must be assigned to the Melocrinitidae. However, the Girardeau species does not fit into any known melocrinitid genus because of the arm structure and its variation. If better material were available, a new genus would be proposed for *A. ? heterodactylus.* Lacking such material, the Girardeau form is questionably grouped with *Alisocrinus* on stratigraphic criteria. *Alisocrinus* is the only melocrinitid which occurs in Ordovician rocks.

The evolution of *A. ? heterodactylus* is also conjectural. Based on the previously annotated similarities and age relationships, the writer postulates descent from *Glyptocrinus dyeri* or one of its allies. The Girardeau crinoid is from the Richmond whereas the glyptocrinids are slightly older, Maysville. Possibly, *A. ? heterodactylus* lay in the ancestry of the Scyphocrinitidae, Middle Silurian to Early Devonian. If so, the axillary IIBr2 must have been surpressed. This is the reverse of the normal camerate trend where pinnulate IIBrr2 usually developed into axillary plates. At any rate, *A. ? heterodactylus* was not closely related to any species definitely placed in *Alisocrinus.*

Specific name. — *heterodactylus* in allusion to the arm structure variation.

Types. — Holotype — USNM 164 589. Paratypes — USNM 164 590, 164 591; Ill. St. Mus. 1565a; IGS. 35P—38.

Occurrence. — Girardeau Limestone, Cape Rock and Orchard Creek exposures.

Order MONOBATHRIDA Moore and Laudon, 1943

Suborder TANAOCRININA Moore, 1952a

Superfamily **XENOCRINACEA** Ubaghs, 1953

Family **XENOCRINIDAE** Miller, 1889b

Genus **COMPSOCRINUS** Miller, 1883

Type species. — By original designation, *Glyptocrinus harrisi* Miller, 1881a, p. 74, pl. 1, figs. 4, 4a.

Diagnosis. — An xenocrinid or tanaocrinid genus characterized by two, three, or four unbranched arms per ray; if the half-rays branch, IIBr2 is axillary; in some species, all iBrr are large and regular; in other forms, only the proximal iBrr are large and regular, and the distal iBrr are small and irregular; RR in full lateral contact except for CD interray; column quadrangular or round.

Occurrence. — Upper Ordovician, North America.

COMPSOCRINUS NODOSUS, n. sp.

Plate 79, figure 3; Text-figure 41

Diagnosis. — A species of *Compsocrinus* characterized by nodose and swollen iBrr; CD interray iBrr small, numerous and irregular; lateral interray proximal iBrr large and regular; arms generally two per ray.

Description. — Calyx shape not well known as the material is crushed; calyx moderately wide, distal constriction absent, calyx base narrow; rounded cup walls expand rapidly to IAx level, above which the walls are straight and expand gradually; "size"/cup width equals 1.2; iBrr areas occupy 60% of total width; CD interray much wider than lateral interrays; proximal half-rays expand rapidly up to IIBr2 level, above which the arms are almost vertical.

BB with ill-defined rim. Median-ray ridges prominent on IBrr, less so on distal RR, cannot be traced onto BB. Anal interray ridge strongly convex, continues straight down underlying CD interray B. CD interray iBrr swollen, highly convex; lateral interray iBrr ornamentation less well known, apparently the same as CD interray iBrr.

BB circlet incompletely known, presumably with four plates having sutures in B, C, D, and E ray positions; CD interray B hexagonal with distal side truncated for primanal, height/width is .55; small BB pentagonal, roughly equidimensional.

RR in lateral contact except for CD interray where the primanal intervenes; RR hexagonal, roughly equidimensional, largest dorsal cup plates. IBr1 hexagonal, about equidimensional. IAxx septagonal, height/width approximately .85. Distal lateral interray FBr is IIBr2 or IIBr3 in paratype ("size" 2.6 to 3.0 mm), unknown in holotype ("size" 5.5 to 6.0 mm). Highest inter-half-ray FBr equals IIBr3 in paratype, at least IIBr4 in holotype. Distal preserved CD interray FBr comprises IIBr3 in holotype. IIBrr1 are largest FBrr, hexagonal with inner sides joined, nonpinnulate; IIBrr2 hexagonal, with pinnule on inter-half-ray side; IIBrr3 and commonly IIBrr4 are FBrr, pinnulate, resemble free Brr more than underlying IIBrr. Proximal pinnular of IIBr2 pinnule fixed into calyx.

Lateral interray iBr1 large, roughly hexagonal, reaches

IBr1 level; iBrr2 smaller and less regular, composed of two plates which end at IAx level; higher three to five ranges consist of three or four small, irregular plates which reach IIBr3 or 4 level.

Inter-half-ray iBr1 large, hexagonal, attains IIBr2 level; two smaller plates in next range; two or three higher ranges consist of three or four small irregular plates, reach IIBr3 or 4 level.

Primanal between C and D ray RR, large, six or seven-sided, nearly equidimensional, followed by three to five plates; the central one is an anal series plate, the others comprise CD interray iBrr1; anal series plates large, basically hexagonal, flanked by two or three CD interray iBrr ranges, proximal anal series plates about equidimensional, distal ones wider than high. CD interray iBrr1 consist of one or two large plates; iBrr2 composed of two to five smaller plates; roughly six higher ranges in holotype, each usually with four plates, some ranges with five or six plates, these iBrr small and irregular.

Articular surfaces of ray plates apparently smooth.

Portion of tegmen known, consists of small, undifferentiated, irregular and slightly nodose plates.

Arms poorly known; unbranched, two per ray in paratype; one holotype C ray IIBr2 may be axillary; arms uniserial; all Brr pinnulate except IIBr1; IIBr2 pinnule on interray side; IIBr22 pinnule complete in paratype, long, slender, with 14 pinnulars.

Free Brr seen in paratype, uniserial, relatively high, height/width equals 1.2, somewhat wedge-shaped, Br depth roughly equals width; pinnule facet slightly protuberant. Articular surfaces and food grooves not known. Br surfaces with small irregular sinuous ridges which parallel the arm length axis.

Pinnular length/height ranges from 1.5:1 to 3:1, depth slightly exceeds height; pinnulars taper distally. Food grooves wide, occupy most of pinnular width. Covering plates small, irregular, arranged in four rows across the food grooves; each pinnular bears roughly five ranges of these plates.

Column partly known; distal stem and attachment device not preserved; column round, tapers slightly in distal direction; proximal and distal widths of holotype stem are about 2.5 and 2.0 mm, respectively. Sutures crenulate; articular surfaces not seen.

Remarks. — This species is based on two somewhat flattened crinoids which are partly buried in matrix. The holotype ("size" 5.5 to 6.0 mm) preserves the CD interray and a long column segment. Examination of the calyx shows that the B and C ray RR are in lateral contact. An arm fragment lying to the upper right of the holotype calyx is biserial but seems too slender to belong to the specimen. The arms are only known in the paratype ("size" about 2.6 to 3.0 mm) which consists of a partial crown illustrating several lateral interrays.

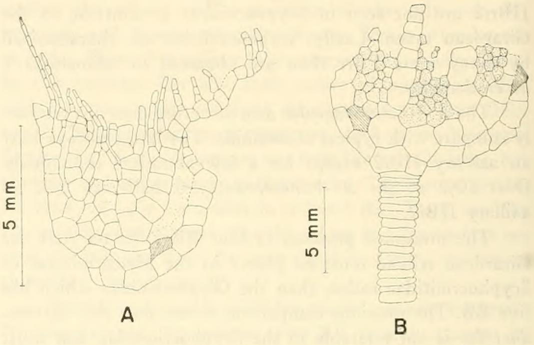

Text-figure 41. — *Compsocrinus nodosus*, n. sp. A. — Paratype, IGS. 35P-12, lateral view, "size" 2.6-3.0 mm, Orchard Creek exposure. B. — Holotype, USNM 164 592, CD interray, "size" 5.5-6.0 mm, Cape Rock exposure. The iBrr are stippled. Broken areas are ruled.

C. nodosus is somewhat transitional between *Tanaocrinus*, *Xenocrinus*, and *Compsocrinus*. The typical compsocrinid characters consist of the relatively large and regular lateral interray proximal iBrr and the arm branching formula. The small numerous and irregular CD interray iBrr closely resemble tanaocrinids and xenocrinids.

The Girardeau form differs from *Compsocrinus harrisi* (Miller) (1881a, p. 74, pl. 1, figs. 4. 4a) in lacking stellate dorsal cup plates and in generally having two rather than four arms per ray. *C. miamiensis* (Miller) (1882, p. 34, pl. 1, fig. 1) is characterized by numerous small spines or nodes on the lateral interray and CD interray iBrr in contrast to the nodose and swollen iBrr of the Girardeau crinoid. Also *C. miamiensis* bears three arms in some rays rather than two arms in all rays. An undescribed compsocrinid from the Richmond near Waynesville, Ohio, shows nodose CD interray iBrr like *C. nodosus* in combination with spinose lateral interray iBrr and arms as in *C. miamiensis*. This transitional species probably indicates that the Girardeau form and *C. miamiensis* are related.

C. nodosus differs from *Tanaocrinus typus* Wachsmuth and Springer (1897, p. 186, pl. 9, figs. 7a-c) in the following: 1. Presence of two arms per ray. The tanaocrinid arms first branch on IIBrr6 to 8, at least one higher bifurcation occurs in some arms; 2. Large proximal iBrr in lateral interrays in contrast to the small and irregular iBrr of *T. typus;* 3. The tanaocrinid is characterized by smooth and flat iBrr whereas nodose and swollen iBrr are found in *Compsocrinus nodosus*.

The Girardeau form may be separated from species of *Xenocrinus* with two arms per ray, such as *X. baeri* (Meek) (see Wachsmuth and Springer, 1897, p. 185, pl. 9, figs. 5a-d) and *X. penicillus* Miller (1881a, p. 72, pl. 1, figs. 3a-c; see Wachsmuth and Springer, 1897, p. 183, pl. 9, figs. 6a,b) by the iBrr. The proximal iBrr of *Compsocrinus nodosus* are large and regular whereas those of the xenocrinids are small and irregular. *Xenocrinus multiramus* Ramsbottom (1961, p. 21, pl. 6, figs. 1-4) has four arms per ray in contrast to the two armed rays of the Girardeau crinoid. Also most xenocrinids exhibit iRR elements which, wholly or partially, separate the RR in the lateral interrays.

Column growth. — The holotype stem segment shows some aspects of the ontogeny. A maximum of four columnal orders is found (numbering of orders after Bather, 1900, text-fig. 17). Orders 3 and 4 are nodose, but the Order 1 is non-nodose. The proximal Order 2 plates are non-nodose whereas the distal plates bear nodose edges. The usual proximal order formula equals: 4-2-3-2-4-2-3-2-4. Although Order 1 is lacking, the other three orders are fully developed. The distal sequence consists of: 4-1-2-1-3-1-2-1-4. Comparison of these formulae indicates that all Order 1 plates grew by intercalation; most likely, Order 4 formed just below the calyx. The origin of Orders 2 and 3 cannot be determined from the sequences; these may have been initiated below the calyx, or by intercalation, or by a combination of both mechanisms. At least 50% of the columnals developed by intercalation.

The thickness of the Order 4, 3, and 2 stem plates was augmented as the columnals were displaced distally. The Order 1 columnal thickness remained constant as far as can be ascertained. This is tabulated below:

	Columnal thickness			
	Order 4	Order 3	Order 2	Order 1
Proximal column	.33 mm	.17 mm	.10 to .17 mm	absent
Mid-length	.47 mm	.33 mm	.25 mm	.25 mm
Distal preserved stem	.70 mm	.50 mm	.25 mm	.25 mm

Specific name. — *nodosus* in allusion to the nodose and swollen iBrr.

Types. — Holotype — USNM 167 592. Paratype — IGS. 35P-12.

Occurrence. — Girardeau Limestone, Cape Rock and Orchard Creek exposures.

Order DIPLOBATHRIDA Moore and Laudon, 1943

Superfamily **DIMEROCRINITACEA** Ubaghs, 1953

Family **DIMEROCRINITIDAE** Bassler, 1938

Genus **PTYCHOCRINUS** Wachsmuth and Springer, 1885

Type species. — By designation of Wachsmuth and Springer, 1897, p. 197, *Gaurocrinus splendens* Miller, 1883, p. 230, pl. 11, figs. 3, 3a.

Diagnosis. — A genus of Dimerocrinitidae with median-ray ridges; uniserial arms; tegmen incompetent, composed of numerous small irregular plates.

Remarks. — Jaekel (1918, p. 41) proposed the Ptychocrinidae for *Ptychocrinus* and several other genera. Moore and Laudon (1943, p. 83) followed this practice, although restricting the family to the type genus; they separated the family from the Dimerocrinitidae for two reasons, the presence of uniserial arms and median-ray ridges. In 1953 (p. 737), Ubaghs grouped *Ptychocrinus* with the Dimerocrinitidae. The writer concurs with Ubaghs because many species of *Dimerocrinites* have median-ray ridges and *Macarocrinus*, usually considered a dimerocrinitid, bears uniserial arms.

Ptychocrinus contains three North American, Upper Ordovician species with the following characters: *P. splendens* (Miller), stellate ridges on the dorsal cup, arms branch on IIBrr13 to 15, most arms bifurcate again on the higher IIIBrr, Girardeau Limestone; *P. fimbriatus* (Shumard), dorsal cup lacks stellate ridges, two arms per ray, Girardeau Limestone; *P. parvus* (Hall) (1867, p. 304; see Hall, 1872, p. 207, pl. 5, fig. 17; Wachsmuth and Springer, 1897, p. 199, pl. 18, figs. 1, 2), dorsal cup lacks stellate ridges, arms four per ray, branching on IIBr2, Maysville, Cincinnati area. These three species are highly divergent. By the standards applied to other Ordovician camerate families, the three crinoids would be placed within different genera. Inasmuch as only three forms are involved, all are retained in *Ptychocrinus*. The two Girardeau ptychocrinids are represented by relatively complete ontogeny sequences composed of 40 to 50 crinoids. The development of *P. parvus* is also partially known. However, these will not be discussed here. Study of the other Girardeau camerate growth sequences has led to the development of better techniques which use the growth rates in more direct fashion. Consequently, the study of ptychocrinid ontogeny is postponed pending later examination by these more sophisticated methods.

Ptychocrinids are most closely allied to *Dimerocrinites* and *Macarocrinus* of the Dimerocrinitidae and *Rhaphanocrinus* (Wachsmuth and Springer, 1885, p. 92(320)) of the Archaeocrinidae. Rhaphanocrinids differ in the presence of iRR (homologous with the iBr1 of ptychocrinids) which separate the RR in lateral interrays. In *Ptychocrinus*, the iBrr1 occur in the usual iBr1 position, and the RR are not separated in lateral interrays. The Ordovician species of *Rhaphanocrinus* closely parallel those of *Ptychocrinus*. The genotype, *Rhaphanocrinus subnodosus* (Walcott) (1884, p. 208, pl. 17, fig. 3; see Wachsmuth and Springer, 1897, p. 259, pl. 11, fig. 2), of the American Trenton, and *R. basalis* (McCoy) (1850, p. 289; see Ramsbottom, 1961, p. 25, pl. 7, figs. 1-7) of the British Caradoc have two arms per ray like *Ptychocrinus fimbriatus*. The Upper Ordovician (Richmond) *Rhaphanocrinus sculptus* (Miller, 1882, p. 37, pl. 1, fig. 2; see Wachsmuth and Springer, 1897, p. 260, pl. 11, fig. 3) shows four arms per ray with the IIBr3 being axillary, a configuration similar to *Ptychocrinus parvus*. *Balacrinus* was proposed by Ramsbotton (1961, p. 24) for *Glyptocrinus basalis* McCoy; the genus was separated from *Rhaphanocrinus* because three rather than two plates follow the iRR. In this, Ramsbottom accepted Wachsmuth and Springer's diagnosis of *Rhaphanocrinus* which stated that the iRR are overlain by two plates. In 1966, the writer examined numerous Museum of Comparative Zoology specimens of *R. subnodosus,* the type species; the iRR are followed by two or three plates. Thus, intraspecific variation in the type species overlaps the genus proposed by Ramsbottom. Consequently, *Balacrinus* is considered a synonym of *Rhaphanocrinus.*

Like *Ptychocrinus,* the Devonian *Macarocrinus* (Jaekel, 1895, p. 36) is characterized by uniserial arms. According to Schmidt (1934, p. 123) and Breimer (1962, pp. 11, 15) the Devonian genus shows differentiated 00 in contrast to the incompetent ptychocrinid tegmen. Breimer (1962, p. 11) assigned the Lower Devonian *Pterinocrinus diensti* Schmidt (1934, p. 128, pl. 22, fig. 1, text-fig. 29) to *Ptychocrinus.* As indicated by Breimer, the arms are uniserial. However, the tegmen is unknown, and it seems preferable to group this form with the Devonian *Macarocrinus* rather than with the Ordovician *Ptychocrinus.*

Dimerocrinites (Phillips, 1839, p. 674) exhibits biserial arms unlike the uniserial ones of *Ptychocrinus.* Actually, *Dimerocrinites* is a highly heterogeneous genus which is in dire need of revision. Such is beyond the scope of this report although a few remarks are presented, largely in the interests of the following section on phylogeny. These are mainly based on the writer's study of specimens at the Smithsonian Institution and British Museum of Natural History rather than the published literature and illustrations which are often misleading. The type species, *D. decadactylus* Phillips (1839, p. 674, pl. 17, fig. 4; see Bather, 1900, text-fig. 123), is strikingly different from the "typical" species assigned to the genus by most authors. The crinoid has rectangular IBrr1 and pentagonal or septagonal IAxx; consequently, the iBr1 is large and extends to the IAx or proximal IIBrr level. The primanal is followed by three plates whereas the iBrr2 consist of two plates. Two arms occur in each ray. All in all, the plate structure of this crinoid is similar to *Gazacrinus* (Miller, 1892, 1894, p. 303).

The Wenlock species, *Dimerocrinites icosidactylus* Phillips (1839, p. 674, pl. 17, fig. 5), is also peculiar. Three or four arms are seen in each ray. The IBr1 and IAx shapes are like the type species. The proximal iBr may occur in the iBr1 position with the RR in lateral contact or in iR orientation where the plate separates the RR and rests on the interray B. Both structures may be found in the same specimen and wide variation exists. Here, the plate structure is similar to *Griphocrinus* (Kirk, 1945, p. 350) although greater variation is observed.

The typical North American and European species of *Dimerocrinites* exhibit predominantly hexagonal IBrr1, pentagonal or septagonal IAxx, and small iBrr1. These possess two arms per ray, such as *D. planus* (Springer, 1926, p. 13, pl. 1, figs. 1-7) of the Middle Silurian of North America, or four arms per ray like *D. whitfieldi* Goldring (1923, p. 85, pl. 1, fig. 2) of the Middle Devonian of New York. The IIBr2 is usually axillary in the latter crinoids.

Ptychocrinus is easily differentiated from the other dimerocrinitid genera as follows: *Eudimerocrinus* (Springer, 1926, p. 14, Middle Silurian) exhibits biserial arms which branch three or four times. The Lower Devonian *Ambicocrinus* (Kirk, 1945, p. 353) bears branched biserial arms and lacks median-ray ridges. *Griphocrinus* (Kirk, 1945, p. 350, Devonian) also has biserial arms and iRR are present in several interrays. The *Cyphocrinus* (Miller, 1892, 1894, p. 51, Middle Silurian) arms are unknown although these are probably recumbent. The dorsal cup is low and widely expanding. The Devonian *Pterinocrinus* (Goldring, 1923, p. 86; see Breimer, 1962, p. 11) shows compound arms with each Br bearing one pinnule on both sides of the arm.

Occurrence. — Upper Ordovician, North American Mid-continent.

PTYCHOCRINUS FIMBRIATUS (Shumard)

Plates 69-72; Text-figure 42

1855. *Glyptocrinus? fimbriatus* Shumard, Geol. Sur. Missouri, Ann. Rept. II, p. 194, pl. A, figs. 10a, b.

1866. *Glyptocrinus fimbriatus* Shumard, Shumard, Cat. Palaeozoic Foss., St. Louis Acad. Sci., Trans., vol. 2, p. 378.

1881. *Glyptocrinus fimbriatus* Shumard, (stated as undeterminable) Wachsmuth and Springer, Rev. Paleocrinoidea, Pt. II, Acad. Nat. Sci. Philadelphia, Proc. 1881, p. 189(363).

1883. *Glyptocrinus fimbriatus* Shumard, Miller, Cincinnati Soc. Nat. Hist., Jour., vol. 6, p. 227.

1889a. *Glyptocrinus fimbriatus* Shumard, Miller, North American Geol. and Paleont., p. 248.

1894. *Glyptocrinus fimbriatus* Shumard, (stated as not a *Glyptocrinus*) Keyes, Missouri Geol. Sur., vol. 4, Paleont., Pt. I, p. 225.
1897. *Glyptocrinus fimbriatus* Shumard, (stated as undeterminable) Wachsmuth and Springer, North American Crin. Camerata, Mus. Comp. Zool., Mem. 20, p. 269.
1915. *Glyptocrinus? fimbriatus* Shumard, Bassler, Bibl. Index American Ord. and Sil. Foss., U.S. Nat. Mus., Bull. 92, p. 554.
1943. *Glyptocrinus fimbriatus* Shumard, Bassler and Moodey, Bibl. Paleoz. Pelmatozoa, Geol. Soc. America, Spec. Paper 45, p. 493.

Diagnosis. — A species of *Ptychocrinus* characterized by two arms per ray; dorsal cup ornamentation consists of median-ray ridges; stellate ridges lacking on iBrr.

Remarks. — *P. fimbriatus* is the most abundant Girardeau camerate, being represented by about 60 definitely assigned crinoids. The smallest and largest known specimens have "sizes" of 1.8 and 11.1 mm.

As shown by the synonymy, considerable confusion existed concerning this crinoid. Shumard based the species on a single poorly preserved crown (holotype, USNM, S. 4161, see Text-fig. 42c of this report) which is partly buried in matrix. The CD interray is not visible and the crinoid represents a "young assemblage" individual ("size" 2.5 mm). Shumard's description and figure disclose no trace of the IBB; consequently the form was assigned to *Glyptocrinus* by Shumard and the subsequent authors who believed generic assignment was possible. Shumard's description and figure are incorrect in several respects: 1. Calyx structure. The IAx in the center ray and the iBrr in the right interray are incorrectly drawn, and the iBrr in the left interray were omitted. 2. The arm structure bears little resemblance to the specimen. As discussed under *Ptychocrinus splendens*, the arm branching structure of the holotype is transitional between *P. fimbriatus* and *P. splendens*. Thus, the holotype is not a satisfactory name bearer for the species. The writer's concept and diagnosis of *P. fimbriatus* is drawn from the normal individuals with two arms per ray. 3. Careful inspection of the holotype (Text-fig. 42c) indicates that IBB are present, these being represented by small triangular plates at the proximal margins of the BB. Therefore, it is not surprising that Shumard failed to recognize the IBB. The presence of IBB plus the fact that Shumard's specimen fits into the growth sequence of undoubted ptychocrinids denotes assignment to *Ptychocrinus*.

During the growth of *P. fimbriatus*, the IBB became more prominent. These are seen as small triangular plates immediately above the proximal columnal in the youngest animals. In this growth stage, the adjacent IBB are not in lateral contact when viewed from the side. Throughout later development, the height and width of IBB were augmented and the plates are in lateral contact in the larger animals.

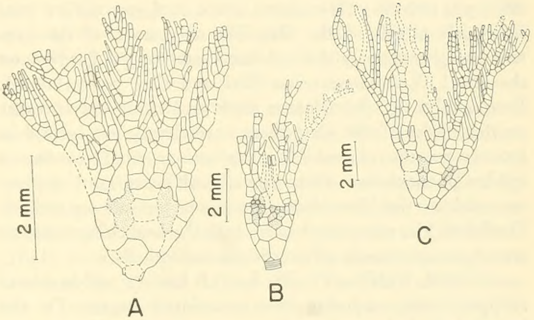

Text-figure 42. — *Ptychocrinus fimbriatus* (Shumard), young crowns, Girardeau Limestone.
A. — Figured specimen, IGS. 35P-64, lateral view of smallest crinoid, "size" 2.0 mm, Orchard Creek exposure.
B. — Figured specimen, USNM 164 612, lateral view, note abnormal ray in center, "size" 2.3 mm, Cape Rock exposure.
C. — Holotype, S. 4161, lateral view, arm branching is transitional between the two Girardeau species of *Ptychocrinus*, "size" about 2.5 mm, Cape Rock exposure.
All iBrr stippled.

The CD interray is unknown in the holotype, although this area is exposed in numerous other specimens. The structure is typical *Ptychocrinus* with the primanal separating the C and D ray RR and resting on the CD interray B. Three plates follow the primanal.

The inside of the calyx showing the grooves which housed the aboral nerve cords is preserved in USNM 164607 (Pl. 71, fig. 5). The distal portion of the aboral nervous system is represented by sharp deep grooves on the IBrr, IIBrr, and pinnules. Branching points occur at the mid-level of the IAxx and on pinnulate Brr. In the latter case, the nerve cord grooves on the pinnule and the associated part of the Br are less pronounced than the aboral nerve cords which lay at the base of the "brachial food grooves." The configuration of the Brr nerve cords resembles that of the free Brr in the Girardeau eopatelliocrinids and alisocrinids except that the branch leading to the pinnule facet is located more distally in *P. fimbriatus*. The aboral nerve cords may be traced on the RR where the grooves are broader and less well defined. Bifurcation occurs at the RR mid-level with the two proximal branches continuing onto the distal parts of the BB. The BB nerve cord grooves are sharper than those of the RR. The remaining proximal part of the nervous system is not visible. The chambered organ must have been located below the distal BB level; probably, the chambered organ lobes were at the IBB level with the lobes in radial orientation (see Bather, 1900, pp. 104-106). The aboral nerve cord grooves are conspicuously absent on the iBrr. The only traces of this system are the vaguely defined horizontal-lateral grooves on the IBrr1 (*i.e.*, connect the IBr1 and iBr1 nerve knots). Presumably, the aboral nerve cords and knots were present on the insides of the iBrr; these were simply not housed in grooves on the plates. *Macrostylocrinus cirrifer* shows a similar phenomenon where the aboral nerve cord grooves occurred on the iBrr of some crinoids but not on others. Doubtless, the nerve cord knots and the branching patterns were homogeneous in all conspecific individuals.

USNM 165073 (Pl. 70, fig. 2) has the calyx plates stripped away exposing the convoluted organ. To the knowledge of the writer, this represents the oldest occurrence of this structure. Most convoluted organs have been described from Mississippian crinoids (see Wachsmuth and Springer, 1897, pp. 142, 143). Generally, later authors have followed Wachsmuth and Springer in considering the convoluted organ as a support for the digestive system (see Ubaghs, 1953, pp. 687-690 for modern summary). Summarizing from Wachsmuth and Springer, Ubaghs, and the writer's observations, in Mississippian crinoids the organ consists of two to four whorls which are coiled to the right as viewed from the tegmen. This corresponds to the gut twist direction in living crinoids. The attachment points for the convoluted organ are not satisfactorily known. When well preserved in Mississippian crinoids, the wall structure is composed of a spicular network, but usually, the organ is strongly encrusted by secondary silica. The internal tegmen food grooves can be traced into the convoluted organ. This is the strongest evidence for the gut support hypothesis. A protective function is eliminated because the camerate crinoid viscera was protected by the calyx plates. The writer visualizes the gut as coiled inside of the convoluted organ with the number and direction of the gut coils and the convoluted organ having been the same. The convoluted organ separated the gut from the aboral nerve cords and chambered organ. Living crinoids have no convoluted organ. The chambered organ is housed under the BB rosette and the axial nerve cords occur within the RR and Brr. The gut is located above the BB rosette and support for the gut, the associated coelems, and other organs is provided by the top of the BB rosette, RR, IBrr, and tegmen (see Nichols, 1962, fig. 2 for diagrammatic cross-section through *Antedon*). To some extent, the modern crinoid BB rosette performs the same function as did the convoluted organ of the camerates, namely separating the gut from the chambered organ. In Recent forms, the aboral nerve cords are isolated from the gut and associated organs, because they are buried inside the calyx plates. Despite the functional similarity, the structures are not homologous. The BB rosette of extant crinoids consists of modified calyx plates. The camerate convoluted organ is a completely separate internal structure which was not derived from the calyx plates.

The convoluted organ is not completely preserved in the Girardeau crinoid. The outermost whorl is visible and the direction of coiling is right as viewed from the tegmen. The proximal margin of the last whorl is marked by a thickened ridge. The convoluted organ appears to be solid, not spicular.

Types. — Holotype — S. 4161. Figured specimens — USNM 164 606-164 612, 165 071-165 078; IGS. 35P-56, 35P-57, 35P-59, 35P-60, 35P-64.

Occurrence. — Girardeau Limestone, Cape Rock and Orchard Creek exposures.

PTYCHOCRINUS SPLENDENS (Miller)

Plates 73-76; Text-figure 43

1883. *Gaurocrinus splendens* Miller, Cincinnati Soc. Nat. Hist., Jour., vol. 6, p. 230, pl. 11, figs. 3, 3a.
1885. *Ptychocrinus splendens* (Miller), Wachsmuth and Springer, Rev. Palaeocrinoidea, Pt. III, sec. 1, Acad. Nat. Sci., Philadelphia, Proc. 1885, p. 101(323).
1889a. *Gaurocrinus splendens* Miller, Miller, North American Geol. and Paleont., p. 247.
1894. *Ptychocrinus splendens* (Miller), Keyes, Missouri Geol. Sur., vol. 4, Paleont., Pt. I., p. 162, pl. 22, fig. 1.
1897. *Ptychocrinus splendens* (Miller), Wachsmuth and Springer, North American Crin. Camerata, Mus. Comp. Zool., Mem. 20, p. 198, pl. 18, figs. 3a, b.
1915. *Ptychocrinus splendens* (Miller), Bassler, Bibl. Index American Ord. and Sil. Foss., U.S. Nat. Mus., Bull. 92, p. 1077.
1917a. *Ptychocrinus splendens* (Miller), Savage, Geol. Sur. Illinois, Bull. No. 23, p. 95, pl. 1, fig. 1.
1943. *Ptychocrinus splendens* (Miller), Bassler and Moodey, Bibl. Paleoz. Pelmatozoa, Geol. Soc. America Spec. Paper 45, p. 657.
1944. *Ptychocrinus splendens* (Miller), Moore and Laudon, *In* Index Foss. North America, p. 187, pl. 72, fig. 19.

Diagnosis. — A species of *Ptychocrinus* characterized by stellate ridges on the iBrr of adults; arms branching on IIBrr13 to 15; arms commonly bifurcate again on IIIBrr30 to 40.

Remarks. — This species is represented by about 50 crinoids which range from about 1.0 to 17 mm in "size". *P. splendens* is the second most abundant Girardeau camerate being exceeded only by *P. fimbriatus*.

As in the patelliocrinids, the young ptychocrinids are similar and difficult to separate. During growth, the two species diverged and the adult animals are easily classified. Therefore, the writer has first grouped the mature crinoids after which the younger specimens were treated.

The adult *P. splendens* are easily separated from *P. fimbriatus* by three characters. *P. splendens* always has stellate ridges on the iBrr; in some specimens, the ridges are augmented by centrally located nodes. *P. fimbriatus* lacks stellate ridges although some animals show numerous small nodes on the iBrr and adjacent ray plates. The arms of mature *P. splendens* almost always branch on IIBrr13 to 15 and commonly on IIIBrr30 to 40. The second bifurcation is observed on most crinoids with "sizes" exceeding 7.0 mm. *P. fimbriatus* bears two unbranched arms per ray regardless of age. Many Girardeau camerates bear traces of pigmentation which presumably represents the coloration when the animals were alive. Like most Girardeau crinoids, *P. splendens* is almost invariably green whereas *P. fimbriatus* is generally dark brown.

The younger crinoids ("sizes" 2.0 to 4.1 mm) are more similar and less easily separated. The stellate ridges of *P. splendens* appeared within the 3.8 to 4.1 mm "size" interval. Apparently, these formed at various times in different individuals as they were lacking in a "size" 4.0 mm animal. Prior to the development of the stellate ridges, the ornamentation of *P. splendens* and *P. fimbriatus* was essentially the same, consisting of median-ray ridges with depressed iBrr areas. The youngest definitely assigned *Ptychocrinus* ("size" 2.0 to 2.8 mm, Text-figs. 42, 43) have about 17 to 27 Brr per arm. If the arms are completely preserved, the IIBrr13 to 15 branch can be located in *P. splendens;* this does not occur in *P. fimbriatus*. The differences in pigmentation are as in the adults.

Two small ("size" 1.0, 1.4 mm, Text-fig. 32a, USNM 164 613) animals are known with 4 to 8 IIBrr per arm. Both specimens are green and are considered *P. splendens*. Aside from the pigmentation, the writer knows of no way to separate these youngest crinoids.

Summarizing the ontogeny of the two Girardeau ptychocrinids: The youngest animals are identical with the exception of pigmentation; *P. fimbriatus* tended to retain the immature characters throughout development. The ornamentation always consisted of median-ray ridges although these became more pronounced with progressive "size" and age. The arms were stabilized at two per ray. *P. splendens* diverged further from the immature configuration during growth. As new Brr formed at the arm tips, branching occurred on IIBrr13 to 15 and eventually on IIIBrr30 to 40. The stellate ridges were initiated at "sizes" ranging from 3.8 to 4.1 mm.

With respect to phylogeny, *P. splendens* is believed to have been derived from the *P. fimbriatus* stock by means of "mutations" (general sense, includes chromosome aberrations, and so forth) which caused the development of arm branching and stellate ridges (see also section on phylogeny). This interpretation is supported by several abnormal crinoids. One young *P. fimbriatus* (IGS. 35P-60, "size" 2.7 mm, Pl. 72, fig. 6) has traces of stellate markings on the iBrr but lacks a IIBrr arm branch. An adult *P. splendens* (USNM 164 596, "size" 9.25 mm, Pl. 75, fig. 4) is typical except for the retarded arm branching. The first bifurcation occurs on IIBr24 in one arm, another is unbranched, and a third is normal. The holotype of *P. fimbriatus* (Text-fig. 42c) shows five arms in which the branching formula can be inferred or determined. Two arms branch on IIBr13 and IIBr15 as in *P. splendens*. The other three arms are unbranched like typical *P. fimbriatus*. Inasmuch as the number of unbranched arms exceeds the branched ones, the crinoid is considered an atypical *P. fimbriatus*. Essentially, these three crinoids are somewhat transitional between the two forms, and such is deemed indicative of close relationship. *P. fimbriatus* is closer to the *Rhaphanocrinus subnodosus* ancestral stock, because both species have two arms per ray and similar dorsal cups. Therefore, *Ptychocrinus splendens* is believed to have constituted an offshoot from the ancestry of *P. fimbriatus*.

At least three young *P. splendens* with aborted rays are known. IGS. 35P-43 ("size" 3.2 mm, Text-fig. 43e). Both arms of one ray and one arm of another failed to develop fully, and these arms have about 14 to 16 Brr whereas the normal ones are composed of roughly 45 plates. The abnormal arm Brr are slightly smaller than the others. The normal dorsal cup plate structure is observed and the aborted arms exhibit no evidence of regeneration, IGS. 35P-42 ("size" 3.4 mm, Text-fig. 43f) possesses one abnormal ray. The fixed IIBrr and free Brr are smaller than those in the normal rays; a IBr1 did not form in the abnormal ray. The aborted arms are much shorter and contain fewer Brr than normal ones. In USNM 164 614 ("size" 3.8 mm), all arms are unusually short and failed to grow normally.

These abnormal crinoids all have low food gathering efficiency (*i.e.,* length of food gathering system/calyx volume) relative to the normal animals of equivalent "size". Aborted adult specimens of this type are unknown. Clearly, these abnormal youngsters did not attain maturity. The large population size of *P. splendens* (see paleoecology) indicates that small selection coefficients constituted effective agents of evolution. Thus, it is concluded that natural selection eliminated these abnormal youngsters.

One of the youngest known *P. fimbriatus* (USNM 164 612, "size" 2.3 mm, Text-fig. 42b) also has an abnormal ray in which the IBr2 is small and only bears a single arm. As in *P. splendens,* all adults are normal and this young *P. fimbriatus* is also believed a victim of natural selection.

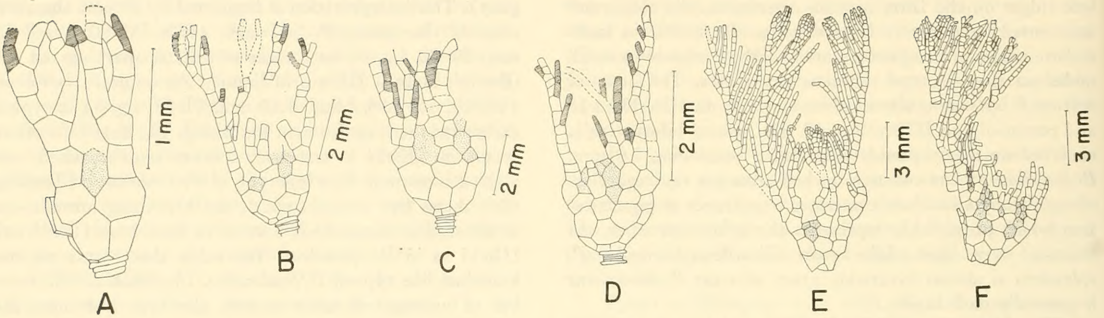

Text-figure 43. — *Ptychocrinus splendens* (Miller), young and abnormal crowns, Girardeau Limestone.
A. — Figured specimen, USNM 164 613, lateral view of one of the smallest crowns, "size" 1.35 mm, Orchard Creek exposure.
B. — Figured specimen, USNM 164 594, lateral view, "size" 2.4 mm, Orchard Creek exposure.
C. — Figured specimen, USNM 164 597, lateral view, "size" 2.5 mm, Cape Rock exposure.
D. — Figured specimen, USNM 164 595, CD interray, "size" 2.8 mm, Cape Rock exposure.
E. — Figured specimen, IGS. 35P-43, lateral view, note aborted arms, "size" 3.2 mm, Orchard Creek exposure.
F. — Figured specimen, IGS. 35P-42, lateral view, note aborted arms, "size" 3.4 mm, Orchard Creek exposure.
All iBrr stippled. Pinnules in A-D obliquely ruled.

Types. — Miller based this species on two syntypes (UC. 6286). The specimen with nearly complete arms which was figured by Miller and most other workers and is illustrated here is designated the lectotype ("size" 4.1 mm, see Pl. 75, fig. 3). The other crinoid ("size" 4.8 mm) becomes the paratype. Figured specimens — USNM 164 594 — 164 603, 164 605, 164 613; IGS. 35P-42, 35P-43, 35P-50. Mentioned specimens — USNM 164 614, 164 612.

Occurrence. — Girardeau Limestone, Cape Rock and Orchard Creek exposures.

PTYCHOCRINID PHYLOGENY

The lineage proposed here must be regarded as preliminary. Essentially, the lines of ancestry and descent are known at the generic, but not at the species level. The phylogeny is based on superposition and qualitative comparative morphology. Unlike the other Girardeau camerate lineages, quantitative techniques have not been used.

Rhaphanocrinus (Middle and Late Ordovician) was probably ancestral to *Ptychocrinus.* The principal change consisted of displacement of the iR to an iBr1 position. This evolution is plausible as it can be seen in the variation of a single form, such as *Dimerocrinites icosidactylus* (British Museum of Natural History specimens studied by writer), *Lyriocrinus melissa* (Hall) (see 1879, p. 139, pl. 15, figs. 18-27) (USNM specimens examined by the writer) and *L. dactylus* (Hall) (see Wachsmuth and Springer, 1897, p. 262, pl. 11, figs. 5a-c) (USNM crinoids seen by the writer). In these species, the proximal iBr may occur in the iR position (*i.e.,* separating the RR and resting on the interray B) or in the iBr1 orientation (plate occurs at the IBr1 level with the RR in lateral contact). For example, *L. melissa* may have from three to five (the latter is the normal number) iRR. The adaptative significance of this change was probably two-fold. Four plates were eliminated from the lateral interrays of the RR circlet. This reduced the number of plates at this level from 10 to six; the primanal was retained in the RR circlet. Such reduction must have increased the strength of the proximal part of the dorsal cup. In addition, the upward displacement of the proximal iBrr most likely simplified the lower part of the aboral nerve cords. Basically, four nerve cord knots were lost at the RR level. Although, the aboral nerve cord grooves have not been seen in an iRR bearing archaeocrinid or rhodocrinitid, this change is inferred with reasonable certainty from the external ornamentation.

Rhaphanocrinus subnodosus of the Trenton is believed ancestral to the Girardeau *Ptychocrinus fimbriatus,* because both species have two arms per ray and similar dorsal cup morphology, if allowance is made for the presence or absence of the iRR elements. *P. splendens* (Girardeau) probably represented an offshoot from the same line; if so, the main change consisted of the development of additional arm branches on the IIBrr13 to 15 and higher Brr. The origin of *P. parvus* (Maysville) with four arms per ray is uncertain. The crinoid may have been derived from *Rhaphano-*

crinus subnodosus (two arms per ray) or pehaps, it was more closely related to *R. sculptus* of the Richmond which is slightly younger than *Ptychocrinus parvus.* These two species possess four arms per ray with branching on the IIBr2 in *P. parvus* and on the IIBr3 in *Rhaphanocrinus sculptus.*

Dimerocrinites (Middle Silurian to Devonian) was clearly derived from *Ptychocrinus* in which the principal advance comprised the formation of biserial from uniserial arms. The mechanism, in terms of the growth rates and adaptative significance, is discussed in the summary of the Girardeau camerate growth and under the Brr development of *Macrostylocrinus pristinus.* The oldest and most primitive *Dimerocrinites* is *D. elegans* Springer (1927, p. 138, pl. 4, fig. 3) of the basal Middle Silurian of Anticosti Island with two arms per ray which are composed of immature biserial Brr. The later species developed wider arms formed of mature biserial Brr. The Early Silurian *Dimerocrinus? vagans* Foerste (1919, p. 13, pl. 2, figs. 6a-e) is probably monocyclic and not a dimerocrinitid.

Most *Dimerocrinites* have mainly hexagonal IBrr1 and septagonal or pentagonal IAxx (*e.g., D. planus,* Middle Silurian). These species were most likely ancestral to those with rectangular IBrr1 and pentagonal or septagonal IAxx like *D. decadactylus* of the Wenlock. Variation in the IBr1 and IAx shapes can be documented in many dimerocrinitids. For example in *D. planus,* examination of 24 USNM specimens shows animals which range from 30 to 100% hexagonal IBrr sides with a mean of about 80%. This denotes genetic instability with respect to this character. Conversely, a hexagonal IBr1 was largely stabilized in the ptychocrinids which indicates that variation in the IBr and IAx shapes postdated the ptychocrinid phase of evolution. The IBrr geometry controls the size of the adjacent iBr1. With a hexagonal IBr1, the iBr1 terminates at the IBr1 midlevel. The formation of a rectangular IBr1 allowed the iBr1 to reach to the mid-IAx or higher levels. This probably reduced the number of iBrr in the calyx and strengthened the dorsal cup. Also this trend possibly simplified the calyx aboral nerve system because some iBrr nerve knots were most likely eliminated.

The origin of the Wenlock *D. icosidactylus* remains unknown. The development of the iRR in some rays may represent a secondary feature which was related to the evolution of a wide dorsal cup.

At the species level, *Ptychocrinus fimbriatus* was probably ancestral to the two arms per ray *Dimerocrinites,* like *D. planus. Dimerocrinites* with four arms per ray may have descended from *Ptychocrinus fimbriatus* (two arms per ray) or *P. parvus* (four arms per ray). Study of the number of arms in various *Dimerocrinites* species shows that most North American forms and *D. decadactylus* of the Wenlock are invariant. The Wenlock *D. icosidactylus* proves an exception and three or four arms may be present in a single ray. This line of reasoning suggests that the arm branching pattern was mainly stabilized in *Dimerocrinites.* In turn, this implies that *P. parvus* was the ancestral stock of the 20-armed *Dimerocrinites.* The similarity of the arm branching pattern may indicate that *Eudimerocrinus* (Middle Silurian) evolved from *Ptychocrinus splendens.* If so, the main changes were the development of more arm branches which increased the food gathering capacity and the area of water filtered by the crinoid, and the evolution of biserial from uniserial arms. These considerations argue for a polyphyletic origin of *Dimerocrinites* and the Dimerocrinitidae.

Subclass INADUNATA Wachsmuth and Springer, 1885

Order DISPARIDA Moore and Laudon, 1943

Superfamily **HOMOCRINICAE** Ubaghs, 1953

Family **CALCEOCRINIDAE** Meek and Worthen, 1869

Genus **CALCEOCRINUS** Hall, 1852

CALCEOCRINUS CONSTRICTUS Brower

Plate 78, figures 2, 3

1966. *Calceocrinus constrictus* Brower, Jour. Paleont., vol. 40, p. 623, pl. 75, figs. 21, 26, 27, text-figs. 2A, E.

Diagnosis. — A species of *Calceocrinus* characterized by unbranched E ray arm, constricted main axils and a robust anal tube.

Remarks. — This crinoid was previously described in detail and it is easily separated from all allied forms by the characters listed above.

Types. — Holotype — IGS. 35P-1: Paratypes — IGS. 35P-2a-c.

Occurrence. — Limestone bed in the Orchard Creek Shale, Mississippi River exposure. Originally, the writer cited the occurrence as the Girardeau Limestone. Later fieldwork (1967) indicated that the crinoids were collected from a limestone layer near the top of the Orchard Creek Shale, and the Girardeau is absent at this locality.

Order CLADIDA Moore and Laudon, 1943

Suborder DENDROCRININA Bather, 1899b

Family **DENDROCRINIDAE** Miller, 1889b

Genus **DENDROCRINUS** Hall, 1852

Type species. — by monotypy, *Dendrocrinus longidactylus* Hall, 1852, p. 193, pl. 42, figs. 7a,b, pl. 43, figs. 1a-k.

Remarks. — *Dendrocrinus* constitutes one of the most important Ordovician dicyclic inadunate groups. Brief survey of the literature and study of many specimens in conjunction with this report indicates that the genus is in dire need of revision. Although a comprehensive study is beyond the scope of this paper, the following preliminary observations are outlined. The last comprehensive treatment of *Dendrocrinus* and its allies was that of Springer (1911, pp. 29-39). Previous to Springer's work, *"Dendrocrinus"* was a highly heterogeneous genus which included almost all Ordovician and some Silurian normal dicyclic inadunates. Springer presented careful and accurate diagnoses of *Dendrocrinus* and the closely related *Cupulocrinus*. As seen below, the *Dendrocrinus* diagnosis is essentially that of Springer.

Dendrocrinus: A genus of Dendrocrinidae characterized by RA lying below the C ray R; X in dorsal cup, lying between the C and D ray RR; RR facets narrow, smooth and horseshoe shaped; anal sac tall, composed of regular plates; arms generally branching isotomously; in some species the distal branches show a tendency to bilateral heterotomy.

Species assigned: Middle Silurian, Niagaran; Rochester Shale, New York: *Dendrocrinus longidactylus* Hall, type species, (1852, p. 193, pl. 42, figs. 7a, b; pl. 43, figs. 1a-k). *D. celsus* Ringueberg (1888, p. 132, pl. 7, fig. 3). Upper Ordovician, Richmond; Ohio, Indiana, Illinois, and Iowa: *Poteriocrinus (Dendrocrinus) caduceus* Hall (1866, p. 4; see Hall, 1872, p. 208, pl. 5, figs. 7, 8). *Poteriocrinites (Dendrocrinus) casei* Meek (1871, p. 295; see Meek, 1873, p. 28, pl. 3bis, figs. 2a-c); syn., *Dendrocrinus kayi* Slocom (1924, p. 335, pl. 29, figs. 1-4). *Poteriocrinites (Dendrocrinus) cincinnatiensis* Meek (1872, p. 312; see Meek, 1873, p. 20, pl. 3bis, figs. 5a,b). Upper Ordovician, Eden; Ohio, Illinois, and Missouri: ? *Dendrocrinus navigiolum* Miller (1880, p. 235, pl. 7, figs. 6, 6a). Upper Ordovician; Ashgill; Great Britain: *Dendrocrinus granditubus* Ramsbottom (1961, p. 15, pl. 4, figs. 1-7). *D. rugocyathus* Ramsbottom (1961, p. 16, pl. 3, figs. 1-5). Middle Ordovician, Trenton; New York and Canada: *D. acutidactylus* E. Billings (1857, p. 266; see E. Billings, 1859, p. 37, pl. 3, figs. 2a,b). *Poteriocrinus alternatus* Hall (1847, p. 83, pl. 28, figs. 1a-f). *Dendrocrinus gregarius* E. Billings (1857, p. 265; see E. Billings, 1859, p. 36, pl. 3, figs. 1a-c). *D. proboscidiatus* E. Billings (1857, p. 267; see E. Billings, 1859, p. 38, pl. 3, figs. 3a-c), *not D. proboscidiatus* W. R. Billings (1887, p. 53). *D. rusticus* E. Billings (1857, p. 270; see E. Billings, 1859, p. 41, pl. 3, figs. 7a, b). Middle Ordovician, Trenton; Kentucky: *Poteriocrinites (Dendrocrinus) dyeri* Meek (1872, p. 314; see Meek, 1873, p. 24, pl. 3bis, figs. 3a, b).

As defined above, *Dendrocrinus* forms a compact and easily identified group. Generally the species are characterized by the following: ornamentation of the anal sac and dorsal cup, *e.g.*, smooth plated, stellate, or with depressed sutures; nature of the Brr, *e.g.*, with rounded or keel shaped backs, high Brr relative to width; structure and shape of the column, *e.g.*, tapering distally or straight, pentagonal or round, composed of alternating nodals and internodals or undifferentiated columnals; and gross nature of the arms and the branching thereof, *e.g.*, with few bifurcations, stout or slender.

The only divergent member of the genus is *D. granditubus*. In this crinoid, the anal sac plates are relatively small and numerous additional rows of plates are intercalated in the distal direction. This results in a more strongly expanded anal sac which is composed of many more rows of plates than in the typical forms, such as *D. longidactylus*. Nevertheless, the regularly plated anal sac of *D. granditubus* clearly denotes assignment to *Dendrocrinus*.

Dendrocrinus is easily distinguished from the allied dendrocrinid genera with narrow RR facets by the structure of the CD interray. In *Bactrocrinites* Schnur (see Schmidt, 1934, p. 56), the RA is either quadrangular or in some species lacking; in addition, the dorsal cup is more slender than in most species of *Dendrocrinus*. *Follicrinus* Schmidt, (1934, p. 74) differs in having a quadrangular RA with a balloon shaped and irregularly plated anal sac similar to that of *Grenprisia* Moore (1962, p. 38). *Parisangulocrinus* Schmidt (1934, p. 59) is characterized by a pentagonal RA which lies beside the C ray R; this genus also possesses diagnostic anal sac ornamentation consisting of well-developed transverse ridges on some or all anal sac plates. Such ornament is unknown in *Dendrocrinus*. In the bizzare dendrocrinid? genus *Esthonocrinus* Jaekel (1918, p. 53), the CD interray is peculiar (see *E. laevior* Jaekel, 1918, p. 53, text-figs. 40a-c). If the writer's interpretation is correct, the plate lying to the left of the C ray R (RV of text-fig. 40b) represents the anal X and a RA is lacking. The anal sac is also peculiar and resembles that of *Cupulocrinus* d'Orbigny (1849, p. 23; see Springer, 1911, p. 29 for diagnosis followed here). It is composed of a prominent row of large plates following anal X; this median row is flanked on both sides by ranges of smaller and more irregular plates. *Grenprisia* Moore (1962, p. 38) differs from *Dendrocrinus* in the possession of wide RR facets, a different type of arm structure, and a small, irregularly plated anal sac which is more or less expanded.

A series of crinoids assigned to *Dendrocrinus* by various writers (see for example, Bassler and Moodey, 1943, pp.

413-416) deviate significantly from the genus as defined above. This group can be diagnosed as a group (genus?) of Dendrocrinidae characterized by wide RR facets but otherwise like *Dendrocrinus.* Species placed here are Upper Ordovician, Richmond: *Poteriocrinus posticus* Hall (1866, p. 5; see Hall, 1872, p. 209, pl. 5, figs. 5, 6), Ohio; *Dendrocrinus minutus* Springer (1927, p. 137, pl. 4, fig. 6), Anticosti Island; *D. ? oswegoensis* Meek and Worthen (1868, p. 333, pl. 4, fig. 4, unnumbered text-fig. on p. 333), Illinois and Iowa. Middle Ordovician, Trenton: *D. proboscidiatus* W. R. Billings (1887, p. 53, fig. prior to p. 49), Ontario and Quebec; *Poteriocrinus gracilis* Hall (1847, p. 84, pl. 28, figs. 2a-f), New York.

These five crinoids form an easily separated suite which is closely allied to *Dendrocrinus.* Within the group the species are defined on similar characters to those previously mentioned for *Dendrocrinus.*

This group is differentiated from *Dendrocrinus* by the RR facets. The arm branching structure and the wide RR facets are similar to *Cupulocrinus,* but the anal tube structure separates this dendrocrinid group from all cupulocrinids. In *Cupulocrinus,* the anal tube is dominated by a median row of large plates tending distally from anal X. This median row of plates is flanked by much smaller and more irregular plates. In the dendrocrinid group, the anal sac is composed of equal sized, regularly arranged plates as in *Dendrocrinus.* In addition, many species of *Cupulocrinus* have flexible crinoid type Brr articulations. See, for example, specimens of *C. humilis* (E. Billings) (1857, p. 270; refer to Springer, 1911, pp. 28-36, pl. 1, figs. 8, 9, pl. 3, figs. 1-3) and *C. jewetti* (E. Billings) (1859, p. 43, text-fig. 15; refer to Springer, 1911, pp. 28-36, pl. 1, figs. 10-12, pl. 3, figs. 5-7). In other cupulocrinid species, the flexible crinoid type articulation has not been observed. For example, *C. conjugans* (E. Billings) (1857, p. 268; see E. Billings, 1859, p. 41, pl. 4, figs. 1, 2; Springer, 1911, p. 37). Such species of *Cupulocrinus* cannot be distinguished from the dendrocrinid group by the arms but must be separated by the anal sac. The dendrocrinid group differs from *Grenprisia* in having a slender, regularly plated anal sac and isotomous arm branching. All other dendrocrinid genera with wide RR facets either lack a RA or possess a quadrangular or pentagonal RA which lies to the side of the C ray R; this contrasts with the pentagonal RA underlying the C ray R of the dendrocrinid group.

Although it is possible that the dendrocrinid group represents a new genus, such is not proposed here. The principal feature distinguishing the group from *Dendrocrinus* is the width of the RR facets. At present, the validity of this character cannot be fully evaluated. Brief study of about 50 specimens of *D. casei* shows that all exhibit narrow RR facets; unfortunately, quantitative figures are not available and the percentage variability cannot be considered. The writer has not investigated the other abundant species of *Dendrocrinus* or the dendrocrinid group in any detail. Thus, whether or not the relative width of the RR facets represents a conservative (and taxonomically usable) character cannot be determined. Consequently, the writer prefers to retain the five species as a group within *Dendrocrinus.*

Certain crinoids assigned to *Dendrocrinus* by various writers cannot be retained in the genus, but must be transferred elsewhere. Included in this category are: *D. similis* E. Billings (1857, p. 267). This species has been illustrated by Wilson (1946, p. 33, pl. 5, fig. 3, text-fig. 2) and transferred to *Iocrinus; Dendrocrinus cambriensis* Hicks (1873, p. 50, pl. 4, figs. 17-20) is now the type and only known species of *Ramseyocrinus* (Bates, 1968); *Dendrocrinus retractilis* Walcott (1884, p. 211, pl. 17, fig. 4). The CD interray of this form is unknown and definite generic assignment cannot be made. The writer suggests assignment to *Merocrinus* based on the wide RR facets, the wide and low dorsal cup, and the wide column and column facet. Certainly, these characters do not indicate assignment to *Dendrocrinus* or the dendrocrinid group. The most peculiar feature of *Merocrinus retractilis* is the slender spirally coiled anal sac which differentiates it from all merocrinids; *Dendrocrinus erraticus* Miller (1881b, p. 316, pl. 8, figs. 1, 1a). Examination of Miller's illustrations and description shows that the RR facets and IBrr are wide; the anal sac is composed of a large row of median plates which is flanked on both sides by smaller and more irregular plates. These features clearly denote assignment to *Cupulocrinus; Homocrinus angustatus* Meek and Worthen (1870, p. 30; see Worthen and Meek, 1875, p. 492, pl. 23, fig. 8). Although the evidence is not conclusive, it seems probable that this species should be placed in *Cupulocrinus.* The anal sac of this crinoid is unknown; however, the wide RR facets and IBrr suggest cupulocrinid affinities; *Dendrocrinus*? *nodobrachiatus* Ringueberg (1890, p. 303, pl. 3, figs. 6, 6a, b). This crinoid is poorly known and cannot be definitely assigned to a genus. According to the original description, either closely spaced heterotomous ramules or pinnules are present. The RA underlies the C ray R and the RR facets appear to be wide with three IBrr per ray. At present, the most appropriate placement appears to be in *Grenprisia;* obviously, the crinoid cannot be referred to *Dendrocrinus* or the dendrocrinid group.

The species of *Cupulocrinus* are divided into two end member types. Type 1 includes forms which lack flexible crinoid type patelloid processes on the Brr and have IBrr which are high relative to width. The best example is *C. conjugans* (E. Billings) (1857, p. 268; see E. Billings, 1859, p. 41, pl. 4, figs. 1, 2; Springer, 1911, p. 37). Type 2 species have patelloid processes and relatively wide IBrr. Examples are *C. humilis* (E. Billings) (1857, p. 270; see Springer, 1911, p. 28, pl. 1, figs. 8, 9, pl. 3, figs. 1-3) and *C. jewetti* (E. Billings) (1859, p. 43, text-fig. 15; see Springer, 1911, p. 28, pl. 1, figs. 10-12, pl. 3, figs. 5-7). The two groups are not discontinuous and intergradation is common. Basically, a continuous cupulocrinid spectrum exists, although the full details have not yet been ascertained.

A gradational sequence ranges from the typical *Dendrocrinus* to *Cupulocrinus* as follows: *Dendrocrinus*, RR facets narrow, IBrr relatively high, smooth Brr articulation surfaces, and anal tube consisting of equal sized, regularly arranged plates. Dendrocrinid group. Like *Dendrocrinus* but with wide RR facets. *Cupulocrinus*, Type 1. Similar to the dendrocrinid group but with wider IBrr and typical cupulocrinid anal sac (*i.e.*, median row of large plates, flanked by smaller and more irregular plates). *Cupulocrinus*, Type 2. As the previous group but with patelloid processes and relatively wider IBrr.

Such morphological gradation suggests evolutionary relationship. All four groups appeared at about the same stratigraphic horizon during the Middle Ordovician Trenton Stage; thus, stratigraphic position does not clarify the ancestral stock. However, based on the evolutionary trends shown by other dicyclic inadunate crinoids, the writer believes that *Dendrocrinus* lies morphologically closest to the ancestral form. This reasoning is based on the fact that most primitive dicyclic inadunates have narrow RR facets and smooth Brr articular surfaces, whereas more advanced forms show wide RR facets and more sophisticated Brr articulations. The geographic distribution of the four groups of cupulocrinids and dendrocrinids indicates that evolution of the group took place in the North American mid-continent and Appalachian area. All four groups first occurred in the Trenton of North America in the Cincinnati-Ontario-Quebec area. Elsewhere, these crinoids are only known from Great Britain. *Cupulocrinus sepulchrum* Ramsbottom (1961, p. 14, pl. 4, figs. 8, 9) appeared in the Caradoc of Montgomeryshire at a horizon roughly equivalent to the North American Trenton. The anal sac of this crinoid is peculiar in having two median rows of large plates rather than one as in other *Cupulocrinus;* the plates flanking these rows have not been observed. This form could be referred to *Cupulocrinus* (Type 1) or to the dendrocrinid group. The latter is suggested by the stellate ornament on the anal sac plates, a character which the writer has not observed in *Cupulocrinus*. At any rate, only one of the four groups lived during the Middle Ordovician in Great Britain. Later, in the Ashgill (Late Ordovician) two groups are found: *Dendrocrinus*, represented by *D. granditubus* and *D. rugocyathus;* and *Cupulocrinus*, probably Type 2, represented by *C. heterobrachialis* Ramsbottom (1961, p. 12, pl. 5, figs. 1-5) and *C. gracilis* Ramsbottom (1961, p. 13, pl. 5, figs. 6, 7). At first glance, these species seem to belong to *Cupulocrinus*, Type 1; however, inspection of the photographs shows that the Brr of both species have the appearance of unweathered *Cupulocrinus*, Type 2 Brr. Therefore, the writer assigns these species to Type 2 rather than Type 1 as suggested by Ramsbottom (1961, p. 12). Consideration of the morphology, stratigraphic position, and the incomplete representation of the four groups in Great Britain denotes that these crinoids were immigrants from North America rather than products of parallel evolution endemic to Great Britain.

As pointed out by Springer (1911, pp. 34-37; 1920, pp. 88-90), *Protaxocrinus* Springer (1906, pp. 515, 519) was derived from *Cupulocrinus*, Type 2, as evidenced by both morphological and stratigraphical grounds. The earliest species of *Protaxocrinus*, *P. laevis* (E. Billings) (1857, p. 278; see Springer, 1911, p. 11, pl. 3, figs. 10, 11; Springer, 1920, p. 348, pl. 45, figs. 2-7) and *P. elegans* (E. Billings) (1857, p. 278; see Springer, 1911, p. 11; Springer, 1920, p. 346, pl. 45, fig. 1) occur with species of *Cupulocrinus*, Type 2 in the Trenton of Quebec and Ontario, although the protaxocrinids are much less common. The principal changes necessary during the transition of *Cupulocrinus*, Type 2 to *Protaxocrinus* were reduction of the BB from five to three and decrease and stabilization of the number of IBrr per ray. The geographic distribution suggests that this evolution took place in North America; later during the Ashgill (Late Ordovician), *Protaxocrinus* emigrated to Scotland where it is represented by *P. girvanensis* Ramsbottom (1961, p. 19, pl. 6, figs. 14, 15).

The position of *Esthonocrinus* with respect to *Dendrocrinus* and *Cupulocrinus* is conjectural. As previously mentioned, the RR facets are narrow as in *Dendrocrinus* whereas the anal sac is of cupulocrinid type. This implies that *Esthonocrinus* could represent a link in the dendrocrinid-cupulocrinid lineage. In the writer's opinion, this is not the case because of two considerations. The geographic occurrence of *Esthonocrinus* (Ordovician, Estonia; Jewe Limestone) is far removed from the North American center of evolution of the dendrocrinid-cupulocrinid line. The lack of RA (assuming the writer's previous interpretation is correct) or lack of RA underlying the C ray R (the only other possibility) in *Esthonocrinus* is interpreted to indicate that this genus is somewhat removed from the North American lineage.

DENDROCRINUS CASEI Meek

Plate 77, figures 1, 2, 4

1848. *Pentacrinite* Christy, Letters on Geology, pl. 2.
1871. *Dendocrinus casei* Meek, American Jour. Sci., ser. 3, vol. 2, p. 295.
1873. *Poteriocrinites (Dendrocrinus) casei* Meek, Meek, Geol. Sur. Ohio, vol. 1, pt. 2, p. 28, pl. 3bis, figs. 2a-c.
1879. *Dendrocrinus casei* Meek, Wachsmuth and Springer, Rev. Palaeocrinoidea, Pt. I, Acad. Nat. Sci. Philadelphia, Proc. 1879, p. 76.
1889. *Poteriocrinites (Dendrocrinus) caseyi* [*sic*] Meek, Lesley, Geol. Sur. Pennsylvania, Rept. Prog. 2, p. 739, unnumbered figure.
1889a. *Dendrocrinus casii* [*sic*] Miller, North American Geol. and Paleont., p. 238.
1893. *Dendrocrinus casii* [*sic*] Foerste, American Geol., vol. 12, pp. 270, 340, fig. on p. 340.
1897. *Dendrocrinus casei* Meek, Wachsmuth and Springer, North American Crin. Camerata, Mus. Comp. Zool., Mem. 20, p. 128, table C, text-fig. 14 (incorrectly cited as text-fig. 13 in text).
1899a. *Dendrocrinus casei* Meek, Bather, Geol. Mag., dec. 4, vol. 6, p. 35, text-fig. 13.
1900. *Dendrocrinus casei* Meek, Bather, Lankester's Treat. Zool., Pt. 3, p. 120, text-fig. 26-3.
1908. *Dendrocrinus casei* Meek, Cumings, Indiana Geol. Surv. Ann. Rept. 36, p. 717, pl. 4, figs. 2a,b.
1910. *Dendrocrinus casei* Meek, Grabau and Shimer, North American Index Foss., vol. 2, p. 505.
1915. *Dendrocrinus casei* Meek, Bassler, Bibl. Index American Ord. and Sil. Foss., U.S. Nat. Mus., Bull. 92, p. 395.
1924. *Dendrocrinus kayi* Slocom, Iowa Geol. Sur. vol. 29, p. 335, pl. 29, figs. 1-4.
1926. *Dendrocrinus kayi* Slocum, Thomas and Ladd, Univ. Iowa, Studies, vol. 11, p. 18, pl. 3, fig. 22.
1943. *Dendrocrinus casei* Meek, Bassler and Moodey, Bibl. Paleoz. Pelmatozoa, Geol. Soc. America, Spec. Paper 45, p. 414.
1943. *Dendrocrinus kayi* Slocum, Bassler and Moodey, Bibl. Paleoz. Pelmatozoa, Geol. Soc. America, Spec. Paper 45, p. 415.

Diagnosis. — A species of *Dendrocrinus* with strongly pentalobate column; dorsal cup steeply conical with moderately heavy single or multiple stellate ridges; anal tube plates with stellate ornament; anal tube plates moderately wide; Brr of average height relative to width for *Dendrocrinus*, Brr sharp backed.

Description. — Crown large, incompletely known; dorsal cup equidimensional with straight sides; sides expanding upward at about 70°; dorsal cup plates with relatively heavy (for *Dendrocrinus*) single or multiple stellate ridges; ridge pattern standard, ridges are thickening of plates and do not involve plate folding; dorsal cup plates otherwise smooth; articular surfaces between adjacent dorsal cup plates smooth; anal sac with plicate (modified stellate) ornamentation; median-ridges of sac plates variable but always wider and heavier than lateral ridges; lateral ridges finer with steep sides; ridges not involving folding of anal sac plates; anal sac plates otherwise smooth with flat articular surfaces; anal sac nonporous.

IBB circlet of moderate height, equal to approximately 20% of dorsal cup height; IBB somewhat wider than high, pentagonal with flat base.

BB circlet high, equalling about 40% of dorsal cup height; BB somewhat wider than high; lateral BB hexagonal; CD interray B septagonal with distal surface truncated for reception of anal X, largest B in dorsal cup.

RR circlet high, equal to approximately 40% of dorsal cup height; RR pentagonal with variable height and width; RR facets narrow, equal to about ½ RR width, facets horseshoe shaped with surface sloping outward at about 40° below horizontal, surfaces gently concave; distal surface of RR just below facet thickened to form supporting rim.

RA pentagonal with width greater than height, distally supporting C ray R, laterally adjoining anal X and CD interray B; anal X hexagonal, wider than high, distal surface of anal X slightly above D ray R, somewhat below C ray R.

Anal sac incompletely known, composed of regular plates with largest plates proximally located; all sac plates much wider than high with relative width increasing distally, sac plates at same level equal sized; anal X bears first tube plate which is "axillary" and gives rise to two rows of plates; another row begins with a large plate between the C ray R and the first tube plate; the last two rows originate above an "axillary" lying between the D ray R, anal X, and the first tube plate; tube plate rows may branch again close to dorsal cup or not, when branching occurs the third, fourth, or fifth plate in the row is "axillary", other rows possess at least eight or nine plates without branching; each side of anal sac composed of six or seven rows of plates at mid-level of IIBrr.

Arms incompletely known with proximal IIIBrr being highest Brr known, composed of smooth Brr with acute angled or keeled dorsal sides (sharp-backed); nonaxillary Brr rectangular, uniserial with IBrr and proximal IIBrr equidimensional; distal IIBrr and IIIBrr becoming higher than wide; axillary Brr spear-shaped with distal width greater than proximal width; all Brr with smooth articular facets; each ray branching isotomously at least twice; IBrr range from 3 to 6 with last axillary; IIBrr equal 7 or 8 with distal Brr axillary; IIIBrr series incompletely known.

Column incompletely known; strongly pentagonal with thickened and protuberant edges; proximal eight or so columnals tapering relatively rapidly; more distal parts of column tapering weakly; all columnals thin with protuberant edges thickened; most columnals somewhat nodose with thicker columnals being the most nodose; column with alternating thick and thin columnals, or columnals not differentiated, commonly every fourth or fifth columnal is distinctly thicker and more nodose; articular surfaces of columnals not seen.

Remarks. — Three partial crowns from the Orchard Creek exposure are assigned to *D. casei.* One individual (S. 5434, Pl. 77, fig. 2, center of photograph) exhibits an arm which is smaller than the normal rays. Although the RR facet associated with the small arm is not completely known, it appears to be much smaller and somewhat constricted relative to the normal arm bearing RR facets. Possibly, the abnormal ray was regenerated or the structure of this arm may have been related to reduced or retarded growth rates.

The Girardeau individuals differ slightly from the typical Richmond Stage material from Ohio and Indiana in having slightly heavier dorsal cup stellate ridges and anal sac median and lateral ridges. However, the writer has examined about 50 Springer Collection individuals of *D. casei* from the Cincinnati area. These show considerable variation in ornamentation and some specimens possess the same type of heavy ornamentation exhibited by the Girardeau crinoids. Hence, the writer considers the Missouri specimens conspecific with the Ohio material.

Meek described the species as always possessing five, six, or seven IBrr per ray. Study of the Cincinnati crinoids discloses wide variation and the IBrr range from two to 12 with the average being 5.2 with a percentage standard deviation of 32%. Although the Girardeau sample is much smaller and the observed range is less, the mean is approximately the same (5.1, percentage standard deviation of 19%). The wide variation suggests that the number of IBrr is a poor taxonomic character in Ordovician dendrocrinoids; however, such cannot be definitely stated until more species can be examined.

In his original description of the holotype (in Chicago Museum of Natural History) and only known crown of *D. kayi,* Slocom compared the Maquoketa crinoid with the Ohio Valley specimens of *D. casei* as follows:

> This species somewhat resembles *D. casei* from a similar horizon in the Ohio Valley but (relative to *D. casei*) the ridges are fewer in number and more prominent, the proportions of the height to the width of the calyx are different and the primibrachs and secundibrachs of a much smaller specimen consist of about a half more plates than in this species.

Consideration of the number of IBrr (three to five in *D. kayi* versus two to 12 in *D. casei*), shows clear overlap and indicates that the two species cannot be distinguished by this character. The multiple stellate ridges and relatively wide dorsal cup, which are supposedly characteristic of *D. kayi,* can also be seen in some Cincinnati individuals of *D. casei,* for example S. 2265. Also, many Ohio individuals of *D. casei* possess wide CD interrays, a feature stressed by Slocom in the description of *D. kayi.* In view of the above, the writer has not been able to separate the two species; accordingly, *D. kayi* is placed in the synonymy of *D. casei.*

D. rugocyathus Ramsbottom (1961, p. 16, pl. 3, figs. 1-5) from the Ashgill of Great Britain is closely related to *D. casei.* The principal differences are that in the former species: the stellate ridges on the dorsal cup are heavier; the median series (distal to anal X) of anal tube plates is heavier and the proximal anal tube plates seem higher; and the higher order Brr are probably higher (relative to width) and more sharp backed than in *D. casei.* Although these characters have not yet been fully evaluated with respect to variation in the North American form, *D. rugocyathus* is believed a valid species.

Figured specimens. — S. 5432 - 5434.

Occurrence. — Girardeau Limestone, Orchard Creek exposure. Upper Ordovician, Richmond Stage; numerous localities in Ohio and Indiana. Maquoketa Group, Brainard Shale; various localities in Iowa.

DENDROCRINUS CURVIJUNCTUS, n. sp.

Plate 77, figure 3

Diagnosis. — A species of *Dendrocrinus* with weakly pentagonal column composed of nodals and internodals, column tapering weakly; dorsal cup steeply conical with slightly rounded base; dorsal cup and anal sac plates slightly convex with somewhat depressed sutures; Brr faintly nodose.

Description. — Crown of moderate size, incompletely known; dorsal cup steeply conical with height approximately equal to width; base of cup slightly rounded; dorsal cup sides expanding upward at about a 70° angle; dorsal cup and anal tube plates weakly convex with somewhat depressed sutures.

IBB circlet high, equal to approximately 30% of cup height; C and D ray IBB are only IBB observed, pentagonal, small, about equidimensional.

BB circlet high, highest circlet in cup, equalling approximately 40% of cup height; BC and DE interray BB partially preserved, hexagonal; CD interray B septagonal, distally truncated for reception of anal X, much higher than wide.

RR circlet high, equal to 30% of cup height; D ray R approximately equidimensional with RR facet occupying about 2/3 width of R; C ray R much wider than high, with narrow RR facet occupying about ½ width of R; RR facets weakly horseshoe shaped, sloping gently outward, surface of RR facets not observed.

RA pentagonal, much wider than high, distally supporting C ray R, laterally adjoining anal X and CD interray B; anal X pentagonal, about equidimensional, lying beside C ray R.

Anal sac incompletely known, composed of regular plates with largest plates proximally located; all sac plates equal-sized at same level, plates variable in height and width, generally equidimensional; proximal portion of sac apparently consisting of three rows of plates; two of these rows begin above anal X; third row initiated on D ray side of anal X; distal parts of anal sac not well known, apparently the three proximal rows branch once or twice near the base of the sac.

Arms incompletely known, composed of faintly nodose uniserial Brr with depressed sutures; non-axillary Brr rectangular with parallel sides; axillary Brr spear-shaped with distal width greater than proximal width; IBrr about twice as wide as high, definitely nodose; IBrr4 axillary, bearing two isotomous branches; higher Brr preserved only in D ray; IIBrr approximately equidimensional, less nodose than IBrr; IIBrr5 axillary, probably branching isotomously; five IIIBrr preserved on left branch of D ray, similar to IIBrr; IIBrr and IIIBrr poorly preserved; Brr articular surfaces not well known, probably smooth, certainly lacking distinct articular ridges and ligamental pits; Brr with gently concave ventral surface; Amb tracts deep, width equal to about ¼ Br width.

Column incompletely preserved, weakly pentagonal, composed of alternating definitely nodose, thicker columnals (nodals) and thinner, less nodose columnals (internodals); all columnals lack cirri; articular surfaces not observed; proximal two columnals taper rapidly; remaining portion of column tapering very weakly.

Remarks. — This species is represented by one partial crown showing the dorsal cup and portions of the arms, anal sac, and column. Although the anal sac is not completely known, the preserved portions of the sac indicate that each of the three proximal rows of plates branches once or twice close to the dorsal cup. Despite this relatively rapid branching, the distal portion of the anal sac is not expanded as in *D. granditubus* Ramsbottom (1961, p. 15, pl. 4, figs. 1-7).

D. curvijunctus is most closely comparable with a series of Trenton species; the affinities of this crinoid with Cincinnatian forms are much less pronounced.

Comparison with Trenton forms: *D. rusticus* E. Billings (see E. Billings, 1859, p. 41, pl. 3, figs. 7a,b) seems to be the most closely allied taxon from the New York-Ontario-Quebec area; however, the Girardeau crinoid differs in a less-tapering column with more pronounced nodals and internodals. *D. acutidactylus* E. Billings (see E. Billings, 1859, p. 37, pl. 3, figs. 2a,b) is separated by its more slender arms with narrow backed Brr and the rounded column. In *D. proboscidiatus* E. Billings (see E. Billings, 1859, p. 38, pl. 3, figs. 3a-c), the Brr are also sharp backed, the anal tube plates plicate, and the column tapers more rapidly. *D. alternatus* (Hall) (1847, p. 83, pl. 28, figs. 1a-f) differs in possessing a round stem with strongly differentiated nodals and internodals. The Girardeau crinoid shows a pentagonal stem which is differentiated into nodals and internodals in contrast to the round stem with undifferentiated columnals of the Kentucky species *D. dyeri* (Meek) (see Meek, 1873, p. 24, pl. 3bis, figs. 3a,b).

The only remotely similar Cincinnatian crinoid is the Maysville form, *D. cincinnatiensis* (Meek) (see Meek, 1873, p. 20, pl. 3bis, figs. 5a,b). However, in the Ohio species, the stem is strongly pentagonal with well-developed proximal-distal sutures. *D. longidactylus* Hall (1852, p. 193, pl. 42, figs. 7a,b, pl. 43, figs. 1a-k) from the Middle Silurian of New York differs in the presence of narrower RR facets with more slender arms and strongly plicate anal sac plates.

Specific name. — *curvijunctus* in allusion to the curved dorsal cup base in the vicinity where the stem joins the calyx.

Holotype. — IGS. 35P-7.

Occurrence. — Girardeau Limestone, Orchard Creek exposure.

DENDROCRINUS ? n. sp. aff. **D.** ? **NAVIGIOLUM** Miller

Plate 78, figure 1

Diagnosis. — A dendrocrinid with column bearing cirri in distal portions, proximal part of column pentagonal, distal part of column round; columnals weakly differentiated; dorsal cup slender with broad and weak median-ray ridges; arms slender, composed of smooth Brr; each ray branching once or twice isotomously.

Description. — Crown relatively small, slender, with fragile arms and column; dorsal cup small, steeply conical, with height much greater than width; dorsal cup sides straight, expanding upward at angles ranging from 70 to 75°; dorsal cup plates smooth; sutures not incised; dorsal cup with broad and weak median-ray ridges; median-ray ridges indistinct on IBB, better developed on BB and RR, median-ray ridges single on proximal parts of IBB, bifurcating on distal part of IBB with the two branches crossing IBB-BB sutures; single median-ray ridges on proximal portion of BB, at distal portion of BB, ridges divide again, cross BB-RR sutures and converge on RR facets.

IBB circlet high, equal to approximately 30% of cup height; IBB slightly higher than wide, pentagonal with flat base.

BB circlet high, largest in dorsal cup, equal to about 45% of cup height; BB much higher than wide, all BB observed hexagonal; CD interray B either not differentiated in size and shape or not observed.

RR circlet relatively low, smallest in dorsal cup, equalling about 25% of dorsal cup height; RR pentagonal with width distinctly greater than height; RR facets narrow, occupying about 50% of RR width, facet horseshoe shaped, surface of facet not observed.

Posterior interray either not differentiated or not seen; anal sac unknown.

Arms composed of smooth Brr with non-incised sutures; non-axillary Brr rectangular, uniserial; axillary Brr pentagonal, spear-shaped with distal width exceeding proximal width; proximal Brr approximately equidimensional (IBrr); distal Brr (IIBrr, IIIBrr, and IVBrr if present) becoming slightly higher than wide; Brr articulation surfaces not seen; each ray branching isotomously two or three times; IBrr comprise 6 with IBrr6 axillary; IIBrr ranging from 7 to 9 with distal IIBrr always axillary; IIIBrr forming terminal Brr in some cases, in other branches IIIBrr7 (approx.) is axillary and gives rise to short branches composed of IVBrr.

Column complete, approximately 30 mm long; proximal 10 mm weakly pentagonal; columnals in this portion of column undifferentiated with smooth or faintly nodose sides, individual columnals ranging from .2 to .3 mm in thickness; distal 20 mm of column round, composed of undifferentiated columnals with smooth sides, columnals of this region ranging from .15 to .30 mm thick; distal 10 mm of stem with irregularly distributed cirri, cirrus bearing columnals probably with one cirrus each; cirri round with ill-defined cirral sutures, number of cirrals per cirrus unknown, cirri of variable length but relatively short compared with most crinoids, cirri directed upward as in *Goniocrinus,* not outward or downward as in most crinoids; articular facets of columnals, cirrus bearing columnals and cirrals unknown.

Remarks. — Three poorly preserved Girardeau specimens, two of which consist of crowns with all or part of the column whereas the third individual is a dorsal cup showing a short column segment, are assigned to this species. All three crinoids are imbedded in and somewhat obscured by the hard, fine-grained argillaceous matrix. No trace of a CD interray can be observed in any of the three individuals; possibly, the CD interray is not differentiated from the other interrays or a RA and X may be present. If one of the specimens could be isolated from the matrix, the nature of the CD interray could be determined; however, this has not been attempted due to the hardness of the matrix.

Inasmuch as the CD interray is unknown, the generic position of this crinoid is uncertain. Morphologically, the species could be assigned to either *Esthonocrinus* or *Dendrocrinus.* As in the similar case of *D.? constrictus,* this form is questionably grouped with *Dendrocrinus* on paleogeographical considerations. The slender dorsal cup with relatively high BB and short RR suggests assignment to *Bactrocrinites.* However, this genus is not known below the Devonian; thus, stratigraphic distribution does not indicate placement within *Bactrocrinites.*

The most similar dendrocrinid to the Girardeau crinoid is *Dendrocrinus? navigiolum* Miller (1880, p. 235, pl. 7, figs. 6,6a) from the Eden of the Cincinnati area. Both species have similar dorsal cups and IBrr. The higher parts of the arms are unknown in the Cincinnati form and no comparison of these can be presented. The main difference between the two forms is the column. In both, the basic column shape and structure is similar; however, the column of the Girardeau crinoid has distal cirri which are lacking in *D? navigiolum.* The writer has examined only two specimens referable to the latter species, the holotype which is in the Chicago Natural History Museum and one Springer Collection individual. The CD interray cannot be determined in either specimen, a situation similar to the Girardeau form.

D. celsus Ringueberg (1888, p. 132, pl. 7, fig. 3) from the Niagaran of New York may be separated from *D?* n. sp. aff. *D.? navigiolum* by its tapering column with wider columnals and the lack of median-ray ridges. The Kentucky Trenton *D. dyeri* (Meek) (see Meek, 1873, p. 24, pl. 3bis, figs. 3a,b) differs in lacking median-ray ridges, the presence of many more arm bifurcations, and having a completely round column. Although the Girardeau form clearly represents a new species, it is not formally described due to the relatively poor preservation of the available material.

The most peculiar feature of *D.?* n. sp. aff. *D.? navigiolum* is the upward directed cirri on the distal part of the column. Possibly, the peculiar cirri orientation could represent a death position, thus being different from the original living configuration. However, a living orientation is indicated by the fact that all cirri show the same upward inclination. The adaptive significance of such cirri is open to question. If the cirri were used for grasping the substrate, the expected orientation would be at right angles to or downward from the column. In some crinoids *(e.g. Goniocrinus)* with upward directed cirri, the cirri cover the crown and probably served to protect the crown or perhaps agitate the water for more efficient feeding. Considering the distal position of the short cirri in the Girardeau crinoid, this is obviously incorrect. Possibly, the cirri were used to grasp upright objects, such as the columns of other crinoids or submarine plants. This cannot be proven with the available material and the relatively short cirri and their orientation argue against such an explanation.

Types. — Figured specimen — IGS. 35P - 5.

Mentioned specimens. — IGS. 35P - 6, 8258.

Occurrence. — Girardeau Limestone, Orchard Creek exposure.

DENDROCRINUS ? CONSTRICTUS, n. sp.

Plate 79, figure 1

Diagnosis. — A large dendrocrinid characterized by steeply conical dorsal cup with centrally constricted IBB circlet; dorsal cup plate ornamentation composed of fine, irregular, sinous ridges with elliptical or slit-shaped pits between them; column tapering rapidly, consisting of wide, undifferentiated columnals.

Description. — Dorsal cup large, approximately 23 mm high, conical with width slightly greater than height; dorsal cup sides straight, steep, expanding upward at about a 70° angle; dorsal cup plates with sharply incised sutures; all dorsal cup plates ornamented with fine sinous irregularly bifurcating ridges, near plate sutures these are at right angles to the sutures as in cystoid pore rhombs, farther away from plate sutures the ridges trend in any direction; small elliptical or slit-shaped pits lie between the ridges, long axes of pits parallel adjacent ridges, pits surficial, not penetrating plates; central portion of IBB circlet distinctly constricted; BB and RR with broad ill-defined median-ray ridges, single on proximal portion of BB, dividing near distal part of BB, then crossing BB-RR sutures with two adjacent ridges converging on RR facets.

IBB circlet high, equal to approximately 30% of cup height; IBB slightly wider than high, pentagonal with rounded proximal sides.

BB circlet high, equal to about 45% of height of cup; BB largest dorsal cup plates, somewhat higher than wide; lateral BB hexagonal; CD interray B septagonal, distally truncated for reception of anal X.

RR circlet smallest in dorsal cup, equalling about 25% of dorsal cup height; RR pentagonal with width greater than height; RR facets narrow, occupying about 40% of RR width, facets horseshoe-shaped, sloping outward at approximately 30° angle, facets with marginal rims; dorsal rim or ridge weak, scarcely differentiated from central area of facet; ventral ridge relatively sharp, distinct, easily separated from central portion of facet, ventral ridge with central groove in median area of facet; central part (ligament pit) of RR facets gently concave.

RA and C ray R unknown; anal X partially preserved, approximately equidimensional, probably hexagonal.

Anal sac and arms unknown.

Column incompletely preserved, round, rapidly tapering in distal direction; columnals wide, straight sided, not nodose, columnals undifferentiated; axial canal round; columnal articulation surfaces not seen; proximal three columnals with edges arched, arched portions of columnals fitting into indentations between adjacent IBB, degree of arch of the three proximal columnals decreases in distal direction and distal side of third columnal is straight; all remaining columnals with parallel proximal and distal surfaces.

Remarks. — This species is based on one specimen, a partial dorsal cup showing the proximal portion of the column. The CD interray is not completely preserved and the nature of the C ray R and RA cannot be determined. A hexagonal anal X can be seen resting on the truncated CD interray B; the shape and level of anal X clearly indicates that a RA was present. However, the shape of the RA is unknown because the C ray R and distal portion of the CD interray B are not preserved. Therefore, the generic position of this crinoid is uncertain; morphologically, this species could be assigned to either *Esthonocrinus* or *Dendrocrinus.* However, the geographic occurrence of *Esthonocrinus* (restricted to the Baltic Sea area) is far removed from that of the Cape Limestone form. Therefore, on the basis of paleogeographical considerations, the Missouri crinoid is tentatively referred to *Dendrocrinus.*

D. ? constrictus is easily differentiated from *Esthonocrinus laevior* Jaekel (1918, p. 53, text-fig. 40) and *E. compactus* Jaekel (1918, p. 53) by the strong constriction of the IBB circlet. The Cape Limestone species is somewhat similar to several species from the Trenton of Canada, *i.e., Dendrocrinus gregarius* E. Billings (see E. Billings, 1859, p. 36, pl. 3, figs. 1a-c), *D. proboscidiatus* E. Billings (see E. Billings, 1859, p. 38, pl. 3, figs. 3a-c), and *D. rusticus* E. Billings (see E. Billings, 1859, p. 41, pl. 3, figs. 7a,b); however, the Missouri crinoid shows a characteristic surface ornamentation and a constricted IBB circlet, both of which are lacking in the Trenton forms. In *D. celsus* Ringueberg (1888, p. 132, pl. 7, fig. 3) from the Niagaran of New York, the dorsal cup is more slender, the IBB circlet is not constricted, and the plates are smooth.

One of the most notable features of *D. ? constrictus* is the large size of the dorsal cup (height, 23 mm). This is by far the largest Ordovician dendrocrinid known. Generally, the dorsal cup height of most adult Ordovician dendrocrinids averages 10 mm or less; the second largest individual which the writer has observed is a crown referable to *D. proboscidiatus* W. R. Billings (1887, p. 53, unnumbered fig.) from the Trenton of Ottawa in which the dorsal cup is about 13 or 14 mm high. Probably, the large size, robust habit, and thick plates of the Missouri crinoid were related to the shallow water, highly agitated depositional environment of the Cape Limestone. Such a depositional environment is indicated by the coarse-grained calcarenite lithology and the predominantly robust brachiopod fauna of the Cape Formation in the Missouri outcrop belt. This occurrence is in contrast to that of the smaller Trenton and Cincinnatian dendrocrinids which generally occur in much finer-grained argillaceous limestones or limestones. The implication is that the high degree of continuous agitation aided the crinoids in feeding and respiration by furnishing a continuous supply of food and fresh oxygen. This, in turn, allowed the development of a larger animal. On the other hand, in wholly or partially quiet water environments, the slower renewal rate of food and oxygen probably favored smaller crinoids.

Specific name. — *constrictus* in allusion to the central constriction of the IBB circlet.

Holotype. — USNM 164 593, probably collected by E. O. Ulrich.

Occurrence. — Upper Ordovician, Cincinnatian; Maquoketa Group, Cape Limestone. The original locality label associated with this specimen reads: Fernvale Limestone (Cape Limestone), Cape Girardeau, Missouri. Although no author is indicated, the label was clearly written by Ulrich and presumably he collected the holotype. Study of the Ulrich collections in the United States National Museum shows the only Cape Limestone sections in Cape Girardeau which were extensively collected by Ulrich are on Main Street to the north of Broadway. Probably, the holotype was found at one of these outcrops.

Subclass FLEXIBILIA Zittel, 1879

Order TAXOCRININIDA Springer, 1913

Family **TAXOCRINIDAE** Angelin, 1878

Genus **PROTAXOCRINUS** Springer, 1906

Type species. — By designation of Springer, 1906, pp. 515, 519, *Taxocrinus ovalis* Angelin, 1878, p. 8, pl. 20, figs. 13, 14.

Diagnosis. — A genus of Taxocrinidae with large pentagonal RA underlying C ray R; IBB visible from side; two IBrr; arms branching isotomously twice or more.

Remarks. — *Protaxocrinus* is closest to the typically Devonian genus, *Eutaxocrinus* (Springer, 1906, pp. 493, 519; see Springer, 1920, p. 357). Both genera have similar dorsal cup habits, two IBrr per ray, and in most species, isotomously branching arms. The most striking difference is the CD interray structure in which the eutaxocrinid RA is almost invariably absent; when this plate is present, it lies in an upper oblique position in contrast to the primitive RA location under the C ray R seen in protaxocrinids.

Gnorimocrinus (Wachsmuth and Springer, 1879, p. 50; see Springer, 1920, p. 353) is easily distinguished by its widely expanding crown and small quadrangular RA.

All other taxocrinids differ greatly from protaxocrinids in the: CD interray structure; presence of more than two IBrr per ray; usually lower dorsal cup in which the IBB are low or not visible from the side; and basically different arm structure in the case of *Onychocrinus* (see Springer, 1920, p. 417).

Occurrence. — Middle Ordovician; Canada. Upper Ordovician; Great Britain. Middle Silurian; Mid-continent North America; Island of Gotland. Lower Devonian; Central Appalachians.

PROTAXOCRINUS GIRARDEAU Springer

Plate 78, figure 4; Plate 79, figure 4

1920. *Protaxocrinus girardeau* Springer, The Crinoidea Flexibilia, Smithsonian Inst. Pub. 2501, p. 349, pl. 45, fig. 8.
1943. *Protaxocrinus girardeau* Springer, Bassler and Moodey, Bibl. Paleoz. Pelmatozoa, Geol. Soc. America, Spec. Paper 45, p. 653.

Diagnosis. — A species of *Protaxocrinus* with narrow dorsal cup and high IBB circlet; dorsal cup plates smooth; arms branching two or three times; Brr with round backs and smooth sides; distal Brr relatively high.

Description. — Crown of moderate size; dorsal cup steeply conical with wide flat base, width greater than height; dorsal cup sides straight, expanding upward at about a 65° angle; dorsal cup plates smooth, with somewhat incised sutures.

IBB circlet high for *Protaxocrinus*, equalling about 30% of dorsal cup height, circlet composed of three plates, two large and one small; sutures located in AE, BC, and CD interrays; small IB with sutures in BC and CD interrays, small IB pentagonal, equidimensional; large IBB basically pentagonal with distal face truncated for reception of overlying B, large IBB much wider than high.

BB circlet high, equal to approximately 35% of dorsal cup height; lateral BB equidimensional, pentagonal with curved proximal edge when underlain by large IB, hexagonal when underlain by IBB suture; CD interray B largest in dorsal cup, with width slightly greater than height, septagonal with distal surface truncated for reception of anal X; articular surfaces between lateral BB and BB and RR partially observed, apparently smooth.

RR circlet high, equalling about 35% of dorsal cup height; RR basically pentagonal with distal-lateral margins truncated for reception of small iBrl, RR approximately equidimensional; RR facets wide, nearly equal to total width of RR, surface of facets not seen.

RA pentagonal with width greater than height, lying below C ray R, beside anal X and CD interray B; anal X hexagonal with height exceeding width, lying above truncated CD interray B and laterally adjoining RA and proximal part of C ray R.

Anal sac not seen.

The iBrr1 small, height greater than width, definitely located in dorsal cup, reaching to proximal portion of IBrl, iBrl followed by irregular perisomic-type plates of unknown structure.

Arms known except for distal tips, composed of smooth Brr with more or less incised or depressed sutures; nonaxillary Brr uniserial, rectangular; proximal Brr distinctly wider than high; distal Brr (highest IIIBrr or IVBrr) becoming nearly equidimensional; axillary Brr pentagonal, spear-shaped with distal width greater than proximal width; articular surfaces not seen; mid-dorsal portions of sutures not strongly depressed as in more progressive taxocrinids, this denotes lack of well-developed patelloid process; IBrr comprise 2 with second axillary, bearing two IIBrr series; IIBrr ranging from 4 to 6, with last always axillary; IIIBrr series commonly unbranched, in such cases 6 to 10 IIIBrr can be seen; in others IIIBrr may branch in which IIIBrr7 is axillary; in the only three nearly complete half-rays, one quarter-ray branches while the other remains unbranched; only several IVBrr observed; terminal IIIBrr or IVBrr not seen.

Only proximal portions of column known, represented by about 7 mm in holotype, approximately 30 mm preserved in figured specimen; column round, tapering slowly for *Protaxocrinus;* columnals generally wide with height equalling 14 to 20% of width; some columnals much thicker with height ranging up to about 50% width; proximal 5 mm of column in figured specimen bearing irregularly distributed nodes or rootlet bases; nodes ranging from 0 to 3 per columnal; in figured specimen the column bends about 120° about 6 mm below the dorsal cup; this is attributed to the presence of two wedge-shaped columnals located at the point of curvature; lumen round with diameter equalling about 20% columnal diameter; articular surface of most columnals with well-developed outer crenularium occupying from 50 to 67% of columnal diameter, crenularium represented by culmina (radiating ridges) which are separated by crenellae (narrow furrows); inner portion of columnal surface smooth, slightly concave, sloping toward lumen; when crenularium is present suture between adjacent columnals is crenulate (symplexy) with culmina fitting into adjacent crenellae of next columnal; in some columnals crenellae and culmina are lacking and the suture surface between such columnals is straight; articular surfaces of such columnals unknown.

Remarks. — This species is based on two specimens consisting of complete crowns with portions of the column. One specimen (holotype) was found at the Orchard Creek exposure whereas the second (figured specimen) comes from the Cape Rock exposure. Unfortunately, the latter individual was not available to Springer in time to be figured in his Flexibilia monograph; however, this specimen was briefly mentioned in the text (Springer, 1920, p. 349).

This figured specimen is important because it illustrates several morphological features which are not present in the holotype and discloses pertinent information about the mode of life. The stem shows a 120° bend about 6 mm below the dorsal cup. This appears to be caused by two large wedge-shaped columnals (width, 1.3 mm; maximum height, .4 mm; minimum height, .2 mm) located at the point of curvature. In addition, the distal preserved 5 mm of the stem exhibits small irregularly distributed nodes. These probably represent rootlet bases; this is indicated by the small partly-buried rootlets in the matrix immediately adjacent to this part of the column. Certainly, the irregular distribution of the nodes indicates that these are not stereom covered cirrus scars. Most likely, this individual lived with the distal part of the stem recumbent on the substrate as in calceocrinids (See Brower, 1966 for discussion of the Calceocrinidae mode of life). In the Girardeau flexible, the crown and the proximal 6 mm of the column was probably permanently elevated above the substrate.

Lane and Webster (1966, pp. 14, 15-22) observed similar bent stems in the Permian flexibiles *Nevadacrinus* (Taxocrinidae) and *Trampidocrinus* (Sagenocrinitidae), and they reached the same conclusions with respect to the life habits. Lane and Webster believed that the bent column of the Permian crinoids probably constituted an adaptation to rough water, principally because the crown was located close to the sea floor in a zone of reduced agitation.

Perhaps, this was also the case for the Girardeau individual which lived in a habitat that was intermittently agitated. The wide stratigraphic separation and distant relationships of the Girardeau and Permian flexibles indicate that the bent stem adaptation developed independently in the three genera. Although 7 to 8 mm of the column are preserved in the holotype, no trace of a wedge-shaped columnal or bent column is seen. Perhaps, the column was straight or the bend may have been located farther down the stem.

Protaxocrinus girardeau is most closely related to the Trenton species *P. laevis* (Billings) (1857, p. 278; see Billings, 1859, p. 47, pl. 4, fig. 3a; Springer, 1920, p. 348, pl. 45, figs. 2-7); both forms show similar dorsal cups and arm branching structure. The Girardeau crinoid can be distinguished by the much more narrow distal arm Brr. In *P. girardeau* the arms branch two or three times in contrast to the invariable three branchings of *P. laevis*. According to Springer (1920, p. 349), the Girardeau form differs from the Trenton species in having five rather than three or four IIBrr. This is not the case because the IIBrr of the Trenton crinoid range from two to five (mean 4.1) whereas the Girardeau individuals show four to six IIBrr with an average of 4.6 plates.

P. girardeau is easily separated from the other Ordovician species of *Protaxocrinus*, *P. elegans* (Billings) (1857, p. 278; see Billings, 1859, p. 47, pl. 4, figs. 4a,b; Springer, 1920, p. 346, pl. 45, fig. 1) and *P. girvanensis* Ramsbottom (1961, p. 19, pl. 6, figs. 14, 15), by its round backed Brr with smooth sides. The Girardeau species differs from all Silurian and Devonian forms in the more narrow dorsal cup with high IBB circlet.

Types. — Holotype — S. 1778. Figured specimen — S. 5435.

Occurrence. — Girardeau Limestone, Orchard Creek and Cape Rock exposures.

Order SAGENOCRINIDA Springer, 1913

Family **ICHTHYOCRINIDAE** Angelin, 1878

Genus **CLIDOCHIRUS** Angelin, 1878

Type species. — By monotypy, *C. pyrum* Angelin, 1878, p. 12, pl. 22, fig. 23.

Diagnosis. — A genus of Ichthyocrinidae with RA underlying C ray R; anal X in cup, proximal margin rests on CD interray B; C and D rays in contact above anal series; IBB low, generally visible from side; BB large, forming part of cup wall; dorsal cup large relative to the arms.

Remarks. — The most characteristic features of *Clidochirus* are the stout inadunate or lecanocrinid type dorsal cup, and the CD interray structure in which the RA underlies the C ray R and a well-developed anal X is present. According to Strimple (1963, p. 113), a RA is lacking in two species of *Clidochirus*, *C. gratiosus* Strimple (1963, p. 113, pl. 8, figs. 9, 10, pl. 9, fig. 7) and *C. keyserensis* Springer (1920, p. 298, pl. 37, figs. 9-11). Study of Springer's illustrations (see figs. 9a, b) and the types of the latter clearly indicate that a RA is present. A RA is apparently absent in *C. gratiosus* Strimple (see pl. 9, fig. 7); probably this species should be referred to an undescribed genus.

Two taxa from the Upper Devonian of Iowa assigned to *Clidochirus* by Bassler and Moodey (1943, p. 366), *C. iowensis* Thomas (1924, p. 465, pl. 42, figs. 19-34, pl. 43, figs. 10-44) and *C.? maximus* Thomas (1924, p. 467, pl. 42, figs. 35-37), are known only from disarticulated plates. The former is based on a series of plates ranging from the IBB to IIBrr. A RA has not been identified in the isolated plates. Most likely, this crinoid should not be assigned to *Clidochirus* as defined here; the writer suggests that this species may be congeneric with *C. gratiosus*. *C.? maximus* is known only from an isolated IAx; obviously, there is no basis for assignment to *Clidochirus* or any other genus and the writer considers this name to be without foundation.

Clidochirus is easily distinguished from *Ichthyocrinus* (Conrad, 1842, p. 279; see Springer, 1920, p. 264), *Synaptocrinus* (Springer, 1920, p. 301) and *Metichthyocrinus* (Springer, 1906, p. 479; see Springer, 1920, p. 320) by the characteristic CD interray structure and the lecanocrinid rather than the typical ichthyocrinid crown habit. Although *Cleistocrinus* Springer (1920, p. 272) has a clidochirid type CD interray, cleistocrinids differ in the absence of the IBB and in the reduced dorsal cup in which the BB and RR are covered by the column.

Occurrence. — Upper Ordovician; Mid-continent, North America. Lower Silurian; Mid-continent, North America. Middle Silurian; Mid-continent, North America; Island of Gotland. Lower Devonian; Appalachian Province, North America.

CLIDOCHIRUS SERRULATUS, n. sp.

Plate 79, figure 2; Text-figure 44

Diagnosis. — A species of *Clidochirus* with crown of average shape; dorsal cup relatively high, arms short for genus; adjacent rays and half-rays united by strongly zigzag suture to level of proximal IIIBrr; all plates smooth; arms branching twice with terminal Brr composed of IIIBrr.

Description. — Crown small, higher than wide, expanding gradually in proximal portions, distally flat; dorsal cup much wider than high; dorsal cup sides slightly rounded, expanding distally at an angle of about 55°; dorsal cup plates smooth, sutures not incised; articular surfaces not observed.

IBB circlet low, height equalling approximately 15% of dorsal cup height; circlet incompletely known, probably composed of three plates as in normal flexible crinoids; only IBB sutures observed in CD interray position; IBB much wider than high; IBB-BB sutures partly anchylosed.

BB circlet high, equal to about 43% of dorsal cup height; BB hexagonal, roughly equidimensional; CD interray B septagonal, equidimensional, with distal face truncated for reception of anal X.

RR circlet high, equalling about 42% of dorsal cup height; RR pentagonal with width distinctly greater than height; RR facets wide, equalling total width of RR; surface of facets not seen.

RA not completely observed, probably pentagonal; suture with C ray R partially obscured by matrix, course of observed part of suture indicates RA underlies C ray R, RA lying beside anal X and CD interray B; anal X pentagonal, equidimensional, located above truncated CD interray B, flanked by C and D ray RR; distal level of anal X lies below RR facets.

The iBrr are absent, IBrr in lateral contact; tegmen not seen.

Proximal Brr laterally joined along zig-zag sutures to form FBrr; zig-zag sutures most prominent on IIBrr and IIIBrr when forming FBrr, less well developed or absent on IBrr; highest FBrr between D and E rays is proximal portion of IIIBrr2; adjacent half-ray Brr united by zig-zag suture to level of proximal part of IIIBrr1; highest quarter-ray FBrr equals proximal portion of IIIBrr1 or IIIBrr2; large iBr present between C and D rays, reaching to proximal level of IIBrr1; distal to IIBrr1, C and D rays joined to level of proximal part of IIBrr4; non-axillary FBrr hexagonal with zig-zag sides; axillary FBrr septagonal with zig-zag sides; free non-axillary Brr rectangular, uniserial; terminal Brr bullet-shaped with rounded tips; IBrr wide with height equalling about 42% of width; distal Brr gradually becoming relatively higher; IIIBrr with height equalling about 58% width; FBrr lateral articular surfaces smooth; proximal or distal articular surfaces of free Brr or FBrr not seen; Brr sutures straight denoting lack of prominent patelloid process; each ray branches equally twice; IBrr comprise 2 in C and E rays; IBr1 axillary in D ray; IIBrr consist of 4 with last axillary, bearing two series of IIIBrr; IIIBrr8 to IIIBrr10 terminal.

Only proximal part of column known, represented by approximately 8 mm in holotype; proximal 1 to 2 mm tapering rapidly; distal portions with slight taper; column round, generally composed of alternating nodals and internodals; proximal internodals with straight sides, internodals becoming more nodose distally; nodals distinctly thicker than internodals with height averaging about 27% of width; average internodal height equalling approximately 12% of width; articular surfaces not observed; suture between adjacent columnals crenulate, denoting presence of crenularium on columnal articular surfaces.

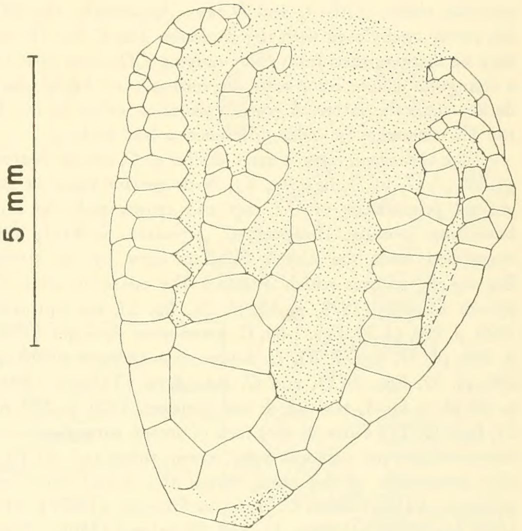

Text-figure 44. — Holotype of *Clidochirus serrulatus*, n. sp., IGS. 35P-8, D ray dorsal cup height 2.9 mm, Girardeau Limestone, Orchard Creek exposure. Matrix stippled. Fused IBB sutures shown by dotted lines. IBB sutures determined by change in calcite color indicated by continuous lines. Inferred sutures denoted by dashed lines.

Remarks. — *C. serrulatus* is based on a single specimen from the Orchard Creek exposure. Unfortunately, the crown is partly buried in matrix and certain aspects of the morphology must be inferred to some degree. The generic assignment of this crinoid is difficult for two reasons. As mentioned in the generic diagnosis, one of the characteristic features of *Clidochirus* is the location of the RA under the C ray R. The RA is not completely visible in the holotype because its right side is partly buried under matrix. Nevertheless, the trend of the observed part of the C ray R-RA suture clearly indicates that this plate underlies the R. The IBB circlet is incompletely known and traces of these plates are only visible in the C and D rays. Apparently, the IBB are partly anchylosed with the B circlet. The C ray IB can only be distinguished from the overlying CD interray B by a change in calcite color with the former plate being much darker than the latter. A similar situation exists in the D ray IB, although the color difference is less striking.

The Girardeau form is most similar to *C. ulrichi* Foerste (1919, p. 17, pl. 2, figs. 1a, b); both species agree in the general proportions of the cup and crown and the arm branching formula. However, *C. serrulatus* is easily distinguished from the Lower Silurian form by its strong Brr zig-zag sutures which interlock the adjacent arms. *C. pyrum* Angelin (1878, p. 12, pl. 22, fig. 23, see Springer, 1920, p. 296, pl. 37, figs. 1-6), *C. americanus* Springer (1920, p. 298, pl. 37, figs. 7, 8), *C. keyserensis* Springer (1920, p. 298, pl. 37, figs. 9-11), and *C. schucherti* (Talbot) (1905, p. 30, pl. 3, fig. 1, text-fig. 4; see Springer, 1920, p. 299, pl. 37, figs. 12, 13) differ in the: lack of strong sutural connections between the adjacent arms; crown shape and the relative proportion of the arms versus the dorsal cup; and presence of IVBrr. Both *C. gratiosus* Strimple (1963, p. 113, pl. 8, figs. 9, 10, pl. 9, fig. 7), and *C? greenei* (Miller, 1892, 1894, p. 306, pl. 8, fig. 3) resemble the Girardeau form in the interlocking of the adjacent arms; however, *C. serrulatus* is easily separated by the crown shape. In addition, *C.? greenei* shows three IBrr in each ray, a character which is unique to this species. *C. iowensis* Thomas (1924, p. 465, pl. 42, figs. 19-34, pl. 43, figs. 10-44) is known only from isolated plates, and in the writer's opinion, the generic assignment of this crinoid is questionable. *C. iowensis* differs from *C. serrulatus* in showing granulose rather than smooth RR and Brr.

Specific name. — *serrulatus* in allusion to the strong zig-zag sutural connections between the adjacent arms.

Holotype. — IGS. 35P-8.

Occurrence. — Girardeau Limestone, Orchard Creek exposure.

EVOLUTION OF *CLIDOCHIRUS* AND ITS ALLIES

Clidochirus serrulatus is the oldest and most primitive species in the genus. Based on morphological comparison and stratigraphic position, the principal clidochirid evolutionary trends were the following: *C. serrulatus* is by far the smallest species. The maximum size was attained by the Middle Silurian *C. pyrum* and *C.? greenei*; the later Devonian crinoids range somewhat smaller. In the Late Ordovician and the Early and Middle Silurian forms (excepting *C.? greenei*), the dorsal cup is relatively large in relation to the whole crown, and the gross habit of these crinoids is similar to that of asaphocrinids, anisocrinids, and some primitive lecanocrinids. In the Early Devonian species, *C. schucherti* and *C. keyserensis,* the dorsal cup became reduced with respect to the crown size; consequently, the habit of these crinoids paralleled typical ichthyocrinids in which the dorsal cup is small with the rays expanding upward rapidly. *C. serrulatus* shows the smallest number of Brr; the highest Brr consist of the IIIBr and about 45 Brr are present in each ray. A similar structure is seen in the Early Silurian *C. ulrichi.* However, most post-Ordovician species have IVBrr and as many as 200 Brr may be found in a single ray. The anal X of the Girardeau form is small and only reaches the distal portions of the adjacent RR. In later species, the CD interray became simplified because of the increase in the anal X size; this commonly terminates at the IBr1 or IAx level and in a few cases higher Brr.

Other ichthyocrinids were derived from *Clidochirus* or its immediate ancestors (see Text-fig. 45). The principal changes consisted of: simplification of the CD interray caused by loss of the RA and anal X; similar trends can be documented in many other flexible stocks, for example, lecanocrinids, synerocrinids, and homalocrinids; and development of the typical ichthyocrinid crown habit. This was accomplished by reduction of the dorsal cup, partly due to decrease in size of the individual cup plates (especially the IBB and BB) and partly caused by covering the dorsal cup plates with the proximal columnal. Also important to the ichthyocrinid habit was the evolution of rapidly expanding rays with numerous Brr; however, this was partially a consequence of the previously mentioned dorsal cup reduction. The progressive formation of the ichthyocrinid habit is considered plausible for most Ichthyocrinidae because such evolution can be seen within *Clidochirus.*

In *Ichthyocrinus* (Middle Silurian; North America, Gotland, Great Britain; Early Devonian; North America, Boehemia), the ichthyocrinid habit is well developed. All traces of the anal X disappeared although the primitive type RA remained under the C ray R. The *Ichthyocrinus* CD interray structure and stratigraphic relations clearly testify to descent from *Clidochirus.*

Synaptocrinus (Middle Devonian; Appalachian Province, North America) closely resembles *Ichthyocrinus.* The former differs mainly in having a strongly differentiated CD interray B and in lack of the RA. The phyletic position of synaptocrinids remains obscure because it is uncertain whether the differentiation of the CD interray B represents a primitive or advanced character. The writer considers

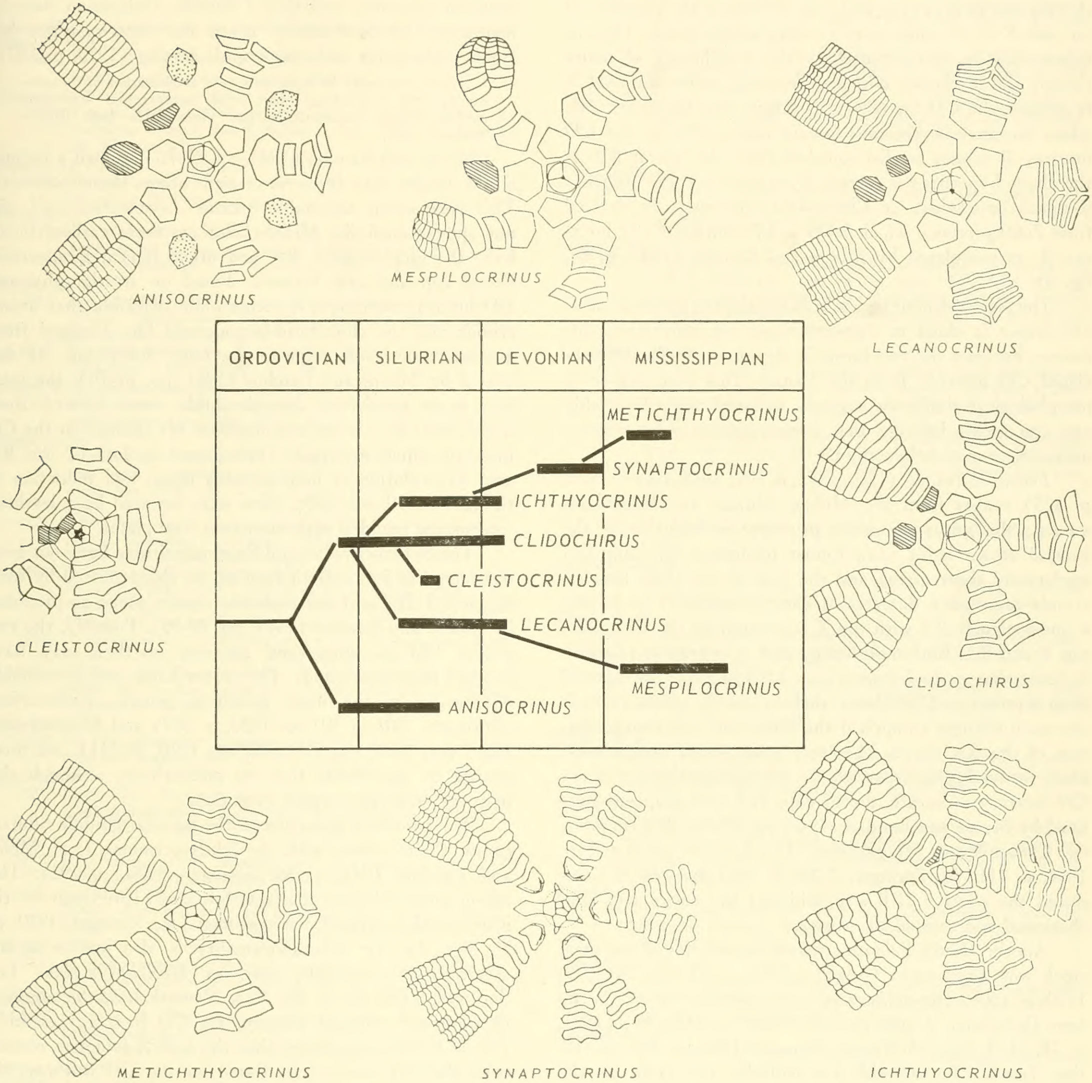

Text-figure 45. — Evolution of *Clidochirus* and its allies. Plate diagrams from Springer (1920). Ring denotes extent of proximal columnal. RA and X ruled. The iBrr of *Anisocrinus* stippled.

this feature as primitive and that it denotes the presence of an anal X in the immediate ancestry of the genus. This interpretation is substantiated by the morphology of many flexible and inadunate crinoids. Generally, when the anal X is present, the CD interray B is larger than the other BB; when the anal X becomes lost in most crinoids, the CD interray B cannot be distinguished from the lateral BB. If the above hypothesis is correct, *Synaptocrinus* was probably a direct descendent of *Clidochirus* and was not derived from *Ichthyocrinus,* which lacks a differentiated CD interray B, as postulated by Moore and Laudon (1943, p. 67, fig. 9).

The North American Early Mississippian genus *Metichthyocrinus* is allied to *Synaptocrinus;* the only basic difference between the two forms is the absence of a differentiated CD interray B in the former. This high degree of morphological similarity suggests evolutionary relationship and the writer believes that synaptocrinids were directly ancestral to metichthyocrinids.

Lecanocrinus, s.l. (Hall, 1852, p. 199; see Springer, 1920, p. 125) ranges from the Middle Silurian to Middle Devonian; the genus resembles primitive clidochirids in the general crown habit (*i.e.,* robust inadunate like cup and moderately short arms) and the lack of the iBrr. Lecanocrinids principally differ from early *Clidochirus* in having a quadrangular RA with the X supported by the CD interray B and RA. Both morphology and stratigraphic relations indicate that early *Lecanocrinus, s.l.* was probably derived from a primitive *Clidochirus,* such as the Girardeau crinoid; the main changes comprised the migration and transformation of the RA shape. The later lecanocrinid genera most likely evolved from *Lecanocrinus, s.l.* through changes in the CD interray structure, dorsal cup, and arm shape as outlined by Moore and Laudon (1943, pp. 67-76). For example, the Carboniferous *Mespilocrinus* (de Koninck and Le Hon, 1854, p. 111; see Springer, 1920, p. 190) lost the RA, reduced the relative IBB size, widened the dorsal cup, and shortened and twisted the arms.

Another Early Paleozoic major sagenocrinitid ancestral stock was *Anisocrinus* (Angelin, 1878, p. 13; see Springer, 1920, p. 160). The oldest and most primitive species is the Late Ordovician *A. oswegoensis* (Miller and Gurley) (1894, p. 33, pl. 3, figs. 15-17; see Springer, 1920, p. 164, pl. 10, figs. 7a-c). This crinoid is essentially the same as the Girardeau *Clidochirus,* except that small iBr1 and iBr2 are present. Middle Silurian anisocrinids greatly increased the height and width of the iBr1. The similar stratigraphic positions and morphological resemblance between *Anisocrinus oswegoensis* and *Clidochirus serrulatus* denote relationship and both are believed to have descended from a common ancestor, probably a Middle Ordovician dicyclic inadunate. Springer clearly noted the close relations between clidochirids and anisocrinids stating (1920, p. 160):

> *Anisocrinus* may be described as a combination of *Lecanocrinus* and *Clidochirus* with solid interbrachial structures added. (Both lecanocrinids and clidochirids lack iBrr — author's note.)

Moore and Laudon (1943, pp. 67-76) implied a lecanocrinid origin for *Anisocrinus* and other Homalocrinidae. This view seems untenable because *Lecanocrinus, s.l.* did not appear until the Middle Silurian; these earliest forms have the quadrangular RA and other typical lecanocrinid dorsal cup and arm features. Based on stratigraphy and CD interray structure, it seems more plausible that anisocrinids and the clidochirid-lecanocrinid line diverged from a common ancestor prior to the Late Ordovician. As discussed by Moore and Laudon (1943, pp. 67-76), the later and more specialized homalocrinids were derived from *Anisocrinus* by various combinations of: changes in the CD interray which eventually culminated in loss of the RA and X; evolution of heterotomous arms; and reduction in the iBrr size. Eventually, these were replaced by a leathery integument studded with numerous tiny plates.

The Synerocrinidae and Sagenocrinitidae have not been considered in detail. Both families are characterized by well-developed iBrr and are probably closely allied as proposed by Moore and Laudon (1943, pp. 67-76). Possibly, the two groups had an anisocrinid ancestor or they may have evolved from taxocrinids. The crown habit and presumably adaptation of the most primitive genera, *Temnocrinus* (Springer, 1902, p. 94; see 1920, p. 207) and *Meristocrinus* (Springer, 1906, pp. 515, 519; see 1920, p. 211), are more similar to taxocrinids than to anisocrinids, although this may represent convergent evolution.

Most workers have placed the peculiar Middle Silurian genus, *Cleistocrinus,* with the Ichthyocrinidae (*e.g.,* Moore and Laudon, 1943, p. 76; Springer, 1920, p. 292). This seems correct despite the fact that small iBrr occur on the inside of the calyx of one specimen (see Springer, 1920, pl. 38, figs. 1a, d); this abnormality is also known in undoubted ichthyocrinids, such as *Metichthyocrinus* (see Springer, 1920, pl. 39, fig. 9b). Nevertheless, the origin of *Cleistocrinus* remains obscure. Its CD interray resembles that of *Clidochirus* except that the anal X is not in contact with the CD interray B. Based on the CD interray, the writer postulates clidochirid ancestry. As pointed out by Springer (1920, pp. 292, 293), *Cleistocrinus* was highly specialized because the IBB were lost by resorption and the BB and RR are completely covered by the proximal columnal. This specialization, at least partially, represented the normal ichthyocrinid tendency to reduce the dorsal cup.

REFERENCES

Allee, W. C., Emerson, A. E., Park, Orlando, Park, Thomas, and Schmidt, K. P.

1949. *Principles of animal ecology.* W. B. Saunders Co., Philadelphia and London, pp. xii and 837.

Allen, J. R. L.

1968. *Current ripples, their relation to patterns of water and sediment motion.* North-Holland Publ. Co., Amsterdam, pp. xiii and 433.

Angelin, N. P.

1878. *Iconographia Crinoideorum in Stratis Suecia Siluricis Fossilium.* Holmiae, 62 pp, 29 pls.

Banse, K.

1964. *On the vertical distribution of zooplankton in the sea. In* Progress in Oceanography, Volume 2, edited by Mary Sears. Macmillan Co., New York, pp. 55-125.

Bassler, R. S.

1915. *Bibliographic index of American Ordovician and Silurian fossils.* United States Nat. Mus., Bull. 92, vols. 1 and 2, pp. vii and 1221, pls. 1, 2.

1938. *Fossilium Catalogus I: Animalia. Pars. 83: Pelmatozoa Palaeozoica.* Gravenhage, 194 pp.

Bassler, R. S. and Moodey, M. W.

1943. *Bibliographic and faunal index of Paleozoic Pelmatozoan echinoderms.* Geol. Soc. America, Spec. Paper 45, 734 pp.

Bather, F. A.

1892. *British fossil crinoids. VIII Cyathocrinus: C. acinotubus Ang. and C. vallatus sp. nov., Wenlock Limestone.* Ann. Mag. Nat. Hist., ser. 6, vol. 9, pp. 202-226, pl. 13, 7 text-figs.

1893. *The Crinoidea of Gotland, Part I. The Crinoidea Inadunata.* K. Svenska Vetenskaps - Akad. Handl., Bd. 25, No. 2, 199 pp., 10 pls., 20 text-figs.

1899a. *Review of Wachsmuth and Springer's monograph on crinoids. Fifth notice - The anal plates.* Geol. Mag., Dec. 4, vol. 6, pp. 31-44, 19 text-figs. *Sixth notice - The classification of camerate crinoids.* pp. 117-127.

1899b. *A phylogenetic classification of the Pelmatozoa.* Rept. British Assoc. Adv. Sci., 1898, pp. 916-923.

1900. *Chapter XI. The Crinoidea. In* A Treatise on Zoology, edited by E. Ray Lankester. Adam and Charles Black, London, pp. 94-204, 127 figs.

Bates, D. E.

1968. *On "Dendrocrinus" cambriensis Hicks, the earliest known crinoid.* Palaeont., vol. 11, pp. 406-409, pl. 76.

Biese, Walter

1927. *Ueber die Encriniten der Unteren Muschelkalkes von Mitteldeutschland.* Preuss. Geol. Landesanstalt, Abh., n.F., Heft 103, 119 pp., 4 pls., 6 text-figs.

Billings, E.

1857. *New species from Silurian rocks of Canada.* Canadian Geol. Sur., Rept. Progress 1853-1856, pp. 256-345.

1859. *Canadian organic remains Decade IV Crinoidea of the Lower Silurian rocks of Canada.* Geol. Sur. Canada, Decade IV, pp. vi and 7-66, 10 pls., 18 text-figs.

Billings, W. R.

1887. *A new genus and three new species of crinoids.* Ottawa Field Naturalist's Club, Trans., vol. 1, pp. 49-54, 1 pl.

Boolootian, R. A.

1966. *Chapter 25. Reproductive physiology. In* Physiology of Echinodermata, edited by R. A. Boolootian, Interscience Pub., New York, pp. 561-613, 37 text-figs.

Breimer, Albert

1962. *A monograph on Spanish Palaeozoic Crinoidea.* Eduard Ijdo N. V., Leiden, 189 pp., 16 pls.

1969. *A contribution to the paleoecology of Palaezoic stalked crinoids.* Koninklijke Neder. Akad. van Wetenschappen, ser. B., Proc., vol. 72, pp. 139-150.

Brower, J. C.

1965. *The genus Steganocrinus.* Jour. Paleont., vol. 39, pp. 773-793, pls. 91-94, 7 text-figs.

1966. *Functional morphology of Calceocrinidae with description of some new species.* Jour. Paleont., vol. 40, pp. 613-634, pl. 75, 2 text-figs.

1967. *The actinocrinitid genera Abactinocrinus, Aacocrinus and Blairocrinus.* Jour. Paleont., vol. 41, pp. 675-705, pls. 75-78, 9 text-figs.

1969. *Chapter 12. Crinoids. In* History of Redwall Limestone of Northern Arizona, edited by E. McKee and R. Gutschick, *et al.* Geol. Soc. America Mem., 114, pp. 475-542, pls. 64-67, text-figs. 79-86.

Cain, J. D. Blyth

1968. *Aspects of the depositional environment and palaeoecology of crinoidal limestones.* Scottish Jour. Geol., vol. 4, pp. 191-208, 1 pl., 5 text-figs.

Carpenter, P. H.

1884. *Report on the Crinoidea collected during the voyage of H.M.S. Challenger, during the years 1873-1876. Part I. General morphology, with descriptions of the stalked crinoids.* Challenger Rept., Zoology, vol. 11, pt. 26, xii and 442 pp., 62 pls., 21 text-figs.

Carpenter, W. B.

1866. *Researches on the structure, physiology, and development of Antedon (Comatula, Lamk.) rosaceus. — Part I.* Phil. Trans., Roy. Soc. London., vol. 156, pp. 671-756, pls. 31-43.

1876. *On the structure of Antedon rosaceus.* Roy. Soc. London, Proc., vol. 24, pp. 451-455.

1884. *On the nervous system of the Crinoidea.* Roy. Soc. London, Proc., vol. 37, pp. 67-76.

Chadwick, H. C.

1907. *Antedon.* Liverpool Mar. Biol. Comm., Mem. 15, 47 pp., 7 pls.

Christy, David

1848. *Letters on geology.* J. M. Christy, Printer, Rossville, U.S.A., pp. 72 and 11, Stratigraphic Sections, 5 pls.

Clark, A. H.

1915. *A monograph of the existing crinoids Volume I. The comatulids Part I.* United States Nat. Mus., Bull. 82, 406 pp., 17 pls., 602 figs.

1921. *A monograph of the existing crinoids Volume I. The comatulids Part 2.* United States Nat. Mus., Bull. 82, 795 pp., 57 pls., 1364 figs.

Clark, H. L.

1915. *The comatulids of Torres Strait: with special reference to their habits and reactions.* Dept. Marine Biol., Carnegie Inst., Washington, vol. 7, pp. 97-125.

Conrad, T.

1842. *Observations on the Silurian and Devonian Systems of the United States, with descriptions of new organic remains.* Acad. Nat. Sci. Philadelphia, Jour., vol. 8, pp. 228-280, pl. 15.

Cuénot, L.

1948. *Classe des Crinöides. In* Traité de Zoologie, edited by Pierre-P Grassé. Masson et Cie, Paris, pp. 31-74, text-figs. 38-98.

Cumings, E. R.

1908. *The stratigraphy and paleontology of the Ordovician rocks of Indiana. In* 32nd Ann. Rept., Geol. Sur. Indiana, pp. 605-1188, 55 pls., 16 text-figs., maps.

Ehrenberg, Kurt

1929. *Pelmatozoan root-forms (fixation).* American Mus. Nat. Hist., Bull., vol. 59, 76 pp., 42 text-figs.

Feder, H. M. and Christensen, A. M.

1966. *Chapter 5. Aspects of asteroid biology. In* Physiology of Echinodermata, edited by R. A. Boolootian. Interscience Pub., New York, pp. 87-127, 7 text-figs.

Fell, H. B.

1966. *Chapter 2. Ecology of crinoids. In* Physiology of Echinodermata, edited by R. A. Boolootian. Interscience Pub., New York, pp. 49-62.

Foerste, A. F.

1893. *The reproduction of arms in crinoids.* American Geol., vol. 12, pp. 270-271, 340, 1 text-fig. on p. 340.

1919. *Echinodermata of the Brassfield (Silurian) Formation of Ohio.* Bull. Scientific Lab., Denison Univ., vol. 19, pp. 3-31, 6 pls.

Gislén, Torsten

1924. *Echinoderm studies.* Zoologiska Bidrag från Uppsala, Bd. 9, Zoologische Beiträge aus Uppsala, 316 pp., 355 text-figs.

Goldring, Winifred

1923. *The Devonian crinoids of the State of New York.* New York St. Mus., Mem. 16, 670 pp., 60 pls., 63 figs.

Grabau, A. W. and Shimer, H. W.

1910. *North American index fossils. Volume II.* A. G. Seiler and Co., New York, pp. xiv and 909, 1937 text-figs.

Grant, Verne

1963. *The origin of adaptations.* Columbia Univ. Press, New York, viii and 606 pp., 103 text-figs.

Grave, B. H.

1934. *Further studies on the longevity and swimming ability of Spermatozoa.* Biol. Bull. Woods Hole Marine Biol. Lab., vol. 67, pp 513-518.

Hall, James

1847. *Palaeontology of New York. Volume I Containing descriptions of the organic remains of the Lower Division of the New York System.* C. Van Benthuysen, Albany, New York, xxiii and 339 pp., 87 pls.

1852. *Palaeontology of New York. Volume II Containing descriptions of the organic remains of the Lower Middle Division of the New York System.* C. Van Benthuysen, Albany, New York, vii and 362 pp., 83 pls.

1866. *Descriptions of new species of Crinoidea and other fossils from the Lower Silurian strata of the age of the Hudson River Group and Trenton Limestone.* Albany, New York, 17 pp., reprinted with plates, see Hall, 1872.

1867. *Descriptions of some new species of Crinoidea and other fossils from the Lower Silurian strata, principally of the Hudson River Group. In* New York St. Mus. Nat. Hist., 20th Ann. Rept., p. 304.

1868. *Descriptions of new or little-known species of fossils from rocks of the age of the Niagara Group. In* New York St. Mus. Nat. Hist., 20th Ann. Rept. (revised edition), pp. 347-438, pls. 10-25.

1872. *Description of new species of Crinoidea and other fossils from strata of the age of the Hudson River Group and Trenton Limestone. In* New York St. Mus. Nat. Hist., 24th Ann. Rept., pp. 205-224, pls. 5-8.

1879. *The fauna of the Niagara Group, in central Indiana. In* New York St. Mus. Nat. Hist., 28th Ann. Rept., pp. 99-203, pls. 3-34.

Hallam, A.

1967. *The interpretation of size-frequency distributions in molluscan death assemblages.* Palaeont., vol. 10, pp. 25-42, 11 text-figs.

Hicks, H.

1873. *On the Tremadoc rocks in the neighbourhood of St. David's, South Wales, and their fossil contents.* Quart. Jour. Soc., London, vol. 29, pp. 39-52, pls. 3-5.

Hudson, G. H.

1911. *Studies of some early Siluric Pelmatozoa. In* New York St. Mus., Bull. 148, pp. 195-272, 7 pls., 36 text-figs.

Hyman, L. H.

1955. *The Invertebrates: Echinodermata.* McGraw-Hill Book Co., New York, pp. vii and 763, 280 figs.

Jaekel, Otto

1895. *Beiträge zur Kenntnis der Palaeozoischen Crinoiden Deutsch-lands.* Palaeont. Abh., n. F., v. 3 (der Ganzen Reihe, Bd. 7), 116 pp., 10 pls., 29 text-figs.

1902. *Uber Verschiedene Wege Phylogenetischer Entwickelund.* Int. Zool. Cong. Berlin 1901, Verh. V., pp. 1058-1117, (60 pp.) 28 text-figs.

1918. *Phylogenie und System der Pelmatozoen.* Palaeontologischen Zeitschrift, Band III, Heft. 1, 128 pp., 114 figs.

Jeffords, R. M. and Miller, T. H.

1968. *Ontogenetic development in Late Pennsylvanian crinoid columnals and pleuricolumnals.* Univ. Kansas, Paleont. Contrib., Echinodermata, Art. 10, 18 pp., 4 pls., 5 text-figs.

Johnson, R. G.

1964. *The community approach to paleoecology. In* Approaches to Paleoecology, edited by John Imbrie and N. D. Newell, John Wiley and Sons, Inc., New York, pp. 107-134.

Keyes, C. R.

1894. *Paleontology of Missouri, Part 1.* Missouri Geol. Sur. vol. 4, 271 pp., 32 pls., 8 figs.

Kirk, Edwin

1911. *The structure and relationships of certain eleutherozoic Pelmatozoa.* United States Nat. Mus., Proc., vol. 41, 137 pp., 11 pls.

1929. *The status of the genus Mariacrinus Hall.* American Jour. Sci., vol. 18, pp. 337-346.

1945. *Four new genera of camerate crinoids from the Devonian.* American Jour. Sci., vol. 243, pp. 341-355.

Koenig, J. W.

1965. *Ontogeny of two Devonian crinoids.* Jour. Paleont., vol. 39, pp. 398-413, 6 text-figs.

Koenig, J. W. and Meyer, D. L.

1965. *Two new crinoids from the Devonian of New York.* Jour. Paleont., vol. 39, pp. 391-397, 4 text-figs.

Koninck, L. G. De and Le Hon, H. S.

1854. *Recherches sur les crinoïdes du Terrain Carbonifère de la Belgique.* Acad. Roy. Belgique, Mém., vol. 28, 217 pp., 8 pls.

Lane, N. G.

1963a. *Meristic variation in the dorsal cup of monobathrid camerate crinoids.* Jour. Paleont., vol. 37, pp. 917-930, 5 text-figs.

1963b. *The Berkeley crinoid collection from Crawfordsville, Indiana.* Jour. Paleont., vol. 37, pp. 1001-1008, pl. 128, 2 text-figs.

1968. *The adaptive significance of balance in Paleozoic stalked crinoids* (abstract). Geol. Soc. America, Abstract Volume for 1968, p. 169.

Lane, N. G. and Webster, G. D.

1966. *New Permian crinoid fauna from southern Nevada.* Univ. California Pub. Geol. Sci., vol. 63, 60 pp., 13 pls., 19 text-figs.

Laudon, L. R.

1933. *The stratigraphy and paleontology of the Gilmore City Formation of Iowa.* Univ. Iowa, Stud. Nat. Hist., vol. 15, No. 2, 74 pp., 7 pls., 7 text-figs.

1967. *Ontogeny of the Mississippian crinoid Platycrinites bozemanensis (Miller & Gurley), 1897.* Jour. Paleont., vol. 41, pp. 1492-1497, pls. 193, 194, 7 text-figs.

Laudon, L. R. and Beane, B. H.

1937. *The crinoid fauna of the Hampton Formation at LeGrand, Iowa.* Univ. Iowa, Stud. Nat. Hist., vol. 17, No. 6, pp. 225-272, pls. 15-19, 7 text-figs.

Lesley, J. P.

1889. *A dictionary of the fossils of Pennsylvania and neighboring states.* Geol. Sur. Pennsylvania, Rept. Prog. 2, xiv and 1283 pp., text-figs.

Linck, O.

1954. *Die Muschelkalkseelilie Encrinus lilliiformis.* Ergebnisse einer Grabung. Aus der Heimat, 62, H. 11/12 Öhringen.

1965. *Stratigraphische, Stratinomische und Ökologische Betrachtungen zu Encrinus liliiformis Lamarck.* Jb. Geol. Landesanst. Baden-Württ. 7, pp. 123-148, Freiburg i. Br.

Macurda, D. B., Jr.

1966. *The ontogeny of the Mississippian blastoid Orophocrinus.* Jour. Paleont., vol. 40, pp. 92-124, pls. 11-13, 10 text-figs.

1968. *Ontogeny of the crinoid Eucalyptocrinites.* Jour. Paleont., vol. 42, No. 5, pt. 2, pp. 99-118, 10 text-figs.

Magnus, D. B. E.

1967. *Ecological and ethological studies and experiments on the echinoderms of the Red Sea.* Stud. Trop. Oceanogr. Miami, vol. 5, pp. 635-664.

Martin, J. A., Knight, R. D., and Hayes, W. C.

1961. *Ordovician System. In* The Stratigraphic Succession in Missouri, edited by W. B. Howe and J. W. Koenig. Missouri Geol. Sur. and Water Resources, vol. 40, 2d ser., pp. 20-32.

Martin, J. A., Larsen, K. G., and Muilenburg, G. A.

1961. *Silurian System. In* The Stratigraphic Succession in Missouri, edited by W. B. Howe and J. W. Koenig. Missouri Geol. Sur. and Water Resources, vol. 40, 2d ser., pp. 32-35.

McCoy, Frederick

1850. *Contributions to British palaeontology, Chapter 7, Silurian Radiata.* Ann. Mag. Nat. Hist., 2d ser., vol. 6, pp. 270-289.

Meek, F. B.

1871. *Article 37. On some new Silurian crinoids and shells.* American Jour. Sci., ser. 3, vol. 2, pp. 295-302.

1872. *Descriptions of new western Palaeozoic fossils, mainly from the Cincinnati Group of the Lower Silurian Series of Ohio.* Acad. Nat. Sci. Philadelphia, Proc. 1871, pp. 308-336.

1873. *Fossils of the Cincinnati Group.* Geol. Sur., Ohio, vol. 1, pt. II, Palaeont., 175 pp., pls. 1-14, 3bis.

Meek, F. B. and Worthen, A. H.

1868. *Fossils of the Cincinnati Group. In* Illinois Geol. Sur., vol. 3, pp. 324-343, pl. 4, 4 text-figs.

1869. *Descriptions of new Crinoidea and Echinoidea from the Carboniferous rocks of the western states, with a note on the genus Onychaster.* Acad. Nat. Sci. Philadelphia, Proc. 1869, pp. 67-83.

1870. *Descriptions of new species and genera of fossils from the Palaeozoic rocks of the western states.* Acad. Nat. Sci. Philadelphia, Proc. 1870, pp. 22-56.

Menzel, D. W.

1967. *Particulate organic carbon in the deep sea.* Deep-Sea Res., vol. 14, pp. 229-238.

Menzel, D. W. and Goering, J. J.

1966. *The distribution of organic detritus in the ocean.* Limnol. and Oceanog., vol. 11, pp. 333-337.

Meyer, D. L.

1965. *Plate growth in some platycrinid crinoids.* Jour. Paleont., vol. 39, pp. 1207-1209, 1 text-fig.

Miller, J. S.

1821. *A natural history of the Crinoidea or lilyshaped animals, with observations on the genera Asteria, Euryale, Comatula, and Marsupites,* Bristol, 150 pp., 50 pls.

Miller, S. A.

1880. *Description of four new species and a new variety of Silurian fossils.* Cincinnati Soc. Nat. Hist., Jour., vol. 3, pp. 232-236.

1881a. *Description of some new and remarkable crinoids and other fossils of the Hudson River Group and notice of Strotocrinus bloomfieldensis.* Cincinnati Soc. Nat. Hist., Jour., vol. 4, pp. 69-77, 1 pl.

1881b. *Subcarboniferous fossils from the Lake Valley mining district of New Mexico with descriptions of new species and description of new species of fossils from the Hudson River Group and remarks on others.* Cincinnati Soc. Nat. Hist., Jour., vol. 4, pp. 306-319, pls. 7, 8.

1882. *Description of two new genera, and eight new species of fossils from the Hudson River Group, with remarks on others.* Cincinnati Soc. Nat. Hist., Jour., vol. 5, pp. 34-44, 2 pls.

1883. *Glyptocrinus redefined and restricted, Gaurocrinus, Pycnocrinus and Compsocrinus established and two new species described.* Cincinnati Soc. Nat. Hist., Jour., vol. 6, pp. 217-235, pl. 11.

1889a. *North American geology and palaeontology.* Cincinnati, Ohio, 664 pp., 1191 figs.

1889b. *The structure, classification and arrangement of American Palaeozoic crinoids into families. In* 16th Ann. Rept. Indiana Geol. Sur., pp. 302-326.

1891, 1892. *Palaeontology. In* 17th Ann. Rept. Geol. Sur., Indiana, 103 pp. (611-705), 20 pls. Advance publication 1891, report published 1892.

1892, 1894. *Palaeontology. In* 18th Ann. Rept. Geol. Sur., Indiana, 79 pp. (257-356), 12 pls. Advance Publication 1892, report published 1894.

Miller, S. A. and Gurley, W. F. E.

1894. *Upper Devonian and Niagara crinoids.* Illinois St. Mus. Nat. Hist., Bull. 4, 37 pp., 3 pls.

1897. *New species of crinoids, cephalopods and other Palaeozoic fossils.* Illinois St. Mus. Nat. Hist., Bull. 12, 59 pp., 5 pls.

Moore, A. R.

1924. *The nervous mechanism of coordination in the crinoid Antedon rosaceus.* Jour. Gen. Physiol., vol. 6, pp. 281-288.

Moore, H. B.

1934. *A comparison of the biology of Echinus esculentus in different habitats, Part I.* Mar. Biol. Ass., United Kingdom, Jour., vol. 19, pp. 869-886.

1935. *A comparison of the biology of Echinus esculentus in different habitats, Part II.* Mar. Biol. Ass., United Kingdom, Jour., vol. 20, pp. 109-128, 10 text-figs.

1966. *Chapter 4. Ecology of echinoids. In* Physiology of Echinodermata, edited by R. A. Boolootian. Interscience Pub., New York, pp. 73-85.

Moore, R. C.

1940a. *Relationships of the family Allagecrinidae, with description of new species from Pennsylvanian rocks of Oklahoma and New Mexico.* Denison Univ., Jour. Sci. Lab., Bull., vol. 34, pp. 55-127, pls. 2, 3, 14 text-figs.

1940b. *Early growth stages of Carboniferous microcrinoids and blastoids.* Jour. Paleont., vol. 14, pp. 572-583, 3 text-figs.

1948. *Evolution of the Crinoidea in relation to major paleogeographic changes in earth history.* 18th Internat. Geol. Cong., Great Britain, Rept. 1948, pt. 12, pp. 27-53, 18 text-figs.

1952a. *Crinoids. In* Invertebrate Fossils, by R. C. Moore, C. G. Lalicker, and A. G. Fischer, McGraw-Hill, New York, pp. 604-652, 34 text-figs.

1952b. *Evolution rates among crinoids.* Jour. Paleont., vol. 26, pp. 338-352, 13 text-figs.

1962. *Ray structure of some inadunate crinoids.* Univ. Kansas, Paleont., Contrib., Echinodermata, Art. 5, 47 pp., 4 pls., 17 text-figs.

Moore, R. C. and Ewers, J. D.

1942. *A new species of Synbathocrinus from Mississippian rocks of Texas, with description of ontogeny.* Bull. Denison Univ., Jour. Sci., Lab., vol. 37, pp. 92-106, 27 text-figs.

Moore, R. C. and Jeffords, R. M.

1968. *Classification and nomenclature of fossil crinoids based on studies of dissociated parts of their columns.* Univ. Kansas, Paleont. Contrib., Echinodermata, Art. 9, 86 pp., 28 pls., 6 text-figs.

Moore, R. C. and Laudon, L. R.

1943. *Evolution and classification of Paleozoic crinoids.* Geol. Soc. America. Spec. Paper 46, 167 pp., 14 pls.

1944. *Class Crinoidea. In* Index Fossils of North America, edited by H. W. Shimer and R. R. Shrock. Massachusetts Institute of Technology Press, New York, pp. 137-209, pls. 52-79.

Moore, R. C. and Miller, T. H.

1968. *Morphological features of crinoid columns.* Univ. Kansas, Paleont. Contrib., Echinodermata, Art. 8, 30 pp., 4 pls., 5 text-figs.

Müller, J.

1855. *In* Zeiller, F. and P. W. Wirtgen, *Bemerkungen über die Petrefacten der älteren Devonischen Gebirge vom Rheine, Insbesondere über die in der Umgegend von Goblenz Vorkommenden Arten.* Verh. Nat. Hist. Ver. Preuss., Rheinlande und Westphalen., pp. 1-28, 79-85, pls. 1-9a, 10-12.

Nichols, David

1960. *The histology and activities of the tube-feet of Antedon bifida.* Quart. Jour. Microscopical Sci., vol. 101, pt. 2, pp. 105-117, 8 figs.

1962. *Echinoderms.* Hutchinson Univ. Lib., London, 200 pp., 26 figs.

'Orbigny, Alcide, d

1849. *Prodrome de paléontologie stratigraphique universelle des Animaux Mollusques et Rayonnés.* Victor Masson, Paris, pp. lx and 394.

Paul, C. R. C.

1968. *Macrocystella Callaway, the earliest glyptocystitid cystoid.* Palaeont., vol. 11, pp. 580-600, pls. 111-113, 15 text-figs.

Phillips, John

1839. *Silurian Encrinites. In* The Silurian System, Part 2, by R. I. Murchison. London, pp. 670-675, pls. 17, 18.

Pryor, W. A. and Ross, C. A.

1962. *Geology of the Illinois parts of the Cairo, LaCenter, and Thebes quadrangles.* Illinois St. Geol. Sur. Circular 332, 39 pp., 2 pls.

Ramsbottom, W. H. C.

1961. *A monograph on British Ordovician Crinoidea.* Palaeontographical Society Monograph, vol. for 1960, 36 pp., 8 pls.

Raup, D. M.

1966. *Chapter 16. The Endoskeleton. In* Physiology of Echinodermata, edited by R. A. Boolootian. Interscience Pub., New York, pp. 379-395, 6 text-figs.

Regnéll, G.

1959. *Données concernant le développement ontogénétique des Pelmatozoaires du Paléozoïque (Échinodermes).* Soc. Géol. France, Bull. 7 sér., t. 1, 1959, pp. 773-783, 6 text-figs.

Ringueberg, E. N. S.

1882. *Description of two new species of crinoids from the shales of the Niagara Group, at Lockport, New York.* Cincinnati Soc. Nat. Hist., Jour., vol. 5, pp. 119-121, pl. 5, figs. 3, 4.

1888. *Some new species of fossils from the Niagara Shales of western New York.* Acad. Nat. Sci. Philadelphia, Proc. 1888, pp. 131-136, pl. 7.

1890. *The Crinoidea of the Lower Niagara Limestone at Lockport, New York, with new species.* New York Acad. Sci., Ann., vol. 5, pp. 301-306, pl. 3.

Rouse, Hunter

1961. *Fluid mechanics for hydraulic engineers.* Dover Publ. Inc., New York, pp. xvi and 422, 245 figs.

Rowley, R. R.

1904. *The Echinodermata of the Missouri Silurian and a new brachiopod.* American Geol., vol. 34, pp. 269-282, pl. 16.

Satterfield, I. R.

1971. *Conodonts and stratigraphy of the Girardeau Limestone (Ordovician) of southeast Missouri and southwest Illinois.* Jour. Paleont., vol. 45, pp. 265-273, pl. 34, 3 text-figs.

Savage, T. E.

1908. *On the Lower Paleozoic stratigraphy of southwestern Illinois.* American Jour. Sci., 4th ser., vol. 25, pp. 431-443.

1917a. *Stratigraphy and paleontology of the Alexandrian Series in Illinois. Part I. In* Illinois St. Geol. Sur. Bull. No. 23, pp. 67-160, pls. 3-9.

1917b. *The Thebes Sandstone and Orchard Creek Shale and their faunas in Illinois.* Illinois Acad. Sci., Trans., vol. 10, pp. 261-275, 2 pls.

Schmidt, W. E.

1930. *Die Echinodermen des Deutschen Unterkarbons.* Preuss. Geol. Landesanstalt, Abh., n.F., Heft 122, pt. 1, 92 pp., 3 pls., 20 text-figs.

1934. *Die Crinoideen des Rheinischen Devons, I Teil: Die Crinoideen des Hunsrückschiefers.* Preuss. Geol. Landesanstalt, Abh.. n.F., Heft 163, 149 pp., 34 pls., 29 figs.

1937. *Fósiles Paleozoicos de la Cordillera Oriental. In Estudios Geológicos y Paleontológicos sobre la Cordillera Oriental de Colombia.* República de Columbia, Ministerio de Industrias y Trabajo, Dept. Minas y Petróleos, 6 pp., 2 pls.

1941. *Die Crinoideen des Rheinischen Devons II Teil: A Nachtrag zu: Die Crinoideen des Hunsrückschiefers. B. Die Crinoideen des Unterdevons bis zur Cultrijugatus—Zone (mit Ausschluss des Hunsrückschiefers.* Reichsstelle für Bodenforschung Abh., n.F., Heft 182, 253 pp., 26 pls., 62 text-figs.

Seilacher, A., Drozdzewski, G., and Haude, R.

1968. *Form and function of the stem in a pseudoplanktonic crinoid (Seirocrinus).* Palaeont., vol. 11, p. 275-282, pl. 48, 3 text-figs.

Shumard, B. F.

1855. *Dr. Shumard's report. In* Missouri Geol. Sur. Ann. Rept. II, edited by G. C. Swallow, pp. 137-208, pls. A-C.

1866. *A catalogue of the Palaeozoic fossils of North America (Echinodermata).* St. Louis Acad. Sci.., Trans., vol. 2, pp. 334-407.

Sieverts, Hertha

1927. *Ueber die Crinoidengattung Marsupites.* Preuss. Geol. Landesanstalt, Abh., n.F., Heft. 108, 73 pp., 5 pls.

Simpson, G. G., Roe, Anne, and Lewontin, R. C.

1960. *Quantitative zoology.* Harcourt, Brace and Co., New York, vii and 440 pp., 64 text-figs.

Slocom, A. W.

1924. *Crinoid descriptions. In* New Echinoderms From the Maquoketa Beds of Fayette County, Iowa, by A. W. Slocom and A. F. Foerste. Iowa Geol. Sur., vol. 29, pp. 320-344, pls. 29, 30, text-figs. 55-58.

Sokal, R. R. and Sneath, P. H. A.

1963. *Principles of numerical taxonomy.* W. H. Freeman and Co., San Francisco and London, pp. x and 359.

Springer, Frank

1902. *On the crinoid genera Sagenocrinus, Forbesiocrinus, and allied forms.* American Geol., vol. 30, pp. 88-97.

1906. *Discovery of the disk of Onychocrinus and further remarks on the Flexibilia.* Jour. Geol., vol. 14, pp. 467-523, pls. 4-7.

1911. *On a Trenton echinoderm fauna at Kirkfield, Ontario.* Canada, Dept. of Mines, Geol. Sur. Branch, Mem. 15-P, 47 pp., 5 pls., 3 text-figs.

1913. *Chapters on Blastoids and Crinoids. In* Zittel-Eastman Textbook on Paleontology, translated and edited by C. R. Eastman, 2nd edition. Macmillan and Co., London, pp. 161-243, text-figs. 252-346.

1917. *On the crinoid genus Scyphocrinus and its bulbous root Camarocrinus.* Smithsonian Institution, Pub. 2440, 74 pp., 9 pls., 19 text-figs.

1920. *The Crinoidea Flexibilia.* Smithsonian Institution, Pub. 2501, 486 pp., pls. A-C, 1-76.

1926. *American Silurian crinoids.* Smithsonian Institution, Pub. 2871, pp. 1-143, 167-239, 33 pls.

1927. *Descriptions of new species of Crinoidea. In* Geology of Anticosti Island, by W. H. Twenhofel. Canadian Geol. Sur. Mem. 154, pp. 137, 138, pl. 4, figs. 3-6.

Strimple, H. W. and Koenig, J. W.

1956. *Mississippian microcrinoids from Oklahoma and New Mexico.* Jour. Paleont., vol. 30, pp. 1225-1247, 4 text-figs.

Strimple, H. W.

1963. *Crinoids of the Hunton Group.* Oklahoma Geol. Sur., Bull. 100, 169 pp., 12 pls., 30 text-figs.

Swan, E. F.

1966. *Chapter 17. Growth, autotomy, and regeneration. In* Physiology of Echinodermata, edited by R. A. Boolootian, Interscience Pub., New York, pp. 397-434.

Talbot, Mignon

1905. *Revision of the New York Helderbergian crinoids.* American Jour. Sci., 4th ser., vol. 20, pp. 17-34, 4 pls., 4 text-figs.

Teichert, Curt

1949. *Permian crinoid Calceolispongia.* Geol. Soc. America, Mem. 34, 132 pp., 26 pls., 24 text-figs.

Templeton, J. S. and Willman, H. B.

1963. *Champlainian Series (Middle Ordovician) in Illinois.* Illinois St. Geol. Sur. Bull. 89, 260 pp.

Termier, Henri and Termier, Geneviève

1949. *Hiérarchie et corrélations des charactères chez les crinoïdes fossiles.* Serv. Carte Géol. l'Algérie, Bull., sér. 1, Paléont., No. 10, 90 pp., 8 pls.

Thomas, A. O.

1924. *Echinoderms of the Iowa Devonian.* Iowa Geol. Sur. Ann. Rept., vol. 29, pp. 387-550, pls. 35-54, text-figs. 60-80.

Thomas, A. O. and Ladd, H. S.

1926. *Additional cystoids and crinoids from the Maquoketa Shale of Iowa.* Univ. Iowa Studies, vol. 11, pp. 5-18, 6 pls.

Thompson, Sir Wyville

1865. *On the embryogeny of Antedon rosaceus (Comatula rosacea of Lamarck).* Phil. Trans., Roy. Soc. London, vol. 155, pp. 513-544, pls. 23-27.

Ubaghs, Georges

1953. *Classe des Crinoïdes. In* Traité de Paléontologie, edited by Jean Piveteau, Masson et Cie, Paris, pp. 658-773, 166 figs.

1958. *Recherches sur les Crinoïdes Camerata du Silurian de Gotland (Suède) Partie III: Melocrinicae, avec des remarques sur l'évolution des Melocrinidae.* Arkiv f. Zoologi, K. Svenska Vetens.-Akad., ser. 2, Bd. 11, No. 16, pp. 259-306, 5 pls., 18 text-figs.

Ulrich, E. O.

1926. *Relative values of criteria used in drawing the Ordovician-Silurian boundary.* Geol. Soc. America Bull., vol. 37, pp. 279-348.

Van Sant, J. F. and Lane, N. G.

1964. *Crawfordsville (Indiana) crinoid studies.* Univ. Kansas Paleont. Contrib., Echinodermata, Art. 7, 136 pp., 8 pls., 41 text-figs.

Wachsmuth, C. and Springer, F.

1879. *Revision of the Palaeocrinoidea, Pt. 1.* Acad. Nat. Sci. Philadelphia, Proc. 1879, 153 pp., pls. 15-17.

1881. *Revision of the Palaeocrinoidea, Pt. 2.* Acad. Nat. Sci. Philadelphia, Proc. 1881, pp. 237 (178-411), pls. 17-19.

1885. *Revision of the Palaeocrinoidea, Pt. 3., sec. 1 and 2.* Acad. Nat. Sci. Philadelphia, Proc. 1885, pp. 334 (226-360, 64-227), pls. 4-9.

1889. *Cited as In Press Authors of Allocrinus and A. typus. In* North American Geology and Palaeontology, by S. A. Miller, Cincinnati, Ohio, p. 222.

1897. *The North American Crinoidea Camerata.* Mus. Comp. Zool., Mem., vols. 20, 21, 897 pp., 83 pls., 23 text-figs.

Walcott, C. D.

1884. *Descriptions of new species of fossils from the Trenton Group of New York. In* New York St. Mus. 35th Ann. Rept., pp. 207-214, pl. 17.

Wanner, Johannes

1916. *Die Permischen Echinodermen von Timor Teil I.* Paläont. von Timor, Lief. 6, Teil 11, 329 pp., pls. 96-114 (1-19), 88 text-figs.

Weller, J. M. and Ekblaw, G. F.

1940. *Preliminary geologic map of parts of the Alto Pass, Jonesboro, and Thebes quadrangles.* Illinois St. Geol. Sur., Rept. of Investigations, No. 70, 26 pp., 1 pl.

Weller, Stuart

1900. *The paleontology of the Niagaran Limestone in the Chicago area; The Crinoidea.* Chicago Acad. Sci. Nat. Hist. Sur., Bull. 4, pt. 1, 153 pp.

Wilson, A. E.

1946. *Echinodermata of the Ottawa Formation of the Ottawa-St. Lawrence Lowland.* Canada, Dept. of Mines and Res., Geol. Sur. Bull. 4, 61 pp., 6 pls., 2 text-figs.

Worthen, A. H.

1866. *Chapter 4. Devonian and Silurian Systems. In* Geol. Sur. Illinois vol. I - Geology, pp. 119-152.

Worthen, A. H. and Meek, F. B.

1875. *Palaeontology of Illinois, Section II. Descriptions of invertebrates. In* Illinois Geol. Sur., vol. 6, pp. 489-532, pls. 23-33, 3 text-figs.

Wright, James

1950-1954. *A monograph of the British Carboniferous Crinoidea, Volume I.* Palaeontographical Soc. Mono., xxx and 190 pp., 67 pls., 108 text-figs.

Zenker, J. C.

1833. *Organische Reste (Petrefacten) aus der Altenburger Braunkohlen - Formation, dem Blankenburger Quadersandstein und Böhmischen Übergangsgebirge.* Beitrage Natur. Urwelt, vii and 67 pp., 7 pls.

Zittel, K. A. von

1879. *Handbuch der Paläontologie, Vol. 1, Paläozoologie.* R. Olderbourg, Munchen and Leipzig, Abt. 1, 765 pp., 557 text-figs.

PLATES

EXPLANATION OF PLATE 59

Figure		*Page*
1, 2.	*Eopatelliocrinus scyphogracilis,* n. gen., n. sp.	333

Girardeau Limestone, Cape Rock exposure.
1. Paratype, USNM 164 542, lateral view of largest crown, "size" 9.6 mm, × 3.8.
2. Paratype, USNM 164 544, lateral view of "adult" assemblage crown, "size" 6.6 mm, × 5.3.

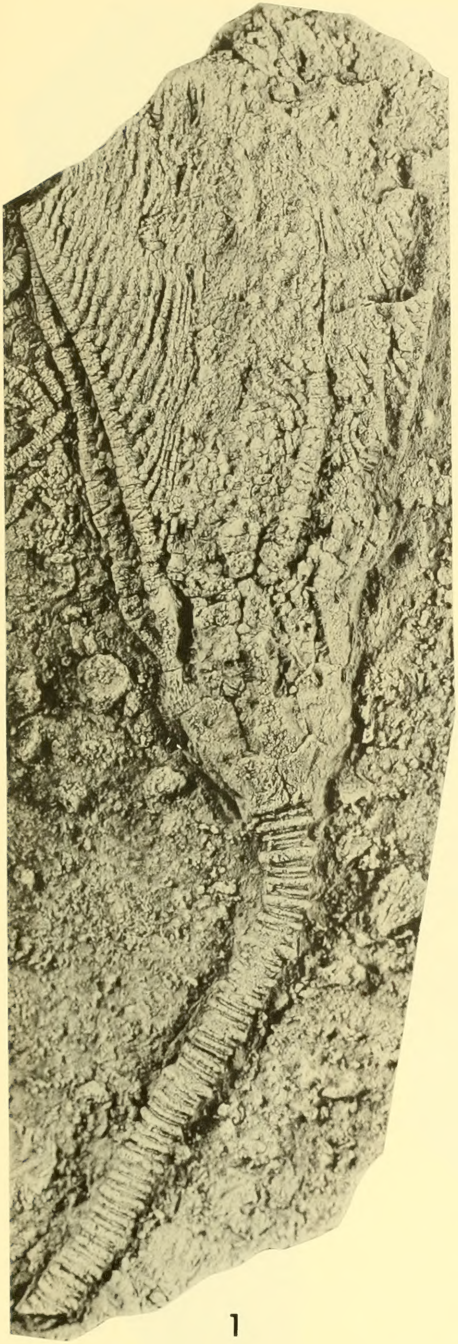

1

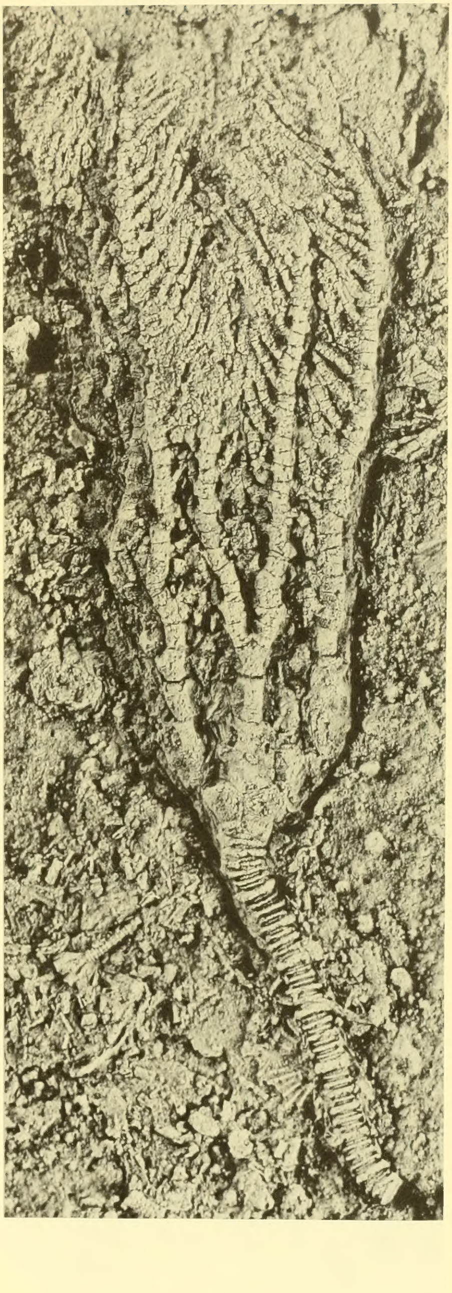

2

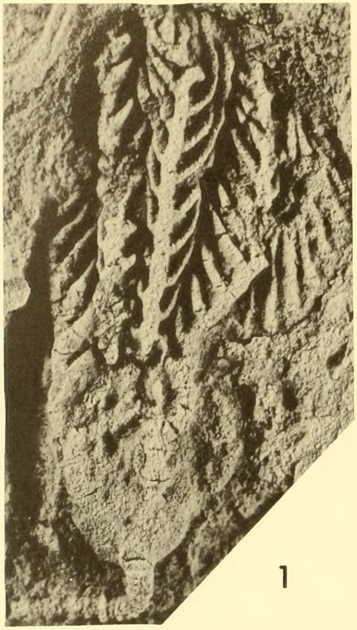
1

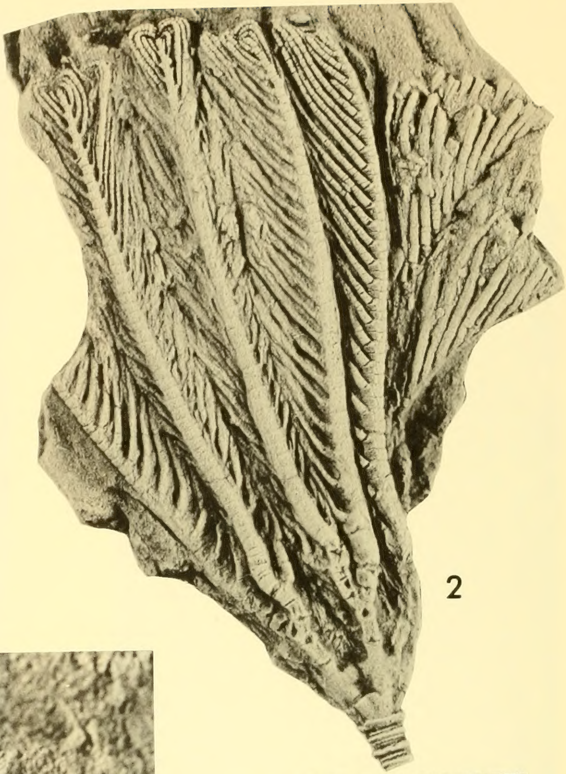
2

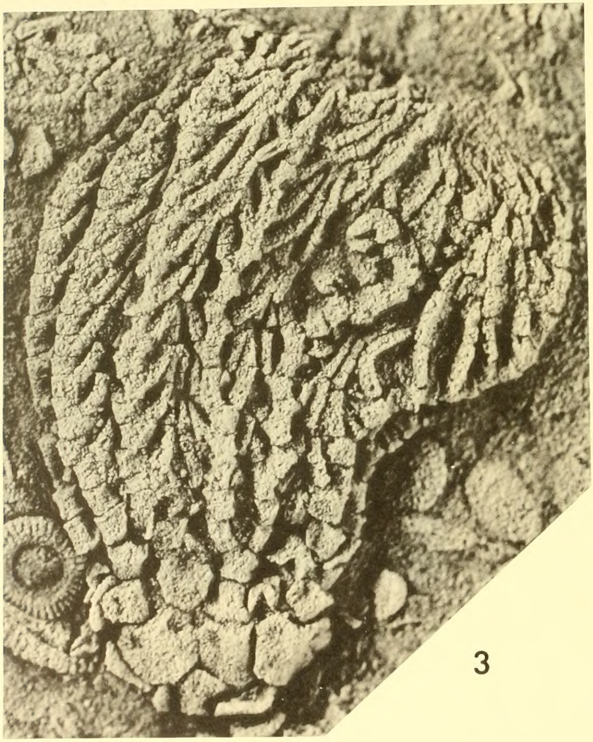
3

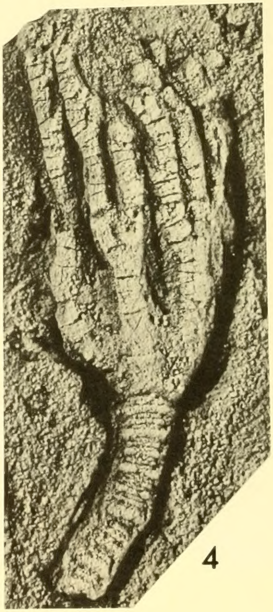
4

EXPLANATION OF PLATE 60

Figure		*Page*
1-4.	*Eopatelliocrinus scyphogracilis,* n. gen., n. sp.	333

Girardeau Limestone.
1. Paratype, USNM 164 549, lateral view of "young assemblage" crinoid, "size" 2.6 mm, × 11, from high density "young assemblage" garden, Orchard Creek exposure.
2. Holotype, USNM 164 541, lateral view of "adult assemblage" animal, "size" 4.8 mm, × 5.4, Cape Rock exposure.
3. Paratype, USNM 164 550, E ray view of "young assemblage" crown on slab with 1, "size" 2.5 mm, × 13.
4. Paratype, USNM 164 548, lateral view of "young assemblage" animal, "size" 2.6 mm, × 10, Cape Rock exposure.

EXPLANATION OF PLATE 61

Figure		*Page*
1-4.	*Eopatelliocrinus latibrachiatus,* n. gen., n. sp.	333

Girardeau Limestone.
1. Paratype, USNM 164 560, probably E ray of "adult assemblage crown, "size" 3.8 mm, × 7.9, from high density "young assemblage" garden, Cape Rock exposure.
2. Paratype, IGS. 35P-21, lateral view of "young assemblage" crown, "size" 1.8 mm, × 10, from high density "young assemblage" garden, Orchard Creek exposure.
3. Holotype, USNM 164 556, C ray of "adult assemblage" crown, "size" 4.0 mm, × 7.8, Cape Rock exposure.
4. Paratype, USNM 164 558, C ray of largest crown, "size" 5.0 mm, × 6.2, on same slab with 1.

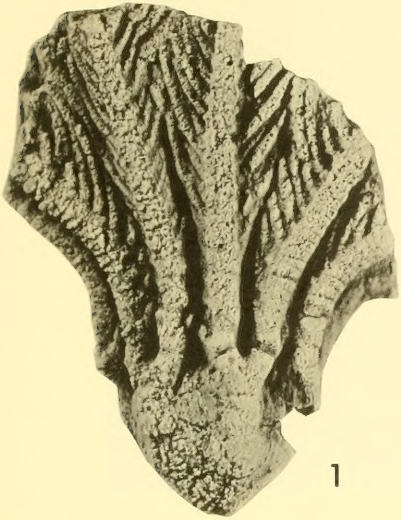

1

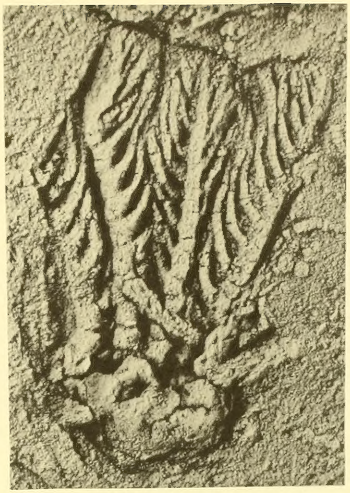

2

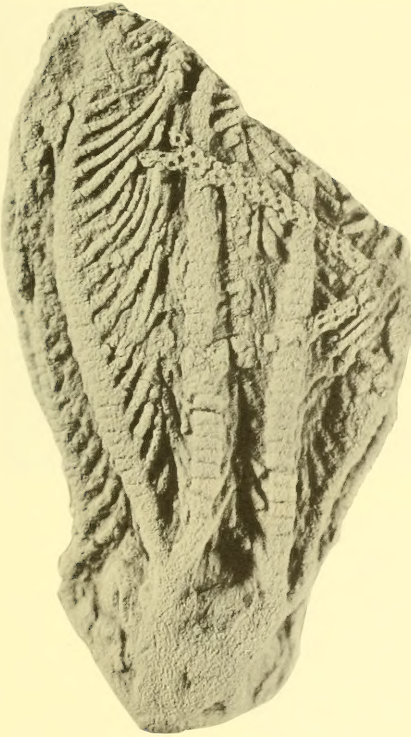

3

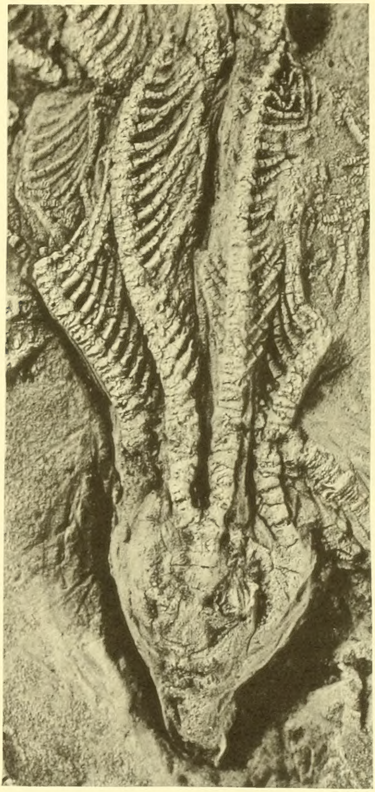

4

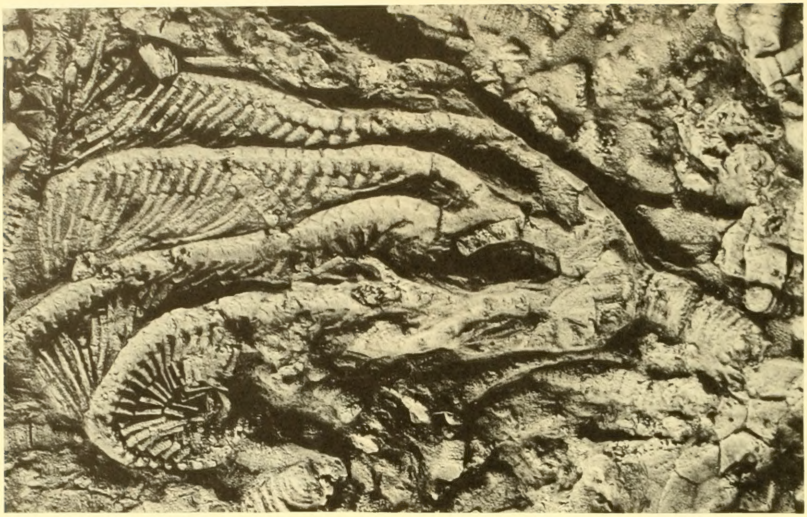

3

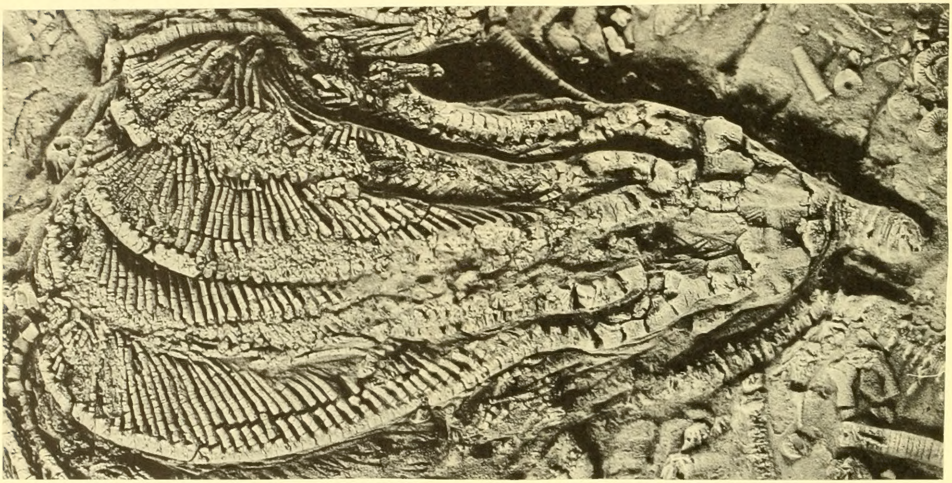

2

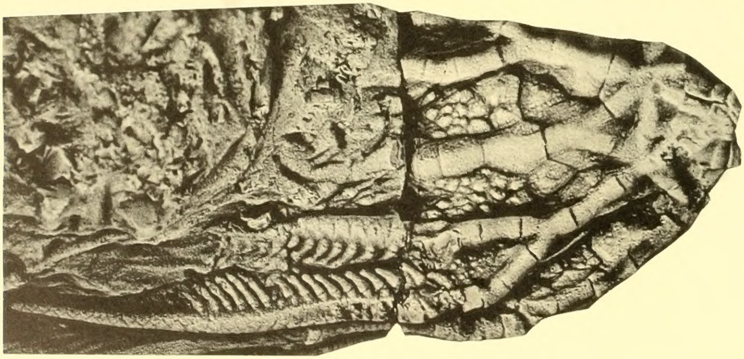

1

EXPLANATION OF PLATE 62

Figure *Page*

1-3. *Macrostylocrinus pristinus*, n. sp. 371

Girardeau Limestone, Orchard Creek exposure.
1. Paratype, USNM 164 568, CD interray of "adult assemblage" crown, "size" 9.2 mm, × 4.9.
2. Holotype, USNM 164 565, E ray? view of "adult assemblage" crown, "size" 7.3 mm, × 4.2, from high density "adult assemblage garden".
3. Paratype, USNM 164 570, E ray of "adult assemblage" crinoid, "size" 7.0 mm, × 5, from same slab as 2.

EXPLANATION OF PLATE 63

Figure		*Page*
1-4.	*Macrostylocrinus pristinus,* n. sp.	371

Girardeau Limestone.
1. Paratype, IGS. 35P-26, lateral view of "young assemblage" animal, "size" 1.7 mm, × 11, from high density "young assemblage" garden, Orchard Creek exposure.
2. Paratype, USNM 164 577, D ray view of "young assemblage" crinoid, "size" 2.4 mm, × 13, from high density "young assemblage" garden, Orchard Creek exposure.
3. Paratype, USNM 164 574, CD interray?, "transitional crinoid", "size" 4.4 mm, × 6, Cape Rock exposure.
4. Paratype, USNM 164 567, lateral view, "adult assemblage" crinoid, "size" 10.2 mm, × 4.6, Orchard Creek exposure.

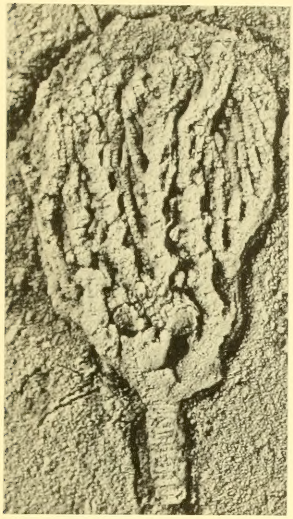
1

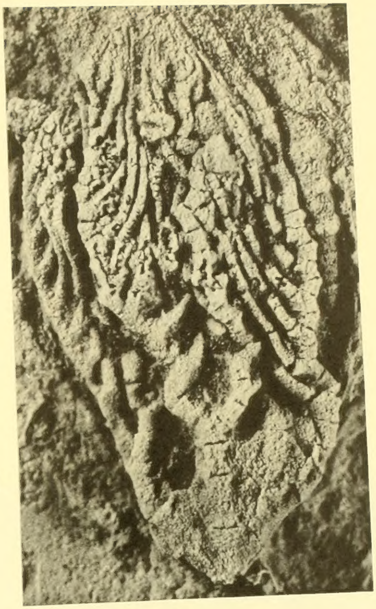
2

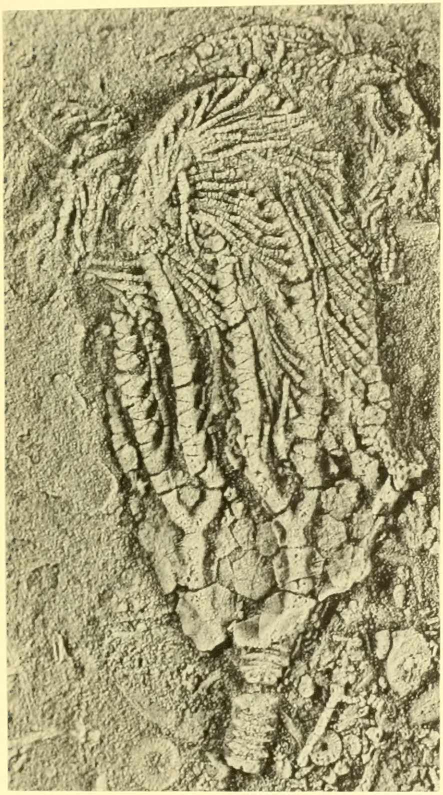
3

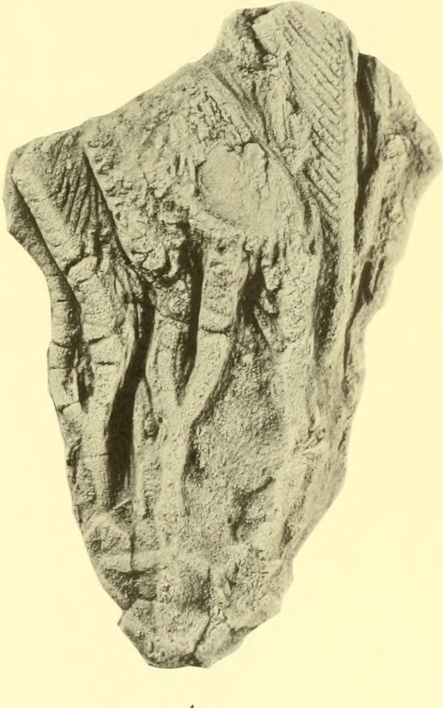
4

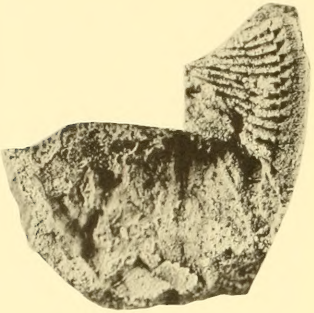

1

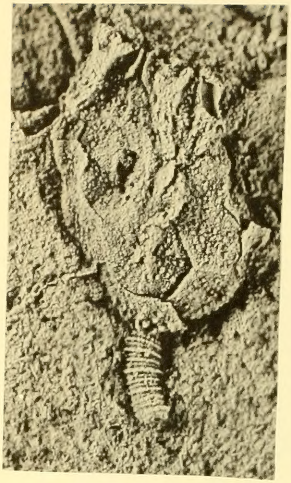

2

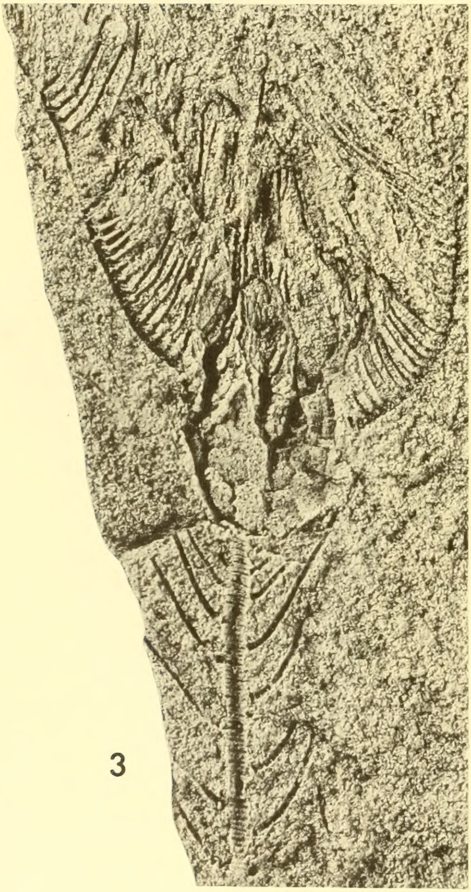

3

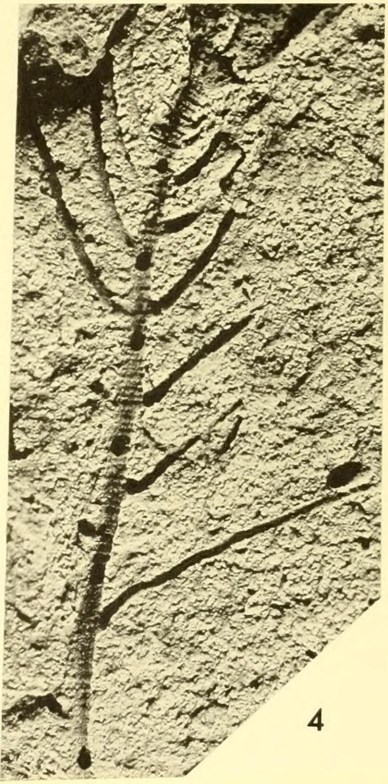

4

EXPLANATION OF PLATE 64

Figure		*Page*
1-4.	*Macrostylocrinus cirrifer* Ramsbottom	363

Ashgillian; Upper Drummock Group, "Starfish Bed"; Thraive Glen, 5 miles NE of Girvan, Scotland.

1. Figured specimen, HM. E. 3586, external mold of poorly preserved calyx with biserial arm, × 6.
2. Paratype, RSM. 1958.1.244, rubber squeeze of external mold, lateral view, "size" 5.8 mm, × 5.5.
3. Paratype, HM. E. 3599a, external mold of crown, lateral view, "size" 3.4 mm, × 5.
4. Figured specimen, HM. E. 3492a, external mold of stem and calyx, holes along axis of column represent cirri, × 8.

EXPLANATION OF PLATE 65

Figure		*Page*
1-7.	*Macrostylocrinus cirrifer* Ramsbottom	363

Ashgillian; Upper Drummock Group, "Starfish Bed"; Thraive Glen, 5 miles NE of Girvan, Scotland.

1-3. Holotype, HM. E. 3585a, internal mold of calyx, "size" 6.1 mm, × 7. 1. C ray twisted to show CD interray. 2. Tegmen, CD interray in base of photograph. 3. C ray oriented to show CD interray iBrr.

4. Paratype, HM. E. 3588, internal mold, base of calyx, × 6.

5, 6. Paratype, HM. E. 3584, internal mold of calyx, "size" 6.8 mm. 5. Lateral view, × 6. 6. Calyx base, × 8.

7. Figured specimen, HM. E. 3602, internal mold of crown, C ray, "size" 3.9 mm, × 6.2.

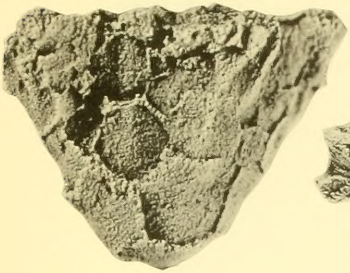

1

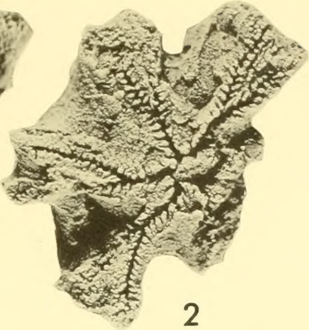

2

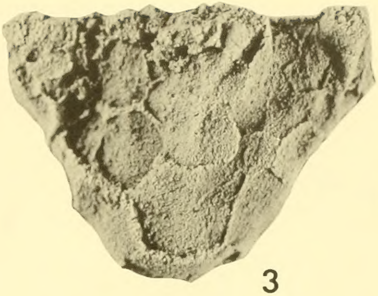

3

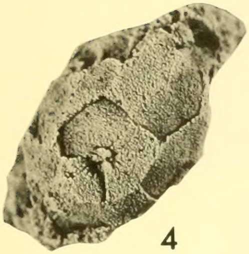

4

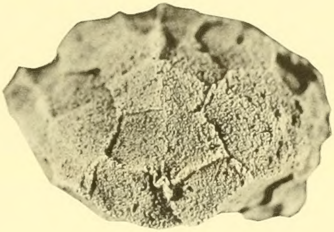

5

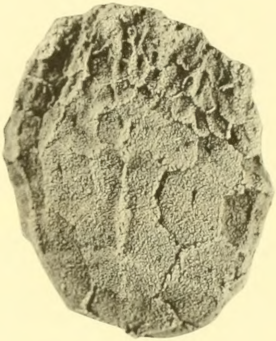

6

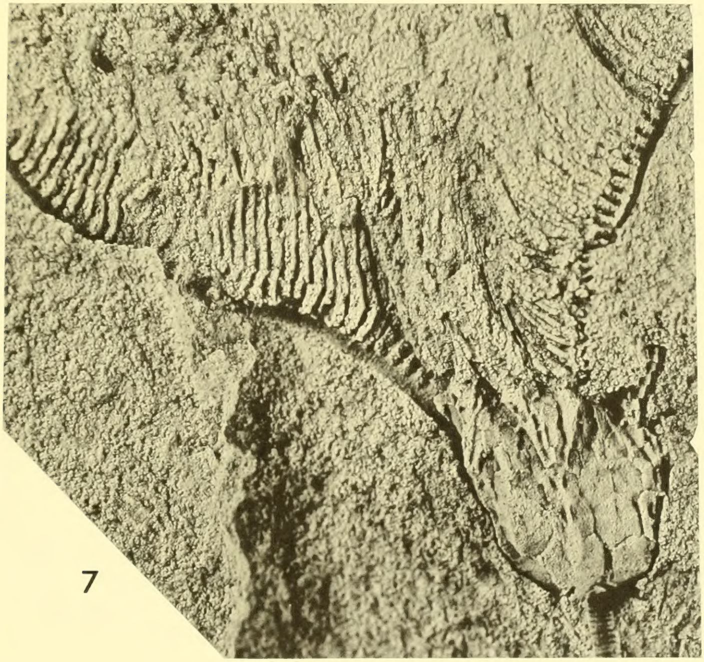

7

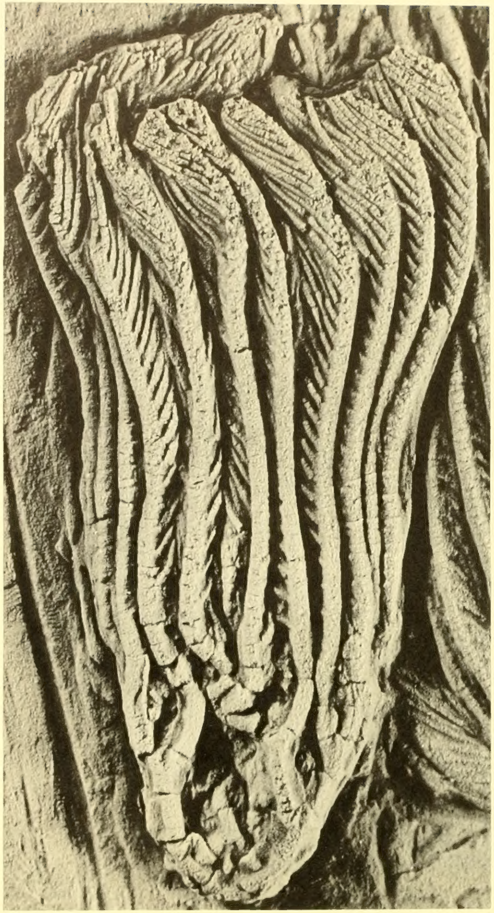

1

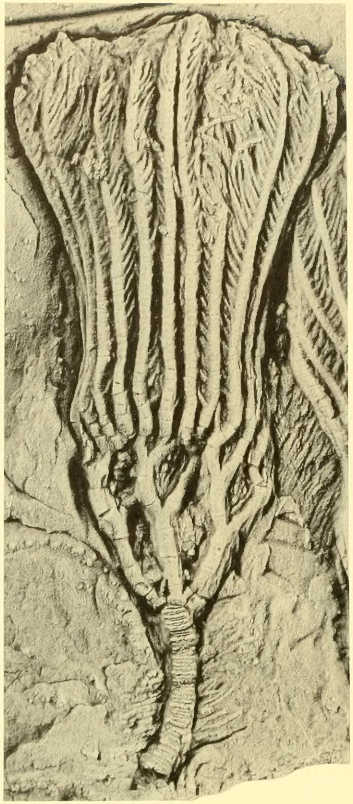

2

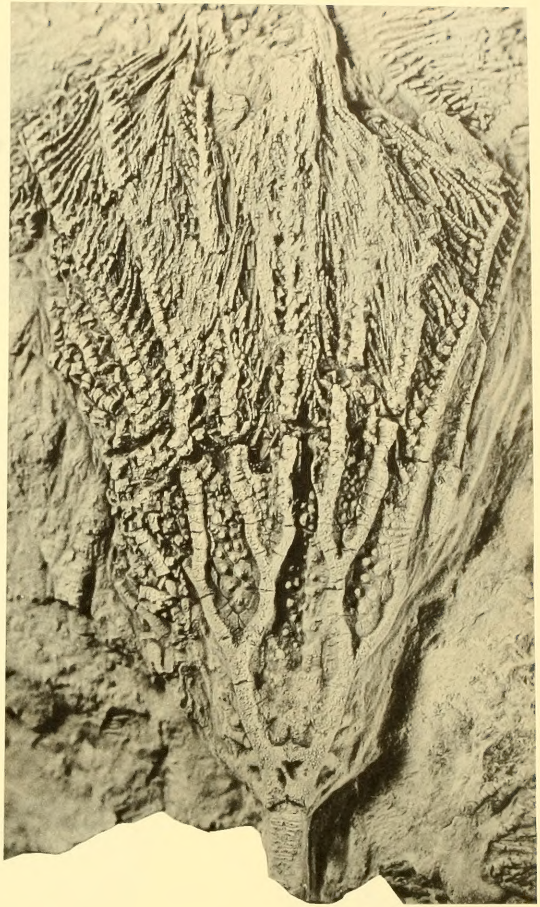

3

EXPLANATION OF PLATE 66

Figure *Page*

1-3. *Alisocrinus tetrarmatus*, n. sp. 408

Girardeau Limestone, Cape Rock exposure.
1. Paratype, YPM. 27029, CD interray, "adult assemblage" crinoid, with only three arms in the C ray, "size" 5.5 mm, × 5.5.
2. Paratype, YPM. 27028, lateral view, "adult assemblage" crown, "size" 6.4 mm, × 3.
3. Holotype, USNM 164 579, lateral view, "adult assemblage" crinoid, "size" 9.0 mm, × 3.6.

EXPLANATION OF PLATE 67

Figure *Page*

1-5. *Alisocrinus tetrarmatus,* n. sp. 408

Girardeau Limestone.

1. Paratype, IGS. 35P-36, C and D rays?, "young assemblage" crinoid with one three armed ray, "size" 2.0 mm, × 10, from "young assemblage" high density slab, Orchard Creek exposure.

2. Paratype, IGS. 35P-35, lateral or CD interray view of smallest "young assemblage" crinoid, "size" 1.1 mm, × 10, from same slab as 1.

3. Paratype, USNM 164 587, lateral view of "young assemblage" crown, "size" 3.4 mm, × 8.8, Cape Rock exposure.

4. Paratype, USNM 164 580, C ray of "adult assemblage" crinoid, "size" 4.2 mm, × 4.3, Orchard Creek exposure.

5. Paratype, Univ. Ill. X 4672, lateral view of "young assemblage" animal, "size" 2.4 mm, × 7.5, low density assemblage, Cape Rock exposure.

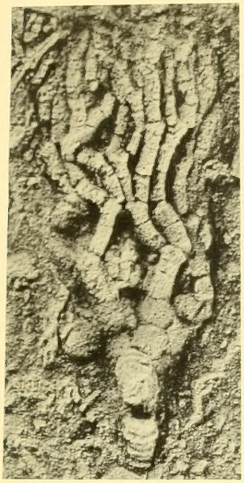

1

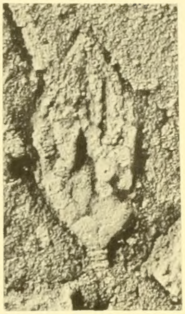

2

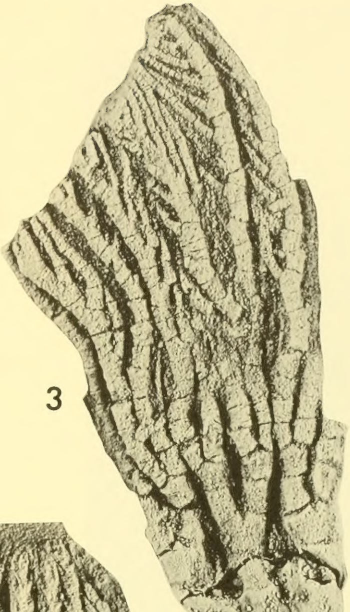

3

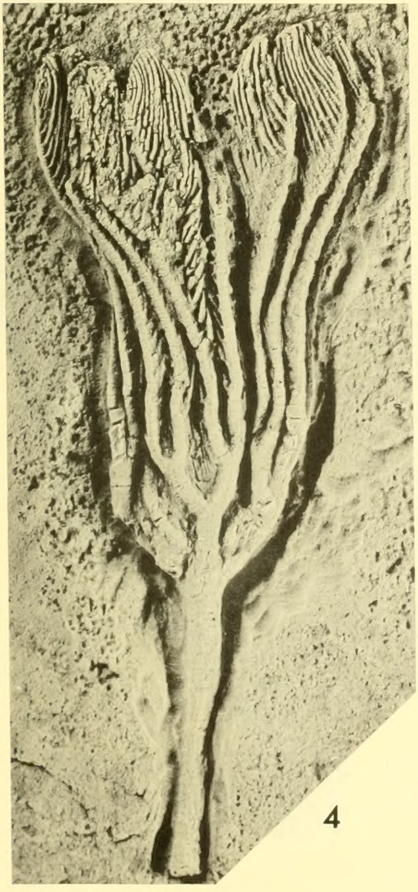

4

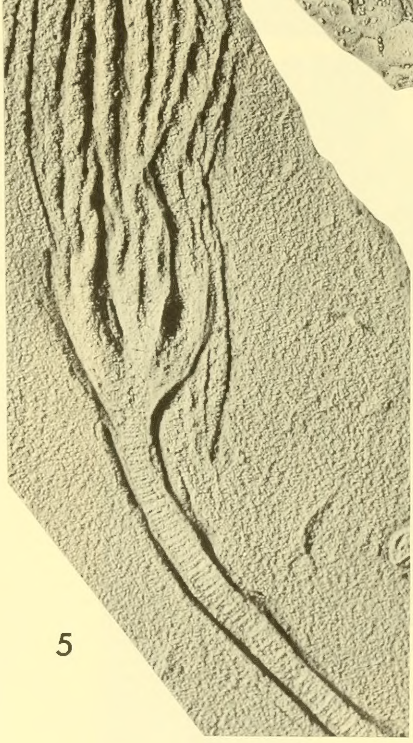

5

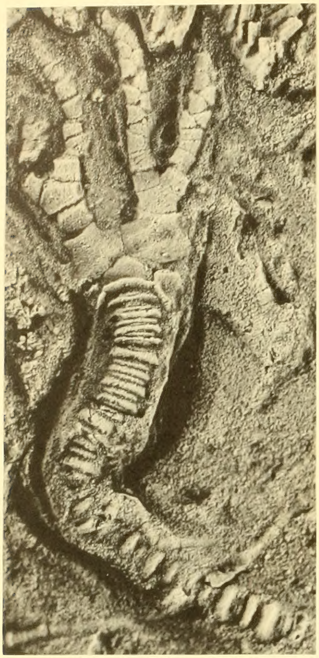
1

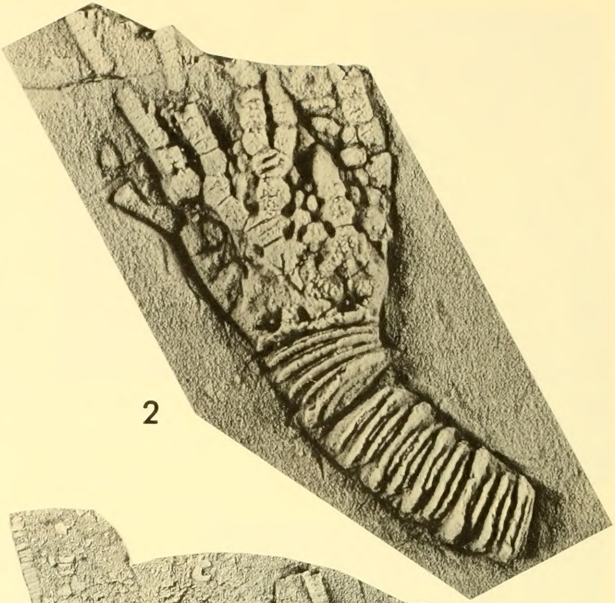
2

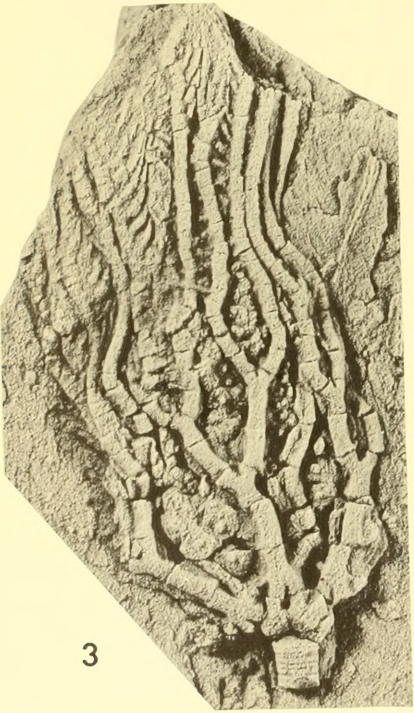
3

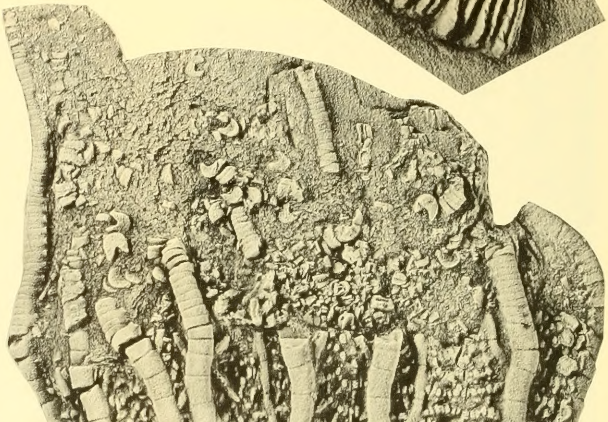
4

EXPLANATION OF PLATE 68

Girardeau Limestone camerates

Figure		*Page*
1.	*Culicocrinus? girardeauensis*, n. sp.	398
	Holotype, IGS. 8258, A and E rays?, "size" 2.6 mm, × 8.5, from high density "young assemblage" slab, Orchard Creek exposure.	
2, 4.	*Alisocrinus? heterodactylus*, n. sp.	437
	2. Paratype, USNM 164 590, D ray, "size" 4.2 mm, × 5.7, low density garden, Cape Rock exposure. 4. Holotype, USNM 164 589, lateral view, "size" 16.6 mm, × 2.2, Cape Rock exposure.	
3.	*Alisocrinus tetrarmatus*, n. sp.	408
	Paratype, USNM 164 581, D ray of "adult assemblage" crinoid, "size" 5.8 mm, × 5.1, Cape Rock exposure.	

EXPLANATION OF PLATE 69

Figure		*Page*
1, 2.	*Ptychocrinus fimbriatus* (Shumard)	446

Girardeau Limestone.

1. Figured specimen, USNM 165 071, lateral view of "adult assemblage" crown, "size" 8.5 mm, × 4.4, Orchard Creek exposure.
2. Figured specimen, USNM 164 611, CD interray of "adult assemblage" crown, "size" 6.9 mm, × 4.2, Cape Rock exposure.

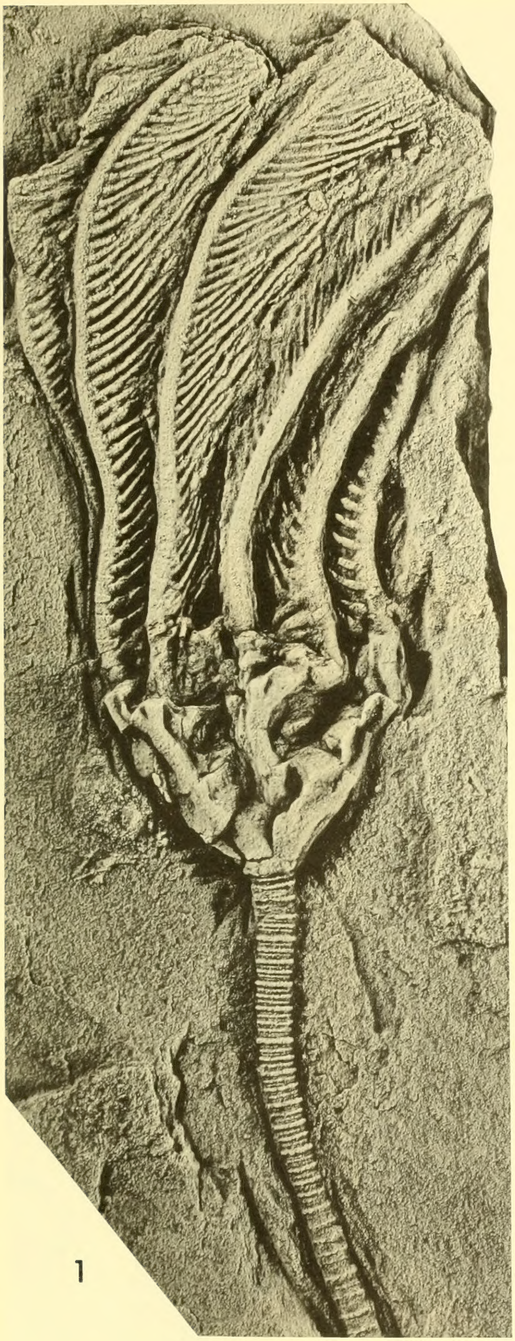

1

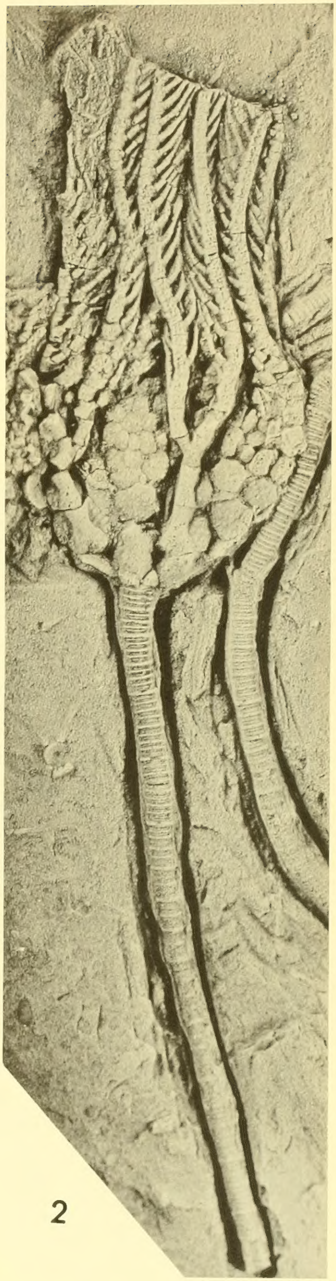

2

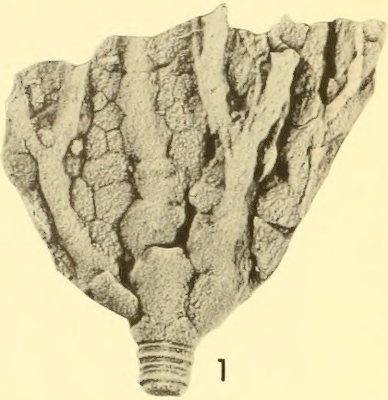
1

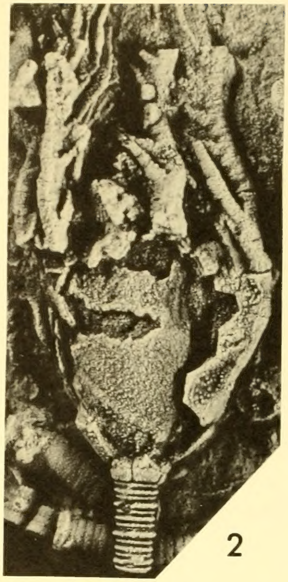
2

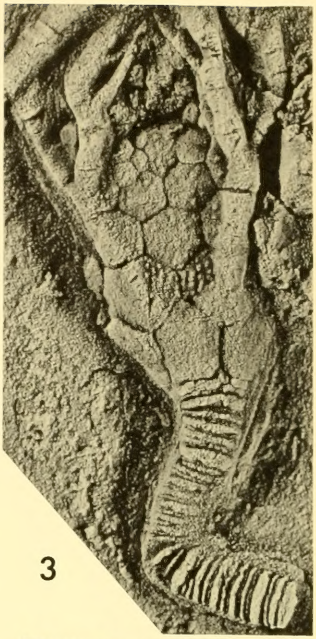
3

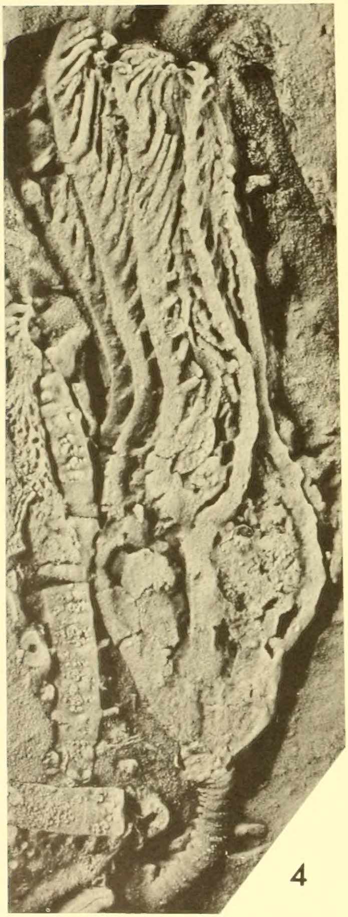
4

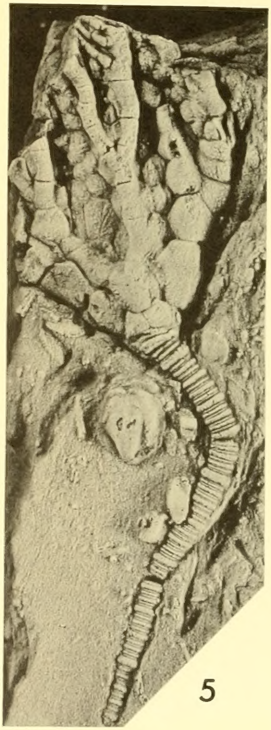
5

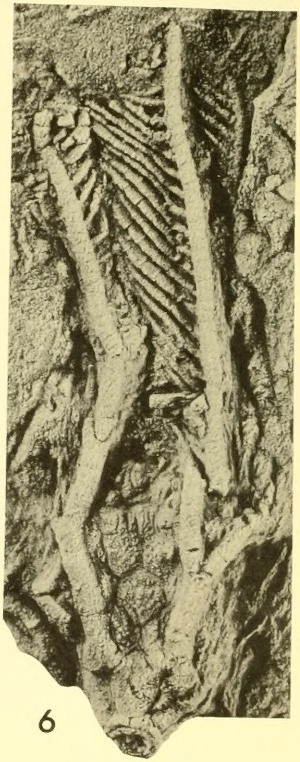
6

EXPLANATION OF PLATE 70

Figure		*Page*
1-6.	*Ptychocrinus fimbriatus* (Shumard)	446

Girardeau Limestone.
1. Figured specimen, USNM 164 609, CD interray of "adult assemblage" calyx, "size" 7.6 mm, × 5.4, Cape Rock exposure.
2. Figured specimen, USNM 165 073, lateral view showing convoluted organ, × 6, Orchard Creek exposure.
3. Figured specimen, IGS. 35P-56, lateral view of "adult assemblage" calyx, "size" 7.6 mm, × 6.3, Orchard Creek exposure.
4. Figured specimen, IGS. 35P-57, lateral view of "adult assemblage" crown, "size" 7.5 mm, × 6, Cape Rock exposure.
5. Figured specimen, USNM 164 610, D ray view of "adult assemblage" calyx, "size" 8.6 mm, × 4.1, Cape Rock exposure.
6. Figured specimen, USNM 164 606, lateral view of "adult assemblage" crown, "size" 7.1 mm, × 4.8, probably Cape Rock exposure.

EXPLANATION OF PLATE 71

Figure		*Page*
1-5.	*Ptychocrinus fimbriatus* (Shumard)	446

Girardeau Limestone.

1. Figured specimen, USNM 165 078, lateral view of "adult assemblage" calyx, × 5, from high density "adult assemblage" garden, Orchard Creek exposure.
2. Figured specimen, USNM 165 076, lateral view of "adult assemblage" calyx, "size" 8.2 mm, × 5.5, from same slab as 1.
3. Figured specimen, USNM 165 075, lateral view of "adult assemblage" crown, "size" 7.1 mm, × 6.3, from same slab as 1.
4. Figured specimen, USNM 165 077, lateral view of part of "adult assemblage" crown, "size" 10.8 mm, × 4.6, from same slab as 1.
5. Figured specimen, USNM 164 607, interior view of "adult assemblage" dorsal cup showing aboral nervous system grooves, "size" 10.3 mm, × 6.2, locality unknown.

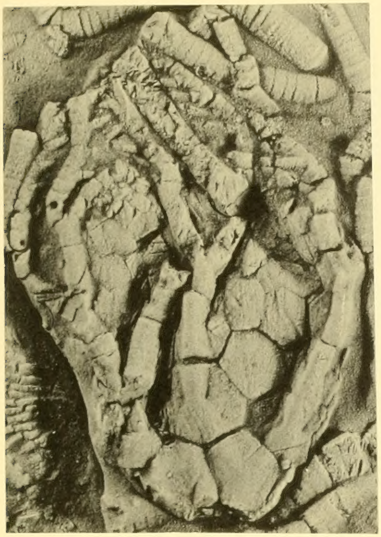
1

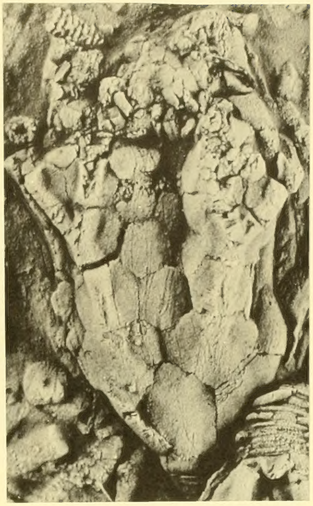
2

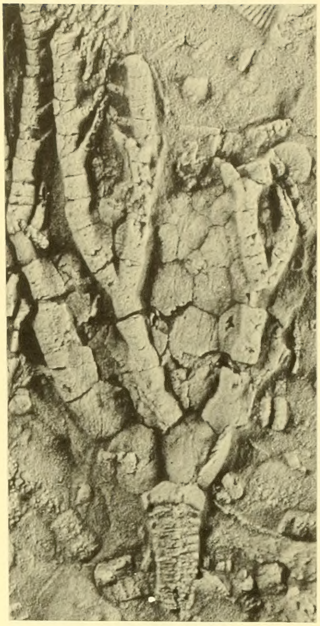
3

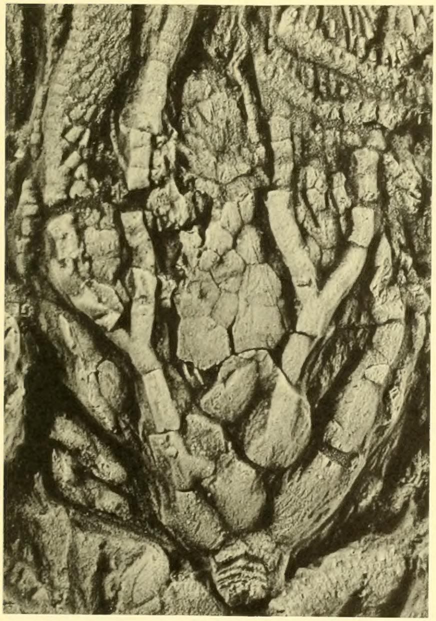
4

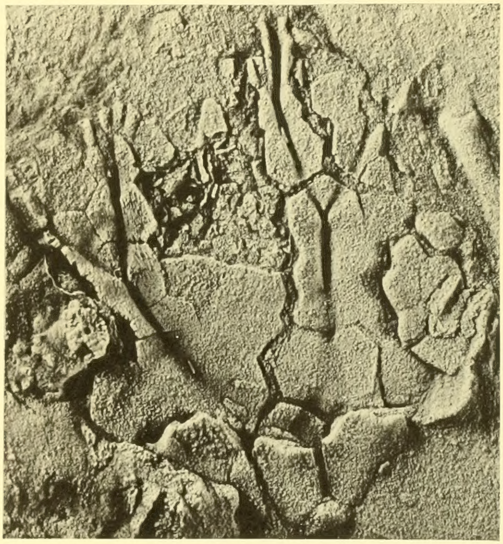
5

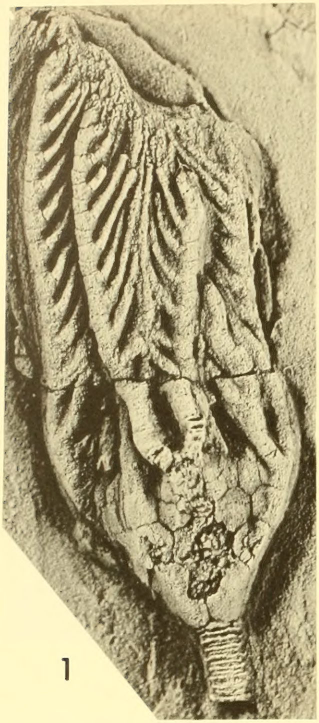
1

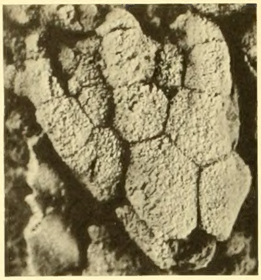
2

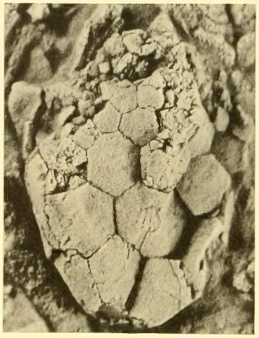
3

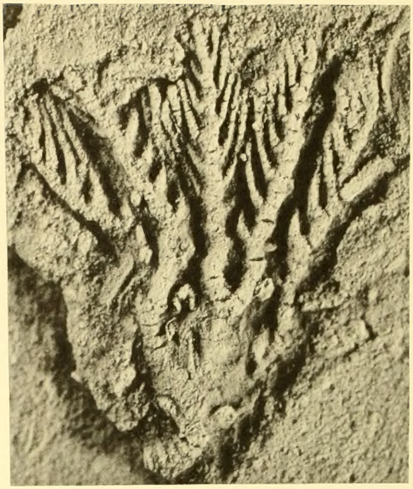
4

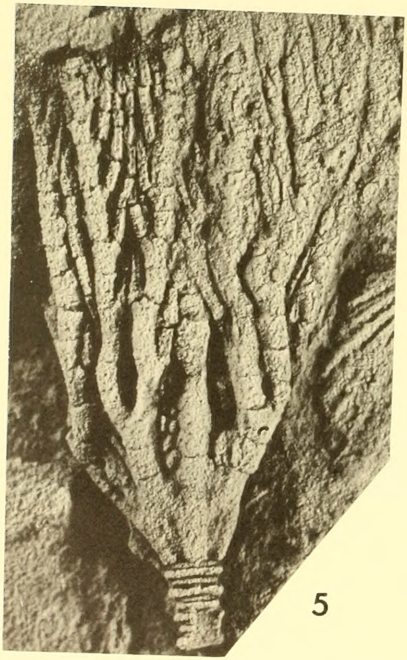
5

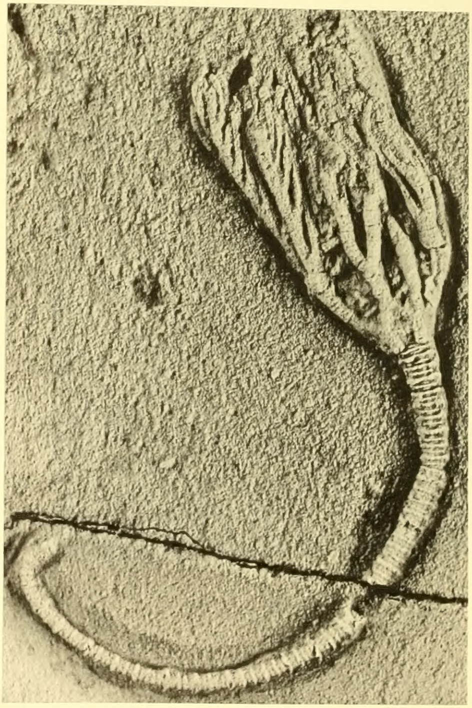
6

EXPLANATION OF PLATE 72

Figure		*Page*
1-6.	*Ptychocrinus fimbriatus* (Shumard)	446

Girardeau Limestone.

1. Figured specimen, IGS. 35P-59, C ray of "young assemblage" crown, "size" 4.0 mm, × 8, Orchard Creek exposure.
2. Figured specimen, USNM 165 072, CD interray of "young assemblage" calyx, "size" 3.6 mm, × 12, Orchard Creek exposure.
3. Figured specimen, USNM 165 074, lateral view of "transitional" calyx, "size" 5.4 mm, × 7, from high density "adult assemblage" slab, Orchard Creek exposure.
4. Figured specimen, IGS. 35P-64, lateral view of smallest "young assemblage" crown, "size" 2.0 mm, × 3, from high density "young assemblage" garden, Orchard Creek exposure.
5. Figured specimen, USNM 164 608, CD interray of "young assemblage" crown, "size" 2.4 mm, × 12, Cape Rock exposure.
6. Figured specimen, IGS. 35P-60, D ray of "young assemblage" animal showing calyx ornamentation like *P. splendens* (Miller) and arm structure like *P. fimbriatus*, "size" 2.7 mm, × 6.7, Orchard Creek exposure.

EXPLANATION OF PLATE 73

Figure		*Page*
1, 2.	*Ptychocrinus splendens* (Miller)	448

Girardeau Limestone, Orchard Creek exposure.

1. Figured specimen, USNM 164 601, lateral view of mature crown, "size" 12.7 mm, × 3.3.
2. Figured specimen, IGS. 35P-50, lateral view of mature crown, "size" 8.0 mm, × 3.6, from high density adult crinoid garden.

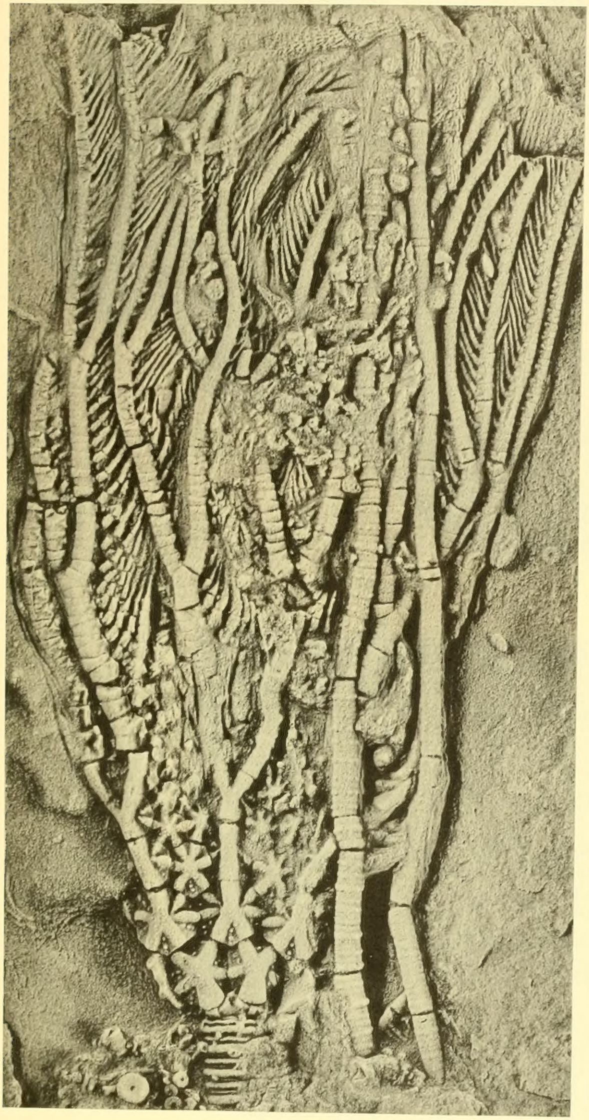

1

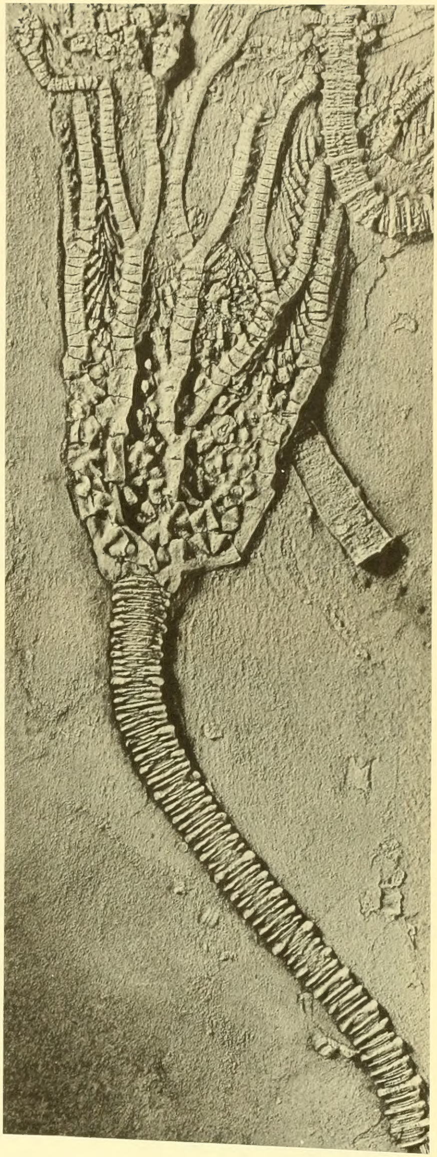

2

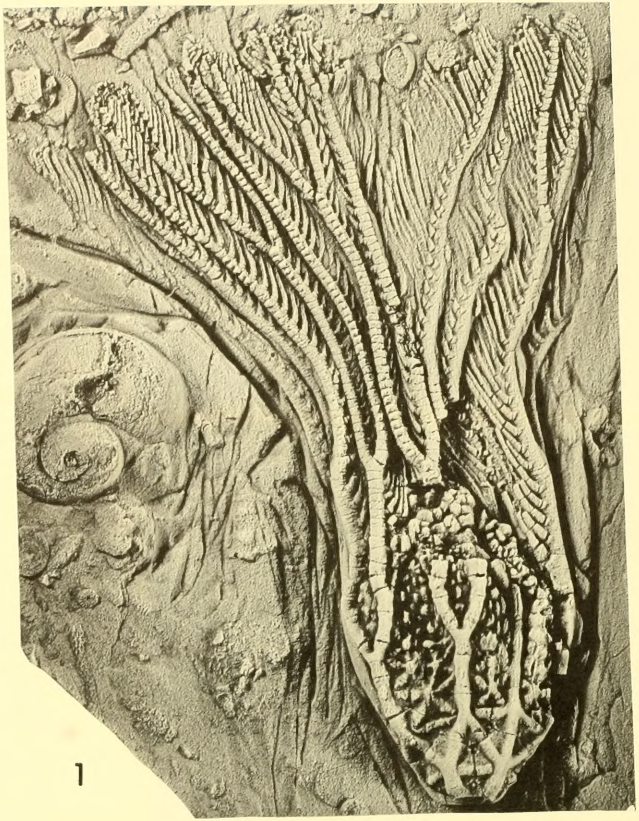

1

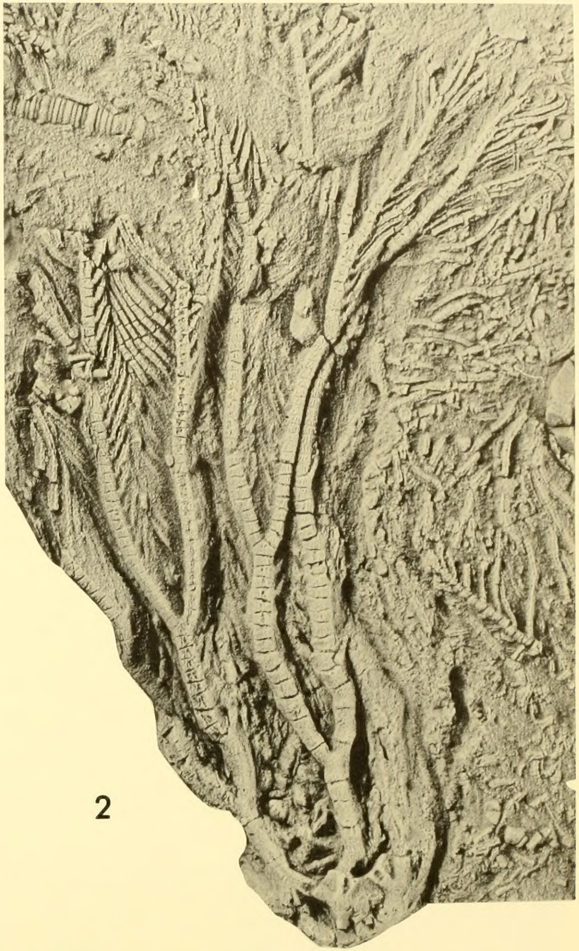

2

EXPLANATION OF PLATE 74

Figure *Page*

1, 2. *Ptychocrinus splendens* (Miller) 448

Girardeau Limestone.
1. Figured specimen, USNM 164 598, lateral view of mature crown, "size" 6.9 mm, × 5.5, Orchard Creek exposure.
2. Figured specimen, USNM 164 602, D ray of adult crown, "size" 7.6 mm, × 4.5, Cape Rock exposure.

EXPLANATION OF PLATE 75

Figure		*Page*
1-4.	*Ptychocrinus splendens* (Miller)	448

Girardeau Limestone.
1. Figured specimen, USNM 164 605, lateral view of mature calyx, × 5.2, from high density "adult assemblage" garden, Orchard Creek exposure.
2. Figured specimen, USNM 164 603, C ray view of young crown, "size" 3.85 mm, × 6.2, Orchard Creek exposure.
3. Lectotype, UC. 6286, lateral view of young crown, "size" 4.1 mm, × 4.9, Cape Rock exposure.
4. Figured specimen, USNM 164 596, lateral view of mature crown, note abnormal arm branching as discussed in text, "size" 9.25 mm, × 3.9, Cape Rock exposure.

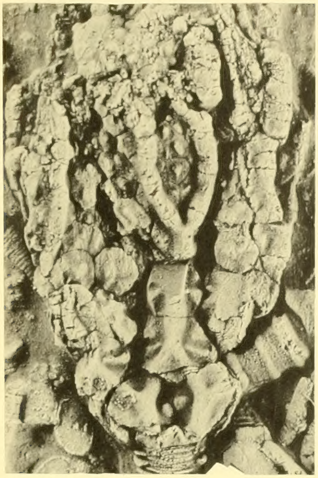

1

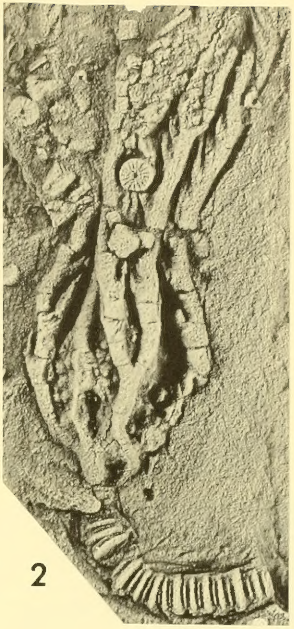

2

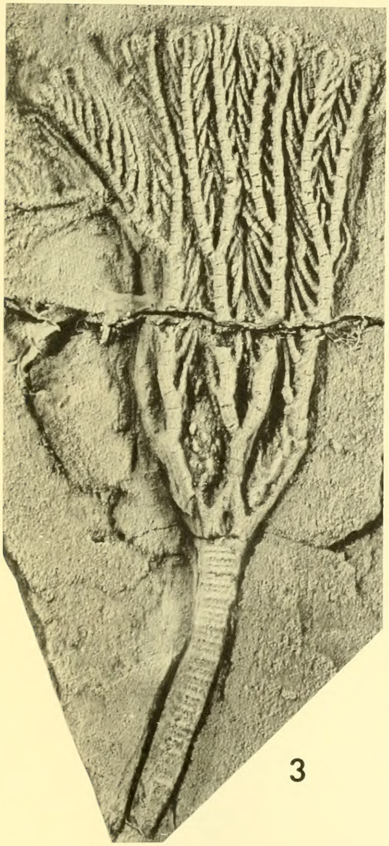

3

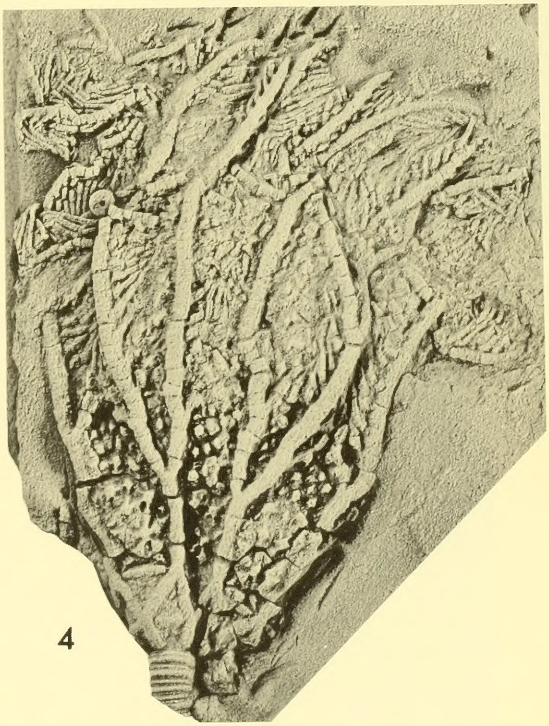

4

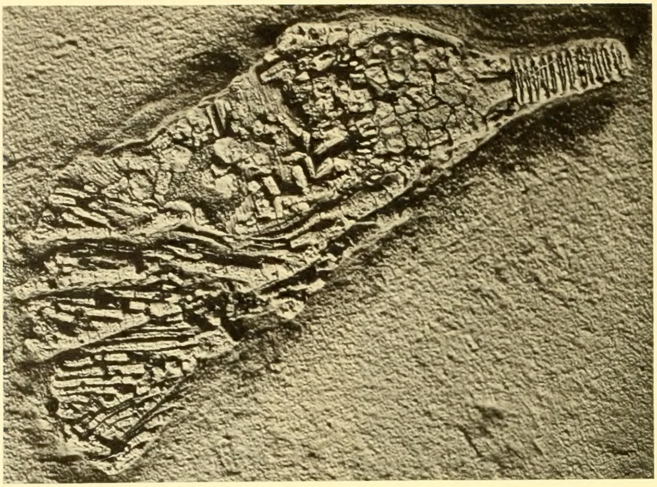

3

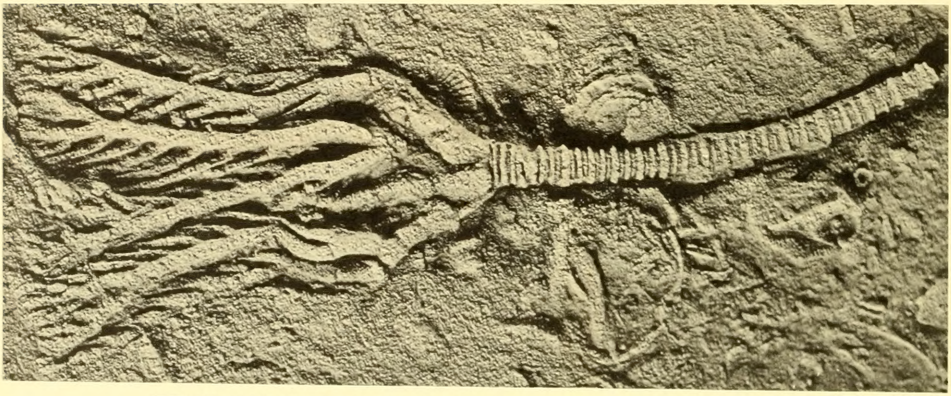

2

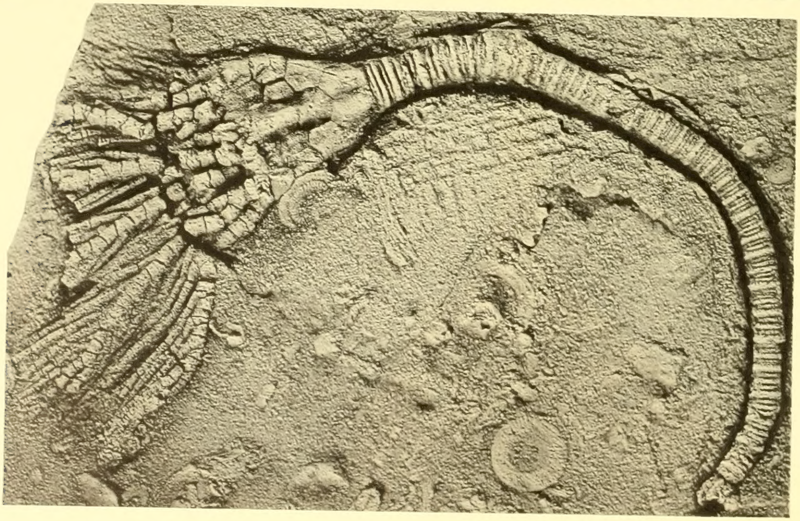

1

EXPLANATION OF PLATE 76

Figure		*Page*
1-3.	*Ptychocrinus splendens* (Miller)	448

Girardeau Limestone.
1. Figured specimen, USNM 164 599, lateral view of young crown, "size" 4.0 mm, × 6.2, Cape Rock exposure.
2. Figured specimen, USNM 164 600, CD interray view of young crinoid, "size" 2.8 mm, × 8.6, Cape Rock exposure.
3. Figured specimen, IGS. 35P-42, lateral view of young crown showing abnormal arms, "size" 3.4 mm, × 6, Orchard Creek exposure.

EXPLANATION OF PLATE 77

Dendrocrinus, Girardeau Limestone, Orchard Creek exposure.

Figure		*Page*
1, 2, 4.	*D. casei* (Meek)	455
	Figured specimens. 1. S. 5433, C ray of crown, cup height 7.2 mm, × 4.2. 2. S. 5434, lateral view with possibly regenerated arm in center ray, × 4.1. 4. S. 5432, CD interray of calyx, cup height 9.1 mm, × 3.8.	
3.	*D. curvijunctus,* n. sp.	456
	Holotype, IGS. 35P-7, CD interray, cup height 4.5 mm, × 4.7, from low density hard substrate assemblage.	

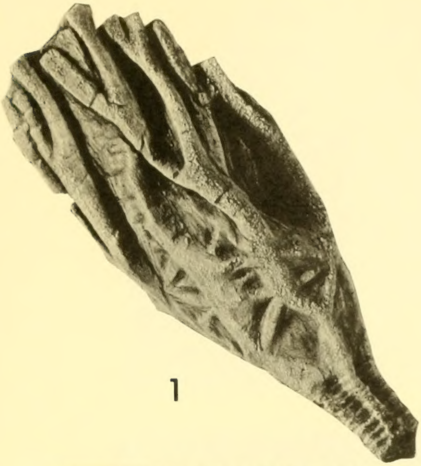
1

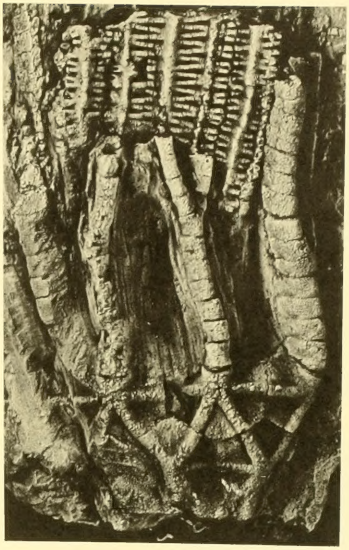
2

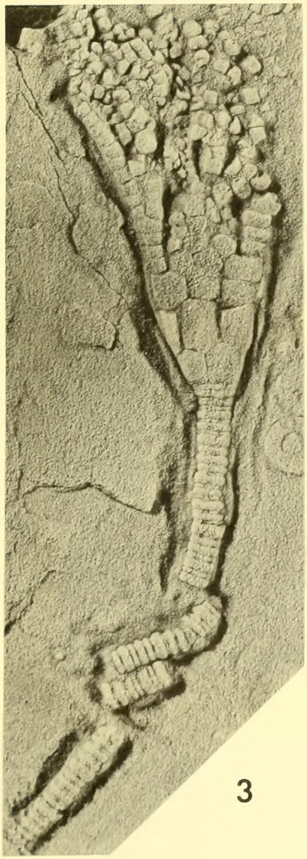
3

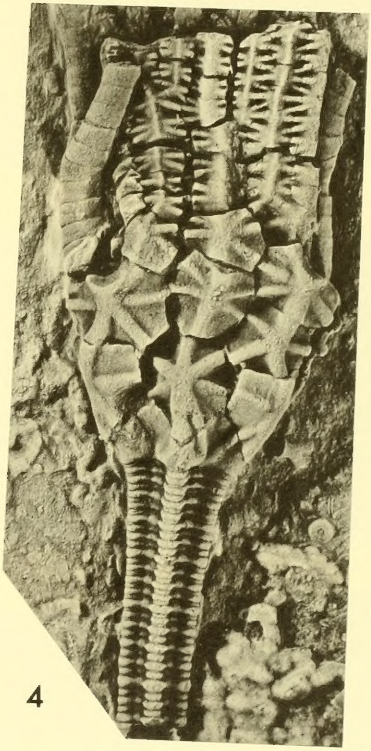
4

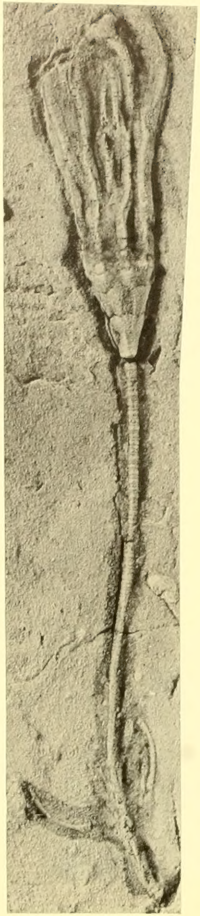
1

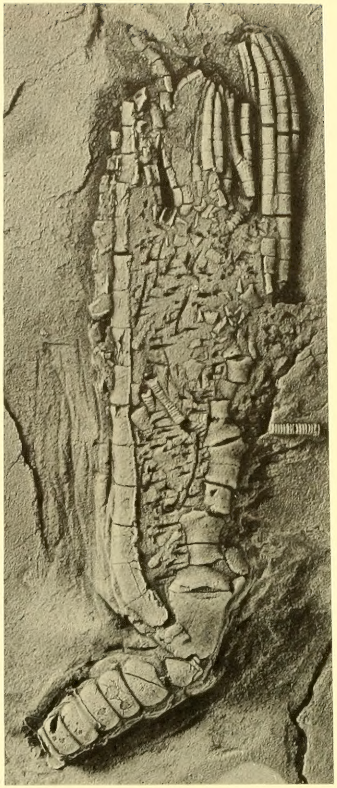
2

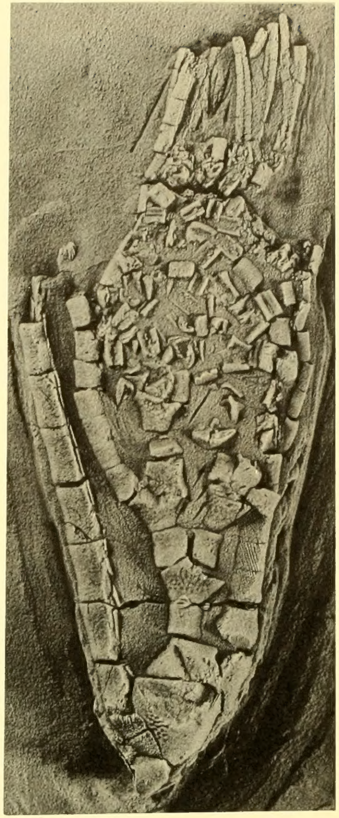
3

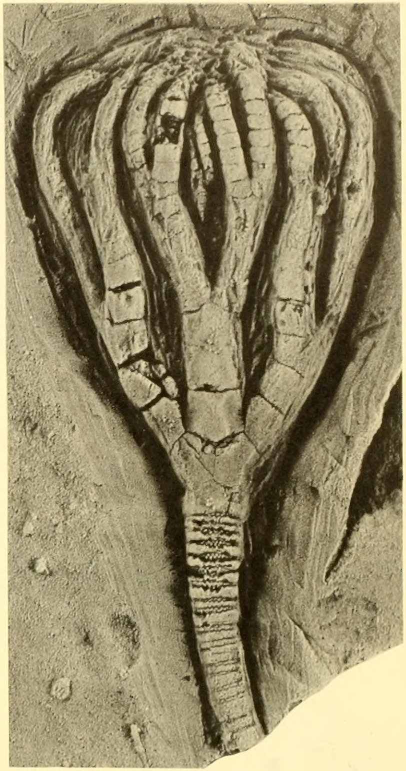
4

EXPLANATION OF PLATE 78

Various inadunates and flexibles

Figure *Page*

1. *Dendrocrinus*?, n. sp. aff. *D*? *navigiolum* Miller 457

Figured specimen, IGS. 35P-5, lateral view of complete individual, cup height 5.3 mm, × 3, from low density hard substrate assemblage, Girardeau Limestone, Orchard Creek exposure.

2, 3. *Calceocrinus constrictus* Brower 451

Limestone bed near top of Orchard Creek Shale, Mississippi River exposure.
2. Paratype, IGS. 35P-2a, A ray, crown height 34 mm, × 3.4.
3. Holotype, IGS. 35P-1, A ray, crown height 32 mm, × 4.2.

4. *Protaxocrinus girardeau* Springer 460

Holotype, S. 1778, lateral view of crown, cup height 4.35 mm, × 4.9, Girardeau Limestone, Orchard Creek exposure.

EXPLANATION OF PLATE 79

Various crinoids

Figure		*Page*
1.	*Dendrocrinus? constrictus,* n. sp. Holotype, USNM 164 593, lateral view, cup height 23 mm, × 2.1, Cape Limestone, probably one of Main Street outcrops, Cape Girardeau, Missouri.	459
2.	*Clidochirus serrulatus,* n. sp. Holotype, IGS. 35P-8, D ray view of crown, cup height 2.9 mm, × 5.3, Girardeau Limestone, Orchard Creek exposure.	462
3.	*Compsocrinus nodosus,* n. sp. Holotype, USNM 164 592, CD interray, the arm fragments in the upper right of the photograph are not conspecific with the calyx, "size" 5.5 - 6.0 mm, × 3.1, Girardeau Limestone, Cape Rock exposure.	443
4.	*Protaxocrinus girardeau* Springer Figured specimen, S. 5435, D and E rays, cup height 4.5 mm, × 4.1, Girardeau Limestone, Orchard Creek exposure.	460

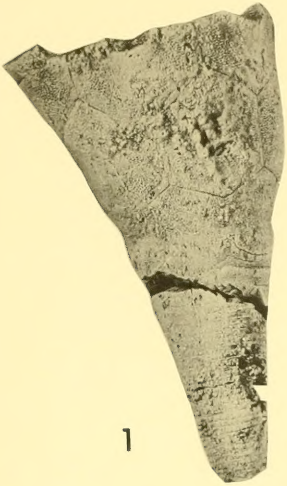

1

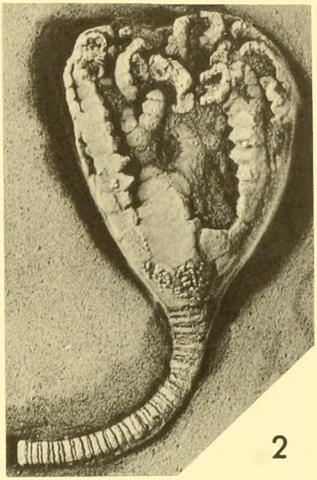

2

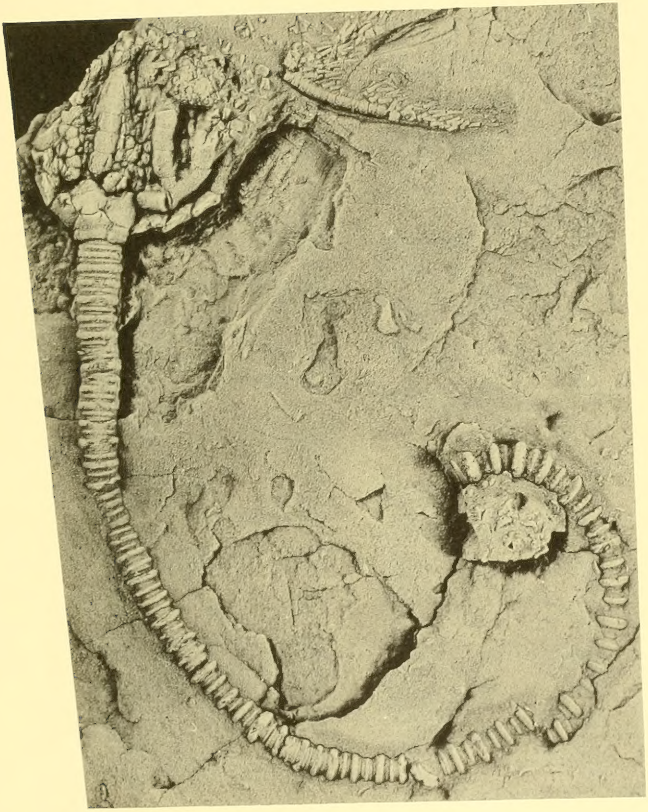

3

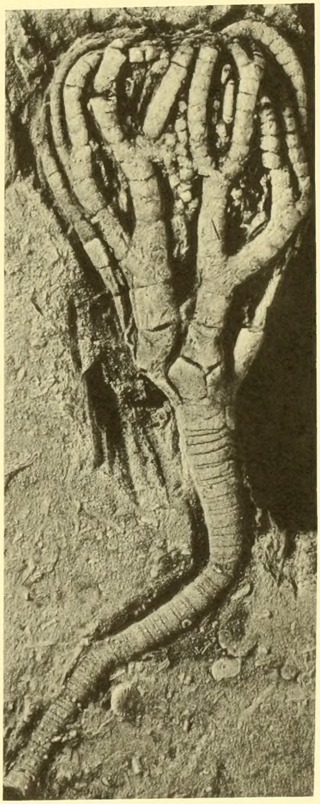

4

INDEX

Note: Page numbers are in light face type. Plate numbers are in bold face type.

A

acinotubus,
  Cyathocrinus 294
acutidactylus,
  Dendrocrinus 452, 457
adriatica,
  Antedon 301, 302, 308, 310
Agaricocrinus 367
Agassiz, A. 287
Alisocrinus 265, 330, 407-443
Allee, W. C. 278
Allen, J. R. L. 268, 467
Allocrinus 401
alternatus,
  Dendrocrinus 457
  Poteriocrinus 452
alternicirrus,
  Isocrinus 288
Ambicocrinus 446
Amblacrinus 399
americanus,
  Clidochirus 464
  Platycrinites 307
Angelin, N. P. 332-333, 399, 401, 408, 460, 462, 464, 466
Angelinocrinus 332
anglicus,
  Macrostylocrinus 405
  Promelocrinus 432-437
angulatus,
  Metacrinus 288
angustatus,
  Homocrinus 453
Anisocrinus 330, 465, 466
Antedon 270, 281, 285, 293-294, 300, 364, 418
Anticosti Island, Middle Silurian, Canada 451, 453
Apiocystites ? 400
Arbacia 279, 281
archaeocrinid, unidentified species 263-264, 283
Archaeocrinus sp. 264
Ashgill Series, Scotland 365, 371, 395, 452, 454, 456
aureatus,
  Alisocrinus 408
  Mariacrinus 432

B

bacca, Lyonicrinus 407
Bactrocrinites 452, 458
baeri, Xenocrinus 294, 445
Bala Beds, England 331
Balacrinus 446
Banse, K. 322
basalis,
  Glyptocrinus 446
  Rhaphanocrinus 446
Bassler, R. S. 332, 447-448, 452, 455, 460, 462
Bates, D. C. 453
Bather, F. A. 285, 294-295, 298, 327, 360, 364, 400, 445-447, 455
Bathycrinus 282-283, 288
Beach River Formation, Tennessee 401
Benbolt Limestone, Virginia and Tennessee 269
Biese, W. 298
bifida, Antedon 272, 278, 284, 287, 293, 298-310, 323
Billings, E. 452-454, 457, 459, 462
Billings, W. R. 452-453, 460
Bogatacrinus 399
Boolootian, R. A. 272, 278
bozemanensis, Platycrinites 307-308, 311, 313, 399
Brainard Shale, Iowa 456
Brassfield Limestone, Ohio 400-401, 407
Breimer, A. 270-271, 283, 285-287, 318-319, 397-399, 446
Briarocrinus 332
Bridge, J. 263
Brower, J. C. 263-266, 326, 396, 451, 461
Burlington Limestone, Illinois, Iowa and Missouri 286, 292, 367
burlingtonensis, Platycrinites 307

C

caduceus, Poteriocrinus (Dendrocrinus) 452
Cain, J. D. Blyth 284
Calceocrinus 451
Calceolispongia 364
Camarothechia ? 264
cambriensis, Dendrocrinus 453
campana, Pisocrinus cf. 298-299
Canistrocrinus 264
Cantharocrinus 399
Cape Girardeau, Missouri 265, 460
Cape Limestone, Missouri 263, 459-460
Cape Rock exposure, near Cape Girardeau, Missouri 263, 265, 277, 281, 333-336, 374, 396, 409, 432, 437, 443-448, 450, 462
Carabocrinus 269
Caradoc Stage, Montgomeryshire, England 446, 454
carleyi,
  Alisocrinus 408, 432-437
  Mariacrinus 408, 431
Carpenter, P. H. 287-290, 294, 298, 364
Carpenter, W. B. 287, 296, 298, 302, 309, 364
Carpocrinus ? n. sp. 264
casei,
  Dendrocrinus **77** 263-264, 282-283, 453-456
  Poteriocrinites (Dendrocrinus) 452, 455
caseyi,
  Poteriocrinites (Dendrocrinus) 455
casii, Dendrocrinus 455
celsus,
  Dendrocrinus 452, 458, 460
Chadwick, H. C. 287
Chazyan Stage 331
chiastodactylus, Patelliocrinus 333
Christy, D. 455
Chytrocrinus 400
Cincinnati area, Ohio 263-264, 432
Cincinnatian Series 263-264, 460
cincinnatiensis,
  Dendrocrinus 457
  Poteriocrinites (Dendrocrinus) 452
cirrifer, Macrostylocrinus **64, 65** 293-294, 298, 300, 310, 331, 334, 363-372, 395-396, 401-407, 410, 448
Clark, A. H. 272, 278, 281, 283, 287, 294, 296, 299-300, 302-305, 309-310, 321, 364
Clark, H. L. 269, 271
Cleistocrinus 462, 465, 466
Clidochirus 265, 330, 462-466
Comactina 302, 304
compactus, Esthonocrinus 459
Compsocrinus 265, 443-445

conjugans, Cupulocrinus 450
Conrad, T. 462
constrictus,
  Calceocrinus ... **78** 263, 451
  Dendrocrinus **79** 263, 458-460
Cooper, G. A. 263
Cordylocrinus 399
Crawfordsville crinoid beds, near Crawfordsville, Indiana 275, 282, 288, 322
Ctenocrinus 437
Cuénot, L. 298, 364
Culicocrinus 265, 303, 397-400, 407
Cumingia 279
Cumings, E. R. 455
Cupulocrinus 452-454
curvijunctus, Dendrocrinus **77** 263-265, 282-283, 456, 457
Cyathocrinus 364
Cyphocrinus 313, 446
cystoid, unidentified species 273
Cyttarocrinus 399

D

dactylus, Lyriocrinus 450
decadactylus,
  Dimerocrinites 446, 451
  Glyptocrinus 263, 294, 307, 312, 341, 408, 416, 430, 432-436
Decorah Shale, Twin Cities, Minnesota 269
decorus, Isocrinus . 285, 287-288, 298
dendrocrinid, undescribed species ...... Table 3
Dendrocrinus ... **77** 264-265, 451-460
depressus, Megistocrinus 307
Diabolocrinus 269
Diaphorostoma 264
diensti, Pterinocrinus 446
Dimerocrinites 330-331, 445-446, 451
discoideus, Platycrinites 383
douglassi "var." serpens, Rhodocrinites 307
Dudley, England 432
duplicatus, Patelliocrinus 333
dyeri,
  Dendrocrinus 457-458
  Glyptocrinus 296, 307, 312, 346, 416-417, 442-443
  Poteriocrinites (Dendrocrinus) .. 452

E

Eden Stage 331, 452, 458
Edgewood Limestone, Illinois and Missouri 263, 266, 332
Ehrenberg, K. 288
elegans,
  Dimerocrinites .. 451
  Protaxocrinus 454, 462
  Scyphocrinites .. 442
Encrinites 314
Encrinus 287-288
Eopatelliocrinus ... 312, 329-363, 394-397, 400-407, 417, 425
Eretmocrinus 383
eriensis, Cyttarocrinus 305
erraticus, Dendrocrinus 453
Esthonocrinus 452, 454, 458, 459
Estonia 454, 459
Eucalyptocrinites . 282, 300, 310
Eucheirocrinus 264
Eudimerocrinus ... 330, 446, 451
Eutaxocrinus 460
exsculptus, Onychocrinus ...... Table 3
extensus, Woodocrinus 289

F

fasciatus, Macrostylocrinus 396
Feder, H. M. 305
Fell, H. B. 270, 283-286, 304, 322
Field Museum of Natural History, Chicago, Illinois (U.C.) 265, 450
fimbriatus,
  Glyptocrinus 446-447
  Ptychocrinus **69, 70, 71, 72** 263-264, 273-278, 282, 293, 308-312, 319-323, 416-418, 445-451
Foerste, A. F. 400-403, 451, 455, 464
Follicrinus 452
fulminatus,
  Patelliocrinus 333
  Promelocrinus .. 408, 432-437
fusibrachiatus, Macrostylocrinus 370

G

Gamachian Stage .. 264-265
Gaussberg, Antarctica 304
Gazacrinus 446
Gilbertsocrinus 288
Girardeau Limestone, Illinois and Missouri 263-269, 276, 320, 333-334, 396, 400-401, 409, 432-434, 437, 443-451, 456-459, 462-464
girardeau, Protaxocrinus **78, 79** 263-265, 283, 460-462
girardeauensis, Culicocrinus? **68** 263-265, 283, 327-329, 398-407
girvanensis, Protaxocrinus 454, 462
Gislén, T. 284-287, 318, 320, 322, 434
Gissocrinus 364
Glyptocrinus 288, 329-332, 408, 432, 447
Gnorimocrinus 460
Goldring, W. 287, 289, 307, 399, 434, 446
Goniocrinus 459
goniodactylus, Gissocrinus 294, 295
Gotland Island, Scandinavia 432, 460-464
gotlandicus, Loveniocrinus 363
Grabau, A. W. 455
gracilis,
  Cupulocrinus 454
  Poteriocrinus 453
granditubus, Dendrocrinus ... 452, 454, 457
Grant, V. 281
gratiosus, Clidochirus 462, 464
Grave, B. H. 279
greenei, Clidochirus ? 464
gregarius, Dendrocrinus 452, 459
Grenprisia 452, 453
Griphocrinus 446

H

Hall, J. 263, 370, 396, 408, 445, 450-453, 457, 466
Hallam, A. 272, 305, 322
Hand, Bryce 268
Hapalocrinus 398, 399, 407
Haplocrinus ? 264
harrisi,
  Compsocrinus 444
  Glyptocrinus 443
heterobrachialis, Cupulocrinus 454
Heterocrinus 288

heterodactylus, Alisocrinus ? .. **68** 263-265, 273, 278, 283, 310-316, 324, 416, 420-422, 434, 437-443
Hicks, H. 453
Homoespira 264
Hudson, G. H. 364
humilis, Cupulocrinus 453, 454
Hunterian Museum, University of Glasgow, Scotland (HM.) 265, 364-371
huntsvillae, Platycrinites 307
Hybocrinus 269
Hydroides 279
Hyman, L. H. 272, 279, 282-283, 293, 298, 300, 302, 364

I

Ichthyocrinus 462-466
icosidactylus, Dimerocrinites .. 446, 450-451
Illinois Geological Survey, Champaign-Urbana, Illinois (IGS.) 265, 273, 333-336, 356-357, 373-374, 377, 383, 384, 396, 400, 409-410, 421, 432, 437, 443-451, 457, 459, 463-464
Illinois State Museum, Springfield, Illinois (Ill. St. Mus.) 265, 443
immaturus, Aorocrinus .... Table 3
Inadunata, three unidentified species 263-264
inagilis, Hallocrinus ? 364
insperatus, Glyptocrinus 332
insperatus "var." carinatus, Glyptocrinus 332, 363
insperatus "var." pentagonus, Glyptocrinus 332
iola, Aorocrinus ...... Table 3
iowensis, Clidochirus 462, 464
Isocrinus 282

J

Jaekel, O. 290, 332, 363, 398-401, 405, 408, 445-446, 452, 459
japonicus, Comanthus 272
Jeffords, R. M. 298, 370
Jewe Limestone, Estonia 454
jewetti, Cupulocrinus 453-454
Johnson, R. G. 274
jugans, Cupulocrinus 453

K

kayi, Dendrocrinus 452, 455-456
kerguelensis, Promachocrinus 278, 301-308, 418
Keyes, C. R. 447-448
keyserensis, Clidochirus 462, 464
Kiel Bay, Germany 322
Kier, Porter 270-271
Kirk, Edwin 283, 288-290, 407, 408, 431-432, 446
Knobstone Group, Kentucky 383
Koenig, J. W. 305, 307, 418, 419
Koninck, L. G. de .. 466
konincki, Mespilocrinus 287

L

laevior, Esthonocrinus 452, 459
laevis,
  Alisocrinus 408, 431-432
  Macrostylocrinus 370, 401-407
  Protaxocrinus 454, 462
Lane, N. G. 275, 282-283, 286-288, 293, 322, 364, 396, 461
latibrachiatus, Eopatelliocrinus ... **61** 263-265, 273, 276-278, 283, 296, 308, 310, 314, 316, 320, 321, 324, 328, 332-363, 373, 374, 378, 384, 393-397, 401-407, 420, 423, 424, 427, 440-442
Laudon, L. R. 307-308, 311, 313, 399
Laurel Limestone, Indiana 401
Laurelocrinus 401
Lecanocrinus 465, 466
Lesley, J. P. 455
Liebe, R. M. 264
lilliformis, Encrinus 298, 383
Linck, O. 287, 299
Llandovery Stage .. 329
longidactylus, Dendrocrinus 451, 452, 457
Loveniocrinus 363
Lyonicrinus 399

M

Macarocrinus 445
maclaeranus, Isocrinus 288
Macrocystella 285
macrodactylus, Woodocrinus 289, 321
Macrostylocrinus .. 264-265, 329, 332, 363-397, 400-407
Macurda, D. B. 282, 293, 300, 310
Magnus, D. B. E. 270, 271, 319
Maquoketa Group (Richmond), Iowa 263-266, 456, 460
Mariacrinus ? 264
Marsupites 364
Martin, J. A. 264
maximus, Clidochirus ? 462
Maysville Stage 443, 445, 450
McCoy, Frederick .. 446
mediterranea, Antedon 272, 301-302, 310
Meek, F. B. 442, 452-458
meeki, Macrostylocrinus 370, 405, 406
melissa, Lyriocrinus 450
Menzel, D. W. 322
meridionalis, Comactina 299-304, 308, 418
Meristocrinus 466
Mespilocrinus 465, 466
Metacrinus 282, 284, 285, 294-297
Metichthyocrinus .. 462, 465, 466
Meyer, D. L. 271, 287, 293, 340
miamiensis, Compsocrinus 444
Miller, J. S. 293
Miller, S. A. 399, 408, 443-455, 458, 464, 466
minutus, Dendrocrinus 453
minutus, Lophocrinus 364
Moore, A. R. 298, 364
Moore, H. B. 278, 293, 305
Moore, R. C. 285, 290, 298, 313, 314, 330, 370, 401, 418, 430, 432, 437, 445, 448, 452, 466
Müller, J. 397, 399
multiramus, Xenocrinus 311, 445

INDEX

N

nana, Iridometra 287
navigiolum,
  Dendrocrinus ? 452, 458
  Dendrocrinus ? n. sp. aff. **78** 263-265, 282, 283, 400, 457-459
Nevadacrinus 461
Niagaran Series 452, 458, 459
Nichols, David 294, 298, 309, 323, 363, 364, 369
nodobrachiatus,
  Dendrocrinus ? 453
nodosus,
  Compsocrinus **79** 263-265, 283, 327, 443, 444, 445
  Platycrinus 397

O

obconicus, Macrostylocrinus 366, 396
Oenochoacrinus 400
onealli,
  Reteocrinus 294
Onychocrinus 460
d'Orbigny, A. 399
Orchard Creek exposure, near Thebes, Illinois 263-267, 277, 281, 333-336, 374, 396, 400, 409, 432, 443-450, 456-459, 462-464
Orchard Creek Formation, Illinois and Missouri 263-269, 451
ornatus,
  Glyptocrinus 401-407, 432-436
  Macrostylocrinus 363, 370, 371, 396, 401-407
  Patelliocrinus 397, 401-407
  Physetocrinus 369
ornigranulatus,
  Platycrinites 307
oswegoensis,
  Anisocrinus 466
  Dendrocrinus 289, 453
ovalis,
  Eucalyptocrinites Table 3
  Taxocrinus 460

P

Palaeocrinus 269
Parisangulocrinus 452
Parkinson, R. 264
parrae, Isocrinus 288
parvus,
  Ptychocrinus 307, 445, 446, 450-451
Patelliocrinus 329, 332-333, 396-397, 400-407
paucidactylus,
  Ctenocrinus 287, 289, 307, 434, 435
Paul, C. R. C. 283, 285
penicillus,
  Xenocrinus 445
Pentacrinite 455
pentangularis,
  Callicrinus 404
Pentland Hills, near Edinburgh, Scotland 298, 299, 331, 405
Periechocrinites 294
petasus, Antedon 284, 310, 434
Phillips, J. 446
Pisocrinus 298
planus,
  Dimerocrinites 385, 446, 451
"platycrinid" 401-407
Platycrinites 407
Pleurocrinus 399
posticus,
  Poteriocrinus 453
pristinus, Macrostylocrinus **62, 63** 263-265, 273-277, 283, 297, 308-314, 320, 324-326, 362, 370-397, 401-407, 414, 417, 425-430, 451
proboscidalis,
  Cactocrinus 369
proboscidiatus,
  Dendrocrinus 452, 453, 459-460
Proetus 264
prolixa,
  Hathrometra 308
Promachocrinus 304
Promelocrinus 330, 333, 408, 432
Protaxocrinus 265, 454, 460-462
Protozeuga 264
Pryor, W. A. 265, 267
Pterinocrinus 446
Ptychocrinus 264, 265, 304, 330-331, 445-451
punctatus,
  Hybocrinus 300
purpureatus,
  Strongylocentrotus 278, 279
pustulosus, Macrostylocrinus ? 370, 371
putillus,
  Climacograptus 264
pyrum, Clidochirus 462, 464

R

Racine Dolomite, Bridgeport, Illinois 366, 396
radiatus,
  Promelocrinus 408, 432-437
Ramsbottom, W. H. C. 311, 363, 395, 445-446, 452, 454, 456, 457, 462
Ramseyocrinus 453
Raup, D. M. 300, 301
recumbens, Macrostylocrinus 363
regalis,
  Platycrinites Table 3
  Strotocrinus 369
Regnéll, G. 418
regularis,
  Culmicrinus 364
retractilis,
  Dendrocrinus 453
  Merocrinus 453
rex, Acanthocrinus 287
Rhaphanocrinus 304, 330, 331, 445-446, 450
Rhizocrinus 282, 283, 288
rhomboidalis,
  Laptaena 264
Richmond Stage 264, 265, 329, 330, 432, 436, 437, 443-446, 451-456
Ringueberg, E. N. S. 370, 407, 431, 452, 453, 458, 460
Rochester Shale, New York 323, 396, 401, 432, 434, 452
Ross, C. A. 264
Rouse, Hunter 268
Rowley, R .R. 332
Royal Scottish Museum, Edinburgh, Scotland (RSM.) 265, 366-371
rugocyathus,
  Dendrocrinus 452, 454, 456
rugosus,
  Patelliocrinus 397
rusticus,
  Dendrocrinus 457, 459

S

Saccocoma 285
Salamans Creek exposure, Illinois 265, 267
sarsii,
  Hathrometra 272, 278, 301-308, 418
Satterfield, I. R. 264
Savage, T. E. 263-265, 448
savignyi,
  Heterometra 270, 271, 319
Schmidt, W. E. 364, 399, 446, 452
Schuchertella 264
schucherti,
  Clidochirus 464

sculptus,
  Rhaphanocrinus 446, 451
Scyphocrinites 442, 443
scyphogracilis,
  Eopatelliocrinus **59, 60** 263-265, 271, 278, 283, 297, 308, 310, 314, 316, 319-321, 324-327, 332-362, 372-379, 384, 388, 390, 392-395, 401-407, 410, 414, 420, 423-429, 441
Seilacher, A. 287, 288, 298, 299
Seirocrinus 288, 290, 298
semiradiatus, Macrostylocrinus 396
sepulchrum,
  Cupulocrinus 454
serrulatus,
  Clidochirus **79** 263, 265, 283, 462-464, 466
Sexton Creek Limestone, Illinois and Missouri 263, 266
Shumard, B. F. 264, 446, 447
Sieverts, H. 364
similis,
  Dendrocrinus 453
Simpson, G. G. 292
Slocom, A. W. 452, 455, 456
Sokal, R. R. 328
spectabilis,
  Melocrinus ? 408, 432
spinosus,
  Culicocrinus 399
splendens,
  Gaurocrinus 445, 448
  Ptychocrinus **73, 74, 75, 76** 263, 264, 271-279, 283, 296, 310-312, 319-323, 330, 346, 416-418, 445, 447, 448-451, 450
Springer Collection, Smithsonian Institute (S.) 401, 408, 432, 447, 448, 456, 462
Springer, F. 264, 271, 299, 302-304, 313, 370, 371, 396-408, 431-432, 442, 446, 451-454, 460-462, 464-466
Sprinkle, J. 278
"Starfish Bed", Thraive Glen, near Girvan, Scotland 363-368, 371, 396
Steganocrinus 329
Stelidiocrinus 332
Streblocrinus 419
Strimple, H. W. 418, 462, 464
suberectus, Girardeaucrinus 264
subglobosus,
  Glyptocrinus 442
  Macrostylocrinus 366
subnodosus,
  Rhaphanocrinus 446, 449-451
stullensis,
  Graffhamicrinus 383
Swan, E. F. 278
Synaptocrinus 462, 464-466, 465

T

Talbot, M. 464
Tanaocrinus 444
Teichert, C. 364
Teleiocrinus 313, 369
Temnocrinus 466
Templeton, J. C. 264
tenuistriata,
  Cornulites 264
Termier, H. 298
tetrarmatus, Alisocrinus **66, 67, 68** 263-265, 273-278, 283, 308-326, 330, 352, 408-436
Thallocrinus 399
Thebes, Illinois 265
Thebes Sandstone, Illinois 263-269
Thomas, A. O. 455, 462, 464
Thompson, Sir W. 298, 302 305
Timor, Indonesia 314, 331
Trampidocrinus 461
Trenton Stage 329, 331, 401, 432, 436, 446, 450, 452-454, 457-462
typus,
  Tanaocrinus 444
  Tanaocrinus cf. 264

U

Ubaghs, G. 287, 309, 331-333, 363, 364, 408, 432, 437, 445, 448
Ulrich, E. O. 263, 264, 460
ulrichi,
  Clidochirus 464
umbrosus,
  Teleiocrinus 311, 313
unicornis,
  Dorycrinus 383
Unitacrinus 285
United States National Museum (USNM) 273, 274, 316, 333-336, 340, 353, 356, 357, 361, 373, 374, 382-385, 392, 393, 396, 401, 409, 410, 432, 437-439, 443-451, 460
University of Illinois (Univ. Ill.) 409, 432
Upper Drummock Group, Scotland 365, 371

V

vagans,
  Dimerocrinus ? 451
Van Sant, J. F. 286, 318

W

Wachsmuth, C. 293, 294, 298, 307, 309, 311, 313, 369, 370, 400, 403, 408, 416, 417, 431, 432, 442-450, 455, 460
Walcott, C. D. 446, 453
Waldron Shale, Indiana and Tennessee 396, 432
Wanner, Johannes 293
warreni,
  Alisocrinus 329, 408, 431-437
  Mariacrinus 407
Weaver, T. 288
Weller, J. M. 263, 264
Weller, S. 366, 396, 404
Wenlock Stage, England 329, 405, 446, 451
whitfieldi,
  Dimerocrinites 446
Wilson, A. E. 453
Woodocrinus 285, 287-289, 299, 317
Worthen, A. H. 263-264, 400
Wright, J. 288, 299
wyville-thompsoni,
  Isocrinus 288

X

Xenocrinus 264, 444, 445

Y

Yale, Peabody Museum (YPM.) 265, 409-410, 422, 432

Z

Zenker, J. C. 442
von Zittel, K. A. 407

L.	(Nos. 225-230). 518 pp., 42 pls. Venezuela and Florida cirripeds, Antarctic forams, Linnaean Olives, Camerina, Ordovician conodonts, Niagaran forams.	18.00
LI.	(Nos. 231-232). 420 pp., 10 pls. Antarctic bivalves, Bivalvia catalogue.	18.00
LII.	(Nos. 233, 236). 387 pp., 43 pls. New Zealand forams, Stromatoporoidea, Indo-Pacific, Miocene-Pliocene California forams.	18.00
LIII.	(Nos. 237-238). 488 pp., 45 pls. Venezuela Bryozoa, Kinderhookian Brachiopods.	18.00
LIV.	(Nos. 239-245). 510 pp., 50 pls. Dominican ostracodes, Texan pelecypods, Wisconsin mollusks, Siphocypraea, Lepidocyclina, Devonian gastropods, Miocene Pectens Guadaloupe.	18.00
LV.	(Nos. 246-247). 657 pp., 60 pls. Cenozoic corals, Trinidad Neogene mollusks.	18.00
LVI.	(Nos. 248-254). 572 pp., 49 pls. American Foraminifera, North Carolina fossils, coral types, Belanski types, Venezuelan Cenozoic Echinoids, Cretaceous Radiolaria, Cymatiid gastropods.	18.00
LVII.	(Nos. 255-256). 321 pp., 62 pls. Jurassic ammonites.	18.00
LVIII.	(Nos. 257-262). 305 pp., 39 pls. Cretaceous Radiolaria, Cretaceous Foraminifera, Pacific Silicoflagellates, North American Cystoidea, Cincinnatian Cyclonema, new species Vasum.	18.00
LIX.	(No. 263). 314 pp. Bibliography of Cenozoic Echinoidea.	18.00
LX.	(Nos. 264-267). 335 pp., 68 pls. Jurassic-Cretaceous Radiolaria, cirripeds, Bryozoa, palynology.	18.00
LXI.	(Nos. 268-270). 365 pp., 31 pls. Mollusks, Murex catalogue, Cretaceous Radiolaria.	18.00
LXII.	(Nos. 271-274). 375 pp., 44 pls. Trace fossils, ammonoids, Silicoflagellates, microfauna.	18.00
LXIII.	(Nos. 275-277). 320 pp., 56 pls. Chitinozoa, Spumellariina, Mexican Ammonites	18.00

Palaeontographica Americana

Volume I.	See Johnson Reprint Corporation, 111 Fifth Ave., New York, N. Y. 10003 Monographs of Arcas, Lutetia, rudistids and venerids.	
II.	(Nos. 6-12). 531 pp., 37 pls. Heliophyllum halli, Tertiary turrids, Neocene Spondyli, Paleozic cephalopods, Tertiary Fasciolarias and Paleozoic and Recent Hexactinellida.	23.00
III.	(Nos. 13-25). 513 pp., 61 pls. Paleozoic cephalopod structure and phylogeny, Paleozoic siphonophores, Busycon, Devonian fish studies, gastropod studies, Carboniferous crinoids, Cretaceous jellyfish, Platystrophia and Venericardia.	28.00
IV.	(Nos. 26-33). 492 pp., 72 pls. Rudist studies Busycon, Dalmanellidae Byssonychia, Devonian lycopods, Ordovican eurypterids, Pliocene mollusks.	28.00
V.	(Nos. 34-47). 445 pp., 101 pls. Tertiary Arcacea, Mississippian pelecypods, Ambonychiidae, Cretaceous Gulf Coastal forams.	32.00
VI.	(Nos. 38-41). 444 pp., 83 pls. Lycopsids and sphenopsids of Freeport Coal, Venericardia, Carboniferous crinoids, Trace fossils.	35.00
VII.	(Nos. 42-45). 257 pp., 58 pls. Torreites Sanchezi, Cancellariid Radula, Ontogeny, sexual dimorphism trilobites, Jamaician Rudists.	23.50

BULLETINS OF AMERICAN PALEONTOLOGY

Vols. I-XXIII. See Kraus Reprint Corp., 16 East 46th St., New York, N. Y. 10017, U.S.A.

XXIV.	(Nos. 80-87). 334 pp., 27 pls. Mainly Paleozoic faunas and Tertiary Mollusca.	12.00
XXV.	(Nos. 88-94B). 306 pp., 30 pls. Paleozoic, Mesozoic, and Miocene fossils.	12.00
XXVI.	(Nos. 95-100). 420 pp., 58 pls. Florida Recent, Texas and South America Cretaceous, Cenozoic fossils.	14.00
XXVII.	(Nos. 101-108). 376 pp., 36 pls. Tertiary mollusks, Paleozoic Venezuela, Devonian fish.	14.00
XXVIII.	(Nos. 109-114). 412 pp., 34 pls. Paleozoic cephalopods, Cretaceous Eocene, forams.	14.00
XXIX.	(Nos. 115-116). 738 pp., 52 pls. Bowden forams and Ordovician cephalopods.	18.00
XXX.	(No. 117). 563 pp., 65 pls. Jackson Eocene mollusks.	16.00
XXXI.	(Nos. 118-128). 458 pp., 27 pls. Mollusks, crinoids, corals, forams, Cuban localities.	16.00
XXXII.	(Nos. 129-133). 294 pp., 39 pls. Silurian cephalopods, crinoids, Tertiary forams, Mytilarca.	16.00
XXXIII.	(Nos. 134-139). 448 pp., 51 pls. Devonian annelids, Tertiary mollusks, Ecuadoran stratigraphy paleontology.	16.00
XXXIV.	(Nos. 140-145). 400 pp., 19 pls. Forams, cephalopods, ostracods, conularid bibliography.	16.00
XXXV.	(Nos. 146-154). 386 pp., 31 pls. Forams, cephalopods, mollusks, ostracods.	16.00
XXXVI.	(Nos. 155-160). 412 pp., 53 pls. Forams, Eocene fish, rudists.	16.00
XXXVII.	(Nos. 161-164). 486 pp., 37 pls. Antillean Cretaceous Rudists, Canal Zone Foraminifera, Stromatoporoidea.	16.00
XXXVIII.	(Nos. 165-176). 447 pp., 53 pls. Forams, ostracods, mollusks, Carriacou, fossil plants.	18.00
XXXIX.	(Nos. 177-183). 448 pp., 36 pls. South American forams, Panama Caribbean mollusks.	16.00
XL.	(No. 184). 996 pp., 1 pl. Type and Figured Specimens P.R.I.	18.00
XLI.	(Nos. 185-192). 381 pp., 35 pls. Forams, mollusks, carpoids, Corry Sandstone.	16.00
XLII.	(No. 193). 673 pp., 48 pls. Venezuelan Cenozoic gastropods.	18.00
XLIII.	(Nos. 194-198). 427 pp., 29 pls. Ordovician stromatoporoids, Indo-Pacific camerinids, Mississippian forams, Cuban rudists.	16.00
XLIV.	(Nos. 199-203). 365 pp., 68 pls. Puerto Rican, Antarctic, New Zealand forams, Lepidocyclina, Eumalacostraca.	16.00
XLV.	(No. 204). 564 pp., 63 pls. Venezuela Cenozoic pelecypods.	18.00
XLVI.	(Nos. 205-211). 419 pp., 70 pls. Forams, Crustacea, brachipods, Recent mollusks.	16.00
XLVII.	(Nos. 212-217). 584 pp., 83 pls. Forams, mollusks, polychaetes, ammonites.	18.00
XLVIII.	(No. 218). 1058 pp., 5 pls. Catalogue of the Paleocene and Eocene Mollusca of the Southern and Eastern United States.	18.00
XLIX.	(Nos. 219-224). 671 pp., 83 pls. Peneroplid and Australian forams, North American carpoids, South Dakota palynology, Venezuelan Miocene molluska, *Voluta*.	18.00

SMITHSONIAN INSTITUTION LIBRARIES

SMITHSONIAN INSTITUTION LIBRARIES

BOUND BY

SMITHSONIAN INSTITUTION LIBRARIES
3 9088 01356 8316